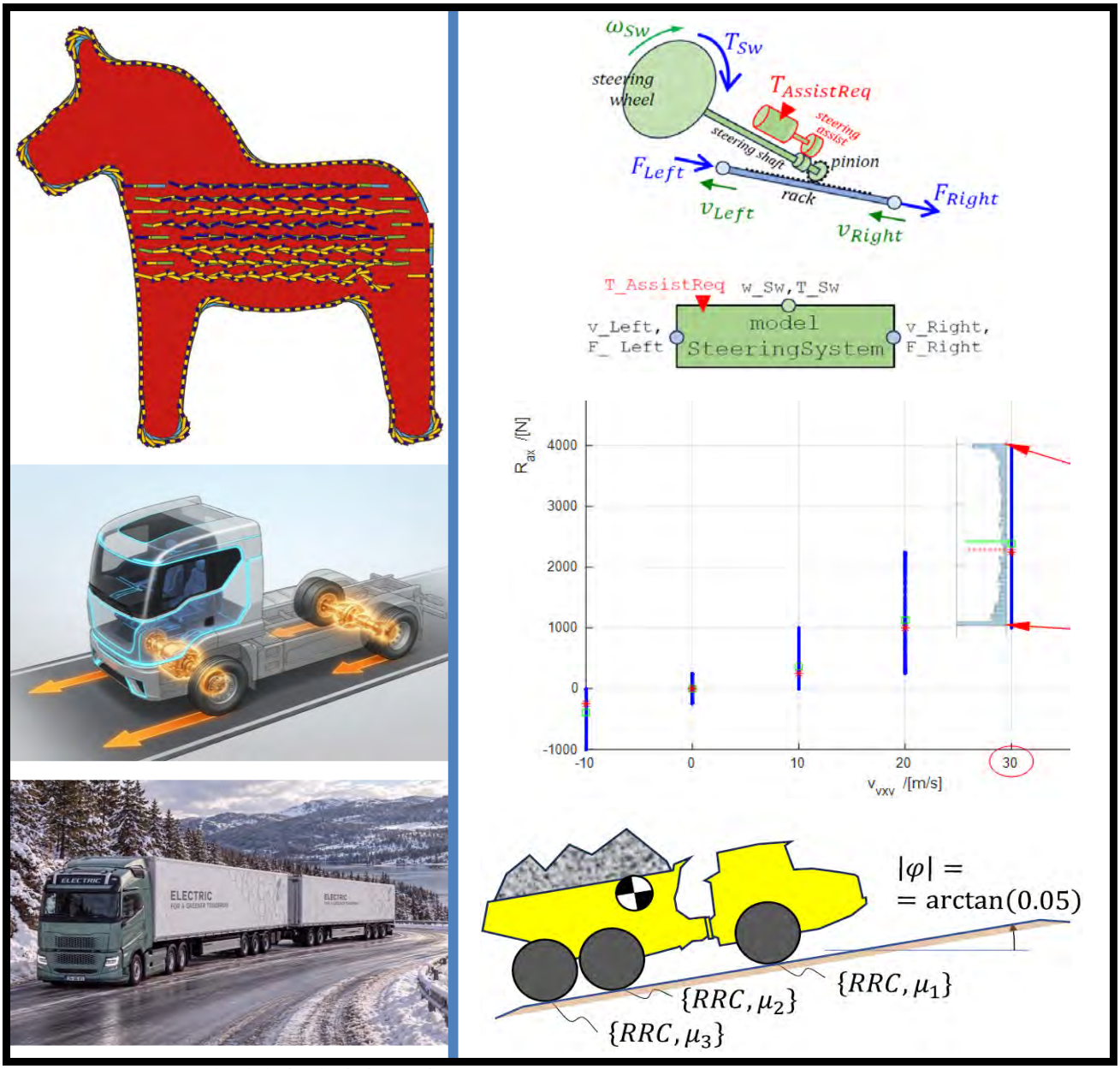
CHALMERS

VEHICLE MOTION ENGINEERING



Latest version *2026-10-05 16:58* (incl. unfinished material): https://www.dropbox.com/scl/fi/76jtg7b3erlkyhf0p7srw/VehicleMotionEngineering.pdf?rlkey=hzv3wntgs7kops474wsgb1g3c&dl=0

All annual editions are found here: https://research.chalmers.se/en/person/bengtja and here: https://dx.doi.org/10.5281/zenodo.23164683

Bengt Jacobson et al,
Vehicle Dynamics Group, Division Vehicle and Autonomous Systems,
Department of Mechanics and Maritime Sciences, Chalmers University of Technology, www.chalmers.se

CC BY NC SA

Recommended citation: Jacobson, Bengt et al., *Vehicle Motion Engineering*. Chalmers University of Technology. https://dx.doi.org/10.5281/zenodo.23164683

Prefaces

Preface 2026

Minor updates/additions, such as: about parameterisation of axle kinematic performance, energy losses from aerodynamics with varying operating conditions, local tyre stiffnesses, tyre wear, and power losses in tyre due to rolling resistance and slip.

/Bengt Jacobson Göteborg, October 2026

Preface 2025

The List of contents removed again, with advice to use pdf reader with pdf-bookmark browser.
Many contribute to this book, and new for present edition are:

Yansong Huang, Volvo Cars and Chalmers
Zhaohui Ge, Chalmers
Sachin Janardhanan, Volvo Trucks and Chalmers
Mattias Hjort, VTI

My apologies to contributors I have forgotten. Remind me, and I will add you to next Preface!

/Bengt Jacobson Göteborg, Oktober 2025

Preface 2024

The pre-title "Compendium in" is removed in this edition, with reference to that the AI chatbot ChatGPT proposed that it is a book than a compendium.
Many contribute to this book, and new for present edition are:

Alireza Marzbanrad, Volvo Trucks

My apologies to contributors I have forgotten. Remind me, and I will add you to next Preface!

/Bengt Jacobson, Göteborg, *October 2024*

Preface 2023

The List of contents have been removed because the Compendium in pdf format has pdf bookmarks, by which you get a better good overview and can more navigate easily.
Many contribute to this compendium, and new for present edition are:

Umur Erdinc, Volvo Trucks and Chalmers

My apologies to contributors I have forgotten. Remind me, and I will add you to next Preface!

/Bengt Jacobson, Göteborg, October 2023

Preface 2022

Many contributes to this compendium. I try to mention them under a section heading where they mainly have contributed.
My apologies to contributors I have forgotten. Remind me, and I will add you to next Preface!

/Bengt Jacobson, Göteborg, October 2022

Preface 2021

In this edition, the compendium has changed name from Vehicle dynamics to Vehicle Motion Engineering. The marking with § has been removed. Many contribute to this compendium, and new for version 2021 are:

Ingemar Johansson, Vehicle Engineering, Chalmers
Mats Jonasson, Vehicle Dynamics, Chalmers
Edo Drenth, Haldex Brakes
Per Johannessen Per, Volvo Trucks
Toheed Ghandriz, Vehicle Dynamics at Chalmers

My apologies to contributors I have forgotten. I can add you to next version! */Bengt Jacobson, Göteborg, October 2021*

Preface 2020

From and including 2020, Chalmers does not print the compendium on paper. Therefore, the two variants, "Printed on paper" and "Digital only" introduced 2019, are not equally motivated. So, the material marked with "#Digital only" from 2019 is kept, and still with blue text, but now marked "§ ". The reader should understand the extra material as possible to jump over for a basic understanding but recommended if aiming for more advanced knowledge.

Many contribute to this compendium, and new for version 2020 is that contributors are mentioned in the beginning of the section where their contribution was primarily done:

Jelena Andric and Majid Astaneh, Chalmers
Pinar Boyraz, Vehicle Safety at Chalmers (in memorial)
Adam Brandt, Vehicle AeroDynamics at Chalmers and CEVT
Fredrik Bruzelius, Vehicle Dynamics at Chalmers and VTI
Niklas Fröjd, Volvo Trucks
Toheed Ghandriz, Vehicle Dynamics at Chalmers
Anders Hedman, Volvo Trucks
Inge Johansson, Volvo Trucks
Ingemar Johansson, CEVT and Vehicle Engineering at Chalmers
Mats Jonasson, Volvo Cars and Vehicle Dynamics at Chalmers
Mikko Karisaari, Oulo University, Finland
Waltteri Koskinen, student at Tampere University, Finland
Leo Laine, Volvo Trucks and Chalmers
Mathias Lidberg, Vehicle Dynamics at Chalmers
Luigi Romano, Vehicle Dynamics at Chalmers
Dragan Sekulić, Vehicle Dynamics at Chalmers
Alexey Vdodin, Vehicle AeroDynamics at Chalmers

My apologies to contributors I have forgotten. I can add you to next version! */Bengt Jacobson, Göteborg, October 2020*

Preface 2019

The compendium 2019 is published in 2 variants: "Printed on paper" and "Digital only". Both are available as pdf-file. The "Digital only" variant contains some additional material; search for "#DigitalOnly". The numbered items (figures, equations, etc) in the "Digital only" variant does not have numbering, in order to keep same numbers of each item between the variants. However, note that page numbering varies between the variants.

Thanks to Tobias Brandin, Fredrik Bruzelius, Edo Drenth, Niklas Fröjd, Toheed Ghandriz, Patrick Gruber, Mats Jonasson, Mathias Lidberg, Anders Lindström, Oscar Ljungcrantz, Peter Nilsson, Luigi Romano, Juliette Utbult and errata reporting from students. Sorry, if I forgot some contributor! */Bengt Jacobson, Göteborg, October 2019*

Preface 2018

One large rearrangement is done: Subsystem descriptions has been collected from Chapter 3, 4 and 5 to 2.3-2.7. Also, minor changes and additions has been done throughout all chapters. Many thanks to, among other, Niklas Fröjd Volvo GTT, Toheed and Fatemeh Ghandriz, Ingemar Johansson CEVT, Mats Jonasson VCC, Mathias Lidberg, Simone Sebben, Alexey Vdovin. Thanks also to many students that have found and reported errors in the previous edition.

/Bengt Jacobson, Göteborg, October 2018

Preface 2017

This edition has various smaller changes and additions. Thanks to Fredrik Bruzelius (VTI), Tobias Brandin (VCC), Niklas Fröjd (Volvo GTT), Assar Jarlsson (Kinnarps), Pär Pettersson (Chalmers), among others. Thanks also to many students that have found and reported errors in the previous edition. */Bengt Jacobson, Göteborg, October 2017*

Preface 2016

This edition has various changes and additions. Some of these are: Chapter 1: Control engineering, Chapter 2: Tyre models, Driver models, Chapter 3: Propulsion systems, Varying road pitch, Non-reactive truck suspensions, Chapter 4: Track-ability, Articulated vehicles, and Cambering vehicles.

Thanks to Cornelia Lex (TU Graz), Fredrik Bruzelius (VTI), Niklas Fröjd, Anders Hedman, Kristoffer Tagesson, Peter Nilsson, Sixten Berglund (Volvo GTT), Tobias Brandin, Edo Drenth, Mats Jonasson (VCC), Mathias Lidberg, Artem Kusachov, Anton Albinsson, Manjurul Islam, Pär Pettersson, Ola Benderius (Chalmers), Mats Sabelström, and Roland Svensson among others.

/Bengt Jacobson, Göteborg, October 2016

Preface 2015

This edition has various changes and additions. Some of these are: brush model with parabolic pressure distribution, typical numerical data for heavy vehicle, added "2.2.3 Tyre", "4.5.3.2 Example of explicit form model", more about tyre relaxation, introduction of neutral steering point, introduction of steady state roll-over wheel lift diagram. Thanks to Anton Albinsson, Edo Drenth (VCC), Gunnar Olsson (LeanNova), Manjurul Islam, Mathias Lidberg, Mats Jonasson (VCC), Niklas Fröjd (Volvo GTT), Ola Benderius, Pär Pettersson, and Zuzana Nedelkova among other. */Bengt Jacobson, Göteborg, 2015*

Preface 2014

This edition has various small changes and additions. The largest changes are: Function definitions added and major update of sections 2.3, 4.1.1, 0, 6.1.1.

Thanks to Lars Almefelt from Chalmers, Jan Andersson from VCC, Kristoffer Tagesson from Volvo GTT and Gunnar Olsson from Leannova and Karthik Venkataraman. */Bengt Jacobson, Göteborg, 2014*

Preface 2013

This edition has various small changes and additions. The largest additions were in: Functional architecture, Smaller vehicles, Roll-over, Pendulum effect in lateral load transfer and Step steer.

Thanks to Gunnar Olsson from LeanNova, Mathias Lidberg, Marco Dozza, Andrew Dawkes from Chalmers, Erik Coelingh from Volvo Cars, Fredrik Bruzelius from VTI, Edo Drenth from Modelon, Mats Sabelström, Martin Petersson and Leo Laine from Volvo GTT. */Bengt Jacobson, Göteborg, 2013*

Preface 2012

A major revision is done. The material is renamed from "Lecture notes" to "Compendium". Among the changes it is worth mentioning: 1) the chapters about longitudinal, lateral and vertical are more organised around design for vehicle functions, 2) a common notation list is added, 3) brush tyre model added, 4) more organised and detailed about different load transfer models, and 5) road spectral density roughness model is added.

Thanks to Adithya Arikere, John Aurell, Andrew Dawkes, Edo Drenth, Mathias Lidberg, Peter Nilsson, Gunnar Olsson, Mats Sabelström, Ulrich Sander, Simone Sebben, Kristoffer Tagesson, Alexey Vdovin and Derong Yang for review reading.

/Bengt Jacobson, Göteborg, 2012

Preface 2011

Material on heavy vehicles is added with help from John Aurell. Coordinate system is changed from SAE to ISO. Minor additions and changes are also done. */Bengt Jacobson, Göteborg, 2011*

Preface 2007

This document was developed as a result of the reorganization of the Automotive Engineering Master's Programme at Chalmers in 2007. The course content has been modified in response to the redistribution of vehicle dynamics and power train education.

These lecture notes are based on the original documents developed by Dr Bengt Jacobson. The text and examples have been reformatted and edited but the author is indebted to the contribution of Dr Jacobson. */Rob Thomson, Gothenburg, 2007*

=== === ===

Keywords: Vehicle Engineering, Automotive Engineering, Vehicle Dynamics, Vehicle Motion, Energy, Modelling, Modelica, Simulation

Cover: From last year of vehicle dynamics education and research at Chalmers:
Left column, from top: From cover of Zhaohui Ge's licentiate thesis, Sachin Janardhanan's PhD thesis, and Umur Erdinç's PhD thesis. Zhaohui's picture consists of many small vehicle trajectories for reversing long heavy combinations vehicles, reversing in a horse (dalahäst) shape. **Right column:** Figures from book and exams given by Vehicle Dynamics group at Chalmers.

Göteborg, Sweden, 2026-10-05 16:58

© Copyright: Chalmers University of Technology, Bengt Jacobson

1 INTRODUCTION

1.1 What is Vehicle Motion Engineering

Vehicle Motion Engineering an engineering subject about motion of vehicles in user-relevant operations. Previous versions of the same book were called Vehicle Dynamics compendium. The power and energy from actuators are also included as well as the algorithms that control them. The subject is applied, and applied on a certain group of products, i.e., vehicles. The subject always uses terms, theories, and methods from Mechanical/Machine engineering, but often also from Control/Signal engineering and Human behavioural science.

1.2 About this book

This book was originally written for the course "MMF062 Vehicle Motion Engineering" at Chalmers University of Technology. The book now covers more than included in that course; both in terms of subsystem designs and in terms of some teasers for more advanced studies of vehicle dynamics. Therefore, it is also useful for the more advanced course "TME102 Vehicle Modelling and Control" and other courses and project work.

The reader of this book is assumed to have knowledge of mathematics and mechanics, to the level of a Bachelor of Engineering degree. Previous knowledge in dynamic systems, often taught well in Control Engineering courses, is useful.

The overall objective of the book is to educate vehicle dynamists, i.e., engineers that understand and can contribute to development of good motion and energy functionality of vehicles. The book focuses on road vehicles, primarily passenger cars and commercial vehicles. Smaller road vehicles, such as bicycles and single-person cars, are only very briefly addressed. It should be mentioned that there exist a lot of ground-vehicle types not covered at all, such as: off-road/construction vehicles, tracked vehicles, horse wagons, hovercrafts, or railway vehicles.

The book is public as a pdf file, see links on the cover page. The main editor, bengt.jacobson@chalmers.se, is happy to supply background material (Matlab scripts, Modelica models, etc) on demand. In principle to anyone on the planet, but priority is to support students or previous students at Chalmers.

Chapter 1 introduces automotive industry and the overall way of working there (1.3, 1.4). Then, Section 1.5 defines required pre-knowledge from "product-generic" engineering. Section 1.5.4.1.8 and onwards comes back to specific for vehicles.

The vehicle is a component or subsystem in a superior transport system consisting of other road users, roads, and transport missions. A vehicle is also, itself, a system within which many components or subsystems interact. Chapter 2 describes what interacts with a vehicle from outside, like aerodynamics and driver. Vehicle dynamics is about how to quantitatively predict and analyse the complete vehicle's behaviour. To do that, a vehicle dynamist must quantitatively understand how most of the vehicle's subsystems works, but not how to design (or engineer) these subsystems. Therefore, Chapter 2 also describes the subsystems relevant for vehicle dynamics (see also Figure 2-2):

- Wheels and Tyre in 2.2
- Suspension in 2.3 (and 3.4.5.2 and 4.3.7.11)
- Propulsion in 2.4
- Braking System in 2.5
- Steering System in 2.6
- Environment Sensing System in 2.8

Functions are needed for requirement setting (1.4), design engineering and verification (1.6.5, 1.6.6). The overall order within the book is that models/methods/tools needed to understand each function are placed before the functions. Chapters 3-5 describes (complete vehicle) "functions", organised after vehicle motion directions:

- Chapter 3: Longitudinal dynamics
- Chapter 4: Lateral dynamics
- Chapter 5: Vertical dynamics

1.3 Automotive engineering

This section is about the context where Vehicle motion engineering is mainly applied, i.e., the automotive industry. *OEM* means Original Equipment Manufacturer and is, within the automotive industry, used for a vehicle manufacturer. OEM is a legal status in some countries. In the automotive industry, the word Supplier means supplier to an OEM. A *Tier1* supplies directly to an OEM. A *Tier2* supplies to a Tier1 and so on. Primarily, suppliers supply parts and subsystems to the OEMs, but suppliers can also supply competence, i.e., consultant services.

From an engineering view, an OEM does Product Development and Manufacturing. But it is good to remember that there is also Purchasing, Marketing & Sales, After Sales, etc. However, Product Development is the main area where the vehicles are designed. It is typically divided into Powertrain, Chassis, Body, Electrical and (Complete) Vehicle Engineering. Vehicle Dynamics competence is mainly needed in Chassis, Powertrain, and Vehicle Engineering.

On supplier side, Vehicle Dynamics competence is mainly needed for system suppliers that supplies propulsion, brake, steering and suspension systems. Additional to OEMs and suppliers, Vehicle Dynamics competence is also needed in authorities for legislation and testing as well as research institutes.

There are engineering associations for automotive engineering. FISITA (Fédération Internationale des Sociétés d'Ingénieurs des Techniques de l' Automobile, www.fisita.com) is the umbrella organisation for the national automotive societies around the world. Examples of national societies are IMechE (United Kingdom), JSAE (Japan), SAE (USA), SAE-C (Kina), SATL (Finland), SIA (France), SVEA (Sweden, www.sveafordon.com) and VDI FVT (Germany). There is a European level association also, EAEC.

1.3.1 Vehicle Dynamics Engineers' Industry Roles

The activity type that sets the pace in automotive industry are vehicle programme or projects. It defines the **technology** to be developed, the **time** and **cost** aspects. The work is organised around such programmes, both at vehicle manufacturers and their sourced subsystem supplier. One way to exemplify such is Figure 1-1. Engineers with vehicle dynamics profile are typically active at departments called Chassis, Complete Powertrain, Electrical or Vehicle Engineering. They are responsible for deliverables to vehicle programme in the form of:

- **Hardware**: Geometry, Strength and function per subsystem, ECUs
- **Software**: SW in, and communication, between subsystems, Functions such as ABS, ESC, ACC
- **Requirement setting and verification**: Handling, Driveability, Brake performance, Ground clearance, Ride comfort, Energy consumption. Verification in **real and virtual tests**.

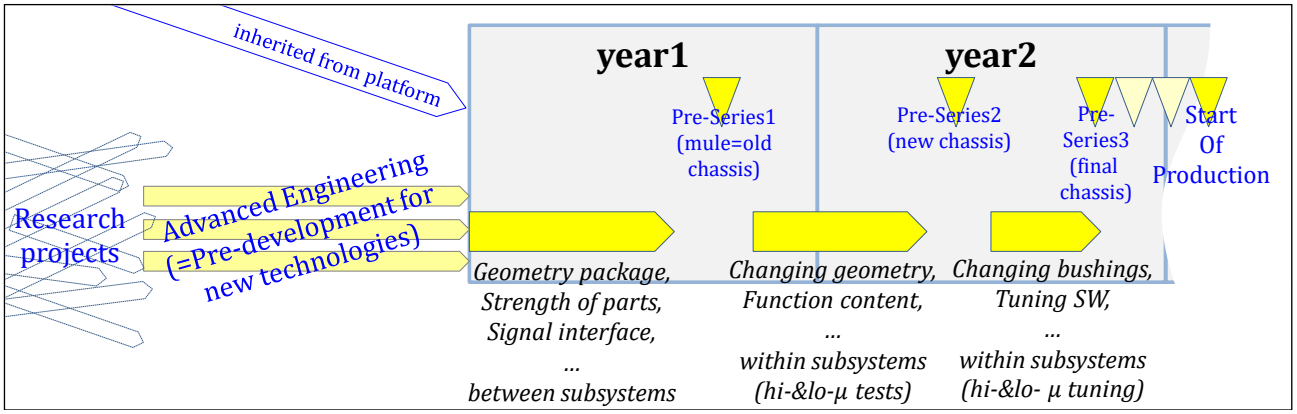


Figure 1-1: An example of vehicle programme and Vehicle Dynamics related activities.

A system to define levels within development is the Technology Readiness Level (TRL), see https://en.wikipedia.org/wiki/Technology_readiness_level. The TRL levels is sometimes grouped to: Research (TRL1..3), Development (TRL4..6) and Deployment TRL7..9.

1.3.1.1 Vehicle programme size and life length

A vehicle programme typically aims on a volume of 10..100 thousands of vehicles per year, manufactured over 3-10 years, where the smaller volumes and the longer manufacturing times are more typical for heavy vehicles. An alternative to traditional vehicle programmes is to develop smaller series, for few selected customers, pilot projects. Some claim that, for paradigm shifts like automated driving and electromobility, smaller commercial pilots are more suitable than large vehicle programmes. The software in the vehicles, can even be updated after sales, which is a continuous development, leaving the concept of only develop towards a certain production start date.

1.4 Requirement Setting

Contribution from Ingemar Johansson, CEVT and Vehicle Engineering at Chalmers

Development of complex products, as vehicles, is driven by **Requirements**, coming from:

- Manoeuvres/Vehicle operations/Use cases, representative for the need of the customers/users
- Legislation from the authorities and Rating from consumer organisation, and
- Engineering constraints from the manufacturer's platform/architecture on which the vehicle should be built, to enable reuse of previous good solutions.

One way of organising requirements is to also define **Attributes**, and **Functions**. The terms are not strictly defined and may vary between vehicle manufacturers and over time. With this said, it is assumed that the reader understands 1.4 as approximate and exemplifying.

In the whole book, both attributes and functions concern the **complete vehicle**, not the subsystems within the vehicles and not the superior level of the transportation system with several vehicles in a road infrastructure.

Attributes and Functions are used to establish processes and structures for requirement setting and verification within a vehicle engineering organisation. Such processes and structures are important to enable a good overall design of such a complex product as a vehicle intended for mass production at affordable cost. Figure 1-2 gives an overview, with reference to the V-process https://en.wikipedia.org/wiki/V-Model, of how a vehicle is developed. Note that these kinds of figures are very idealized, and one should neither trust the process too much nor neglect them. A vehicle is a very complex product. First, it has several levels of functions and subsystems. Secondly, it is difficult to keep a clean hierarchical order between functions and subsystems. Thirdly and most conceptually

difficult, is the fact that each subsystem gets requirements from many functions as showed by the dashed lines; this makes the complexity explode.

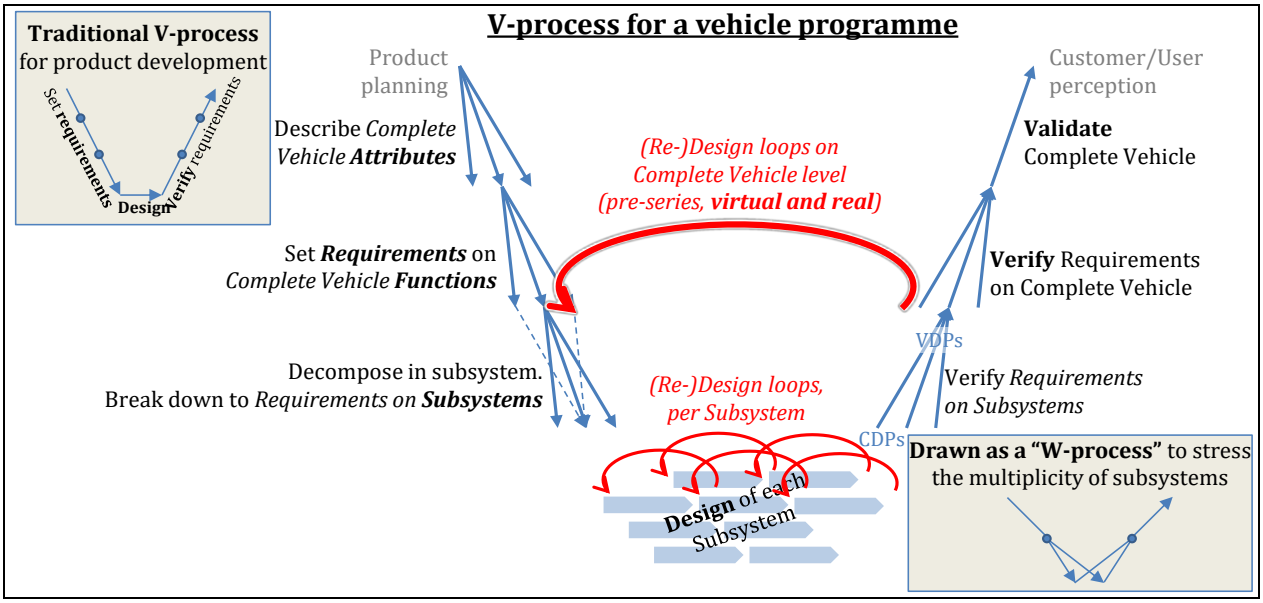


Figure 1-2: V-process for a vehicle program. Faster design loops gives faster (more "agile") development. Note that virtual verification on complete vehicle level can be made either assuming values on concrete or virtual design parameters (CDPs or VDPs), see Figure 1-6.

The "agility" (https://en.wikipedia.org/wiki/Agile_software_development) of the development must be high for complex products as vehicles to keep development time down. Terms, as *agile development*, vary over time and between different parts of industry.

In automotive engineering, the subsystems maturity levels are traditionally called A-, B-, and C-samples, where A-sample is the first version. The division into these sample levels becomes lesser clear with today's development of mechatronic subsystems, where the control algorithms can be updated much more frequent.

1.4.1 Attributes

An attribute is a high-level aspect of how the users perceive the vehicle. Attributes which are especially relevant for vehicle dynamics are listed in Table 1-3. The table is much generalised and the attributes in it would typically need to be decomposed into sub-attributes when used in the engineering organisation of an OEM. Also, not mentioned in the table, are attributes which are less specific for vehicle dynamics, such as Affordability (low cost for user), Quality (functions sustained over vehicle lifetime), Styling (appearance, mainly visual), etc.

An Attributes is a way to group functions, especially useful for an OEM organisation and vehicle development programs. Functions are a way to group requirements. **Legal** requirements are often, but not always, possible to trace back to, primarily, one specific attribute. Requirements arising from OEM-internal **platform and architecture constraints** are often more difficult to trace in that way. Hence, "platform/architecture" is a "requirement container", beside the attributes.

Table 1-3: Attributes relevant for Vehicle Dynamics / Vehicle Motion.

↓Attribute	Description↓
Transport Efficiency	This attribute means to maximize output from and minimize costs for transportation. Transport output can be measured in $person \cdot km$, $ton \cdot km$ or $m^3 \cdot km$. The costs are mainly energy costs and time, but also wear of vehicle parts influence. The attribute is most important for commercial vehicles but becomes increasingly important also for passenger vehicles. The attribute is mainly addressing long-term vehicle usage pattern, typically 10 min to 10 hours. There are diverse ways to define such usages, e.g. (Urban / Highway / Mixed) driving cycles. So far, the attribute is mainly required and assessed by the vehicle customers/users. The attribute can also be seen to include "Environmental Efficiency", which means low usage of natural resources (mainly energy) and low pollution, per performed transport task. This is to a substantial extent required and assessed by society/legislation.
Safety	Minimizing risk of property damages, personal injuries and fatalities both in vehicle and outside, while performing the transportation. This attribute is to a considerable extent required and assessed by society/legislation. In some markets, mainly developed countries, it is also important for vehicle customers/users.
User Experience (or Driver Experience)	How the occupants (often the driver) experience the vehicle during transport; from relaxed transport (comfort) to active driving (sensation). This attribute contains sub-attributes as: • **Ride comfort**. Ride comfort often refers to vibrations and harshness of the occupants' motion, primarily vertical but secondly longitudinal and lateral. So, V and H in NVH (=Noise, Vibration and Harshness) is included. If expanding to "comfort" it would include also N (noise) and compartment air conditioning, but these sub-attributes are less related to vehicle dynamics. • **Performance** describes how the vehicle can perform at the limits of its capabilities: acceleration, deceleration, and cornering. Most often, it refers to longitudinal limitations due to propulsion and brake systems limitations. • **Driveability, Handling and Roadholding** describes how the vehicle responds to inputs from driver and disturbances, and how driver gets feedback from vehicle motion e.g., through steering feel. It is also the corresponding response aspects for a "virtual driver", i.e., a control algorithm for automated driving. Driveability often refers to longitudinal (acceleration, braking gear shifting). Handling and Roadholding often refer to lateral manoeuvres. • **Trust** in automated driving becomes increasingly important and needs to be balanced; high trust but not over-trust. This attribute is to a considerable extent required and assessed by the vehicle customers/users, both through own experience but also indirectly via assessments by experts, e.g. in motor journals.

1.4.2 Functions

In this book, a *function* is more specific than an attribute. A function should define *measures* of something the (complete) vehicle does, so that one can set (quantitative) *requirements* on each measure, see 1.4.3. The function is not primarily fulfilled by any specific subsystem. However, the realisation of a function in a certain vehicle programme, normally only engages a limited subset of all subsystems. So, the function will there pose requirements on those subsystems. Hence, it is easy to mix up whether a function origin from an attribute or a subsystem. One way to categorise functions is to let each function belong to the subsystem which it mainly implies requirements on rather than the source attribute. Categorizing functions by subsystems tends to lead to "carry-over" function realisations from previous vehicle program, which can be good enough in many cases. Categorizing functions by source attribute facilitates more novel function realisations, which can be motivated in other cases.

The word "function" has appeared very frequently lately along with development of electrically controlled systems. The function "Accelerator pedal driving" in 3.5.2.2 has always been there, but when the design of it changed from mechanical cable and cam to electronic communication and algorithms (during 1990's) it became much more visible as a function, sometimes referred to as "electronic throttle". The design, or realization, of the same function was changed. The change of design enabled, or was motivated by, improvement of some sub-functions, e.g., idle speed control which works better in a wider range of engine and ambient temperature.

Some section headings in the book have an **asterisk "*"**. This marks that the section contains a function. The "**Function definition**" is given in the semantic form in Eq [1.1].

A generic "Function definition":

{The Function} *is* {***a Measure***} *for some* {***Fixed Conditions***} *and some* {***Parameterized Conditions***}. [1.1]

One example is:

> ***Braking Distance*** *is the* ***distance travelled during braking*** *with* ***{fully applied brake pedal*** *from* ***100 km/h straight*** *driving to* ***stand-still}*** *and* {*road peak* ***friction coefficient 0.5*** *on* ***level*** *ground* ***without headwind*** *and vehicle loaded with* ***kerb weight and 100 kg on the roof***}.

The word "conditions" should be understood as a manoeuvre, operation or use case. It is often possible and efficient to define multiple measures from one "condition" by varying the parameterized conditions.

The {*Measure*} should be one unambiguously defined measure (such as time, velocity or force) of something the vehicle does. The {*Measure*} is ideally a continuous, objective and scalar physical quantity, subjected for setting a requirement on the vehicle. The {*Fixed Conditions*} should be unambiguously defined and quantified conditions for the vehicle and its surroundings. The keyword "*certain*" identifies the {*Parameterized Conditions*}, which need to be fixed to certain numerical values or probabilistic distributions, before using the Function definition for requirement setting, see 1.4.3.

Since the term "Function" is defined very broadly in the book, these definitions become very different. One type of Function definition can be seen in "3.2.5.1 Top speed *", which includes a well-defined measure. Another type of Function definition is found in "3.5.2.4 Anti-Lock Braking System, ABS *" and "4.3.3 Under-, Neutral- and Over-steering *". Here, the definitions are more on free-text format, and an exact measure is not so well defined.

1.4.2.1 Organising Functionality

There is, of course, not any single physically correct or incorrect way to organise the total functionality in a vehicle into a finite list or structure of functions. However, defining functions is helpful when organising the development in a vehicle programme or when inheriting functionality between vehicle programmes. Examples of categorisation of functions are:

- Function break-down in tree-structure from **attributes**. This facilitates development from user needs and is often argued as the best.
- Functions assigned to the **(sub-)system** which the function mainly belong (purchase-wise or technology-wise). Such categories can be, e.g., Brake functions and Steering functions.
- Functions sorted in **"Customer** functions**"** and **"Support** functions**"**. A Support function is typically used by many customer functions, see "1.6.4.2 Vehicle Function Architecture".
- Functions sorted in **Standard** and **Option** in the product to end customer.
- **Dynamic** vs **Driver-informing** functions, differentiated by whether the function actuates vehicle motion or only inform/warn driver.

1.4.2.1.1 Vehicle Motion Functions Broken-down from Attributes

An example of tree-structure, starting from the attributes in Table 1-3, is given below. The attributes are broken down towards functions. The level where a Function description can be formulated would be the deepest on each branch in this tree-structure. In some places, "subjective assessment" can replace the unit, because far from all functions/requirements are measurable. The example tree-structure below does not reach the Function description level.

- **Transport Efficiency**
  (These measures require a certain transport operation to be defined, see 3.3.1.)
  The inverse of *Transport efficiency* is *Transport cost* in $[€/m]$ or $[€/(ton \cdot km)]$. This is the sum of several terms:
  - *Energy consumption costs*; which depends on energy $[€/Nm]$ or fuel price $[€/m^3]$, see 3.3.5.1
  - *Transport time costs*; which depends on driver salary for goods transports and on occupant travel time cost $[€/h]$ for passenger transports, see 3.3.5.2
  - *Component wear costs;* e.g. tyre wear (2.2.9), battery degradation, etc. The cost can be quantified via a life quantity (e.g. $[m]$ tread thickness for tyres) and a DegradationQuantity (e.g. $[m/s]$ for tyres) and a Replacement cost $[€/replacement]$.
- **Safety**
  (These measures require a certain manoeuvre or traffic scenario. When adding several measures, one has to consider severity and probability of those.)
  - *Speed reduction before collision*; in $[m/s]$
  - *Avoidance speed*; in [m/s] maximum entry speed to the traffic scenario, or to a cone track, lane change or tightening curve
  - *Longitudinal Deceleration*; in [s] for decelerating from one speed to another speed in a straight-line or curve.
- **User Experience**
  - **Ride comfort**
    - *Vertical stationary oscillations*; in vertical amplitude per road displacement amplitude $[(m/s^2)/m]$ for a certain irregularity of road at certain speed
    - *Vertical and longitudinal transient shock*; in $[m/s^3]$ vertical and longitudinal peak when driving over certain cleat on road in certain speed
  - **Performance**
    - Longitudinal Acceleration ([s] for accelerating from certain speed to another certain speed)
    - Lateral SteadyState Acceleration $[m/s^2]$ when driving in certain radius)
  - **Driveability, Handling and Roadholding**
    - Longitudinal Acceleration margins $[m/s^2]$ or *subjective assessment* peak or average during certain transport task)
    - Transport time ([s] or *subjective assessment* around a certain handling track)
    - Pedal response $[(m/s^2)/m]$ or $[(m/s^2)/N]$) for step pedal apply
    - Steering wheel response ([(rad/s)/deg]) or *subjective assessment* for step or oscillating steering
  - **Trust** (requirements here are far from well established)
    - *Subjective assessment* after longer (maybe ≥a week) use of the vehicle. Many and/or well-trained test users needed. A questionnaire can be used to organise subjective assessment in different traffic situation, low/high speed, light/dark, dry/slippery road, longitudinal interaction with other road users, lateral interaction with lane edges, etc.

1.4.3 Requirements

A requirement shall be such that it is possible to verify how well a product fulfils it. A requirement on the complete vehicle is typically formulated as:

A generic "Requirement" (referring to a certain "Function definition"): [1.2]

The vehicle *shall fulfil*
{the Function measure} {< or > or ≈} {number [unit]}.

One example is:

The vehicle *shall fulfil* ***Braking Distance < 30 [m]***.

Examples (with included function descriptions):

The vehicle *shall…*

- *… accelerate from 50 to 100 km/h in* ***<5 s*** *when full acceleration pedal. On level road.*
- *… decelerate from 100 to 0 km/h in* ***<35 m*** *when brake pedal is fully applied, without locking any rear wheel. On straight and level road.*
- *… turn with outermost edge on a diameter* ***<11m*** *when turning with full steering at low speed.*
- *… have a characteristic speed of* ***70 km/h (±10 km/h).*** *On level ground and high-friction road conditions and any recommended tyres.*
- *… give a weighted RMS-value of vertical seat accelerations* $<1.5\,m/s^2$ *when driving on road with class B according to ISO 8608 in 100 km/h.*
- *… keep its body* ***above a 0.1 m*** *high peaky two-sided bump when passing the bump in 50 km/h.*

To limit the amount of text and diagrams in the requirements it is useful to refer to ISO and OEM specific standards. Also, it is good to document the purpose and/or use cases with the requirement.

The above listed requirements stipulate the function of the vehicle, which is the main approach in this book. Alternatively, a requirement can stipulate the design of the vehicle, such as "The vehicle shall weigh <1600 kg" or "The vehicle shall have a wheel base of 2.5 m". The first type (above listed) can be called *Performance based requirement*. The latter type can be called *Design based requirement* or *Prescriptive requirement* and such are rather "means" than "functions", when seen in a function vs mean hierarchy. It is typically desired that requirements are Performance based, else they would limit the technology development in the OEM and/or the society.

1.4.3.1 Absolute or Relative Requirements

The requirements above are expressed as *absolute*, in the sense that they can be verified for one single vehicle. This is necessary for legal requirements. However, it is very difficult to develop verification methods, especially virtual methods, as good as needed for absolute requirement verification. Hence, it is common to compare between two or multiple designs, in which one uses *relative* requirements. The comparison is typically a comparison of the same defined measure with a competitor vehicle or previous development loop. Rewriting the first listed requirement from above gives this example of relative requirement:

> ***The vehicle*** *shall accelerate from 50 to 100 km/h in* ***smaller time than*** *a certain competitor (or our vehicle design in previous development loop) when full acceleration pedal.*

1.4.3.2 Experiment Matrix

This section claims that an *Experiment Matrix* (or *Test Matrix*) often is useful and proposes how to reason when generate such a matrix.

In the previous description of requirements, it was assumed that one set of numerical parameters can represent all relevant manoeuvre/operation. In most cases this could lead to overfitting of design parameters, so that the vehicle does not perform well in real use. Therefore, one often need to vary the manoeuvre/operation parameters over multiple experiments. We can use an *Experiment Matrix* to select variations within the manoeuvre/operation space. Before deciding the experiment matrix, it is often good to start from a *Manoeuvre/Operation Parameter Span Matrix*. Figure 1-4 shows an example.

Manoeuvre/Operation Parameter Span Matrix

Manoeuvre			Road					Use	
initial speed v_{x0} [km/h]	acceleration [m/s^2]	...	(down) grade	radius [m]	road-to-tyre peak friction	road friction variation	...	Payload [ton]	...
80	-8		0	∞	0.8 (hi)	constant		0	
	-2		5 deg	$\frac{v_{x0}}{3}$	0.2 (lo)	split, left/right=lo/hi		25	
						step up			
						step down			

Experiment Matrix (or Test Matrix)

Experiment									
Name1	22	-8		0	∞	0.8	constant		25	
Name2	22	-8		0	∞	0.8	constant		0	
Name3	22	-8		0	∞	0.2	constant		25	
Name4	22	-8		0	22/3	0.2	constant		25	
Name5	22	-8		0	22/3	0.2	step up		25	

Figure 1-4: An example of "Span Matrix" and "Experiment Matrix" for brake performance. The "span matrix" here can generate up to $1 \cdot 2 \cdot 2 \cdot 2 \cdot 2 \cdot 4 \cdot 2 = 128$ *experiments. An "experiment matrix" shows which of them are chosen, here only 5.*

Note that variation of (vehicle) *design parameters* is very essential to find best product design. So, each experiment needs to be performed for many vehicle designs. This can be documented either as adding more columns and rows to the experiment matrix or in a *vehicle design alternative matrix*, separate from the experiment matrix. The latter way is proposed with the motivation that vehicle design alternatives rather belong to the design/optimization process than the requirement setting, see Figure 1-10. If separate experiment matrix with n rows and vehicle design alternative matrix with m rows, the total number of experiments to carry out will be maximum $n \cdot m$.

Also note that the required numerical value of the requirement measure (e.g. braking distance) typically change between the experiments (e.g. differently long braking distance is required for different road friction).

1.4.4 Requirement Setting in Hierarchical Products

In Figure 1-2, it is indicated that requirements on the vehicle is decomposed into requirements on subsystems. There are several examples of this in vehicles; requirements on vehicle might have to be broken down into requirements on, e.g.:

- Actuators (prime mover, transmission, brake, steering)
- Environment sensors (video cameras, radars, GPS receivers, etc)
- Suspensions (front axle suspension, rear axle suspension),
- Body (for aerodynamic and strength and compliance)

Of these subsystems, the suspensions are probably the ones which is most complex to handle as subsystems in the development process, because the designs of the suspensions influence very many requirements on the vehicle. Also, the two axle suspensions, front and rear, are designed by different engineers but they together influence the vehicle motion. Therefore, the suspension system is used as challenging example below.

To decompose a requirement on the vehicle in requirements on two or more subsystems is a high level design decision in itself. No concrete design parameters ("hardpoints" etc) are decided, but functionality ("K&C measures") is decided and distributed between subsystems, in the example: between front and rear axle. The K&C measures are 1st a *design decision* of which of front and rear that

should do what. 2nd, to the design of each axle, they become *(incoming requirements)*. A design decision on one level generate the requirement to the next level, see https://en.wikipedia.org/wiki/Function%E2%80%93means_tree. In Figure 1-6, the K&C measures gets a 3rd role, namely the *actual or achieved values* in each design loop. Note that In Figure 1-6 not only shows one design, but also how design can be varied for optimization.

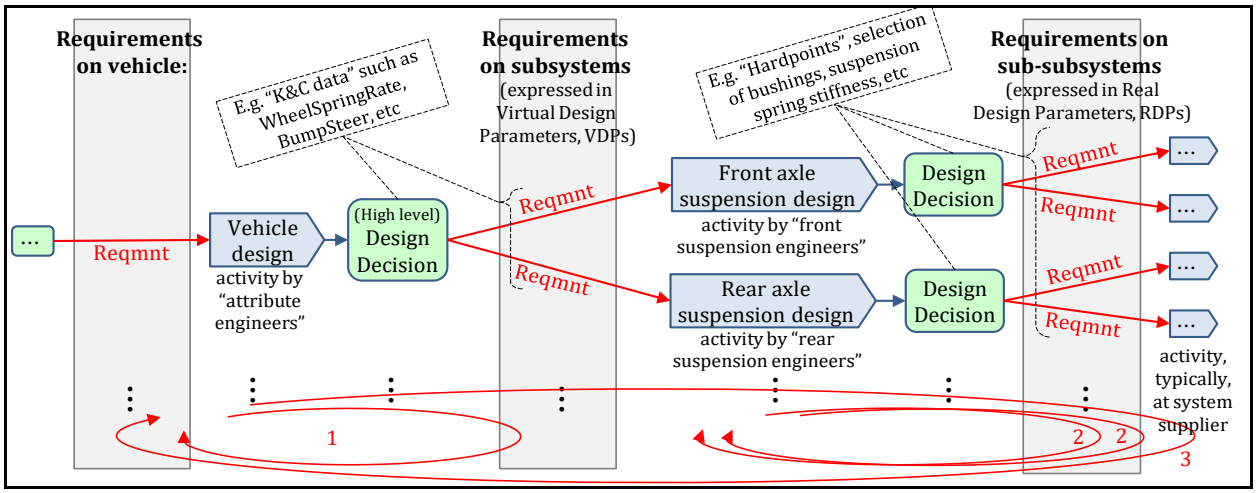


Figure 1-5: Requirement decomposition during development (Synthesis or Reverse/Inverse use of models) activity. Here exemplified with front and rear axle. Curved red arrows indicate different design loops.

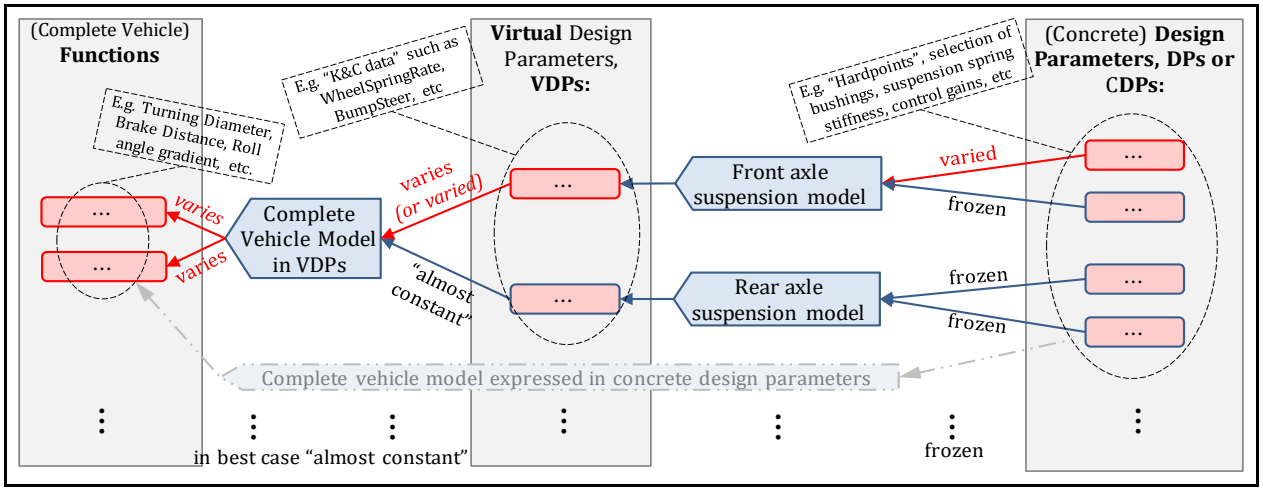


Figure 1-6: As Figure 1-5 but arrows show Analysis (or Forward use of models). The influence from right to left is a "natural causality" of how parameters influence the requirement fulfilment. It is indicated that, for a certain design task, some parameters are frozen, and some are to be varied to optimize (or to find a satisfying) design. The double-dotted alternative gives less traceability of the requirement decomposition (the VDPs) and require longer development cycles due to more complex models and simulation tools.

Note that different experience and different computation/simulation models are useful in the first and second design step. In each design step, the models needed must verify how well a certain design of a system fulfils the requirements on the same system, where the system can be ether complete vehicle, front suspension or rear suspension. When all low-level design is done, a 3rd type of model is useful, to verify how well certain designs of all subsystems fulfil the requirements on the complete vehicle. The last-mentioned verification is traditionally done in prototype vehicles, but with a good virtual verification architecture in at the vehicle manufacturer, it becomes increasingly possible to do virtually. The following figure is a development of Figure 1-2 to show the 3 verification/design loops, which typically requires different models and computations. Note that number 3 also requires organisation and databases and tools, i.e. a virtual verification architecture.

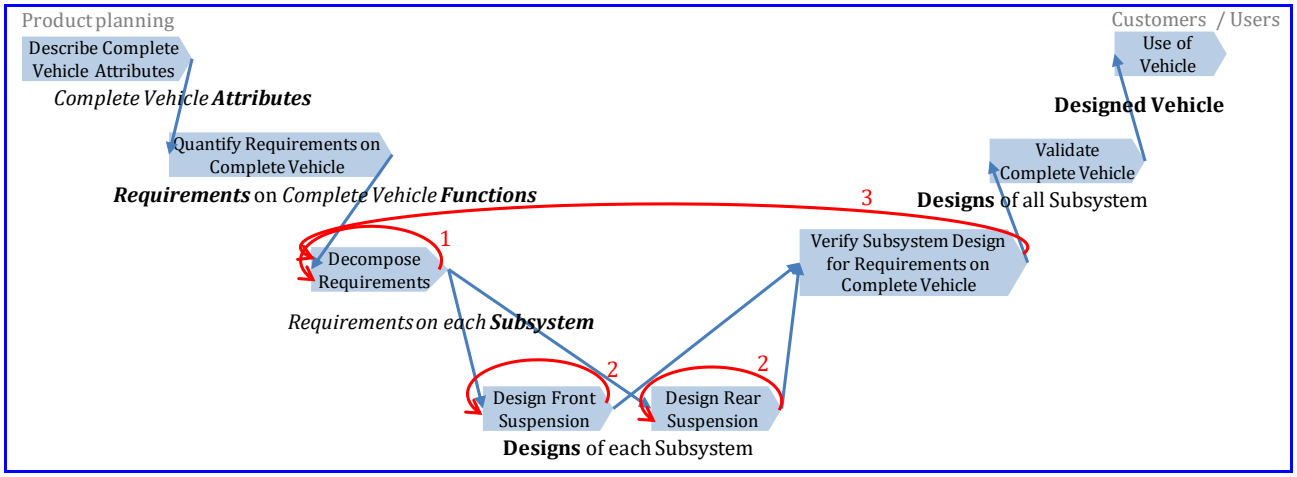


Figure 1-7: V-process where 3 types of verification are shown: 1, 2, and 3. Red arrows indicate the same design loops as in previous Figure 1-5. Compare also with Figure 1-2 and Figure 1-11.

1.4.5 Product Safety

Contribution from Per Johannesson, Volvo Trucks
Contribution from Mats Jonasson, Volvo Cars and Vehicle Dynamics at Chalmers

It becomes increasingly important for vehicle manufacturers to take responsibility of their products. The main reason is that numbers and complexity of sensors, actuators and control functions increases. The risks are often connected to how vehicle moves, i.e. to vehicle dynamics/vehicle motion. The number of risks increase both because the systems becomes more complex and because more information is available on-board. The availability of information can mean that it is ethically wrong to **not** act on it, e.g. to **not** automatically brake if camera detects a possible pedestrian ahead. An acceptable excuse to **not** brake could however, e.g., be that braking would mean a more severe risk due to causing a collision from rear-coming traffic. All functions needs to be safe, so generally the risk have to be minimized. For safety functions (e.g. ABS, airbag, etc), however, there is also the safety benefit, which motivates also an analysis of combined risk and benefit.

Failure Mode Effect Analysis (FMEA) has been around for a long time and it is applicable on any design in any product, and not only safety aspects. Basically, one identifies things that can go wrong with a certain conceptual design early in development and decide how to follow it up during the development. The follow-up normally includes to formulate requirements on the design. ISO26262 (ISO 26262, 2011-2012) describes a similar way of working, but it more specialized on traffic safety hazards and vehicles as products. ISO26262 (ISO 26262, 2011-2012) is developed driven by that software meets mechanics in mass-produced products (vehicles) intended for everyday use by almost everyone.

A very brief description of (ISO 26262, 2011-2012) follows here, see also figure below. A certain *Item* (part, subsystem or function) is identified for *Hazard Analysis* early in product development. Hazards are defined and assessed to a certain *Automotive Safety Integrity Level (ASIL)* in a *Risk Assessment*. The ASILs, listed with increasing severity, are QM, ASIL-A, ASIL-B, ASIL-C, ASIL-D. The levels ASIL-A to ASIL-D require *Safety Requirements* managed under an ISO26262 process during the continued development, while the QM does not. A Safety Requirement is a requirement on the design which reduces the ASIL to a tolerable level.

Conceptually, one can calculate ASIL for a certain hazard: $ASIL = Risk = Severity \cdot (Exposure \cdot Controllability)$;. For instance, loss of acceleration has generally lower *Severity* than loss of deceleration. For instance, the *Exposure* becomes lower if the hazards only appears in sharp turns or if there is redundancy in the solution. For instance, a hazard during automated driving increases the ASIL via the *Controllability* factor, since human driver is then less alert and less likely to control the situation.

ISO26262 describes how the work should be documented. The documentation can be asked for in a legal court case.

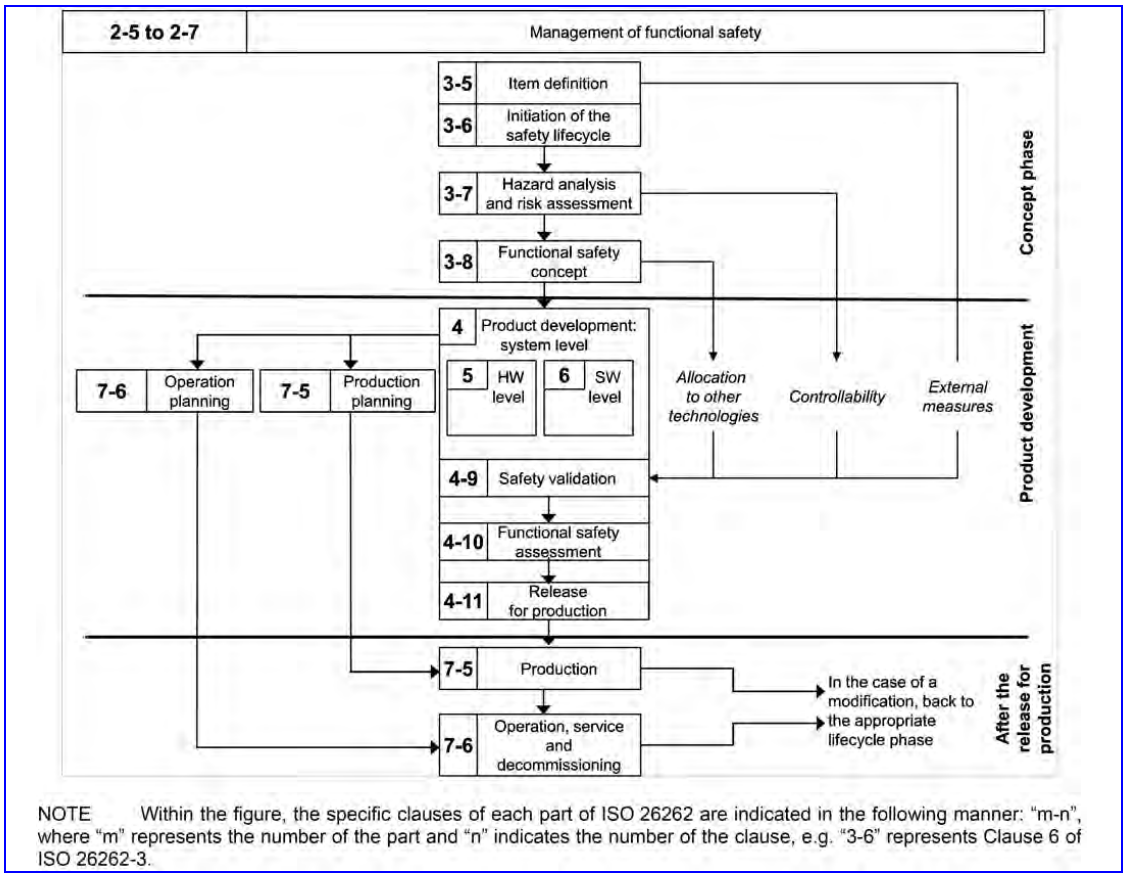


Figure 1-8: Overview of the safety life cycle, from (ISO 26262, 2011-2012).

1.4.6 Models, methods, and tools

The attributes, functions and requirements are top level entities in vehicle development process. But to design and verify, the engineers need knowledge in form of models, methods and tools.

As mentioned above, some sections in the book have an asterisk "*" in the section heading, to mark that they explain a function, which can be subject for complete vehicle requirement setting. The remaining section, without an asterisk "*", are there to give the necessary knowledge (models, methods and tools) to verify (including understand) the function and the requirements on it. It is the intention that the necessary knowledge for a certain function appears before the description of that function. One example is that the "2.4 Propulsion", "3.2.1 Traction diagram" and "3.2.2 Energy consumption and power losses

Consumed energy is a substantial part of the transportation **cost** [€], typically one third for goods transports. We can only quantify consumed energy as an integral over an interval, in time t or in travelled distance s. So, an engineer, a driver, or a control algorithm must consider energy cost in a **predictive** way, predicting to a moving horizon or the end of a whole transport mission. Corresponding for consumed power, or power loss, is that it is a (momentaneous or instantaneous) **cost rate** or cost gradient, $[€/s]$ or $[€/m]$. Energy **consumption** and especially power **loss**, can only be modelled for each **part** (battery, prime mover, transmission, wheel, …) and/or for each **phenomenon** (rolling resistance, aerodynamic resistance, …).

Requirements on energy consumption typically refers to a driving cycle or operating cycle, see 3.3.1 and 3.3.5.1. In such cycles, the operating conditions varies. In 3.2, we study Steady state functions, as opposed to cycles. Therefore, the operating conditions are constant. However, in both steady state and cycles, the quantities in Table 3.1 are useful. Note similarities and differences between EPD and PPS." are placed before "3.2.5.1 Top speed *". Functions only appear in Chapters 3, 4 and 5.

1.5 General engineering

Engineering (or Design Engineering, in Swedish often "Ingenjörsvetenskap", in German "Ingenieurwissenschaft"), as a science has an important portion of *Synthesis.* As support for synthesis, it also relies on *Analysis*, *Inverse analysis* or *(Nature) Science*, see Figure 1-9. Figure 1-10 distinguishes between Analysis and Synthesis, which shows that Analysis is a step in the whole design loop. The actual Design step requires Synthesis. The overall purpose is to propose a design, e.g. numerical values of *Design parameters* of a product. The distinction between Analysis and Inverse Analysis can be made when there is a natural causality ("cause-effect-direction").

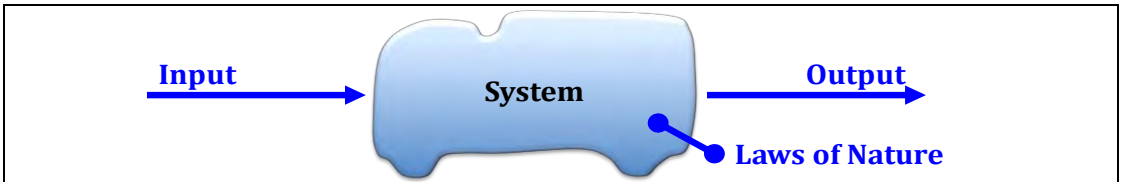
In 1.5 some useful general methods and tools are described. Parts of these are probably repetition for some of the reader's previous education, in mechanical and control engineering. In the end of 1.5, there is a stronger connection to the vehicle engineering.

1.5.1 Model Based Engineering

An analysis, as in Figure 1-10, can use either real or virtual verification. For real verification one need to build prototypes. For *Virtual Verification*, models are needed. A (dynamic) model is a representation of something from real-world varying over a time interval, such as a car during longitudinal acceleration from 0..100 km/h. Models are always based on assumptions, approximations and/or simplifications. However, when using models as a tool for solving a particular problem, the models at least must be able to reproduce the engineering problem one is trying to solve. Also, models for engineering must reflect design changes in a representative way, so that new designs can be evaluated. Too detailed models tend to be a less useful, since they require and produce a lot of data.

The models typically used in vehicle dynamics can be called *physical dynamic* models (many alternative names: cyber-physical, functional, lumped, discretized, system, DAE-model, ODE-models, etc.). The models are typically multi-domain type, involving mechanics, hydraulics, pneumatics, electrics, chemical, control algorithms, electronic, computation, driver's actions, etc. Examples of modelling methods which more seldom are used directly in vehicle dynamics are: Finite Elements, Computational Fluid Dynamics, CAD geometry models, etc.

Physical models are assumed. As opposite to this, one can think of formulating a mathematical model without motivation from established physics. Without a physical model, the parameters are generally not interpretable to real design parameters; an indication of this is when the modeller does not know the units of parameters and internal variables in the model. Real tests are needed to find the values of the parameters; the process to find these parameters can be called *(parameter) tuning*. Alternative methods for tuning are regression, machine learning, etc. Such models can only be used for interpolation in variables and parameters, not extrapolation. For vehicle engineering, the vehicle model can generally be physical, so that its real-world design parameters can be identified. However, a driver model can be useful also without strict physical model since the driver is not to be designed during vehicle engineering. But it is important to consider that the driver do change its behaviour when vehicle design parameters are changed, which is an example of co-variation of parameters, which is easy to forget.



Given	Find	Process
Input, Laws of Nature, System	Output	Analysis
Output, Laws of Nature, System	Input	Inverse Analysis
Input, Output, System	Laws of Nature	(Nature) Science (induction)
Input, Output, Laws of Nature	System	Engineering Design (Synthesis)

Dixon, J.R., (1966) Design Engineering, Inventiveness, analysis and Decision Making

Figure 1-9: Engineering Design and related activities. Picture from Stefan Edlund, Volvo Trucks.

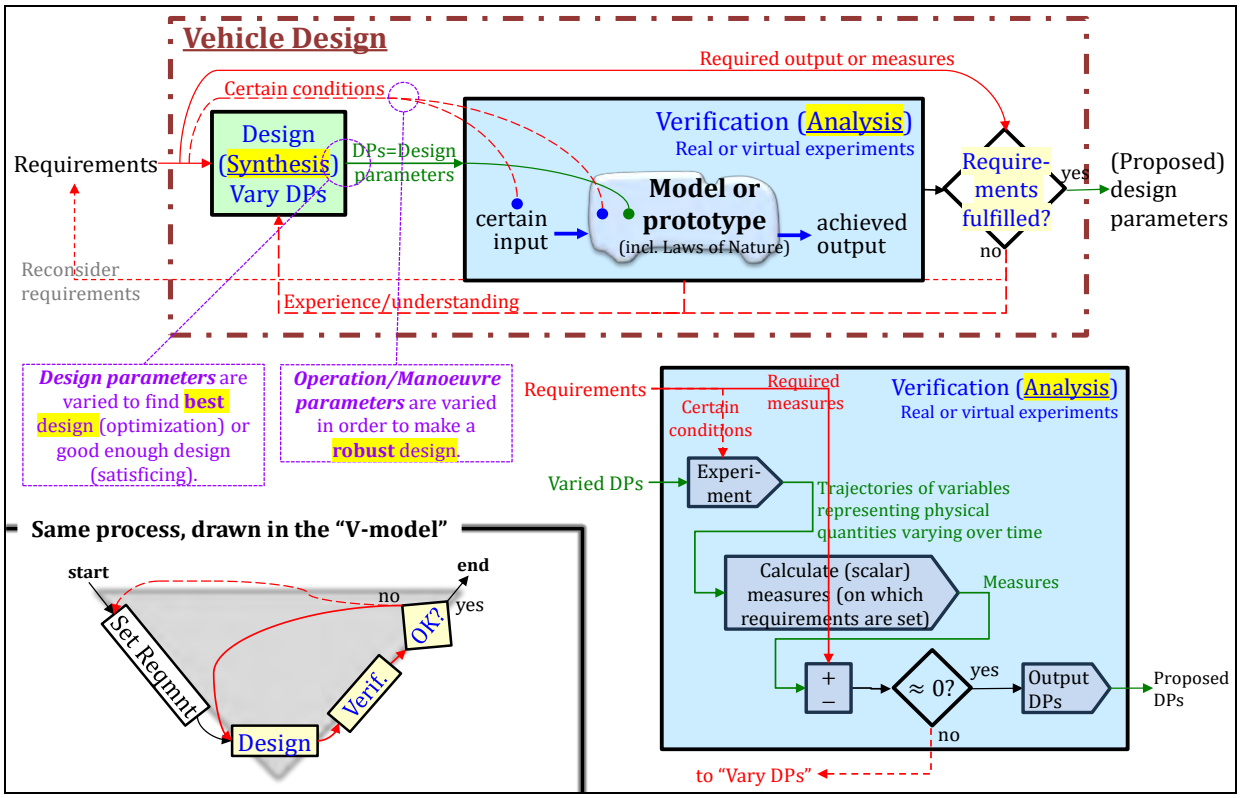


Figure 1-10: How Analysis/Synthesis and Design/Operation parameters appears in Vehicle Design. For V-model, see Figure 1-2.

Figure 1-10 shows development on only one level, while Figure 1-11 shows multiple (two) levels.

The requirements on vehicle level and subsystem level should be expressed in different physical measures. It facilitates that design loops in early phases of development can be done without the multiple subsystem design loops. This requires special complete vehicle models, see lower part of Figure 1-11 (and Figure 1-5 and Figure 1-6). These models must be parameterized with virtual design parameters (or requirements on the subsystems). It also requires a good experience of how well the virtual design parameters can be fulfilled.

In later loops, see upper part of Figure 1-11, the complexity of dependency between subsystem designs is inevitable. The latter requires more of the data bases on the company, both to store design parameters and models and to secure compatibility between submodels developed in different simulation tools. In the very late loops, the models must be replaced with real prototype vehicles.

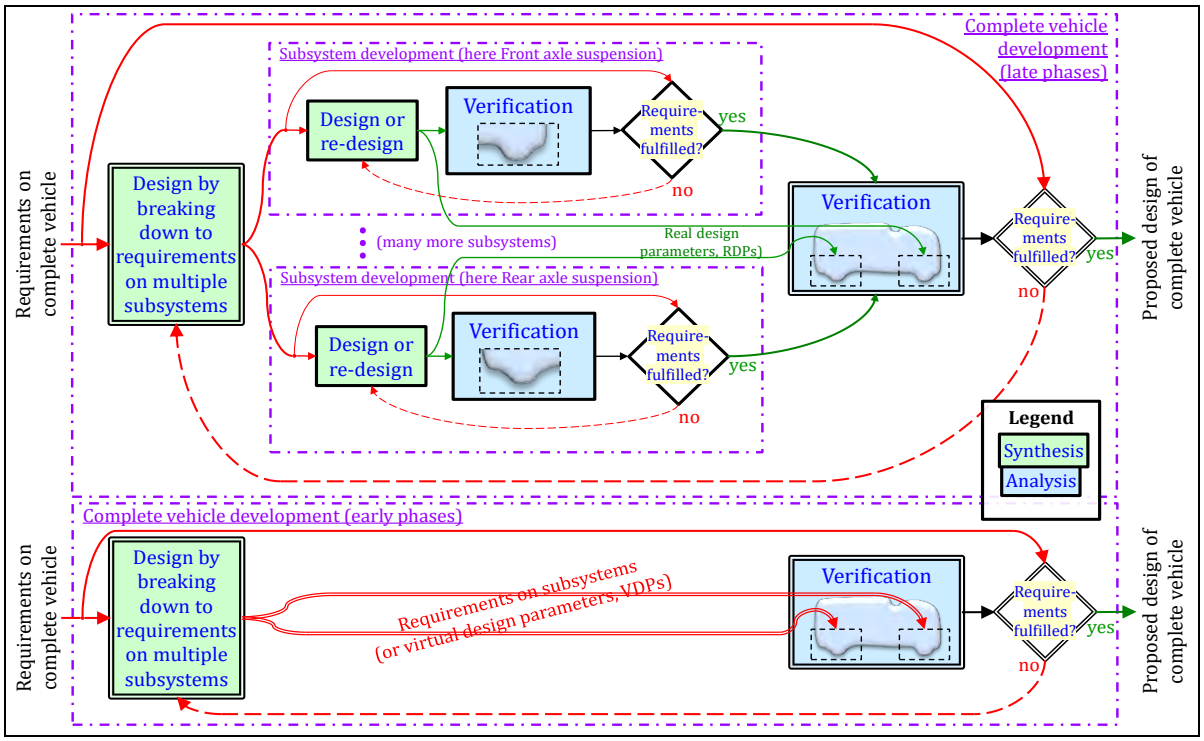


Figure 1-11: How V-model with development loops can be applied for a product decomposed in multiple subsystems. Upper: A complete process, including internal design loops for each subsystem. Lower: A faster process, excluding internal design loops for each subsystem. Note that the complete vehicle models require different parametrization and that the lower can only be done virtually, not with real world prototypes.

(Virtual) Verification on complete vehicle level can be of two types, using either real or virtual design parameters (RDP or VDP), see Figure 1-5 and Figure 1-6. The latter allows easier simulation models which can facilitate faster development loops.

1.5.1.1 Stages in (Dynamic) Model Based Engineering

Each block Figure 1-12 visualises a stage in model-based engineering, co-existing with the complement, *real-world prototype testing*. One can identify **modelling** in 3 stages in the overall process: *1.5.1.1.3 Physical Modelling, 1.5.1.1.4 Mathematical modelling,* and *1.5.1.1.5 Explicit Form Modelling.* See Figure 1-12. The book spends most effort on the first 2 of those 3. For example, see Figure 1-51.

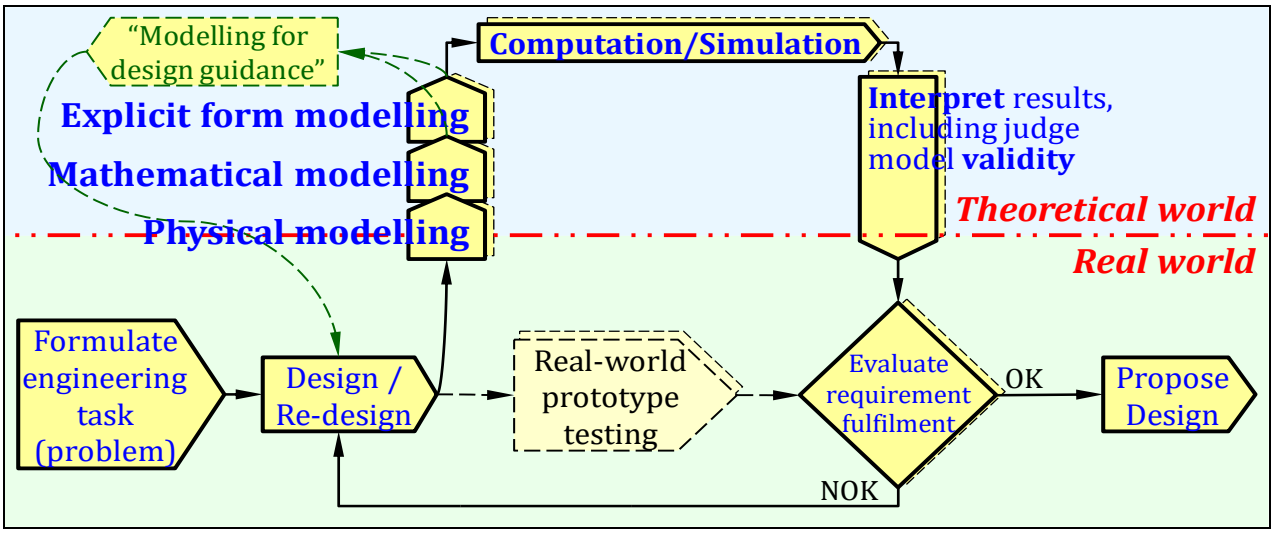


Figure 1-12: (Dynamic) Modelling stages. Real versus Theoretical world. The dashed boxes in the background indicate that same design must fulfil multiple requirements, which might require multiple models.

1.5.1.1.1 Formulating the Engineering Design Task

Based on a problem description, one formulates the **engineering design task**, which describes the required design decisions (if possible, appoint design parameters) for an existing vehicle or a concept.

There is no model yet, but the object for modelling, e.g., a certain vehicle, must be specified. The specification of such object is therefore *model-independent*, e.g., photos, (manufacturing) drawings, or parameter sets. Such parameter set is a *model-independent parameter set*. It is mentioned in Figure 1-12 that multiple models might be needed. It is then important that their model parameters are interpreted from the same parameter set, so that the same product is evaluated. That is why the word "*model-independent*" is important.

Also, requirements on how the output of the system should react in certain vehicle operations (or manoeuvres or situations) must be identified. Requirements can be either constraints (something<number) and/or optimization (some scalar to be minimized).

The conceptual idea with requirements in vehicle industry is that they are set independently of the design solution. However, the general requirements are seldom neither enough for a certain engineering design task; one often must reformulate or add requirements. The operation parameters often have a range/spread/stochasticity to design for, see Figure 1-10. Examples of such parameters describe traffic situation, driver, tyre/road characteristics, weather, see 1.5.1.3.1. The range can be searched for in feedback or logged data from customers and accident statistics. But it is also very important with experienced engineering judgment, to forecast how the problem will appear in a future context, with a future fleet of vehicles and a future road infrastructure. Design methodology can be used to reason about and categorize parameters (e.g., Taguchi's: "signal, response, noise and control factors").

One design task is typically influenced by several requirements and can therefore need multiple models of the same system. This stresses the importance of parameterization, which help to secure that the same design is assessed in the different models.

1.5.1.1.2 Design

Design (or Synthesis, as opposed to Analysis) is a creative part where experience and intuition is important.

1.5.1.1.3 Physical Modelling

In this stage, one should generate a ***physical model***, which in this book means drawings and text. The name *physical model* is used in this book, because "physical" marks that it is not completely mathematical yet, but it has an interpretation to physical phenomena.

> English "*physical*" can mean either "*real-world*" or "*physics-based*", so a less ambiguous name could be "*physics-based model*". In languages, e.g., {Swedish, German} there are different words, {fysisk, physisch} is different from {fysikalisk, physikalisch}. Alternative names could be *engineering model* or *phenomenological model*. Some would not even call it a model, but this book aims at underlining that a drawing is the first stage of modelling, where many (conscious or unconscious) decisions are made, such as which physical phenomena to model.

Free-body diagrams (1.5.2.1), data flow diagrams (1.5.1.1.3.2) and operating conditions (1.6.2) are important ingredients in the physical model of a vehicle. However, also other domains than mechanics are often needed, such as hydraulics, electrics, driver and control algorithms. The physical model shall clarify assumptions/approximations/simplifications, e.g., rigid/elastic, inertial/massless, continuous/time sampled algorithms, small angles, etc. Discrete dynamics (1.5.1.4), such as ideal dry friction, backlash or end stop, does not exist in real world, so such assumptions are typical examples of clear differences between real system and physical model. On the contrary, continuous dynamics does not exist in a real digital controller, which is discrete through time sampling. So, modelling the controller as continuous is also a clear difference between real system and physical model.

The physical model should consider what phenomena is needed to be captured for intended variations (e.g. which design parameters), decided by the engineering task. The (model) parameters and variables are defined in the drawing but might need additional text. The interpretation from the *model-independent parameter set* (from 1.5.1.1.1) to the model parameters requires a lot of experience of the product, which here is vehicle. A physical model is often not executable, but it can be. One example of executable format is a model build in an MBS tool, see 1.5.4.1.4 and Figure 1-54.

1.5.1.1.3.1 Deductive vs inductive definition of parameters

Parameters can be categorized as design parameters or operation parameters. Wether a parameter is one or the other, can depend on the purpose of the model. Design parameters describe something that the engineer is about to propose a value on. Design parameters must be defined in a way, so the engineer understands them, in a physical or *deductive* way. This means that the design parameters should be defined based on physical phenomena which the engineer understands/believes in, maybe such as a friction coefficient or a length. With such a deductive definition, the engineer can understand how to change the parameter, and within which range it can be varied. Operation parameters rather describe the environment where the product under design operates. It is best if also they can be deductively defined, but it is not equally important and, sometimes, an inductive definition can better represent a certain operation environment.

An example of deductive definition of a parameter is: Rolling radius of a tyre is the length of the tyre belt. A non-deductive (inductive or empirical) definition is: Rolling radius is $1/(2 \cdot \pi)$ of the length that the wheel rolls if rolling one revolution without slip. The former is necessary for an engineer desiging the tyre. If it gives an accurate enough model, it is also better for an engineer designing the tyre slip control algorithm, because it increases the understanding of how the tyre behaves.

1.5.1.1.3.2 Drawing

Drawing is a very important tool for engineers to understand and explain. Very often, the drawing contains free body diagrams, FBD, see 1.5.2.1, but also other diagrams are useful to mix in. Block diagram with signal flow is one such other useful diagram. Geometric drawing in scale is yet an other useful diagram. On top of normal drawing conventions for engineering drawings, it is also important to draw motion and forces. The notation for this is proposed in Figure 1-13.

It is often necessary to include more than just speeds and forces in the drawings. In vehicle dynamics, these could be: power flow and signal or data flows. These can preferably be drawn as arrows, but of another kind than the motion and force arrows.

When connecting components with signal flow, the resulting diagram is a *data flow diagram* or *block diagrams*. Physical components and physical connections can be included in such diagram, and if arrows between them it would represent data flow or causality. Physical components can also be connected by "Physical connections", which does not have a direction, see 1.5.1.1.3.2.1. It should be noted that a *(computation) flow charts* and *(discrete) state diagram* represent something quite different from data flow diagrams, even if they may look similar; in state diagrams, an arrow between two blocks represents a transition from one (discrete) state or operation mode, to another, see Figure 1-14.

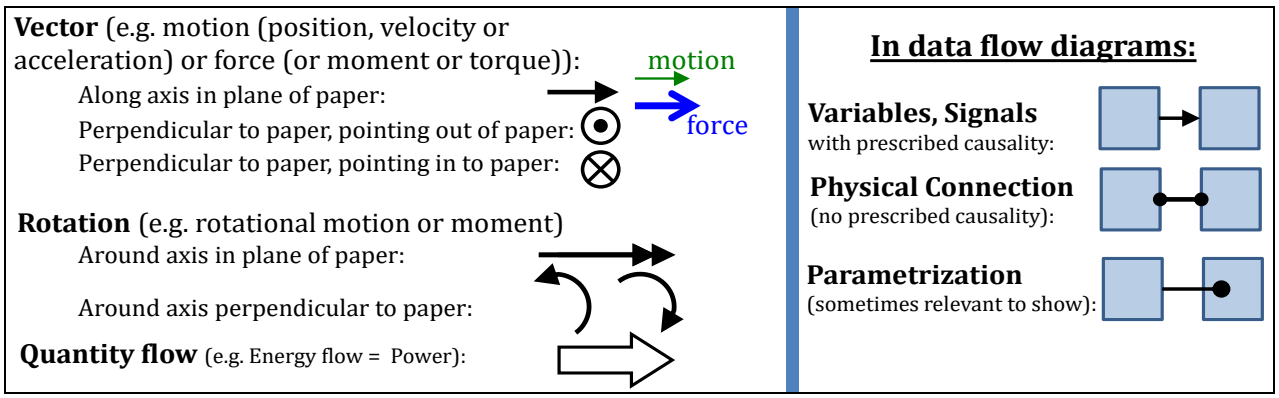


Figure 1-13: Arrow-like drawing.

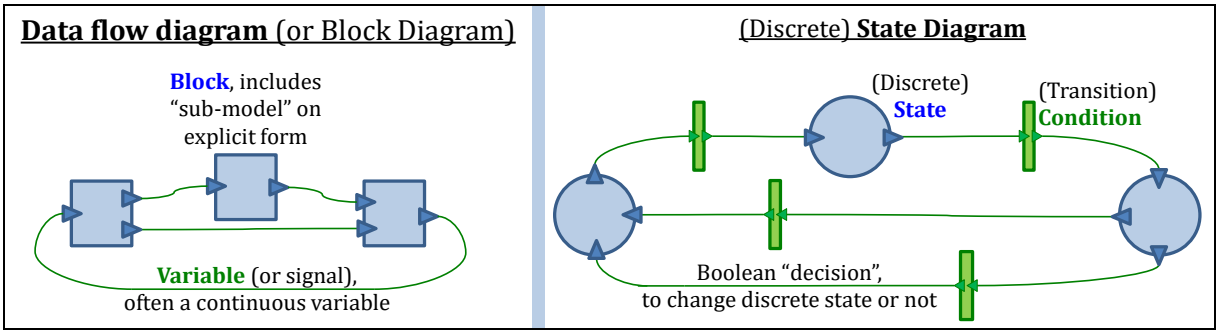


Figure 1-14: Data flow diagram vs State Diagram. Flow Charts are similar to State Diagrams.

1.5.1.1.3.2.1 Measures in Drawings

To define physical quantities in words is generally ambiguous; different people understand them differently and from time to time. So, it is much safer to define them in drawings. Figure 1-15 shows some examples. One has to differ between a minus sign in front of the variable name in the drawing, $-L_2$, and whether the numerical value of the variable is positive or negative.

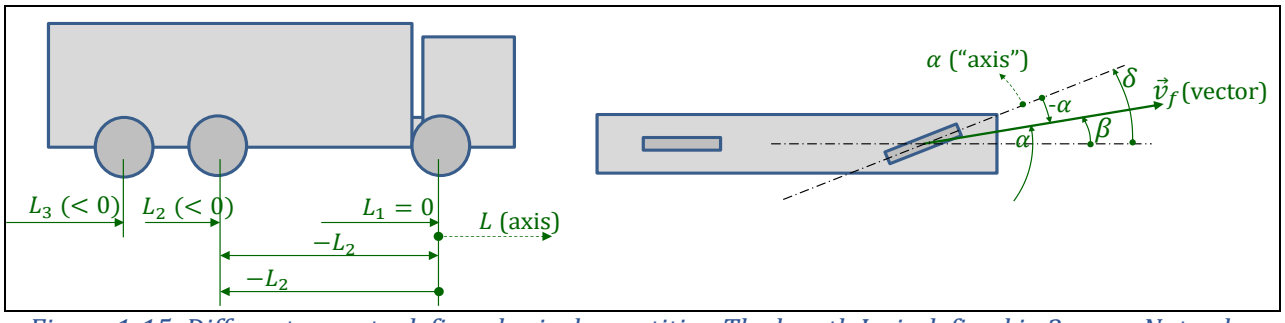


Figure 1-15: Different ways to define physical quantities. The length L_2 is defined in 3 ways. Note also different types of arrows: "axis", "vector" and other, where other are "meassurements".

Defining forces and moments in a drawing is special in the sense that they always appear as action and reaction, see 1.5.2.1.1. and 1.5.1.1.6.

1.5.1.1.4 Mathematical modelling

In this stage, one should generate a **mathematical model**, which means equations. Basically, mathematical modelling is about finding the right equations; equally many as unknowns. It can be difficult to draw an exact border between physical and mathematical modelling. It is often efficient to develop them in iterations, i.e., to allow yourself to go back and update the physical model while you develop the mathematical model. When introducing a variable (such as a force or velocity) in the mathematical model, it is often good to check that it is well defined in the physical model.

For large systems, such as vehicle dynamics, it is often desired and possible to use well-established physical or engineering phenomena for the subsystems. These phenomena can be equilibrium, elasticity, dry friction etc., see 1.5.2.4. This way of modelling is sometimes refered to as *deductive*, as opposed to *inductive*.

For dynamic systems, the unknowns are unknown variables of time. In the mathematical model, the assumptions are transformed into equations. For dynamic systems, the equations form a "DAE" (Differential-Algebraic system of Equations). It is seldom necessary to introduce derivatives with respect to other independent variables, such as positions, i.e. one does seldom need PDE (Partial Differential Equations). The general form of a DAE:

- $\boldsymbol{f_{DAE}}(\dot{\boldsymbol{z}}, \boldsymbol{z}, t) = \boldsymbol{0}$;

Here, the function $\boldsymbol{f_{DAE}}$ is an operator which include only algebraic operations. An alternative notation would be to use a function $\boldsymbol{f_{DAE2}}$, being an operator including both algebraic and differential operations:

- $\boldsymbol{f_{DAE2}}(\boldsymbol{z}(t), t) = \boldsymbol{0}$;

To distinguish between whether a physical quantity is a variable ($z = z(t)$) or a parameter ($p \; such \; that \; \dot{p} = 0$), see more in 1.5.1.3, is a very important modelling decision. This can be underlined by using an operator $\boldsymbol{f_{DAE3}}$ instead:

- $\boldsymbol{f_{DAE3}}(\boldsymbol{z}(t), t, \boldsymbol{p}) = \boldsymbol{0}$;,

The Mathematical model is *acausal*, i.e. describes relations between the variables and parameters, not how and in which order to compute. A Mathematical model can be equations on a piece of paper or in a word processing format and then it is not executable. However, writing the Mathematical model in the standardized format *Modelica* (https://www.modelica.org/) makes it executable with Modelica tools, see 1.5.4.1.5.

An example of a model on Modelica format is given in [1.3], where $\boldsymbol{f_{DAE3}}$ is defined between "`equation`" and "`end`". No explicit dependence of time t is in the example. The $\boldsymbol{z}$ is {`v, F, x`}. The $\boldsymbol{p}$ is {`m, c, F0`}. (For a modelling context of this example model, see Figure 1-51.)

```
model ExampleModel
  parameter Real m, c, F0;
  Real v, F, x;
equation
  m*der(v) = -F;
  v = der(x);
  F = F0+c*x;
end ExampleModel;
```

[1.3]

The $\boldsymbol{z}$ are the (dependent) variables and t is time (independent variable). The mathematical model is complete only if there are equally many (independent) equations in $\boldsymbol{f_{DAE}}$ as there are variables in $\boldsymbol{z}$, $\dim(\boldsymbol{f_{DAE}}) = \dim(\boldsymbol{z})$. (Since DAE, we don't count $\dot{\boldsymbol{z}}$ and $\boldsymbol{z}$ as different variables.) Note that one can be interested if treating also cases where $\dim(\boldsymbol{f_{DAE}}) < \dim(\boldsymbol{z})$. It is when $\dim(\boldsymbol{z}) - \dim(\boldsymbol{f_{DAE}})$ of the variables in $\boldsymbol{z}$ can be considered as known, so called, input variables $\boldsymbol{u}(t)$. The notation "(t)" marks that $\boldsymbol{u}$, generally, might have to be known DAE variables, i.e. their time derivatives also have to be known.

1.5.1.1.4.1 Mathematics and Notation/Naming Conventions

See also 1.10.

Generally, a variable is denoted x or $x(t)$, where t is the independent variable time. In contexts where one means that variable's value at a certain time instant, t_0, it can be denoted $x(t_0)$. In contexts where one wants to mark that the variable's time history over a time interval (infinitely many values over an infinite or finite time interval) is referred to, it can be denoted $x(\cdot)$.

One cannot see from the notation if p is a variable or parameter. If one want to underline that it is a parameter, one can add the equation $\dot{p} = 0$;.If underlining that it is a variable, one can use $p(t)$.

Differentiation (of x) with respect to time t: $\frac{dx}{dt} = \dot{x} = der(x)$.

> **Differentiation** (of x) with respect to y, holding something constant (or invariant) is, mathematically, called **partial differentiation** and is often denoted $\frac{\partial x}{\partial y}$. Another notation, which often is more precise in physics or engineering, is, e.g., $\frac{dx}{dy}\Big|_{holding\ z\ constant}$ or $\frac{dx}{dy}\Big|_{z\equiv z_0}$. One can keep the "curved d" (∂) notation, as $\frac{\partial x}{\partial y}\Big|_{z\equiv z_0}$, but it is somewhat double and therefore unnecessary.

Matrices (two-dimensional arrays) are denoted with bold letters, often uppercase $\boldsymbol{A}$. Column and row vectors (one-dimensional arrays) are denoted with bold, often lowercase $\boldsymbol{b}$. When elements in arrays are written, brackets are used: $\begin{bmatrix} x & y \\ y & z \end{bmatrix}$.

Geometric vector (or physical vector, or spatial vector), denoted by $\vec{v}$. To use geometric vectors in calculations, they are often expressed as one-dimensional arrays with components. It has to be clear for each component, which direction it is expressed in, e.g. by a subscript, e.g. $\boldsymbol{v_{xyz}} = [v_x, v_y, v_z]$.

Parentheses avoid ambiguity, e.g., $(a/b) \cdot c$ or $a/(b \cdot c)$, but not just $a/b \cdot c$. The last expression becomes different if executed from left or from right. There are, e.g., programming languages that executes in different directions.

Multiplication symbols (* or · or × or •) also avoid ambiguity, e.g. $a \cdot bx$, not abx (assuming bx is one variable, not two). Another avoided ambiguity is when using operators, e.g., it shows the difference between $f(x)$ and $f \cdot (x)$. Therefore, present book does not omit multiplication signs. Present book denotes multiplication between scalars and matrices equally, using "·". Multiplication between geometric vectors is denoted: Cross multiplication, denoted $\vec{a} \times \vec{b}$ and scalar multiplication, denoted $\vec{a} \bullet \vec{b}$.

Stringent use of parentheses and multiplication symbol enables use of **variable notations with more than one token**, which is often needed to avoid misunderstandings in contexts of multiple disciplines with different notation tradition. It is common in programming but also used in this book.

An **interval** has a notation with double dots. Example: Interval between a and b is denoted $a..b$.

An **explanation**, between consecutive steps in a derivation of equations, is written in curly brackets {}. Example: $x + y = \{a + b = b + a\} = y + x$; or $x + y = \{addition\ is\ commutative\} = y + x$.

The approximately equal token (≈) between numerical values simply means a **rounding**, often from left to right, $\pi \approx 3.14$. In present book it is also used between symbolic expressions in derivations where **limitations of validity** are introduced, e.g., $\cdots = \sin(\alpha) \approx \{\alpha\ is\ small\} \approx \alpha = \cdots$;.

The identity token (≡) can be used differently in different context. In this book, which is about dynamics, it is used to emphasize that the equality **holds over time**.

An **inverse function** is denoted with superscript inv, $y = f(x); \Leftrightarrow x = f^{inv}(y)$. The use of superscript -1 can cause an ambiguity whether f^{-1} means inverse function or inverted function value $(1/f)$. When a name of the inverse function is available, it can be used, e.g. $\arctan(\cdots)$ instead of $\tan^{\mathrm{inv}}(\cdots)$.

Fourier and Laplace **transform** of function $f(t)$ are denoted $\mathcal{F}\big(f(t)\big)$ and $\mathcal{L}\big(f(t)\big)$, respectively:

$$\mathcal{F}\big(f(t)\big) = \int_{-\infty}^{+\infty} f(t) \cdot e^{-j\cdot\omega\cdot t} \cdot dt\,; \quad where\ \omega \in Re$$

$$\mathcal{L}\big(f(t)\big) = \int_{0}^{\infty} f(t) \cdot e^{-s\cdot t} \cdot dt\,; \quad where\ s = \sigma + j\cdot\omega \quad where\ \sigma\ and\ \omega\ \in Re$$

There are many practical rules for manipulation transformed differential equations, such as $\mathcal{F}\left(\dot{f}(t)\right) = j\cdot\omega\cdot\mathcal{F}\big(f(t)\big)$; and $\mathcal{L}\left(\dot{f}(t)\right) = s\cdot\mathcal{L}\big(f(t)\big) - f(0)$;. For Laplace transform, more examples are given in Table 1.1 and Table 1.2.

Table 1.1: Examples of function in time domain and the corresponding in Fourier domain.

Function description	*Function in time domain, $f(t)$*	*Function in Fourier domain, $\mathcal{F}\big(f(t)\big)$*
Constant	c	$\mathcal{F}(c) = c\cdot\left\{\begin{matrix} dirac\ delta \\ pulse\ in\ f=0 \end{matrix}\right\} = c\cdot\delta(0);$
Derivative	$\dot{f}(t)$	$\mathcal{F}\big(\dot{f}(t)\big) = (i\cdot\omega)^n\cdot\mathcal{F}\big(f(t)\big);$

Table 1.2: Examples of function in time domain and the corresponding in Laplace domain.

Function description	*Function in time domain, $f(t)$*	*Function in Laplace domain, $\mathcal{L}\big(f(t)\big)$*
Unit impulse	$\delta(t)$	$\mathcal{L}\big(\delta(t)\big) = 1$
Unit step	$\sigma(t)$	$\mathcal{L}\big(\sigma(t)\big) = 1/s$
Unit ramp	$t\cdot\sigma(t)$	$\mathcal{L}\big(t\cdot\sigma(t)\big) = 1/s^2$
Exponential	$e^{-\alpha\cdot t}$	$\mathcal{L}(e^{-\alpha\cdot t}) = 1/(s+\alpha)$
Sine	$sin(\omega\cdot t)$	$\mathcal{L}(sin(\omega\cdot t)) = \omega/(s^2+\omega^2)$
Cosine	$cos(\omega\cdot t)$	$\mathcal{L}(cos(\omega\cdot t)) = s/(s^2+\omega^2)$

An example: The dynamic model $\dot{y} = \frac{d}{dt}\big(y(t)\big) = gain\cdot u(t)$; looks as follows, if written Fourier transformed or Laplace transformed: $y(\omega) = gain\cdot u(\omega)/(-j\cdot\omega)$; or $y(s) = gain\cdot u(s)/s$;, respectively.

A **main character** with subscripts is a proposed notation. The main character is preferably selected as what is widely used, e.g. F for force and v for translational velocity. Then the concept of subscripts becomes important.

The **order within subscripts** can be debated, e.g. should a longitudinal (x) force (F) on rear axle (r) should be denoted F_{rx} or F_{xr}. The intention in this book is to order subscript in the following order:

- the physical vehicle part (here rear axle) as 1st subscript
- the specification (longitudinal, x) as 2nd

This leads to F_{rx}. If there are needs for specification:

- detailed specifications, such as coordinate system, e.g. wheel coordinate (w), it will be the 3rd subscript

Then we get F_{rxw}. Further specifications, such as design case, e.g. without (0) or with (1) a certain technical solution, one can suitably add a 4th subscript, leading to F_{rxw0} and F_{rxw1}. If subscripts have >1 token, it can sometimes be good to use comma, e.g. $F_{rear,x,wheel,with}$ or use "camel case", e.g., $F_{Rear,xWheelWith}$.

In a complex product as a vehicle, it is often difficult to avoid >1 main character. Examples of such in the book are RRC=Rolling resistance coefficient and $\Delta\delta$=additional steering angle. The risk to misunderstand those as $R\cdot R\cdot C$ and $\Delta\cdot\delta$, respectively, is reduced by the above recommendation to always use multiplication sign.

Naming of variables (signals), parameters and function components (blocks) is often important in large products as vehicles. Some naming needs to be readable for many engineers, such as CAN signals. Hence, companies developing their own naming standards. But also, the standardization organisation AUTOSAR has released a naming standard, with intention to be accepted by both vehicle manufacturers and system suppliers.

1.5.1.1.4.2 Parameterisation

It is not only a question of finding suitable equations, but also to decide *parameterisation*. Parameterisation includes decision of **which** quantities that shall be modelled as parameters as opposed to variables and how parameters are **defined and related to each other** and, finally, the **numerical** values.

To point out the parameters, $\boldsymbol{p}$, they can be included in the DAE form as $\boldsymbol{f}_{\boldsymbol{DAE}}(\dot{\boldsymbol{z}}(t), \boldsymbol{z}(t), t, \boldsymbol{p}) = \boldsymbol{0}$;.

1.5.1.1.4.3 Selection of output variables

Selection of *output variables* is important so that output variables are enough to evaluate the requirements on the system. Selecting too many might cause unnecessarily complex models which are hard to extract design insights from, while selecting too few can jeopardize the reusability of the model for other design tasks.

Output variables can often be processed to a *measure* during the studied operation/manoeuvre. Such measures are typically scalar value. An example is energy consumption, which is processed from power consumption, e.g., $T \cdot \omega$ or $U \cdot I$, by integration over the simulated vehicle operation/manouvre. The processing can be post-processing after the simulation, but it can also be part of the dynamic model. If part of the dynamic model, the measure appears as the final value of an *output variable*. From engineering perspective, such output variables are special since they cause "function measures" on which requirements can be set, see 1.4.2.

1.5.1.1.4.4 Differentiation Order

Above, the ODEs are assumed to be of first order. There is a strong tradition to in mechanical engineering to model with 2nd order differential equations, where accelerations of inertial bodies appear as 2nd derivative of position. However, numerical methods for solving first order differential equations are much more mature and Vehicle Dynamics mainly aims at such. Hence, the book aims at first order differential equations.

It is easy to go from few equations to higher order to many first order differential equations; variables appearing in 2nd order derivative $\ddot{z}_i$ are replaced with $\dot{z}_{new,j}$ and one equation $\dot{z}_i = z_{new,j}$; is added. The opposite is not generally as easy, but often possible. An example is a linear model $\dot{\boldsymbol{z}} = \boldsymbol{A} \cdot \boldsymbol{z}$;, which can be converted from many 1st order to fewer 2nd order becomes as follows:

$$\underbrace{\begin{bmatrix}\dot{\boldsymbol{z}}_1\\ \dot{\boldsymbol{z}}_2\end{bmatrix}}_{\dot{\boldsymbol{z}}} = \underbrace{\begin{bmatrix}\boldsymbol{A}_{11} & \boldsymbol{A}_{12}\\ \boldsymbol{A}_{21} & \boldsymbol{A}_{22}\end{bmatrix}}_{\boldsymbol{A}} \cdot \underbrace{\begin{bmatrix}\boldsymbol{z}_1\\ \boldsymbol{z}_2\end{bmatrix}}_{\boldsymbol{z}}; \Rightarrow \left\{\begin{matrix}\text{differentiate}\\ \text{equation for } \dot{\boldsymbol{z}}_1\end{matrix}\right\} \Rightarrow \left\{\begin{matrix}\text{eliminate}\\ \boldsymbol{z}_2 \text{ (and } \dot{\boldsymbol{z}}_2)\end{matrix}\right\} \Rightarrow$$

$$\Rightarrow \ \ddot{\boldsymbol{z}}_1 - \left(\boldsymbol{A}_{11} + \boldsymbol{A}_{12} \cdot \boldsymbol{A}_{22} \cdot \boldsymbol{A}_{12}^{-1}\right) \cdot \dot{\boldsymbol{z}}_1 + \boldsymbol{A}_{12} \cdot \left(\boldsymbol{A}_{22} \cdot \boldsymbol{A}_{12}^{-1} \cdot \boldsymbol{A}_{11} - \boldsymbol{A}_{21}\right) \cdot \boldsymbol{z}_1 = \boldsymbol{0};$$

Another way to go from higher order to lower order differential equations is to go via Laplace transform. This is exemplified on same equations as above, but only for scalar $\boldsymbol{z}_1$ and $\boldsymbol{z}_2$:

$$\underbrace{\begin{bmatrix}\dot{\boldsymbol{z}}_1\\ \dot{\boldsymbol{z}}_2\end{bmatrix}}_{\dot{\boldsymbol{z}}} = \underbrace{\begin{bmatrix}A_{11} & A_{12}\\ A_{21} & A_{22}\end{bmatrix}}_{\boldsymbol{A}} \cdot \underbrace{\begin{bmatrix}z_1\\ z_2\end{bmatrix}}_{\boldsymbol{z}}; \Rightarrow \left\{\begin{matrix}\text{Laplace}\\ \text{transform}\end{matrix}\right\} \Rightarrow \ s \cdot \begin{bmatrix}z_1\\ z_2\end{bmatrix} = \begin{bmatrix}A_{11} & A_{12}\\ A_{21} & A_{22}\end{bmatrix} \cdot \begin{bmatrix}z_1\\ z_2\end{bmatrix}; \ \Rightarrow$$

$$\Rightarrow \ \left(\begin{bmatrix}A_{11} & A_{12}\\ A_{21} & A_{22}\end{bmatrix} - s \cdot \boldsymbol{I}\right) \cdot \begin{bmatrix}z_1\\ z_2\end{bmatrix} = \boldsymbol{0}; \ \Rightarrow \{\text{eliminate } z_2\} \Rightarrow$$

$$\Rightarrow \ s^2 \cdot z_1 - (A_{11} + A_{22}) \cdot s \cdot z_1 + (A_{11} \cdot A_{22} - A_{12} \cdot A_{21}) \cdot z_1 = 0; \ \Rightarrow$$

$$\Rightarrow \left\{ \begin{matrix} \text{inverse} \\ \text{Laplace} \\ \text{transform} \end{matrix} \right\} \Rightarrow \ \ddot{z}_1 - (A_{11} + A_{22}) \cdot \dot{z}_1 + (A_{11} \cdot A_{22} - A_{12} \cdot A_{21}) \cdot z_1 = 0;$$

1.5.1.1.4.5 Affine and Linear form (ABCD form)

Contribution from Fredrik Bruzelius, Vehicle Dynamics at Chalmers and VTI

In some cases, the model can be written on an *Affine (Explicit) Form*:

- $\dot{\boldsymbol{x}} = \boldsymbol{k}_{\dot{\boldsymbol{x}}} + \boldsymbol{A} \cdot \boldsymbol{x} + \boldsymbol{B} \cdot \boldsymbol{u}; \quad \boldsymbol{y} = \boldsymbol{k}_{\boldsymbol{y}} + \boldsymbol{C} \cdot \boldsymbol{x} + \boldsymbol{D} \cdot \boldsymbol{u}$; where $\boldsymbol{A}, \boldsymbol{B}, \boldsymbol{C}, \boldsymbol{D}$ are matrices.

Note that the notation $\boldsymbol{x}, \boldsymbol{y}, \boldsymbol{u}$, introduced in 1.5.1.1.9.3, is used already here in 1.5.1.1.4.5. This is to comply with notation well established in control engineering, which is relevant for 1.5.1.1.4.5.

If the constant terms $\boldsymbol{k}_{\dot{\boldsymbol{x}}}$ and $\boldsymbol{k}_{\boldsymbol{y}}$ are zero the special case *Linear form* (or *ABCD form*) is at hand:

- $\dot{\boldsymbol{x}} = \boldsymbol{A} \cdot \boldsymbol{x} + \boldsymbol{B} \cdot \boldsymbol{u}; \quad \boldsymbol{y} = \boldsymbol{C} \cdot \boldsymbol{x} + \boldsymbol{D} \cdot \boldsymbol{u}$; where $\boldsymbol{A}, \boldsymbol{B}, \boldsymbol{C}, \boldsymbol{D}$ are matrices.

To find the numerical solution $\boldsymbol{y}(t)$ it does not matter much which of the above forms that is used. To detect instability, one compute eigen-values of $\boldsymbol{A}$ and $\boldsymbol{A}$ is same in both forms. So far, the *affine* form is enough. However, many methods in frequency analysis, control engineering and signal processing requires the *linear* form. The **property** *linear*, which we are after with the **form** *linear*, can be described as that the effect from two superimposed input signals superimposes as: $[\dot{x}, y] = f_{\dot{x}y}(u_1 + u_2) = \{using\ the\ special\ property\} = f_{\dot{x}y}(u_1) + f_{\dot{x}y}(u_2)$;. The constant terms would ruin this property, because the effect from constant terms would obviously appear twice in $f_{\dot{x}y}(u_1) + f_{\dot{x}y}(u_2)$ but only once in $f_{\dot{x}y}(u_1 + u_2)$. So, it is often motivated to look for a *linear* form.

If $\boldsymbol{A}$ is non-singular we can find a form which is linear *in state derivatives* by offsetting $\boldsymbol{x}$ by replacing $\boldsymbol{x}$ with $(\boldsymbol{x_0} + \boldsymbol{x_{ofA}})$, where $\boldsymbol{x_0} = -\boldsymbol{A^{-1}} \cdot \boldsymbol{k}_{\dot{\boldsymbol{x}}}$;. The result becomes:

- $\dot{\boldsymbol{x}}_{\boldsymbol{ofA}} = \boldsymbol{A} \cdot \boldsymbol{x}_{\boldsymbol{ofA}} + \boldsymbol{B} \cdot \boldsymbol{u}; \quad \boldsymbol{y} = \underbrace{(\boldsymbol{k}_{\boldsymbol{y}} + \boldsymbol{C} \cdot \boldsymbol{x_0})}_{\boldsymbol{k_{yofA}}} + \boldsymbol{C} \cdot \boldsymbol{x}_{\boldsymbol{ofA}} + \boldsymbol{D} \cdot \boldsymbol{u}$;

If $\boldsymbol{A}$ is singular but $\boldsymbol{B}$ is non-singular, we can find a form which is linear *in state derivatives* by offsetting $\boldsymbol{u}$ by replacing $\boldsymbol{u}$ with $(\boldsymbol{u_{ofB}} + \boldsymbol{u_0})$, where $\boldsymbol{u_0} = -\boldsymbol{B^{-1}} \cdot \boldsymbol{k}_{\dot{\boldsymbol{x}}}$;. The resulting form becomes:

- $\dot{\boldsymbol{x}} = \boldsymbol{A} \cdot \boldsymbol{x} + \boldsymbol{B} \cdot \boldsymbol{u}_{\boldsymbol{ofB}}; \quad \boldsymbol{y} = \underbrace{(\boldsymbol{k}_{\boldsymbol{y}} - \boldsymbol{D} \cdot \boldsymbol{B}^{-1} \cdot \boldsymbol{k}_{\dot{\boldsymbol{x}}})}_{\boldsymbol{k_{yofB}}} + \boldsymbol{C} \cdot \boldsymbol{x} + \boldsymbol{D} \cdot \boldsymbol{u}_{\boldsymbol{ofB}}$;

It is often enough to find a form which is linear *in state derivatives*, as shown above. However, if both $\boldsymbol{A}$ and $\boldsymbol{D}$ are non-singular, we can find a *Linear Form,* i.e. linear in both state derivatives and outputs, i.e. without both $\boldsymbol{k}_{\dot{\boldsymbol{x}}}$ and $\boldsymbol{k}_{\boldsymbol{y}}$. This is done by offsetting $\boldsymbol{u}$ by replacing $\boldsymbol{x}$ with $(\boldsymbol{x_{ofAD}} + \boldsymbol{x_0})$ and $\boldsymbol{u}$ with $(\boldsymbol{u_{ofAD}} + \boldsymbol{u_0})$, where $\begin{bmatrix} \boldsymbol{x_0} \\ \boldsymbol{u_0} \end{bmatrix} = -\begin{bmatrix} \boldsymbol{A} & \boldsymbol{B} \\ \boldsymbol{C} & \boldsymbol{D} \end{bmatrix}^{-1} \cdot \begin{bmatrix} \boldsymbol{k}_{\dot{\boldsymbol{x}}} \\ \boldsymbol{k}_{\boldsymbol{u}} \end{bmatrix}$;. The resulting form becomes:

- $\dot{\boldsymbol{x}}_{\boldsymbol{ofAD}} = \boldsymbol{A} \cdot \boldsymbol{x}_{\boldsymbol{ofAD}} + \boldsymbol{B} \cdot \boldsymbol{u}_{\boldsymbol{ofAD}}; \quad \boldsymbol{y} = \boldsymbol{C} \cdot \boldsymbol{x}_{\boldsymbol{ofAD}} + \boldsymbol{D} \cdot \boldsymbol{u}_{\boldsymbol{ofAD}}$;

(The used terms, *affine* and *linear*, can be confusing because the common meaning of the word linear can include a constant term, while absence of constant term would instead be called *proportional*.)

If the model is affine (or linear), $\boldsymbol{A}, \boldsymbol{B}, \boldsymbol{C}, \boldsymbol{D}$ can be found by identification of the coefficients for the components of $\boldsymbol{x}$ and $\boldsymbol{u}$. Manual manipuations or symbolic tools can be used. If the model is non-linear, one can sometimes motivate to neglect small terms so that the model becomes affine. A more general and automated way to find an affine model is to make a Taylor expansion (symbolic or numerical) around $(\boldsymbol{x_0}, \boldsymbol{u_0}, t_0)$. If the model is affine and there is no explicit dependency of t, the Taylor expansion will be exact:

$$\dot{\boldsymbol{x}} = \boldsymbol{f_{ODE}}(\boldsymbol{x}, \boldsymbol{u}) = \{affine\} =$$

$$= \boldsymbol{f_{ODE}}(\boldsymbol{x_0}, \boldsymbol{u_0}) + \left(\frac{\partial \boldsymbol{f_{DAE}}}{\partial \boldsymbol{x}}\right)\Big|_{\substack{\boldsymbol{x}=\boldsymbol{x_0}\\ \boldsymbol{u}=\boldsymbol{u_0}}} \cdot (\boldsymbol{x} - \boldsymbol{x_0}) + \left(\frac{\partial \boldsymbol{f_{DAE}}}{\partial \boldsymbol{u}}\right)\Big|_{\substack{\boldsymbol{x}=\boldsymbol{x_0}\\ \boldsymbol{u}=\boldsymbol{u_0}}} \cdot (\boldsymbol{u} - \boldsymbol{u_0}) = \{affine\} =$$

$$= \boldsymbol{f_{ODE}}(\boldsymbol{x_0}, \boldsymbol{u_0}) + \boldsymbol{A} \cdot (\boldsymbol{x} - \boldsymbol{x_0}) + \boldsymbol{B} \cdot (\boldsymbol{u} - \boldsymbol{u_0}); \quad \text{where } \boldsymbol{A} \text{ and } \boldsymbol{B} \text{ independent of } \boldsymbol{x_0} \text{ and } \boldsymbol{u_0} \quad \Rightarrow$$

$$\Rightarrow \quad \dot{\boldsymbol{x}}_{\boldsymbol{of}} = \boldsymbol{f_{ODE}}(\boldsymbol{x_0}, \boldsymbol{u_0}) + \boldsymbol{A} \cdot \underbrace{(\boldsymbol{x} - \boldsymbol{x_0})}_{\boldsymbol{x_{of}}} + \boldsymbol{B} \cdot \underbrace{(\boldsymbol{u} - \boldsymbol{u_0})}_{\boldsymbol{u_{of}}};$$

If $(\boldsymbol{x_0}, \boldsymbol{u_0})$ is a steady state condition it means same as that $\boldsymbol{f_{ODE}}(\boldsymbol{x_0}, \boldsymbol{u_0}) = 0$, so the constant term linearization gets the form *linear in state derivatives* $\dot{\boldsymbol{x}}_{\boldsymbol{of}}$. Similar Taylor expansion can be done with $\boldsymbol{g}$ for outputs $\boldsymbol{u}$, to find a linear (or at least affine) from also for outputs.

Models with explicit dependency of t are treated in (Bruzelius, 2004).

Note that the model was assumed to be affine. This meant that $\boldsymbol{A}$ and $\boldsymbol{B}$ becomes independent of $\boldsymbol{x_0}$ and $\boldsymbol{u_0}$, as opposed to a non-linear model, see 1.5.1.1.9.1.

1.5.1.1.4.6 Closed Form Solution of Model on Affine Form

It will here be shown that a closed form solution can be found for the affine form. This is an alternative to simulation. The following example shows how to find the solution for $\dot{\boldsymbol{x}} = \boldsymbol{k} + \boldsymbol{A} \cdot \boldsymbol{x}$; with $\boldsymbol{x}(0) = \boldsymbol{x_0}$.

Make an ansatz: $\boldsymbol{x} = \boldsymbol{x_{const}} + \boldsymbol{V} \cdot \left[e^{\lambda_1 \cdot t}, e^{\lambda_2 \cdot t}, \cdots, e^{\lambda_{\dim(x)} \cdot t}\right]^T = \boldsymbol{x_{const}} + \boldsymbol{V} \cdot \boldsymbol{e}^{\boldsymbol{\lambda} \cdot t}; \quad \Rightarrow$

$\Rightarrow \quad \dot{\boldsymbol{x}} = \boldsymbol{V} \cdot \mathbf{Diag}\left(\left[\lambda_1 \cdot e^{\lambda_1 \cdot t},\ \lambda_2 \cdot e^{\lambda_2 \cdot t},\ \cdots,\ \lambda_{\dim(x)} \cdot e^{\lambda_{\dim(x)} \cdot t}\right]\right) = \boldsymbol{V} \cdot \mathbf{Diag}\left(\lambda_1,\ \lambda_2,\ \cdots,\ \lambda_{\dim(x)}\right) \cdot \boldsymbol{e}^{\boldsymbol{\lambda} \cdot t} = \boldsymbol{V} \cdot \boldsymbol{D} \cdot \boldsymbol{e}^{\boldsymbol{\lambda} \cdot t};$

Insert: $\boldsymbol{V} \cdot \boldsymbol{D} \cdot \boldsymbol{e}^{\boldsymbol{\lambda} \cdot t} = \boldsymbol{k} + \boldsymbol{A} \cdot \left(\boldsymbol{x_{const}} + \boldsymbol{V} \cdot \boldsymbol{e}^{\boldsymbol{\lambda} \cdot t}\right);$

Identify constant terms: $\mathbf{0} = \boldsymbol{k} + \boldsymbol{A} \cdot \boldsymbol{x_{const}}; \quad \Rightarrow \quad \boldsymbol{x_{const}} = -\boldsymbol{A}^{-1} \cdot \boldsymbol{k};$

Identify exponential terms: $\lambda_i \cdot \boldsymbol{I} = \boldsymbol{A}; \quad \forall i \quad \Rightarrow \quad [\boldsymbol{V_{norm}}, \boldsymbol{D}] = \text{eig}(\boldsymbol{A}); \quad and \quad \boldsymbol{V} = \boldsymbol{V_{norm}} \cdot \mathbf{diag}(\boldsymbol{m});$ $\boldsymbol{V_{norm}}$ is a matrix with normalized eigenvectors as columns. $\boldsymbol{m}$ is a column vector with magnitudes of eigenvectors.

The solution before fulfilling initial conditions becomes: $\boldsymbol{x} = -\boldsymbol{A}^{-1} \cdot \boldsymbol{k} + \boldsymbol{V_{norm}} \cdot \mathbf{Diag}(\boldsymbol{m}) \cdot \boldsymbol{e}^{\boldsymbol{\lambda} \cdot t};$

Fulfilling initial conditions $\boldsymbol{x_0}$: $\boldsymbol{x_0} = -\boldsymbol{A}^{-1} \cdot \boldsymbol{k} + \boldsymbol{V_{norm}} \cdot \mathbf{Diag}(\boldsymbol{m}) \cdot \boldsymbol{e}^{\boldsymbol{\lambda} \cdot 0} = -\boldsymbol{A}^{-1} \cdot \boldsymbol{k} + \boldsymbol{V_{norm}} \cdot \boldsymbol{m}; \quad \Rightarrow$ $\boldsymbol{m} = \boldsymbol{V}_{\boldsymbol{norm}}^{-1} \cdot (\boldsymbol{x_0} + \boldsymbol{A}^{-1} \cdot \boldsymbol{k}) = \boldsymbol{V}_{\boldsymbol{norm}}^{T} \cdot (\boldsymbol{x_0} + \boldsymbol{A}^{-1} \cdot \boldsymbol{k});$

So, the solution becomes: $\boldsymbol{x} = -\boldsymbol{A}^{-1} \cdot \boldsymbol{k} + \boldsymbol{V_{norm}} \cdot \mathbf{Diag}\left(\boldsymbol{V}_{\boldsymbol{norm}}^{T} \cdot (\boldsymbol{x_0} + \boldsymbol{A}^{-1} \cdot \boldsymbol{k})\right) \cdot \boldsymbol{e}^{\boldsymbol{\lambda} \cdot t};$

1.5.1.1.4.7 Inline Integration or Difference Equation Formulation

The methods in mind above, e.g. "Euler forward with constant time step", assumes a loop over time where each a time-sequential step includes an update of time and state variables. In this context there is one important assumption, the derivative approximation. If one, already in the Mathematical model, assumes a time step Δt (or any numerical grid $\boldsymbol{t_{grid}} = [t_0, t_1, \cdots, t_N]$) and replaces each occurrence of the state derivatives with its derivative approximation one get a system of difference equation instead of a system of differential equations. So, the solution over a whole/longer time interval (a macro step) consisting of multiple micro time steps, is iteratively found at once, i.e. without the stepwise looping over time. It is useful for co-simulation. The method is also used in predictive control, 1.5.3.2, i.e. optimization over a time interval.

Using the derivative approximation for "Euler forward" gives $\boldsymbol{x}(t_{now} + \Delta t) = \boldsymbol{x}(t_{now}) + \Delta t \cdot \dot{\boldsymbol{x}}_{\boldsymbol{now}};$ (or shorter $\boldsymbol{x_{i+1}} = \boldsymbol{x_i} + (t_{i+1} - t_i) \cdot \dot{\boldsymbol{x}}_{\boldsymbol{i}};$). So, one can reformulate:

$$\boldsymbol{f_{DAE}}(\dot{\boldsymbol{z}}, \boldsymbol{z}, t) = \mathbf{0}; \quad \text{where } \boldsymbol{z} = [\boldsymbol{x}, \boldsymbol{y}]$$

to:

$$\boldsymbol{f_{DAE}}\left(\left[(\boldsymbol{x_{i+1}} - \boldsymbol{x_i})/(t_{i+1} - t_i), [\boldsymbol{x_i}, \boldsymbol{y_i}]\right], \boldsymbol{z_i}, t_i\right) = \mathbf{0}; \quad \text{for } i = 0,1,\cdots,N$$

This is a system of ordinary algebraic equations. The $\dot{\boldsymbol{y}}_{\boldsymbol{i}}$ exists only if we have "High order" (see 1.5.1.5). We can eliminate such as described in 1.5.1.5. Then, with $\boldsymbol{f}_{\boldsymbol{DAE}} = [\boldsymbol{f}_{\boldsymbol{xDAE}}, \boldsymbol{f}_{\boldsymbol{yDAE}}]$:

$$\boldsymbol{f}_{\boldsymbol{xDAE}}((\boldsymbol{x}_{\boldsymbol{i+1}} - \boldsymbol{x}_{\boldsymbol{i}})/(\boldsymbol{t}_{\boldsymbol{i+1}} - \boldsymbol{t}_{\boldsymbol{i}}), \boldsymbol{x}_{\boldsymbol{i}}, \boldsymbol{y}_{\boldsymbol{i}}, t_i) = \boldsymbol{0}; \quad \text{for } i = 0,1,\cdots,N-1$$

$$\boldsymbol{f}_{\boldsymbol{yDAE}}(\boldsymbol{x}_{\boldsymbol{i}}, \boldsymbol{y}_{\boldsymbol{i}}, t_i) = \boldsymbol{0}; \quad \text{for } i = N$$

We assume initial values x_0 and time grid $[t_0, t_1, \cdots, t_N]$ are known. Then there are $\mathrm{N} \cdot \dim(\boldsymbol{x}) + (N+1) \cdot \dim(\boldsymbol{y})$ unknowns and equally many equations. An example (same as in Figure 1-51) is here given. The m and c are parameters. The Mathematical model is the following DAE with 3 unknowns (v, x, F) and 3 (differential algebraic) equations:

$$m \cdot \dot{v} = -F;$$
$$\dot{x} = v;$$
$$F = c \cdot x;$$

Rewritten to system of system of difference equations with $N \cdot 2 + (N+1) \cdot 1 = 3 \cdot N + 1$ unknowns $(v_1, v_2, \cdots, v_N, \quad x_1, x_2, \cdots, x_N, \quad F_0, \cdots, F_N)$ and $2 \cdot N + 1 \cdot (N+1) = 3 \cdot N + 1$ equations:

$$\boldsymbol{f}_{\boldsymbol{xDAE}} = \begin{bmatrix} \frac{v_{i+1} - v_i}{t_{i+1} - t_i} + F_i \\ \frac{x_{i+1} - x_i}{t_{i+1} - t_i} - v_i \end{bmatrix} = \boldsymbol{0}; \quad \text{for } i = 0,1,\cdots,N-1$$

$$\boldsymbol{f}_{\boldsymbol{yDAE}} = [F_i - c \cdot x_i] = \boldsymbol{0}; \quad \text{for } i = 0,1,\cdots,N$$

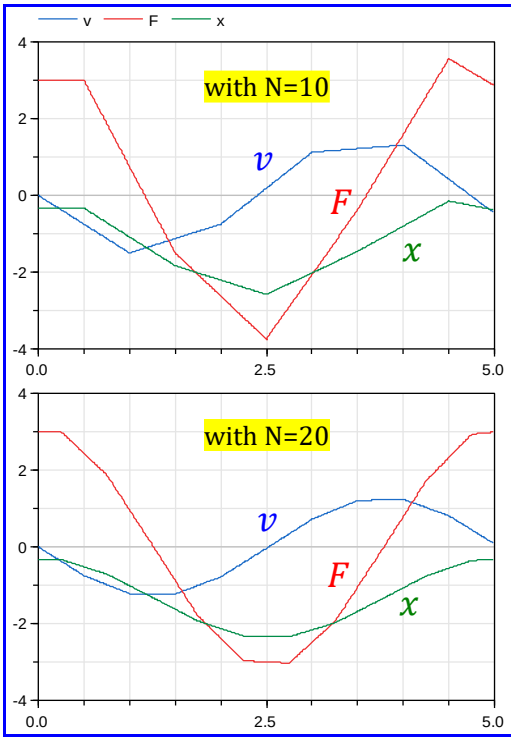
There are many ways to solve such (algebraic) system of equation. One do not need a dynamic tool, since the independent variable time is removed. In case of a linear dynamic model $\dot{\boldsymbol{x}}(t) = \boldsymbol{A} \cdot \boldsymbol{x}(t);$, one can assembly a large algebraic system of equations with "another $\boldsymbol{A}$ matrix", here called $\boldsymbol{A}_{\boldsymbol{large}}$:

$$\boldsymbol{A}_{\boldsymbol{large}} \cdot [\boldsymbol{x}_{\boldsymbol{array}}; \boldsymbol{y}_{\boldsymbol{array}}] = \boldsymbol{b};$$

Note that $\boldsymbol{x}(t) = [x_1(t), \cdots, x_{\dim(x)}(t)]$ means an array of variables, while $\boldsymbol{x}_{\boldsymbol{array}}$ means a longer array (or column vector) $\boldsymbol{x}_{\boldsymbol{array}} = [[x_1(t_0), \cdots, x_1(t_N)], \cdots, [x_{\dim(x)}(t_0), \cdots, x_{\dim(x)}(t_N)]]$. Our example, with $N = 2$, becomes:

$$\underbrace{\begin{bmatrix} \begin{bmatrix} 1 & 0 \\ -1 & 1 \end{bmatrix} & \begin{bmatrix} 0 & 0 \\ 0 & 0 \end{bmatrix} & \begin{bmatrix} -t_0 + t_1 & 0 & 0 \\ 0 & -t_1 + t_2 & 0 \end{bmatrix} \\ \begin{bmatrix} 0 & 0 \\ t_1 - t_2 & 0 \end{bmatrix} & \begin{bmatrix} 1 & 0 \\ -1 & 1 \end{bmatrix} & \begin{bmatrix} 0 & 0 & 0 \\ 0 & 0 & 0 \end{bmatrix} \\ \begin{bmatrix} 0 & 0 \\ 0 & 0 \\ 0 & 0 \end{bmatrix} & \begin{bmatrix} 0 & 0 \\ -c & 0 \\ 0 & -c \end{bmatrix} & \begin{bmatrix} 1 & 0 & 0 \\ 0 & 1 & 0 \\ 0 & 0 & 1 \end{bmatrix} \end{bmatrix}}_{\boldsymbol{A}_{\boldsymbol{large}}} \cdot \underbrace{\begin{bmatrix} \begin{bmatrix} v_1 \\ v_2 \end{bmatrix} \\ \begin{bmatrix} x_1 \\ x_2 \end{bmatrix} \\ \begin{bmatrix} F_0 \\ F_1 \\ F_2 \end{bmatrix} \end{bmatrix}}_{\boldsymbol{x}_{\boldsymbol{array}}} = \underbrace{\begin{bmatrix} \begin{bmatrix} v_0 \\ 0 \end{bmatrix} \\ \begin{bmatrix} x_0 + (t_1 - t_0) \cdot v_0 \\ 0 \end{bmatrix} \\ \begin{bmatrix} c \cdot x_0 \\ 0 \\ 0 \end{bmatrix} \end{bmatrix}}_{\boldsymbol{b}};$$

However, a Modelica tool is a dynamic tool and it can be useful, because a Mathematical model in Modelica can, with minor code editing, be changed to a difference equation. The "traditional" Modelica model in Figure 1-52 can be edited to a variant with difference equations as shown in the following figure. (Some Modelica tool have this rewriting as a build-in and selectable automatic feature, typically used for real time simulation.) Another derivative approximation is used in the figure, to show that also "implicit" approximations as "midpoint" can be used.




```
model ExampleModel_InlineIntegration
  parameter Real m=2, c=3;
  Real v, x, F;

  parameter Real F0=4, v0=0, x0=-1/3;
  Real v_array[N+1], F_array[N+1], x_array[N+1];
  Real derv_array[N-1 +1], derx_array[N-1 +1];
  parameter Integer N=20;  //=2; //
  parameter Real t0=0, tend=5, t_array[:]=linspace(t0,tend,N+1);
  //Note: Modelica indexes vectors from 1, while the compendium indexes
initial value with 0. Therefore "+1"
equation
//Equations with "constant variables":
  v_array[1]=v0; x_array[1]=x0; // derv_array[3]=33; F_array[11]=111;
  //Derivative approximations:
  for i in (0 +1):(N-1 +1) loop
    if i==1 then
      //Forward 1st order derivative aproximation:
      derv_array[i]=(v_array[i+1]-v_array[i])/(t_array[i+1]-t_array[i]);
      derx_array[i]=(x_array[i+1]-x_array[i])/(t_array[i+1]-t_array[i]);
    else
      //Midpoint 1st order derivative aproximation:
      derv_array[i]=(v_array[i+1]-v_array[i-1])/(t_array[i+1]-t_array[i-1]);
      derx_array[i]=(x_array[i+1]-x_array[i-1])/(t_array[i+1]-t_array[i-1]);
    end if;
  end for;
  for i in (0 +1):(N-1 +1) loop
     m*derv_array[i] = -F_array[i]; //instead of m*der(v)=-F;
     derx_array[i]   = +v_array[i]; //instead of der(x)=v;
  end for;
  for i in (0 +1):(N +1) loop
     F_array[i] = F0 + c*x_array[i];  //instead of F = F0 + c*x;
  end for;

//Equations with "variable variables":
  v = Modelica.Math.Vectors.interpolate(t_array,v_array, time);
  x = Modelica.Math.Vectors.interpolate(t_array,x_array, time);
  F = Modelica.Math.Vectors.interpolate(t_array,F_array, time);
end ExampleModel_InlineIntegration;
```

Figure 1-16: Example from Figure 1-52 implemented as difference equation model in Modelica.

The row "`v_array[1]=v0; x_array[1]=x0;`" in Figure 1-52 indicate an initial value problem, which is the most common problem, i.e., where the state variables are known at initial time (indexed `i=1`). But **note** that the solution method very simply allows knowing some other variables at other time instants instead, e.g. "`derv_array[3]=33; F_array[11]=111;`".

Finally, it should be remembered that the form described above is "contaminated" by containing the derivative approximation, so it is a mix of "1.5.1.1.5 Explicit Form Modelling" and "1.5.1.1.6 Computation".

1.5.1.1.4.8 Stability

When only looking at the mathematical model as a step towards a numerical simulation, we might often not reflect on whether the system is *stable* or *unstable*. However, we will find out when/if we do simulation (1.5.1.1.6) or stability analysis (1.5.1.1.9.2). However, it is worth to know about *instability* already while working with the mathematical model, because it can sometimes explain "non-intuitive properties" of the DAE equations. One example of non-intuitive is that models for high-speed steady state cornering (4.3) tell that one should steer to the right when turn left. This is only when the longitudinal speed v_x is larger than a certain speed, see 4.3.5. The explanation is that the operating conditions are unstable; one need to "balance" to stay on a (instable) equilibrium. Other examples are keeping the balance when steering a one-track vehicle (4.5.2.3) or low speed reversing with articulated vehicles (4.2.6).

1.5.1.1.5 Explicit Form Modelling

In this stage, one should generate an **Explicit Form model**, which means equations rearranged to assignment statements, i.e. to an explicit form (algorithm) which outputs the state derivatives. The explicit form model is generally causal. You probably recognize this formulation as "ODE" (Ordinary Differential Equation) or "IVP" (Initial Value Problem). So, the general form is:

- $\dot{\boldsymbol{x}} \leftarrow \boldsymbol{f}_{\boldsymbol{ODE}}(\boldsymbol{x}, \boldsymbol{u}, t); \quad \boldsymbol{y} \leftarrow \boldsymbol{g}(\boldsymbol{x}, \boldsymbol{u}, t);$

(Here, the function $\boldsymbol{f}_{\boldsymbol{ODE}}$ is an operator which include only algebraic operations.)

We have essentially the same set of equations in the Mathematical model as in the Explicit Form model. However, seen as Explicit Form model, we count x and $\dot{x}$ as different variables. So far, this

means that we have too few equations. To keep equality between number of variables and equations, we can count in also the equations $x \leftarrow \int \dot{x} \cdot dt;$.

The $\boldsymbol{x}$ is the state variables, $\boldsymbol{u}$ is the input variables $\boldsymbol{u}(t)$, and $\boldsymbol{y}$ the output variables. In the mathematical model, there was no distinction between different dependent variables in $\boldsymbol{z}$. However, to reach the explicit model, each variable in $\mathbf{z}$ has to be identified as belonging to either of $\boldsymbol{x}$, $\boldsymbol{y}$ or $\boldsymbol{u}$. Simply speaking, states $\boldsymbol{x}$ are the variables which appears both as z_i and $\dot{z}_i$, inputs $\boldsymbol{u}$ are variables that cannot be solved for within the system of equations and outputs $\boldsymbol{y}$ are the remaining variables. Since the state variables are identified, the *Explicit Form* is sometimes called *State Space Form*.

A *Dataflow Diagram* a.k.a. *Block Diagram* (see Figure 1-24 and Figure 1-51) is a graphical representation of the explicit form. It is drawn using blocks with input and output ports and arrows representing signals between; integration is represented by integration blocks with $\dot{\boldsymbol{x}}$ as input and $\boldsymbol{x}$ as output.

One can see a Dataflow Diagram as representing the system in time domain as signals $u(t)$ sent between blocks $f(u(t), t)$. Alternatively, one can also see a Dataflow Diagram as representing the system in frequency domain as signals $z(s)$ existing between blocks $f(u(s), s)$. Here, s is the Laplace variable. One should not mix these views. The first view suits best if combined with physical submodels where there is also physcial connections. The latter is more abstract and possibly more close to a Mathematical model; it is questionable if there should be arrows on the lines between the blocks, because the lines does not really represent a data flow.

1.5.1.1.5.1 Causality

Systems can be modelled with **Natural causality**. For mechanical systems, this is when forces on the masses (or motion of the compliance's ends) are prescribed as functions of time. Then the velocities of the masses (or forces of the compliances) become state variables and must be solved through time integration. The opposite is called **Inverse dynamics** and means that velocities of masses (or forces of compliances) are prescribed. For instance, the velocity of a mass can be prescribed and then the required forces on the mass can be calculated through time differentiation of the prescribed velocity. Cf. Analysis and Inverse Analysis in Figure 1-9.

1.5.1.1.5.2 Black-box explicit form

The explicit form can also be of *black-box* type, meaning that the algorithm to calculate $\dot{x}$ is not human-readable. That is useful when companies need to share odels for simulation. A standard for such format is Functional Mock-Up Interface, FMI, see 1.5.4.1.6.

1.5.1.1.5.2.1 Semi-Explicit form

If the explicit form cannot be found, there are time integration methods also for solving the semi-explicit form: $\dot{\boldsymbol{x}} \leftarrow \boldsymbol{f}_{\boldsymbol{semi}}(\boldsymbol{x}, \boldsymbol{y}, \boldsymbol{u}(t), t);\ \mathbf{0} = \boldsymbol{g}_{\boldsymbol{semi}}(\boldsymbol{x}, \boldsymbol{y}, \boldsymbol{u}(t), t);$.

A generalisation of the semi-explicit form is when we cannot even find explicit expression for all state derivatives $\dot{\boldsymbol{x}}$. We can still formulate an Explicit form model, but then using "implicit form expressions". As extreme example, when no variables can be solved for:

- $[\dot{\boldsymbol{x}}, \boldsymbol{y}] \leftarrow solve\left(\boldsymbol{f}_{\boldsymbol{ODE,impl}}(\dot{\boldsymbol{x}}, \boldsymbol{x}, \boldsymbol{y}, \boldsymbol{u}(t), t) = \mathbf{0}\right);$

The operator "*solve*" is here meant to be implemented as a (numerical) iteration during the Computation (compare 1.5.1.7.3). The only difference to the original $\boldsymbol{f}_{\boldsymbol{DAE}}$ is that the states $\boldsymbol{x}$ are identified among the variables $\boldsymbol{z}$. But, it should also be noted that this is no general cure to avoid doing Mathematical manipulations, because far from all iterations succeed; so, explicit form expressions should be strived for as far as possible! Often, some parts of the Explicit form can be explicit form and only a few variables appear in a *solve* expression. When implicit expressions appear in the Explicit form model, we have a situation where causality is not defined for the involved variables, although the model is on an overall Explicit form.

1.5.1.1.5.2.2 Implicit form

If neither explicit or semi-explicit form cannot be found, there are time integration methods also for solving the implicit form: $\boldsymbol{residual} \leftarrow \boldsymbol{f_{implicit}}(\dot{\boldsymbol{x}}, \boldsymbol{x}, \boldsymbol{y_1}, \dot{\boldsymbol{y}}_2, \boldsymbol{y_2}, \boldsymbol{u}(t), t)$;. The difference with the model in 1.5.1.1.3.2 is that the states $\boldsymbol{x}$ are identified. The $\boldsymbol{residual} = \boldsymbol{0}$; is solved numerically and iteratively yielding $\{\dot{\boldsymbol{x}}, \dot{\boldsymbol{y}}_1, \boldsymbol{y_1}, \boldsymbol{y_2}\}$ at each model evaluation. Then $\boldsymbol{x} \leftarrow \int \dot{\boldsymbol{x}} \cdot dt$;. Both $\dot{\boldsymbol{y}}_2$ and $\boldsymbol{y_2}$ are found without time integration, which means that $\dim(\boldsymbol{y_1})$ extra equations are needed compared to $\boldsymbol{f_{DAE}}$ in 1.5.1.1.3.2. These are found through differentiation of some equations, see more 1.5.1.5.

An alternative solution method time integrates also $\boldsymbol{y_2} \leftarrow \int \dot{\boldsymbol{y}}_2 \cdot dt$; without fulfilling the extra equations. Instead the extra equations are used to correct $\boldsymbol{x}$ and $\boldsymbol{y_2}$ to eachother between each time step. This is used in many MBS tools, such as Adams, see 1.5.4.1.4.

1.5.1.1.6 Computation

Computation, is to find a numerical solution for all variables, also called *(time) trajectories*. Several ways can be of interest, e.g.:

- *(Time domain) Simulation* (e.g. Initial value problem, IVP or End value problem, EVP). There are many advanced pre-programmed integration methods which one can use without knowing the details. It is often enough to understand the concept of the simplest "Euler forward with constant time step", in which the state variables are updated in each time step, Δt, as follows:
  $\dot{\boldsymbol{x}}_{\boldsymbol{now}} \leftarrow \boldsymbol{f_{ODE}}(\boldsymbol{x}(t_{now}), \boldsymbol{u}(t_{now}), t_{now})$; (Explicit form model)
  $\boldsymbol{x}(t_{now} + \Delta t) \leftarrow \boldsymbol{x}(t_{now}) + \Delta t \cdot \dot{\boldsymbol{x}}_{\boldsymbol{now}}$; (Derivative approximation)
  Typically, the time step Δt is varied by the integration methods itself to minimize computation time, but maintaining a certain accuracy. The Δt should neither be mixed up with the *output interval* (how dense in time the simulation results are logged) nor the *sample time* in time discrete systems, see 1.5.1.4. A general advice to check that you have got a correct enough solution is to tune the tolerance to as large as possible without changing the character of the solution. Examples of, so called forward and backward methods are given in Figure 1-17.

```
model DiscreteIntegrator
  parameter Real SampleTime=0.5;
  Real u, yc,   udF, ydF, prederydF,  udB, ydB, derydB;
initial equation
  yc=0.2; pre(ydF)=yc; pre(ydB)=yc;
equation
  //input:
  u=0.1*sin(2*time);
  //model (continuous):
  der(yc)=-yc+u;

  //discrete, EulerFwd: pre(deryd)=(yd-pre(yd))/SampleTime
  when sample(0, SampleTime) then
    udF=u;
    prederydF = -pre(ydF)+pre(udF); //model
    ydF=pre(ydF)+prederydF*SampleTime;
  end when;

  //discrete, EulerBwd: deryd = (yd-pre(yd))/SampleTime
  when sample(0, SampleTime) then
    udB=u;
    derydB = -ydB+udB; //model
    ydB=pre(ydB)+derydB*SampleTime;
  end when;
end DiscreteIntegrator;
```

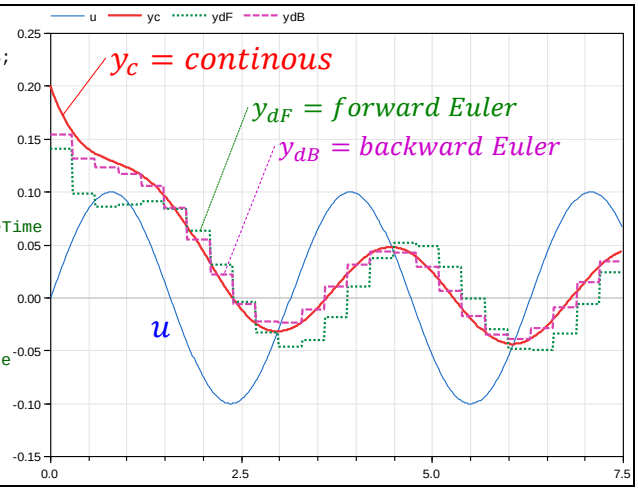


Figure 1-17: A continuous dynamic model, $\dot{y}_c = -y_c + 0.1 \cdot sin(2 \cdot t)$; and two discretizations: Euler Forward (y_{dF}) and Euler Backward (y_{dB}).

- For linear or linearized models and simple excitation one can find the solution without time integration, by using the *"matrix exponential"*, $e^{\boldsymbol{Matrix}}$: The solution to a linear system without input, $\dot{z} = A \cdot z$;, starting from a given initial state $\boldsymbol{x}(0) = \boldsymbol{x_{iv}}$ is found as $\boldsymbol{x}(t) = e^{\boldsymbol{A} \cdot t} \cdot \boldsymbol{x_{iv}}$;. An alternative way, using a solution ansatz, is shown in 4.5.4.1.
- *Frequency domain analyses.* Linear models or models linearized around an operating condition by differentiating and $A_{ij} = df_i/dx_j$ and $B_{ik} = df_i/du_k$. The matrices are very useful for eigen-modes, eigen-frequencies, step response, stability, or use as model base in model-based control design methods.
- *Stability analysis* is to study when small disturbances lead to large response and how. (In linear models, when limited disturbances lead to unlimited solutions, typically oscillating or

exponentially increasing.) Stability analysis is normally done for one operating point $[\boldsymbol{x_0}, \boldsymbol{u_0}]$, around which one linearizes. Instability is detected as when any eigenvalue to $\boldsymbol{A}$ has positive real parts. If there are inputs ($\dim(\boldsymbol{u}) > 0$), the stability is "for the open loop system", e.g. for the vehicle without driver. If the equations for $\boldsymbol{u}$ is included in the model, there will be no $\boldsymbol{B}$ matrix, and the stability is then "for the closed loop system", e.g. for the vehicle with driver. Adding a driver can make the system (vehicle with driver) more or less stable.

- *Optimization*. Either optimizing a finite number of defined design parameters or time trajectories, e.g., $u(t)$. There are many optimization methods, ranging from trial-and-error to exhaustive search and mathematically/numerically advanced, gradient based or evolutionary inspired methods. More about optimization in 1.5.1.1.9.3.

1.5.1.1.6.1.1 Knowing other than initial (state) value problems

It should be mentioned that the explicit form can be used also for other than knowing the initial (state) values. We use a simple mass-spring system as example:

$$m \cdot \dot{v} = -F; \quad and \quad \dot{F} = c \cdot v; \quad where\ the\ states\ are\ \{v, F\}$$

- **Initial (state) value problem** (as reference): $v|_{t=0} \quad and \quad F|_{t=0}$ are known.
- **Initial values known, but other than the states**. E.g. we know $v|_{t=0} \quad and \quad \dot{v}|_{t=0}$. Then we can first solve $F|_{t=0}$ from the algebraic equation at initial time $t = 0$: $m \cdot \dot{v}|_{t=0} = F|_{t=0}; \quad and \quad \dot{F}\big|_{t=0} = c \cdot v|_{t=0};$. When we know $F|_{t=0}$, it can be solved as the Initial (state) value problem.
- **End (state) value problem**: $v|_{t=t_{end}} \quad and \quad F|_{t=end}$ are known. Then we can do a variable transformation $\tau = t_{end} - t;$:

$$\{m \cdot \dot{v} = -F; \quad \dot{F} = c \cdot v;\} \Rightarrow \left\{m \cdot \frac{dv}{dt} = -F; \ \frac{dF}{dt} = c \cdot v;\right\} \Rightarrow \{\tau = t_{end} - t;\} \Rightarrow$$

$$\Rightarrow \left\{m \cdot \frac{dv}{d\tau} \cdot \frac{d\tau}{dt} = -F; \ \frac{dF}{d\tau} \cdot \frac{d\tau}{dt} = c \cdot v; \ \right\} \Rightarrow \left\{m \cdot \frac{dv}{d\tau} \cdot (-1) = -F; \ \frac{dF}{d\tau} \cdot (-1) = c \cdot v;\right\} \Rightarrow$$

$$\Rightarrow \left\{m \cdot \frac{dv}{d\tau} = F; \ \frac{dF}{d\tau} = -c \cdot v; \ \tau = t_{end} - t;\right\} \Rightarrow \{m \cdot v' = F; \ F' = -c \cdot v; \ t = t_{end} - \tau;\}$$

The last 2 first equations can be solved as an initial (state) variable problem with the independent variable τ, as opposed to t. The true time t is solved as a algebraic part of the system for each τ instant using the 3rd equation: $t = t_{end} - \tau;$.

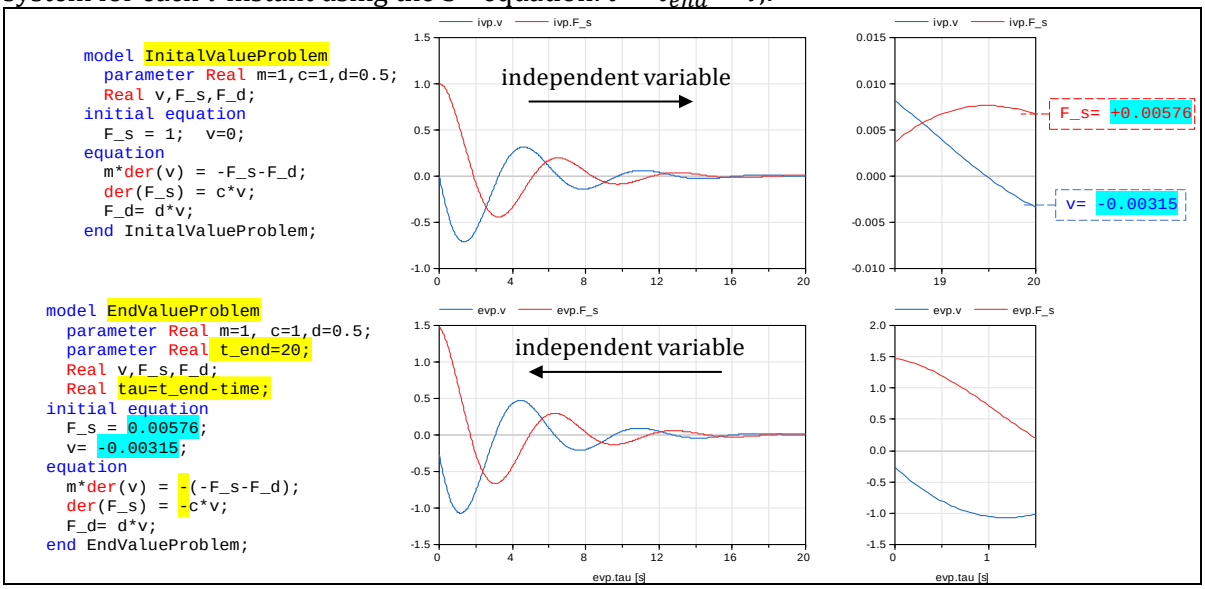


Figure 1-18: Solving same mathematical model as IVP and EVP. The end values from the IVP are used as end values in the EVP. EVP is numerically sensitive, since model is instable in reverse time. (Modelica is used, where the name of the independent variable is always "time", so t and τ swopped, sorry!)

- **Mixed values known at mixed times**: In principle, any variables at any time can be given, and there would still be one unique solution. Note that the number of given values must be equally

many as the state variables. However, exactly how to re-formulate and solve such a general problem can be very complex and no general method is given in this book.

1.5.1.1.6.2 Tests with analogue system, e.g., scale models

The computation discussed above is often a way to avoid building real prototypes, as in early phases of development of complex, often large, products. Prior to good digital computers, one could make use of tests with a smaller and/or less complex real prototype. Or, one put big effort in solving the equations for one (often non-dimensional) case and then re-calculated the result to the full-scale product. The re-calculation between requires that the differential equations are well known. An example of where scale-down real models are used is fluid forces on boats hulls. An example of where solutions to non-dimensional equations are usefully re-calculate to real system is hydrodynamic bearings. In the following, it will be discussed in what extent this is a useful technique for road vehicles.

The assumed situation is that we want to check how a certain design of a (full-sized) vehicle will work for a certain maneuver by testing a maneuver with a smaller (down-)scaled vehicle. So, we need to propose a design of the down-scaled vehicle, the maneuver to be performed with the scaled vehicle, and how to transform the result from the scaled vehicle to how the full-sized vehicle would behave in the maneuver with the full-sized vehicle.

The simple one track model in Eq [4.55] will be used, with the simplification that $F_{fxw} = 0$ and $v_x > 0$ and $C_f = C_r = C_a$ and $l_f = l_r = l_a$:

$$\frac{d}{dt}\underbrace{\begin{bmatrix} v_y \\ \omega_z \end{bmatrix}}_{\boldsymbol{x}} = \underbrace{\begin{bmatrix} -\dfrac{2\cdot C_a}{m\cdot v_x} & v_x \\ 0 & -\dfrac{2\cdot C_a\cdot l_a^2}{J\cdot v_x} \end{bmatrix}}_{\boldsymbol{A}} \cdot \underbrace{\begin{bmatrix} v_y \\ \omega_z \end{bmatrix}}_{\boldsymbol{x}} + \underbrace{\begin{bmatrix} \dfrac{C_a}{m} \\ \dfrac{C_a\cdot l_a}{J} \end{bmatrix}}_{\boldsymbol{B}} \cdot \underbrace{\delta_f}_{u};$$

Now, we make an experiment with the scaled vehicle, i.e., we apply $u_s(t_S)$ and find $x_s(t_S)$ which satisfies $\frac{d}{dt_s}\boldsymbol{x_S} = \boldsymbol{A_S}\cdot\boldsymbol{x_S} + \boldsymbol{B_S}\cdot u_s$. The design of the scaled vehicle is given by $\{\boldsymbol{A_s}, \boldsymbol{B_s}\}$ defined as $\{\boldsymbol{A}, \boldsymbol{B}\}$ but with the scale vehicle design parameters: $\{C_{aS}, m_S, v_{xS}, l_{aS}, J_S\}$. Make an ansatz of proportional scaling: $\{\boldsymbol{x_s}, u_s, t_s\} = \{\boldsymbol{S_x}\cdot\boldsymbol{x}, S_u\cdot u, S_t\cdot t\}$. Then we would like to find out which **scale vehicle design** (which $\{\boldsymbol{A_s}, \boldsymbol{B_s}\}$), which **excitation scaling** (which S_u), and which **time scaling** (S_t) that satisfies:

$$\frac{d}{dt}\boldsymbol{x} = \boldsymbol{A}\cdot\boldsymbol{x} + \boldsymbol{B}\cdot u;\ \Rightarrow\ \frac{d}{dt_S}\frac{dt_S}{dt}\left(\boldsymbol{S_x^{-1}}\cdot\boldsymbol{x_s}\right) = \boldsymbol{A}\cdot\left(\boldsymbol{S_x^{-1}}\cdot\boldsymbol{x_s}\right) + \boldsymbol{B}\cdot(S_u^{-1}\cdot u_s);\ \Rightarrow$$

$$S_t\cdot\boldsymbol{S_x^{-1}}\cdot\frac{d}{dt_S}\boldsymbol{x_s} = \boldsymbol{A}\cdot\boldsymbol{S_x^{-1}}\cdot\boldsymbol{x_s} + \boldsymbol{B}\cdot\frac{1}{S_u}\cdot u_s;\ \Rightarrow$$

$$\frac{d}{dt_S}\boldsymbol{x_s} = \underbrace{\frac{1}{S_t}\cdot\boldsymbol{S_x}\cdot\boldsymbol{A}\cdot\boldsymbol{S_x^{-1}}}_{\boldsymbol{A_S}}\cdot\boldsymbol{x_s} + \underbrace{\frac{1}{S_t}\cdot\boldsymbol{S_x}\cdot\boldsymbol{B}\cdot\frac{1}{S_u}}_{\boldsymbol{B_S}}\cdot u_s;\ \Rightarrow$$

Identify relations between design parameters:

$$\boldsymbol{S_x}\cdot\begin{bmatrix} -\dfrac{2\cdot C_a}{m\cdot v_x} & v_x \\ 0 & -\dfrac{2\cdot C_a\cdot l_a^2}{J\cdot v_x} \end{bmatrix} = \begin{bmatrix} -\dfrac{2\cdot C_{aS}}{m_S\cdot v_{xS}} & v_{xS} \\ 0 & -\dfrac{2\cdot C_{aS}\cdot l_{aS}^2}{J_S\cdot v_{xS}} \end{bmatrix}\cdot\boldsymbol{S_x}\cdot S_t;$$

$$\boldsymbol{S_x}\cdot\begin{bmatrix} \dfrac{C_a}{m} \\ \dfrac{C_a\cdot l_a}{J} \end{bmatrix} = \begin{bmatrix} \dfrac{C_{aS}}{m_S} \\ \dfrac{C_{aS}\cdot l_{aS}}{J_S} \end{bmatrix}\cdot S_u\cdot S_t;$$

We have the $2\cdot 2 + 2\cdot 1 = 6$ scalar equations and $5+4+1+1 = 11$ unknown scalars $\{\{C_{aS}, m_S, v_{xS}, l_{aS}, J_S\}, \boldsymbol{S_x}, S_u, S_t\}$. So, we should be able to select 11-6=5 of the scale vehicle design parameters freely, e.g., all these $\{C_{aS}, m_S, v_{xS}, l_{aS}, J_S\}$ can be selected for an easy build of the scaled vehicle. The remaining 6 $\{\boldsymbol{S_x}, S_u, S_t\}$ should be possible to calculate.

However, the equations are not independent or trivial. Also, a full $\boldsymbol{S_x}$ would mix lateral velocity and yaw velocity, so the intuition of the scale vehicle test becomes poor, so we might want to constrain $\boldsymbol{S_x}$ to be a diagonal matrix, so that $v_{yS} = S_{vy} \cdot v_y$ and $\omega_{zS} = S_{\omega z} \cdot \omega_z$. Both these lead to constraints on how to build the scaled vehicle; $\{C_{aS}, m_S, v_{xS}, l_{aS}, J_S\}$ must be selected in a certain way to make the scale test result well and usefully interpretable.

So, if we reduce to a diagonal $\boldsymbol{S_x} = \mathrm{diag}(S_{vy}, S_{\omega z})$ and tear down the matrix equation to scalar equations:

$$\begin{bmatrix} S_{vy} & 0 \\ 0 & S_{\omega z} \end{bmatrix} \cdot \begin{bmatrix} -\frac{2 \cdot C_a}{m \cdot v_x} & v_x \\ 0 & -\frac{2 \cdot C_a \cdot l_a^2}{J \cdot v_x} \end{bmatrix} = \begin{bmatrix} -\frac{2 \cdot C_{aS}}{m_S \cdot v_{xS}} & v_{xS} \\ 0 & -\frac{2 \cdot C_{aS} \cdot l_{aS}^2}{J_S \cdot v_{xS}} \end{bmatrix} \cdot \begin{bmatrix} S_{vy} & 0 \\ 0 & S_{\omega z} \end{bmatrix} \cdot S_t;$$

$$\begin{bmatrix} S_{vy} & 0 \\ 0 & S_{\omega z} \end{bmatrix} \cdot \begin{bmatrix} \frac{C_a}{m} \\ \frac{C_a \cdot l_a}{J} \end{bmatrix} = \begin{bmatrix} \frac{C_{aS}}{m_S} \\ \frac{C_{aS} \cdot l_{aS}}{J_S} \end{bmatrix} \cdot S_u \cdot S_t;$$

$$\begin{bmatrix} -\frac{2 \cdot C_a}{m \cdot v_x} \cdot S_{vy} & v_x \cdot S_{\omega z} \\ 0 & -\frac{2 \cdot C_a \cdot l_a^2}{J \cdot v_x} \cdot S_{\omega z} \end{bmatrix} = \begin{bmatrix} -\frac{2 \cdot C_{aS}}{m_S \cdot v_{xS}} \cdot S_{vy} \cdot S_t & v_{xS} \cdot S_{\omega z} \cdot S_t \\ 0 & -\frac{2 \cdot C_{aS} \cdot l_{aS}^2}{J_S \cdot v_{xS}} \cdot S_{\omega z} \cdot S_t \end{bmatrix};$$

$$\begin{bmatrix} \frac{C_a}{m} \cdot S_{vy} \\ \frac{C_a \cdot l_a}{J} \cdot S_{\omega z} \end{bmatrix} = \begin{bmatrix} \frac{C_{aS}}{m_S} \cdot S_u \cdot S_t \\ \frac{C_{aS} \cdot l_{aS}}{J_S} \cdot S_u \cdot S_t \end{bmatrix};$$

$$\begin{cases} -\frac{2 \cdot C_a}{m \cdot v_x} \cdot S_{vy} = -\frac{2 \cdot C_{aS}}{m_S \cdot v_{xS}} \cdot S_{vy} \cdot S_t; \\ v_x \cdot S_{\omega z} = v_{xS} \cdot S_{\omega z} \cdot S_t; \\ 0 = 0; \\ -\frac{2 \cdot C_a \cdot l_a^2}{J \cdot v_x} \cdot S_{\omega z} = -\frac{2 \cdot C_{aS} \cdot l_{aS}^2}{J_S \cdot v_{xS}} \cdot S_{\omega z} \cdot S_t; \\ \frac{C_a}{m} \cdot S_{vy} = \frac{C_{aS}}{m_S} \cdot S_u \cdot S_t; \\ \frac{C_a \cdot l_a}{J} \cdot S_{\omega z} = \frac{C_{aS} \cdot l_{aS}}{J_S} \cdot S_u \cdot S_t; \end{cases}$$

$$\begin{cases} \frac{C_a}{m \cdot v_x} = \frac{C_{aS}}{m_S \cdot v_{xS}} \cdot S_t; \\ v_x = v_{xS} \cdot S_t; \\ \frac{C_a \cdot l_a^2}{J \cdot v_x} = \frac{2 \cdot C_{aS} \cdot l_{aS}^2}{J_S \cdot v_{xS}} \cdot S_t; \\ \frac{C_a}{m} \cdot S_{vy} = \frac{C_{aS}}{m_S} \cdot S_u \cdot S_t; \\ \frac{C_a \cdot l_a}{J} \cdot S_{\omega z} = \frac{C_{aS} \cdot l_{aS}}{J_S} \cdot S_u \cdot S_t; \end{cases}$$

The "influence matrix" for these 5 equations and 9 unknowns can be written:

S_t	S_u	S_{vy}	$S_{\omega z}$	C_{aS}	m_S	v_{xS}	l_{aS}	J_S
$\neq 0$	0	0	0	$\neq 0$	$\neq 0$	$\neq 0$	0	0
$\neq 0$	0	0	0	0	0	$\neq 0$	0	0
$\neq 0$	0	0	0	$\neq 0$	0	$\neq 0$	$\neq 0$	$\neq 0$
$\neq 0$	$\neq 0$	$\neq 0$	0	$\neq 0$	$\neq 0$	0	0	0
$\neq 0$	$\neq 0$	0	$\neq 0$	$\neq 0$	0	0	$\neq 0$	$\neq 0$

The equations give some limitations. For instance, we cannot solve it for $\{S_t, S_u, S_{vy}, S_{\omega z}, C_{aS}\}$ because the left-most matrix is singular. But we can solve it for $\{S_{vy}, S_{\omega z}, C_{aS}, m_S, v_{xS}\}$:

$$\begin{cases} \frac{C_a}{m \cdot v_x} = \frac{C_{aS}}{m_S \cdot v_{xS}} \cdot S_t; \\ v_x = v_{xS} \cdot S_t; \\ \frac{C_a \cdot l_a^2}{J \cdot v_x} = \frac{2 \cdot C_{aS} \cdot l_{aS}^2}{J_S \cdot v_{xS}} \cdot S_t; \\ \frac{C_a}{m} \cdot S_{vy} = \frac{m}{C_a} \cdot \frac{C_{aS}}{m_S} \cdot S_u \cdot S_t; \\ \frac{C_a \cdot l_a}{J} \cdot S_{\omega z} = \frac{C_{aS} \cdot l_{aS}}{J_S} \cdot S_u \cdot S_t; \end{cases}$$

Eliminate v_{xS} by using up 2nd equation as $v_{xS} = \frac{v_x}{S_t}$:

$$\begin{cases} \frac{C_a}{m \cdot v_x} = \frac{C_{aS}}{m_S \cdot v_x} \cdot S_t^2; \\ \frac{C_a \cdot l_a^2}{J \cdot v_x} = \frac{2 \cdot C_{aS} \cdot l_{aS}^2}{J_S \cdot v_x} \cdot S_t^2; \\ \frac{C_a}{m} \cdot S_{vy} = \frac{m}{C_a} \cdot \frac{C_{aS}}{m_S} \cdot S_u \cdot S_t; \\ \frac{C_a \cdot l_a}{J} \cdot S_{\omega z} = \frac{C_{aS} \cdot l_{aS}}{J_S} \cdot S_u \cdot S_t; \end{cases}$$

Eliminate m_S by using up 1st equation as $m_S = \frac{C_{aS} \cdot m}{C_a} \cdot S_t^2$:

$$\begin{cases} \frac{C_a \cdot l_a^2}{J} = \frac{2 \cdot C_{aS} \cdot l_{aS}^2}{J_S} \cdot S_t^2; \\ \frac{C_a}{m} \cdot S_{vy} = \frac{S_u}{S_t}; \\ \frac{C_a \cdot l_a}{J} \cdot S_{\omega z} = \frac{C_{aS} \cdot l_{aS}}{J_S} \cdot S_u \cdot S_t; \end{cases}$$

Eliminate C_{aS} by using up 1st equation as $C_{aS} = \frac{C_a \cdot l_a^2 \cdot J_S}{2 \cdot J \cdot l_{aS}^2 \cdot S_t^2}$:

$$\begin{cases} S_{vy} = \frac{m}{C_a} \cdot \frac{S_u}{S_t}; \\ S_{\omega z} = \frac{l_a}{2 \cdot l_{aS} \cdot S_t^2} \cdot S_u \cdot S_t; \end{cases}$$

So, we have to build, drive and interpret the scaled vehicle with:

$$v_{xS} = \frac{v_x}{S_t};$$

$$C_{aS} = \frac{C_a \cdot l_a^2 \cdot J_S}{2 \cdot J \cdot l_{aS}^2 \cdot S_t^2};$$

$$m_S = \frac{C_{aS} \cdot m}{C_a} \cdot S_t^2;$$

$$S_{vy} = \frac{m}{C_a} \cdot \frac{S_u}{S_t};$$

$$S_{\omega z} = \frac{l_a}{2 \cdot l_{aS} \cdot S_t^2} \cdot S_u \cdot S_t;$$

But the following can be freely selected: $\{S_t, S_u, l_{aS}, J_S\}$.

Do an example using realistic parameters, realistic for both the full-sized and scaled vehicle, [$SI\ units\ and\ rad$] are used:

$\{C_a, m, v_x, l_a, J\} = \{98000 \quad 2000 \quad 20 \quad 1.5 \quad 1100\}$

$\{S_t, S_u, l_{aS}, J_S\} = \{10 \quad 1 \quad 0.2 \quad 0.05\}$

$v_{xS} = \frac{v_x}{S_t} = 2\ [m/s]$; (sounds reasonable for the down-scaled car)

$C_{aS} = \frac{C_a \cdot l_a^2 \cdot J_S}{2 \cdot J \cdot l_{aS}^2 \cdot S_t^2} = 1.25\ [N/1]$; (needs careful selection of "toy car wheels")

$m_S = \frac{C_{aS} \cdot m}{C_a} \cdot S_t^2 = 2.56\ [kg]$; (sounds reasonable for the down-scaled car)

$S_{vy} = \frac{m}{C_a} \cdot \frac{S_u}{S_t} = 0.002\ \left[\frac{m/s}{m/s}\right]$;

$$S_{\omega z} = \frac{l_a}{2 \cdot l_{aS} \cdot S_t^2} \cdot S_u \cdot S_t = 0.375 \left[\frac{rad/s}{rad/s}\right];$$

The example pointed out that the model is a key to be able to design a scaled vehicle and how to use it. One can imagine that other manoeuvres or studies can require quite different things of the model to be useful, so down-scaling vehicles has its limitations. (Although: Using down-scaled models can have many other benefits, like education and understanding of how what influences what in a vehicle and how to work with designing HW and SW.)

1.5.1.1.6.3 Evaluate Requirement Fulfilment

This is often called *Requirement Verification* and means to find out *how well the vehicle fulfils the requirements* with the tested design parameters. Prior to that, and especially in the first design loop, the *Model Validity* should be evaluated. (One can also do "*Requirement Validation*" which is to judge whether a suitable selection of requirements was selected in 1.5.1.1. This requires much experience.)

Often, there is an old design which was the cause for the whole engineering task and then there might be test data to validate model with. Such validity check will be for one certain design. If directly comparing one simulation with one test it is an **absolute model validity**. If comparing the change between two tests where something has been changed, it is a **relative model validity**, e.g. telling if the model reflects design parameter changes well. The relative model validity is often more important than the absolute. Since one often don't know exactly how the model is going to be used, it can be a good habit to include a boolean auxiliary variable for validity. Typically, one would plot some (1-10) physical quantities as function of time, for multiple (>2) different design parameter values in the same diagram.

One clear reason to set the validity "false" is when the physical model assumptions are not met, such as if a wheel lifts from ground (assuming equations to handle wheel lift is not included). In other cases, it can be more of an engineering judgement on what threshold to set the validity false. Then, if validity is false during only a tiny fraction of the whole studied time, it is again a judgement whether to disqualify the simulation result or not. The Modelica function for building in validity checks in the models is `assert` which can be used to either terminate the simulation or give a warning.

Evaluation of **requirement fulfilment** (or Analysis, as opposed to Synthesis) involves understanding and interpretation of the computation results to real world. New requirements can appear, typically when new constraints become active with the new design.

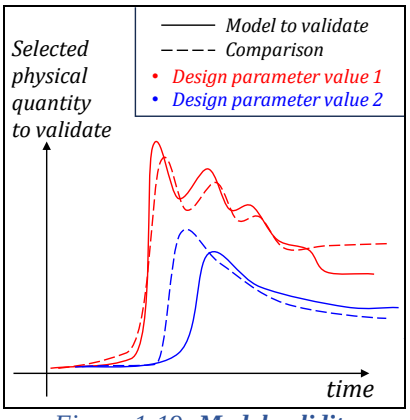


*Figure 1-19: **Model validity** judgement. Compare with measurements, validated model, or experience. Check influence of design parameters.*

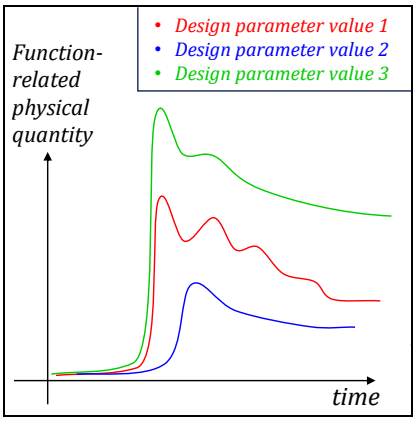


*Figure 1-20: **Analyse** (understand, at least learn) the influence of design parameters.*

Requirement:
Function measure **> 32** [unit2]

Design parameter [unit1]	**Function measure** [unit2]	**Requirement fulfilment**
7	30	no
8	35	yes
10	36	yes, best
11	34	yes

*Figure 1-21: **Requirement fulfilment** to find acceptable or best design(s).*

1.5.1.1.7 Redesign

Redesign is Design, but in design loop number >2. The results from the first design loop are important to learn from. In some cases, one can inversely calculate the new design or use numerical methods to optimize to a new better design.

1.5.1.1.8 Final Design

Final design, meaning a concrete proposal of design, such as a numerical design parameter value or a drawing or control algorithm.

1.5.1.1.9 Modelling for Design Guidance

The activity "Modelling for Design Guidance" in Figure 1-12 marks another "branch" than the straight-forward computation/simulation for virtual verification described in 1.5.1.1 to 1.5.1.1.8. It refers to activities that leads to a mathematical model with purpose to generate knowledge that can support the design. Examples of such adjustments are:

- Linearization of the model, 1.5.1.1.9.1, helps control or estimator designs and frequency and modal analyses.
- Stability analysis, 1.5.1.1.9.2, helps understanding on a more general level.
- Optimization, 1.5.1.1.9.3, can be used both during product development and during product use.

A very general names of such models could be "design guidance models", which would be complementary with "plant models" or "models for virtual verification". As specializations within all "Design guidance models", we can typically find:

- *Control design models*, used for controller design
- *Estimator design models*, used for estimator design
- *Optimization models*, used in the optimization (when optimizing with more mathematical optimization methods than just trial and error or machine learning)

For design guidance, we often need "clean" simulation models. Such are models where only a few physical phenomena are modelled as opposed to "general purpose models". General purpose models typically have all dofs and all subsystems modelled. Clean models might be 1D or 2D models with idealized models of the subsystems, mechanically and control-wise. The clean models can often give an general understanding of which physical phenomena that is mainly causing a problem and/or how a certain design parameter influence a requirement measure. Reduced order/modal restricted models which can be simulated in the vehicle for on-line/off-line predictions/predictive optimization.

With "clean" models, one can even reach a *Closed form expression* or *Analytical expression*, $\dot{\boldsymbol{x}} = \boldsymbol{f}_{\boldsymbol{ClosedForm}}(\boldsymbol{x}, \boldsymbol{u})$. In some cases, one can even find *Closed form solution* or *Analytical solution*, $\boldsymbol{z} = \boldsymbol{f}_{\boldsymbol{ClosedForm}}(t)$;. Examples where closed form solutions are possible are linear models with inputs $\boldsymbol{u}(t)$ expressed as a simple time functions, such as step, harmonic and/or exponential functions, see examples in 4.4.3.1, 4.5.4.1 and 5.4.

To reach closed form expressions/solutions, one often must, after the mathematical model, reduce the number of equations by eliminating variables. This can help to understand the behaviour of the whole system. The Mathematical model is still important since it documents better which physical phenomena has been modelled. The differentiation order can often increase when eliminating variables, so that $\ddot{\boldsymbol{z}}, \dddot{\boldsymbol{z}}, \cdots$ appears in the equations.

1.5.1.1.9.1 Linearization of Non-Linear Model

A general model is not affine and consequently also not linear. They are often called *non-linear* (but *non-affine* would be more correct, because an affine model is normally not called non-linear). There are many reasons to why models are non-linear: examples of *continuous* non-linearities are terms of the type x_i^2, $x_i^{0.5}$, $x_i \cdot x_j$, $x_i \cdot u_j$, $\sin(x_i)$. There are also *discrete* non-linearities, such as time sampling or discrete physical phenomena like dry friction, back-lash, etc. Note the difference between an **affine model** resulting from physical model without additional approximations, and a **linearization of a**

non-linear model. The latter means that there are more approximations than what was done in the physical model. These additional approximations normally have less physical interpretation.

In order to find the numerical solution, one typically does not gain anything on finding an affine form. But there are reasons for such form; basically the same reasons as mentioned in 1.5.1.1.4.5 for finding the linear form of a linear model.

If non-linear model, but only continuous non-linearities, one can *linearize* the models via Taylor expansion and get an **approximate** model, a *linearization on affine form*. A Taylor expansion to find an approximate model in affine form, corresponding as in 1.5.1.1.4.5, would look like:

If the model is non-linear but there is no explicit dependency of t, the Taylor expansion will be exact:

$$\dot{\boldsymbol{x}} = \boldsymbol{f_{ODE}}(\boldsymbol{x}, \boldsymbol{u}) \approx$$

$$\approx \boldsymbol{f_{ODE}}(\boldsymbol{x_0}, \boldsymbol{u_0}) + \left(\frac{\partial \boldsymbol{f_{DAE}}}{\partial \boldsymbol{x}}\right)\Big|_{\substack{\boldsymbol{x}=\boldsymbol{x_0} \\ \boldsymbol{u}=\boldsymbol{u_0}}} \cdot (\boldsymbol{x} - \boldsymbol{x_0}) + \left(\frac{\partial \boldsymbol{f_{DAE}}}{\partial \boldsymbol{u}}\right)\Big|_{\substack{\boldsymbol{x}=\boldsymbol{x_0} \\ \boldsymbol{u}=\boldsymbol{u_0}}} \cdot (\boldsymbol{u} - \boldsymbol{u_0}) = \left\{ \begin{matrix} non- \\ linear \end{matrix} \right\} =$$

$$= \boldsymbol{f_{ODE}}(\boldsymbol{x_0}, \boldsymbol{u_0}) + \boldsymbol{A}(\boldsymbol{x_0}, \boldsymbol{u_0}) \cdot (\boldsymbol{x} - \boldsymbol{x_0}) + \boldsymbol{B}(\boldsymbol{x_0}, \boldsymbol{u_0}) \cdot (\boldsymbol{u} - \boldsymbol{u_0}); \;\; \Rightarrow$$

$$\Rightarrow \quad \dot{\boldsymbol{x}}_{\boldsymbol{of}} = \boldsymbol{f_{ODE}}(\boldsymbol{x_0}, \boldsymbol{u_0}) + \boldsymbol{A}(\boldsymbol{x_0}, \boldsymbol{u_0}) \cdot \underbrace{(\boldsymbol{x} - \boldsymbol{x_0})}_{\boldsymbol{x}_{\boldsymbol{of}}} + \boldsymbol{B}(\boldsymbol{x_0}, \boldsymbol{u_0}) \cdot \underbrace{(\boldsymbol{u} - \boldsymbol{u_0})}_{\boldsymbol{u}_{\boldsymbol{of}}};$$

If $(\boldsymbol{x_0}, \boldsymbol{u_0})$ is a steady state condition it means same as that $\boldsymbol{f_{ODE}}(\boldsymbol{x_0}, \boldsymbol{u_0}) = 0$, so the linearization gets the form *linear in state derivatives* $\dot{\boldsymbol{x}}_{\boldsymbol{of}}$ and inputs $\boldsymbol{u}_{\boldsymbol{of}}$, i.e. without constant term. Similar Taylor expansion can be done with $\boldsymbol{g}$ for outputs $\boldsymbol{u}$, to find a linear (or at least affine) from also for outputs.

Note that the model was assumed to be non-linear. This meant that $\boldsymbol{A}$ and $\boldsymbol{B}$ became dependent of $\boldsymbol{x_0}$ and $\boldsymbol{u_0}$. For an affine model this was not the case, see 1.5.1.1.4.5. The consequence is that the model can be stable around one $(\boldsymbol{x_0}, \boldsymbol{u_0})$ and instable around another. Therefore, many methods for frequency analysis, control engineering and signal processing is not so applicable if the system is strongly non-linear.

1.5.1.1.9.2 Stability Analysis

Stability is when all components in $\boldsymbol{x}$ stays limited (finite) with limited (finite) $\boldsymbol{u}$ and over long but finite time. Stability for a linear model or linearization of a non-linear model is guaranteed if the real part of all eigenvalues of $\boldsymbol{A}$ are negative. For a linear model, the $\boldsymbol{A}$ matrix does not depend on $\boldsymbol{x}$, so the stability is relatively easy checked. For a non-linear model one would typically linearize around the initial value and check sign of real part of all eigenvalues. However, this is not enough, since the solution can "slip away" to a regime where the signs of real part of the eigenvalues changes. The following picture gives some examples.

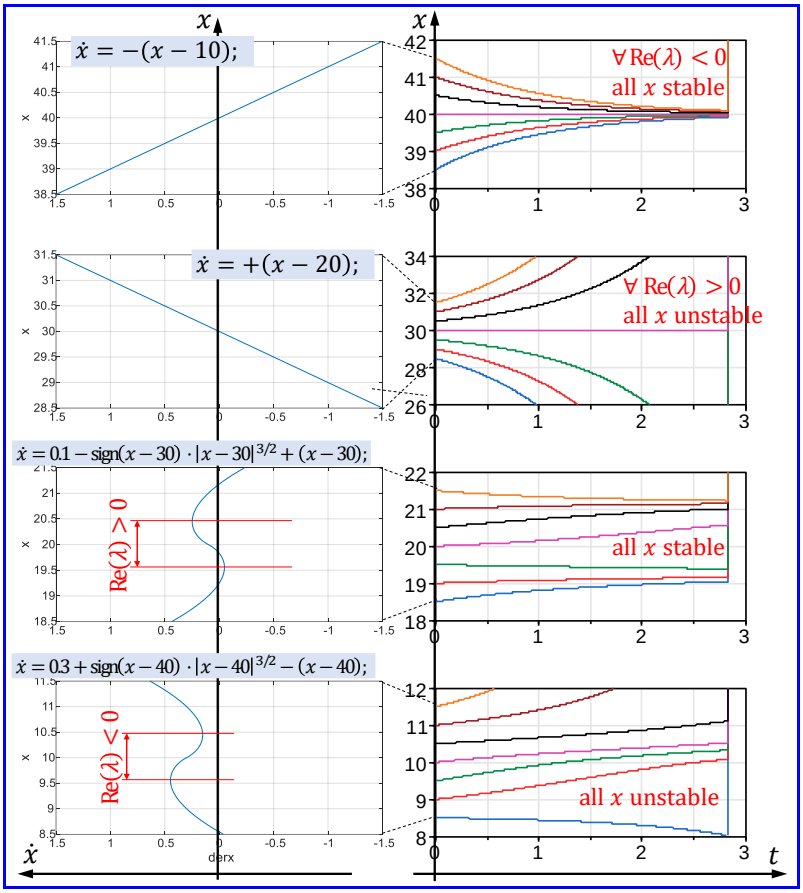


Figure 1-22: 1st and 2nd rows: Linear models. Stability or instability same for all x and follwos what $Re(\lambda)$ indicates. 3rd: Non-linear model. Stability regimes are larger than $Re(\lambda)$ indicates. 4th row: Non-linear model. Stability regimes are smaller than $Re(\lambda)$ indicates.

The influence of varying $\boldsymbol{u}$ will now be treated. Stability is easiest understood for a model without $\boldsymbol{u}$. However, if we have a $\boldsymbol{u}$, one often assumes $\boldsymbol{u}$ is limited, slowly varying and independent of $\boldsymbol{x}$, e.g. $\boldsymbol{u}$ is constant. Then it still holds to look only on eigenvalues of $\boldsymbol{A}$ in $\boldsymbol{A} \cdot \boldsymbol{x} + \boldsymbol{B} \cdot \boldsymbol{u}$. The only additional note here is that $\boldsymbol{A}$ can depend on $\boldsymbol{u}$ even if $\boldsymbol{u}$ is constant. An example is the influence from propulsion force on lateral dynamics, F_{fyw} in 4.4.2.

However, if $\boldsymbol{u}$ is depending on $\boldsymbol{x}$, e.g., $\boldsymbol{u} = \boldsymbol{CL} \cdot \boldsymbol{x}$; we have a closed loop system. Then we have to look on eigenvalues of $\boldsymbol{A_{CL}}$ in $\boldsymbol{A} \cdot \boldsymbol{x} + \boldsymbol{B} \cdot \boldsymbol{u} = \boldsymbol{A} \cdot \boldsymbol{x} + \boldsymbol{B} \cdot \boldsymbol{CL} \cdot \boldsymbol{x} = (\boldsymbol{A} + \boldsymbol{B} \cdot \boldsymbol{CL}) \cdot \boldsymbol{x} = \boldsymbol{A_{CL}} \cdot \boldsymbol{x}$. This can change the stability totally. A vehicle dynamics related case of this is that we can either assess lateral stability for vehicle alone, with input steering angle limited and independent or, opposite, assess lateral stability for vehicle with a closed loop driver, who steers as a direct function of the vehicle motion, 0. Another situation when the $\boldsymbol{A}$ matrix changes is when a drvier model includes an own state variable, e.g., a time delay. Then, both $\boldsymbol{x}$ and $\boldsymbol{A}$ grows with one dimension.

1.5.1.1.9.3 Optimization

The formulation of the optimization task is important. The book argues for that one should start with the formulation as *engineering task*, before jumping into a certain numerical optimization method.

One can differ between:

- *Parameter optimization:*
  Find $\boldsymbol{p_{free}}$ *that minimizes* $Cost(\boldsymbol{z}, \boldsymbol{p})$ *such that* $\boldsymbol{Constr}(\boldsymbol{z}, \boldsymbol{p}) < \boldsymbol{0}$
- *Trajectory optimization*:
  Find $\boldsymbol{z_{free}} = \boldsymbol{z_{free}}(t)$ *that minimizes* $Cost(\boldsymbol{z}, \boldsymbol{p})$ *such that* $\boldsymbol{Constr}(\boldsymbol{z}, \boldsymbol{p}) < \boldsymbol{0}$
- where $\boldsymbol{p_{free}} \subseteq \boldsymbol{p}$ and $\boldsymbol{z_{free}} \subseteq \boldsymbol{z}$ and the dynamic model $\boldsymbol{f_{DAE}}(\boldsymbol{z}, t, \boldsymbol{p}) = \boldsymbol{0}$; shall be fulfilled

Parameter optimization has (a finite number of) *design parameters* $\boldsymbol{p_{free}}$, while trajectory optimization has (a finite number of) *design trajectories* $\boldsymbol{z_{free}}(t)$. Elements in $\boldsymbol{p_{free}}$ are constant values, either continuous, such as final gear ratio, or discrete, such as front or rear axle propulsion.

For trajectory optimization, $\boldsymbol{z_{free}}(t)$ are trajectories, typically, trajectories of request signals to actuators, such as requested engine torque, or other trajectories, such as longitudinal velocity (as function of time or longitudinal position). In a first stage, we have a mathematical model with DAE equations: $\boldsymbol{f_{DAE}}(\boldsymbol{z}, t, \boldsymbol{p}) = \boldsymbol{0}$;. In a second step, closer to computation, we divide $\boldsymbol{z} = \{\boldsymbol{x}, \boldsymbol{y}, \boldsymbol{u}\}$ and reformulate to ODE equations: $\dot{\boldsymbol{z}} = \boldsymbol{f_{ODE}}(\boldsymbol{z}, t, \boldsymbol{p})$;. In a next step, we often discretize the independent variable t, which makes a vector over time of each variable, e.g. $\boldsymbol{x_i} = \{x_i(t_1), x_i(t_2), \cdots\}$.

Each trajectory has an <u>in</u>finite number of values, which makes a big difference. Parameter optimization can be to find the best gear ratios ($\boldsymbol{p_{free}} = [r_1, r_2, \dots, r_6]$) and the cost function f includes a simulation of the dynamic system, e.g., modelled by a driver model and a vehicle model. The latter can be to find the best pedal and gear selection trajectories ($\boldsymbol{z_{free}} = [pedal(t), gear(t)]$). Evaluation of the cost and constraint functions then includes a simulation of a vehicle model with guessed driver trajectories instead of a closed loop driver model. An optimization problem can also be of both types, i.e., include both *design parameters* $\boldsymbol{p}$ and *design trajectories* $\boldsymbol{z}(t)$.

Assume that the $Cost$ has the unit [€]. We typically have $Cost[€] = Constant[€] + \int CostRate[€/s] \cdot dt$. However, for some cases of trajectory optimization, when the state variables in the model is independent of $\boldsymbol{z_{free}}$, one can reduce the optimization problem to a *Momentaneous Trajectory Optimization*, which can be seen as a 3rd category of optimization. It is then the $CostRate[€/s]$ that is minimized, and the optimization problem collapses to what to do at present time instant t_0. We can then find a 3rd category of optimization, *momentaneous variable optimization:*

- $Momentaneous\ Trajectory\ Optimization$:
  $Find\ \boldsymbol{z_{free}}(t_0) \quad that\ minimizes\ CostRate\big(\boldsymbol{z_{free}}(t_0), \boldsymbol{p}\big) \quad such\ that\ \boldsymbol{Constr}(\boldsymbol{z}, \boldsymbol{p}) < \boldsymbol{0} \in \mathbb{R}^1$

This might look very similar to the *parameter optimization* because both $\boldsymbol{p_{free}}$ and $\boldsymbol{z_{free}}(t_0)$ are finite numbers of scalars. However, $\boldsymbol{p_{free}}$ is to be decided <u>during product development</u> while $\boldsymbol{z_0}$ and $\boldsymbol{z}(t)$ must be computed <u>during product use</u>.

See also "1.5.3.2 Momentaneous or Predictive Control".

1.5.1.1.9.3.1 An example

See also "3.5.2.3.1 Predictive CC".

An optimization task could be to minimize the cost for a vehicle, via a dynamic model for a typical driving mission, $\boldsymbol{f}(\dot{\boldsymbol{z}}, \boldsymbol{z}, t, \boldsymbol{p}) = \boldsymbol{0}$. With a certain $(\boldsymbol{p_{free}}, \boldsymbol{z_{free}})$, we can find the solution $\boldsymbol{z}(t)$. If we also have a cost model, as below, we can express the cost for the mission as follows. The s denots position along the mission, P denots power, E denots energy, Sal denotes (driver) salary:

$$Cost\big(\boldsymbol{p_{free}}, \boldsymbol{z_{free}}\big)[€] = \underbrace{\frac{s_{End}\big(\boldsymbol{p_{free}}, \boldsymbol{z_{free}}\big)[m]}{s_{Life}\big(\boldsymbol{p_{free}}, \boldsymbol{z_{free}}\big)[m]} \cdot PartCost_0\big(\boldsymbol{p_{free}}\big)[€]}_{PartCost_1(\boldsymbol{p})\,[€]} +$$

$$+ \underbrace{\int_{t=0}^{t_{End}\left(\boldsymbol{p_{free}}, \boldsymbol{z_{free}}\right)} \underbrace{Prize_{E0}\left[\frac{€}{J}\right] \cdot P_{Cons}\big(\boldsymbol{p_{free}}, \boldsymbol{z_{free}}\big)\left[\frac{J}{s}\right]}_{CostRate_{t,Energy}[€/s]} \cdot dt[s]}_{Cost_{E1}(\boldsymbol{p},\boldsymbol{z})[€]} +$$

$$+ \underbrace{\int_{t=0}^{t_{End}\left(\boldsymbol{p_{free}}, \boldsymbol{z_{free}}\right)} \underbrace{Prize_{Sal0}\left[\frac{€}{s}\right]}_{CostRate_{t,Salary}[€/s]} \cdot dt[s]}_{Cost_{Sal1}\left(\boldsymbol{p_{free}}, \boldsymbol{z_{free}}\right)[€]} \approx$$

$$\approx \underbrace{\frac{s_{EndApprox}(\boldsymbol{p_{free}})}{s_{LifeApprox}(\boldsymbol{p_{free}})} \cdot PartCost(\boldsymbol{p_{free}})[€] +}_{PartCost_1(\boldsymbol{p})\,[€]}$$

$$+ \underbrace{\int_{t=0}^{t_{End}(\boldsymbol{p_{free}},\boldsymbol{z_{free}})} \underbrace{\left(Cost_{E0}\left[\frac{€}{Nm}\right] \cdot P_{Cons}(\boldsymbol{p_{free}},\boldsymbol{z_{free}})\left[\frac{Nm}{s}\right] + \right.}_{CostRate(\boldsymbol{p_{free}},\boldsymbol{z_{free}})[€/s]} \underbrace{\left. +Cost_{Sal0}\left[\frac{€}{s}\right] \right)}_{CostRate(\boldsymbol{p_{free}},\boldsymbol{z_{free}})[€/s]} \cdot dt[s]}_{UseCost(\boldsymbol{p_{free}},\boldsymbol{z_{free}})[€]};$$

The $CostRate$ for energy is above expressed as $CostRate_t[€/s] = Prize[€/J] \cdot Power[J/s]$ which is logical when time is independent variable. However, in transportation, the distance along a route can be an alternative independent variabel and then it is often useful to express $CostRate$ for energy as $CostRate_s[€/m] = Prize[€/J] \cdot EnergyRate[J/m]$ and integrated to $Cost_{Energy}[€] = \int CostRate_s[€/m] \cdot ds[m]$;. The unit of $EnergyRate$ can, alternatively, be $[J/m = N]$. It is not measurable in practice as any force, but the value can then be compared with forces like air resistance force. The $CostRate$ for driver salary is natural to have as $CostRate_t$ in Europe and $CostRate_s$ in North America, since the drivers are paid per time and distance, respectively. Adding $CostRate$ for wear or component degradation is yet another aspect, not included in example formula above.

The engineering task must be reformulated to a *computation task*. In that step, some adjustments are often made to be able to use a particular existing mathematical and numerical method for optimization:

- Objectives can be changed from constraints to cost. Then, some of the scalar inequality or equality constraints in $\boldsymbol{Constr}(\boldsymbol{z},\boldsymbol{p}) < \boldsymbol{0}$ or $\boldsymbol{f}(\dot{\boldsymbol{z}},\boldsymbol{z},t,\boldsymbol{p}) = \boldsymbol{0}$ are removed and instead one term $w \cdot\ g(\boldsymbol{p})$ is added to the cost function $f_{cost}(\boldsymbol{p})$ for each scalar constrained removed. The resulting optimum will not be the same for any values of w; the $Cost$ will be larger, and the constraint will only be approximately fulfilled.
- For trajectory optimization: The trajectories are often discretized, either as $\boldsymbol{z}$ values over a grid in time or as parameters of curve fits of $\boldsymbol{z}(t)$. Then, when coming to the computation task, the difference between parameter and trajectory optimization vanishes and the same computational methods can be used. The dynamic model $\boldsymbol{f}$ then appears as equality constraints as opposed to inside the cost function, which changes the computation task to:

  $$Find \cdots \quad that\ minimizes\ Cost(\cdots)\ or\ CostRate(\cdots) \quad such\ that \begin{cases} \boldsymbol{Constr}(\cdots) < \boldsymbol{0} \\ and\ \boldsymbol{f}(\cdots) = \boldsymbol{0} \end{cases}$$

  This re-formulation is necessary if the method is of collocation type, see 1.5.1.1.9.3.1.2.

In the engineering task the distinctions Cost (or CostRate) vs Constraints and Cost (or CostRate) vs Model are often important and a good selection of what is what requires vehicle engineering experience and insight in the actual problem. Cost (or CostRate), Constraints and Model are often mixed up in the computation task, which easily leads to misunderstandings between vehicle engineers and computation engineers. In worst case, it leads to a numerically optimal solution, but of the wrong engineering optimization problem.

1.5.1.1.9.3.1.1 Single- or Multi-Objective Optimization

One can say that optimization can only optimize a scalar cost. One can, of course, weight several costs together to one cost: $f = w_1 \cdot f_1 + w_2 \cdot f_2$;. This can be called be called *multi-objective optimization*. It is then important to understand the units. Consider f_{cost} as having the unit [€], which leads to that you have to be able to set a number on the weigths $[w_1, w_2, \cdots]$ with units $[€/unit_{f1}, €/unit_{f2}, \cdots]$. This is often difficult to motivate, which makes the interpretation of the found optimum difficult to use for direct design decisions.

However, for parameter optimization, there is a useful variant of multi-objective optimization. It is to not take the optimization all the way to one optimum but stay at a relation between design

parameters. One can then draw a *Pareto front*, i.e., a relation between design parameters which forms an envelope in a diagram with the scalar costs on the axes. The same relations can be drawn in a diagram with design parameters on the axes, which reduces the dimension of the space in which one should look for the best design parameters.

1.5.1.1.9.3.1.2 Shooting and Collocation Methods for Optimization

A divider among (trajectory) optimization methods is between those who iteratively find the solution $\boldsymbol{x}$ through simulation (time integration) and iteratively update $\boldsymbol{u}$ between those simulations (*shooting methods*) and those who solves iteratively for both $\boldsymbol{x}$ and $\boldsymbol{u}$ at the same time (*collocation methods*). Single shooting and multiple shooting are examples of shooting methods.

Shooting methods are often preferable to elaborate with the formulation of the engineering optimization problem, because they can be applied on most forms of mathematical model. Collocation methods can require the problem on a certain mathematical form (e.g., linear, quadratic, continuous), which leads to a risk that one solves another problem than what was engineering-wise intended.

Using collocation methods, one uses the mathematical model to generate the equality constraint $\boldsymbol{f}$. One discretizes the model in time, which converts the differential equations into difference equations, using a certain derivative approximation, such as $(\boldsymbol{x_{k+1}} - \boldsymbol{x_k})/\Delta t = \dot{\boldsymbol{x}}_{\boldsymbol{k}} = \boldsymbol{f}(\boldsymbol{x_k}, \boldsymbol{u}(t_k), t_k) = \boldsymbol{f}(\boldsymbol{x_k}, \boldsymbol{u_k}, k \cdot \Delta t)$;. From computational point of view, the problem is then converted from trajectory optimization to an optimization of a finite number of trajectory values $z_i(t_j)$. Typically, very simple derivative approximations are used, compared to today's integration methods for simulation. However, it is relatively easy to use also implicit derivative approximations which can be very computational efficient.

1.5.1.1.9.3.1.3 Dynamic programming, DP

Dynamic programming, DP, is a method which is neither shooting nor collocation. DP follows the dynamic process in a grid in $\{Time, RequestSignal(s)\}$ or $\{Time, StateVariable(s)\}$. Also, other grid variables can be used. The cost calculation for each path in the grid can be evaluated with small simulations, which makes DP resemble of shooting methods. The selection of best combination of paths is made for the whole horizon, which makes DP resemble of collocation methods. The absolute optimum, for that grid, is always found. That makes the methods useful, at least for assessing how good a more computational lean method is working. DP can also work as real time solution, but the computational time increases rapidly with number of states. Reference (Jacobson & Spickenreuther, 2003) explains the method with a gear shifting optimization as example.

1.5.1.1.9.3.1.4 Optimization during Product Use

We can distinguish between optimization during product development and optimization during product use. For the latter case, there are often high demands on computation speed and robustness of the models. This can, to some extent, be met by simplification of the models, e.g., by neglecting physical phenomena and/or linearization. One must understand the product well, its design and use, to avoid simplifying in a way that the "optimal solution to the wrong problem" is computed.

1.5.1.2 Approximations

As mentioned above, assumptions (or simplifications or approximations) are made during *Physical modelling*. These can be directly motivated by **vehicle design**, such as assuming that some part is rigid or massless. They can also be directly motivated by the **manoeuvre** to be studied with the model. Examples of approximations during Physical modelling are massless bodies, steady state conditions and small angles. These have implications on the *Mathematical modelling* stage: some fictive forces do not appear in the equations, and $angle$ replaces $\sin(angle)$ in the equations. Note that the angle has to be in radians. Note also that, if one do unit check including angular units, $angle \approx \sin(angle)$ should be checked as having unit=1 and not unit=radians.

We can also assume that some variables or parameters are *small*. If a term in the final Explicit form model gets a high order, one can approximate mathematically by removing it. For example, a term $small^N$ where $N \geq 2$ can be removed if the other terms have $N < 2$. Note that such approximations can not be done in an *equation* (during Physical or Mathematical modelling), but in the final *expression* (in Explicit form model). For example, a term with order $small^N$ in Mathematical model, it can end up in denominator in final Explicit form model, which correspond to order $small^{-N}$. Removing terms can also be done by keeping only the first terms in a Taylor expansion of $\boldsymbol{f_{ODE}}$ in the Explicit form: $\boldsymbol{f} \approx \boldsymbol{f_0} + (\boldsymbol{df/dx})|_{\boldsymbol{x_0},\boldsymbol{u_0}} \cdot (\boldsymbol{x} - \boldsymbol{x_0}) + (\boldsymbol{df/du})|_{\boldsymbol{x_0},\boldsymbol{u_0}} \cdot (\boldsymbol{u} - \boldsymbol{u_0})$;.

1.5.1.3 Constants, Parameters, and Variables of Quantity and Signal type

Variables and **Signals** vary with time during an experiment with the model. **Constants** and **parameters** do not. The book uses the definition from Modelica, www.modelica.org and 1.5.4.1.5 to distinguish between variables and parameters: Variables can vary with time while parameters can not.

In most cases, the variables and parameters have physical interpretations, e.g. a corresponding (physical or engineering) **quantity** with a known unit. Units are central for engineering. A $quantity = \{measure\} \cdot [unit]$; such as $Length = L = \{L\} \cdot [m] = 2 \cdot [m]$;. The $\{measure\}$ is here the numerical value.

> The relation and notation with { } and [ ] are proposed in (ISO 80000-1) means that a mathematical, but not physical, form of an equation should use $\{L\}$ and not L. It also means that a physical form of the same equation should use L. It is sometimes worth to think of, for instance when we approximate $\sin(\{angle\}) \approx \{angle\} = angle/[rad]$. Another example is axis labels in a diagram, if the axis shows the measure $\{L\}$, the axis label should be $\{L\} = L/[m]$.

If using a consistent set of units, such as SI-units, each equation can be seen as either a relation between quantities or relation between measures. The book assumes SI-units, (ISO 80000-3),where else is not stated. Angle units are not stipulated by SI since they are dimensionless ($ArcLength/Radius = m/m = 1$), but the recommendation is to use radians.

It is recommended to not use numerical constants directly in the equations unless they are dimensionless=unitless, such as often π and 2 are in equations.

1.5.1.3.1 Constants and Parameters

A parameter can be changed between experiments. A constant does not even change between experiments. Typical constant is π or gravity constant g. Typical parameters are vehicle wheelbase and road friction coefficient. Note that most important characteristics of a parameter p in a dynamic model is that it does **not** depend on the independent variable time t, i.e. $\dot{p} = 0$;.

A parameter is normally a scalar (0D) quantity, e.g., vehicle mass. However, it can also have more dimensions, e.g., the 1D parameter road unevenness (description of how road vertical position z_r varies with longitudinal position along road x). The latter one can be seen as a continuous function (infinite number of points) but it is often implemented with a finite number of scalar parameters, e.g. through a "grid" or other finite parameterization such as $\{frequency; amplitude\}$.

From vehicle engineering point of view there is a significant difference also between *Design parameters* and *Operation/Manoeuvre parameters*. The *Design parameters* are varied to fulfil the requirements as good as possible. (Note that not all of the design parameters are subject to variation in all engineering tasks. E.g., if designing one part of the vehicle, the other parts are considered as fixed.) The *Operation/Manoeuvre parameters* should also be varied, but as disturbances for which the vehicle need to be robust.

It is often natural to have different parameter sets to describe the design and operation/manoeuvre and another for use in the equations. For example, the kerb weight (design) and load (operation) are good for description while the total weight (sum of kerb and load) is the parameter that appears in the

equations. Therefore, the parameters that appears in the equations cannot always be categorized as either design or operation/manoeuvre parameters. It is easy to forget that the selection of parameters and the relations between parameters are often an equally important part of the engineering problem, as the relations between variables (the equations) is for the dynamic system. A good question to ask oneself is often: Is the comparison "fair" if I vary parameters as I do?

1.5.1.3.1.1 About selection of parameters

To get a useful model it is important to select parameters which can be validated in real world tests, but preferably tests of parts of the system, not the whole system, because it increases the validity range of the model.

A simple example is that it is more useful with coefficient of friction μ as parameter, than the friction force F_{fr} itself. Using μ as parameter, requires also that the model uses the well-established physical/engineering $F_{fr} = \mu \cdot N$;, where N is the contact normal force. Using F_{fr} as parameter, the model would get an unnecessary small "validity range". This small range is troublesome since it would require a new test, if the product is redesigned so that N is changed. An alternative problem could be that one does not realize that a new test is needed, so one instead uses the same value of F_{fr}.

1.5.1.3.2 Variables

The independent variable in dynamic systems is time t. In the following, variables refer to the othe (dependent) variables.

Variables vary during the studied time interval. If not else is mentioned, we assume continuous variation, but variables can also vary in discrete levels, 1.5.1.4. Time derivatives of (continuous) variables cannot be assumed to zero, which is important when going from DAE to ODE formulation since some DAE equations might need to be differentiated. In Mathematical model (DAE), a variable and its time derivatives are counted as one variable. In Explicit model (ODE), one can count each time derivative of a variable as an additional variable, but then one also should count each integration ($z_i = \int \dot{z}_i \cdot dt$;) as one equation.

From vehicle engineering point of view, the *Operation/Manoeuvre* can stipulate a constant value of some variables. Mathematically, it is then a parameter (parameter $z = 7$;), but as vehicle engineers it can be better to think of it as a variable z with an initial value, coming from the *Operation/Manoeuvre*, such as $z_0 = 7$; and an extra equation $\dot{z} = 0$;. The initial value is then an *Operation/Manoeuvre parameter* and not a *Design parameter*. A typical example could be longitudinal speed, v_x.

The book mainly deals with simulation, but it can be noted that, during parameter optimization, $p_{opt} = \min_p \left(functional\left(Model(\cdots, p)\right)\right)$;, one does several simulations with same model. Some model parameters are *varied* between simulations and these parameters could therefore be called variables. To avoid such semantic confusion, it is proposed to call them *optimization variables* when talking about them in the optimization context. In simulation context, they are simply parameters or *design parameters*.

A very important special case of variables are **state variables** or **states**. State variables are given initial values and then updated through integration along the time interval studied. (Continuous) States are updated through time integration. Which variables to use as states is **not** uniquely defined by the physical (or mathematical) model. See 1.5.2.1.2.

1.5.1.3.3 Signals

Since vehicle dynamics so often requires models of the control algorithms, one often use the words variable and signal interchangeable. It is suggested to reflect over the difference:

While a variable can be of the type **(physical) quantity**, such as velocity v_x, it can also be of **signal** type, such as requested velocity v_{xReq}. A signal can represent an ODE variable with prescribed causality. So, a variable is typically not represented by a signal before the modelling stage "1.5.1.1.5

Explicit Form Modelling". However, signals **can** appear already in mathematical model (DAE), typically as interface on models of mechatronic subsystems or subsystems consisting purely of algorithms (software). For such signals, the causality is normally prescribed already in the mathematical model and one have to differ between **differentiation orders**, so that z_i and $\dot{z}_i$ are counted as two variables. A strict way to implement this is given in the Modelica modelling format, see 1.5.4.1.5.

1.5.1.3.4 Mechatronics

A *Mechatronic* system contains both algorithms and physical equations. It means that it has to be connected by both signals and physical variables. Also, it can contain parameters of both types: algorithms parameters (e.g. gain values) and physical (e.g. response time for actuator). In vehicles, the mechatronic subsystems are typically Propulsion, Brake and Steering system.

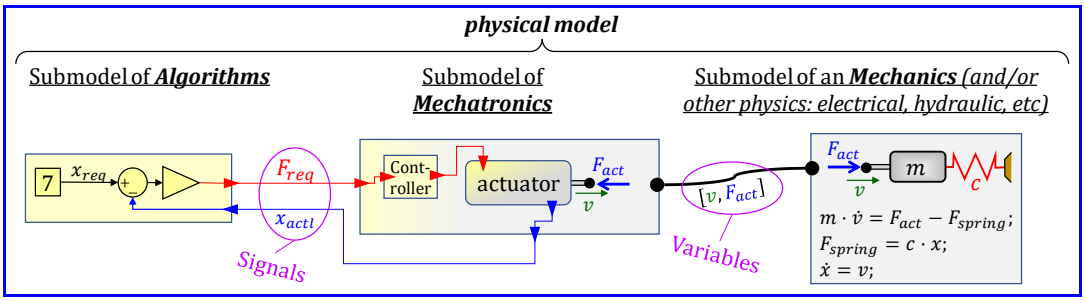


Figure 1-23: Mechatronics submodels have both signals and physical interfaces.

1.5.1.4 Algebraic Loops or Simultaneous Equations

One problem that can appear when generating the Explicit form model is *Algebraic loops*. The name is most intuitively understood when Data flow diagram is used for the Explicit form model, see 1.5.4.1.2. Then, an Algebraic loop is a signal loop which does not include and integrator blocks; meaning that each branch of the loop needs input from the other to calculate its output. Algebraic loops can also be called *Simultaneous equations*. The smallest possible can actually be one single equation, e.g. a transcendent equation, such as "$x = \sin(x)$;", which has no closed form solution.

A simple mechanical example where two equations need to be solved before each other is given in Figure 1-24. The example is a vehicle decelerating with locked wheels; Vertical forces are needed to calculate friction forces, which are needed to calculate acceleration, which is needed to calculate vertical forces.

Loops appear often between bigger chunks of equations than in Figure 1-24, namely between modules in the model. The decomposition in certain modules is often desired for model modularity. A typical other example where a loop occurs is when doing quasi-steady state assumptions about roll moment distribution between axles (4.3.7.11.3).

Loops can always be solved by setting up an iteration in each evaluation of time derivatives. This can sometimes be accepted, but it gives poor computational speed. Other ways are to handle the loops by sacrificing simplicity in model is to model an additional elasticity or inertia between the modules, or simply a (non-physical) filter. "Memory blocks" can work but are not recommended, since the simulations will be dependent on solver. Best is if the loop can be symbolically solved, as in Figure 1-24.

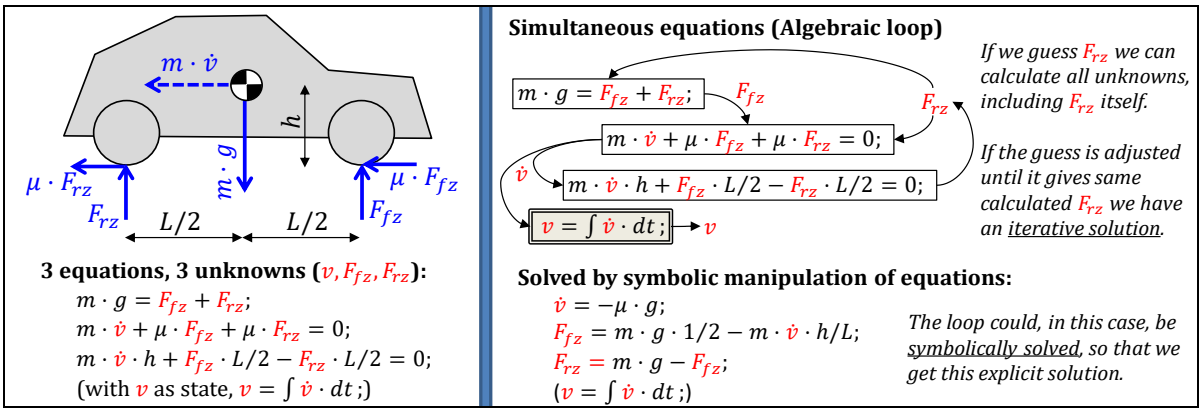


Figure 1-24: An example of Algebraic loop, also called Simultaneous equations.

1.5.1.5 High Index

A possible problem for a mathematical model is High index. A simple mechanical example of High index system of equations is when two inertias are rigidly connected, see Figure 1-25, where a working causality cannot be found with retained modularity. Similarly to algebraic loops, it can be solved with equation manipulations, but for high index problems, the manipulations include differentiation of some equations. It is tempting to try a "differentiating" block ($\dot{v}_2 = (d/dt)v_2$; instead of $v_2 = \int \dot{v}_2 \cdot dt$; in Figure 1-25) but that will not work. Other examples where high index occurs is when modelling purely rolling wheels (3.3.2.1.1).

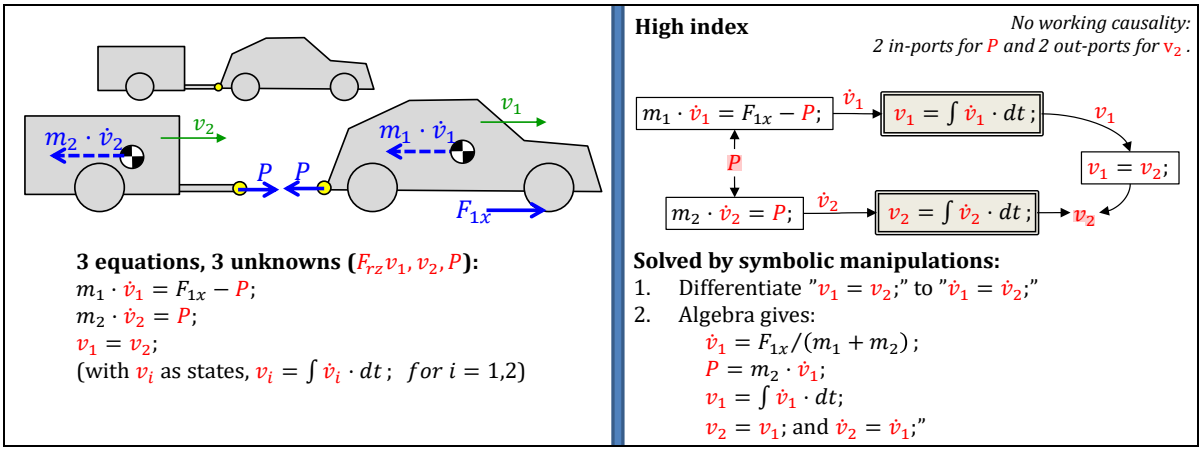


Figure 1-25: An example of a High index model; an accelerating rigidly connected car and trailer.

1.5.1.6 Time Sampling and Time Events

In vehicle dynamics, the dynamics occurring in the digital control is essential. A control algorithm can of course be modelled with continuous equations, but the effect of time sampling and signal communication delays are often essential to include. A mathematical method to model this phenomenon is "time events".

Time events are similar to, but not same as, discrete dynamics in 1.5.1.4. The similarity is that both time events and state events (used for discrete dynamics) uses transition conditions, $\boldsymbol{h} > \boldsymbol{0}$. But for time events, the transition conditions are only a function of time $\boldsymbol{h}(t)$. Time events appear since algorithms are executed on digital processors or are delayed sin signal communication. Time events are generally more established and easier to get physically consistent than the more general *state events*, $\boldsymbol{h} = \boldsymbol{h}(\boldsymbol{x_c}, \boldsymbol{x_d}, \boldsymbol{u}, t)$.

In Modelica, a continuous model with its time sampled controller can be modelled as in Figure 1-26. The example is speed control of a vehicle in uphill. The longer sample time gives an unstable solution.

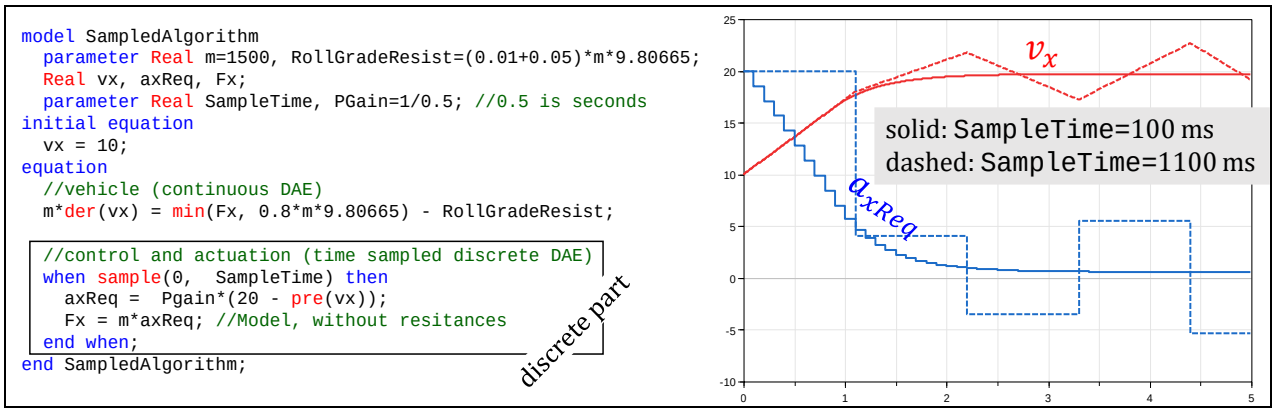


Figure 1-26: Dynamic model with time sampled part.

1.5.1.6.1 Discretization of Continuous Models

When a simulation tool solves a dynamic model it typically does time discretization, but as engineers we still see the model as continuous. However, continuous dynamic models often have to be intentionally (time) discretized; as they shall become parts of the product, the vehicle. The integral part of a PID controller is one example. Another example is when an algorithm is derived as continuous, which is often the case with filters and estimators, 1.5.3.5. Yet another example is when the algorithms shall perform simulations of dynamic models which are derived as continuous. An example of converting a continuous dynamic model to a time discrete is shown in Figure 1-17.

1.5.1.7 Discrete Dynamics

Contribution from: Fredrik Bruzelius, Vehicle Dynamics at Chalmers and VTI

Only continuous dynamics, as opposed to **discrete dynamics**, were considered in 1.5.1.1.3.2 to 1.5.1.1.6. Discrete dynamics modelling can be used for computational efficient models of, e.g., ideal dry friction or ideal backlash but also to model time sampled (digital) systems. See Figure 1-27. The way the states evolve over time differs between continuous and discrete dynamics: During the modelling, the continuous states, $\boldsymbol{x_c}$, should be thought of as changing continuously. In the computation there has to be a discretization in time steps since computers are digital (not analogue). Hence the $\boldsymbol{x_c}$ are updated only between each time step but thought of as continuously changing in between. The update is based on the state derivatives, $\dot{\boldsymbol{x}}_{\boldsymbol{c}}$, and a derivative approximation, e.g. $\dot{\boldsymbol{x}}_{\boldsymbol{c}} = (\boldsymbol{x_c}(t + \Delta t) - \boldsymbol{x_c})/\Delta t$;. Discrete states, $\boldsymbol{x_d}$, should be thought of as constant except that they stepwise change value at the time instants *when* one of the *transition conditions* becomes true (not between these time instants!). These time instants are called *(state) events*, and can be implemented as *when* event indicators, $\boldsymbol{h}(\boldsymbol{x_c}, \boldsymbol{x_d}, \boldsymbol{u}(t), t) > 0$, becomes true.

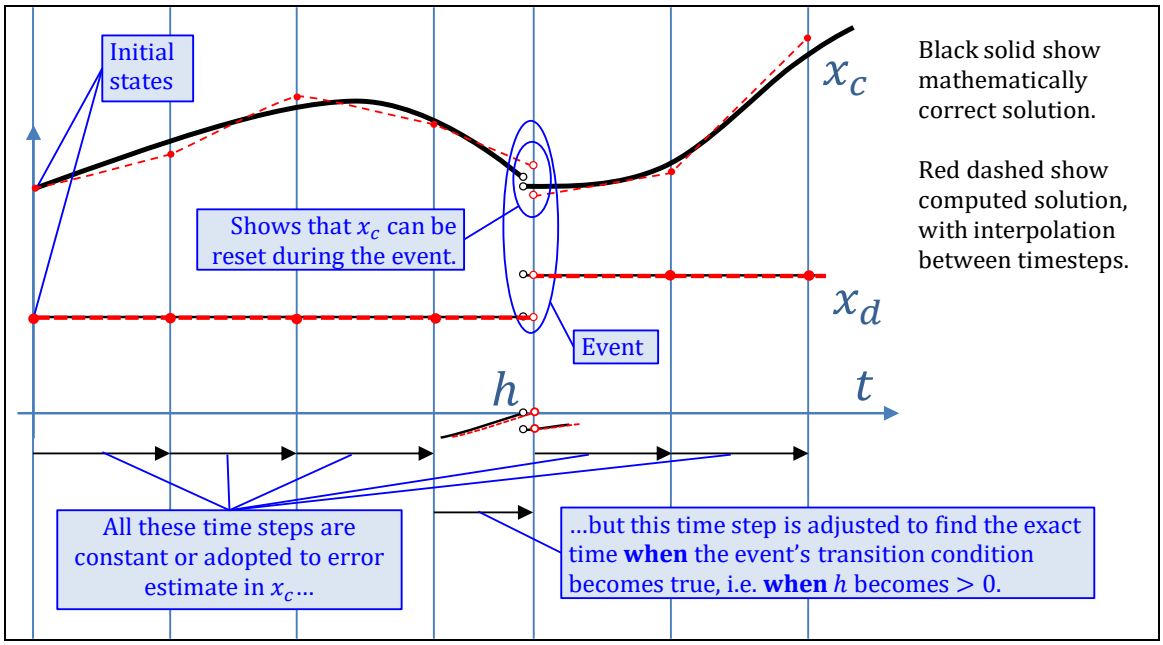


Figure 1-27: A visualization of a solution with both continuous and discrete states. Error of the computed solution appears in the variable's dimension (but not in time) for the continuous states, while it appears in time (but not in the variable's dimension) for the discrete states.

At a first glance, the x_c should not change in the events, but are two reasons why one sometimes model them to change (stepwise) at an event: one is to reinitialize to physically obvious values (e.g. a bouncing ball need to start from the surface it bounces at when the bounce happens) and the other is if one change physical model at an event, e.g. introduce an inertia or elasticity. The latter can be powerful to solve an engineering task, but the engineer has to be especially observant on how credible the numerical solution is, because the simulation tools can typically not estimate errors in such model. The latter way is here described as one model, but in another context, it can be seen as "splicing" of several models.

A system which includes both types (*hybrid dynamics*) evolves as follows:

$\boldsymbol{x_c}(t + \Delta t) \leftarrow \boldsymbol{x_c} + \Delta t \cdot \dot{\boldsymbol{x}}_{\boldsymbol{c}} = \boldsymbol{x_c} + \Delta t \cdot \boldsymbol{f_c}(\boldsymbol{x_c}, \boldsymbol{x_d}, \boldsymbol{u}(t), t)$; and

when $\boldsymbol{h}(\boldsymbol{x_c}, \boldsymbol{x_d}, \boldsymbol{u}(t), t) > \boldsymbol{0}$ *then* $\boldsymbol{x_d}(t^+) \leftarrow \boldsymbol{f_d}(\boldsymbol{x_c}, \boldsymbol{x_d}, \boldsymbol{u}(t), t)$;.

Note that a "knee" (discontinuous derivative but continuous value) in an equation does generate an event, but no discrete state, since no "memory" is needed. But a step (mathematical discontinuity in value) or a hysteresis (mathematical function with multiple values depending on which branch is active) generate state event with discrete state. See examples in 2.4.4.

One can see discrete dynamics as if the physics get stuck on the steep part of a step or in a branch in a hysteresis, until when an exit condition becomes true. Examples where this occur is dry friction, one-way clutches, back-lashes, diodes, etc. Another example appears if one changes physical models, e.g. remove a mass or compliance, during some parts of the simulation, governed by certain events.

Discrete dynamics is not as well established in most basic engineering education as continuous dynamics.

1.5.1.7.1 Event Iteration and Chattering

Several discrete state transitions can occur during same time instant, which calls for *event iteration* one time instant, i.e. during zero time. An example is when a friction element switches state from positive slipping to sticking and to negative slipping during one time instant. A typical problem with these models is that transition conditions are such that event iteration does not converge, so called *chattering*.

It can be needed to reinitialize continuous state variables ($\boldsymbol{x_c}(t^+) = \cdots$) in events, e.g. motivated by impact dynamics. There is a risk that the numerical solution gets stuck in undesired high frequency switching of discrete states which also can lead to chattering.

Chattering can be caused by coding errors of the event handling or inconsistent physical modelling.

1.5.1.7.2 Finite State Machines

Examples of state events which typically appear in control algorithms or driver models are *(finite) state machines*. These are easier in the way that typically do not have event iteration, but only one state transition should happen in each time sample. This reduces the risk of chattering, or at least makes the chattering to appear with the sample time, not during a time instant.

1.5.1.7.3 Discrete Dynamics Implementation in Tools

Here is an example of how discrete states can be modelled (or implemented) in Modelica. The example is purely mathematical and without physical interpretation.

```
Model example_DiscreteState
  Real y, x_c (start=0);
  Integer x_d (start=0);
equation
  //Eqs defining continuous variables y and x_c (but can use the discrete variable):
  y = x_c^2;
  der(x_c) = if (x_d == 0) then -1 else +1;
  //Eq defining discrete variable x_d (how it is updated at state events):
  when     (pre(x_d) == 1 and x_c > +1) then    x_d = 0; reinit(x_c,+2);
  elsewhen (pre(x_d) == 0 and x_c < -1) then    x_d = 1; reinit(x_c,-2);
  end when;
end example_DiscreteState;
```

For tools that do not handle discrete events, the same model can be implemented with the discrete state x_d declared as continuous variable, which causes also some other changes. In Modelica:

```
Model example2_DiscreteState
  Real y, x_c (start=0);
  Real x_d (start=0); //Discrete state declared as conntiuous variable
equation
  //Eqs defining continuous variables y and x_c (but can use the discrete variable):
  y = x_c^2;
  der(x_c) = if (x_d == 0) then -1 else +1;
  der(x_c)=0;
  //Eq defining discrete variable x_d (how it is updated at state events):
  when     (abs(x_d-(+1))<0.5 and x_c > +1) then    reinit(x_d,0); reinit(x_c,+2);
  elsewhen (abs(x_d-( 0))<0.5 and x_c < -1) then    reinit(x_d,1); reinit(x_c,-2);
  end when;
end example2_DiscreteState;
```

1.5.1.7.4 Discrete Dynamics in Dataflow Diagram Based Tools

Here is the same example as in 1.5.1.7.3, but modelled (or implemented) in a Dataflow Diagram based tool, Simulink. Many tools do not have direct support for discrete dynamics. A way to use an "Integrator block for continuous states" can be used to handle "updates of a discrete state x_d" is shown in the figure below. Another way is to use a Matlab function block with this function inside:

```
persistent xd %persistent makes xd be remembered since last function call
if xd~=nextxd
   xd=nextxd;
end
```

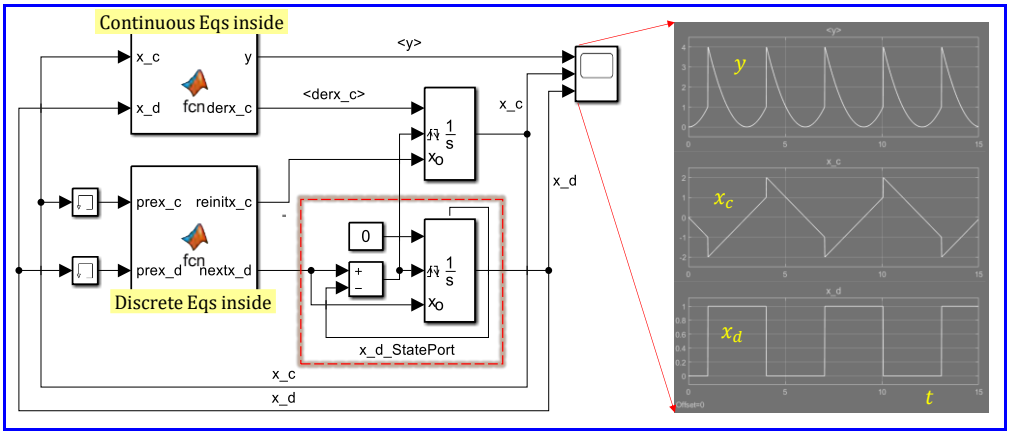


Figure 1-28: Same model as shown in Modelica format, but here implemented in the Dataflow Diagram Based Tool "Simulink". The red dashed box shows how updating of a discrete state x_d can be modelled. Note $\dot{x}_d \equiv 0$;, but x_d is reset at some time instant.

1.5.2 Mechanical/Machine Engineering

Vehicle dynamics originates from Mechanical or Machine engineering (in Swedish "Maskinteknik", in German "Machinenbau"). Therefore, it is important to be fluent with the following mechanical basic quantities and relations:

- Torque = $T = Force \cdot Lever$; (or Moment=$M = Force \cdot Length$;)
- Power = Force · Translational velocity: $P = F \cdot v$;
  (or Power = Torque · Rotational velocity: $P = T \cdot \omega$;)
  (or in other domains: Power=Voltage·Current; Power=Flow·Pressure; etc)
- Energy = time integral of Power: $E = \int P \cdot dt$; or: $E = \int F \cdot dx$; or: $E = \int T \cdot d\varphi$;.
- (Torque) Ratio = Output torque/Input torque: $ratio_T = T_{out}/T_{in}$;
- (Rotational velocity) Ratio = Input velocity /Output velocity: $ratio_\omega = \omega_{in}/\omega_{out}$;
- (Power) Efficiency = Useful power/Used power: $\eta = P_{Useful}/P_{Used}$;
- Efficiency (in a wider meaning): $\eta = Usedful/Used$;

Translational velocities, rotational velocities, forces, and moments are vector quantities. If formulating equations with geometric vectors and $\vec{r}$ denotes position vectors:

- $\vec{v}_A = \vec{v}_0 + \vec{\omega} \times (\vec{r}_A - \vec{r}_0)$; (for a rigid body)
- $\vec{T}_A = (\vec{r}_A - \vec{r}_0) \times \vec{F}_A$;

Interfaces in mechanical systems are recommended to use $[F, v]$ or $[T, \omega]$, which is a "factorized power interface", see 1.5.2.1.2. Note that Mechanical or Machine engineering, includes also other physical domains than mechanical, such as electric, hydraulic, etc.

1.5.2.1 Free-Body Diagrams

In the physical model, see 1.5.1.1.3, a *free-body diagram, FBD,* is often central. See example in Figure 1-30 and Figure 1-31. Also, division into subsystems by introducing *cuts* or *connections*. It is often practical to identify moment-free connection points, etc. The subsystem split typically goes through:

- Connection point between towing unit and towed unit (typical interface quantities: 2 positions (with their derivative, velocities) and 2 forces).
- Driveshaft close to each wheel (typical interface quantities: 1 shaft torque, 3 forces, and 2 angles (steering and shaft rotation), sometimes 1 wheel camber angle).
- Surface between driver's hand and steering wheel (typical interface quantities: 1 angle and 1 torque).
- Sensed signals and request signals, which cuts out control algorithms as subsystem.

One can draw FBDs with two purposes: To understand the real-world problem/manoeuvre or to help formulating (equilibrium) equations.

- A FBD with the 1st purpose, typically has force arrows with the actual force directions. It is then logical to name them $|F|$ or just write an explicit numerical value.
- A FBD with the 2nd purpose has force arrows as the corresponding forces are defined positive and named F (or $-F$, if drawn as defined negative). The reasoning about naming with $|F|, F, -F$ or numerical value also applies to other signed or vector quantities: velocities, displacements, and distances; in translation and rotation. Most FBDs in the book is of this type. Note: If drawing the complete force play the FBD contains the same information as the equilibrium equations of the freed part!

It is recommended to **not** draw two forces acting at the same point of part and having same direction, F_1 and F_2. With such unsuitable drawing, it is very easy to set up wrong equations, e.g., for friction limitation.

Forces in a cut can have the same name, e.g., the name F_{fz0} appears twice in Figure 1-30 as force acting on the body and on the wheel. This should be understood as one force, broken down to its *dual force appearances*, action and reaction, see Newton's 3rd law (Newton, 1687-07-05). The two appearances should have the same notation on both sides of the cut, or one must add one equation which tells that the two notations are equal. Also note that the moment T_f is not marked in the FBD to the left in Figure 1-30. This is because T_f is "inside" this FBD. Therefore, it is not possible to draw it unambiguously without splitting the FBD in two FBDs, as done to the right in Figure 1-30.

Note that there is another situation where one sometimes sees 2 forces with the same name. This is when the modeller uses same notation for 2 forces which he knows will be equal. An example would be to denote F_{fz0} and F_{fz} with same name when acting on the wheel in Figure 1-30. If using such notation, one has to keep in mind that the naming itself hides an assumption; equilibrium without any other forces. So, this way of naming is **not** generally recommended. It can be a short-cut for the experienced modeller if the model should not be used later and not by another person. However, it is a dangerous way of modelling for the less experienced modeller.

When using FBD as a help to set up equilibrium equations, a short-cut that can be to express a force in other, in a way that equilibrium is already fulfilled in the FBD. This eliminates one equilibrium equation. An example of this could be to use F_{fz} instead of F_{fz0} in Figure 1-30, which would make the vertical force equilibrium for the front axle ($F_{fz} - F_{fz} = 0$) unnecessary and not useful.

1.5.2.1.1 Forces in a Cut or Connection

The same force (or moment) appears as action and reaction on each side of a cut, see 3rd law in (Newton, 1687-07-05). There are two ways of denoting forces and moments in a cut:

- Using **single cut force notation**: Same force (and moment) notation in both part's FBD.
- Using **multiple cut forces notation**: Different force (and moment) notation in each part's FBD.

The latter is more systematic, but requires extra variables and equations, saying that the cut is in equilibrium. It is also more general since it can handle more than two parts in a cut (which makes the name *connection* between *connectors* more understandable than *cut*). The latter is also a way to allow notations in local coordinate systems for each part. However, the first is probably easiest for intuition since it follows the concept of that a force in a cut always has one action and one reaction. The book uses both ways. Example is given in 1.6.1.1.

1.5.2.1.2 Physical Connections and Factorized Power Interface

When connecting physical quantities (as opposed to connect signals), it is recommended to use interface variables which factorize power P, e.g., velocity v and force F, because $P = v \cdot F$. Similar factorization is found in other domains, on a general form $P = \mathit{effort} \cdot \mathit{flow}$. (In thermodynamics, there are two flow variables, e.g., mass flow and enthalpy flow, which is not treated in this book.) Connection via such "factorized power interfaces" is sometimes referred to as "power bonds". Effort and flow often

get opposite causality in the explicit form model, except in high index models, see 1.5.1.5, or in some inverse problem formulations, e.g., backward simulation in 3.3.5.7.1.1. Multi-dimensional flow (e.g., $\{F_x, F_y\}$) or other derivative orders, e.g., $\{position, force\}$ instead of $\{velocity, force\}$ also work.

Using factorized power interfaces reduces the risk of modelling errors, e.g., mixing up physical quantities (e.g., F for force) with signals **referring to** the quantities (e.g., $F_{Req}, F_{Actl}, F_{Est}$ which all refer to F but they are signals). In Modelica tools, there are often checks that models are "balanced", which is closely related to using proper physical connections and physically correct number of equations.

When connecting physical components in a data flow diagram with "Physical connections", there can be two main concepts:

- Connections to "cuts" or "nodes" **between** components, see Figure 2-97. Here, each node has typically potential and flow variables (velocities and forces in Mechanical systems). And there are only two components connected to each node. The node variables appear in both components' equations. The connection itself generates these equations: "Potential variable in node and both connected components are equal" and "Flow variable in node and both connected components are equal".
- Connections between "connectors" **on** components, see Figure 2-98 and Figure 2-121. Such a connection can connect more than two components. The equations in each component are formulated in the connector's variables. The connection itself generates these equations: "Effort variables are equal" and "Sum of flow variables are zero". This is used in most Modelica tools and Modelica libraries.

The first is often the easiest (least number of equations and variables) if one knows the system's topology and operation/use well. The latter is a more systematic which easier handles larger models or if one is less experienced in the system's topology and operation/use. The latter is supported in the standard modelling language Modelica, see 1.5.4.1.5 and the open book on internet in (Tiller, 2019) and (Åberg, 2021).

1.5.2.2 Selection of State Variables

From 1.5.1.3.2, we know state variables have to be selected and that selection is not unique. For mechanical systems, one often selects positions x_m and velocities v_m of (inertial and rigid) bodies as state variables. Inertial means "having mass", which is why subscript m is used. However, it is also possible and sometimes preferable, to replace these positions with forces F_s in (massless and elastic) bodies, a.k.a. as springs or compliances. Subscript s is chosen from spring. With mass-spring system as example, the two alternatives become:

- $\underline{v_m, x_m}$ states: $[\dot{v}_m = F_s/m\,;\quad F_s = c \cdot x_m;\quad \dot{x}_m = v_m;]$ (or $[\ddot{x}_m = F_s/m\,;\quad F_s = c \cdot x_m;]$) and
- $\underline{v_m, F_s}$ states: $[\dot{v}_m = F_s/m;\quad \dot{F}_s = c \cdot v_m;\quad x_m = F_s/c\,;]$, respectively.

We now drop the subscripts, $x_m = x, F_s = F, \cdots$. The latter alternative is especially relevant when position x is not of interest, typically in propulsion systems. If v, F states, one equation ($x = F/c$) can then be omitted which can simplify. It is also often easier to express steady state initial conditions for a pre-tensioned system, e.g., wheel suspension where spring forces can be states. A drawback might be that, if overdetermined pre-tensioned systems (e.g. mass suspended in two springs: $[\dot{v} = (F_1 + F_2)/m;\ \dot{F}_1 = c_1 \cdot v; \dot{F}_2 = c_2 \cdot v;\ x = F_1/c_1\,;\ x = F_2/c_2\,;]$), more states than necessary will be used, which means that positions (x) can be calculated in two ways ($x = F_1/c_1\,;\ x = F_2/c_2\,;$). These two ways can drift apart. The drift can be eliminated by completely disregard the original spring constitutions ($x = F_1/c_1\,;\ x = F_2/c_2\,;$) and instead use position as a state ($\dot{x} = v;$). The mathematical system is then effectively:

- $\underline{v, F, x}$ states: $[\dot{v} = F/m\,;\quad \dot{F} = c \cdot v;\quad \dot{x} = v;]$.

Another warning, when using force in elasticity as state in models with discrete event is that a reset of another state in the model might require also resetting the force state. That occurs when a deformation is changed stepwise in an event.

One can see the latter alternative as if the states are the variables which represents the two energy forms kinetic and potential energy, as in Lagrange mechanics.

1.5.2.3 Varying the Order of the ODE

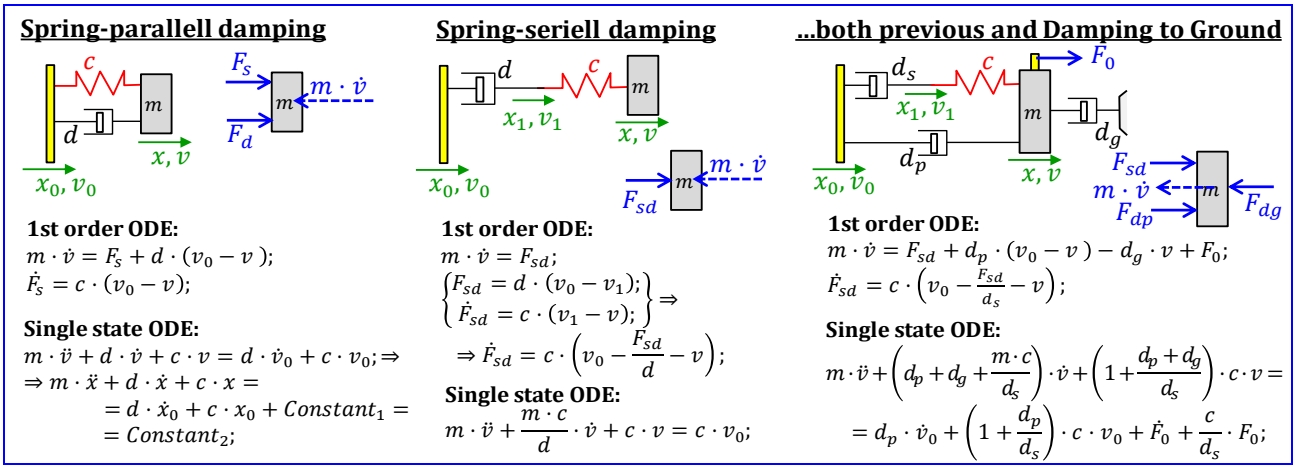


Figure 1-29: Examples of damped mass and spring systems, as 1st order ODEs and single state ODEs.

1.5.2.3.1 Dimensionality

Above, we have assumed one dimension, i.e. the forces and velocities were 1D. (Note that forces and vectors are vector quantities, so they were still vectors, but 1D vectors. This is not always enough to in engineering, because the products should work in real world, which has 3 geometrical dimensions. So, in each point or node in a mechanical system: $\{\vec{v}, \vec{\omega}\} = \left\{\{v_x, v_y, v_z\}, \{\omega_x, \omega_y, \omega_z\}\right\}$ and $\{\vec{F}, \vec{M}\} = \left\{\{F_x, F_y, F_z\}, \{M_x, M_y, M_z\}\right\}$.

The 1D equations above ($F = m \cdot \dot{v}, \dot{F} = c \cdot v;$) do have 3D variants, where mass m and stiffness c are 3×3 matrices. See 1.5.2.4.

1.5.2.4 Equation Types

The step from physical model (see 1.5.1.1.3) to mathematical model (1.5.1.1.3.2) means basically to identify variables and parameter and find the relationship between them, i.e. the equations. Models for Vehicle Dynamics always includes mechanics. A deductive way to find equations for the mechanical parts is to select between 3 main types of equations:

- *Equilibrium*,
- *Compatibility* (or *Congruence* or *Kinematics*), and
- *Constitution*.

Equilibrium and Compatibility are generally the first to be questioned in Physical model, e.g., whether a part shall be modelled as inertial and rigid or massless and compliant. Constitution comes then and it is generally even more debatable, e.g., whether a damping (energy loss) shall be modelled as dry friction, viscous (linear) or other, e.g., quadratic, relation?

1.5.2.4.1 Equilibrium

Contribution from Dragan Sekulić

In present section, equilibrium means equilibrium of forces (including moments). The word equilibrium is, elsewhere, used as equilibrium of other quantities, such as power, energy, electric current, mass flow, etc..

Equilibrium gives relations between forces (including moments), see (Newton, 1687-07-05).

For a **static** system **or** a system **without mass inertia**, (static) equilibria will be kept: Sum of forces in any direction is zero: $\sum \boldsymbol{F} = \boldsymbol{0}$; and Sum of moments around any axis is zero: $\sum \boldsymbol{M} = \boldsymbol{0}$;.

For a **dynamic** system **with mass inertia**, there are inertia effects. Inertia effects can be seen as "fictive forces" and "fictive moments" (or "d'Alembert forces or moments"). Typically, the fictive forces are $F_{fict} = m \cdot a$ (where a =translational acceleration) and the fictive moments are $M_{fict} = J_{CoG} \cdot \dot{\omega}$. These are counter-directed to a and $\dot{\omega}$, respectively. We can find the equations either as "Dynamic equilibrium":

- Sum of forces, including F_{fict}, in any direction is zero: $\sum_{\boldsymbol{incl.fict}} \boldsymbol{F} = \boldsymbol{0}$;
- Sum of moments **around any axis**, including both M_{fict} and "$lever \times F_{fict}$", is zero: $\sum_{\boldsymbol{incl.fict}} \boldsymbol{M} = \boldsymbol{0}$;

or as "Equations of motion", a.k.a. "Newton's 2nd law":

- Sum without fictive in a direction must be equal to $m \cdot a$: $\sum_{\boldsymbol{excl.fict}} \boldsymbol{F} = \boldsymbol{m} \cdot \boldsymbol{a}$;
- Sum without fictive **around axis through CoG** in direction of $\dot{\omega}$ have to be equal to $J_{CoG} \cdot \dot{\omega}$: $\sum_{\boldsymbol{CoG,excl.fict}} \boldsymbol{M} = \boldsymbol{J_{CoG}} \cdot \dot{\boldsymbol{\omega}} + \boldsymbol{\omega} \times (\boldsymbol{J_{CoG}} \cdot \boldsymbol{\omega})$;

The way to use fictive forces enable us to represent and understand the inertial dynamics already when we draw the free-body diagram, i.e. before we even introduce equations.
Note: Fictive forces are different from traditional forces in that they cannot easily be seen as a couple of action and reaction force.
The J_{CoG} is the mass moment of inertia matrix in CoG along the same coordinate axes as ω is expressed in. In this book, the alternative with "Dynamic equilibrium" is mainly used. The fictive forces are introduced in the free-body diagrams with dashed arrows, see Figure 1-30 and Figure 1-31. (Note: Fictive forces are different from traditional forces in that they cannot easily be seen as a couple of action and reaction force.) Advantage with "Dynamic equilibrium" is easiness to form moment equilibria since it can be taken around any axis (example in Figure 1-31). It is also easier to include motion effects within a part of the system (such as $J_f \cdot \dot{\omega}_f$ and $J_r \cdot \dot{\omega}_r$ in Figure 1-30). The general form for the fictive forces is:

$$\vec{F}_{fict} = \frac{d}{dt}(translational\ momentum) = \frac{d}{dt}(m \cdot \vec{v}) = m \cdot \frac{d}{dt}\vec{v} = m \cdot \frac{d}{dt}\left(\frac{d}{dt}\vec{r}\right) =$$
$$= m \cdot \dot{\boldsymbol{v}} - \underbrace{m \cdot 2 \cdot \boldsymbol{\omega} \times \boldsymbol{v}}_{Coriolis\ force} - \underbrace{m \cdot \boldsymbol{\omega} \times (\boldsymbol{\omega} \times \boldsymbol{r})}_{Centrifugal\ force} - \underbrace{m \cdot \dot{\boldsymbol{\omega}} \times \boldsymbol{r}}_{Euler\ force};$$

The $\vec{r}$ is the *position vector*. The Coriolis and Euler forces can often be assumed as zero in examples in this book due to no motion within the vehicle and rigidity of rotating bodies. The general form for the fictive moments is:

$$\vec{M}_{fict} = \frac{d}{dt}(rotational\ momentum) = \frac{d}{dt}(\boldsymbol{J_{CoG}} \cdot \vec{\omega}) = \boldsymbol{J_{CoG}} \cdot \dot{\boldsymbol{\omega}} + \underbrace{\boldsymbol{\omega} \times (\boldsymbol{J_{CoG}} \cdot \boldsymbol{\omega})}_{Gyroscopic\ moment};$$

The term $\boldsymbol{\omega} \times (\boldsymbol{J_{CoG}} \cdot \boldsymbol{\omega})$ can often be assumed as zero in examples in this book due to symmetries and rotation in one plane at the time.

Note: As seen in the latter paragraphs above, "Dynamic equilibrium" becomes more difficult for general 3D motion. In those cases, "Equations of motion", a.k.a. "Newton's 2nd law", might be easier.

Figure 1-30 and Figure 1-31 show examples of free-body diagrams (FBDs) with all forces, including fictive forces. With such FBDs, the equilibrium equations are implicitly defined.

In Figure 1-30, the mass of the wheels can be included in the FBD of the vehicle body and rear axle, but not the FBD of the front axle. The moment of inertia is marked as $J_i \cdot \dot{\omega}_i$, but in practice we can often neglect these terms in the FBD of the whole vehicle (but not for the FBD of the wheel, where they are often essential in the equilibrium $J_i \cdot \dot{\omega}_i = T_i - F_{ix} \cdot WheelRadius$;), see more in 3.3.6.2.

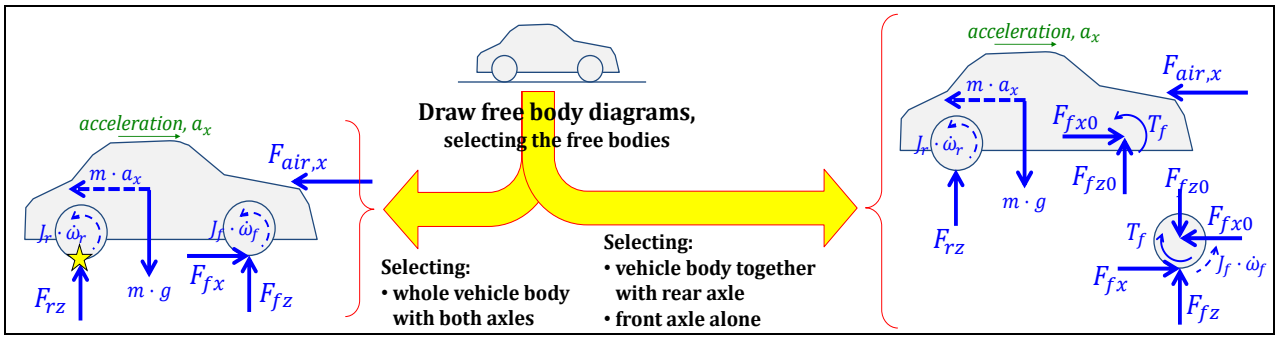
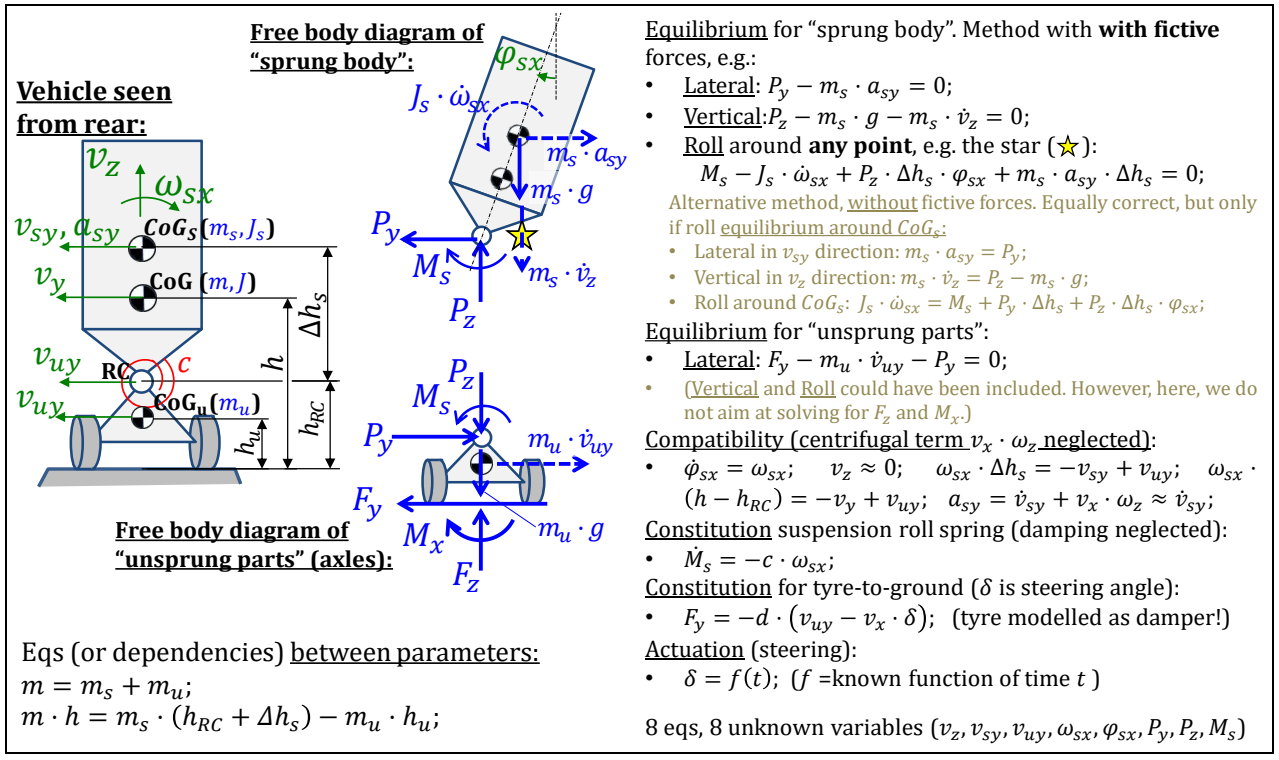


Figure 1-30: Free body diagram. The dashed arrows marks "fictive" force or moment. The star is a way to mark around which point(s) moment equilibrium is taken in the later stage "Mathematical model". The fictive moments $J_f \cdot \dot{\omega}_f$ and $J_r \cdot \dot{\omega}_r$ are often neglectable in equilibrium for whole vehicle, but significant in equilibrium for individual wheels.

In Figure 1-31, the prescribed motion actuation (steering angle $\delta(t)$) and good road grip result in 4 states, e.g. $[v_y, \omega_{sx}, M_s, \varphi_{sx}]$ or $[v_{sy}, \omega_{sx}, M_s, \varphi_{sx}]$. If unsprung parts have only a neglectable portion of the total vehicle mass, it can be easier to use $m_u = 0$ and replace m_s with the total vehicle mass. However, J_s should not be changed, because it is still only the sprung body that rolls.



Eqs (or dependencies) between parameters:
$m = m_s + m_u;$
$m \cdot h = m_s \cdot (h_{RC} + \Delta h_s) - m_u \cdot h_u;$

Equilibrium for "sprung body". Method with **with fictive** forces, e.g.:
- Lateral: $P_y - m_s \cdot a_{sy} = 0;$
- Vertical: $P_z - m_s \cdot g - m_s \cdot \dot{v}_z = 0;$
- Roll around **any point**, e.g. the star (☆):
  $M_s - J_s \cdot \dot{\omega}_{sx} + P_z \cdot \Delta h_s \cdot \varphi_{sx} + m_s \cdot a_{sy} \cdot \Delta h_s = 0;$

  Alternative method, without fictive forces. Equally correct, but only if roll equilibrium around CoG_s:
  - Lateral in v_{sy} direction: $m_s \cdot a_{sy} = P_y;$
  - Vertical in v_z direction: $m_s \cdot \dot{v}_z = P_z - m_s \cdot g;$
  - Roll around CoG_s: $J_s \cdot \dot{\omega}_{sx} = M_s + P_y \cdot \Delta h_s + P_z \cdot \Delta h_s \cdot \varphi_{sx};$

Equilibrium for "unsprung parts":
- Lateral: $F_y - m_u \cdot \dot{v}_{uy} - P_y = 0;$
- (Vertical and Roll could have been included. However, here, we do not aim at solving for F_z and M_x.)

Compatibility (centrifugal term $v_x \cdot \omega_z$ neglected):
- $\dot{\varphi}_{sx} = \omega_{sx};$ $v_z \approx 0;$ $\omega_{sx} \cdot \Delta h_s = -v_{sy} + v_{uy};$ $\omega_{sx} \cdot (h - h_{RC}) = -v_y + v_{uy};$ $a_{sy} = \dot{v}_{sy} + v_x \cdot \omega_z \approx \dot{v}_{sy};$

Constitution suspension roll spring (damping neglected):
- $\dot{M}_s = -c \cdot \omega_{sx};$

Constitution for tyre-to-ground (δ is steering angle):
- $F_y = -d \cdot (v_{uy} - v_x \cdot \delta);$ (tyre modelled as damper!)

Actuation (steering):
- $\delta = f(t);$ (f =known function of time t)

8 eqs, 8 unknown variables $(v_z, v_{sy}, v_{uy}, \omega_{sx}, \varphi_{sx}, P_y, P_z, M_s)$

Figure 1-31: Free body diagrams for combined translation and rotation. The figure also shows the two ways of setting up equilibria, with and without fictive forces. Angle φ_x is assumed small.
(To make as clear example as possible for roll: Centrifugal term $v_x \cdot \omega_z$ neglected. And, the d is written as a general damping coefficient, while, in 2.2.4, it can be found that $d = C_y / v_x$;.)

A Modelica implementation of the model in Figure 1-31 is here shown:

```
model RollDynamics_Sprung_Unpsrung
 ... //declaration of parameters and variables
equation
  //Equilibrium for sprung body:
  m_s*der(v_sy)-P_y=0;
  -m_s*g-m_s*der(v_z)+P_z=0;
  M_s -J_s*der(w_sx) +P_z*Dh_s*phi_sx
          +m_s*der(v_sy)*Dh_s =0;

  //Equilibrium for unsprung parts:
  m_u*der(v_sy) -F_y +P_y =0;
  F_z=P_z;
  P_y*h_RC +m_u*der(v_uy)*h_u +M_x -M_s =0;

  //Compatibility:
  der(phi_sx)=w_sx;
  v_z=0;
  w_sx*Dh_s=-v_sy+v_uy;
  w_sx*(h-h_RC)=-v_y+v_uy;

  //Constitution:
  der(M_s)=-c*w_sx;
  F_y=-d*(v_uy-v_x*delta);
end RollDynamics_Sprung_Unpsrung;
```

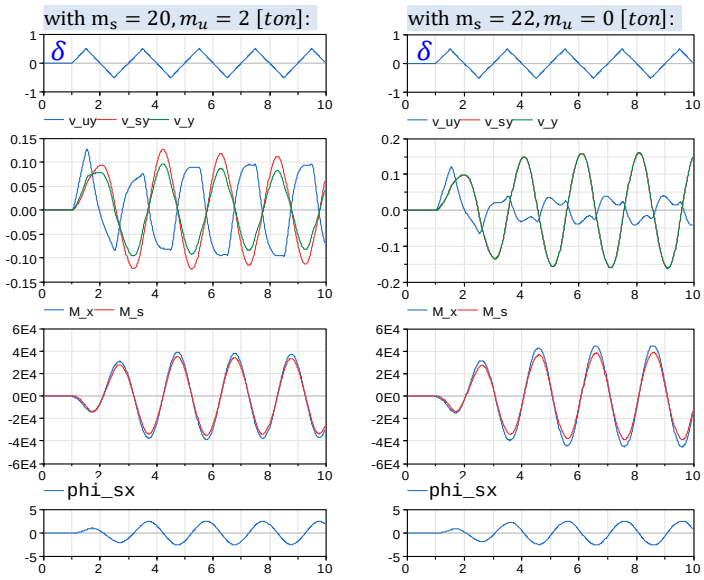


Figure 1-32: A Modelica implementation of the model in Figure 1-31 and two simulation results.

1.5.2.4.1.1 Centrifugal Forces in General 3D Motion

Centrifugal force terms appear as $m \cdot v_i \cdot \omega_j$ where $i \neq j$, i.e. for rotation perpendicular to translational velocity:

$$\begin{bmatrix} a_x \\ a_y \\ a_z \end{bmatrix} = \begin{bmatrix} \dot{v}_x \\ \dot{v}_y \\ \dot{v}_z \end{bmatrix} + \begin{bmatrix} 0 & +v_z & -v_y \\ -v_z & 0 & +v_x \\ +v_y & -v_x & 0 \end{bmatrix} \cdot \begin{bmatrix} \omega_x \\ \omega_y \\ \omega_z \end{bmatrix} = \begin{bmatrix} \dot{v}_x \\ \dot{v}_y \\ \dot{v}_z \end{bmatrix} + \begin{bmatrix} 0 & -\omega_z & +\omega_y \\ +\omega_z & 0 & -\omega_x \\ -\omega_y & +\omega_x & 0 \end{bmatrix} \cdot \begin{bmatrix} v_x \\ v_y \\ v_z \end{bmatrix} =$$

$$= \begin{bmatrix} \dot{v}_x + v_z \cdot \omega_y - v_y \cdot \omega_z \\ \dot{v}_y - v_z \cdot \omega_x + v_x \cdot \omega_z \\ \dot{v}_z + v_y \cdot \omega_x - v_x \cdot \omega_y \end{bmatrix} \approx \left\{ \begin{matrix} in\ most\ relevant \\ vehicle\ operations: \\ v_x \gg v_y\ and\ v_x \gg v_z \end{matrix} \right\} \approx \begin{bmatrix} \dot{v}_x \\ \dot{v}_y \\ \dot{v}_z \end{bmatrix} + \begin{bmatrix} 0 \\ +\omega_z \\ -\omega_y \end{bmatrix} \cdot v_x;$$

In most vehicle operations, the most important centripetal acceleration terms are: $\omega_z \cdot v_x$ (see Eq [4.50]) and $\omega_y \cdot v_x$ (see Eq [3.31]).

1.5.2.4.1.2 Force-equivalence and coordinate transformation

A special case is force-equivalence and coordinate transformation of forces and moments between different coordinate systems, e.g. Eq [1.7]. Such equation looks like an equilibrium, but it is different because no physics is involved, only mathematics. The physical influence from different force-equivalent sets of forces and moments is the same only if the body is rigid; if the body is compliant and/or includes mechanisms, it matters more where on the body the forces act.

Force equivalence is used e.g. in Figure 2-64 and Figure 2-142. A set of forces are equivalent with some other set if they can be replacing each other in the free body diagram. It is recommended to not draw the two set of forces in the same free body diagram, since they are alternative to each other.

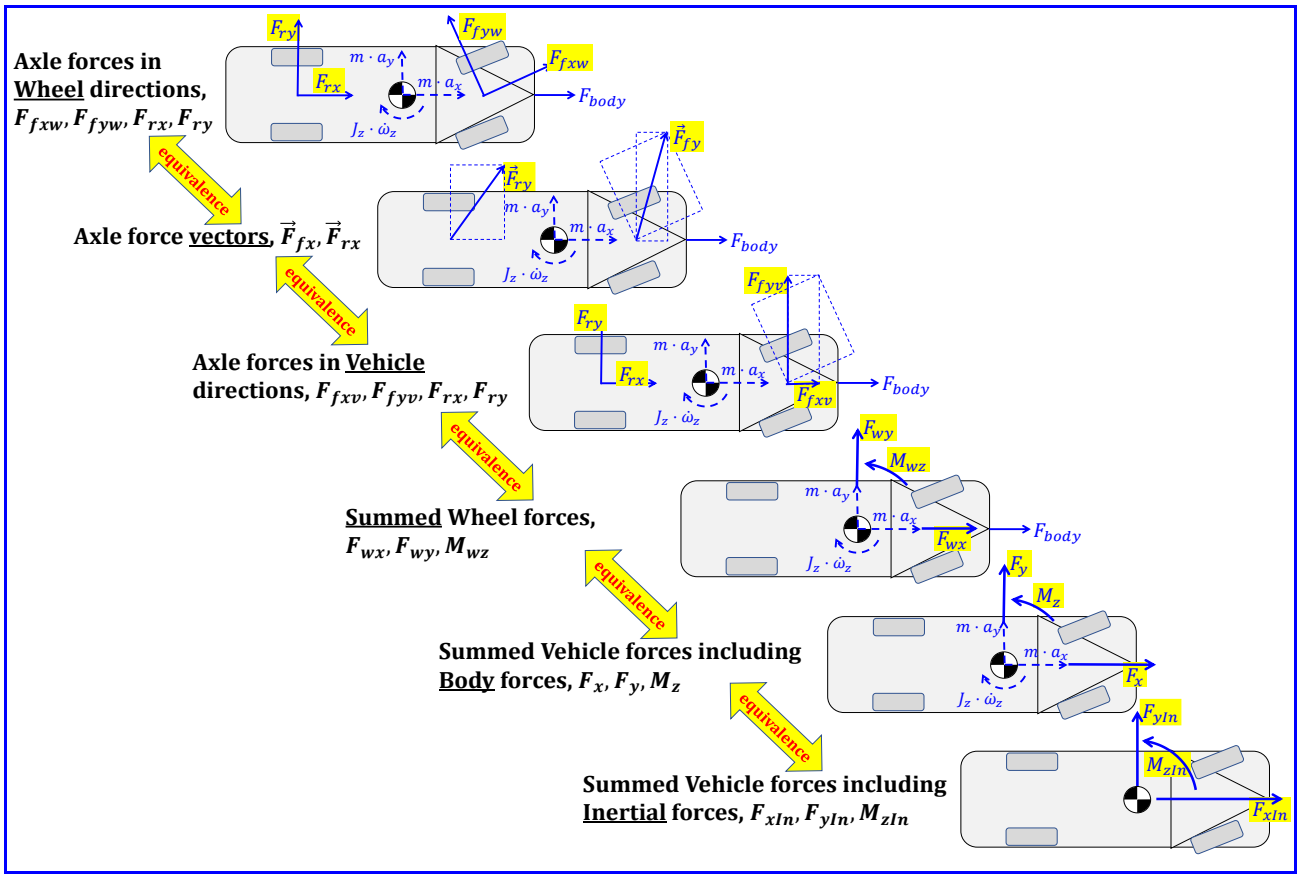
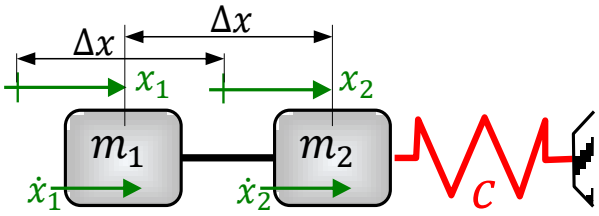


Figure 1-33: Coordinate transformation between force-equivalent of forces (and moments) on a vehicle

1.5.2.4.1.3 Lagrange Mechanics

An alternative to Newton mechanics is Lagrange mechanics, which sometimes is an easier method to find the same equations. Lagrange mechanics is basically to express kinetic energy (T) and potential energy (V) in (position) coordinates, Cartesian or Generalized. With Lagrange mechanics, the equilibrium is not formulated in forces (or moments) but in partial derivatives of energy (kinetic energy surplus, called the *Lagrangian*$= L = T - V$) with respect to these coordinates and their derivatives. One can see this as "equilibria of projected energy". Lagrange mechanics does not use the factorisation of power into $P = F \cdot v$, so it undermines the categorization in 1.5.2.4.1..1.5.2.4.1.2; the compatibility and constitution will be mixed in from start. So, the modularity corresponding to physical components in the system often gets lost. Also, energy generating and energy dissipating components has to be treated with special care, especially dry friction. Next figure shows an example of how the Lagrange method can be applied on a simple system. The system has no external forces, i.e. it has no non-constraint forces. It neither has energy exchange nor energy dissipation inside itself. Hence, the energy in the system is constant. The example is the same as the one which Newton method is applied on in Figure 1-53.

Table 1-34: Example of deriving Mathematical model using Lagrange method



Lagrange 1st kind	***Lagrange 2nd kind***
(Cartesian) Coordinates: $\boldsymbol{r} = [x_1, x_2]$; *Energies:* $T = \frac{m_1 \cdot \dot{x}_1^2}{2} + \frac{m_2 \cdot \dot{x}_2^2}{2}$;, $V = \frac{c \cdot x_2^2}{2} + V_0$; *and* $L = T - V$; *We have to, intuitively, identify* ***Constraints****:* $f_1 = x_2 - x_1 - \Delta x = 0$;	*We have to, intuitively, select* ***Generalized coordinates****:* $\boldsymbol{q} = [q_1] = [x_1]$; *Energies:* $T = \frac{(m_1+m_2) \cdot \dot{q}_1^2}{2}$;, $V = \frac{c \cdot (q_1 + \Delta x)^2}{2} + V_0$; *and* $L = T - V$;
Lagrange equations (≈ "equilibria of projected energy"): $\frac{\partial L}{\partial \boldsymbol{r_k}} - \frac{d}{dt}\left(\frac{\partial L}{\partial \dot{\boldsymbol{r}}_{\boldsymbol{k}}}\right) + \sum_{i=1}^{C} \lambda_i \cdot \frac{\partial f_i}{\partial \boldsymbol{r_k}} = \boldsymbol{0}$; ⇒ $\Rightarrow \begin{bmatrix} \frac{\partial L}{\partial x_1} \\ \frac{\partial L}{\partial x_2} \end{bmatrix} - \frac{d}{dt}\left(\begin{bmatrix} \frac{\partial L}{\partial \dot{x}_1} \\ \frac{\partial f_1}{\partial \dot{x}_2} \end{bmatrix}\right) + \lambda_1 \cdot \begin{bmatrix} \frac{\partial f_1}{\partial x_1} \\ \frac{\partial f_1}{\partial x_2} \end{bmatrix} = \begin{bmatrix} 0 \\ 0 \end{bmatrix}$; ⇒ $\Rightarrow \begin{bmatrix} 0 \\ -c \cdot x_2 \end{bmatrix} - \begin{bmatrix} m_1 \cdot \ddot{x}_1 \\ m_2 \cdot \ddot{x}_2 \end{bmatrix} + \lambda_1 \cdot \begin{bmatrix} -1 \\ +1 \end{bmatrix} = \begin{bmatrix} 0 \\ 0 \end{bmatrix}$;	*Lagrange equations (≈ "equilibria of projected energy"):* $\frac{d}{dt}\left(\frac{\partial L}{\partial \dot{q}_j}\right) = \frac{\partial L}{\partial q_j}$; ⇒ $\Rightarrow \frac{d}{dt}\left(\frac{\partial L}{\partial \dot{x}_1}\right) = \frac{\partial L}{\partial x_1}$; ⇒ $\Rightarrow (m_1 + m_2) \cdot \ddot{q}_1 = -c \cdot (q_1 + \Delta x)$;
Eliminate to independent coordinates, using the Constraints. Here, eliminate $x_2 = x_1 + \Delta x$;, *i.e. solve for* x_1 *and (the Lagrange multiplier)* λ_1*:* $\ddot{x}_1 = -c \cdot \frac{x_1 + \Delta x}{m_1 + m_2}$; *(2nd order ODE)* $\lambda_1 = c \cdot \frac{m_1}{m_1 + m_2} \cdot (x_1 + \Delta x)$; *(algebraic equation)*	*Transform to Cartesian coordinates:* $\ddot{x}_1 = -\frac{c \cdot (x_1 + \Delta x)}{m_1 + m_2}$; *(2nd order ODE)*

We can identify λ_1 as the constraint force F_1 from the Newton mechanics. But, f_1 can be formulated in many ways which leads to other interpretations, e.g. multiplying f_1 by 2 gives $\lambda_1 = F_1/2$ instead. So, more generally, the Lagrange multipliers are linear combinations of constraint forces. Lagrange mechanics formulates the equations in kinetic and potential energy in a way which has similarities with using velocities of bodies and forces in compliances as state variables, as described in 1.5.2.1.2.

1.5.2.4.2 Compatibility

Compatibility (or Kinematics) gives relations between motions (positions, velocities, accelerations, …). One example is $Speed = Radius \cdot Rotational\ speed$; for a purely rolling wheel or $\beta_f \approx (v_y + l_f \cdot \omega_z)/v_x$; for body side slip angle over front axle for a vehicle body moving in road plane.

Compatibility can also be expressed as relation between positions, as opposed to velocities. That is often done when nonlinear relations, such as when angles are changing significantly. We can still use velocity relations but add positions as state variables, see 1.5.2.4.3.3.

1.5.2.4.2.1 Coordinate Transformation

A coordinate transformation of motion quantities is the equations relating different coordinate systems or, simply, different notation. This can look as a compatibility equation, but it is different because no physics is involved, only mathematics.

1.5.2.4.3 Relation between Equilibrium and Compatibility for Mechanisms

Consider a mechanism, meaning something which only interacts with its surrounding via velocities v, including rotational velocities ω, and forces F, including moments M. Assume these are pairwise $[v_i, F_i]$ for $i = 1, \cdots, N$. Examples are a transmission and a suspension linkage, see Figure 1-35.

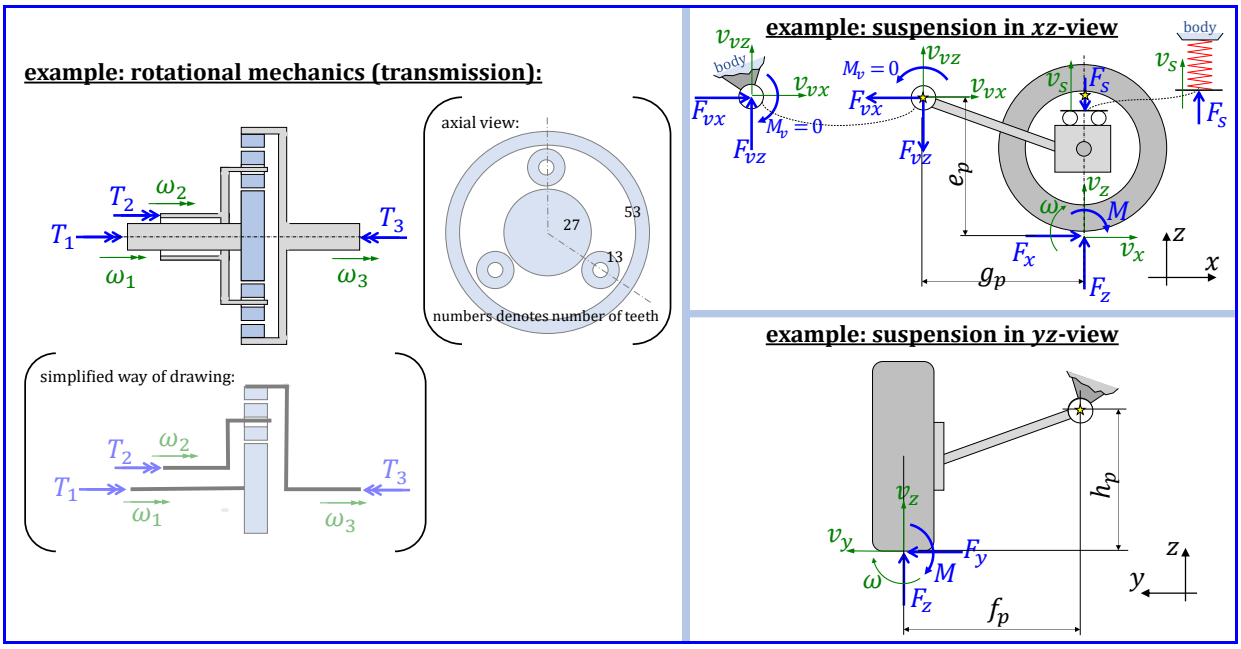


Figure 1-35: Examples for relation between Equilibrium and Compatibility for Mechanisms

Assume further that the mechanism does neither includes energy storage nor power dissipation. We would typically need velocity equations and force equations. For a certain position, or pose, these equations are proportional:

$$\boldsymbol{v_F} = \underbrace{\boldsymbol{R_v}}_{N_{FDof} \times N_{vDof}} \cdot \boldsymbol{v_v}; \text{ and } \boldsymbol{F_v} = \underbrace{\boldsymbol{R_F}}_{N_{vDof} \times N_{FDof}} \cdot \boldsymbol{F_F};$$

where $\boldsymbol{v} = [\boldsymbol{v_v^T} \quad \boldsymbol{v_F^T}]^T = [v_1, \cdots, v_N]^T$ and $\boldsymbol{F} = [\boldsymbol{F_v^T} \quad \boldsymbol{F_F^T}]^T = [F_1, \cdots, F_N]^T$.

The N_{vDof} is the number of motion degrees of freedom and N_{FDof} is the number of force degrees of freedom. The N is the number of interfaces and $N_{vDof} + N_{FDof} = N$.

We can derive $\boldsymbol{R_v}$ and $\boldsymbol{R_F}$ from compatibility and (forces) equilibrium, respectively. However, we can alternatively find one of $\boldsymbol{R_v}$ and $\boldsymbol{R_F}$ from the other, using **power** equilibrium, see (Jacobson B. , 1993). Here is the proof in short: The power input in each node is $P_i = v_i \cdot s_i \cdot F_i$; where $s_i = +1$ or -1 if $v_i \cdot F_i$ is power to and from the mechanism, respectively. The power equilibrium becomes:

$$P_{in} = \sum_{i=1 \cdots N} (v_i \cdot s_i \cdot F_i) = \boldsymbol{v^T} \cdot \underbrace{\text{diag}([s_1, s_2, \cdots, s_N])}_{\boldsymbol{S}=\text{diag}([\boldsymbol{S_v}, \boldsymbol{S_F}])} \cdot \boldsymbol{F} = 0; \Rightarrow$$

$$\Rightarrow [\boldsymbol{v_v^T} \quad \boldsymbol{v_F^T}] \cdot [(\boldsymbol{S_v} \cdot \boldsymbol{F_v})^T \quad (\boldsymbol{S_F} \cdot \boldsymbol{F_F})^T]^T = 0;$$

$$\Rightarrow [\boldsymbol{v_v^T} \quad (\boldsymbol{R_v} \cdot \boldsymbol{v_v})^T] \cdot [(\boldsymbol{S_v} \cdot \boldsymbol{R_F} \cdot \boldsymbol{F_F})^T \quad (\boldsymbol{S_F} \cdot \boldsymbol{F_F})^T]^T = 0;$$

$$\Rightarrow \boldsymbol{v_v^T} \cdot \left(\boldsymbol{S_v} \cdot \boldsymbol{R_F} + \boldsymbol{R_v^T} \cdot \boldsymbol{S_F}\right) \cdot \boldsymbol{F_F} = 0; \Rightarrow \boldsymbol{S_v} \cdot \boldsymbol{R_F} = -\boldsymbol{R_v^T} \cdot \boldsymbol{S_F};$$

$$\Rightarrow \boldsymbol{R_F} = -\boldsymbol{S_v} \cdot \boldsymbol{R_v^T} \cdot \boldsymbol{S_F}; \text{ or } \boldsymbol{R_v} = -\boldsymbol{S_F} \cdot \boldsymbol{R_F^T} \cdot \boldsymbol{S_v};$$

One example of when this is useful is for a transmission, such as a planetary gear with many shafts, where $\boldsymbol{v_v} = [\omega_1, \omega_2, \cdots, \omega_3]$ are the rotational velocities of as many shafts as there are motion degrees of freedom. The relations between all the shafts' velocities can be found, through rather simple kinematic equations, and becomes $\boldsymbol{v_F} = \boldsymbol{R_v} \cdot \boldsymbol{v_v}$;. The relations between the shaft torques is then,

without setting up equilibria, $\boldsymbol{F_v} = \boldsymbol{R_F} \cdot \boldsymbol{F_F}$, with $\boldsymbol{R_F} = -\boldsymbol{S_v} \cdot \boldsymbol{R_v^T} \cdot \boldsymbol{S_F}$;. Neither translational velocities nor forces are present in this transmission example.

Another example is suspension linkage. For a suspension on a non-steered axle, one often use vertical velocity of the wheel hub as $\boldsymbol{v_v} = [v_{Hub,z}]$, i.e. a scalar. With kinematic equations, one can find $\boldsymbol{v_F} = \boldsymbol{R_v} \cdot \boldsymbol{v_v}$, where $\boldsymbol{v_F}$. The $\boldsymbol{R_v}$ has dimension 5×1. The relation between the forces is then, without setting up equilibria, $\boldsymbol{F_v} = \boldsymbol{R_F} \cdot \boldsymbol{F_F}$, with $\boldsymbol{R_F} = -\boldsymbol{S_v} \cdot \boldsymbol{R_v^T} \cdot \boldsymbol{S_F}$;. The $\boldsymbol{R_F}$ has dimension 1×5, so the $\boldsymbol{F_v} = [F_z]$ becomes a linear combination of $\boldsymbol{F_F} = [F_x, F_y, M_x, M_y, M_z]$. For a steered axle $\boldsymbol{v_v} = [v_{Hub,z}, v_{Rack}]$.

In the examples in Figure 1-35, these equations correspond to:

1.5.2.4.3.1 Transmission example:

We select 3 cuts which are the 3 shaft ends: $\{\{\omega_1, T_1\}, \{\omega_2, T_2\}, \{\omega_3, T_3\}\}$. The positive directions of the speeds and torques are chosen so that $P_i = \omega_i \cdot T_i$ becomes the power from left to right, which is assumed to be the engineer's intended "design direction" for the power transmission. The selection leads to $S_1 = S_2 = +1$ and $S_3 = -1$. $\boldsymbol{S} = \mathbf{diag}(\{+1, +1, -1\})$.

$$\text{Compatibility} \Rightarrow \quad \frac{\omega_1 - \omega_2}{\omega_3 - \omega_2} = -\frac{53}{27}; \Rightarrow \quad \underbrace{[\omega_1]}_{\boldsymbol{v_F}} = \underbrace{\begin{bmatrix} \frac{80}{27} & \frac{-53}{27} \end{bmatrix}}_{\boldsymbol{R_v}} \cdot \underbrace{\begin{bmatrix} \omega_2 \\ \omega_3 \end{bmatrix}}_{\boldsymbol{v_v}};$$

Then we have selected that cut 1 is the "F cuts" and cuts 2 and 3 are "v cuts". So:

$$\text{Power equilibrium} \Rightarrow \quad \boldsymbol{R_F} = -\boldsymbol{S_v} \cdot \boldsymbol{R_v^T} \cdot \boldsymbol{S_F}; \Rightarrow \quad \boldsymbol{R_F} = -\underbrace{\begin{bmatrix} \underbrace{+1}_{S_2} & 0 \\ 0 & \underbrace{-1}_{S_3} \end{bmatrix}}_{\boldsymbol{S_v}} \cdot \begin{bmatrix} \frac{80}{27} & \frac{-53}{27} \end{bmatrix}^T \cdot \underbrace{[+1]}_{\boldsymbol{S_F} = S_1} = \begin{bmatrix} \frac{-80}{27} \\ \frac{-53}{27} \end{bmatrix};$$

$$\text{Insertion} \Rightarrow \quad \underbrace{\begin{bmatrix} T_2 \\ T_3 \end{bmatrix}}_{\boldsymbol{F_v}} = \underbrace{\begin{bmatrix} \frac{-80}{27} \\ \frac{-53}{27} \end{bmatrix}}_{\boldsymbol{R_F}} \cdot \underbrace{[T_1]}_{\boldsymbol{F_F}}; \quad \text{(which is also deriveable from (force) equilibrium)}$$

1.5.2.4.3.2 Suspension in xz-view example:

We select 6 cuts: $\{\{v_x, F_x\}, \{v_z, F_z\}, \{\omega, M\}, \{v_{vx}, F_{vx}\}, \{v_{vz}, F_{vz}\}, \{v_s, F_s\}\}$. The selected signs give the S_i, in same order, as $\{+1, +1, +1, -1, -1, -1\}$. Here, the positive directions were chosen as if power transmission was from the wheel's ground contact to vehicle body.

$$\text{1 force and 2 moment equilibria} \Rightarrow \left\{ \begin{matrix} F_x - F_{vx} = 0; \\ M + (F_s - F_z) \cdot g_p - F_x \cdot e_p = 0; \\ M - F_{vz} \cdot g_p - F_x \cdot e_p = 0; \end{matrix} \right\} \Rightarrow \underbrace{\begin{bmatrix} F_{vx} \\ F_z \\ F_{vz} \end{bmatrix}}_{\boldsymbol{F_v}} = \underbrace{\begin{bmatrix} 0 & 1 & 0 \\ 1 & \frac{-e_p}{g_p} & \frac{1}{g_p} \\ 0 & \frac{-e_p}{g_p} & \frac{1}{g_p} \end{bmatrix}}_{\boldsymbol{R_F}} \cdot \underbrace{\begin{bmatrix} F_s \\ F_x \\ M \end{bmatrix}}_{\boldsymbol{F_F}};$$

Then we have selected which are the "F cuts" and which are the "v cuts". So:

$$\text{Power equilibrium} \Rightarrow \quad \boldsymbol{R_v} = -\boldsymbol{S_F} \cdot \boldsymbol{R_F^T} \cdot \boldsymbol{S_v}; \Rightarrow$$

$$\Rightarrow \boldsymbol{R_v} = -\begin{bmatrix} -1 & 0 & 0 \\ 0 & +1 & 0 \\ 0 & 0 & +1 \end{bmatrix} \cdot \begin{bmatrix} 0 & 1 & 0 \\ 1 & \frac{-e_p}{g_p} & \frac{1}{g_p} \\ 0 & \frac{-e_p}{g_p} & \frac{1}{g_p} \end{bmatrix}^T \cdot \begin{bmatrix} -1 & 0 & 0 \\ 0 & +1 & 0 \\ 0 & 0 & -1 \end{bmatrix} = \begin{bmatrix} 0 & 1 & 0 \\ 1 & \frac{e_p}{g_p} & \frac{-e_p}{g_p} \\ 0 & \frac{-1}{g_p} & \frac{1}{g_p} \end{bmatrix};$$

Insertion ⇒ $\underbrace{\begin{bmatrix} v_s \\ v_x \\ \omega \end{bmatrix}}_{\boldsymbol{v_F}} = \underbrace{\begin{bmatrix} 0 & 1 & 0 \\ 1 & \frac{e_p}{g_p} & \frac{-e_p}{g_p} \\ 0 & \frac{-1}{g_p} & \frac{1}{g_p} \end{bmatrix}}_{\boldsymbol{R_v}} \cdot \underbrace{\begin{bmatrix} v_{vx} \\ v_z \\ v_{vz} \end{bmatrix}}_{\boldsymbol{v_v}}$;

This (kinematic) relation between velocities can also be derived from compatibility, but it is often easier via these matrix operations. It also gives the insight that force and velocity relations in a mechanism are each other's transposed relations, if neither power accumulation nor losses in the mechanism.

1.5.2.4.3.3 Suspension in *yz*-view example:

In this example, we show another approach: We include the body in the mechanism and select 3 cuts: $\{\{v_y, F_y\}, \{v_z, F_z\}, \{\omega, M\}\}$. The selected signs give the S_i, in same order, as $\{+1, +1, +1\}$. Here, the positive directions were chosen as if power input in the wheel's ground contact; and there is no power output cut, since the body is included in the mechanism.

There is only 1 equilibria which only involves the cut forces and it is the moment equilibrium of the wheel and link around "$\star$": $\{M + F_z \cdot f_p + F_y \cdot h_p = 0;\} \Rightarrow \underbrace{[F_z]}_{\boldsymbol{F_v}} = \underbrace{\begin{bmatrix} \frac{-h_p}{f_p} & \frac{-1}{f_p} \end{bmatrix}}_{\boldsymbol{R_F}} \cdot \underbrace{\begin{bmatrix} F_y \\ M \end{bmatrix}}_{\boldsymbol{F_F}}$;

Then we have selected which are the "F cuts" and which are the "v cuts". So:

Power equilibrium ⇒ $\boldsymbol{R_v} = -\boldsymbol{S_F} \cdot \boldsymbol{R_F^T} \cdot \boldsymbol{S_v}; \Rightarrow \boldsymbol{R_v} = -\begin{bmatrix} +1 & 0 \\ 0 & +1 \end{bmatrix} \cdot \begin{bmatrix} \frac{-h_p}{f_p} & \frac{-1}{f_p} \end{bmatrix}^T \cdot [+1] = \begin{bmatrix} \frac{-h_p}{f_p} \\ \frac{-1}{f_p} \end{bmatrix}$;

Insertion ⇒ $\underbrace{\begin{bmatrix} v_y \\ \omega \end{bmatrix}}_{\boldsymbol{v_F}} = \underbrace{\begin{bmatrix} \frac{-h_p}{f_p} \\ \frac{-1}{f_p} \end{bmatrix}}_{\boldsymbol{R_v}} \cdot \underbrace{[v_z]}_{\boldsymbol{v_v}}$;

If angles are large and we want to follow what happens in a dynamic model, we would have to use a position variable as state variable, e.g. h_z, with the additional equations $\dot{h}_p = -v_z$; and $\dot{f}_p = \frac{h_p}{f_p} \cdot v_z$;.

A drawback with this (which is to avoid compatibility in positions) is that the measure $\sqrt{h_p^2 + f_p^2}$ may vary a bit due to numerical imperfections in a numerical simulation.

1.5.2.4.3.4 Discussion of examples

For the suspension examples, it is intuitive to use $\boldsymbol{v_v} = [v_z]$, because one usual think of the suspension as mainly allowing vertical deformation. There are also needs for extensions:

Expanding to 3D, which would expand to $\boldsymbol{v} = [v_x \quad v_y \quad v_z \quad \omega_x \quad \omega_y \quad \omega_z]^T$

For a steered axle: to $\boldsymbol{v_v} = [v_z \quad \omega_z]^T$

In case of a rigid axle: Treat both wheels on an axle together, which means: $\boldsymbol{v} = [v_{lx} \quad v_{ly} \quad v_{lz} \quad \omega_{lx} \quad \omega_{ly} \quad \omega_{lz} \quad v_{rx} \quad v_{ry} \quad v_{rz} \quad \omega_{rx} \quad \omega_{ry} \quad \omega_{rz}]^T$, where subscript l and r refers to *left* and *right*. There can be constraints between these variables, e.g. $\omega_{lx} = \omega_{rx}$ if non-steered rigid axle.

If the system studied has energy storage or power dissipation included, they can often be defined as outside the mechanism, only leading to more interfaces. However, if the energy dissipation is of dry friction type, this is not easily possible. Instead, the geometry can be adjusted via a geometry interpretation of dry friction, using a friction angle which defines a corrected geometry, see (Mägi,

Jacobson, & Resev, 1998). Note that the proportional relations, i.e., $\boldsymbol{R_v}$ and $\boldsymbol{R_F}$, are only valid close around a certain position state or pose.

One can integrate the velocities to positions (including angles), so $\boldsymbol{R_v}$ and $\boldsymbol{R_F}$ can be updated during the simulation. For that reason, it is a large advantage with symbolically expressed $\boldsymbol{R_v}$ and $\boldsymbol{R_F}$.

1.5.2.4.4 Constitution

Constitution are relations between forces (including moments) and motions, e.g.

- For a (linear) spring: $Force = F_0 + c \cdot Deformation$; or $\frac{d}{dt} Force = c \cdot DeformationSpeed$;. Metallic materials typically follow such linear behaviour, cf. Hooks law, if not deformed too much or too fast.
- For a (linear) damper: $Force = d \cdot DeformationSpeed$;. Shearing of thin liquid films typically follows such linear behaviour, e.g., in lubricated bearing where shear force is proportional to sliding speed.
- For a dry friction contact: $Force = Constant \cdot sign(SlidingSpeed)$;. This is the most common friction model in mechanical engineering, explained by adhesion between molecules and hysteresis when material is deforming over micro level asperities. So, the proportionality constant depends on both cooperating bodies material and surface roughness. Note: When a friction contact sticks, the equation switches to a compatibility equation ($SlidingSpeed = 0$;). The $Constant$ for dry friction is often called friction coefficient and denoted μ. The μ has the unit either [1], $[N/N]$, or $[N_{xy}/N_z]$. The separation in N_{xy}="Newtons in contact plane" and N_z="Newtons perpendicular to contact plane" can sometimes help the understanding.
- For a more general model component: $Force = function(Position, Speed)$;. Even more general would include models of actuators: $Force = function(Position, Speed, Signal)$;, where $Signal$ often is a request signal, e.g., $ForceRequest$.

This book uses c for stiffness [N/m or N/(m/s)] and d for damper coefficient [N/(m/s) or Nm/(rad/s)]. It is often used in German and Swedish engineering, while k and c, is more often used in English-speaking engineering.

1.5.2.4.4.1 Higher dimensionality

Above in 1.5.2.4.4, only the 1D variants of constitutive equations was presented. As higher dimension equilibrium equations were presented in 1.5.2.4.1, also higher dimension variants of constitutive equations can be needed. One such is the 2D variant of linear spring constitution:

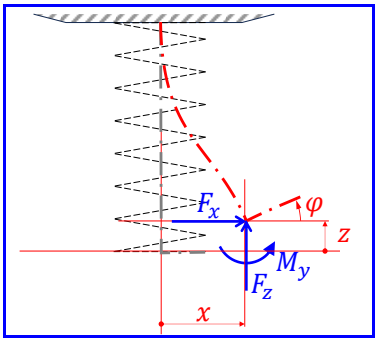


Figure 1-36: 2D spring model in xz-plane.

$$\begin{bmatrix} F_x \\ F_z \\ M_y \end{bmatrix} = \begin{bmatrix} c_{xx} & c_{xz} & c_{x\varphi} \\ c_{zx} & c_{zz} & c_{z\varphi} \\ c_{\varphi x} & c_{\varphi z} & c_{\varphi\varphi} \end{bmatrix} \cdot \begin{bmatrix} x \\ z \\ \varphi \end{bmatrix} = \left\{ \begin{matrix} energy \\ conservation \end{matrix} \right\} = \begin{bmatrix} c_{xx} & c_{xz} & c_{x\varphi} \\ c_{xz} & c_{zz} & c_{z\varphi} \\ c_{x\varphi} & c_{z\varphi} & c_{\varphi\varphi} \end{bmatrix} \cdot \begin{bmatrix} x \\ z \\ \varphi \end{bmatrix}; \quad [1.4]$$

This will be referred to when rolling resistance is discussed in 2.2.2.2.3.

1.5.2.4.5 Algorithms and Other Equation Types

The listing of equation types in 1.5.2.4.1, 1.5.2.4.1.3 and 1.5.2.4.4 is a help but not claimed to be complete. There are other equation types that can appear, e.g., from electrical and chemical

engineering. Among these others, “control algorithms and driver models” are especially important for vehicle dynamics, so they will be discussed here in 1.5.2.4.5.

Via sensors and actuators, control algorithms can operate with the mechanics, mechatronics. The control algorithms with their interface to sensors and actuators is here included in the equation type “algorithms”. We also include models of how the human driver controls and experience the mechanical quantities. This equation type cannot be sorted into the traditional 1.5.2.4.1..1.5.2.4.1.2. Conceptually, any quantities that can be sensed or actuated in, and outside of, the subject vehicle can occur in these equations. (Finite) State machines are often useful when modelling (and designing) algorithm-based functions but also the driver, see discrete state machine in 1.5.1.4.

A model of control algorithm can often be the same artefact as the design of it, especially if using a modelling tool that allows automatic generation of real-time code, like Simulink. However, note that the algorithms in real system is implemented in a time discrete digital computation platform and digital communication, so using a time continuous version as model is an approximation in itself. For best fidelity, the models need to be formulated as time discrete dynamics. Then one can properly represent the influence from the design parameter sample time on the vehicle functions.

1.5.3 Control Engineering

Vehicle dynamics is more and more influenced by electronics, where algorithms are the main artefact to engineer. For this reason, this section introduces some relevant theory and methods and their *connection to vehicle models as they are described in vehicle dynamics*. From Figure 1-37, we realize that there are many types of Vehicle Level Algorithms, and the Vehicle Motion Controller is maybe the most central for vehicle dynamics. It should be underlined that the control structure in today’s vehicles are not as clean and structured as in Figure 1-37, very much depending on that vehicle level control is distributed in several ECUs, each belonging to its own subsystem.

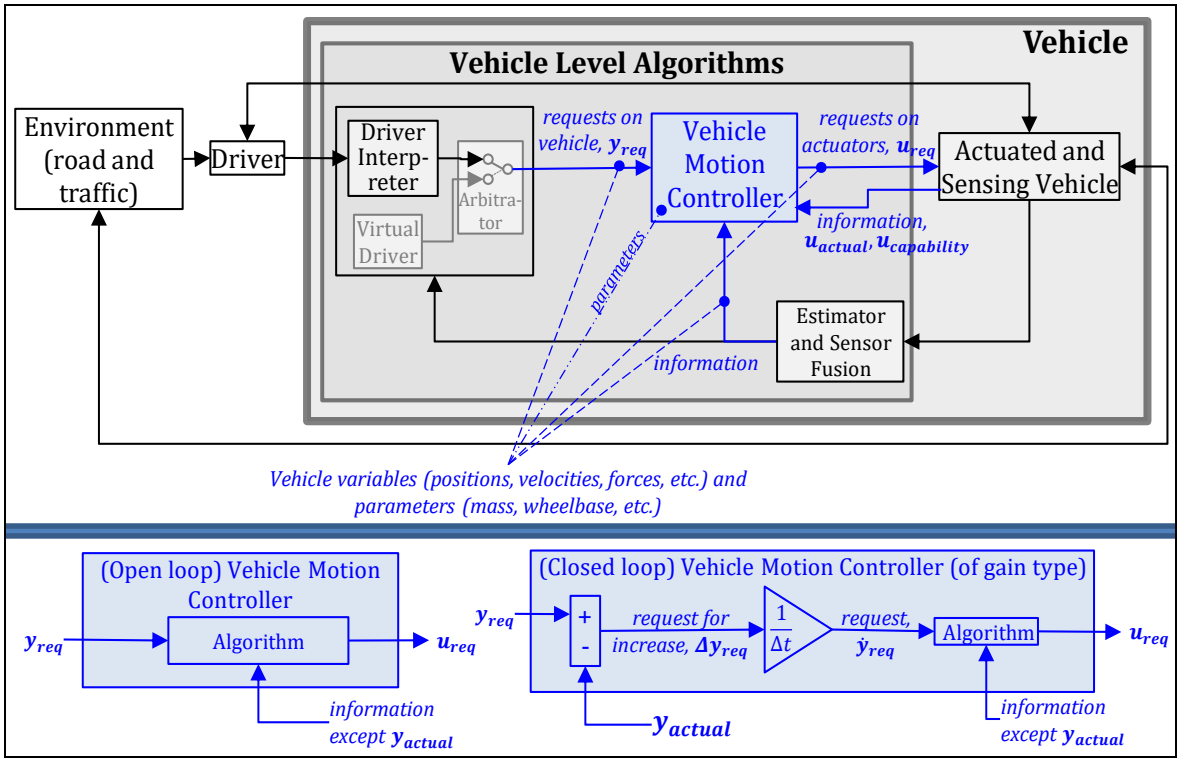


Figure 1-37: Context for Vehicle Level Algorithms and Vehicle (Motion) Controller. “Virtual Driver” takes vehicle driver into account and closes the loop in vehicle speed and lateral position.

Control algorithms can be designed without utilizing knowledge about the controlled system, such as neural networks, tuned only on observations on how the system responds. However, in this section we only consider Model based controllers. For those, the input and output signals, as well as parameters

inside, has a clear physical interpretation in vehicle quantities, as well as units, see Figure 1-38. For instance, the requests on vehicle, $\boldsymbol{y_{req}}$, is typically forces or acceleration, $\left[F_x[N]; F_y[N]; M_z[Nm]\right]$ or $\left[\dot{v}_x[m/s^2]; \dot{v}_y[m/s^2]; \dot{\omega}_z[rad/s^2]\right]$ or velocities $\left[v_x[m/s]; v_y[m/s]; \omega_z[rad/s]\right]$. The model base is helpful when tuning the controller parameters. Moreover, the model base helps to find a consistency between derivatives order in the controller and the controlled system, such as if P, I or D gains should be used in a PID-controller.

The $\boldsymbol{y_{Req}}$ contains typically vehicle **motion** variables (positions, velocities, accelerations, forces) but other vehicle variables, such as energy or power variables can be added, e.g. $\boldsymbol{y_{Req}} = \left[F_x; F_y; M_z; \dot{E}_{buff}\right]$, where E_{buff} is energy level (or state of charge SoC) in an energy buffer.

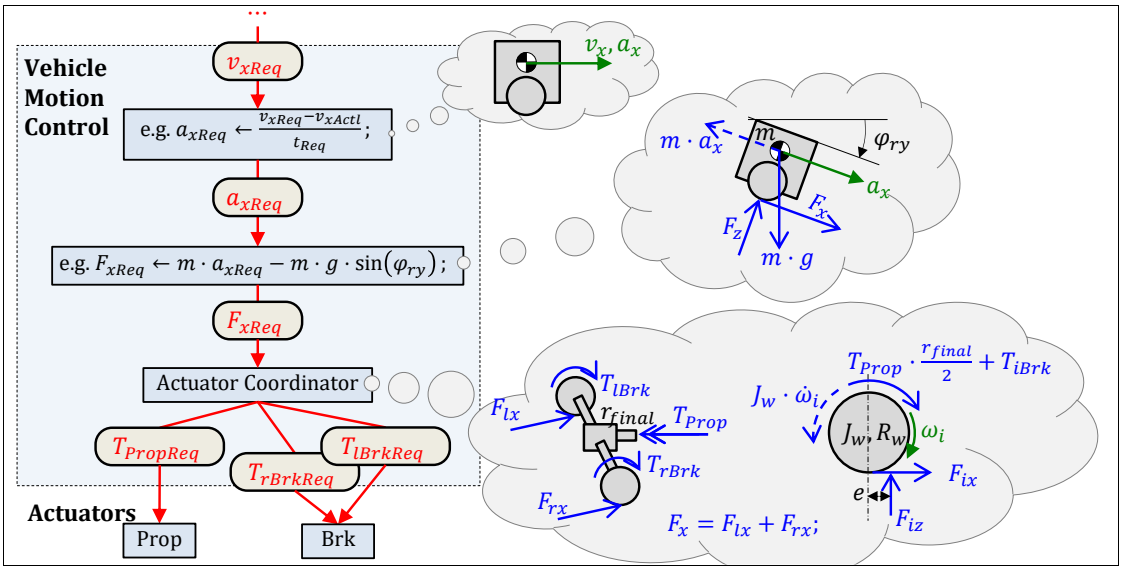


Figure 1-38: Request flow in Vehicle Motion Control. Each block has its own Physical model, which explains the its interface quantities (variables and parameters).

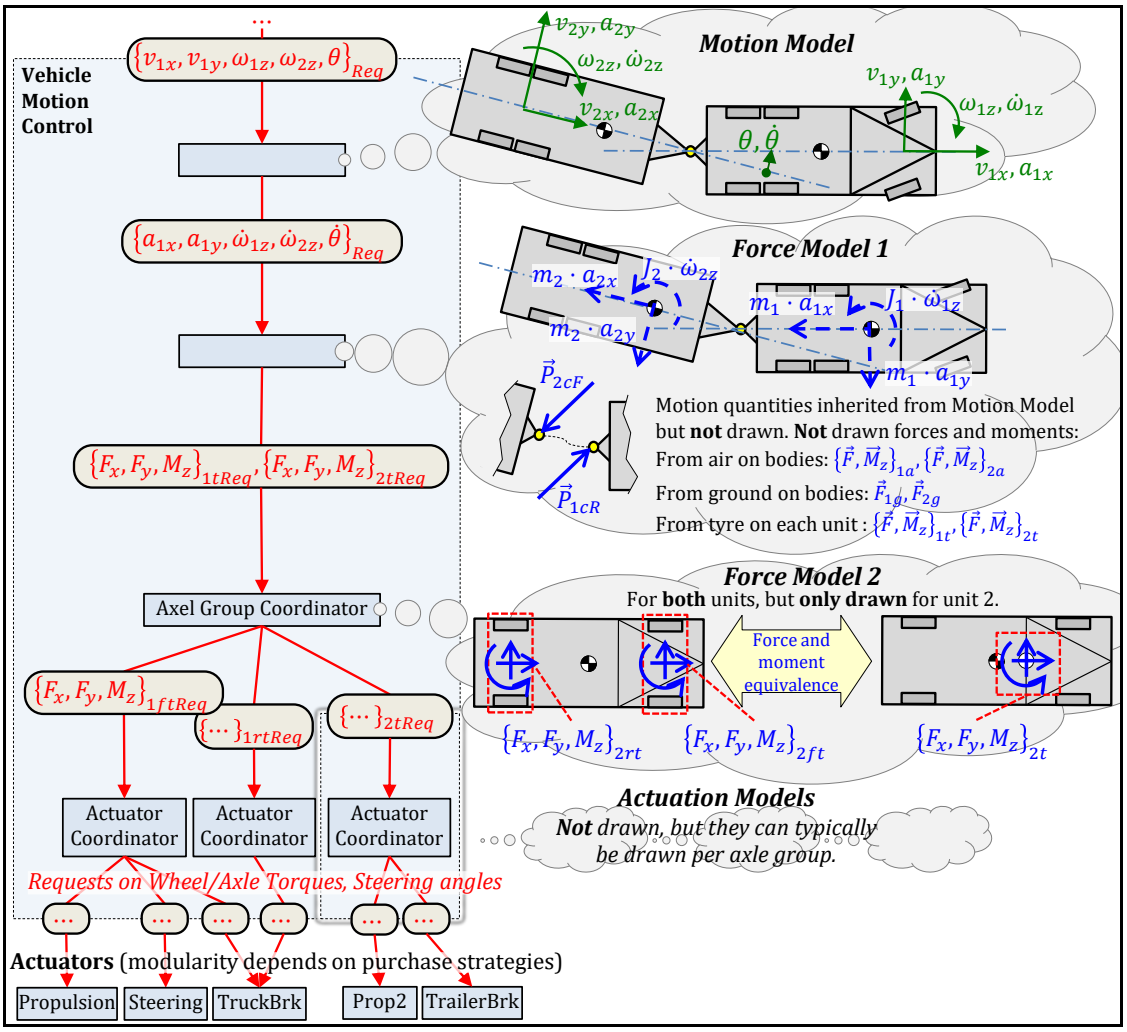


Figure 1-39: Like Figure 1-38, but for a more complex vehicle.

1.5.3.1 Decision Making or Execution

Nowadays, one can often hear *Decision-making algorithms* as an expression. It means some kind of rules for when to transit between discrete states, such as transit from LaneFollowing to LaneChange in automated driving or switching from Wheel Torque Control to Wheel Speed Control for ABS/TC-like functions. The complement to *Decision making* can be called *Actuation execution* and it would typically mean the computation of continuous request signals, such as Steering Wheel Angle Request or Brake Pressure Request, in the two above examples.

1.5.3.2 Momentaneous or Predictive Control

If the controller considers the future (predicted) of its input $\boldsymbol{y_{req}}$ and/or output $\boldsymbol{u_{req}}$, the controller uses ***Predictive control***. If the controller was designed to consider both its input $\boldsymbol{y_{req}}$ and output $\boldsymbol{u_{req}}$ at same time instant, the controller uses ***Momentaneous control*** (or *Instantaneous control*). This categorization is often useful. The future of the input cannot be known, so future of inputs $\boldsymbol{u_{req}}$ should be seen as prediction e.g., expressed in time or desired path ahead. A predictive controller generally needs a model of the environment and vehicle such that the consequences (cost [€] and possibly constraints [*pass or fail*] can be predicted for different candidates of $\boldsymbol{u_{req}}$. See 3.5.2.3.1.

A reason to do predictive control, as opposed to the simpler momentaneous control, is that the control objective requires some strategic planning over future time. One example can be fuel consumption, where the objective is an integral over future time, $Fuel = \int FuelRate \cdot dt$;, where a high $FuelRate$ can be good initially (momentaneously) to minimize $Fuel$. Another example is how to keep high

transport speed while negotiating a curve, where it is generally more strategically optimal to brake before steering. The objective is an integral $Position = \int Velocities \cdot dt$;. See (Ross,2015).

In the context of predictive control using models (a.k.a. Model Predictive Control (MPC)), there are typically 3 time intervals to differ between, listed in decreasing size:

- **Prediction horizon**: This is the future time period over which predictions are made and control actions planned.
- **Sampling time**: Also known as the time between predictions are made and control actions are updated.
- **Grid size within each prediction**: This refers to the discretization of the prediction horizon into smaller time steps or intervals, e.g. used for prediction through simulation of a dynamic model of the system.

In 1.5.3.3 and 1.5.3.4, momentaneous control will be assumed unless else is stated.

An example of difference can be that the driver interpreter can output momentary $\boldsymbol{y_{req}}$ such as $[F_x; F_y; M_z]$ or $[\dot{v}_x; \dot{v}_y; \dot{\omega}_z]$ and an energy management in line with this would output $[\dot{E}_{buff}]$. A predictive version of $\boldsymbol{y_{req}}$ is typically $[F_x(t); F_y(t); M_z(t)]$ or $[v_x(t); v_y(t); \omega_z(t)]$ and $[E_{buff}(t)]$, where $\cdots(t)$ marks that the request is then a plan ahead in time. The plan can also be in travelled distance ahead, $\cdots(s)$.

1.5.3.3 Open or Closed Loop Control

As indicated already in Figure 1-37, a ***Closed Loop control*** uses the actual value ($\boldsymbol{y_{actual}}$) of the requested quantity $\boldsymbol{y_{req}}$. Else it is an ***Open Loop control***, which can also be called *Feed Forward control* or *Inverse Model Control*.

A driver is in the loop can correct errors, so Open Loop often works well enough. Especially if the driver is given good feedback, e.g., good steering feel. When automation of driving there is a motivation to go towards more Closed-loop control. However, there can be architectural benefits to close the loop in the Virtual driver instead of the Vehicle Motion Controller, see Figure 1-37, so that same algorithms can used in Vehicle Motion Controller for manual and for automatic driving.

A more including definition of closed loop controller is that the controller uses any signal from the controlled object, not exclusively whether it uses v_{actual}. With that definition, almost all controllers become closed loop controllers. An example is an open-loop controller for a cruise control function: $F_{x,req} \leftarrow m \cdot \dot{v}_{x,req} + F_{x,res}$;. Here, the requested vehicle quantity is acceleration ($\dot{v}_{x,req}$) but the used information about the vehicle is not $\dot{v}_{x,actual}$ but estimated mass (m) and estimated driving resistance force ($F_{x,res}$). These estimated quantities are typically updated much slower than the request control loop, but they are still a kind of closed loop. With the initial definition, it is open loop controller, but with the more including definition it would be a closed loop controller.

The cruise controller example above is an example of Open Loop control where the *Inverse model* is very clear: $\dot{v}_x \leftarrow (F_x - F_{x,res})/m$;. The most common implementation of Closed Loop is when the control error is calculated as an intermediate quantity. In the cruise control example, it would be $\dot{v}_{x,error} \leftarrow \dot{v}_{x,actual} - \dot{v}_{x,req}$; or with opposite sign it is rather a differential request $\Delta\dot{v}_{x,req} \leftarrow \dot{v}_{x,req} - \dot{v}_{x,actual}$ $(= -\dot{v}_{x,error})$;. A ***Gain controller*** could then be: $F_{x,req} \leftarrow Gain \cdot \Delta\dot{v}_{x,req}$;. This can be called a P-control on acceleration or D-control on velocity. The model connection is not obvious since one cannot directly see that $Gain$ corresponds to mass and resistance force is not even present. A similar gain controller could be formulated in another differentiation order, such as velocity instead of acceleration: $F_{x,req} \leftarrow Gain \cdot \Delta v_{x,req}$;. This can be called P-control on velocity, I-control on acceleration or D-control on position. The model ($F_x = m \cdot \dot{v}_x$;) combined with the controller ($F_{x,req} \leftarrow Gain \cdot \Delta v_{x,req}$;) points out that $Gain$ should be seen as $mass/time$, where $time$ is the time to when $v_{x,req}$ should be reached. Interpretation of gains to physical quantities with units is encouraged, since it facilitates tuning and reuse of the controller. Such interpretation requires a physical model.

It is typical for automotive engineering, that algorithms are reused, and sometimes incrementally developed, from one platform or vehicle programme to the next. Hence, given a certain controller, it is

very relevant to understand/derive its model base, for efficient parameter setting. However, it is important to realize that it is not generally possible to derive the model base from a given controller. So, the controller really has to be developed from a physical model. So, the documentation of which physical model is used is very important output from the control design, beside the controller itself. The documentation should include model equations and declarations of variables and parameters so that next vehicle programme can inherit this as document.

1.5.3.4 Degree of Over-Actuation

Already before designing the controller, it is often clear what vehicle requests $\boldsymbol{y_{req}}$ and actuateable quantities $\boldsymbol{u_{req}}$ there are. The number (or dimension=dim) of those enables one categorization:

- If $dim(\boldsymbol{u_{req}}) = dim(\boldsymbol{y_{req}})$, the vehicle is (formally) **Neutral actuated**.
- If $dim(\boldsymbol{u_{req}}) < dim(\boldsymbol{y_{req}})$, the vehicle is (formally) **Under-actuated** ($\boldsymbol{u_{req}}$ is over-determined)
- If $dim(\boldsymbol{u_{req}}) > dim(\boldsymbol{y_{req}})$, the vehicle is (formally) **Over-actuated** ($\boldsymbol{u_{req}}$ is under-determined). In a function architecture, this requires a Coordinator in 1.6.4.2.

Consider that the vehicle model is $\boldsymbol{f_{DAE}}(\boldsymbol{x}, \boldsymbol{u}, \boldsymbol{y}, t) = 0$;, or in explicit form $[\dot{\boldsymbol{x}} \quad \boldsymbol{y}] = [\boldsymbol{f_{ODE}}(\boldsymbol{x}, \boldsymbol{u}, t) \quad \boldsymbol{g}(\boldsymbol{x}, \boldsymbol{u}, t)]$;. With such a model, we can include saturations (actuators saturated or road friction saturated) and dependencies between actuators (e.g. >1 torque actuator acting on one wheel). Instead of dimension, we define the property "*rank of the model*" as the number of dimensions that the vehicle motion can be influenced in by the available actuators. Using a linearization of the model, we can find $\boldsymbol{B}$ such that:

$$\boldsymbol{y} \approx \boldsymbol{g}(\boldsymbol{x_0}, \boldsymbol{u_0}, t_0) + \boldsymbol{B}(\boldsymbol{x_0}, \boldsymbol{u_0}, t_0) \cdot (\boldsymbol{u} - \boldsymbol{u_0}) = \boldsymbol{g_0} + \boldsymbol{B}(\boldsymbol{x_0}, \boldsymbol{u_0}, t_0) \cdot (\boldsymbol{u} - \boldsymbol{u_0});$$

$$where\ \boldsymbol{B}\ has\ \dim(\boldsymbol{y})\ rows\ and\ \dim(\boldsymbol{u})\ columns\ and\ B_{ij} = \frac{\partial g_i}{\partial u_{reqj}};$$

$$"Rank\ of\ model" = \operatorname{rank}(\boldsymbol{B}).$$

The controller should then aim at finding $\boldsymbol{u_{req}}$ so that $\boldsymbol{y_{req}} - (\boldsymbol{g_0} - \boldsymbol{B} \cdot \boldsymbol{u_0}) = \boldsymbol{B} \cdot \boldsymbol{u_{req}}$;. We identify "virtual requests" $\boldsymbol{v_{req}} = \boldsymbol{y_{req}} - (\boldsymbol{g_0} - \boldsymbol{B} \cdot \boldsymbol{u_0})$; of same dimension as $\boldsymbol{y_{req}}$, so $\boldsymbol{v_{req}} = \boldsymbol{B} \cdot \boldsymbol{u_{req}}$;.

The rank of $\boldsymbol{B}$ (or any matrix) is the number of non-zero diagonal elements in the middle matrix $\boldsymbol{S}$ in the singular value decomposition of $\boldsymbol{B}$, $svd(\boldsymbol{B}) = \boldsymbol{U} \cdot \boldsymbol{S} \cdot \boldsymbol{V}^T$;. Using the rank, we can define degree of over-actuation in a way which better helps us differ between different control design types, see also Figure 1-40:

- If $\dim(\boldsymbol{u_{req}}) = \operatorname{rank}(\boldsymbol{B})$, the vehicle is (effectively) **Neutral actuated**.
  Conceptually, $\boldsymbol{u_{req}}$ could be calculated from $\boldsymbol{v_{req}}$, using the model, which would be an Inverse model control design: $\boldsymbol{u_{req}} \leftarrow \boldsymbol{B^{-1}} \cdot \boldsymbol{v_{req}}$;.
- If $\dim(\boldsymbol{u_{req}}) < \operatorname{rank}(\boldsymbol{B})$, the vehicle is (effectively) **Under-actuated** ($\boldsymbol{u_{req}}$ is over-determined). If actuators cannot be added and requests cannot be disregarded, one has to apply optimization, e.g., to minimize $f_{cost} = \left\| \boldsymbol{y_{req}} - \boldsymbol{g}(\boldsymbol{x}, \boldsymbol{u_{req}}, t) \right\|$; with some weigths on the components. There is generally a unique optimum. If we can use the linear model and set weight factors, we can rewrite to minimizing the $f_{cost} = \left\| \boldsymbol{W_v} \cdot (\boldsymbol{v_{req}} - \boldsymbol{B} \cdot \boldsymbol{u_{req}}) \right\|_2$;, where $\boldsymbol{W_v}$ is a square weight matrix. Optimizing in *Least Square sense* (a.k.a. using the *Pseudo-inverse*) gives $\boldsymbol{u_{req}} = ((\boldsymbol{W_v} \cdot \boldsymbol{B})^T \cdot \boldsymbol{W_v} \cdot \boldsymbol{B})^{-1} \cdot (\boldsymbol{W_v} \cdot \boldsymbol{B})^T \cdot \boldsymbol{W_v} \cdot \boldsymbol{v_{req}} = (\boldsymbol{W_v} \cdot \boldsymbol{B})^{\dagger} \cdot \boldsymbol{W_v} \cdot \boldsymbol{v_{req}}$;.
- If $\dim(\boldsymbol{u_{req}}) > \operatorname{rank}(\boldsymbol{B})$, the vehicle is (effectively) **Over-actuated** ($\boldsymbol{u_{req}}$ is under-determined). Conceptually, there is no way to convert the problem to a Neutral actuated case (without disregarding actuators or adding requests), but one can find and approximate solution through optimization. Trying an optimization as for the under-actuated vehicle will not work well, since there are generally no unique solutions, i.e. $((\boldsymbol{W_v} \cdot \boldsymbol{B})^T \cdot \boldsymbol{W_v} \cdot \boldsymbol{B})$ is singular). One way to handle it would be to use some random way to find one $\boldsymbol{u_{req}}$ among all non-unique optima. This can lead to jumping $\boldsymbol{u_{req}}$ in time, which is undesirable. A second way is to convert the

problem to a Neutral actuated case by simply prescribing suitably many components in $\boldsymbol{u_{req}}$: $u_{req,i} = u_{des,i}$, where subscript *des* means desired. A third way is to to convert the problem into a Neutral- or Under-actuated case by adding equations for each and all components in $\boldsymbol{u_{req}}$, typically: $\boldsymbol{u_{req}} = \boldsymbol{0}$. To use zero is difficult to motivate directly from vehicle motion/actuation perspective but it can be thought of as a way to guaranteeing unique mathematical solutions, which is good.
Combining second and third way gives an optimization problem with cost function as follows: $f_{cost} = \left\|\boldsymbol{W_{motion}} \cdot \left(\boldsymbol{v_{req}} - \boldsymbol{B} \cdot \boldsymbol{u_{req}}\right)\right\|_2 + \sum\left\|W_{act,i} \cdot \left(u_{req,i} - u_{des,i}\right)\right\|_2 + \left\|\boldsymbol{W_{smooth}} \cdot \boldsymbol{u_{req}}\right\|_2$;.
The $\boldsymbol{W}$ matrices are diagonal matrices with weight factors. For solving such mathematical problems there are well established subroutines for **Control allocation, CA,** which can also take constraints into account.

A visualisation of these cases and solution is given in Figure 1-40.

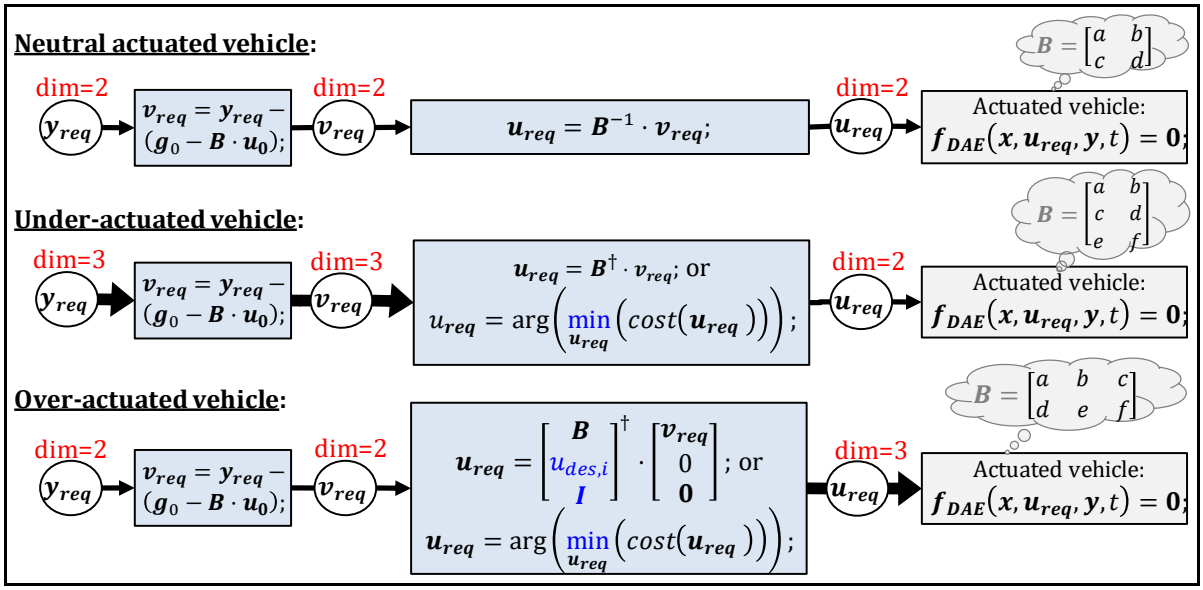


Figure 1-40: Visualisation of possible conceptual controllers for vehicles with different degree of over-actuation. Superscript $\cdots^{\dagger}$ denotes "quasi-inverse". Weighting is not shown.

1.5.3.4.1 Momentaneous Optimization

Note that the weighting is not shown in Figure 1-40. The weighting is probably the most difficult, in some sense, one has to compare costs for different motion components, so if simple weight matrix, its components should typically have the units $[€/N]$ in longitudinal and $[€/N]$ in lateral which is very difficult to set and might vary with such as distance to lead vehicle and distance to road edge. Also, if y_{req} includes energy related requests, the units can be of type $[€/J]$ depending on the fuel or electric energy price. So, the approach described above is very mathematical and a bit naive when we see the original engineering problem.

Instead of a naive weighting "outside" the model, we can include the cost as a variable already in our model. The cost will then appear more intuitive and less artificial. Typically, one sees two types of cost variables: *cost* in [€] and *costRate* in $[€/s]$. For transport costs (fuel, driver salary, etc) these are often very natural. For motion they are still very difficult to grasp, which suggest looking for ways to see motion requests as constraints (to fulfil exactly) and transport costs as costs (to be minimized).

Looking only at transport costs, one realizes that the overall goal is to minimize the *cost* [€], but that has to be done predictive, i.e. by integrating *costRate* $[€/s]$ over a longer time, see 1.5.3.2 and 1.5.3.4.2. However, if the motion constraints should be fulfilled as constraints over the time, it is probably a good idea to minimize *costRate* $[€/s]$ momentanously (at each time instant) such that the momentaneous motion constraints are fulfilled.

An example of such optimization is given here: A vehicle with two propulsion motors, subsrcitps 1 and 2, is modelled as:

$$m \cdot a_x = F_x;$$
$$F_x = ratio \cdot (T_1 + T_2);$$
$$\omega_1 = \omega_2 = ratio \cdot v_x;$$
$$fuelRate = f_1(T_1, \omega_1) + f_2(T_2, \omega_2);$$
$$costRate = fuelRate \cdot fuelPrice;$$

The $\boldsymbol{v_{Req}} = [a_{xReq}]$ and $\boldsymbol{u_{Req}} = [T_1, T_2]$.

Minimizing $costRate$ under constraint of fulfilling motion request a_{xReq}:

$$\{T_1, T_2\} = \arg\left(\min_{T_1,T_2}\left(costRate(T_1, T_2)\right) \quad subject\ to \quad m \cdot a_{xReq} = ratio \cdot (T_1 + T_2);\right);$$
$$\text{where} \quad costRate(T_1, T_2) = \left(f_1(T_1, ratio \cdot v_x) + f_2(T_2, ratio \cdot v_x)\right) \cdot fuelPrice;$$

There are methods to find the optimum for certain forms of the $costRate$ and the constraint. One example is quadratic programming (e.g., Matlab command `quadprog`), which assumes that $costRate$ can be formulated on a quadratic form:

$$costRate = \frac{1}{2} \cdot \boldsymbol{u_{Req}^T} \cdot \boldsymbol{Q} \cdot \boldsymbol{u_{Req}} + \boldsymbol{f^T} \cdot \boldsymbol{u_{Req}}; \quad subject\ to \quad \boldsymbol{B} \cdot \boldsymbol{u_{Req}} = \boldsymbol{v_{Req}};$$

This form includes both linear and quadratic terms, so coefficient can often be found which makes a rather good approximation.

1.5.3.4.2 Momentaneous and Predictive Optimization

The above in the 1.5.3.4 could be applied also for predictive control if we think of $\boldsymbol{u_{req}}$ and $\boldsymbol{y_{req}}$ as having N times more elements, where N is the number of time instants considered in the prediction. The model can be applied N times, and if it contains state variable, a time integration method is needed to make the sequences of each variable consistent. If model is linear and optimization is to be applied, there are cooking-book methods, such as **Model Predictive Control (MPC)**, see e.g. Ref (Ross,2015), describes MPC. Simply adding more time instants adds equally many equations as unknowns ($\boldsymbol{u_{req}}$), so it does not change the degree of over-actuation. However, if the variation of $\boldsymbol{u_{req}}(t)$ is parameterised (e.g. $\boldsymbol{u_{req}}(t) = \boldsymbol{p}$; or $\boldsymbol{u_{req}}(t) = \boldsymbol{p_1} + \boldsymbol{p_2} \cdot t$;), the problems becomes as under-actuated, which is more well-conditioned and can be solved in a least square sense.

Over actuated passenger car can appear if each wheel has controllable actuation, see (Jonasson, 2009).

1.5.3.5 Filtering, Estimation and Differentiation

Filtering is often used to reduce noise in measurements of variables. The result is a smoother signal of the same quantity. We can also use filters to do variable *estimation*. This is good because it can avoid a sensor which can be expensive. Such filter can be called *estimators* (or *observers*) and they are typically based on a physical model so that input is one quantity and output is another quantity, e.g. $F_{est} = m \cdot a_{est} = m \cdot d/dt\ (v_{sensed})$;, where d/dt require a filter to implement.

The result from the filter can either be needed on-line as input to a controller in real-time (during use of the vehicle) or off-line (post-processing) after the measurement. On-line filters can only use the history of the signal which is why they always cause some time delay. Off-line filters can use the logged signal both before and after, by which time delays can be avoided.

Having a model, one can differ between if it is a variable or a parameter that is estimated. (Whether a physical quantity is a variable or a parameter is cannot be uniquely decided in the real world.) Generally speaking, *variable estimation* is more typically on-line filtering while *parameter estimation* can have more of off-line character. Off-line can log several data samples and then find (the constant) parameter value, best fitted for the whole sample period, e.g. in least square sense. Parameter

estimation can also be recursive, which means that each new sample is weighted with previous parameter estimate; so the estimate is a memory, i.e. a state.

1.5.3.5.1 Filter and differentiator

Figure 1-41 shows an example of an on-line filter is a first order filter. Figure also shows a simple (approximate) differentiator. Figure shows both continuous and discrete implementation in a block diagram format. Implementation of discrete integration using "`when sample()`" statements and the `pre()` operator in Modelica was shown in 1.5.1.4.

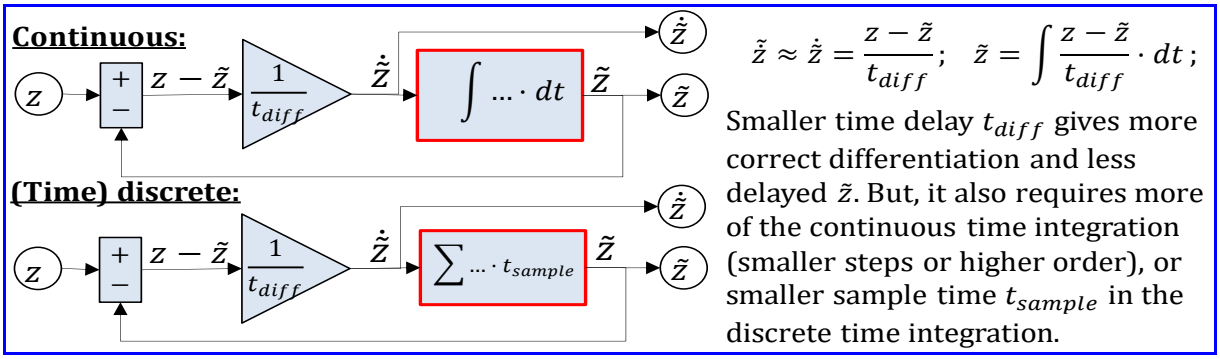


Figure 1-41: Example of differentiator (output $\dot{\tilde{z}}$) and on-line filter (output y) as block diagram. Upper: Continuous. Lower: (Time) Discrete. A smaller t_{diff} "drives" the $\tilde{z}$ faster to z. (In Simulink, the continuous integrator block is named "$1/s$" and the discrete one is named "$t_{sample}/(z-1)$".)

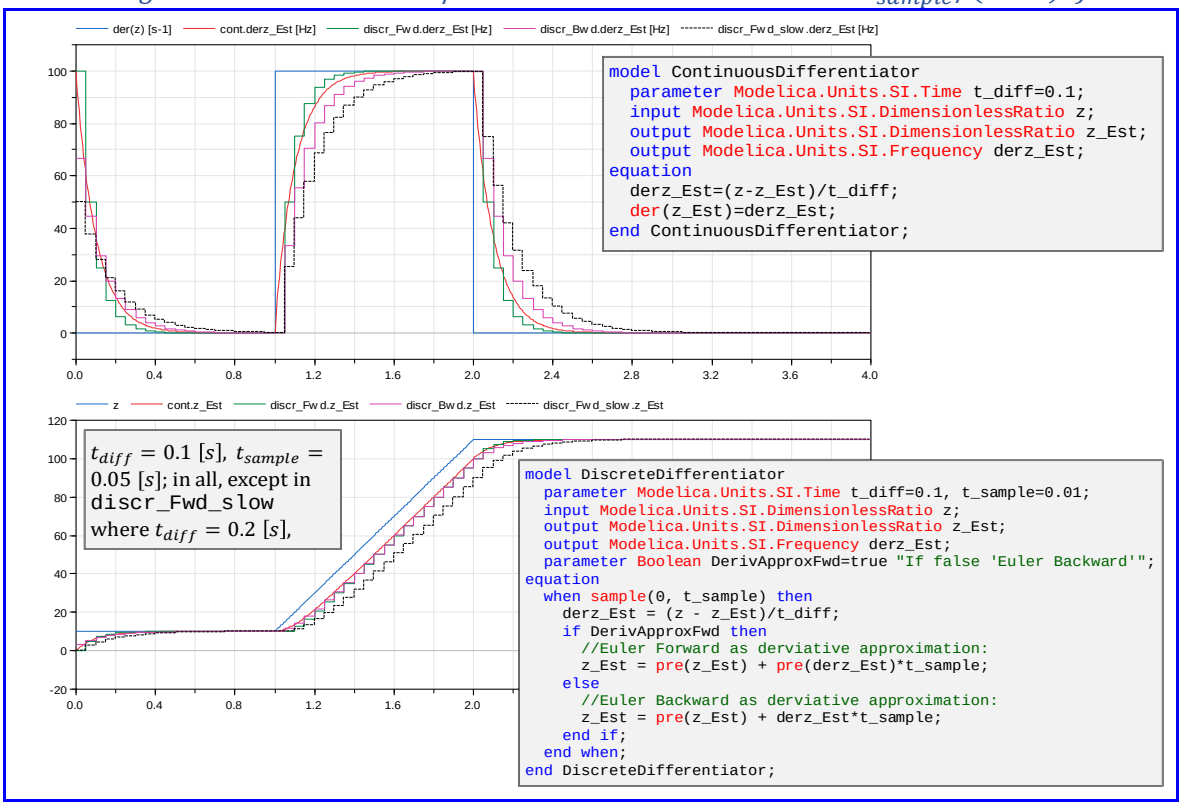


Figure 1-42: Example of continuous and discrete differentiators.

In dynamic models for simulation, one should avoid differentiation because it introduces delays which can lead to numerically unstable or wrong solutions. Off-line differentiation is much less troublesome. However, if the derivative is not fed back, the problems become isolated with less risk for troubles.

1.5.3.5.1.1 Higher order differentiators

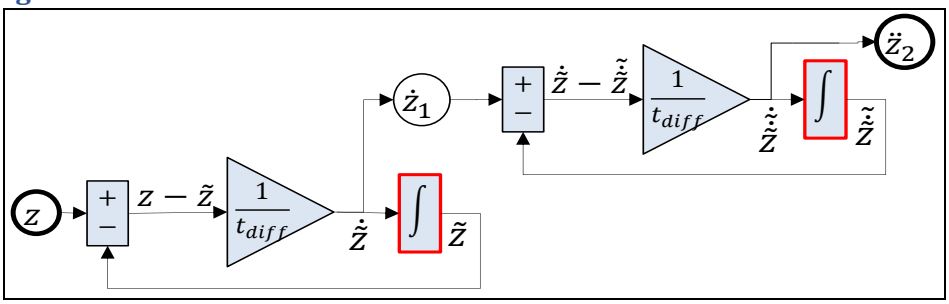


Figure 1-43: Example of 2nd order differentiator (output $\ddot{z}_2 \approx \frac{d^2}{dt^2}(input\ x) = \ddot{z}$).

1.5.3.5.2 Inverse model estimator

Physical-model-based variable estimators (or State Observers) can be designed as simulation of a model driven by the sensed inputs $\boldsymbol{u_{sens}}$.

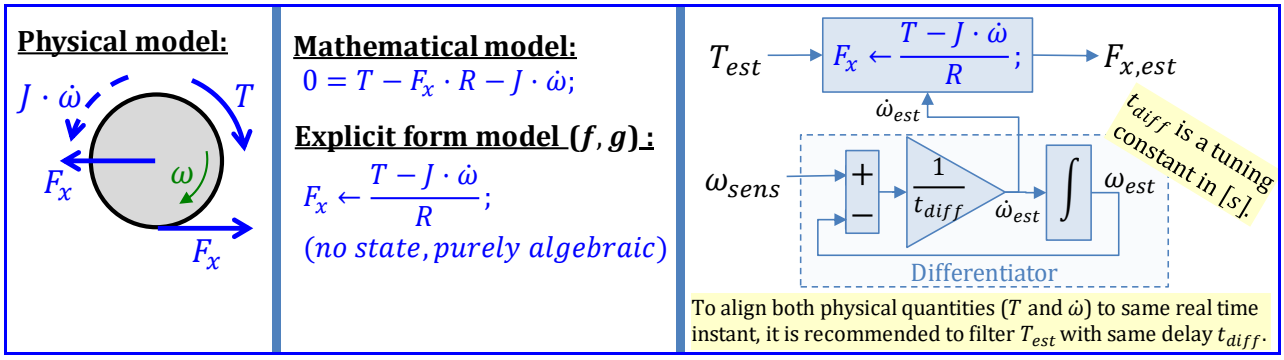


Figure 1-44: Concept and example of Physical-model-based variable estimators involving a differentiator.

```
model FxEst_Diff_Cont
  parameter Real DifferentiationTime=0.1;
  input Real w;
  Real w_est, T_est, Fx_est;
  input Real T, R, J;
equation
  der(w_est) = (w - w_est)/DifferentiationTime;
  der(T_est) = (T - T_est)/DifferentiationTime;
  0 = T_est - Fx_est*R - J*der(w_est);
end FxEst_Diff_Cont;

model FxEst_Diff_Discr
  parameter Real SampleTime=0.05;
  parameter Real DifferentiationTime=0.1;
  input Real w;
  Real w_est, T_est, Fx_est;
  input Real T, R, J;
  Real derw_est, derT_est;
equation
  when sample(-1000, SampleTime) then
    derw_est = (w-pre(w_est))/ DifferentiationTime;
    w_est=pre(w_est)+
     ((pre(derw_est)+derw_est)/2)*SampleTime;

    derT_est = (T-pre(T_est))/DifferentiationTime;
    T_est=pre(T_est)+
     ((pre(derT_est)+derT_est)/2)*SampleTime;
  end when;
  0 = T_est - Fx_est*R - J*derw_est;
end FxEst_Diff_Discr;
```

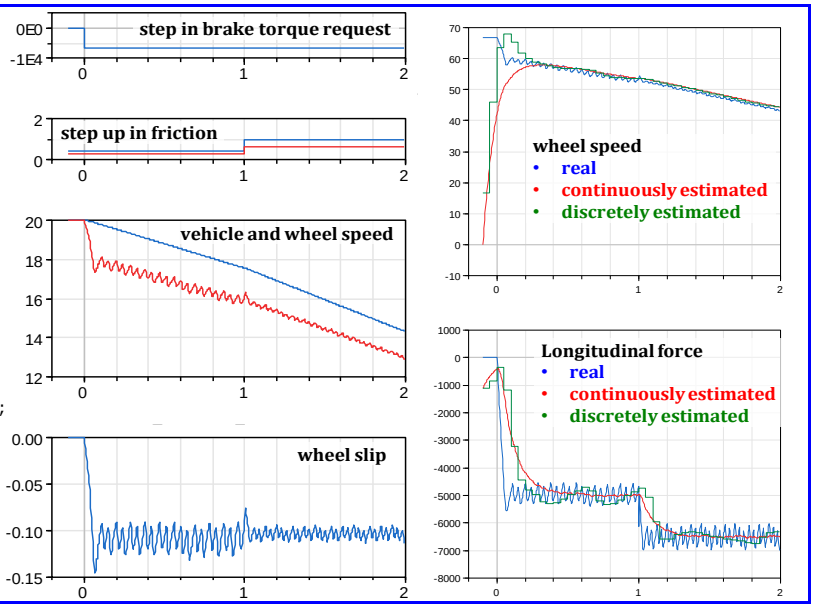


Figure 1-45: Continuous and discrete implementation of estimator in Figure 1-44. Tested with a one-wheel vehicle model with ideal, but sampled, sensing of wheel speed and wheel brake torque. Implicit midpoint or Trapezoidal rule (or Tustin approximation) used as derivative approximation for the discrete integration.

1.5.3.5.3 Estimator and predictors using model and measurement

Contribution from Carl Emvin, Chalmers

The estimator above uses a model and a measurement (if we see the estimated torque T_{est} as a measurement). However, the model and the measurement complement each other; none of them is enough to generate the desired estimate, $F_{x,est}$.

With a dynamic model we can "estimate the future", which might also be called "predict". When prediction, there is always a share of uncertainty. For prediction, we will need a dynamic model, i.e. how the system evolves over time (ahead). If we also have a measurement we can use both a dynamic and a model and a measurement. These both are enough to generate one estimate each, so there is a need to weight the dynamic model and the measurement together. *Luenberger* and *Kalman* filtering are names for such methods.

Model (on explicit form) for estimator design:

$$\dot{x} = f(x);$$
$$y_{est} = g_{est}(x);$$
$$y_{meas} = g_{meas}(x);$$

If we know the initial state, we can either estimate without using the y_{meas}:

$$x \leftarrow \int \dot{x} \cdot dt = \int f(x) \cdot dt \quad "simulation";$$
$$y_{est} \leftarrow g_{est}(x);$$
$$y_{meas} \leftarrow g_{meas}(x) \quad "what\ we, ideally, should\ measure";$$

So, we can calculate what we, ideally, should measure. However, due to errors, it will not be same as a measured y_{meas}. Believing both the model $\dot{x} = f(x)$; and the measurements blindly would lead to an unbalanced model (fewer unknown variables than equations). This suggests that we should add an unknown variable, an error. However, we add 2 unknown variables ($StateDerError$and $MeasError$) and 1 equation. These 2 unknowns and the 1 equation can be seen as "1 added error mechanism". The error mechanism has the effect of "driving" the states towards the states that corresponds to the measurements. The "driving" is something that happens over time in a similar way as the "driving" in the differentiator in Figure 1-41. Then the model is balanced:

$$\dot{x} = f(x) + StateDerError;$$
$$y_{est} = g_{est}(x);$$
$$y_{meas} = g_{meas}(x) + MeasError;$$
$$StateDerError = L \cdot MeasError;$$

The L tells how much the $MeasError$ influences the $\dot{x}$. Eliminating both $MeasError$ and $StateDerError$ yields:

$$\dot{x} = \underbrace{f(x)}_{\dot{x}_1} + \underbrace{L \cdot \left(y_{meas} - g_{meas}(x)\right)}_{\dot{x}_2};$$
$$y_{est} = g_{est}(x);$$

Now the estimator becomes:

$$x \leftarrow \int \dot{x} \cdot dt = \int (f(x) + L \cdot (y_{meas} - g_{meas}(x))) \cdot dt \quad "simulation";$$
$$y_{est} \leftarrow g_{est}(x);$$

...or, as dataflow block diagram:

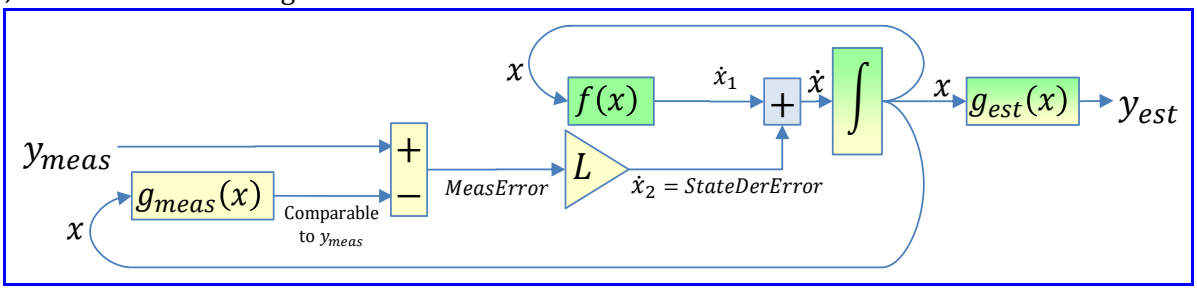


Figure 1-46: Concept and example of a Luenberger estimator. The term StateDerError "drives" y_{est} to values which are consistent with the measurements y_{meas}.

The green part alone is a pure simulation model which outputs the quantity which should be estimated y_{est}. The yellow part alone is a 1st order filter of a measured variable to the states x and then converting them to the quantity which should be estimated y_{est}. The whole Luenberger estimator shows how they can be weighted together by selecting/tuning a value on L.

The L is a tuning function of the estimator. The L has the dimension "state unit per measurement unit per time", so a correct sign and large magnitude value "drives" the estimator faster towards the measurement. The L does not have to be constant, so one can change L depending on how much one trust the measurement for different conditions.

Kalman filter can be seen as extension or specialisation of Luenberger. Kalman filter often uses the notation K instead of L, but they both appear in a calculation in the same way as shown for L in Figure 1-46. With the theory for Kalman filters, one can calculate L from known stochastic distribution of the errors.

1.5.3.5.3.1 Use as estimator

The above-described model-based filter is useful to estimate the momentaneous value ("now-value") of parameters and variables. Examples from vehicle motion engineering can be parameters as gross mass (m) and centre of gravity heigth (h) and variables as vertical wheel forces (F_z) and lateral body velocity over ground (v_y).

The filter uses the dynamic model $f(x)$ to react fast in transients time periods and the measurement model $g_{meas}(x)$ to "drive" back the estimate to measurements during less transient time periods where the measurements give a better estimate.

1.5.4 Tools

This section presents some tools and methods for modelling and computation.

1.5.4.1.1 General Mathematics Tools

Contributions from Mats Jonasson, Volvo Cars and Vehicle Dynamics at Chalmers
Examples of tool: Matlab, Matrixx, Python

We will take Matlab as example. Matlab is a commercial computer program for general mathematics. It is developed by Mathworks Inc. The book will use some simple Matlab code to describe models in this book. The following are useful for dynamic models:

General help function, here shown for function "inv" `>> help inv`
Solve linear systems of equations, $\boldsymbol{A} \cdot \boldsymbol{x} = \boldsymbol{b}$: `>> x=inv(A)*b;`
Solve non-linear systems of equations, $\boldsymbol{f}(\boldsymbol{x}) = \boldsymbol{0}$: `>> x=fsolve('f',...);`
Solve ODE as initial value problems, $\dot{\boldsymbol{x}} = \boldsymbol{f}(t, \boldsymbol{x})$: `>> x=ode23('f',x0,...);`

Find Eigen vectors (V) and Eigen values (D) to systems: $\boldsymbol{D} \cdot \boldsymbol{V} = \boldsymbol{A} \cdot \boldsymbol{V}$: `>> [V,D]=eig(A);`
Find $\boldsymbol{x}$ which minimizes $f(\boldsymbol{x})$ under constraints $\boldsymbol{A} \cdot \boldsymbol{x} \leq \boldsymbol{b}$: `>> x=fmincon(f,x0,A,b);`
Find the $\boldsymbol{x}$ which minimizes $0.5 \cdot \boldsymbol{x}^T \cdot \boldsymbol{H} \cdot \boldsymbol{x} + \boldsymbol{f}^T \cdot \boldsymbol{x}$: `>> x=quadprog(H,f);`

Matlab is mainly numerical, but also has a symbolic toolbox:

```
>> syms x a; Eq=a/x+x==0; solve(Eq,x)  %symbolically solve equation
ans = +(-a)^(1/2)
      -(-a)^(1/2)

>> diff(a/x+x,x)  %symbolically differentiate expression
ans = 1 - a/x^2

>> int(x^3+log(x),x)  %symbolically integrate expression
ans = (x*(4*log(x) + x^3 - 4))/4

>> F = laplace(f) %F = Laplace transform of the expression f
>> f = ilaplace(F) %f = inverse Laplace transform of the expression F
      >> clear all; syms f t F s a w; f=a*sin(w*t); F=laplace(f), f=ilaplace(F)
      F = (a*w)/(s^2 + w^2)
      f = a*sin(t*w)

>> partfrac(f,x) %is the partial fraction decomposition of the expression f
      >> clear all; syms f x; f=(7*x+3)/(5*x^2-3*x+0.5); partfrac(f,x)
      ans = (14*x + 6)/(10*x^2 - 6*x + 1)
      >> clear all; syms f x; f=(7*x+3)/(5*x^2-3*x+0.5);
            partfrac(f,x,'Factormode','complex')
      ans = (0.7 - 5.1i)/(x - 0.3 - 0.1i) + (0.7 + 5.1i)/(x - 0.3 + 0.1i)
>> ABCD=ss(A,B,C,D); %creates an object ABCD representing the linear state
            space model "A,B,C,D", see 1.5.1.1.4.5
>> step(ABCD) %computes step response of the model ABCD, see Figure 1-49.
```

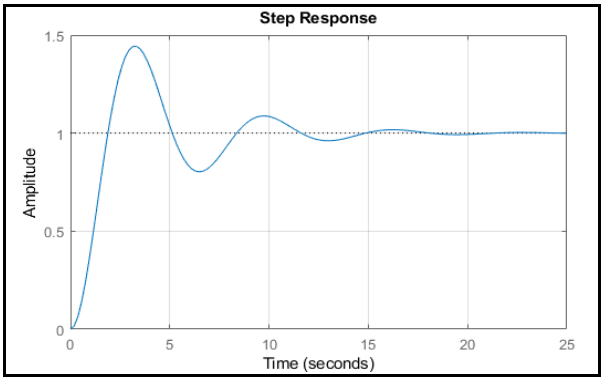


Figure 1-49: Plot resulting from Matlab commands `ss` and `step`:

```
>> clear all; ABCD=ss([-0.5,-1;1,0],[1;0],[0,1],[0]); step(ABCD), grid on
```

Of special interest for dynamic systems is that Matlab has a built-in function for "matrix exponential", mentioned in 1.5.1.1.6. E.g., if $\dot{\boldsymbol{x}} = \boldsymbol{A} \cdot \boldsymbol{x}$; with $\boldsymbol{x}(0) = \boldsymbol{x}_{\boldsymbol{iv}}$ the solution is $\boldsymbol{x}(t) = e^{\boldsymbol{A} \cdot t} \cdot \boldsymbol{x}_{\boldsymbol{iv}}$ which can simply be computed as:

```
>> x=expm(A*t)*x_iv;  %with A as (square) matrix
```

1.5.4.1.1.1 Algorithmic solving

The Matlab symbolic function `solve`, see above, is very useful for the step from Mathematical model in 1.5.1.1.4 to Explicit form model in 1.5.1.1.5. You need to select states (`x`) and introduce symbolic variables also for their derivatives (`derx`). The system of equation is the solved for state derivatives (`derx`) while the states (`x`) are considered as known. However, `solve` can only solve for each unknown and misses to utilize "algorithmic solutions". An algorithmic solution is a sequence of assignment statements which must be evaluated in the given order. It is often more computational and

coding efficient. So, `solve` is limited, but here is a home-made script which does an algorithmic solution. It can sometimes be useful for elaborating with different ways to model a real system.

```
%script: AlgorithmicSolve.m
clear all
syms p1 p2 x derx y;
Equations=[x==y^x, derx*x==y+p2];
UnknownsWithElimOrder=[derx, y]; %elaborate with the order within this vector

codeLines = strings(1, numel(UnknownsWithElimOrder));
eqsCurrent = Equations %;
for i = 1:numel(UnknownsWithElimOrder)
    v = UnknownsWithElimOrder(i) %;
    %Find first equation which contains the variable to eliminate:
    idx = find(arrayfun(@(eq) has(eq, v), eqsCurrent), 1);
    if isempty(idx), error('No equation contains %s', char(v)), end
    % Isolate the variable:
    isolatedEq = isolate(eqsCurrent(idx), v);   rhsExpr = rhs(isolatedEq);
    % Add the assignment statement:
    codeLines(i) = sprintf('%s := %s;', char(v), char(rhsExpr)) %;
    % Eliminate (substitue) in remaining equations:
    eqsCurrent(idx) = []; % remove the used equation
    eqsCurrent = subs(eqsCurrent, v, rhsExpr) %;
    % pause; %Uncomment for elaborating with elimination order
end
disp('Algorithmic solution:')
for i=numel(UnknownsWithElimOrder):-1:1,   disp(codeLines(i)),   end;
disp('Solution with common solve as comparison:') %Can be commented out
sol=solve(Equations,UnknownsWithElimOrder)
    % derx: (p2 + x^(1/x)*exp(-(pi*k*2i)/x))/x
    %    y: x^(1/x)*exp(-(pi*k*2i)/x)
```

If the system of equations is singular, it may indicate that the chosen states are not suitable or that some equations need to be replaced by their differentiated versions. The script above, together with guiding error messages, can be seen as a micro-version of a Modelica compiler, see 1.5.4.1.5.1 and (Elmqvist, 2014). Modelica compilers perform similar steps but on a much larger scale, including BLT (Block Lower Triangular) decomposition, tearing of algebraic loops, and systematic handling of higher-index DAEs.

1.5.4.1.1.2 Solving Linear Dynamic System using `expm`

```
clear all;


m=1500;
f_heave=1; c=round(m*(2*pi*f_heave)^2,-3)
damping=0.3; d=round(damping*(2*sqrt(c*m)),-2)


figure(1), clf
%derx=A*x; x=[v_z;F_s;z];
%x=expm(A*t)*x_iv;
A=inv(diag([m,1,1]))*[-d 1 0; -c 0 0; 1 0 0];
x_iv=[0;1000;0];
for N=[7,100]
    t_vec=[linspace(0,2,N)];
    x_mat=[];
    for i=1:length(t_vec)
        t=t_vec(i);
        x_mat(:,i)=expm(A*t)*x_iv;
    end
    for j=1:length(x_iv)
      subplot(length(x_iv),1,j), plot(t_vec,x_mat(j,:)),
hold on, grid on
    end
end
ylabel('t /[s]')
subplot(length(x_iv),1,1), ylabel('v_z /[m/s]')
subplot(length(x_iv),1,2), ylabel('F_s-m*g /[N]')
subplot(length(x_iv),1,3), ylabel('z /[m]')
```

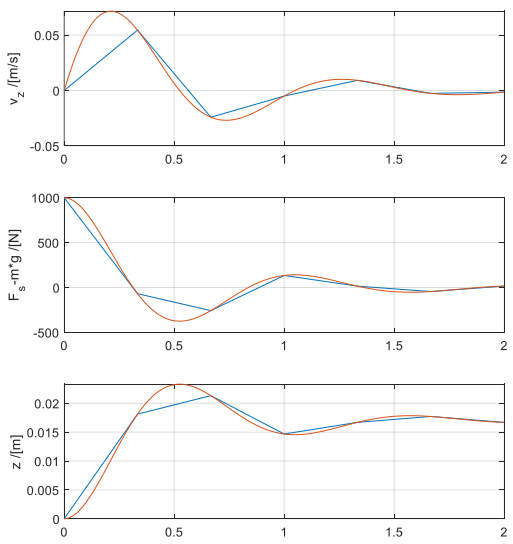


Figure 1-50: An example in Matlab code, where `expm` is used to find the solution.

1.5.4.1.1.3 Simulation by Programming Integration

In Figure 1-51, the Matlab function `f` shows an implementation of an explicit form model:

```
function [derv,derx, F] = f(t, v,x)
```

```
   m=2; c=3;
   F=c*x;
   derv=-F/m;
   derx=v;
end
```

The following Matlab script simulates it (using simplest possible derivative approximation, Newton forward) and plots the result.

```
>> clear all; dt=0.001; t_vec=[0:dt:5]; v_vec=0; x_vec=1; F_vec=[];
for i=1:length(t_vec)
   [derv,derx,F_vec(i)]=f(t_vec(i),v_vec(i),x_vec(i));
   v_vec(i+1)=v_vec(i)+derv*dt;
   x_vec(i+1)=x_vec(i)+derx*dt;
end
figure(1), clf
plot(t_vec',[v_vec(1:end-1);F_vec;x_vec(1:end-1)]')
grid on, legend('v','F','x')
```

The states `x, v` has to be given initial values. The output variable F is not a state and has to be treated slightly different.

1.5.4.1.1.4 Simulation of a model on explicit form using built-in Integration Methods

There are many other built-in integration methods in Matlab, e.g. `euler, ode23, ode45` and ode23s. The same example as above can also be simulated with such, here exemplified with `ode23`:

```
>> clear all; [t_vec,States]=ode23('f2',[0 5],[0 1]);
figure(1), clf, plot(t_vec,States), grid on, legend('v','x')
```

A wrapper function f2 has to be defined to meet the interface format for ode23:

```
function [derStates] = f2(t, States)
   [derv,derx, F] = f(t, States(1),States(2));
    derStates=[derv;derx];
end
```

1.5.4.1.2 Dataflow Diagram Based Tools

Examples of tools: Simulink, Systembuild, Altair Activate, Xcos, Modelica Block library

In these tools, the Explicit form model (or an ODE) is built with a graphical representation, around "integrator blocks", often marked "1/s" or "$\int$ ". An example using Simulink is shown in Figure 1-51. Simulink is designed for designing/modelling signal processing and control design. It can also be used for modelling the physics of the controlled systems. There are no dedicated vehicle dynamics tools/libraries from Mathworks (but there are in-house developed specific libraries in automotive companies).

From this type of tools, it is often possible to automatically generate real time code, which is more and more used instead of typing algorithms. It can be used for rapid prototyping of control functions, or even for generation of executable code for production ECUs.

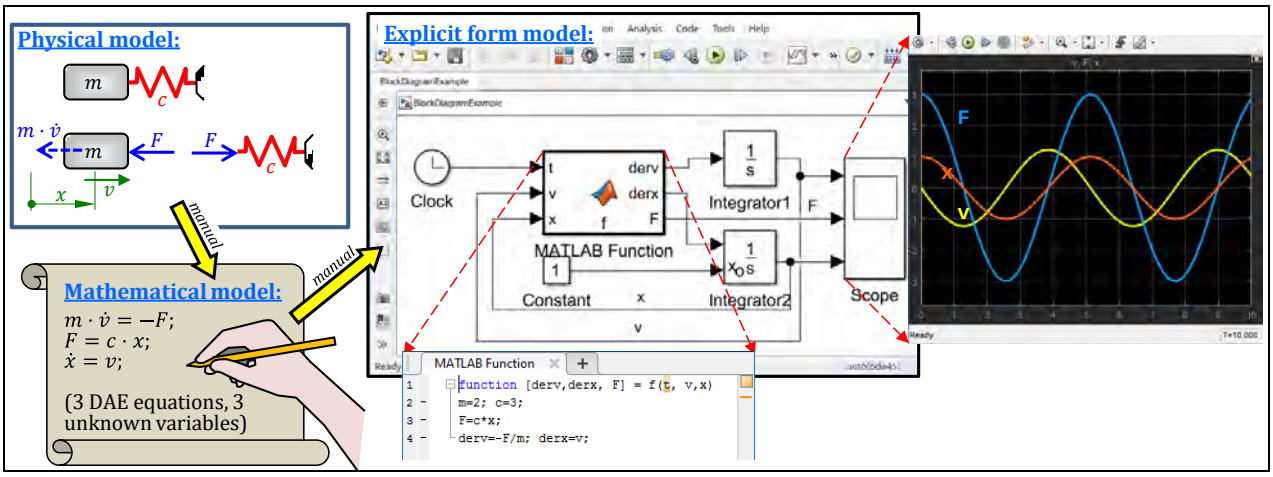


Figure 1-51: Graphical modelling using Simulink for Explicit form model.

1.5.4.1.3 Vehicle Dynamics Specialized Simulation Tools

Examples of tools: CarMaker, TruckMaker, veDYNA, CarSim, TruckSim, Vehicle Dynamics Library

These tools are frequently used in professional vehicle development. They contain multi-purpose and relatively advanced models of vehicles. It is also important that they contain models of drivers and environments (ground, road, traffic, cone-tracks, …). They are prepared for parameter changes. However, they are generally less prepared for modelling conceptually new designs, which can make these tools less useful for vehicle manufacturers and advanced research. For this reason, many of these tools offer also an interface to Simulink or FMU, so that the user can add in their own vehicle models or export parts to other tools.

1.5.4.1.4 MBS Tools

Examples of tools: Adams, Simpack, LMS Virtual Lab, Simscape Multibody, Modelica with Mechanics library.

These are general 3D mechanics modelling and simulation tools, so called MBS (Multi-Body Simulation) tools. As one example, Adams contains libraries of general bodies, joints and force elements. But there are toolboxes in Adams for vehicle dynamics, where template models and special components (such as tyre models and driver models) are available for vehicles dynamics. The models are very advanced and accurate for 3D mechanics, and there are import/export interfaces to Simulink.

1.5.4.1.5 Acausal modelling tools

1.5.4.1.5.1 Modelica based modelling tools

Examples of tools: Dymola, Maplesim, System-Modeler, AMESim, Optimica Studio, Jmodelica, OpenModelica (https://openmodelica.org/), OMwebbook (http://omwebbook.openmodelica.org/static/DynamicWebbook/), Modelon Impact, and 1.5.4.1.1.1

Modelica is not a tool but a globally standardized format for lumped dynamic models on DAE form (or Mathematical form, see 1.5.1.1.3.2). See also (Elmqvist, 2014). There are several tools which supports the format. So, Modelica models are *tool-independent*. Specification of Modelica is found at https://www.modelica.org/. When learning Modelica, http://www.xogeny.com/ is helpful.

An example of a Modelica model is given in Figure 1-52. A "crash course" in Modelica, to understand the simple examples used in this book.

> A Modelica model is *acausal*, i.e., it consists of *equations* as opposed to consist of *assignment statements*. So, Modelica is an executable Mathematical model format. All variables and parameters are declared, not only equations.
>
> Declaration must distinguish between which are parameters and variables is a necessary part for a DAE model, see "`parameter Real`" and "`Real`", respectively. When modelling real physical systems, one declares real physical quantities, e.g. a force, and in such declaration, `Real` can be replaced with `Modelica.Units.SI.Force`. Unit declarations are used to give the user warning for inconsistency checks.
>
> Equations are declared under key word `equation`. The operator `der` means differentiation with respect to time and replaces the "d/dt" or "dot above" in equations. Declaring `x` as a parameter, implicitly tells that `der(x)=0;`.

The model format is also object oriented, which means that libraries of model components are facilitated through, e.g., inheritance (marked extends) and instantiations of models in models (with `BaseModelName instanceName(Parameter1=7);` in declaration part), as "sub models". The libraries often use also a graphical layer, which is also standardized. There are some open-source libraries for various physical domains, such as hydraulic, mechanics, thermodynamics and control. There are also commercial libraries, where we find vehicle dynamics relevant components: Vehicle Dynamics Library and Powertrain Library. Some simple Modelica code will be used to describe models in this book.

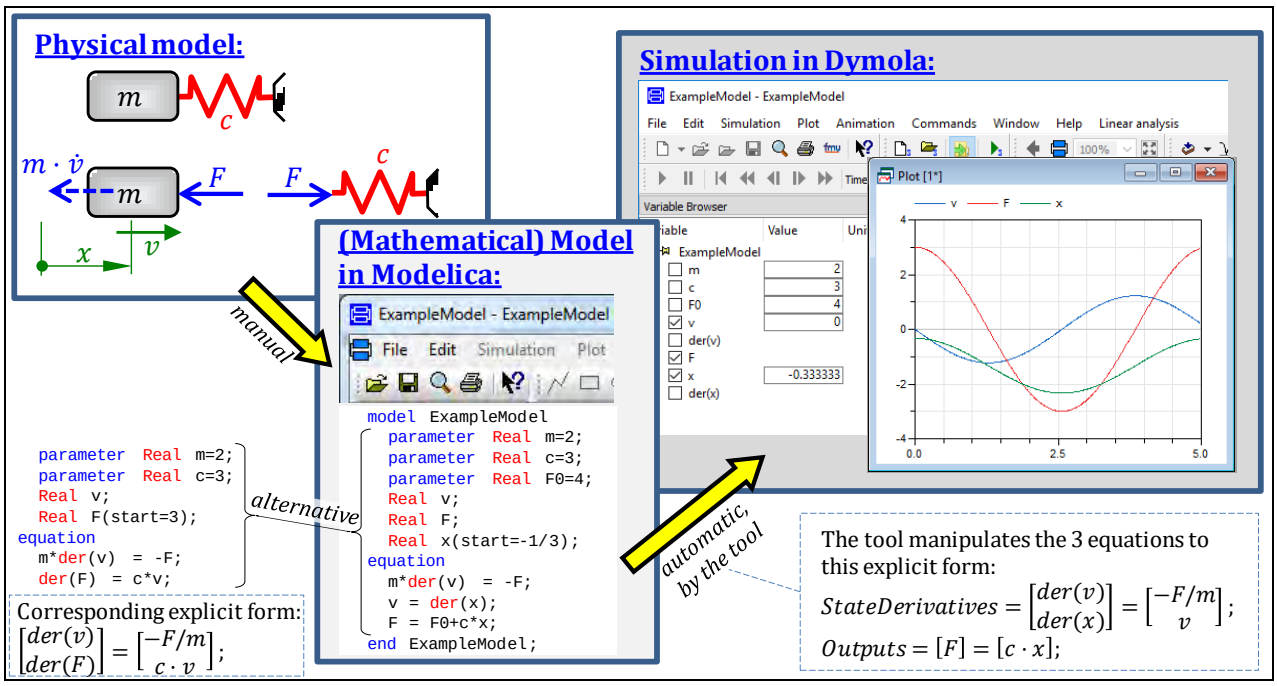


Figure 1-52: Example of model in Modelica format (using the tool Dymola). Two alternative models are given, leading to either [x, v] or [v, F] as states. Same example model as in Figure 1-51.

Mathematical modelling is more efficient than Explicit form modelling, since the engineer does not need to spend time on symbolic/algebraic manipulation of the equations. This is especially true when a model is reused in another context which changes the causality or for so called "higher index problems", see Figure 1-53. In this book, many models are only driven to Mathematical model, since it is enough if assuming there are modern tools as Modelica tools available. One the other hand, an explicit form model has the value of capturing the causality, i.e. the cause-to-effect chain. The causality can sometimes facilitate the understanding and in that way help the engineer, which is why at least one and rather complete model is shown as explicit form model, see 4.5.3.2.

One can also declare variables with prescribed causality, i.e. signals, in Modelica. Declaration of input signal: "`input Real z;`". Modelica can also handle sampled signals and discrete states.

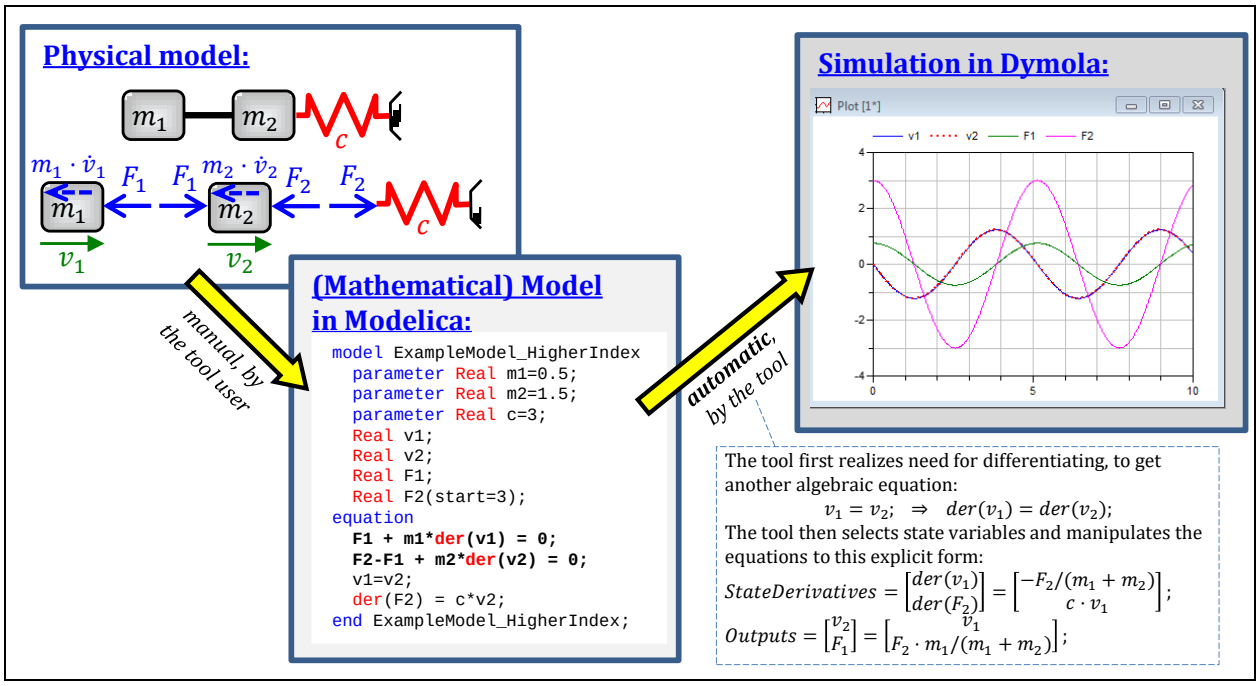


Figure 1-53: Example of "higher index problem" model in Modelica format.

1.5.4.1.5.2 Modelica standardized and open component libraries

Figure 1-54 shows a usage of the Mechanical translational 1D library.

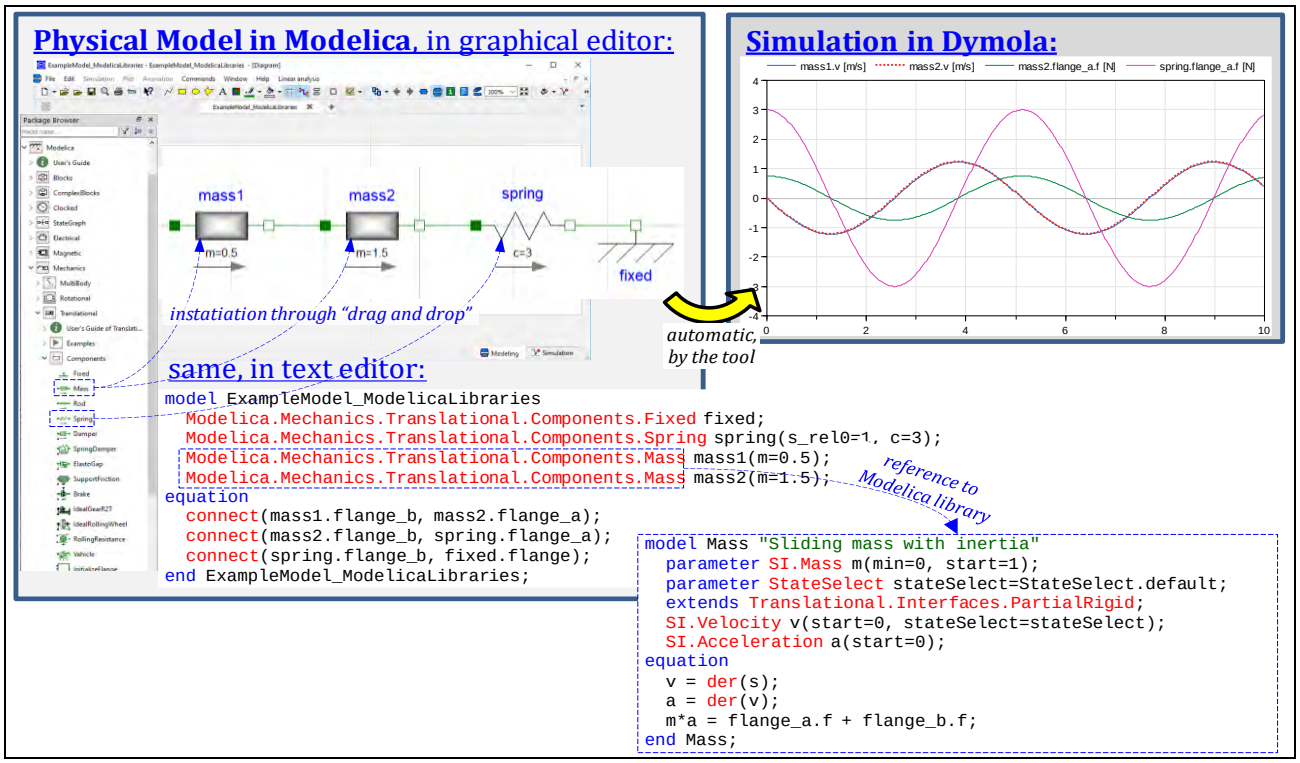


Figure 1-54: Example of model in Modelica format, using a standard Modelica library.

1.5.4.1.5.3 Small home-built Modelica component library

This section shows a simple example of a component library in Modelica, see Figure 1-55. We call it the "small home-built example". It should give an understanding of "what's under the hood" in the library example in Figure 1-54.

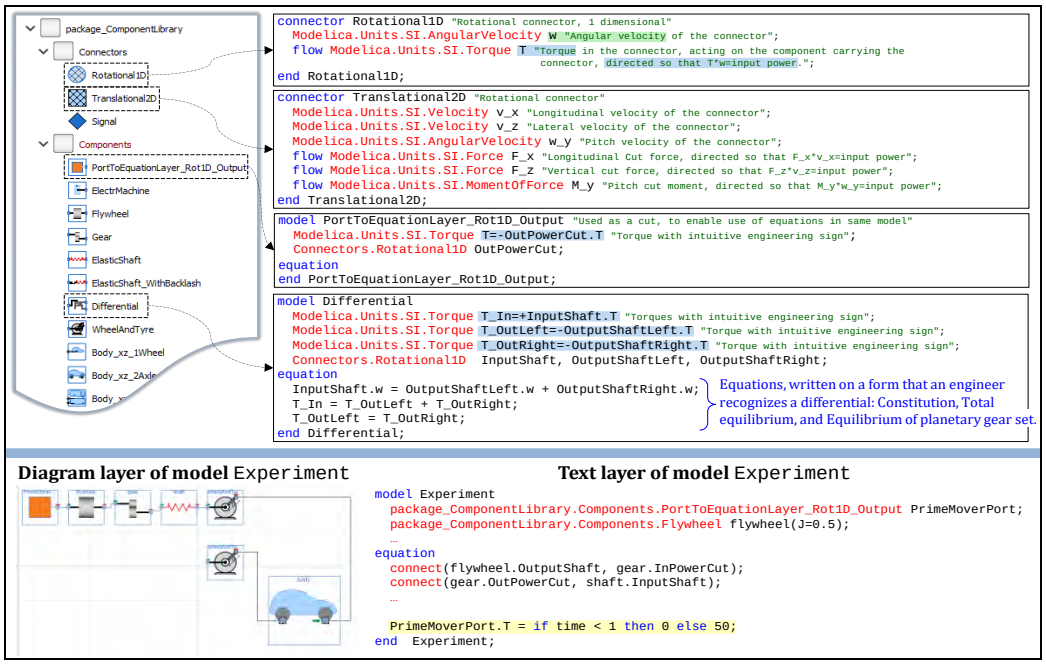


Figure 1-55: Example of a small home-built Modelica library. Higlighted: Green: Velocities, Blue: Torques, Yellow: Pure equations instead of component (here: Model of Driver or Control algorithm).

In the Modelica standard, there is also ways to define a component icon for each component and do the connections by drawing lines on the screen. Therefore, the models above can also be given a graphical modelling environment, see model `Experiment` in the bottom of Figure 1-55. The Modelica standard stipulates that each connector generates equations: all ordinary variables (as angular velocity `w`) in the connected connectors are set equal, while the sum of all flow variables (as torque `T`) in the connected connectors are set to zero. This calls for a sign change to get intuitive sign convention for an engineer, see Figure 1-55. If one want to mix both components (graphical modelling) and text (code) in same model, Figure 1-55 proposes a special component, see "`PortToEquationLayer_Rot1D_Output`" in Figure 1-55.

Adding simplest possible vehicle body could be done by building a wheel with one Mechanical Rotational 1D connector and one Mechanical Translational 1D connector. Further, to include load transfer between two axles on the vehicle, one could use a Mechanical Translational 1D connector, and so on.

It shall be noted that the example in Figure 1-55 models the propulsion system as beside, not in, the vehicle body. Therefore, reaction torques from the propulsion system on the body will not be modelled. The reaction torques are typically pitching or rolling torques for a transversally or longitudinally mounted propulsion component.

1.5.4.1.5.4 Web-based Modelica tools

There are open source and commercial tools for modelling and simulation via web. *OMwebbook* and *Modelon Impact* are examples of each, respectively. Using OMwebbook for the example in Figure 1-52 is shown in Figure 1-56.

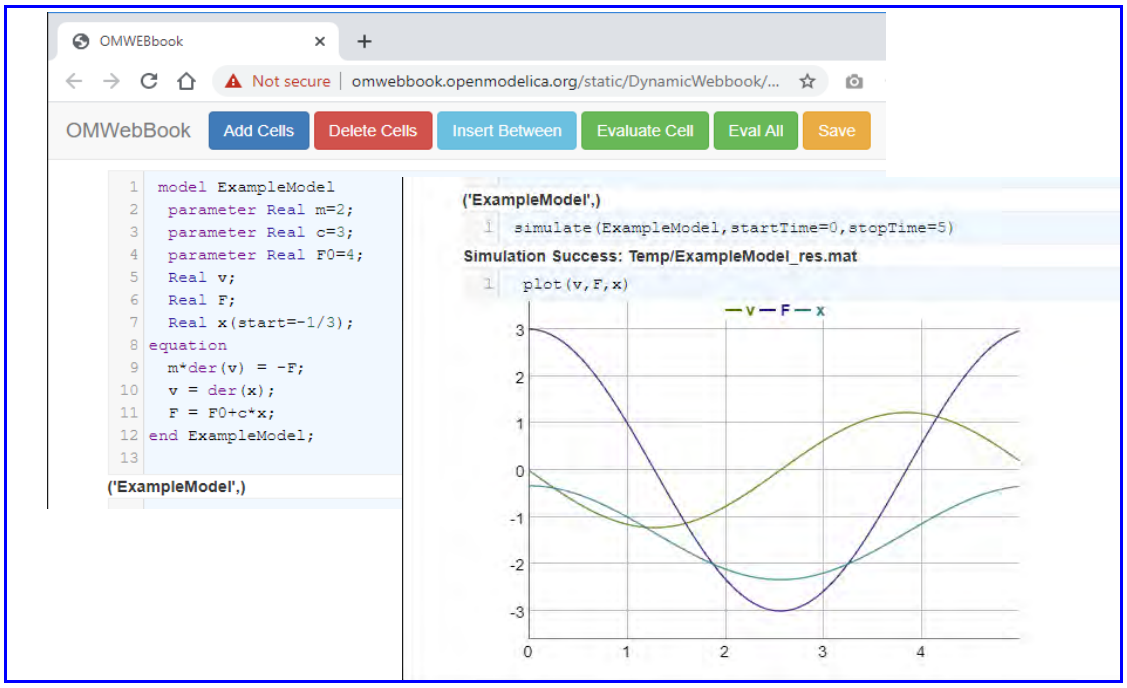


Figure 1-56: Modelica format, using OMwebbook, for same example model as in Figure 1-52

1.5.4.1.6 FMI Supporting Simulation Tools

Examples of tools: Most of the tool examples in 1.5.4.1.5, but also Simulink, CarMaker

FMI (Functional Mock-up Interface) is not a tool but a globally standardized format for dynamic models on explicit form (see https://fmi-standard.org/). There are several tools which supports this format. FMI enables model exchange (export and import) between tools. It also allows hiding Intellectual Property (IP) by using "black-box format", i.e. models compiled (not human-readable). The IP is important for exchange between OEMs and suppliers. The black-box model exchange requires extra robust models to generate the FMU (Functional Mock-up Unit) from, because the user of the model cannot be expected to debug it. An FMU is an Explicit form model on FMI format.

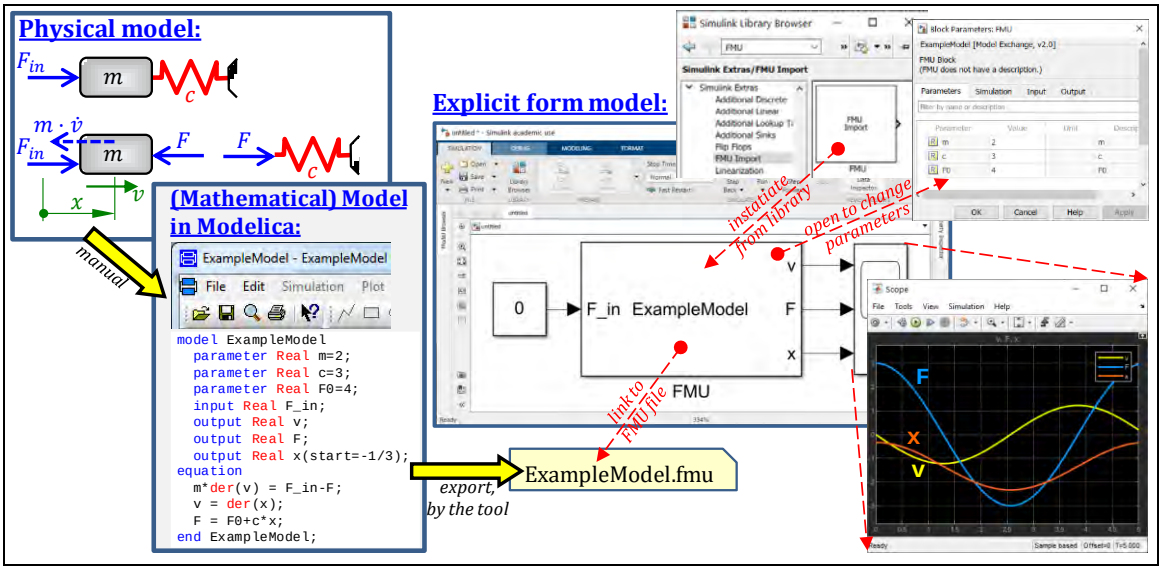


Figure 1-57: Example of Mathematical model in Modelica, export to Explicit form as FMU-file imported to Simulink. Same example model as in Figure 1-51, but with a force F_{in}.

1.5.4.1.6.1 Model Exchange and Co-Simulation FMUs

FMUs can be either of Model Exchange type (requires external solver) or Co-Simulation type (includes an own solver for the own states).

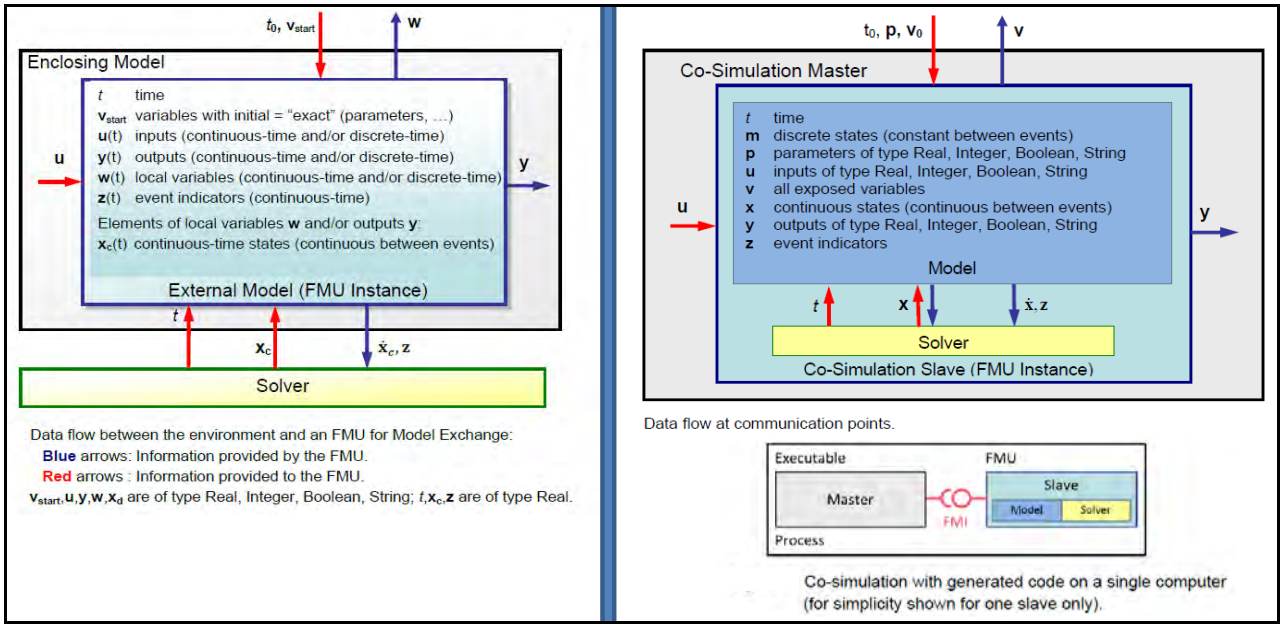


Figure 1-58: FMI standard models. Left: FMU for Model Exchange. Right: FMU for Co-Simulation.

There are also add-on standards for combining several FMUs in an hierarchy (System Structure and Parameterization SSP) and for co-simulation with FMUs (Distributed Co-Simulation Protocol DCP).

1.5.4.1.7 Modularity in Models

Another aspect of modelling is the modularity. For complex products as vehicles, it is often important to keep a modularity in the models, which reflects the subsystems in the product. This is for reuse of subsystem models and co-operation between engineering teams at vehicle manufacturer and suppliers. Reuse cuts modelling time, but also improves the models over time since bugs are found when models are used. Modularity is also important for replacing one subsystem model with a real ECU with software or splitting model between several processors for increasing the computational capability. Methods for above motivated "co-simulation" are typically based on that each module are on explicit form but also include its own time integrator. This can create big challenges in numerical stability and accuracy of the whole system.

1.5.4.1.7.1 Co-Simulation and Real-time Simulation

Co-Simulation is when merging models containing their own time integration code. It can be caused by different modelling environments or that the models have to be kept confidential. Co-simulation means that several systems, e.g. several FMUs, integrates on their own in small (micro) time steps, but exchange interface variables only at certain larger (macro) time steps. There is a standard also for this communication, see https://dcp-standard.org/.

The opposite to co-simulation is *Mono-Simulation*. In *Mono-simulation*, there is only one numerical time integration method (solver) and it can access the whole model at once; all derivatives are calculated together: $\dot{\boldsymbol{x}} = \boldsymbol{f}_{\boldsymbol{ODE}}(\boldsymbol{x}, t)$. Then, there is a wide range of well-developed codes and the error is kept under control by automatic time step variation during the simulation.

Real-time simulation (or *On-line simulation*) is when the model need to be synchronized with something from the real world, such as a human driver, a test rig with a real subsystem or just an electronic hardware (1.6.6.2.1). Opposite can be called *Off-line-Simulation*. Real-time simulation is similar to co-simulation in the way that there is not one over-arching integration solver for the whole system.

Co-Simulation and Real-time simulation very often they appear at the same time. Many challenges appear, such as keeping integration error under control, computation fast enough for real time, synchronising variables, etc.

1.5.4.1.7.2 Co-Modelling

An alternative way where models of sub-systems are connected on Mathematical form, as opposed to Explicit form. It could be called "co-modelling" (or "acausal co-simulation") and make it easier to organize libraries of models since one would not need to keep different versions of part models for different causality on interface variables. However, co-modelling would require a globally accepted and used standard of Mathematical modelling format, which does not exist yet; Modelica is the closest to reach such status. It would also be important to encrypt such models, for confidentiality. There is a proposal for an encryption standard of Modelica, called SEMLA (Standardized Encryption of Modelica Libraries and Artifacts).

1.5.4.1.8 Bond Graphs Tools

Contribution from Pinar Boyraz, Vehicle Safety at Chalmers

Examples of tools: Modelica with Bond graphs libraries, https://www.20sim.com/features/model-libraries/bondgraphs/, ...

Bond graphs is a method to graphically model with arrows for flow and effort, see 1.5.2.1.2. It can be used without any tool (non-executable drawing) but it has also been programmed in some tools.

1.6 Vehicle Engineering

1.6.1 Vehicle Motions and Coordinate Systems

A vehicle's (motion) degrees of freedom are named as in marine and aerospace engineering, such as heave, roll, pitch and yaw, see Figure 1-59. Figure 1-59 also defines the 3 main geometrical planes, such as transversal plane and symmetry plane. For ground vehicles, the motion *in-road-plane (irp)* is the primary motion, and has the dofs longitudinal, lateral and yaw. The remaining degrees of freedom (dof) describes the *out-of-road-plane (oorp)* motion. Also, the forces and moments on the vehicle body can be categorized in irp forces (longitudinal forces, lateral forces and yaw moments) and oorp (vertical forces, roll moments and pitch moments). Along each dof one defines velocity, such as longitudinal velocity v_x in $[m/s]$ and yaw velocity (or yaw rate) ω_x in $[rad/s]$.

The consistent use of parameters that describe the relevant positions, velocities, accelerations, forces, and moments (torques) for the vehicle are critical. Unfortunately, there are sometimes disparities between the nomenclature used in different textbooks, scientific articles, and technical reports. It is important to apply coordinate system from (ISO 8855). It is the predominant coordinate system used nowadays.

Historically, a coordinate system with other positive directions, Reference (SAEJ670), has been applied. (For geometric design, e.g., suspension hardpoints and body shapes, and aero dynamics, the (ISO 4130) is more used. It has x rearwards, y to the right and z upwards.)

The distinction of vehicle fixed and inertial (= earth fixed = world fixed) coordinate systems is important. Figure 1-60 depicts the four most relevant reference frames in vehicle dynamics: the inertial, the vehicle, the wheel corner and the wheel reference frames. All these different coordinate systems allow for the development of equations of motion in a convenient manner.

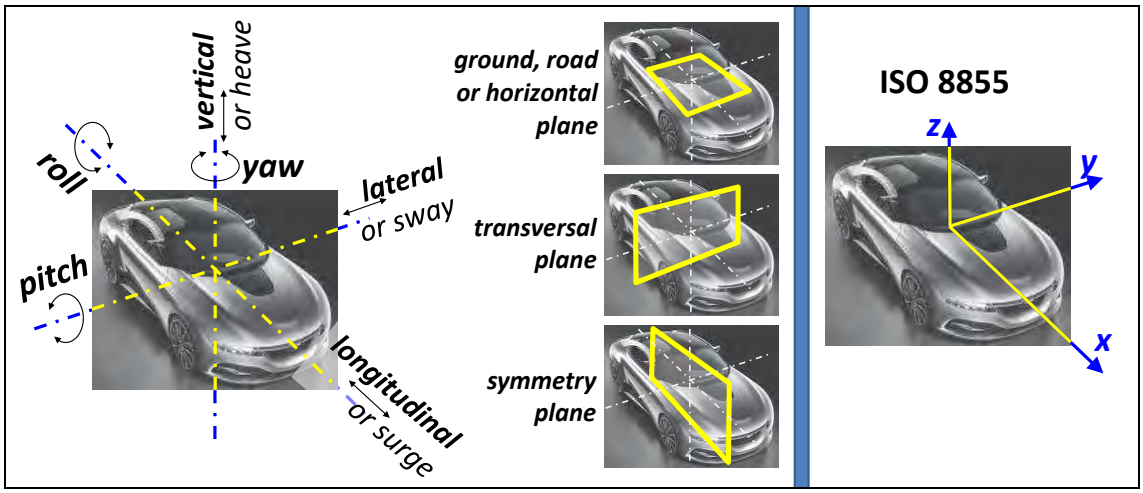


Figure 1-59: Left: Vehicle (motion) degrees of freedom and important planes. Right: ISO coordinate system

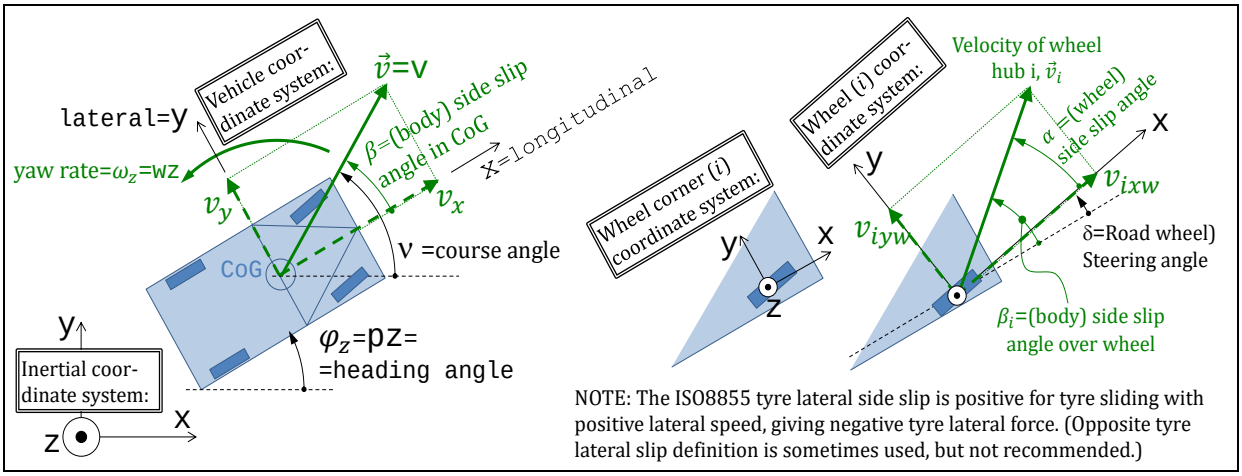


Figure 1-60: Coordinate systems and motion quantities in ground plane.

The orientation of the axes of an inertial coordinate system is typically either along the vehicle direction at the beginning of a manoeuvre or directed along the road or lane. Road or lane can also be curved, which calls for curved longitudinal coordinate.

Origin for a vehicle coordinate system is often centre of gravity of the vehicle, but other points can be used, such as mid front axle (ground contact or wheel centre height), mid of front bumper, outer edge of body with respect to certain obstacle, etc. Figure 1-60 defines velocities $\vec{v}$. Note that they are relative to inertial system, "velocities over ground", not relative to the other coordinate systems. However, the velocity components v_x, v_y are depent of which coordinate system $\vec{v}$ is decomposed in. Positions are often not included in the models. When positions are needed, e.g. for lane markings, road edges, other moving vehicles and varying friction, they are typically defined in inertial coordinate systems but algorithms on-board the vehicle use positions expressed in vehicle coordinate system.

In ISO and Figure 1-60, wheel side slip is defined so that it is positive for positive lateral speed. This means that lateral tyre forces on the wheel will be negative for positive side slip. Some would rather want to have positive force for positive side slip. Therefore, one can sometimes see the opposite definition of wheel side slip, as e.g., in (Pacejka, 2005). It is called the "modified ISO" sign convention.

Often there is a need to number each unit/axle/wheel. The numbering in Figure 1-61 is proposed. It should be noted that non-numeric notations are sometimes used, especially for two axle vehicles without secondary units. Then front=f, rear=r. Also, to differentiate between sides, left=l and right=r.

Using these motion dofs and coordinates for modelling is further described in 1.6.2.

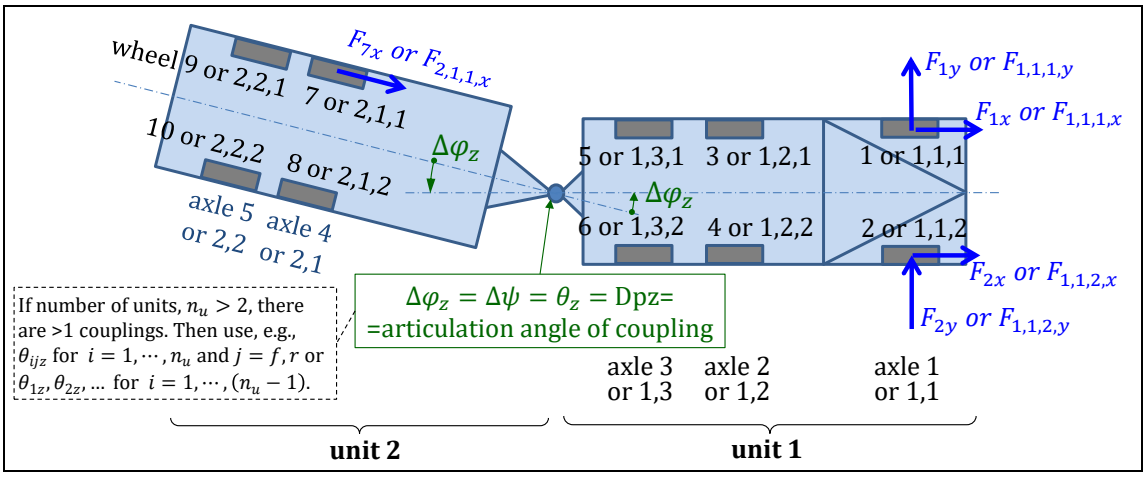


Figure 1-61: Proposed numbering of units, axles, wheels and articulation angle. Example shows a rigid truck with trailer.

If multiple units: $\theta_{ifz} = \theta_{i-1,rz} = \varphi_{iz} - \varphi_{i-1,z}$;, so the rule is "articulation (yaw) angle in front coupling on a unit i is the yaw angle of the unit ahead, relative to the unit i". This can be extended to articulation articulation roll angles: $\theta_{ifx} = \theta_{i-1,rx} = \varphi_{ix} - \varphi_{i-1,x}$; to articulation pitch angles: $\theta_{ify} = \theta_{i-1,ry} = \varphi_{iy} - \varphi_{i-1,y}$;. See also 4.5.2.2.

1.6.1.1 Couplings

Coupling forces can be denoted using "single cut force notation" or "multiple cut forces notation", see 1.5.2.1.1. Coupling, in 1.6.1.1, means moment-free 2D connection between bodies. Similar reasoning is made for transmission coupling in 2.4.1.

1.6.1.1.1 Single cut force notation

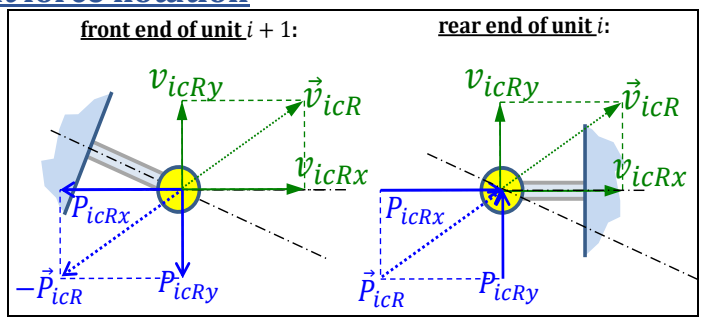


Figure 1-62: Coupling force notation, using "single cut force notation", for the coupling named "icR" (for unit i, coupling Rear).

For single cut force notation, it can be an alternative to replace subscript "icR" with a sequential numbered identifier of the coupling within the vehicle, e.g. $c1, c2, \cdots, c(n_u - 1)$, where n_u are the number of units.

1.6.1.1.2 Multiple cut forces notation

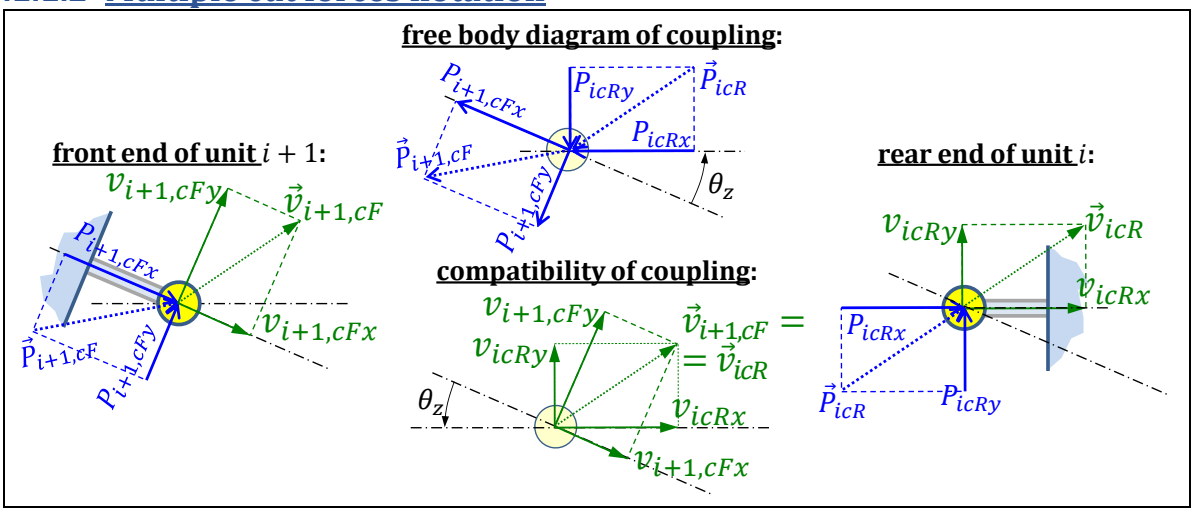


Figure 1-63: Coupling force notation, using "multiple cut forces notation", for the coupling between unit i and $i+1$. Subscripts: "icR" as in Figure 1-62 and "$i+1, cF$" after unit $i+1$, coupling Front.

For multiple cut forces notation, introduces more notations than needed to describe the physical real-world situation. Hence one need extra transformation equations in Eq [1.5] and Eq [1.6]. Also, extra equations are needed to set the front coupling forces of the first unit and the rear coupling forces of the last unit to zero.

Compatibility:

Compatibility, from unit i to unit $i+1$:

$$\begin{bmatrix} v_{i+1,cFx} \\ v_{i+1,cFy} \end{bmatrix} = \begin{bmatrix} \cos(\theta_z) & -\sin(\theta_z) \\ \sin(\theta_z) & \cos(\theta_z) \end{bmatrix} \cdot \begin{bmatrix} v_{icRx} \\ v_{icRy} \end{bmatrix}; \quad [1.5]$$

Same equation, but expressed as from unit $i+1$ to unit i:

$$\begin{bmatrix} v_{icRx} \\ v_{icRy} \end{bmatrix} = \begin{bmatrix} \cos(\theta_z) & \sin(\theta_z) \\ -\sin(\theta_z) & \cos(\theta_z) \end{bmatrix} \cdot \begin{bmatrix} v_{i+1,cFx} \\ v_{i+1,cFy} \end{bmatrix};$$

Force equilibrium of coupling (or *Force equivalence* between forces on the two units):

From unit i to unit $i+1$:

$$\begin{bmatrix} P_{i+1,cFx} \\ P_{i+1,cFy} \end{bmatrix} = -\begin{bmatrix} \cos(\theta_z) & -\sin(\theta_z) \\ \sin(\theta_z) & \cos(\theta_z) \end{bmatrix} \cdot \begin{bmatrix} P_{icRx} \\ P_{icRy} \end{bmatrix}; \quad [1.6]$$

Same equation, but expressed as from unit $i+1$ to unit i:

$$\begin{bmatrix} P_{icRx} \\ P_{icRy} \end{bmatrix} = -\begin{bmatrix} \cos(\theta_z) & \sin(\theta_z) \\ -\sin(\theta_z) & \cos(\theta_z) \end{bmatrix} \cdot \begin{bmatrix} P_{i+1,cFx} \\ P_{i+1,cFy} \end{bmatrix};$$

1.6.1.2 Wheel Orientation

For steered wheels, there are often reason to translate forces and velocities between vehicle coordinate system and wheel coordinate system, see Figure 1-64 and Eq [1.7].

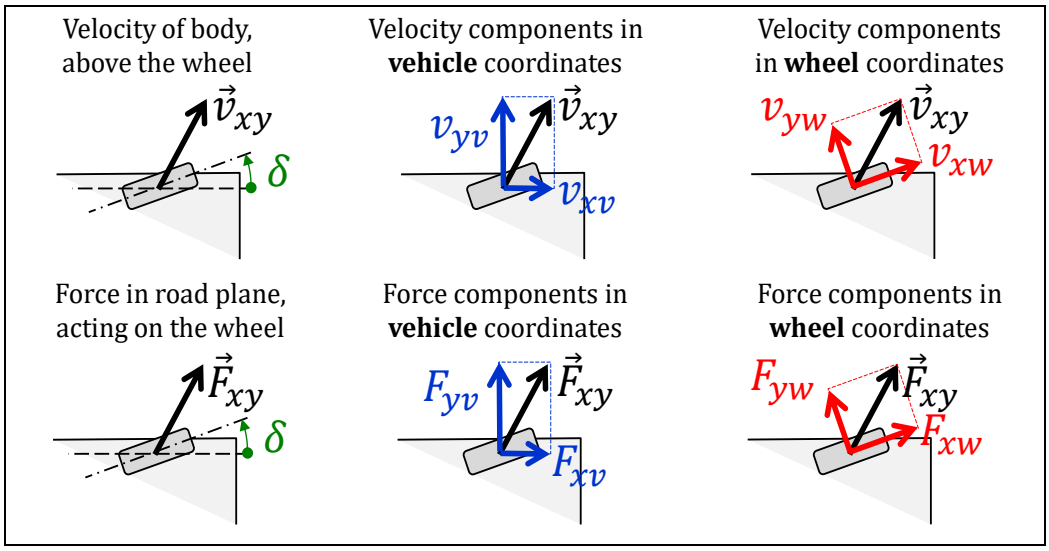


Figure 1-64: Transformation between forces and velocities in vehicle coordinate system and wheel coordinate system.

Transformation from wheel coordinates to vehicle coordinates:

$$\begin{bmatrix} v_{xv} \\ v_{yv} \end{bmatrix} = \begin{bmatrix} \cos(\delta) & -\sin(\delta) \\ \sin(\delta) & \cos(\delta) \end{bmatrix} \cdot \begin{bmatrix} v_{xw} \\ v_{yw} \end{bmatrix}; \quad and \quad \begin{bmatrix} F_{xv} \\ F_{yv} \end{bmatrix} = \begin{bmatrix} \cos(\delta) & -\sin(\delta) \\ \sin(\delta) & \cos(\delta) \end{bmatrix} \cdot \begin{bmatrix} F_{xw} \\ F_{yw} \end{bmatrix};$$

Or, same relation, but expressed as from vehicle coordinates to wheel coordinates:

$$\begin{bmatrix} v_{xw} \\ v_{yw} \end{bmatrix} = \begin{bmatrix} \cos(\delta) & \sin(\delta) \\ -\sin(\delta) & \cos(\delta) \end{bmatrix} \cdot \begin{bmatrix} v_{xv} \\ v_{yv} \end{bmatrix}; \quad and \quad \begin{bmatrix} F_{xw} \\ F_{yw} \end{bmatrix} = \begin{bmatrix} \cos(\delta) & \sin(\delta) \\ -\sin(\delta) & \cos(\delta) \end{bmatrix} \cdot \begin{bmatrix} F_{xv} \\ F_{yv} \end{bmatrix}$$

[1.7]

1.6.1.3 Axle Position Relative to Vehicle Body

It can also be useful to define axle positions (translatory positions and angular orientations). For a rigid axle, it has a direct physical meaning. For an axle with individual wheel suspension, it can be a virtual mean value of left and right wheels direction.

A sign convention, aligned with articulation angles (between units) and steering angles, would be: Relative roll angle of an axle=$\theta_{jx} = \varphi_{jx} - \varphi_x$;, so the rule is "axle orientation of axle j is relative to the vehicle body". This can be extended to translatory position and orientation in yaw and pitch.

1.6.1.4 Wheel position relative to vehicle body

The wheel's (or wheel hub's) vertical position (or velocity) upwards relative to the vehicle body is called *jounce*. The term *rebound* refers to the same but in opposite direction.

1.6.1.5 Slip of Tyres and Wheels

Slip (longitudinal s_x and lateral s_y) for a tyre or wheel will be defined in Chapter 2, see Eq [2.2], Eq [2.43] and 2.2.4.1.1.1. Slip is central for relating tyre forces in ground plane F_x, F_y to vehicle and wheel motion and wheel vertical force F_z. Note that rotational speed of each wheel ω_i comes in as additional variables to Figure 1-60. Slip is a dimensionless velocity, "sliding velocity divided by a reference velocity", so the unit is either [1] or $[(m/s)/(m/s)]$. It appears as an intermediate variable to compute forces: $[F_x, F_y] = \boldsymbol{f_s}(F_z, s_x, s_y) = \boldsymbol{f_s}\left(F_z, s_x(\omega, v_x), s_y(\omega, v_y)\right) = \boldsymbol{f_v}(F_z, \omega, v_x, v_y)$;. One can sometimes define slip also for an axle or even for an axle group, but it becomes less strict, since ω, v_x, v_y can generally differ between the wheels within the axle or axle group.

When $\omega \to 0$, both $|s_x| \to \infty$ and $|s_y| \to \infty$. Note also that the slip is rather a mathematical auxiliary variable than a physical quantity. This becomes obvious for $\omega = 0$ or $\text{sign}(\omega \cdot v_x) = -1$, for which the slip becomes obsolete for F_x, F_y.

1.6.1.5.1 Slip angle

The direction of the vector $\vec{v} = [v_x, v_y]$ can be meassured with the slip angle $\alpha = \text{arctan2}(v_y, v_x)$. If the wheel has no longitudional slip ($R \cdot \omega = v_x$), α is also a measure of the lateral slip s_y. See 2.2.4.1.1.2.

1.6.1.6 Compatibility between Tyre and Vehicle

When implementing lateral tyre models in a vehicle model for lateral dynamics, there are two major ways of formulating the compatibility that relates vehicle motion (body slip angle β) to wheel side slip ($s_{iy} \approx \tan(\alpha)$) via wheel steering angle (δ). One way is to express longitudinal and lateral velocity components with sine and cosine, as done in Eqs [4.3], [4.6] and [4.51]. The other way is to use the angle sum $\beta_i = \delta_i + \alpha_i$;.

$$\begin{bmatrix} v_{xv} \\ v_{yv} \end{bmatrix} = \begin{bmatrix} \cos(\delta) & -\sin(\delta) \\ \sin(\delta) & \cos(\delta) \end{bmatrix} \cdot \begin{bmatrix} v_{xw} \\ v_{yw} \end{bmatrix}; \quad or \quad \begin{cases} \sqrt{v_{xv}^2 + v_{yv}^2} = \sqrt{v_{xw}^2 + v_{yw}^2}; \\ \underbrace{\text{arctan2}(v_{yv}, v_{xv})}_{\beta} = \delta + \underbrace{\text{arctan2}(v_{yw}, v_{xw})}_{\alpha}; \end{cases} \quad [1.8]$$

If approximating with small angles, it is easier to approximate to a linear vehicle model, see 4.3.2.1 and 4.4.2.2. For reversing, the angles β, α are close to $\pm\pi$ instead of close to 0.

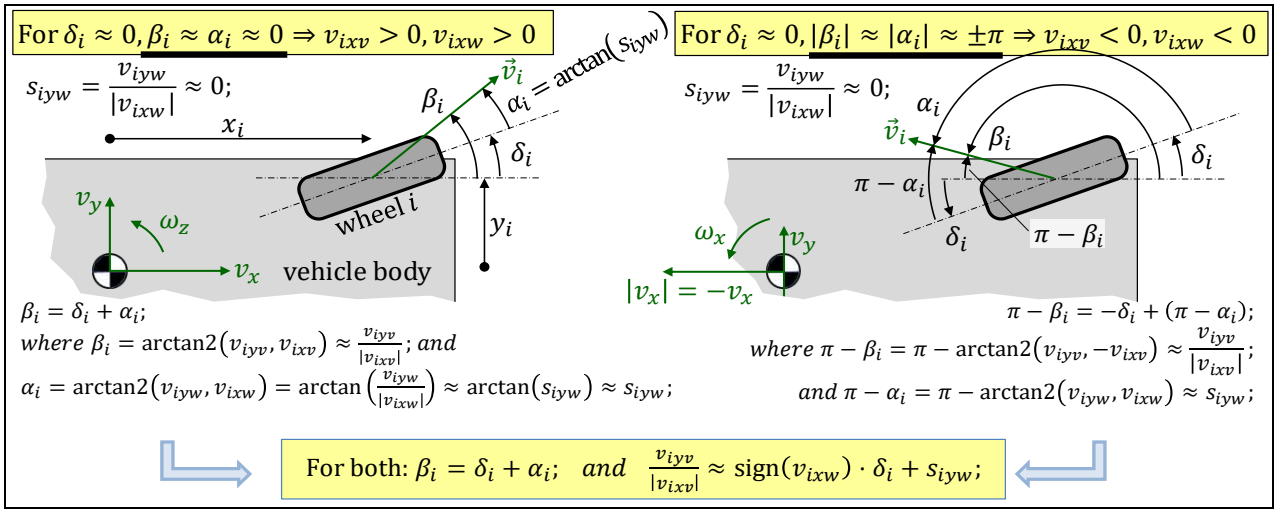


Figure 1-65: Approximate compatibility relation for small side slip, $v_{yw} \approx 0$. All angles δ, β, α are defined within $[-\pi, +\pi]$. Left: For forward driving. Right: For reversing.

1.6.1.7 Path, Orientation, Pose and Trajectory

A ***path*** can be $x(y)$ or $y(x)$ for centre of gravity where x and y are coordinates in the road plane. To cope with all paths, it is often necessary to use a curved path coordinate instead, s, i.e. $x(s)$ and $y(s)$. A path do have an orientation of itself φ_{rz}, defined through $\arctan(\varphi_{rz}) = dy/dx = (dy/ds) \cdot (1/(dx/ds)) = y'/x'$;. However, a vehicle following the path does not need to point along the path.

The vehicle also has a varying orientation, $\varphi_z(x)$ or $\varphi_z(s)$, which often is often relevant, but the term "path" does necessarily include this. In those cases, it might be good to use an expression "***path with orientation***" instead.

If the vehicle is articulated, it has not only the orientation as additional variable over the path. It also has the articulation angle θ in each articulation point. The set of articulation angles $\boldsymbol{\theta}$ describes the "pose", so the total description would be $[x;\ y;\ \varphi_z;\ \boldsymbol{\theta}]$ and called "***path with orientation and pose***".

A ***(time) trajectory*** is a more general term than a path and it brings in the dependence of time, t. One typical understanding is that trajectories can be $[x(t);\ y(t);\ \varphi_z(t); \boldsymbol{\theta}(t)]$. But also, other quantities, such as steer angle or vehicle propulsion force can be called trajectory: $\delta(t)$ and $F_x(t)$, respectively. The word "trace" is sometimes used interchangeably with trajectory.

1.6.1.7.1 Path with Orientation

The path and path with orientation was introduced in 1.5. The path, in global coordinate system, is related to vehicle speeds, in vehicle fix coordinates, as given in Figure 1-66 and Equation [1.9].

Knowing $(v_x(t), v_y(t), \omega_z(t))$, we can determine "path with orientation" $(x(t), y(t), \varphi_z(t))$, by time integration of the right-hand side of the equation. Hence, the positions are typically "state variables" in lateral dynamics models.

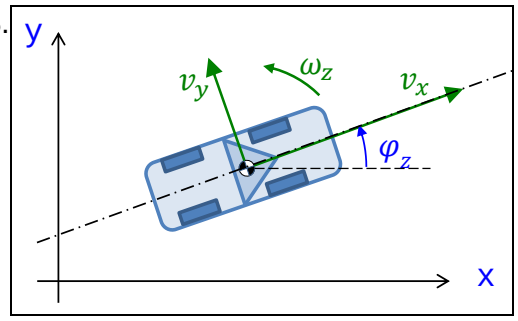


Figure 1-66: Model connecting "path with orientation" to velocities in vehicle coordinate system.

$$\begin{bmatrix}\dot{x}\\ \dot{y}\end{bmatrix} = \begin{bmatrix}\cos(\varphi_z) & -\sin(\varphi_z)\\ \sin(\varphi_z) & \cos(\varphi_z)\end{bmatrix} \cdot \begin{bmatrix}v_x\\ v_y\end{bmatrix};$$

$$\dot{\varphi}_z = \omega_z; \qquad [1.9]$$

It should be noted that in some problems, typically manoeuvring at low speed, the real time scale is of less interest. Then, the problem can be treated as time independent, e.g. by introducing a coordinate, s, along the path, as in Equation [1.10].

$$x' = \frac{v_x}{\dot{s}} \cdot \cos(\varphi_z) - \frac{v_y}{\dot{s}} \cdot \sin(\varphi_z);$$
$$y' = \frac{v_y}{\dot{s}} \cdot \cos(\varphi_z) + \frac{v_x}{\dot{s}} \cdot \sin(\varphi_z);$$
$$\varphi_z{}' = \frac{\omega_z}{\dot{s}};$$

where prime notes differentation with respect to s [1.10]

Here, $\dot{s}$ can be thought of like an arbitrary time scale, with which all speeds are scaled. One can typically choose $\dot{s} = 1\ [m/s]$. However, in this book we will keep notation t and the dot notation for derivative.

1.6.1.8 Length and Width Dimensions

For passenger cars, the length and width dimensions are rather constant and simple to define in a way that they always are positive: This can simplify the understanding and intuition for equations. For heavy vehicle, the situation is more complex and varying which motivates a more systematic way of denoting dimensions. The numerical values of the dimensions then often becomes negative. Two such conventions are shown in Figure 1-67.

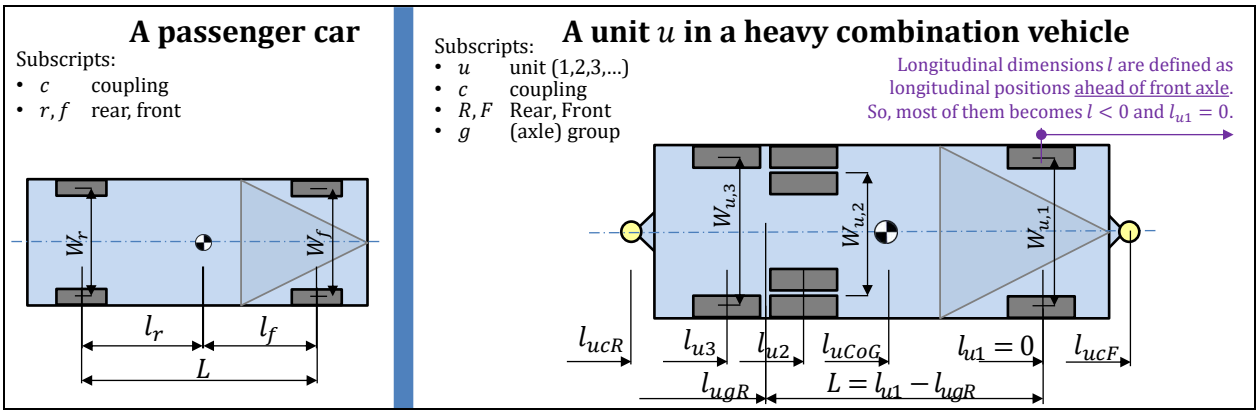


Figure 1-67: Two examples of dimension definitions and notation.

1.6.2 Complete Vehicle Modelling Concepts

Commercial model libraries for vehicle motion, see 1.5.4.1.3, often uses very detailed models on the most advanced levels listed in 1.6.2. If all their parameters are set as the studied vehicle, their numerical output becomes very accurate for most driving operations. For understanding, and as base for control design, the less advanced levels in 1.6.2 can often be more efficient to use. It is then important to select among the different less advanced level so that the right physical phenomena for the studied driving operation are modelled.

The (Dynamic) Equilibria (or Equation of Motion) can be seen as the main equations in a mathematical model of a complete vehicle. A summarizing view of this is given in Eq [1.11].

In the left approximations, only the most important centrifugal effects, $m \cdot v_x \cdot \omega_i$, are included see also Eqs [3.37] and [4.50]. The sums refer to forces and moments acting on the vehicle body; from tyre/ground caused by actuation and rolling resistance, from gravity and from aerodynamics. Equations for forces and moments in the summations are not given here, but are needed for the model to be complete, i.e. "simulate-able".

In-road-plane (irp) equilibria:

$$\begin{cases} m \cdot \dot{v}_x \approx m \cdot (\dot{v}_x - v_y \cdot \omega_z) \approx m \cdot (\dot{v}_x - v_y \cdot \omega_z + v_z \cdot \omega_y) = \sum forces_x ; \\ m \cdot (\dot{v}_y + v_x \cdot \omega_z) = \sum forces_y ; \\ J_z \cdot \dot{\omega}_z = \sum moments_z ; \end{cases}$$

Out-of-road-plane (oorp) equilibria:

$$\begin{cases} m \cdot (\dot{v}_z - v_x \cdot \omega_y) \approx m \cdot (\dot{v}_z - v_x \cdot \omega_y + v_y \cdot \omega_x) = \sum forces_z ; \\ J_x \cdot \dot{\omega}_x = \sum moments_x ; \\ J_y \cdot \dot{\omega}_y = \sum moments_y ; \end{cases} \quad [1.11]$$

Chapter **3** and **4** requires complete vehicle models that can measure complete vehicle functions expressed in *irp* motion.

1.6.2.1 Model Characterizations

A major categorization, see Eq [1.11] and 1.6.2.3 and 1.6.2.4, of vehicle models is whether the model considers *only* **irp** motion or *also* **oorp** motion. Another important categorization is to differ between **one-track** and **two-track** models, see 1.6.2.3.2.

1.6.2.1.1 Dynamic Operating Condition

A third important categorization is which "dynamic operating conditions" that characterizes the operation/manoeuvre. Categories for such are below defined based on the irp motion of the vehicle body.

1.6.2.1.1.1 Static

Static condition means that vehicle does not moves irp. All velocities and accelerations are zero. So, all terms on left side in Eq [1.11] are neglected. Force play in longitudinal direction can still be non-zero, due to e.g. gravitational force and pre-tension between axles and wheels.

1.6.2.1.1.2 Low speed

Low speed condition means that vehicle moves with low speed irp: forward, reverse or stand-still. Also, accelerations are low. Fictive forces ($mass \cdot acceleration$) are neglected in the models. All terms on left side in Eq [1.11] are neglected.

1.6.2.1.1.3 Steady State

Steady State condition means that time history is irrelevant for the quantities studied. Seen as a manoeuvre over time, the studied quantities are constant. Explained for a certain model, it means that the influence of the derivatives of the corresponding variables, that else would generate state variables, is neglected. In physical model of a mechanical system this often means that "*mass · acceleration* " or "*force derivative/stiffness* " is neglected (in mathematical model: equation "$\dot{z}_i = 0$;" is added, in explicit form model: "$\dot{z}_i$" is replaced with "0"). If only some quantities are treated in this way, one might call the conditions steady state with respect to these quantities. Only the $m \cdot v_i \cdot \omega_j$ terms (centrifugal forces) on left side in in Eq [1.11] are kept.

1.6.2.1.1.4 Transient

Transient (or Transient State, as opposed to Steady State) condition means that time history is relevant; i.e. there are delays, represented by "state variables" when simulated. All terms on the left side in in Eq [1.11]are kept. Note that also cases with low velocities but large accelerations belongs here, and not in 1.6.2.1.1.2.

1.6.2.1.1.5 Stationary Oscillating

Stationary Oscillating condition is a special case of transient, where cyclic variations continue over long time with a repeated pattern. Long time means to that all none-cyclic components of the variation is damped out. The pattern is often modelled as harmonic (sinus and cosine variations in time) with constant amplitudes and phases. Example is sinusoidal steering with small enough steering amplitude, see 4.4, but also driving with over an undulated road surface, see Chapter 5. All terms on left side in in Eq [1.11] are kept, as for transient operation.

1.6.2.1.1.6 Quasi-Steady State

Quasi-Steady State condition have a more diffuse meaning. It can refer to steady state with respect to some quantities, i.e. some terms on left side in in Eq [1.11] are neglected but not all. Alternatively, it can refer to that the quantities are prescribed to an explicit function of time, e.g. $v_x = f(t)$; meaning that also $\dot{v}_x$ is known. The latter is sometimes also known as "inverse dynamics".

1.6.2.1.2 Other Characterizations

Let us also briefly list some other possible categorizations for Chapter 3 and 4:

- Categorization referring to **small angles** ($\sin(angle) = 1; \cos(angle) = 0;$) or not, applied to steering/articulation angles and/or tyre/body side-slip angles.
- Categorization referring to **tyre models** are further explained in 2.2.7.
- One can also categorize referring to **subsystem models**.
  - The suspension can add states per wheel or axle i, at least the vertical spring force F_{si}.
  - The propulsion and brake system can be actively controlled. They give wheel torques $\boldsymbol{T}(t) = [\omega_1, \omega_2, \cdots]$. Such models often add one state per wheel or axle i, the rotational speed ω_i.
  - Chapter 3 uses different models of propulsion, brake and suspension. E.g., the propulsion system can add more states: engine delay, gear shifting, torsional shaft, control algorithms.
  - Chapter 4 adds the steering subsystem, with its control algorithms. Also, more about model categorisation is found in 4.1.1.

Chapter **5** is very different since it treats vehicle functions expressed in *out-of-road-plane* motion. So, most models in Chapter **5** uses only the oorp equations, i.e. not the irp equations, above.

To make the overall model simulate-able one needs some form of driver model and environment model. A rather complete example model is described in 4.5.3.2.

1.6.2.2 1D Models

In some cases, it can be enough to model motion in 1 dimension. Some examples are:

- **Longitudinal 1D** in 3.2 and 3.3, it can be enough to model v_x: $m \cdot \dot{v}_x = \sum forces_x$;.
- **Roll 1D** in 4.3.7.13, it can be enough to model ω_x: $J_x \cdot \dot{\omega}_x = \sum moments_x$;
- **Heave 1D** in 5.4, it can be enough to model v_z: $m \cdot \dot{v}_z = \sum forces_z$;

1.6.2.2.1 One-Wheel Longitudinal 1D Models

For Longitudinal 1D model it is common that all wheels (or axles) are lumped to one wheel, see Figure 1-68. The lumping means that torques from all wheel torque actuators (propulsion, brake, …) are summed to one torque which acts on one fictive wheel. The fictive wheel carries the whole vertical force from all wheels. It should be noted that we also, implicitly, assume that all wheels rotate equally fast. The rolling resistance coefficient and slip characteristics of the fictive wheel are, for instance, taken as a weighted mean between all wheels, weighted with vertical load of each wheel. This kind of vehicle model can**not** well represent driving situation with significant wheel slip, different ground conditions (grade, peak friction, …) under wheels, non-Ackermann steering geometry or articulation angles between vehicle units.

1.6.2.2.2 Per-Axle and Per-Axle-Group Longitudinal 1D Models

To repair the mentioned short-comings with the One-Wheel Longitudinal 1D Model, more axles and axle groups can be modelled separately, see Figure 1-68. (The motion is still 1 dimensional, but the force play is 2D; so one can think about these as "1.5D models", but that is no established nomenclature.)

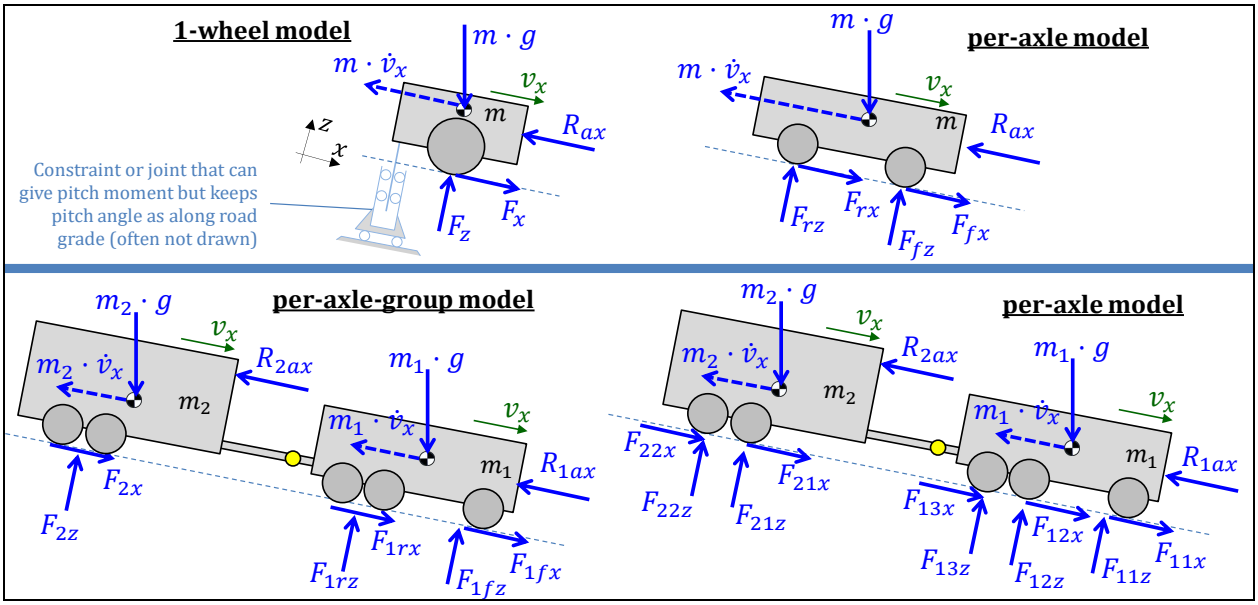


Figure 1-68: Different longitudinal 1D models.

1.6.2.3 In-road-plane Models, 2D

When modelling longitudinal dynamics, one has to involve at least v_x. When modelling lateral dynamics, one has to involve at least v_y and ω_z. So, models in xy-plane (irp) are often useful. (Other 2D models, in xz- or zy-planes, can also be relevant, e.g. for load transfer.)

1.6.2.3.1 Particle and Body Models

A particle model is similar to a 1D-model but can move in 2D and have forces in 2D. In cases such as threat estimation in 3.5.2.8 and 4.6.2.5, a particle model can be of use. The alternative is a body model,

see Figure 1-69. A particle model cannot resolve F_z per wheel or axle, which means that tyre slip, neither s_x nor s_y, can be properly captured which is a problem for both longitudinal and lateral dynamics. The force $\vec{F}$ can be decomposed in global directions $[F_X, F_Y]$ or $[F_{xg}, F_{yg}]$. Other decompositions are road $[F_{xr}, F_{yr}]$, path $[F_{xp}, F_{yp}]$ or vehicle $[F_{xv}, F_{yv}]$. Road can be tracked using a map. Path can be tracked by remembering position from previous time history. Vehicle heading is most difficult, since a particle model do not capture yaw dynamics well.

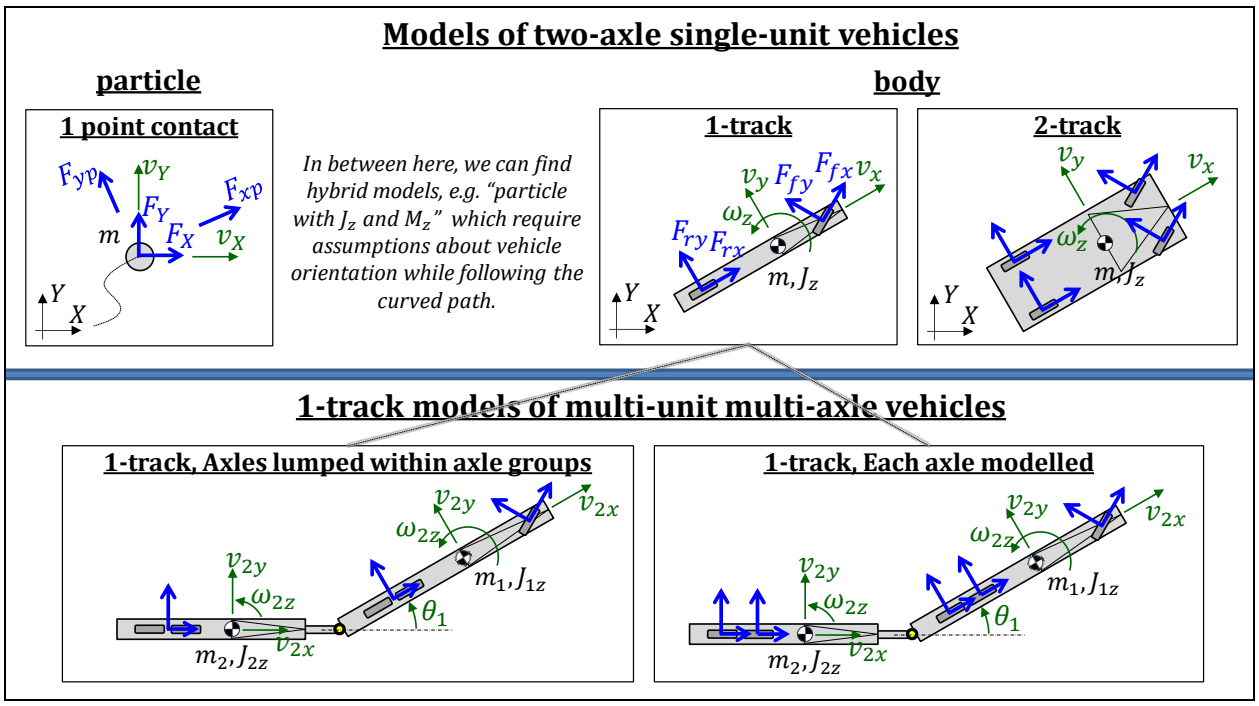


Figure 1-69: Different in-road-plane vehicle model concepts. The forces are from tyre contacts, acting on vehicle body. Fictive forces (m · acceleration) and body forces (gravity and aerodynamic) are not drawn.

1.6.2.3.2 One-Track and Two-Track Models

The models can assume that each wheel on the axles have their own ground contact (two-track models) or if there is only one "virtual tyre" modelled per axle (one-track model or single-track model or "bicycle model"). See Figure 1-69 and Figure 1-70. For multi-axle vehicles, one can even simplify one step further and model only one "virtual tyre" per axle group, see Figure 1-69. It should be noted that the simplifications have limitations, they are not suitable when the forces of the different tyres are significantly different, e.g. differences in actuated wheel torques or different wheel side slips.

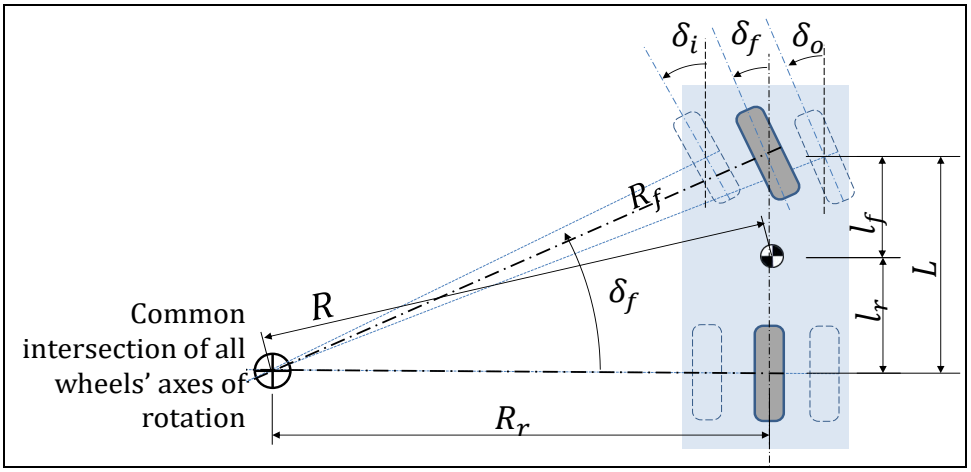


Figure 1-70: Collapsing a two-track vehicle to a one-track model.

Lateral dynamics phenomena which one-track models do not capture well are, e.g.:

- Deviations from Ackerman geometry within an axle, see 2.6.1.
- Roll motion
- Lateral load shift (4.3.7.2) and combined tyre slip (4.3.7.6).
- Added yaw moment due to left/right-asymmetric wheel torque, such as ESC interventions.

The in-road-plane (irp) models does not capture the out-of-road-plane motion, v_z, ω_x, ω_y. However, they can still capture the transfer of loads (vertical forces on wheels).

For longitudinal dynamics, one-track models are often enough. For longitudinal functions in "3.2 Steady state functions" and "3.3 Functions for (longer) transports", even particle models are often enough. But, it is important to understand the validity limit of the model!

1.6.2.4 Adding Out-of-road-plane Motion

One can combine equations from several 2D views (xy-, xz- and yz-plane) without adding all cross-coupling effects from strict 3D rigid body dynamics theory. An example of a two-track model including both irp and oorp motion is given in 4.5.3.

1.6.2.4.1 7-dof models

Here is an example of that nomenclature can overlap between "sub-communities" of vehicle motion engineering: The name "7-dof model" can mean either of:

- "7-dof **handling** model", which has the dofs $\{longitudinal, lateral, yaw, 4\ wheel\ rotations\}$. The states can be, at least and for example: $\{v_x, v_y, \omega_z, \omega_{fl}, \omega_{fr}, \omega_{rl}, \omega_{rr}\}$.
- "7-dof **ride** model", which has the dofs $\{vertical, pitch, roll, 4\ wheel\ vertical\}$. The states can be, at least and for example: $\{v_z, \omega_y, \omega_x, z_{fl}, z_{fr}, z_{rl}, z_{rr}\}$.

1.6.2.4.2 14-dof models

The name "14-dof model", typically means a model with the dofs $\{\{longitudinal, lateral, yaw\}, \{vertical, roll, pitch\}, 4\ wheel\ rotations, 4\ wheel\ vertical\}$. The states can be, at least and for example: $\{\{v_x, v_y, \omega_z\}, \{v_z, \omega_x, \omega_y\}, \{\omega_{fl}, \omega_{fr}, \omega_{rl}, \omega_{rr}\}, \{z_{fl}, z_{fr}, z_{rl}, z_{rr}\}\}$.

1.6.3 Vehicle Dynamics Terms

1.6.3.1 Load Levels

The weight of the vehicle varies through usage. For many vehicle dynamic functions, it is important to specify this load level.

Kerb weight is the total weight of a vehicle with standard equipment, all necessary operating consumables (e.g., motor oil and coolant), a full tank of fuel, while not loaded with either passengers or cargo. Kerb weight definition differs between different governmental regulatory agencies and similar organizations. For example, many European Union manufacturers include a 75 kg driver to follow European Directive 95/48/EC.

Payload is the weight of carrying capacity of vehicle. Depending on the nature of the mission, the payload of a vehicle may include cargo, passengers or other equipment. In a commercial context, payload may refer only to revenue-generating cargo or paying passengers.

Gross Vehicle Weight/Mass (GVW/GVM) is the maximum operating weight/mass of a vehicle as specified by the manufacturer including the vehicle's chassis, body, engine, engine fluids, fuel, accessories, driver, passengers and cargo but excluding that of any trailers.

Other load definitions exist, such as:

- *"**Design Weight**"* (for passenger vehicles, this is typically Kerb weight plus 1 driver and 1 passenger, 75 kg each, in front seats)
- *"**Instrumented Vehicle Weight**"* (includes equipment for testing, e.g. out-riggers)

- ***"Road-allowed GVW/GVM"*** is the maximum GVW/GVM for a certain road, limited by the strength of the road and bridges. It is applicable for heavy trucks.

For vehicle dynamics it is often also relevant to specify where in the vehicle the load is placed because it influences how vertical forces under the wheels/axles distribute as well as moments of inertia.

1.6.3.2 Open-Loop and Closed-Loop Test Manoeuvres

Two expressions used in vehicle dynamics are "Open-loop" and "Closed-loop" test manoeuvres.

An **open-loop** manoeuvre refers to the case where the driver controls (steering wheel, brake pedal and accelerator pedal) are operated in a specific sequence, i.e. as functions of time. A typical case is a sine wave excitation of the steering wheel. The time history of the steering wheel angle is defined as a function that is independent of the road environment or driver input. This type of manoeuvre can be relevant to design for, and it tells some but not all about the real-world driving cases. Theoretical simulation and real testing with a steering robot are examples of how such studies can be made.

A **closed-loop** manoeuvre refers to the case when (human) driver feedback via driver controls is included. This represents real-world driving better. In real vehicle or driving simulator testing, a real driver is used. This enables collection of the drivers' subjective experience. In cases of simulation, a "driver-model" is needed. A driver-model can have varying levels of complexity but in all cases simulates the response of a human driver to different effects, such as lateral acceleration, steering wheel torque, various objects appearing outside the vehicle, etc.

A test with real vehicle, carried out with a steering-robot (and/or pedal robot) can also be called closed-loop if the robot is controlled with a control algorithm which acts differently depending on the vehicle states, i.e. if the algorithm is a driver model.

With increasing level of automation, there is sometimes a need for distinguishing between closed/open loop with respect to human driver or automated driver.

1.6.3.2.1 Closing Loop via Human and/or Virtual Driver

The concepts of open- and closed-loop control are demonstrated in figure below. The important difference to note is that in open-loop control there is no feedback to the driver. The figure also shows a "Virtual driver" which represents today's automated driving functions based on environment sensing, such as adaptive cruise control (section 3.5.2.3) and lane keeping aid (section 4.6.2.2). Closed loop control incorporates the different types of feedback to the driver. Drivers automatically adapt to the different feedback. Understanding driver response to different feedback, and expressing it in mathematical descriptions, is an active area of research, particularly for driver support functions.

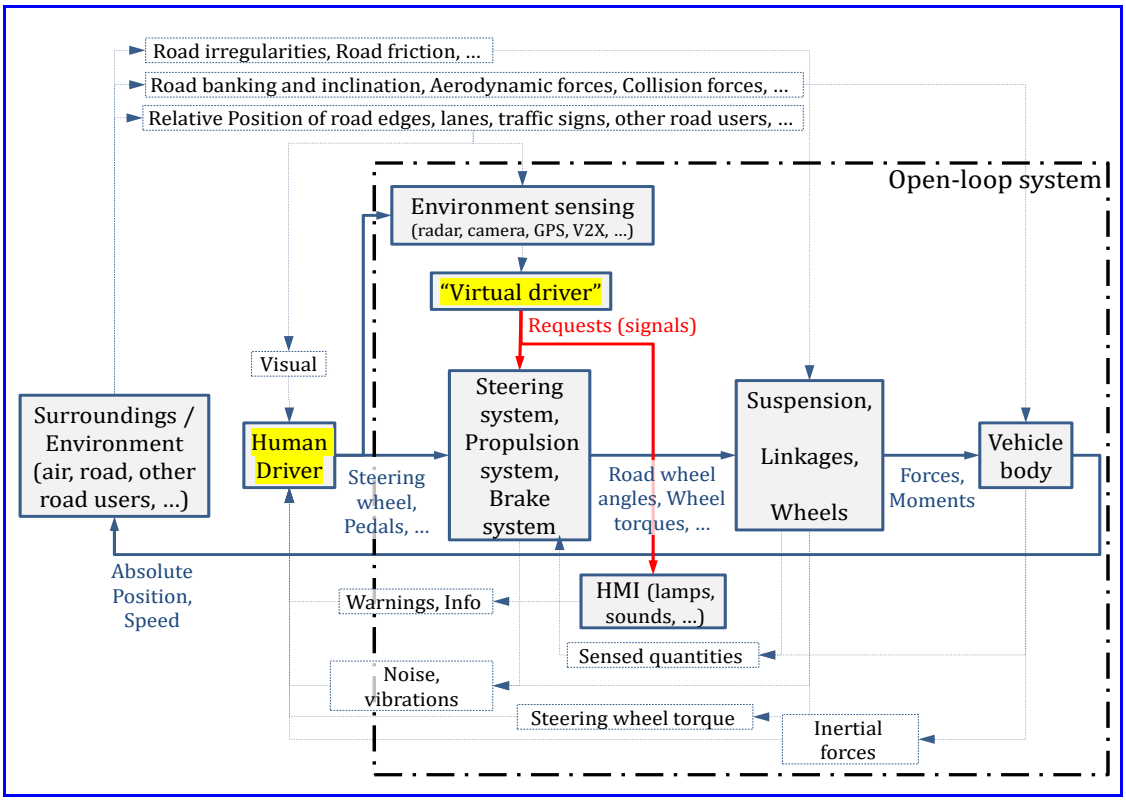


Figure 1-71: Open and closed loop representations of vehicle dynamic systems

1.6.3.3 Objective and Subjective Measures

Two main categories of finding measures are:

- *An **Objective*** measure is a physical measure calculated in a defined and unique way from data which can be logged in a simulation or from sensors in a real test.
- *A **Subjective*** assessment is a rating measure set by a test driver (e.g. on a scale 1-10) in a real-vehicle test or driving simulator test.

One generally strives for objective measures. However, many relevant functions are so difficult to capture objectively, such as Steering feel and Comfort in transient jerks, so subjective assessments are needed and important.

1.6.3.4 Stable and Unstable

Often, in the automotive industry and vehicle dynamics, the words "stable" and "unstable" have a broad meaning, describing whether high lateral slip on any axle is present or not. Sometimes it is used for roll-over instability. Also, the articulation angle can be unstable when reversing in low speed with a trailer. Stability analysis in a stricter physics/mathematical meaning is touch upon in 0.

It is useful to know about this confusion of words. An alternative expression for the wider meaning is "loss of control" or "loss of tracking" or "directional unstable", which can include that vehicle goes straight ahead, but road bends.

1.6.3.5 Subject and Object Vehicle

The ***subject vehicle*** is the vehicle that is studied, and often under development. It is practical to have a name for it, since one often studies one specific vehicle, but it may interact with other in a traffic situation. Alternative names are ***host vehicle***, ***ego vehicle*** or simply ***studied vehicle***.

Other vehicles are called ***object vehicles*** or ***opponent vehicles***. A special case of object vehicle is ***lead vehicle*** which is ahead of, and travels in same direction as, subject vehicle. Another special case is ***on-coming vehicle*** which is ahead of, and travels in opposite direction as, subject vehicle.

1.6.3.6 Active Safety, ADAS and AD

The expression *Active Safety* is used in Automotive Engineering with at least two different meanings:

- Active Safety can refer to the vehicle's ability to avoid accidents, including both when the driver is in control (such as ABS and ESC, but also steering response) and functions with automatic interventions based on sensing of the vehicle surroundings (such as AEB and LKA). See http://en.wikipedia.org/wiki/Active_safety. Active Safety can even include static design aspects, such as designing the wind shield and head light for good vision/visibility.
- Alternatively, Active Safety can refer to only the functions with automatic interventions based on sensing of the vehicle surroundings. In those cases it is probably more specific to use *Advanced Driver Assistance Systems (ADAS)* instead, see http://en.wikipedia.org/wiki/Advanced_Driver_Assistance_Systems. ADAS does not only contain safety functions, but also comfort functions like CC and ACC.

Functions that off-load the driver normal tasks during driving can be sorted under *Automated Driving, AD*. Fully automated driving, e.g. transportation without human driver on-board, is probably a far future vision. On the other hand, it is already a reality that some portion of the driving tasks are automated in the latest vehicle on the market, such as Adaptive cruise control, see 3.5.2.3, and Lane Keeping Aid, see 4.6.2.2. If both those are active at the same time, we have already automated driving. Definitions of automation levels 0-5 is found in Reference (SAE_J3016, 2016). Today's version of these systems normally has a way to hand-back responsibility to driver rather immediately in hazardous situations. Future automated driving functions will need to always have a safe-stop function. The way to compete between vehicle manufacturers will probably be to avoid hand-backs (maximize up-time) and to allow as long "hand-back times" as possible. So, vehicle dynamics will be important in the development, especially for safety reasons for automated driving in higher speeds; hazardous situations where human driver selects to take back the driving.

1.6.4 Vehicle Architectures

Vehicles are often designed in platforms, i.e. parts of the design solutions are reused in several variants. Typical variants may be different model years or different propulsion system. To be able to reuse solutions, the vehicles have to be built using the same *architecture*.

A **mechanical** (or geometric) architecture may include design decisions about certain type of wheel suspension on front and rear axle. An **electrical and electronic** architecture may include design decisions about electric energy supply system (battery voltage etc.) and electronic hardware for computers (Electronic Control Units, ECUs) and how they are connected in networks, such as Controller Area Network, CAN.

The mechanical architecture influences vehicle dynamics functions. However, it is noteworthy that also the electronic architecture also is very important for the vehicle dynamics, through all electronic sensors, actuators and control algorithms. One example of this importance is the ABS control of the friction brake actuators. Architectures for functions are therefore motivated, see 1.6.4.2.

1.6.4.1 Subsystems

The architectures are dependent on the business model for how to purchase and integrate subsystems to a vehicle. Hence, it is relevant to define the subsystems. For vehicle motion functionality, the relevant subsystems (or "motion support devices") are typically:

- Propulsion system
- Brake system
- Wheel suspension
- Wheels and tyres
- Steering system
- Environment sensing system

Each of these can typically be purchased as one subsystem. Each typically have mechanical and signal interface to the remaining vehicle. Different vehicle manufacturers can have different strategies for signal interface and how much the subsystems are allowed to be dependent of each other.

1.6.4.2 Vehicle Function Architecture

As the number of electronically controlled functions increase, an architecture for vehicle functionality, or "Function Architecture", becomes necessary to meet fast introduction of new functionality and to manage different variety of vehicle configurations. A function architecture is a set of design rules for how functions interact with each other (e.g., signalling between control functions). Also, the decomposition in subsystems should be reflected in this architecture, see 1.6.4.1. An older expression which is related to function architecture is *cybernetics*. Examples (from Vehicle Dynamics/Motion function domain, often including energy) of modern expressions which are related are Integrated Chassis Control (GM), Integrated Vehicle Dynamics Control (Ford), Complete Vehicle Control (Volvo) and Vehicle Dynamics Integrated Management (Toyota). There is no exact and generally well accepted definition of a function architecture. Some concepts for how to discuss and decide a function architecture are shown sin Figure 1-72.

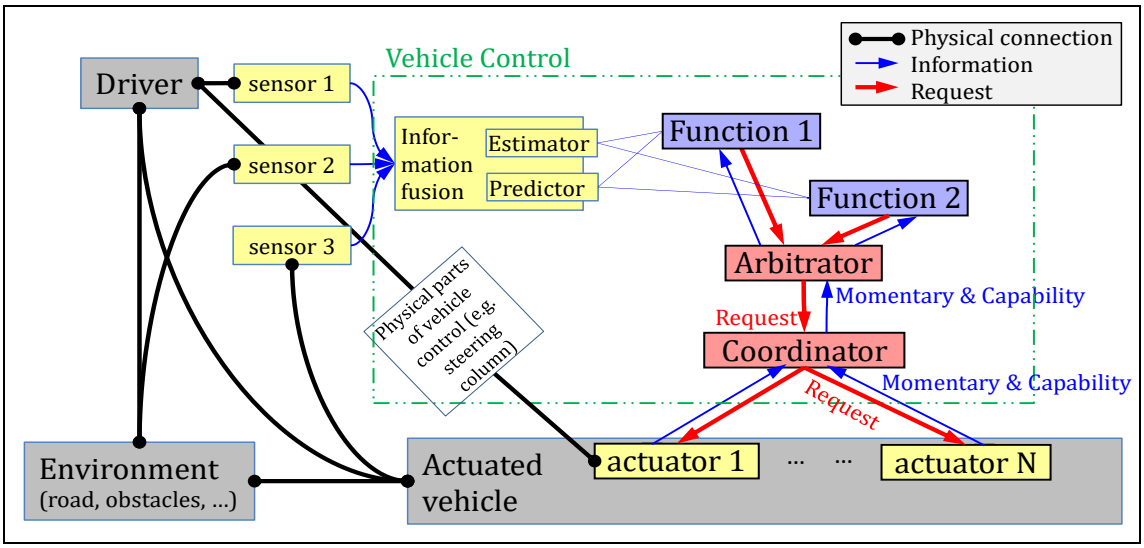


Figure 1-72: Concepts of a vehicle motion (and energy) function architecture. Arbitrators, Coordinators and Actuators are the most important architectural objects for vehicle dynamics (vehicle motion).

The words *Requirement*, 1.4.3, and *Request* are used as follows in this book: Both ask for something. A **Requirement** asks for a measure of a whole transport operation or manoeuvre and it is set (by an engineer) during the development of the vehicle. A **Request** asks for a quantity and it is set (calculated by an algorithm) during the use of the vehicle. Based on *Requirements*, the function developing engineers, formulates the algorithms that will calculate the *Requests*.

One example of way to visualize a reference architecture is given in Figure 1-73. To have a function architecture becomes more and more important, driven by increasing content of electronic control in vehicles. The interface between vehicle and motion support devices (or subsystems, or actuators and sensors) depends on which function architecture that each vehicle manufacturer and subsystem supplier has agreed.

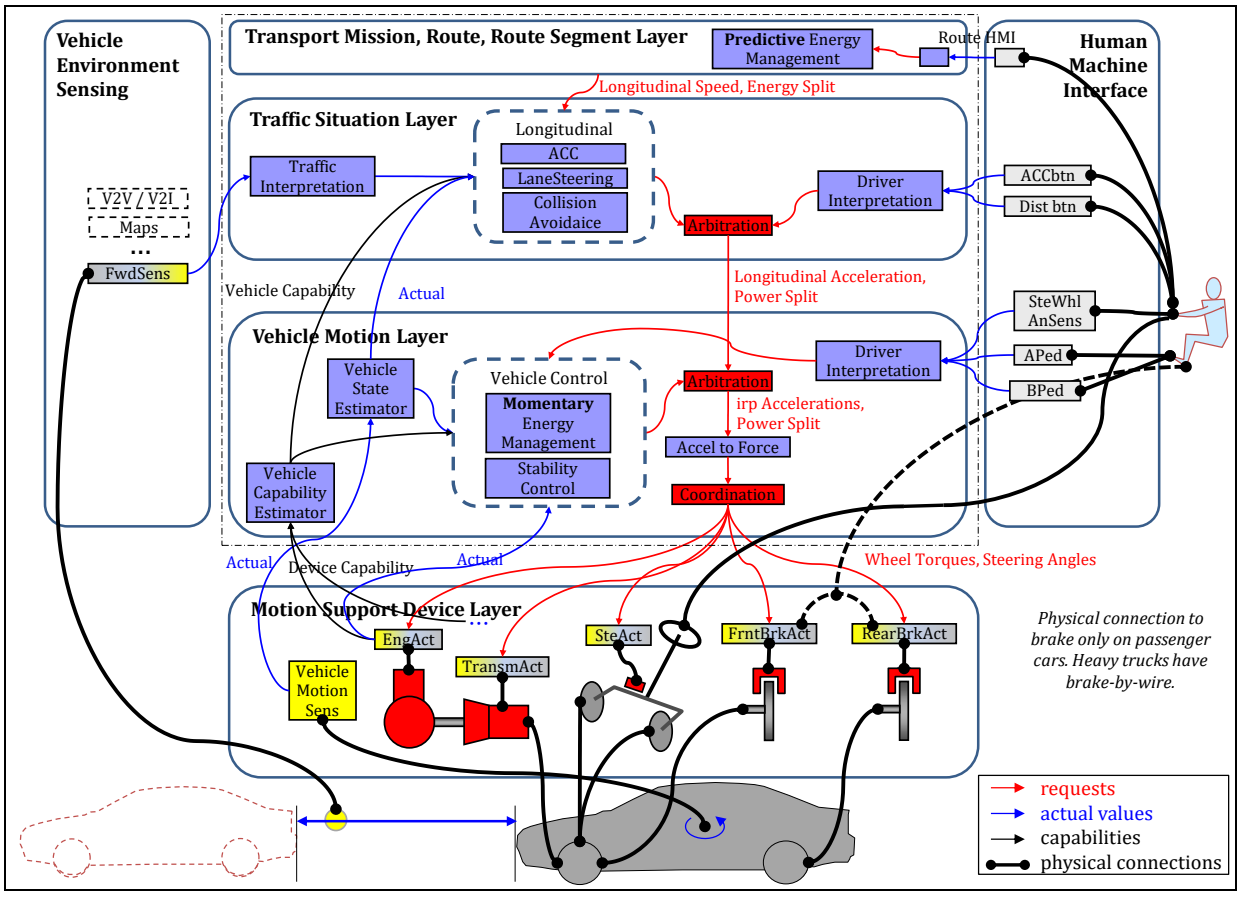


Figure 1-73: One example of reference architecture of vehicle motion functionality. Red arrows: Requests, Blue arrow: Information, Black lines with dot-ends: physical connection.

In order to be able to formulate design rules in reference architecture of functionality the following are relevant questions:

- Which physical quantities should be represented on the interface between Devices (Sensors and Actuators) and Vehicle Level Functionality?
- Partitioning within a reference architecture of vehicle motion functionality could be realised as shown in Figure 1-73. Different Layers/Domains are defined:
  - **Human Machine Interface** Domain: This includes the sensors/buttons which the driver uses to request services from the vehicle's embedded motion functionality.
  - **Vehicle Environment** Domain: Includes surrounding sensors mounted on vehicle but also communication with other vehicles (V2V) and infrastructure (V2I) and map information.
  - **Route** Layer: Planning the whole transport mission, horizon 10..1000 km. These functions exist mainly for commercial traffic and might be done outside the subject vehicle.
  - **Traffic Situation** Layer: Interpret the immediate surrounding traffic which the vehicle is in, road/lanes and other road users, horizon ≈100..300 m. Example of functions: adaptive cruise control, collision avoidance, and lane steer support.
  - **Vehicle Motion** Layer: This includes the Energy management, powertrain coordination, brake distribution, and vehicle stability such as ESC, ABS. Horizon ≈10..30 m This layer also estimates the vehicle states e.g. v_x, v_y, ω_z. In addition, this layer would be able to give vehicle level capability of max/min acceleration and their derivative.
  - **Motion Support Device** Layer: This includes the devices/actuators that can generate vehicle motion. This layer is also consisting sensors which could include the capability and status of each device e.g. max/min wheel torque.
- Formalisation of different types of:
  - Blocks, e.g. **Controller**, **Information Fusion**, **Arbitrator** and **Coordinator**.

        - Both arbitrators and coordinators have inputs and outputs as requests, typically expressed in same physical quantity. An arbitrator has more requests in that out and a coordinator has more requests out than in.
    - Signals, e.g. **Request** or **Information**. Information can be, e.g., **Actual** (or Status) and **Capability**.
        - A request signal is sent because the sender wants something to be done, e.g., a torque to be applied or an HMI lamp to light up.
        - An information signal is sent because the receiver wants to know something, e.g., what torque is applied (actual), what torque can be applied (capability) or is an HMI button pressed (actual).
    - **Parameters** used in Functional blocks. One can differ between Physical parameters (or Model parameters) and Tuning parameters. Some parameters can be common across the whole vehicle, which enables a kind of communication between blocks without normal signals, but instead exchanging values during start-up of the system.

Each signal should have a definition of which physical quantity and unit it refers to. For signals of Actual type, there also needs a concept to handle how accurate they are; e.g. as a tolerance or sending an upper and lower value between the physical quantity shall be. The definition of physical quantity is very important, not the least for Request signals. An example is, if using tyre longitudinal slip as quantity, sender and receiver of signal have to agree on slip definition. Since there are many slip definitions around, it might suggest using wheel rotational speed instead, which is less ambiguous.

The functionality is then allocated to ECUs, and signals allocated to network communication. The reference architecture can be used for reasoning where the allocation should be done. Which functionality is sensitive for e.g. time delay and thus should be allocated in the same ECU? Detailed control algorithm design is not stipulated by a reference architecture. Instead the reference architecture assists how detailed control algorithms be managed in the complete problem of controlling the vehicle motion. Whether solutions of Functional Safety (ISO 26262, 2011-2012) is represented in a reference architecture of functionality can vary.

Vehicles consisting of several units add special challenges, especially if the units are actuated. A heavy truck trailer is always actuated with at least brakes.

1.6.4.3 Virtual Vehicle Architecture

Virtual vehicle architecture, VVA, here refers to how to organize complete vehicle models, which can replace some real vehicle pre-series. VVA is a set of rules how a vehicle model should be modularized, such as variable/signal interfaces, parameterization, format- and toolchains. The vision is that a whole project organisation, within an OEM and its suppliers, could deliver modules to virtual pre-series and that these modules would fit together. The FMI format, see 1.5.4.1.6, is one example of what could facilitate this.

1.6.5 Verification Methods with Real Vehicle

1.6.5.1 In Traffic

Driving on public roads in real traffic is the most realistic way to verify how well a vehicle fulfils the requirements during real use. It can be used for completely new vehicle models; or new systems, mounted on old models. The drivers can be either ordinary drivers (FOT=Field Operational Test) or test drivers (expeditions). A general existing vehicle population can also be studied by collecting data, e.g. as Accident Statistics Databases.

1.6.5.2 On Test Track

For vehicles and systems which are not yet allowed on public roads, or tests which are very severe or need a high degree of repeatability, test are carried out at test tracks. There are specialized test tracks for certain conditions, such as hot climate or slippery surfaces.

1.6.5.3 Rapid Prototyping, RP

Rapid prototyping here refers to rapid prototyping of control algorithms. The method is to have a real vehicle but especially equipped with a real-time computer with I/O to the vehicle. Changes of control algorithms can be done in a laptop on-board and then new versions can be downloaded to the real-time computer and tested a minute later. This enables a really quick development loop.

1.6.5.4 Augmented Reality, AR or Manipulated Environment

This is a new method. A typical example is: A real driver drives a real vehicle on a real road/test track. Some additional (virtual/simulated) traffic objects are presented to driver, e.g. on a head-up display. The same objects can be fed into the control functions, as if they were detected by the vehicle's camera/radar, which enables functions such as automatic braking to be triggered.

1.6.5.5 Objective Measures and Subjective Assessment

The vehicle can be instrumented so that measurements can be logged and later compared with requirements. Also, the tests can be performed with driving robot, so that the manoeuvres are well repeated.

However, driving also with human driver has its own value; the subjective assessments can be registered via interviews and debriefing after performed tests. A typical scale used for subjective rating or assessment is shown in Figure 1-74.

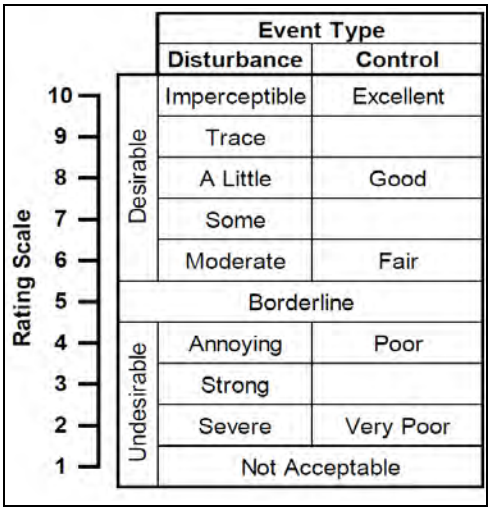


Figure 1-74: Subjective rating scale (SAE J1441, 2016.)

1.6.6 Verification Methods with Virtual Vehicle

This section introduces different methods called "XIL=X in the Loop". The loop referred to is then the representation of the whole system, except for the X. The loop is typically a simulation model, but there can also be hardware.

1.6.6.1 Testing with Real Driver

1.6.6.1.1 DIL =Driver in the Loop

Verification with a driving simulator (or DIL) is when a real human, not a driver model, uses real driver devices (pedals, steering wheel) to influence a simulation model of the remaining system (vehicle and environment). The loop is closed by giving the human feedback through display of what would be visible from driver seat, including views outside windscreen.

Feedback can be further improved by adding a motion platform to the driver's seat, sound, vibrations in seat, steering wheel torque, etc. The vehicle model run in the simulator can utilize HIL, SIL and MIL, from 0, for some part of the vehicle model. Driving simulator can be compared to other verification methods, see Table 1-75. Subjective scale from Figure 1-74 can be used.

Table 1-75: Comparison of verification methods for complete vehicle functions

			Alternative verification methods		
			Office simulation	**Driving simulator**	**Real vehicle test**
Requirements	**Test new technology before it is built (save time and money)**		+	-	- -
	Design parameter sweep/optimization		+!	-	- -
	Repeatable and Parallelized testing		+	+	-
	Safe testing		+	+	-
	Representative integration in vehicle		-	+!	++
	Represen-tative behaviour	w.r.t. to vehicle	-	-	+!
		w.r.t. driver	-	+!	+
		w.r.t. to surroundings (road & traffic)	- - (env. sens)	- (env. sens)	+!

1.6.6.2 Testing using Driver Model

Generally, this means that driver, vehicle and environment are modelled and simulated. To perform a serious test there is also need to put effort on test scripts so that the model is run in the intended test manoeuvre and result is pre-processed. For verification of functions involving with algorithms, the HIL, SIL and MIL below are different ways to represent the algorithm in the vehicle model.

1.6.6.2.1 HIL = Hardware in the Loop Simulation

The hardware is often one or several ECUs (Electronic Control Units). If several ECUs are tested, the hardware can also contain the communication channel between them, e.g. a CAN bus. The hardware is run with real-time I/O to simulation model of the remaining system (vehicle, driver and environment).

In some cases, there is also mechanical hardware involved, such as if the ECU is the brake system ECU, the actual hydraulic part of the brake system can also be included in the HIL set-up, a so called "wet brake ECU HIL".

For HIL, there can be two types of hardware involved: The hardware under test or test object, the H in HIL) and hardware that helps representing the rest of the system, i.e. a part of the loop (the L in HIL). Also, the test object is typically an ECU or a mechanical hardware such as brake system or similar.

1.6.6.2.2 SIL = Software in the Loop Simulation

The software is often one or several computer programs (intended for download in electronic control units). The software is run with synchronized time discrete I/O to a simulation model of the remaining system (vehicle, driver and environment).

The software is often used in compiled format (black box format) so that the supplier of the software can retain his intellectual property.

1.6.6.2.3 MIL = Model in the Loop Simulation

The model, or more correctly, a control algorithm, is a conceptual form of the computer programs (intended for download in electronic control units). The control algorithm is run with I/O to a simulation model of the remaining system (vehicle, driver and environment).

The control algorithms can appear in compiled format so that the supplier of the control algorithms can retain his intellectual property. Then it is hard to tell the difference between MIL and SIL.

1.7 Heavy Trucks

The following section describes heavy trucks, mainly as compared to passenger vehicles.

1.7.1 General Differences

Trucks are normally bought and owned by companies, not private persons. Each truck is bought for a specialized transport task. Life, counted in covered distance, for trucks is typically 10 times passenger cars. The lifetime cost of fuel is normally 5 times the vehicle cost, compared to passenger car where these costs are about equal. The cost for driver salary is a part of mileage cost, typically same magnitude as fuel cost. If investment cost for vehicle and repairs are distributed over travelled distance, these are typically also of same magnitude. So, the cost for a transport typically comes from one third fuel, one third driver salary and one third vehicle investment and repairs.

In the book, the word *combination vehicle* is used as for a combination of several *vehicle units*. One vehicle unit can be, e.g., a truck, a full-trailer, a semi-trailer, a centre-axle-trailer, or a converter dolly. The word *vehicle* is avoided unless as a general word is motivated, not distinguishing between combination vehicle or vehicle unit. (There is, at least, one alternative terminology, which instead uses *vehicle combination* and *vehicle*, respectively.)

1.7.2 Vehicle Dynamics Differences

A truck has 5..10 times less power installed per vehicle weight. Trucks have their centre of gravity much higher, meaning that roll-over occurs at typically 4 m/s^2 lateral acceleration, as compared to around 10 m/s^2 for passenger cars. Trucks have centre of gravity far behind mid-point between axles, where passenger cars have it approximately symmetrical between the axles. Trucks are often driven with more units after, see Figure 1-76. The weight of the load in a truck can be up to 2..4 times the weight of the empty vehicle, while the maximum payload in passenger cars normally are significantly lower than the empty car weight. Another difference is that a heavy vehicle often have very roll-compliant body (frame). The compliance also varies a lot depending on what is built/loaded on the frame. Trucks often have many steered axles, while passenger cars normally are only steered at front axle. The view for the driver (and environment sensors) is from higher up and without inner rear mirror. The lateral margins in lane are much smaller.

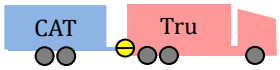
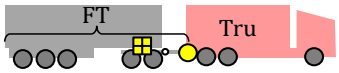
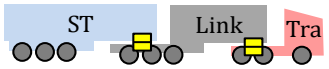
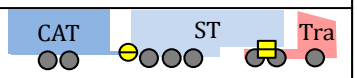
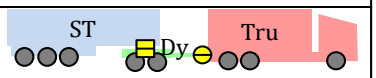
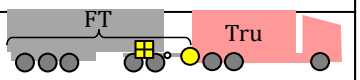
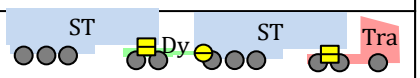
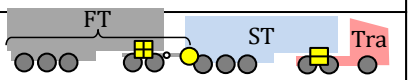
Another difference is that it is not as easy as for two-axle vehicles, to find the vertical loads under each axle. This is both with and without longitudinal load transfer. The load varies a lot in mass and position, there is often multiple axles in each axle group and there can be a vertical force exchange between the units. See 4.5.2.2.2.2.

1.7.3 Definitions

In Figure 1-76, we can find the following units:

- Towing units: Tractor or Rigid (Truck)
- Towed units: Full trailer (FT), Semi-trailer (ST), Centre-axle trailer (CAT), (Converter) Dolly
- The couplings between the units can of 2 types:
  - **Fifth-wheel coupling** (e.g. between Tractor and Semi-trailer). Designed to take force in all 3 directions. Furthermore, it is designed to be roll-rigid, but free in pitch and yaw.
  - A **Turntable** is similar to a fifth wheel but has a rolling bearing instead of a pitch-hinged greased surface, which leads to less yaw friction and no pitch degree of freedom. In converter dollies, one often sees both, fifth wheel on top of turntable.
  - **Hitch coupling** or **Drawbar coupling** (e.g. between Rigid and Full trailer). Designed to take forces in longitudinal and lateral directions, but only minor in vertical direction. Also, it is rotationally free in all 3 directions. A full-trailer has pitch-moment-free rear end of drawbar. A converter dolly or centre-axle-trailers have pitch-rigid rear end of drawbar.

- There is often a need for several axles close to each other, to manage a high vertical force. Such group of axles is called “axle group”, “axle arrangement” or “running gear”.

Conventional CVs	Tractor-ST	Tractor-SemiTrailer	16.5 m, 40 t	
	Truck CAT	Truck-CentreAxleTrailer	18.75 m, 40 t	
	Truck FT	Truck-FullTrailer	18.75 m, 40 t	
Existing LCVs	B-double or Tractor B-double	Tractor-LinkTrailer-SemiTrailer	25.25 m, 60 t	
	Tractor-ST-CAT	Tractor-SemiTrailer-CentreAxleTrailer	25.25 m, 60 t	
	Nordic CV	Truck-Dolly-SemiTrailer	25.25 m, 60 t	
		Truck-FullTrailer	24 m, 60 t	
Prospective LCVs	A-double	Tractor-SemiTrailer-Dolly-SemiTrailer	31.5 m, 80 t	
		Tractor-SemiTrailer-FullSemiTrailer	≈30 m, 80 t	
	C-double	Truck-CentreAxleTrailer-CentreAxleTrailer	27.5 m, 66 t	
	AB-double or Truck B-double	Truck-Dolly-LinkTrailer-SemiTrailer	34 m, 90 t	

○	vertical-free, pitch-free, roll-free (hitch coupling on pitch-free drawbar)
⊖	vertical-rigid, pitch-free , roll-free (hitch coupling on pitch-rigid drawbar)
⊟	vertical-rigid, pitch-free, roll-rigid (fifth-wheel coupling)
⊞	vertical-rigid, pitch-rigid, roll-rigid (turn-table coupling)
	(all above couplings are longitudinal-rigid, lateral-rigid, yaw-free)

Figure 1-76: An overview of combination vehicles (CVs). Based on (Kharrazi , 2012). The FullTrailer is registered as one unit, but it can be modelled as two units with a coupling between.

1.8 Construction equipment

Construction equipment comprises heavy, self-propelled work machines designed for earthmoving, material handling, and site operations in construction, infrastructure development, and mining. Unlike road vehicles, their primary purpose is not transportation but the generation of mechanical work through digging, loading, lifting, compacting, or manoeuvring on irregular and often temporary surfaces.

1.8.1 Machine types and functions

Typical categories include excavators, wheel loaders, articulated haulers, rigid dump trucks, dozers, compactors, graders, and pavers. These machines generally employ hydrostatic or highly reduced drivetrains to deliver large tractive forces at low speeds. Articulated frames or tracked undercarriages are used to maintain mobility and stability across soft, uneven, or highly variable ground. Work functions rely on high-flow hydraulic actuators capable of producing large forces, which create strong dynamic couplings between the machine, the surrounding soil, and the working tools.

1.8.2 Motion characteristics and dynamics

Although their operating speeds are low (often below 40 km/h), the dynamic challenges arise from handling large masses, variable payloads, and ground-dependent reaction forces. Machines experience significant load shifts, high torque peaks, and abrupt changes in resistance due to soil interaction. Stability—both static and dynamic—is critical, especially for machines performing lifting or reaching motions with long hydraulic arms.

1.8.3 Safety and control systems

Modern construction equipment is strongly mechatronic. Sensor systems are used for load-moment limiting, machine positioning, ground interaction monitoring, and collision avoidance. Increasingly, machines integrate automated or semi-autonomous functions for digging, grading, and haul-cycle optimization. Safety is governed by machinery-specific regulations and worksite requirements, with particular emphasis on tip-over prevention, overload protection, and safe human–machine interaction.

1.8.4 Differences from road vehicles

Compared to heavy road vehicles, construction equipment varies widely in geometry, kinematics, and force distribution. They are optimized for power, traction, and control of ground-tool interaction rather than transport speed or long-distance efficiency. As a result, their design principles, motion models, and functional requirements differ fundamentally from those used for trucks and buses.

1.9 Smaller vehicles

This section is about smaller vehicles, meaning bicycles, electric bicycles, motorcycles and car-like vehicles for 1..2 persons. The last vehicle type refers to vehicles which are rare today, but there are reasons why they could become more common: Increasing focus on energy consumption and congestion in cities can be partly solved with such small car-like vehicles, of which the Twizy in Figure 1-77 is one example. All vehicles in Figure 1-77 can be referred to as Urban Personal Vehicle (UPVs), because they enable personalised transport in urban environments. The transport can be done with low energy consumption per travelled person and distance, compared to today's passenger cars. The transport will also give higher levels of flexibility and privacy for the travelling persons, compared to today's public transportation. If such vehicles also could be shared between users, this concept will even more help congestion in cities but might require automation of booking and maybe even automation of driving. The term *Micromobility vehicles* is sometimes used for the bicycle-like UPVs, but it normally excludes the car-like UPVs.

Beside UPVs there could be considered smaller Urban Freight Vehicles (UFVs), but driver salary costs would then be very high per transported mass (or volume) of goods. So, UFVs might need to wait for automation of driving.

Figure 1-77 show some UPVs. UPVs/UFVs may require some categorizations:

- Climate and user type: Sheltered **or** open.
- Transport and user type: Short travels (typically urban, 5-10 km, 50 km/h) **or** long travels (typically inter-urban, 10-30 km, 100 km/h).
- Chassis concept:
  - Narrow (e.g. normal bicycles and motorcycles) **or** wide (at least one axle with 2 wheels, resulting in 3-4 wheels on the vehicle). Note that UPVs in both categories are typically still less wide than passenger cars.
  - Roll moment during cornering carried by suspension roll stiffness or roll moment during cornering avoided by vehicle cambering. The first concept can be called "Roll-stiff vehicle". The second concept can be called "Cambering vehicle" or "Leaning vehicle". One-tracked vehicles are always Cambering vehicles. two-tracked are normally Roll-stiff, but there are examples of Cambering such (see upper right in Figure 1-77). See Figure 1-78.

- (This book does only consider vehicles which are "Pitch-stiff", i.e. such that can take the pitch moment during acceleration and braking. Examples of vehicles not considered, "Pitching vehicles", are: one-wheeled vehicles as used at circuses and two-wheeled vehicles with one axle, such as Segways.)

- Note that also Roll-stiff Vehicles camber while cornering, but **outwards** in curve and only **slightly**, while Cambering Vehicles cambers **inwards** in curve and with a **significant** angle. Cambering Vehicles is more intricate to understand when it comes to how wheel steering is used. In a Roll-stiff Vehicle, the wheel suspension takes the roll-moment (maintains the roll equilibrium), which means that driver can use wheel steering solely for making the vehicle steer (follow an intended path). In Cambering Vehicles, the driver has to use the wheel steering for both maintaining the roll equilibrium and following the intended path. A model is given in **4.5.2.3**. Figure 1-78 shows some possible conceptual design of a cambering vehicle. It is not possible to do a partly roll-stiff and partly cambering vehicle, unless one uses suspension springs with negative stiffness, i.e. the suspension would need to consume energy to tilt the vehicle inward in curve.

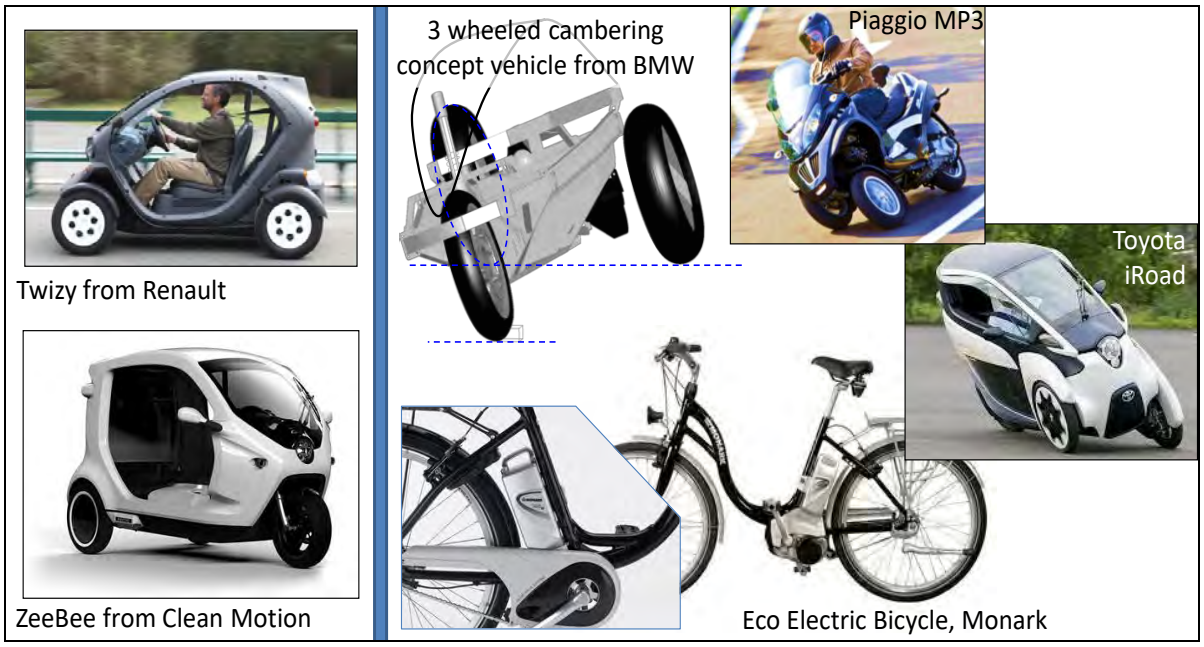


Figure 1-77: Examples of Urban Personal Vehicles. Left: "Roll-stiff". Right: "Cambering". From www.motorstown.com, www.cleanmotion.se, www.monarkexercise.se, www.nycscootering.com.

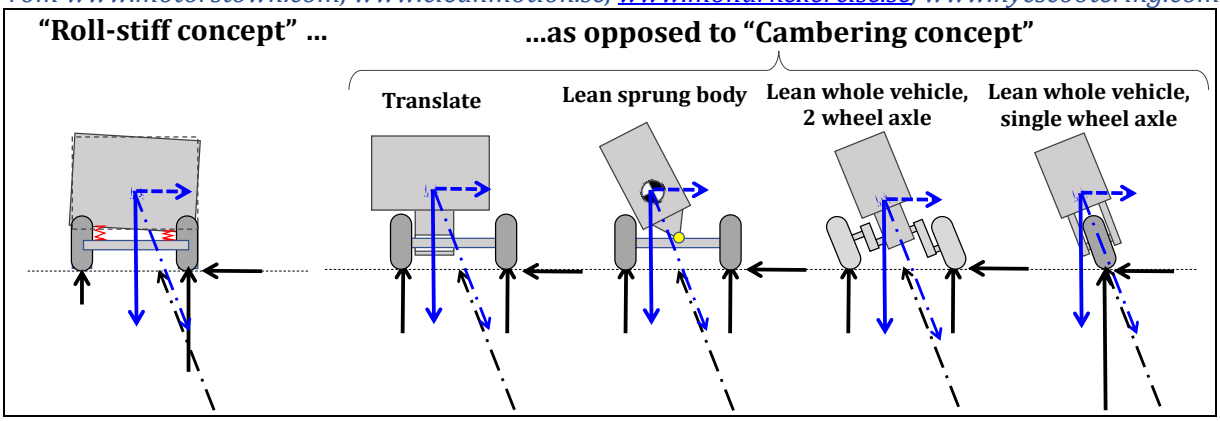


Figure 1-78: How Cambering vehicles avoid taking the roll moment while cornering. The vehicles are viewed from rear and turns to the left. The dash-dotted arrows mark the resulting forces which are equal between the 5 concepts.

1.10 Notations and units

See also 1.101.5.1.1.4.1.

Tables in this section show notation of parameters, variables and subscripts used in this book. The intention of this book is to follow International Standards (ISO 8855), but deviations from this is sometimes used, especially motivated by conflicts with areas not covered by (ISO 8855). Some alternative notations are also shown, to prepare the reader for other frequently used notation in other literature.

The units are mainly chosen as SI units and radians. The SI system does not have any unit for (monetary) value or cost, which is needed for engineering. It is a logical way to give an objective function, for selection or optimization, a unit.

Table 1-79: Notations

Categorization			Notation				
			Recommended		Alternatives		
		Subject for notation	in code	*by hand*		Unit	Description / Note
1. General	Basic	Monetary value or cost	C	C		€	for optimization
	Basic	Monetary value or cost rate	CR	CR		€/s	or €/m, for optimization
	Basic	(Shaft) Torque	T	T	M	Nm	
	Basic	Coefficient of friction	mu	μ	mue, muh	1=N/N	
	Basic	Damping coefficient	d	d	c,k,D	N/(m/s) or Nm/(rad/s)	
	Basic	Density	roh	ρ			
	Basic	Efficiency	eta	$h\eta$		1=W/W	Ratio between useful/output power and used/input power
	Basic	Energy	E	E	W	Nm=J	
	Basic	Force	F	F	f	N	
	Basic	Gravity	g	g		m/s^2	9.80665 average on Earth
	Basic	Height	h	h	H		
	Basic	Imaginary unit	j	j	i	-	j*j=-1
	Basic	Mass	m	m	M	kg	
	Basic	Mass moment of inertia	J	J	I	$kg*m^2$	Subscript can be given to denote around which axis
	Basic	Moment (of forces)	M	M	T	Nm	Not for shaft torque
	Basic	Power	P	P		W=Nm/s=J/s	
	Basic	Ratio	r	r	u, i (ISO8855)	Nm/(Nm) or (rad/s)/(rad/s)	Ratio between input and output rotational speed, or output and input torque, in a transmission
	Basic	Rotational speed	w	ω	ω	rad/s	
	Basic	Shear stress	tau	τ		N/m^2	
	Basic	Stiffness coefficient	c	c	C, k, K	N/m or Nm/rad	
	Basic	Strain	eps	ε		m/m	
	Basic	Translational speed	v	v	V	m/s	
	Basic	Wave length	lambda	λ		m	
	Basic	Width	W	W	w	m	Can be track width, vehicle width, tyre width, …
	Dynamics	(Time) Frequency	f	f		1/s=periods/s	
	Dynamics	Angular (time) frequency	w	ω	ω	rad/s	
	Dynamics	Angular spatial frequency	W	Ω		rad/m	
	Dynamics	Dependent variables in a dynamic system	z	z		<various>	Both state variables and output variables
	Dynamics	Input variables in a dynamic system	u	u		<various>	
	Dynamics	Mean Square value	MS	MS			
	Dynamics	Output variables in a dynamic system	y	y		<various>	
	Dynamics	Power spectral density	G	Φ	PSD		
	Dynamics	Root Mean Square value	RMS	RMS			
	Dynamics	Spacial frequency as radians per travelled distance	W	Ω		rad/m	
	Dynamics	Spatial frequency	fs	f_s		1/m=periods/m	
	Dynamics	States variables in a dynamic system	x	x		<various>	
	Dynamics	Time	t	t	τ,T	s	The independent variable in a dynamic system
	Operators	Transfer function	H	H			
2. Vehicle	1. General	Air resistance coefficient	cd	c_d	Cd	1	
	1. General	Cornering stiffness or lateral tyre stiffness	Cy	C_y	C_α	N/rad or N/1	$dF_y/da = dF_y/ds_y$ at $a=s_y=0$
	1. General	Longitudinal tyre stiffness	Cx	C_x		N/1	df_{yw}/ds_x at $s_x=0$

Table 1-80: Notations

Categorization			Notation				
			Recommended		Alternatives		
		Subject for notation	in code	*by hand*		Unit	Description / Note
2. Vehicle	1. General	Mass	m	m	M	kg	
	1. General	Rolling resistance coefficient	f	f		1=N/N	
	1. General	Track width	W	W		m	
	1. General	Tyre stiffness	C	C	c	N/1	*dF/ds* at *s=0*
	1. General	Understeer gradient	Ku	K_u	Kus, kus, U (ISO8855)	N/(N/rad) = rad/(m/s^2)	
	1. General	Vehicle side slip angle	b	β	β	rad	If no subscript, undefined or CoG
	1. General	Wheel base	L	L	l, lf+lr, WB	m	
	1. General	Wheel radius	R	R	r, Rw	m	
	2. Road	Curvature	kappa	κ	roh, ρ	rad/m=1/m	road or path
	2. Road	Curve radius	R	R	r, roh, ρ	m	road or path
	2. Road	Road bank angle	pxr	φ_{xr}			Positive when right side of ground is lower than left side ground
	2. Road	Road inclination angle	pyr	φ_{yr}		rad	Positive downhill
	2. Road	Vertical position of road	zr	z_r	z, Z	m	
	3. Motion	Vehicle acceleration, in interial system	ax, ay, az	a_x, a_y, a_z		m/(s^2)	decomposed in vehicle coordinates direction
	3. Motion	Time derivatives of each component v_x, v_y, v_z	dervx, dervy, dervz	$\dot{v}_x, \dot{v}_y, \dot{v}_z$	der(vx), der(vy), der(vz)	m/(s^2)	decomposed in vehicle coordinates direction
	3. Motion	Vehicle position	x,y,z	x, y, z	r=[rx,ry,rz] or [X,Y,Z]	m	often position of Center of Gravity, CoG
	3. Motion	Vehicle velocity, in interial system	vx,vy,vz	v_x, v_y, v_z	u,v,w	m/s	decomposed in vehicle coordinates direction
	4. Forces	Forces and moments on vehicle	Fx, Fy, Fz, Mx, My, Mz	$F_x, F_y, F_z, M_x, M_y, M_z$		[N, N, N, Nm, Nm, Nm]	From ground, air, towed units, colliding objects, etc. May appear also for in road plane: F=[Fx, Fy, Mz]
	4. Forces	Forces on one wheel, axle or side from ground	Fix,Fiy,Fiz	F_{ix}, F_{iy}, F_{iz}	lowercase f	N	Subscript "i" is placeholder for particular wheel, axle or side. May appear also extended with moments: [Fx, Fy, Fz, Mx, My, Mz]
	4. Forces	Forces on one wheel, axle or side from ground	Fixv, Fiyv,Fizv	$F_{ixv}, F_{iyv}, F_{izv}$	lowercase f	N	in vehicle coordinate system
	4. Forces	Forces on one wheel, axle or side from ground	Fixw,Fiyw,Fizw	$F_{ixw}, F_{iyw}, F_{izw}$	lowercase f	N	in wheel coordinate system
	5. Angles	Camber angle	g	γ	γ	rad	Sign convention positive when either of "rotated as wheel roll angle" or "top leaning outward vs vehicle body".
	5. Angles	Low speed or Ackermann speed steering wheel angle	dswA	δ_{swA}		rad	The angle required for a certain vehicle path curvature at low speeds
	5. Angles	Euler rotations		ψ, θ, φ		rad	Order: yaw, pitch, roll
	5. Angles	Roll, pitch, yaw angle	px, py, pz	$\varphi_x, \varphi_y, \varphi_z$	φ, θ, ψ	rad	Angles, not rotations. Roll and Pitch normally small
	5. Angles	Vehicle angular velocity, in interial system	wx, wy, wz	$\omega_x, \omega_y, \omega_z$	$[\dot{\varphi}, \dot{\theta}, \dot{\psi}], [\dot{\varphi}, \dot{\theta}, \Omega]$	rad/s	decomposed in vehicle coordinates direction (roll, pitch, yaw)
	5. Angles	Steering angle	d	δ	delta	rad	May refer to steering wheel, road wheel or axle
	5. Angles	Steering angle of road wheels	drw	δ_{rw}	RWA	rad	Normally an average of angles on front axle

Table 1-81: Notations

Categorization			Notation				
			Recommended		Alternatives		
		Subject for notation	**in code**	***by hand***		**Unit**	**Description / Note**
2. Vehicle	5. Angles	Steering angle of steering wheel	dsw	δs_w	SWA	rad	
	6. Slip	Tyre (lateral) slip angle	a	α	alpha	rad	a=arctan(sy)
	6. Slip	Tyre lateral slip	sy	s_y		1= (m/s)/(m/s)	sy=tan(a)
	6. Slip	Tyre longitudinal slip	sx	s_x	$\kappa, -\kappa$		
	6. Slip	Tyre slip	s	s			
	7. Subscript	axle	a	a			used e.g. as Ca=cornering stiffness for any axle
	7. Subscript	centre of gravity	CoG	CoG	COG, cog, CG, cg		
	7. Subscript	front	f	f	F, 1		Often used as double subscript, e.g. fr=front right
	7. Subscript	inner	i	i			Often means with respect to curve
	7. Subscript	left	l	l	L		Often used as double subscript, e.g. fl=front left
	7. Subscript	outer	o	o			Often means with respect to curve
	7. Subscript	rear	r	r	R, 2		Often used as double subscript, e.g. fr=rear right
	7. Subscript	road	r	r			
	7. Subscript	road wheel	rw	rw	RW		E.g. drw=road wheel steering angle
	7. Subscript	sprung mass	s	s			
	7. Subscript	steering wheel	sw	sw	SW, H (ISO8855)		E.g. dsw=steering wheel angle
	7. Subscript	unsprung mass	u	u	us		
	7. Subscript	vehicle	v	v			used e.g. as F1v to denote wheel force on wheel 1 in vehicle coordinates
	7. Subscript	wheel	w	w			used e.g. as F1w to denote wheel force on wheel 1 in wheel coordinates
3. Subsystem in vehicles	1. Propulsion	Engine torque	Te	T_e		Nm	
	1. Propulsion	Propulsion torque	Tprop	T_{prop}		Nm	often expressed at wheel
	2. Brake	Brake torque	Tbrk	T_{brk}		Nm	
	3. Steering	Steering wheel torque	Tsw	T_{sw}	SWT	Nm	
	4. Suspension	Caster angle	CA			rad	
	4. Suspension	Caster offset	c			m	
	4. Suspension	Kingpin inclination angle	KPI			rad	
	4. Suspension	Pneumatic trail	t			m	
	4. Suspension	(Wheel) Camber angle		φ_{Camber}		rad	

1.11 Typical Numerical Data

The purpose of the tables in this section is to give approximate numerical values of parameters. Vehicle parameters are often dependent on each other; changing one leads to that it is suitable to change others. The parameters are given with the intention to be consistent with each other, for each vehicle example. The tables balance between being generic and specific, which is difficult. Therefore, please consider the table as very approximate.

Table 1-82: Typical values of parameters, common for typical passenger cars and heavy trucks.

Parameter	Notation	Typical Value		Unit
		Passenger car	Heavy truck	
Air density	roh	1		kg/(m^3)
Earth gravity	g	9.80665		m/(s*s)
Road friction, at dry asphalt	mu	1.0		N/N
Road friction, at wet asphalt		0.6		
Road friction, at snow		0.3		
Road friction, at wet ice		0.1		
Tyre Cornering Coefficient (lateral slip coefficient), i.e. slip stiffness normalized with vertical load	CCy	15..25	5..10	(N/rad)/N = (N/1)/N
Ratio of tyre longitudinal and lateral slip coeffcient stiffness	CCx/CCy	1.5..2		1

1.11.1For Passenger Vehicles

Table 1-83: Typical data for a passenger vehicle.

Group/Type	Parameter	Notation	Typical Value	Unit	Note / Typical / Range / Relation to other
Vehicle	Length, bumper to bumper		5.00	m	
Vehicle	Longitudinal distance from CoG to front axle	lf	1.3	m	40-50% of wheel base: lf=0.55*L;
Vehicle	Mass	m	1700	kg	
Vehicle	Moment of inertia for yaw rotation	Jzz	2900	kg*m*m	Radius of gyration is sligthly less (0.9) than half wheel base: =m*(0.9*L/2)^2
Vehicle	Unsprung mass	mus	200	kg	Sum of 4 wheels with suspensions
Vehicle	Track width	W	1.70	m	
Vehicle	Wheel base	L	2.90	m	
Vehicle	Projected area in a transversal view	Afront	2	m^2	For calculation of air resistance. Examples: Volvo XC90 has 2.78 m^2, Volvo S60 has 2.27 m^2
Vehicle	Aerodynamic coefficients	cd, clf, clr	0.31, 0.10, 0.07	1	For calculation of longitudinal resistance and lift force over front and rear axle
Wheel and Tyre	Rolling resistance		0.01	N/N	
Wheel and Tyre	Wheel radius		0.30	m	
Wheel and Tyre	Wheel rotational inertia	Jw	0.5	kg*m*m	For one wheel
Wheel and Tyre	Tyre vertical stiffness	ct	250 000	N/m	For one wheel
Propulsion	Engine inertia		0.5	kg*m*m	
Propulsion	Transmission ratio, highest gear		5.00	rad/rad= Nm/Nm	Engine to wheel. In magnitude of 5.
Propulsion	Transmission ratio, lowest gear		10.00	rad/rad= Nm/Nm	Engine to wheel. In magnitude of 10.
Brake	Brake proportioning, front/rear		70/30	N/N or Nm/Nm	Often tuned so that braking both axles when braking 0.8*g
Steering	Steering ratio		16	rad/rad	Steering wheel to Road wheel
Suspension	Suspension heave stiffness (without roll)	cs	100 000	N/m	Vertical stiffness at wheel. Sum of 4 wheels. So that bounce frequency f is between 1 and 2 Hz: sqrt(c/m)=f*2*pi; Bump stop at (3..4)*g when fully loaded.
Suspension	Suspension roll stiffness, only from anti-roll-bars	carb	14 000	N/m	Vertical stiffness at wheel. Sum of both axles.
Suspension	Suspension damping	ds	13 000	N/(m/s)	Wheel rate. Sum of 4 wheels. Some 40..60% of critical damping: d = (0.4..0.6)*2*sqrt(c*m); 2..3 times softer in compression than rebound.

1.11.2For Heavy Vehicles

Compared to passenger cars, trucks differ much more in size and configuration, see Figure 1-76. Also, a certain individual vehicle also differs much more between empty and fully loaded. Globally, “Tractor with Semitrailer” is the most common heavy vehicle, which is why it is used as example.

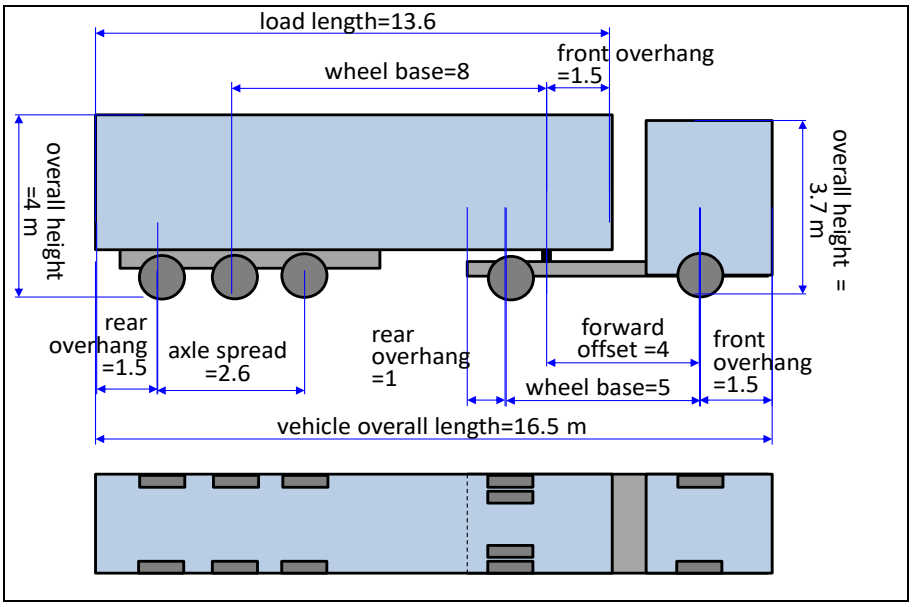


Figure 1-84: Typical data for a heavy vehicle, exemplified with "Tractor with Semi-trailer"

Table 1-85: Typical data for a heavy vehicle

Group/Type	Parameter	Typical Value		Unit	Note / Typical / Range / Relation to other
		Empty	With max payload		
Vehicle	Trackwidth, centre-to-centre for single tyres	2.25		m	Outer tyre edge 2.55
Vehicle	Projected area in a transversal view	10.0		m^2	For calculation of air resistance
Vehicle	Aerodynamic coefficient	0.5..0.7		1	c_d coefficient in aero dynamic resistance formula (normal truck 0.4, long combination truck 0.6)
Vehicle	Frame torsional compliance, per meter frame	1/2.5		(rad/MNm)/m	A stiff and rigidly connected "body build" can stiffen a lot
Tractor	CoG heigth	1.00		m	
Tractor	Mass (total), tractor	7500		kg	
Tractor	Moment of yaw inertia	22500		kg*m*m	Around unit CoG
Tractor	Unsprung mass	1700		kg	Sum of all axles at unit
Semitrailer	CoG heigth	1.00	2.00	m	
Semitrailer	Mass (total), semi-trailer	10000	32500	kg	
Semitrailer	Moment of yaw inertia	150000	500000	kg*m*m	Around unit CoG
Semitrailer	Unsprung mass	2400		kg	Sum of all axles at unit
Wheel and Tyre	Wheel radius	0.50		m	0.4-0.5
Wheel and Tyre	Wheel rotational inertia	10.0		kg*m*m	For one wheel, single tyre
Wheel and Tyre	Rolling resistance	0.005		N/N	Or less, 0.003
Propulsion	Engine max power	370		kNm/s=kW	
Propulsion	Engine inertia	5		kg*m*m	
Propulsion	Transmission ratio, highest gear	3		1=rad/rad=Nm/Nm	Engine to wheel
Propulsion	Transmission ratio, lowest gear	30			Engine to wheel
Steering	Steering ratio	20		rad/rad	Steering wheel to Road wheel
Steering	Steering wheel rotational inertia	0.04		kg*m^2	Steering wheel to Road wheel

2 VEHICLE INTERACTIONS AND SUBSYSTEMS

2.1 Introduction

The study of vehicle dynamics starts with the interfaces between the vehicle and its environment, see Figure 2-1. The vehicle tyres are the primary force interface for all motion (in road plane, i.e. acceleration, steering, braking) but also undesired disturbances (out-of- road plane, i.e. road unevenness, road bumps, etc.). Additionally, the aerodynamic loads on the vehicle will create forces that are often undesirable (wind resistance, side gusts, etc.) but can sometimes be exploited for better contact with the road (down-force). An example of extreme interactions to the vehicle is the impact forces from a crash. An interaction of another kind is the driver. One often divides the whole system into 3 parts: vehicle, driver and environment, see Figure 2-1. Driver and environment can often be clustered as 2.10 Driving and transport application, which includes all outside subject vehicle. Some aerodynamic models are given in 2.9. Driver models are discussed with some selected example models, see 2.10.2.

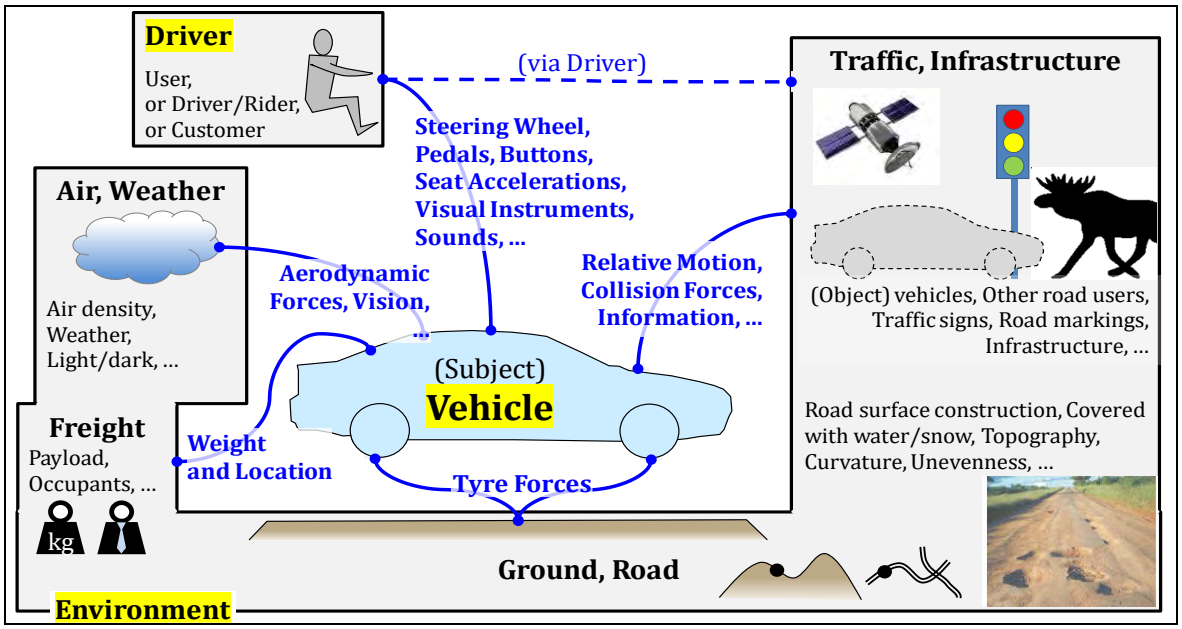


*Figure 2-1: How the **vehicle** interacts with **driver** and **environment**.*

The chapter also contains descriptions of the subsystems which are most relevant for Vehicle Dynamics, with focus on Wheels and Tyres, see Figure 2-2.

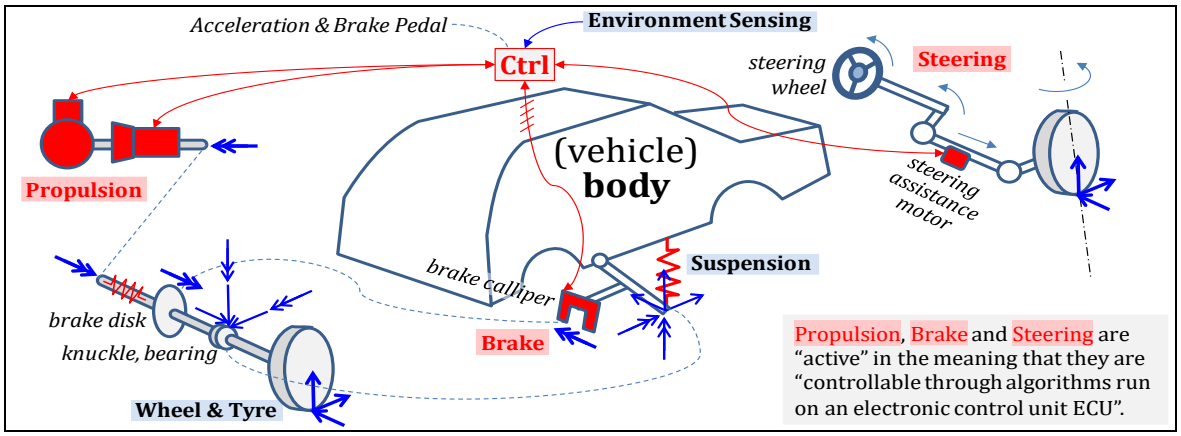


Figure 2-2: Vehicle with the 6 Vehicle Dynamics relevant subsystems: Wheels and Tyres, Suspension, Propulsion, Brake, Steering, and Environment Sensing. Towed units, with similar subsystems, are not shown.

The Environment Sensing System is described as a subsystem, see 2.7. There are also a lot of other sensors in the vehicle, sensing the conditions in the subject vehicle, see 3.5, 4.6 and 5.10. These sensors are often more established and therefore often treated as included in a certain subsystem, such as wheel (rotational) speed sensors are often a part of the brake system.

2.1.1 Wheel torque actuation system

The propulsion and brakes are cooperating to actuate the wheel torques. The proposed nomenclature in this book is:

- **Wheel torque actuation system** (one per vehicle or per vehicle unit) consists of one
  - **Propulsion system**, consisting of one or multiple
    - **Powertrains** which consist of one
      - **Prime mover** (e.g. combustion engine or electric machine) and
      - **Drivetrain** which consist of
        - **Main transmission** (e.g. gearbox, propulsion shaft)
        - **Distribution transmission** (e.g. differential, drive shaft)
  - **Braking system** which consists of one
    - **Friction brake systems** (e.g., pump, valves, brake callipers, brake discs) and
    - **Parking brake system** (often integrated in friction brake system) and, often,
    - **Retarders** (e.g. hydraulic retarder, electromagnetic retarder)

Note that the expressions "per vehicle or per vehicle unit" above, reveals the ambiguity whether a braked tractor with braked trailer has one or two braking systems, as well as whether a propelled tractor with propelled trailer has one or two propulsion systems.

2.1.2 References for this Chapter

- Tyres: (Pacejka, 2005), (Rill, 2006), and (Michelin, 2003)
- Vehicle Aerodynamics: Reference (Barnard R. , 2010)
- Driver models: *"Chapter 38 Driver Models in Automobile Dynamics Application"* in Reference (Ploechl, 2013)

2.2 Wheels and Tyres

2.2.1 Introduction

The wheels and tyres of a vehicle have the following overall purposes, see also Figure 2-3:

- Carry the vertical load F_z. (Involved in suspension.)
- Carry lateral force F_y, so that the wheel "tracks" with $v_y \approx 0$. (Involved in steering.)

- Transmit torque T to F_x with $P_{Loss} = T \cdot \omega - F_x \cdot v_x$ with $P_{Loss} \approx 0$. (Involved in propulsion and braking.)

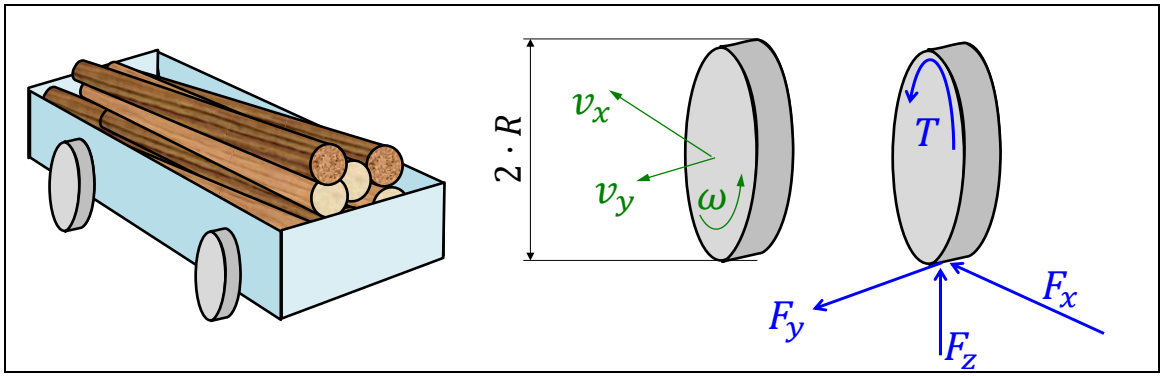


Figure 2-3: The overall purposes with each wheel with tyre

To minimize negative effects, it is also important that the wheels and tyres:

- Operate with minimum **energy** loss, minimum tyre **wear**, minimum **particle emissions**, and minimum **noise**.
- Isolate **disturbances**, mainly vertical. This includes also that the wheel should not cause disturbances, which overall means that the wheel and tyre should be round and balanced.

2.2.1.1 Wheel Integration in Suspension

To understand the "force flows" of a wheel, it is good to understand the conceptual integration, regarding shaft, brake disks and wheel bearings. Cars typically have their inner bearing rings rotating with the wheel, while trucks instead have outer rings rotating, see Figure 2-4.

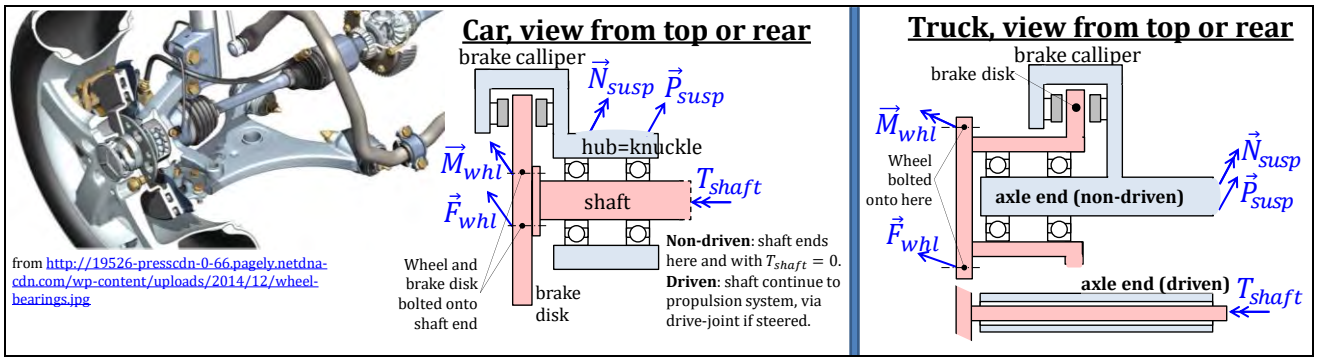


Figure 2-4: Concepts of wheels are typically integrated. All vectors are 3D, while moment $\vec{N}_{xz}$ is 2D in the wheels xz-plane and moment T_{shaft} is perpendicular to the same plane.

2.2.1.2 Tyre Design

Before discussing the mechanics of tyre and road interactions, the physical structure of the wheel assembly should be understood. Consisting of a steel rim and an inflated rubber toroid, pneumatic tyres were invented and patented by Robert William Thomson in 1845 and are essentially the only type of tyre found on motor vehicles today.

The physical construction of the tyre carcass affects the response of the tyre to different road loadings. The carcass is a network of fabric and wire reinforcement that gives the tyre the mechanical strength. The structure of the carcass can be different: Bias-ply, Bias-ply Belted, and Radial-ply, see Figure 2-5. Bias-ply tyres were the first types of pneumatic tyres to be used on motor vehicles. Radial ply tyres followed 1946 and became the standard for passenger cars and is today also dominating also on trucks.

Note how the bias-ply constructions have textile structures oriented at an angle to the tyre centreline along the x-z plane. This angle is referred to as the crown angle and is further illustrated in Figure 2-5.

Note the textile orientation for the bias-ply and radial tyres. Also note the difference in crown angles between the two tyre constructions. This difference plays an important part in the rolling resistance characteristics of the tyre which is 2.2.1.6.

The tyre components in Figure 2-5 have been constructed to provide the best tyre performance for different loading directions. Trade-offs are necessary between handling performance and comfort, between acceleration and wear, as well as between rolling resistance and desired friction for generating forces in ground plane. The rubber components and patterns incorporated in the tread are critical to the friction developed between the tyre and road under all road conditions (wet, dry, snow, etc.). Friction is most relevant in longitudinal and lateral vehicle dynamics. The belts define the circumferential strength of the tyre and thus braking and acceleration performance. The sidewall and plies define the lateral strength of the tyre and thus influence the lateral (cornering) performance of the vehicle. The sidewall as well as the inflation pressure are also significant contributors to the vertical stiffness properties of the tyre and affect how the tyre transmits road irregularities to the remainder of the vehicle. A tyre that has strong sidewalls will support vertical load well, but at the cost of vertical compliance.

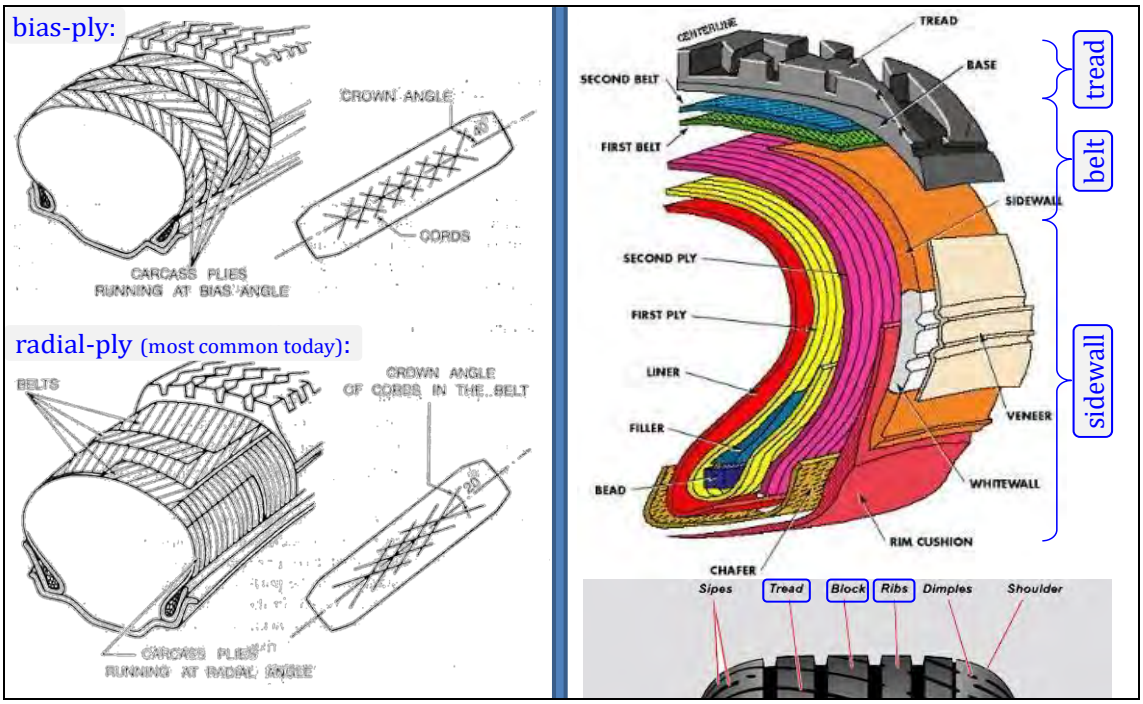


Figure 2-5: Left: Carcass Construction, (Wong, 2001). Left top: Bias-ply construction. Left bottom: Radial construction. Right: Radial Tyre Structure, (Cooper Tire & Rubber Co., 2007).

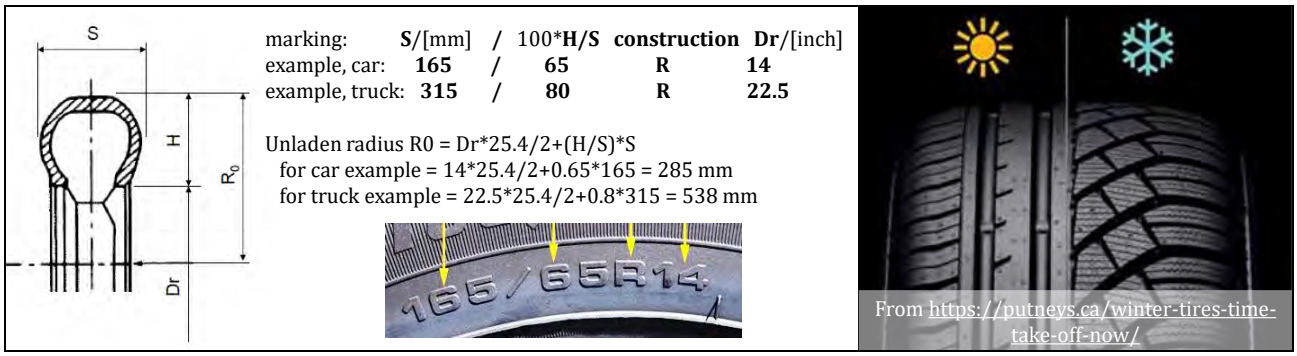


Figure 2-6: Left: Tyre marking (radial tyre). Right: Typical summer and winter tread patterns.

2.2.1.3 Wheel Angles

A wheel or a tyre is best described in its own coordinate system, see Figure 2-7. The 3 forces and 3 moments are acting on the wheel from the ground. The other quantities, such as slip angle α and camber angle ε_w, in Figure 2-7 are examples of variables which have influence on the forces and moments in the coming chapters.

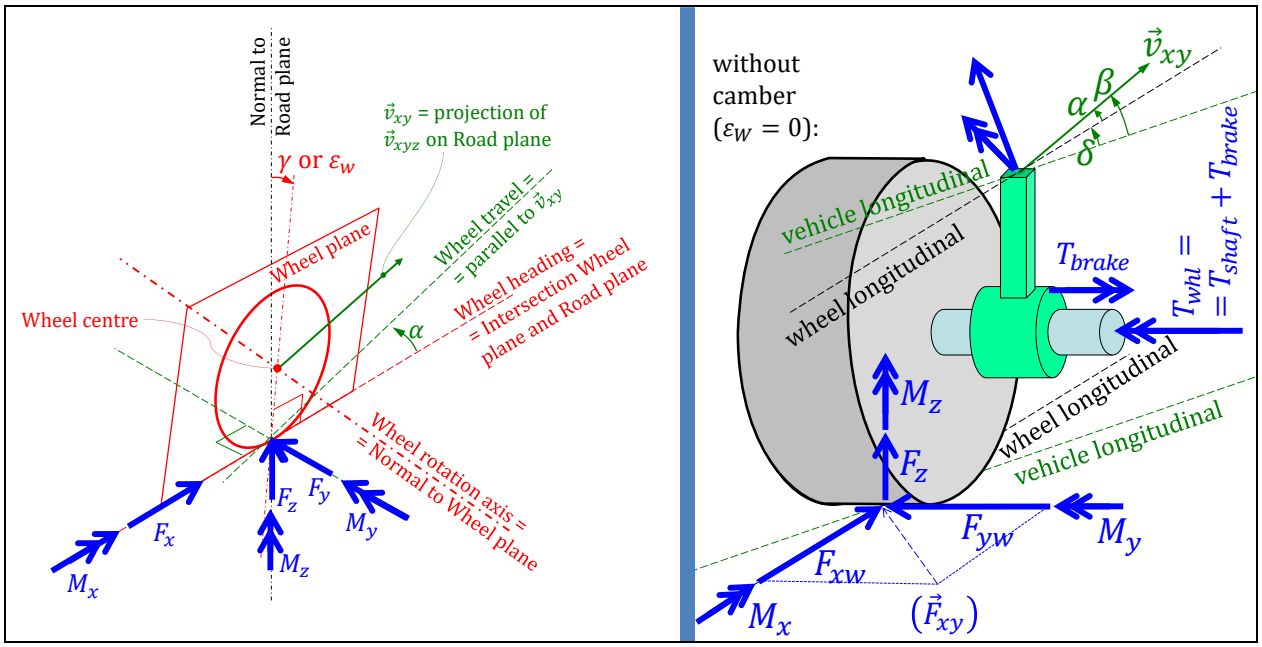


Figure 2-7: Left: Tyre coordinate system from (ISO 8855). Forces and moments on tyre from ground on tyre. Right: How T_{shaft} (from propulsion) and T_{brake} (from brake) sums up to a T_{whl} and how T_{whl} is related to tyre F_x. Also, how β and δ (from suspension) sums up to α and how it is related to tyre F_y.

2.2.1.3.1 Steer Angle

A wheel on a vehicle has a *Steer angle*, δ. The Steer angle is the angle from vehicle longitudinal axis to the wheel plane about the vehicle vertical axis (ISO 8855). Assuming vehicle xy-plane is parallell to road plane, this angle is same as angle from vehicle longitudinal axis to the intersection between wheel plane and road plane.

2.2.1.3.2 Camber Angle

A wheel on a vehicle on a road surface has a *Camber angle*. The Camber angle is the roll angle between the wheel and the road, see (ISO 8855). So, the Camber angle is both due to how the wheel is mounted on the vehicle and roll angle of the road, wheel camber and road camber. Assuming vehicle xy-plane is parallel to road plane, the typical symmetry within an axle means that camber angle typically has opposite signs on left and right wheel. However, for two-track vehicles, one can often see the sign convention that a wheel top leaning outward from vehicle body is negative, regardless of on left or right side.

2.2.1.3.3 Steer and Camber

If a wheel has both significant Steer angle and significant Camber angle at the same time, these angles alone does not define the orientation, since steering-before-cambering gives another orientation than cambering-before-steering. One way is to express the orientation in a rotational angle around the steering axis, see 2.2.1.3.5. An alternative is to use the concept of Euler rotations.

2.2.1.3.4 Castor Angle

A wheel, suspended to be steered, has a *Castor angle* (or *Caster angle*). This is the angle between the vehicle vertical axis and the projection of the steering axis (2.2.1.3.5) on the vehicle xz-plane (ISO 8855). Castor angle is positive when top of steering axis is inclined rearward. Castor angle provides an additional aligning torque, see 0 and 0, and changes the Camber angle when the wheel is steered.

2.2.1.3.5 Steering Axis Inclination

A wheel, suspended to be steered, has a *Steering axis inclination* (or *Kingpin inclination*). This is the angle between the vehicle vertical axis and the projection of the steering axis (2.2.1.3.5) on the vehicle yz-plane (ISO 8855). *Steering axis inclination* is positive when top of steering axis is inclined inward. See also 0.

2.2.1.3.6 Static Toe Angle

A wheel on an axle has a *Static toe angle* (a.k.a. *Toe-in*). The Static toe angle is the angle between vehicle longitudinal axis and the wheel plane about the vehicle vertical axis, with the vehicle at rest and steering in the straight-ahead position (ISO 8855). Positive Static toe angle (a.k.a. *Toe-in* or *"−Toe-out"*) is when forward portion of the wheel is closer to the vehicle centreline than the wheel centre. So: $\delta_{l,Toe-in} = -\delta_l|_{\delta_{sw}=0}$; and $\delta_{r,Toe-in} = +\delta_r|_{\delta_{sw}=0}$;. Typically, left and right wheel on same axle has same Static toe angle. Toe-in is often discussed as an *axle* property rather than a *wheel* property: *Axle* (Static) Toe-in $= \delta_{axle,Toe-in} = \delta_{l,Toe-in} + \delta_{r,Toe-in} = -\delta_l|_{\delta_{sw}=0} + \delta_r|_{\delta_{sw}=0}$;.

One could define an "instantaneous toe angle", for an axle during arbitrary vehicle operation (non-rest and non-zero steering), as $-\delta_{left} + \delta_{right}$. This will have a different value than Static toe angle due to suspension linkage geometry and elasticity in suspension bushings, e.g. vary with δ_{sw}, $F_{axle,y}$ and $F_{axle,x}$. See also 2.6.1.1.1 Ackermann percentage.

Toe (regardless of toe-in or toe-out) generally generates opposing lateral forces on left and right side leading to propulsion energy loss and tyre wear. Toe-out on front axle and toe-in on rear axle makes the vehicle more yaw stable (less over-steered). Tone-in on front axle makes vehicle more yaw agile but it also improves on-centre steering feel. Normal design choice for a passenger car is positive Static toe angle (Toe-in) on both axles, and more on front axle.

2.2.1.4 Wheel radii

The wheel has a nominal radius R_{Nom} e.g. according to its marking. However, in vehicle motion engineering we need to investigate the details and then we can define many different radii, or radius-like lengths. The two main such are:

- Effective radius R_e, which is used for velocity relations, such as $v_x = R_e \cdot \omega$;, and
- Loaded radius R_l, which is used for torque equilibrium, such as $T = F_x \cdot R_l$;

2.2.1.5 Tyre Model Architecture

This section describes how a tyre model can be instantiated once per wheel and integrated in a model together with models of vehicle, driver, and environment, see Figure 2-8. It does not define a variable flow (causality) between the wheel and the tyre model; such causality depends on how the wheel inertias and elasticity is modelled. This sectionFigure 2-8 differs between parameters and variables, in context of dynamic study, i.e. in time domain. Within each simulation, parameters are constant, but variables can vary. If design optimization, as opposed to simulation, the design parameters also has a role of variables (i.e. they are varied) in the optimization, but not in time domain. This section follows approximately the STI tyre model interface standard (Besselink, 2011), but not in all details.

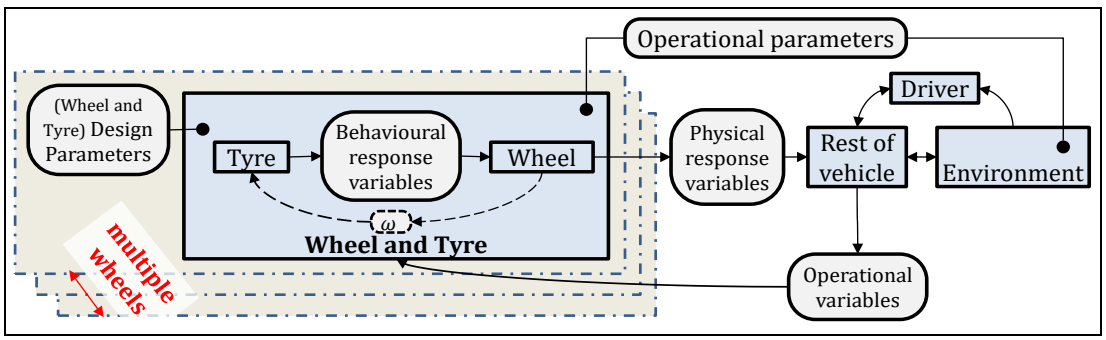


Figure 2-8: How wheel and tyre models can come into a model context.

2.2.1.5.1 (Wheel and Tyre) Design Parameters

We limit ourselves to today's traditional pneumatic tyres. Then the design is captured by:

- Carcass/Material: Rubber quality and plies arrangement.
- Tread/Grooves: Groove pattern, Groove depth, Tread depth, Spikes pattern (if spikes)
- Main dimensions: Outer radius, Width, Aspect ratio
- Installation parameters: Inflation pressure

2.2.1.5.2 Operational Parameters

These are operating conditions which vary slowly, and in this description assumed to be constant during one manoeuvre/driving cycle. These are:

- Road surface (dry/wet, asphalt/gravel/snow/ice, …)
- Road compliance and damping (hard/soft, …)
- Wear state of tyre
- Age of tyre
- Temperature

2.2.1.5.3 Operational Variables

These are operating conditions which vary quickly, and in this description assumed to be variable in time during one manoeuvre/driving cycle. These are:

- Tyre velocities (v_x, v_y, ω) or Tyre slip (s_x and s_y (or α) and sign(ω))
  The ω can be thought of as internal within "Wheel and Tyre", see dashed in Figure 2-8.
- Vertical tyre force, (F_z)
- Wheel torque ($T_{yActuation} = T_{Propulsion} + T_{Brake}$)
- Camber angle

The wheel's rotational velocity, ω, can be contained in *Wheel and Tyre model* instead of inside *Model of rest of the vehicle*, which would mean that ω will not be part of the *Operational variables* interface.

Tyre forces in road plane (F_x, F_y) can be given instead of tyre slip. Another alternative is to give the corresponding actuation, e.g., wheel shaft torque and wheel steer angle relative to wheel course angle. With those setups, the response variables in 2.2.1.5.4.

Vertical tyre force can be modelled as arbitrarily varying in time or as an offset amplitude for different frequencies where offset is from a mean value. The mean value would then be a parameter instead of a variable. The latter alternative can be more efficient if simulating a longer driving cycle, where following each road wave would be very computational inefficient.

2.2.1.5.4 Response Variables

Response refers to response to Operational variables changes.

2.2.1.5.4.1 Physical Response Variables

The variables from tyre model to model of rest of the vehicle is essential the forces and moments, see Figure 2-7:

- Longitudinal and lateral forces (F_x, F_y)
- Roll moment or Overturning moment (M_x)
- Rolling resistance moment ($M_{yRollResist}$)
- Spin moment or Aligning moment (M_z)

Other responses are:

- Wear rate [worn rubber mass or tread depth per time unit]
- Loaded radius (R_l =the lever for F_x around wheel center)
- Rolling radius (or Effective radius= $R_e = v_{Belt}/\omega \approx BeltCircumference/\pi$)

Note: The radii are important for modelling. Both R_l and R_e are not clear radii, but the are "radius-like" lengths; lengths because they are defined as "lever of force" (R_l) and "ratio between translatory and rotational velocities" (R_e), respectively.

2.2.1.5.4.2 Behavioural Response Variables

The Responses can be modelled as Behavioural variables:

- Slip characteristics (slip stiffnesses C_{sx}, C_{sy} $[N/1]$, peak friction coefficient, … and/or other parameters in physical or empirical tyre slip model, as in 2.2.3.4 and 0)
- Rolling resistance coefficient (RRC)
- Vertical stiffness and damping coefficients
- Wear coefficient, Relaxation lengths or deformation stiffnesses $[N/m]$, …

One can select to not introduce Behavioural response variables but only use Physical response variables. If Behavioural response variables are introduced, one should consider them as special from DAE point of view, e.g., they can be difficult to differentiate. Also, they require an agreed definition to be interpreted, which is the reason to why they are not proposed as interface variables to the vehicle model.

2.2.1.6 How Tyres Carries Vertical Load

Figure 2-9 shows how a pneumatic tyre carries the vertical load partly by change of stress from a pretensioned (inflated) condition. It can be seen as change of stress in 3 parts: the lower sidewall, the upper sidewall and the "balloon" consisting of belt and air. In a traditional bicycle or motorbike wheel, the pre-tensioned spokes have a similar role as the air and rubber parts of a pneumatic tyre.

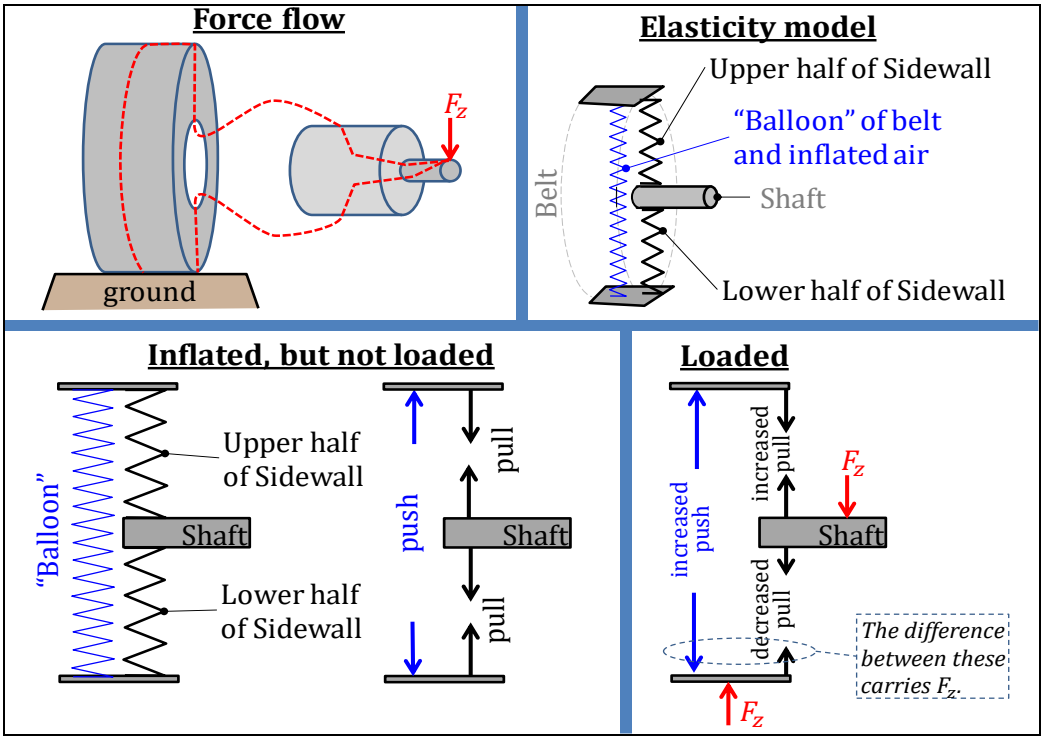


Figure 2-9: A pneumatic tyre is pre-tensioned by inflation pressure. This figure explains how the wheel and tyre takes (vertical) load through sidewall parts and the balloon.

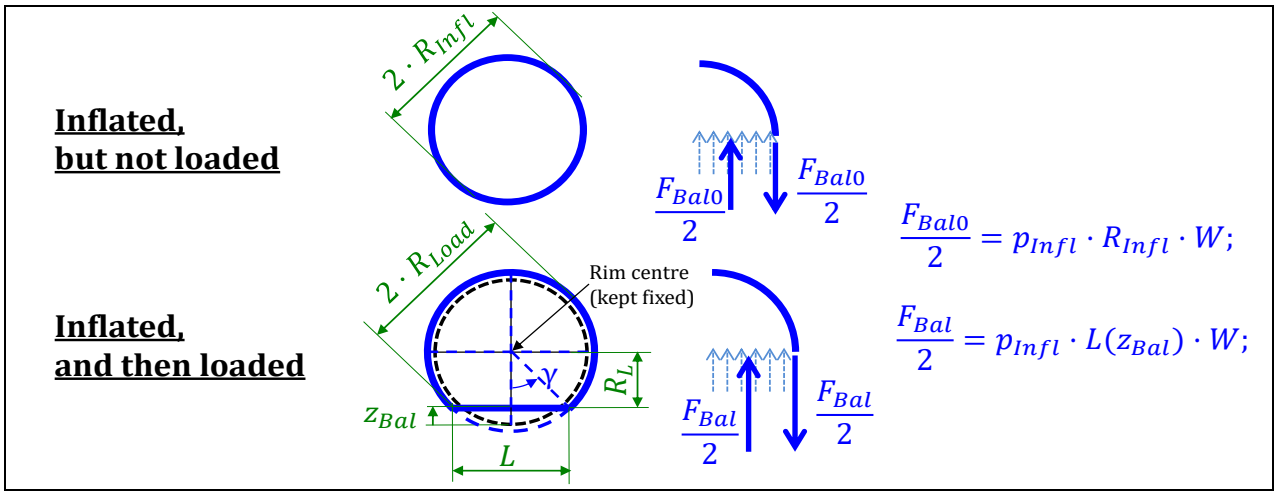


Figure 2-10: Model of how the force in "balloon" F_{Bal} changes with vertical deformation of "balloon" z_{Bal}. The balloon increases its tension in belt, from F_{Bal0} to F_{Bal}, but not significantly through increase of its inflation pressure p_{Infl}.

Assuming circumference of belt is constant and that the deformed shape is a circle arc plus a chord length L:

$$2 \cdot \pi \cdot R_{Infl} = 2 \cdot (\pi - \gamma) \cdot R_{Load} + L;$$

$$\cancel{R_{Load}} - \left(z_{Bal} \cancel{+ R_{Load}} - R_{infl}\right) = R_{Load} \cdot \cos(\gamma)\,;$$

$$\frac{L}{2} = R_{Load} \cdot \sin(\gamma)\,;$$

[2.1]

Elimination of γ and R_{Load} in Eq [2.1] gives a function $L(z_{Bal})$, which is the constitutive relation for the balloon as a vertical spring.

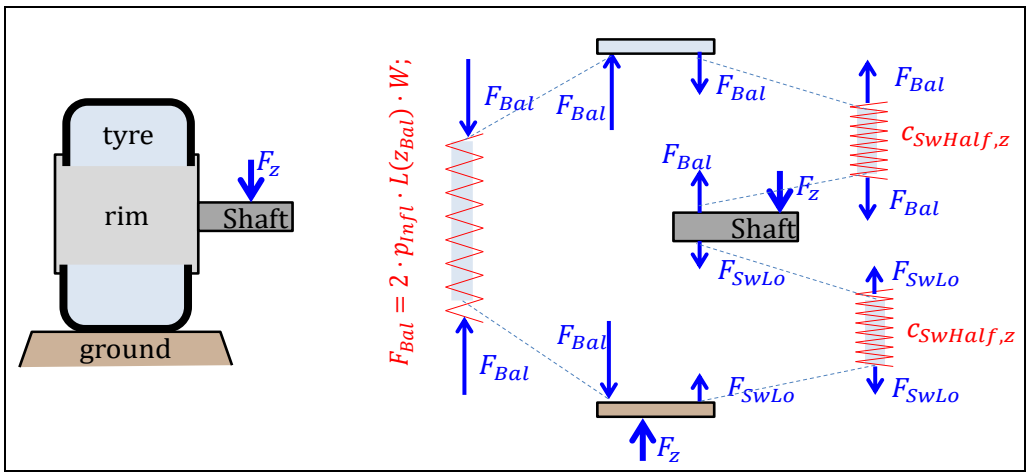


Figure 2-11: Vertical elasticity model of wheel.

2.2.1.7 The wheel as a transmission

The whole wheel, rim and tyre, can be seen as a transmission from rotational mechanical power to translational mechanical power. The shaft is on the rotating side; where we find rotational speed, ω, and the torque, T. The torque T is then the sum of torque on the propulsion shaft and torque on the brake disk or drum. The wheel hub is on the translating side of the transmission; were we find translating speed, v_x, and force, $F_{hub,x}$. See Figure 2-12. Normally, we approximate and denote $F_{ground,x} = F_{hub,x} = F_x$ and $F_{ground,z} = F_{hub,z} = F_z$.

If we neglect deformation of tyre/ground and sliding, we find the intended function of the wheel:

$v_x = radius \cdot \omega$; and $F_x = T/radius$;

There will be force losses (see 2.2.2) and speed losses (see 2.2.3) which makes a propelling wheel, i.e. $F_x \cdot v_x > 0$, require $T > F_x \cdot radius$ and $\omega > \omega/radius$. These losses also make a braking wheel, i.e. $F_x \cdot v_x < 0$, deliver $T < F_x \cdot radius$ and $\omega < \omega/radius$.

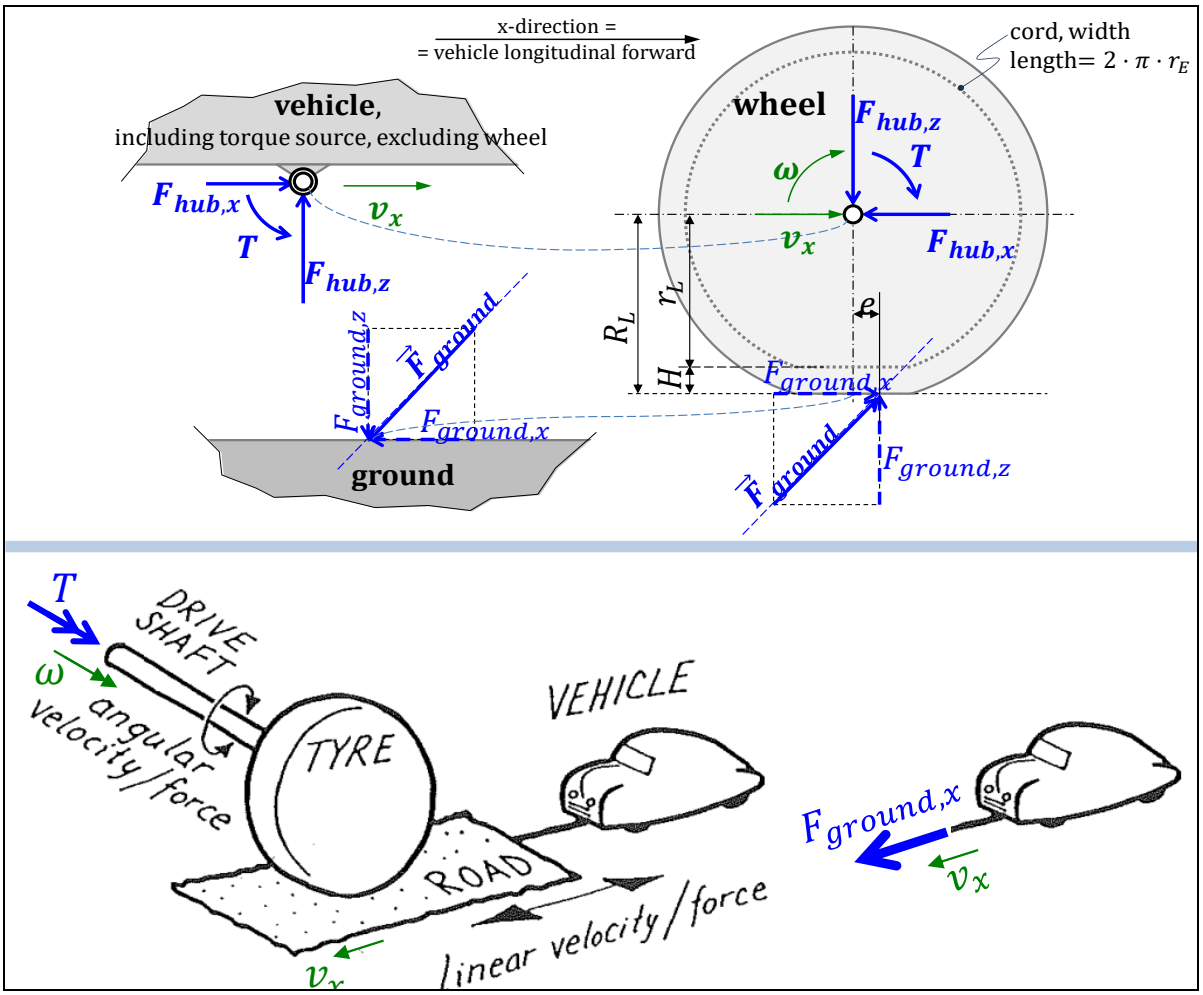


Figure 2-12: Upper: A wheel as a transmission from rotational $[\omega; T]$ to translational $[v_x; F_{hub,x}]$. Lower: A visualization from Ref. (Jacobson B. , 1993).

The longitudinal force in ground plane F_x, depends on the design of the tyre, the ground surface and the operational variables, such as velocities $[v_x, \omega]$ and vertical force F_z. The tyre can be under *braking*, *free rolling*, *pure rolling* or *propulsion/traction*, listed in order of increasing F_x and increasing T.

Elimination of γ and L in Eq [2.1] gives a function $R_{Load}(z_{Bal})$, which gives us the radius-like lever $R_l = R_{Load} + H$.

2.2.1.7.1 Losses

This section aims at giving a top-level view of the combined effect of force and speed losses. Therefore, the section uses models which are derived later in the book.

The force losses can be modelled with rotational equilibrium of the wheel around rim center:

$T = F_x \cdot radius + F_x \cdot e$; $where\ radius = R_L$;

The speed losses can be modelled with the brush model, which in a simple form yields:

$$F_x = C_x \cdot \frac{radius \cdot \omega - v_x}{|radius \cdot \omega|}; \quad where\ radius = r_E;$$

The power loss, from definition of power, yields:

$$P_{Loss} = T \cdot \omega - F_x \cdot v_x;$$

With these 3 equations, we can study P_{Loss} in the traction diagram ($\{v_x, F_x\}$-diagram). E.g., the solution for $\omega > 0$ becomes:

$$P_{Loss}(v_x, F_x) = -\frac{v_x \cdot (F_x^2 \cdot r_E + C_x \cdot F_z \cdot e + C_x \cdot F_x \cdot R_L - C_x \cdot F_x \cdot r_E)}{F_x \cdot r_E - C_x \cdot r_E};$$

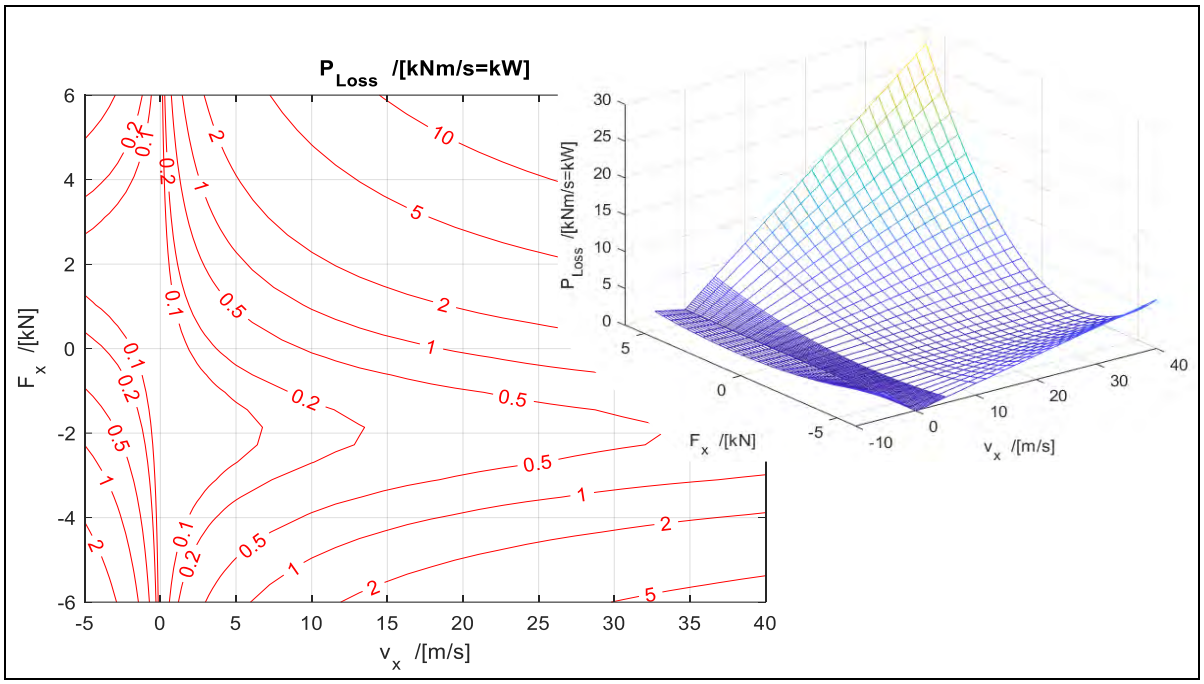


Figure 2-13: Power losses for a wheel modelled with rolling resistance and slip losses. Parametrized with numerical values typical for a passenger car. Note that saturation due to road friction is not included, which would increase losses dramatically for large $|F_x|$.

2.2.1.7.2 Efficiencies

Efficiency η often means power efficiency, it is $\eta = P_{useful}/P_{used}$. For a transmission there are two such when power is coming out in the intended output end and when power goes backward, into the intended output end. For a wheel, with subscript $Prop$ for intended power transfer from propulsion system to vehicle body and Brk for intended power transfer from vehicle body to propulsion system (for reduction of vehicle speed and/or regeneration of energy to storage):

$$\eta_{Prop} = \frac{P_{useful}}{P_{used}} = \frac{+F_x \cdot v_x}{+T \cdot \omega}; \quad and \quad \eta_{Brk} = \frac{P_{useful}}{P_{used}} = \frac{-T \cdot \omega}{-F_x \cdot v_x};$$

With those definitions and the equations from 2.2.1.7.1 these power efficiencies can be analysed.

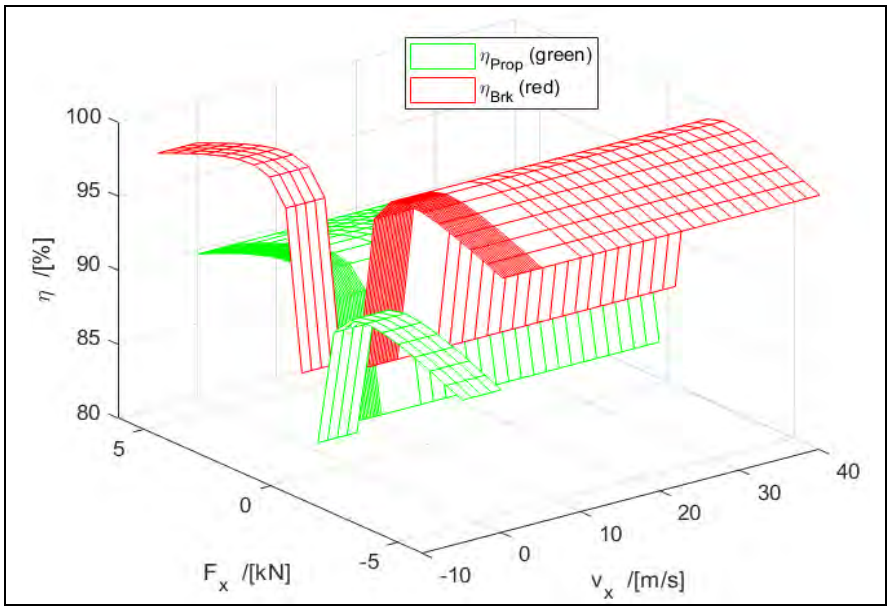


Figure 2-14: Power efficiencies for a wheel. Parametrized with numerical values typical for a passenger car. Note that saturation due to road friction is not included, which would decrease both η_{Prop} and η_{Brk} dramatically for large $|F_x|$.

For transmissions, one often factorizes the (power) efficiency η in speed and torque efficiencies: $\eta = \eta_\omega \cdot \eta_T$. The η is always $\leq 1 = 100\%$ and the distribution of losses between η_ω and η_T depends on what nominal ratio is assumed. For a wheel and tyre, the corresponding becomes a factorization;

$\eta = \eta_v \cdot \eta_F$; (if, as below, same nominal radius R_{Nom} is used in velocity and force equations.)

$$where \begin{bmatrix}\eta_v \\ \eta_F\end{bmatrix} = \begin{cases} = \{F_x \cdot v_x > 0\} = \begin{bmatrix}\eta_v \\ \eta_F\end{bmatrix}_{Prop} = \begin{bmatrix}\frac{v_x}{v_{xNom}} = \frac{v_x}{R_{Nom}\cdot\omega} \\ \frac{F_x}{F_{xNom}} = \frac{F_x}{T/R_{Nom}}\end{bmatrix}; \\ = \{F_x \cdot v_x < 0\} = \begin{bmatrix}\eta_v \\ \eta_F\end{bmatrix}_{Brk} = \begin{bmatrix}\frac{\omega}{\omega_{Nom}} = \frac{\omega}{v_x/R_{Nom}} \\ \frac{T}{T_{Nom}} = \frac{T}{R_{Nom}\cdot F_x}\end{bmatrix}; \end{cases}$$

Check: $\eta_{Propv} \cdot \eta_{PropF} = \frac{v_x}{R_{Nom}\cdot\omega} \cdot \frac{F_x}{T/R_{Nom}} = \frac{+v_x\cdot F_x}{+\omega\cdot T} = \eta_{Prop}$; and $\eta_{Brkv} \cdot \eta_{BrkF} = \frac{\omega}{v_x/R_{Nom}} \cdot \frac{T}{R_{Nom}\cdot F_x} = \frac{-\omega\cdot T}{-v_x\cdot F_x} = \eta_{Brk}$;. This was expected and, hopefully, it gave an understanding of the factorization into velocity and force efficiency.

Note that R_{Nom} is a 3rd "ratio-like" parameter for a wheel, beside R_L and r_E. The value of R_{Nom} depends on what one expects from the wheel, which can be different.

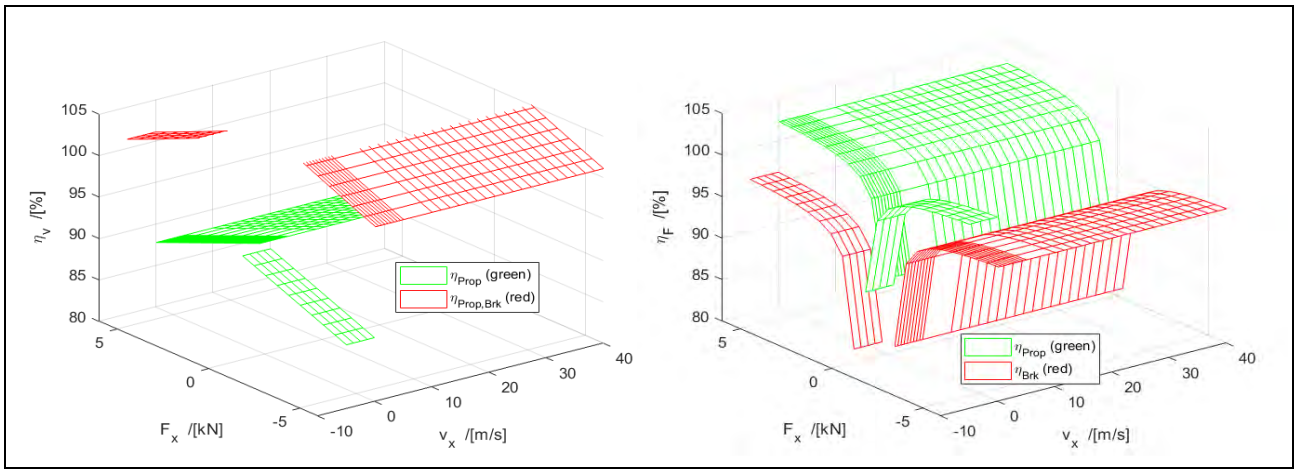


Figure 2-15: Velocity and force efficiencies for a wheel. Parametrized with numerical values typical for a passenger car. Note that saturation due to road friction is not included, which would decrease both η_{vProp} and η_{vBrk} dramatically for large $|F_x|$.

2.2.1.8 Tyre Rolling and Radii

Ideal rolling is shown in Figure 2-16 a). This relationship does not hold when the tyre is deflected as in Figure 2-16 b). Not even the deflected radius can be assumed to be a proportionality constant between angular and translational velocity, since the tyre contact surface slides, or slips, versus the ground. Then, an even more true picture of a rolling tyre looks like Figure 2-16 c), where the deformation at the leading edge also is drawn. This means that v_x is only $\approx R \cdot \omega$ and only for limited slip levels.

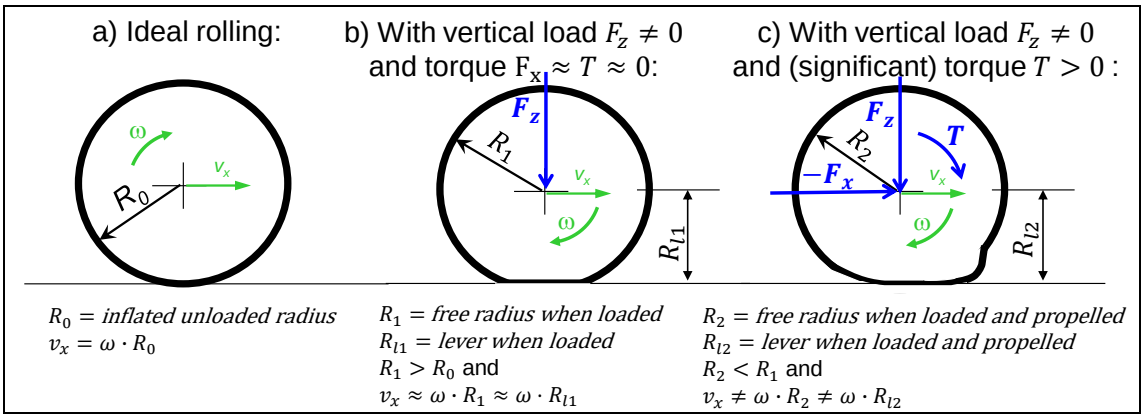


Figure 2-16: Radius and velocity relations of a tyre. R_0 and R_l are not the same across a), b) and c).

There is a relative velocity between tyre and the road surface. The ratio between this relative velocity and a reference velocity is defined as the "tyre slip", see also 1.6.1.5. The reference velocity can be the circumferential speed or the translational velocity of the tyre, depending on the application. For a driven wheel, the slip definition in Eq [2.2] is often used and for braked wheels Eq [2.3] is often used. This is to avoid division by small numbers in take-off and brake tests, respectively. The physical model in 2.2.3.1 reveals that Eq [2.2] is the physically most motivated.

$$s_x = \frac{R \cdot \omega - v_x}{|R \cdot \omega|}; \qquad [2.2]$$

$$s_x = \frac{R \cdot \omega - v_x}{|v_x|}; \qquad [2.3]$$

The longitudinal slip is alternatively denoted σ_x, κ, or λ. Sometimes specific names are used for slip in Eq [2.2] and Eq [2.3]: theoretical and practical slip, respectively. When only studying braking, some uses the opposite sign definition, so that the numerical value of the slip becomes positive during

braking. In conclusion: slip is not a uniquely intuitive physical quantity, so it is often important to agree on which slip definition to use.

With the definition in Eq [2.2] and a model for how tyre longitudinal force varies with R, ω and v_x (Eq [2.22] taken as example) we get Figure 2-17, which shows cuts in Figure 2-46.

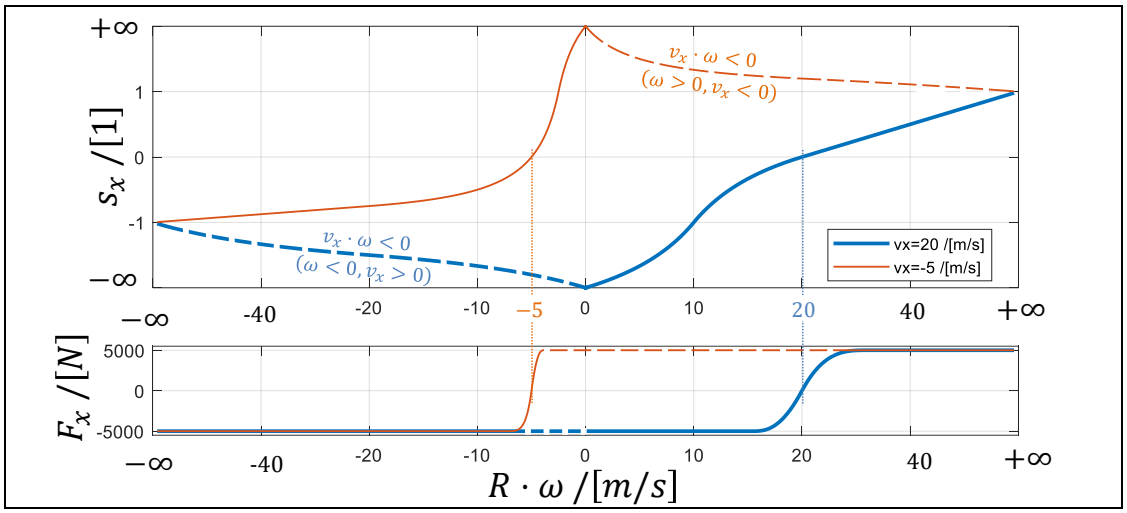


Figure 2-17: Slip s_x and force F_x as function of $R \cdot \omega$ for constant v_x. $C_x = 50\ [kN/1]$ and $\mu \cdot F_z = 5000\ [N]$. Semi-inverted scales around $|R \cdot \omega| = 20$ and $|s_x| = 1$. Dashed shows where definition of s_x is not relevant, since F_x is not dependent of s_x, since $v_x \cdot \omega < 0$.

In 2.2.3.1, we will see some reasons to model as proportional, $F_x \propto s_x$. But, already in Figure 2-18, we can note that there will be a need to saturate due to maximum friction force $\mu \cdot F_z$.

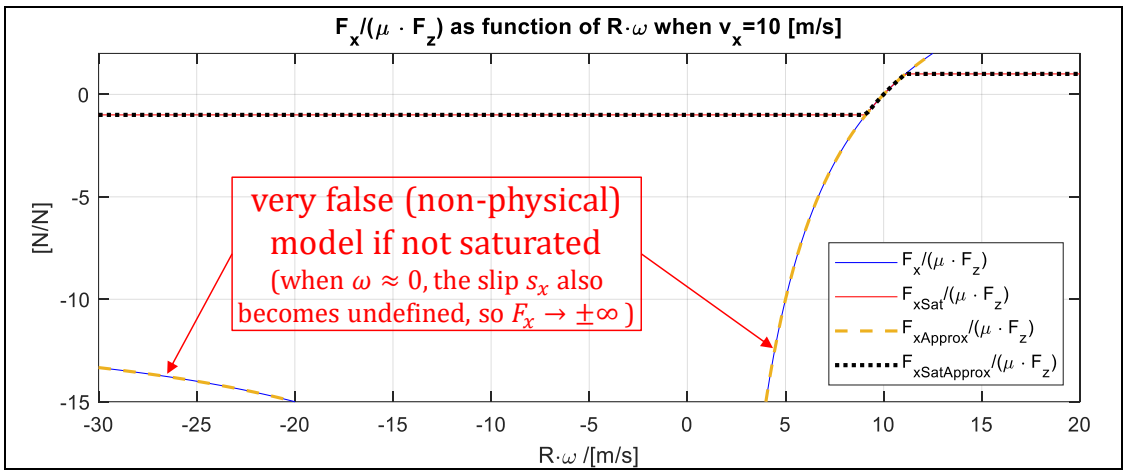


Figure 2-18: F_x as function of $R \cdot \omega$ for constant $v_x = 10\ m/s$. $C_x = 50\ [kN/1]$ and $\mu \cdot F_z = 5000\ [N]$.

It is not obvious which R to use of Eqs [2.2] and [2.3], e.g. R_0, R_1, R_2, R_{l1}, or R_{l2}. However, this book recommends the free radius (R_1 or R_2), rather than the loaded radii (R_{l1} or R_{l2}) because the free radii are better average value of the radius around the tyre and the tyre's circumference is tangentially stiff, so speed has to be same around the circumference.

2.2.1.9 Tyre Contact Length

The contact length L represents the deformation shape. The L is not a design parameter, but an intermediate parameter or variable, explaining both rolling resistance and tyre forces from slip. One way to model L in a physical way is shown in Figure 2-19. The tyre belt is modelled as circumferentially rigid (constant length), which gives:

$$2 \cdot \pi \cdot R_{free} = \frac{2 \cdot \pi - 2 \cdot \gamma}{2 \cdot \pi} \cdot 2 \cdot \pi \cdot R_{F_z} + L;$$
$$\left(R_{free} - \Delta z\right)^2 + (L/2)^2 = R_{F_z}^2;$$
$$\frac{L/2}{R_{free} - \Delta z} = \tan(\gamma);$$

[2.4]

Additionally, we need a model for the vertical deformation. Simplest possible is a linear spring:

$$F_z = c_z \cdot \Delta z;$$

[2.5]

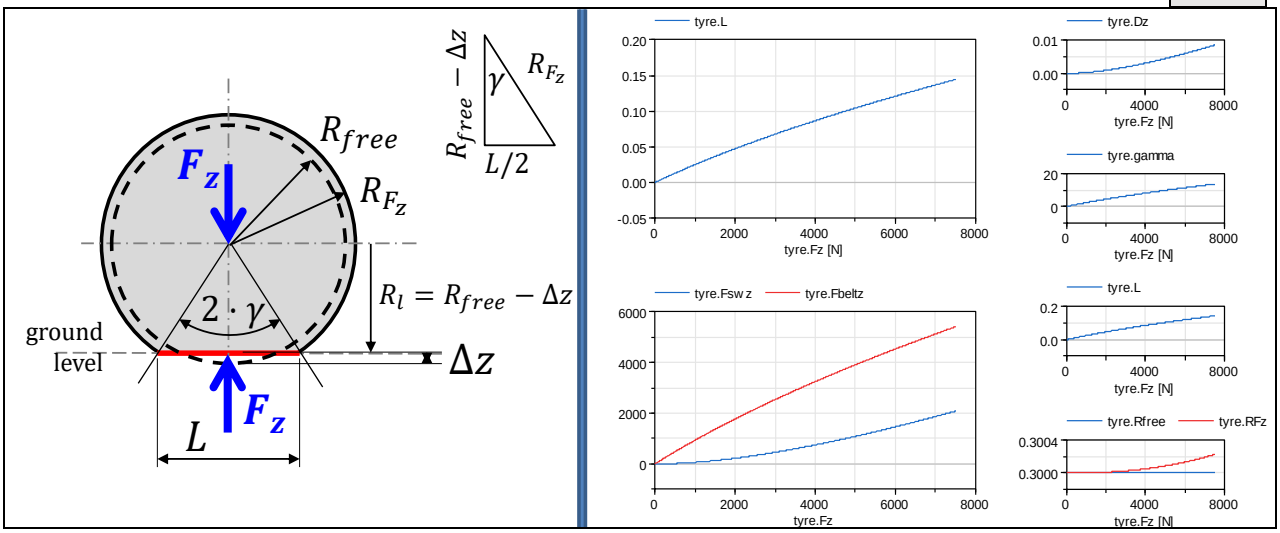


Figure 2-19: Left: Physical model. Right: Example result of model defined by Eqs [2.4] and [2.6].

A typical usage of this model is to know variable F_z and parameters R_{free} and c_z. This leaves 4 unknown variables $(\Delta z, \gamma, L, R_{F_z})$ and equally many equations. An explicit solution is easy for Δz, but difficult for the remaining 3 variables $[\gamma, L, R_{F_z}]$. For a single operation conditions, one can solve by iteration. For whole simulations, it is more computational efficient to pre-process numerically in a table for how $[\Delta z, L, R_{F_z}]$ varies with γ (for certain R_{free}, which typically not varies during a simulation). For each time instant during simulation, interpolation in this table gives $[\gamma, L, R_{F_z}]$ from known Δz.

The stiffness c_z can be found for an existing tyre with a certain inflation pressure, but it is far from a design parameter. Also, the linear model is often too simplified. To improve this, alternative vertical deformation models can be used. If studying only single operation conditions, Finite Element models are suitable. But for simulations, a more computational efficient solution is almost a necessity. The model in Eq [2.6] can replace Eq [2.5]. This is simple but indicates the mechanisms for how sidewall stiffness and inflation pressure come into play: Assume that the vertical load is carried by sidewalls $(F_{sw,z})$ and the belt area between the sidewalls $(F_{belt,z})$. Assume belt has no bending stiffness and sidewalls follow Hertz contact theory (2.2.3.1.3, where constant k_{sw} has unit $[N/m^2]$):

$$F_z = F_{sw,z} + F_{belt,z};$$
$$F_{belt,z} = p_{infl} \cdot W \cdot L; \quad (W = \text{tyre width},\ p_{infl} = \text{tyre inflation pressure})$$
$$F_{sw,z} = k_{sw} \cdot L^2;$$

[2.6]

So, Eq [2.6] can be solved for $[L, F_{sw,z}, F_{belt,z}]$. Then [2.4] can be solved for $[\gamma, \Delta z, R_{F_z}]$, using iterations or preprocessing with swept γ and interpolation, very similar as described above. The model is plotted for varying F_z in Figure 2-19.

The k_{sw} is a radial stiffness of the sidewall. The set $[W, k_{sw}, p_{infl}]$ is closer to design parameters than the parameter $[c_z]$.

When driving on soft ground, the deformation of the ground adds variables, beside L, that influences rolling resistance and forces in ground plane. Driving on soft ground is not well covered in this book, except shortly in 2.2.2.4.5. Present section assumes rigid ground.

2.2.2 Rolling resistance of tyres

2.2.2.1 Definition of Rolling resistance

Rolling resistance is a phenomena which can be quantified as $EnergyLoss[Nm]$ or $PowerLoss[Nm/s]$ or $TorqueLoss\ [Nm]$ or $ForceLoss\ [N]$ or $ForceOffset\ [m]$ in the tyre. The first two quantifications (and definitions of Rolling Resistance Coefficient RRC below) includes both force and speed losses, while the other only includes torque (or force) losses.

RRC is the rolling resistance divided by something that gives a dimensionless measure. For a wheel and tyre on flat, level and hard ground, the RRC becomes:

- **Energy definition**: $RRC_E\left[\frac{Nm}{N\cdot m}\right] = \frac{EnergyLoss}{F_z\cdot|Distance|} = \frac{\int|T\cdot\omega - \vec{F}_{xy}\bullet\vec{v}_{xy}|\cdot dt}{F_z\cdot\int|\vec{v}_{xy}|\cdot dt} = \\ = \begin{Bmatrix}no\ late\text{-}\\ral\ slip\end{Bmatrix} = \frac{\int|T\cdot\omega - F_x\cdot v_x|\cdot dt}{F_z\cdot\int|v_x|\cdot dt};$
- **Power definition**: $RRC_P\left[\frac{Nm/s}{N\cdot(m/s)}\right] = \frac{PowerLoss}{F_z\cdot|Speed|} = \frac{T\cdot\omega - \vec{F}_{xy}\bullet\vec{v}_{xy}}{F_z\cdot|\vec{v}_{xy}|} = \\ = \begin{Bmatrix}no\ late\text{-}\\ral\ slip\end{Bmatrix} = \frac{T\cdot\omega - F_x\cdot v_x}{F_z\cdot|v_x|} = \frac{T\cdot\omega - F_x\cdot v_x}{F_z\cdot v_x}\cdot\mathrm{sign}(v_x);$
- **Torque definition**: $RRC_T\left[\frac{Nm}{N\cdot m}\right] = \frac{TorqueLoss}{F_z\cdot R_{Nom}} = \frac{T_{RR}}{F_z\cdot R_{Nom}} = \frac{T - F_x\cdot R_l}{F_z\cdot R_{Nom}}\cdot\mathrm{sign}(\omega) = RRC_F;$
- **Force definition**: $RRC_F\left[\frac{N}{N}\right] = \frac{(Longitudinal)ForceLoss}{F_z} = \frac{T/R_l - F_x}{F_z}\cdot\mathrm{sign}(\omega);$
- **Force offset definition**: $RRC_e\left[\frac{m}{m}\right] = \frac{(Vertical)ForceOffset}{R_{Nom}} = \frac{e\cdot\mathrm{sign}(\omega)}{R_{Nom}};$

The RRC is relatively constant for a tyre, so it gives a good approximation to model RRC as a (constant) **parameter** for a certain tyre if the operating conditions do not change too much.

However, for models that should reflect more varied operating conditions, e.g., variation of $F_z, v_x, temperature, etc$, much more is needed. If, at all, using the RRC in the model, it will have to be a **variable**. Some variations can be expressed as physical models, but one almost always need some tuning to measurements, either from vehicles tests or from tyre test rigs. When taking such experimental data as input to modelling, it is of little use that measurement engineers and modelling engineers only exchange values of RRC and operating conditions; one need to also agree on the definition of RRC.

Energy definition RRC_E and power definition RRC_P have the advantage that they do not rely on any radius. But they are not very useful in most vehicle dynamics models since they do not resolve into force and velocity. It should be mentioned that (ISO28580, 2018) only treats $T = 0$ and proposes RRC_E. (Schuring, 1980) uses same definition but admits that T can be $\neq 0$. Generally, RRC_E and RRC_P reflect only the sum of speed and force losses, so they vary more than the other. So, the book uses the other definitions: RRC_T, RRC_F and RRC_e.

A model of the slip losses can be inserted. If we use one simple model from 2.2.3, $F_x = C_x\cdot s_x = CC_x\cdot F_z\cdot s_x = CC_x\cdot F_z\cdot\frac{R_b\cdot\omega - v_x}{|R_b\cdot\omega|}$;, the RRC_P becomes as follows, which initiate yet another radius, the belt radius R_b. Inserting all this gives a model with 2 equations which models the tyre using all these radii:

The set of radii is now R_l, R_{Nom}, R_b, R_e. The R_l is the lever for the F_x, often called “loaded radius”. The R_b is the ratio v_x/ω when $F_x = 0$, often well represented by circumference of the belt divided by $2\cdot\pi$.

The R_e is the ratio v_x/ω when $T = 0$, so $R_b \approx R_e$. The R_{Nom} is introduced to make the RRC dimensionless. So R_{Nom} can be chosen very freely, e.g., some (constant) nominal radius from tyre manufacturer.

2.2.2.2 Physics explanation of Rolling Resistance

There is no well-established physics-based mode of rolling resistance. In the following, two possible explanations are given, see Figure 2-21 and Figure 2-22**Error! Reference source not found.**. They consider only tyres on hard and flat ground and moderate speeds, both positive and negative. On soft ground, there are mechanisms as in 2.2.2.4.5. And, at very high speeds, there is inertial impact mechanism which causes energy loss. The explanation models below mainly take on the challenge to explain why a rolling resistance moment appears opposite to roll direction, also when speed is close to zero.

The overall explanation of rolling resistance for pneumatic tyres on hard flat surfaces is that the pressure distribution is offset in rolling direction. In Figure 2-21, radial damping and friction is the cause for the offset, see 2.2.2.2.2. Figure 2-21 also shows another offset phenomenon; that the whole contact patch is moved forward due to longitudinal force and shearing of the sidewalls. The latter phenomenon also includes a elasticity-motivated shift of the effective vertical force F_z within the moved contact patch, see 2.2.2.2.3.

The rolling resistance coefficient is almost the same for very low speeds; even when the wheel starts rolling from zero speed, after gradually increasing the torque up to the rolling resistance moment.

2.2.2.2.1 Losses due to different phenomena

2.2.2 is about power or energy losses in the tyre due to rolling resistance. Since we look at steady state operation conditions, the difference between power and energy is only that energy is the time integral understand rolling resistance as one of several phenomena that contributes to power loss.

The tyre can be used in operating conditions where we aim to transmit rotational power $T \cdot \omega \geq 0$ to translational power $F_x \cdot v_x$. Then, the nominal (expected or conceptually intended) output power is $(F_x \cdot v_x)_{Nom} = T \cdot \omega$. The design principle of a wheel makes it possible to also decompose into nominal force and velocity: $(F_x \cdot v_x)_{Nom} = F_{xNom} \cdot v_{xNom}$; where $F_{xNom} = T/R_{Nom}$ and $v_{xNom} = R_{Nom} \cdot \omega$. The power loss is $P_{Loss} = T \cdot \omega - F_x \cdot v_x$.

(The tyre can alternatively be used in operating conditions when the aimed power direction is opposite, e.g. when regenerating kinetic energy from vehicle to battery: when we aim to transmit translational power to rotational power. Then the nominal output power is $(T \cdot \omega)_{Nom} = F_x \cdot v_x$. We can still use the design principle of a wheel and decompose into: $(T \cdot \omega)_{Nom} = T_{Nom} \cdot \omega_{Nom}$; where $T_{Nom} = F_x \cdot R_{Nom}$ and $\omega_{Nom} = v_x/R_{Nom}$. The power loss is still $P_{Loss} = T \cdot \omega - F_x \cdot v_x$.)

The ways by which $F_x \cdot v_x \leq F_{xNom} \cdot v_{xNom}$ can happen are:

- $F_x \leq F_{xNom}$, which we call force losses
- $v_x \leq v_{xNom}$, which we call velocity losses

Force losses can be explained with an offset of the vertical force in the tyre-to-ground contact (called rolling resistance in 2.2.2). An additional phenomenon that contributes is if the wheel has a camber angle, which gives a “spin torque” in the tyre-to-ground contact. Both ”steals” force. (One can include the latter in rolling resistance.)

Velocity losses can be explained with wheel-longitudinal slip s_x (as introduced in 2.2.3). An additional phenomenon is wheel-lateral slip s_y (as introduced in 2.2.4).

2.2.2.2.2 Radial friction as explanation of the vertical force offset

Contribution from Matthias Hjort, VTI

The radial friction in Figure 2-21 can explain an offset pressure distribution. The e normally increase with F_x. But, as mentioned in the bottom of the figure, there is a phenomenon acting in the other

direction. It is very difficult to find for numbers on the total effect e/F_x, but it is typically positive and one can find numbers of couple of mm per $F_x = 1\ kN$.

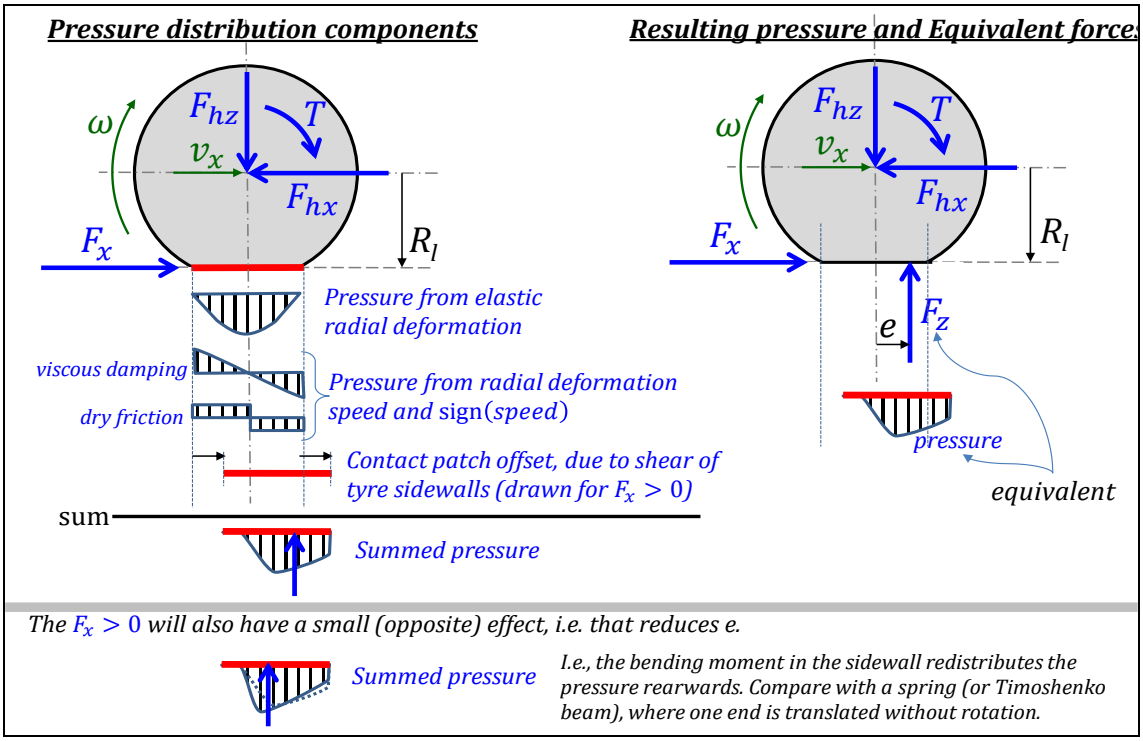


Figure 2-21: Normal force distribution on a tyre. The measure e is the force offset. In steady state, the forces in hub and contact patch are the same: $F_{hx} = F_x$ and $F_{hz} = F_z$.

An experiment as in Figure 2-22 gives us a possibility estimate the dry friction portion of the radial≈vertical force. The difference between increase and decrease of Δz is denoted ΔF_z.

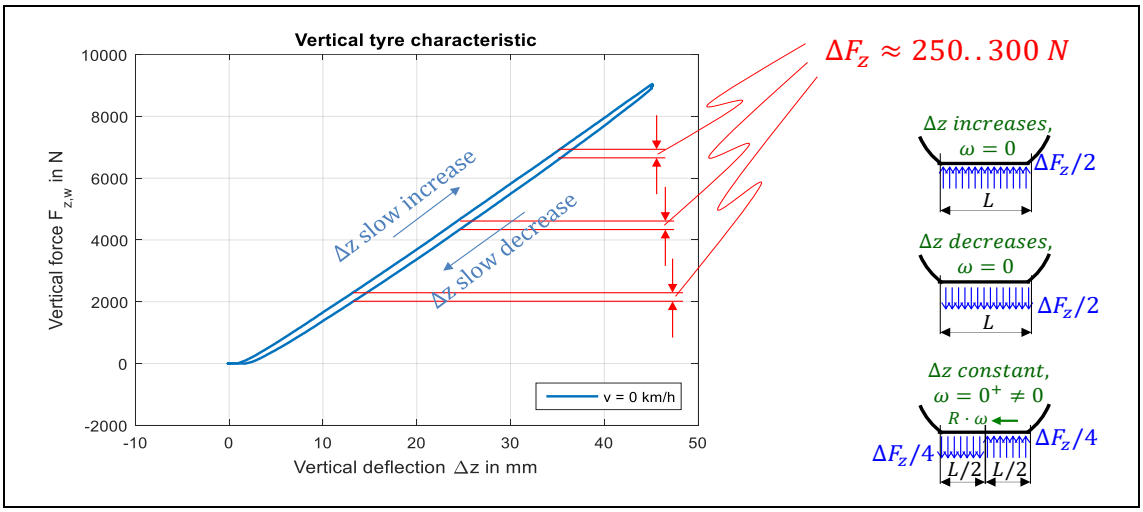


Figure 2-22: Vertical force F_z vs deformation Δz from a compression test of a non-rolling tyre. The wheel had $v_x = \omega = 0$ and Δz was varied slowly.

The ΔF_z can be used to estimate the rolling friction torque T_{RR} and RRC. We assume values for a typical passenger car with a certain $\{F_z, L\}$:

$$T_{RR} = 2 \cdot \frac{\Delta F_z}{4} \cdot \frac{L}{4} = \Delta F_z \cdot \frac{L}{8} \approx \{250..300\} \cdot \frac{\{0.075..0.15\}}{8} \approx \{3..6\}\ [Nm];$$

$$RRC_T = \frac{T_{RR}}{F_z \cdot R_{Nom}} = \frac{\{3..6\}}{5000 \cdot 0.3} = \{0.002..0.004\} \left[\frac{Nm}{N \cdot m}\right];$$

A typical value of RRC is 0.005..0.01, so the $RRC_T = \{0.002..0.004\}$ from the compression test of a non-rolling tyre explains about half of it.

We can assume that a "deformation friction pressure" p_μ is the part of pressure needed to shorten and stretch the contact point towards and from the rim. The phenomena can be modelled (seen as) either radial friction elements in the sidewalls and/or friction when squeezing rubber in the tyre tread into and out from the road texture (e.g. between stones in the asphalt). The contact pressure part from such phenomena would be $= p_\mu \cdot \text{sign}(deformation\ velocity)$, so it is $\pm p_\mu$ depending on if before or after the contact pressure peak. If peak symmetric in contact and $L \propto \sqrt{F_z}$ with $L = k \cdot \sqrt{F_z}$.

$$\underbrace{RRC \cdot R}_{e} \cdot F_z = p_\mu \cdot \underbrace{W \cdot \frac{L}{2}}_{Area} \cdot \underbrace{\frac{L}{4}}_{Lever} = \frac{p_\mu \cdot W \cdot L^2}{8} = \frac{p_\mu \cdot W \cdot k^2 \cdot F_z}{8}; \quad \Rightarrow$$

$$\Rightarrow \quad RRC = \frac{e}{R} = \frac{p_\mu \cdot W \cdot k^2}{8 \cdot R}; \qquad [2.7]$$

So, the RRC would increase width W and decrease with R. The p_μ is a parameter with physical motivation. The p_μ can still be a function of such as tyre temperature and road texture. With typical values for tyres, one gets $p_\mu = 100..1000\ \left[\frac{N}{m^2}\right] = 0.1..1\ [MPa]$. Keep in mind that p_μ represents two phenomena: Friction in the sidewalls (independent of road) and Friction in the road texture (depends on both tyre and road). Combined with Reference (Ejsmont & et al, 2017) one can find an indication of that p_μ (and RRC) typically increases with 50% if changing from even to rough asphalt. So, assuming asphalt texture varies within that range, some 75% of p_μ (and RRC) comes from tyre sidewalls and 25% from tyre tread and road texture. When getting RRC from tyre test machines, it is therefore relevant to know what texture the tyre has been tested against.

2.2.2.2.3 2D spring as explanation of the vertical force offset

There will also be an elastic deformation which contributes to the offset.

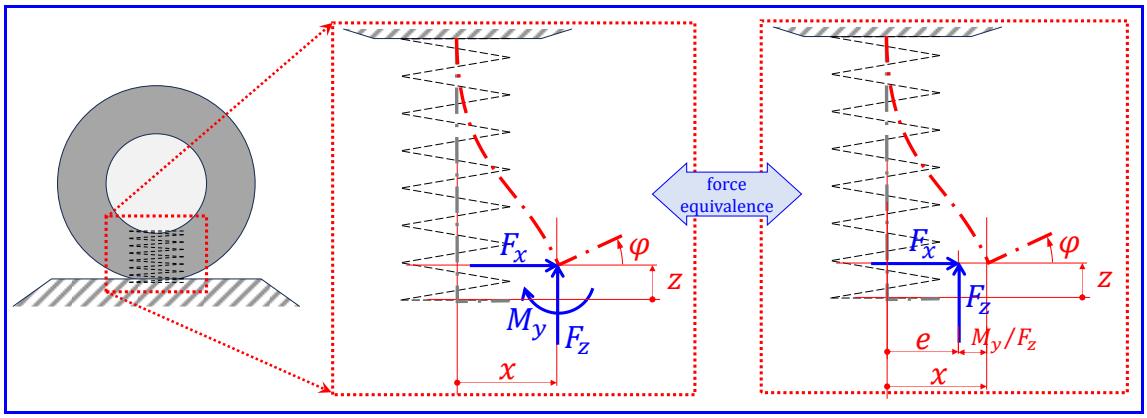


Figure 2-23: 2D spring model of a tyre's lower part of sidewall.

We use the model From 1.5.2.4.4.1 :

$$\begin{bmatrix} F_x \\ F_z \\ M_y \end{bmatrix} = \begin{bmatrix} c_{xx} & c_{xz} & c_{x\varphi} \\ c_{xz} & c_{zz} & c_{z\varphi} \\ c_{x\varphi} & c_{z\varphi} & c_{\varphi\varphi} \end{bmatrix} \cdot \begin{bmatrix} x \\ z \\ \varphi \end{bmatrix} = \left\{ \begin{matrix} \{x, \varphi\} = \{0,0\} \\ should\ give \\ \{F_x, M_y\} = \{0,0\} \end{matrix} \right\} = \begin{bmatrix} c_{xx} & 0 & c_{x\varphi} \\ 0 & c_{zz} & 0 \\ c_{x\varphi} & 0 & c_{\varphi\varphi} \end{bmatrix} \cdot \begin{bmatrix} x \\ z \\ \varphi \end{bmatrix}; \qquad [2.8]$$

Assuming that F_z is known and $\varphi = 0$ gives: $e = x - \frac{M_y}{F_{z0}} = \frac{F_z - c_{x\varphi}}{F_z \cdot c_{xx}} \cdot F_x = \left(1 - \frac{c_{x\varphi}}{F_z}\right) \cdot \frac{F_x}{c_{xx}};$

2.2.2.2.4 Summing up both phenomena

The phenomena from 2.2.2.2.2 and 2.2.2.2.3 superimpose to:

$$e = e_{\mu} + e_{2Dspring} = \frac{p_{\mu} \cdot W \cdot k^2}{8} \cdot \text{sign}(\omega) + \left(1 - \frac{c_{x\varphi}}{F_z}\right) \cdot \frac{F_x}{c_{xx}};$$

2.2.2.3 Mathematical Representation of Rolling Resistance

The rolling resistance force is defined as the loss of longitudinal force on the vehicle body, as compared to the longitudinal force which would have been transferred with an ideal wheel. Assuming force equilibria in longitudinal and vertical direction, $F_{hub,z} = F_{ground,z} = F_z$ and $F_{hub,x} = F_{ground,x} = F_x$, see Figure 2-12.

$$RRC = \left|\frac{T/R - F_x}{F_z}\right|; \qquad [2.9]$$

F_x denotes the longitudinal force on the wheel, T denotes the applied torque and R denotes the tyre radius. For a free rolling tyre, where $T = 0$, RRC becomes simply $-F_x/F_z$. One often sees definitions of RRC which assumes free rolling tyre; but Eq [2.9] is also valid when $T \neq 0$, which is useful.

A free body diagram of the forces on the wheel can be used to explain the rolling resistance. Consider Figure 2-21 which represents a free rolling wheel under steady state conditions. The inertia of the wheel is neglected.

Longitudinal and vertical force equilibria are already satisfied, due to assumptions above. However, moment equilibrium around wheel hub requires:

$$T - F_x \cdot R_l - F_z \cdot e = 0 \Rightarrow F_x = \frac{T}{R_l} - \frac{e}{R_l} \cdot F_z; \qquad [2.10]$$

This result suggests that the force F_x, which pushes the vehicle body forward, is the term T/R_l (arising from the applied torque T) minus the term $F_z \cdot e/R_l$. The term can be seen as a force F_{roll} and referred to as the rolling resistance force. We seldom know neither R_l or e, but they are rather constant and the form of Eq [2.10] is same as Eq [2.9] if:

$$RRC = |e/R|; \qquad [2.11]$$

Eq [2.11] is a definition of rolling resistance coefficient based on physical mechanisms internally in the tyre with road contact, while Eq [2.9] is based on quantities which are measurable externally, see Eq [2.9]. Sometimes one sees $RRC = -F_x/F_z$ as a definition, but that is not suitable since it assumes absence of torque.

It is not obvious which radius to use. R_l can be motivated because R_l is the lever for F_x. However, in 2.2.1.7.2, we found arguments for using other radii. If same radius is used, for slip and rolling resistance, we can fully see the tyre as a transmission with the nominal ratio R and zero energy loss if $RRC = 0$ and $s_x = 0$.

It is important to refer to this phenomenon as rolling **resistance** as opposed to rolling **friction**. It is not friction in the basic sense of friction, because $F_x \neq -RRC \cdot F_z$ except for the special case when un-driven wheel ($T = 0$). Figure 2-24 shows an un-driven and pure rolling.

Rolling resistance is a torque loss. Other torque losses, which can be included or not in tyre rolling resistance, are:

- losses associated with friction in gear meshes,
- drag losses from oil in the transmission,
- wheel bearing (and bearing sealings) torque losses,
- drag from brake discs,
- drag losses from aerodynamic around the wheel, and
- uneven road in combination with suspension damping that dissipates energy.

These should, as rolling resistance, be subtracted from propulsion/brake torque. However, sometimes they are included as part of the tyres rolling resistance coefficient, which can be misleading. The wheel bearing torque loss have two torque terms: one is proportional to vertical load on the wheel (adds

typically 0.0003 to rolling resistance coefficient), and the other is of constant magnitude but counter-directed to rotation speed. The former term can be included in rolling resistance coefficient. The aerodynamic losses due to wheel rotation are special since they vary with wheel rotational speed, meaning that they (for constant vertical load) are relevant to include when studying the variation of rolling resistance coefficient with vehicle speed. A summarizing comment is that one has to be careful with where to include different torque losses, so that they are included once and only once.

2.2.2.4 Variation of Rolling Resistance

Several parameters will affect the rolling resistance moment (or Rolling resistance coefficient). Design parameters, see Figure 2-8:

- Tyre material. Natural rubber often gives lower rolling resistance.
- Radial tyres have more flexible sides, giving lower rolling resistance also bias ply have a greater crown angle causing more internal friction within the tyre during deflection.
- Geometry:
  - Diameter. Large wheels often have lower coefficient of rolling resistance
  - Width
  - Groove depth
  - Tread depth
- Higher inflation pressure gives lower rolling resistance on hard ground but higher rolling resistance on soft ground (and vice versa), see Figure 2-26 and Figure 2-27.

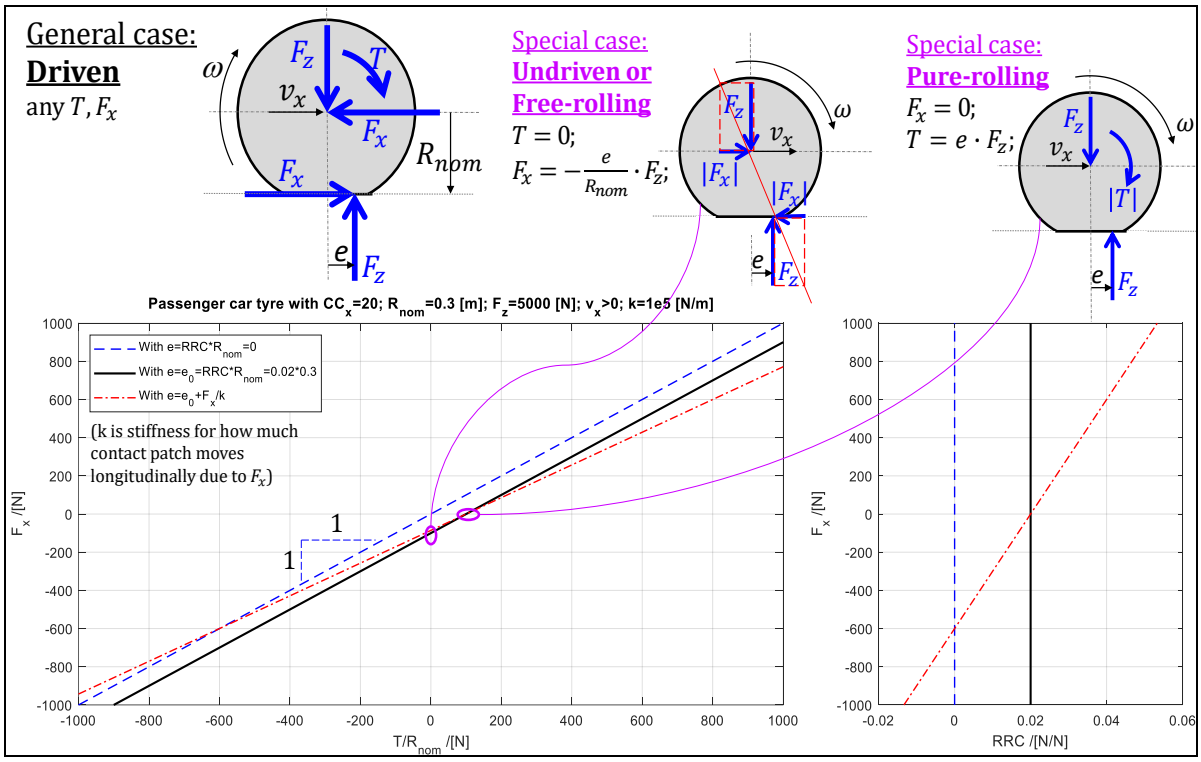


Figure 2-24: Driven wheel with rolling resistance. Special cases "Free-rolling" and "Pure rolling".

Operational parameters, see Figure 2-8:

- Elevated temperatures give low rolling resistance, via increased inflation pressure. Tyres need to roll approximately 30 km before the rolling resistance drop to their lowest values.
- Road/ground, sometimes covered: Clean asphalt, Asphalt with water/leaves/sand/..., Loose/hard gravel, Snow/ice. Soft ground or covered hard ground increases rolling resistance.
- Wear state. Worn tyres have lower rolling resistance than new ones (less rubber to deform).

Operational variables, see Figure 2-8:

- Vertical force.
- Speed. Rolling resistance increases with vehicle speed due to rubber hysteresis and air drag.

- Tyre loads (propulsion/braking and lateral forces)

Approximately for modern tyres (written year 2020): Passenger car tyres have $RRC = 0.005..0.01$, Truck tyres have $RRC = 0.003..0.005$. The lower values are "eco-tyres" and can have some trade-off with vertical comfort and road grip.

Note that some of the below mentioned variations can correlate, e.g. increased speed leads to higher tyre temperature after the tyre warm-up.

2.2.2.4.1 Variation of Tyre Type

Trucks tyres have a much lower rolling resistance coefficient than passenger vehicle tyres, approximately half. Tyres have developed in that way for trucks, because their fuel economy is so critical.

2.2.2.4.2 Variation of Vertical Force

In a first approximation, the rolling resistance force is proportional to vertical force, i.e. RRC is constant.

However, note that increased vertical load leads to warming up the tyres. The warm-up process is typically slow, with time constant of 0.5..1 hour. See2.2.2.4.3.

This, and parasitic bearing and brake drag losses, $torque = \text{sign}(\omega) \cdot constant$, and tyre lateral slip losses, explains why commercial vehicles lift axles when driven with low payload.

2.2.2.4.3 Variation of (Tyre) Temperature

RRC typically decreases with temperature due to less friction in the tyre material when warm. A temperature change of 1 $deg\ C$ can change RRC with typically 0.6%, so it is a significant influence.

It should be noted that it is the temperature of the tyre, not the ambience. The temperature of the tyre changes relatively slowly, following thermodynamics:

$$\frac{d}{dt}Temp_{Tyre} = function_1\left(Temp_{Tyre}, Temp_{Ambience}, P_{LossTyre}, Cooling, \cdots\right);$$

Studying steady state $Temp_{TyreSS}$, one can set $\frac{d}{dt}Temp_{Tyre} = 0$ and solve for $Temp_{Tyre}$:

$$Temp_{TyreSS} = function_2\left(Temp_{Ambience}, P_{LossTyre}, Cooling, \cdots\right);$$

The $Cooling$ depends, e.g., on air flow around the tyre and rain on tyre.
The $P_{LossTyre}$ depends on the rolling resistance coefficient itself and vertical load and speed.

Studying short ($\approx 10 - 20\ minutes$) but fast ($\approx 100\ km/h$) transport missions, where one start from cold tyres, one should rather use the cold temperature than the steady state temperature. It makes a large difference in energy consumption.

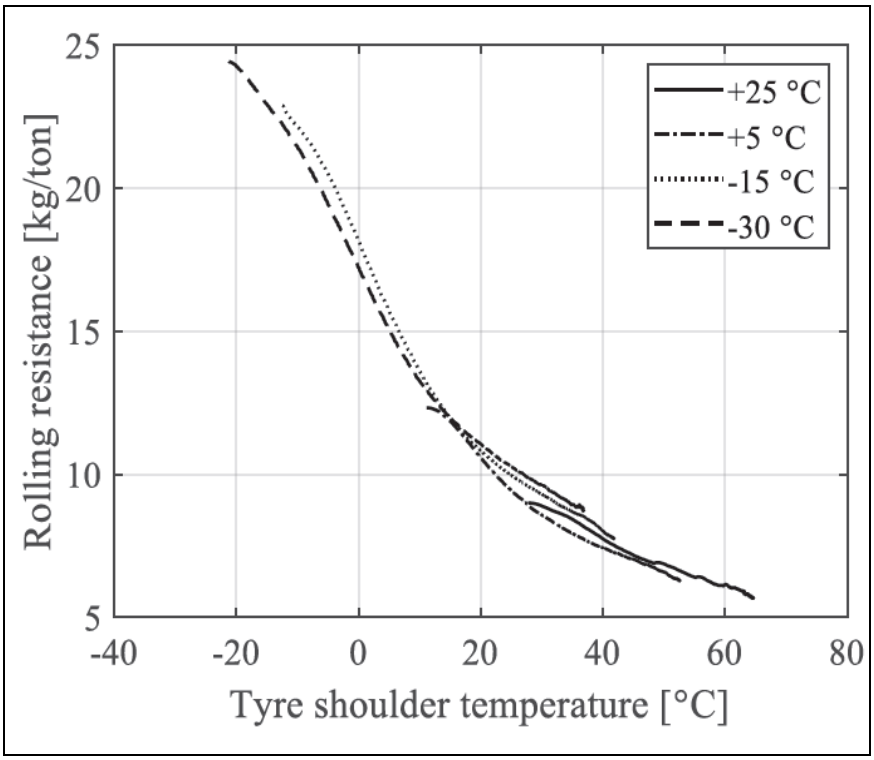


Figure 2-25: Rolling resistance coefficient variation with tyre temperature for a truck tyre. From Reference (Hyttinen, 2023).

2.2.2.4.4 Variation of Speed

As an example, left part of Figure 2-26 shows the influence of speed and tyre construction on rolling resistance. The sudden increase in rolling resistance at high speed is important to note since this can lead to catastrophic failure in tyres. The source of this increase in rolling resistance is a high energy standing wave that forms at the trailing edge of the tyre/road contact.

There are some empirical relationships derived for the tyre's rolling resistance. It is advisable to refer to the tyre manufacturer's technical specifications when exact information is required. This type of information is usually very confidential and not readily available. Some general relationships have been developed, from (Wong, 2001):

Radial-ply passenger car tyres: $RRC = 0.0136 + 0.04 \cdot 10^{-6} \cdot v^2$
Bias-ply passenger car tyres: $RRC = 0.0169 + 0.19 \cdot 10^{-6} \cdot v^2$
Radial-ply truck tyres: $RRC = 0.006 + 0.23 \cdot 10^{-6} \cdot v^2$
Bias-ply truck tyres: $RRC = 0.007 + 0.45 \cdot 10^{-6} \cdot v^2$

As seen in Figure 2-26, a rule of thumb is that rolling resistance coefficient is constant up to around 100 km/h.

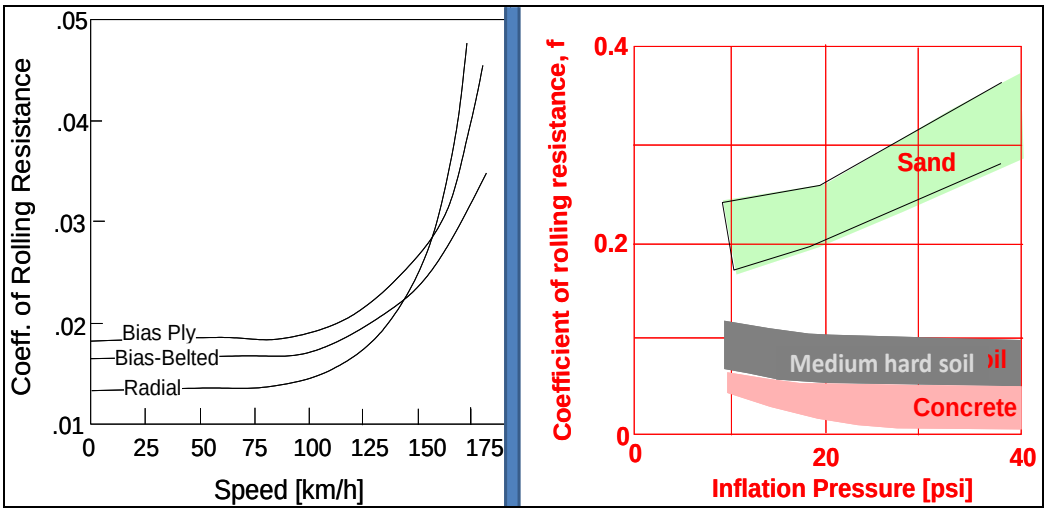


Figure 2-26 : Left: Rolling resistance coefficient variation with speed for different tyre types (Gillespie, 1992). Right: Range of Coefficient of Rolling Resistance for different road/ground material.

2.2.2.4.5 Variation of road surface

The road or ground can mainly vary in two ways: how **rigid** and how **slippery** it is. It is not solely a question of the road, because such rigidness should be judge relative to tyre inflation pressure and such slipperiness should be judged relative to tyre tread pattern, including whether the tyre has spikes or not.

Right part of Figure 2-26 shows that the rolling resistance changes a lot due to different road/ground material and inflation pressures. As can be expected, a range of values exist depending on the specific tyre and surface materials investigated. On hard ground, the rolling resistance decreases with increased inflation pressure, which is in-line with the explanation model used above, since higher pressure intuitively reduces the contact surface and hence reduces e. On soft ground the situation is reversed, which requires a slightly different explanation model, see Figure 2-27. On soft ground, the ground is deformed so that the wheel rolls in a "wheel-local up-grade" with inclination angle φ. Intuitively, a higher inflation pressure will lead to more deformation of the ground, leading to a steeper φ.

The phenomena in Figure 2-27 is a plastic deformation of the ground, so if a vehicle has several tyres which takes the same path on ground, the rolling resistance will be different due to a memory (a state variable) in the ground.

The "wheel-local up-grade" in Figure 2-27 follows each tyre so that it is constant in time for each tyre. This is a difference to simply uneven (rigid) road, where the wheels experience alternating wheel-local up- and ground-grade. In average, the alternating up and down does not generate rolling resistance in tyre, but it can cause energy-loss in wheel suspension and consequently this contributes to energy consumption for the vehicle.

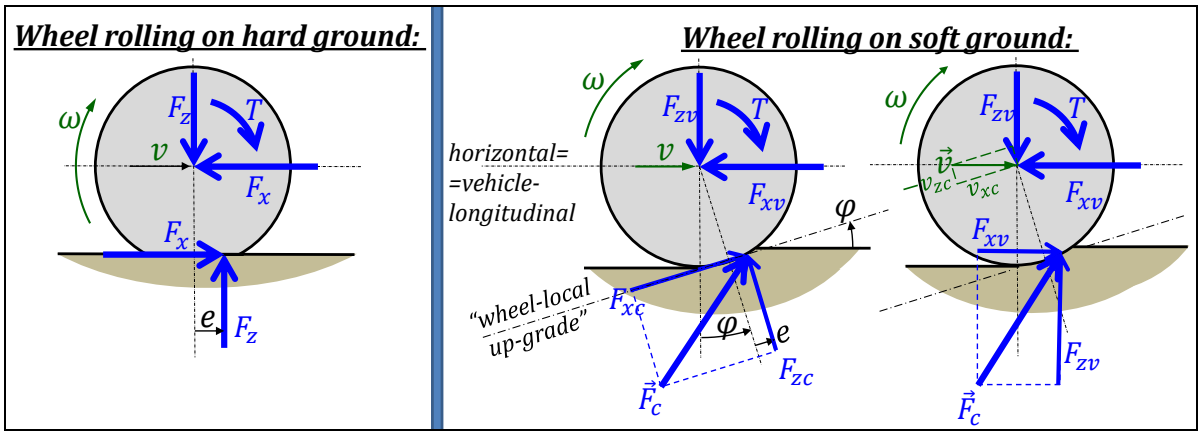


Figure 2-27 : Rolling resistance explanation for hard and soft ground. Subscripts: c=contact, v=vehicle.

2.2.2.4.6 Variation of Longitudinal Force, Propulsion and Braking

Figure 2-21 shows a longitudinal offset forward of **contact patch**, increasing with longitudinal force F_x. But also, the pressure distribution **shape** can change with longitudinal force F_x. If pressure shape change, it would be for, at least, two reasons: the belt in the rear of the contact would be stretched which would lift it from ground, which would contribute to an even larger offset of the equivalent normal force F_z. If one sees the shear rubber under wheel as a spring in $\{z, x\}$-plane which end is translating, there can be a bending moment which motivates reduction of the offset of the equivalent normal force F_z. (Compare with a 2D spring: $[F_z \quad F_x \quad M_y]^T = \boldsymbol{C_{3\times3}} \cdot [z \quad x \quad \varphi_y]^T$.) So, the change of e due to longitudinal force F_x is far from obvious to model.

However, there are phenomena which suggest that RRC depends on F_x. The phenomenon is not well studied, since RRC is often given for free-rolling tyres, but according to Figure 2-29 RRC increases with positive F_x and decreases with negative F_x. The wheel radius also decreases with magnitude of force. For negative forces, these two effects have opposite influence, so the change is less for negative force, as seen in Figure 2-29.

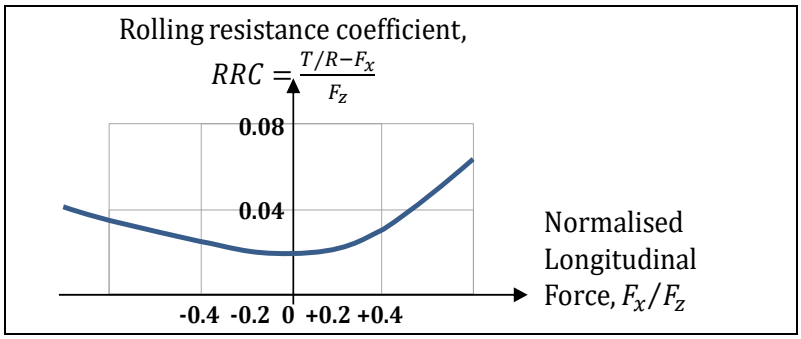


Figure 2-29 : Rolling resistance dependency of longitudinal tyre force. Inspired by (Wong, 2001)

2.2.2.4.7 Separation of Actuated Wheel Torque and Rolling Resistance

Contribution from Toheed Ghandriz, Vehicle Dynamics

The force play in FBD numbered 3 in figure below is primarily proposed for understanding. But there are sometimes reasons to use FBD numbered 4, where the torques T and $F_{ground,z} \cdot e$ from Figure 2-12 are treated separately and converted to one force each. Such reason is that $T = T_{Act}$ is possible to control (actuatable) while $F_{ground,z} \cdot e = T_{RR}$ is not.

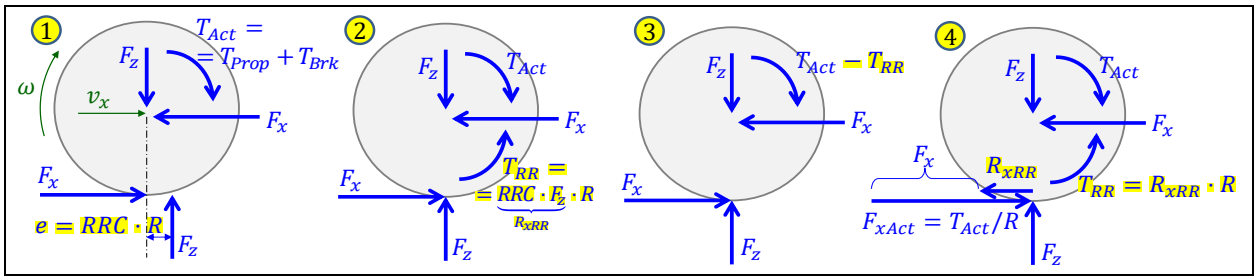


Figure 2-30: Force equivalent FBDs with both rolling resistance (RR) and actuation (Act). Wheel is modelled inertia free in both translation and rotation. F_{xAct} and R_{xRR} is a virtual decomposition of the real force F_x.

The decomposition of F_x in F_{xAct} and R_{xRR} means a deviations from the advice in 1.5.2.1 to not draw two forces acting at the same point of part and having same direction. Then note:

- The tyre models where force depends on slip (2.2.3..2.2.7) applies to F_x, not to F_{xAct}.
- The R_{xRR} is not a separate physical force acting on the vehicle. It is $F_x = F_{xAct} - R_{xRR}$ that physically acts on the vehicle and should appear in vehicle equilibrium.

So, R_{xRR} is very different from aero dynamic resistance force and grade resistance forces, which are physical forces acting on the vehicle.

2.2.2.5 Energy Losses on Uneven or Deformable Ground

Previous treats flat and rigid ground, except that uneven or deformable ground is briefly mentioned in 2.2.2.4.5. If ground is rigid but uneven, there will be "local up- and down-hills". Such will also appear if the ground is deformable, but they will be more of "local uphills which follows each wheel". If ground is uneven, it will additionally cause energy losses in the suspension damper. Uneven ground, if wheel takes longitudinal or lateral forces, also increase the slip losses due to large variations in normal force.

Figure below introduces the directions *global* (e.g. $m \cdot g$ and F_{icv}), *vehicle* or *road* (e.g. F_{zv}) and *contact* e.g. F_{zc}). The rolling resistance coefficients in this section will be "**effective** rolling resistance coefficients", which means that they are different, typically larger, than the contact-local coefficient RRC_c from the force offset e.

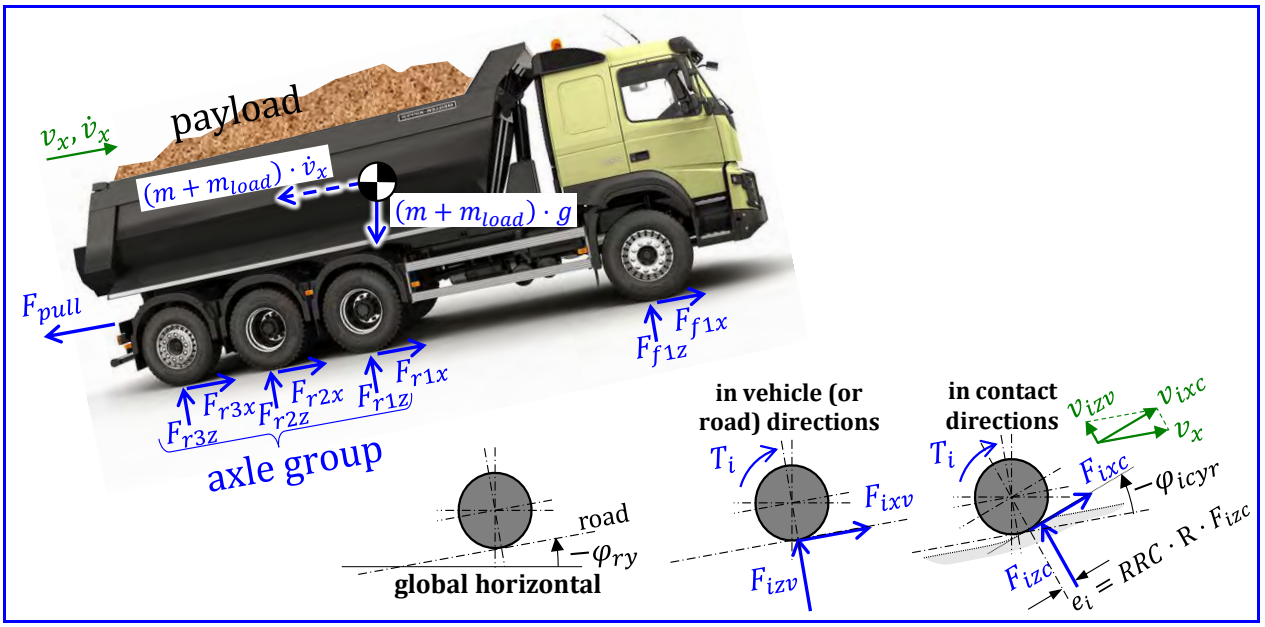


Figure 2-31: Explanation of rolling resistance as wheel rolling in a "local uphill". The "global uphill" or "road" is marked to distinguish between φ_{ry} (angle of road around y) and φ_{iycr} (angle under wheel i of the contact around y relative to road).

2.2.2.5.1 Uneven and Rigid Ground

2.2.2.5.1.1 Force Losses

Moment equilibrium of the wheel gives:

$$0 = T_i - F_{ixc} \cdot R - F_{izc} \cdot e_i;$$

If we model the "local", or contact-local, rolling resistance as on rigid ground, $e = RRC_c \cdot R$, we get:

$$0 = T_i - F_{ixc} \cdot R - F_{izc} \cdot RRC_c \cdot R; \Rightarrow \left\{ \begin{matrix} force \\ equivalence \end{matrix} \right\} \Rightarrow$$

$$\Rightarrow \quad 0 = T_i/R - \left(F_{ixv} \cdot \cos(-\varphi_{icyr}) + F_{izv} \cdot \sin(-\varphi_{icyr})\right) - \left(F_{izv} \cdot \cos(-\varphi_{icyr}) - F_{ixv} \cdot \sin(-\varphi_{icyr})\right) \cdot RRC_c; \Rightarrow$$

$$\Rightarrow \quad 0 = T_i/R + F_{ixv} \cdot \left(-\cos(-\varphi_{icyr}) + \sin(-\varphi_{icyr}) \cdot RRC_c\right) + F_{izv} \cdot \left(-\sin(-\varphi_{icyr}) - \cos(-\varphi_{icyr}) \cdot RRC_c\right); \Rightarrow$$

$$\Rightarrow \quad F_{ixv} = \frac{T_i/R - F_{izv} \cdot (\sin(-\varphi_{icyr}) + \cos(-\varphi_{icyr}) \cdot RRC_c)}{\cos(-\varphi_{icyr}) - \sin(-\varphi_{icyr}) \cdot RRC_c} \approx \left\{ \begin{matrix} small \\ |\varphi_{icyr}| \end{matrix} \right\} \approx \frac{T_i/R - F_{izv} \cdot (-\varphi_{icyr} + RRC_c)}{1 + \varphi_{icyr} \cdot RRC_c} \approx$$

$$\left\{ \begin{matrix} small\ |\varphi_{icyr}|\ and \\ small\ |RRC_c| \end{matrix} \right\} \approx T_i/R - F_{izv} \cdot \left(-\varphi_{icyr} + RRC_c\right);$$

One can define a rolling resistance in the vehicle direction, RRC_v:

$$RRC_v = \frac{ForceLoss}{VerticalForce} = \frac{T_i/R - F_{ixv}}{F_{izv}} \approx \frac{T_i/R - \left(T_i/R - F_{izv} \cdot (-\varphi_{icyr} + RRC_c)\right)}{F_{izv}} \approx RRC_c + \left(-\varphi_{icyr}\right);$$

Note that negative φ_{icyr} is a "local downhill", so RRC_v is the sum of two positive values if "local uphill", which should be intuitive correct. If the ground is **uneven and rigid**, there are equally much local downhill as local uphill on average; also if the road has a "global grade". Then, on average, there is no influence of φ_{icyr}, so $\overline{RRC_v} \approx RRC_c$.

2.2.2.5.1.2 Speed Losses

It should be intuitive to use the longitudinal slip model, see 2.2.3, in the contact directions: $F_{ixc} = C_{ix} \cdot s_{ix} = CC_{ix} \cdot F_{izc} \cdot s_{ix};$. Inserting the slip definition $s_{ix} = (R \cdot \omega_i - v_{ixc})/|R \cdot \omega_i|$; gives:

$$F_{ixc} = CC_{ix} \cdot F_{izc} \cdot \frac{R \cdot \omega_i - v_{ixc}}{|R \cdot \omega_i|}; \Rightarrow \left\{ \begin{matrix} force \\ equivalence \end{matrix} \right\} \Rightarrow$$

$$\Rightarrow \left(F_{ixv} \cdot \cos(-\varphi_{icyr}) + F_{izv} \cdot \sin(-\varphi_{iyc})\right) =$$

$$= CC_{ix} \cdot \left(F_{izv} \cdot \cos(-\varphi_{icyr}) - F_{ixv} \cdot \sin(-\varphi_{icyr})\right) \cdot \frac{R \cdot \omega_i - \left(v_x \cdot \cos(-\varphi_{icyr})\right)}{|R \cdot \omega_i|} \Rightarrow$$

$$\Rightarrow \left\{ \begin{matrix} small \\ |\varphi_{icyr}| \end{matrix} \right\} \Rightarrow \left(F_{ixv} + F_{izv} \cdot \left(-\varphi_{icyr}\right)\right) \approx CC_{ix} \cdot \left(F_{izv} - F_{ixv} \cdot \left(-\varphi_{icyr}\right)\right) \cdot \frac{R \cdot \omega_i - (v_x)}{|R \cdot \omega_i|}; \Rightarrow$$

$$\Rightarrow F_{ixv} - F_{izv} \cdot \varphi_{icyr} \approx CC_{ix} \cdot \left(F_{izv} + F_{ixv} \cdot \varphi_{icyr}\right) \cdot s_{ix}; \Rightarrow$$

$$\Rightarrow F_{ixv} - CC_{ix} \cdot F_{ixv} \cdot \varphi_{icyr} \cdot s_{ix} \approx CC_{ix} \cdot F_{izv} \cdot s_{ix} + F_{izv} \cdot \varphi_{icyr}; \Rightarrow$$

$$\Rightarrow F_{ixv} \approx F_{izv} \cdot \frac{CC_{ix} \cdot s_{ix} + \varphi_{icyr}}{1 - CC_{ix} \cdot s_{ix} \cdot \varphi_{icyr}} = \left\{ \begin{matrix} small\ |CC_{ix} \cdot s_{ix}| \\ and\ small\ |\varphi_{icyr}| \end{matrix} \right\} = F_{izv} \cdot \left(CC_{ix} \cdot s_{ix} + \varphi_{icyr}\right);$$

Note that negative φ_{icyr} is a "local downhill", so φ_{icyr} helps in creating F_{ixv} which reduces the required F_{ixv} and, hence the required T_i. If the ground is **uneven and rigid**, there are equally much local downhill as local uphill as average over a longer route, also if the road has a "global grade". Then, over a longer route, there is no influence of φ_{icyr}, so $F_{ixv} \approx F_{izv} \cdot CC_{ix} \cdot s_{ix};$. So, it does not influence vehicle function *energy consumption* over longer routes. But it can, of course, but it can influence the vehicle function to travers a certain position on a route, e.g. a slippery and high bump under the drive wheels can stop the vehicle. It can, however, influence the vehicle function *route traversal*, since a slippery and high bump under the drive wheels may prevent the vehicle from passing a certain position along the route.

The same modelling concept can be used with saturated $F_{ixc} = \text{sign}(s_{ix}) \cdot \min(CC_{ix} \cdot |s_{ix}|; \mu) \cdot F_{izc};$ and then one can study traction problems due to uneven ground; i.e. when the vehicle gets stuck.

2.2.2.5.2 Losses in Suspension Damping

Above concluded that uneven and rigid does not cause energy losses over longer routes. However, unevenness can still cause energy loss due to increased motion in vehicle suspension dampers.

2.2.2.5.3 Deformable ground

If the ground is deformable (soft) it deforms due to the force from the tyre. The ground is generally more plastic than elastic, so a simplification is that deformation is completely plastic.

2.2.3 Longitudinal tyre force and slip

The longitudinal force, F_x, between the tyre and ground influences the vehicle propulsion and braking performance. We can see it as a depending on the sliding between the tyre and the ground.

First, compare friction characteristics for a translating block of rubber with a rolling wheel of rubber. Figure 2-32 shows the basic differences between classical dry-friction, or Coulomb friction, of such sliding block and the basic performance of a rolling tyre. Experiments have shown that the relative speed between the tyre and the road produces a frictional force that has an initial linear region that builds to a peak value. After this peak is achieved, no further increase in the tangential (friction) force is possible. There is not always a peak value, which is shown by the dashed curve in the figure. The slope in the right diagram will be explained in 2.2.3.1, using the so called "tyre brush model".

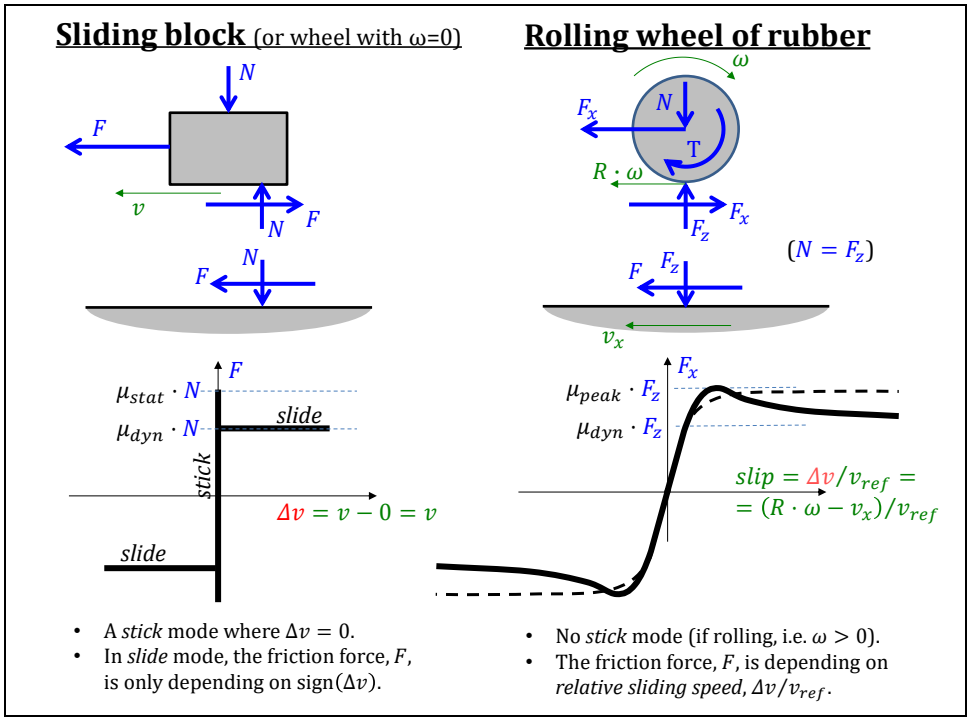


Figure 2-32: Friction characteristics.

2.2.3.1 Brush model for longitudinal force and slip

The brush model is frequently used to explain how tyre develop forces in ground plane, see e.g. Refs (Pacejka, 2005) and (Svendenius, Tire Modeling and Friction Estimation, 2007). The brush model is a physically based model that uses shear stress and dry friction at a local level, i.e. for each contact point in the contact patch. Models for pressure distribution (e.g. Hertz's contact theory), wear (e.g. Reye-Archard wear law), and power loss between sliding surfaces are examples of other well established models which can be applied in a "deductive" way to the brush model. Figure 2-33 shows the starting point for understanding the brush model.

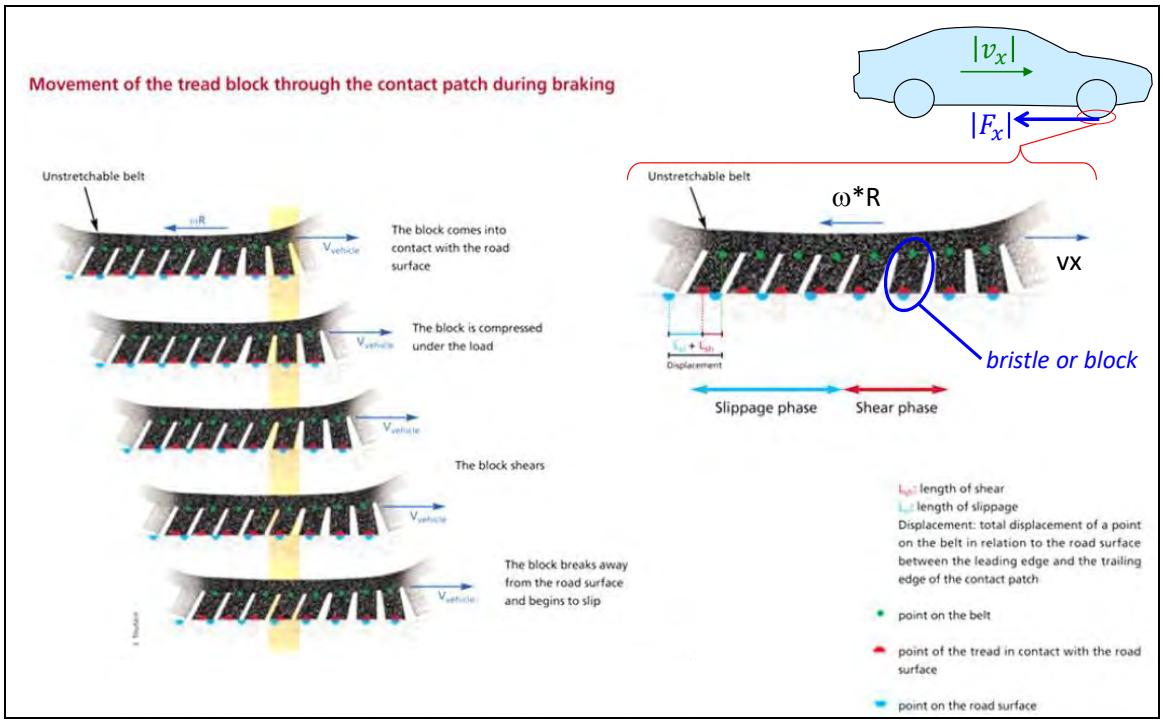


Figure 2-33: Tyre ground contact for braked tyre. Origin to a "Brush model". Picture from Michelin.

2.2.3.1.1 Uniform Pressure Distribution and Known Contact Length

A first simple variant of the brush model, uses the following assumptions:

- Sliding and shear stress only in **longitudinal** direction (as opposed to combined longitudinal and lateral)
- Uniform and known **pressure distribution** over a constant and known contact length (as opposed to using a contact mechanics-based approach, which can calculate pressure distribution and contact length L.)
- **Contact length** is known (as opposed to function of vertical force).
- No difference between **static and dynamic** coefficient of friction
- Only studying the **steady state conditions**, as opposed to including the transition between operating conditions. Here, "steady state" refers to the distributions of tyre tread shear deformation $\gamma(\xi)$ and shear stress $\tau(\xi)$, which are assumed to not vary with time.

At first, we also assume that the tread is built up of N bristles of rubber. Each bristle is assumed as a sheared piece of rubber without force interaction between neighbouring bristles. If there is no sliding between rubber and ground, the shear stress of the element develops as in Hooke's law: $F_i = \tau_i \cdot Area_i = G \cdot \gamma_i \cdot Area_i$;. The $Area_i = W \cdot L/N$, but we let $N \to \infty$, we can use a continuous model: $dF = \tau \cdot dArea = \tau \cdot W \cdot d\xi$;, where W is width of tyre and ξ a coordinate along the belt in the contact, see Figure 2-34. Figure 2-34 also shows that we assume friction contact between bristle and ground. (The bristles can alternatively be seen as bending beams fixed in the belt end or rigid beams connect with rotational springs in the belt end.)

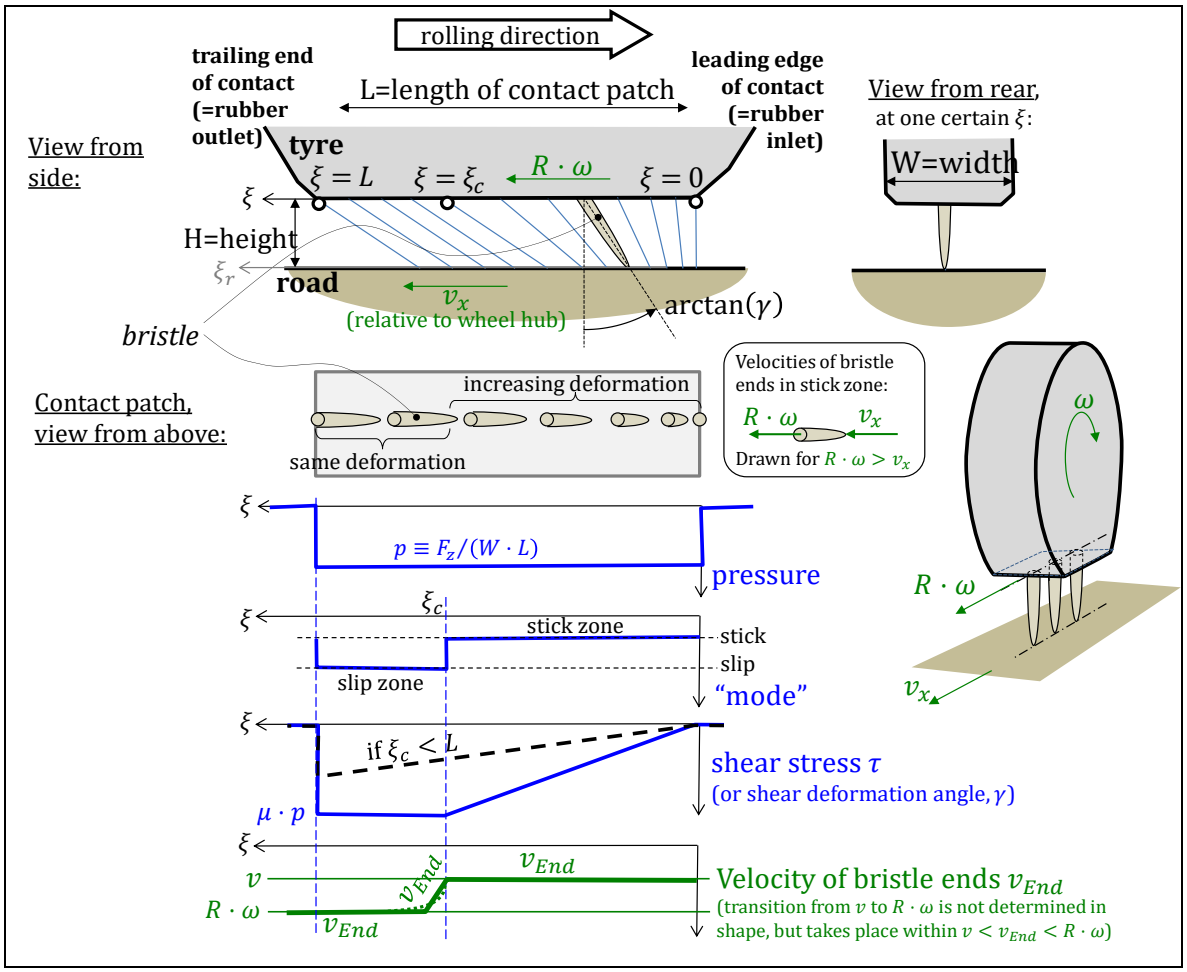


Figure 2-34: Physical model for simple brush model for longitudinal slip. Drawn for propelled tyre. The bristles represent the rubber tread, not including elasticity in sidewall. Drawn for $R \cdot \omega > v_x$.

If we assume no sliding:

$$\tau = G \cdot \gamma;$$
$$where\ \tau = shear\ stress, G = shear\ modulus, \gamma = shear\ deformation\ (= \tan(shear\ angle));$$

When a bristle enters the contact patch, it lands un-deformed, i.e. with $\gamma = 0$. The further into contact, along coordinate ξ, we follow the element, the more sheared will it become. Since the ground end of the element sticks to ground, the increase becomes proportional to the speed difference Δv and the transport time t_{transp}, which is the time it takes for a bristle to reach the coordinate ξ:

$$\gamma = \frac{\int_{t=0}^{t=t_{transp}} \Delta v \cdot dt}{H} = \left\{ \begin{matrix} \Delta v = \\ = R \cdot \omega - v_x \end{matrix} \right\} = \frac{R \cdot \omega - v_x}{H} \cdot \int_{t=0}^{t_{transp}} dt = \left\{ \begin{matrix} \xi = v_{transp} \cdot t_{transp}; \\ v_{transp} = |R \cdot \omega|; \end{matrix} \right\} =$$
$$= \frac{R \cdot \omega - v_x}{H} \cdot \int_{t=0}^{\xi/|R \cdot \omega|} dt = \frac{R \cdot \omega - v_x}{H} \cdot \int_{t=0}^{\xi/|R \cdot \omega|} dt = \frac{R \cdot \omega - v_x}{H} \cdot \frac{\xi}{|R \cdot \omega|} = \frac{1}{H} \cdot \underbrace{\frac{R \cdot \omega - v_x}{|R \cdot \omega|}}_{s_x} \cdot \xi;$$

Note that, assuming the elastic bristles are on the wheel (not on the ground) leads to that the slip definition in Eq [2.2], not Eq [2.3], falls out. Eq [2.2] makes the model singular when we want it to be singular ($\omega = 0$) while Eq [2.3] would mask that desired singularity and introduce a false singularity at $v_x = 0$. That the model becomes singular at $\omega = 0$ is a healthy warning from physics, via mathematics, to us that we need to handle $\omega = 0$ with special care. The situation $v_x = 0$ is not very special if $\omega \neq 0$.

The force is the and integral of τ from $\xi = 0$ to $\xi = L$:

$$F_x = \int_{W \cdot L} \tau \cdot dA = W \cdot \int_{\xi=0}^{L} G \cdot \gamma \cdot d\xi = W \cdot \mathrm{G} \cdot \int_{\xi=0}^{L} \frac{1}{H} \cdot s_x \cdot \xi \cdot d\xi = \frac{G \cdot W}{H} \cdot s_x \cdot \int_{0}^{L} \xi \cdot d\xi =$$

$$= \underbrace{\frac{G \cdot W \cdot L^2}{2 \cdot H}}_{C_x} \cdot s_x = C_x \cdot s_x; \qquad (Note: This\ assumes\ \textbf{\textit{no sliding}}\ in\ contact.)$$

Note that this model simplifies F_x from a function of 2 variables (ω and v_x) to 1 variable (s_x). With this definition of slip, s_x, we automatically handle ω and v_x both positive and ω and v_x both negative. The case when ω and v_x have different signs ($\omega \cdot v_x < 0$) is special and will be handled below.

(It is possible to reach Eq [2.13] via integration over ξ_r instead. Then, one uses $v_{transport} = |v_x|$. After a more complex derivation, the resulting slip definition $s_x = (R \cdot \omega - v_x)/|R \cdot \omega|$ falls out in the final expression for F_x, i.e. Eq [2.13]. Despite this, one often sees $s_x = (R \cdot \omega - v_x)/|v_x|$.)

If friction limit is not reached ($|\tau| < \mu \cdot p$) within the whole contact, this model is valid. The risk for sliding is highest at $\xi = L$ so the validity can be formulated $|\tau(L)| < \mu \cdot p = \mu \cdot \frac{F_z}{W \cdot L} \Rightarrow \frac{G}{H} \cdot |s_x| \cdot L < \mu \cdot \frac{F_z}{W \cdot L} \Rightarrow |s_x| < \frac{\mu \cdot F_z}{2 \cdot C_x} \Leftrightarrow |F_x| < \frac{\mu \cdot F_z}{2}$.
So, if that condition is not fulfilled, the friction limit is reached within the contact, i.e. at a break-away point at $\xi = \xi_c < L$. Then, we have to split the integral in two. The point ξ_c is defined by $\tau(\xi_c) = \frac{G}{H} \cdot s_x \cdot \xi_c = \frac{2 \cdot C_x}{W \cdot L^2} \cdot s_x \cdot \xi_c = \mu \cdot p; \Rightarrow \xi_c = \frac{\mu \cdot p \cdot W \cdot L^2}{2 \cdot C_x \cdot s_x} = \frac{\mu \cdot F_z \cdot L}{2 \cdot C_x \cdot s_x};$. For $\xi > \xi_c$, the rubber element will slide with a constant $\tau = \mu \cdot p$.

$$F_x = W \cdot \int_0^L \tau \cdot d\xi = W \cdot \int_0^{\xi_c} \frac{2 \cdot C_x}{W \cdot L^2} \cdot s_x \cdot \xi \cdot d\xi + W \cdot \int_{\xi_c}^{L} \mu \cdot p \cdot d\xi =$$

$$= \frac{2 \cdot C_x}{L^2} \cdot s_x \cdot \frac{\xi_c^2}{2} + \mu \cdot p \cdot W \cdot (L - \xi_c) = \left\{ p = \frac{F_z}{W \cdot L}; \quad and \quad \xi_c = \frac{\mu \cdot F_z \cdot L}{2 \cdot C_x \cdot s_x}; \right\} =$$

$$= \underbrace{\frac{\mu^2 \cdot F_z^2}{4 \cdot C_x \cdot s_x}}_{F_{x,stick}} + \underbrace{\mu \cdot F_z \cdot \left(1 - \frac{\mu \cdot F_z}{2 \cdot C_x \cdot s_x}\right)}_{F_{x,slip}} = \mu \cdot F_z \cdot \left(1 - \frac{\mu \cdot F_z}{4 \cdot C_x \cdot s_x}\right); \quad for\ s_x > \frac{\mu \cdot F_z}{2 \cdot C_x} \qquad [2.12]$$

The force terms, $F_{x,stick}$ and $F_{x,slip}$, from each of stick and slip regions are identified. These two terms are separately shown plotted in Figure 2-38.

The case when ω and v_x have different signs leads to that $\xi_c = 0;$, since the bristles will deform in the opposite direction; slip over the whole contact or *macro slip*. So, the whole contact has $\tau = \mu \cdot p$, which leads to $F_z = \mu \cdot F_z;$. Hence, the total expression for F_x becomes as in Eq [2.13]. We also add subscript x on G and H, to prepare for a corresponding model for lateral forces, in 2.2.4.

$$F_x = \begin{cases} = \text{sign}(R \cdot \omega - v_x) \cdot \mu \cdot F_z = \text{sign}(s_x) \cdot \mu \cdot F_z; & if\ \omega \cdot v_x < 0 \\ = C_x \cdot s_x; & else\ if\ |s_x| \le \frac{\mu \cdot F_z}{2 \cdot C_x} \Leftrightarrow |F_x| \le \frac{\mu \cdot F_z}{2} \\ = \text{sign}(s_x) \cdot \mu \cdot F_z \cdot \left(1 - \frac{\mu \cdot F_z}{4 \cdot C_x} \cdot \frac{1}{|s_x|}\right); & else \end{cases} \qquad [2.13]$$

$$where\ C_x = \frac{G_x \cdot W \cdot L^2}{2 \cdot H_x};\ dimension: [force] \quad and \quad s_x = \frac{R \cdot \omega - v_x}{|R \cdot \omega|};$$

Eq [2.13] is plotted in Figure 2-38. Eq [2.13] is also called Dugoff tyre model. It exists also as lateral slip and combined slip tyre model, see (Dugoff, Fancher, & Segel, 1969).

It is important to reflect over which of the physical quantities that reasonably must be modelled as varying. This will of course depend on the driving manoeuvre studied, but here is a typical situation: The slip s_x and normal load F_z are typical varying and defined by the vehicle model. The quantities

μ, G_x, W, H_x are often reasonably constant, so they can be parameters. However, it is often **not** reasonable to assume that the contact length L is constant. L is rather a function of F_z: $L(F_z)$;.

The case when $\omega \cdot v_x < 0$ is unusual and can only occur when $|s_x| > 1$. An example is when vehicle moves rearward with $v_x = -1\ m/s$, would be that the wheel spins forward, e.g. with $R \cdot \omega = 1\ m/s$. Then $s_x = +2$ and $F_x = \mu \cdot F_z$. Also, if increase to $R \cdot \omega = +\infty\ m/s$, we get same $F_x = \mu \cdot F_z$, but with $s_x = +\infty$. One can also note that there is another $R \cdot \omega$, for same v_x, which gives $s_x = +2$. This is $R \cdot \omega = -1/3\ m/s$ and then $F_x = \mu \cdot F_z \cdot (1 - \mu \cdot F_z/(8 \cdot C_x))$, which is $< \mu \cdot F_z$. So, F_x is uniquely defined for any (ω, v_x), but F_x has double solutions for some s_x, when $|s_x| > 1$.

If we instead hold a certain forward vehicle speed, e.g. $v_x = 1\ m/s$, and study how F_x varies with ω, we can identify 4 specific levels of ω:

- Full rearward traction: $R \cdot \omega = -\infty\ m/s$. This gives $s_x = -\infty$, with different signs on ω and v_x, and $F_x = -\mu \cdot F_z$;
- Locked wheel: $R \cdot \omega = 0\ m/s$. This also gives $s_x = -\infty$ and $F_x = -\mu \cdot F_z$;
- Pure rolling wheel: $R \cdot \omega = 1\ m/s$. This gives $s_x = 0$ and $F_x = 0$;
- Full forward traction: $R \cdot \omega = +\infty\ m/s$. This gives $s_x = +1$ and $F_x = \mu \cdot F_z \cdot (1 - \mu \cdot F_z/(4 \cdot C_x)) \approx \{typically\} \approx (0.95..0.98) \cdot \mu \cdot F_z$, which is $< \mu \cdot F_z$;

The first case is achievable, with an electric motor braking but not with friction brakes, where ω and v_x have different signs. The last case shows that we cannot reach $\mu \cdot F_z$ in the direction the vehicle moves, since there will always be a small part on the inlet side of the contact where the shear stress has not reached $\mu \cdot p$. In practice, we can see it as $\approx \mu \cdot F_z$, but when using the model mathematically, it can be good to note such small phenomena.

2.2.3.1.1.1 Power losses due to slip

We identify two different slip losses:

$$P_{LossSlip} = P_{LossSlipZone} + P_{LossStickZone};$$

The first slip loss is the loss we find in a micro view, for each bristle sliding relative to the ground in the **slip zone**. It can be mentioned that a constant sliding speed is assumed across the slip zone.

Below, we will derive an expression of how $P_{SlipLoss}$ depends on operating condition $\{\omega, T, v_x, F_x\}$. Note that we distinguish between R_E and R_L. These two radii (or radius-like length measures) were discussed briefly in 2.2.1.7.2 and they will be addressed again.

$$\begin{aligned} P_{LossSlipZone} &= \int_{\min(\xi_{Crit}, L)}^{L} \tau \cdot (R_E \cdot \omega - v_x) \cdot W \cdot d\xi = \int_{\min(\xi_{Crit}, L)}^{L} \mu \cdot p \cdot (R_E \cdot \omega - v_x) \cdot W \cdot d\xi = \\ &= \int_{\min(\xi_{Crit}, L)}^{L} \mu \cdot \frac{F_z}{W \cdot L} \cdot (R_E \cdot \omega - v_x) \cdot W \cdot d\xi = \\ &= \mu \cdot F_z \cdot \left(1 - \frac{\min(\xi_{Crit}, L)}{L}\right) \cdot (R_E \cdot \omega - v_x); \end{aligned}$$

The second slip loss is the energy stored elastically in bristles in the **stick zone**. It is regarded as a loss in a macro view (whole tyre) although it is initially stored. This is motivated by that we assume that the stored energy is lost due to damping in the tread material on the way around the wheel before the same bristle enters the contact patch again after approximately one wheel revolution.

$$P_{LossStickZone} = \int_0^{\min(\xi_{Crit},L)} \tau \cdot (R_E \cdot \omega - v_x) \cdot W \cdot d\xi = \int_0^{\min(\xi_{Crit},L)} G \cdot \gamma \cdot (R_E \cdot \omega - v_x) \cdot W \cdot d\xi =$$
$$= \int_0^{\min(\xi_{Crit},L)} G \cdot \frac{1}{H} \cdot \frac{R_E \cdot \omega - v_x}{|R_E \cdot \omega|} \cdot \xi \cdot (R_E \cdot \omega - v_x) \cdot W \cdot d\xi =$$
$$= \frac{G \cdot W}{H} \cdot \frac{(R_E \cdot \omega - v_x)^2}{|R_E \cdot \omega|} \cdot \int_0^{\min(\xi_{Crit},L)} \xi \cdot d\xi = = \frac{G \cdot W}{H} \cdot \frac{(\min(\xi_{Crit},L))^2}{2} \cdot \frac{(R_E \cdot \omega - v_x)^2}{|R_E \cdot \omega|};$$

So:

$$P_{LossSlip} = \mu \cdot F_z \cdot \left(1 - \frac{\min(\xi_{Crit},L)}{L}\right) \cdot (R_E \cdot \omega - v_x) + \frac{G \cdot W}{H} \cdot \frac{(\min(\xi_{Crit},L))^2}{2} \cdot \frac{(R_E \cdot \omega - v_x)^2}{|R \cdot \omega|}$$
$$= \left[\mu \cdot F_z \cdot \left(1 - \frac{\min(\xi_{Crit},L)}{L}\right) + \frac{G \cdot W}{H} \cdot \frac{(\min(\xi_{Crit},L))^2}{2} \cdot s_x\right] \cdot (R_E \cdot \omega - v_x);$$

Using $C_x = \frac{G \cdot W \cdot L^2}{2 \cdot H}$, we get:

$$P_{LossSlip} = \left[\mu \cdot F_z \cdot \left(1 - \frac{\min(\xi_{Crit},L)}{L}\right) + C_x \cdot \left(\frac{\min(\xi_{Crit},L)}{L}\right)^2 \cdot s_x\right] \cdot (R_E \cdot \omega - v_x);$$

Using $\xi_{Crit} = \frac{\mu \cdot F_z \cdot L}{2 \cdot C_x \cdot s_x}$, we can split in:

If $\xi_{Crit} > L \quad \Leftrightarrow \quad |s_x| < \frac{\mu \cdot F_z}{2 \cdot C_x} \quad \Leftrightarrow \quad |F_x| \leq \frac{\mu \cdot F_z}{2}$:

$$P_{LossSlip} = \left[\mu \cdot F_z \cdot \left(1 - \frac{L}{L}\right) + C_x \cdot \left(\frac{L}{L}\right)^2 \cdot s_x\right] \cdot (R_E \cdot \omega - v_x) = \underbrace{C_x \cdot s_x}_{F_x} \cdot (R_E \cdot \omega - v_x);$$

If $\xi_{Crit} < L \quad \Leftrightarrow \quad |s_x| > \frac{\mu \cdot F_z}{2 \cdot C_x} \quad \Leftrightarrow \quad |F_x| > \frac{\mu \cdot F_z}{2}$:

$$P_{LossSlip} = \left[\mu \cdot F_z \cdot \left(1 - \frac{\min(\xi_{Crit},L)}{L}\right) + C_x \cdot \left(\frac{\min(\xi_{Crit},L)}{L}\right)^2 \cdot s_x\right] \cdot (R_E \cdot \omega - v_x) =$$
$$= \left[\mu \cdot F_z \cdot \left(1 - \frac{\frac{\mu \cdot F_z \cdot L}{2 \cdot C_x} \cdot \frac{1}{s_x}}{L}\right) + C_x \cdot \left(\frac{\frac{\mu \cdot F_z \cdot L}{2 \cdot C_x} \cdot \frac{1}{s_x}}{L}\right)^2 \cdot s_x\right] \cdot (R_E \cdot \omega - v_x)$$
$$= \left[\mu \cdot F_z \cdot \left(1 - \frac{1}{C_x} \cdot \frac{\mu \cdot F_z}{2} \cdot \frac{1}{s_x}\right) + \frac{1}{C_x} \cdot \left(\frac{\mu \cdot F_z}{2}\right)^2 \cdot \frac{1}{s_x}\right] \cdot (R_E \cdot \omega - v_x) =$$
$$= \underbrace{\mu \cdot F_z \cdot \left[1 - \frac{\mu \cdot F_z}{4 \cdot C_x} \cdot \frac{1}{s_x}\right]}_{F_x} \cdot (R_E \cdot \omega - v_x);$$

To get an expression with validity range $\forall\{\omega, v_x\}$, we also need to distinguish when $\omega \cdot v_x < 0$. Then slip losses are more easily: sliding force $\mu \cdot F_z \cdot \text{sign}(R_E \cdot \omega - v_x)$ times sliding velocity $(R_E \cdot \omega - v_x) = s_x \cdot |R_E \cdot \omega|$. Then we directly get:

$$P_{LossSlip} = \underbrace{\mu \cdot F_z \cdot \text{sign}(R_E \cdot \omega - v_x)}_{F_x} \cdot (R_E \cdot \omega - v_x);$$

We reach, $\forall\{\omega, v_x\}$:

$$P_{LossSlip} = F_x \cdot (R_E \cdot \omega - v_x); \quad \text{where } F_x \text{ from Eq. [2.13]}$$

Note that, for both a propelling wheel and for a braking wheel ($F_x < 0$ and $R_E \cdot \omega < v_x$), $P_{SlipLoss}$ becomes positive which is follows 2nd law of thermodynamics.

The initial assumptions about the two loss terms can be applied also for other, more advanced, brush tyre models, such as parabolic pressure distribution. The expression $P_{SlipLoss} = F_x \cdot (R_E \cdot \omega - v_x)$; will still be valid, but the expression for F_x changes.

The result in present section (2.2.3.1.1.1) is:

$P_{LossSlip} = F_x \cdot (R_E \cdot \omega - v_x)$; where a force-vs-slip model, e.g., Eq. [2.13], can be used to express F_x	[2.14]

Note: Eq [2.42] in "2.2.3.8.1 Power loss analysis" shows similar expression with the difference that R_L replaces R_E. Let us look at one operation case: $v_x > 0$, $F_x > 0$, and positive parentheses ($R_E \cdot \omega > R_L \cdot \omega > v_x$): the expression with R_L gives a lower value on $P_{LossSlip}$ because $R_L < R_E$. So, [2.14] overestimates the power losses due to slip.

See also 2.2.1.7

2.2.3.1.2 Longitudinal slip stiffness

In summary for many models, the following is a good approximation (compared to tests) for small longitudinal slip, and certain normal load and certain friction coefficient:

$$F_x = C_x \cdot s_x; \qquad [2.15]$$

For the brush model, or any other model which describes $F_x(s_x, F_z, \mu, \dots)$, one can define the "Longitudinal tyre (slip) stiffness" C_x, which have the unit $N = N/1 = N/((m/s)/(m/s))$. It is the derivative of force with respect to slip when at $s_x = s_y = 0$:

$$C_x = \left(\frac{d}{ds_x} F_x(s_x)\right)\Big|_{s_x=0}; \qquad [2.16]$$

Note that C_x is not a stiffness in the conventional sense (force per deformation) but a force per slip, where slip is velocity per velocity. A tyre also has a deformation stiffness. Often, it is obvious which stiffness is relevant, but to be unambiguous one can use the wording: "slip stiffness" C_x with unit [N/1=N/((m/s)/(m/s))] and "deformation stiffness" with unit [N/m].

With the brush models with both pressure distributions, Eq [2.13] and Eq [2.22], we get the $C_x = G \cdot W \cdot L^2/(2 \cdot H)$. With $G = 0.5\ [M\,N/m^2]$ (typical shear modulus in rubber), $W = L = 0.1..0.12\ [m]$ (typical sizes of contact patch for passenger car) and $H = 0.01\ [m]$ (approximate tyre tread depth) one gets $\approx 25[kN] < C_x = G \cdot W \cdot L^2/(2 \cdot H) <\approx 40[kN/1]$. Empirically, we can measure C_x for passenger car tyres around $25..50\ [kN/1]$. This indicates that the brush model models the essential physical phenomena and that the sheared part (the bristles) is rather only the tread than the whole elastic part sidewall and tread together.

2.2.3.1.2.1 Local longitudinal slip stiffness

Reference (ISO 8855) defines and denotes the longitudinal slip stiffness $C_x = (dF_x/ds_x)|_{F_x=0} = (dF_x/ds_x)|_{s_x=0}$. The more general gradient dF_x/ds_x including $s_x \neq 0$, i.e., including $F_x \neq 0$, is **not** defined or denoted in Reference (ISO 8855). Present book aims at using the name and notation "**local** longitudinal slip stiffness" and C'_x.

The word "local" refers to "local along variation in s_x". So, to underline that it is not a constant, it can be clarifying to denote it $C'_x(F_x)$ or $C'_x(s_x)$, or even $C'_x(F_x, \cdots)$ or $C'_x(s_x, \cdots)$. Generally, C'_x decreases with increasing $|F_x|$.

The C'_x is useful for design of wheel torque control, e.g., for linearizing. A Taylor expansion gives:

$$F_x \approx F_{x0} + \frac{dF_x}{d\omega}\cdot(\omega-\omega_0) = F_{x0} + \left.\frac{dF_x(\omega,v_x)}{d\omega}\right|_{\omega=\omega_0,v_x=v_{x0}}\cdot(\omega-\omega_0) =$$

$$= F_{x0} + \underbrace{\left.\frac{dF_x(s_x)}{ds_x}\right|_{s_x=s_{x0}}}_{C_x'(s_{x0})}\cdot\left.\frac{ds_x}{d\omega}\right|_{\omega=\omega_0,v_x=v_{x0}}\cdot(\omega-\omega_0) = F_{x0} + C_x'(s_{x0})\cdot\left(\frac{d}{d\omega}\frac{R\cdot\omega - v_{x0}}{|R\cdot\omega|}\right)\Big|_{\omega=\omega_0}\cdot(\omega-\omega_0) =$$

$$= F_{x0} + C_x'(s_{x0})\cdot \mathrm{sign}(\omega_0)\cdot\left(\frac{d}{d\omega}\left(1-\frac{v_{x0}}{R\cdot\omega}\right)\right)\Big|_{\omega=\omega_0}\cdot(\omega-\omega_0) =$$

$$= F_{x0} + C_x'(s_{x0})\cdot \mathrm{sign}(\omega_0)\cdot\frac{v_{x0}}{R}\cdot\left.\frac{--1}{\omega_0^2}\right|_{\omega=\omega_0}\cdot(\omega-\omega_0) =$$

$$= F_{x0} + C_x'(s_{x0})\cdot \mathrm{sign}(\omega_0)\cdot\frac{v_{x0}}{R}\cdot\frac{1}{\omega_0^2}\cdot(\omega-\omega_0) = F_{x0} + C_x'(s_{x0})\cdot\frac{v_{x0}}{|R\cdot\omega_0|}\cdot\frac{1}{\omega_0}\cdot(\omega-\omega_0) =$$

$$= F_{x0} + \frac{C_x'(s_{x0})\cdot v_{x0}}{|R\cdot\omega_0|}\cdot\left(\frac{\omega}{\omega_0}-1\right);$$

Note that C_x' has an important variation with lateral utilization of tyre contact, e.g., $C_x'(s_x, F_y)$. This is not included in present section but in 2.2.5.4.

2.2.3.1.3 Influence of Vertical Load and Friction in Brush Model

The vertical load on the tyre affects the force generation, F_x. For large slip our dry friction model motivates that F_x is proportional to F_z. This is also a good approximation for small slip, via $C_x \propto F_z$. Then, one can define the Longitudinal Slip Stiffness Coefficient, CC_x:

$$F_x = C_x\cdot s_x = CC_x\cdot F_z\cdot s_x; \qquad [2.17]$$

The contact length L will reasonably vary according to some deformation model. Hertz's contact theory for line contact motivates that $L \propto \sqrt[2]{F_z}$. This is implemented as $L^2 = F_z/k$, where k is a material modulus with dimension *force/area*, gives:

$$C_x = C_x(F_z) = \frac{G_x\cdot W\cdot L^2}{2\cdot H_x} = \frac{G_x\cdot W\cdot F_z/k}{2\cdot H_x} = \underbrace{\frac{G_x\cdot W}{2\cdot H_x\cdot k}}_{CC_x}\cdot F_z; \qquad [2.18]$$

So, the assumption $L \propto \sqrt[2]{F_z}$ explains why $C_x \approx CC_x\cdot F_z \propto F_z$;. This can be verified with experiments, see Figure 2-82. A small tendency for digressive increase ($\partial^2 C_x/\partial F_z^2 < 0$) can be found. A definition of CC_x from a general $F_x(F_z, s_x)$ will include F_{z0}, which is a vertical force around which the model should be used.

$$CC_x = \left.\left(\frac{d}{dF_z}C_x(F_z)\right)\right|_{F_z=F_{z0}} = CC_x(F_{z0}); \qquad [2.19]$$

The result is summarised in Figure 2-35. Increasing μ only increases the saturation level, while leaving the slope at lower s_x constant, or possibly slightly increased. Variation of F_z involves the contact length model. The assumption "$L \propto \sqrt[2]{F_z}$" simply scales the curve in force direction. Overall, it can be concluded that there are arguments for two conceptual ways how the tyre characteristics changes, varied vertical force and varied friction coefficient, see Figure 2-35.

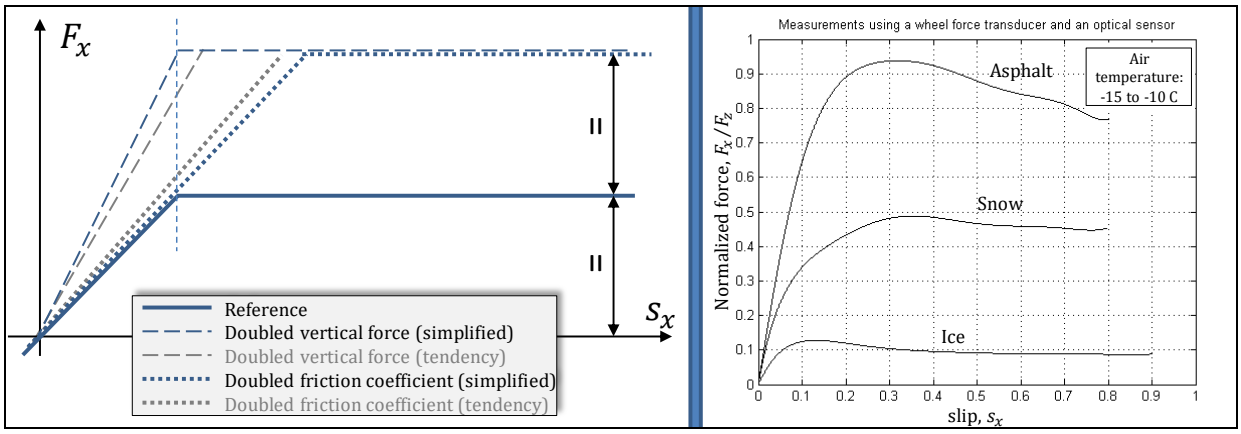


Figure 2-35: How tyre characteristics typically vary due to varying vertical force and road friction. Left: Theory. Right: Measurements with varying friction, i.e. varying surfaces, from PhD course by Ari Tuononen, Aalto university, Finland, Saariselkä, Finland 2014-03-15..22.

Now we have discussed the influence of vertical force and tyre-to-road friction on $F_x(s_x)$ if $S_y \equiv 0$. We see also how the variation of (local) longitudinal slip stiffness $C'_x(s_x)$. Similar for lateral $F_y(s_y)$ and $C'_y(s_y)$ if $s_x \equiv 0$ in 0. For combined slip, where $s_x \neq 0$ and $s_y \neq 0$, see 2.2.5.4.

2.2.3.1.4 Influence of Different Static and Dynamic Friction

A common model for friction is that coefficient of friction to remain sticking, μ_{stick}, is higher than the coefficient of friction when slipping has started, μ_{slip}. This is sometimes called "stiction", $k_{stiction} = \mu_{stick}/\mu_{slip}$. If this is implemented in the model, the brush model can explain why the overall $F_x(s_x)$ often has a peak, as indicated already in Figure 2-32.

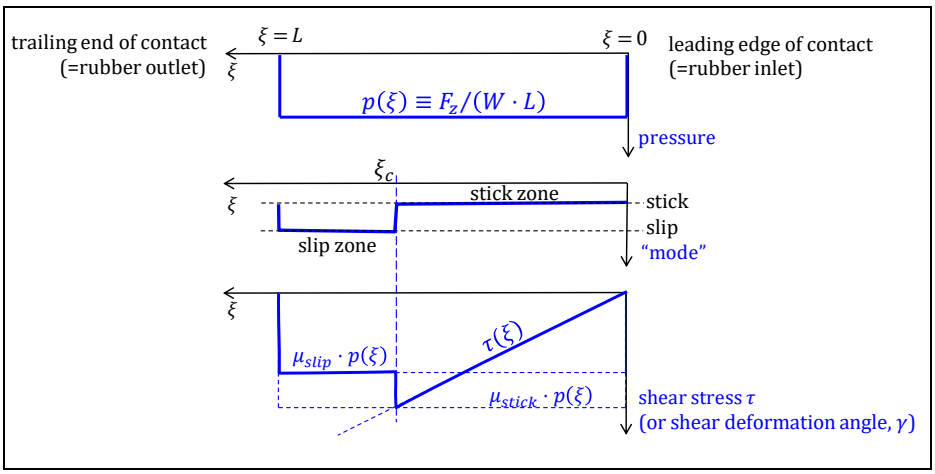


Figure 2-36: Brush model with different static and dynamic friction and uniform pressure distribution.

The differing between μ_{stick} and μ_{slip}, affects like this: $F_{x,slip} = W \cdot \int_{\xi_c}^{L} \mu_{slip} \cdot p \cdot d\xi$; and $\xi_c = \frac{\mu_{stick} \cdot F_z \cdot L}{2 \cdot C_x \cdot s_x}$;.

$$F_x = \begin{cases} = \text{sign}(s_x) \cdot \mu_{slip} \cdot F_z; & if\ \omega \cdot v_x < 0 \Leftrightarrow 1 < |s_x| < \infty \\ = C_x \cdot s_x; & else\ if\ |s_x| \leq \dfrac{\mu_{stick} \cdot F_z}{2 \cdot C_x} \Leftrightarrow |F_x| \leq \dfrac{\mu_{stick} \cdot F_z}{2} \\ = \text{sign}(s_x) \cdot \mu_{slip} \cdot F_z \cdot \left(1 - \dfrac{F_z}{2 \cdot C_x \cdot |s_x|} \cdot \mu_{stick} \cdot \left(1 - \dfrac{\mu_{stick}}{2 \cdot \mu_{slip}}\right)\right); & else \end{cases} \quad [2.20]$$

$$where\ C_x = \frac{G_x \cdot W \cdot L^2}{2 \cdot H_x};\ \ dimension: [force] \quad and\ s_x = \frac{R \cdot \omega - v_x}{|R \cdot \omega|};$$

This model only gives a peak if $k_{stiction} > 2$, see Figure 2-40. The model explains that a peak can occur, but the shape of the curve does not correlate well with tyre measurements. The model can work to explain some phenomena on vehicle level, but a better model can be found if assuming parabolic pressure distribution, see 2.2.3.1.5.

2.2.3.1.5 Different pressure distributions

The uniform pressure distribution is mainly for understanding how the brush model works. The parabolic pressure distribution fits much better with experiments and it is much more frequent used.

However, both uniform and parabolic distributions are: symmetrical around wheel centre. A reflection is that, in the rolling resistance parts, we realized that the distribution can be offset due to losses radial deformation of sidewalls, and the whole contact patch can be moved due to F_x. These mechanisms are fully physical so they could be included in the brush model, but they are not (yet) in this book.

Note: We can note that the symmetrical distributions gives an anti-symmetric $F_x(s_x)$, i.e. $F_x(s_{x1}) = -F_x(-s_{x1})$, which would not necessarily be true if the distribution is modelled to vary (move and change shape and change contact length) with F_x.

2.2.3.1.5.1 Brush Model with Parabolic Pressure Distribution

Hertz's contact theory for line contact motivate an elliptical pressure distribution. A parabolic pressure distribution approximates an elliptical and it gives an alternative brush model, as compared to the one appearing from uniform pressure.

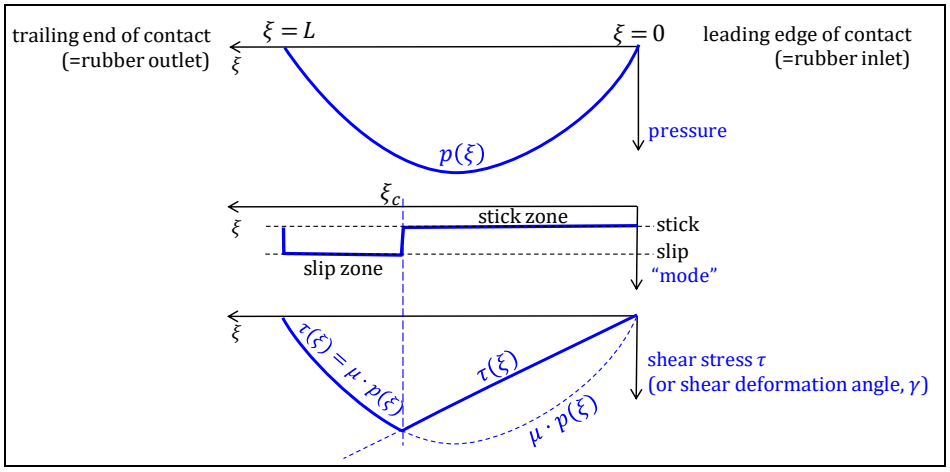


Figure 2-37: Brush model with parabolic pressure distribution. Equal static and dynamic friction.

The coefficients in the parabolic pressure function have to be chosen such that $\int_0^L p(\xi) \cdot W \cdot d\xi = F_z$ and $p(0) = p(L) = 0$;:

$$p(\xi) = \frac{6 \cdot F_z}{W \cdot L} \cdot \frac{\xi}{L} \cdot \left(1 - \frac{\xi}{L}\right); \qquad [2.21]$$

If we do the corresponding derivation as for the uniform pressure distribution, e.g. assuming a stick and slip zones, the location of where slip starts, ξ_c, becomes:

$$\tau(\xi_c) = \frac{G}{H} \cdot s_x \cdot \xi_c = \mu \cdot p(\xi_c) = \mu \cdot \frac{6 \cdot F_z}{W \cdot L} \cdot \frac{\xi_c}{L} \cdot \left(1 - \frac{\xi_c}{L}\right); \Rightarrow \xi_c = L - \frac{G \cdot W \cdot L^3 \cdot s_x}{6 \cdot \mu \cdot H \cdot F_z};$$

The slip where ξ_c appears outside $0 < \xi_c < L$ is when ξ_c becomes < 0, which is when the whole contact slips:

$$\xi_c = L - \frac{G \cdot W \cdot L^3 \cdot s_x}{6 \cdot \mu \cdot H \cdot F_z} = L \cdot \left(1 - \frac{C_x \cdot s_x}{3 \cdot \mu \cdot F_z}\right) < 0; \Rightarrow s_x > \frac{3 \cdot \mu \cdot F_z}{C_x};$$

Total longitudinal force, F_x, becomes:

$$F_x \cdot \text{sign}(s_x) = \begin{cases} = \mu \cdot F_z & if\ \omega \cdot v_x < 0 \\ = C_x \cdot |s_x| - \dfrac{(C_x \cdot |s_x|)^2}{3 \cdot \mu \cdot F_z} + \dfrac{(C_x \cdot |s_x|)^3}{27 \cdot (\mu \cdot F_z)^2}; & else\ if\ |s_x| < \dfrac{3 \cdot \mu \cdot F_z}{C_x} \Leftrightarrow \\ & \Leftrightarrow |F_x| \le \mu \cdot F_z \\ = \mu \cdot F_z; & else \end{cases}$$

$$where\ C_x = \frac{G \cdot W \cdot L^2}{2 \cdot H};\ \ dimension: [force] \quad and\ s_x = \frac{R \cdot \omega - v_x}{|R \cdot \omega|};$$

[2.22]

The shape of this curve becomes as shown in Figure 2-38. The uniform pressure distribution model is drawn as reference. Note that the parabolic pressure distribution does not give any linear part, but the derivative at $s_x = 0$ is same, $C_x = G \cdot W \cdot L^2/(2 \cdot H)$.

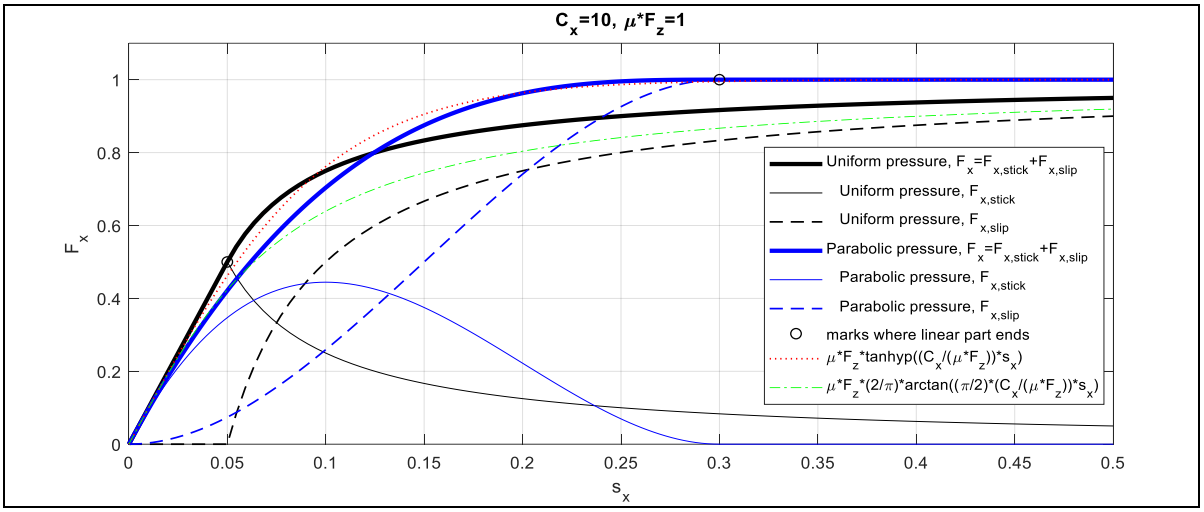


Figure 2-38: Shape of force-to-slip relation derived with brush model with different pressure distributions. Also, the force terms from stick- and slip-regions are shown. The arctan and tanhyp curves are examples of curve-fitting to same dF_x/ds_x in $s_x = 0$.

2.2.3.1.6 Different Static and Dynamic Friction

We now introduce different μ_{stick} and μ_{slip}.

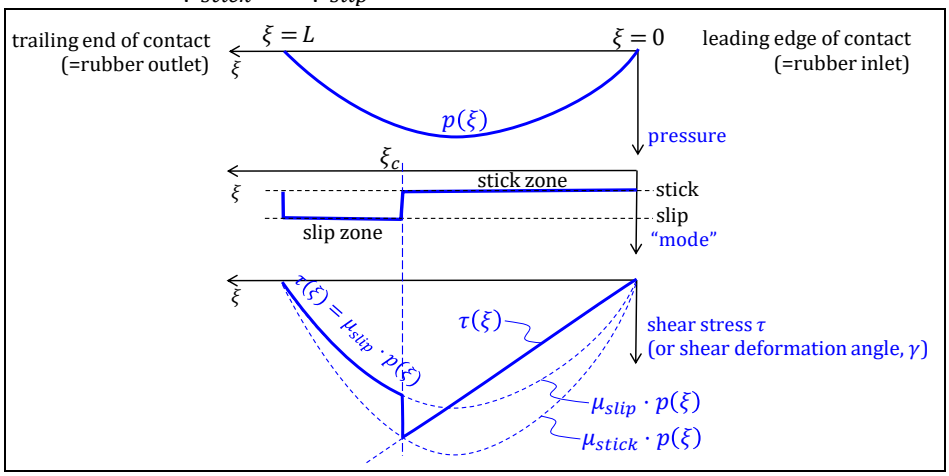


Figure 2-39: Brush model with parabolic pressure distribution and different static and dynamic friction.

We also identify each force term, for stick and slip regions, as follows:

$$F_{x,stick} = W \cdot \int_0^{\xi_c} \tau(\xi) \cdot d\xi = W \cdot \int_0^{\xi_c} \frac{2 \cdot C_x}{W \cdot L^2} \cdot s_x \cdot \xi \cdot d\xi = \left\{ \xi_c = L \cdot \left(1 - \frac{C_x \cdot s_x}{3 \cdot \mu_{stick} \cdot F_z}\right); \right\} =$$
$$= \cdots = C_x \cdot \left(1 - \frac{C_x \cdot s_x}{3 \cdot \mu_{stick} \cdot F_z}\right)^2 \cdot s_x;$$
$$F_{x,slip} = W \cdot \int_{\xi_c}^{L} \mu_{slip} \cdot p \cdot d\xi = \mu_{slip} \cdot W \cdot \int_{\xi_c}^{L} p \cdot d\xi = \left\{ \begin{matrix} p = \frac{6 \cdot F_z}{W \cdot L} \cdot \frac{\xi}{L} \cdot \left(1 - \frac{\xi}{L}\right); \\ \xi_c = L \cdot \left(1 - \frac{C_x \cdot s_x}{3 \cdot \mu_{stick} \cdot F_z}\right); \end{matrix} \right\} =$$
$$= \cdots = \mu_{slip} \cdot F_z \cdot \left(3 - 2 \cdot \frac{C_x \cdot s_x}{3 \cdot \mu_{stick} \cdot F_z}\right) \cdot \left(\frac{C_x \cdot s_x}{3 \cdot \mu_{stick} \cdot F_z}\right)^2;$$
$$Both\ expressions\ valid\ only\ for\ s_x < \frac{3 \cdot \mu_{stick} \cdot F_z}{C_x};$$

[2.23]

The force terms, $F_{x,stick}$ and $F_{x,slip}$, from each of stick and slip regions are identified for $s_x < 3 \cdot \mu_{stick} \cdot F_z / C_x$. When slip is larger, $s_x > 3 \cdot \mu_{stick} \cdot F_z / C_x$, the whole contact slips, $F_{x,stick} = 0$; and $F_{x,slip} = \mu_{slip} \cdot F_z$;. If we sum to $F_x = F_{x,stick} + F_{x,slip}$ we get:

$$F_x = \begin{cases} = \text{sign}(R \cdot \omega - v_x) \cdot \mu_{slip} \cdot F_z; & if\ |s_x| > \frac{3 \cdot \mu_{stick} \cdot F_z}{C_x} \\ = C_x \cdot s_x - \left(2 - \frac{\mu_{slip}}{\mu_{stick}}\right) \cdot \frac{\text{sign}(s_x) \cdot (C_x \cdot s_x)^2}{3 \cdot \mu_{stick} \cdot F_z} + \left(3 - 2 \cdot \frac{\mu_{slip}}{\mu_{stick}}\right) \cdot \frac{(C_x \cdot s_x)^3}{27 \cdot (\mu_{stick} \cdot F_z)^2}; & else \end{cases}$$
$$where\ C_x = \frac{G \cdot W \cdot L^2}{2 \cdot H};\ \ dimension: [force] \quad and\ s_x = \frac{R \cdot \omega - v_x}{|R \cdot \omega|};$$

[2.24]

Note that s_x does not needed to be computed when the first branch "$F_x = \text{sign}(s_x) \cdot \mu_{slip} \cdot F_z$;" is valid.

Typical values of friction coefficients that give good resemblance with measurements are $k_{stiction} = 1.1..2.0$, see experiment with tyre tread sample in (Ludwig & Kim, 2017). Note that the peak of the curve neither appears at $F_x/F_z = \mu_{slip}$ nor $F_x/F_z = \mu_{stick}$. For example, the curve with $[\mu_{slip}\ \ \mu_{stick}] = [1\ \ 2]$ peaks at $F_x/F_z \approx 6300/5000 \approx 1.26$, which is far from $\mu_{stick} = 2$.

Eq [2.24] gives same peak $F_{x,peak}$ and asymptotic $F_{x,slip}$ independent of C_x. The peak slip $s_{x,peak}$ becomes independent of $C_x/F_z = CC_x$, which is often constant:

$$F_{x,peak} = \pm F_z \cdot \underbrace{\mu_{stick} \cdot \frac{4 - 3 \cdot \frac{\mu_{slip}}{\mu_{stick}}}{\left(3 - 2 \cdot \frac{\mu_{slip}}{\mu_{stick}}\right)^2}}_{\mu_{peak}};\ \text{ and }\ s_{x,peak} = \frac{\pm 3 \cdot F_z}{C_x} \cdot \frac{\mu_{stick}}{3 - 2 \cdot \frac{\mu_{slip}}{\mu_{stick}}} = \frac{\pm 3}{CC_x} \cdot \frac{\mu_{stick}}{3 - 2 \cdot \frac{\mu_{slip}}{\mu_{stick}}};$$

The model and analysis can be transferred to lateral slip, except that there is often a tendency that $C_y/F_z \neq CC_y$, but rather that C_y/F_z decreases with F_z. Hence, $s_{y,peak}$ increases with F_z.

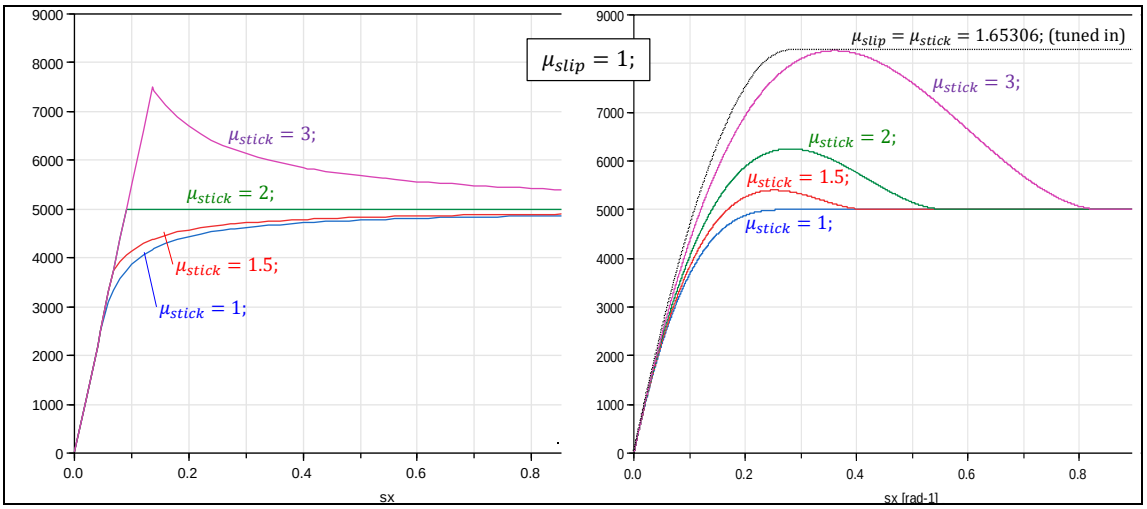


Figure 2-40: Brush model with uniform (left) and parabolic (right) pressure, varying μ_{stick}/μ_{slip}.

On low friction (snow, ice) the ratio μ_{Stick}/μ_{Slip} is normally smaller, which explains why the peak in force is normally less pronounced.

2.2.3.1.7 Different slip definitions influence on tyre characteristics estimation

The slip definition (i.e. $v_{transp} = R \cdot \omega$ or $v_{transp} = v_x$ in $s = (R \cdot \omega - v_x)/v_{transp}$) matters for the curve's transition shape to saturation. If the tyre behaves as the physically well motivated $v_{transp} = R \cdot \omega$, and we use the same definition for estimation of $\{CC_x, \mu\}$, the estimation will of course be correct. But if we use the other definition, $v_{transp} = v_x$, for the estimation there will be an error. See Figure 2-41.

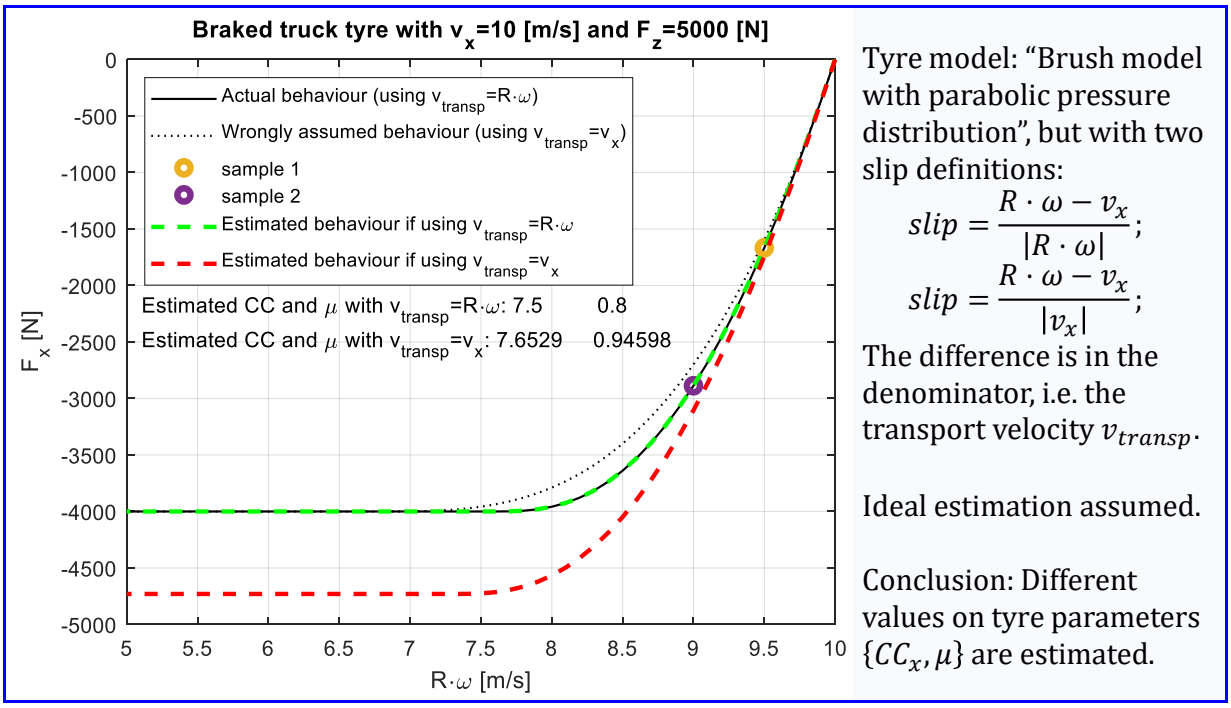


Figure 2-41: Effect of slip definition on friction estimation

2.2.3.2 Measurements

Some examples of measurements are given Figure 2-42. It is important to understand that there is a big spread between different tyres (e.g. studded or not, as shown in the figure) and that the physical phenomena we try to measure and model is not only the tyre, but the contact between one certain tyre and one certain ground surface (e.g. ice, as shown in figure). Additionally, there is one certain wheel suspension which can cause different high frequency oscillations which affect the averaged measured

signals. The figure shows both longitudinal and lateral grip, so both relevant for 2.2.3 and 2.2.4, but not the combined situation in 2.2.5.

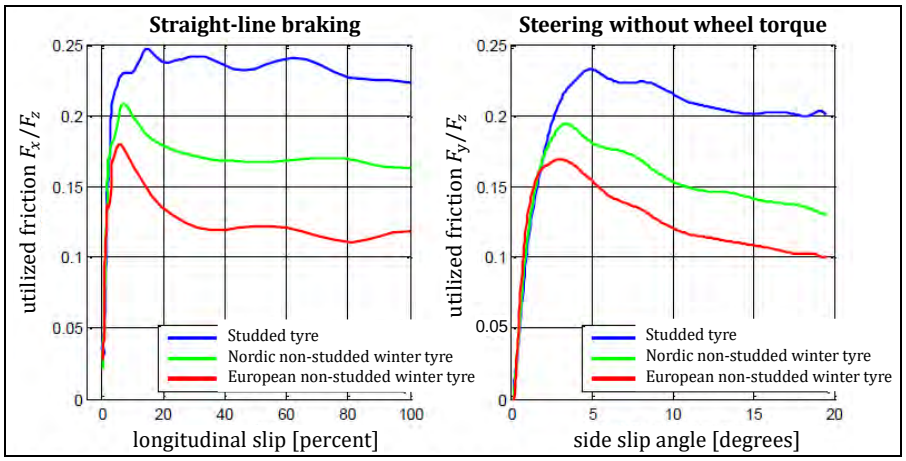


Figure 2-42: Typical measurements for passenger car tyres on ice. From Hjort and Eriksson, VTI report 875, 2015. https://www.vti.se/en/Publications .

2.2.3.3 Parameter Fitting in Physical Tyre Models

The brush model variants presented above are *physical tyre models*. They can to some extent represent changing tyre design parameters and changing ground properties. It is almost impossible to know the correct numerical values of the real design parameters, such as G_x, W, H_x in $C_x = G_x \cdot W \cdot L^2/(2 \cdot H_x)$ or μ. But if one has experimental data, one can at least fit C_x and μ, to one experiment. Changing C_x or μ then makes sense. However, L is no design parameter, but a variable dependent of F_z. So, if also changing F_z, one would need more experimental data with variation in F_z or a model for $L = L(F_z)$. The book argues for using slip definition from Eq [2.2] when fitting parameters in physical tyre models.

2.2.3.4 Curve Fit Tyre Models

The brush model is a *physical tyre model*. However, if a model is required which is numerically accurate for one specific tyre of which one have experimental data, and there is no need for changing tyre design parameters and ground properties, one can use a *curve fit tyre model* instead. Curve fit models are inductive, as opposed to deductive; they do not bother to comply with well-established physical and engineering phenomena as elasticity and dry friction. The advantage with curve fit models is that almost any experiment result can be represented by tuning model parameters. The disadvantage it less validity when extrapolating from a certain experiment, e.g. changing parameters or operating conditions.

Those “Curve Fit Tyre Models” often uses a mathematical curve approximation, such as trigonometric and exponential forms instead of models as in Eq [2.13]. Most curve fit tyre models use the "collapse from 3 to 2 independent variables", by which is meant that the fitted curves have 2 independent variables: $[F_x, F_y] = func\left(s_x(R \cdot \omega, v_x), s_y(R \cdot \omega, v_x)\right)$; instead of $[F_x, F_y] = func(\omega, v_x, v_y)$;. This selection of number of independent variables is typically the only very physical assumption in the curve fit models. It is important that **same** slip definition is used when numerical parameter values are fitted as when the tyre model is used, e.g. for simulation.

Note that curve fit models are not necessarily physically dimensional correct. E.g., the difference $B \cdot x - \arctan(B \cdot x)$ in Eq [2.25] is a difference between two different physical dimensions: *force* $[N]$ and $\arctan(force\ [N])$. This means that one should only use a curve fit model with the units it is defined for.

2.2.3.4.1 Magic Formula Tyre Model

The most well-known curve fit tyre model is probably the "Magic Formula". It was proposed by Hans Pacejka, 1934-2017. It is described, e.g., in (Bakker, 1987). The curve fit has the general form shown in Eq [2.25]:

$$Force = y(x) = D \cdot \sin\left(C \cdot \arctan\left(B \cdot x - E \cdot (B \cdot x - \arctan(B \cdot x))\right)\right) + S_V;$$
$$Slip = s = x = X + S_H; \qquad [2.25]$$

The variable *Slip* is the tyre slip, either longitudinal slip s_x or lateral slip s_y with unit [1]. The parameters are: D $[N]$ is peak factor, B [1] is stiffness factor, C [1] is shape and E $[1/rad]$ is curvature factor. The parameters $S_V[N]$ and $S_H[1]$ simply shifts the curve so that it passes through the origin, which might not be the case for measurement data, since there can be errors in tyre radius and correction for rolling resistance.

A unit identification, starting from that $Force$ is in $[N]$ and x in [1], leads to: $S_V[N]$ and $D[N]$. For a strict unit consistency, we must assume some unwritten constants with value 1, e.g., the $1[rad]$ as in the following:

$$C[1] \cdot \arctan\left(\frac{\underbrace{B[1] \cdot x[1]}_{[1]} - E\left[\frac{1}{rad}\right] \cdot \left(\underbrace{B[1] \cdot 1[rad] \cdot x[1]}_{[rad]} - \underbrace{\arctan\left(\underbrace{B[1] \cdot x[1]}_{[1]}\right)}_{[rad]} \right)}{[1]} \right)$$

The need of the unitary constant $1[rad]$ is an effect of that the Magic formula is a mathematical curve fit. The Magic formula is often given without the $1[rad]$, while including $1[rad]$ would be more physical since then it would at least be unit consistent.

For the lateral tyre models later in the book, a similar Magic formula exists. The need of the constant $1[rad]$ remains the same, regardless of if lateral slip is measured in dimensionless lateral slip s_y or a tyre sideslip angle α. This remains as $1[rad]$ because the trigonometric functions in magic formula ($\sin(\cdots)$, $\arctan(\cdots)$) does not come from any physical geometry of the tyre but is just a mathematical fit of a single variable curve of how F varies with slip.

The influences of the parameters are shown in Figure 2-43.

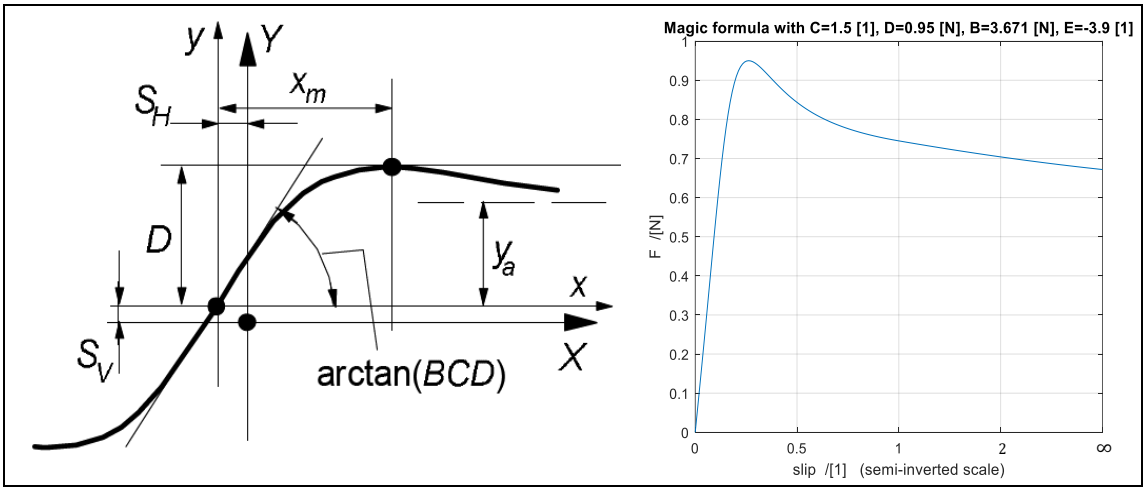


Figure 2-43: Left: Magic Formula Tyre Parameters, (Pacejka, 2005). Right: Example parameterisation.

New versions of Magic Formula Tyre Model are subsequently released. The latest and most complex versions use around 150 or 200 parameters.

2.2.3.4.2 TMsimple and TMeasy Tyre Models

TMsimple and TMeasy are two other curve fit models. TMsimple is shown in Eq [2.26] (without influence of vertical force). Both are shown in Figure 2-44. TMsimple is a simplified variant of TMeasy. For example, in TMsimple, it is not possible to set the maximum force value to a specific slip. TMeasy is described in Ref (Hirschberg, Rill, & Weinfurter, 2007).

$$F(s) = F_{max} \cdot \sin\left(B \cdot \left(1 - e^{-|s|/A}\right) \cdot \mathrm{sign}(s)\right);$$
$$where\ B = \pi - \arcsin(F_\infty / F_{max});\ and\ A = F_{max} \cdot B / C;$$
$$with\ F_{max}, F_\infty\ and\ C \text{ as in Figure 2-44} \qquad [2.26]$$

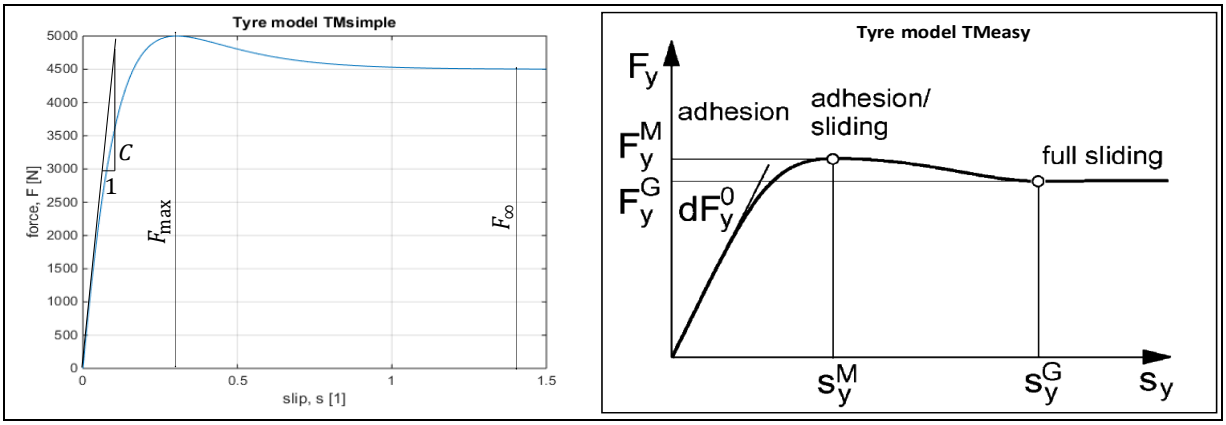


Figure 2-44: Left: TMsimple (Lex, 2015). Right: TM-Easy Tyre Model, (Hirschberg, Rill, & Weinfurter, 2007).

2.2.3.4.3 Curve fit models using tanhyp(⋯)

Figure 2-38 indicates that tanhyp(⋯) (see also Ref (Metzler, Tavernini, Gruber, & Sorniotti, 2020)) gives a better curve fit than arctan(⋯). However, that conclusion is drawn without introducing different static and dynamic friction coefficients, see 2.2.3.1.6. Figure 2-40 shows that the curve shape is influenced by how different μ_{slip} and μ_{stick} are.

Here is the tanhyp(⋯) model for longitudinal force, given both as the force $F_x(s_x)$ and the local longitudinal slip stiffness $C_x'(s_x)$:

$$F_x(s_x) = \mu \cdot F_z \cdot \mathrm{sign}(s_x) \cdot \mathrm{tanhyp}\left(\frac{C_x}{\mu \cdot F_z} \cdot s_x\right) = \mu \cdot F_z \cdot \mathrm{sign}(s_x) \cdot \mathrm{tanhyp}\left(\frac{CC_x}{\mu} \cdot s_x\right);$$
$$C_x'(s_x) = \frac{dF_x}{ds_x} = \mu \cdot F_z \cdot \frac{CC_x}{\mu} \cdot \left(1 - \mathrm{tanhyp}^2\left(\frac{CC_x}{\mu} \cdot s_x\right)\right); \qquad [2.27]$$

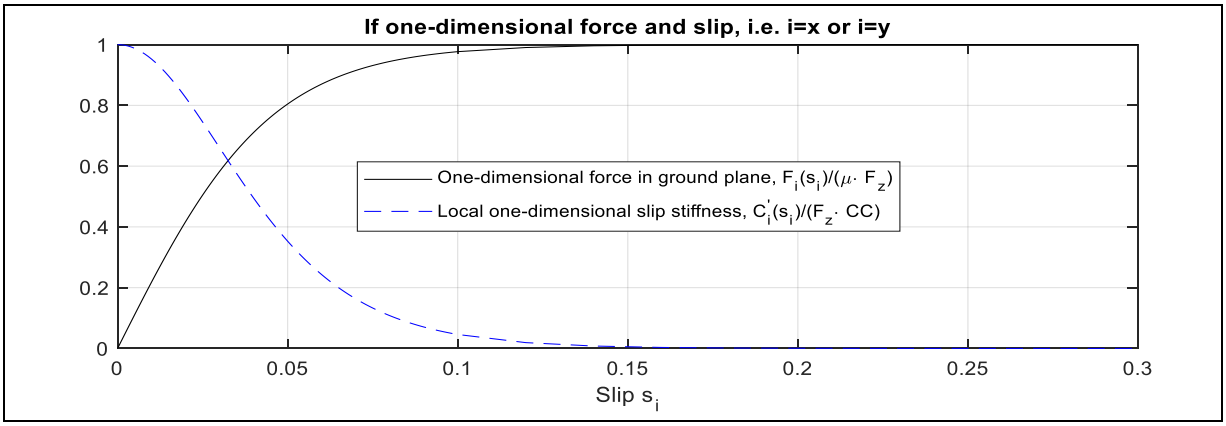


Figure 2-45: The curve fit model using tanhyp(⋯).
We can use it either with $i = x$ (longitudinal) or $i = y$ (lateral).

2.2.3.5 More Advanced Models

There are numerous of more advanced tyre models, such as Swift and FTire. They mix physical and curve fit parameters. FTire is almost a finite element model and demands very many parameters.

2.2.3.6 Very Simple Tyre Models

There are many more models with different degree of curve fitting to experimental data. However, one can often have use for very simple curve fits, such as:

- Linearized: $F_x = C_x \cdot s_x$
- Linearized and saturated: $F_x = \text{sign}(s_x) \cdot min(C_x \cdot |s_x|; \mu \cdot F_z)$. This means approximating the curve $F\_x(s_x)$ with 3 spliced lines with the 2 borders $s_x = \pm \mu \cdot F_z / C_x$. One can also splice in more lines, so that the model stays piecewise linear.
- Ideal rolling: $s_x = 0; \Leftrightarrow R \cdot \omega = v_x;$ (as if linear with $C_x \to \infty$).
  The force F_x is still in the wheel (or tyre) model. So, this wheel model does not mind whatever value F_x has in $-\infty < F_x < +\infty$. It will depend on what surroundings the wheel model is connected to.
- Ideal rolling and saturated: $if\ stick\ s_x = 0;\ else\ F_x = \mu \cdot F_z;$ Discrete state switching: $when\ s_x < 0\ then\ stick \leftarrow true;\ elsewhen\ F_x > \mu\ then\ stick \leftarrow false;$ (Approximately described.)

2.2.3.7 Transients and Relaxation

Contribution from Luigi Romano, Vehicle Dynamics at Chalmers

Both the physical and empirical tyre models assume steady state condition in the contact patch, meaning steady state deformation pattern and steady state sliding speed distribution. These models also result in that the force F_x is a function of v_x/ω, often hidden in an auxiliary variable called slip $s_x = s_x(v_x/\omega)$.

Transients between different steady state conditions take some time which is why the phenomena is called *relaxation*. Often in Vehicle Dynamics, the relaxation is such a quick process that it can be assumed to take place instantaneously, i.e., the algebraic relation $F_x = F_x(s_x)$ can be used. But sometimes it is relevant to model the transients more carefully. Transients are triggered by variations; variations in slip (v_x and/or ω), vertical force (F_z) and/or surface conditions (e.g., expressed in varying μ). Transients can also appear for constant conditions (constant v_x, ω, F_z, μ) if the tyre and its suspension constitute a system that comes into stick-slip oscillations.

Note that also start from stand-still and deceleration to stand-still are examples of strong transients in slip. We can see this in Figure 2-17 where we see that the smaller $|v_x|$, the steeper the curve $F_x(\omega)$ becomes during sign change. So, if $v_x = 0$, the $F_x(\omega)$ will have same step-form as a dry friction contact in Figure 2-32.

Similarly, we see infinitely steep gradients near $\omega = 0$ in Figure 2-46. If using slip, we experience this as a mathematical singularity; slip approaches $\pm\infty$ when ω approaches zero. Modelling transients often solve both the mentioned transients in slip, vertical force and surface conditions as well as driving situations involving/close to stand-still. The physical phenomena to be modelled is elasticity; in tyre sidewalls and/or in contact patch.

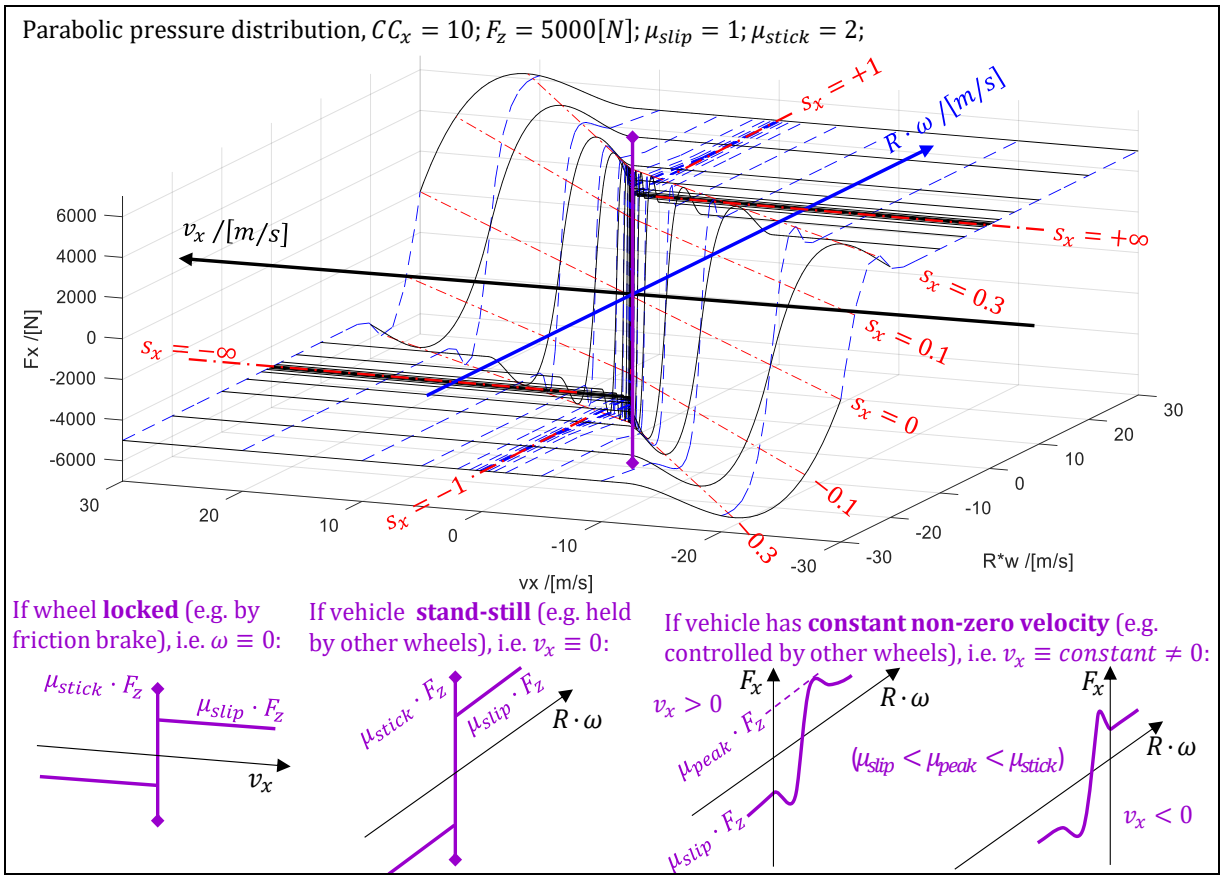


Figure 2-46: Eq [2.24] plotted over the $[R \cdot \omega, v_x]$-plane.

As a very general (but not yet physically motivated) model, we can sketch a model with a 1st order time delay with time constant τ of the force:

$$\dot{F}_x = (1/\tau) \cdot (f_{SS}(s_x, F_z, \mu, \cdots) - F_x);$$

where $f_{SS}(s_x, F_z, \mu, \cdots)$ is the force according to a steady state model, e.g. Eq [2.13]. [2.28]

Alternatively, one can also express the delay as a 1st order time delay of the slip, as follows:

$$F_x = f_{SS}(s_{x,delayed}, F_z, \mu, \cdots);$$

$$\dot{s}_{x,delayed} = (1/\tau) \cdot (s_x - s_{x,delayed});$$

where $f_{SS}(s_{x,delayed}, F_z, \mu, \cdots)$ is the force according to a steady state model, e.g. Eq [2.13] [2.29]

The time constant is often expressed through a "relaxation length" L_r as follows:

$$\tau = \frac{L_r}{v_{Transport}} = \frac{L_r}{|R \cdot \omega|};$$

However, we can motivate the size of L_r with more physical phenomena, which will be discussed in 2.2.3.7.1 (rearranging the deformation pattern within the contact, which changes with time constant $L/|R \cdot \omega|$) and 2.2.3.7.2 (changing the overall sliding velocity of the contact, which changes with time constant $F_x/\dot{F}_x$). Both are combined in 2.2.3.7.3.

2.2.3.7.1 Transients due to contact patch

The force F_x will not follow the steady state function $f_{SS}(s_x, F_z, \mu, \cdots)$ directly, but with some form of delay or transient. One physical phenomenon that causes such delay is that the bristles in the contact patch need to adopt to a new deformation pattern.

Following the brush model, the physically correct way would be to extend the equations to a partial differential equation (*PDE*), with derivatives with respect to both time and position along the contact patch, ξ, see 2.2.3.7.5.

A less mathematical, but still physical, motivation would be to use the Eq [2.28] with a time delay deduced from the following physical reasoning: The change in force requires all bristles in the slip zone in the contact patch to adopt to a new deformation pattern. So, in principle, all bristles have to be replaced. So, the time it takes to replace these bristles is assumed to:

$$\tau = \frac{L_r}{v_{Transport}} = \frac{L_{r,patch}}{|R \cdot \omega|} = \frac{\xi_c}{|R \cdot \omega|} \approx \begin{Bmatrix} average \\ \xi_c \approx L/2 \end{Bmatrix} \approx \frac{L/2}{|R \cdot \omega|}; \qquad [2.30]$$

Often, one uses a much larger relaxation length, like a certain fraction ($\approx 25..50\%$) of the tyre circumference, but that comes from experiments, so it contains all physical phenomena. In 2.2.3.7.3 and Eq [2.38], the two main phenomena are modelled, so the $L_r \approx 25..50\%$) of the tyre circumference there.

2.2.3.7.2 Transients due to elastic sidewall

Figure 2-47 shows a physical model which can model how the force change is delayed during quick changes in slip. The model can also handle vehicle stand-still. This type of model is often called a *rigid ring tyre model* because the belt is modelled as a rigid ring, or *single contact point* model. The ring is here massless but has mass and rotational inertia. The longitudinal and vertical support are here rigid, but they can be modelled as compliant. If no significant inertia in wheel hub, the driveshaft compliance will be series coupled with the rotational compliance, c_{sw}. The torque T_{rim} is the sum of torque from propulsion system and brake system. Damper elements can be added beside the compliances.

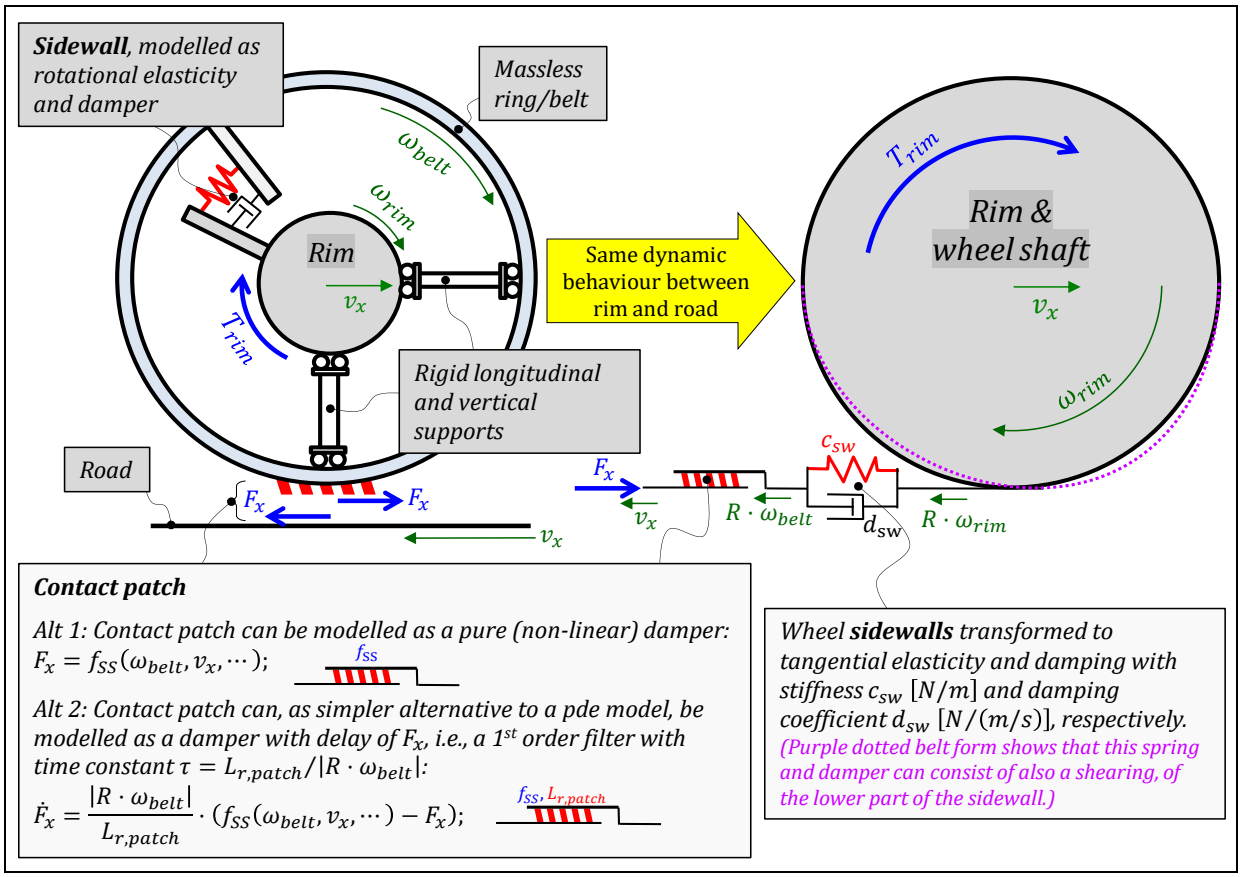


Figure 2-47: Tyre model including both the contact patch and the rotational elasticity of tyre sidewalls.

If we neglect delay in the contact patch model, or $L_{r,patch} \to 0$, we get this mathematical model:

$$
\begin{aligned}
&F_x = F_{xs} + F_{xd};\\
&\dot{F}_{xs} = c_{sw} \cdot (R \cdot \omega_{rim} - R \cdot \omega_{belt});\\
&F_{xd} = d_{sw} \cdot (R \cdot \omega_{rim} - R \cdot \omega_{belt});\\
&F_x = f_{SS}(s_{x,belt}, F_z, \mu, \cdots); \quad where \quad s_{x,belt} = \frac{R \cdot \omega_{belt} - v_x}{|R \cdot \omega_{belt}|};
\end{aligned}
\qquad [2.32]
$$

Note that Eq [2.32] can be seen as 2 models, sidewall and belt with contact patch. These two are simply connected in the physical connecting node $\{\omega_{belt}, F_x\}$. So, *the sidewall does not need to be seen as involved in the relaxation. And, if the rim inertia is not to be considered (e.g. for low speed and start and stop), also elastic parts of the wheel torque actuators (propulsion and brake subsystems) and the suspension subsystem, can be seen as involved in the transients of the force F_x between tyre and ground.*

If Eq [2.32] is used in a system where ω_{rim} and v_x are input variables to tyre, the force F_{xs} will become a state variable. It is then not a problem that slip is undefined for $\omega = 0$, because the explicit form of equations will become as follows, using the inverse of the f_{ss}. Note that we simplify by only considering the case when $\omega_{belt} \cdot v_x > 0$ and $d_{sw} = 0$. And the model validity is limited to $F_x, F_z, \mu, \ldots$ such that uniquely defines $s_{x,belt}$, which, e.g., disqualifies f_{SS} with a peak.

$$
\begin{aligned}
&s_{x,belt} \leftarrow f_{SS,inv}(F_x, F_z, \mu, \cdots);\\
&\omega_{belt} \leftarrow \frac{v_x}{R \cdot (1 - s_{x,belt} \cdot \mathrm{sign}(v_x))}; \quad (only\ valid\ for\ \omega_{belt} \cdot v_x > 0)\\
&\dot{F}_x \leftarrow c_{sw} \cdot (\omega_{rim} - \omega_{belt});\\
&where\ f_{ss,inv}\ is\ the\ inverse\ of\ function\ f_{SS}\ such\ that\ s_{x,belt} = f_{SS,inv}(F_x, F_z, \mu, \cdots);
\end{aligned}
\qquad [2.33]
$$

One avoids the mathematical problem to divide by $\omega = 0$ in the slip definition. However instead, one can get the mathematical problems that the f_{SS} is not possible to **invert** for $|F_x| > \max_{s_{x,belt}}(|f_{SS}(\cdots)|)$ and that f_{ss} is not possible to invert **uniquely** for $F_x \approx \pm\mu_{Peak} \cdot F_z$. The physically correct modelling cures would be to model wheel lift and separate in different discrete modes (between and outside peaks), respectively.

2.2.3.7.3 Transients due to both contact patch and elastic sidewall

Figure 2-47 can be used again, but now with contact patch delay, i.e., $L_{r,patch} > 0$.

$$
\begin{aligned}
&F_x = F_{xs} + F_{xd};\\
&\dot{F}_{xs} = c_{sw} \cdot (R \cdot \omega_{rim} - R \cdot \omega_{belt});\\
&F_{xd} = d_{sw} \cdot (R \cdot \omega_{rim} - R \cdot \omega_{belt});\\
&\dot{F}_x = \frac{|R \cdot \omega_{belt}|}{L_{r,patch}} \cdot \left(f_{SS}(s_{x,belt}, F_z, \mu, \cdots) - F_x\right); \quad where \quad s_{x,belt} = \frac{R \cdot \omega_{belt} - v_x}{|R \cdot \omega_{belt}|};
\end{aligned}
\qquad [2.34]
$$

Now we will assume that the tyre is to be modelled in same model environment as in Eq [2.33], with ω_{rim} and v_x as input variables. We concretize with the simple tyre model $F_x = C_x \cdot s_{x,belt};$, which is same as using $f_{SS}(s_{x,belt}, F_z, \mu, \cdots) = C_x \cdot s_{x,belt}; with\ constant\ C_x;$ and $d_{sw} > 0$.

$$
\begin{aligned}
&\dot{F}_{xs} \leftarrow \frac{c_{sw} \cdot (F_x - F_{xs})}{d_{sw}};\\
&\dot{F}_x \leftarrow -\frac{|F_{xs} - F_x + R \cdot d_{sw} \cdot \omega_{rim}| \cdot \left(F_x + \frac{C_x \cdot d_{sw} \cdot \left(v_x - \frac{F_{xs} - F_x + R \cdot d_{sw} \cdot \omega_{rim}}{d_{sw}}\right)}{|F_{xs} - F_x + R \cdot d_{sw} \cdot \omega_{rim}|}\right)}{L_{r,patch} \cdot d_{sw}};\\
&s_{x,belt} \leftarrow -\frac{(d_{sw} \cdot v_x + (F_x - F_{xs}) - d_{sw} \cdot R \cdot \omega_{rim})}{|F_{xs} - F_x + d_{sw} \cdot R \cdot \omega_{rim}|};
\end{aligned}
\qquad [2.35]
$$

If adding assumption that $d_{sw} = 0$ and $c_{sw} > 0$ and $R \cdot \omega_{rim} > 0$:

$$
\begin{aligned}
&\dot{F}_x \leftarrow -\frac{c_{sw} \cdot (C_x \cdot v_x + (F_x - C_x) \cdot R \cdot \omega_{rim})}{C_x - F_x + L_{r,patch} \cdot c_{sw}};\\
&\omega_{belt} \leftarrow \frac{C_x \cdot v_x + L_{r,patch} \cdot R \cdot c_{sw} \cdot \omega_{rim}}{R \cdot (C_x - F_x + L_{r,patch} \cdot c_{sw})};\\
&s_{x,belt} \leftarrow \frac{F_x \cdot v_x + L_{r,patch} \cdot c_{sw} \cdot (R \cdot \omega_{rim} - v_x)}{C_x \cdot v_x + L_{r,patch} \cdot c_{sw} \cdot R \cdot \omega_{rim}};
\end{aligned}
\qquad [2.36]
$$

We note that, when $d_{sw} = 0$, one state variable disappears (F_x instead of $\{F_{xs}, F_x\}$). In none of the alternatives it is any problem with singularities when $\omega \to 0$ (as in the slip definition, where ω is in the denominator).

If one brings in a more general model $F_{SS} = f_{SS}(s_x, F_z, \mu, \cdots)$, one can see that it is used inversely, i.e., calculating slip from force, or more general calculating ω_{belt} from force. This indicates the problem of using tyre models with a peak, because then one need a discrete state variable to differ between if below or above peak, which leads too far for this book.

For the brush model with uniform pressure distribution, Eq [2.13], the inverted function $f_{SS,inv}$ (such that $s_x = f_{SS,inv}(F_{SS}, F_z, \mu, \cdots);$) becomes as follows, including such saturation:

$$s_x = g(F_x, F_z, \mu) = \begin{cases} = \dfrac{F_x}{C_x}; & for\ |F_x| \le \dfrac{\mu \cdot F_z}{2}; \\ = \dfrac{\mu \cdot F_z}{4 \cdot C_x} \cdot \dfrac{\text{sign}(F_x)}{1 - \dfrac{|F_x|}{\mu \cdot F_z}}; & for\ |F_x| < 0.95 \cdot \mu \cdot F_z; \\ = \dfrac{\mu \cdot F_z}{4 \cdot C_x} \cdot \dfrac{\text{sign}(F_x)}{1 - 0.95}; & else \end{cases}$$

$$where\ C_x = \frac{G \cdot W \cdot L^2}{2 \cdot H};\ \ dimension: [force]$$

[2.37]

2.2.3.7.4 Relation between slip stiffness, deformation stiffness, and relaxation length

Now, the Eqs [2.35] and [2.36] includes both the phenomena contact patch relaxation and the phenomena sidewall elasticity. These are two different phenomena that is intuitively present at the same time in the real world. The dynamics of the first is captured in L_r and the dynamics of the latter is captured in c_{sw}. Since we seldom can measure the ω_{belt}, it is seldom we can resolve any measured delays into those 2 parameters. A common way to model the overall transients of a tyre is, therefore, to include both phenomena in a formula on the same form as Eq [2.35]:

$$\dot{F}_x = (1/\tau) \cdot \left(f_{SS}\left(s_{x,rim}, F_z, \mu, \cdots\right) - F_x\right);$$

where $f_{SS}\left(s_{x,rim}, F_z, \mu, \cdots\right)$ is the force according to a steady state model, e.g., Eq [2.13]. The slip $s_{x,rim} = \frac{R \cdot \omega_{rim} - v_x}{|R \cdot \omega_{rim}|}$;. The time delay, $\tau = \frac{L_{r,patch,sw}}{v_{Transport}} = \frac{L_{r,patch,sw}}{|R \cdot \omega_{rim}|}$, where the $L_{r,patch,sw}$ is a relaxation length, but not the same as in Eqs [2.28] and [2.29]. The $s_{x,rim}$ and $L_{r,patch,sw}$ are not

[2.38]

If one identifies the numerical value of $L_{r,patch,sw}$ from real world tests, it becomes typically 25..50% of the tyre circumference. The physical interpretation of Eq [2.38] is not straightforward since it combines the 2 phenomena in 1 formula arranged for only one of them.

If we concretize with the same tyre model as used to derive Ed [2.36], $F_x = C_x \cdot s_x$; and assume $R \cdot \omega_{rim} > 0$, Eq [2.38] becomes:

$$\dot{F}_x = (1/\tau) \cdot \left(C_x \cdot s_{x,rim} - F_x\right) = \frac{R \cdot \omega_{rim}}{L_{r,patch,sw}} \cdot \left(C_x \cdot \frac{R \cdot \omega_{rim} - v_x}{R \cdot \omega_{rim}} - F_x\right);$$

[2.39]

We will now force the quasi-physical relaxation model in Eq [2.28] and Eq [2.38] to follow the more physically motivated model in Eq [2.28]. We now require L_r in Eq [2.28] to give the same $\dot{F}_x$ as $\{c_{sw}, L_{r,patch}\} = \{c_{sw}, 0\}$ gives with in Eq [2.36]. Then is requires: $L_r \approx \frac{C_x}{c_{sw}} \left[\frac{N/1}{N/m} = m\right]$;.

This points out a relation between tyre longitudinal slip stiffness $C_x[N/1]$, longitudinal deformation stiffness $c_{sw}[N/m]$, and "relaxation length" L_r. At a first glance, it might be difficult to believe in such a relation, but here is an explanation: The main part of the relaxation is due to sidewall elasticity, not due to the rearrangement of bristles in the contact patch. So, the simplified model with the relaxation length L_r explains the relaxation with the phenomena which is of least importance. Hence, we get this (initially weird) relation. It can, e.g., be used to estimate a value of c_{sw} from tests where C_x and L_r are identified using the approximative assumption $s_{xRim} = s_x$. So, in a way, we do 2 "errors" that cancel out each other, leading to an approximative relation $L_r \approx \frac{C_x}{c_{sw}}$.

2.2.3.7.5 Expansion of Brush Model to Partial Differential Equation

The brush model derived in 2.2.3.1 was derived for steady state deformation pattern, i.e., the deformation was only $\gamma(\xi)$, not $\gamma(\xi, t)$. The models in 0 and 2.2.3.7.2 starts from such and add time

derivatives only on wheel or tyre level, i.e. on variables like F_x and s_x. These models fit well as parts in larger dynamic models of the whole vehicle and one can use ordinary simulation methods for dynamic system, 1.5.1.1.6.

Modelling with a transient deformation pattern, i.e., $\gamma(\xi, t)$, is a way to understand phenomena for single tyres, even if it is less computational efficient to do so for a model of a whole vehicle. The model becomes a partial differential equation, PDE, as opposed to ODE. A PDE can be implemented in a tool for ODE if one discretizes the PDE to ODE. One can also discretize already in the Physical model, i.e. "following each bristle" as visualised in Figure 2-48.

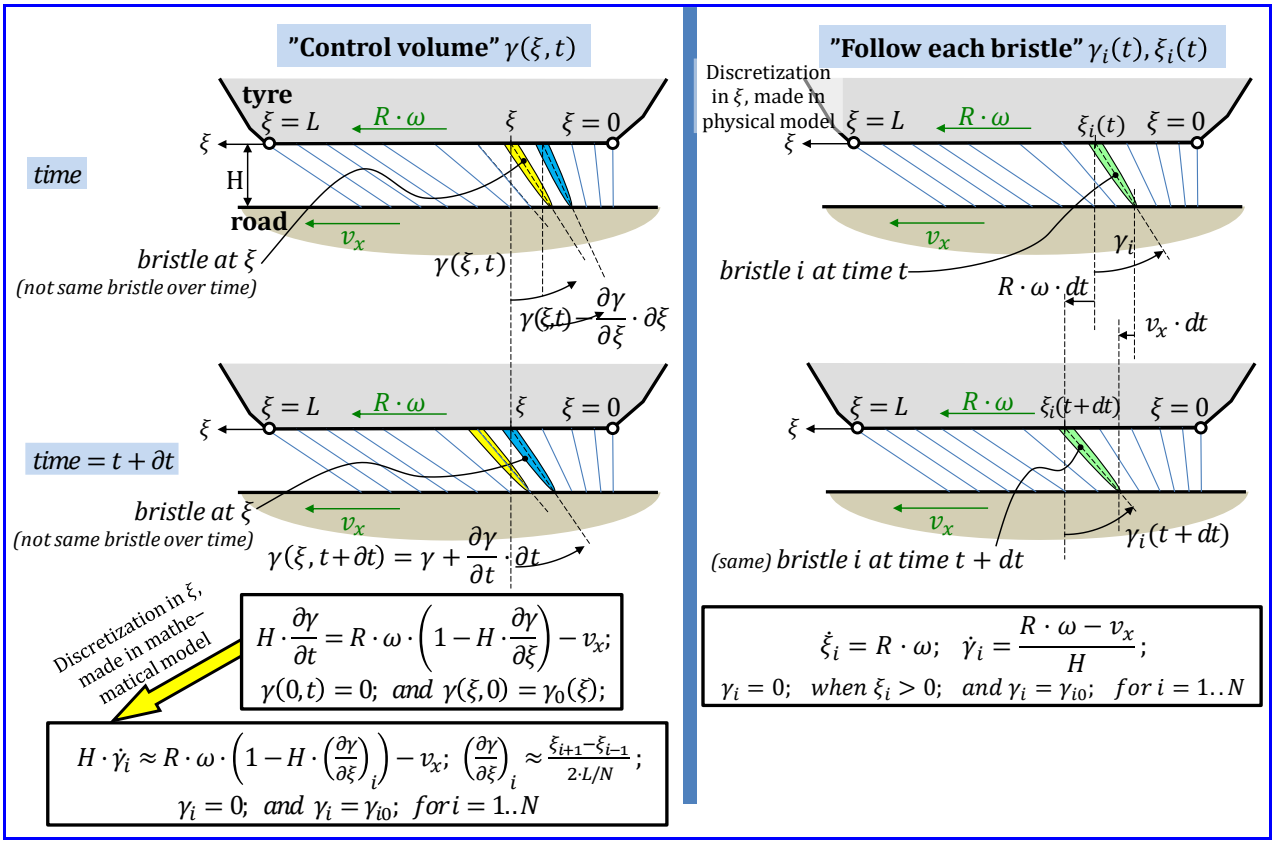


Figure 2-48: Two views of how bristle deformation varies in space and time. Left: Eulerian approach, using a "control volume" i in which new bristles comes in and moves out. Right: Lagrangian approach, following a certain bristle through the contact.

Note that the figure only shows model and equation for the stick zone. With the model derived from "following each bristle", it is straight-forward to implement also stick, slip and transitions for each bristle. Figure 2-49 shows how the bristles moves and deforms over time and space for one example. With the model derived from the control volume, it is less easy to do this, but for many driving cases one can assume that there is exactly one break-away point ξ_c as in the steady state model. Reference (Romano, Bruzelius, & Jacobson, Unsteady-state brush theory, 2020) does this for a start from stand-still and brake to stand-still, showing that the model in 0 can be motivated starting from the PDE from the "control volume".

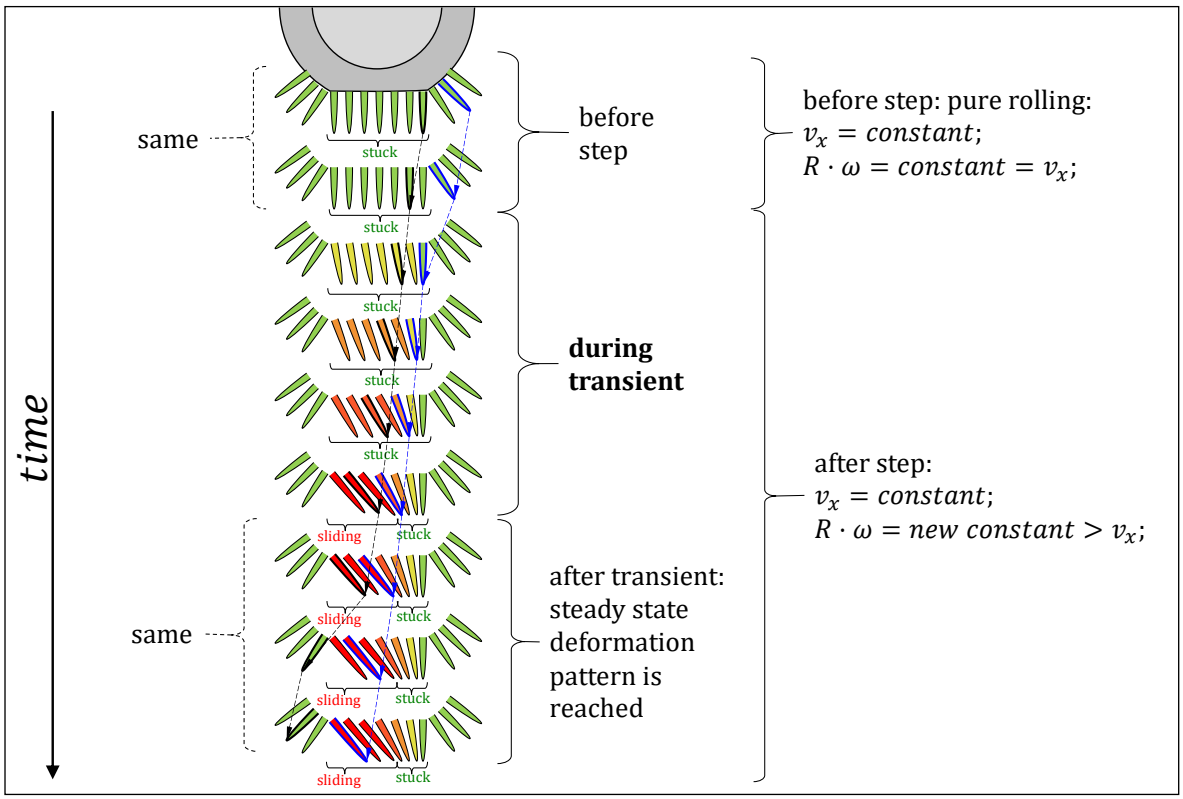


Figure 2-49: Model that follows each bristle over time. Example shows a step change in ω from $R \cdot \omega = v_x$ to $R \cdot \omega > v_x$.

The Modelica model in [2.41] shows an implementation of this modelling concept using parabolic pressure distribution, different static and dynamic friction and contact discretized in N=10 bristles. Figure 2-50 and Figure 2-51 shows an example simulation with this model. Comparison with the corresponding steady state model shows transient tends to overestimate F_x. Comparison with the "relaxed" steady state, using Eqs [2.28] and [2.29], shows that the relaxation length ξ_c seems most reasonable. Note that delay time τ was limited to stay $> 1\ ms$; else $|F_x|$ becomes instable and $\gg \mu_{stick} \cdot F_z$ for large $|s_x|$.

```
model Tyre_Transient
  parameter Modelica.Units.SI.Length R=0.3, H=0.01, W=0.1, L=0.1;
  parameter Modelica.Units.SI.ModulusOfElasticity G=0.5e6;
  parameter Modelica.Units.SI.Force F_z=5000;
  parameter Modelica.Units.SI.DimensionlessRatio mu_stick=1.5, mu_slip=0.7;

  input Modelica.Units.SI.Velocity v_x;
  input Modelica.Units.SI.AngularVelocity w;
  Modelica.Units.SI.Force F_x;
  Modelica.Units.SI.Velocity v_sliding[N] "Sliding velocities 1..N between lower bristle ends and ground";
  Modelica.Units.SI.Force F_ix[N] "Longitudinal forces 1..N on lower bristle ends from ground";
  Modelica.Units.SI.Force F_iz[N] "Vertical forces 1..N on bristles";
  Modelica.Units.SI.Position xi[N] "Position of points 1..N on the belt";
  Modelica.Units.SI.Position xi_lo[N] "Position of lower bound for points 1..N on the belt";
  Modelica.Units.SI.Position xi_up[N] "Position of upper bound for points 1..N on the belt";
  Real DiscrState[N] "Discrete state for contacts 1..N between lower bristle ends and ground";

  //Auxilliary, not necessarily physical:
  parameter Integer N=10;
  Modelica.Units.SI.Force mu_stick_F_iz[N, mu_slip_F_iz[N];
initial equation
  DiscrState = zeros(N);
  xi = ((L/N)/2)*ones(N) + (0:(N - 1))*L/N;
  F_ix = zeros(N);
equation
  //between wheel and contact patch:
  F_x = sum(F_ix);
  der(xi) = R*w*ones(N);

  //pressure distribution:
  for i in 1:N loop
    xi_lo[i] = if noEvent(xi[i] <= min(xi)) then 0 else xi[i] - 0.5*L/N;
    xi_up[i] = if noEvent(xi[i] >= max(xi)) then L else xi[i] + 0.5*L/N;
    F_iz[i] = (6*F_z/L)*( ((xi_up[i]^2/(2*L))-
                  (xi_up[i]^3/(3*L^2))) - ((xi_lo[i]^2/(2*L))-(xi_lo[i]^3/(3*L^2))));
    mu_stick_F_iz[i] = mu_stick*F_iz[i];
    mu_slip_F_iz[i] = mu_slip*F_iz[i];
  end for;

  //shearing and dry friction:
  for i in 1:N loop
    if noEvent(abs(DiscrState[i]-(0))<0.5) then
      v_sliding[i] = 0;
      der(F_ix[i]) = (G*W*L/N)*(R*w-v_x)/H;
    else
      der(F_ix[i]) = DiscrState[i]*mu_slip*der(F_iz[i]);
      v_sliding[i] = R*w + (H*N/(G*W*L))*der(F_ix[i]) - v_x;
    end if;
    der(DiscrState[i]) = 0;

    when xi[i] > L then
    //when a bristles leaves, its xi[i] is reused as xi[i] for a new bristle entering:
      reinit(xi[i], 0);
      reinit(DiscrState[i], 0);      reinit(F_ix[i], 0);
    elsewhen abs((DiscrState[i])-(0)) < 0.5 and F_ix[i] > +mu_stick*F_iz[i] then
      reinit(DiscrState[i],+1);      reinit(F_ix[i], +mu_slip*F_iz[i]);
    elsewhen abs((DiscrState[i])-(0)) < 0.5 and F_ix[i] < -mu_stick*F_iz[i] then
      reinit(DiscrState[i],-1);      reinit(F_ix[i], -mu_slip*F_iz[i]);
    elsewhen abs((DiscrState[i])-(-1)) < 0.5 and v_sliding[i] > 0 then
      reinit(DiscrState[i], 0);
    elsewhen abs((DiscrState[i])-(+1)) < 0.5 and v_sliding[i] < 0 then
      reinit(DiscrState[i], 0);
    end when;
  end for;
end Tyre_Transient;
```

[2.41]

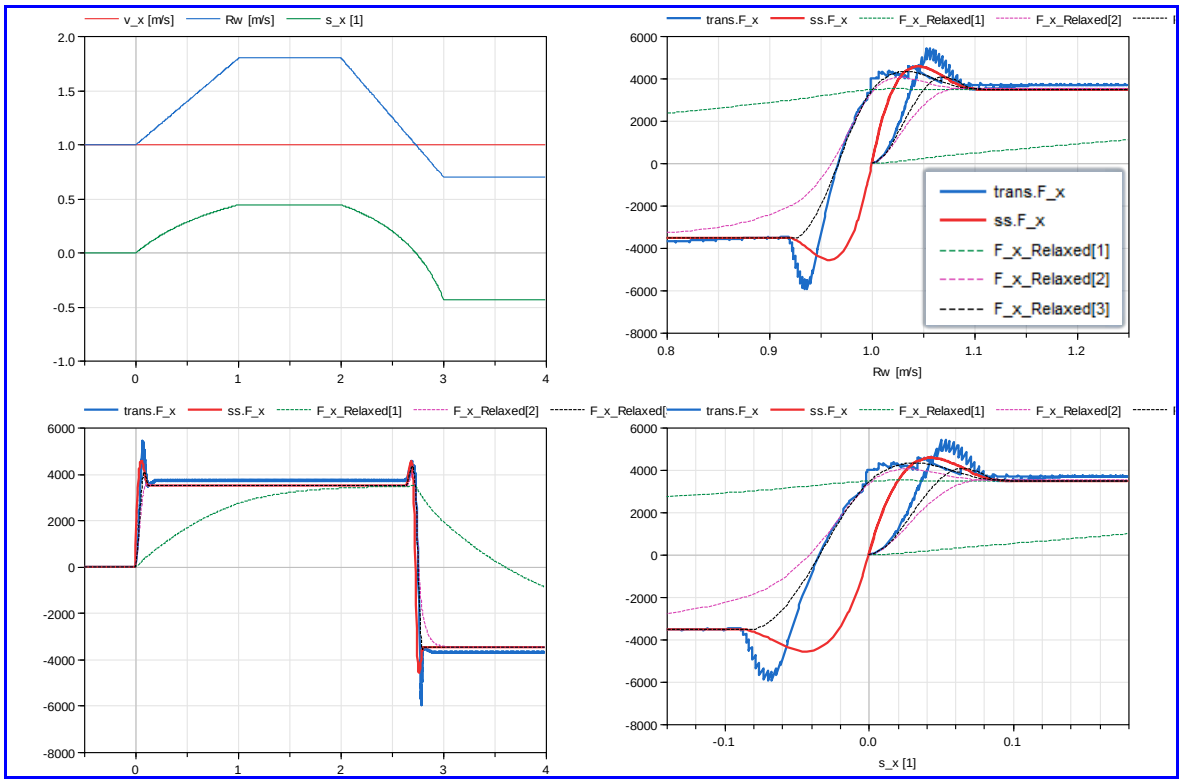


Figure 2-50: Simulation example. Transient tyre model (`trans`), compared with steady state (`ss`) and the "relaxed" steady state. Relaxation lengths are: [1] half circumference, [2] half contact patch and [3] half ξ_c.

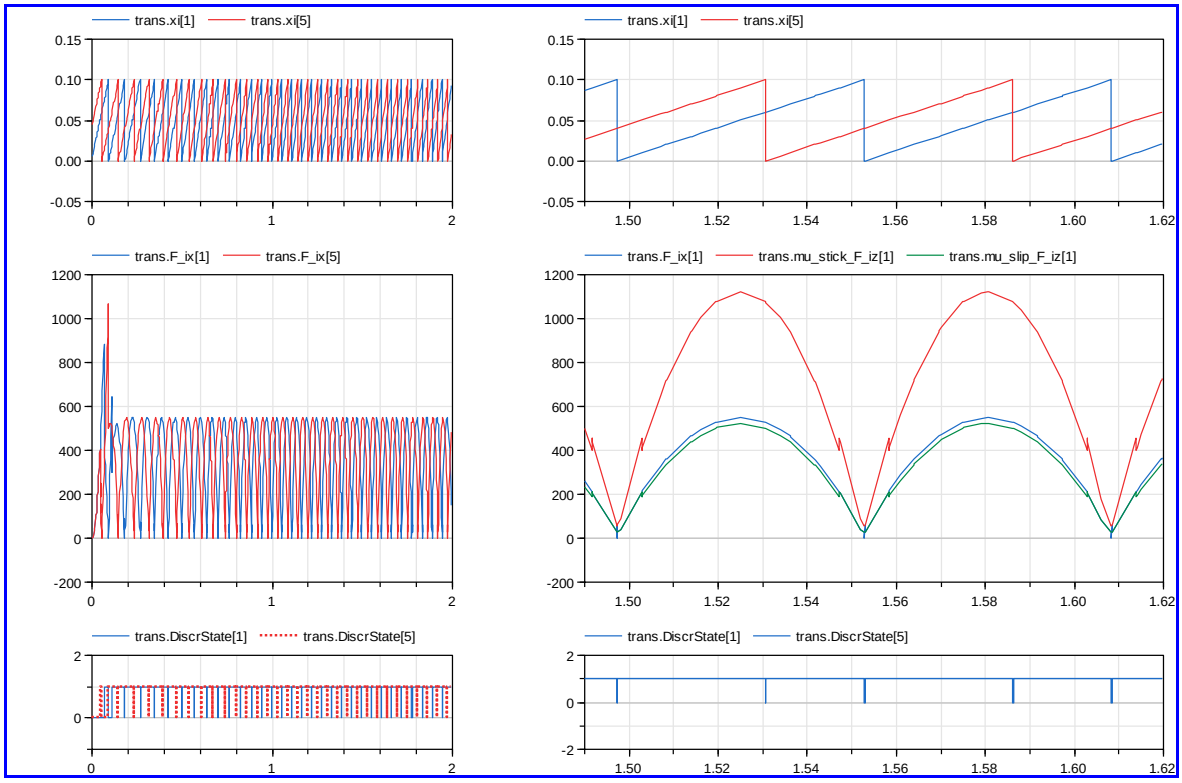


Figure 2-51: Simulation example. Shows how the discretized bristles work.

2.2.3.8 Rolling resistance and longitudinal force and slip

So far, the models in 2.2.3 have not included rolling resistance. But in reality, both appear at the same time. As we regard rolling resistance as a torque, not a force, it does not affect the $F_x(s_x)$ curve. But the rolling resistance does move the $T(s_x)$ curve vertically in the diagram. The curve moves upwards if the wheel is rolling forward and downwards if rolling rearwards, see Figure 2-52. Utilizing $F_x = C_x \cdot s_x = (CC_x \cdot F_z) \cdot s_x = -RRC \cdot F_z$; gives $s_x = -RRC/CC_x \approx 0.01/10 = 0.001$;.

The $F_x(s_x)$ curve is normally the suitable view for vehicle level studies, while the $T(s_x)$ curve is sometimes needed for involving a model of the propulsion and brake systems. As mentioned in 2.2.1.7.2, one can select different R in the slip definition. Figure 2-52 uses an R for slip definition such that $F_x = 0$ for $s_x = 0$, i.e. for pure rolling. Often, for wheel slip control (ABS, TC, …), one instead uses a radius for slip definition such that $T = 0$ for $s_x = 0$, i.e. for free-rolling. That is because it is much easier to know when $T = 0$ than when $F_x = 0$. When $T = 0$, the motion can make it look as if the wheel was rolling at a slightly different radius$= v_x/\omega = R \cdot (1 + \text{sign}(\omega) \cdot RRC/CC_x) \approx (0.999 \; or \; 1.001) \cdot R$ which is the Rolling radius R_e in 2.2.1.7.2.

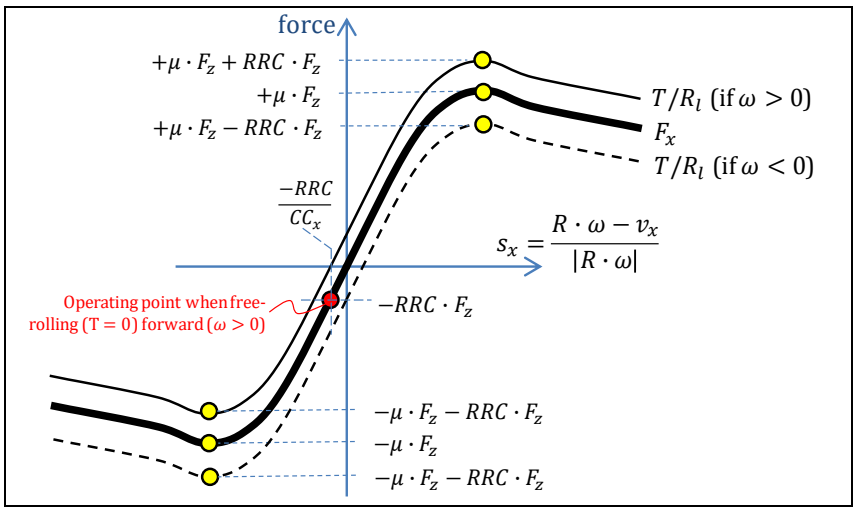


Figure 2-52: Longitudinal tyre force (F_x) and normalized wheel torque (T/R_l). Slip s_x defined so that curve $F_x(s_x)$ passes through diagram origin, which means that $T(s_x)/R_l$ does not.

2.2.3.8.1 Power loss analysis

Contributions from Jochen Rauh, former Daimler, Mats Jonasson and Juliette Torinsson, Chalmers

See also 2.2.1.7.

We start from a physical model to understand the quantities. Soft tyre on hard flat ground is assumed.

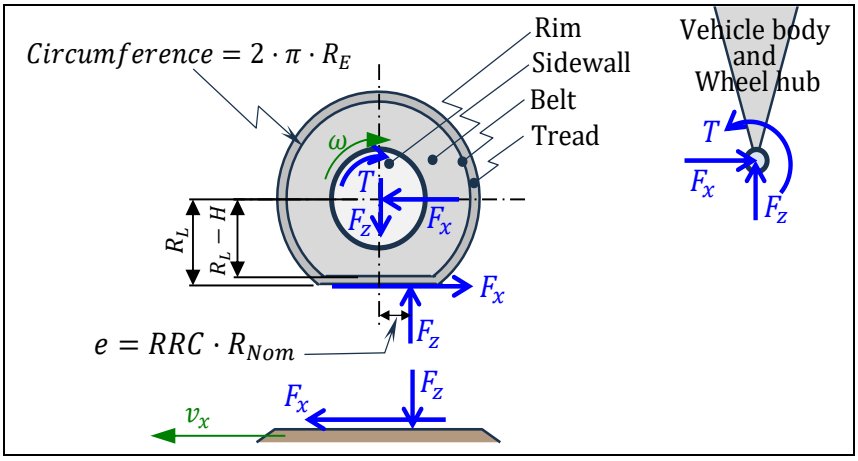


Figure 2-53: Physical model for analysis of power losses in a wheel, keeping consistency with physical models which explains rolling resistance (torque losses) and slip losses (velocity losses). Note that velocities are relative to vehicle body and wheel hub.

In the following, we will deductively use well established expressions:

$$P_{Loss} = \underbrace{T \cdot \omega}_{P_{in}} - \underbrace{F_x \cdot v_x}_{P_{out}} \quad "Power\ equilibrium";$$

$$T = F_x \cdot R_L + \underbrace{F_z \cdot e}_{T_{RR}} \quad "Torque\ equilibrium";$$

We will identify different terms in the power loss. We define the power exchange between the shaft and the rim as positive when flowing **to** the rim, P_{in}. We define power exchange between the wheel hub and the rim as positive when going **from** the rim, P_{out}.

$$P_{Loss} = \underbrace{T \cdot \omega}_{P_{in}} - \underbrace{F_x \cdot v_x}_{P_{out}} = \{T = F_x \cdot R_L + F_z \cdot e;\} = (F_x \cdot R_L + F_z \cdot e) \cdot \omega - F_x \cdot v_x =$$

$$= \underbrace{F_z \cdot e \cdot \omega}_{T_{RR} \cdot \omega = P_{LossRR}} + \underbrace{F_x \cdot (R_L \cdot \omega - v_x)}_{P_{LossSlip}};$$

We identified P_{LossRR} as what intuitively is a power loss due to the rolling resistance torque, $P_{LossRR} = T_{RR} \cdot \omega$. The remaining is identified as a loss due to slip, called $P_{LossSlip}$.

Note 1: The exact model of rolling resistance is not important as long as it is physically explainable. We can, e.g., think of it as the simple model: $e = RRC \cdot R_{Nom};$.

Note 2: While F_x is a function of $s_x = (R_E \cdot \omega - v_x)/|R_E \cdot \omega|$, where R_E is used as opposed to R_L one can be surprised that the $P_{LossSlip}$ as expressed in R_L as opposed to R_E, see 2.2.3.1.1.1. However, if we can use a tyre force(slip) model we see how R_E joins R_L in the expression, so both appears:

$$P_{LossSlip} = F_x \cdot (R_L \cdot \omega - v_x) = \left\{e.g.\ F_x = CC_x \cdot F_z \cdot \frac{R_E \cdot \omega - v_x}{|R_E \cdot \omega|};\right\} =$$

$$= CC_x \cdot F_z \cdot \frac{(R_E \cdot \omega - v_x) \cdot (R_L \cdot \omega - v_x)}{|R_E \cdot \omega|};$$

So, we have divided the total power loss in the wheel into rolling resistance loss (a.k.a. force or torque loss), and slip loses (a.k.a. velocity losses) using the vertical force offset $e = RRC \cdot R_{Nom}$ and CC_x from the brushmodel, respectively.

$$P_{Loss} = P_{LossRR} + P_{LossSlip};$$

where:

$P_{LossRR} = F_z \cdot e \cdot \omega;$

$P_{LossSlip} = F_x \cdot (R_L \cdot \omega - v_x);$

where a model for the pressure distribution and losses due to radial friction, e.g., Eq [2.7], can be used to express the offset e, and

where a force-vs-slip model, e.g., Eq. [2.13], can be used to express $F_x(v_x, \omega)$ which makes $P_{LossSlip}$ dependent of both R_L and R_E.

[2.42]

Note, the above expressions derived from power equilibrium leads to a different expression than we found in 2.2.3.1.1.1 in the derivation based on integral over contact patch of shear stress and sliding velocity.

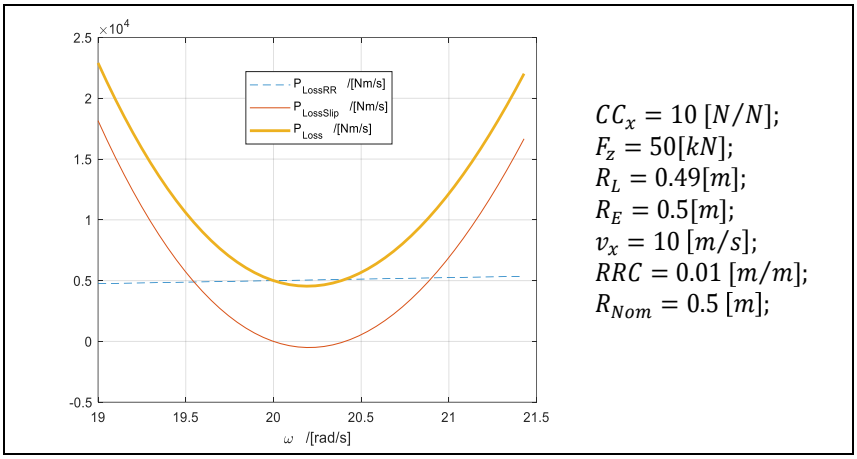


Figure 2-54: Numerical test of Eq [2.42]. The slip loss becomes negative for $v_x/R_E < \omega < v_x/R_L$.

See also 2.2.1.7.

2.2.4 Lateral tyre force and slip

After a vehicle starts moving, controlling the direction of travel becomes a high priority for the operator. For wheeled vehicles, the primary mode to control travel direction is to change the orientation of the tyre, i.e., to apply a steering angle. Tyres generate a lateral force when they are oriented at an angle different to the direction of the vehicle motion. The tyre typically deforms as in Figure 2-55.

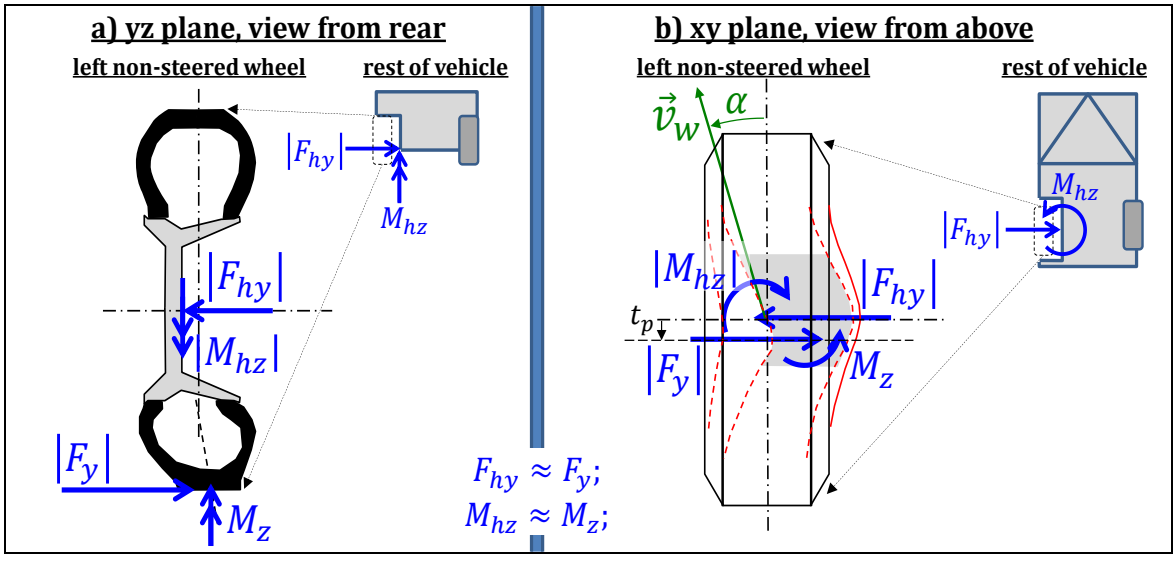


Figure 2-55: Deformation and forces of a tyre with lateral force F_z (and yaw moment M_z). Wheel side slip angle is α.

It is essential to distinguish between the steer angle and wheel (lateral or side) slip angle of the tyre. Lower right part of Figure 1-60 shows this difference. The steer angle, δ or d, is the angle between vehicle longitudinal direction and tyre longitudinal direction. The wheel side slip angle, α is the angle between tyre longitudinal direction and the tyre translational velocity (=wheel hub velocity).

Assuming no longitudinal tyre slip, $R \cdot \omega = v_x$, the relation between the lateral force of a tyre and the wheel side slip angle is typically as shown in Figure 2-60. The behaviour of the curve is similar to that exhibited for longitudinal forces Figure 2-43 and Figure 2-44. It becomes even more similar if lateral slip angle is replaced by lateral wheel slip, s_y, which is $= \tan(\alpha) \approx \alpha$ for small lateral slip.

$$s_y = \frac{v_y}{|R \cdot \omega|} = \begin{Bmatrix} if\ s_x = F_x \approx 0 \\ \Leftrightarrow R \cdot \omega \approx v_x \end{Bmatrix} \approx \frac{v_y}{|v_x|} \cdot \text{sign}(v_x \cdot \omega) = \{if\ v_y \approx 0\}$$
$$\approx \tan(\alpha) \cdot \text{sign}(v_x \cdot \omega) = \{if\ v_x \cdot \omega > 0\} \approx \tan(\alpha)\,; \qquad [2.43]$$

Using magnitude in denominator $|R \cdot \omega|$ gives same sign of s_y and F_y for all combinations of signs of ω and v_y, which leads to easier formulas. Note the 3 assumptions above:

- No combined slip (only lateral): $F_x = 0$
- Small slip: $v_y \approx 0$, and
- Rotational speed have same sign as longitudinal speed: $v_x \cdot \omega > 0$

See also 2.2.4.1.1.2.

2.2.4.1 Brush model for lateral force and slip

With corresponding simplification as in 2.2.1.6, we now use the brush model to also explain the lateral properties.

2.2.4.1.1 Model with Independent Bristles

Figure 2-56 shows the model for pure lateral slip (no longitudinal slip) and should be compared to Figure 2-34. The difference is that the model for lateral slip has the deformation of the bristles perpendicular to drawing in the upper left view in the figure.

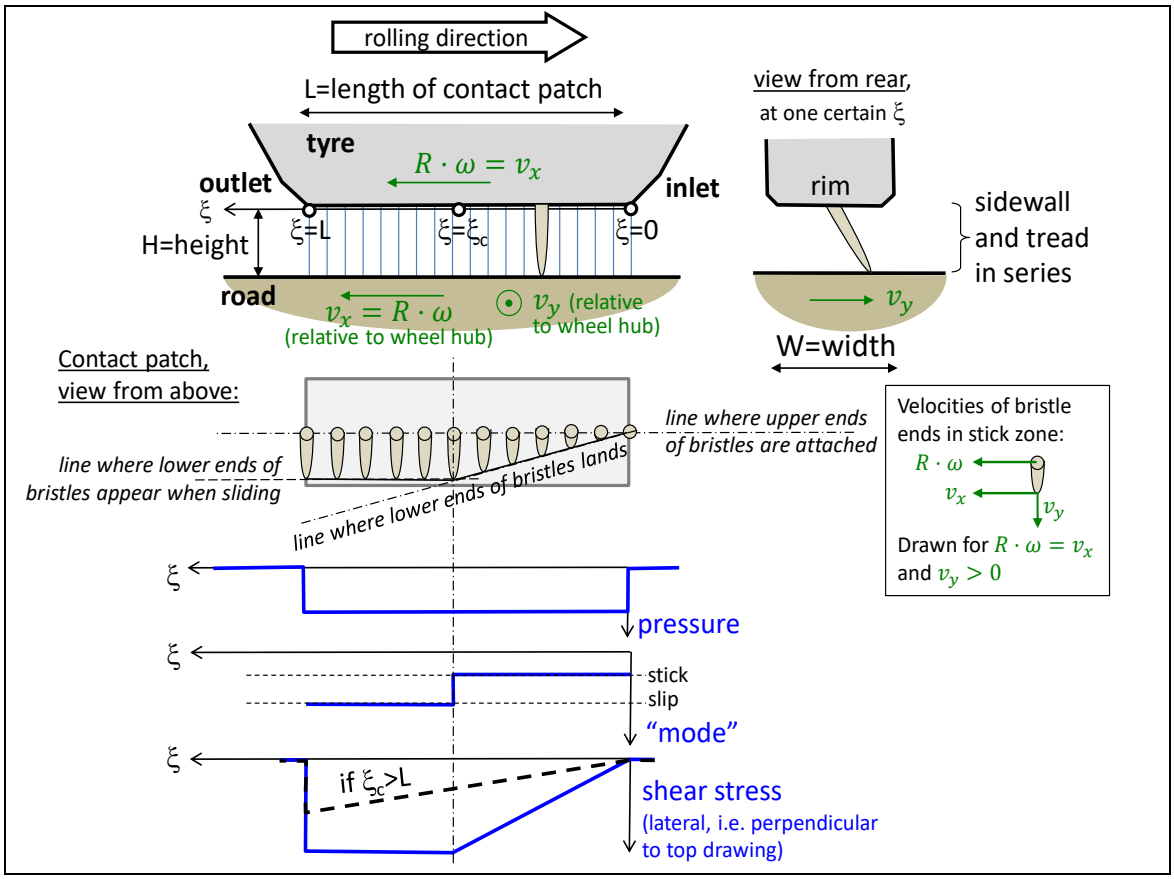


Figure 2-56: The brush model's physical model for lateral slip. The bristles are to be thought of as the ***tread in series with sidewall*** *lateral elasticity.*

Each bristle in Figure 2-56 is thought of as a part of the tread in series with a part of the sidewall. Further, the bristles are considered as independent of each other, which is debatable. However, it is enough for a quantitative explanation of the brush model for lateral slip. The derivation of model equations becomes similar as for the longitudinal model:

$$\tau_y = G_y \cdot \gamma_y = G_y \cdot \frac{\Delta v_y \cdot t(\xi)}{H_y} = G_y \cdot \frac{-v_y \cdot t(\xi)}{H_y} = \left\{ \begin{matrix} t(\xi) = \xi / v_{Transport}; \\ v_{Transport} \approx |R \cdot \omega|; \end{matrix} \right\} =$$

$$= G_y \cdot \frac{-v_y \cdot \xi}{H_y \cdot |R \cdot \omega|} = -\frac{G_y}{H_y} \cdot \frac{v_y}{|R \cdot \omega|} \cdot \xi = \left\{ C_y = \frac{G_y \cdot W \cdot L^2}{2 \cdot H_y};\ s_y = \frac{-v_y}{|R \cdot \omega|}; \right\} = -\frac{2 \cdot C_y}{W \cdot L^2} \cdot s_y \cdot \xi;$$

Note that subscript y has been introduced where we need to differ towards the longitudinal brush model. (In 2.2.4.1.1.2, we will introduce two variants, s_{yt} and s_{yw}. In present derivation, s_y would be denoted s_{yt}.) Correspondingly, subscript x should be used in longitudinal model. As for longitudinal model, we must express the force differently for when friction limit is not reached within the contact and when it is.

$$F_y = \begin{cases} = -C_y \cdot s_y; & if\ |s_y| \le \frac{\mu \cdot F_z}{2 \cdot C_y} \Leftrightarrow |F_y| \le \frac{\mu \cdot F_z}{2} \\ = -\operatorname{sign}(s_y) \cdot \mu \cdot F_z \cdot \left(1 - \frac{\mu \cdot F_z}{4 \cdot C_y} \cdot \frac{1}{|s_y|}\right); & else \end{cases}$$

$$where\ C_y = \frac{G_y \cdot W \cdot L^2}{2 \cdot H_y};\ \ dimension: [force] \quad and\ s_y = \frac{v_y}{|R \cdot \omega|};$$

(Only valid for pure lateral slip, i.e.: $v_x = R \cdot \omega$, and $\operatorname{sign}(v_x \cdot \omega) > 0$.)

[2.44]

Note that the lateral tyre slip s_y is the sliding speed of tyre over ground in lateral direction, divided by the **same** "transport speed" as for longitudinal slip, i.e. the longitudinal transport speed $R_w \cdot \omega$. Note also that the lateral force F_y and lateral tyre slip are counter-directed, which is logical since it is of friction nature.

2.2.4.1.1.1 Parabolic Pressure Distribution

If we assume a parabolic pressure distribution and derive very similar as in 2.2.3.1.5, we get this:

$$-F_y \cdot \text{sign}(s_y) = \begin{cases} = \mu \cdot F_z & if\ \omega \cdot v_x < 0 \\ = C_y \cdot |s_y| - \dfrac{(C_y \cdot |s_y|)^2}{3 \cdot \mu \cdot F_z} + \dfrac{(C_y \cdot |s_y|)^3}{27 \cdot (\mu \cdot F_z)^2}; & else\ if\ |s_y| < \dfrac{3 \cdot \mu \cdot F_z}{C_y} \Leftrightarrow \\ & \Leftrightarrow |F_y| \leq \mu \cdot F_z \\ = \mu \cdot F_z; & else \end{cases}$$

$$where\ C_y = \frac{G_y \cdot W \cdot L^2}{2 \cdot H_y};\ \ dimension: [force] \quad and\ s_y = \frac{v_y}{|R \cdot \omega|};$$

(Only valid for pure lateral slip, i.e.: $v_x = R \cdot \omega$;) [2.45]

2.2.4.1.1.2 Lateral Slip and Slip Angle

The lateral **tyre** slip $s_{yt} = v_{yw}/|R \cdot \omega|$ in Eq [2.44] and Eq [2.47] can be compared with lateral **wheel** slip angle $\alpha = \arctan2(v_{yw}, v_{xw})$ from Figure 2-55:

- "Lateral **wheel** slip"$= s_{yw} = v_{yw}/|v_{xw}|$, is how the wheel (the hub) translates over ground expressed in wheel coordinates. Note that s_{yw} is independent of wheel rotational speed, so it is not useful to model combined tyre slip phenomena.
  - If $v_y \approx 0$ and $v_x > 0$, then $s_{yw} = v_{yw}/|v_{xw}| = \tan(\alpha)$.
  - If $v_y \approx 0$ and $v_x < 0$, then $s_{yw} = v_{yw}/|v_{xw}| = \tan(\pm\pi - \alpha)$.

  One could use subscript h (hub) instead of w (wheel) which might underline that the rotational speed influence is not included. The s_{yw} (or s_{yh}) used in the vehicle motion model **cannot** take the wheels' torque actuation subsystems so accurately into account, since the rotational speed influence is **not** included.
- "Lateral **tyre** slip" $= s_{yt} = v_{yw}/|R \cdot \omega|$, is the slip used in the constitutive relation $F_{yw} = F_{yw}(s_{yt})$.

  One could use subscript ω (rotational speed) instead of t (tyre) which might underline that the rotational speed influence is included. The s_{yt} (or $s_{y\omega}$) used in the vehicle motion model takes the wheels' torque actuation subsystems more accurately into account, since the rotational speed influence is included.
- If no longitudinal tyre slip $s_x = 0$, i.e. if $R \cdot \omega = v_x$, we have $s_{yw} = s_{yt}$. Then s_{yw} can be used in the constitutive relation without any approximation.

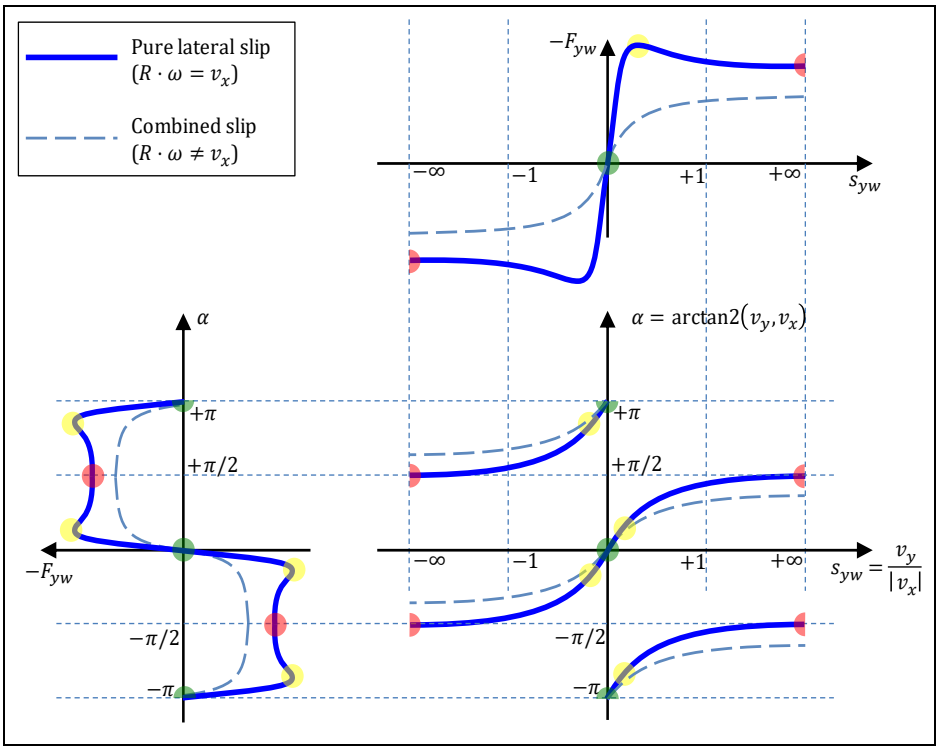


Figure 2-57: Comparison of expressing operating conditions in $F_{yw}(s_{yw})$ or $F_{yw}(\alpha)$.

For a linearization, the most correct way is that lateral force is $F_y \propto s_{yt}$, as opposed to $F_y \propto \alpha$. Often one finds $F_y \propto \alpha$ as starting point in the literature, but this book uses $F_y \propto s_{yt}$. (In (Pacejka, 2005), pp184-185, there is also a note that s_{yt} is more appropriate than α.)

A difference is how one linearizes a vehicle model in v_y and ω_z. A non-steered axle i modelled with $F_{iy} \propto \alpha_i$, needs to be approximated with $\alpha_i = arctan(v_{iyv}, v_{ixv}) \approx v_{iyv}/v_{ixv}$ for $v_x > 0$ (or with $\alpha_i = \pi - arctan2(v_{iyv}, v_{ixv}) \approx \pi - v_{iyv}/v_{ixv}$ for $v_x < 0$, see Figure 1-65) to make the vehicle model linear, see derivation of Eq [4.54]. However, with $F_{iy} \propto s_{iy}$; the vehicle model becomes linear without further approximations.

2.2.4.1.2 Model with Dependent Bristles, String Model

Opposed to the assumption in 2.2.4.1.1, the lateral deformations of the bristles are dependent on each other, especially since the tread is mounted on the belt and the belt is rather like a string. So, we assume a certain deformation of the sidewall, expressed in ε_{in} and ε_{out} for the belt, or "string", in Figure 2-58. This gives a slightly different model compared to 2.2.4.1.1. Models with such belt deformation are called "tyre string models". The shape of the string is dependent on the sidewall elasticity, e.g., tyre profile height, but also of the side force itself. So, the model is intrinsically implicit; the string shape influences the side force and the side force influences the string shape.

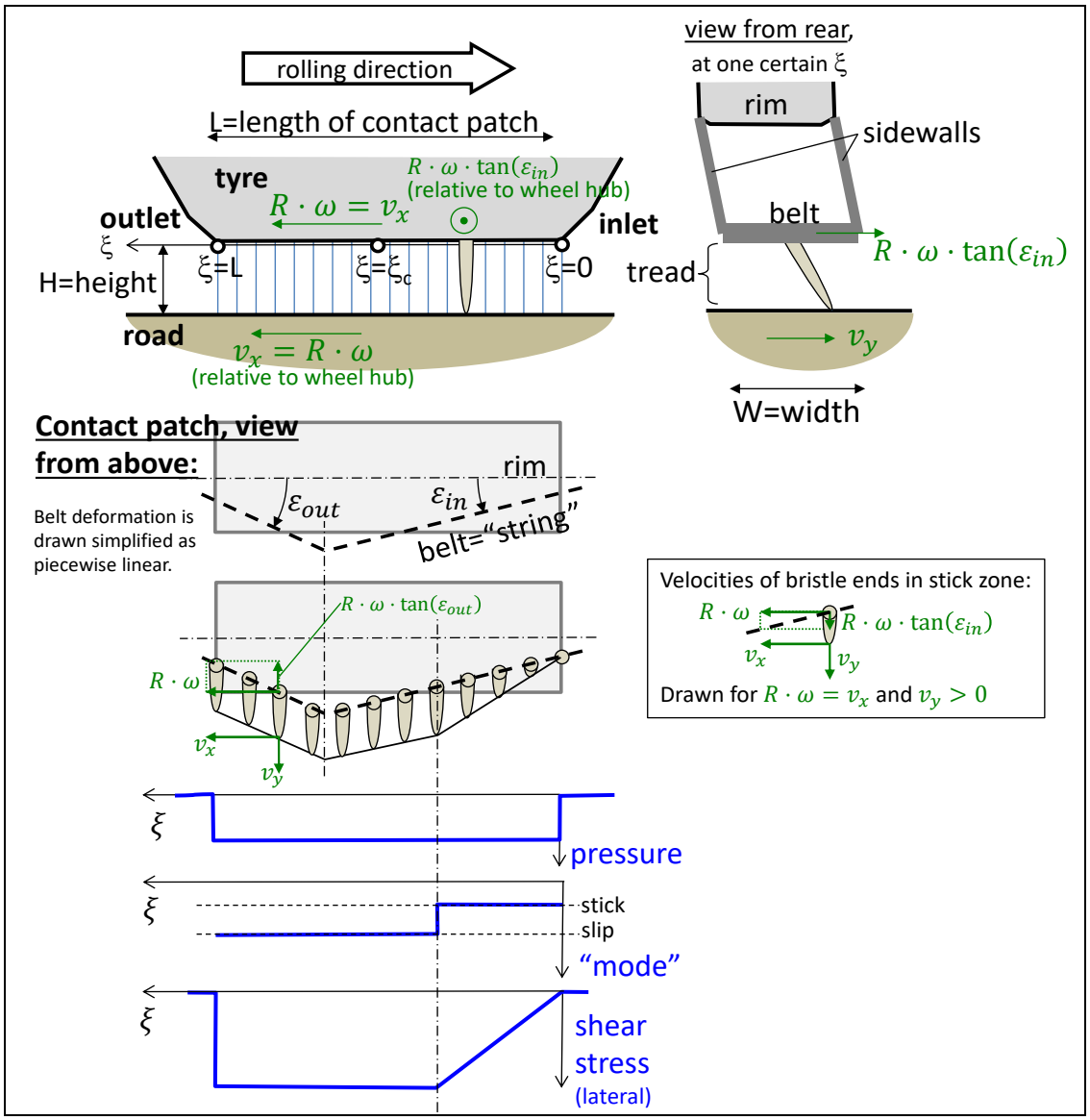


Figure 2-58: Tyre sidewall deformation and tread deformation with the belt (the "string") in between. The drawn bristles are here assumed to represent only tread parts, while the sidewall is treated as an elastic structure between rim and belt.

The derivation of model equations becomes similar as for the longitudinal model. Here is an intermediate result, an expression for the shear stress τ_y:

$$\tau_y = G_{y,tr} \cdot \gamma_y = G_{y,tr} \cdot \frac{\Delta v_y \cdot t(\xi)}{H_{y,tr}} = G_{y,tr} \cdot \frac{\left(R \cdot \omega \cdot \tan(\varepsilon_{in}) - v_y\right) \cdot t(\xi)}{H_{y,tr}} =$$

$$= \left\{ \begin{matrix} t(\xi) = \xi / v_{Transport}; \\ v_{Transport} \approx |R \cdot \omega|; \end{matrix} \right\} = G_{y,tr} \cdot \frac{\left(R \cdot \omega \cdot \tan(\varepsilon_{in}) - v_y\right) \cdot \xi}{H_{y,tr} \cdot |R \cdot \omega|} =$$

$$= \frac{G_{y,tr}}{H_{y,tr}} \cdot \left(\tan(\varepsilon_{in}) \cdot \operatorname{sign}(\omega) - \underbrace{\left(\frac{v_y}{|R \cdot \omega|} \right)}_{s_y} \right) \cdot \xi = \left\{ C_{y,tr} = \frac{G_{y,tr} \cdot W \cdot L^2}{2 \cdot H_{y,tr}} \right\} =$$

$$= -\frac{2 \cdot C_{y,tr}}{W \cdot L^2} \cdot \underbrace{\left(s_y - \tan(\varepsilon_{in}) \cdot \operatorname{sign}(\omega) \right)}_{s_{y\varepsilon}} \cdot \xi;$$

Comparing to 2.2.4.1.1, we can note that subscript tr is added to underline that $C_{y,tr}$ and $G_{y,tr}/H_{y,tr}$ now means only the tread, not including the sidewall. Sidewall elasticity is instead handled with ε_{in}.

The variable $s_{y\varepsilon}$ is an auxiliary mathematical variable introduced only to make the expressions more manageable; it will be eliminated later.

$$F_y = \begin{cases} = -C_{y,tr} \cdot s_{y,\varepsilon}; & if\ |F_y| \le \dfrac{\mu \cdot F_z}{2} \\ = -\operatorname{sign}(s_{y,\varepsilon}) \cdot \mu \cdot F_z \cdot \left(1 - \dfrac{\mu \cdot F_z}{4 \cdot C_{y,tr}} \cdot \dfrac{1}{|s_{y,\varepsilon}|}\right); & else \end{cases}$$

$$where\ C_{y,tr} = \frac{G_{y,tr} \cdot W \cdot L^2}{2 \cdot H_{y,tr}};\ \ dimension: [force]$$

$$and\ s_y = \frac{v_y}{|R \cdot \omega|}\ \ and\ s_{y,\varepsilon} = s_y - \tan(\varepsilon_{in}) \cdot \operatorname{sign}(\omega)\,;$$

Now, this model is still **implicit** because ε_{in} depends on $\tau(\xi)$. Introducing simplest possible (linear) constitutive equation for this dependency as in Eq [2.46]:

$$\int \tau \cdot d\xi = F_y = -C_{sw,\varepsilon,in} \cdot \tan(\varepsilon_{in})\,; \qquad [2.46]$$

Eq [2.46] makes it possible to derive the following **explicit** model:

$$F_y = \begin{cases} = -\dfrac{C_{sw,\varepsilon,in} \cdot C_{y,tr}}{C_{sw,\varepsilon,in} + C_{y,tr}} \cdot s_y; & if\ |F_y| \le \dfrac{\mu \cdot F_z}{2} \\ = -sign(s_y) \cdot \mu \cdot F_z \cdot \dfrac{1 + \dfrac{C_{sw,\varepsilon,in} \cdot |s_y|}{\mu \cdot F_z} - \sqrt{\left(1 - \dfrac{C_{sw,\varepsilon,in} \cdot s_y}{\mu \cdot F_z}\right)^2 + \dfrac{C_{sw,\varepsilon,in}}{C_{y,tr}}}}{2}; & else \end{cases} \qquad [2.47]$$

$$where\ s_y = \frac{v_y}{|R \cdot \omega|};\ \ and\ C_{y,tr} = \frac{G_{y,tr} \cdot W \cdot L^2}{2 \cdot H_{y,tr}};\ \ dimension: [force]$$

(Only valid for pure lateral slip, i.e.: $v_x = R \cdot \omega$;)

It should be noted that the constitutive relation in Eq [2.46] only states how the string is angled. It is still physically consistent to separately add, outside the tyre model, a constitutive equation for the lateral translational deformation of the sidewall; something as $F_y = c_{sw,transaltion} \cdot \delta_{tyre,y}$;, where $\delta_{tyre,y}$ would be the lateral deformation between wheel rim and contact patch. Such sidewall elasticity would appear in series with the lateral tyre slip force model, in a similar way as the torsional sidewall elasticity in 0 appeared in series with the longitudinal tyre slip force model.

2.2.4.1.3 Comparison of the Bristle Models

Eq [2.47] (dependant bristles) is to be compared to Eq [2.44] (independent bristles). Using $C_{ysw} = C_{sw,\varepsilon,in} \cdot C_{y,tr}/(C_{sw,\varepsilon,in} + C_{y,tr})$; the models are identical up to $\mu \cdot F_z/2$ and have the same asymptote for $s \to \infty$. See Figure 2-59.

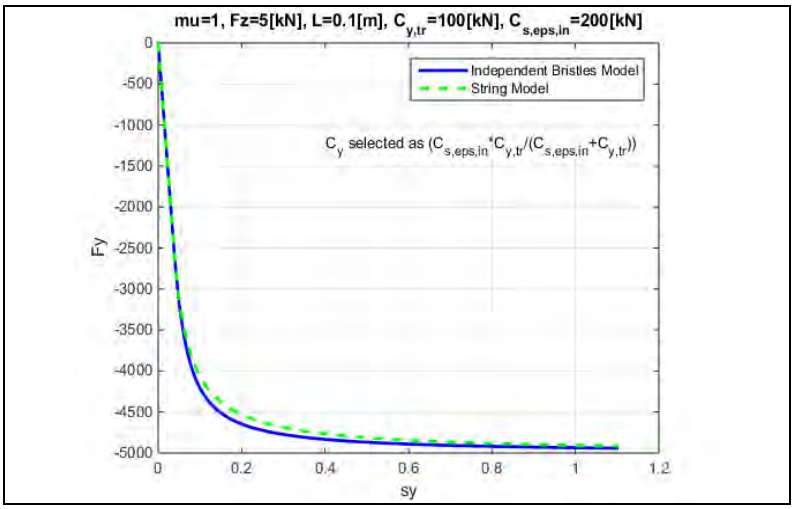


Figure 2-59: Comparison of model with independent and dependent bristles (String model).

The influence of vertical load F_z was discussed in 2.2.3.1.2 but is better explained with dependent bristles. Assumes that only the tread stiffness $C_{y,tr}$ (and not $C_{sw,\varepsilon,in}$) varies with contact length, and that this variation is proportional, $C_{y,tr}(F_z) \propto F_z$;, as we found in 2.2.3.1.2. This indicates a digressive characteristic of $C_y(F_z)$, which is also observed in measurements.

The model with dependent bristles is probably more correct. Anyway, we will use the other most in this book, since it is much easier to combine with the longitudinal model (Eq [2.13]) to model combined (longitudinal and lateral) slip.

One can note that the difference between tyre slip $s_y = s_{yt} = v_y/|R \cdot \omega|$ and $s_{yw} = v_y/|v_x|$ was neglected. It will have some influence if the tyre is exposed to combined longitudinal and lateral slip. One can understand that from realizing that the tyre tread relates to a slip stiffness $[N/(m/s/(m/s)]$ while the side wall relates to a deformation stiffness $[N/m]$..

2.2.4.2 Lateral Tyre Slip Stiffness

In summary for many models (and tests!) the following is a good approximation for small lateral slip (and negligible longitudinal slip and constant normal load):

$$F_y = -C_y \cdot s_y; \quad \text{or} \quad F_y = -C_\alpha \cdot \alpha; \qquad [2.48]$$

For the brush model, or any other model which describes $F_y(s_y, F_z, \mu, \dots)$ or $F_y(\alpha, F_z, \mu, \dots)$, one can define the "Lateral tyre slip stiffness" or "Tyre Cornering Stiffness", C_y or C_α, which have the unit N/1 or N/rad. It is the derivative of force with respect to slip or slip angle. Reference (ISO 8855) defines the cornering stiffness as C_α for slip angle $\alpha = 0$. It is implicit that also $s_x = 0$. And $\alpha = 0$ when $s_y = 0$:

$$C_\alpha = -\left(\frac{\partial}{\partial \alpha} F_y\right)\Big|_{\alpha=s_x=0} \quad = \quad C_y = -\left(\frac{\partial}{\partial s_y} F_y\right)\Big|_{s_y=s_x=0}; \qquad [2.49]$$

When using only small slip, it does not matter if the cornering stiffness is defined as the slope in an F_y versus α diagram or F_y versus $s_y = tan(\alpha)$ diagram. Therefore, the notation for cornering stiffness varies between C_α and C_y. Cornering stiffness has the unit N which can be interpreted differently: as $[N = N/1 = N/((m/s)/(m/s))\,]$ or as $[N = N/rad]$.

The longitudinal tyre slip stiffness, C_x, is normally larger than the lateral tyre slip stiffness, C_y, which can be explained with that the tyre is less stiff in lateral direction. Since it is the same rubber one could argue that both G and H should be the same, but both due to longitudinal grooves in the tread and due to lateral deformable sidewall, it is motivated to introduce different subscripts: $(G/H)_x > (G/H)_y$.

One could elaborate with different friction coefficients μ_x and μ_y, but in this book it is claimed that friction is well modelled as isotropic. More about this in 2.2.4.7.5.

The cornering tyre forces initially exhibit a linear relation with the slip angle. A non-linear region is then exhibited up to a maximum value. In Figure 2-60, the maximum slip angle is only 16 degrees (or $s_y = \tan(16\ deg) = 0.29$) and one can expect that the tyre forces will drop as the slip angle approaches 90 degrees.

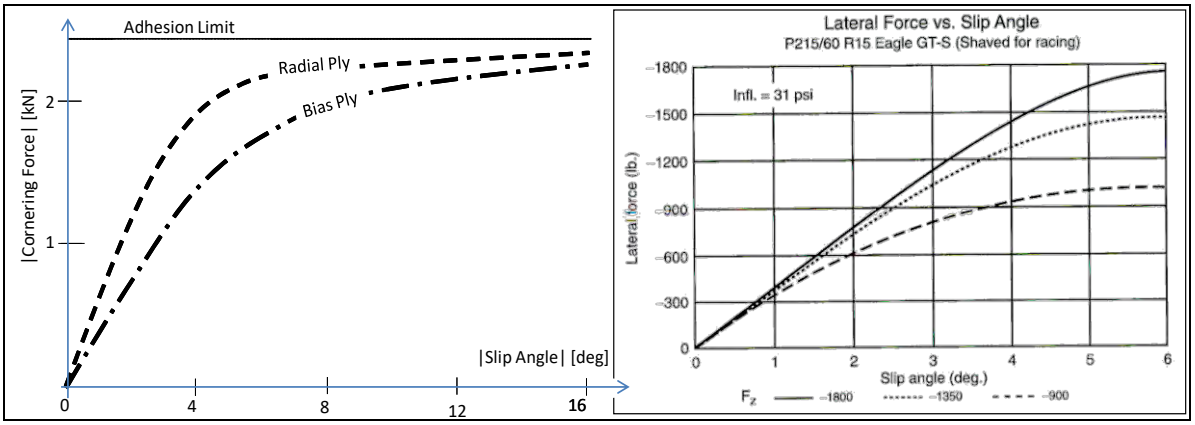


Figure 2-60: Left: Influence of tyre design. Right: Influence of inflation pressure, (Gillespie, 1992).

2.2.4.2.1.1 Local lateral slip stiffness

Reference (ISO 8855) defines and denotes the lateral slip stiffness $C_y = \left(dF_y/ds_y\right)\big|_{F_y=0} = \left(dF_y/ds_y\right)\big|_{s_y=0}$. The more general gradient dF_y/ds_y including $s_y \neq 0$, i.e., including $F_y \neq 0$, is **not** defined or denoted in Reference (ISO 8855). Present book aims at using the name and notation "**local** lateral slip stiffness" and C'_y. Compare to 2.2.3.1.2.1.

The word "local" refers to "local along variation in s_y". So, to underline that it is not a constant, it can be clarifying to denote it $C'_y(F_y)$ or $C'_y(s_y)$, or even $C'_y(F_y, \cdots)$ or $C'_y(s_y, \cdots)$. Generally, C'_y decreases with increasing $|F_y|$.

The C'_y is useful for design of vehicle yaw control, e.g. for linearization. A note here is that we typically do not do this per wheel, but for a whole axle (left and right wheel) or even an axle group (front or rear, where each can include multiple axles). The C'_y for an axle group is approximately the sum of C'_y for many wheels.

2.2.4.3 Influence of Vertical Load

As discussed for longitudinal slip and the rolling resistance behaviour of tyres, the vertical load on the tyre affects the force generation. The general behaviour of the tyre's cornering performance as the vertical load changes is presented in Figure 2-60. These figures show that the cornering stiffness is influenced by vertical load. A first approximation is that $C_y \propto F_z$ with proportionality coefficient $CC_y = CC_\alpha$, the Cornering Coefficient (or Lateral Slip Stiffness Coefficient):

$$F_y = C_y \cdot s_y = CC_y \cdot F_z \cdot s_y; \quad \text{or} \quad F_y = C_\alpha \cdot \alpha = CC_\alpha \cdot F_z \cdot \alpha; \qquad [2.50]$$

We have the linearized in two ways: with respect to F_z and s_y. Slightly better than proportional with respect to F_z is $F_y \approx -CC_{yNom} \cdot (F_z - F_{zNom}) \cdot s_y$; where subscript *Nom* is the tyre's nominal load. Some examples are shown in Figure 2-61 and Figure 2-62. A physically motivated influence from F_z can use combined slip, see 2.2.5.4.

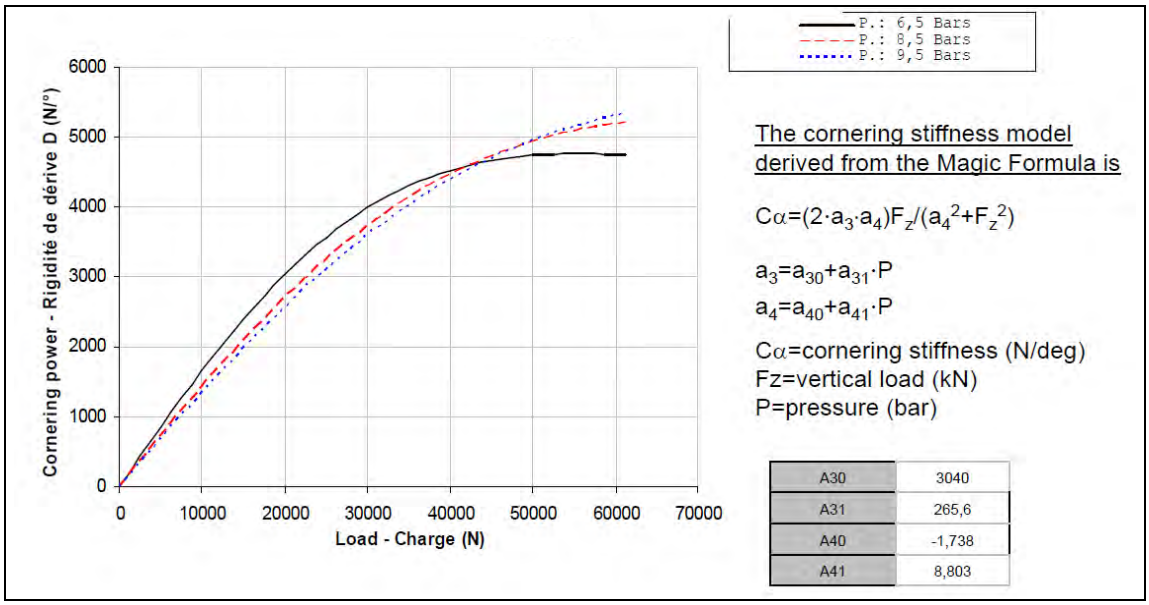


Figure 2-61: Example of cornering stiffness versus vertical load for a truck tyre 295/80R22.5.

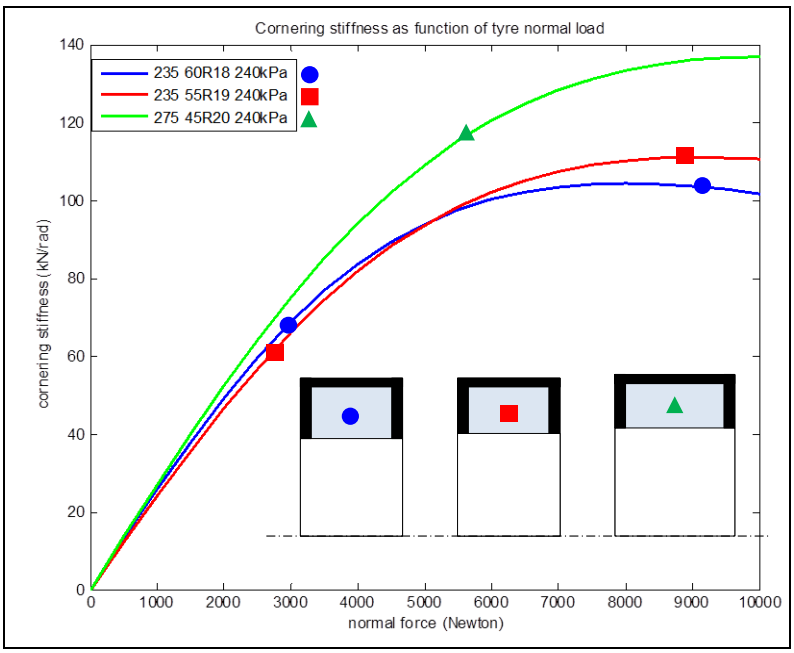


Figure 2-62: Cornering stiffness versus vertical load for some passenger car tyres. From flat track tests.

2.2.4.4 Influence of Tyre Wear

Worn tyres get smaller groove depth and bristle height H. So, worn tyres should be more slip stiff.

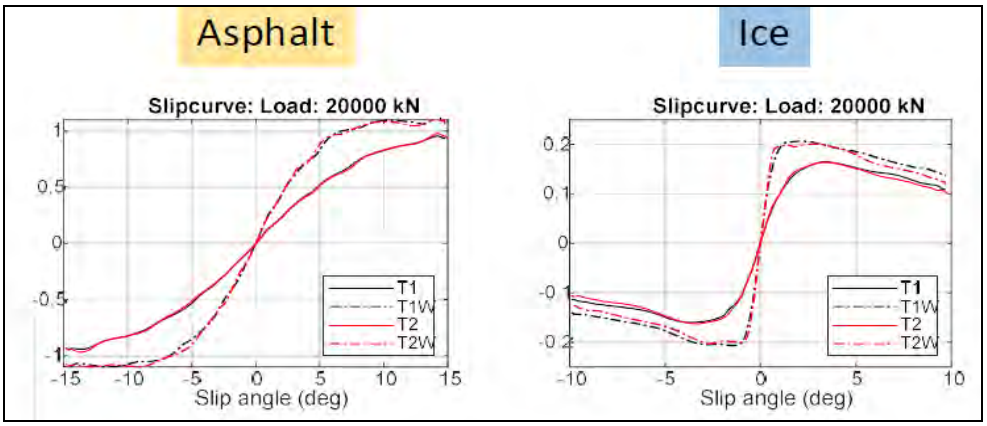


Figure 2-63: Preliminary measurements of lateral slip stiffness for twin-mounted trailer tyres for heavy vehicles. Two tyres, "1" and "2", are measured. "W" means worn to a small groove depth but still legal. From Mattias Hjort and Sogol Kharrazi, VTI.

2.2.4.5 Curve Fit Tyre Models for Lateral Slip

The general form of the lateral force versus lateral slip curve is also suitable for the Magic Formula, TM-Easy, or similar curve fitting approach when sufficient test data is available.

2.2.4.6 Transients and Relaxation

As for longitudinal, there transients between the steady state conditions, see 2.2.3.7.

Below is a model for the transient due to changing the deformation pattern in the contact patch. As in 0, the model is not fully physical, but only exploits a 1st order filter.

$$\dot{F}_y = \frac{1}{\tau} \cdot \left(f_{SS}(s_y, F_z, \mu, \cdots) - F_y \right); \quad [2.51]$$

where $f_{SS}(s_y, F_z, \mu, \cdots)$ is the force according to a steady state model. The slip $s_y = \frac{v_y}{|R \cdot \omega|}$;. The time delay, $\tau = \frac{L_{r,patch}}{v_{Transport}} = \frac{L_{r,patch}}{|R \cdot \omega|}$ and $L_{r,patch}$ is a relaxation length.

The relaxation length $L_{r,patch}$ is, intuitively, of the same magnitude as the stick zone ξ_c, since the stick zone is what has to be "rolled over" before a new deformation pattern of bristles can appear.

In same way as for longitudinal in 2.2.3.7, one can also involve the elasticity of the tyre sidewall. In lateral, this elasticity is the same as modelled as $F_y = -C_{sw,\varepsilon,in} \cdot \tan(\varepsilon_{in})$; in Eq [2.46]. If we identify the relaxation length in Eq [2.51] from real experiments, and the experiments do not take into account that there is difference between $s_y = \frac{v_y}{|R \cdot \omega|}$ and $s_{y,\varepsilon} = s_y - \tan(\varepsilon_{in}) \cdot \sin(\omega)$, we typically get a relaxation length around 25. .50% of the tyre circumference. It includes more than just the patch transients, so the name should then rather be $L_{r,patch,sw}$.

2.2.4.7 Other Forces and Moments in Lateral Use of Tyre

(This section has strong connection with 2.6.2.)

The deformations of the tyre during cornering are quite complex when compared to the case of pure longitudinal motion, see Figure 2-55. Hence, there are more effects than simply a lateral force. Some of these will be discussed in the following.

2.2.4.7.1 Tyre Aligning Moment due to Lateral Shear

In the lowest diagram in Figure 2-56, one can see that shear stress is concentrated to the outlet side of the contact patch for small slip angles. So, the equivalent lateral force acts behind the centre of wheel rotation for small slip angles. As seen in Figure 2-55 b) it acts at a position t_p behind the wheel's y axis.

The distance t_p is called the pneumatic trail, see also Figure 2-64, and the resulting yawing moment around a vertical axis through centre of the contact patch will be $= F_y \cdot t_p$, which is often called the tyre aligning moment, M_z. The moment is named after that is normally acts to align the wheel in direction of zero side slip. Figure 2-64 shows $M_z = F_y \cdot t_p$, but also a similar moment, $F_y \cdot (t_p + c)$. Additional effects from τ_x are not drawn.

If the tyre is on a steered axle, the aligning moment influence on steering wheel torque is important. When finding that influence, the moment around the steering axis intersection with ground is the important moment $= F_y \cdot (t_p + c)$, which can be called the steering moment. The distance c is the mechanical trail, which is built into the suspension linkage design. One typically designs the suspension so that $c > 0$, which makes the whole steering moment act in the same direction as the aligning moment. If driver takes his hands from steering wheel in a curve, and/or if steering power assistance is lost, the steering will tend to steer in the direction of body motion above the steered axle, which is normally relatively smooth and safe.

Figure 2-64 shows the combined response of lateral force and slip angle. It is interesting to note that the steering torque reaches a peak before the maximum lateral force capacity of the tyre is reached. It can be used by drivers to find, via steering wheel torque, a suitable steer angle which gives a large lateral force but still does not pass the peak in lateral force. The reason why pneumatic trail can become slightly negative is because pressure centre is in front of wheel centre, see Figure 2-21.

2.2.4.7.1.1 Tyre Aligning Moment in due to Lateral Shear in Brush Model

A model for (yawing) aligning moment around a vertical axle through centre of contact point, M_z, will now be derived. Any model for lateral shear stress can be used, but we will here only use the uniform pressure distribution and independent bristles in 2.2.4.1.1. A corresponding expression as Eq [2.44] is derived, but for M_z instead of F_y.

$$M_z = -W \cdot \int_0^L \tau \cdot \left(\xi - \frac{L}{2}\right) \cdot d\xi = \cdots =$$

$$= \begin{cases} = -\mathrm{C_y} \cdot \dfrac{L}{6} \cdot s_y; & for\ F_y < \dfrac{\mu \cdot F_z}{2} \Leftrightarrow s_y < \dfrac{\mu \cdot F_z}{2 \cdot C_y} \\ = -\dfrac{\mu^2 \cdot F_z^2 \cdot L}{8 \cdot C_y \cdot s_y} \cdot \left(1 - \dfrac{\mu \cdot F_z}{3 \cdot C_y \cdot s_y}\right); & else \end{cases}$$

$$where\ C_y = \frac{G_y \cdot W \cdot L^2}{2 \cdot H_y};$$

[2.52]

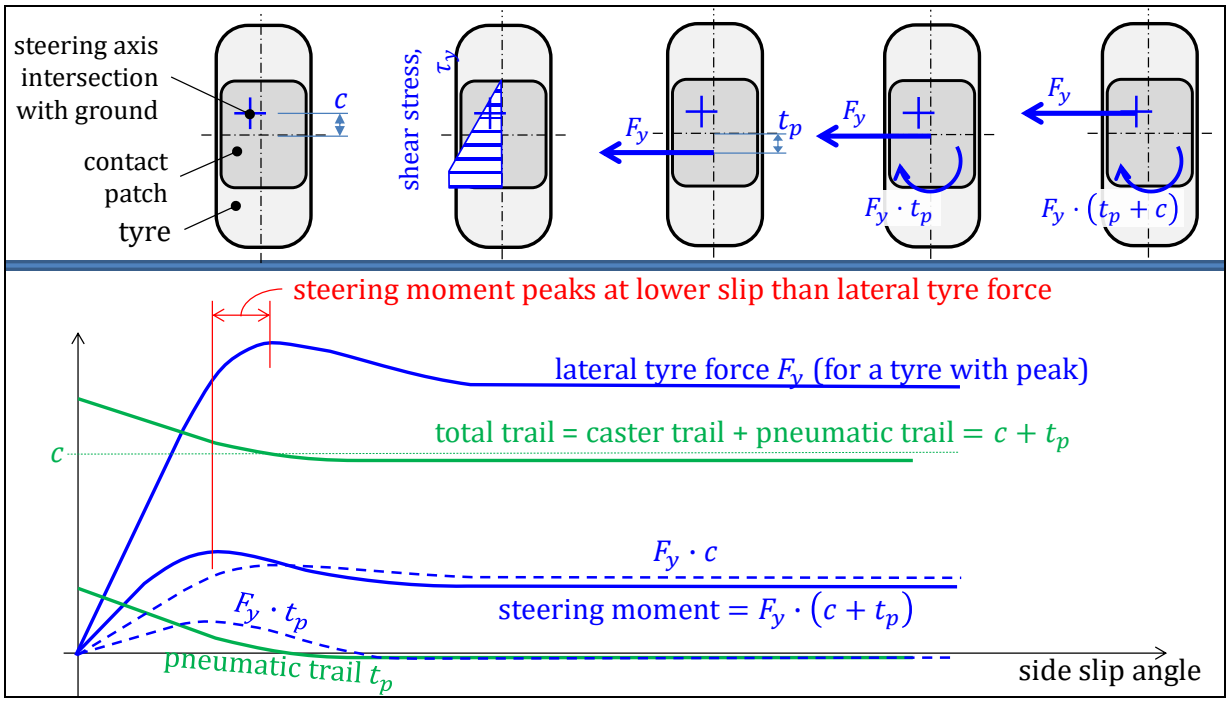


Figure 2-64: General Response of Steering torque to Side slip angle. Tyre aligning moment = $F_y \cdot t_p$ is one part of the steering moment= $F_y \cdot (t_p + c)$.

The curve of Eq [2.52] is plotted in Figure 2-65.

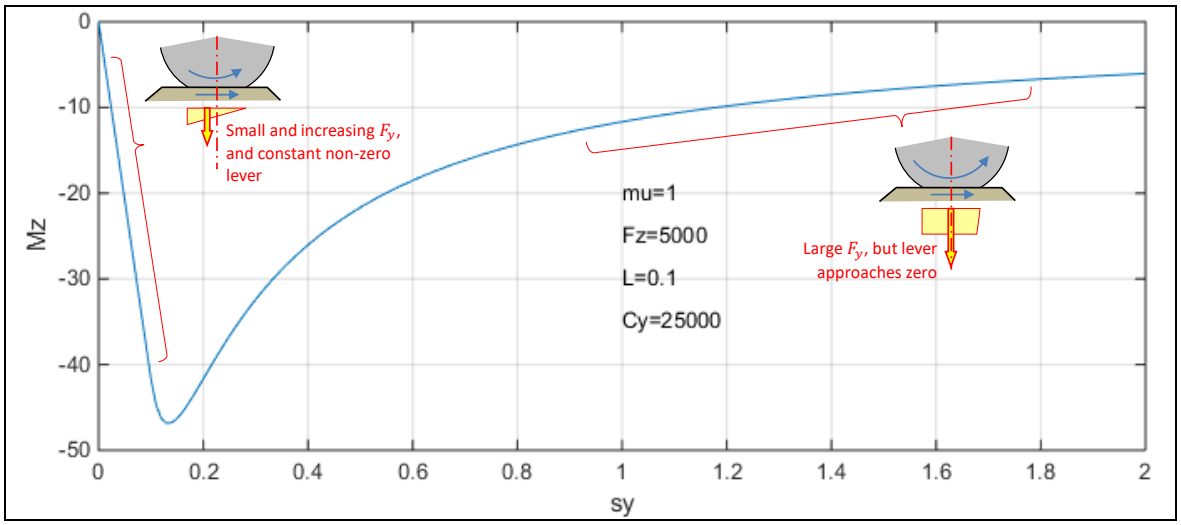


Figure 2-65: Aligning moment (M_z) around contact patch center for uniform pressure distribution.

The lateral force and the aligning torque can be used to calculate the steering forces. If also the steering assistance is known, the steering wheel torque can be calculated. It can be noted that the model does not include the moment from steering rotation itself, i.e. the torque counteracting $\dot{\delta}$.

2.2.4.7.2 Both Lateral and Longitudinal Shear

Figure 2-64 does not show effects from τ_x, but Figure 2-67 shows influence from both τ_x and τ_y. The none-symmetry in shear stress around wheel centre in Figure 2-67 can appear as steady state; non-symmetry in τ_y due to brush model and in τ_x due to non-symmetric vertical pressure.

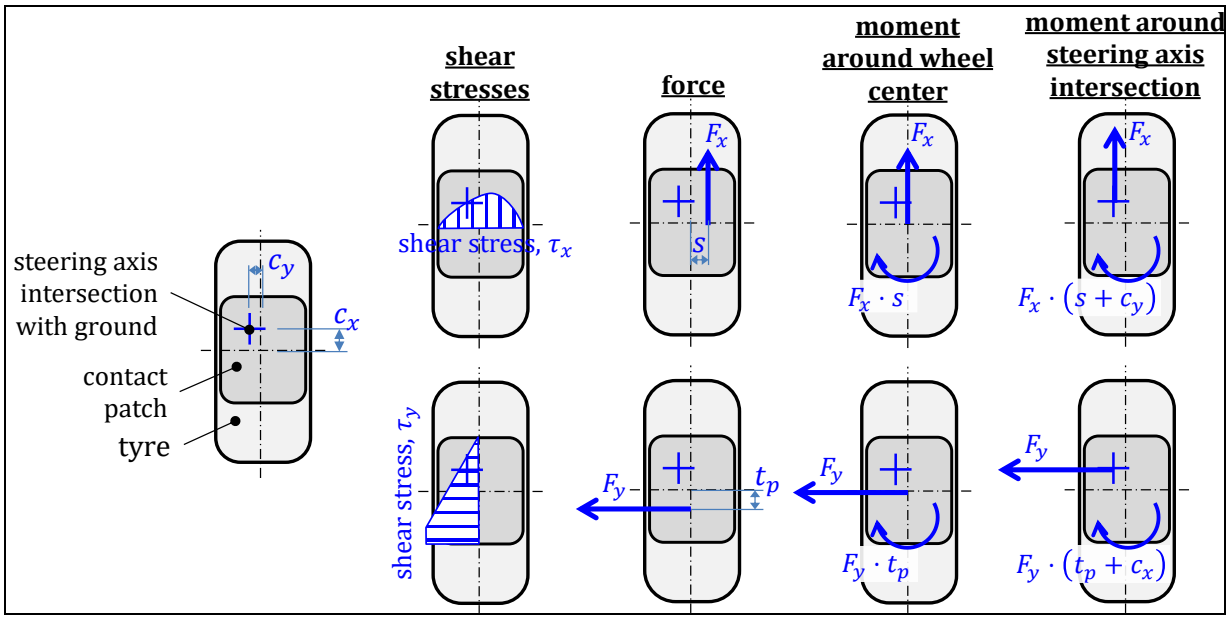


*Figure 2-66: Influence from both lateral and longitudinal shear stress on aligning moment. The wheel yaw velocity relative to ground is **not** considered.*

2.2.4.7.3 Tyre Torque from Steering Angle Change

There is an additional phenomenon that generates shear stresses in tyre contact patch. This is typically at low speed and steering a lot, e.g. at parking manoeuvres. Then, the wheel develops additional F_x, F_y, M_z in the contact patch due to wheel yaw velocity $\omega_{whl,z}$, sometimes called *wheel turn slip,* or *tyre turn slip*. The additional moment M_z is sometimes called *bore torque*. The typical vehicle operation is at low speed when changing the wheel steering angles while the forward motion and wheel (pitch) velocity is neglectable, so the F_x, F_y, M_z from slip s_x and s_y is neglectable.

The yaw velocity of the wheel relative to ground $\omega_{wheel,z} \approx \dot{\delta}_{wheel}$. One way to model it is, are conceptually an elastic torsional spring in series with friction. But if assuming the shear stiffness in the contact patch is high, the tyre slides relative to the gound in all locations in contact patch, so:

$$\{\tau_x, \tau_y\} = \mu \cdot p(\xi,\eta) \cdot \frac{\{x_{MP} - x, y_{MP} - y\}}{\sqrt{(x_{MP} - x)^2 + (y_{MP} - y)^2}} \cdot \text{sign}(\omega_{wheel,z}); \quad where\ \omega_{wheel,z} \approx \dot{\delta}_{wheel};$$

$$F_x = \int_A \tau_x \cdot dA; \quad and \quad F_y = \int_A \tau_y \cdot dA; \quad and \quad M_z = \int_A \tau_y \cdot \sqrt{(x_{MP} - x)^2 + (y_{MP} - y)^2} \cdot dA;$$

2.2.4.7.4 Camber Force

Camber force (also called Camber thrust) is the lateral force caused by the cambering of a wheel. Camber thrust $F_{yCamber}$ is approximately linearly proportional to camber angle φ_{wx} for small angles: Camber thrust= $F_{yCamber} = -C_{Camber} \cdot \varphi_{wx}$. The camber stiffness, C_{Camber}, is typically 5..10 % of the cornering stiffness. The tyre lateral forces due to lateral slip F_{ySlip} and due to camber $F_{yCamber}$ are superimposable when they are small:

$$F_y = F_{ySlip} + F_{yCamber} = -C_y \cdot s_y - C_\gamma \cdot \varphi_{wx}; \qquad [2.53]$$

F_{ySlip} and $F_{yCamber}$ use same friction contact to ground so the sum will be saturated by $\mu \cdot F_z$.

A physical model for camber thrust can be derived very similarly to how models in 2.2.3.1 and 2.2.4.1, see Figure 2-68: Brush modes for Camber force (or Camber thrust) $F_{yCamber}$. There action line of $F_{yCamber}$ is often ahead of contact patch centre, which is called Camber Lead.

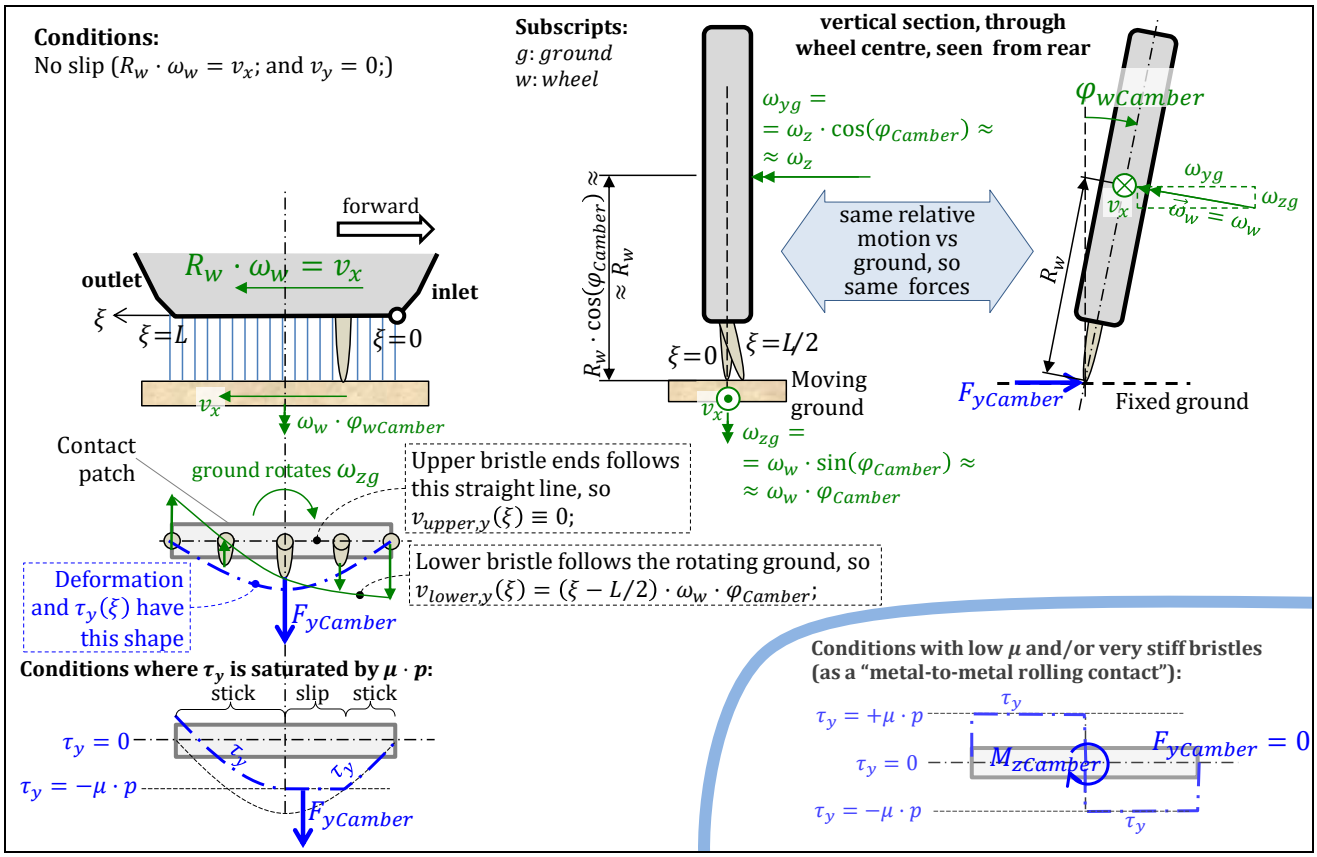


Figure 2-68: Brush modes for Camber force (or Camber thrust) $F_{yCamber}$. Think of ground as rotating opposite to the vertical component of wheel rotation $\vec{\omega}_w$.

$$\tau_y(\xi) = G_y \cdot \gamma_y(\xi) = \left\{ \begin{matrix} it\ takes\ time\ t_\xi \\ for\ a\ bristle \\ from\ inlet\ to\ \xi \end{matrix} \right\} = G_y \cdot \frac{\int_0^{t_\xi} \left(v_{lower,y} - v_{upper,y}(\xi) \right) \cdot dt_\xi}{H_y} = G_y \cdot \frac{\int_0^{t_\xi} \left((\xi - L/2) \cdot \omega_{zg} - 0 \right) \cdot dt_\xi}{H_y} =$$

$$\left\{ \begin{matrix} \xi = v_{transp} \cdot t_\xi = \\ = R_w \cdot \omega_w \cdot t_\xi \end{matrix} \right\} = \frac{G_y}{H_y} \cdot \omega_{zg} \cdot \int_0^{t_\xi} \left(R_w \cdot \omega_w \cdot t_\xi - L/2 \right) \cdot dt_\xi = \frac{G_y}{H_y} \cdot \omega_{zg} \cdot \left[R_w \cdot \omega_w \cdot \frac{t_\xi^2}{2} - \frac{L}{2} \cdot t_\xi \right]_0^{t_\xi} = \frac{G_y}{2 \cdot H_y} \cdot \omega_{zg} \cdot$$

$$\left(R_w \cdot \omega_w \cdot \frac{t_\xi^2}{2} - L \cdot t_\xi \right) = \left\{ t_\xi = \frac{\xi}{R_w \cdot \omega_w};\ \omega_{zg} \approx \omega_w \cdot \varphi_{Camber} \right\} = \frac{G_y}{2 \cdot H_y} \cdot \omega_w \cdot \varphi_{Camber} \cdot \left(R_w \cdot \omega_w \cdot \left(\frac{\xi}{R_w \cdot \omega_w} \right)^2 - L \cdot \right.$$

$$\left. \frac{\xi}{R_w \cdot \omega_w} \right) = \frac{G_y}{2 \cdot H_y} \cdot \frac{1}{R_w} \cdot (\xi^2 - L \cdot \xi) \approx \frac{G_y}{2 \cdot H_y \cdot R_w} \cdot \varphi_{Camber} \cdot (\xi^2 - L \cdot \xi);$$

Integration $F_{yCamber} = \int_0^L \tau_y(\xi) \cdot d\xi$; gives:

$$F_{yCamber} = -C_{Camber} \cdot \varphi_{Camber};\quad where\ C_{Camber} = \frac{G_y \cdot W \cdot L^3}{12 \cdot H_y \cdot R_w};$$

[2.54]

Note: Only valid when no part of the contact patch is saturated by friction.

Checking with typical values for a passenger car tyre gives: $C_{Camber}/C_y = \left(G_y \cdot W \cdot L^3/(12 \cdot H_y \cdot R_w)\right)/\left(G_y \cdot W \cdot L^2/2 \cdot H_y\right) = L/(6 \cdot R_w) \approx 0.1/(6 \cdot 0.3) \approx 0.05 = 5\%$; which is of same magnitud as 5..10%, which was mentioned in beginning of 2.2.4.7.4.

Since the model is physical down to a level of shear stress in each part of the contact patch, it can be extended to include longitudinal and lateral tyre slip.

2.2.4.7.5 Overturning Moment

The contact patch is deflected laterally from the centre of the carcass. This creates an overturning moment M_x due to the offset position of the normal force. The lateral force F_y also contributes to the overturning moment.

2.2.5 Combined Longitudinal and Lateral Slip

Operation of vehicles often involves a combination of steering/cornering and braking/propulsion. Two relatively clean and relevant examples are:

- Loss of side grip due to increased magnitude of wheel torque or longitudinal tyre slip. Typically, this is when increasing propulsion or braking while cornering
- Loss of longitudinal grip due to increased lateral tyre force or tyre side slip. Typically, this is when steering while braking or accelerating.

The first example is maybe most clear; one have to be more careful when changing wheel torques in a curve. Engineering for these manoeuvres requires models of vehicle and wheels/shafts but also tyres. These tyre models have to represent combined slip, i.e. how $[F_x, F_y]$ varies with (s_x, s_{yt}) or (s_x, s_{yw}), where $s_{yt} = v_y/|R \cdot \omega|$ and $s_{yw} = v_y/|v_x|$.

If the tyre has isotropic adhesion properties in the lateral and longitudinal direction, one can assume that the maximum force magnitude F_{xy} is determined by the maximum resultant friction force, $\mu \cdot F_z$.

$$F_{xy}{}^2 = F_x{}^2 + F_y{}^2 \leq (\mu \cdot F_z)^2 \Rightarrow \left(\frac{F_x}{F_z}\right)^2 + \left(\frac{F_y}{F_z}\right)^2 \leq \mu^2 \qquad [2.55]$$

Equation [2.55] can be plotted as a circle, called the "Friction Circle". Since the lateral and longitudinal properties are not isotropic (due to carcass deflection, tread patterns, camber, etc) the shape may be better described as a "Friction Ellipse" or simply "Friction limit".

When not cornering, the tyre forces are described by a position between -1 (braking) and +1 (acceleration) along the $F_x/(\mu \cdot F_z)$ axis. Note that the scales of both axes are normalized to the maximum value for friction.

The "actuation" of the wheel means the propulsion, braking and steering (and sometimes suspension control) of the wheel. An ideal actuation allows all conditions within the boundaries of the friction circle to be achieved anytime during a vehicle manoeuvre. An example of limitation in actuation is a wheel on a non-steered rear axle, which cannot reach any of the lateral parts of the circle; unless the vehicle slides laterally.

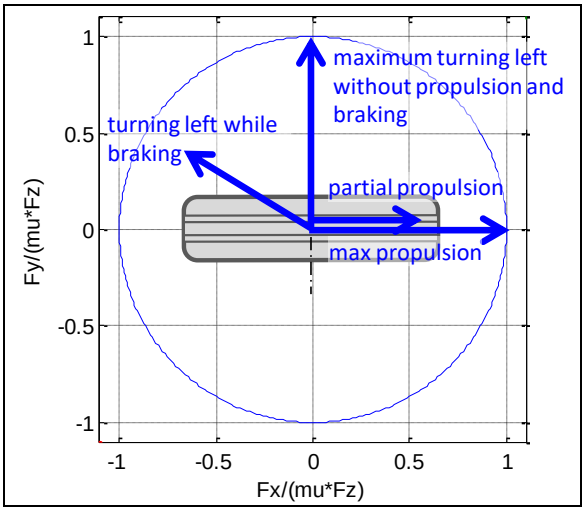


Figure 2-69: Friction Circle with some examples of utilization. View from above, forces on tyre.

At the boundary of the friction circle, tyres become more sensitive to changes in slip. It is therefore extra important to model the direction of the force in relation to shear deformation and relative slip motion in the tyre contact patch. Here, isotropic shear and friction properties are assumed:

$$\frac{lateral\ sliding\ speed}{longitudinal\ sliding\ speed} = \frac{v_y}{R \cdot \omega - v_x} = -\frac{F_y}{F_x}; \qquad [2.56]$$

When considering a combined slip model, one can establish the "total slip" $s_{xyt} = s$, through the definition $s_{xyt}^2 = s^2 = s_x^2 + s_{yt}^2$;. Then, it can be tempting to look for a function $F_{xy} = f(s_{xyt})$; and then decompose F_{xy} into F_x and F_y through $[F_x; F_y] = [+s_x/s_{xyt}\,; -s_{yt}/s_{xyt}] \cdot F_{xy}$. This is not fully physical, which is easiest understood by looking at the brush model for uniform pressure distribution: When s_{xyt} is small enough, there will be no slip in the contact, because $\tau < \mu \cdot p$ in whole contact. For such conditions and isotropic linear deformation model of the bristles, the longitudinal and lateral models from before are valid. Then F_x is independent of s_{yt} and F_y is independent of s_x. So, using s_{xyt} gives a

non-physical dependence. Anyway, such approximate models can be useful for conditions with larger slip, see 2.2.5.3.1.

2.2.5.1 Isotropic and uniform pressure brush model with independent bristles

The longitudinal model Eq [2.13] and the lateral model with independent bristles in 2.2.4.1.1 will now be used with the anisotropy $C_x \neq C_y$;. This is motivated by that sidewall contributes more to lateral bristle elasticity than to longitudinal bristle elasticity. With significantly different tread grooves in longitudinal and lateral direction, one could motivate also difference in friction coefficient μ, but here we assume same μ in both directions. The derivation of mathematical model comes from the physical model inFigure 2-70. It becomes very similar to the derivation for the pure longitudinal and lateral models.

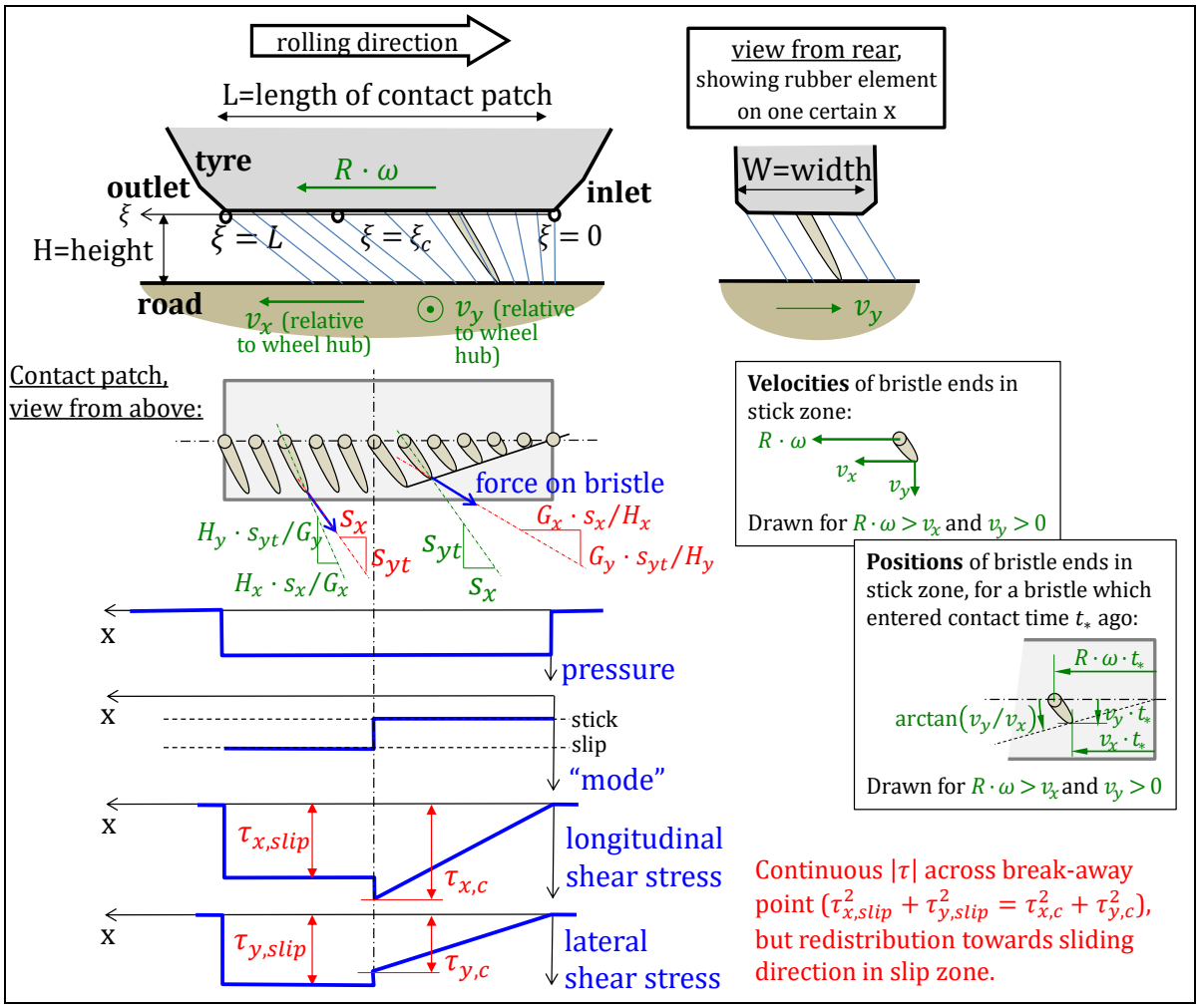


Figure 2-70: Physical model for deriving brush model for combined slip.

For the stick zone:

$$\tau_x = \frac{2 \cdot C_x}{W \cdot L^2} \cdot s_x \cdot \xi; \quad and \quad \tau_y = \frac{2 \cdot C_y}{W \cdot L^2} \cdot s_{yt} \cdot \xi;$$

If no slip in contact:

$$F_x = W \cdot \int_0^L \tau_x \cdot d\xi = W \cdot \int_0^L \frac{2 \cdot C_x}{W \cdot L^2} \cdot s_x \cdot \xi \cdot d\xi = \frac{2 \cdot C_x}{L^2} \cdot s_x \cdot \int_0^L \xi \cdot d\xi = \frac{2 \cdot C_x}{L^2} \cdot s_x \cdot \frac{L^2}{2} = C_x \cdot s_x;$$

$$F_y = W \cdot \int_0^L \tau_y \cdot d\xi = W \cdot \int_0^L \frac{2 \cdot C_y}{W \cdot L^2} \cdot s_{yt} \cdot \xi \cdot d\xi = \frac{2 \cdot C_y}{L^2} \cdot s_y \cdot \int_0^L \xi \cdot d\xi = \frac{2 \cdot C_y}{L^2} \cdot s_{yt} \cdot \frac{L^2}{2} = C_y \cdot s_{yt};$$

Now, if there is a break-away point (ξ_c) where slip starts, we can find it from $\tau(\xi_c) = \mu \cdot p; \;\Rightarrow\; \tau_x^2 + \tau_y^2 = \mu^2 \cdot p^2;$. Introducing an auxiliary parameter, $k = C_x/C_y$, and an auxiliary variable, $s_k = \sqrt{(k \cdot s_x)^2 + s_{yt}^2}$, gives the following break-away point:

$$\tau(\xi_c) = \mu \cdot p; \;\Rightarrow\; \tau_x^2 + \tau_y^2 = \mu^2 \cdot p^2; \;\Rightarrow \cdots \Rightarrow\; \xi_c = \frac{\mu \cdot F_z \cdot L}{2 \cdot C_y \cdot s_{kt}};$$

The forces, when $0 < \xi_c < L$ and $\omega \cdot v_x > 0$ becomes:

$$F_x = W \cdot \int_0^L \tau_x \cdot d\xi = W \cdot \int_0^{\xi_c} \frac{2 \cdot C_x}{W \cdot L^2} \cdot s_x \cdot \xi \cdot d\xi + W \cdot \int_{\xi_c}^L \tau_{x,slip} \cdot d\xi =$$

$$= W \cdot \int_0^{\xi_c} \frac{2 \cdot C_x}{W \cdot L^2} \cdot s_x \cdot \xi \cdot d\xi + W \cdot \int_{\xi_c}^L \mu \cdot p \cdot \frac{s_x}{s} \cdot d\xi = \cdots = \frac{C_x \cdot s_x \cdot \xi_c^2}{L^2} + \frac{\mu \cdot F_z \cdot s_x}{L \cdot s} \cdot (L - \xi_c); \quad \text{and}$$

$$-F_y = W \cdot \int_0^L \tau_y \cdot d\xi = \left\{ \begin{matrix} analogously \\ with\ x\ direction \end{matrix} \right\} = \cdots = \frac{C_y \cdot s_y \cdot \xi_c^2}{L^2} + \frac{\mu \cdot F_z \cdot s_y}{L \cdot s} \cdot (L - \xi_c);$$

Arranging for all combinations of (v_x, v_y, ω), we find Eq[2.57].

$$\begin{bmatrix} F_x \\ F_y \end{bmatrix} = \begin{cases} = \begin{bmatrix} +\mu \cdot F_z \cdot \frac{s_x}{s} \\ -\mu \cdot F_z \cdot \frac{s_{yt}}{s} \end{bmatrix}; & if\ \omega \cdot v_x < 0 \\ = \begin{bmatrix} +C_x \cdot s_x \\ -C_y \cdot s_{yt} \end{bmatrix}; & else\ if\ s_k \le \frac{\mu \cdot F_z}{2 \cdot C_y} \Leftrightarrow F_{xy} = \sqrt{F_x^2 + F_y^2} \le \frac{\mu \cdot F_z}{2} \\ = \begin{bmatrix} +\left(\left(\frac{\xi_c}{L}\right)^2 \cdot C_x \cdot s_x + \mu \cdot F_z \cdot \frac{L - \xi_c}{L} \cdot \frac{s_x}{s}\right) \\ -\left(\left(\frac{\xi_c}{L}\right)^2 \cdot C_y \cdot s_{yt} + \mu \cdot F_z \cdot \frac{L - \xi_c}{L} \cdot \frac{s_y}{s}\right) \end{bmatrix}; & else \end{cases} \qquad [2.57]$$

$$where\ s_x = \frac{R \cdot \omega - v_x}{|R \cdot \omega|}; \quad s_{yt} = \frac{v_y}{|R \cdot \omega|}; \quad s_{xyt} = \sqrt{{s_x}^2 + {s_{yt}}^2};$$

$$k = \frac{C_x}{C_y}; \quad s_k = \sqrt{(k \cdot s_x)^2 + {s_{yt}}^2}; \quad \xi_c = \frac{\mu \cdot F_z \cdot L}{2 \cdot C_y \cdot s_k}; \quad C_x = \frac{G \cdot W \cdot L^2}{2 \cdot H};$$

The terms with $(\xi_c/L)^2$ comes from shear stress in the stick zone, and the direction is in proportion to the stiffnesses C_x and C_y (anisotrop elasticity). The terms with $(L - \xi_c)/L$ comes from the shear stress in the slip zone and it is counter-directed to the relative velocity between the surfaces (isotropic friction).

Figure 2-71 shows results from the model. It can be observed that F_x is independent of s_y and F_y is independent of s_x for $F_{xy} \le \mu \cdot F_z/2$. This is a reasonable consequence of that no sliding occurs for $F_{xy} \le \mu \cdot F_z/2$ which means that forces F_x and F_y are purely defined by the elasticity, not the friction.

Figure 2-71 shows, for $s_{yt} \approx 0.01..0.04$, that F_y increases with utilization of $|F_x|$ at some areas. This is a redistribution of force from longitudinal to lateral, due to that the tyre stiffer in longitudinal than lateral.

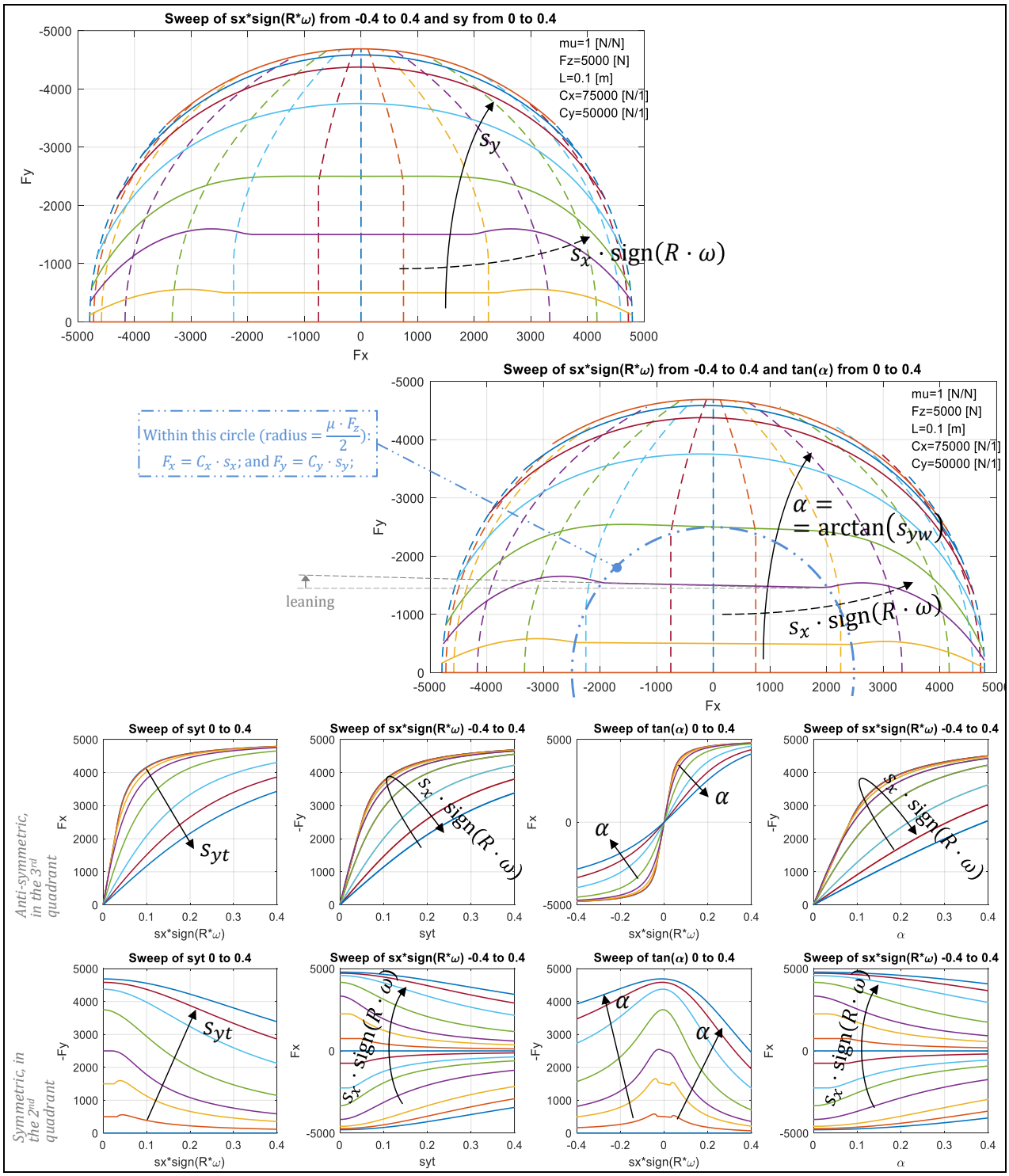


Figure 2-71: Tyre $F(s)$ with iso-curves for longitudinal slip s_x and lateral tyre slip $s_y = v_y/|R_w \cdot \omega|$ (5 left diagrams) and for $s_x = (R_w \cdot \omega - v_x)/|R_w \cdot \omega|$ and slip angle $\alpha = arctan(v_x/v_y)$ (5 right diagrams). Tyre model from Eq [2.57] used. Levels used for slip and tan(slip angle): $0, \pm 0.01, \pm 0.03, \pm 0.05, \pm 0.1, \pm 0.2, \pm 0.3, \pm 0.4$. ($s_y = s_{yt}$)

Note that, for $F_{xy} = \sqrt{F_x^2 + F_y^2} \leq \frac{\mu \cdot F_z}{2}$, F_x is independent of s_{yt} and F_y of s_x. This is because for such low slip and uniform pressure distribution, there is no slipping part in the contact patch. It is the slipping part that creates the "cross-dependence" that F_x depends on s_{yt} and F_y on s_x. The independence appears as the perpendicular iso-s_x and iso-s_y curves for $F_{xy} < \mu \cdot F_z$ in the upper diagrams in Figure 2-71.

For small s_x, it is still a good model that $F_x = F_x(s_x) \propto s_x$ and $F_y = F_y(s_{yt}) \propto s_{yt}$. Then: $F_y = -C_y \cdot s_{yt} = -C_y \cdot v_y/(R_w \cdot \omega) = \{s_x = (R_w \cdot \omega - v_x)/(R_w \cdot \omega)\} = -C_y \cdot v_y \cdot (1 - s_x)/v_x = -C_y \cdot (1 - s_x) \cdot s_{yw}$;. Increasing s_x from 0 to small positive s_x means reduction of $|F_y|$, which should be intuitive since utilization of friction in one direction reduce force in the other. However, decreasing s_x from 0 to small negative s_x means increase in $|F_y|$, which can be counter intuitive. However, the explanation is that the "transport speed" $R \cdot \omega$ decreases, which means a "slip stiffer" tyre. The increase in F_y for small braking is seen in Figure 2-72: slight brake torque on a wheel improves lateral grip!

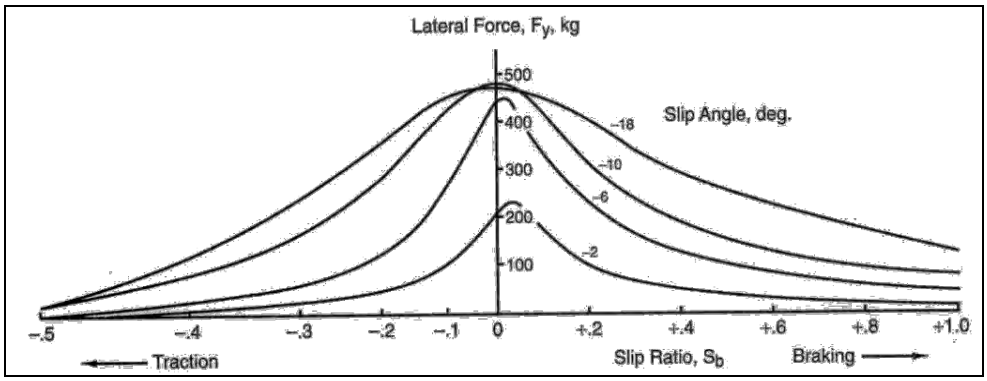


Figure 2-72: Combined longitudinal and lateral Slip. (Tyre) Slip angle $\alpha = arctan(v_y/|v_x|) = arctan(s_{yw})$ is constant for each curve.

2.2.5.2 Anisotropy, Parabolic Pressure, Stick and Slip Friction, Independent Bristles

Section 2.2.5.1 is for uniform pressure distribution and same friction coefficient for stick and slip. We will now change to the more realistic parabolic distribution and replace μ with μ_{stick} and μ_{slip}. The model gets one more parameter and therefore more tunable to experiments, see Eq [2.58].

$$\begin{bmatrix} F_x \\ F_y \end{bmatrix} = \begin{cases} = \begin{bmatrix} +\mu_{slip} \cdot F_z \cdot \frac{s_x}{s} \\ -\mu_{slip} \cdot F_z \cdot \frac{s_{yt}}{s} \end{bmatrix}; & if\ \omega \cdot v_x < 0 \quad or \quad s_k > \frac{3 \cdot \mu_{stick} \cdot F_z}{C_y} \\ = \begin{bmatrix} +\left(C_x \cdot s_x \cdot \left(\frac{\xi_c}{L}\right)^2 + \mu_{slip} \cdot F_z \cdot \left(1 - 3 \cdot \left(\frac{\xi_c}{L}\right)^2 + 2 \cdot \left(\frac{\xi_c}{L}\right)^3\right) \cdot \frac{s_x}{s}\right) \\ -\left(C_y \cdot s_{yt} \cdot \left(\frac{\xi_c}{L}\right)^2 + \mu_{slip} \cdot F_z \cdot \left(1 - 3 \cdot \left(\frac{\xi_c}{L}\right)^2 + 2 \cdot \left(\frac{\xi_c}{L}\right)^3\right) \cdot \frac{s_{yt}}{s}\right) \end{bmatrix}; & else \end{cases} \quad [2.58]$$

$$where \quad s_x = \frac{R \cdot \omega - v_x}{|R \cdot \omega|}; \quad s_{yt} = \frac{v_y}{|R \cdot \omega|}; \quad s_{xyt} = \sqrt{{s_x}^2 + {s_{yt}}^2}; \quad k = \frac{C_x}{C_y};$$

$$s_k = \sqrt{(k \cdot s_x)^2 + {s_{yt}}^2}; \quad \frac{\xi_c}{L} = 1 - \frac{C_y \cdot s_k}{\mu_{stick} \cdot 3 \cdot F_z}; \quad C_x = \frac{G \cdot W \cdot L^2}{2 \cdot H};$$

Eq [2.58] is plotted for steady state conditions in Figure 2-73. We can, for instance, see how $F_y(s_{yt})$ is weakened by increased $|s_x|$. This is very important for yaw and body side slip control by braking and traction of individual wheels/axles. Since the model captures both longitudinal and lateral, it can also be reformulated to how $F_y(s_{yt})$ is influenced by F_x. However, the formula for this becomes probably rather messy, and involves elimination of $R \cdot \omega$. It would also make sense to change from using slip stiffnesses C $[N/1]$ to slip stiffness coefficients CC $[N/N]$, by using $C = CC \cdot F_z$ and eliminate L by a contact model, $L \propto \sqrt{F_z}$. Physically based models are very useful because their validity range is larger; one can vary more variables over larger ranges.

However, using Eq [2.58] in a vehicle simulation, often becomes singular. This is either when $R \cdot \omega = 0$ (locked wheel, which means that s_x and s_y becomes not physically interpretable) or when

$(R \cdot \omega - v_x)^2 + v_y^2 = 0$ (direction of relative velocity becomes not physically interpretable). A way to avoid such computational problems is to introduce a small positive velocity parameter, v_ε, and divde by $\max(|R \cdot \omega|; v_\varepsilon)$ instead of $|R \cdot \omega|$ and $\max(\sqrt{(R \cdot \omega - v_x)^2 + v_y^2}; v_\varepsilon)$ instead of $\sqrt{(R \cdot \omega - v_x)^2 + v_y^2}$. However, one should keep in mind that this gives a tyre model which cannot fully stop if the road has a slope, longitudinally or laterally. It also does not model that the break-away force for a non-rotating tyre on a stand-still vehicle is $F_{xy} = \mu_{stick} \cdot F_z$. If one need to model such, e.g. for start in uphill or banked road, the tyre model needs to be developed to a dynamic model with discrete states.

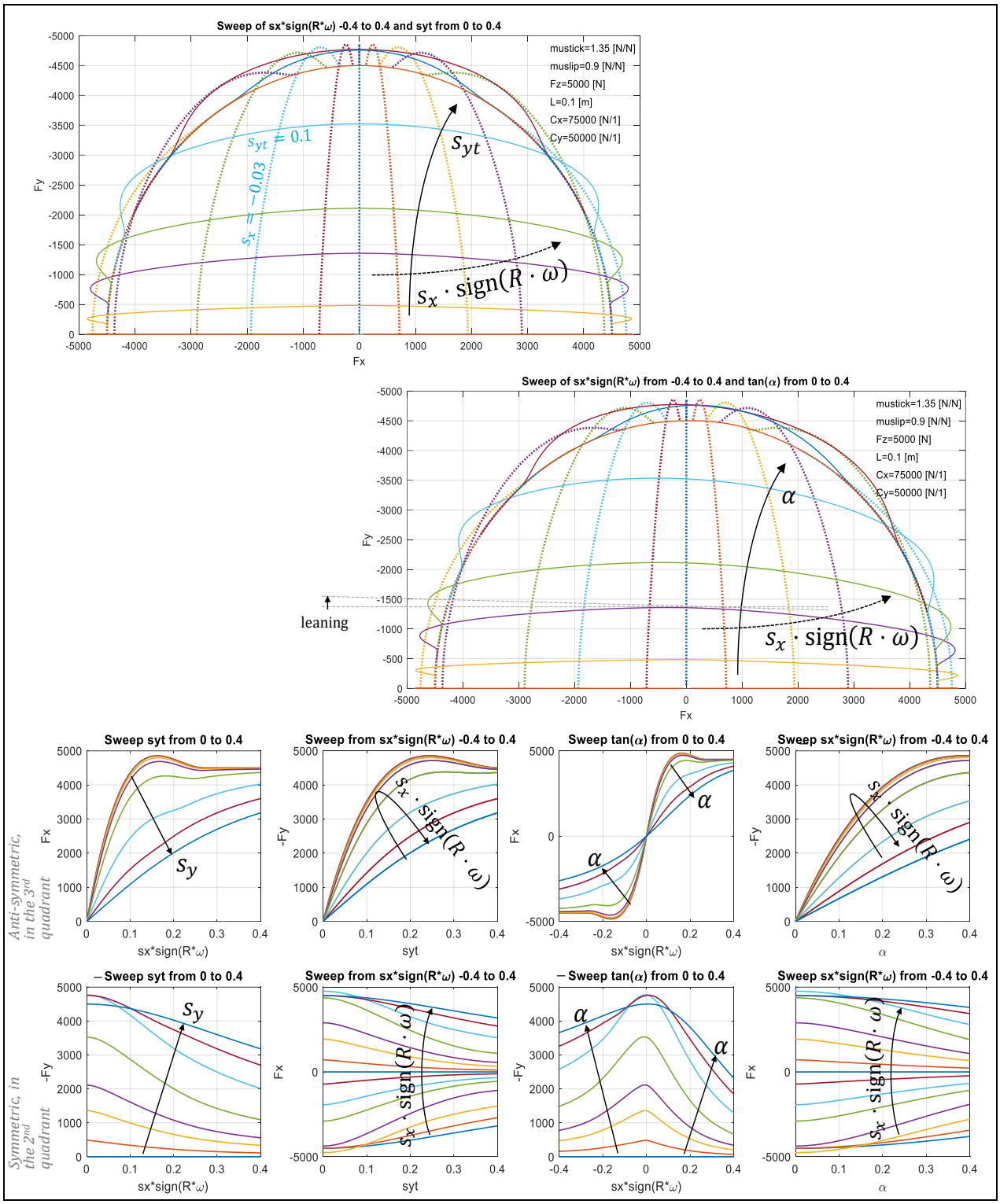


Figure 2-73: Tyre $F(s)$ with iso-curves for longitudinal slip s_x and lateral tyre slip $s_y = v_y/|R_w \cdot \omega|$ (5 left diagrams) and for $s_x = \frac{R_w \cdot \omega - v_x}{|R_w \cdot \omega|}$ and slip angle $\alpha = arctan(v_x/v_y)$ (5 right diagrams). Tyre model from Eq [2.58] and Eq [2.68] used. Levels used for slip and tan(slip angle): $0, \pm 0.01, \pm 0.03, \pm 0.05, \pm 0.1, \pm 0.2, \pm 0.3, \pm 0.4$. ($s_y = s_{yt}$)

If s_x is varied while $s_{yt} \equiv 0$ in Eq [2.58], leads exactly to the longitudinal slip model with peak (Eq [2.24]). Similar peak in F_y is found for varying s_{yt} while $s_x \equiv 0$. The peaks in F_x and F_y are equally large, but the peak in F_y occurs at larger slip: $s_{y,peak} > s_{x,peak}$. Also, for combined slip, a maximum in F_{xy} occurs, but on a "2-dimensional ridge" in the "cake plot" in Figure 2-74.

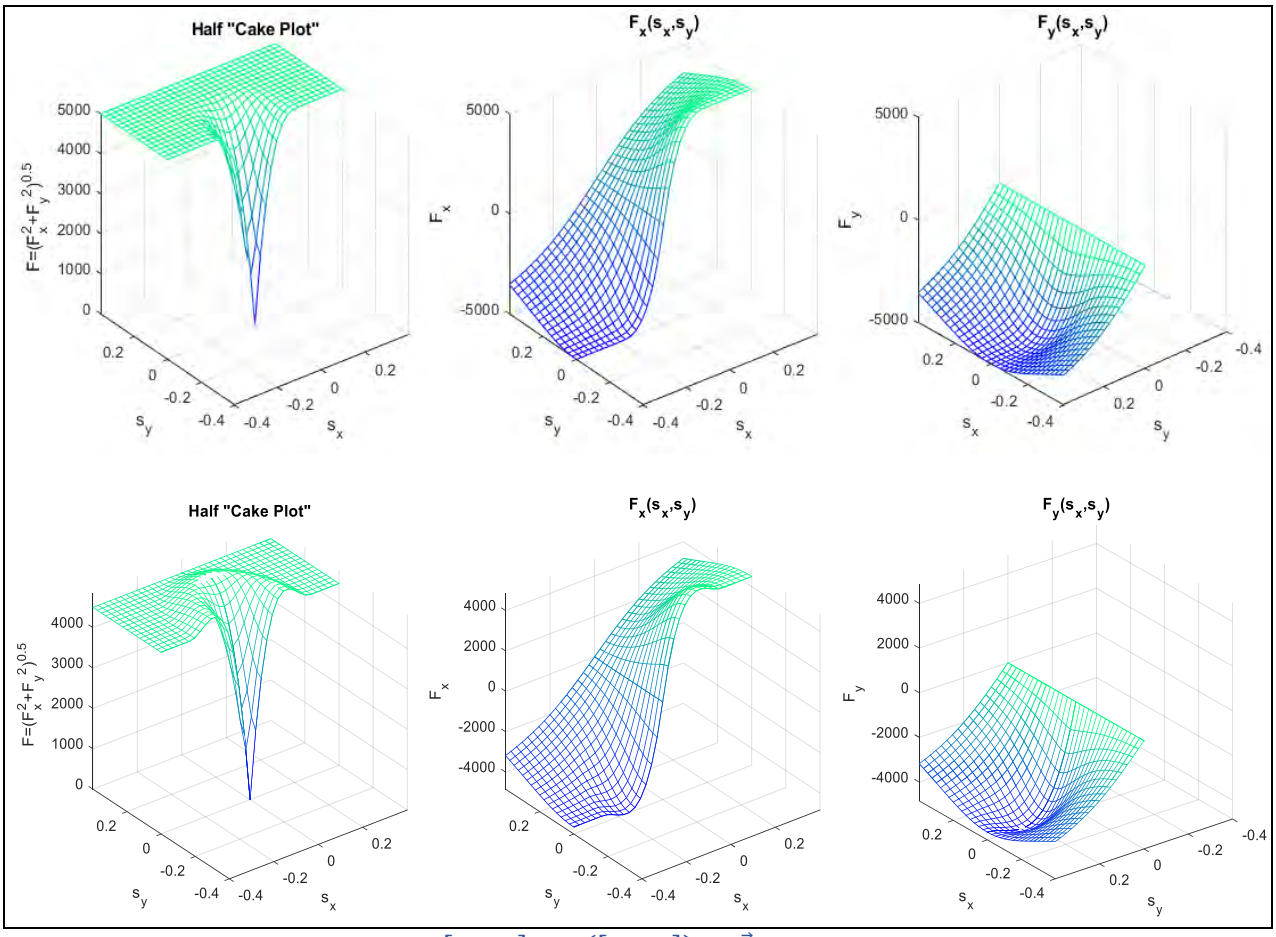


Figure 2-74: Plots of the vector field $[F_x, F_y] = f([s_x, s_y])$ or $\vec{F} = f(\vec{s})$, using the results from Figure 2-71 (above) and Figure 2-73 (below). "Cake-plot" is an expression from (Weber, 1981). ($s_y = s_{yt}$)

We can now look at the local lateral slip stiffness C'_y. For pure lateral slip we had $C'_y(s_{yt})$, but here, with combined slip, we have $C'_y(s_x, s_{yt})$. It also depends on what we hold constant during the partial differentiation $C'_y = \partial F_y / \partial s_{yw}$. In Figure 2-75, this is exemplified with holding s_x or F_x constant. Read more about this in 2.2.5.4.

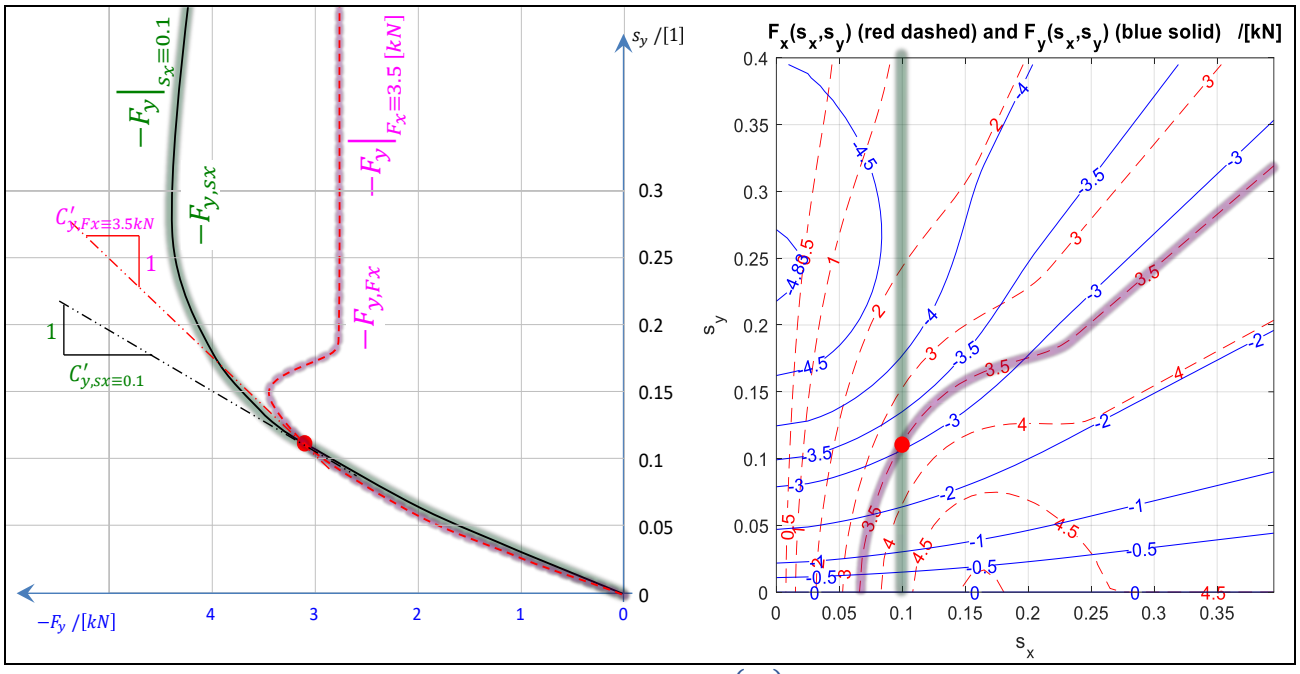


Figure 2-75: Right: From Figure 2-74. Left: Approximate $F_y(s_y)$, holding s_x constant (green shaded) and holding F_x constant (magenta shaded), which gives different F_y and C'_y.

2.2.5.3 Approximate combined slip models

2.2.5.3.1 Scalar force function based combined slip model

A simple but rather physically motivated combined slip model can be based on "total slip, s_{xy}", as shown in Eq[2.59].

$$\begin{bmatrix}F_x\\F_y\end{bmatrix}=\begin{bmatrix}+s_x\\-s_y\end{bmatrix}\cdot\frac{F_{xy}}{s_{xy}}=\begin{bmatrix}R_w\cdot\omega-v_x\\-v_y\end{bmatrix}\cdot\frac{F_{xy}}{\sqrt{(R_w\cdot\omega-v_x)^2+(v_y)^2}};$$

$$where\ s_{xy}^2=s^2=s_x^2+s_y^2;\quad where\ s_x=\frac{R_w\cdot\omega-v_x}{|R_w\cdot\omega|};\quad and\quad s_y=\frac{v_y}{|R_w\cdot\omega|};$$

$$and\ F_{xy}=\begin{cases}=\mu\cdot F_z; & if\ v_x\cdot\omega<0\\=f(\mu,F_z,s_{xy}); & else\end{cases}$$

$$where, e.g.,\ f=f(s_{xy});, e.g., f=\{\text{Eq [2.13], [2.20], [2.22] or [2.24]}\};\ \text{or}$$

$$f=\begin{cases}=F_z\cdot\min(CC_{xy}\cdot s_{xy};\mu);\\=\mu\cdot F_z\cdot\tanh\left((CC_{xy}/\mu)\cdot s_{xy}\right);\\=\cdots;\end{cases}$$

$$where\ CC_{xy}\approx\{typically\}\approx 5..20\ [N/N];$$

[2.59]

With Eq[2.59], anisotropy cannot be modelled. Inspired by Eq [2.57] and Eq [2.58], we can therefore adjust it to Eq [2.60], using μ_k instead of s_{xy}. Eq [2.60] can be tuned to experiment data which has different CC_x and CC_y.

$$\begin{bmatrix} F_x \\ F_y \end{bmatrix} = \begin{bmatrix} +s_x \\ -s_y \end{bmatrix} \cdot \frac{F_{xy}}{s_{xy}} = \begin{bmatrix} R_w \cdot \omega - v_x \\ -v_y \end{bmatrix} \cdot \frac{F_{xy}}{\sqrt{(R_w \cdot \omega - v_x)^2 + (v_y)^2}};$$

$$where\ s_{xy}^2 = s^2 = s_x^2 + s_y^2;\quad where\ s_x = \frac{R_w \cdot \omega - v_x}{|R_w \cdot \omega|};\quad and\quad s_y = \frac{v_y}{|R_w \cdot \omega|};$$

$$and\ F_{xy} = \begin{cases} = \mu \cdot F_z; & if\ v_x \cdot \omega < 0 \\ = f(\mu, F_z, s_k); & else \end{cases}$$

$$where,\ f = f(s_k) = \{as\ Eq\ [2.59], \text{except replacing } s_{xy} with\ s_k\};$$

$$where\ s_k = \sqrt{(k \cdot s_x)^2 + {s_y}^2};\quad k = CC_x/CC_y\,;$$

$$where, typically, CC_y \approx 5..15\ [N/N]\ and\ k \approx 1.5$$

[2.60]

2.2.5.3.1.1 Combined slip model on inverted form

A common usage of combined slip is that (F_x, v_x, v_y) are known and we look for $[F_y, \omega] = func\,(F_x, v_x, v_y)$;. We will try to find that function using Eq[2.59] with $f = \mu \cdot F_z \cdot \text{tanhyp}\left((CC_{xy}/\mu) \cdot s_{xy}\right)$;:

$$s_x = \frac{R_w \cdot \omega - v_x}{|R_w \cdot \omega|};\quad s_y = \frac{v_y}{|R_w \cdot \omega|};\quad s_{xy}^2 = s_x^2 + s_y^2;$$

$$F_{xy} = \mu \cdot F_z \cdot \text{tanhyp}\left(\frac{CC_{xy}}{\mu} \cdot s_{xy}\right);\quad F_x = +\frac{s_x}{s_{xy}} \cdot F_{xy};\quad F_y = -\frac{s_y}{s_{xy}} \cdot F_{xy};$$

So, 6 equations and 6 unknowns ($s_x, s_y, s_{xy}, \omega, F_{xy}, F_y$). We limit to solve for $\omega > 0$ and eliminate ω, F_{xy}, and s_{xy}:

$$s_y = \frac{v_y}{v_x} \cdot (1 - s_x);$$

$$F_x = +\frac{s_x}{\sqrt{s_x^2 + s_y^2}} \cdot \mu \cdot F_z \cdot \text{tanhyp}\left(\frac{CC_{xy}}{\mu} \cdot \sqrt{s_x^2 + s_y^2}\right);$$

$$F_y = -\frac{s_y}{\sqrt{s_x^2 + s_y^2}} \cdot \mu \cdot F_z \cdot \text{tanhyp}\left(\frac{CC_{xy}}{\mu} \cdot \sqrt{s_x^2 + s_y^2}\right);$$

So, 3 equations and 3 unknowns $\{s_x, s_y, F_y\}$. Formally, we can solve for F_y and then find the eliminated, e.g. ω, from equations before the elimination. However, the equation system of 3 equations is transcendent so a symbolic solution cannot be found. (Compare with equation $\sin(x) = x$, which cannot be symbolically solved). We can arrange an iterative numerical solution to find $\{s_x, s_y, F_y\}$.

2.2.5.3.2 Friction circle inspired simplification of combined slip model

A combined slip model for cases when one knows F_x without involving s_x is shown in Eq [2.61]. See also (Svendenius, Tire Modeling and Friction Estimation, 2007) (Svendenius, 2003). The expression for F_y is useful when we know the wheel torque, e.g., by prescribed propulsion or braking and do not consider the wheel rotational inertia, then $F_x = T/R_w$. The expression for F_x in Eq [2.61] shows the corresponding, less usual, case when F_y is known without involving s_y. These models are not fully physically motivated, but can instead be considered "a mathematical scaling, inspired by the friction ellipse-like curves in Figure 2-73". It is a rather good approximation when $F_{xy} \approx \mu \cdot F_z$. But for $F_{xy} \approx 0$, it is less good to scale with $\mu \cdot F_z$ since the forces F_x and F_y are then more dependent of the shear elasticity than of friction and consequently rather independent of each other.

$$F_y = \sqrt{1-\left(\frac{F_x}{\mu \cdot F_z}\right)^2} \cdot \left(F_y(s_y)|_{F_x=s_x=0}\right); \quad and$$

$$F_x = \sqrt{1-\left(\frac{F_y}{\mu \cdot F_z}\right)^2} \cdot \left(F_x(s_x)|_{F_y=s_y=0}\right);$$

[2.61]

Eq [2.63] shows a "concept of scaling" which often also is applied on the slip stiffness coefficients CC_i:

$$CC_x(s_y) = \sqrt{1-\left(\frac{F_y}{\mu \cdot F_z}\right)^2} \cdot \left(CC_x|_{F_y=s_y=0,F_z=F_{z0}}\right) = \sqrt{1-\left(\frac{F_y(s_y)}{\mu \cdot F_z}\right)^2} \cdot CC_x;$$

$$CC_y(s_x) = \sqrt{1-\left(\frac{F_x}{\mu \cdot F_z}\right)^2} \cdot \left(CC_y|_{F_x=s_x=0,F_z=F_{z0}}\right) = \sqrt{1-\left(\frac{F_x(s_x)}{\mu \cdot F_z}\right)^2} \cdot CC_y;$$

[2.62]

2.2.5.3.2.1 Comparison with Physically Motivated Model

Figure 2-76 shows how causality can be changed and why Eq [2.61] and Eq [2.63] are approximations.

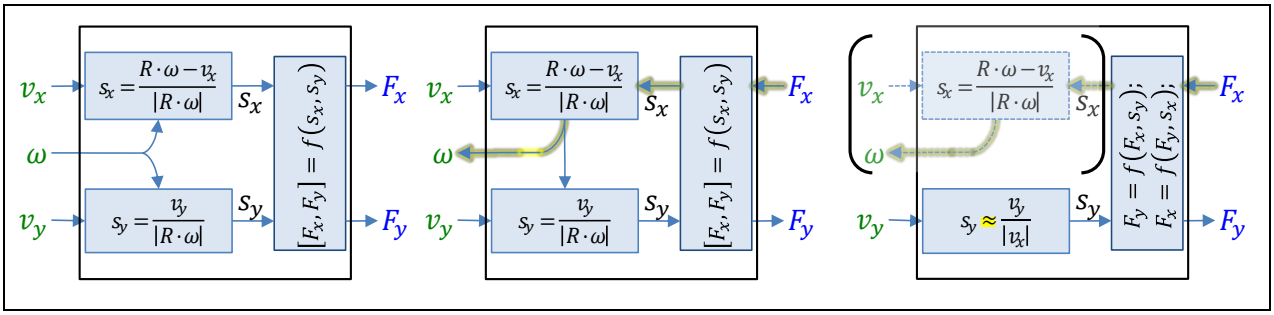


Figure 2-76: Left and middle shows how causality can be changed for a physically motivated model, such as in Eq [2.57] and Eq [2.58], even if the middle generates an algebraic loop. The right shows how Eq [2.61] and Eq [2.63] "cheats", by using an s_y definition which assumes $R \cdot \omega \approx v_x$, which is only motivated without combined slip.

Figure 2-77 compares the resulting approximative forces from Eq [2.61] with the forces from the physical motivated model Eq [2.58]. The approximation is overall good, but least good when both s_x and s_y are small.

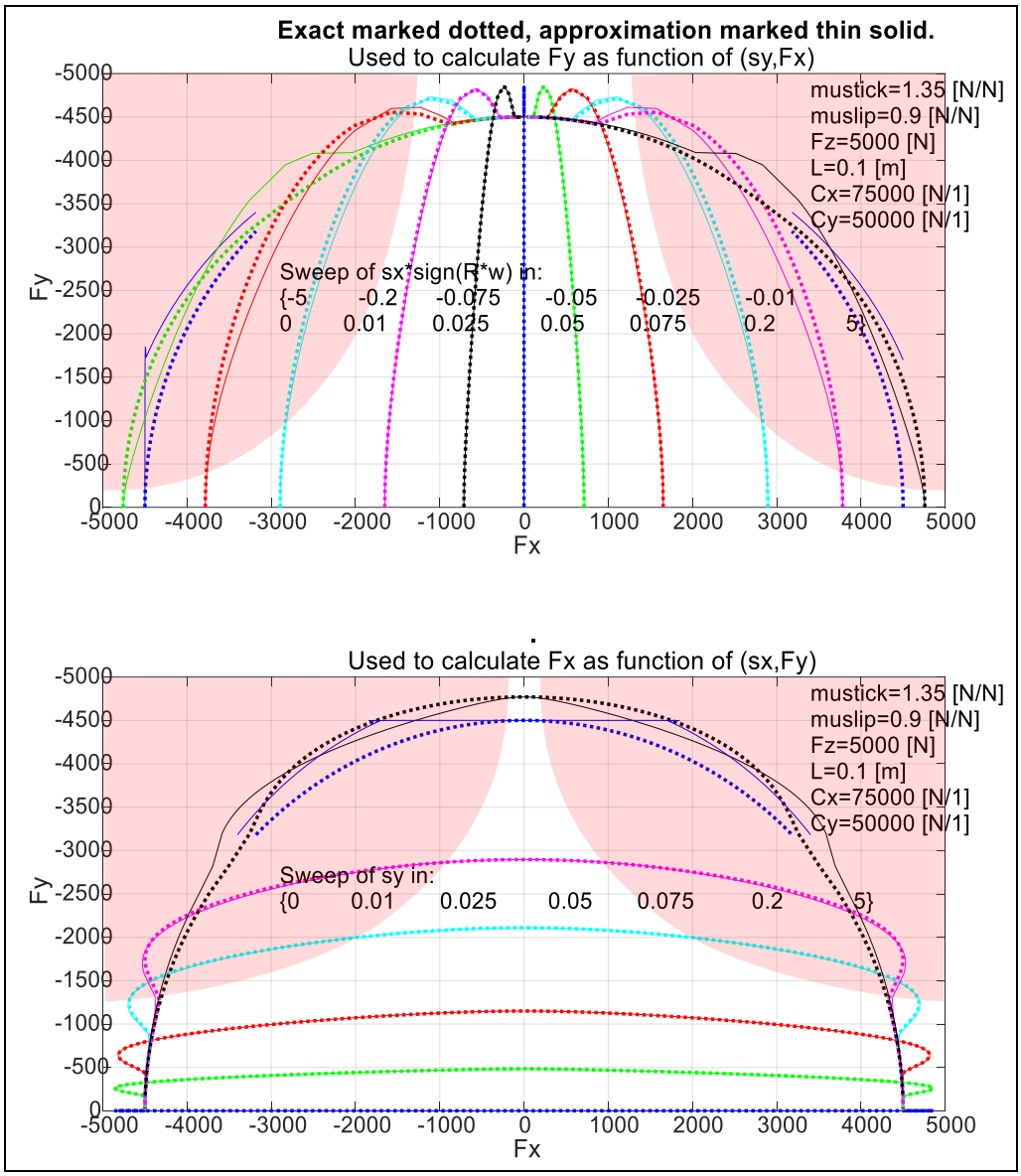


Figure 2-77: Comparison, where "exact" (bold dotted) means Eq [2.58] and "approximation" (thin solid) means Eq [2.61]. The red shaded areas shows where the approximation is judged as worst.

2.2.5.4 Local slip stiffnesses during combined slip

Generally, the (local) slip stiffnesses $\{C'_x, C'_y\}$ *decrease with increasing* $\{|F_y|, |F_x|\}$*, respectively. These two local slip stiffnesses are important for control design of longitudinal wheel slip control (ABS, TC, ...) and lateral slip control of yaw (ESC, ...), respectively.*

The simplest possible brush models (with uniform pressure) distribution (Eq [2.57]) suggests that $F_x \propto s_x$ and F_x is *independent* of s_y (and $F_y \propto s_y$ and F_y is *independent* of s_x) for $F_{xy} < 0.5 \cdot \mu_{Peak} \cdot F_z$. So, $C'_y \approx C_y$ is often a good enough approximation for forces $F_{xy} <\approx (0.25..0.5) \cdot \mu_{Peak} \cdot F_z$ which simplifies the analyses a lot.

The not fully physically deducted combined slip model, Eq [2.61], can be differentiated to find local slip stiffnesses, C'_x and C'_y:

$$C'_{x,F_y}(s_x,F_{y0}) = \left.\frac{dF_x}{ds_x}\right|_{F_y=F_{y0}} = \frac{\partial}{\partial s_x}\left(\sqrt{1-\left(\frac{F_{y0}}{\mu\cdot F_z}\right)^2}\cdot\left(F_x(s_x)|_{F_y=0}\right)\right) =$$

$$= \sqrt{1-\left(\frac{F_{y0}}{\mu\cdot F_z}\right)^2}\cdot\frac{\partial}{\partial s_x}\left(F_x(s_x)|_{F_y=0}\right) = \sqrt{1-\left(\frac{F_{y0})}{\mu\cdot F_z}\right)^2}\cdot C_x; \quad [2.63]$$

$$C'_{y,F_x}(s_y,F_{x0}) = \left.\frac{dF_y}{ds_y}\right|_{F_x=F_{x0}} = \cdots = \sqrt{1-\left(\frac{F_{x0}}{\mu\cdot F_z}\right)^2}\cdot C_y;$$

Holding F_j constant, as indicated in $(dF_i/ds_i)|_{F_j=F_{j0}}$, indicate that the F_{j0} is a known constant or elsehow a known function of time; i.e., controlled or requested. But there are reasons to consider s_j as requested. This, applied to C'_y and C'_x, will be studied in 2.2.5.4.1 and 2.2.5.4.2, respectively.

2.2.5.4.1 Local lateral slip stiffness varies during combined slip

Contributions from Umur Erdinc, Volvo Trucks and Sachin Janardhanan, Volvo Trucks and Chalmers

For, e.g., C'_y, this would mean that F_x is requested denoted F_{x0}. The lateral part of Eq [2.63] shows C'_y for *(longitudinal) force control* which is close to *torque control*, see 4.6.2.2.4 [2.64].

$$C'_{y,T}(s_y,T_0) = C'_{y,T}(s_y,F_{x0})|_{F_{x0}\ expressed\ in\ T_0} = \left(\sqrt{1-\left(\frac{F_{x0}}{\mu\cdot F_z}\right)^2}\cdot C_y\right)\Bigg|_{F_{x0}\ expressed\ in\ T_0} =$$

$$= \left\{\begin{matrix} T_0 = F_x\cdot R + F_z\cdot RRC\cdot R; \\ (wheel\ rotational\ equilibrium) \end{matrix}\right\} = \sqrt{1-\left(\frac{\frac{T_0}{R}-F_z\cdot RRC}{\mu\cdot F_z}\right)^2}\cdot C_y = \sqrt{1-\left(\frac{T_0/R}{\mu\cdot F_z}-\frac{RRC}{\mu}\right)^2}\cdot C_y; \quad [2.64]$$

Torque control is often used for the wheel torque actuator subsystems, i.e. propulsion and brake systems together.

But 4.6.2.2.4 exemplifies two control modes: *torque control* but also *(longitudinal) slip control*. These two modes will give two different values of C'_y, which can be denoted $C'_{y,T}$ and C'_{y,s_x}, respectively.

It is more difficult to find an expression for $C'_{y,sx}$. We start differentiating:

$$C'_{y,s_x}(s_y,s_{x0}) = \left.\frac{dF_y}{ds_y}\right|_{s_x=s_{x0}} = \frac{\partial}{\partial s_y}\left(\sqrt{1-\left(\frac{F_y(s_y,s_{x0})}{\mu\cdot F_z}\right)^2}\cdot\left(F_y(s_y)\right)\Big|_{F_x=0}\right) = \cdots;$$

2.2.5.4.2 Local longitudinal slip stiffness varies during combined slip

A parallel distinction could be between *(lateral) force control* and *(lateral) slip control*, C'_{x,F_y} and C'_{x,s_y}, respectively. Normally we consider the steering as *(lateral) slip control* because we come from a long tradition of human steering via a 1-displacement-dof steering subsystem which, implicitly control the lateral slip through a prescribed steering angle. But with controllable steering systems, e.g., electrical power assisted steering (EPAS) or steer-by-wire (SbW) one could consider a "dual-request-interface" also laterally.

The longitudinal part of Eq [2.63] is very similar to *(lateral) force control*:

$$C'_{x,F_y}(s_y,F_{y0}) = C'_{x,F_y}(s_y,F_{y0})\Big|_{F_{y0}\ expressed\ in\ F_{yAssist}} =$$

$$= \left(\sqrt{1-\left(\frac{F_{y0})}{\mu\cdot F_z}\right)^2}\cdot C_x\right)\Bigg|_{F_{y0}\ expressed\ in\ F_{yAssist}} = \left\{\begin{matrix} F_{y0} = F_{yDrvr} + F_{yAssist}; \\ \left(\begin{matrix}\text{if SbW or driver has hands off the} \\ \text{steering wheel: } F_{yDrvr} = known = 0\end{matrix}\right)\end{matrix}\right\} =$$

$$= \sqrt{1-\left(\frac{F_{yDrvr}+F_{yAssist}}{\mu\cdot F_z}\right)^2}\cdot C_y; \qquad [2.65]$$

It is more difficult to find an expression for controlled slip, $C'_{x,sy}$ and $C'_{y,sx}$. We start differentiating:

$$C'_{i,s_j}(s_i,s_{j0}) = \frac{dF_i}{ds_i}\Big|_{s_j=s_{j0}} = \frac{d}{ds_i}\left(\sqrt{1-\left(\frac{F_j(s_j,s_{i0})}{\mu\cdot F_z}\right)^2}\cdot\left(F_i(s_i)|_{F_j=s_j=0}\right)\right) = \cdots;$$

We see that both factors depends on s_x, which involves the whole combined slip model, $\{F_x,F_y\} = \boldsymbol{F_{xy}}(s_x,s_y)$. The present book does not go further but leaves these local slip stiffnesses to 2.2.5.4.3, where we use a more physically motivated combined slip model.

2.2.5.4.3 Slip stiffness with a scalar force function based combined slip model

Eqs [2.63] and [2.62] uses a friction circle inspired scaling. A more physically motivated model would have a larger validity range. One such model is the combined slip model which uses a *scalar force function*, $F_{xy} = f(s_{xy})$ and force direction counter-directed to sliding velocity $F_x/F_y = s_x/s_y$.

Below, we will derive expressions for local lateral slip stiffness $C'_y = \partial F_y/\partial s_y$ from such combined slip model. We will now also distinguish between $s_{yt} = v_y/|R\cdot\omega|$ and $s_{yw} = v_y/|v_x| = \tan(\alpha)$. We need to decide/understand which of s_{yw} and s_{yt} to differentiate with respect to. We take as engineering example that we want a C'_y for use in a model with the vehicles lateral motion. Then we want to express how F_y varies with the vehicle motion v_y, so we partially differentiate F_y with respect to s_{yw}.

We also need to decide/understand what to hold constant in the partial differentiation. We take as engineering example that we, for a given $\{v_x,v_y\}$. There are two very relevant alternative assumptions:

- ideal longitudinal slip control holds $s_x \equiv s_{x0}$ in the partial differentiation.
- ideal longitudinal force control holds $F_x \equiv F_{x0}$ in the partial differentiation.

There can be a big difference between holding s_x or F_x constant, see Figure 2-75. If we hold F_x constant we typically lower the local slip stiffness, $C'_{yFx} < C'_{ysx}$. We keep both for a while, because both F_x and s_x can be natural to request from the wheel torque actuator system. Now, we can come a bit further:

$$C'_y = \frac{-\partial F_y}{\partial s_{yw}} = \frac{-\partial F_y}{\partial v_y}\cdot\frac{\partial v_y}{\partial s_{yw}} = |v_x|\cdot\frac{-\partial F_y(v_y,\omega)}{\partial v_y} = \begin{cases} = -|v_x|\cdot\frac{d}{dv_y}\left(F_y(v_y,\omega)\big|_{s_x\equiv s_{x0}}\right) = C'_{y,sx}; \\ or \\ = -|v_x|\cdot\frac{d}{dv_y}\left(F_y(v_y,\omega)\big|_{F_x\equiv F_{x0}}\right) = C'_{y,Fx}; \end{cases}$$

$$C'_{y,sx} = -|v_x|\cdot\frac{d}{dv_y}\left(F_y(v_y,\omega)\big|_{s_x\equiv s_{x0}}\right) = \left\{\begin{matrix} use\ s_{x0} = (R\cdot\omega - v_x)/|R\cdot\omega| \\ to\ hold\ s_x \equiv s_{x0}\end{matrix}\right\} =$$

$$= -|v_x|\cdot\frac{d}{dv_y}\left(F_y\left(v_y,\frac{v_x/R}{1\mp s_{x0}}\right)\right) = -|v_x|\cdot\frac{d}{dv_y}\left(F_{y,sx}(v_y)\right);$$

$$C'_{y,Fx} = -|v_x|\cdot\frac{d}{dv_y}\left(F_y(v_y,\omega)\big|_{F_x\equiv F_{x0}}\right) = \left\{\begin{matrix} use\ F_x(v_y,\omega) = F_{x0} \\ to\ hold\ F_x \equiv F_{x0}\end{matrix}\right\} =$$

$$= -|v_x|\cdot\frac{d}{dv_y}\left(F_y\left(v_y,F_{xInv}(v_y,F_{x0})\right)\right) = -|v_x|\cdot\frac{d}{dv_y}\left(F_{y,Fx}(v_y)\right);$$

Now, we use the following tyre model as example:

$$F_{xy} = \mu \cdot F_z \cdot \text{tanhyp}\left(\frac{CC_{xy}}{\mu} \cdot s_{xyt}\right); \quad F_x = \frac{s_x}{s_{xyt}} \cdot F_{xy}; \quad F_y = \frac{-s_{yt}}{s_{xyt}} \cdot F_{xy};$$

$$s_x = \frac{R \cdot \omega - v_x}{|R \cdot \omega|}; \quad s_{yt} = \frac{v_y}{|R \cdot \omega|}; \quad s_{xyt} = \sqrt{s_x^2 + s_{yt}^2}; \quad T = F_x \cdot R_w;$$

We can eliminate the auxiliary slip variables and express it in physical variables.

$$F_x = +\mu \cdot F_z \cdot \frac{R \cdot \omega - v_x}{\sqrt{v_y^2 + (R \cdot \omega - v_x)^2}} \cdot \text{tanhyp}\left(\frac{CC}{\mu} \cdot \frac{\sqrt{v_y^2 + (R \cdot \omega - v_x)^2}}{|R \cdot \omega|}\right);$$

$$F_y = -\mu \cdot F_z \cdot \frac{v_y}{\sqrt{v_y^2 + (R \cdot \omega - v_x)^2}} \cdot \text{tanhyp}\left(\frac{CC}{\mu} \cdot \frac{\sqrt{v_y^2 + (R \cdot \omega - v_x)^2}}{|R \cdot \omega|}\right); \quad [2.66]$$

We can now plot $F_y(s_{yt}), F_y(s_{yw}), F_x(s_{yt})$, and $F_x(s_{yw})$.

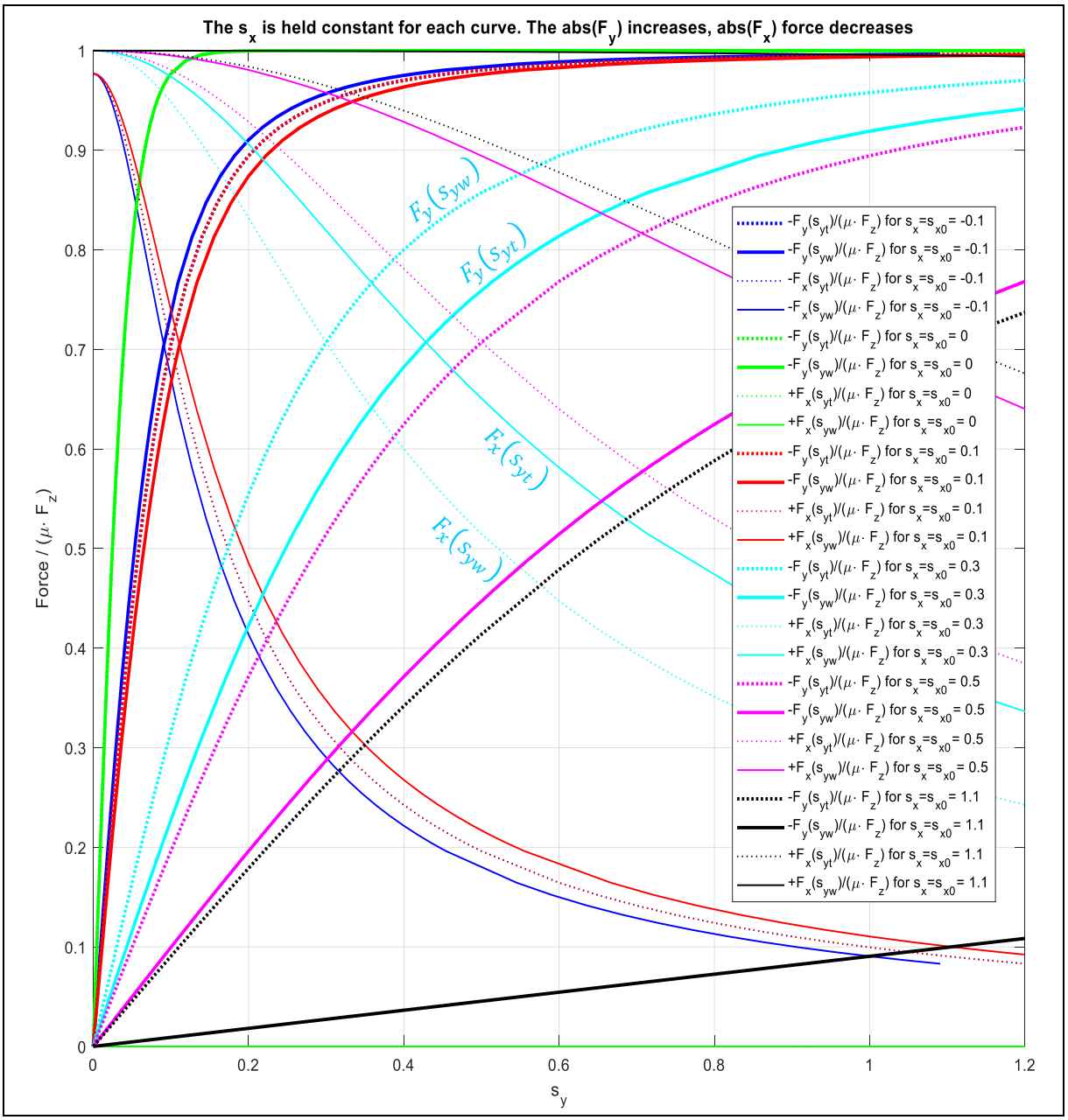


Figure 2-78: The F_y as function of lateral slip, both s_{yt} and s_{yw}. The slope in the plot is then the local slip stiffness for constant s_x, i.e., $-dF_y/ds_{yw}\big|_{s_x \equiv s_{x0}}$.

We can express the local lateral slip stiffness for holding s_x constant during the partial differentiation, $C'_{y,sx}$, by directly differentiation of F_y with respect to v_y. The expression will be branched by sign(ω):

$$\frac{C'_{y,sx0,\omega>0}}{|v_x|\cdot\mu\cdot F_z} = -\left(\frac{v_y^2}{\left(\frac{s_{x0}^2\cdot v_x^2+(s_{x0}-1)^2\cdot v_y^2}{(s_{x0}-1)^2}\right)^{1.5}} - \frac{1}{\sqrt{\left(v_x+\frac{v_x}{s_{x0}-1}\right)^2+v_y^2}}\right)\cdot \tanhyp\left(\frac{\frac{CC}{\mu}\cdot|s_{x0}-1|\cdot\sqrt{\left(v_x+\frac{v_x}{s_{x0}-1}\right)^2+v_y^2}}{|v_x|}\right)+$$
$$+\frac{\frac{CC}{\mu}\cdot v_y^2\cdot|s_{x0}-1|\cdot\left(\tanhyp^2\left(\frac{\frac{CC}{\mu}\cdot|s_{x0}-1|\cdot\sqrt{\left(v_x+\frac{v_x}{s_{x0}-1}\right)^2+v_y^2}}{|v_x|}\right)-1\right)\cdot(s_{x0}-1)^2}{|v_x|\cdot(s_{x0}^2\cdot v_x^2+(s_{x0}-1)^2\cdot v_y^2)};$$

$$\frac{C'_{y,sx0,\omega<0}}{|v_x|\cdot\mu\cdot F_z} = -\left(\frac{v_y^2}{\left(\frac{s_{x0}^2\cdot v_x^2+(s_{x0}+1)^2\cdot v_y^2}{(s_{x0}+1)^2}\right)^{1.5}} - \frac{1}{\sqrt{\left(v_x-\frac{v_x}{s_{x0}+1}\right)^2+v_y^2}}\right)\cdot \tanhyp\left(\frac{\frac{CC}{\mu}\cdot|s_{x0}+1|\cdot\sqrt{\left(v_x-\frac{v_x}{s_{x0}+1}\right)^2+v_y^2}}{|v_x|}\right)+$$
$$+\frac{\frac{CC}{\mu}\cdot v_y^2\cdot|s_{x0}+1|\cdot\left(\tanhyp^2\left(\frac{\frac{CC}{\mu}\cdot|s_{x0}+1|\cdot\sqrt{\left(v_x-\frac{v_x}{s_{x0}+1}\right)^2+v_y^2}}{|v_x|}\right)-1\right)\cdot(s_{x0}+1)^2}{|v_x|\cdot(s_{x0}^2\cdot v_x^2+(s_{x0}+1)^2\cdot v_y^2)};$$

[2.67]

This can be plotted, see Figure 2-79.

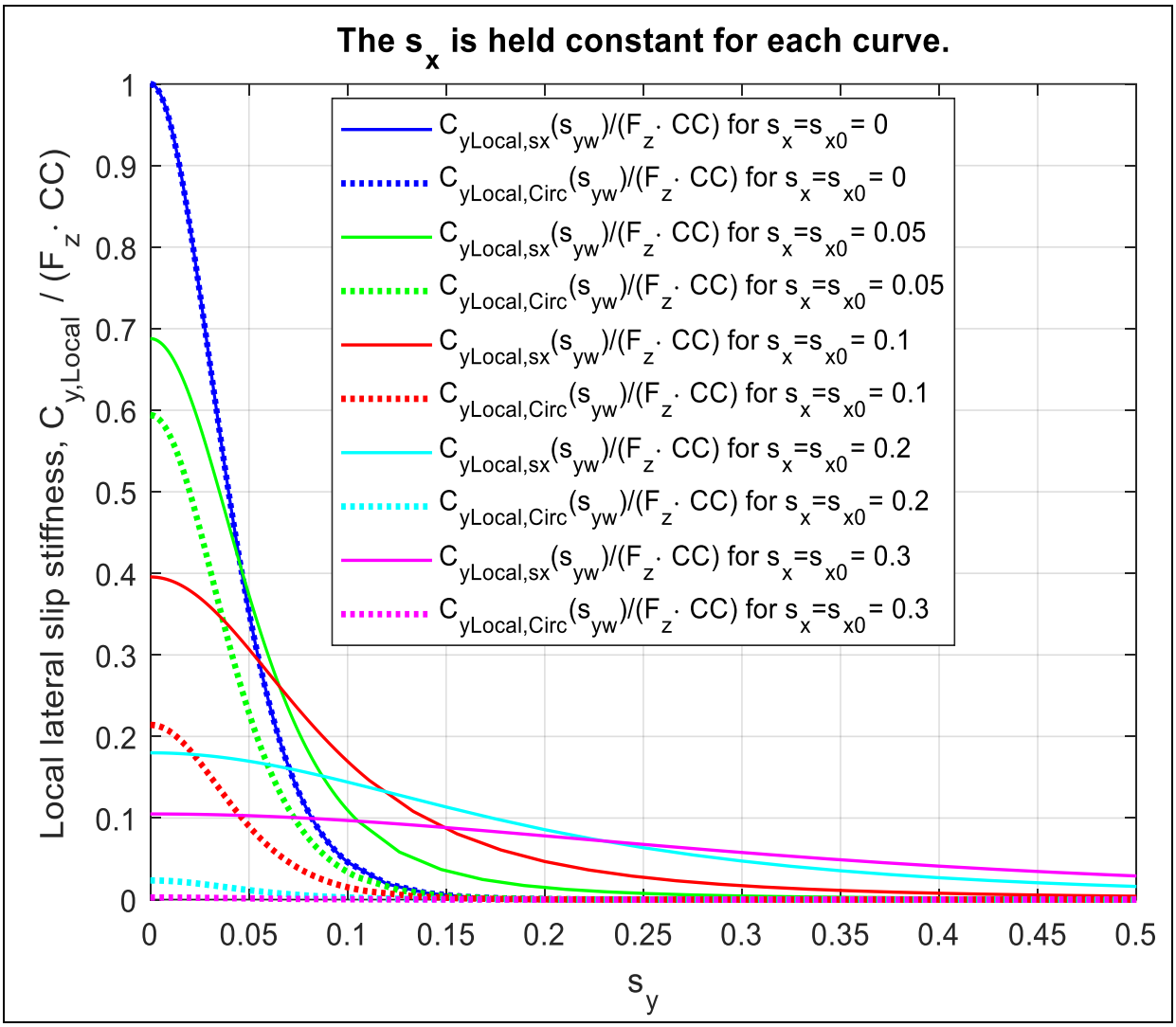


Figure 2-79: The local lateral slip stiffness $C'_{y,sx0} = dF_y/ds_{yw}\big|_{s_x \equiv s_{x0}}$ variation with $\{s_x, s_{yt}\}$ and with $\{s_x, s_{yw}\}$. The local slip stiffness from Eq [2.63] is drawn for comparison and subscripted "Circ".

The local slip stiffness from Eq [2.63] is drawn as comparison. It is very unprecise except for $s_x = 0$ and $s_x >\approx 1$.

The local slip stiffness for holding $F_x \equiv F_{x0}$ constant during the partial differentiation, $C'_{y,Fx0}$, is more difficult. Matlab Symbolic Toolbox (R2023b) cannot even find the expression for ω (to hold $F_x \equiv F_{x0}$). The present book does not go further to try to solve $C'_{y,Fx0}$. Instead, here comes a motivation for modelling as if $s_x \equiv s_{x0}$ was held. When studying Figure 2-75, one can see that controlling to constant s_x is most important for larger slip, after the curve intersection. So, there we should definitely use s_x control. For smaller slip, F_x control is better but only slightly better. So, a switching controller, dual-request-interface, as in 4.6.2.2.4, is motivated both for a large lateral force margin and a large (local) lateral slip stiffness. For vehicles with a good implementation of such dual-request-interface, the variation of (local) slip stiffness is therefore better approximated with $C'_{y,sx0}$ than with $C'_{y,Fx0}$.

2.2.5.5 Constant vehicle motion

Figure 2-80 shows the constant condition $\alpha = 0.1\ [rad]$. It is a useful view when we want to allocate wheel torque in a curve, motivated by that the vehicle motion, $\{v_x, v_y\}$ does not change so quickly, so it makes sense to lock $\alpha = \arctan(v_y/v_x)$ in the allocation algorithms.

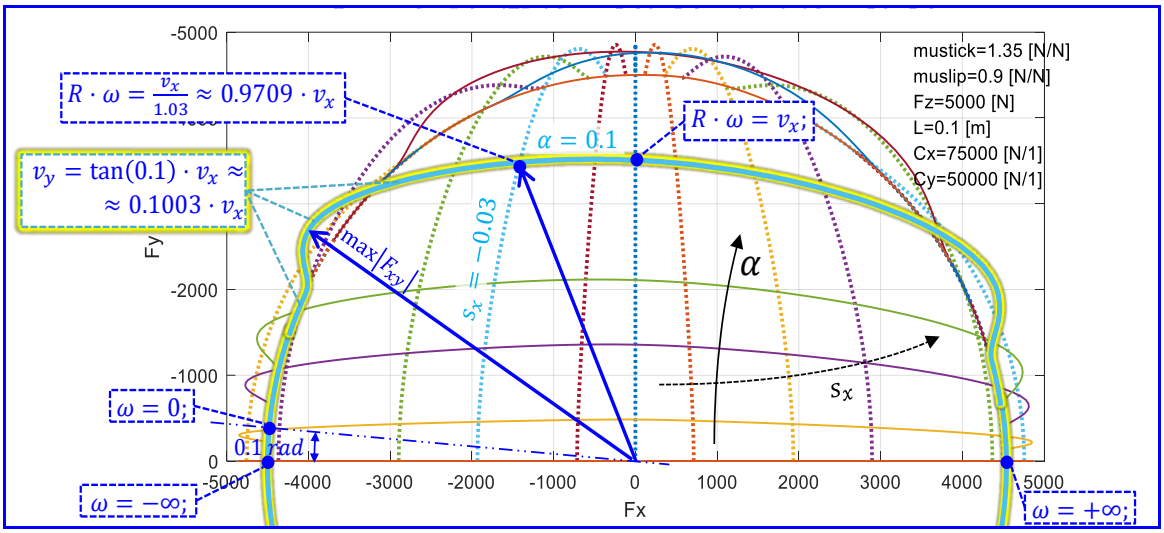


Figure 2-80: Part from Figure 2-73. Shows specific conditions: (rotationally) locked ($\omega = 0$), infinite spin ($\omega = \pm\infty$), and max$|F_{xy}|$. The max$|F_y|$ appears at slight negative $F_x \approx -500\ N$. Yellow glowed curve shows constant $\alpha = 0.1\ [rad]$.

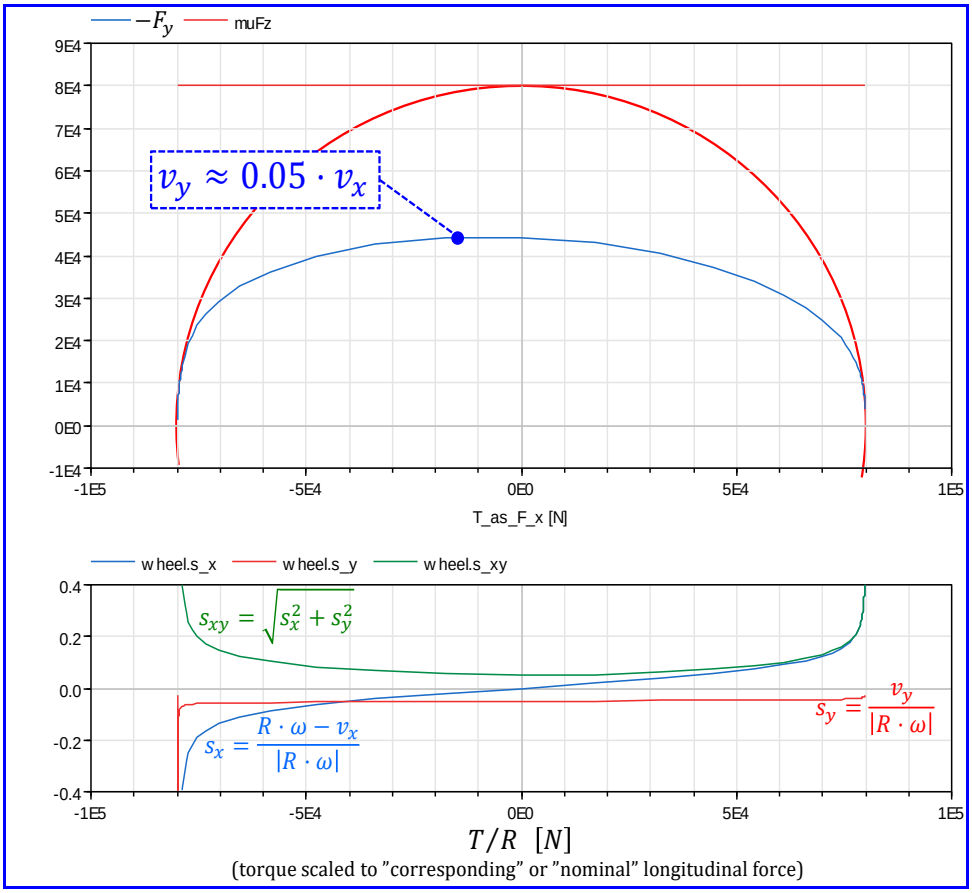


Figure 2-81: Similar as Figure 2-80, but with simpler model (Eq [2.59] with tanhyp(⋯)) and not numerically same conditions. Also, only one operating curve is drawn, for constant $v_y = 0.05 \cdot v_x$.

These thoughts are for the performance of a single wheel to a whole axle group in 2.7.

2.2.5.6 Influence of Vertical Force

Contribution from Niklas Fröjd, Volvo Trucks

Figure 2-82 shows experiment data on how slip stiffness varies with vertical force.

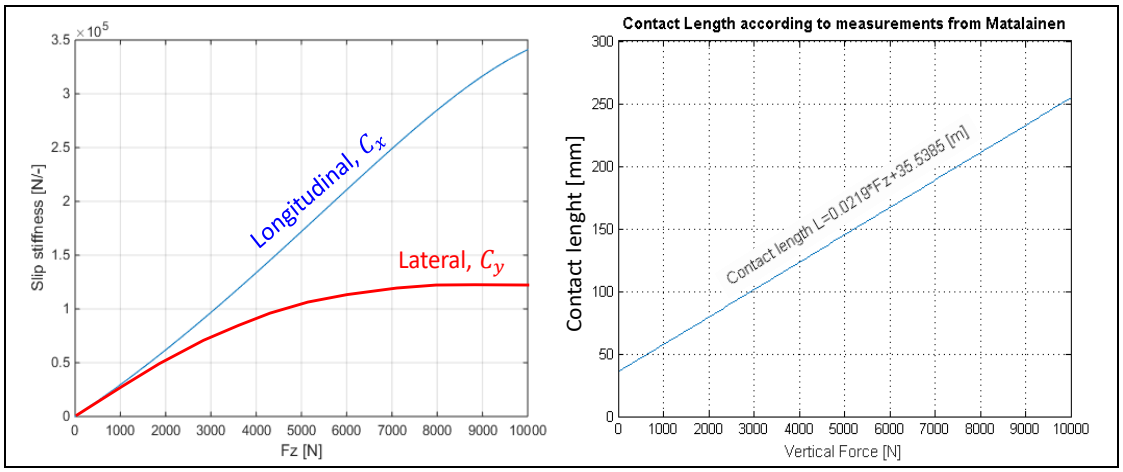


Figure 2-82: Measurements for varying vertical force. Left: Slip stiffnesses. Right: Contact length.

2.2.5.6.1 Explanation of Higher Slip Stiffness Longitudinal than Lateral

The model in 2.2.4.1.1.1 explains why tyre is more slip stiff in longitudinal than lateral direction, i.e. why $C_x > C_y$. We can then assume iso-tropic brush bristles in both friction and shear stiffness, i.e. $C_{tr,x} = C_{tr,y} = C_{tr}; \Rightarrow C_x = C_{tr}$; and $C_y = C_{sw,\varepsilon,in} \cdot C_{tr}/(C_{sw,\varepsilon,in} + C_{tr})$;. From experiments, we typically find $C_x/C_y = \{at\ nominal\ F_z = F_{zNom}\} = C_{xNom}/C_{yNom} = CC_{xNom}/CC_{yNom} = k_{Nom} =$ 1.5 . . 2. This could be explained with the model if $C_{sw,\varepsilon,in}/C_{tr} = 1/(k_{Nom} - 1) = 2 \,..\, 1$. This shows that neither of $C_{sw,\varepsilon,in}$ nor C_{tr} is neglectable.

2.2.5.6.2 Model for how Lateral Slip Stiffness is Digressive with Vertical Force

The model in 2.2.4.1.1.1 can also explain why lateral slip stiffness C_y is digressive with F_z, as indicated already in 2.2.3.1.3. The explanation is found by utilizing that the contact length L has to be same for longitudinal and lateral.

The C_{tr} was found to be proportional to F_z, due to that contact length increase proportional to $\sqrt{F_z}$. A very conceptional reasoning of how $C_{sw,\varepsilon,in}$ could vary with F_z follows now: We defined $C_{sw,\varepsilon,in} = \varepsilon_{in}/F_y$. For a fix lateral deformation $\varepsilon_{in} \approx\propto 1/L$ and $F_y \approx\propto L$. So, $C_{sw,\varepsilon,in} \propto 1/L^2 \propto 1/F_z$. With $C_x \propto F_z$ and $C_{sw,\varepsilon,in} \propto 1/F_z$, and given $C_x = C_{xNom}$ and $C_y = C_{yNom}$ at given nominal $F_z = F_{zNom}$, the model gives Eq [2.68] and Figure 2-83. So, by knowing F_{zNom} and measuring C_{xNom} and C_{yNom} one gets k_{Nom} as $k_{Nom} = C_{xNom}/C_{yNom}$ and thereby a quantified model of $C_x(F_z)$ and $C_y(F_z)$.

$$C_x = \frac{F_z}{F_{zNom}} \cdot C_{xNom}; \quad and \quad C_y = \frac{F_z}{F_{zNom} + \frac{k_{Nom} - 1}{F_{zNom}} \cdot F_z^2} \cdot C_{xNom}; \qquad [2.68]$$

We can now identify slip stiffness coefficients from 2.2.3.1.3 and 0: $CC_x = C_{xNom}/F_{zNom}$ works well. But, since F_y is no longer linear with F_z, CC_y cannot be identified. The influence from F_z on F_y is captured by two parameters, CC_x and k_{Nom}, instead of just one, CC_y.

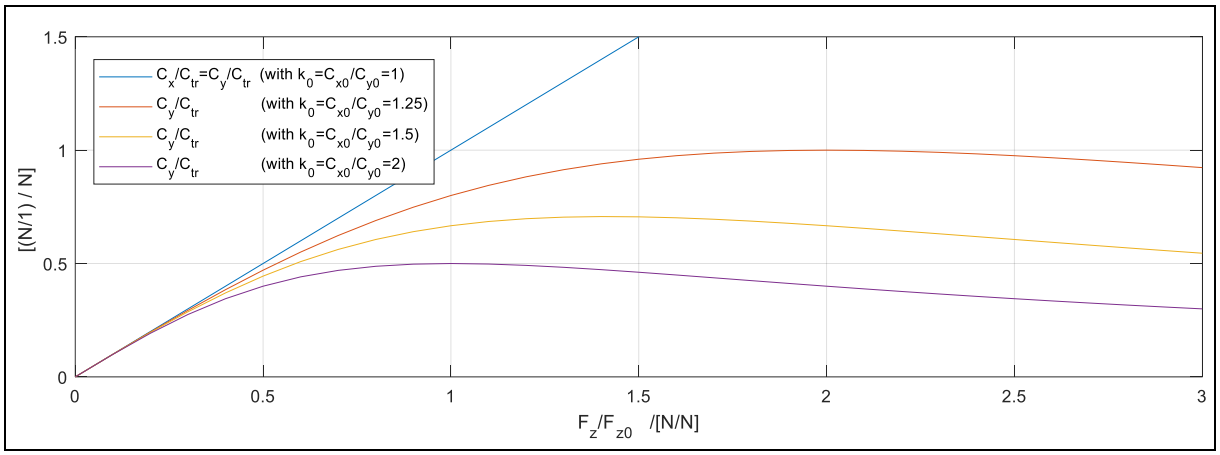


Figure 2-83: Model with Dependent Bristles explains that Lateral Slip Stiffness is digressive with F_z. The C_{tr} is (direction independent) slip stiffness due to tread (tr).

The C_x and C_y can be substituted into Eq [2.58].

2.2.6 Transients and Relaxation

As for longitudinal and lateral, there transients between the steady state conditions, see 2.2.3.7 and 2.2.4.6.

Below is a model for the transient due to changing the deformation pattern in the contact patch. As in 0 and 2.2.4.6, the model is not fully physical, but only exploits one 1st order filter per direction.

$$[\dot{F}_x;\ \dot{F}_y] = \frac{1}{\tau}\cdot[(f_{SSx}(s_x, s_y, F_z, \mu, \cdots) - F_x);\ (f_{SSy}(s_x, s_y, F_z, \mu, \cdots) - F_y)]; \quad [2.69]$$

where $[f_{SSx};\ f_{SSy}]$ are the forces according to steady state models. The slips are $s_x = \frac{R\cdot\omega - v_x}{|R\cdot\omega|}$; and $s_y = \frac{v_y}{|R\cdot\omega|}$;. The time delay, $\tau = \frac{L_{r,patch}}{v_{Transport}} = \frac{L_{r,patch}}{|R\cdot\omega|}$ and $L_{r,patch}$ is a relaxation length.

The relaxation length $L_{r,patch}$ is, intuitively, of the same magnitude as the stick zone ξ_c, since the stick zone is what has to be "rolled over" before a new deformation pattern of bristles can appear.

In same way as for longitudinal in 2.2.3.7, one can also involve the elasticity of the tyre sidewall. The transients due to contact patch are due to that the bristles are replaced and it is the same bristles that carry shear stress both longitudinally and laterally, so it is only one scalar τ and one scalar $L_{r,patch}$. The elasticities of the sidewall are, however, due to 2 different deformations one longitudinal (pitch rotation of tyre) and one lateral (yaw deformation of sidewall): $\dot{F}_x = c_{sw}\cdot(\omega_{rim} - \omega_{belt})$; and $F_y = -C_{sw,\varepsilon,in}\cdot\tan(\varepsilon_{in})$;. So, if we identify the relaxation length in Eq [2.69] from real experiments, we can get different relaxation lengths if we look at delays of longitudinal and lateral force. Typically, these relaxation lengths become around 25..50% of the tyre circumference. It includes more than just the patch transients, so the name should then rather be $L_{r,patch,sw}$, and, as noted, they can be different for longitudinal and lateral.

Most reasoning in 2.2.3.7 is applicable also for combined slip relaxation.

2.2.7 Summary of Tyre Force vs Slip Models

Categorization of tyre models for longitudinal force and slip:

- No lateral slip:
  - Ideally rolling ($R\cdot\omega \equiv v_x$; leaving F_x to be defined by other than the tyre)
  - Linear $F_x = +C_x\cdot s_x = +CC_x\cdot F_z\cdot s_x$;
  - Saturated due to road friction:
    - Simplest, saturated linear: $F_x = +\text{sign}(s_x)\cdot\min(C_x\cdot|s_x|,\ \mu\cdot F_z)$;

    - General: $F_x = f_x(\mu, F_z, s_x)$;
- Influence from lateral slip: $F_x = f(s_x, F_z, F_y)$;

Categorization of tyre models for lateral force and slip:

- No longitudinal slip:
    - Ideally tracking ($v_y \equiv 0$; leaving F_y to be defined by other than the tyre)
    - Linear $F_y = -C_y \cdot s_y = -CC_y \cdot F_z \cdot s_y$;
    - Saturated due to road friction:
        - Simplest, saturated linear: $F_y = -\operatorname{sign}(s_y) \cdot \min(C_y \cdot |s_y|,\ \mu \cdot F_z)$;
        - General: $F_y = f_y(\mu, F_z, s_y)$;
- Influence from longitudinal slip: $F_y = f(s_y, F_z, F_x)$;

A general Combined force and slip model: $[F_x, F_y] = f(s_x, s_y, F_z)$; or $[F_x, F_y] = f(\omega, v_x, v_y, F_z)$;.

2.2.8 Vertical Properties of Tyres

The most important vertical property of a tyre is probably the stiffness. It mainly influences the vertical dynamics, see Chapter **5**. For normal operation, the vertical force of the tyre can be assumed to vary linearly with vertical deflection. This linearity is consistent with Hertz's contact theory for line contact, see also 2.2.3.1.3. If comparing a tyre with different pressures, the stiffness increases approximately linear with pressure. See Figure 2-84.

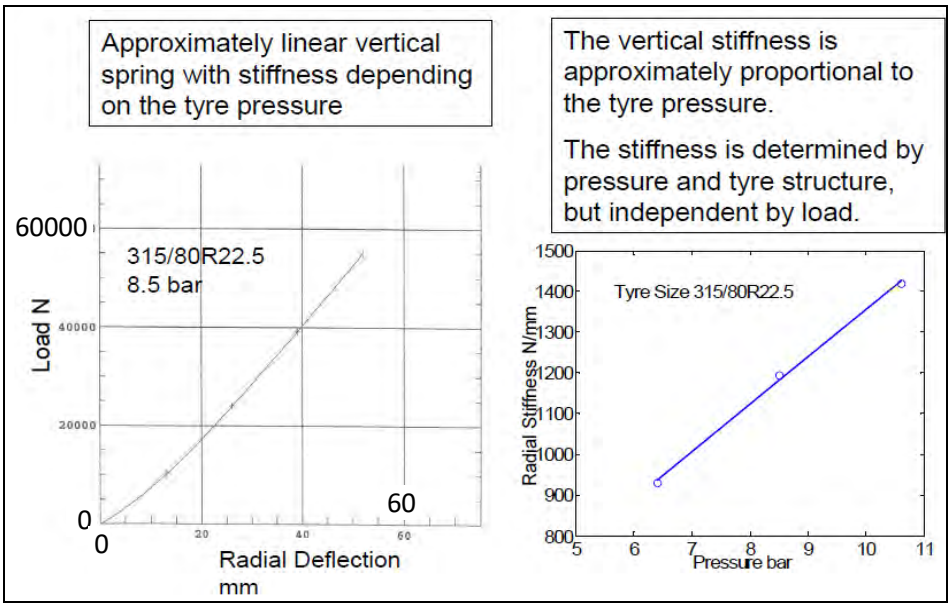


Figure 2-84: Vertical properties of a truck tyre.

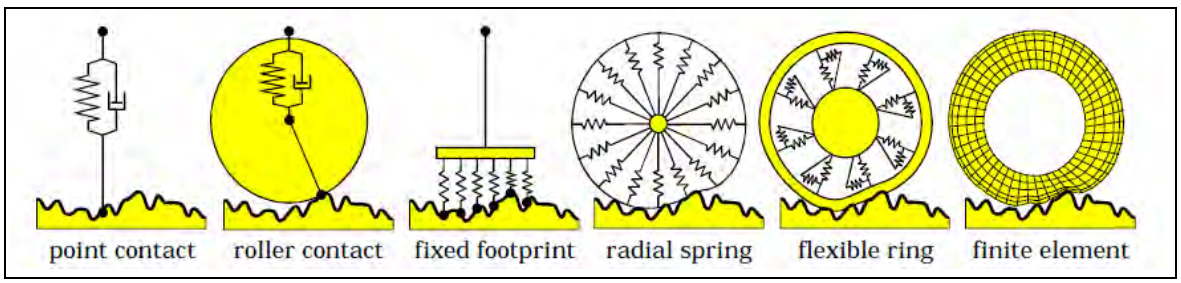


Figure 2-85: Different tyre models which will filter road irregularities differently. Picture from Peter Zegelaar, Ford Aachen.

2.2.9 Tyre Wear

Contributions from Sachin Janardhanan, Volvo Trucks and Chalmers and Mats Jonasson, Chalmers

There are many other aspects of how tyres perform, e.g., wear. Wear models are often based on the Archard's (or Reye's) wear hypothesis: Amount of worn material is proportional to normal force times sliding distance where sliding occurs. With dry friction, we can replace normal force with friction force. Wear rate (worn material per time) can be measured as *tread thickness wear rate* [m/s], *volumetric wear rate* [m^3/s], or *mass wear rate* [kg/s]. We use volumetric below and the notation $WearRate\ [m^3/s]$. The proportionality constant becomes $k_w[m^2/N]$. The k_w will depend on tyre tread material, ground surface roughness, tyre temperature, presence of water, etc. Different approaches to apply this to tyres and expanding to temperature dependency etc. is found for instance in Reference (Grosch & Schallamach, 1961). In this book, we also introduce $ShaveArea[m^2] = WearRate\ [m^3/s]/|R \cdot \omega|\ [m/s]$ is a function of slip below. The $ShaveArea$ can be imagined as the cross-sectional area of a continuous strip of tyre material shaved off by the road surface as the wheel rotates.

The wear only (or mainly) happens on the bristle tips when they slide relative to the ground. This is in the slip zone in the contact patch. On these bristles' tips, the wear law should be applied. In the stick part, the bristles only bends elastically so there is no slip between rubber and ground and consequently not wear, as intended by Archard.

It is very common that one uses models which do **not** differ between stick and slip zone but simply uses a relative speed between belt and ground, not between bristle tips and ground. Present book claims this is unnecessary **inaccurate**. However, since it is so common it is shown in eq [2.75]. Eq [2.75] also assumes a **linear** tyre model, $F_{xy} = C \cdot s_{xy};$. Such models are often used, e.g. in Ref. (J. Lepine, 2022).

$$WearRate[m^3/s] \propto FrictionForce \cdot SlidingSpeed \Rightarrow$$
$$\Rightarrow WearRate[m^3/s] = k_w[m^2/N] \cdot F_{xy}[N] \cdot \Delta v[m/s] =$$
$$= k_w \cdot F_{xy} \cdot \sqrt{(R \cdot \omega - v_x)^2 + v_y^2} = k_w \cdot F_{xy} \cdot s_{xy} \cdot |R \cdot \omega|;$$
$$ShaveArea[m^2] = k_w \cdot F_{xy} \cdot s_{xy} \approx \left\{ \begin{matrix} assume\ linear \\ tyre\ model \end{matrix} \right\} \approx k_w \cdot C \cdot s_{xy}^2 \approx \frac{k_w}{C} \cdot F_{xy}^2;$$
$$\text{where } F_{xy} = \sqrt{{F_x}^2 + {F_y}^2};\ \ s_{xy} = \sqrt{{s_x}^2 + {s_y}^2};$$

[2.70]

When considering that wear **only in the slip zone**, we cannot use a constitutive equation on tyre level, $F_{xy} = function(v_x, v_y, \omega)$, because we must differ between the stick and slip zone. Therefore, the pressure distribution $p(\xi)$ in the contact patch must be considered. In the previous derivations of the different tyre models, we have decomposed in $F_x = F_{xStick} + F_{xSlip}$, which is here directly useful if we also limit to **pure longitudinal** slip. The F_{xSlip} is the force in the slip zone. We need also Δv. It is reasonable to assume same sliding velocity between bristle tips and ground over the whole slip zone and that it is same as between belt and ground, namely: $\Delta v = \sqrt{(R \cdot \omega - v_x)^2 + v_y^2} = |R \cdot \omega - v_x|$.

For **uniform pressure distribution** we use Eq [2.12] and derive as follows:

$$WearRate[m^3/s] \propto FrictionForce \cdot SlidingSpeed \Rightarrow$$
$$\Rightarrow WearRate[m^3/s] = k_w[m^2/N] \cdot F_x[N] \cdot \Delta v[m/s] =$$
$$= k_w \cdot F_{xSlip} \cdot |R \cdot \omega - v_x| = k_w \cdot F_{xSlip} \cdot |s_x| \cdot |R \cdot \omega|;$$

$$ShaveArea[m^2] = k_w \cdot |F_{xSlip}| \cdot |s_x| = \{\text{Eq [2.12][2.13]}\} = \begin{Bmatrix} when\ there\ \boldsymbol{is}\ a \\ slip\ zone, i.e., \\ |s_x| > \mu \cdot F_z/(2 \cdot C_x) \end{Bmatrix}$$
$$== k_w \cdot \mu \cdot F_z \cdot \left|1 - \frac{\mu \cdot F_z}{2 \cdot C_x \cdot s_x}\right| \cdot |s_x|;$$
$$ShaveArea[m^2] = \begin{Bmatrix} when\ there\ is\ \boldsymbol{no} \\ slip\ zone, i.e., \\ |s_x| < \mu \cdot F_z/(2 \cdot C_x) \end{Bmatrix} = 0;$$

[2.71]

And, for **parabolic pressure distribution** we use Eq [2.12] and derive as follows:

For $s_x < \frac{3 \cdot \mu \cdot F_z}{C_x}$:

$$ShaveArea[m^2] = k_w \cdot |F_{xSlip}| \cdot |s_x| = \begin{Bmatrix} \text{Eq [2.23]} \\ \mu_{stick} = \mu_{Slip} = \mu \end{Bmatrix} =$$
$$= k_w \cdot \mu \cdot F_z \cdot \left|\left(3 - 2 \cdot \frac{C_x \cdot s_x}{3 \cdot \mu \cdot F_z}\right) \cdot \left(\frac{C_x \cdot s_x}{3 \cdot \mu \cdot F_z}\right)^2\right| \cdot |s_x|;$$

For $s_x > \frac{3 \cdot \mu \cdot F_z}{C_x}$:

$$ShaveArea[m^2] = k_w \cdot \mu \cdot F_z \cdot |s_x|;$$

[2.72]

The curves for $ShaveArea/k_w$ as a function of s_x are shown below. Since $ShaveArea/k_w$ has the unit $[m^2]/([m^2/N]) = N$, it may be interpreted metaphorically as the cutting force required in the imagined planing or milling process.

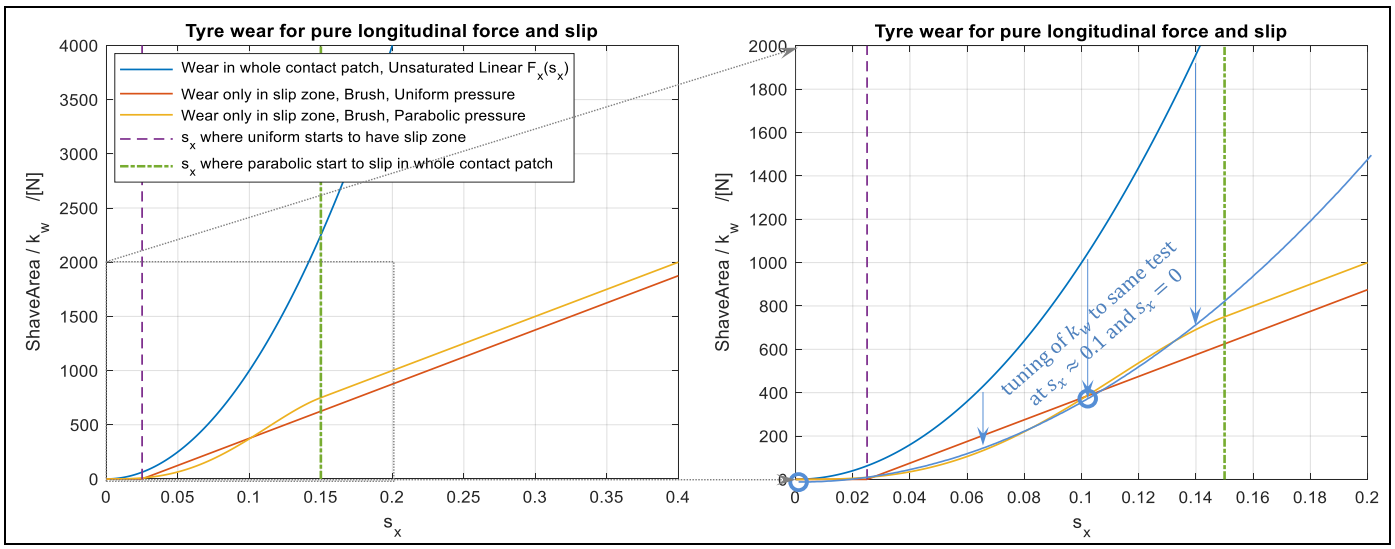


Figure 2-86: Three different models of tyre wear for a tyre with pure longitudinal slip.

The wear proportionality constants k_w for the different models will get different numerical values if estimated from the same wear test in a tyre test machine. So, there are reasons to believe that the k_w from a test with just a tyre tread material sample scraped to the same surface would show rather similar values as the two models "Wear only in slip zone" but very different values compared to estimation from the model "Wear only in slip zone".

2.2.10 Power losses due to tyre slip

Studying the brush model, power is lost in two places in tyre-to ground contact:

- In the **slip zone**, i.e., where $\xi > \xi_c$. Friction shear stresses under sliding, both longitudinal and lateral.
- **After the slip zone**, where the stored elastic energy in the bristles is dissipated when the bristles bend back to their radial direction. The energy is dissipated in the damping in the material.

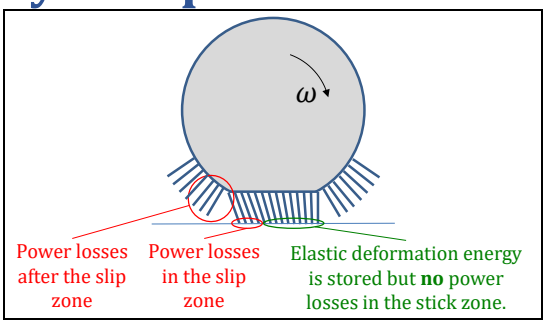


Figure 2-87: Power loss due to tyre slip.

In total, the power loss is the scalar product (•) between sliding force and sliding velocity:

$$P_{loss} = \vec{F}_{xy} \bullet \vec{v}_{Belt,xy} = \underbrace{F_{xw} \cdot (R \cdot \omega - v_{xw})}_{P_{loss,x}} + \underbrace{-F_{yw} \cdot v_{yw}}_{P_{loss,y}} =$$

$$= F_{xw} \cdot \frac{R \cdot \omega - v_{xw}}{|R \cdot \omega|} \cdot |R \cdot \omega| - F_{yw} \cdot \frac{v_{yw}}{|R \cdot \omega|} \cdot |R \cdot \omega| =$$

$$= \left(F_{xw} \cdot s_x - F_{yw} \cdot s_{yt}\right) \cdot |R \cdot \omega| \approx \left\{\begin{matrix}\text{if } R \cdot \omega \approx \\ \approx v_{xw}\end{matrix}\right\} \approx \left(F_{xw} \cdot s_x - F_{yw} \cdot s_{yt}\right) \cdot |v_{xw}|;$$

There are two terms: power loss due to longitudinal and lateral slip, respectively. If $F_{xw} = C_x \cdot s_x$, and $F_{yw} = -C_y \cdot s_y$:

$$P_{loss} = \left(C_x \cdot s_x^2 + C_y \cdot s_y^2\right) \cdot |v_{xw}| = \{\text{or}\} = \left(\frac{F_{xw}^2}{C_x} + \frac{F_{yw}^2}{C_y}\right) \cdot |v_{xw}|; \qquad [2.74]$$

So, one can select between expressing the power loss in $F \cdot s$, F^2, or s^2.

If approximating with $C_x \approx CC_x \cdot F_z$, and $C_y \approx -CC_y \cdot F_z$:

$$P_{loss} = \left(CC_x \cdot s_x^2 + CC_y \cdot s_y^2\right) \cdot F_z \cdot |v_{xw}| = \{\text{or}\} = \left(\frac{F_{xw}^2}{CC_x} + \frac{F_{yw}^2}{CC_y}\right) \cdot \frac{1}{F_z} \cdot |v_{xw}|; \qquad [2.75]$$

We have assumed a linear model ($F \propto s$) which is a reasonable assumption for normal driving, and therefore reasonable for most energy consumption assessments. If, instead, peak friction is reached, it is not suitable to assume $R \cdot \omega \approx v_{xw}$ and the force $\left|\vec{F}_{xy}\right|$ will be $\mu \cdot F_z$ and counter-directed the sliding velocity, so:

$$P_{loss} = \vec{F}_{xy} \bullet \vec{v}_{Belt,xy} = \mu \cdot F_z \cdot \left|v_{Belt,xy}\right| = \mu \cdot F_z \cdot \sqrt{(R \cdot \omega - v_{xw})^2 - v_{yw}^2};$$

2.3 Suspension System

Suspension can mean suspension of wheels (or axles), suspension of sub-frame and drivetrain and suspension of cabin (for heavy trucks). This section considers only wheel and axle suspension. Suspension design is explained in 2.3, but also used as example in 1.4.4 and used in complete vehicle models in 3.4.5-3.4.7, 4.3.7.11, and 4.5.3.

Suspension influences road grip and ride comfort, so merely all vehicle motion, Chapters 3..5. The influence is through how **vertical forces** and **camber and steer angles** on the wheels change with **body motion** (heave, roll, pitch), **road unevenness** (bumps, potholes, waviness) and **wheel forces in ground plane** (from Propulsion, Braking and Steering subsystems). Important is also that suspension influences the material stresses (extreme values and fatigue), both in the suspension itself and other in other parts of the vehicle body. Figure 2-88 shows one way to see the suspension systems role.

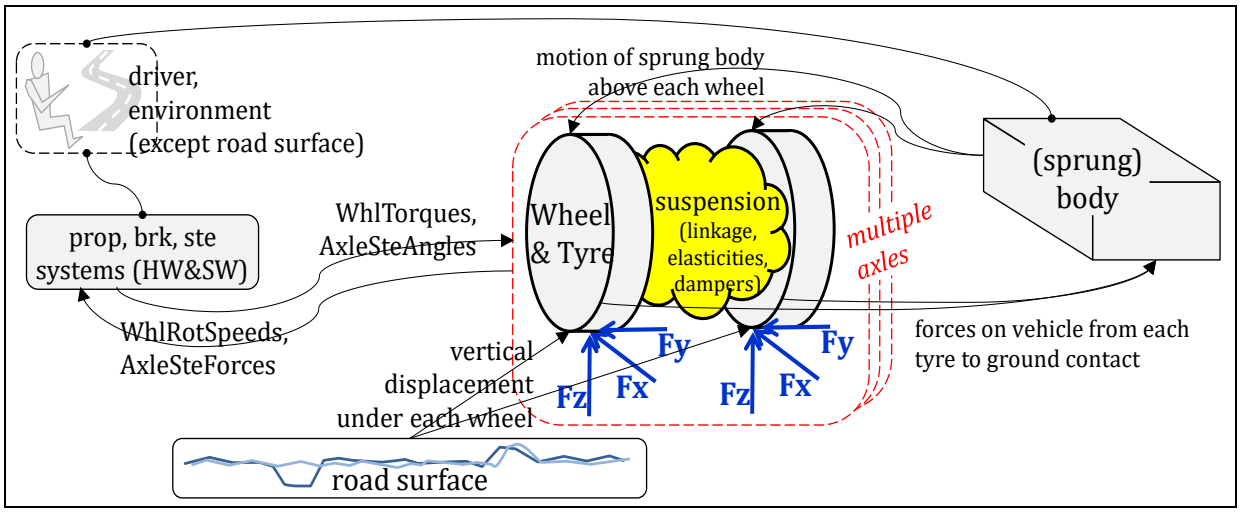


Figure 2-88: Wheel/axle suspension described as modular sub-model per axle. It may be noted that both wheel model (main geometry such as wheel radius) and tyre model (how F_x and F_y vary with tyre slip and F_z) is a part of each Wheel & Tyre sub-model.

The simplest view we can have of a suspension system is that it is an individual suspension between the vehicle body and each wheel, consisting of one linear spring and one linear damper in parallel. Chapter 5 uses this simple view for analysis models, because it facilitates understanding and it is enough for a first order evaluation of the functions studied (comfort, road grip and fatigue load) during normal driving on normal roads.

The full 3D aspect of suspension is not covered here in 2.3. Instead, a division into 2D is done in 2.3.3 Suspension -- Heave and Pitch and 2.3.4 Suspension -- Heave and Roll, aiming at Longitudinal and Lateral dynamics, respectively. The full 3D aspects are briefly addressed in 4.5.3.2.5 and 0. See also (Blundell & Harty, 2014).

2.3.1 Components in Suspension

Each wheel can rotate in its hub. Each hub can be individually suspended to the body or left and right hub can be mounted on a rigid beam which is suspended to the body. The suspension parts are below grouped in: Linkage, Elasticities and Dampers. One might count in additional parts in the suspension, such as bearings, shafts, brake parts, etc.

2.3.1.1 Linkage

Linkage, which has the purpose to constrain the relative motion between wheel and body via kinematics to one dof (approximately vertical translation), or, for a steered axle, also allow one more dof (approximately yaw rotation) per axle. One way to understand the function of the linkage is that it defines the relation between motion (velocities and positions) of the wheels and the body. Another way is that the linkage defines how forces in the wheel-to-ground contacts are brought to the body. These two functions are not independent design decisions, since the relations are the transpose of each other, see 1.5.2.4.3.

The linkage consists of links (or members) and joints; mainly ball joints, but sometimes others, such as hinge joints. The coordinates (“hard-points”) of these joints are the real design parameters, but the dynamic behaviour of a complete vehicle model can be expressed in much fewer parameters, namely the “effective pivot points”. These effective points are used in 2.3.3 and 2.3.4.

2.3.1.2 Compliances

Springs are examples of compliances (or elasticities). The springs develop forces when the wheels are vertically displaced relative to the body. There is often one spring per wheel but also an anti-roll bar per axle. The anti-roll bar connects left and right wheel to each other to reduce body roll.

Springs often have a rather linear relation between the vertical displacement and force of each wheel, but there are exceptions:

- **Anti-roll bars** make the two sides on an axle dependent of each other (still linear). Anti-roll bars can be used on both individual wheel suspensions and rigid axle suspensions.
- The springs are intentionally designed to be non-linear in the compressed end of their stroke with **bump stops**. Bump stops at passenger cars are typically designed at $(3.5..4) \cdot g$ vertical acceleration when vehicle is fully loaded. (A somewhat opposite non-linearity appears in the rebound end of the stroke, due to wheel lift. Here it is the contact force with ground that is saturated to zero, not the spring force. The difference is the damping force.)
- In context of bump stop, it is relevant to mention an almost opposite phenomena in the other end of the deformation range; a wheel cannot take vertical pulling forces to the ground. This is called **wheel lift**, and it is the saturation of force under the tyre to zero, as opposed to becoming negative.
- The compliances can be non-linear during the whole stroke, e.g., **air-springs** and **leaf-springs**. Air-springs are non-linear due to the nature of compressing gas. Ideal gas can often be assumed: $p \cdot V = n \cdot R \cdot T;\ \Rightarrow\ \ Force = n \cdot R \cdot T/(L_0 - Compression)$;.
- The compliances can be **controllable** during operation of the vehicle. This can be to change between the pre-load level to adjust for varying roads and varying weight of vehicle cargo. When controlled in a shorter time scale, e.g., for compensating in each oscillation cycle, it is described in 2.3.1.4.

The springs are the main compliance, but also other smaller compliances are present and makes the effective stiffness lower: the links themselves, the bushings in the joints between the links and the brackets where the links are connected to the body. For the complete vehicle model, the tyres vertical compliance adds to the suspension compliance.

2.3.1.3 Dampers

Dampers have the purpose to dissipate energy from any oscillations of the vertical displacement of the wheel relative to the body. High damping damps oscillations, but high damping also increases the shock force transmittance (with this reasoning, the name “shock-absorber” is misleading). The most common design is the hydraulic piston type. Simplest understanding or modelling is a linear relation between the vertical deformation speed and force. But the following non-linearities should be mentioned:

- The dampers are normally intentionally designed to be different in different deformation direction. Typical values for passenger cars are about 3 times more damping in rebound (extension) than compression (bump). For heavy vehicles, the difference is often even larger, maybe a factor 5 or 10.
  An intuitive explanation to the asymmetry can be found by comparing driving over different transient unevenness, a bump or a hole. In both cases, large spring stiffness and large damping cooperate to transfer the road unevenness and worsen comfort. But average damping cannot be too low, since damping damps oscillations. When driving over a bump, the force can be very large due to the bump stop in the spring. When driving over a hole, the force is limited by wheel lift from ground. The spring, including bump stop and wheel lift, is therefore generally stiffer for a bump than for a hole. So, to compensate for this, the damping is made opposite: more damping when driving over a hole, i.e. rebound (extension).
- Damping in **leaf springs** is non-linear since they work with dry friction.
- The dampers can be designed to be **controllable** during operation of the vehicle. This can be used to change the damping characteristics to adjust for varying roads or varying weight of

vehicle cargo. When controlled in a shorter time scale, e.g., for compensating in each oscillation cycle, it is described in 2.3.1.4.

2.3.1.4 Controlled force elements

Elements in which the force can be varied during the driving operation can be categorized either as controlled springs or controlled dampers. Therefore, it is given a separate section with heading *Controlled **force elements***.

An alternative name is active suspension. The term **active** may cause confusion in categorization because it can refer to that the element is **energized** (not only dissipating energy but also receiving energy) or that the **control algorithms** are active while driving. Active control algorithms can be combined with either energized or non-energized elements.

Algorithm-controlled **energized** force elements: The is the more advanced system and is only found on some few very high-end vehicles on market. The element can be a hydraulic piston where the pressure difference between the two chambers is pressurized with a pump. Such can typically be in parallel with a spring and hence it can replace the normal damper. An example is https://www.tenneco.com/assets/1/7/ACOCAR_Brochure.pdf. Another use is to have a position actuator in series with an elasticity. An example is https://www.bwigroup.com/active-stabilizer-bar-systems/. How it affects the vehicle comfort and grip is shown 2.3.1.4.

Algorithm-controlled **non-energized** force elements: This is also advanced but is found on more, still high-end, vehicles on market. It is also called "semi-active suspension". The typical realization is a damper, in which the hydraulic orifice can be varied. One example is https://www.media.volvocars.com/se/sv-se/media/pressreleases/5257.

Both can affect energy consumption.

2.3.2 Axle and Wheel Rates

All compliances (springs, bushings, etc) contribute to the stiffness between the body and the wheels. The wheels are not independent of each other; we have especially a connection between left and right due to the anti-roll bars. Therefore, we define both axle (compliance) rate and wheel (compliance) rate, see Figure 2-89. We can also call these *Effective stiffnesses* of the axle and wheel, respectively.

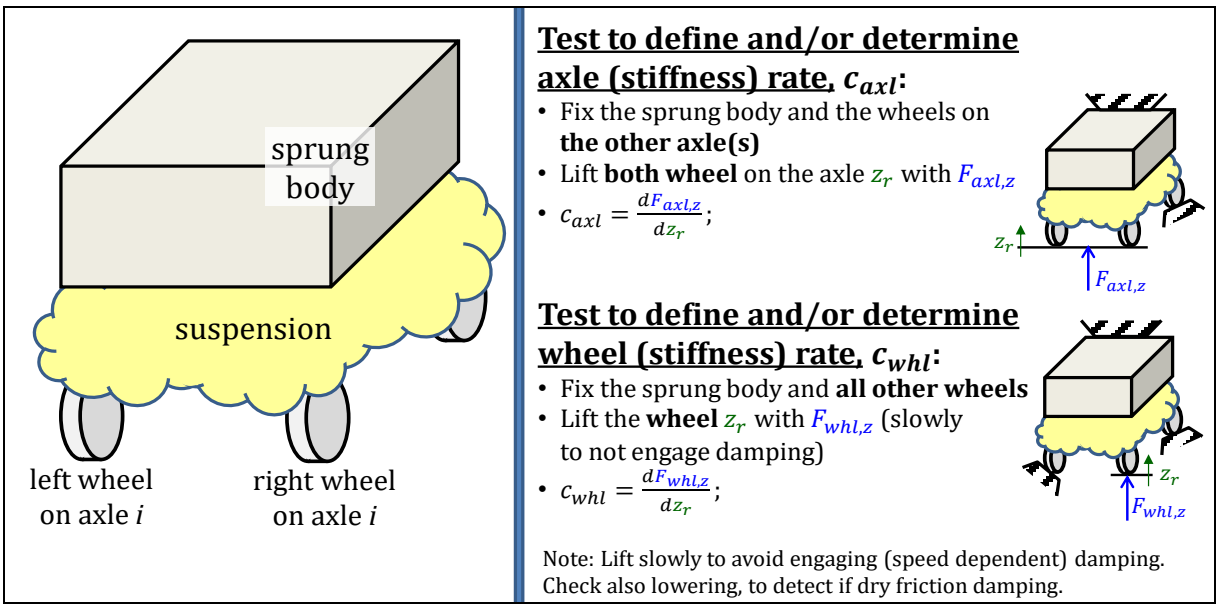


Figure 2-89: Definition of axle and wheel (stiffness) rates.

Alternatively to lifting one wheel, the axle can be rolled (without lifting the midpoint of the axle): $z_{left} = z_r = \varphi_{rx} \cdot W/2$; and $z_{right} = -z_r = -\varphi_{rx} \cdot W/2$;. It is then natural to find the measure axle

roll stiffness $c_{roll}[Nm/rad] = F_{whl,z} \cdot W/\varphi_{rx};$, instead of $c_{whl}[N/m]$. If the vehicle is symmetric and track width is known, these measures carry the same information and $c_{roll} = c_{whl} \cdot W^2/2;$.

With these definitions, the vertical wheel forces for a two-axle vehicle will be as follows. It is assumed that the vehicle is symmetrical and that there are connections between the wheels only as anti-roll bars on each axle. The body is fixed and road under the wheels are displaced with z_{rij}. Notation $c_{i,axl}$ is axle rate and $c_{i,whl}$ is wheel rate for axle i. The time derivative of spring force $\dot{F}_{sij}$ and vertical velocities are used to avoid involving pre-tension in the springs.

$$\begin{bmatrix} \dot{F}_{s1l} \\ \dot{F}_{s1r} \\ \dot{F}_{s2l} \\ \dot{F}_{s2r} \end{bmatrix} = \begin{bmatrix} \boldsymbol{C_{w1}} & \boldsymbol{0} \\ \boldsymbol{0} & \boldsymbol{C_{w2}} \end{bmatrix} \cdot \begin{bmatrix} v_{r1lz} \\ v_{r1rz} \\ v_{r2lz} \\ v_{r2rz} \end{bmatrix}; \quad where\ \boldsymbol{C_{wi}} = \begin{bmatrix} c_{i,whl} & -\left(c_{i,whl} - \frac{c_{i,axl}}{2}\right) \\ -\left(c_{i,whl} - \frac{c_{i,axl}}{2}\right) & c_{i,whl} \end{bmatrix};$$

If both body and road under the wheels is moving, we simply exchange $[v_{1lz} \quad v_{1rz} \quad v_{2lz} \quad v_{2rz}]^T$ with $[v_{r1lz} \quad v_{r1rz} \quad v_{r2lz} \quad v_{r2rz}]^T - [v_{1lz} \quad v_{1rz} \quad v_{2lz} \quad v_{2rz}]^T$. The axle roll stiffness becomes $c_{i,roll} = \left(c_{i,whl} - c_{i,axl}/4\right) \cdot W^2$; [Nm/rad] for $\dot{M}_{s1x} = c_{i,axl} \cdot \omega_{r1x}$.

Similarly, for axle i, we can define axle (damping) rate $d_{i,axl}$, wheel (damping) rate $d_{i,whl}$ and axle roll damping $d_{i,roll}$. However, $d_{i,axl}$ is often simply $2 \cdot d_{i,whl}$ since there are typically no dampers connecting left and right wheel. Corresponding 4×4 damping matrix becomes a diagonal matrix, since $d_{i,axl}$ normally is $2 \cdot d_{i,whl}$.

If we know the design parameters (stiffness and location of the actual spring) we can calculate the rates. This will be exemplified in 2D and briefly discussed for general (3D) below.

2.3.2.1 Explanation in 2D

A very simplified suspension is assumed in Figure 3-59. The stiffnesses c_f and c_r are the *axle spring rates* (or *effective stiffnesses* of each axle). The real spring may have another stiffness c_{real}, but its effect on vertical force is captured in the effective stiffness. An example of how the effective stiffness is found for a 2D model (heave and pitch) from a real suspension design is given in Figure 2-90.

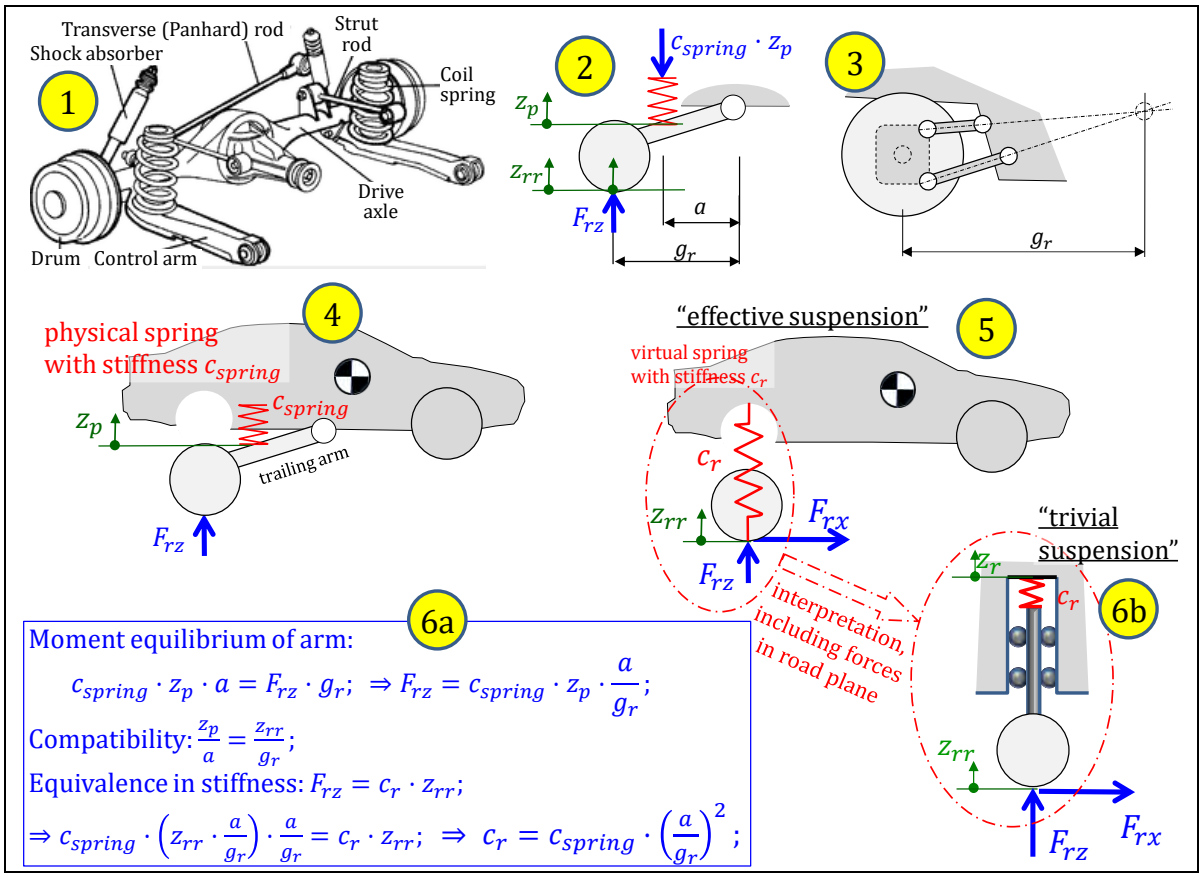


Figure 2-90: From suspension design spring stiffness to effective stiffness. 6a: Final Mathematical model. 6b: Interpretation ("Reverse modelling") back from Mathematical to Physical model, showing "Trivial (linkage) suspension".

Note that the factor $(a/g_r)^2$ is not the only difference between effective and real stiffness, but the effective can also include compliance from other parts than just the spring, such as bushings and tyre. There will also be a need for a corresponding effective damping coefficient, see 3.4.5.2.2, or axle (damping) rate. How forces in road plane is transferred is not well captured in this model, see F_{rx} in Figure 2-90. Compared to suspension models later in book, Figure 2-90 ends with a "trivial (linkage) suspension model". In 3.4.5.2, the suspension linkage is better modelled, which allows validity for F_{ix} (propulsion and braking). Corresponding for F_{iy} is modelled in 4.3.7.11.3.

2.3.2.2 Expansion to 3D

It should be noted that above is one of 2 possible 2D views of explaining effective stiffness. A similar reasoning could be done in view from rear. Then we would see the same physical spring but other levers (a and b). So, that view would give another value of effective stiffness. A realistic model for both F_{ix} and F_{iy} has to use **pivot axis in 3D** instead. If a prototype is available, one can also measure effective stiffness, because it is the actual stiffness that one would feel if one tries to lift the wheel by grabbing the tyre-to-ground contact surface. In a first approach one can explain a 3D model as moment equilibrium around a moment-free pivot axis. However, for a general 3D motion, there should be a screw joint along the pivot axis, see mathematical formulation of equilibrium in 4.5.3.2.5. The lead of the screw is often assumed to be zero and it is no examples below where a non-zero lead is identified in an example suspension.

2.3.2.3 Example: Requirements on suspension

Contribution from Yansong Huang, Chalmers Vehicle Dynamics and Volvo Cars

To make vehicle development efficient one decomposes it into hierarchical levels, see 1.4.4, the requirements on vehicle motion need to be broken down (cascaded) to requirements on lower level, i.e. requirements on subsystems in the vehicle. Two such subsystems are the front and rear axle suspension. The kinematic properties of each axle are a very important example of requirements, which need compatibility equations to be formulated.

Only the *first order* suspension kinematics is shown above. The expression "first order" above comes from that the velocities are proportional to each other, which is only true in a certain *design position* $pos_0 = [z_0, y_{Ste0}]$, where z is the vertical position of wheel hub relative to vehicle body (jounce) and y_{Ste} is the lateral position of the tie rod outer end relative to its position in zero steering. If we look at one of the hub positions, such as steering angle $\varphi_{Ste,z}$. Since $\varphi_{Ste,z}$ is related to steering angle rate $\omega_{Ste,z}$ through $\omega_{Ste,z} = \dot{\varphi}_{Ste,z}$, the full kinematic relation can be written and approximated as follows. Note that it is simplified by assuming a given constant $y_{Ste} = y_{Ste0}$, typically $y_{Ste0} = 0$, so that φ_z only varies with z:

$$\varphi_z = f(z);$$

The curve $\varphi_z(z)$ can be numerically found for a range of z values if all geometry is known. So, numerically we can require **points on the curve** (e.g. 3 numerical points (z, φ_z)) and numerically iterate to find a geometry which fulfils these requirements.

Now, a key trick to express the requirements in another way is to derive expressions as below, for the derivatives is to assume a design position and a constant vertical velocity v_z. However, the v_z is cancelled out, so "constant v_z" is only an imagined test to characterize the suspension.

$$\varphi_z = f(z); \quad \Rightarrow \quad \dot{\varphi}_z = \frac{df}{dz} \cdot \dot{z} \quad \Rightarrow \quad \frac{\dot{\varphi}_z}{\dot{z}} = \frac{\omega_z}{v_z} = \frac{df}{dz} = 1stDeriv(z);$$

$$\varphi_z = f(z); \quad \Rightarrow \quad \ddot{\varphi}_z = \frac{d^2f}{dz^2} \cdot \dot{z}^2 \quad \Rightarrow \quad \frac{\ddot{\varphi}_z}{\dot{z}^2} = \frac{\dot{\omega}_z}{v_z^2} = \frac{d^2f}{dz^2} = 2ndDeriv(z);$$

$$\varphi_z = f(z) = 0thDeriv(z);$$

The other way to formulate requirements is to require numerical values on the **derivatives** in a certain design position z_0. If we require equally many derivatives as points on curves, we have the same number of design dofs. However, with this approach we can often find the geometry by algebraic solutions which is much quicker and precise than numerical iteration.

Both ways to formulate requirements on an axle have about the same chances to fulfil requirements from vehicle motion on the axles. Both uses *virtual design parameters* as an intermediate level between vehicle motion and suspension geometrical design. The two first derivative $0thDeriv$ and $1stDeriv$ is often used; e_p/g_p in 1.5.2.4.3.2 is an example of $1thDeriv$. But Reference (Huang, 2025) successfully explores this also for higher order derivatives. (Huang, 2025) shows how it is used both upstream (to formulate requirements from vehicle motion to axles) and downstream (to calculate suspension geometry to full the requirements). Unlike the simplified reasoning above, (Huang, 2025) shows this for passenger cars, with complete axles (with left and right wheel), including both jounce and steering and, to some extent, also the compliance (e.g. from bushings). Choice of derivatives and highest order of their derivatives for each suspension motion dof is not trivial and therefore also discussed in (Huang, 2025). Selection of vehicle motion manoeuvres and measures is also cruicial. To enable a clearer cut between vehicle motion and suspension design, the following approximation can be used in those complete vehicle simulations which are needed to set requirements on the axles:

$$\varphi_z \approx 0thDeriv(z_0) + 1stDeriv(z_0) \cdot (z - z_0) + 2ndDeriv(z_0) \cdot (z - z_0);$$

2.3.3 Suspension -- Heave and Pitch

2.3.3.1 Examples of Suspension Designs

In Figure 3-61, a "trailing arm" is drawn both for front and rear axle. For rear axle, that is a realistic design even if other designs are equally common. However, for front axle a so-called McPherson suspension is much more common, see Figure 2-91. Figure 2-92 shows a suspension for a heavy vehicle.

2.3.3.1.1 Different order of kinematic measures

In Figure 2-91 and Figure 2-92, distance measures *e* and *g* are defined. The ratio between these vertical and longitudinal measures are axle measures, also known as *anti-dive ratio* and *anti-squat ratio*. They constrain the relation between longitudinal and vertical velocities of the hub relative to the vehicle body to be constant. Note that this constant ratio is only a good approximation around a certain "design height". When the jounce (vertical position of hub relative to vehicle body) comes further from the design height, the constraint changes and in fact it is generally non-linear. There we call the simple ratio a "first order kinematic axle measure" or "first order kinematic target" for an axle. For advanced development of suspensions one uses both 1st and 2nd order targets, maybe even 3rd order in some cases. (Alternatively, one can develop for only 1st order targets but at several design heights.)

2.3.4 Suspension -- Heave and Roll

2.3.4.1 Examples of Suspension Designs

There are axles with dependent wheel suspensions, which basically look as the roll centre axle model in Figure 4-39 , i.e. that left right wheel are rigidly connected to each other. Then, there are axles with dependent wheel suspensions, which look more like the model with wheel pivot points in Figure 4-39. For these, there are no (rigid) connections between left and right wheel.

Many axles have a so-called anti-roll bar, which is an elastic connection between left and right side. It is connected such that if the wheel on one side is lifted, it also lifts the wheel on the other side. Note that, if an anti-roll bar is added to an independent wheel suspension it is still called independent, because the connection is not rigid.

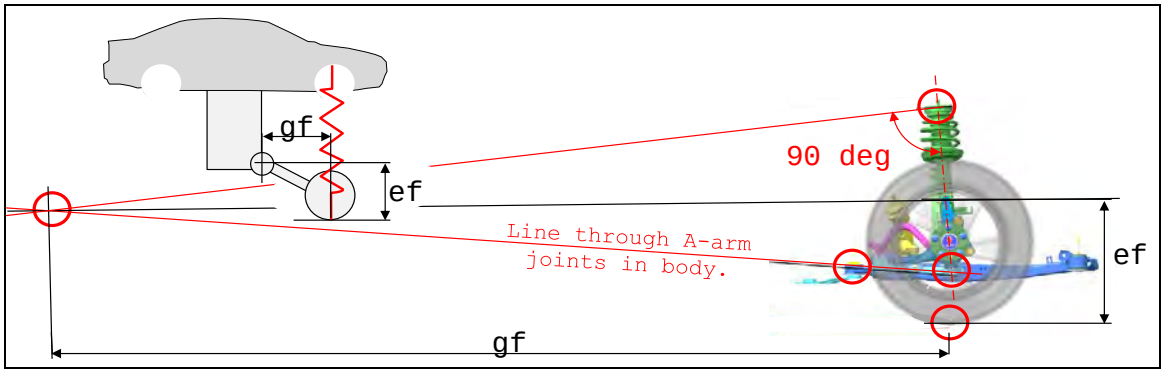


Figure 2-91: Example of typical front axle suspension, and how pivot point is found. The example shows a McPherson suspension. From Gunnar Olsson, LeanNova.

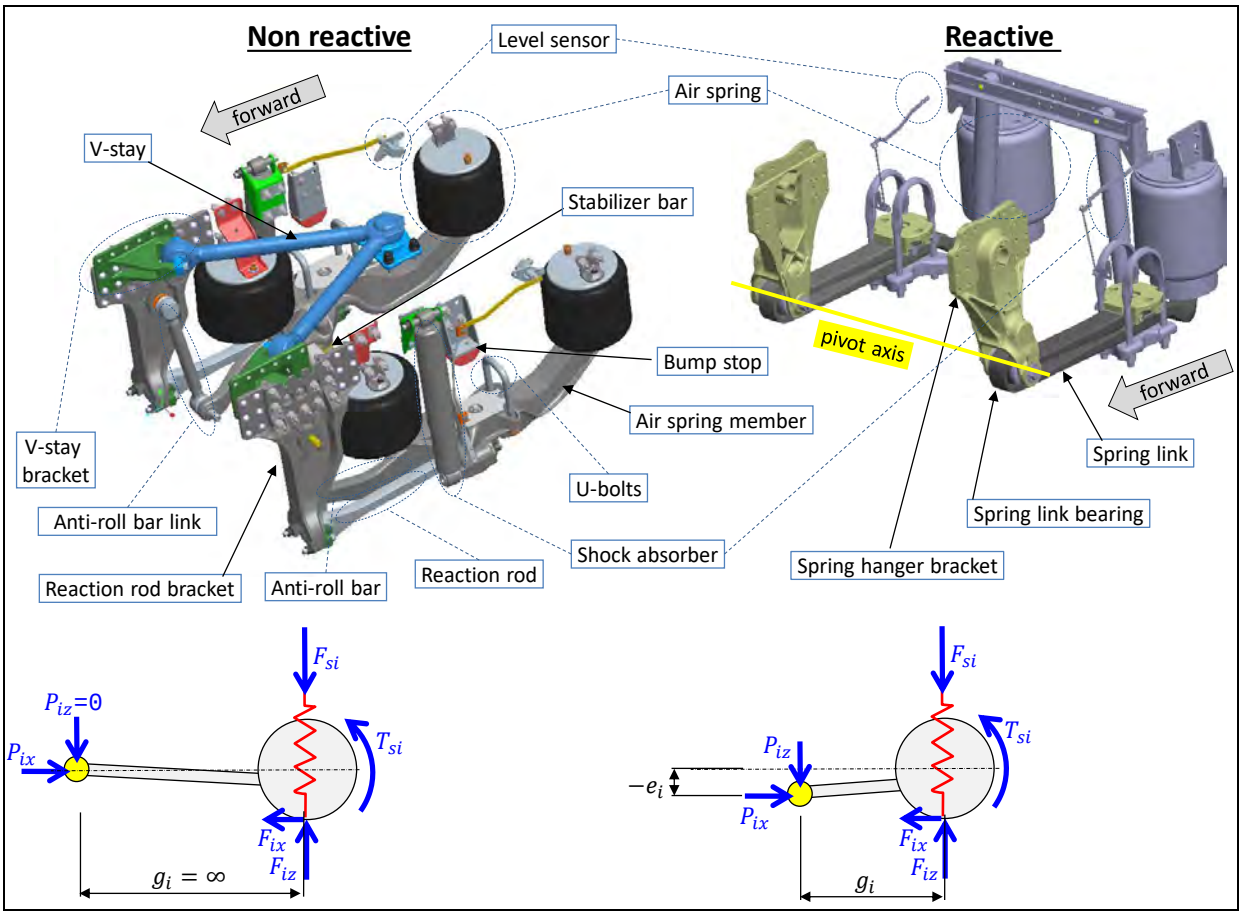


Figure 2-92: Axle suspensions/installations for one rear axle on a heavy vehicle.

Figure 2-93 and Figure 2-94 show design of two axles with independent wheel suspensions. Figure 2-95 shows an axle with dependent wheel suspension. These figures show how to find wheel pivot points and roll centre. In the McPherson suspension in Figure 2-94, one should mention that the strut is designed to take bending moments. For the rigid axle in Figure 2-95, one should mention that the leaf spring itself takes the lateral forces. Symmetry between left and right wheel suspension is a reasonable assumption and it places the roll centre symmetrically between the wheels, which is assumed in the previous models and equations regarding roll centre.

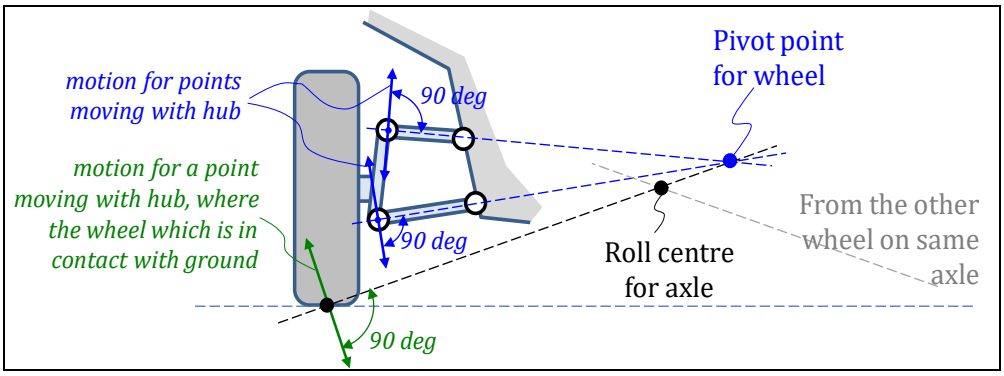


Figure 2-93: Example of how to appoint the pivot point for one wheel, and roll centre height, for an axle with double wishbone suspension.

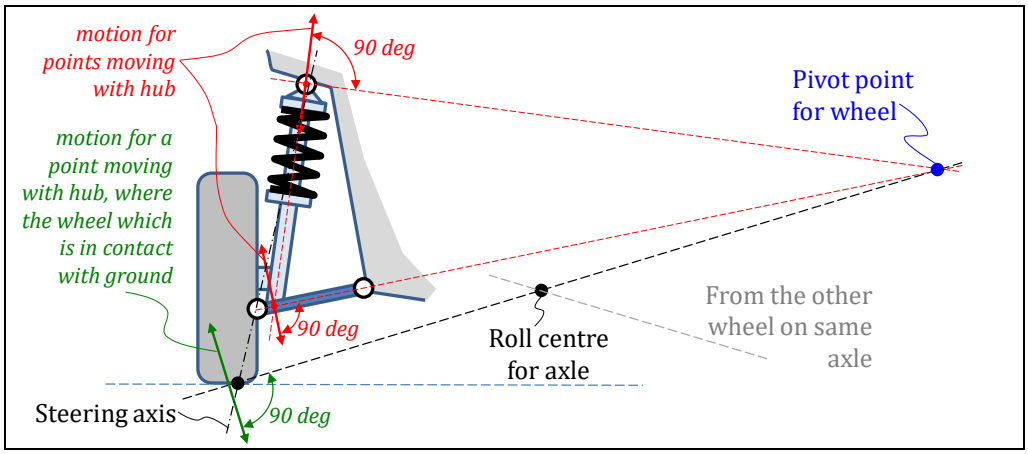


Figure 2-94: Example of how to appoint the pivot point for one wheel, and roll centre height, for axle with double McPherson suspension.

Generally, an axle with leaf springs gives roll centre height on approximately same as wheel radius, see Figure 2-95. An axle with V-stay, Figure 2-92, gets the rollcentre in the V-stay. With individual wheel suspension one has much larger flexibility, and typical chosen designs are 30..90 mm front and 90..120 mm rear.

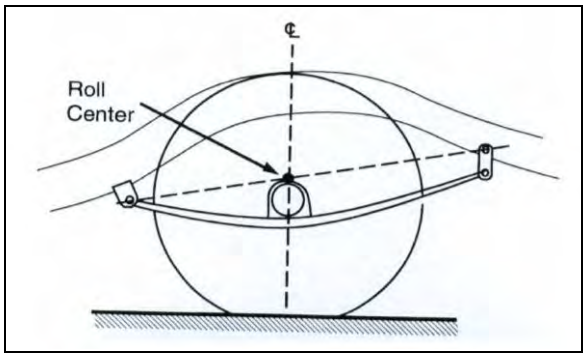


Figure 2-95: Example of how to appoint the pivot point for one wheel and roll centre for axle with rigid axle suspended in leaf springs. From (Gillespie, 1992).

The target for roll centre height is a trade-off. On one side, high roll centre is good because it reduces roll in steady state cornering. On the other side, low roll centre height is good because it gives small track width variations due to vehicle heave. Track width variations are undesired, e.g. because it makes the left and right tyre lateral force fight against each other, leaving less available friction for longitudinal and lateral grip. Roll centre is normally higher rear than front. One reason for that is that the main inertia axis leans forward, and parallelism between roll axis and main inertia axis is desired.

2.4 Propulsion System

A generalised propulsion system is shown in Figure 2-96, along with a specific example of a conventional one. There are 1+2=3 control degrees of freedom marked for the generalized one (e.g. engine power, transmission ratio and storage power) while there is only 1+1=2 for the conventional. The larger number of control degrees of freedom comes from that there are 2 drivetrains, e.g. an ICE as prime mover and an electric machine inside the transmission. Most of 2.4 assumes a single drivetrain, except Figure 2-96 and 2.4.7, which assumes multiple drivetrains. This book distinguishes between propulsion systems and drivetrains, where there is exactly one propulsion system for a whole vehicle, but it can consist of one or more drivetrains.

Note that the approach in Figure 2-96 uses a one-wheel 1D longitudinal model, see 1.6.2.2.1.

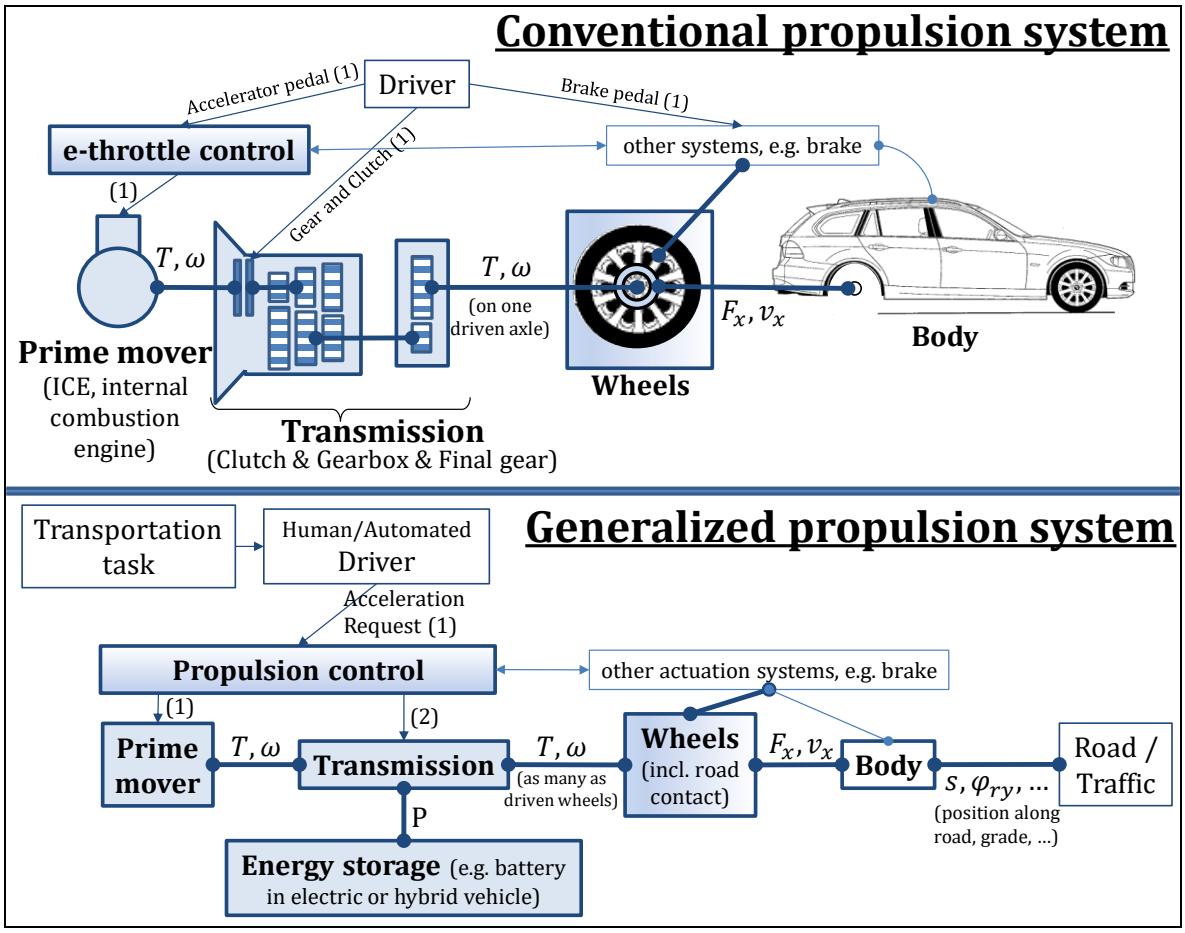


Figure 2-96: Propulsion system models, as appearing in a vehicle model

2.4.1 Modelling Concepts

It is often suitable to model propulsion systems as in "1.6.1.1.1 Single cut force notation", see Figure 2-97.

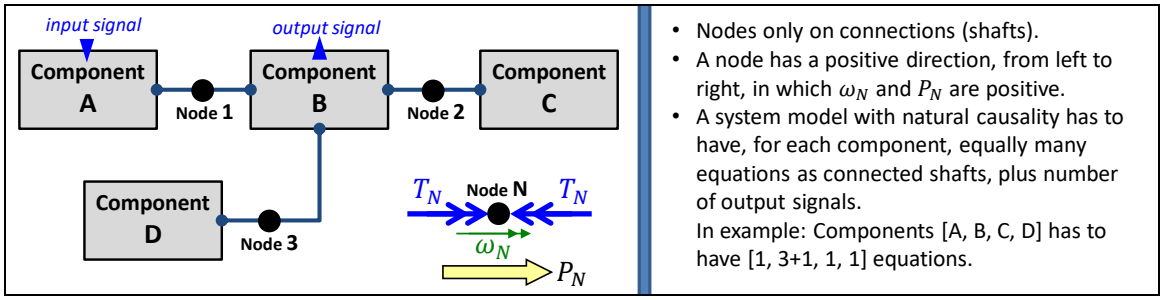


Figure 2-97: Proposed notation and sign conventions for Propulsion system models, following "1.6.1.1.1 Single cut force notation". A cut results in a "node". In each node there is one force (or torque): T_N.

The alternative would be as shown in Figure 2-98. It might be better if the model should resolve moments in different directions in 3D (not shown in Figure 2-98), such as can be relevant e.g. for conical gear transmissions.

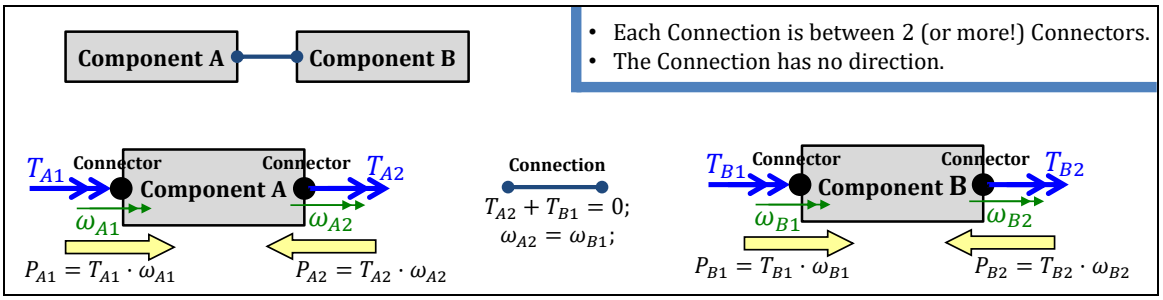


Figure 2-98: Alternative notation and sign conventions for Propulsion system models, following "1.6.1.1.2 Multiple cut forces notation". A cut results in a "connection". In each connection there can be multiple (>1) force (or torque): $\{T_{A2}, T_{B1}\}$.

2.4.2 Prime movers

The conversion of stored energy to power occurs in the prime mover, see Figure 2-96. Details of the conversion processes and transmission of power to the tyres are not covered in this book. Some basic background is still necessary to describe the longitudinal performance of the vehicle. The main information that is required is a description of the torque applied to the wheels over time and/or as a function of speed. Additional, for control of most efficient transport, we need some relation of the power efficiency. So, there are 3 types of useful relations for any prime mover:

- 2.4.2.1 Capabilities of prime movers
- 2.4.2.2 Throttling of the prime mover
- 2.4.2.3 Efficiency and consumption

2.4.2.1 Capabilities of prime movers

Sketches of how the capability (maximum and minimum torque) varies with speed for different prime movers, e.g. internal combustion engines (ICEs) and electric machines/motors (EMs), are shown in Figure 2-99.

An ICE can only output power ($T \cdot \omega > 0$) in a narrow speed range in one speed direction. (There are ICEs which operate rather well also in reverse, such as some two-stroke ICEs.) Outside this range, the ICE works more like a damper, meaning that $\text{sign}(T \cdot \omega) < 0$ and $|T|$ increases with $|\omega|$. The curves for an EM in Figure 2-99 show that the main speciality, compared to ICEs, is that their operation ranges, in both speed and torque, are nearly mirrored in speed and torque axes. An ICE can, in practice, not operate in quadrant 2 and 3.

Other properties that make EMs different to ICEs are: quick and accurate response, well known actual torque and that it is much more realistic to divide them into several drivetrains, which can operate on different wheels/axles. And, again, EMs can operate in all 4 quadrants!

Prime movers are limited in torque ($T < T_{Max}$) by the maximum mechanical stress of the material. Prime movers are limited in power loss ($P_{Loss} < P_{LossMax}; \Rightarrow P = T \cdot \omega < P_{LossMax}/(1-\eta)$). The capabilities of ICEs can also be limited by too high emissions.

Limitation in power loss is for operation over long time in normal ambient conditions where the heating reaches a steady state temperature. Higher torques $|T|$ can be handled if good cooling and for shorter periods of time.

For EMs, used at moderate $|\omega|$, the power loss limit is reached for moderate $|T|$, where η is typically almost constant (0.80..0.95). For the power loss limit one can therefore find a parameter P_{Max} for the machine which well approximates the power loss limit as a power limit: $P = T \cdot \omega < P_{Max} \approx P_{LossMax}/(1-\eta)$. For EMs, used at very high $|\omega|$, the power efficiency becomes very small, so a limited electric energy supply gives a $T_{Max} < 0$, i.e. the machine brakes.

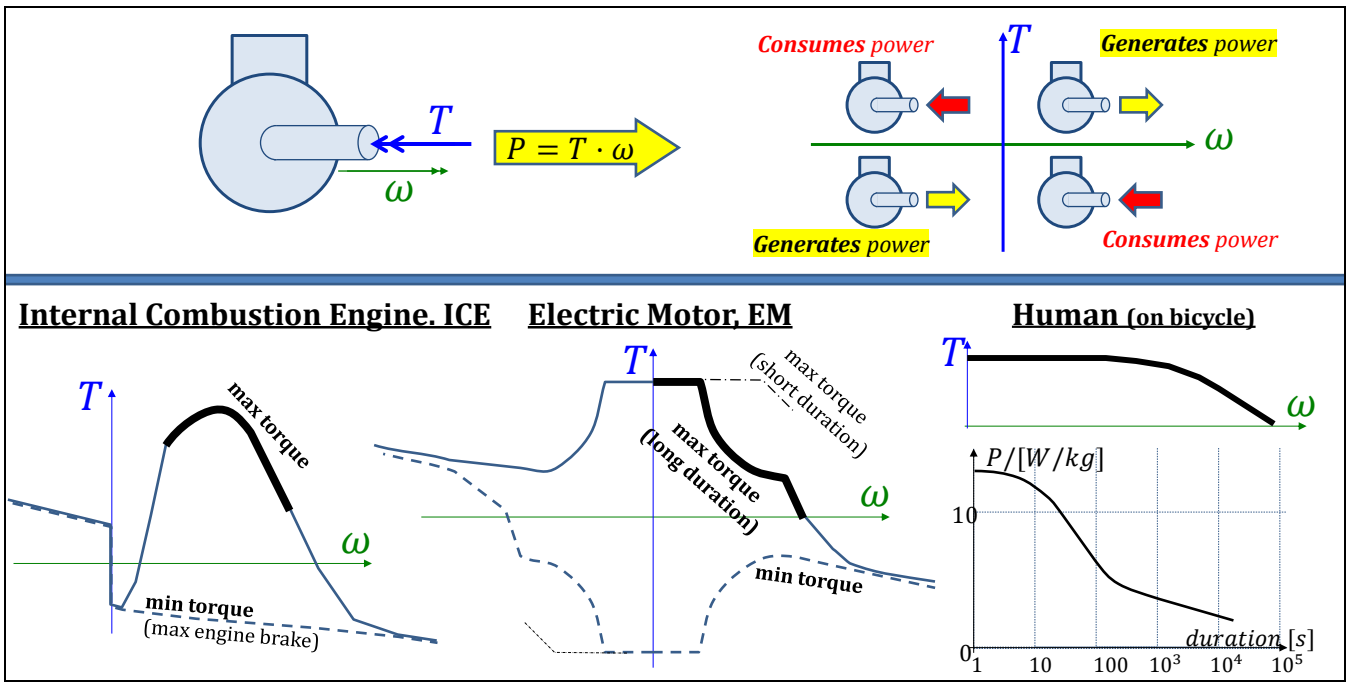


Figure 2-99: Torque Characteristics of 3 Prime Movers: ICE, EM and Human

A bicycle uses the human body as prime mover. It reminds of an EM in that it has torque from zero speed. The duration dependency is high, with maximum power ≈ 10 W/kg up to a minute duration and ≈ 2 W/kg for an hour duration.

2.4.2.2 Throttling of the prime mover

First about the word "throttling": The word comes from Otto (petrol) ICEs, in which the throttling was made through varying the opening angle of the air inlet value (a throttle) in the carburettor. In Diesel ICEs, and today's Otto ICEs, it is done by varying the amount of injected fuel per stroke.

Now, the vehicle level control often has a request interface where torque (or, less usual, speed) on the output shaft of the prime mover can be requested. However, to develop the algorithms to calculate this request, the vehicle engineer often needs to understand one level lower, which is how the "throttling" is made. This motivates 2.4.2.2.

The ICE and EM in Figure 2-99 can be complemented with "constant throttling" curves, as in Figure 2-100. The straight lines in the EM are conceptually from a model (from 2.4.2.3.2) with constant resistance in resistors.

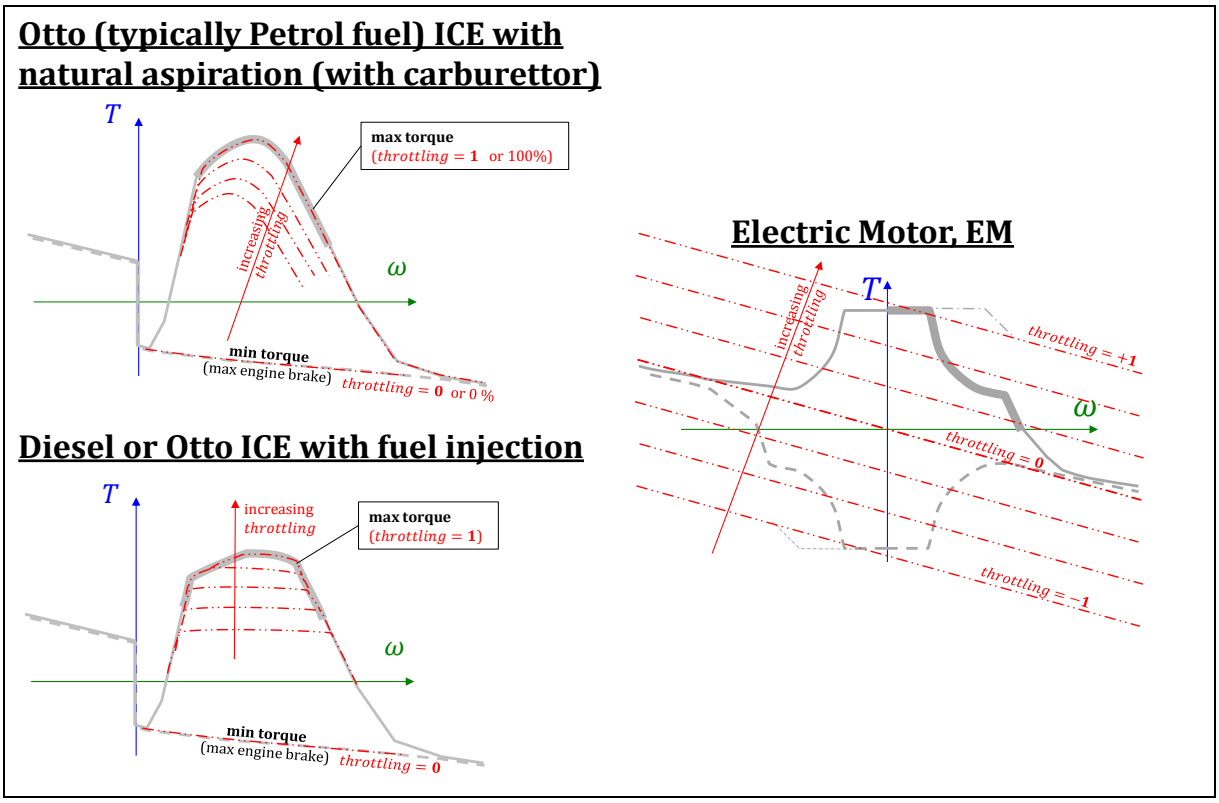


Figure 2-100: Throttling characteristics. The exact curves depend on how "throttling" is defined, which is here: throttle angle for naturally aspirated ICEs, mass of fuel injected per stroke fuel for injection ICEs, and effective voltage for EMs.

To simulate a course-of-events, such as a gear shift, we would need to prescribe the throttling, i.e., it will be an input variable. Conceptually, the explicit form of the model equation would be:

$$T \leftarrow function(\omega, throttling);$$

If starting from a torque request T_{Req}, the simulation model would include first use an inversion of the function above:

$$throttling \leftarrow function_{Inv}(\omega, T_{Req});$$

In many studies, the delay due to transients when changing torque from the prime mover can be neglected. Then we can skip to calculate the $throttling$ and instead use min, max, and the capabilities $T_{Min}(\omega)$ and $T_{Max}(\omega)$:

$$T = \max\Big(\min\Big(T_{Req}, T_{Max}(\omega)\Big), T_{Min}(\omega)\Big);$$

2.4.2.3 Efficiency and consumption

The *(power) efficiency* (η) is the *useful power* (=output on shaft=$T \cdot \omega$) divided with the *consumed power*, P_{Cons}. For ICEs, the consumed power is proportional to the *fuel rate* in $[kg/s]$ or $[m^3/s]$. For battery EMs, the consumed power is the decrease rate of stored energy, where rate means "per time". For EMs supplied from the grid (which is unusual, but an example is a trolley bus), the consumed power is the power that one pays for.

Note that one can instead define *energy efficiency*, i.e. *useful energy* divided with *consumed energy*. If averaging power efficiency over time and neglecting energy storages in the prime mover, such as kinetic rotational energy, the numerical value of the two efficiencies will be the same. However, the book prefers momentary quantities, i.e. power, to make it possible to study the vehicle motion (force and velocity) over time.

The *fuel rate* $[kg/s]$ is the amount of injected fuel per time. If fuel rate is multiplied with the *specific energy content* of the fuel, c, in $[J/kg]$, one gets the *consumed power* in $[J/s]$. If the useful power is divided with the consumed power, one gets the power efficiency. So, the *specific fuel consumption* $[kg/J]$ is inversely proportional to power efficiency for a given fuel.

$$\eta = \frac{P_{Useful}}{P_{Cons}} = \frac{P_{Useful}\left[\frac{J}{s}\right]}{FuelRate\left[\frac{kg}{s}\right] \cdot c\left[\frac{J}{kg}\right]}; \Rightarrow \left\{\begin{matrix} for\ a\ given\ fuel: \\ c = constant \end{matrix}\right\} \Rightarrow$$

$$\Rightarrow \quad \eta \propto \frac{P_{Useful}}{FuelRate}\left[\frac{J}{kg}\right] = \frac{1}{SpecificFuelConsumtion\left[\frac{kg}{J}\right]};$$

$$where\ c = SpecificEnergyContent\ in\ [J/kg]\ or\ [J/m^3] \qquad [2.76]$$

The efficiency is dependent on the operating point in the speed vs torque diagram, or map, for the prime mover. An example of a specific fuel consumption map for an ICE is given in Figure 2-101. The curves for constant specific fuel consumption are shaped exactly as the curves for constant efficiency curves. The corresponding 3D plots would show "a hollow and a mountain", respectively. Maps with similar function can be found for other types of prime movers, such as the efficiency map for an EM, see Figure 2-102.

Figure 2-101 and Figure 2-102 also show that the efficiencies can be transformed to the traction diagram. The maps for different gears partly overlap each other, which show that an operating point of the vehicle can be reached using different gears. The most fuel or energy efficient way to select gear is to select the gear which gives the lowest specific fuel consumption, or highest efficiency. Such a gear selection principle is one way of avoiding specifying the gear selection as a function over time in the driving cycle. For vehicles with automatic transmission, that principle can be programmed into the control algorithms for the transmission. However, the gear selection is often a trade-off with acceleration reserve, see 3.3.5.6, which argues for lower gear. Assuming very tightly stepped transmission, or CVT, gives that a high efficiency can be kept down to around 0.3 of maximum power.

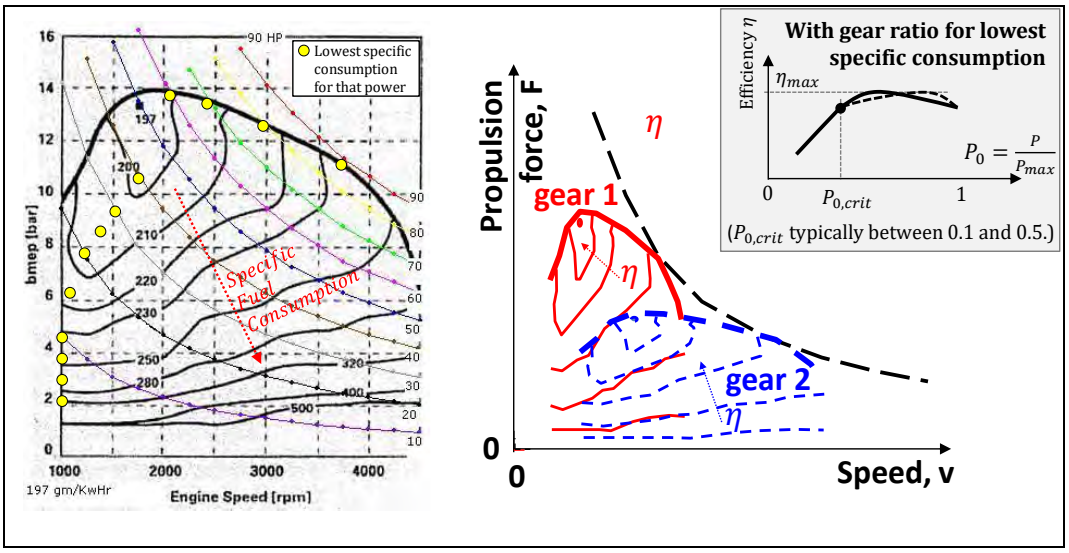


Figure 2-101: Left: Fuel consumption map. Curves with constant specific fuel consumption $[g/(kW \cdot h)]$, which is $\propto 1/efficiency$. Middle: Specific fuel consumption curves transformed to Traction Diagram, for different gears. Right: How efficiency with efficiency-optimal gear ratio drops significantly when $P < P_{0,crit} \cdot P_{max}$.

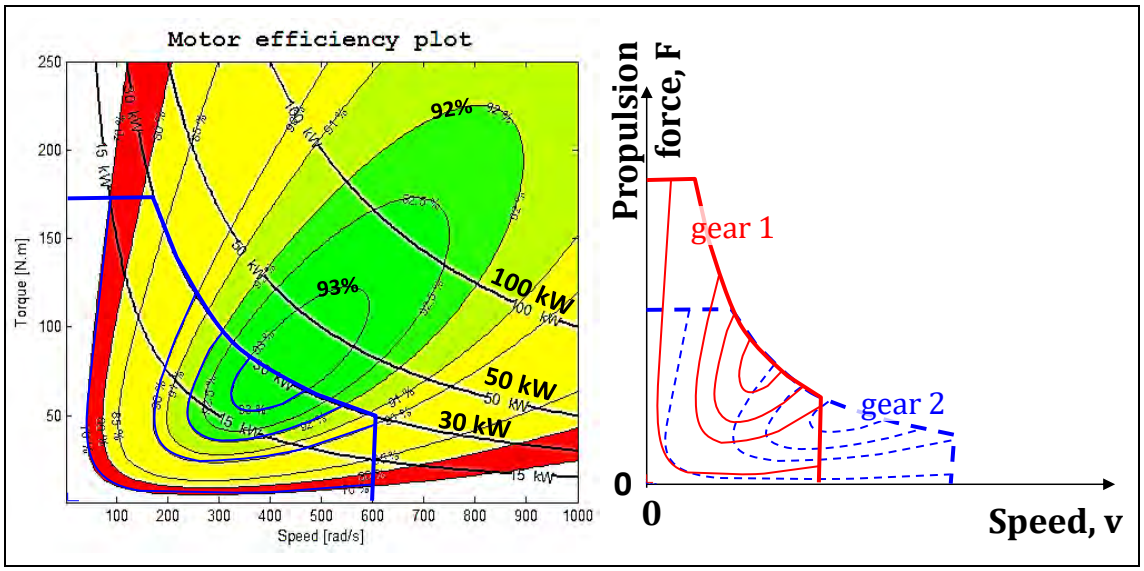


Figure 2-102: Left: Efficiency map for a typical brushless DC motor, from (Boerboom, 2012). Elliptic curves show where efficiency, in [1/W/W], is constant. Right: The efficiency curves can also be transformed in Traction Diagram, see 3.2.1, for a given gear.

2.4.2.3.1 Power loss and efficiencies in electric machines

Power is well defined in any physical domain, so the *power loss* in a machine is apparently $P_{Loss} = P_{in} - P_{out}$;. We have defined directions of $\{U, I, \omega, T\}$ so that $P_{Loss} = U \cdot I - T \cdot \omega$;.

The definition of *(power) efficiency* is less apparent. This is because the definition of η is varying, approximately following the quadrants, see Figure 2-103. The efficiencies η_{Mtr} and η_{Gen} are both defined as $\eta = P_{Useful}/P_{Used}$;, but $Useful$ and $Used$ have different meaning for motor and generator.

When treating more than one quadrant, it is therefore less risk for misunderstandings to work with maps for $P_{Loss}(\omega, T)$ than for $\eta(\omega, T)$. Also, P_{Loss} varies less, it is always positive and finite.

Note that quadrant 1 and 3 (or 2 and 4) are very symmetric, while quadrant 1 and 4 (or 2 and 3) are not as symmetric. So, the diagram has a "symmetry with flip": mirrored in both ω axis and T axis. Note in Figure 2-104, that there are areas in the diagram where the machine can be seen as either a motor with negative efficiency or a generator with negative efficiency. There we could call it "power dissipator", which means that power must be put in to both the electrical connection and the mechanical connection (the shaft).

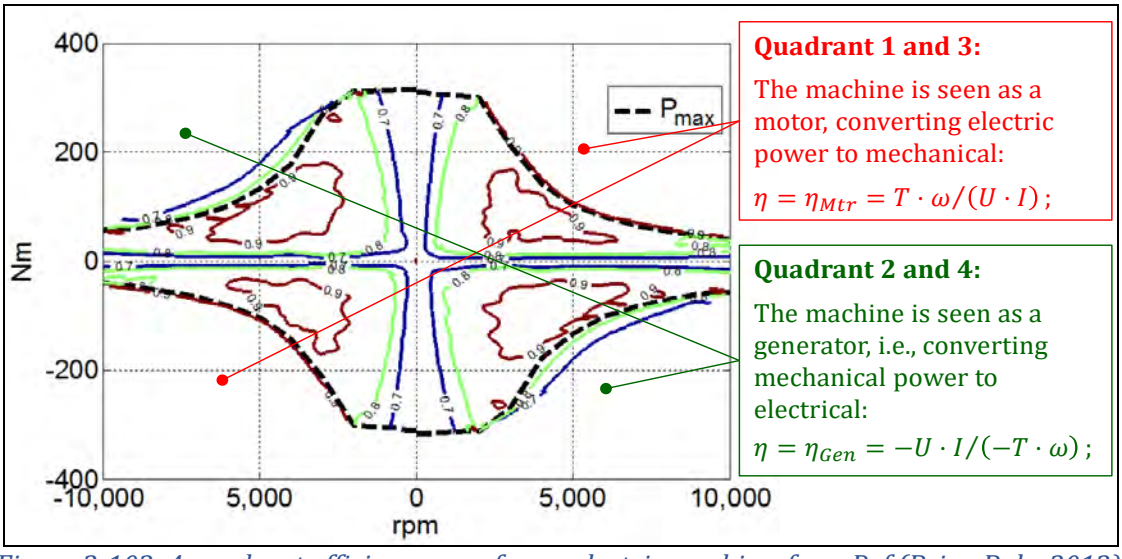


Figure 2-103: 4 quadrant efficiency map for an electric machine, from Ref (Brian Bole, 2012).

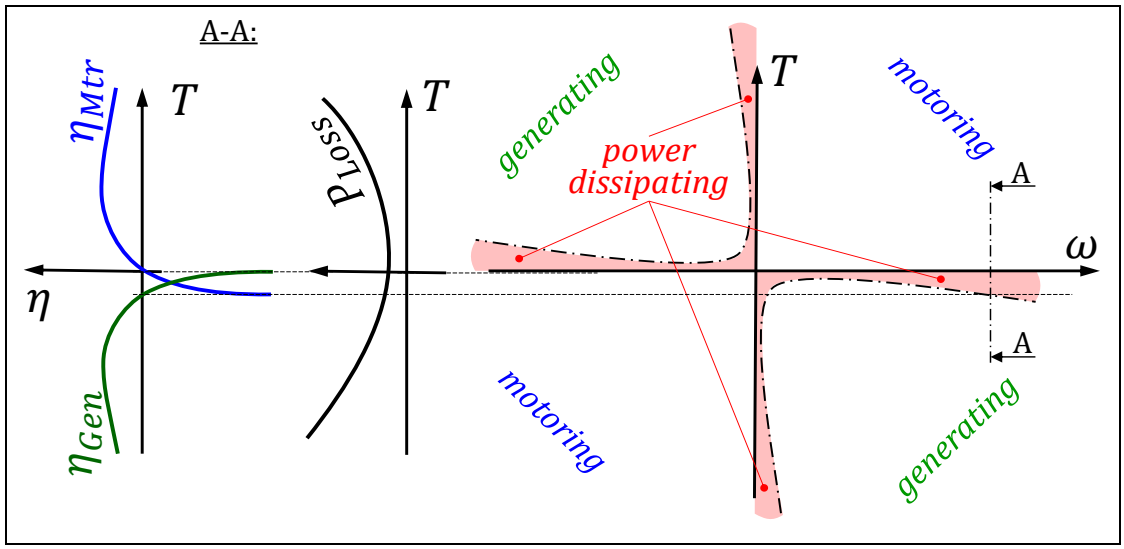


Figure 2-104: En electric machine can operate in motoring, generating, or power dissipating.

2.4.2.3.2 Model of power losses in an electric machine

A model of the losses ($\{\eta_{Mtr}(\omega,T)\ and\ \eta_{Gen}(\omega,T)\}$, or $P_{Loss}(\omega,T)$) is useful when studying selection of gears and coordination of multiple electric drivetrains. For this, interpolation in a map from empiric measurements can be used. However, a physically motivated model can have advantages in computation performance and validity range. The models presented in 2.4.2.3.2 are not physically accurate in details, e.g., bearing in mind that the current is not a direct current, but alternating current due to the throttling. However, physical phenomena (resistances) are used, which makes the model decent in all operating conditions, e.g., power losses are always ≥ 0 since the resistances has positive real values.

Similar search for simple and tuneable EM efficiency models is found in, e.g., Reference (Mahmoudi, Soong, Pellegrino, & Armando, 2015). As in the book, these map P_{Loss} as opposed to η. The book is slightly more physical, since the book makes some of the modelling using resistors, not only mathematical expressions.

2.4.2.3.2.1 Initial model, physical

The model should have a minimum of parameters, but many enough to make the model tuneable to experiments, which is typically a handful of parameters. The model should be used instead of a map, which typically has many more parameters, typically hundreds of values in a dense $\{T,\omega\}$-grid. If we would like to tune for a certain peak efficiency η_{MtrOpt} at a certain $\{\omega,T\}$, it is likely that less resistors would be enough, e.g. Figure 2-105.

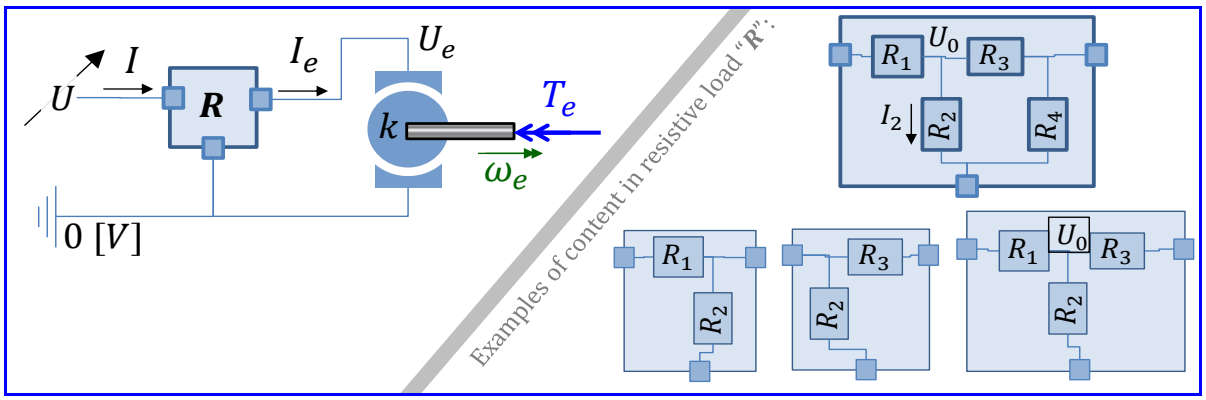


Figure 2-105: Physical model of power losses in an electric machine using an ideal motor and some electrical resistors, each with voltage drop proportional to current.

A mathematical model, using the 4-resistor content of the resistive load ***R*** in Figure 2-105:

$$\begin{aligned} U - U_0 &= R_1 \cdot I; \\ U_0 &= R_2 \cdot I_2; \\ U_0 - U_e &= R_3 \cdot (I - I_2); \\ U_e &= R_4 \cdot (I - I_2 - I_e); \\ T_e \cdot \omega &= U_e \cdot I_e; \\ T_e &= k \cdot I_e; \end{aligned} \qquad [2.77]$$

Elimination of all variables except the interface variables $\{U, I, T_e, \omega_e\}$ is the same as eliminating the internal variables $\{U_0, U_e, I_2\}$. It gives a model with only 2 equations:

$$\begin{bmatrix} U \\ I \end{bmatrix} = \begin{bmatrix} a & b \\ c & d \end{bmatrix} \cdot \begin{bmatrix} \omega_e \\ T_e \end{bmatrix}; \qquad [2.78]$$

$$\text{where } \begin{bmatrix} a & b \\ c & d \end{bmatrix} = \begin{bmatrix} \left(1 + \frac{R_1}{R_2} + \frac{R_1}{R_4} + \frac{R_3}{R_4} + \frac{R_1 \cdot R_3}{R_2 \cdot R_4}\right) & \left(R_1 + R_3 + \frac{R_1 \cdot R_3}{R_2}\right) \\ \left(\frac{1}{R_2} + \frac{1}{R_4} + \frac{R_3}{R_2 \cdot R_4}\right) & \left(1 + \frac{R_3}{R_2}\right) \end{bmatrix} \cdot \begin{bmatrix} k & 0 \\ 0 & \frac{1}{k} \end{bmatrix};$$

The linearity of this model leads to straight line throttling curves, as in Figure 2-100.

Definition of the "auxiliary variable" P_{eLoss}:

$$\begin{aligned} P_{eLoss} = U \cdot I - T_e \cdot \omega_e &= \{insert\ expressions\ for\ U\ and\ I\} = \\ &= (b \cdot T_e + a \cdot \omega_e) \cdot (d \cdot T_e + c \cdot \omega_e) - T_e \cdot \omega_e = \\ &= \underbrace{a \cdot c}_{A} \cdot \omega_e^2 + \underbrace{b \cdot d}_{B} \cdot T_e^2 + \left(\underbrace{b \cdot c + a \cdot d}_{C} - 1\right) \cdot T_e \cdot \omega_e = \\ &= A \cdot \omega_e^2 + B \cdot T_e^2 + (C - 1) \cdot T_e \cdot \omega_e = \\ &= (A \cdot \omega_e^2 + B \cdot T_e^2 + (C - 1) \cdot T_e \cdot \omega_e) \cdot \frac{T_e \cdot \omega_e}{T_e \cdot \omega_e} = \\ &= \left(A/(T_e/\omega_e) + B \cdot T_e/\omega_e + (C - 1)\right) \cdot T_e \cdot \omega_e = \\ &= P_{eLoss}(T_e/\omega_e, T_e \cdot \omega_e, \{A, B, C\}); \end{aligned}$$

$$where \begin{cases} A = \left(\frac{1}{R_2} + \frac{1}{R_4} + \frac{R_3}{R_2 \cdot R_4}\right) \cdot \left(1 + \frac{R_1}{R_2} + \frac{R_1}{R_4} + \frac{R_3}{R_4} + \frac{R_1 \cdot R_3}{R_2 \cdot R_4}\right) \cdot k^2; \\ B = \left(R_1 + R_3 + \frac{R_1 \cdot R_3}{R_2}\right) \cdot \left(1 + \frac{R_3}{R_2}\right) \cdot \frac{1}{k^2}; \\ C = \left(1 + \frac{R_3}{R_2}\right) \cdot \left(1 + \frac{R_1}{R_2} + \frac{R_1}{R_4} + \frac{R_3}{R_4} + \frac{R_1 \cdot R_3}{R_2 \cdot R_4}\right) + \left(\frac{1}{R_2} + \frac{1}{R_4} + \frac{R_3}{R_2 \cdot R_4}\right) \cdot \left(R_1 + R_3 + \frac{R_1 \cdot R_3}{R_2}\right); \end{cases}$$

The parameters (either it is the 5 parameters $\{k, R_1, R_2, R_3, R_4\}$, 4 parameters $\{a, b, c, d\}$, or the 3 parameter $\{A, B, C\}$) help to get one approximate understanding of an electric machine, but it is often difficult to find each of the parameter values from separate measurements. For vehicle engineering, as opposed to a machine designer, it is often more important to have a model which is tuneable to well represent the power efficiency, and well represent it over a larger range of operating points. So, we will now try to express the P_{eLoss} in what we can read out from an efficiency map (from experiment with the machine in a subsystem rig) rather than expressed in the $\{A, B, C\}$.

First, express the auxiliary variables for power efficiencies, motoring and generating:

$$\begin{aligned} \eta_{eMtr} = \frac{P_{Useful}}{P_{Used}} = \frac{T_e \cdot \omega_e}{U \cdot I} = \frac{T_e \cdot \omega_e}{T_e \cdot \omega_e + P_{eLoss}} = \frac{1}{1 + \frac{P_{eLoss}}{T_e \cdot \omega_e}} = \frac{1}{A/(T_e/\omega_e) + B \cdot T_e/\omega_e + C} = \\ = \eta_{Mtr}(T_e/\omega_e, \{A, B, C\}); \end{aligned}$$

$$\begin{aligned} \eta_{eGen} = \frac{P_{Useful}}{P_{Used}} = \frac{-U \cdot I}{-T_e \cdot \omega_e} = 1/\eta_{Mtr} = A/(T_e/\omega_e) + B \cdot T_e/\omega_e + C = \\ = \eta_{Gen}(T_e/\omega_e, \{A, B, C\}); \end{aligned}$$

Then, elaborate with the **location** of the optimum operating points, where η_{eMtr} and η_{eGen} have their optimal (maximum) values. These are candidates to tune from. They are points in the 1-dimensional space of T_e/ω_e, not the 2-dimensional space of $\{T, \omega\}$.

$$\left(\frac{\partial}{\partial(T_e/\omega_e)}\eta_{Mtr}\right)\Big|_{T_e/\omega_e=(T_e/\omega_e)_{MtrOpt}} = 0; \Rightarrow$$

$$\Rightarrow \frac{\frac{A}{(T_e/\omega_e)^2_{MtrOpt}} - B}{\left(C + B\cdot(T_e/\omega_e)_{MtrOpt} + \frac{A}{(T_e/\omega_e)_{MtrOpt}}\right)^2} = 0; \Rightarrow \frac{A}{(T_e/\omega_e)^2_{MtrOpt}} = B;$$

$$\left(\frac{\partial}{\partial(T_e/\omega_e)}\eta_{Gen}\right)\Big|_{T_e/\omega_e=(T_e/\omega_e)_{GenOpt}} = 0; \Rightarrow$$

$$\Rightarrow \frac{A}{(T_e/\omega_e)^2_{GenOpt}} - B = 0; \Rightarrow \frac{A}{(T_e/\omega_e)^2_{GenOpt}} = B;$$

So, the model can only handle that $(T_e/\omega_e)^2_{MtrOpt} = (T_e/\omega_e)^2_{GenOpt}$, but that is a good approximation for most machines. So, we list $(T_e/\omega_e)_{Opt}$ as our first measure which is needed for tuning: $(T_e/\omega_e)_{Opt} = +(T_e/\omega_e)_{MtrOpt} = -(T_e/\omega_e)_{GenOpt}$.

Now, we had 3 parameters and found one equation, so we have 3-1=2 more dofs to tune. We try to do it from the **values** of the optimal efficiencies:

$$\eta_{Mtr}|_{T_e/\omega_e=+(T_e/\omega_e)_{Opt}} = \eta_{MtrOpt}; \Rightarrow \frac{1}{A/(T_e/\omega_e)_{Opt}+B\cdot(T_e/\omega_e)_{Opt}+C} = \eta_{MtrOpt};$$

$$\eta_{Gen}|_{T_e/\omega_e=-(T_e/\omega_e)_{Opt}} = \eta_{GenOpt}; \Rightarrow A/(T_e/\omega_e)_{Opt} + B\cdot(T_e/\omega_e)_{Opt} + C = \eta_{GenOpt};$$

Solving for all $\{A, B, C\}$ gives:

$$A = \frac{1}{4}\cdot\frac{1-\eta_{MtrOpt}\cdot\eta_{GenOpt}}{\eta_{MtrOpt}}\cdot(T_e/\omega_e)_{Opt};$$

$$B = \frac{1}{4}\cdot\frac{1-\eta_{MtrOpt}\cdot\eta_{GenOpt}}{\eta_{MtrOpt}}\cdot\frac{1}{(T_e/\omega_e)_{Opt}};$$

$$C = \frac{1+\eta_{MtrOpt}\cdot\eta_{GenOpt}}{2\cdot\eta_{MtrOpt}};$$

So, we can replace the parameters $\{A, B, C\}$ with parameters $\{(T_e/\omega_e)_{Opt}, \eta_{MtrOpt}, \eta_{GenOpt}\}$ in the expression for P_{eLoss}:

$$P_{eLoss} = \left[\frac{1}{4}\cdot\frac{1-\eta_{MtrOpt}\cdot\eta_{GenOpt}}{\eta_{MtrOpt}}\cdot\left(\frac{(T_e/\omega_e)_{Opt}}{T_e/\omega_e} + \frac{T_e/\omega_e}{(T_e/\omega_e)_{Opt}}\right) + \left(\frac{1+\eta_{MtrOpt}\cdot\eta_{GenOpt}}{2\cdot\eta_{MtrOpt}} - 1\right)\right]\cdot T_e\cdot\omega_e;$$

A model which is useful as a submodel in a larger (vehicle) model becomes as follows. Note that the model does **not** allow resolution in both electrical interface variables U and I, only the product $U\cdot I$. Anyway, the model is useful for following state-of-charge SoC in a battery ($d/dt\,(SoC) = U\cdot I/E_{BattMax}$). We can also find an equation to connect to P_{Loss}, which is useful for optimizing cost rate ($energy\ cost\ rate[€/s] = Prize[Nm/€]\cdot P_{Loss}[Nm/s]$).

$$P_{eLoss} = \left[\frac{1}{4}\cdot\frac{1-\eta_{MtrOpt}\cdot\eta_{GenOpt}}{\eta_{MtrOpt}}\cdot\left(\frac{(T_e/\omega_e)_{Opt}}{T_e/\omega_e} + \frac{T_e/\omega_e}{(T_e/\omega_e)_{Opt}}\right) + \left(\frac{1+\eta_{MtrOpt}\cdot\eta_{GenOpt}}{2\cdot\eta_{MtrOpt}} - 1\right)\right]\cdot T_e\cdot\omega_e; \quad [2.79]$$

$$U\cdot I = T_e\cdot\omega_e + P_{eLoss};$$

2.4.2.3.2.1.1 A numerical example

With $\{(T_e/\omega_e)_{Opt}, \eta_{MtrOpt}, \eta_{GenOpt}\} = \left\{\frac{100}{300}\left[\frac{Nm}{rad/s}\right], 0.95\ \left[\frac{W}{W}\right], 0.90\left[\frac{W}{W}\right]\right\}$, we get:

- $A = 0.0127[Nms]$;
- $B = 0.1145\left[\frac{1}{Nms}\right]$;
- $C = 0.9763\left[\frac{W}{W} = 1\right]$;

The efficiencies are plotted in Figure 2-106. The upper right plot is made with "semi-invert scale" on the T_e/ω_e axis, which shows symmetries around $T_e/\omega_e = (T_e/\omega_e)_{Opt}$ and $T_e/\omega_e = -(T_e/\omega_e)_{Opt}$.

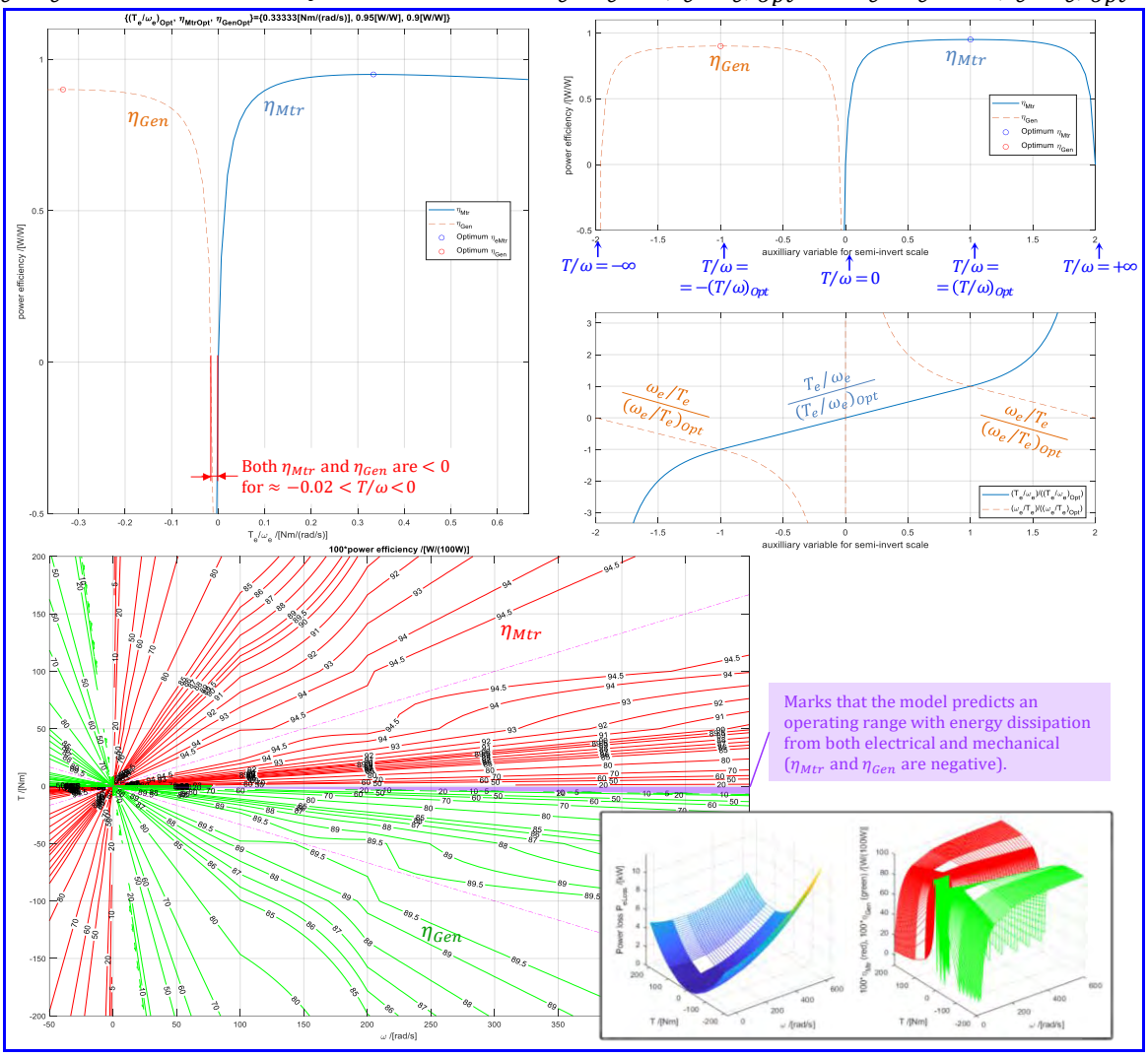


Figure 2-106: Numerical example, using model from Eq [2.87]. The model is smooth, but the grid over $\{\omega_e, T_e\}$ makes the plot unsmooth.

With the model, η_{Mtr} and η_{Gen} vary only with 1 variable, T_e/ω_e, and not with the 2 variables, $\{T_e, \omega_e\}$ or $\{T_e/\omega_e\,, T_e \cdot \omega_e\}$. So, in a $\{\omega_e, T_e\}$ plot, it gives maxima along <u>lines</u> ($T_e/\omega_e = +(T_e/\omega_e)_{Opt}$ and $T_e/\omega_e = -(T_e/\omega_e)_{Opt}$). We can call these optimal lines "ridges".

Experiments with electric machines rather show maximum η_{Mtr} and η_{Gen} in <u>points</u> $\{T, \omega\} = \{T_{MtrOpt}, \omega_{MtrOpt}\}$ and $\{T, \omega\} = \{T_{GenOpt}, \omega_{GenOpt}\}$. So, one would like add something in the model that "bends down" ridges, both for when $|T \cdot \omega| < (T_e \cdot \omega_e)_{Opt}$ and when $|T \cdot \omega| > (T_e \cdot \omega_e)_{Opt}$.

2.4.2.3.2.2 Adding two power loss terms

We add 2 losses:

- An electric machine needs to create an electromagnetic field. This is an **idle** power loss, which is a loss independent of whether $T \cdot \omega = 0$ or $T \cdot \omega \neq 0$. Such idle loss dominates when $T \cdot \omega \approx 0$, so adding it to the model would "bend down" the ridges when $|T \cdot \omega| < (T \cdot \omega)_{Opt}$. We introduce a parameter ΔP_{Loss}.
- We also realise that we need a term in η proportional to $T \cdot \omega$, which requires a term in P_{Loss} proportional to $(T \cdot \omega)^2$. We introduce one such term also, with parameter D.

We use notation without e in the subscripts for the new model. This yields:

$$P_{eLoss} = \left(\frac{A}{T/\omega} + B \cdot \frac{T}{\omega} + (C-1)\right) \cdot T \cdot \omega + \boldsymbol{\Delta P_{Loss}} + D \cdot (T \cdot \omega)^2 =$$
$$= P_{eLoss}\left(\frac{T}{\omega}, T \cdot \omega, \{A, B, C, \boldsymbol{\Delta P_{Loss}}, D\}\right);$$

We can draw a physical model as in Figure 2-107.

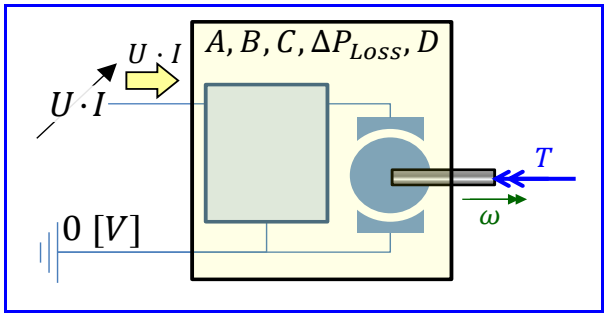


Figure 2-107: Extension of the model in Figure 2-119. The model is quasi-physical, i.e. contains parts which are not well physically motivated, to enable tuning to experiment. Therefore, the internal variables, U_e and I_e, are not interpretable, which is why they are not marked. Also, the resolution into U and I is lost; we only have $U \cdot I$.

The power efficiencies for, motoring and generating, becomes:

$$\eta_{eMtr} = \frac{1}{\frac{A}{T/\omega} + B \cdot \frac{T}{\omega} + C + \frac{\boldsymbol{\Delta P_{Loss}}}{T \cdot \omega} + D \cdot T \cdot \omega} = \eta_{Mtr}\left(\frac{T}{\omega}, T \cdot \omega, \{A, B, C, \Delta P_{Loss}, D\}\right);$$
$$\eta_{eGen} = \frac{A}{T/\omega} + B \cdot \frac{T}{\omega} + C + \frac{\boldsymbol{\Delta P_{Loss}}}{T \cdot \omega} + D \cdot T \cdot \omega = \eta_{Gen}\left(\frac{T}{\omega}, T \cdot \omega, \{A, B, C, \Delta P_{Loss}, D\}\right);$$

The same 3 tuning equations as in 2.4.2.3.2.1 must be fulfilled, i.e.

- $\partial\eta/\partial(T/\omega)|_{\{(T\cdot\omega),(T/\omega)\}=\{(T\cdot\omega)_{Opt},(T/\omega)_{Opt}\}} = 0;$
- $\eta_{Mtr}\left((T \cdot \omega)_{Opt}, (T/\omega)_{Opt}\right) = \eta_{MtrOpt};$
- $\eta_{Gen}\left((T \cdot \omega)_{Opt}, (T/\omega)_{Opt}\right) = \eta_{GenOpt};.$

We have 5 parameters to tune, so we need 5-3=2 additional tuning equations:

- $\partial\eta/\partial(T \cdot \omega)|_{\{(T\cdot\omega),(T/\omega)\}=\{(T\cdot\omega)_{Opt},(T/\omega)_{Opt}\}} = 0;$
- $\eta_{Mtr}\left((T \cdot \omega)_{Opt}/2\,, (T/\omega)_{Opt}\right) = \eta_{MtrHalf};$ (as one example of characteristic point)

So, we can replace the parameters $\{A, B, C, \Delta P_{Loss}, D\}$ with parameters $\{(T/\omega)_{Opt}, \eta_{MtrOpt}, \eta_{GenOpt}, (T/\omega)_{Opt}, \eta_{MtrHalf}\}$ in the expressions for η_{Mtr} and η_{Gen}.

We can find a unique solution for $\{A, B, C, \Delta P_{Loss}, D\}$, e.g. using Matlab Symbolic toolbox:

- $A = -\frac{\left(\frac{T}{\omega}\right)_{Opt} \cdot (8 \cdot \eta_{MtrOpt} - 9 \cdot \eta_{MtrHalf} + \eta_{GenOpt} \cdot \eta_{MtrOpt} * \eta_{MtrHalf})}{4 * \eta_{MtrOpt} * \eta_{MtrHalf}} = 0.0028\ [Nms];$
- $B = -\frac{8 * \eta_{MtrOpt} - 9 * \eta_{MtrHalf} + \eta_{GenOpt} * \eta_{MtrOpt} * \eta_{MtrHalf}}{4 * \left(\frac{T}{\omega}\right)_{Opt} * \eta_{MtrOpt} * \eta_{MtrHalf}} = 0.0248\ \left[\frac{1}{Nms}\right];$
- $C = \frac{\eta_{GenOpt} * \eta_{MtrOpt} + 1}{2 * \eta_{MtrOpt}} = 0.9913\ \left[\frac{W}{W} = 1\right];$
- $\Delta P_{Loss} = \frac{2 * (T \cdot \omega)_{Opt} * (\eta_{MtrOpt} - \eta_{MtrHalf})}{\eta_{MtrOpt} * \eta_{MtrHalf}} = 671.8925\ \left[\frac{Nm}{s}\right];$
- $D = \frac{2 * \eta_{MtrOpt} - 2 * \eta_{MtrHalf}}{(T \cdot \omega)_{Opt} * \eta_{MtrOpt} * \eta_{MtrHalf} f} = 7.4655 \cdot 10^{-7}\ \left[\frac{1}{Nm/s}\right];$

Finally, the resulting model:

$$P_{Loss} = \left(\frac{A}{T/\omega} + B \cdot \frac{T}{\omega} + (C-1)\right) \cdot T \cdot \omega + \Delta P_{Loss} + D \cdot (T \cdot \omega)^2 =$$
$$= A \cdot \omega^2 + B \cdot T^2 + (C-1) \cdot T \cdot \omega + \Delta P_{Loss} + D \cdot (T \cdot \omega)^2; \quad [2.80]$$

$$where: \quad A = -\frac{\left(\frac{T}{\omega}\right)_{Opt} \cdot (8 \cdot \eta_{MtrOpt} - 9 \cdot \eta_{MtrHalf} + \eta_{GenOpt} \cdot \eta_{MtrOpt} * \eta_{MtrHalf})}{4 * \eta_{MtrOpt} * \eta_{MtrHalf}};$$

$$B = -\frac{8 * \eta_{MtrOpt} - 9 * \eta_{MtrHalf} + \eta_{GenOpt} * \eta_{MtrOpt} * \eta_{MtrHalf}}{4 * \left(\frac{T}{\omega}\right)_{Opt} * \eta_{MtrOpt} * \eta_{MtrHalf}};$$

$$C = \frac{\eta_{GenOpt} * \eta_{MtrOpt} + 1}{2 * \eta_{MtrOpt}};$$

$$\Delta P_{Loss} = \frac{2 * (T \cdot \omega)_{Opt} * (\eta_{MtrOpt} - \eta_{MtrHalf})}{\eta_{MtrOpt} * \eta_{MtrHalf}};$$

$$D = \frac{2 * \eta_{MtrOpt} - 2 * \eta_{MtrHalf}}{(T \cdot \omega)_{Opt} * \eta_{MtrOpt} * \eta_{MtrHalf f}};$$

$$U \cdot I = T \cdot \omega + P_{Loss};$$

2.4.2.3.2.2.1 A numerical example

With $\{(T/\omega)_{Opt}, \eta_{MtrOpt}, \eta_{GenOpt}, (T/\omega)_{Opt}, \eta_{MtrHalf}\} =$
$= \left\{\frac{100}{300}\left[\frac{Nm}{rad/s}\right], 0.95\ \left[\frac{W}{W}\right], 0.90\left[\frac{W}{W}\right], 100 \cdot 300\left[\frac{Nm}{rad/s}\right], 0.94\left[\frac{W}{W}\right]\right\}$, we get:

- $A = 0.0053[Nms]$;
- $B = 0.0473\left[\frac{1}{Nms}\right]$;
- $C = 0.9763\left[\frac{W}{W} = 1\right]$;
- $\Delta P_{Loss} = 671.8925\ [W]$;
- $D = 7.4655 \cdot 10^{-7}\ \left[\frac{W}{W^2}\right]$;

The efficiencies are plotted in Figure 2-108.

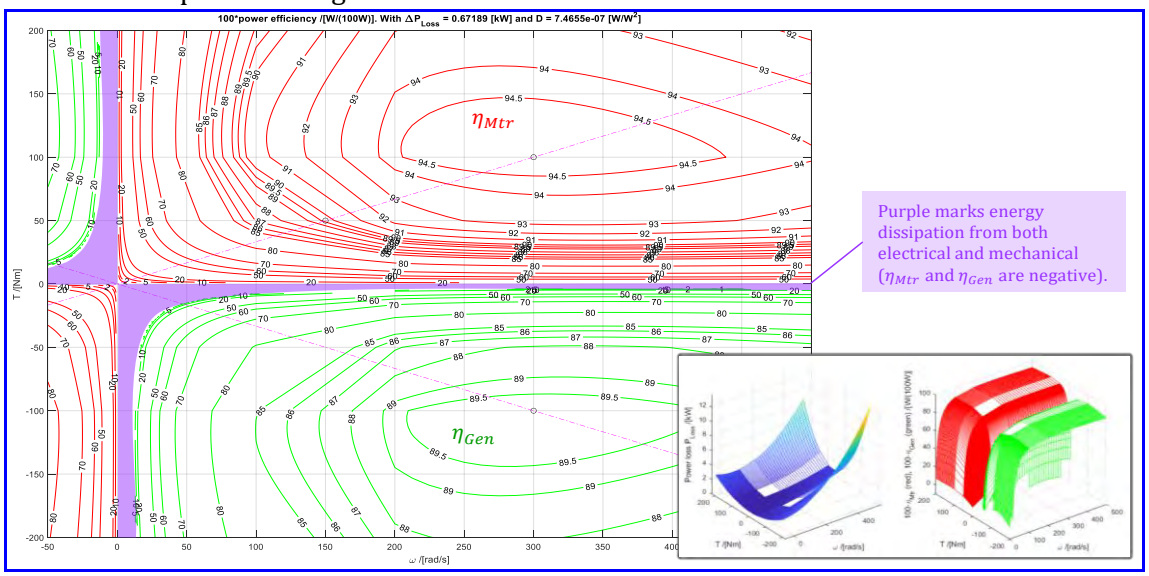


Figure 2-108: Numerical example, using model from Eq [2.80].

Left diagram in Figure 2-109 compares P_{Loss} with $T \cdot \omega$. Curve shapes for constant P_{Loss} and the capability limits, e.g. $T_{CapMax} = \min(T_{Max}, P_{Max}/\omega)$ in 2.4.2.1 are similar. A limitation of generated heat explains why a P_{Max} is a good limitation when ω is far from 0. When ω is closer to 0, there are two

explanations to a T_{Max} is a good limitation: both limitation of generated heat and maximum mechanical stresses in the machine parts.

Right diagram in Figure 2-109 shows how η_{Mtr} and η_{Gen} varies in the operating area where energy is dissipated. Both are negative and they are each others inverted values. The operation area should be avoided from energy saving point of view because it uses energy from battery to brake the vehicle; it is better to use friction brakes.

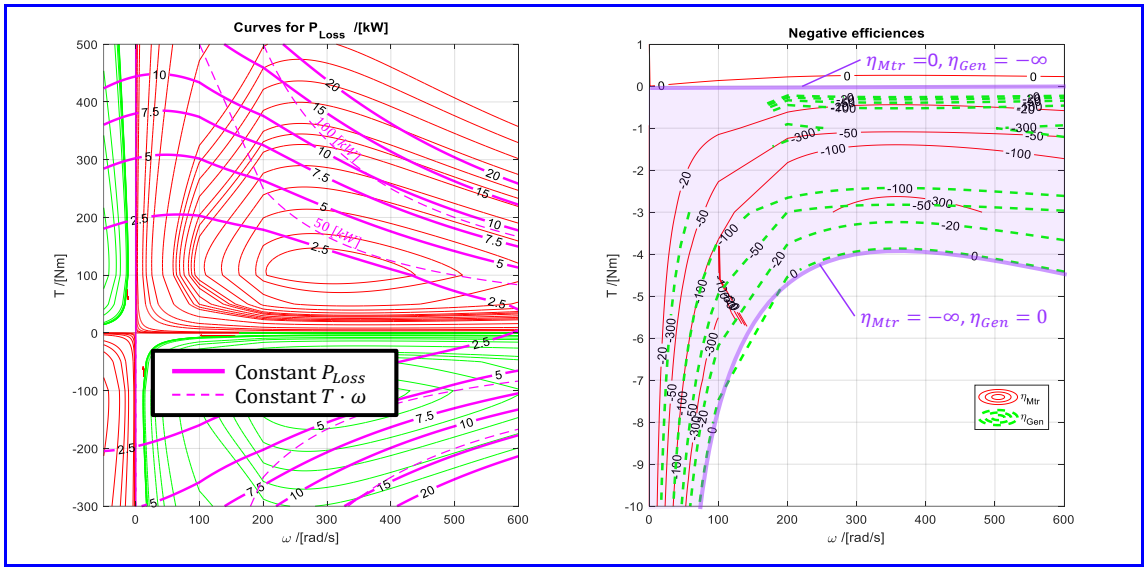


Figure 2-109: Left: Compare P_{Loss} with (mechanical) power $T \cdot \omega$.
Right: Close study of operating range with energy dissipation $\eta_{Mtr} = 1/\eta_{Gen} < 0$.

2.4.3 Transmissions

In some contexts, "transmission" means the 1-dimensional transmission of rotational mechanical power from an input shaft to one output shaft. Such are called "Main transmissions". In other contexts, "transmission" means the system that distributes the energy to/from an energy buffer and to/from multiple axles and/or wheels. Such are called "Distribution transmissions".

2.4.3.1 Main Transmissions

Contributions from Edo Drenth, Haldex Brakes

Main transmission can be either stepped transmissions or continuously variable transmissions, CVTs. Among stepped transmissions, there are manual an automatic. Among automatic, there are those with power transmission interruption during shifting and other with powershifting, see 2.4.3.1.2. Clutches and torque converters can also be part of models of main transmissions, see 2.4.4 and 2.4.4.3.

Most main transmissions use gears, which is here used as example as opposed to CVTs.

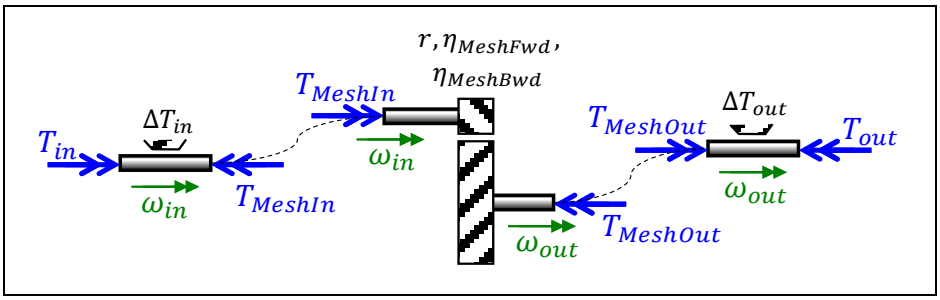


Figure 2-110: Physical model of single gear stage. Parameters are in black text.

The ΔT_i model the "load independent" (a.k.a. "parasitic") losses, arising from bearings, sealings, oil and similar. Note that bearing losses which magnitude is depending on the radial force of the bearing cannot be captured in ΔT_i but instead they can be in the η_{Mesh}.

$$T_{MeshIn} = T_{in} - \Delta T_{in} \cdot \text{sign}(\omega_{in}); \quad where\ \Delta T_{in} > 0$$
if $\omega_{in} = 0$: A discrete state locked becomes true and $\omega_{in} = 0$; replaces the torque equation above and a discrete state locked can.

$$T_{out} = T_{MeshOut} - \Delta T_{out} \cdot \text{sign}(\omega_{out}); \quad where\ \Delta T_{out} > 0$$
if $\omega_{out} = 0$: A discrete state locked becomes true and $\omega_{out} = 0$; replaces the torque equation above.

[2.81]

The $\eta_{MeshFwd}$ and $\eta_{MeshBwd}$ models "the load dependent" losses. Their name comes from that they typically model the friction losses in the gear mesh, e.g. calculated through gear geometry and friction coefficient between the coggs. However, the part of the bearing torque loss which is proportional to radial force can also be approximately included in η_{MeshIn} and $\eta_{MeshOut}$. And, one can often approximate also with $\eta_{MeshFwd} \approx 1/\eta_{MeshBwd} \approx \eta_{Mesh}$.

$$\frac{T_{MeshOut}}{T_{MeshIn}} = \begin{cases} = r \cdot \eta_{MeshFwd} \approx r \cdot \eta_{Mesh}; & if\ \text{sign}(P_{Mesh}) = +1 \\ = r \cdot \eta_{MeshBwd} \approx r/\eta_{Mesh}; & if\ \text{sign}(P_{Mesh}) = -1 \end{cases}$$

$$\frac{\omega_{in}}{\omega_{out}} = r;$$

$$where\ \ r = r_1, r_2, \cdots r_N;$$

$$and\ \ \eta_{MeshFwd}, \eta_{MeshBwd}, \eta_{Mesh}\ are\ \leq 1;$$

$$and\ \ \text{sign}(P_{Mesh}) = \text{sign}(T_{MeshIn} \cdot \omega_{in}) = \text{sign}(T_{MeshOut} \cdot \omega_{out});$$
If $T_{MeshIn} \cdot \omega_{in} = T_{MeshOut} \cdot \omega_{out} = 0$: $T_{MeshIn} = T_{MeshOut} = 0$; replaces both the torque equation and the velocity equation above.

[2.82]

To handle the discrete state events in Eq [2.81] and Eq [2.82] it is suitable to model Eq [2.81] and Eq [2.82] in one model of the whole single gear stage. An implementation of such whole model with state events is found in the Modelica (see see 1.5.4.1.5.) standard model called "Modelica.Mechanics.Rotational.Components.LossyGear".

To model a main transmission with several gear steps one can let the model select different sets of $\{\Delta T_i, \eta\}$ parameters depending on a discrete input, representing the selected gear. The gear changes are then not physically modelled, but it can be enough in some studies, e.g. energy consumption over lon driving cycles with few gear changes.

The discrete state in Eq [2.82] where $T_{MeshIn} = T_{MeshOut} = 0$; normally does not last for for any time duration, while $\text{sign}(P_{Mesh})$ changes between $+1$ and -1. But there is one exception: See 2.4.3.1.3.

2.4.3.1.1 Efficiencies

For any 1-dimensional transmission of rotational mechanical power between two rotating shafts, the power efficiency, $\eta_{power} = P_{out}/P_{in} = T_{out} \cdot \omega_{out}/(T_{in} \cdot \omega_{in})$;, is typically depending on operating condition, so it is not a parameter but a variable. This is even more obvious for energy efficiency, defined over a time interval: $\eta_{energy} = \int P_{out} \cdot dt / \int P_{in} \cdot dt$.

If assuming a nominal ratio, r, the total efficiency can be decomposed in $\eta_{total} = \eta_T \cdot \eta_\omega$;, where $\eta_T = T_{out}/(r \cdot T_{in})$ is the torque efficiency and $\eta_\omega = \omega_{out}/(\omega_{in}/r)$ is the speed efficiency. The efficiency η_{Mesh} in Eq [2.82] is a torque efficicency and can be modelled as a parameter, using basic physical (engineering) parameters, from gear geometry and friction coefficient between the coggs.

2.4.3.1.2 Powershifting Main Transmissions

The most common powershifting transmission is using planetary gears and torque converter, see Figure 2-122 and (Jacobson B. , 1993). During 2000-2010, developments in mechatronics has enabled to leave out the torque converter and the planetary gears resulting in what often meant with powershifting transmissions, see concept in Figure 2-111. In practice, one can often manage with 2 clutches, and instead select different paths through gear wheels with synchronisers. An advanced design of powershifting transmission for a hybrid propulsion system is seen in Figure 2-124. A dummy sequence of shifting is simulated in Figure 2-125.

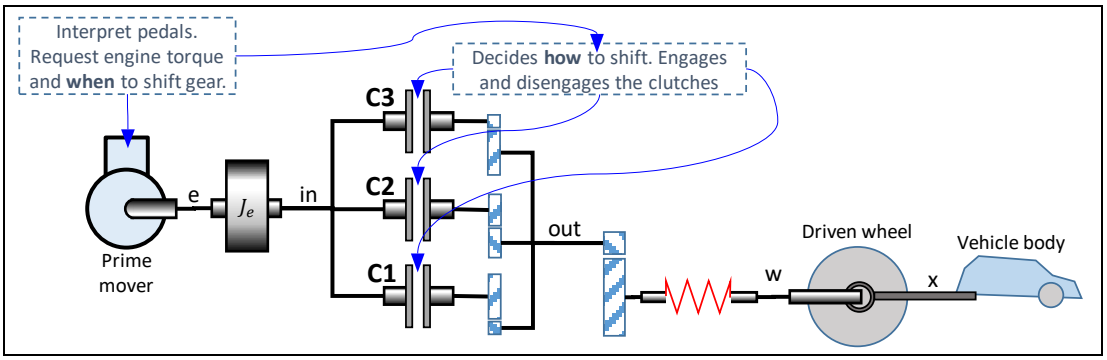


Figure 2-111: Conceptual design of powershifting transmission with 3 gears.

2.4.3.1.3 Neutral Gear

Propulsion system can have the possibility to be in *Neutral Gear*. This means that there is a clutch or coupling that it is disengaged. One cannot find a value of ratio r, because there is no relation between input and output shaft torques which represents *Neutral mode*. We saw this in Eq [2.82], in the discrete state with $T_{MeshIn} \cdot \omega_{in} = T_{MeshOut} \cdot \omega_{out} = 0$, where there is no speed equation using the ratio r, but instead two torque equations: $T_{MeshIn} = T_{MeshOut} = 0$;.

2.4.3.2 Distribution Transmissions

The distribution between prime mover and energy buffer, as well as between multiple axles and/or wheels, can conceptually be done in two mechanical ways, exemplified in the following with distribution between left and right:

- Distribute in certain fractions of (rotational) speed. A **(rotationally) rigid shaft** between left and right wheel is one example of this. We find this in special vehicles, such as go-carts, and in other vehicles as when a **differential lock** is engaged. There are 3 shafts in such an axle: input shafts and two output shafts (to left and right wheel). The equations will be:

$$\begin{aligned} \omega_{in} &= \omega_{left}; \\ \omega_{in} &= \omega_{right}; \\ T_{in} &= T_{left} + T_{right}; \end{aligned} \qquad [2.83]$$

- Distribute in certain fraction of torque. This requires some type of planetary gear arrangement. A conventional **(open) differential** gear is one example of this, where the equations will be:

$$\begin{aligned} \omega_{in} &= \frac{\omega_{left} + \omega_{right}}{2}; \\ T_{left} &= T_{right}; \\ T_{in} &= T_{left} + T_{right}; \end{aligned} \qquad [2.84]$$

The case of multiple (wheel-individual) drivetrains, we can see it as a 3rd generalized way. There are then 2 input shafts, so the common input connector can be an electric connection with voltage U_{in} and current I_{in}, instead of one common input shaft with ω_{in} and T_{in}. Compared to eqs [2.83] and [2.84], we find only 1 equation (not 3): $U_{in} \cdot I_{in} = T_{left} \cdot \omega_{left} + T_{right} \cdot \omega_{right}$;. So, there are 2 control dofs, e.g.

T_{left} and T_{right}, which are known from (requested by) a control algorithm, i.e. via an input port to each machine.

2.4.3.2.1 Torque distribution and vehicle motion

In present section, the torque distribution with open or locked differential will be discussed as if the differential differentiated between left and right wheel on an axle. Similar discussion can be made for open and locked differentials between axles, but these are not further described in present section.

Generally speaking, the open differential is rather straight-forward to use in most vehicle dynamics analyses: The speeds are given by vehicle motion (e.g. curve-outer wheel runs faster than curve-inner wheel, defined by vehicle yaw velocity and track width). The torques are defined by the differential, as half of the propulsion torque at each side.

A locked differential, it is generally more difficult to analyse and understand in a vehicle manoeuvre. Here, the wheels are forced to have same rotational speed, and, in a curve, that involves the tyre longitudinal slip characteristics, so the explicit form solution involves more equations.

So, open/locked differential is the basic concept choice. But there are additions to those: One can build in a friction clutch which is either operated automatically with mechanical wedges or similar or operated by control functions. Another was is to build in one-way clutches which can be coupled in dynamically, see (Lidberg & Alfredsson, 2009). One can also build in an EM which moves torque from one wheel to the other. However, the book does not go further into these designs.

2.4.3.2.2 Flywheels and shafts

Flywheels and shafts are also parts of the distribution transmissions. If oscillations are to be studied, these must be modelled with energy storing components:

- Rotating inertias or Flywheels ($J \cdot \dot{\omega} = T_{in} - T_{out}$;) and
- Elasticities, compliances, or springs: ($\dot{T} = c \cdot (\omega_{in} - \omega_{out})$).

2.4.4 Clutches and Brakes in Transmission

The modelling techniques shown in this section are also applicable also for tyres (2.2) and brakes (2.4.7).

Seen as machine elements, brakes are special cases of clutches, specialized by that one of the clutch halves is fixed. There are brakes on the wheels, but there are also brakes inside the transmission. A tyre operates as a transmission clutch (2.2.1.6) which can stick and slip (0). Also, when operating between forward and rearward rolling, the rolling resistance of the tyre acts as a brake, with stick and slip.

Clutches with dry friction are difficult to model in dynamic systems since they introduce “discrete dynamics”, sticking and slipping, see 1.5.1.4. The conceptual mathematical model of a controlled clutch is given in Figure 2-112 and Eq [2.85]. Here, the interface variables are T, ω_1, ω_2 and c_c. Capacity c_c $[Nm]$ is an input signal representing the magnitude of torque when the clutch slips. (The c_c also called “torque if slipping” T_{slip} in 2.5.1.) In the model below, a discrete state variable, $x_d = -1, 0\ or\ +1$, is introduced to model the discrete dynamics.

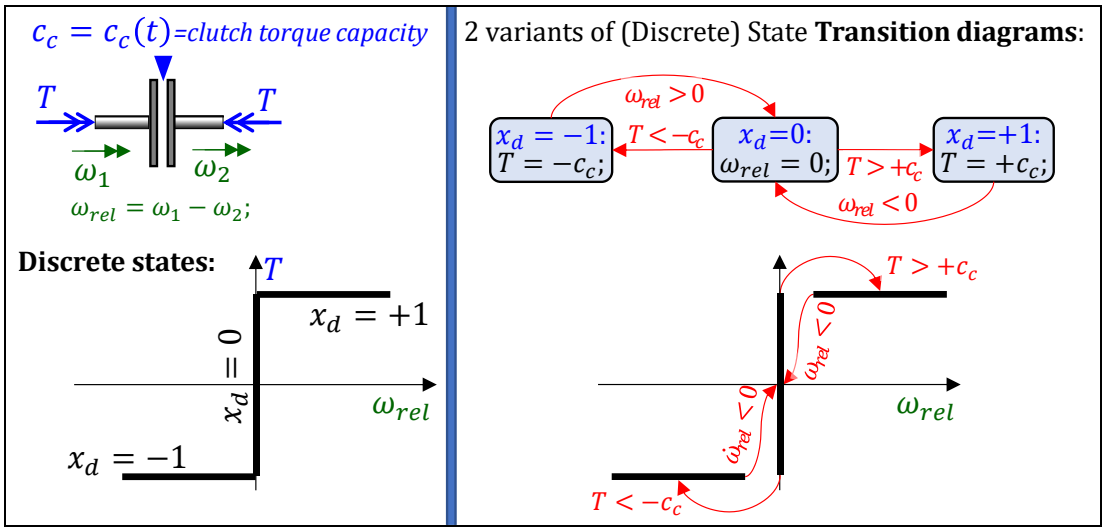


Figure 2-112: Model of a clutch. The x_d is a discrete state, declared as Integer.

(Continuous) Equations, using the discrete state x_d:

$$\begin{cases} if\ x_d = -1\ then & T = +c_c; \\ elseif\ x_d = 0\ then & \omega_{rel} = 0; \\ elseif\ x_d = +1\ then & T = -c_c;\ \ end\ if; \end{cases}$$

(Discrete State) Transition Equation:

$$\begin{cases} when\ (x_d = -1\ \ and\ \ \omega_{rel} > 0)\ then & x_d = 0; \\ elsewhen\ (x_d = 0\ \ and\ \ T < -c_c)\ then & x_d = -1; \\ elsewhen\ (x_d = 0\ \ and\ \ T > +c_c)\ then & x_d = +1; \\ elsewhen\ (x_d = +1\ \ and\ \ \omega_{rel} < 0)\ then & x_d = 0;\ \ end\ when; \end{cases}$$

[2.85]

2.4.4.1 Modelling Format and Tool Aspects

A tool with discrete dynamic support should log at least two values for an event: the value before and after the event. So, there will be 2 identical time values in the time vector. Several transitions can happen during on event, e.g. switching from $x_d = -1$ to $x_d = +1$ without $x_d = 0$ in between in Figure 2-112. For this reason, the simulation tool needs to do "event iteration", which means that the whole model is evaluated repeatedly during the event until no further changes happens. It can be discussed whether intermediate values during the event iteration should be logged or not. Modelica is designed to **not** log those.

2.4.4.2 Different Surroundings for the Clutch

Different implementations can be needed for different surroundings; energy dissipating or generating components (dampers or power sources), kinetic energy storing components (flywheels) or potential energy storing components (elasticities), see examples in Figure 2-113. The challenge is to handle that the set of state variables can change between the different discrete states.

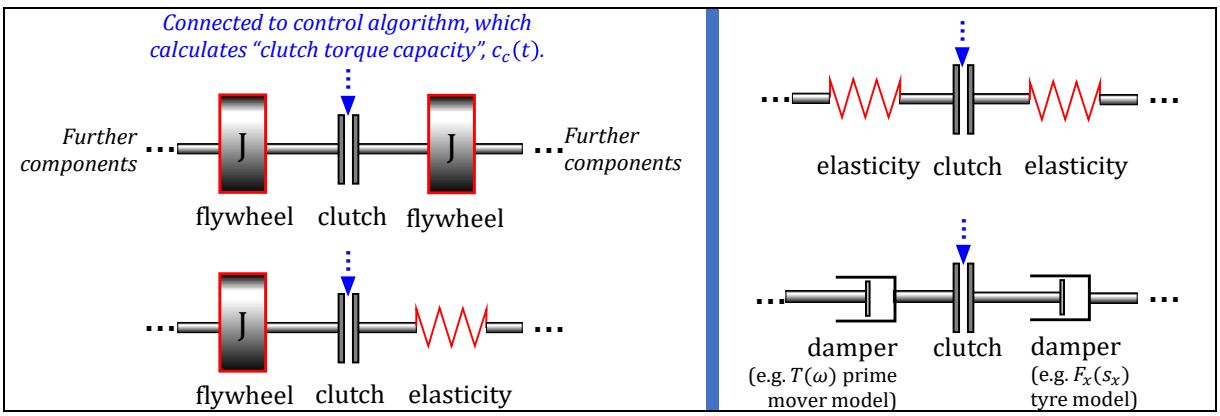


Figure 2-113: Examples of differently modelled surroundings of a clutch.

For complete main transmissions, as automatic transmissions, there are several clutches involved, the implementation of the ideal model in Eq [2.85] can be very demanding. It is modelled in Modelica. The discrete dynamics is modelled with the discrete state (`xd` declared `Integer`) and the operator "`pre(z)`", which holds the z value from last time instant or, in an event, from the last event iteration.

2.4.4.2.1 Clutch and Elasticity in Series

The easiest surrounding to a clutch is in series with elasticity, assuming velocities can be input. Figure 2-114 shows such. It also adds $stiction = st > 1$; a different static and dynamic friction, $\mu_{stick} = st \cdot \mu_{slip}$;.

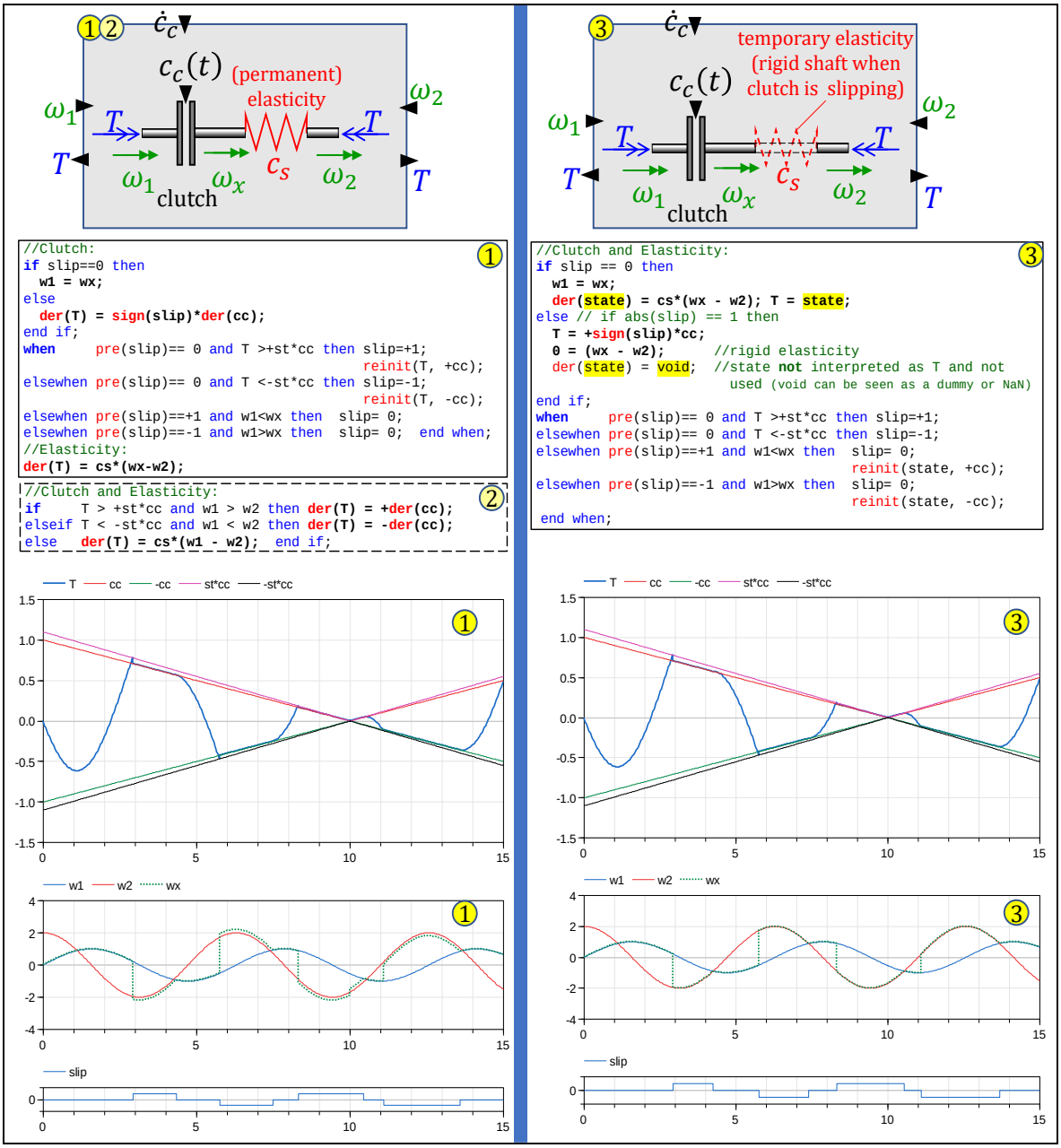


Figure 2-114: Model of clutch and elasticity in series, modelled for speed input from both sides. Implemented in Modelica. Implementation 1,2 and 3. Without discrete state and without `when` (2) only works well (without chattering) for $st = 1.0$. Switched physical model (3) has a state (`state`) depending on the discrete state slip; elasticity is modelled only when `slip=0`.

2.4.4.2.2 Clutch between Inertias

When connecting 2 inertias or 2 elasticities with a clutch is more complicated. For clutch between inertias, it is proposed to use ω_{rel} as state variable, because it makes it easy to keep $\omega_{rel} \equiv 0$ during stick, see Figure 2-115.

Modelling friction between inertias brings up a question which does not appear if elasticity or damper in series with the friction. See Eq [2.85] for the friction contact model, with the discrete states $x_d = -1, 0, or + 1$. Simplify to that one of the inertias is fixed and the other is rotating inertia with an initial speed which is negative. Now we apply a constant positive torque on the latter inertia, such that the speed starts to increase towards zero, i.e., at least larger torque than the dynamic friction torque c_c. If the torque even is larger than the dynamic friction, $st \cdot c_c$, a reasonable model would result in that the x_d switches from $x_d = -1$ to 0 and to $+1$ at the same time instant. Multiple state event switching at the same time instant is called state event propagation. A more debatable case is if the torque is between c_c and $st \cdot c_c$. Then there are two "intuitively legitimate" ways that the model can act, either passing from $x_d = -1$ to 0 and to $+1$ or only from $x_d = -1$ to 0 in one time instant. The latter behaviour, not reaching $x_d = +1$, is more motivated the more compliance (elasticity or damping) the contact surfaces have in the contact plane. It is also more motivated the quicker the "landing", perpendicular to the contact plane, of the two contact surfaces against each other takes place. So, contacts between rigid surfaces (such as dry metal to metal contacts) are prone to be better modelled with the first behaviour, while soft or wet contacts (such as wet clutches in automatic gearboxes or tyre-to-road contacts) are more prone to the better modelled with the latter.

At time instants with multiple discrete state switches, it is not recommended to store the intermediate variable values, i.e. the values after the first switch from $x_d = -1$ to 0, because it will have values which are wrong (not consistent with the intended model), e.g. it can have values of friction force $> st \cdot c_c$ for a large applied torque in the above example. Modelica tools, such as Dymola, typically do not store the intermediate values, but store only the first and last values independent if one or multiple switches of discrete state during the time instant.

Today, the Modelica tools, such as Dymola, supports state event propagation (multiple changes of a discrete state variable at one time instant). So, for simple systems, one does not need to model more than Eq [2.85], i.e. with the discrete states $x_d = -1, 0, or + 1$. However, earlier and for more robustness to complexity (many friction contacts) one can implement the state event propagation more explicitly using a 5-state model, with the discrete states $x_d = -2, -1, 0, +1, or + 2$, as in Figure 2-115. The values $x_d = \pm 1$ are temporary during a state event; it enables a total state transition during one event between $x_d = -2$ and $x_d = +2$, without (wrongly) logging an intermediate $x_d = 0$. With $st < 1$, there is risk for chattering solutions.

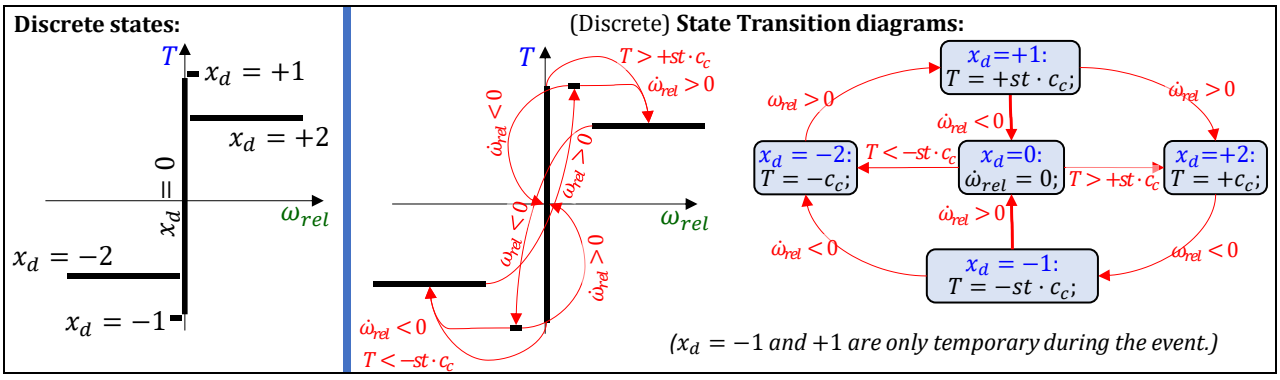


Figure 2-115: Model of a clutch for connection between inertias.

Modelling several friction contacts between rigid inertial bodies is difficult but also have a potential for high computational efficiency, compared to introducing small compliances (stiff elasticities).

2.4.4.2.3 Functional or Inverse Clutch Model

In some cases, it can be suitable to prescribe how the clutch is operates in terms of $\omega_{rel}(t)$ instead of $c_c(t)$. This means that we rather assume a successful engagement as that $\omega_{rel} \to 0$ during an assumed engagement time, than assuming a $c_c(t)$ and find out how long time it takes to engage (or fail to engage. The $\omega_{rel}(t)$ is then declared as input and the (required) torque $T(t)$ and the torque capacity $c_c(t)$ becomes an output. This can simplify the modelling. This is not further discussed in this book but see http://blog.xogeny.com/blog/part-2-kinematic/.

2.4.4.2.4 Friction contact with 2D friction

The previous clutch is a 1D friction with sliding only in one dimension, the relative rotation in the clutch. It is easily extendable to translational motion, which can be useful for example when studying a vehicle in xz-plane and the wheel with only longitudinal sliding and tyre force. To model a more general friction contact, i.e. both dimensions of a contact patch, can be of interest for tyres under combined slip, longitudinal and lateral. The continuous time equations for an ideal friction law for 2D friction is obvious:

if Slip (if sliding):

$|\vec{F}_{xy}| = \mu_{Slide} \cdot F_z(t)$; and $\angle(\vec{F}_{xy}) = \angle(\vec{v}_{Relxy})$; and $\vec{v}_{Relxy} =$ "$determined\ by\ surroundings$";

else (if not Slip, i.e. Stick):

$\vec{v}_{Relxy} = \vec{0}$; and $\vec{F}_{xy} =$ "$determined\ by\ surroundings$";

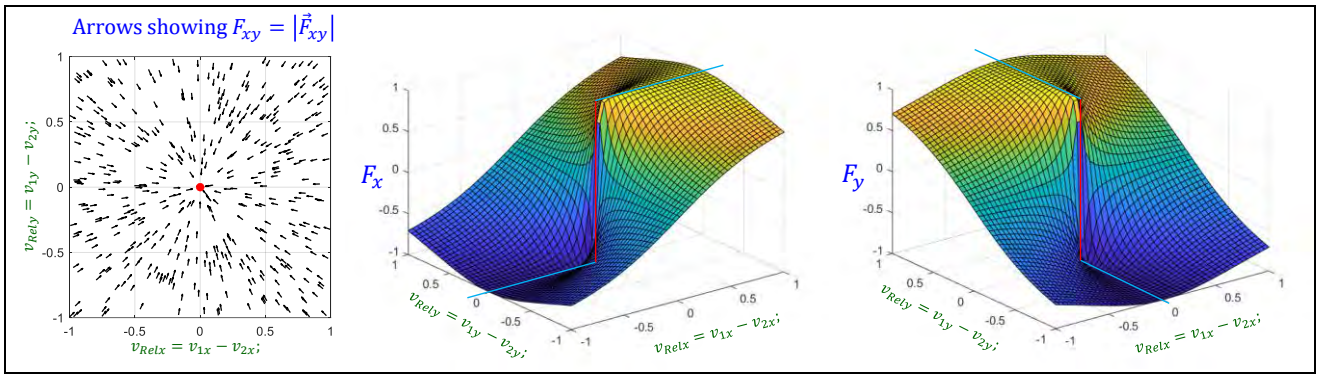


Figure 2-116: Friction force when Slip, i.e. not Stick. The red shows the singularity for $|\vec{v}_{Relxy}| = 0$

The transition condition to Slip (from Stick) is easy: *when* $|\vec{F}_{xy}| > \mu_{Stick} \cdot F_z$;. However, there are two major difficulties:

- A natural way to implement the friction during Slip is $F_x = \mu_{Slide} \cdot F_z(t) \cdot v_{Relx}/|\vec{v}_{Relxy}|$;. Then the continuous time model becomes singular for $|\vec{v}_{Relxy}| = 0$.
- The transition conditions from Slip (to Stick) happens when $|\vec{v}_{Relxy}|$ becomes zero, which corresponds to a zero-crossing for 1D friction but only an zero-arrival from one side for 2D friction. A zero-arrival from one side is less robust to identify numerically.

These difficulties are overcome by using two discrete variables, `Slipx` and `Slipy`, which each can take the value of -1, 0, or +1.

2.4.4.2.4.1 Example

An example will be given. Physical model and Mathematical model (in Modelica) is found Figure 2-117.

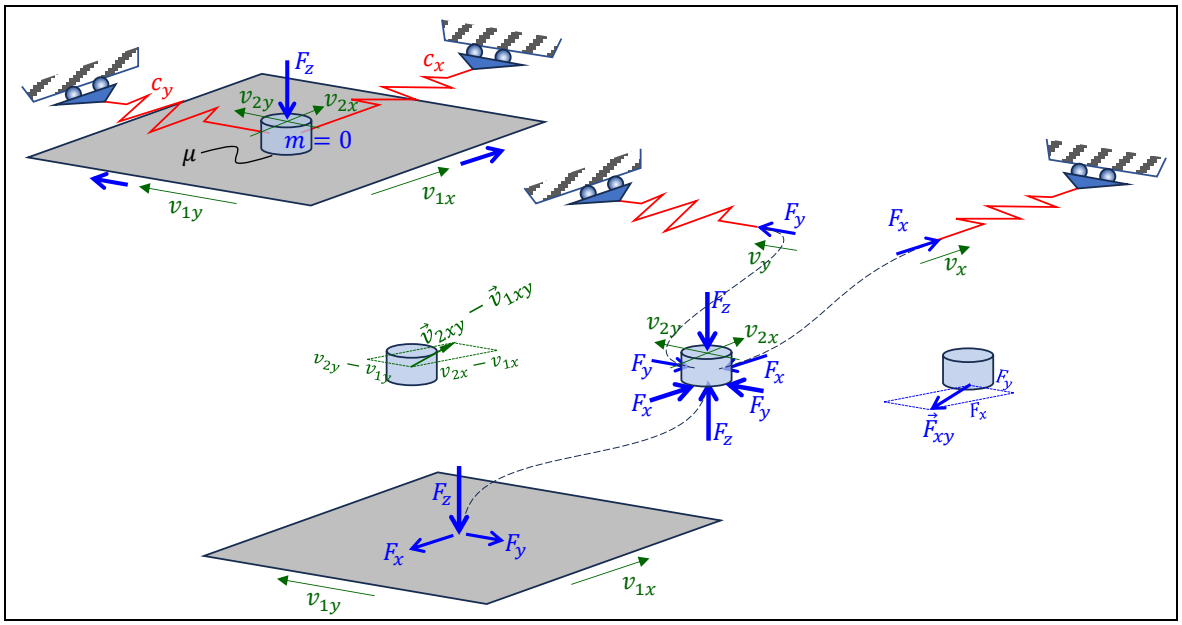


Figure 2-117: Physical model of a system with 2D friction. A massless particle (v_{2x}, v_{2y}) is suspended in two springs (F_{sx}, F_{sy}). The particle is pushed to a plate (F_z). The plate is moved (v_{1x}, v_{1y}).

The two "types of combinations" of discrete variables, $Slip_x$ and $Slip_y$, defines two discrete states: Stick and Slip, used in the explanation below.

2.4.4.2.4.1.1 Analysis of time continuous equations during Stick

Stick means: $if\ |Slip_x| + |Slip_y| = 0$.

The following is the *Mathematical model*. Only the yellow marked equations are different from the other "type of combination", Slip, in 2.4.4.2.4.1.2.

$$
\begin{cases}
\begin{cases}
v_{Relx} = v_{1x}(t) - v_{2x}; \\
v_{Rely} = v_{1y}(t) - v_{2y}; \\
v_{Relx} = 0 \quad "Sticking\ Columb\ friction"; \\
v_{Rely} = 0 \quad "Sticking\ Columb\ friction"; \\
F_{xy} = \sqrt{F_x^2 + F_y^2} \quad "Auxilliary\ variable\ F_{xy} = |\vec{F}_{xy}|"; \\
v_{Relxy} = \sqrt{v_{Relx}^2 + v_{Rely}^2} \quad "Auxilliary\ variable\ v_{Relxy} = |\vec{v}_{Relxy}|";
\end{cases} \\
\begin{cases}
\dot{F}_x = c_x \cdot v_{2x}; \\
\dot{F}_y = c_y \cdot v_{2y};
\end{cases}
\end{cases}
$$

It is a DAE system: 8 equations, 8 unknowns $\{F_x, F_y, F_{xy}, v_{2x}, v_{2y}, v_{Relx}, v_{Rely}, v_{Relxy}\}$. When aiming for Explicit form model, we must select states. We will use state selection $\{F_x, F_y\}$ as example. Then, the ODE will be 8 equations with 8 unknowns $\{\dot{F}_x, \dot{F}_y, F_{xy}, v_{2x}, v_{2y}, v_{Relx}, v_{Rely}, v_{Relxy}\}$.

The *Explicit form model* becomes:

$$\begin{cases} v_{Relx} \leftarrow 0; \\ v_{Rely} \leftarrow 0; \\ v_{2x} \leftarrow v_{1x}(t) - v_{Relx}; \\ v_{2y} \leftarrow v_{1y}(t) - v_{Rely}; \\ v_{Relxy} \leftarrow \sqrt{v_{Relx}^2 + v_{Rely}^2}; \\ \dot{F}_x \leftarrow c_x \cdot v_{Relx}; \\ \dot{F}_y \leftarrow c_y \cdot v_{Rely}; \\ F_{xy} \leftarrow \sqrt{F_x^2 + F_y^2}; \end{cases}$$

2.4.4.2.4.1.2 Analysis of time continuous equations during Slip

Slip means: $if\ \left|Slip_x \cdot Slip_y\right| = 1$.

The following is the *Mathematical model*. Only the yellow marked equations are different from the other "type of combination", Stick, in 2.4.4.2.4.1.1.

$$\begin{cases} \begin{cases} v_{Relx} = v_{1x}(t) - v_{2x}; \\ v_{Rely} = v_{1y}(t) - v_{2y}; \\ \left(F_{FricSlip}(t)\right)^2 = F_x^2 + F_y^2 \quad \text{"Friction force magnitude for slipping Columb friction"}; \\ v_{Relx} \cdot F_y - v_{Rely} \cdot F_x = 0 \quad \text{"} \begin{Bmatrix} \text{Friction force direction for slipping Columb friction, i.e.,} \\ \vec{v}_{Relxy} = (v_{Relx}, v_{Rely}) \text{ co-linear with } \vec{F}_{xy} = (F_x, F_y) \end{Bmatrix} \text{"}; \\ F_{xy} = \sqrt{F_x^2 + F_y^2} \quad \text{"Auxilliary variable } F_{xy} = \left|\vec{F}_{xy}\right| \text{"}; \\ v_{Relxy} = \sqrt{v_{Relx}^2 + v_{Rely}^2} \quad \text{"Auxilliary variable } v_{Relxy} = \left|\vec{v}_{Relxy}\right| \text{"}; \end{cases} \\ \begin{cases} \dot{F}_x = c_x \cdot v_{2x}; \\ \dot{F}_y = c_y \cdot v_{2y}; \end{cases} \end{cases}$$

It is a DAE (Differential-Algebraic system of Equations) with 8 equations, 8 unknowns $\{F_x, F_y, F_{xy}, v_{2x}, v_{2y}, v_{Relx}, v_{Rely}, v_{Relxy}\}$. When aiming for Explicit form model, we must select states. We will use same state selection as for "type Slip", namely $\{F_x, F_y\}$. Then, the algebraic system of equations from the ODE (Ordinary Differential system of Equations) will be 8 equations with 8 unknowns $\{\dot{F}_x, \dot{F}_y, F_{xy}, v_{2x}, v_{2y}, v_{Relx}, v_{Rely}, v_{Relxy}\}$. This system is singular, see 3rd equation with only zeros in the index matrix:

$$\begin{bmatrix} \dot{F}_x & \dot{F}_y & F_{xy} & v_{2x} & v_{2y} & v_{Relx} & v_{Rely} & v_{Relxy} \\ & & & 1 & & 1 & & \\ & & & & 1 & & 1 & \\ 0 & 0 & 0 & 0 & 0 & 0 & 0 & 0 \\ & & & & & 1 & 1 & \\ & & 1 & & & & & \\ & & & & & 1 & 1 & 1 \\ 1 & & & 1 & & & & \\ & 1 & & & 1 & & & \end{bmatrix}$$

But if we replace $\left(F_{FricSlip}(t)\right)^2 = F_x^2 + F_y^2$; with its differentiated version of $2 \cdot F_{FricSlip}(t) \cdot \dot{F}_{FricSlip}(t) = 2 \cdot F_x \cdot \dot{F}_x + 2 \cdot F_y \cdot \dot{F}_y$; it becomes non-singular:

$$\begin{bmatrix} \dot{F}_x & \dot{F}_y & F_{xy} & v_{2x} & v_{2y} & v_{Relx} & v_{Rely} & v_{Relxy} \\ & & & 1 & & 1 & & \\ & & & & 1 & & 1 & \\ 1 & 1 & 0 & 0 & 0 & 0 & 0 & 0 \\ & & & & & 1 & 1 & \\ & & 1 & & & & & \\ & & & & & 1 & 1 & 1 \\ 1 & & & 1 & & & & \\ & 1 & & & 1 & & & \end{bmatrix}$$

The *Explicit form model* becomes, after eliminating unknowns in the order $\dot{F}_x, \dot{F}_y, F_{xy}, v_{2x}, v_{2y}, v_{Relx}, v_{Rely}, v_{Relxy}$:

$$\begin{cases} \dot{F}_x \leftarrow \dfrac{c_y \cdot \left(F_x \cdot c_x \cdot v_{1y} - F_y \cdot c_x \cdot v_{1x} + \dfrac{F_{FricSlip} \cdot F_y \cdot \dot{F}_{FricSlip}}{F_x} \right)}{F_x \cdot c_x \cdot \left(\dfrac{F_y^2 \cdot c_y}{F_x^2 \cdot c_x} + 1 \right)}; \\ \dot{F}_y \leftarrow \dfrac{F_{FricSlip} \cdot \dot{F}_{FricSlip} - F_y \cdot \dot{F}_y}{F_x}; \\ v_{2y} \leftarrow \dfrac{F_y \cdot \dot{F}_x + F_x \cdot c_x \cdot v_{1y} - F_y \cdot c_x \cdot v_{1x}}{F_x \cdot c_x}; \\ v_{2x} \leftarrow \dfrac{F_x \cdot v_{2y} - F_x \cdot v_{1y} + F_y \cdot v_{1x}}{F_y}; \\ v_{Rely} \leftarrow v_{1y} - v_{2y}; \\ v_{Relx} \leftarrow v_{1x} - v_{2x}; \\ F_{xy} \leftarrow \sqrt{F_x^2 + F_y^2}; \\ v_{Relxy} \leftarrow \sqrt{v_{Relx}^2 + v_{Rely}^2}; \end{cases}$$

2.4.4.2.4.1.3 Mathematical model, time continuous and time discrete

Now, we also need to describe the discrete state transitions, both when to transit and what to do in the transition. They are documented in the when clauses below in the Mathematical model (in Modelica):

```
model Test_2DFriction
 …
  Integer Slipx;
  Integer Slipy;
  //Slipx and Slipy are time discrete variables, -1/0/+1. Combinations of them are used to
    identify two discrete states: abs(Slipx)+abs(Slipy)==0 and abs(Slipx)+abs(Slipy)==2
…
equation
  //Operation:
  v_1x = 2*sin(1*time);
  v_1y = 0.5*sin(0.6*time);
  der(F_z) = if time < 9 then -0.1 elseif time < 40 then +0.1 else 0;

  //Friction contact:
  F_FricSlip = mu*F_z;       F_FricCapStick = st*F_FricSlip;
  v_Relx = v_1x - v_2x;      v_Rely = v_1y - v_2y;
  v_Relxy = sqrt(v_Relx^2 + v_Rely^2);       F_xy = sqrt(F_x^2 + F_y^2);
  P_Loss=F_x*v_Relx + F_y*v_Rely;

  if abs(Slipx) + abs(Slipy) == 0 then
    v_Relx = 0;    v_Rely = 0;
  else // if abs(Slipx) + abs(Slipy) == 2 then
    der(F_FricSlip) = der(sqrt(F_x^2 + F_y^2));
    v_Relx*F_y - v_Rely*F_x = 0;
  end if;
```

```
  when abs(pre(Slipx)) + abs(pre(Slipy))==0 and F_xy > F_FricCapStick then
    Slipx = sign(F_x);    Slipy = sign(F_y);
    reinit(F_x, F_x/st);    reinit(F_y, F_y/st);
  elsewhen v_Relxy < v_Eps and abs(pre(Slipx))+abs(pre(Slipy))==2 and P_Loss<0 then
    Slipx = 0;    Slipy = 0;
  elsewhen v_Relxy > v_Eps and pre(Slipx) == +1 and v_Relx < 0 then
    Slipx = -1;    Slipy = pre(Slipy);
  elsewhen v_Relxy > v_Eps and pre(Slipx) == -1 and v_Relx > 0 then
    Slipx = +1;    Slipy = pre(Slipy);
  elsewhen v_Relxy > v_Eps and pre(Slipy) == +1 and v_Rely < 0 then
    Slipx = +pre(Slipx);    Slipy = -1;
  elsewhen v_Relxy > v_Eps and pre(Slipy) == -1 and v_Rely > 0 then
    Slipx = +pre(Slipx);    Slipy = +1;
  end when;
  //Elasticity:
  der(F_x) = c_x*v_2x;  der(F_y) = c_y*v_2y;
…
end Test_2DFriction;
```

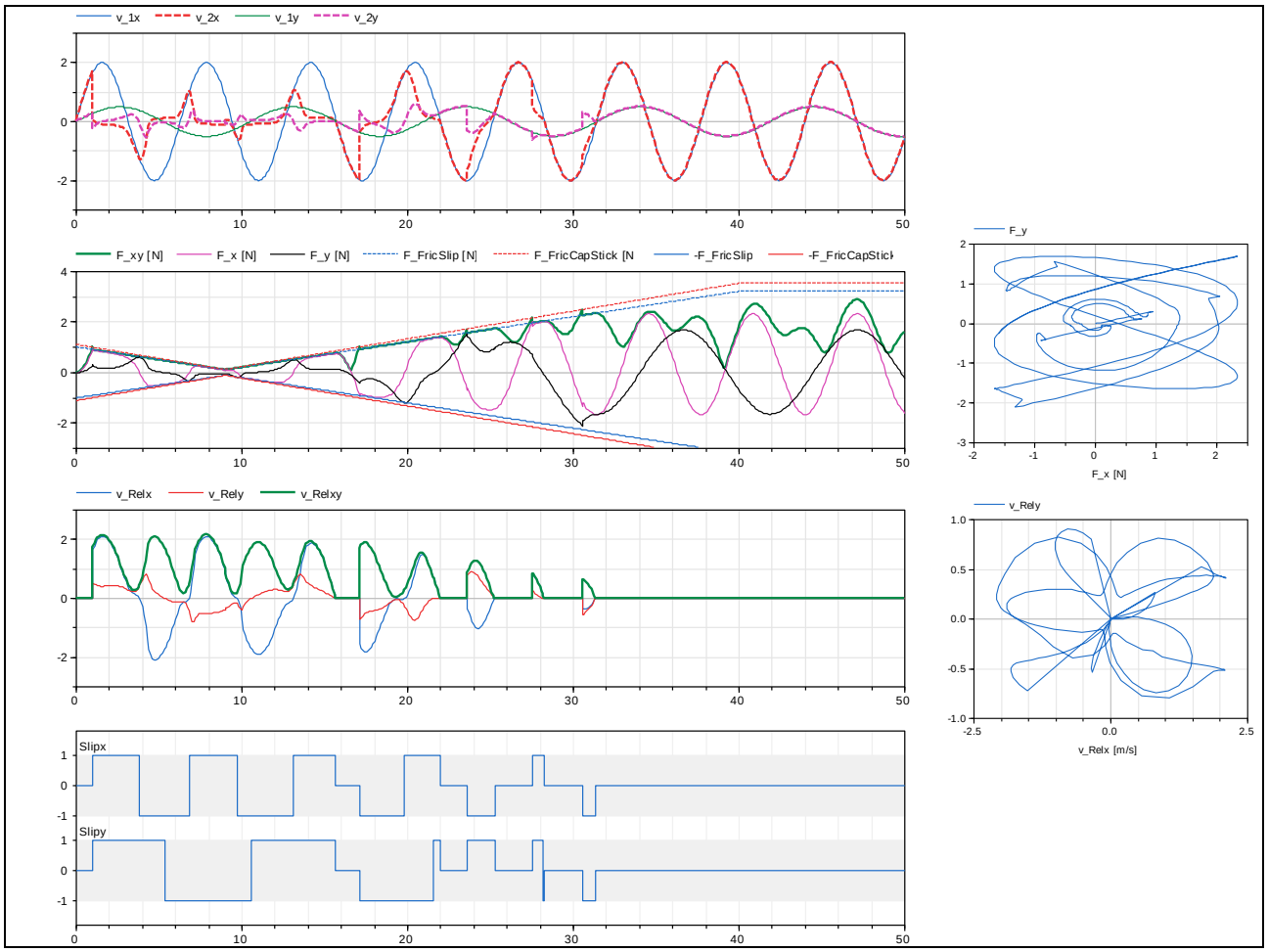


Figure 2-118: Simulation result from Figure 2-117

2.4.4.3 Implementation of Clutches as Stiff Dampers

A way around model implementation problems is to use an approximate clutch model as in Eq [2.88]. The advantage is that it can handle any surrounding without leading to changing set of state variables. The drawback is that it has a trade-off between modelling the intended physics (Eq [2.88]) and the computational efficiency in simulation; the more $d \to \infty$, the closer to the intended model we come, but the simulation time will increase towards infinity. The approximation can be seen as putting a stiff damper in direct series with an ideal clutch. There are also other approximations, which could be seen as putting a stiff spring with stiffness c in series with an ideal clutch. This will work if clutch is surrounded by inertias:

$$T_{left} = T_{right};\quad and\quad \omega_{rel} = \omega_{left} - \omega_{right};$$

$$\frac{T_{left}}{c}\cdot \mathrm{sign}(\omega_{rel}) =$$

$$= \begin{cases} = \min\left(\dfrac{1-\varepsilon}{\varepsilon}\cdot\dfrac{|\omega_{rel}|}{\omega_{nom}}\ ;\ 1+\dfrac{\varepsilon}{1-\varepsilon}\cdot\left(\dfrac{|\omega_{rel}|}{\omega_{nom}}-1\right)\right); & if\ \dfrac{|\omega_{rel}|}{\omega_{nom}} < 1 \\ = \max\left(\dfrac{1}{1+\dfrac{\varepsilon}{1-\varepsilon}\cdot\left(\dfrac{\omega_{nom}}{|\omega_{rel}|}-1\right)}\ ;\ \dfrac{\varepsilon}{1-\varepsilon}\cdot\dfrac{|\omega_{rel}|}{\omega_{nom}}\right); & else \end{cases}$$

[2.86]

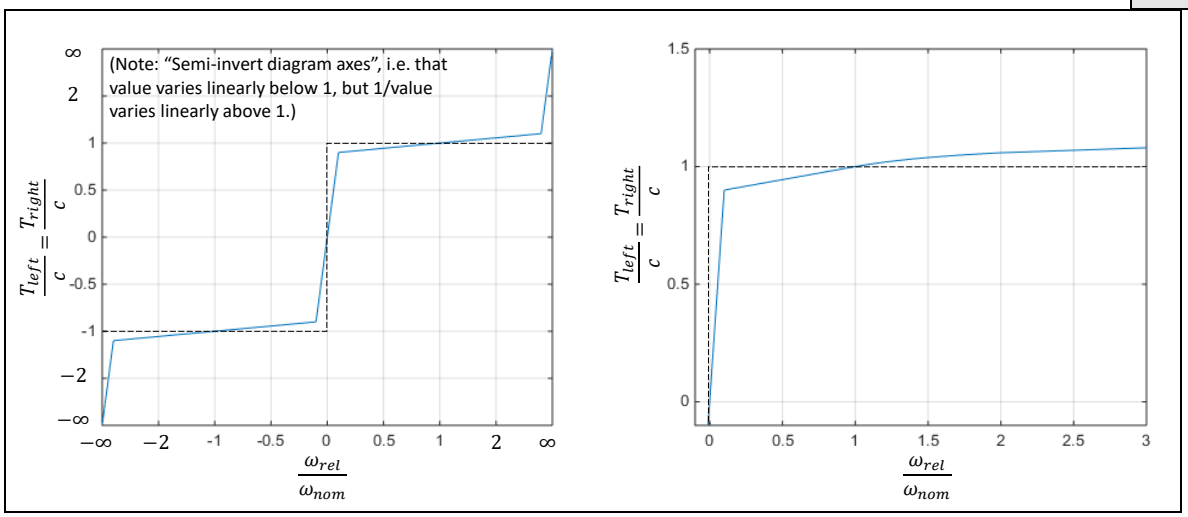


Figure 2-119: Example of approximation of clutch model. Strategies: ω_{nom}= typical slip speed of clutch, $\varepsilon \ll 1$. Dashed curve shows before approximation.

Figure 2-120 shows an example that the ideal and approximate models can give comparable results with respect to torques and speeds. About computational efficiency, the ideal needs around 5 *ms* time step with Euler forward integration, while the approximate needs 100 times smaller time step. If better agreement than in Figure 2-120 is needed, ε needs to be reduced, which slows down the approximation even more. Note also that, for energy dissipation, the approximate model of course calculates a higher energy dissipation, since it assumes the clutch has to slip to transfer torque.

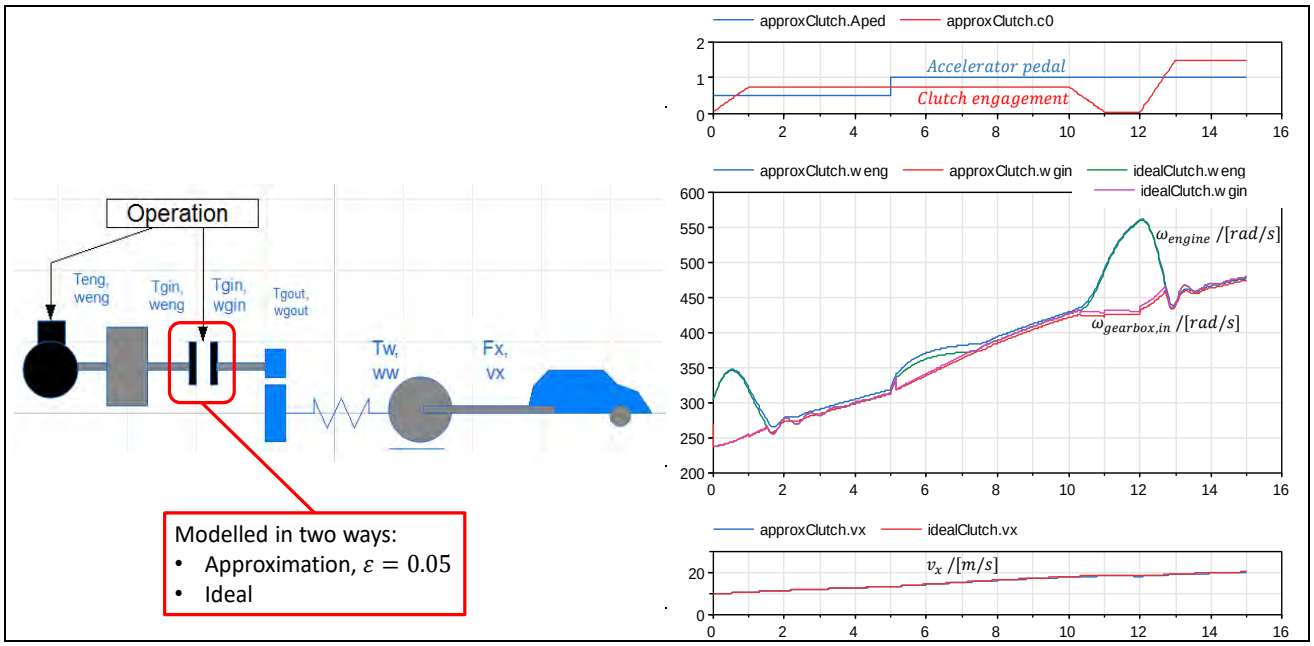


Figure 2-120: Example with clutch, modelled in two ways

There are clutch models also in the standard Modelica (see 1.5.4.1.5) library, see Figure 2-121. Note that the library is built such that the "small inertia" is needed, which forces down computational efficiency during clutch slip.

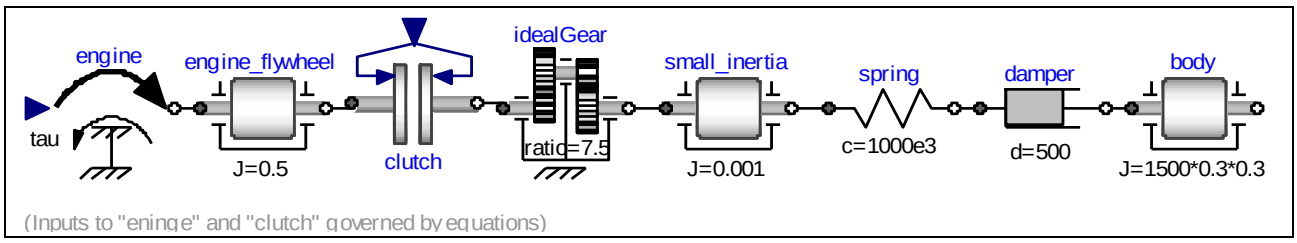


Figure 2-121: Model example with clutch, using standard Modelica library "Modelica.Mechanics.Rotational"

Brakes, one-way clutches and backlashes often causes similar difficulties and can be modelled similarly as clutches.

2.4.5 Hydrodynamic Torque Converters

Hydrodynamic torque converters serve almost same purpose as a clutch, but it is much less complex to model as a member of a dynamic system. Such converters have a pump in input side and turbine on output side. They can operate with substantial slip, and when slip, there is a torque amplification, which leads to that a vehicle with converter have typically good acceleration performance and driveability also without the corresponding lowest gear needed on same vehicle without converter.

The following model gives the steady state characteristics of a hydrodynamic torque converter. Steady state characteristics are often enough but combined with that hydrodynamic torque converters often are possible to lock-up with a clutch, mounted in parallel to the impellers.

$$\frac{T_{out}}{T_{in}} = \mu(\nu);\ \frac{T_{in}}{\omega_{in}^2} = \lambda(\nu);\quad where\ \mu\ and\ \lambda\ are\ functions\ and\ \nu = \frac{\omega_{out}}{\omega_{in}};$$

But if locked-up: $\frac{T_{out}}{T_{in}} = 1;\ \ and\ \frac{\omega_{out}}{\omega_{in}} = 1;$

The moment capacity, λ, is often given on a dimensionless form $\lambda = T_{in}/\left(\omega_{in}^2 \cdot\ OilDensity \cdot OuterRadius^5\right)$.

[2.87]

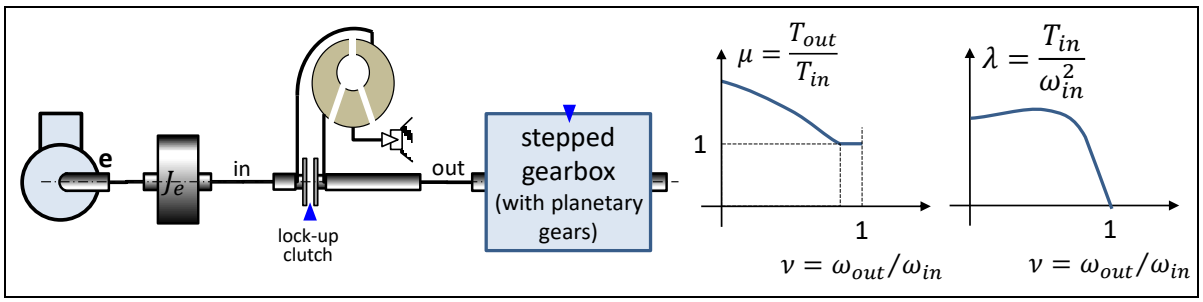


Figure 2-122: Left: Traditional automatic transmission. Right: Conceptual curves of the torque converter.

2.4.6 Energy Storages and Energy Buffers

Contribution from Jelena Andric and Majid Astaneh, Chalmers

Fuel tank for fossil fuel or hydrogen, battery, flywheel, hydro static accumulator and super capacitor are examples of *energy storages*. An *energy buffer* often refers to an energy storage that can not only be emptied (during propulsion), but also refilled by regenerating energy from the vehicle during deceleration. With that nomenclature, a fuel tank is an energy storage, but not an energy buffer. Also, a battery which can only be charged from the grid, and not from regenerating deceleration energy, is not

an energy buffer. Today, the most common energy storage is fossil fuel tank and the most common energy buffer is battery.

Eq [2.88] gives a simple model of an energy buffer. Also, the energy converters to mechanical rotation (electric machines, if energy buffer is a battery) is modelled.

$$\dot{E} = \begin{cases} = (P_{in} - P_{out}) \cdot \eta_{charge}; & for\ P_{in} > P_{out}; \\ = (P_{in} - P_{out}) / \eta_{use}; & else; \end{cases}$$
$$where\ P_{in} = T_{in} \cdot \omega_{in}; and\ P_{out} = T_{out} \cdot \omega_{out}; \quad [2.88]$$

Including how the buffer is connected, one more equation can be found: Typically, $\omega_{in} = \omega_{out}$; or $T_{in} = T_{out}$;.

The model uses stored energy, E. For batteries, one often uses state of charge, SoC, instead. Conceptually, $SoC = E/E_{max}$;, where E_{max} is a nominal maximum charge level.

A first approximation of the efficiencies of modern batteries, can be $\eta_{charge} = \eta_{use} = constant =$ 0.85..0.95, but typically the efficiency is dependent of many things, such as $P_{in} - P_{out}$. The model above does not consider any leakage when buffer is "resting", i.e. when $P_{in} = P_{out}$. Seen over a whole transport operation, the energy is typically both stored in and taken out from the battery, so a "roundtrip efficiency" becomes smaller, only $\eta_{roundtrip} \approx \eta_{charge} \cdot \eta_{use}$.

Another aspect of batteries is the life time. State of health SoH is a way to measure remaining battery life. The $SoH = t/t_{new}$, where t is the time it takes to discharge from full to a certain SoC (or certain voltage) with a certain power output (or certain electric current). Subscript *new* refers to when battery is new. With models for SoH, one can include the battery degradation as a cost and thereby sum it with the cost of energy consumption. The book does not give any of those models in detail, but generally, $SoH = 1$ when battery is new and $d(SoH)/dt = func(P, temp)$ or $= func(d(SoC)/dt\,, temp)$. It is zero for $P = 0$ and decreases with $|P|$.

2.4.6.1 Fuel Cells

Contribution from Leo Laine, Volvo Trucks and Chalmers

From vehicle motion point of view, a fuel cell with hydrogen storage is an energy storage with electric energy output. It has limited change rate of output power, typically a time constant of 10 s, so it is typically combined with a battery. Together with a battery, regeneration and a higher change rate of output power is possible.

2.4.6.2 Size of Energy Buffers

For vehicle dynamics engineers, it can be difficult to get an intuitive understanding of the size of an energy buffer like a battery. Since the storage is often limiting range, speed changes and "road grade flattening", is can help to express energy in the following measures with more vehicle dynamics related units, instead of $[J]$ or $[kWh]$:

- Range: $E_{range}\ [m] = E[J]/F_{resistance}[N] = E/(RRC \cdot m \cdot g + 0.5 \cdot \rho \cdot A \cdot c_d \cdot v^2)$. Note that energy lost in friction brakes are not included.
- Speed change: $E_{speedChange}\ [m/s] = \sqrt{2 \cdot E[J]/m}$. Note that driving resistance in not included.
- Road grade flattening: $E_{roadFlattening}\ [m] = E[J]/(m \cdot g)$. Note that driving resistance in not included.

2.4.7 Special Topology Propulsion Systems

There are two propulsion systems which are topologically special: **Hybrid Propulsion Systems** and **Multiple Electric Drivetrains**. Simply speaking, the first has multiple prime movers (e.g. an ICE and one electrical motor) while latter has multiple sinks (e.g. propulsion on two axles). In both cases, it

often appears something like different driving modes, which can reduce the need of many gears and invoke a need for modes selection, similar/related to gear selecton.

2.4.7.1 Hybrid Propulsion Systems

Hybrid propulsion systems can be categorized in

- series,
- parallel, or
- split.

Let us consider the case with 2 prime movers, PMs. If both the PMs are connected with 1 velocity-dof to the vehicle, it is a parallel hybrid. The force from both PMs are summed to a propulsion force on the vehicle body. If there are 2 velocity-dofs and one of the PMs actuates all the propulsion force on the vehicle body, it is a series hybrid. If there are 2 velocity-dofs and the velocity from them is added to the vehicle velocity, it is a split hybrid. See Figure 2-123. Note that other important aspects are:

- whether the battery can be charged from grid (while parked) or not
- whether there are single or multiple energy storages. If single battery but multiple electric motors, the vehicle is often not called a hybrid vehicle. A futuristic example is if electric propulsion on car and trailer with connection of their batteries so that the batteries acts as one battery. An old example is a single fuel tank but several cylinders in an ICE engine, which is very common and obviously very seldom seen as a hybrid.

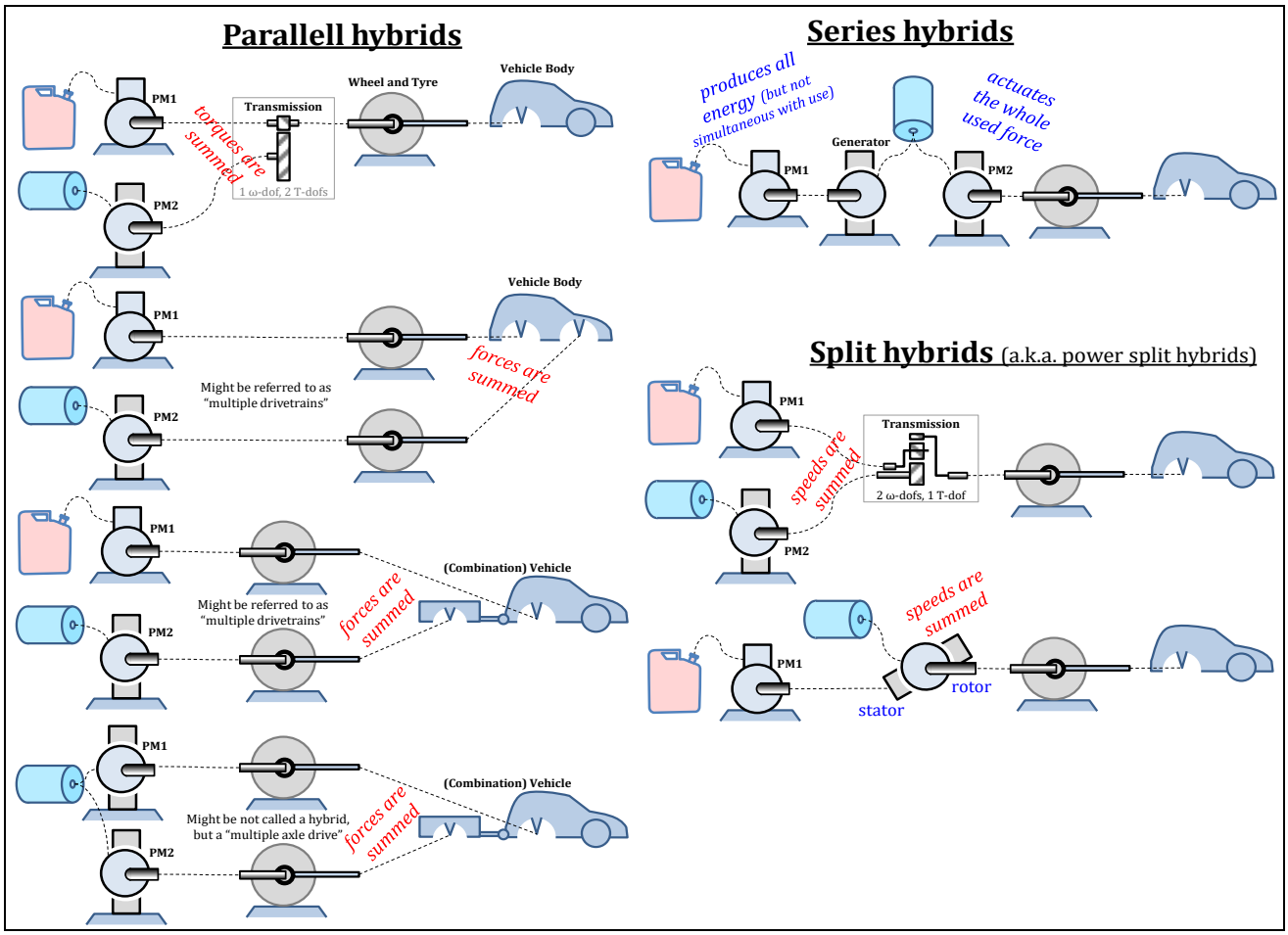


Figure 2-123: Examples of series, parallel and split hybrid propulsion systems.

2.4.7.1.1 Example of Hybrid Propulsion System

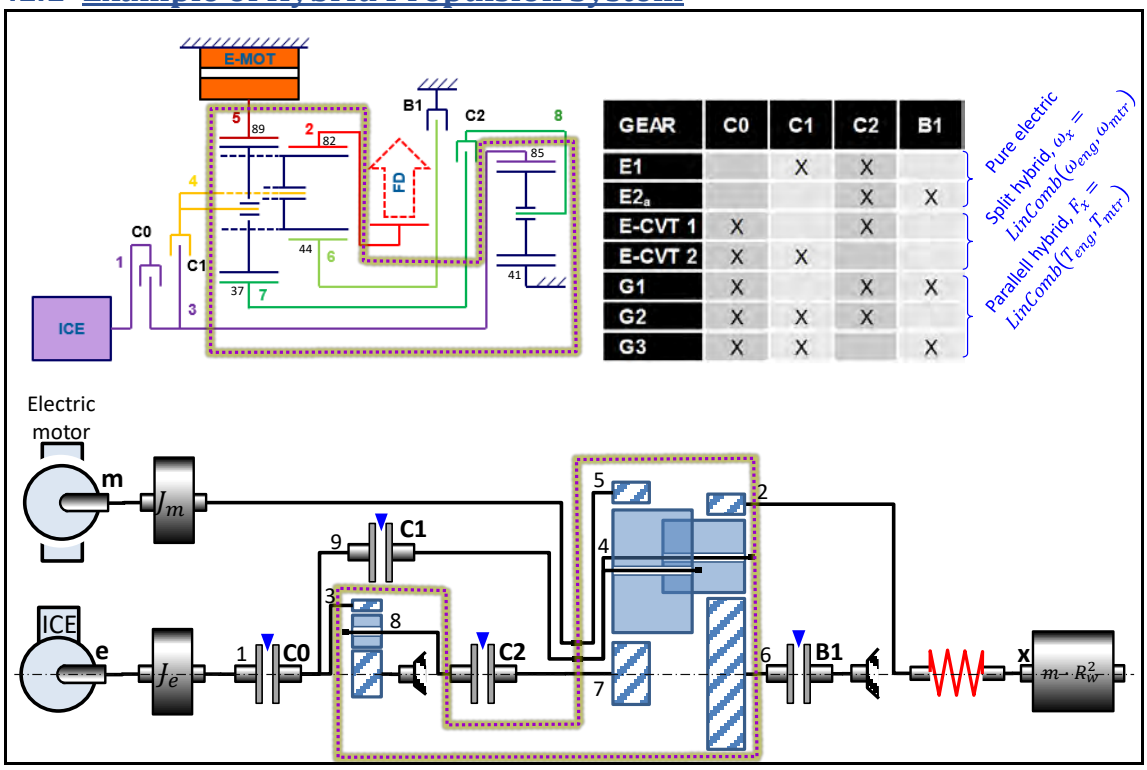


Figure 2-124: Hybrid propulsion system with powershifting, designed using planetary gears. Upper left: Design. Upper right: Gear/Clutch schedule. Lower half: Dynamic model.

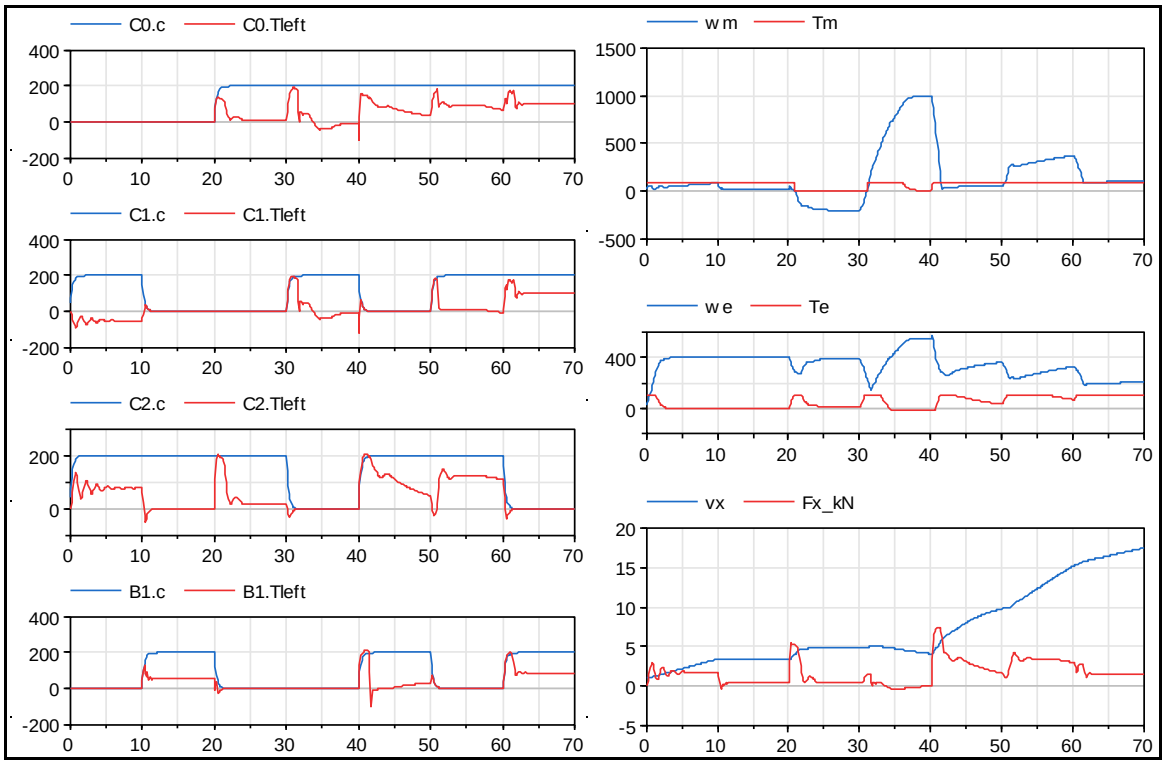


Figure 2-125: Simulation of the transmission in Figure 2-124 (with approximate clutch models from Eq [2.86]). Example sequence of shifts: Simply shift each 10th second, in order as in table in Figure 2-124.

2.4.7.2 Multiple Electric Drivetrains

Electric machines (EMs) requires less complex transmissions than ICEs, since they have a broader speed range, $\omega_{max}/\omega_{min}$ (in principle ∞ since $\omega_{min} = 0$), and therefore require fewer gears. EMs are also less complex than ICEs. They also allow less complex transmissions, since they have a broader

speed range, $\omega_{max}/\omega_{min}$ (in principle ∞ since $\omega_{min} = 0$), which requires fewer gears. If an EM can manage with 1 gear, there is no need for gearboxes, which further contribute to reduce complexity. So, it makes sense to design electric vehicles without gearboxes but allow multiple EMs, i.e. multiple drivetrains. The following is an example where a single electric drivetrain with a 2-gearbox is challenged by a multiple electric drivetrain without gearboxes.

The EM model from 2.4.2.3.2 is used with scaling in torque dimension.

2.4.7.2.1 Single Drivetrain Vehicle

The single drivetrain vehicle is designed as follows: EM for single drivetrain scale with 1 or no scaling. The intersection of $F = P/v$; and the driving resistance defines the top speed, see 3.2.5.1. Lowest ratio (gear 2) is selected for the top speed. We now have design point 1. Highest ratio (gear 1) is then selected so that the constant power hyperbolas are spliced without gap or overlap. This defines design points 2 (startability, 3.2.10.1) and 3 (maximum speed at startability road grade). The efficiency map for each gear can be used to identify gear shift curves for maximum efficiency, as was indicated in Figure 2-102.

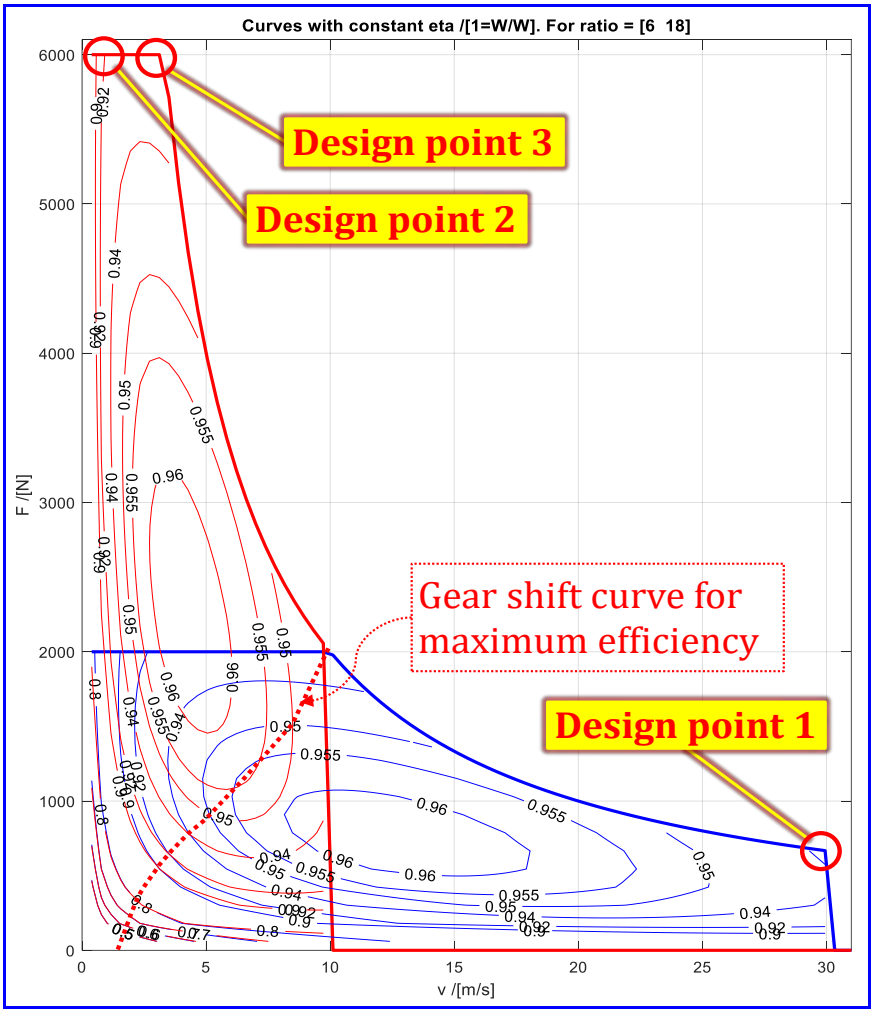


Figure 2-126: Efficiency maps for a Single Drivetrain: 1 electric motor (20 kW) which propels the vehicle via a 2-stepped gearbox.

Vdc:650V	L= 160	i= 15								
38400	81,0	89,1	92,1							
31000	85,4	91,7	94,0	92,9						
25600	87,2	92,8	94,7	95,2						
18000	90,4	94,4	95,8	96,7	96,3	93,9				
12800	91,8	95,1	96,3	97,0	96,7	95,9	94,1			
9400	93,3	95,7	96,5	97,1	97,0	96,1	95,3	94,8	94,4	93,1
6000	93,9	95,9	96,5	97,0	96,9	96,0	94,9	94,5	94,0	93,2
3600	94,4	95,7	96,1	96,5	96,5	95,3	93,9	93,2	92,6	91,5
2400	93,6	94,2	94,3	94,4	94,3	92,7	90,3	89,2	88,2	86,4
1300	91,4	91,6	91,4	91,2	91,1	88,5	84,8	83,2	81,8	79,2
Torque at wheels [Nm]	6	12	20	30	40	50	60	70	80	88
	speed [kph]									

Vdc:650V	l= 110	i= 22/9								
38400	88,0	92,3	94,1							
31000	90,1	93,7	95,1	93,8						
25600	91,8	94,7	95,9	96,1						
18000	93,3	95,6	96,5	96,9	96,2	94,0				
12800	94,6	96,2	96,9	97,1	96,9	96,3	95,5	93,8		
9400	95,1	96,4	96,9	97,1	96,9	96,4	96,4	96,1	95,0	94,8
6000	95,5	96,4	96,7	96,9	96,7	96,1	97,0	97,1	97,1	96,9
3600	95,1	95,4	95,5	95,5	95,5	94,6	97,1	97,1	97,1	96,9
2400	94,7	95,0	95,0	95,0	95,0	94,0	96,8	96,9	96,9	96,7
1300	92,0	91,9	91,6	91,4	91,4	89,6	95,5	95,5	95,5	95,5
Torque at wheels [Nm]	1st gear						2nd gear			
	6	12	20	30	40	50	60	70	80	88
	speed [kph]									

Figure 2-127: Efficiency maps for a heavy vehicle with a Single Drivetrain. Top: 1 gear. Bottom: 2 gears, selected for maximum efficiency. From Reference (Kopplow, 2023).

2.4.7.2.2 Multiple Drivetrain Vehicle

Propulsion system components to the multiple drivetrain vehicle can be designed in many ways. We exemplify with 3 drivetrains, each with an EM scaled with 0.5. The ratios of drive train 1 and 2 are same as for gear 2 in single drivetrain vehicle. The ratio of drivetrain 3 is such that all 3 drivetrains together can reach design point 2. Design point 3 is not fully reached, but other advantages are reached, see figure below.

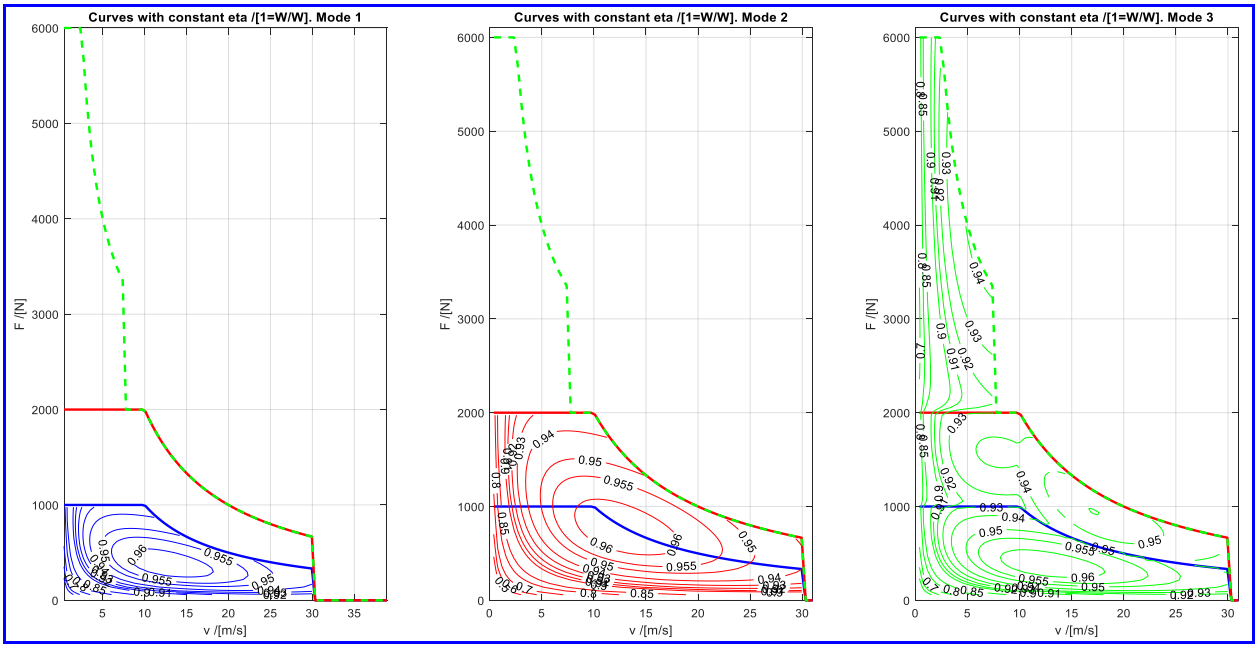


Figure 2-128: Efficiency maps for a Multiple Drivetrains: 3 electric motors (3×10 kW) which parallelly propel the vehicle. No stepped gearboxes. Efficiency maps for 3 Modes are shown.

The figure shows 3 "Modes". A Modes is a selection of which drivetrains (which EMs) to use, and with which distribution, to generate the required force F on the vehicle. The 3 modes in the figure are defined as:

- Mode 1: Use only Drivetrain 1
- Mode 2: Use Drivetrain 1 and 2, with equal force from each
- Mode 3: Use only Drivetrain 1 if it is enough for the required F. If more is needed, add the extra needed from Drivetrain 2. If even more is needed, add as much as needed from Drivetrain 3.

Note, that these modes are defined, they constitute discrete selections which can be compared to gear selection in stepped gearboxes.

Also note that one can define a mode also through momentaneous optimization, such that a "Use a power loss minimizing mix of all Drivetrains", as in Ref (Utbult, Jonasson, Yang, & Jacobson, 2020). Similarly, other optimizations, such as maximum acceleration margin and least cost (e.g., cost of energy, wear, and battery degradation) can be formulated. Such modes can be compared to ratio selection for CVTs.

2.5 Braking System

*Braking can refer to either **wheel torque braking** (intentionally adding wheel torques opposite to direction of motion, using propulsion and/or braking system) or vehicle braking (intentionally adding negative longitudinal forces on the vehicle by any means, including steering left and right wheel equally but opposite, raising an aerodynamic brake shield or releasing a parachute). Braking often results in vehicle deceleration, but not necessary, e.g., if braking on one wheel and propelling on another or if braking in a steep downhill. This section treats only **wheel braking**.*

There are several systems that can brake a vehicle:

- Service brake system (brake pedal and ABS/ESC controller, which together applies brake pads to brake discs/drums)
- Parking brake (lever/button that applied brake pads to brake discs/drums, normally on rear axle on cars but all axles on heavy vehicles)
- Prime mover brakes:
  - Engine braking (ICE operates at "engine brake" as marked in Figure 2-99)
  - Electric machines (machines can be used symmetrical, i.e., both for positive and negative torques, see Figure 2-99)
- Heavy vehicles often have *Retarders*. They normally use hydraulic or Eddy current to dissipate engine, as opposed to dry friction. So, they cannot brake at low speeds or stand-still.
- Large steer angles will decelerate the vehicle, see 3.2.4.3.2.

This section is about **(dry) friction brakes**, meaning Service brakes and Parking brake. In vehicle dynamics perspective, these have the following special characteristics:

- Friction brakes are almost unlimited in force for a limited time since they can lock the wheels for most driving situations and road friction (ICE and electric motors are often limited by their maximum power, since it is often smaller than available road friction.) However, if the friction brakes are used for a long time, the brake lining will start to fade. This means friction coefficient is lowered due to high temperature (oxidation and melting of pad/lining material).
- Friction brakes can only give torque in opposite direction to wheel rotation. (Electric motors can brake so much that wheel spins rearwards.)
- Friction brakes can hold the vehicle at standstill. (Using electric machines for stand-still in a slope, a closed loop control would be necessary, resulting in that vehicle "floats" a little.)

The basic design of a passenger car brake system is a hydraulic system is show in Figure 2-129. Here, the brake pedal pushes a piston, which causes a hydraulic pressure (pressure = pedal force/piston area). The hydraulic pressure is then connected to brake callipers at each wheel, so that a piston at each wheel pushes a brake pad towards a brake disc ($DiscForce = Pressure \cdot PistonArea$). The brake torque on each wheel is then simply: $T = NumberOfFrictionSurfaces \cdot DiscCoefficientOfFriction \cdot DiscRadius \cdot DiscForce$. (Normally, there are 2 friction surfaces since double-acting brake callipers.) By selecting different piston area and disc radii at front and rear, there is a basic hydro mechanical brake

distribution ratio between front and rear axle. There are normally two circuits for redundancy. It should be mentioned that *DiscCoefficientOfFriction* varies a lot; during one strong brake event, it can typically drop 10..25% due to temperature rise and sliding velocity decrease.

Brake systems for heavy trucks are generally based on pneumatics, as opposed to hydraulics, see Figure 2-131. Ref (Tagesson K. , 2017), has a good descriptive chapter about brake systems for heavy vehicles.

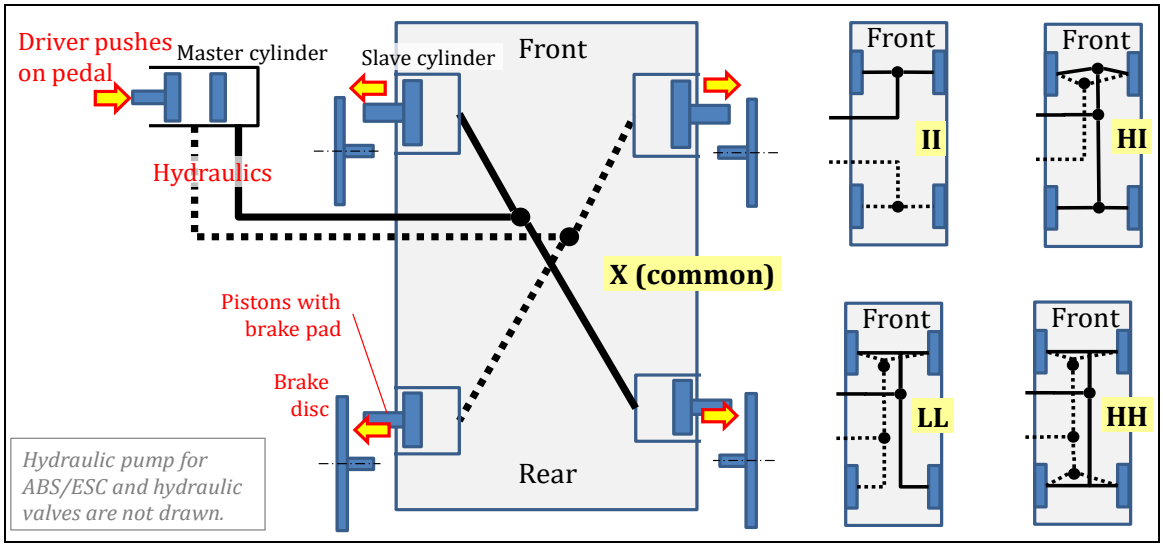


Figure 2-129: Layouts of a hydraulically applied brake system, which is conventional on passenger cars.

Brake systems for modern road vehicles are mechatronic systems, i.e. they contain both mechanical parts and control algorithms. As minimum, one can include the wheel slip control, see 4.6.2.2.4, or ABS/EBD, see 3.5.2.4/3.5.2.5.

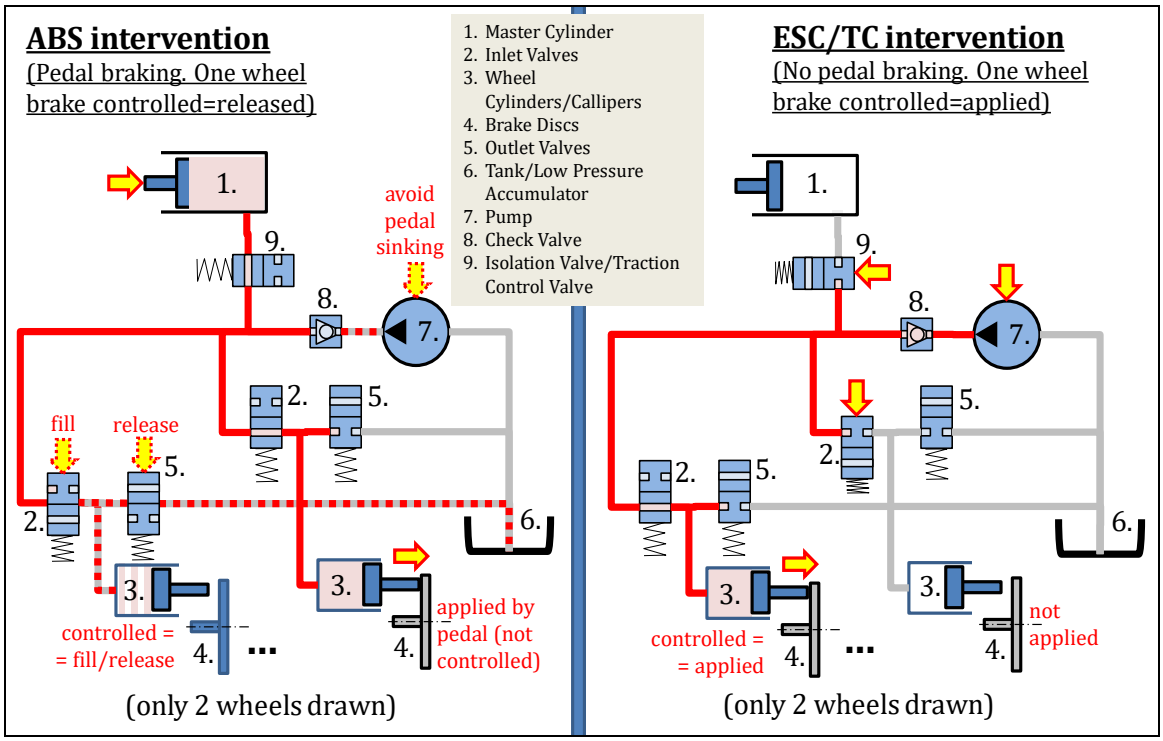


Figure 2-130: Concept of hydraulically applied brake system for ABS/EBD and ESC/TC functions.

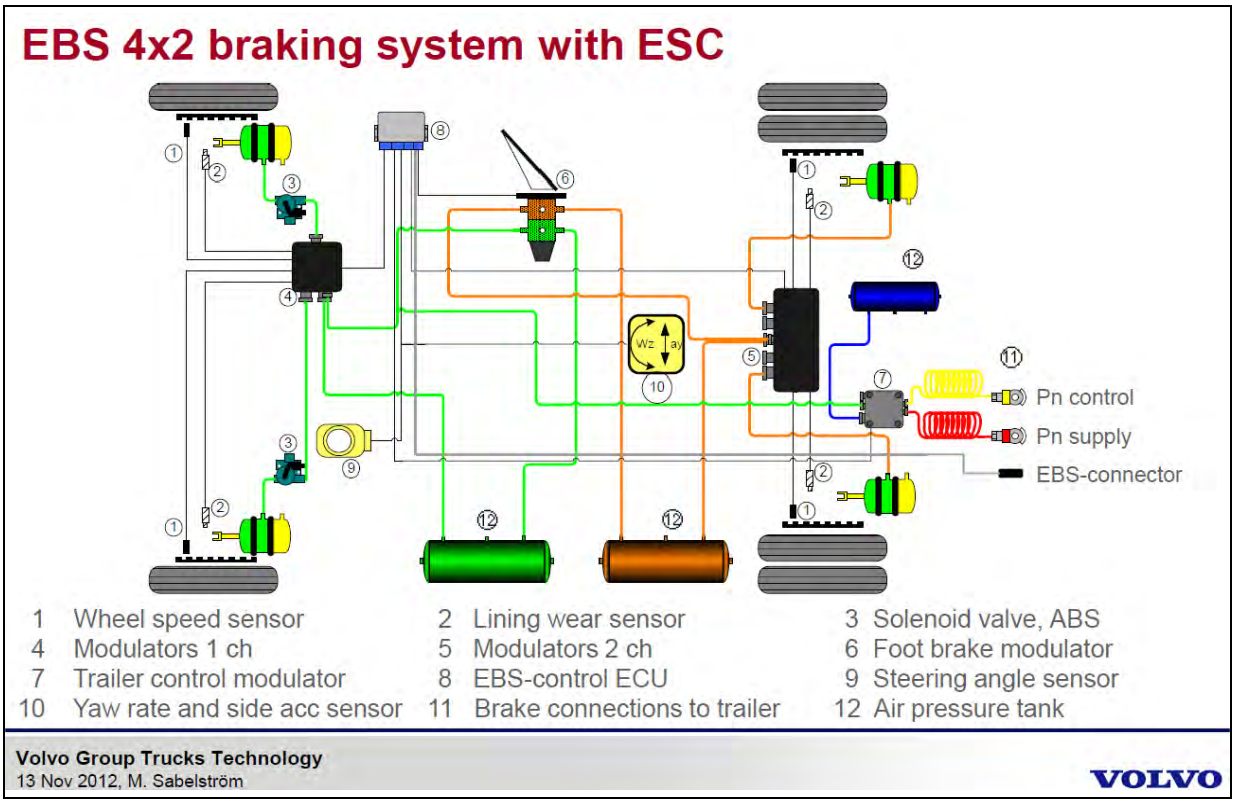


Figure 2-131: Pneumatically applied brake system for heavy vehicles. Electronics Brake System, EBS, from Volvo GTT, Mats Sabelström.

Standard (ISO 11992, 2003) is that the truck decides and sends 1 scalar request rearwards. The physical interpretation of the signal is the fraction of "utilized friction", i.e. $\sum F_x / \sum F_z$. The trailing units simply relay the same signal rearwards.

2.5.1 Wheel Longitudinal Slip Limit Control

For vehicle dynamics, the braking system is both characterized by distribution between wheels and the longitudinal slip control performance of individual wheels, see 3.5.2.4 and 4.6.2.2.4.

Here comes an example of a slip controlled wheel by dry friction brake actuation. It is a development of the the example in Figure 1-45. It is a one wheel vehicle model. Vertical force on wheel is constant. Tyre model as in Eq [2.58] and Eq [2.68]. State variables are $v_x, v_y, \omega, T_{Slip}$. The v_x varies due to the braking. The $v_y \equiv 0$ since purely longitudinal manouvre. The ω varies due to wheel rotational inertia and the brake application. The T_{Slip} is the "torque if slipping" of the brake, i.e. the brake torque $= -\text{sign}(\omega) \cdot T_{Slip}$. (The T_{Slip} is denoted c_c in 2.4.4.) The T_{Slip} is a first order delayed of the $T_{SlipReq}$. The $T_{SlipReq}$ is a signal computed in the (time sampled) algorithm. The model of the brake actuator, including both algorthms and hardware physics is hown in the following and a simulation example in Figure 2-132.

```
⋮
  //Brake Actuator Algo:
  parameter Modelica.Units.SI.Time DifferentiationTime=0.1;
  parameter Modelica.Units.SI.Time SampleTime=0.01;
  parameter Modelica.Units.SI.DimensionlessRatio s_xMin=-0.2;
  Modelica.Units.SI.Velocity v_xEst;
  Modelica.Units.SI.AngularVelocity w_Est;
  Modelica.Units.SI.Torque T_SlipReq, T_Est;
  Modelica.Units.SI.Force F_xEst;
  Modelica.Units.SI.AngularAcceleration derw_Est;
  TorqueRate derT_Est;
  Modelica.Units.SI.DimensionlessRatio s_xEst;

  //Brake Actuator:
  Modelica.Units.SI.Torque T_Slip;
```

```
  parameter Modelica.Units.SI.Time Delay=0.1;
⋮
equation
⋮
  //Actuator.Algo:
  when sample(-1000, SampleTime) then
    //Control algorithm:
    if pre(s_xEst) > s_xMin then  T_SlipReq = F_xSlipReqVeh*R_w;
    else                          T_SlipReq = 0;                    end if;
    //Estimators:
    v_xEst = v_x; // sample and hold
    derw_Est = (w - pre(w_Est))/DifferentiationTime; //Discrete differentiation
    w_Est = pre(w_Est) + ((pre(derw_Est)+derw_Est)/2)*SampleTime; //Trapetziodal approx..
  //w_Est = pre(w_Est) + (pre(derw_Est              )*SampleTime; //Euler forward approx.
  //w_Est = pre(w_Est) + (derw_Est                  )*SampleTime; //Euler backward approx.
    derT_Est = (T_Act - pre(T_Est))/DifferentiationTime; //Discrete differentiation
    T_Est = pre(T_Est) + ((pre(derT_Est) + derT_Est)/2)*SampleTime; //Trapetziodal approx.
    F_xEst = (T_Est - J_w*derw_Est)/R_w; // Physical model base (F_xEst not used in algo!)
    s_xEst = (R_w*w_Est - v_xEst)/abs(R_w*w_Est); // Definition of auxilliary vriable slip
  end when;
  //Actuator.HardPhysical:
  der(T_Slip) = (T_SlipReq - T_Slip)/Delay; // Known problem: Reasonable model only for w>0
  T_Act=-sign(w)*T_Slip; // Known problem: Cannot stick at w=0
⋮
```

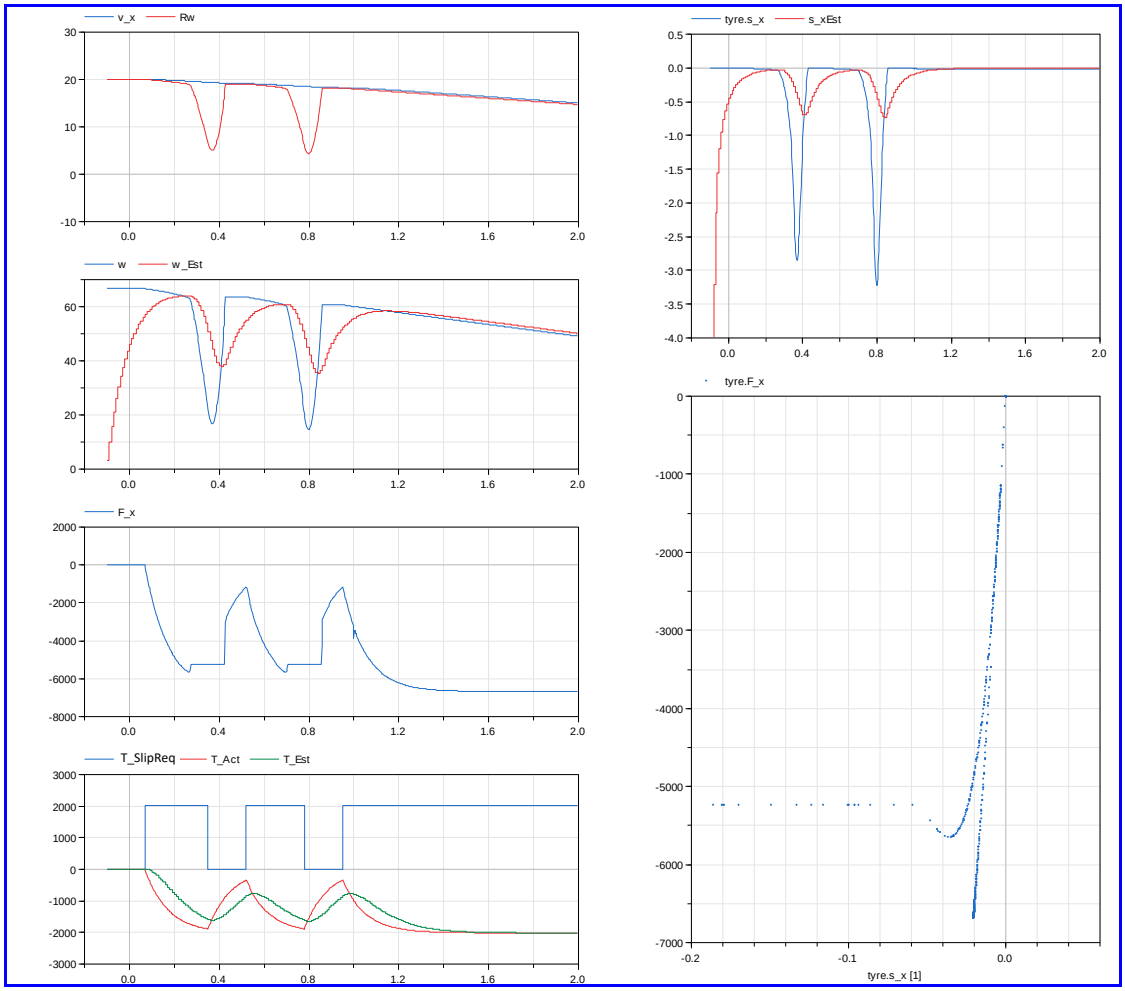


Figure 2-132: Longitudinal slip control simulation example.

2.6 Steering System

*Steering can refer to either **wheel steering** (intentionally changing steer (or yaw) angle of wheels relative to the vehicle body) or **vehicle steering** (intentionally redirecting the vehicle by any means, including also propelling or braking the wheels on side). This section is about **wheel steering**.*

The steering system is here referred to the arrangements (mechanical or by-wire) between steering wheel and the road wheel's steering on the steered axle. It is normally the front axle that is steered. Driver's interaction is two-sided, both steering wheel angle and torque, which is introduced in 2.10. In present section, we will focus on how wheel steer angles are distributed between the wheels.

2.6.1 Chassis Steering Geometry

Contribution from Ingemar Johansson, Vehicle Engineering, Chalmers and Mats Jonasson, Vehicle Dynamics, Chalmers

2.6.1.1 Balancing between parallel and Ackermann steering

For low-speed, Ackermann gives best manoeuvrability and lowest tyre wear. For high-speed, Parallel is better in both aspects. This is because, at high speed, vehicles corner with side slip outwards in curves, which means that the instantaneous centre is further away than Ackermann geometry assumes, i.e. more towards the motion parallel. A balancing between low and high speed leads to that steering geometry is typically chosen between Ackermann and parallel.

In summary: Ackermann geometry means steering angles that leads to *absence of fighting tyre forces*, often between left and right wheel on an axle, or extended to heavy vehicles, it can also be fighting between two axles, typically two or more axles in a non-steered rear axle group. That rules, expressed in *forces*, can mean different steering *geometry* for different longitudinal velocity, curvature, wheel torque distribution, and tyres/axle slip stiffness.

2.6.1.1.1 Ackermann percentage

A measure of the balance between Ackermann and parallel is called "Ackermann percentage", here denoted $AckmPerc$. It is either a function of steering or a scalar measure. Beware of that there are different definitions, but generally: $AckmPerc = ((\delta_i - \delta_o)) / \delta_{ref}$;. It gives 0 for parallell steering, which is good. Normally $\delta_{ref} = (\delta_{iA} - \delta_{oA})$;, which is good because it gives 1 for perfect Ackermann. One also need to connect $\{\delta_{iA}, \delta_{oA}\}$ to the actual angles $\{\delta_i, \delta_o\}$. One way to do this is interpret δ_{ref} as the *axle steering angle*, which is the average angle $\delta_{ref} = ((\delta_i + \delta_o)) / 2$ and $\{\delta_{iA}, \delta_{oA}\}$ as the Ackermann angles for "a vehicle which, at low speed, moves as the corresponding one-track model" which gives a 4th equation. With these 4 equations, we can plot the function $AckmPerc = function(\delta_i, \delta_o, W, L)$;, see example in Figure 2-136. To get one scalar measure, one can, e.g., decide to pick the function value for $\delta_i = 20\ deg$ or a small δ_{sw}. Note that the 4th equation above makes $AckmPerc$ dependent of vehicle data such as W, L and possible steering one the other axles, so $AckmPerc$ is **not** an axle measure, but a vehicle measure.

2.6.1.2 Practical Design

A intended design of an Ackermann steering geometry is shown in Figure 2-134. The practical design of linkage will also make the transmission from steering wheel angle to road wheel steer angle non-linear. This can lead to different degrees of Ackerman steering for small and large steering wheel angles.

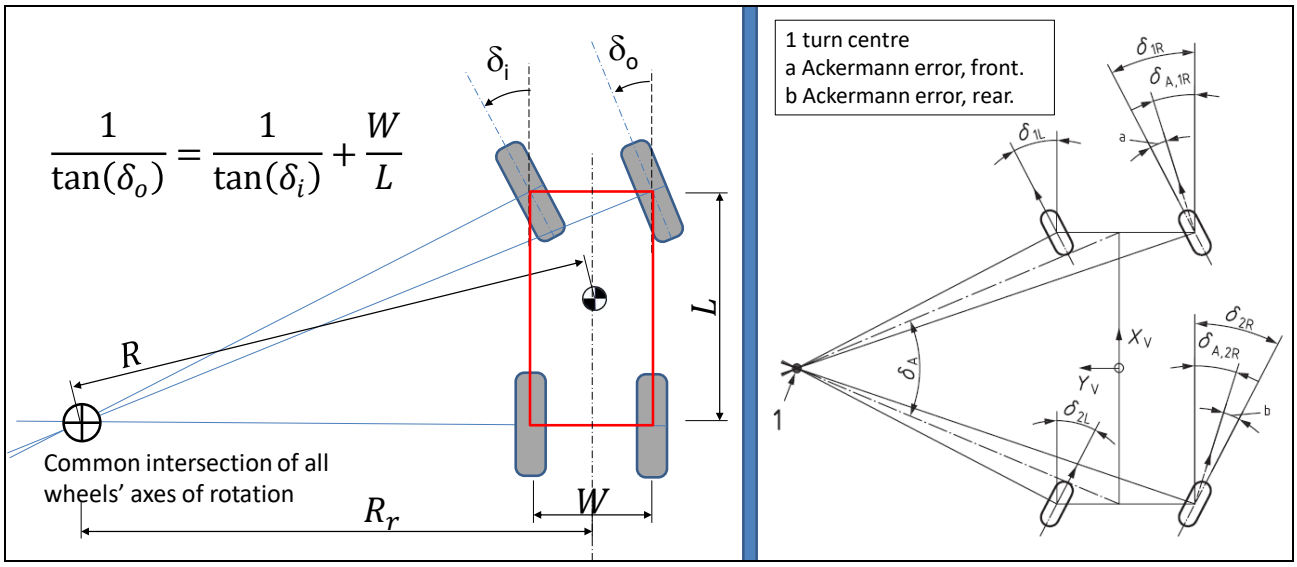


Figure 2-133: Intended design of Ackermann steering geometry. Left: One axle steered. Right: Both axles steered and including "Ackermann errors". From (ISO 8855).

In traditional steering systems, the steering wheel angle has a monotonically increasing function of the steer angle of the two front axle road wheels. This relation is approximately linear with a typical ratio of 15..17 for passenger cars. For trucks the steering ratio is typically 18..22. In some advanced solutions, steering on other axles is also influenced (multiple-axle steering, often rear axle steering). There are also solutions for dynamically adding steer angle through a planetary gear and electric angle-controlled motor on the steering shaft, so called Active Front Steering (AFS). In reference (Tagesson K. , 2017), there is a good descriptive chapter about steering systems for heavy vehicles.

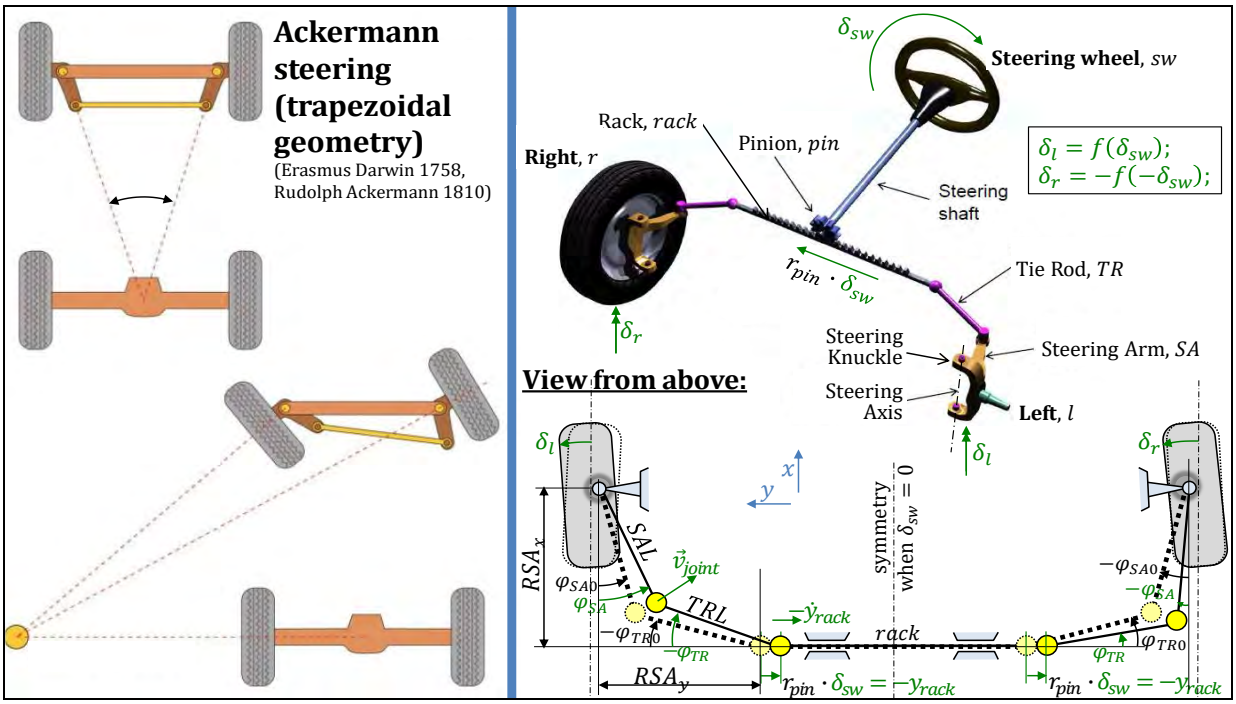


Figure 2-134: Practical designs. Left: Trapezoidal Steering which gives exact Ackermann. Right: Rack Steering, common on passenger cars.

2.6.1.2.1 Ackermann Percentage for Rack Steering

Figure 2-136 plots all angles as function of, e.g., δ_{sw}. One could formulate the geometric relations in algebra, or as in Figure 2-136, in differential equations, using proportionality between time derivatives of angles. The latter method gives simpler equations, but more effort to calculate the initial values.

[Modelica code for one wheel]

```
model SteAn_OneWheel
  constant Real pi=Modelica.Constants.pi;
//Design parameters:
  parameter Boolean Left;
  parameter Modelica.Units.SI.Length SAL, TRL, RSA_x,RSA_y;
  parameter Modelica.Units.SI.Angle d_Toe;
//Physical Variables:
  Modelica.Units.SI.Position y_rack;
  Modelica.Units.SI.Velocity v_jointx,v_jointy;
  Modelica.Units.SI.Angle d, p_TR, p_SA;
initial equation
  d = d_Toe;
  if Left then
    RSA_x=SAL*cos(+p_SA) +TRL*sin(-p_TR);
    RSA_y=SAL*sin(+p_SA) +TRL*cos(-p_TR);
  else ··· end if;
equation
  if Left then
    v_jointx =          0  - TRL*cos(-p_TR)*(der(p_TR));
    v_jointy = der(y_rack) + TRL*sin(-p_TR)*(der(p_TR));
      v_jointx =             + SAL*sin(+p_SA)*der(p_SA);
      v_jointy =             - SAL*cos(+p_SA)*der(p_SA);
  else ··· end if;
  der(d)=der(p_SA);
end SteAn_OneWheel;
```

[Modelica code for axle on vehicle]

```
model SteAn_Axle "Default parameters for a left wheel"
  constant Real pi=Modelica.Constants.pi;
//Design parameters:
  parameter Modelica.Units.SI.Length L_SA=2.5 "Length steering axes to rear axle";
  parameter Modelica.Units.SI.Length W_SA=1.6 "Width between steering axes.";
  parameter Modelica.Units.SI.Length r_pin=0.01 "Pinion ratio";
  parameter Modelica.Units.SI.Length SAL=0.19 "Steering arm length";
  parameter Modelica.Units.SI.Length TRL=0.17 "Tie-rod length";
  parameter Modelica.Units.SI.Position RSA_x=0.2 "Rack to Steering Axis, longitudinal";
  parameter Modelica.Units.SI.Position RSA_y=0.25 "Rack (end) to Steering Axis, lateral";
  parameter Modelica.Units.SI.Angle d_Toe=0.25*pi/180 "Toe(-in) for one wheel";
//Auxilliary parameters:
  parameter Modelica.Units.SI.AngularVelocity sweepRate=1;
  parameter Modelica.Units.SI.Angle d_eps=0.1*pi/180;
//Physical Variables:
  Modelica.Units.SI.Position y_rack;
  Modelica.Units.SI.Angle d_sw;
  Modelica.Units.SI.Angle d_ref, d_lA, d_rA;
//Auxilliary Variables:
  Real AckmPerc;  Boolean Valid;  Modelica.Units.SI.Length R_A;
//Sub models:
  SteAn_OneWheel left( Left=true, SAL=SAL,TRL=TRL,RSA_x=RSA_x,RSA_y=RSA_y,d_Toe=-d_Toe);
  SteAn_OneWheel right(Left=false,SAL=SAL,TRL=TRL,RSA_x=RSA_x,RSA_y=RSA_y,d_Toe=+d_Toe);
equation
  d_sw = sweepRate*time;
  y_rack=-r_pin*d_sw;
    left.y_rack=y_rack;
    right.y_rack=y_rack;
      d_ref=(left.d+right.d)/2;
  if abs(d_ref) > d_eps then
    Valid = true;
    1/tan(d_ref) = R_A/L_SA;
    1/tan(d_lA) = (R_A - W_SA)/L_SA;
    1/tan(d_rA) = (R_A + W_SA)/L_SA;
    AckmPerc = (left.d - right.d)/(d_lA - d_rA);
  else
    Valid = false; R_A = L_SA/d_eps; d_lA = d_eps; d_rA = d_eps; AckmPerc = 0;
  end if;
end SteAn_Axle;
```

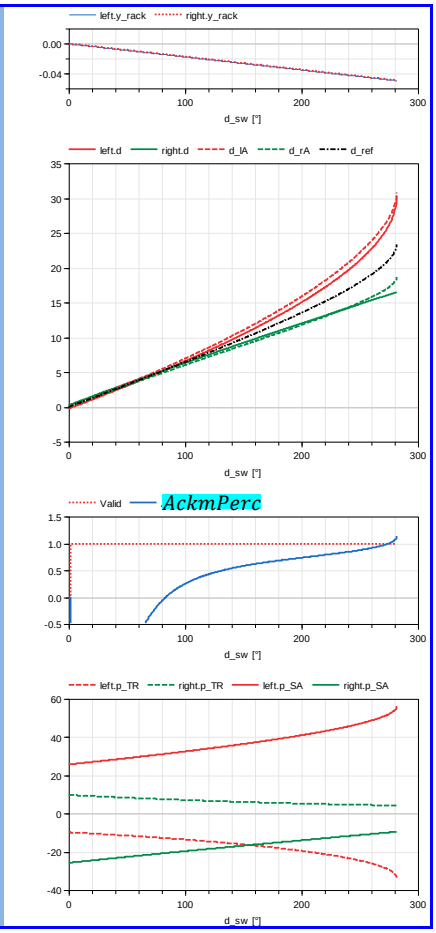


Figure 2-136: Ackermann percentage as function (or curve, i.e., a 1D quantity). Modelica code and resulting plot.

2.6.2 Steering System Forces

The steering wheel torque, T_{sw}, should basically be a function of the tyre/road forces, mainly the wheel-lateral forces. This gives the driver a haptic feedback of what state the vehicle is in. The torque/force transmission involves a servo actuator, which helps the driver to turn the steering system, typically that assists the steering wheel torque with a factor varying between 1 and 10, but less for small T_{sw} (highway driving) than large T_{sw} (parking), see Figure 2-137. Here, the variation in assistance is assumed to be hydraulic and follows a so-called boost curve. At $T_{sw} = 0$, the assistance is ≈0.45/0.55≈1 and for $T_{sw} = 4$ Nm, it is ≈0.9/0.1≈10.

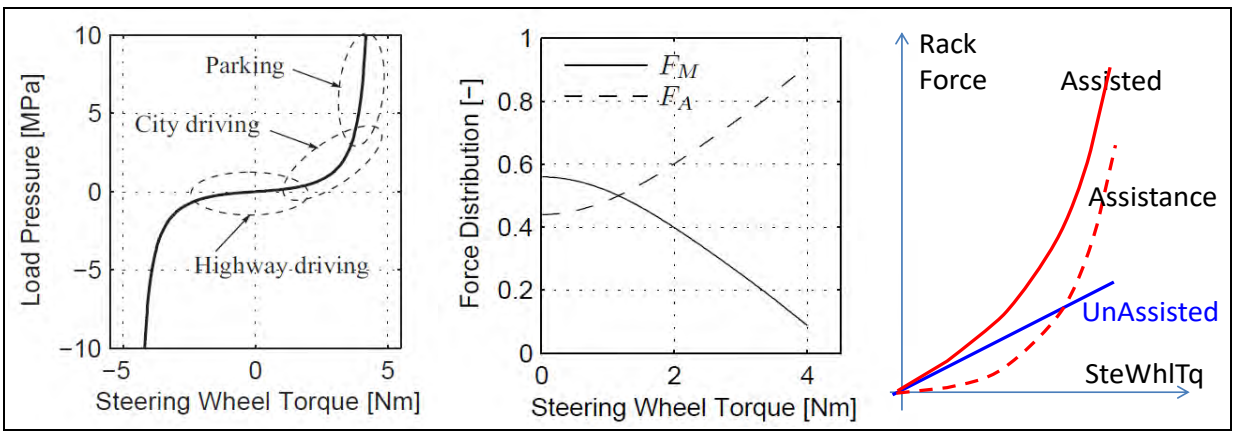


Figure 2-137: Left: Boost Curve with different working areas depending on the driving envelope. Middle: Torque distribution between manual torque, FM, and assisting torque, FA, depending on applied steering wheel torque. From Reference (Rösth, 2007). Right: Unassisted and assisted steering wheel torque.

2.6.2.1 Torque Steer and Brake Steer

For vehicle dynamics, one important effect of a steered axle, is that the lateral force on the axle tries to align the steering in the direction that the body (over the steered axle) moves without tyre side slip. This is designed in via the sign of the castor trail, see Figure 2-138. Also, asymmetry in longitudinal tyre forces (wheel shaft torques and/or brake torques) affects the steering wheel torque. This is analysed in the following.

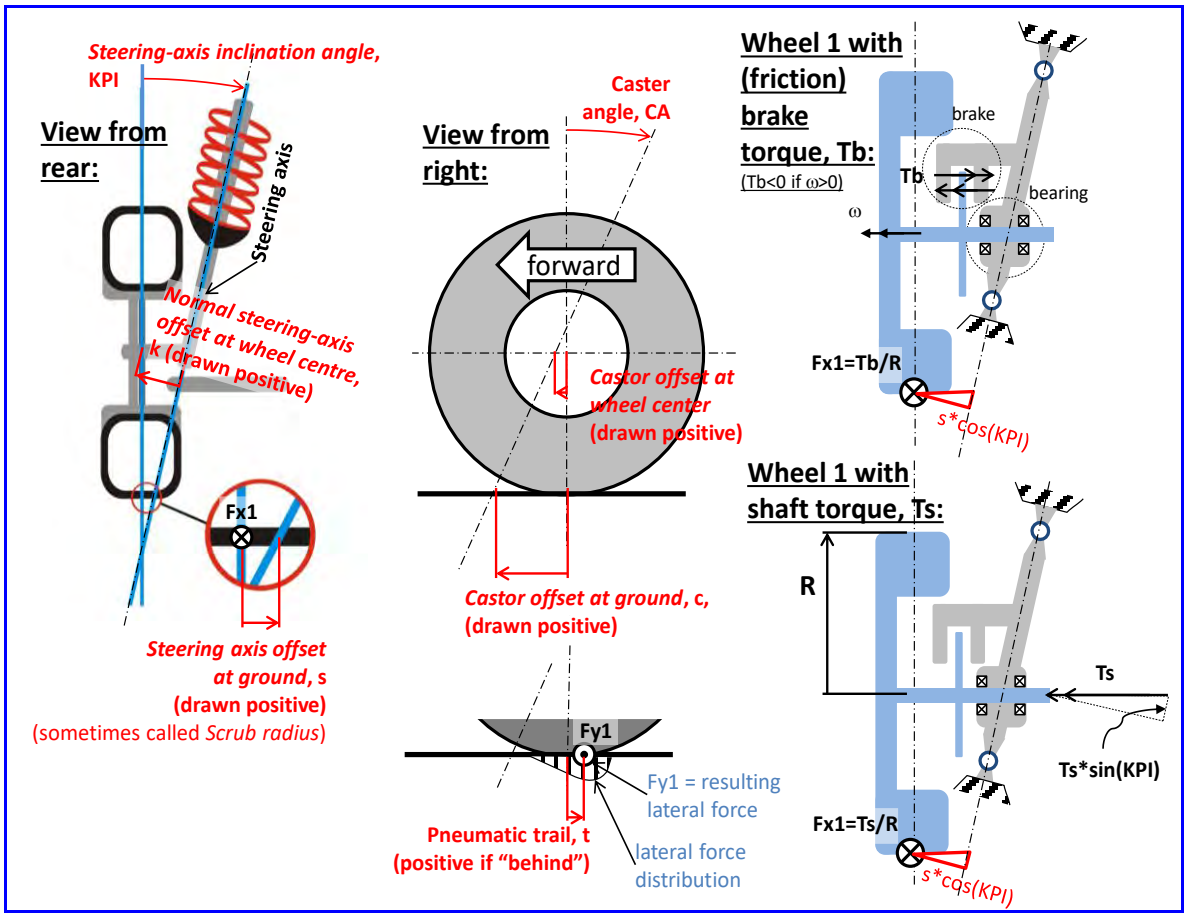


Figure 2-138: Steering geometry and offsets.

On a steered axle, there is a *Steering axis* (or *Kingpin axis*) around which the wheel is rotated when it is steered. The steering axis intersects with the ground plane at a point which normally has an offset from the contact patch centre, both longitudinally and laterally. The offsets are called *Castor offset at ground* and *Steering axis offset at ground*, respectively. (Steering axis offset at ground is sometimes called *Scrub radius*, but that is also used for the resulting distance of both offsets, so it is an ambiguous name.) This figure also defines *Normal steering axis offset at wheel centre*. We will use the 3 latter measures to explain why steering is affected by differences in shaft torque left/right, differences in brake torque left/right, and lateral wheel forces. The steering axis distance from wheel centre in a side view, is called *Castor offset at wheel centre*.

Often, the actual forces between tyre and ground are not in the exact centre of the nominal contact patch, which also creates "effective" version of castor offset and scrub radius. For instance, the *Pneumatic trail* adds to the Castor offset at ground due to the lateral force distribution being longitudinally offset from nominal contact point; so that the lever becomes not only c, but $c + t$. The moment, T_{steer}, on steering system (around Steering axis, turning towards increasing steer angle) is affected by tyre forces on a steered axle as in Equation below.

Castor offset at ground is, on passenger vehicles, 15-20 mm (at motorcycles approximately 100 mm). On rear wheel driven passenger vehicles, it is typically 5 mm due to higher Castor Angle which gives a

beneficial higher Camber angle gain at cornering. On a front wheel driven passenger vehicle, a non-zero castor offset is not chosen due to drive axle lateral displacement. Castor offset gives a self-aligning steering moment, which generally improves the steering feel.

$$T_{steer} = \frac{-(T_{b1}+T_{s1})}{R}\cdot s\cdot\cos(KPI) + \frac{-T_{s1}}{R}\cdot R\cdot\sin(KPI) + \\ + \frac{(T_{b2}+T_{s2})}{R}\cdot s\cdot\cos(KPI) + \frac{T_{s2}}{R}\cdot R\cdot\sin(KPI) + \\ +(-1)\cdot\Big(F_{y1}\cdot(c+t_1)+F_{y2}\cdot(c+t_2)\Big)\cdot\cos(CA) = \\ = \frac{T_{b2}-T_{b1}}{R}\cdot s\cdot\cos(KPI) + \frac{T_{s2}-T_{s1}}{R}\cdot k - \Big(F_{y1}\cdot(c+t_1)+F_{y2}\cdot(c+t_2)\Big)\cdot\cos(CA);$$ [2.89]

The equation shows that difference in both brake torque and shaft torque affects steering and so does the sum of lateral forces. For reducing torque steer and disturbances from one-sided longitudinal forces due to road irregularities, kingpin offset, scrub radius different road friction should be as small as possible, but it is limited by geometrical conflicts between brake disc, bearing, damper, etc.

Positive scrub radius contributes to self-centring, thanks to lifting the car body, see below. Negative scrub radius compensates for split-μ braking, or failure in one of the brake circuits. Hence, the scrub is a balance between these two objectives. Scrub radius is often slightly negative on modern passenger cars. Scrub radius is often positive on trucks, maybe 10 cm, due to packaging.

2.6.2.1.1 Effects from Lifting the Vehicle Body

The geometry in figure shows one part of the lifting effect. This is that if steer angle is changed from zero, it lifts the vehicle body slightly which requires a steering torque. One can see this as a kind of "return spring effect". Figure 2-139 shows how KPI and scrub radius causes the vehicle body to lift a distance $s''' = s\cdot\cos(KPI)\cdot(1-\cos(|\varphi_{steer}|))\cdot\sin(KPI)$. This will require a work $T_{steer}\cdot\varphi_{steer} = F_{iz}\cdot s'''$. This leads to an T_{steer} (additional to Eq above) as follows:

$$(additional)\ T_{steer} = \\ = \sum_{i=left,right}\frac{F_{iz}\cdot s'''}{\varphi_{steer}} = \frac{s\cdot\cos(KPI)\cdot(1-\cos(|\varphi_{steer}|))\cdot\sin(KPI)}{\varphi_{steer}}\cdot F_{axle,z};$$ [2.90]

It should be noted that the Eq is not complete with respect to all "returning effects". There are also effects from Castor angle and Castor trail as well as that the tyre has a width and radius. However, in total, these give rise to a returning steering torque which is depending on the steer angle.

It can also be noted that steering effort for low speed or stand-still is largely influenced by whether brakes are applied or not, due to the magnitude (not sign) of scrub radius.

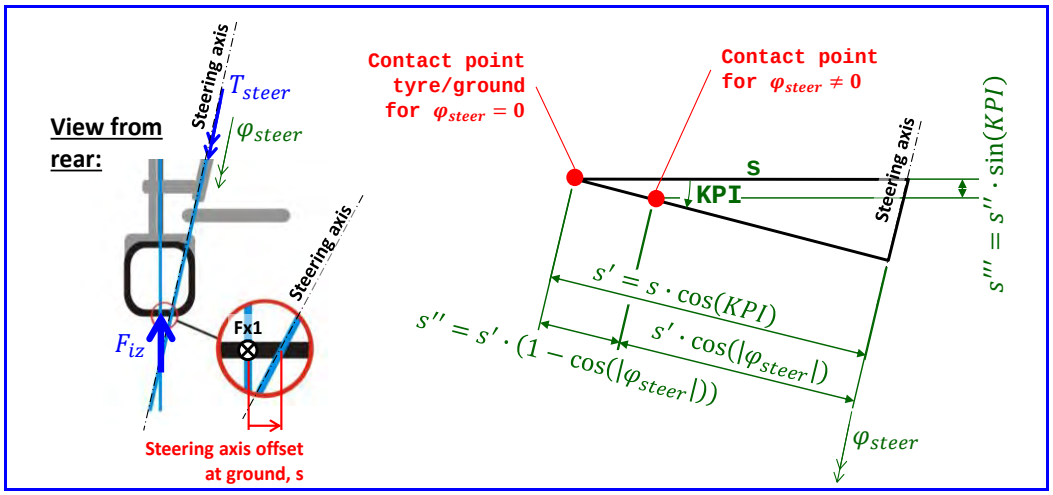


Figure 2-139: Lift effect due to steer angle and positive Steering axis offset at ground.

2.7 Combined effects of subsystems on axles' and axle groups' road grip

Contribution from Sachin Janardhanan, Volvo Trucks and Vehicle Engineering at Chalmers

Figure 2-80 and Figure 2-81 shows how a single wheel with an applied wheel torque operates to apply both longitudinal and lateral forces $\{F_x, F_y\}$ while carrying a known vertical force F_x and moving with constant and known $\{v_x, v_y\}$. It is a good starting point for a one-track vehicle with one wheel per axle, such as a typical motorcycle. When wheels are combined to an axle, they become at least two, left and right. Also, when axles are combined to axle groups, such as double or triple rear axles on a truck. When more than one wheel, the Figure 2-80 and Figure 2-81 are not complete for how the axle or axle group works.

The section 2.7 will point out this difference by showing some corresponding diagrams applicable for an axle or axle groups with different arrangement of suspension, wheel torque application and steering. Simple wheel model (Eq [2.59] with tanhyp(⋯)) is used. Only two wheels are used and the distance between them is neglected, so that the diagrams represents either one axle with neglected trackwidth or two one-wheel axles with neglected axle spread. 4 examples are show in Figure 2-140.

Note that **if** the distance between the wheels (track width and/or axle spread) is **not** neglected, the axle group will not only generate $\{F_x, F_y\}$ but also a yaw moment $\{F_x, F_y, M_z\}$. The yaw moment will be proportional to $F_{1x} - F_{2x}$ if the two wheels represent left and right wheels on an axle. The yaw moment (around centre of axle group) will be proportional to $F_{1y} - F_{2y}$ if the two wheels represent the two axles in the axle group. For one if the axles or axle groups in those force differences are plotted.

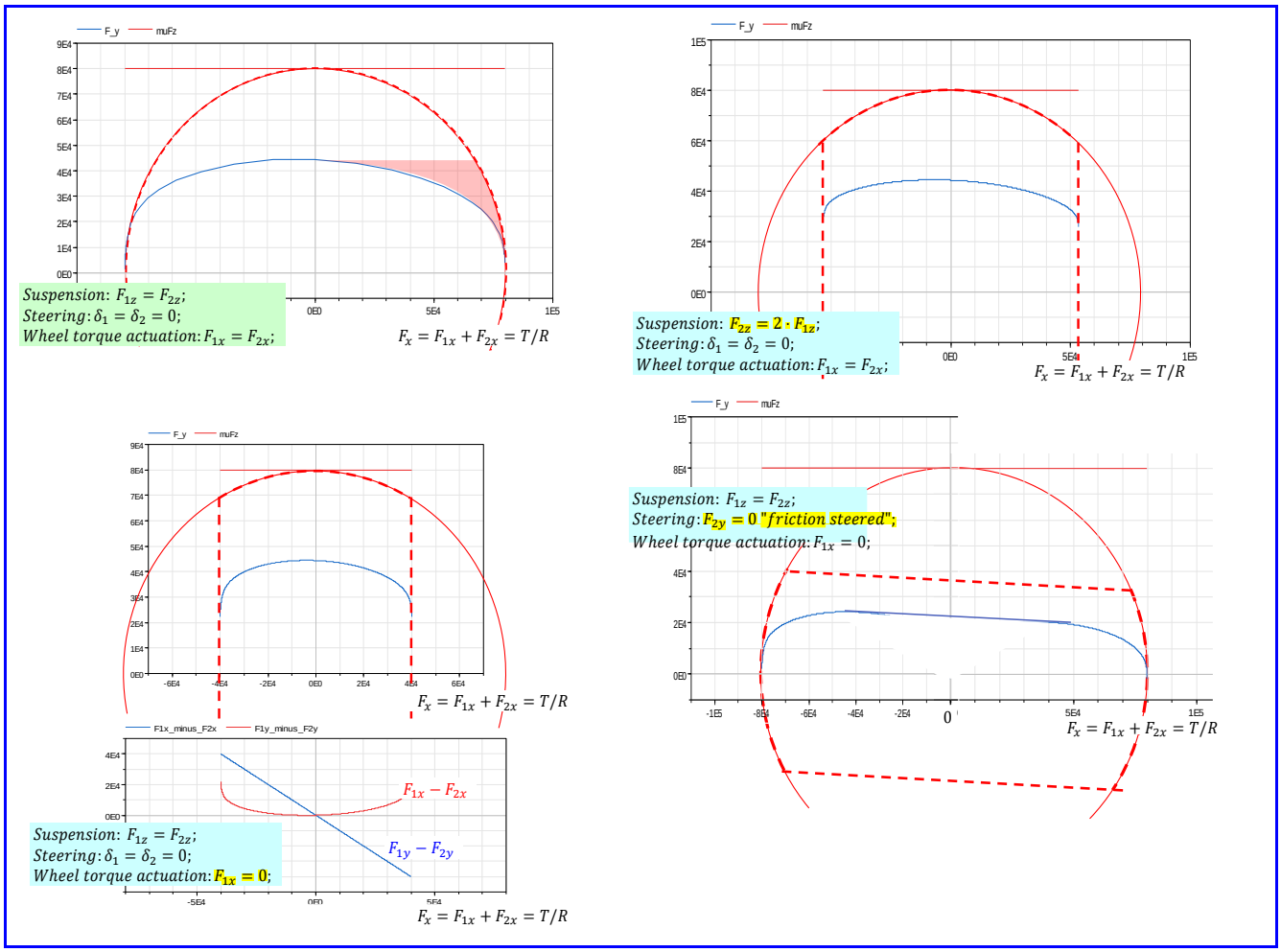


Figure 2-140: Similar as Figure 2-81, but for different axles or axle groups. The curve for $v_y = -0.05 \cdot v_x$ is calculated. Solid red circle is reference from Figure 2-81 (as if one wheel). Red dashed shape is an approximated limitation for the axle or axle group (as if is reaching "the edge of friction" for each wheel with its actuation).

These thoughts are developed from performance of an axle group to lateral stability of a whole vehicle with front and rear axle group in 3.4.4 (for straight-line driving), 4.3.5.1(for steady state high speed cornering), and 4.5.5 (for transient lateral dynamics).

2.8 Environment Sensing System

This subsystem must be mentioned since it is maybe the most important new enabler for today's development of automated driving. The technology to sense (radar, camera, lidar, GPS, etc) is not typically part of vehicle dynamics, but many vehicle dynamics control functions can be invented or improved through usage of the information from the subsystem. Some typically available information is listed in 3.5.1 and 4.6.1. Another vehicle dynamics aspect is that some sensor fusion, but primarily some predictions, can be made using vehicle dynamics models.

2.9 Vehicle aerodynamics

Contribution from Alexey Vdodin, Vehicle AeroDynamics at Chalmers and Adam Brandt, Vehicle AeroDynamics at Chalmers and CEVT

The flow of air around the vehicle body produces different external forces and moments acting on the vehicle. The fluid mechanics will not be covered in this course. However, practical first order models for aerodynamic forces have been established and are presented here.

2.9.1 Longitudinal relative wind velocity

The air moves relative to the vehicle body. This creates a pressure distribution which can be represented as a force-equivalent force vector $\vec{F}_{air}$, see Figure 2-141.

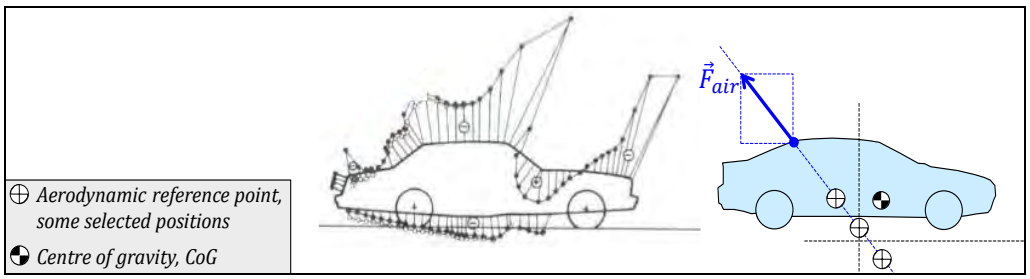


Figure 2-141: Pressure field on body and its force-equivalent force $\vec{F}_{air}$.

Force-equivalence can also be found through other combinations of forces and pitch moments, see Figure 2-142.

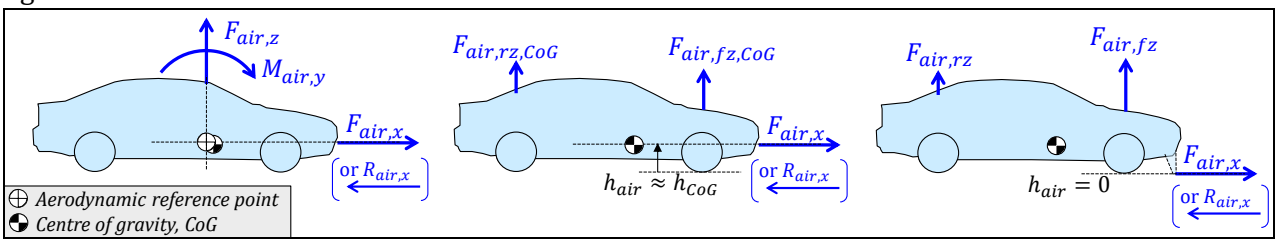


Figure 2-142: Force-equivalent ways to model longitudinal-wind aerodynamic forces in xz-plane. $F_{air,fz}$ and $F_{air,rz}$ differs, but $F_{air,x}$ is the same for all. Values for $\{c_d, c_{lf}, c_{lr}\}$ are often given for reference point in ground plane, as the right-most drawing.

From vehicle motion point of view, variables for aerodynamic forces and moments are naturally defined as positive when acting on vehicle in directions defined positive by (ISO 8855). They are denoted F and M in 2.9. So, $F_{air,x} > 0$ when the wind pushes the vehicle forward. Consequently, $F_{air,x} < 0$ when the wind is resisting forward motion of the vehicle. The longitudinal force play is special in the sense that it often appears in discussions where it is natural to name it "resistance force" (resisting forward motion), which makes it natural to use the opposite sign definition. So, we use a double notation on the longitudinal aerodynamic force: $F_{air,x} = -R_{air,x}$, see Eq [2.91].

2.9.1.1 Longitudinal resistance

Many vehicle functions can be analysed enough by only using the longitudinal resistance force $R_{air,x}$.

$$F_{air,x} = -R_{air,x} = \frac{c_d \cdot \rho \cdot A_{front}}{2} \cdot v_{Relx}^2 \cdot \text{sign}(v_{Relx}); \qquad [2.91]$$

The v_{Relx} is the longitudinal component of the wind velocity relative to the vehicle. The parameters c_d, ρ and A_{front} represent the drag coefficient, the air density and a reference area of the vehicle, respectively. The A_{front} is the area of the vehicle projected on a vehicle transversal plane. The most common case is relative headwind, which makes $\text{sign}(v_{Relx}) = -1$, which makes $F_{air,x} < 0$ and $R_{air,x} = \frac{c_d \cdot \rho \cdot A_{front}}{2} \cdot v_{Relx}^2 > 0$. The $v_{Relx} = v_x - v_{wind,x}$.

Typical values of drag coefficients (c_d) for cars can be found in 1.11.1 and sources such as: (Robert Bosch GmbH, 2004), (Barnard R. , 2010), (Hucho, 1998), and (Schuetz, 2015). These coefficients are derived from coast down tests, wind tunnel tests or CFD (Computational Fluid Dynamics) calculations. The air resistance can often be neglected for city speeds, but not at highway speeds. It should be noted that the c_d varies with the angle of the wind relative to the vehicle; the wind yaw angle typically leads to larger c_d and higher energy consumption, see 2.9.3.

2.9.1.1.1 Wind influence when varying road direction

Contribution from Carl Emvin, Chalmers.VehDyn

If we know the wind magnitude and wind direction but the road direction is unknown, it is reasonable to assume that the wind direction in road coordinates varies stochastically uniformly over all possible directions: $\varphi_{wzr} = U[-\pi, +\pi]$, e.g. if driving in a network of roads. With given wind velocity magnitude $|v_w|$ and given (vehicle-) longitudinal vehicle velocity component v_{vxv}:

$$R_{air,x} = -\frac{c_d \cdot \rho \cdot A_{front}}{2} \cdot v_{Relx}^2 \cdot \text{sign}(v_{Relx});$$

$$v_{Relx} = v_{wxv} = v_{vxv} - |v_w| \cdot \cos(\varphi_{wzr}); \quad where\ \varphi_{wzr} = U[-\pi, +\pi]$$

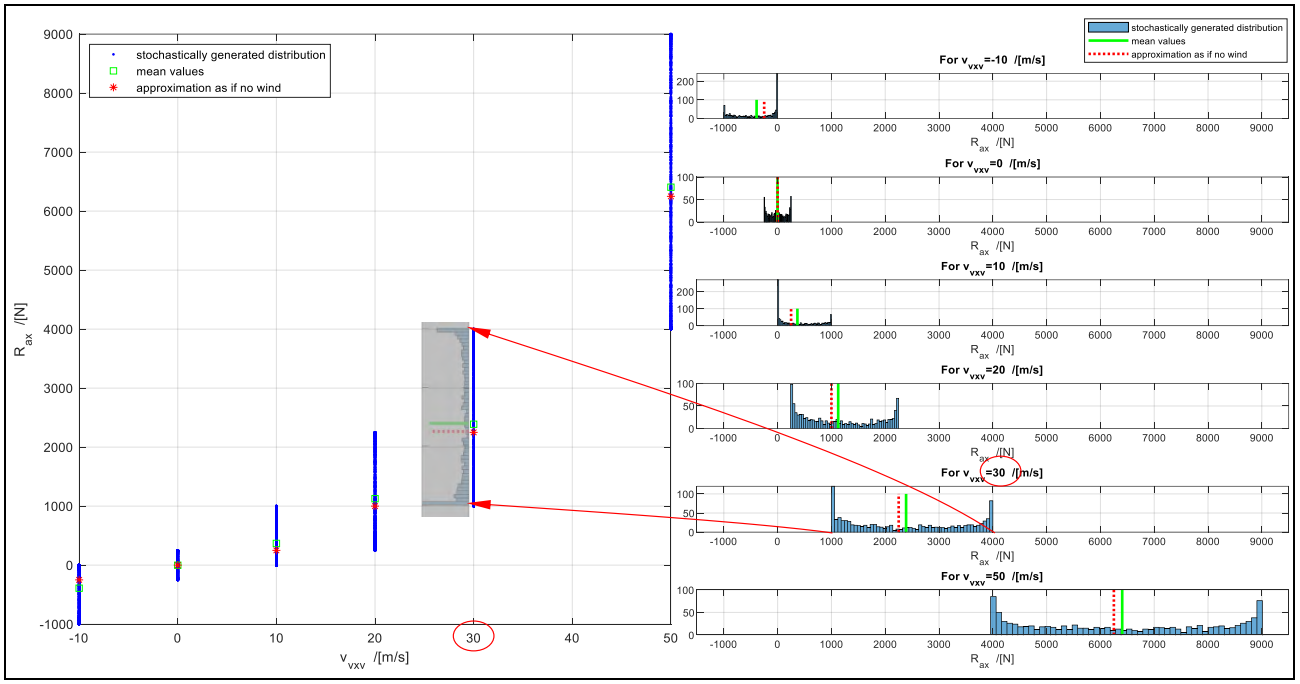


Figure 2-143: $R_{air,x}$ distributions for $v_{vxv} = \{-10\ 0\ 10\ 20\ 30\ 50\}\ [m/s]$ for a typical heavy vehicle. Magnitude of wind velocity vector is constant 10 $[m/s]$. Green is the mean value (of 1000 stochastically generated sample directions). Red is the value if neglecting wind, which is an unsuitable assumption, wrongly motivated with that direction is uniformly distributed $\varphi_{wzr} = U[-\pi, +\pi]$, with mean value zero.

So, the mean of wind velocity vector is zero, but the correct mean value of resistance force $R_{air,x}$ (green in figure) is larger than if we neglect wind (red in figure). Note that the energy consumption becomes consistently underestimated (if $v_{vxv} > 0$).

2.9.1.1.2 Wind influence when wind magnitude varies

Contribution from Carl Emvin, Chalmers.VehDyn

If we know the wind magnitude, wind direction, and the road direction, we can calculate a constant φ_{wzr} along the route. Then the stochastic effect from 2.9.1.1.1 vanish. However, wind velocity vector does vary and stochastic parameters for this can be provided to a vehicle for functions such as "residual range prediction" and "predictive cruise".

There is no well-established standard for which stochastic parameters can be provided but let us assume that wind direction is known and constant while wind magnitude is varying stochastically uniformly as $|v_w| = U(v_{wMin}, v_{wMax})$, where $v_{wMax} \geq v_{wMax} \geq 0$.

$$R_{air,x} = -\frac{c_d \cdot \rho \cdot A_{front}}{2} \cdot v_{Relx}^2 \cdot \text{sign}(v_{Relx});$$

$$v_{Relx} = v_{wxv} = v_{vxv} - |v_w| \cdot \cos(\varphi_{wzr});$$

$$where\ |v_w| = U(v_{wMin}, v_{wMax}); \quad where\ v_{wMax} \geq v_{wMax} \geq 0$$

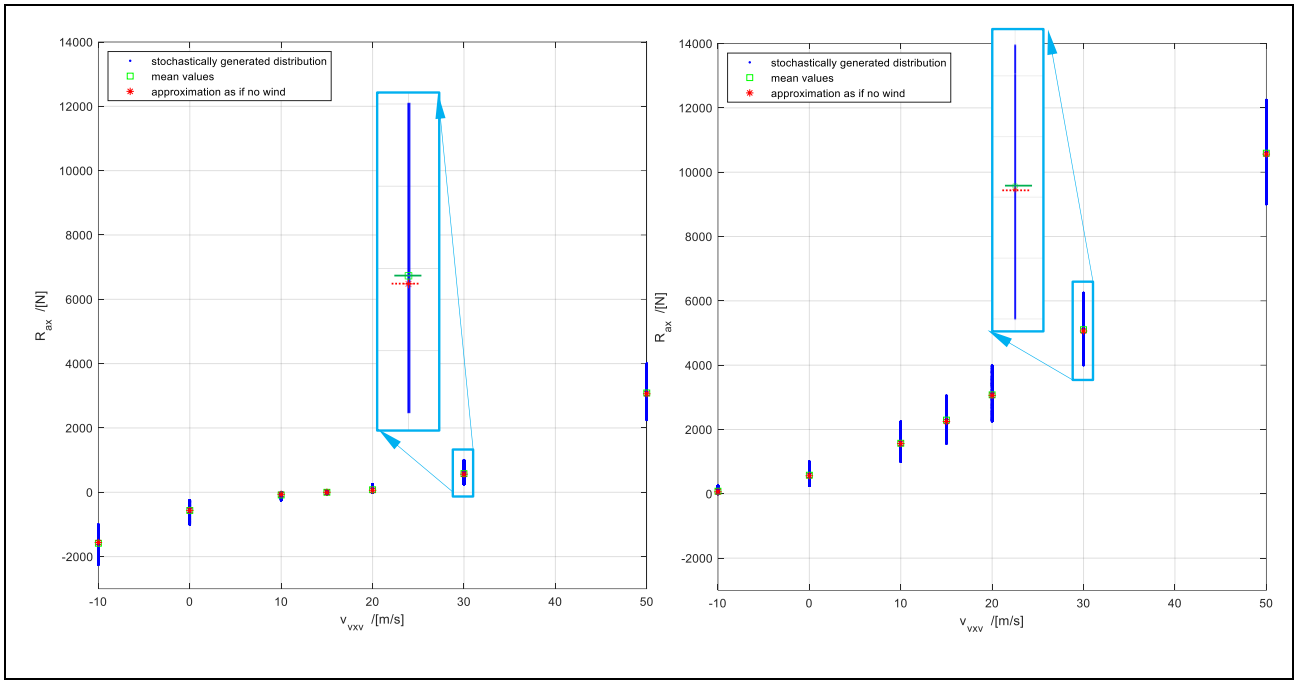


Figure 2-144: $R_{air,x}$ distributions for different v_{vxv} for a typical heavy vehicle. Magnitude of wind velocity vector is uniformly distributed $|v_w| = U(v_{wMin}, v_{wMax}) = U(10,20)$. Left: Tailwind. Right: Headwind. Green is the mean value (of 1000 stochastically generated sample directions). Red is the value if using mean wind magnitude, which is an unsuitable assumption, forgetting that the non-linear transformation of the stochastic variation from $|v_w|$ to $R_{air,x}$.

So, the mean of wind velocity vector is zero, but the correct mean value of resistance force $R_{air,x}$ (green in figure) is larger than if we neglect wind magnitude variation (red in figure). Note that the energy consumption becomes consistently underestimated (if $v_{vxv} > 0$), here as in 2.9.1.1.1.

2.9.1.2 Vertical and pitch from aerodynamics

Since a car structure moving through the air is not unlike an aircraft wing, there are also an aerodynamic lift force and pitch moment. This affects the vertical forces on front and rear axle, and consequently the tyre to road grip. Hence, it affects the lateral stability.

$$F_{air,z} = \frac{c_l \cdot \rho \cdot A_{front}}{2} \cdot v_{Relx}^2; \qquad M_{air,y} = \frac{c_{pm} \cdot L \cdot \rho \cdot A_{front}}{2} \cdot v_{Relx}^2 \cdot \text{sign}(v_{Relx}^2); \qquad [2.92]$$

The coefficient c_l represents the lift characteristics of the vehicle. For extreme vehicle, such as racing cars, one can achieve negative c_l, but often by sacrificing with higher c_d. The forces $F_{air,x}$ and $F_{air,z}$ are assumed to act through the same reference point, often centre of gravity (CoG), which defines $M_{air,y}$.

One can replace $[F_{air,x}, F_{air,z}, M_{air,y}]$ with equivalent $[F_{air,x}, F_{air,fz,CoG}, F_{air,rz,CoG}]$ or $[F_{air,x}, F_{air,fz}, F_{air,rz}]$, Figure 2-142 and Eq [2.93].

$$F_{air,fz} = \frac{c_{lf} \cdot \rho \cdot A_{front}}{2} \cdot v_{Relx}^2; \qquad F_{air,rz} = \frac{c_{lr} \cdot \rho \cdot A_{front}}{2} \cdot v_{Relx}^2; \qquad [2.93]$$

For a reference height h_{air}, often $h_{air} = 0$

For a given vehicle, the values of $\{c_{lf}, c_{lr}\}$ are dependent of reference point height, see Figure 2-142.

2.9.2 Lateral relative wind velocity

When the wind comes from the side, there can be direct influences on the vehicle lateral dynamics. Especially sensitive are long but light vehicles (such as buses or vehicles with unloaded trailers). The problem can be emphasized by sudden winds (e.g. on bridges or exiting a forested area). Besides direct effects on the vehicle lateral motion, side-winds can also disturb the driver through disturbances in the steering wheel feel. Similar expressions to the longitudinal loads are derived for lateral forces and from side-winds.

$$|F_{air,y}| = \frac{c_s \cdot \rho \cdot A}{2} \cdot v_{Rel}^2;$$
$$|M_{air,z}| = \frac{c_{ym} \cdot \rho \cdot A \cdot L}{2} \cdot v_{Rel}^2; \qquad [2.94]$$

Normally, reference area A is frontal projected area and reference length L is the wheelbase for two axle vehicles. Also note that the reference velocity v_{Rel} is normally the longitudinal component of the relative velocity v_{Relx}. In most situations we have wind from an angle which leads to simultaneous longitudinal and lateral relative velocity, see 2.9.3.

2.9.3 Simultaneous longitudinal and lateral relative wind

2.9.3.1 Sign change of relative wind components

The above coefficients $c_d, c_l, c_{pm}, c_{lf}, c_{lr}$ are normally measured or computed for negative v_{Relx}, i.e. negative relative headwind ($v_{Relx} < 0$). For positive relative tailwind ($v_{Relx} > 0$), these coefficients get other numerical values due to absence of symmetry in vehicle body shape across an xy-plane. So, these coefficients are functions of sign(v_{Relx}).

The coefficients c_s, c_{ym} are typically more independent of sign(v_{Relx}) > 0 due to approximate symmetriy in vehicle body shape across an xz-plane.

Some of the equations above in 2.9 are selected to include "sign(⋯)". The corresponding c coefficiencts typically, thereby, retain their (positive) sign. In the other equations, the corresponding c coefficiencts may or may not change sign.

2.9.3.2 Varying relative wind yaw angle

The coefficients $c_d, c_l, c_{pm}, c_{lf}, c_{lr}$ are not only depending of sign(v_{Relx}), as mentioned in 2.9.3, but also $v_{y,rel}$ or relative wind yaw angle $\varphi_{Relz} = \arctan2(v_{Rely}, v_{Relx}) = \arctan2(v_{Wind,y}, v_{Relx})$.

The coefficients c_s, c_{ym} are almost independent of sign(v_{Rely}) but they still vary with relative wind yaw angle φ_{Relz}.

The aerodynamic coefficients can be mapped to represent the influence from wind yaw angle $\varphi_{air,z,rel}$ in different ways, which lead to different formulas for $F_{air,x}, F_{air,y}, F_{air,z}, M_{air,x}, M_{air,y}, M_{air,z}$. It is therefore important to know how the mapping is done before using such a formula in the vehicle dynamics model. The two following bullets shows two examples of models for $F_{air,x} = -R_{air,x}$. The 1st way is well-established in the vehicle aerodynamics community while the 2nd is more general aerodynamics (used in (Askerdal, 2023)).

- $R_{ax} = 0.5 \cdot \rho \cdot A_{front} \cdot c_{df}(\varphi_{Relz}) \cdot {v_{Relx}}^2;$
  where $v_{Relx} = v_x - v_{wind,x}$; *and* $\varphi_{Relz} = \arctan2(v_{Rely}, v_{Relx}) = \arctan2(v_{wind,y}, v_{Relx})$;
- $R_{ax} = R_{axy} \cdot \cos(\varphi_{Relz})$;
  $R_{axy} = |\vec{R}_a| = 0.5 \cdot \rho \cdot A_{Proj}(\varphi_{Relz}) \cdot c_{Proj}(\varphi_{Relz}) \cdot v_{Relxy}^2;$

$$where\ A_{Proj}(\varphi_{Relz}) = A_{front} \cdot |\cos(\varphi_{Relz})| + A_{side} \cdot |\sin(\varphi_{Relz})|;$$

The two aerodynamic drag coefficients c_{df} and c_{Proj} are different, but related via that they should give the same force R_{ax}:

$$0.5 \cdot \rho \cdot A_{front} \cdot c_{df}(\varphi_{Relz}) \cdot {v_{Relx}}^2 = R_{axy} \cdot \cos(\varphi_{Relz});\ \Rightarrow$$

$$\Rightarrow\ 0.5 \cdot \rho \cdot A_{front} \cdot c_{df}(\varphi_{Relz}) \cdot {v_{Relx}}^2 = 0.5 \cdot \rho \cdot A_{Proj}(\varphi_{Relz}) \cdot c_{Proj}(\varphi_{Relz}) \cdot \left(v_{Relx}^2 + v_{Rely}^2\right) \cdot \cos(\varphi_{Relz});\ \Rightarrow$$

$$\Rightarrow\ A_{front} \cdot c_{df}(\varphi_{Relz}) \cdot {v_{Relx}}^2 = \left(A_{front} \cdot |\cos(\varphi_{Relz})| + A_{side} \cdot |\sin(\varphi_{Relz})|\right) \cdot c_{Proj}(\varphi_{Relz}) \cdot \left(v_{Relx}^2 + v_{Rely}^2\right) \cdot \cos(\varphi_{Relz});\ \Rightarrow$$

$$\Rightarrow\ c_{Proj}(\varphi_{Relz}) = \frac{c_{df}(\varphi_{Relz})}{\left(|\cos(\varphi_{Relz})| + \frac{A_{side}}{A_{front}} \cdot |\sin(\varphi_{Relz})|\right) \cdot \cos(\varphi_{Relz})} \cdot \frac{1}{1 + \left(\frac{v_{Rely}}{v_{Relx}}\right)^2} = \frac{c_{df}(\varphi_{Relz})}{\left(|\cos(\varphi_{Relz})| + \frac{A_{side}}{A_{front}} \cdot |\sin(\varphi_{Relz})|\right) \cdot \cos(\varphi_{Relz})} \cdot \frac{1}{1 + \tan^2(\varphi_{Relz})};$$

(Askerdal, 2023)Decompose aerodynamic forces on each unit in an articulated vehicle

A special effect for articulated vehicles (car with caravan, tractor with semi-trailer, etc.) is that there are reasons to decompose the wind force and moment components, or the aerodynamic coefficients, to one for each vehicle unit. This is especially important for lateral force and yaw moment, see Figure 2-146.

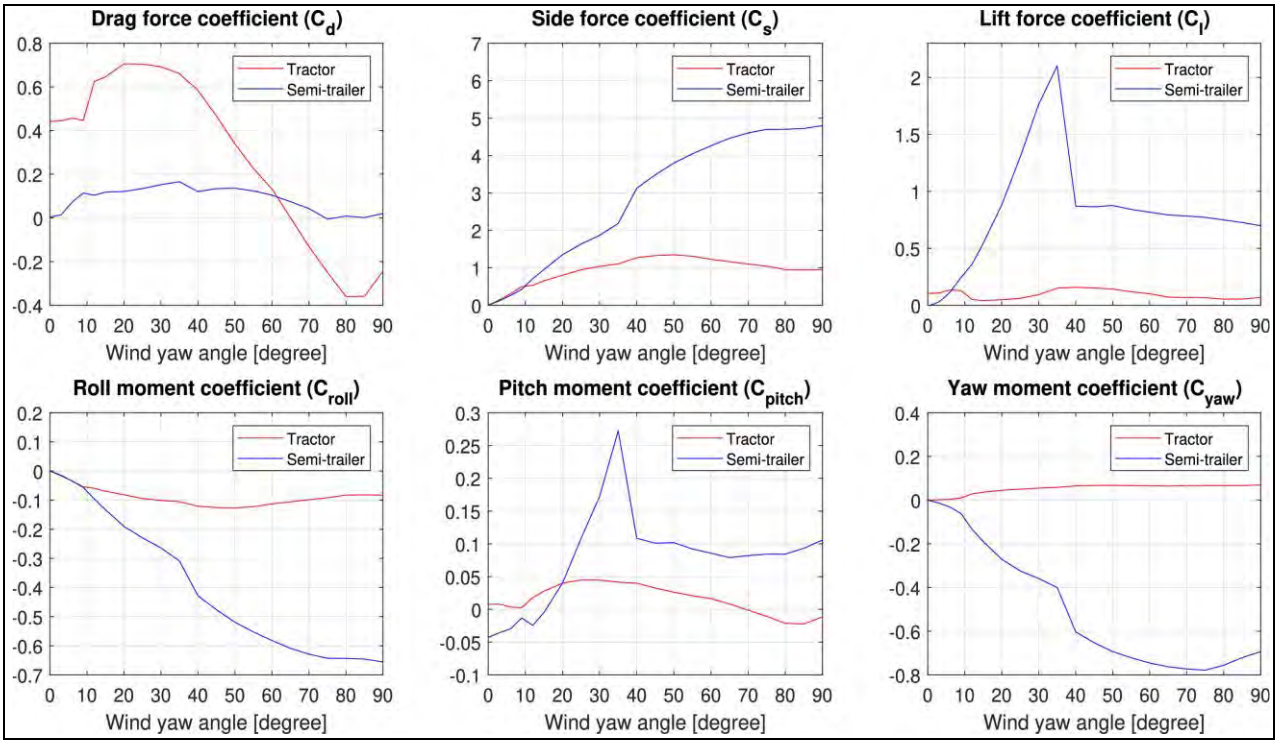


Figure 2-146: Decomposition of aerodynamic coefficients on each vehicle unit for a tractor with a semitrailer. From (Sivaramakrishnan, o.a., 2023).

2.9.3.4 Transient wind variations

Note that the equations still assume steady-state conditions for the aerodynamics; if wind direction relative to vehicle changes quickly (by changing wind direction or yawing vehicle vs ground), there can be transients, which is warned for, but not covered, in this book.

2.10 Driving and transport application

The driver drives and experiences the vehicle in the short time scale through pedals, steering wheel and seat. But the load (cargo weight and position) and choice of route is important on the longer time scale. One can differ between, Ref (Pettersson, 2019):

- ***Transport Application*** is how the vehicle is used by one user/owner during the vehicle's lifetime. It can be commuting 2 × 15 km/day, 5 days/week (e.g. for passenger car) or loading and transporting timber on 10 km forest road + 300 km highway, twice per day (e.g. for a truck). Transport application is important when developing and selling/buying, where one aims at minimizing TCO (Total Cost of Ownership).
- ***Transport Operation*** is how the vehicle is used along a specific route. It is typically 10 min to 10 h driving. Driving Cycles and Operating Cycles in 3.3.1.1 have the purpose to describe (model) the transport operation, except the vehicle and driver.
  Transport Operation is important when operating transports, where one aims at minimizing TCOP (Total Cost of OPeration) or TCOC (Total Cost of Operating Cycle).

2.10.1Mission, Road and Traffic

This section is kept very short, but it is included for completeness, beside 2.10.2. See more in 3.3.1.

2.10.2Driver

To study how different vehicle designs work in a vehicle operation, a driver model is needed. In its easiest form, a driver model can be steering wheel angle $\delta_{stw} \equiv 0$; or $\delta_{stw} = \hat{\delta} \cdot \sin(\omega \cdot t)$;. Another extreme interpretation of what can be called a driver model is an implicit/inverse statement, like "driver will push accelerator pedal so that speed $v_x \equiv 20\ [m/s]$ during the manouvre", which leads to that accelerator pedal position becomes an output, as opposed to input, to the vehicle model. Beyond those very extreme driver models, there is often need for a driver model which react on vehicle states **in relation to an environment or traffic**. In this section, driver models are primarily thought of as models of the driver of the subject vehicle, but when modelling surrounding traffic carefully, each object vehicle can also use a driver model.

The driver interacts with the vehicle mainly through steering wheel, accelerator pedal and brake pedal. In addition to these, there are clutch pedal, gear stick/gear selector, and various buttons, etc., see Figure 2-147, but we focus here on the first 3 mentioned.

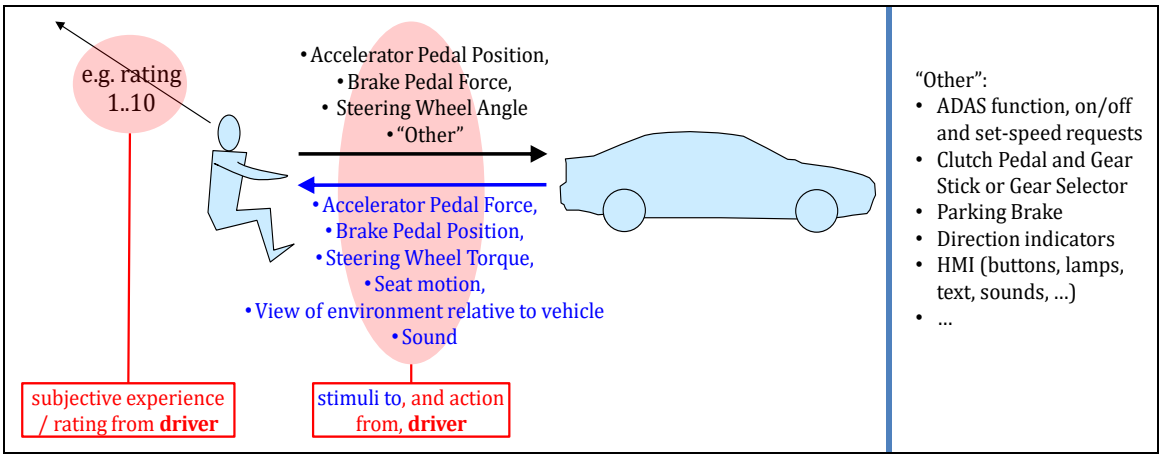


Figure 2-147: Interface of driver, and some commonly assumed causality.

Driver's control of vehicle dynamics, or vehicle motion including position, can be discussed in longitudinal (mainly pedals) and lateral (mainly steering wheel).

Driver reacts on several stimuli, such as motion (mainly through seat), sounds and optical. Among motion, it is primarily the translational accelerations (and their time derivative, jerk) that is sensed by the driver, but also rotational velocities can be sensed by humans. Among the optical, looming (optical expansion of an object in the driver's field of view $[deg/s]$) is often used as a cause for how driver uses the pedals. The optical flow (the pattern of apparent motion of objects, surfaces, and edges in the driver's field of view) is often used as a cause for highest comfortable speed and yaw velocity.

Driver models are here discussed as models of the "human driver" for use in vehicle verification simulations. However, driver models can also be understood as models of "virtual driver", and then they are actually implemented as algorithms in the vehicle product, e.g. as prediction algorithms or automated driving controllers. In the first context, it is often important to vary the driver model (at least its parameters, maybe even its equations) for robustness, as mentioned in Figure 1-9. In the latter context, the driver model of the subject vehicle is rather varied for optimization, see Figure 1-9 again.

An important aspect of driver modelling is how the user (driver or occupant) **experiences** the vehicle. This is often referred to as subjective rating, but for some cases one can establish methods to objectively calculate a measure of how good or bad the experience is. The measure can sometimes be a physical quantity but often it has to be a rating or grading without unit. Examples are "driveability [rating 0-10, high is good]", "steering effort [deg/s, low is good]" and "ride comfort [m/s^2, low is good]", see Figure 1-74.

2.10.2.1 Driver Modelling

As in all modelling, it is important to model, or select model, after what the model should be used for. Driver modelling for "**verification of vehicle functions**" and for implementation in "**driving automation functions**" are similar in that they should react on the vehicle's environment, but there are also differences. Driver models for verification of vehicle functions should be as human-like as possible. They should also judge feedback to driver, such as assessing steering effort. Driver models for use in driving automation functions should also be human-like to facilitate cooperation between human and automated driving, such as hand-over/take-back or simultaneous control. However, there are also reasons to not mimic all aspects from a human driver, such as the human's inability to watch in several directions simultaneously.

A categorization of modelling concept is whether the model uses equations that intend to reflect the **biological** processes human's perception, cognition and neuro-muscular or equations from a **vehicle model**. The first concept (exemplified in 2.10.2.3.3) would rather use angle to obstacle as opposed to distance to obstacle, since humans rather see angles than distances. The latter concept (exemplified in 2.10.2.2.1) assumes that driver has adapted to the specific vehicle and (subconsciously) operates the vehicle in a kind of inverse model thinking. Overall, both concepts can reflect approximately the same driving, but they are differently parameterized; typically, in biological parameters and vehicle parameters, respectively.

Driver can be modelled in 2 parts: Strategic and Operative. A division in Longitudinal and Lateral is also relevant. One can think of different ways of arranging these dimensions on each other; one possible way is shown in Figure 2-148.

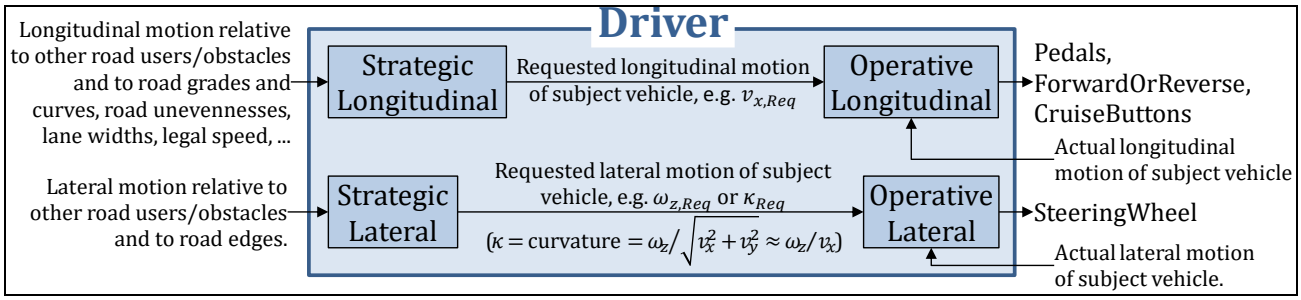


Figure 2-148: One possible arrangement of Strategic vs Operative and Longitudinal and Lateral.

2.10.2.2 Longitudinal Driver Models

Each pedal has both pedal position and pedal force as communication channels to the driver.

In broad terms, the accelerator pedal position is interpreted by a control system as a certain requested engine torque, which means a certain wheel shaft torque on the propelled axle/axles. In some advanced solutions, one could think of using accelerator pedal force as a feedback channel from vehicle to driver.

In broad terms, the brake pedal force gives a certain friction brake torque application on each axle. In some advanced solutions, one could think of changing brake pedal position versus force characteristics as a feedback channel from vehicle to driver. But already with traditional (hydraulic) brake systems for passenger cars, the brake pedal gives a feedback to driver in that ABS interventions are felt.

For electric and hybrid vehicles, the brake pedal can typically influence the propulsion system as well, in that at low levels of pedal braking, the electric propulsion motors give negative wheel shaft torque. This is for regenerating energy. Regenerative braking can even be engaged at low levels of accelerator pedal position.

A model of how the driver operates the pedals is called a longitudinal driver model. But different manoeuvres call for different driver models. Examples of manoeuvres/situations are:

- Full acceleration or deceleration, including driver delays
- Keep constant speed
- Keep distance to lead vehicle
- When a cut-in happens in front of object vehicle: Expand to comfortable/safe gap
- Approach slower object vehicle from behind: Reduce to comfortable/safe gap
- Longitudinal speed control during overtaking
- Longitudinal speed control to stand-still

2.10.2.2.1 Example of Longitudinal Driver Model

An example for approaching a slower vehicle from behind is defined through simple kinematic relations and some assumptions, which indicates how to calculate the required (constant) acceleration to reach a certain safe gap. The safe gap can be defined by “gap needed to exactly avoid collision if braking as object vehicle but with a certain reaction time”. In traffic schools, one is often taught that safe time gap STG is $STG = 3\ [s]$, as a rule of thumb. In Eq, it is shown how such a model is derived, subscripts: *s=subject, o=object, 0=present, p=predicted*. The requested acceleration a_{req} just have to be converted to pedal force or position.

Prediction, of object and subject:

$$s_{op} = s_{o0} + v_o \cdot t_p; \text{ (object vehicle assumed to not accelerate)}$$

$$v_{sp} = v_{s0} + a_{req} \cdot t_p;$$

$$s_{sp} = s_{s0} + v_{s0} \cdot t_p + a_{req} \cdot t_p^2/2;$$

Requirement on prediction at t_p:

$$s_{op} - s_{sp} = (s_o - s_s)_{safe} = v_o \cdot SafeTimeGap = v_o \cdot STG;$$

$$v_{sp} = v_o;$$

Solve for a_{req} and t_p gives the driver model on explicit form:

$$a_{req} = \frac{-(v_o - v_{s0})^2}{2 \cdot (s_{o0} - s_{s0} - STG \cdot v_o)};$$

$$t_p = \frac{2 \cdot (s_{s0} - s_{o0} + STG \cdot v_o)}{v_o - v_{s0}};$$

Use only if $t_p > 0$, else "prediction" happens in passed time.

[2.95]

Examples of applying the driver model in above Eq is shown in Figure below, where also a general PVA-time-diagrams (PVA=position, velocity, acceleration) is shown. PVA-time-diagrams are often useful when studying vehicle operations with other moving objects. Different scenarios can be tested, and driver models can be derived using simple formulas, such as constant speed and constant acceleration.

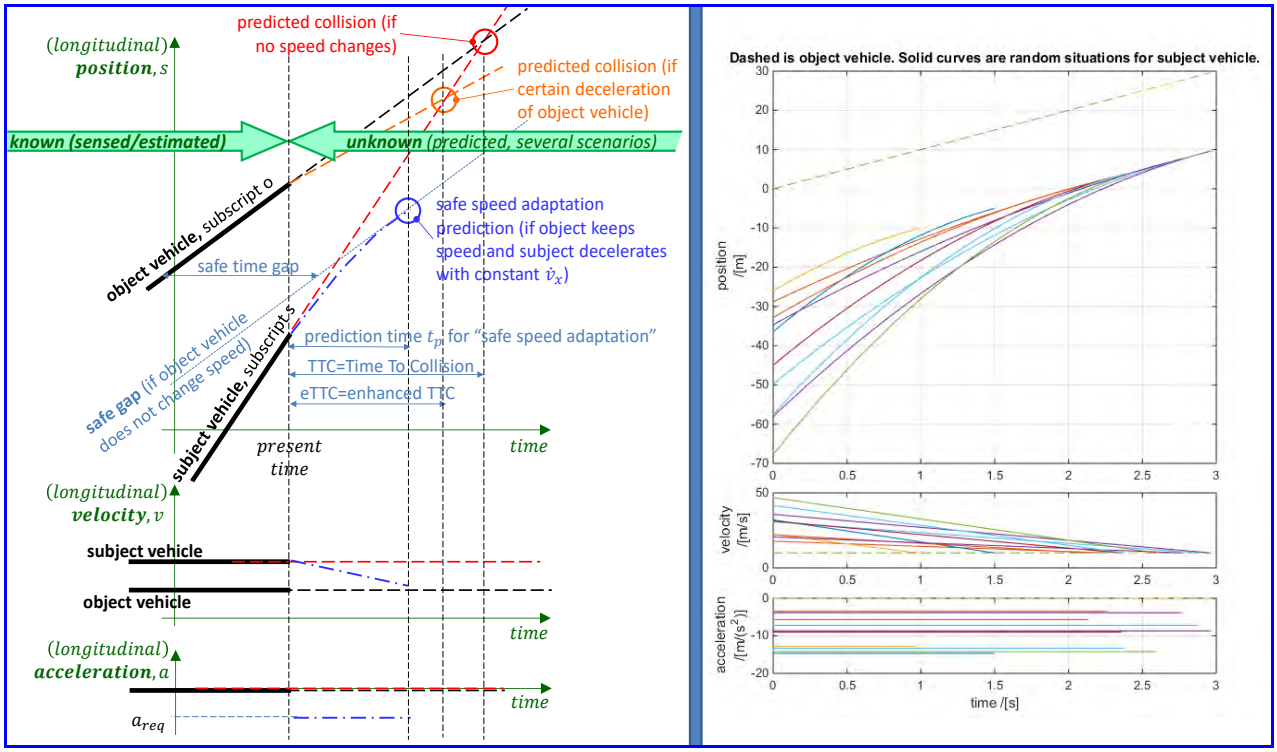


Figure 2-149: Left: PVA-time-diagrams (PVA=position, velocity, acceleration) for studying longitudinal interaction with an object vehicle ahead. Right: PVA diagram for the driver model in Eq above using $SafeTimeGap = 2\ [s]$ and some randomly selected s_{s0} and v_{v0}.

2.10.2.3 Lateral Driver Models

2.10.2.3.1 Causality of Steering Wheel Angle and Torque

The driver interacts with steering wheel through two channels, steering wheel angle and steering wheel torque. The angles of the road wheels are functions of steering wheel angle, almost independent of forces and torques in the steering system. Further, the steering wheel torque is a function of the lateral force on the front axle, reduced with assistance from the power steering or steering servo, but almost independent of the angles.

A frequently used model is that the driver decides a steering wheel angle and expects a certain steering wheel torque, T_{sw}, feedback. Only in very driver-active steering situations, the causality is modelled the other way, e.g. studying what happens if driver takes hands-off, i.e. steering wheel torque =0. It can be that driver uses the effect that steering system returns to $\delta = 0$ without driver torque after a quick step steering by driver.

2.10.2.3.2 Steering Wheel Angle Driver Models

How driver operates the steering wheel can also be called a lateral driver model. But different manoeuvres call for different driver models. Examples of manoeuvres/situations are:

- Going into curve from straight and vice versa
- Turning in intersection
- Avoidance manoeuvre
- Stabilizing vehicle when sudden lose yaw stability, e.g. in curve
- Compensating road unevenness which cause lateral disturbance
- Lateral speed control during overtaking

2.10.2.3.3 Example of Steering Wheel Angle Driver Model Based on Biology

An example of a driver model is the Salvucci and Gray model in Figure and Eq below. It is motivated from human's biological cognition. The steering wheel angle is denoted δ_{stw}.

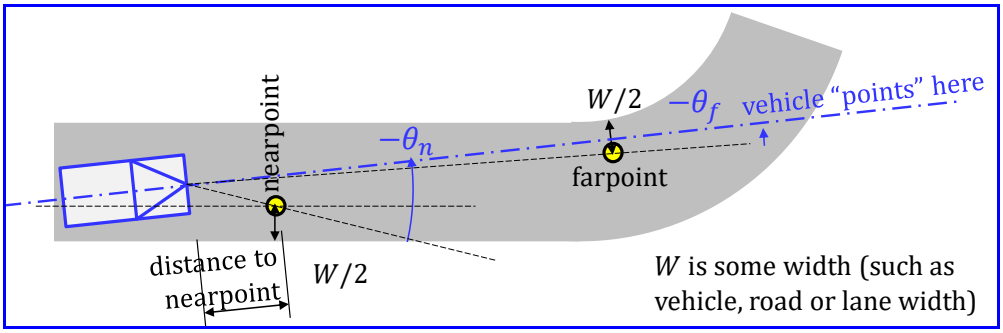


Figure 2-150: Salvucci and Gray model for how driver steers.

$$\dot{\delta}_{stw} = k_f \cdot \dot{\theta}_f + k_n \cdot \dot{\theta}_n + k_I \cdot \theta_n; \;\Leftrightarrow$$

$$\Leftrightarrow \; \delta_{stw}(t) = \delta_{stw}(t_0) + k_f \cdot \theta_f(t) + k_n \cdot \theta_n(t) + k_I \cdot \int_{t_0}^{t} \theta_n(t_0..t) \cdot dt \,; \qquad [2.96]$$

It is not well defined in figure above what it means that vehicle "points". It can be either vehicle heading or vehicle course angle. Probably, the course angle, is most motivated to use. The course angle is different for different points in the vehicle, so one might need to define also a "mind-point" in the vehicle. In many cases the mind-point is the position of the driver.

The 3 k parameters that have to be tuned to certain driver, vehicle and operation. Additionally, the distance to aim-points needs to be tuned, such as if there should be extra margins on top of $W/2$ and whether W is vehicle, road or lane width. Further on, all these assumptions can change during a simulation, e.g. as driving on a windy country road and suddenly a meeting vehicle shows up might

make the far point jump. So, even if the model equation appears simple, it is far from obvious how to tune and use it. Hence, there are variants of it which has only one aim-point. We will refer to the reduced model, with only one aim-point:

$$\dot{\delta}_{stw} = k_a \cdot \dot{\theta} + k_I \cdot \theta; \quad \Leftrightarrow$$
$$\Leftrightarrow \quad \delta_{stw}(t) = \delta_{stw}(t_0) + k_a \cdot \theta(t) + k_I \cdot \int_{t_0}^{t} \theta_n(t_0..t) \cdot dt\,; \qquad [2.97]$$

This kind of model is fed with variables from the vehicle and environment states. A drawback is that the dynamic vehicle behaviour is built into the k parameters, meaning that if vehicle dynamics is changed, e.g. adding a trailer or reducing road friction, the k parameters reasonable have to be re-tuned. If identifying the k parameters as physical parameters, using a dynamic vehicle model, one can reduce the need for such re-tuning.

Above driver model can be categorized as having “look ahead”. Simpler driver model can be based on only where the vehicle is at present time, such as present lateral position in lane. More advanced driver models use a dynamic model for prediction. The vehicle dynamics model is especially needed in predicting models.

3 LONGITUDINAL DYNAMICS

3.1 Introduction

The primary purpose of a vehicle is transportation, which requires longitudinal dynamics. The chapter is organised with one group of functions in each section as follows:

- 3.2 Steady state function
- 3.3 Functions for
- 3.4 Functions in (shorter) events
- 3.5 Control Functions

3.1.1 References for This Chapter

- 2.4 Propulsion and *"Chapter 23. Driveline"* in Ref (Ploechl, 2013)
- *"Chapter 24. Brake System Dynamics"* in Ref (Ploechl, 2013)
- *"Chapter 27 Basics of Longitudinal and Lateral Vehicle Dynamics"* in Ref (Ploechl, 2013)
- *"Chapter 6: Adaptive Cruise Control"* in Ref (Rajamani, 2012)

3.2 Steady state functions

Functions as top speed and grade-ability are relevant without defining a certain time period. For such functions, it is suitable to observe the vehicle in steady state, i.e. independent of time. Those functions are therefore called steady state functions, in this book. The main subsystems that influences here are the propulsion system, see 2.4, and the (Friction) Brake system, see 2.4.7.

3.2.1 Traction diagram

The force generated in the prime mover is transmitted through a mechanical transmission to the wheel which then generates the propulsive forces in the contact patch between tyre and road. In an electric in-wheel motor, the transmission can be as simple as a single-step gear. In a conventional vehicle, it is a stepped transmission with several gear ratios (i.e. a gearbox). Then, the drivetrain can be drawn as in Figure 3-1. The torque and rotational speed of the engine is transformed into force and velocity curves via the mechanical drivetrain and driven wheel. The result is a Traction diagram. The transformation follows the following formula, if losses are neglected:

$$F = ratio \cdot \frac{T}{WheelRadius}; \quad and \quad v = WheelRadius \cdot \frac{\omega}{ratio}; \qquad [3.1]$$

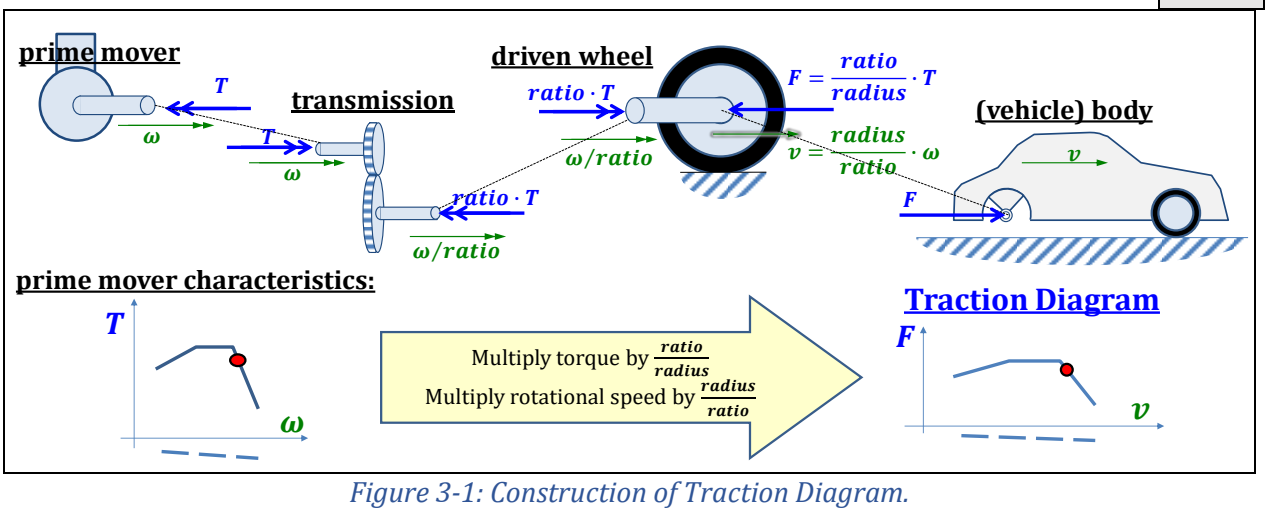


Figure 3-1: Construction of Traction Diagram.

A traction diagram for a truck is given in Figure 3-2, which also shows that there will be one curve for each gear.

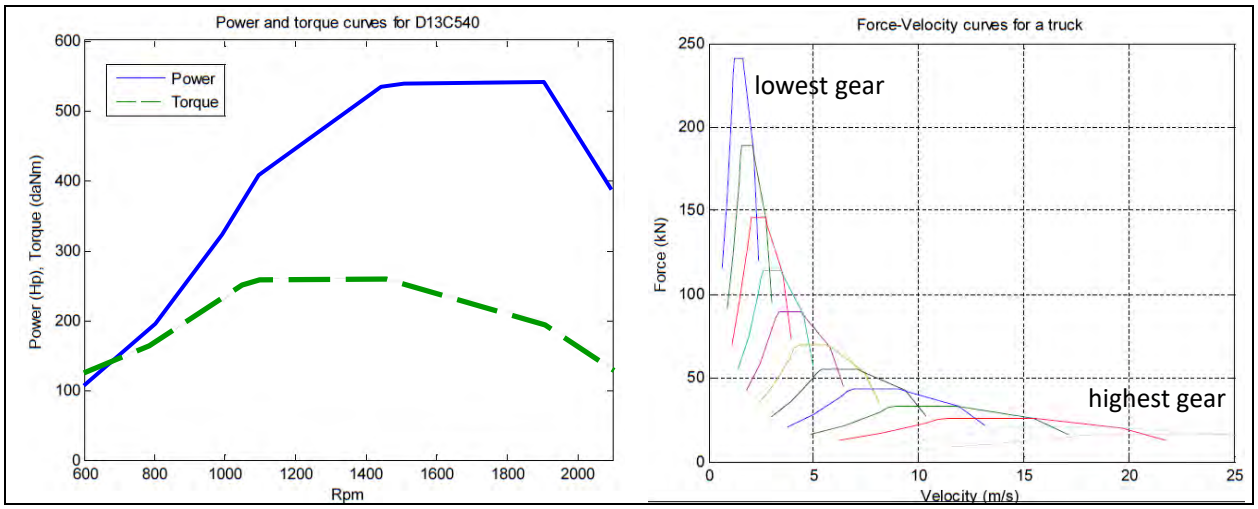


Figure 3-2: Example of engine map and corresponding traction diagram map from a truck. (D13C540 is an I6 diesel engine of 12.8-litre and 540 hp for heavy trucks.)

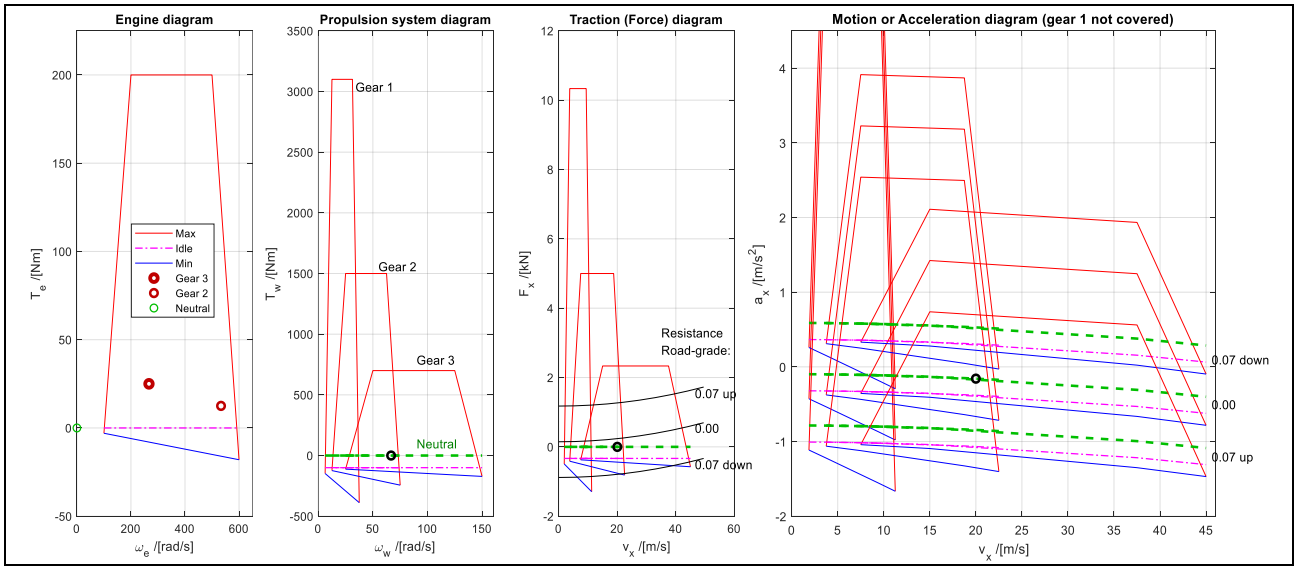


Figure 3-3: Relations between diagrams. The circle markers show alternative gears for one example of downhill operating point, where neutral gear is possible.

Losses in transmission can be included by loss models for transmission, such as:

$$F = \eta_T \cdot ratio \cdot \frac{T}{radius};\ where\ \eta_T \leq 1;$$

$$v = \eta_\omega \cdot radius \cdot \frac{\omega}{ratio};\ where\ \eta_\omega \leq 1;$$

$$where \quad \eta_T \cdot \eta_\omega = \eta_{total} = \frac{P_{vehicle}}{P_{engine}} = \frac{F \cdot v}{T \cdot \omega} \leq 1;$$

[3.2]

This will move the curves in the first quadrant downwards due to $\eta_T < 1$ and to the left due to $\eta_\omega < 1$. Tyre rolling friction is a torque loss mechanism, which on its own yields $\eta_\omega = 1$ and $\eta_T < 1$. Tyre longitudinal slip is a speed loss mechanism, which on its own yields $\eta_\omega < 1$ and $\eta_T = 1$. See 2.2.1.6. The multiplication with η is only demonstrative and should be seen more generic: in many cases the losses are additional instead of multiplicative, e.g. for rolling resistance: $F = ratio \cdot (T - \Delta T)/radius = ratio \cdot (T - f \cdot F_z)/radius$;. Which wheels' F_z to use is discussed in 3.2.2.

A traction diagram is a kind of "one degree of freedom graphical model". The traction diagram is on complete vehicle level, so the force axis represents the sum of forces from all wheels. This can include more than one propulsion system and also brakes.

3.2.1.1 Gear selection

<Gear selection for minimizing power losses (for saving energy) is also discussed in "3.2.2.3 Example with simple actuator coordination

We will now study the vehicle in Figure 3-5. In this example, we do neither include neutral gear nor the brake. This makes the actuator coordination as simple as possible: Only select gear.

The upper diagrams in Figure 3-6, Figure 3-7, Figure 3-8, Figure 3-9, Figure 3-10, and Figure 3-11 are traction diagrams:

- How the following 6 measures vary over the $\{v_x, F_x\}$:
  $P_{Loss}, \eta, PPS_{Loss}, P_{Storage} = P_{Cons}, PPS_{Storage}, CRPS_{Tot}$
  - For each "actuator coordination" ($Gear = 1$ and $Gear = 2$), because for many $\{v_x, F_x\}$, one can drive on either of the gears.
- The optimum values of these 6 measures. Were optimum means minimum of $P_{Loss}, PPS_{Loss}, P_{Storage} = P_{Cons}, PPS_{Storage}, CRPS_{Tot}$ and maximum of η.
- Also, the optimum actuator coordination (i.e. either $Gear = 1$ or $Gear = 2$) is shown.
- Electric machine model from Eq [2.88[2.88]
- Pseudo code for how the $CRPS_{TotOpt}$ diagram was plotted:

```
for v_x = v_x axis
  for F_x = F_x axis
    for Gear = [1 2] %Sweep the free actuator request Gear
      T_Em = ⋯; %The other actuator request T_Em fulfil the F_x
      CRPS_Tot = ⋯;
    end
    select the best CRPS_TotOpt = ⋯ and corresponding Gear_Opt = ⋯
  end
 end
 plot⋯;
```

Note:

- All the 6 measures give the same gear shifting curves, i.e. the same actuator coordination, i.e. the same best gear for a given $\{v_x, F_x\}$.
- These upper diagrams, especially $PPS_{Storage}(v_x, F_x)$, can be used to read out a function measure for "3.2.2.1 Energy consumption for constant operating conditions, with given speed *".
- It can also be used for momentaneous optimization, i.e. real-time computation during vehicle usage. A map, $Gear = map(v_x, F_x)$, independent of the driving resistance, can be pre-processed which strongly reduces the computational load.

The results are independent of the driving resistance. However, 3 examples of driving resistance curves are drawn in the traction diagrams. If we compute best measure (e.g. $CRPS_{Tot}$) along those curves, we get the diagrams in the bottom of each figure. The optimum is marked with a circle, and the circle ends up at different optimum v_x depending on which measure is optimized. These lower diagrams can be used to read out a function measure for "3.2.2.2 Energy consumption for constant operating conditions, with free speed *". It would make sense that the vehicle (or driver) selects a speed from the $CRPS_{Tot}$ diagram.

A more complex actuator coordination, which will be shown in 3.2.2.4. A map, $Gear = map(v_x, F_x)$, can be pre-processed which strongly reduces the computational load in real time.

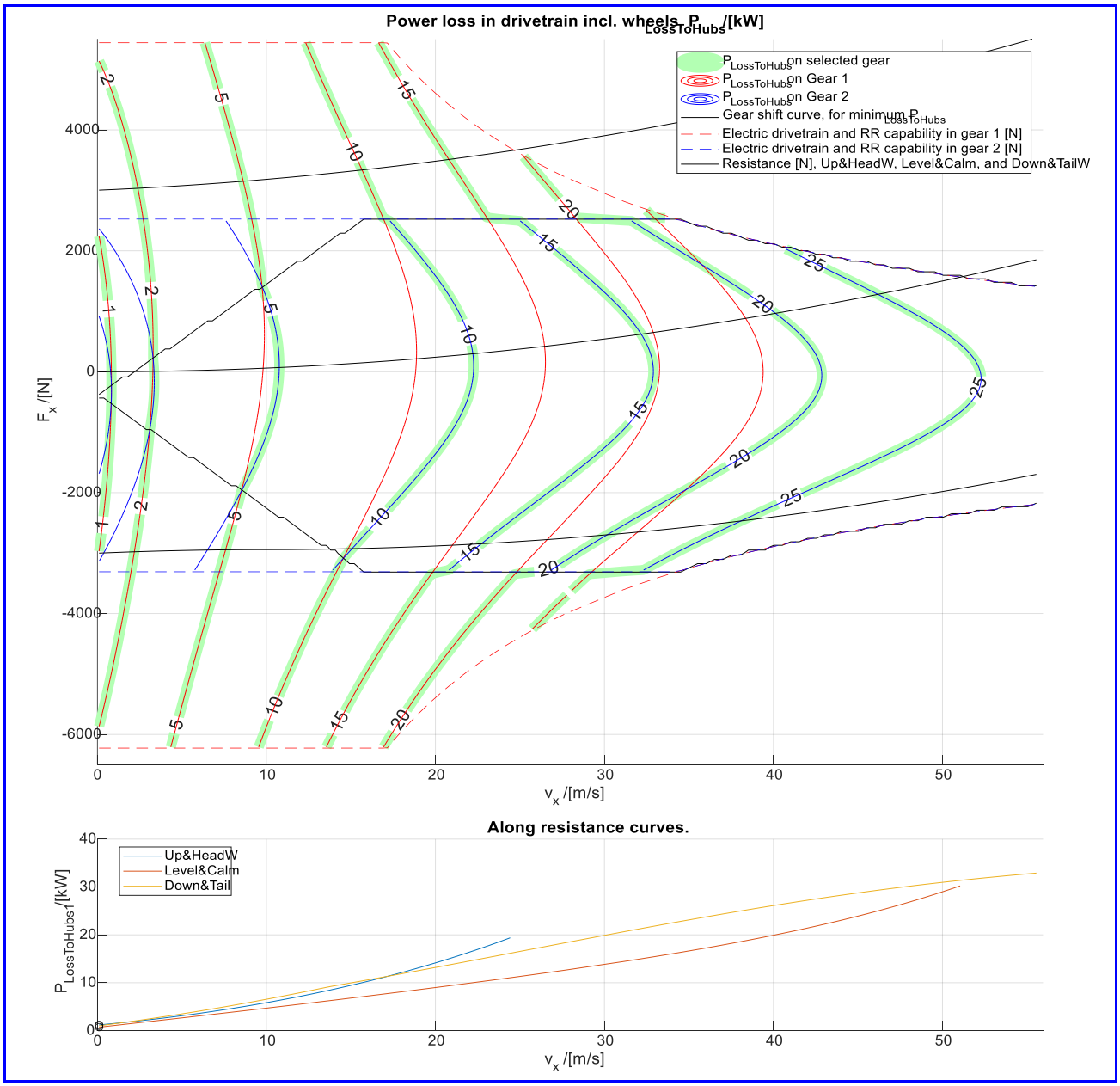


Figure 3-6: Select gear and speed through $min(P_{Loss})$.

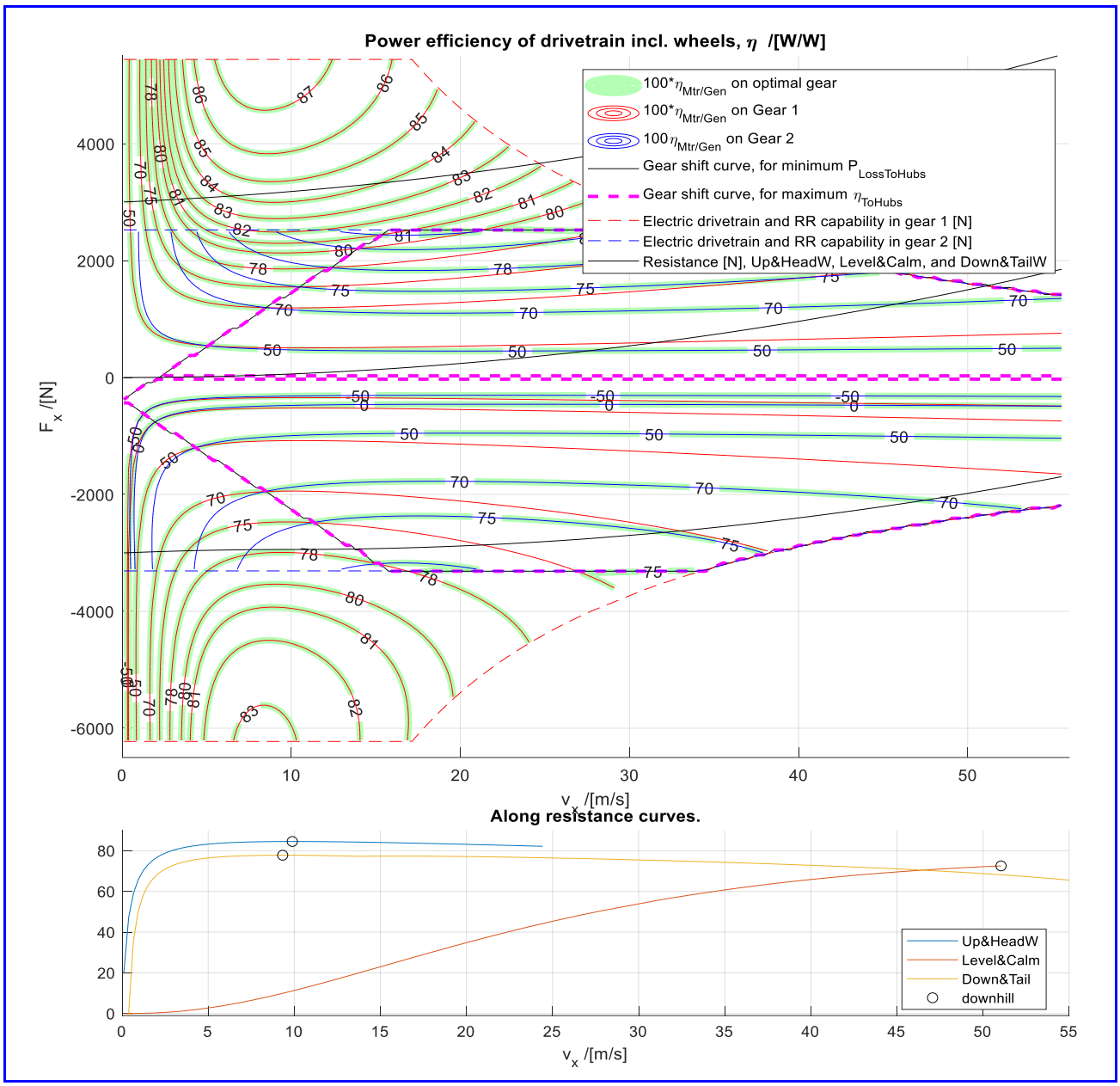


Figure 3-7: Select gear and speed through max($\eta_{DrivetrWheels}$).

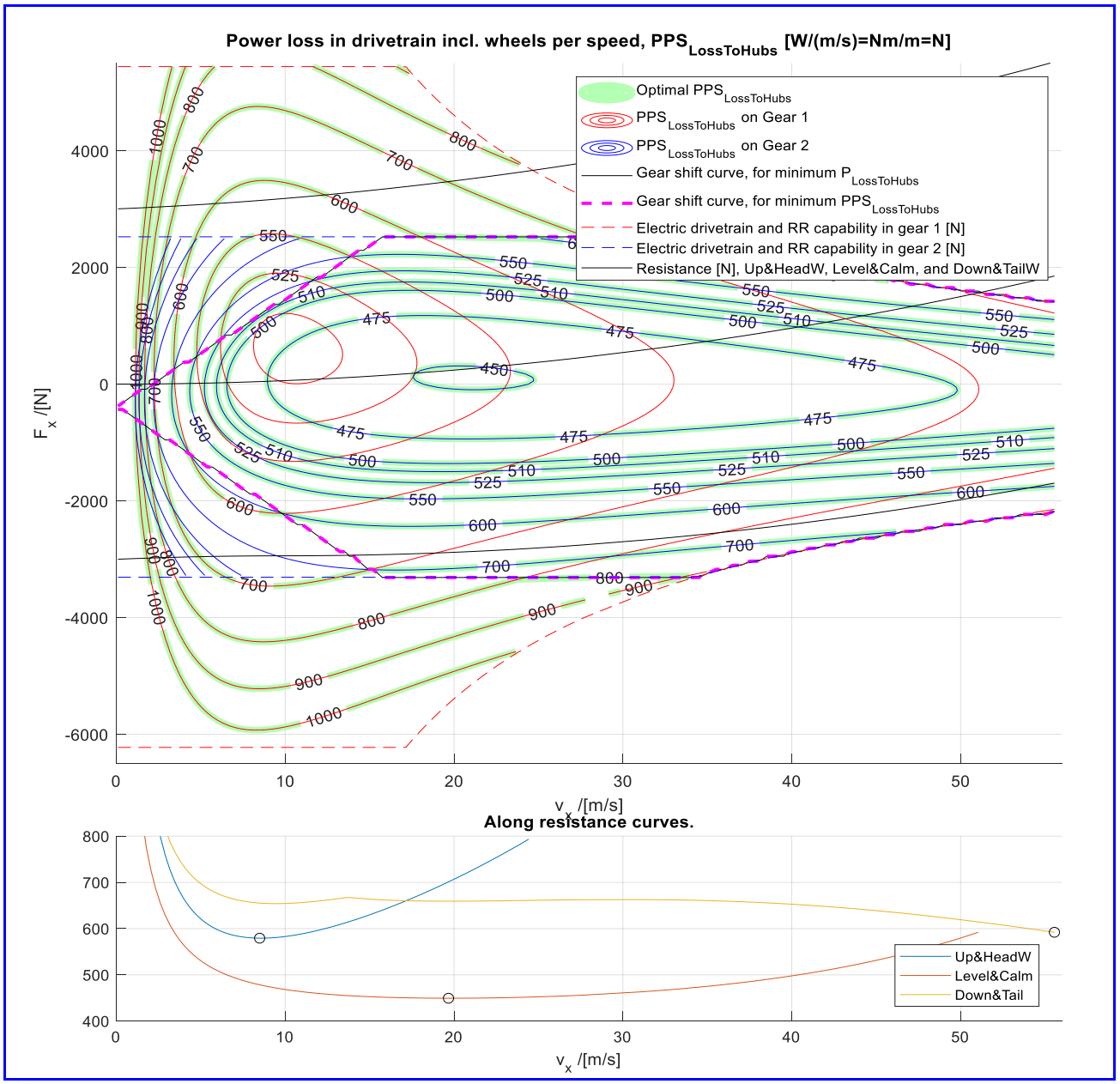


Figure 3-8: Select gear and speed through min(PPS_{Loss}).

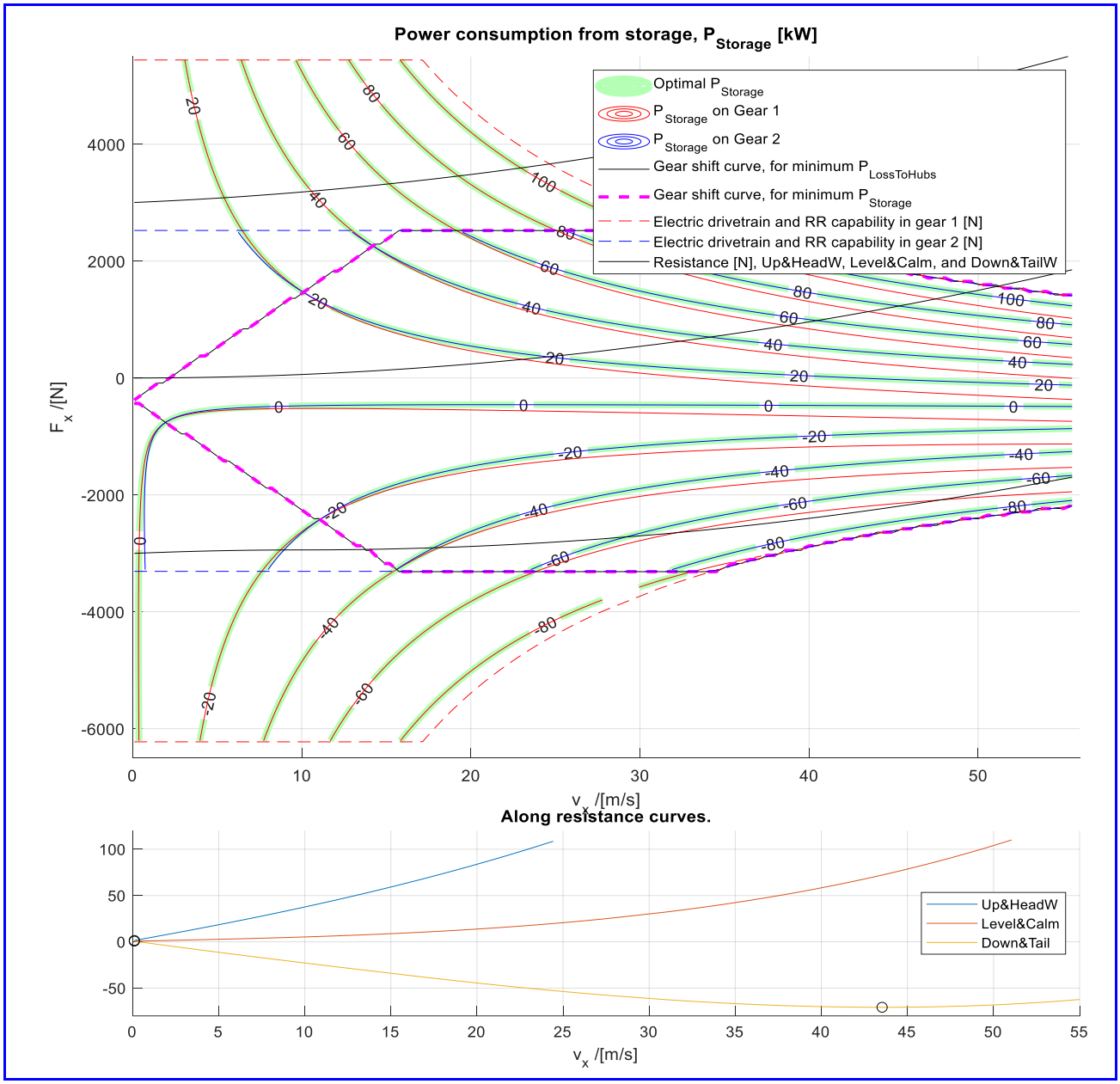


Figure 3-9: Select gear and speed through min($P_{Storage}$).

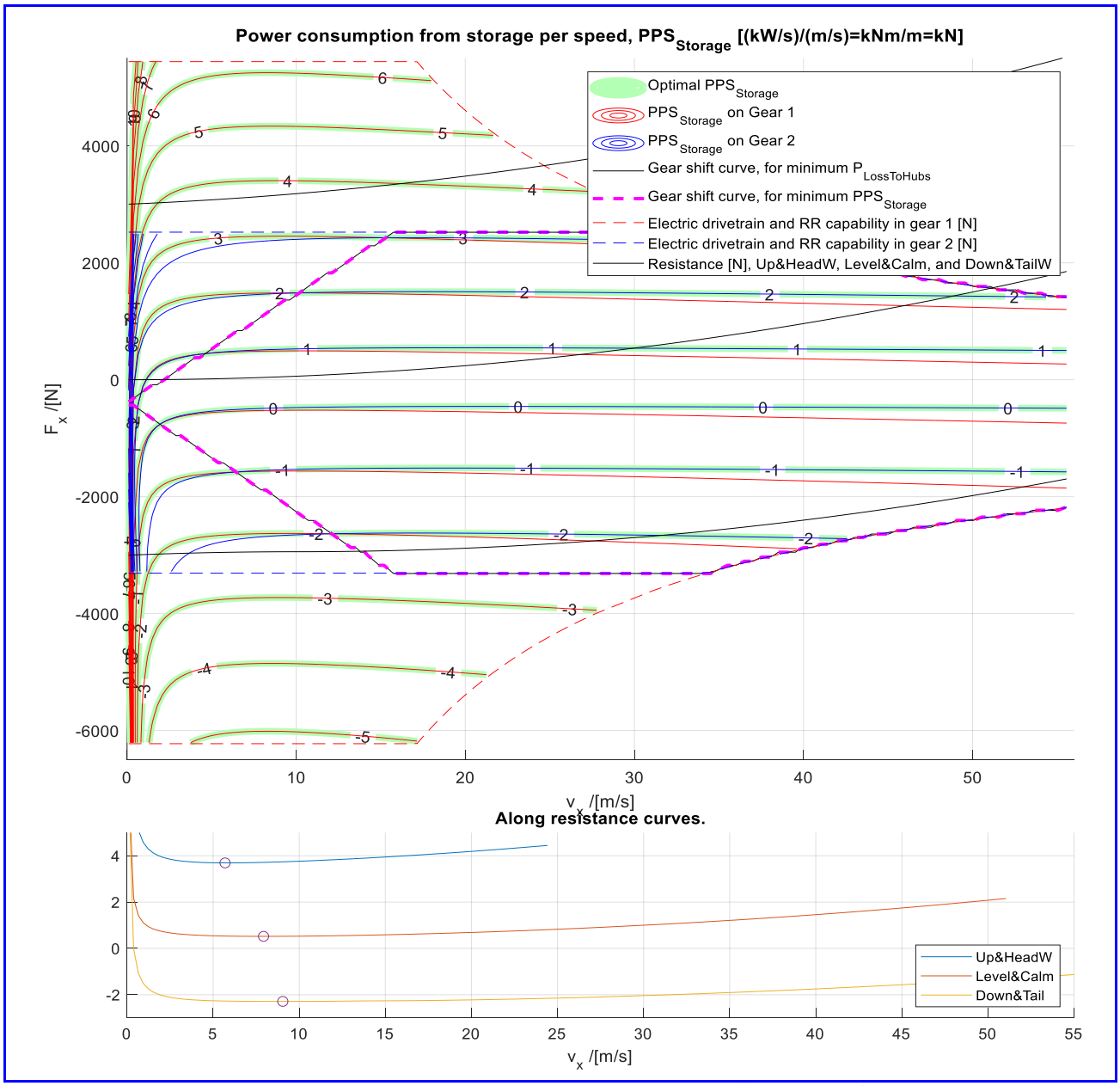


Figure 3-10: Select gear and speed through $min(PPS_{Storage})$.

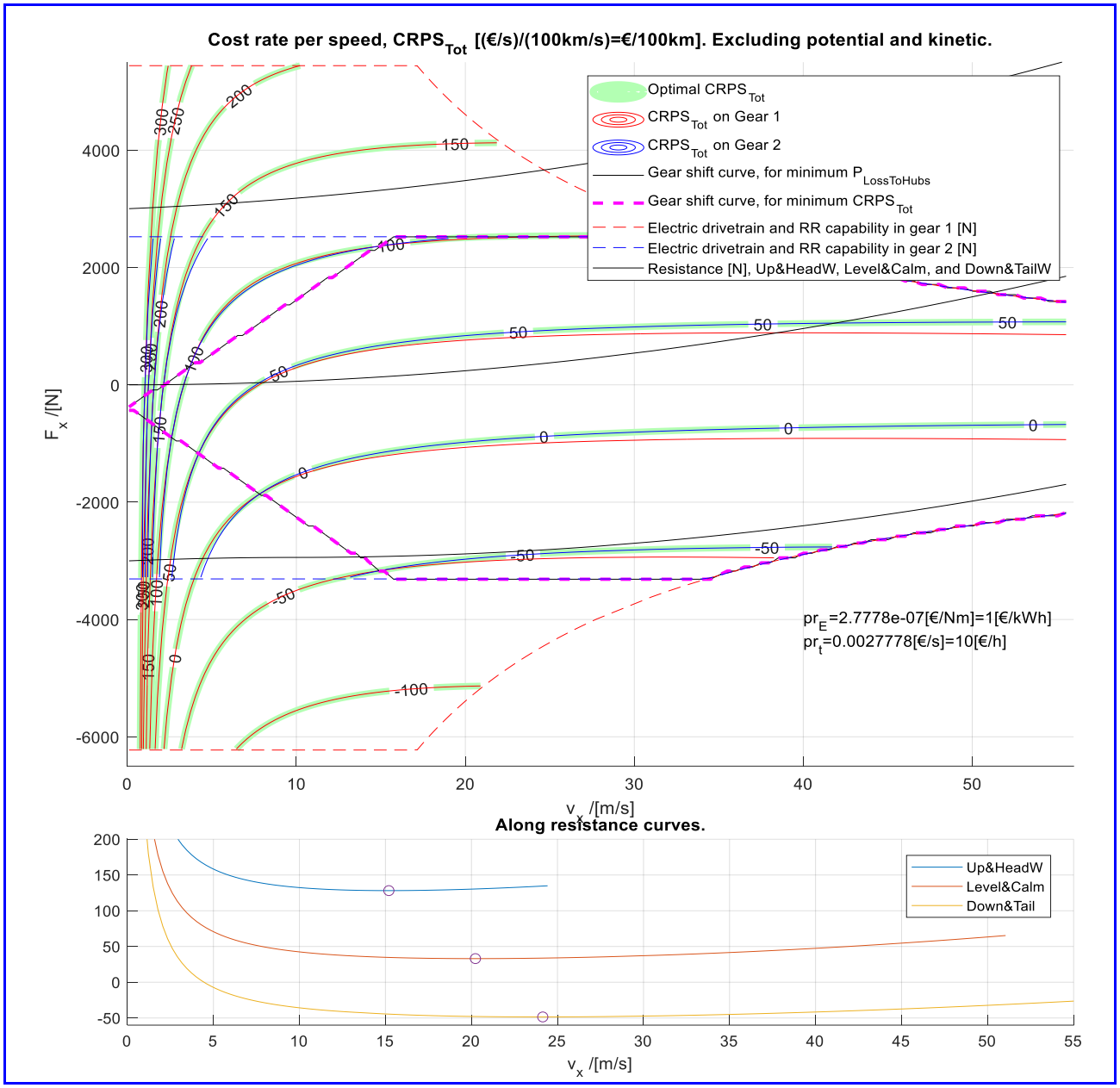


Figure 3-11: Select gear and speed through $min(CRPS_{Tot})$.

Coordination of wheel torque actuators for minimum power ".>

Gear selection is *when* to change from one specific gear to another. It is mainly expressed in operating conditions; one can draw gear selection as curves for each shifting in a traction diagram. If we call that "when" to shift, there is also a question "how" to shift. The "when" is discussed in the following section, while "how" is not covered well in this book, but it is briefly discussed in 2.4.3.1 and exemplified in 2.4.7.1. More about the "how" in (Jacobson B. , 1993).

3.2.1.1.1 Gear selection expressed in steady-state operating conditions

In Figure 3-3, the gear selection was discussed for an operating point defined by 3 quantities: v_x, a_x and $\varphi_{road,y}$. To be noted is that it was discussed also assuming steady state (constant over time). We will now discuss optimal gear selection for only a 2-dimensional diagram, conceptually as in Figure 3-4.

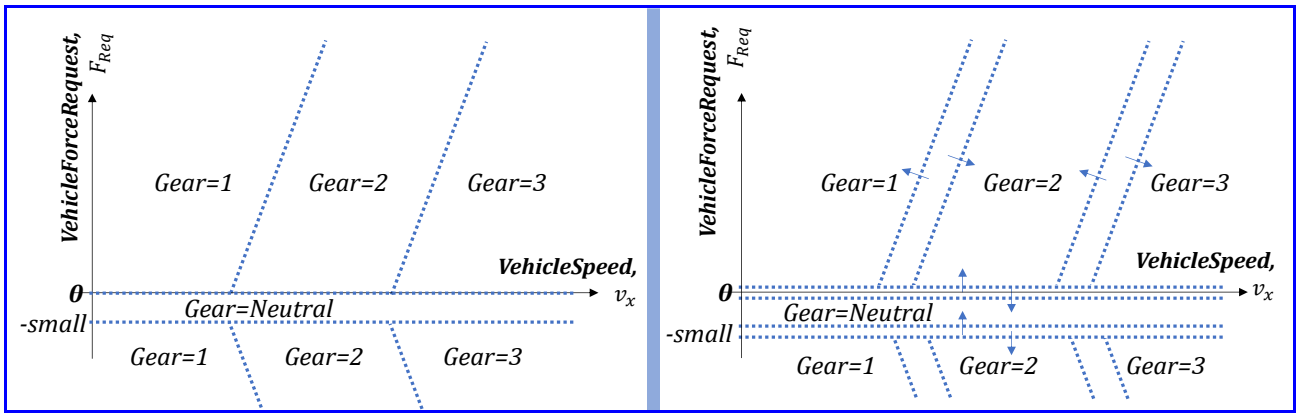


Figure 3-4: Gear selection diagram. Left: Shift curves for "gear i → j" and "gear j → i" approximated as one shift curve. Right: with hysteresis to avoid non-stationary or too frequent shifts

The curves are chosen to create regions for a gear. For $F_{Req} > 0$, one typically selects gear for lowest fuel consumption. For $F_{Req} < -small$, one selects a non-neutral gear to allow engine and retarder braking, to avoid wear and overheating of the friction brakes. If electric propulsion, the engine braking has a positive effect of regenerating energy which save energy over the whole transport operation.

For $0 < F_{Req} < -small$, the engine brake is strong enough so one can do either engine brake or apply brake; Figure 3-4 selects neutral gear, so friction brake is assumed. If engine has much idle losses, it can often be more energy saving to select neutral gear and friction braking, see 2.4.3.1.3.

The curves in the diagram are also depending on other conditions, such as road grade and vehicle gross weight. The diagram only indicates sequential gears, while, especially heavy vehicle with many gears, often jump over gears, e.g. shifting directly from gear 1 to 3. The energy optimality of neutral gear is explained in Figure 3-3.

3.2.1.1.2 Gear Selection for transient operating conditions

The previous description was made for a steady-state operating condition. Transients, i.e. variations over time, add the problem to avoid non-stable gear shifting, and especially that gear is shifted too frequent. This is because each shift causes energy losses, but also other negative consequences such as reduced driveability of the vehicle and lifetime of the propulsion system components.

Too frequent shifting can be avoided by hysteresis in different ways. One way is to define separate up- and down-shift curves, see previous figure. The hysteresis is achieved by putting these curves much enough apart. This can be characterized as using a *memory*.

Another way to avoid too frequent shifting, is to use a *timer* which explicitly forbids shifting within a certain time after the last shift. Using the time partly overcome the problem that the area in the diagram where neutral gear is optimal is very narrow.

So, there is a conflict between selecting neutral gear or not for low energy consumption and avoiding too frequent gear shifts.

With a predictive cruise, 3.5.2.3.1, it is much easier to utilize the neutral gear, since the algorithm can simply look in the prediction and find out if a too frequent gear shift is predicted or not. In this way one can allow neutral gear much more often without the drawbacks of too frequent shifting.

3.2.2 Energy consumption and power losses

Consumed energy is a substantial part of the transportation **cost** [€], typically one third for goods transports. We can only quantify consumed energy as an integral over an interval, in time t or in travelled distance s. So, an engineer, a driver, or a control algorithm must consider energy cost in a **predictive** way, predicting to a moving horizon or the end of a whole transport mission. Corresponding for consumed power, or power loss, is that it is a (momentaneous or instantaneous) **cost rate** or cost gradient, $[€/s]$ or $[€/m]$. Energy **consumption** and especially power **loss**, can only be modelled for each **part** (battery, prime mover, transmission, wheel, …) and/or for each **phenomenon** (rolling resistance, aerodynamic resistance, …).

Requirements on energy consumption typically refers to a driving cycle or operating cycle, see 3.3.1 and 3.3.5.1. In such cycles, the operating conditions varies. In 3.2, we study Steady state functions, as opposed to cycles. Therefore, the operating conditions are constant. However, in both steady state and cycles, the quantities in Table 3.1 are useful. Note similarities and differences between EPD and PPS.

Table 3.1: Quantities for energy (consumption) and power (losses)

Overall definition of different consumptions	**When modelling as losses in physical parts or phenomena, i**	**Note**
Energy, E_{Cons} • in $[J]$, • is an **accumulation** over a time interval: $E_{Cons} = \int P_{Cons} \cdot dt$;	E_{iLoss} is the energy loss in part, or phenomenon, i. If all $(\forall i)$ are modelled: $E_{Cons} = \sum_{\forall i} E_{iLoss}$;	P_{Cons} is the power from the energy storages which we have a cost [€] to fill up, such as fuel tanks and batteries. For a battery, $E_{Cons} = \int \frac{d(E_{Stored})}{dt} \cdot dt$; E_{iLoss} is the energy "loss" in a part or phenomena, where loss means that we cannot use the energy for transport. Important to include in "$\forall i$" are: energy storages, prime movers, transmissions, wheels, friction brakes, aerodynamic resistance, road grades, and auxiliary loads.
Energy per distance, EPD • in $[J/m = N]$, • is an **average** over a time interval: $EPD = E_{Cons}/(\int \dot{s} \cdot dt) =$ $= E_{Cons}/\int ds$;	$EPD_i = E_{iLoss}/(\int \dot{s} \cdot dt) = E_{iLoss}/(\int ds)$; If all $(\forall i)$ parts or phenomena are modelled: $EPD = \sum_{\forall i} EPD_i$;	EPD and EPD_i can be seen as the "equivalent" **average** resistance forces, $R_{iEquivAv}$ $[N]$. These are averaged over a distance interval. $R_{iEquivAv}$ is equivalent with respect to the **energy** loss. Losses E_{iLoss} can be replaced by a constant force acting on the vehicle body, counter-directed to the route direction. $R_{iEquivAv}$ cannot be measured in a real-world test but are useful for comparison between losses in different parts or phenomena.
Power, P_{Cons} • in $[J/s = W]$, • is defined for the vehicle in its transport operation • is a **momentaneous** quantity (for a time **instant**, not an average over a short time interval)	If all $(\forall i)$ parts or phenomena are modelled: $P_{Cons} = \sum_{\forall i} P_{iLoss}$;	Note the difference between the **momentaneous** quantity P_{Cons} and the **average** over a time interval, $P_{ConsAv} = E_{Cons}/(\int dt) = (\int P_{Cons} \cdot dt)/(\int dt)$;. $P_{iLoss} = P_{iIn} - P_{iOut}$; During driving, some (as storages) have $P_{iIn} \equiv 0$, and some (as aerodynamic resistance) have $P_{iOut} \equiv 0$, while some (as prime movers, transmissions and wheels) can have both $P_{iIn} \neq 0$ and $P_{iOut} \neq 0$.
Power per speed, PPS • in $[(J/s)/(m/s) = N]$ • is defined for the vehicle in its transport operation or for a part or phenomenon in the vehicle • is a **momentaneous** quantity: $PPS = P/\dot{s}$;	$PPS_i = P_{iLoss}/\dot{s}$; If all $(\forall i)$ parts or phenomena are modelled: $PPS = \sum_{\forall i} PPS_i$;	PPS and PPS_i can be seen as "equivalent" **momentaneous** resistance forces R_{iEquiv}. These are mot averaged but momentaneous at a time instant. R_{iEquiv} is equivalent with respect to the **power** loss. Losses P_{iLoss} can be replaced by a force acting on the vehicle body, counter-directed to the route direction. R_{iEquiv} cannot be measured in a real-world test but are useful for comparison between losses in different parts or phenomena.

Energy consumption for constant operating conditions can be with given speed and with free speed, see 3.2.2.1 and 3.2.2.2.

3.2.2.1 Energy consumption for constant operating conditions, with given speed *

Function definition: ***Energy (or Fuel) consumption*** *is the amount of energy* $[J]$ *(or fuel* $[kg]$ *or* $[litre]$*) consumed by the vehicle per performed transportation amount. Transportation amount can e.g. be measured in* $[km]$, $[person \cdot km]$, $[ton \cdot km]$, *or* $[m^3 \cdot km]$. *The vehicle operation conditions are given as: Constant* ***given speed*** *as well as constant given other conditions: road gradient, head wind, cargo load, road surface conditions, etc.*

Typical values of the constant operating condition are zero road grade and zero head wind speed. A test scenario is that the vehicle is driven a certain distance, from $s = 0$ to $s = s_{End}$, with the specified constant speed.

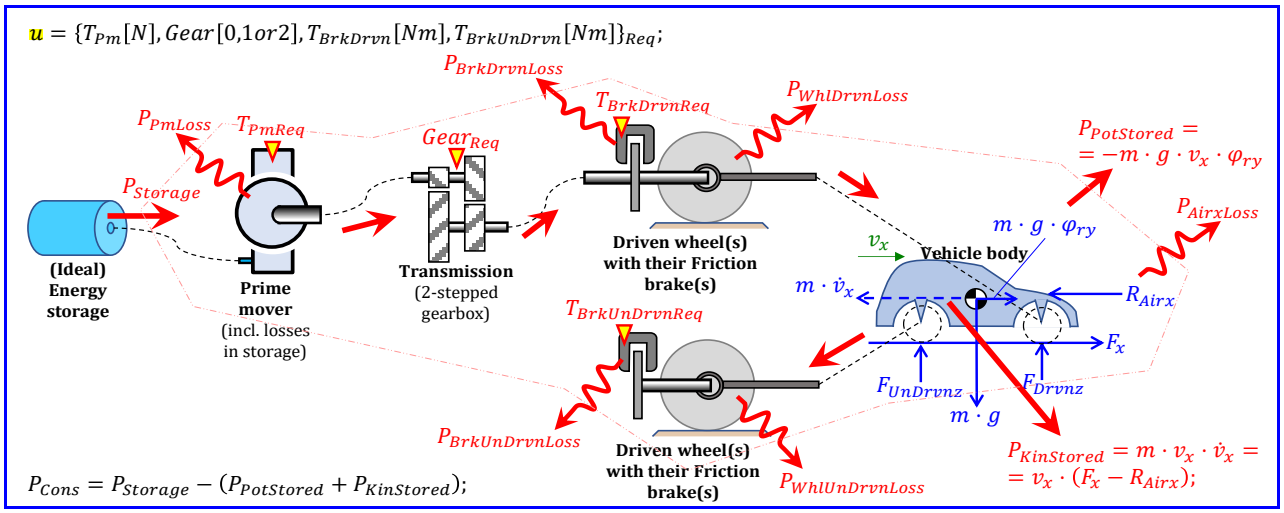


Figure 3-5: Example of power flow in a one-drivetrain vehicle. Dash-dotted curve shows the system border which defines P_{Cons}.

Figure 3-5 shows an example of propulsion systems. The dash-dotted curves show the system borders which defines consumed power P_{Cons}. For steady state we definitely not need to consider $P_{KinStored}$ because it will be zero. We also neglect also $P_{PotStored}$ because it is given by the constant road grade. (When doing predictive cruise, one cannot forget these power flow, and other similar, such as heating the compartment or keeping the pay-load frozen.)

Assuming that there is a main storage of energy (e.g., a fuel tank or a battery), the consumed energy E_{Cons} can be calculated as:

$$E_{Cons} = E_{Storage}\big|_{s=0} - E_{Storage}\big|_{s=s_{End}} - E_{Other}\big|_{s=s_{End}};$$

The $E_{Other}\big|_{s=s_{End}}$ represents valuable remaining energy by the end of the driving, stored somewhere else than in main storage. It could be higher altitude or warmed up passenger compartment. There is no physical law to tell what remaining energy is valuable or not. In the following, we assume $E_{Other}\big|_{s=s_{End}} = 0$.

$$E_{Cons} = E_{Storage}\big|_{s=0} - E_{Storage}\big|_{s=s_{End}};$$

The function definition above is energy "per transportation amount", which can be "per distance". We introduce a notation for *energy per distance*, EPD:

$$EPD = \frac{E_{Cons}}{s_{End} - 0} = \frac{E_{Storage}\big|_{s=0} - E_{Storage}\big|_{s=s_{End}}}{s_{End}};$$

Vehicles can perform the transport operation in a way that v_x is not exactly co-directed with the intended route. Taking this into account would require: $s_{End} - 0 = \int |v_{xy}| \cdot dt$. Examples of such are turns or reversing. However, if we neglect such parts, v_x is co-directed with intended route and we can use $s_{End} - 0 = \int v_x \cdot dt$. Then we can also introduce *energy per speed EPS*:

$$EPD\left[\frac{Nm}{m}\right] = \frac{E_{Cons}}{s_{End} - 0} = \frac{\int P_{Cons} \cdot dt}{s_{End} - 0} = \frac{\int P_{Cons} \cdot dt}{\int v_x \cdot dt} = \left\{\begin{matrix} constant \\ operating\ conditions \end{matrix}\right\} =$$

$$= \frac{P_{Cons} \cdot \int dt}{v_x \cdot \int dt} = \frac{P_{Cons}}{v_x} = PPS\left[\frac{Nm/s}{m/s}\right] \quad (= R_{EquivAv}\,[N]);$$

If many possibilities to operate actuators, many "actuations", we still must decide how to coordinate them, i.e. calculate $\boldsymbol{u}^*$. This can be to blend (allocate) wheel torque actuator torques for minimum $EPD = PPS$, while fulfilling the vehicle longitudinal force equilibrium. An example of actuator coordination is gear selection in a stepped gearbox or ratio selection in a CVT. Such coordination is not directly blending (or allocating) but a form of actuator coordination since we must find $\boldsymbol{u}^*$.

$$\boldsymbol{u}^* = arg\left(\min_{\boldsymbol{u}}\left(PPS(v_x,\boldsymbol{u})\right)\right) = arg\left(\min_{\{T_{PmReq},Gear_{Req}\}}\left(PPS\left(v_x,\{T_{PmReq},Gear_{Req}\}\right)\right)\right);$$

$$where\ PPS(v_x,\boldsymbol{u}) = \sum_{\forall i}\frac{P_{iLoss}(v_x,\boldsymbol{u})}{v_x};\quad which\ is\ = \frac{P_{Cons}(v_x,\boldsymbol{u})}{v_x};$$

$$and\ F_x(v_x,\boldsymbol{u}) = R_{Resist}(v_x,\boldsymbol{u}) = \frac{P_{ResistLoss}(v_x,\boldsymbol{u})}{v_x}\quad "longitudinal\ force\ equilibrium";$$

We can eliminate one component, u_{elim}, in $\boldsymbol{u} = \{u_{elim},\ \boldsymbol{u_{free}}\} = \{T_{PmReq}, Gear_{Req}\}$:

$$\boldsymbol{u}^* = \{T^*_{PmReq}, Gear^*_{Req}\} = \left\{T^*_{PmReq}, arg\left(\min_{Gear_{Req}}\left(PPS\left(v_x,T^*_{PmReq},Gear_{Req}\right)\right)\right)\right\} =$$

$$= \left\{\begin{array}{c} \dfrac{P^{-1}_{ResistLoss}\left(v_x,F_x,\ Gear^*_{Req}\right)}{v_x}, \\ arg\left(\min_{Gear_{Req}}\left(PPS\left(v_x,\dfrac{P^{-1}_{ResistLoss}\left(v_x,F_x,\ Gear_{Req}\right)}{v_x},Gear_{Req}\right)\right)\right) \end{array}\right\};$$

$$where\ PPS(v_x,\boldsymbol{u}) = \sum_{\forall i}\frac{P_{iLoss}(v_x,\boldsymbol{u})}{v_x};\quad which\ is\ = \frac{P_{Cons}(v_x,\boldsymbol{u})}{v_x};$$

By this elimination, we have reduced the free variables, from 2 ($\{T_{PmReq}, Gear_{Req}\}$) to 1 ($Gear_{Req}$), in the trajectory optimization (or optimal control) problem. The total wheel torque actuation does typically also include (friction) brake systems. In the example above, it could mean that $\boldsymbol{u} = \{T_{PmReq}, Gear_{Req}, T_{BrkReq}\}$ before elimination.

So far, we have only counted the cost (rate) for energy. We can add cost (rates) as cost (rate) for transport time. There can also be constraints on driveability, e.g. acceleration capability, and safety, e.g. legal speed, which motivates us to deviate from minimizing the cost rate. But in principle, we have now sketched how the wheel

3.2.2.2 Energy consumption for constant operating conditions, with free speed *

A variant of the function in 3.2.2.1 is if the speed selection is part of the function, as opposed to given:

> *Function definition:* ***Energy (or Fuel) consumption*** *is the amount of energy* $[J]$ *(or fuel* $[kg]$ *or* $[litre]$*) consumed by the vehicle per performed transportation amount. Transportation amount can e.g. be measured in* $[km], [person \cdot km], [ton \cdot km]$, *or* $[m^3 \cdot km]$. *The vehicle operation conditions are given as: Constant (but* ***not given****)* ***speed*** *as well as constant given other conditions: road gradient, head wind, cargo load, road surface conditions, etc.*

We will now aim at finding the (constant but **not given**) **speed** which gives lowest energy consumption over a certain distance. If varying operating conditions and multiple energy storages, we can always end up in a trajectory optimization with state variables an integral cost function *EPD* and the optimal speed becomes a varying trajectory. First, we assume one single energy storage. Then, we can still end up in a trajectory optimization with an integral cost function *EPD* but no state variables and an optimal speed which vary. Then, we fix the operating conditions which enable us to use *PPS* as an algebraic cost function and the optimal speed becomes a constant. This is still a predictive optimization, but it has collapsed to an algebraic optimization. If many actuators, we still must optimize how to use them together, e.g. allocate or blend them to fulfil the vehicle longitudinal force equilibrium and the minimum *PPS*, so the main equation changes to:

$$\{v_x, \boldsymbol{u}\}^* = arg\left(\min_{\{v_x,\boldsymbol{u}\}}(PPS(v_x,\boldsymbol{u}))\right);\quad where\quad \boldsymbol{u} = \{Act_{1Req}, Act_{2Req}, \cdots\};$$

$$where\ PPS(v_x,\boldsymbol{u}) = \sum_{\forall i}\frac{P_{iLoss}(v_x,\boldsymbol{u})}{v_x};\quad which\ is\ = \frac{P_{Cons}(v_x,\boldsymbol{u})}{v_x};$$

$$and\ F_x(v_x,\boldsymbol{u}) = R_{Resist}(v_x,\boldsymbol{u}) = \frac{P_{ResistLoss}(v_x,\boldsymbol{u})}{v_x}\quad "longitudinal\ force\ equilibrium";$$

We can often simplify "$\forall i$" by only including wheel torque actuators. But also with that simplification, we typically have multiple actuators, at least one drivetrain and one friction brake system. But to simplify, we here assume that there is only one drivetrain with one storage and that the operating conditions are such that friction brake is not needed, so we do not even consider to use it. All losses should be included, to really be able to claim that we minimize EPD and E_{Cons} by minimizing PPS, but in the example, we only include some, Em = electric machine, Rr = rolling resistance on driven axles, and $Resist$ = driving resistance = aerodynamic resistance + grade resistance + rolling resistance on nondriven axles:

$$\boldsymbol{u} = \{T_{PmReq}, Gear_{Req}\};\quad and\quad PPS(v_x,\boldsymbol{u}) = \frac{\overbrace{P_{EmLoss}(v,\boldsymbol{u}) + P_{RrDrvnLoss}(v,\boldsymbol{u})}^{P_{DtLoss}(v,\boldsymbol{u})} + P_{ResistLoss}(v,\boldsymbol{u})}{v};$$

$$and\ F_x(v,\boldsymbol{u}) = R_{Resist}(v,\boldsymbol{u}) = \frac{P_{ResistLoss}(v,\boldsymbol{u})}{v}\quad "longitudinal\ force\ equilibrium";$$

There is only one free variable in the optimization, the (discrete) $Gear_{Req}$. Since discrete with limited number of alternative gears, we can do an extensive search optimization, which simply means that we try all gear and select the gear with lowest EPD, $Gear^*_{Req}$. Then all other will also be found, such as the speed v which is then the optimal speed v^*. To minimize EPD will give same optimum as minimize PPS or maximizing the drivetrain power efficiency η_{Dt}. The losses in the driven tyres, such as their tyre slip and rolling resistance, should be included in η_{Dt}.

3.2.2.3 Example with simple actuator coordination

We will now study the vehicle in Figure 3-5. In this example, we do neither include neutral gear nor the brake. This makes the actuator coordination as simple as possible: Only select gear.

The upper diagrams in Figure 3-6, Figure 3-7, Figure 3-8, Figure 3-9, Figure 3-10, and Figure 3-11 are traction diagrams:

- How the following 6 measures vary over the $\{v_x, F_x\}$:
  $P_{Loss}, \eta, PPS_{Loss}, P_{Storage} = P_{Cons}, PPS_{Storage}, CRPS_{Tot}$
  - For each "actuator coordination" ($Gear = 1$ and $Gear = 2$), because for many $\{v_x, F_x\}$, one can drive on either of the gears.
- The optimum values of these 6 measures. Were optimum means minimum of $P_{Loss}, PPS_{Loss}, P_{Storage} = P_{Cons}, PPS_{Storage}, CRPS_{Tot}$ and maximum of η.
- Also, the optimum actuator coordination (i.e. either $Gear = 1$ or $Gear = 2$) is shown.
- Electric machine model from Eq [2.88[2.88]

- Pseudo code for how the $CRPS_{TotOpt}$ diagram was plotted:

```
for v_x = v_x axis
  for F_x = F_x axis
    for Gear = [1 2] %Sweep the free actuator request Gear
      T_Em = ⋯; %The other actuator request T_Em fulfil the F_x
      CRPS_Tot = ⋯;
    end
    select the best CRPS_TotOpt = ⋯ and corresponding Gear_Opt = ⋯
  end
 end
 plot⋯;
```

Note:

- All the 6 measures give the same gear shifting curves, i.e. the same actuator coordination, i.e. the same best gear for a given $\{v_x, F_x\}$.
- These upper diagrams, especially $PPS_{Storage}(v_x, F_x)$, can be used to read out a function measure for "3.2.2.1 Energy consumption for constant operating conditions, with given speed *".
- It can also be used for momentaneous optimization, i.e. real-time computation during vehicle usage. A map, $Gear = map(v_x, F_x)$, independent of the driving resistance, can be pre-processed which strongly reduces the computational load.

The results are independent of the driving resistance. However, 3 examples of driving resistance curves are drawn in the traction diagrams. If we compute best measure (e.g. $CRPS_{Tot}$) along those curves, we get the diagrams in the bottom of each figure. The optimum is marked with a circle, and the circle ends up at different optimum v_x depending on which measure is optimized. These lower diagrams can be used to read out a function measure for "3.2.2.2 Energy consumption for constant operating conditions, with free speed *". It would make sense that the vehicle (or driver) selects a speed from the $CRPS_{Tot}$ diagram.

A more complex actuator coordination, which will be shown in 3.2.2.4. A map, $Gear = map(v_x, F_x)$, can be pre-processed which strongly reduces the computational load in real time.

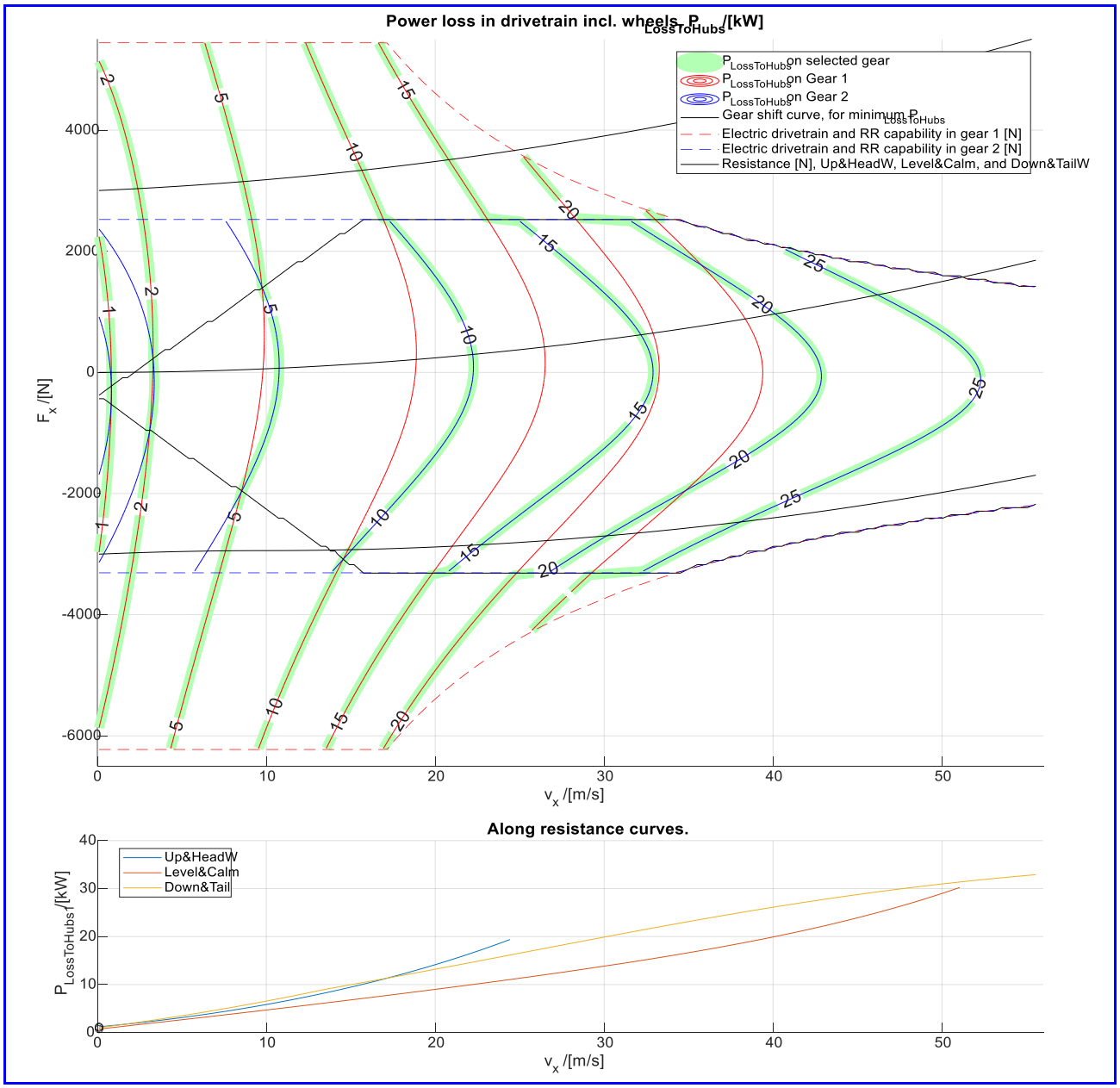


Figure 3-6: Select gear and speed through $min(P_{Loss})$.

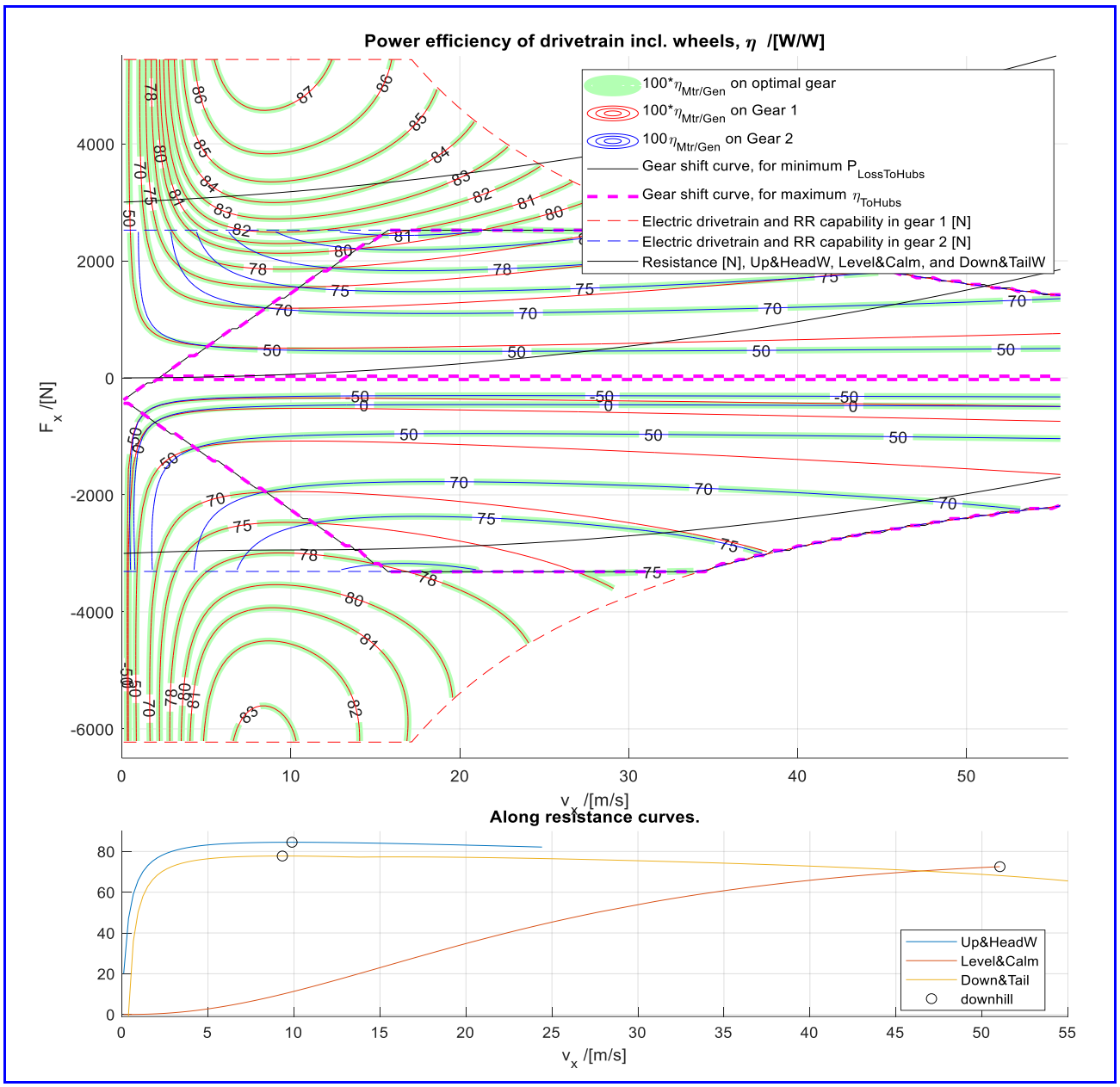


Figure 3-7: Select gear and speed through max($\eta_{DrivetrWheels}$).

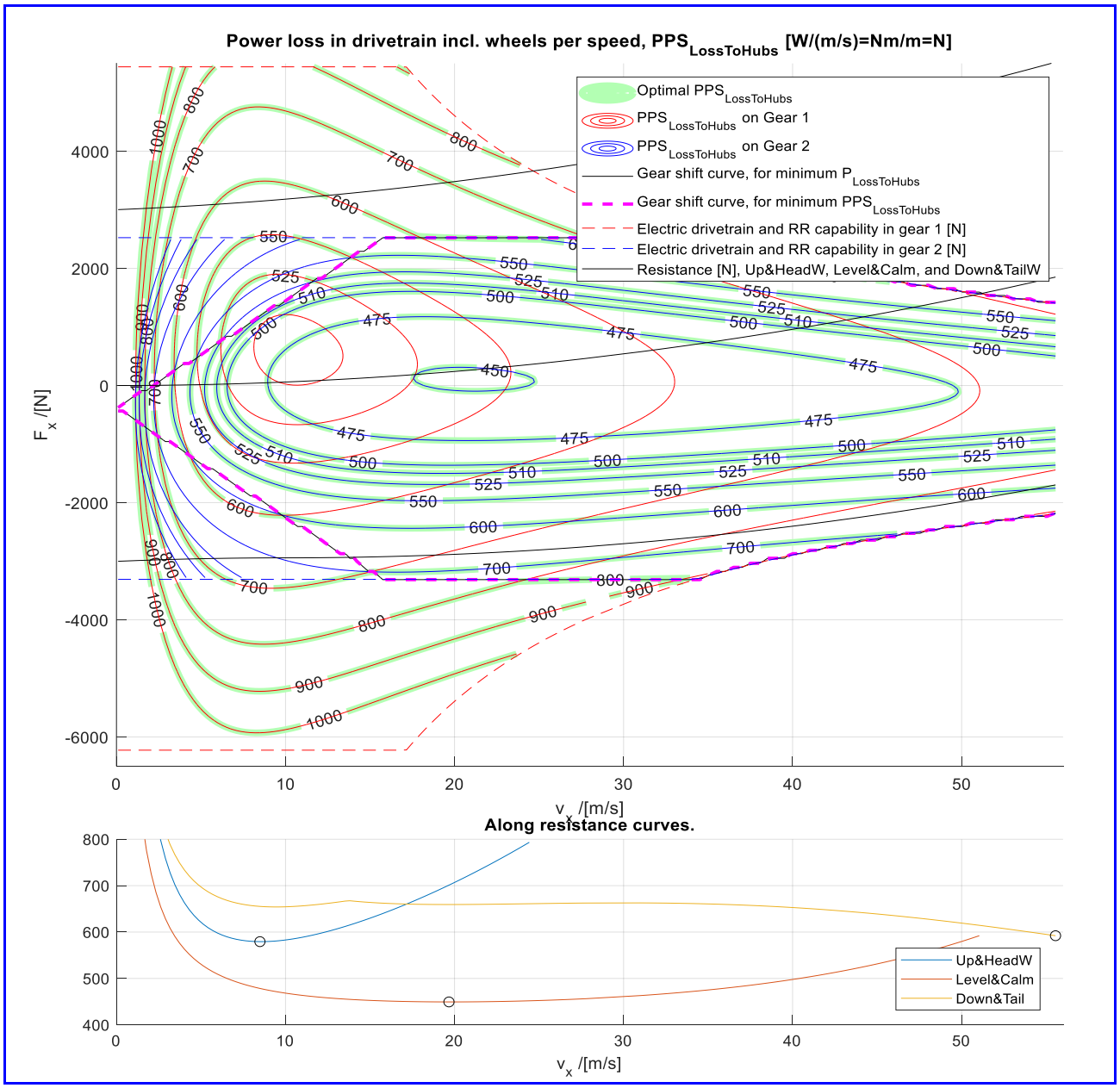


Figure 3-8: Select gear and speed through $min(PPS_{Loss})$.

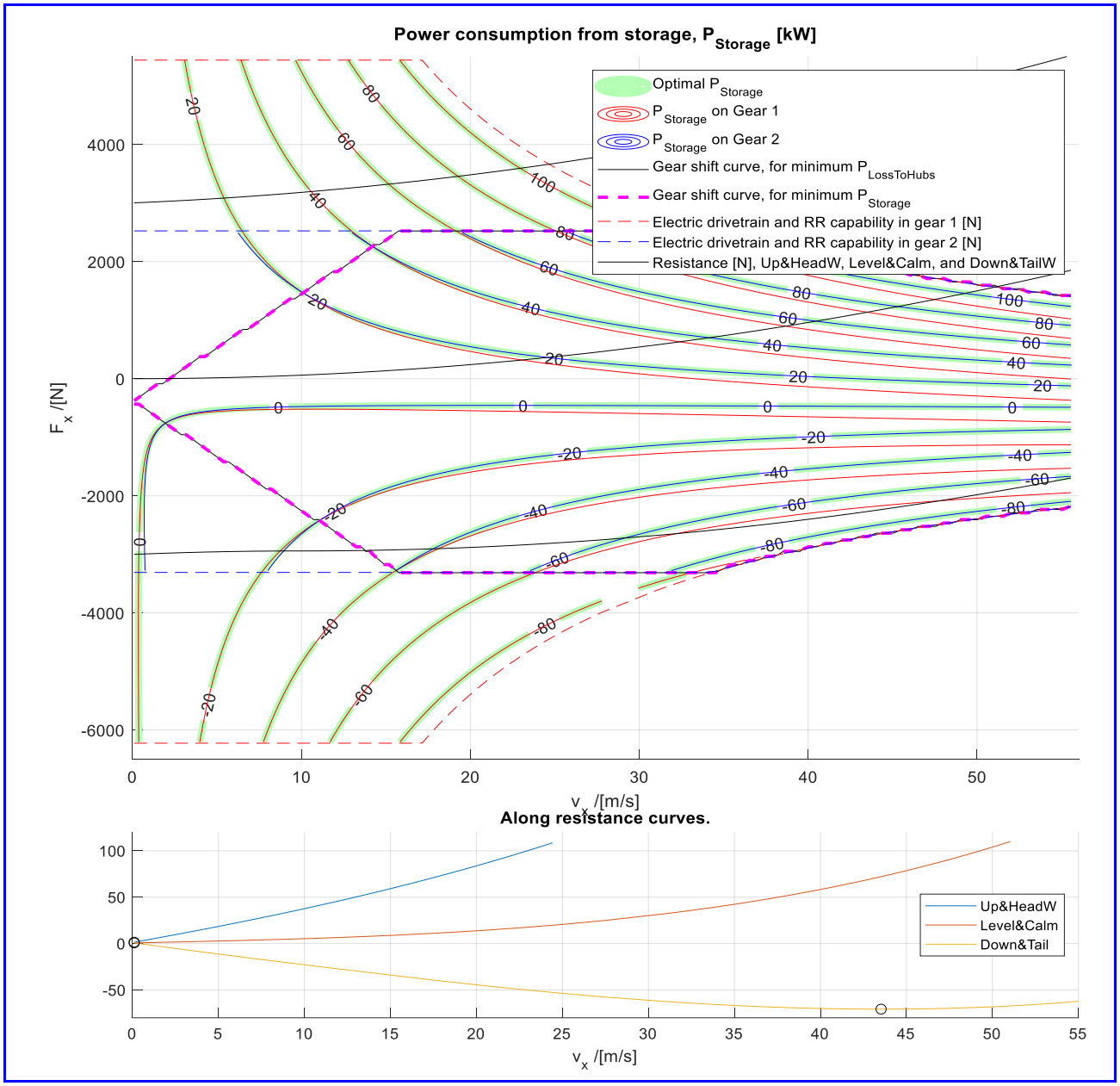


Figure 3-9: Select gear and speed through min($P_{Storage}$).

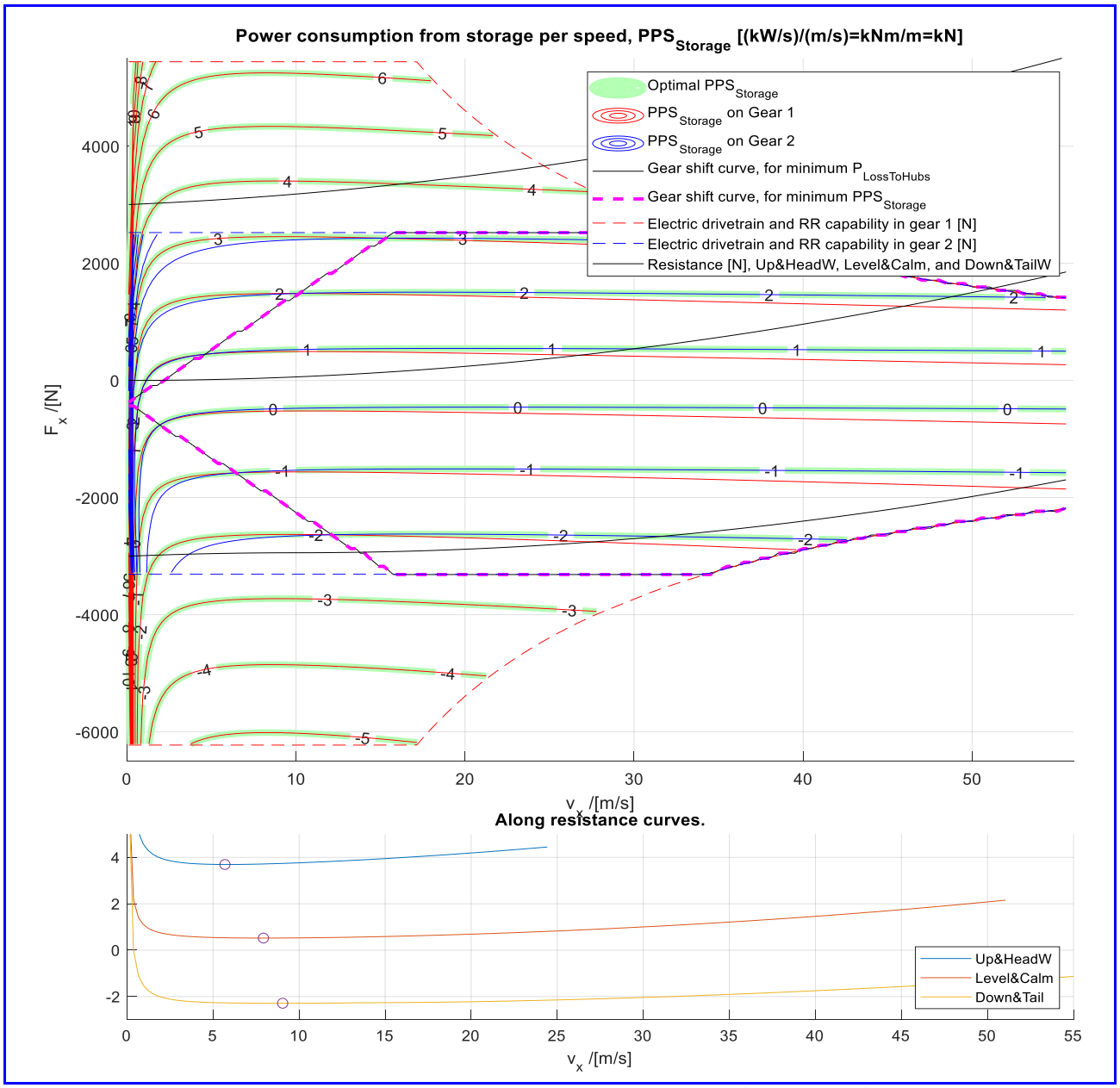


Figure 3-10: Select gear and speed through $min(PPS_{Storage})$.

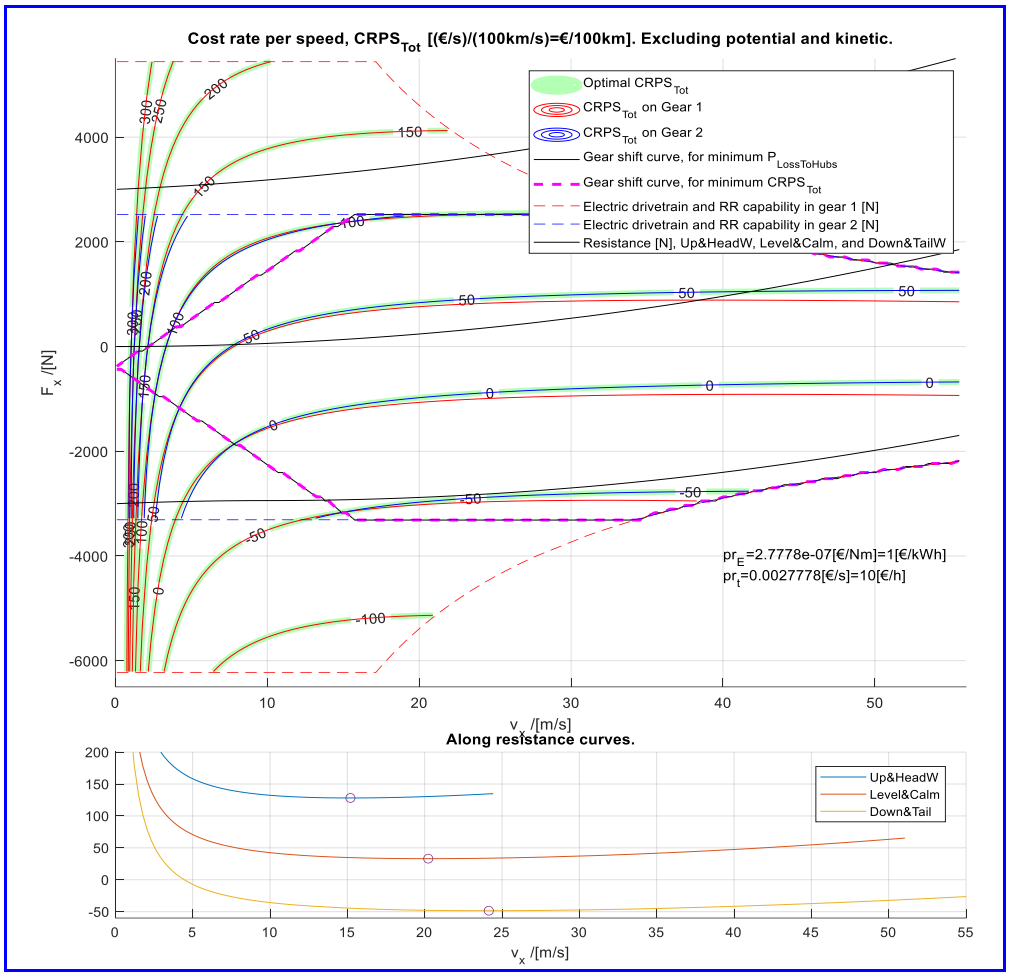


Figure 3-11: Select gear and speed through $min(CRPS_{Tot})$.

3.2.2.4 Coordination of wheel torque actuators for minimum power losses

Vehicles are often over-actuated, see 1.5.3.4. One degree of longitudinal over-actuation is already present for very traditional vehicles during negative actuated force, just because they have one drivetrain which can do engine braking and one friction brake system. A simple gear selection is also a form of over-actuation, because we can operate in one $\{v_x, F_x\}$ on different gears; so gear can, and has to, be selected. With more futuristic multiple-drivetrain vehicles, one can typically foresee more degrees of longitudinal over-actuation.

3.2.2.5 Example with more relevant actuator coordination

We will now study the vehicle in Figure 3-12. It uses same electric machine and gear ratios as the vehicle in Figure 3-5. In this example, we include neutral gear in the sense that each electric machine can be turned off. If turned off it generates no torque, while if turned on it requires power input also if outputting zero torque. So, turning off is "neutral gear" in the sense that the idling torque is avoided. We also include (friction) brake. This concept is more relevant than the example in 3.2.2.3.

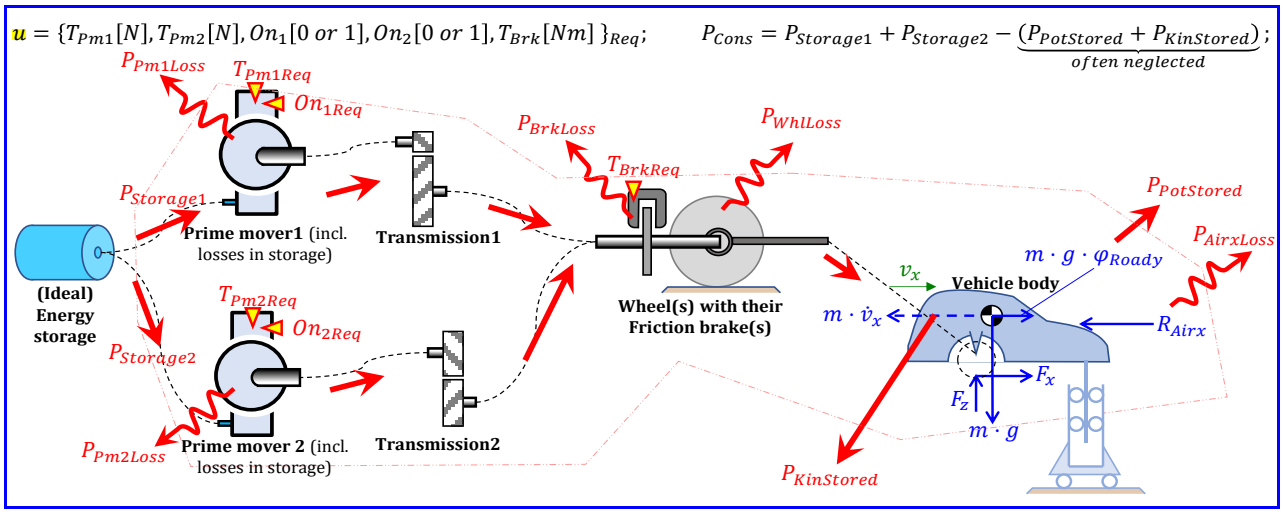


Figure 3-12: Example of power flow in a two-drivetrain vehicle. Not that the vehicle body uses wheels lumped to one.

The $\boldsymbol{u}$ vector is $\boldsymbol{u} = \{On_{Em1}\ [0\ or\ 1], T_{Em1}\ [Nm], On_{Em2}\ [0\ or\ 1], T_{Em2}\ [Nm], On_{Brk}\ [0\ or\ 1], T_{Brk}\ [Nm]\}$.

Pseudo code for how the $CRPS_{TotOpt}$ diagram was plotted:

```
for v_x = v_x axis
  for F_x = F_x axis
    for ⋯ %Sweep the free actuator requests and use the other actuator
          request fulfil the F_x. More complex for clauses than the example
          in 3.2.2.3. But still only around 2 pages of code.
      CRPS_Tot = ⋯;
    end
    select the best CRPS_TotOpt = ⋯; and
          corresponding {On_Em1, T_Em1, On_Em2, T_Em2, On_Brk, T_Brk}_Opt = ⋯;
  end
 end
 plot⋯;
```

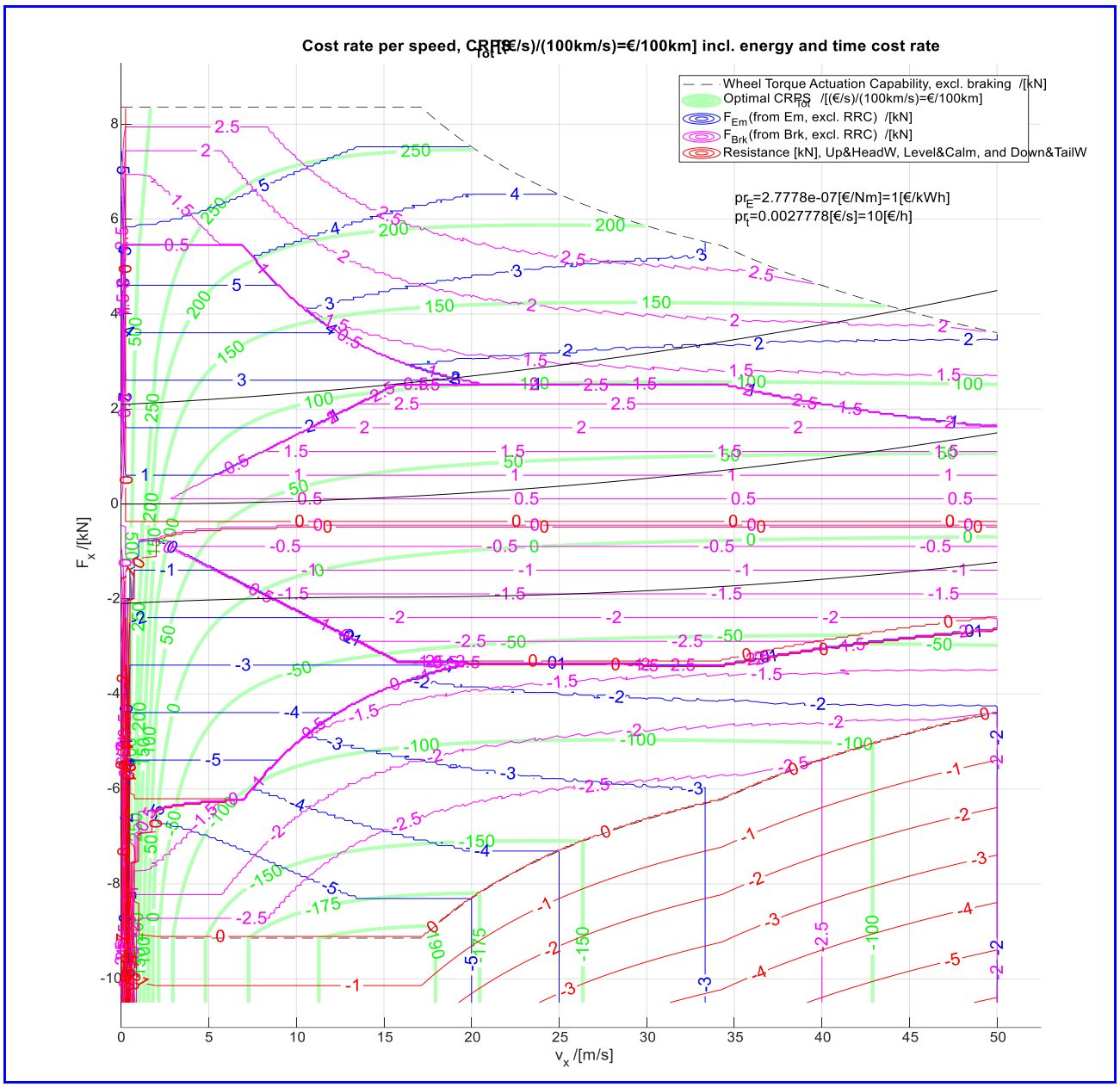


Figure 3-13: Traction diagram with solution for $min(CRPS_{Tot})$

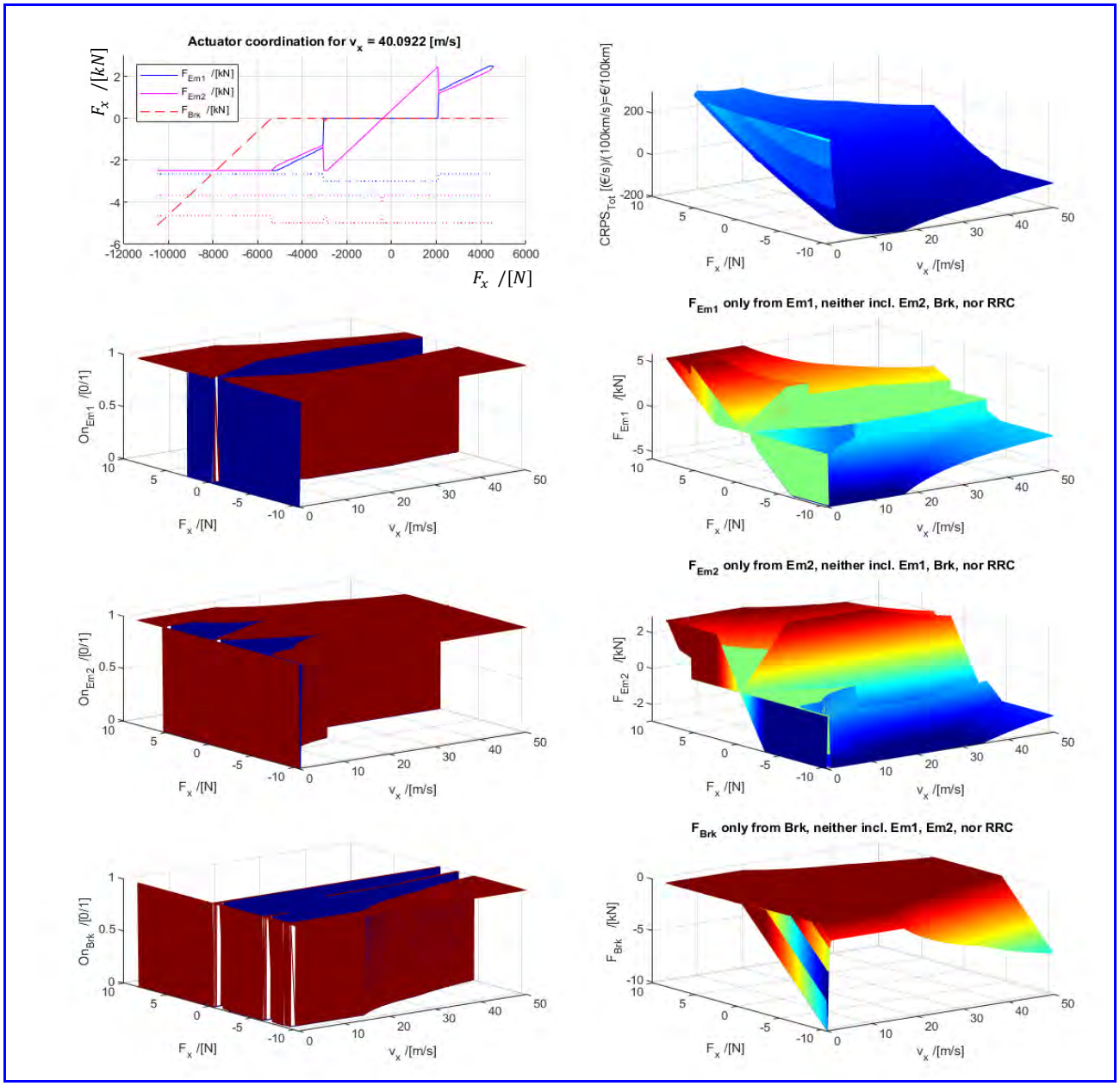


Figure 3-14: Other plots of the optimum actuator coordination.

3.2.2.6 Example with axle-wise friction braking

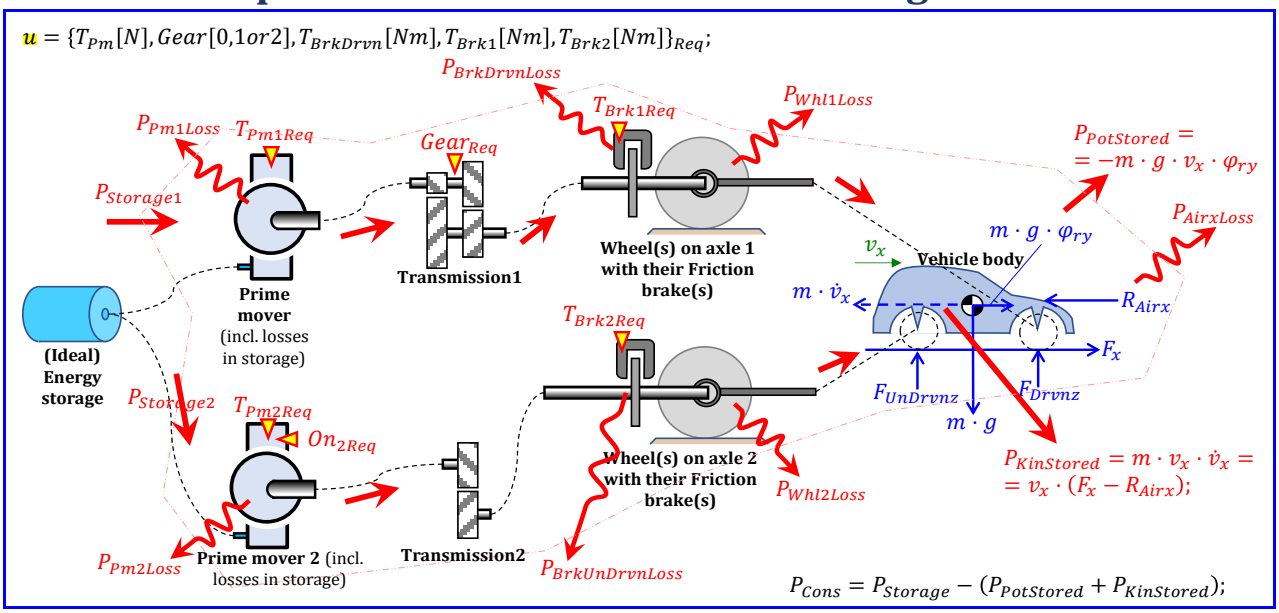


Figure 3-15: Example of power flow in a one-drivetrain vehicle, with 2-axle friction braking. Dash-dotted curve shows the system border which defines P_{Cons}.

In this example, we have added the possibility to distribute friction brake between front and rear axle. Then, we have 1 more control dof for wheel torque actuation; we must decide $\{F_{Brk1}, F_{Brk2}\}$ instead of F_{Brk}. It does not influence the cost rate, but we can utilize it to make friction utilization as equal as possible which improves the yaw balance in the way that the lateral grip is not lost only on one axle, but on both axles, at the same friction. This is better because the vehicle will understeer and oversteer less.

Since we introduce the friction, we can as well introduce a longitudinal acceleration a_x and lateral acceleration a_y and simplest possible model for transfer of vertical axle force and distribution of lateral axle force.

It will give us the same $CRPS_{TotOpt}$ diagram as in Figure 3-16, but another distribution of F_{Brk} to $\{F_{Brk1}, F_{Brk2}\}$, see Figure 3-14 .

Pseudo code for how the diagram in Figure 3-14 was plotted:

```
for Fx = Fx axis
  for … %Sweep the free actuator requests and use the other actuator
        request fulfil the Fx. More complex for clauses than the example
        in 3.2.2.3. But still only around 2 pages of code.
    CRPS_Tot = …;
  end
  select the best CRPS_TotOpt = …;
    and corresponding {On_Em1, T_Em1, On_Em2, T_Em2, On_Brk, T_Brk}_Opt
  for … %Sweep one of {F_Brk1, F_Brk2} and calculate the other so that
        F_Brk1, F_Brk2 = F_Brk select the smallest difference μ_1Util − μ_2Util .
  end
  select the best {F_Brk1, F_Brk2}_Opt = …;
end
plot…;
```

The utilized friction for each axle is calculated $\mu_{iUtil} = \frac{\sqrt{F_{ix}^2 + F_{iy}^2}}{F_{iz}} = \frac{\sqrt{((T_{Emi} + T_{Brki})/Radius)^2 + F_{iy}^2}}{F_{iz}}$;, for $i = 1$ (front axle) and $i = 2$ (rear axle).

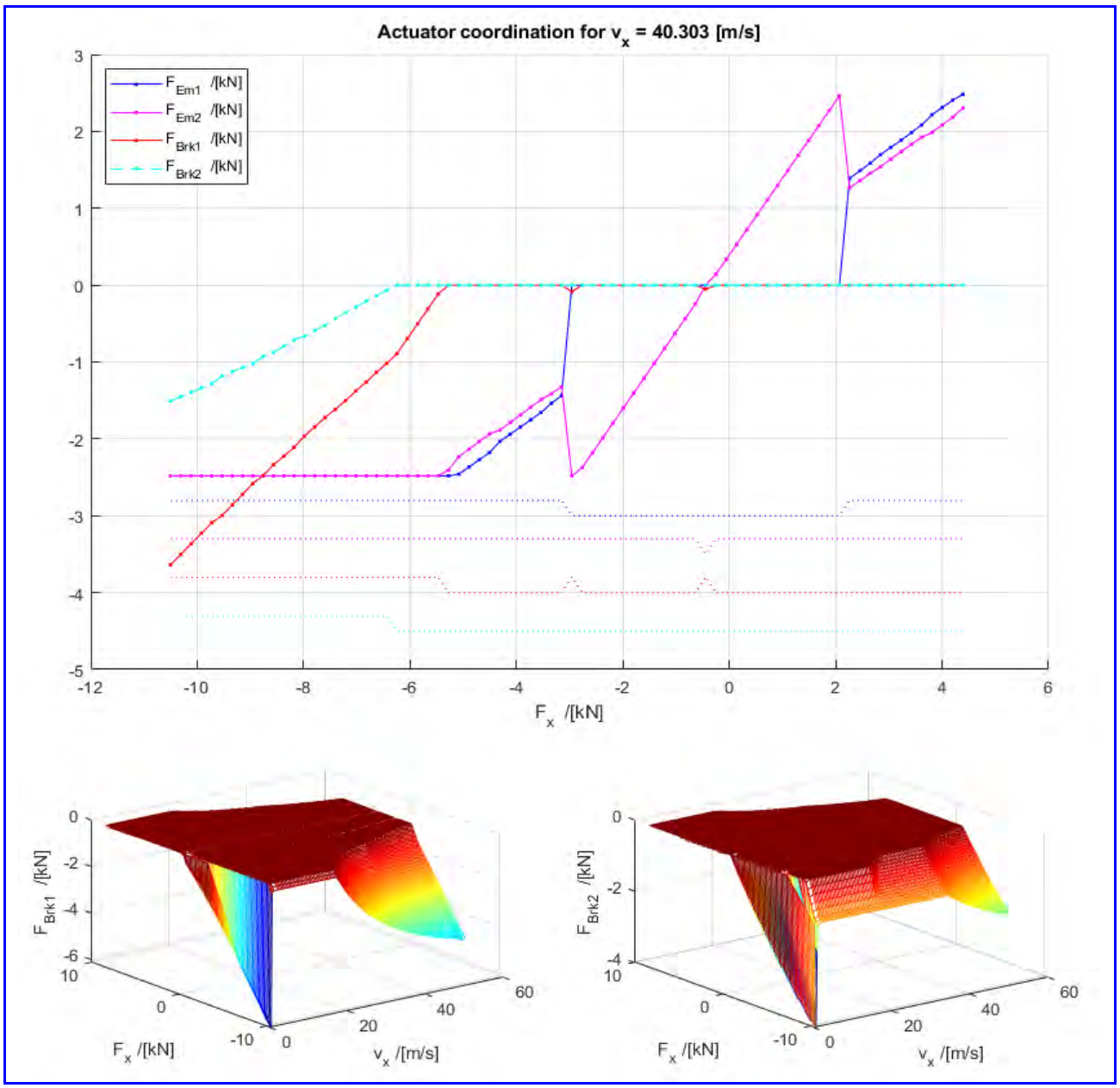


Figure 3-16: Plots of the optimum distribution of friction brake between the two axles. Optimum is here equal friction utilization. Longitudinal driving conditions flat, level ground without aerodynamic forces ($a_x = F_x/m$, $with\ m = 2000\ kg$). Lateral driving conditions $a_y = 2\ m/s^2$.

3.2.3 Transport cost

The attribute behind requirements on energy consumption in 3.2.2 is transport efficiency, which reveals that it is the cost of energy that is important. (Beside this, there are of course also legal requirements which must be met to even sell the vehicle.) One example of significant cost, beside energy cost, is transport time cost. Especially for goods transportation, where the driver salary is rather proportional to time.

3.2.3.1 Definition of quantities

The quantities defined in Table 3.1, can then be duplicated to “cost variants”, see Table 3.2.

Table 3.2: Duplication of quantities in Table 3.1 to "cost variants".

Energy or power quantity from Table 3.1	**"Cost variant"**	**When modelling in physical parts or phenomena,** i
Energy, E_{Cons} • in $[J]$	Cost, $Cost$ • in [€]	$Cost = \sum_{\forall i} Cost_i$;
Energy per distance, EPD • in $[J/m = N]$	Cost per distance, CPD • in $[€/m]$	$CPD = \sum_{\forall i} CPD_i$;
Power, P_{Cons} • in $[J/s = W]$	Cost rate, $CostRate$ • in $[€/s]$	$CostRate = \sum_{\forall i} CostRate_i$;
Power per speed, PPS • in $[(J/s)/(m/s) = J/m = N]$	Cost rate per speed, $CRPS$ • in $[(€/s)/(m/s) = €/m]$	$CRPS = \sum_{\forall i} CRPS_i$;

Note that we model also cost and cost rates, e.g.:

- The energy cost rate for rolling resistance can be modelled as $CostRate_{E,RR} = Pr_E \cdot P_{RR,Loss} = Pr_E \cdot RRC \cdot m \cdot g \cdot v$; where Pr_E is a constant in $[€/J]$.
- The transport time cost rate can be modelled as $CostRate_t = Pr_t \cdot \frac{dt}{dt} = Pr_t$; and
  Then, the transport time cost becomes $Cost_t = \int Pr_t \cdot dt = Pr_t \cdot \int dt = Pr_t \cdot t$;
  where Pr_t is a constant in $[€/s]$.

3.2.3.2 Transport cost for constant operating conditions *

Function definition: ***Transport cost*** *is the cost* [€] *per performed transportation amount. Transportation amount can e.g. be measured in* $[km]$, $[person \cdot km]$, $[ton \cdot km]$, *or* $[m^3 \cdot km]$. *The vehicle operation is defined by a constant speed, including constant road gradient, constant head wind, constant cargo load, constant road surface conditions, etc.*

As for energy consumption, the requirement setting typically refers to a driving cycle or operating cycle, see 3.3.1. In such cycles, the operating conditions varies, and a transport cost for the cycle, can be requirement set.

Finding a cost-optimal constant speed can therefore be quite different from finding an energy-optimal constant speed, as we did in 0. We redo the example from 0, assuming also energy price Pr_E $\left[\frac{€}{kWh}\right]$, time price Pr_t $\left[\frac{€}{h}\right]$, and minimization of cost per distance, CPD instead of energy per distance, EPD.

$$CPD = \frac{Cost}{s_{End} - 0} = \frac{Cost_E + Cost_t}{s_{End} - 0} = \frac{Pr_E \cdot E_{Cons} + Pr_t \cdot \int dt}{s_{End} - 0} =$$
$$= \frac{Pr_E \cdot \int P_{Cons} \cdot dt + Pr_t \cdot t_{End}}{\int v_x \cdot dt} = \frac{Pr_E \cdot P_{Cons} \cdot \int dt + Pr_t \cdot t_{End}}{v_x \cdot \int dt} =$$
$$= \frac{Pr_E \cdot P_{Cons} \cdot \cancel{t_{End}} + Pr_t \cdot \cancel{t_{End}}}{v_x \cdot \cancel{t_{End}}} = \frac{Pr_E \cdot P_{Cons} + Pr_t}{v_x} = Pr_E \cdot \frac{P_{Cons}}{v_x} + \frac{Pr_t}{v_x} =$$
$$= Pr_E \cdot PPS + \frac{Pr_t}{v_x} = CRPS;$$

Instead of Power per speed, PPS, we find Cost rate per speed, $CRPS$.

As when modelling losses of parts or phenomena, it is a challenge to select which parts or phenomena that should be included as costs. Costs for goods transport typically consist of 1/3 energy, 1/3 time and 1/3 wear (maintenance). A motivation to not include the wear in this example is that wear is probably rather proportional to distance, and therefore constant in the optimization of which speed to select.

We should now minimize $CPD = CRPS$.

$$CPD = CRPS = Pr_E \cdot PPS + \frac{Pr_t}{v_x} = \begin{Bmatrix} PPS \text{ from} \\ 0 \end{Bmatrix} =$$

$$= Pr_E \cdot \left(\underbrace{\frac{\rho A c_d}{2} \cdot v_x^2}_{F_x} + \underbrace{RRC \cdot m \cdot g}_{R_{RR,Equiv}} + \underbrace{\frac{P_{EM,Loss}(T,\omega)}{v_x}}_{R_{EM,Equiv}=PPS_{EM}} \right) + \frac{Pr_t}{v_x} ==$$

$$= \underbrace{Pr_E \cdot \left(\underbrace{\frac{\rho A c_d}{2} \cdot v_x^2}_{F_x} + \underbrace{RRC \cdot m \cdot g}_{R_{RR,Equiv}} \right) + \frac{Pr_t}{v_x}}_{varies\ with\ operation\ conditions} + \underbrace{Pr_E \cdot \underbrace{\frac{P_{EM,Loss}(T,\omega)}{v_x}}_{R_{EM,Equiv}=PPS_{EM}}}_{CRPS_{EM}};$$

See Figure 3-17. In the left diagram, we plot the curves for $CRPS_{EM} = CPD_{EM}$ which is independent of the resistance curve. This makes the diagram more useful for any resistance curve, even if one resistance curve is drawn as an example. The right diagram shows the total $CRPS$ for the example resistance curve.

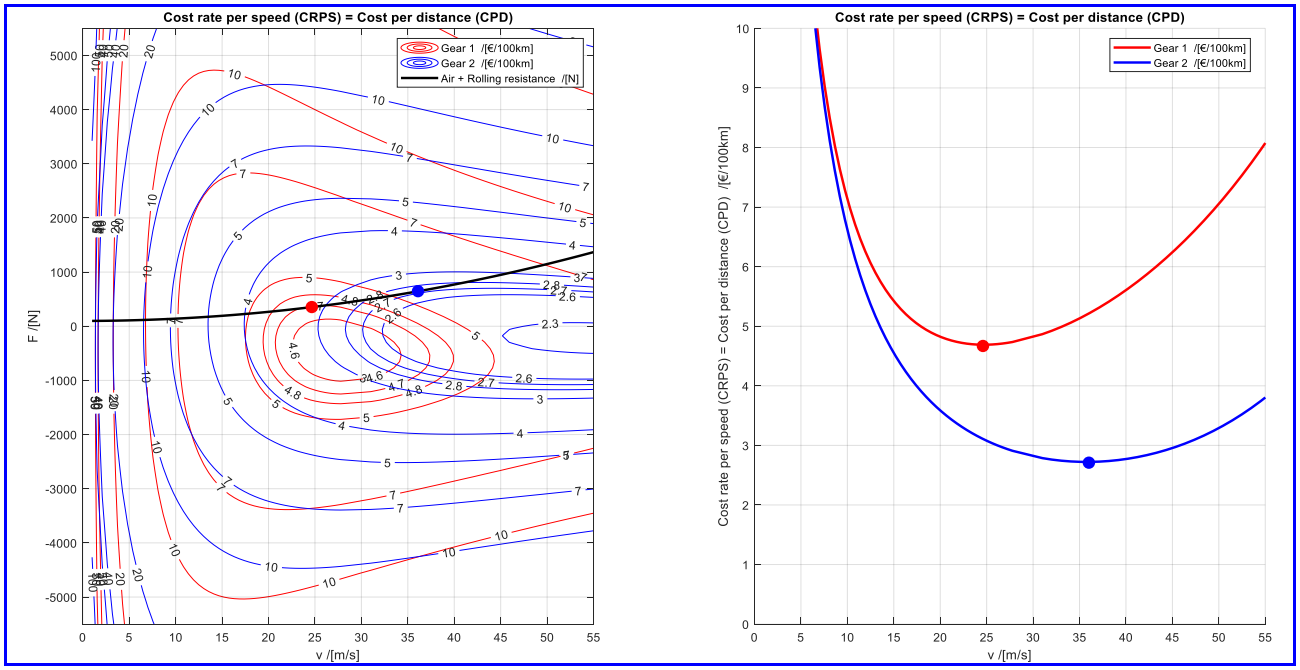


Figure 3-17: Cost rate. Left: Variation in traction diagram with one example of resistance. Right: Variation along resistance curve. Energy price 2€/kWh. Transport time price 2€/h.

3.2.4 Driving resistance

This section describes some parts or phenomena that causes momentaneous power losses (P_{iLoss} $[J/s]$ and PPS_i $[N]$), which causes energy losses over a transport operation (E_{iLoss} $[J]$ and EPD_i $[N/m]$).

3.2.4.1 Resistance from body forces

Some losses can be identified as true forces, visible directly in a free body diagram and measurable in a real vehicle, i.e. their Energy loss per distance, $EPD = R_{Equiv}$ comes from physical forces acting on the vehicle body counter-directed to the route direction. Such are forces from gravity due to road grade and aerodynamic resistance.

Another way to approach this is to study Figure 3-2 and extrapolate that a very low transmission ratio, i.e., a very high gear, we would enable infinite speed, which of course is not realistic. This is because "driving resistance force" is missing in Figure 3-2. Such force can be added to traction diagram as a curve that typically increases with speed. The top speed is found as the intersection between propulsion curve and driving resistance force curve, see Figure 3-18.

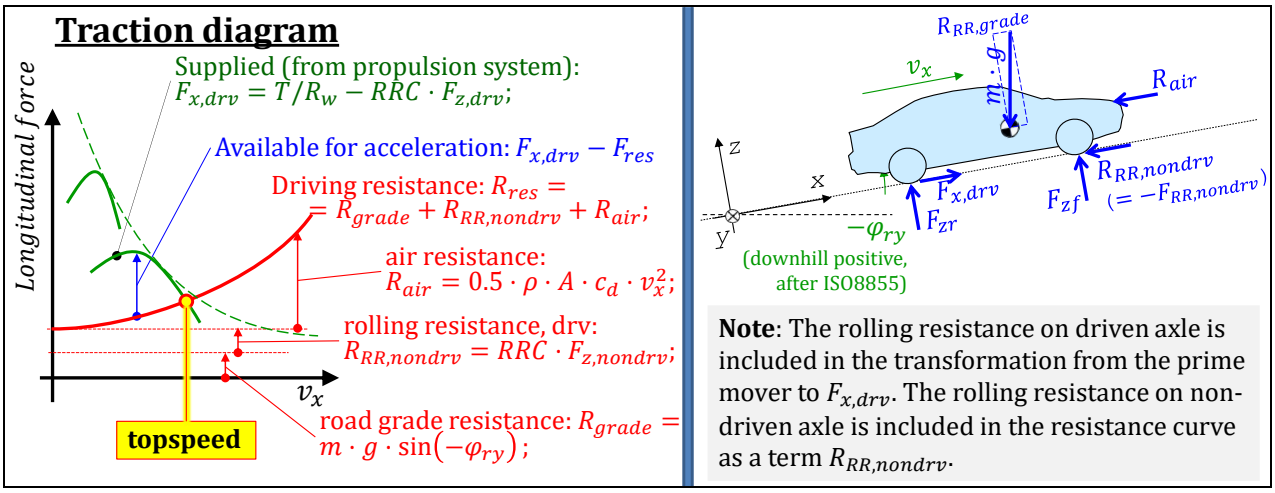


Figure 3-18: Traction diagram. Head wind speed, $v_{wind,x}$, is assumed to be zero. See also Figure 3-28.

One part of the driving resistance force comes from driving uphill: the grade or gravitational load on the vehicle. This is negative when driving down-hill. There is also aerodynamic driving resistance force, see Eq [2.91]. Grade and aero-dynamic resistance are body forces.

3.2.4.2 Rolling resistance

Rolling resistance is a phenomenon that generates a power loss ($P_{RR,Loss}$). Rolling resistance is not a longitudinal force on the vehicle body, but a torque on each wheel i: $F_{ix} = T_i - RRC \cdot F_{iz}$;.

We can express rolling resistance as a power loss per speed (PPS_{RR}) which can be seen as an equivalent resistance force ($R_{RR,Equiv}$). But note, it is **not** a body force as those described in 3.2.4.1.

However, for a non-driven wheel, the rotational equilibrium of the wheel leads to a small negative longitudinal force in tyre-to-road contact. So, rolling resistance can be included in traction diagram in either the "supply" or resistance curve. If one want to use the traction diagram to show the friction limit where a wheel start to spin, $F_{ix} > \mu \cdot F_{iz}$ as in 3.2.9, it is explaining to include rolling resistance in supply curve for driven wheels, but in the resistance curve for the non-driven wheels. In the following, rolling resistance is represented as a torque on driven wheels (which lowers the supply curve) and a longitudinal force on non-driven wheels (which lifts the resistance curve). The traction diagram can then also host a curve for friction limit for spinning driven wheels, as in Figure 3-28.

$$R_{res} = R_{roll} + m \cdot g \cdot \sin(-\varphi_y) + \frac{1}{2} \cdot c_d \cdot \rho \cdot A \cdot (v_x - v_{wind,x})^2;$$

$$R_{roll} = \sum_{\text{non-driven wheels}} RRC \cdot F_{wheel,z};$$

If all wheels are undriven: $R_{roll} = RRC \cdot m \cdot g \cdot \cos(\varphi_y)$;

[3.3]

As seen in Figure 3-18, the supply and resistance curves are drawn in same diagram. The resulting intersection identifies the top speed of the vehicle. This is a stable point in the diagram, so the vehicle condition at top speed is for steady state (no acceleration).

Figure 3-18 also shows that the acceleration divided by the mass can be identified as a vertical measure in the traction diagram. However, one should be careful when using the traction diagram for more than steady state driving. We will come back to acceleration performance later, after introducing the two effects "Load transfer" and "Rotating inertia effect".

3.2.4.3 Tyre slip losses

3.2.4.3.1 Power losses due to negative wheel torque

When negative wheel torque is required, one can either apply this wheel torque with energy dissipation (friction brakes, engine brake, retarder) or with electric propulsion system.

In the first case, there is only losses: $P_{loss} = -T_{Brk} \cdot \omega > 0$;.

In the latter case, ideally, the whole power $-T_{Prop} \cdot \omega > 0$ is recovered to the energy buffer and $P_{loss} = 0$. But, more realistically, only $-(1-\eta) \cdot T_{Prop} \cdot \omega$ is recovered and $P_{loss} = -\eta \cdot T_{Prop} \cdot \omega > 0$; where η is the efficiency for power transmission from translational to rotational and $\eta < 1$. If applying large negative torque, there will be slip losses will make η decrease. In extreme, if such large negative wheel torque is applied that the wheel start rotates rearwards, $\omega \cdot v_x < 0$, power will both be extracted from buffer and the loss will be: $P_{loss} = T_{Prop} \cdot \omega = negative \cdot negative > 0$.

3.2.4.3.2 Power losses due to longitudinal tyre slip

Tyre slip causes power losses, 0. In this section we consider only tyre-longitudinal slip.

Consider a vehicle with $N \geq 3$ wheels. Assume a certain vehicle speed v_x and a certain desired propulsion force $F_x = \sum_{i=1..N}(T_i/R_w)$. Also assume that wheel torques T_i can be distributed according to $N-1$ equations, e.g., $T_1 = T_2; T_3 = T_4 = 0$; for a conventional front axle driven 4-wheeled car. Also assume same longitudinal stiffness coefficient CC_x on all wheels and that out-of-road-plane equilibria and suspension equations defines the vertical forces $F_{1z}..F_{Nz}$. Using Eq [2.81], and assuming all tyres same $CC_{ix} = CC_x$, the power loss due to longitudinal tyre slip can be expressed as:

$$P_{loss,x} \approx CC_x \cdot \sum_{i=1:N}\left(s_{ix}^2 \cdot F_{iz} \cdot |v_{ixw}|\right) \approx CC_x \cdot \sum_{i=1:N}\left(s_{ix}^2 \cdot F_{iz}\right) \cdot |v_x|;$$

where LSRC can be identified: $P_{loss,x} = \underbrace{\frac{CC_x}{m \cdot g} \cdot \sum_{i=1:N}\left(s_{ix}^2 \cdot F_{iz}\right)}_{LSRC} \cdot m \cdot g \cdot |v_x|;$

Or, less dependent of the definition of slip, using $F_{ix} = CC_x \cdot F_{iz} \cdot s_{ix}$:

$$P_{loss,x} \approx \frac{1}{CC_x} \cdot \sum_{i=1:N}\left(F_{ixw}^2 \cdot F_{iz} \cdot |v_{ixw}|\right) \approx \frac{1}{CC_x} \cdot \sum_{i=1:N} \frac{F_{ixw}^2}{F_{iz}} \cdot |v_x|;$$

where LSRC can be identified: $P_{loss,x} = \underbrace{\frac{1}{m \cdot g \cdot CC_x} \cdot \sum_{i=1:N} \frac{F_{ix}^2}{F_{iz}}}_{LSRC} \cdot m \cdot g \cdot |v_x|;$

[3.4]

Longitudinal Slip Resistance Coefficient $LSRC$ is a variable such that the additional power due to longitudinal slip is $LSRC \cdot m \cdot g \cdot v_x$. The $LSRC$ for an axle is comparable with the mean rolling resistance coefficient RRC for on an axle. A difference is that $LSRC$ is a loss of rotational speed, while RRC is a torque loss.

An example with a fore-aft-symmetric 2-axle vehicle, propelled on one axle gives:

$$P_{loss,x} = \frac{1}{CC_x} \cdot \left(F_x^2 \cdot \frac{1}{m \cdot g/2} + 0\right) \cdot |v_x| = \underbrace{\frac{2}{CC_x} \cdot \left(\frac{F_x}{m \cdot g}\right)^2}_{LSRC} \cdot m \cdot g \cdot |v_x|;$$

The same vehicle, but propelled equally much on both axles gives:

$$P_{loss,x} = \frac{1}{CC_x} \cdot \left(F_x^2 \cdot \frac{1}{m \cdot g/2} + F_x^2 \cdot \frac{1}{m \cdot g/2}\right) \cdot |v_x| = \underbrace{\frac{1}{CC_x} \cdot \left(\frac{F_x}{m \cdot g}\right)^2}_{LSRC} \cdot m \cdot g \cdot v_x;$$

So, only half as much energy is lost due to longitudinal tyre slip if propelling on 2 axles instead of 1.

If one uses same one-axle driven vehicle but distribute the same gross weight on a non-driven trailer. First consider a vertical-force-free coupling, as a truck with a full trailer:

$$P_{loss,x} = \frac{1}{CC_x} \cdot \left(F_x^2 \cdot \frac{1}{m \cdot g/4} + 0 + 0 \right) \cdot |v_x| = \underbrace{\frac{4}{CC_x} \cdot \left(\frac{F_x}{m \cdot g} \right)^2}_{LSRC} \cdot m \cdot g \cdot v_x;$$

Then, consider a vertical-force-carrying coupling, as a (rear axle driven) tractor with semitrailer:

$$P_{loss,x} = \frac{1}{CC_x} \cdot \left(F_x^2 \cdot \frac{1}{m \cdot g/4 + m \cdot g/4} + 0 + 0 \right) \cdot |v_x| = \underbrace{\frac{2}{CC_x} \cdot \left(\frac{F_x}{m \cdot g} \right)^2}_{LSRC} \cdot m \cdot g \cdot |v_x|;$$

Then, generalise by using $F_{Drivenx}/F_{Drivenz} = \mu_{DrivenUtil}$ and $F_{Drivenz}/(m \cdot g) = Fraction_{Drivenz}$:

$$P_{loss,x} = \frac{1}{CC_x} \cdot \left(\frac{F_{Drivenx}^2}{F_{Drivenz}} + 0 \right) \cdot |v_x| = \frac{1}{CC_x} \cdot \left(\frac{F_{Drivenx}}{F_{Drivenz}} \right)^2 \cdot \frac{F_{Drivenz}}{m \cdot g} \cdot m \cdot g \cdot |v_x| =$$

$$= \underbrace{\frac{\mu_{DrivenUtil}{}^2 \cdot Fraction_{Drivenz}}{CC_x}}_{LSRC} \cdot m \cdot g \cdot |v_x|;$$

If comparing common heavy vehicles with passenger vehicles, also taking into account that CC_x is typically half for heavy vehicles, the $LSRC$ is generally 2..4 times larger for the heavy vehicles. The difference can be even larger as the weight often needs to be carried by more axles, whereof only one is driven. However, typically, $LSRC$ is in the magnitude of only a percent of RRC.

3.2.4.3.3 Power losses due to lateral tyre slip

(This section requires knowledge from Chapter 4 for full understanding.)

Tyre slip causes power losses, 0. In this section we consider only tyre-lateral slip.

The tyres lateral slip can add driving-resistances compared to what is included in Eq [3.3]. Some driving conditions relevant for assessing energy consumption are covered in the following sections.

3.2.4.3.3.1 Driving straight with wheel toe-angle

An axle i with $\delta_{ToeIn} = \delta_r - \delta_l = 2 \cdot \delta_i$ when driving straight gives rise to the following power loss due to the lateral tyre forces:

$$P_{i,loss} \approx \{symmetry\} \approx 2 \cdot \min\left(CC_y \cdot s_{ijyt}^2,\ \mu \cdot |s_{ijyt}|\right) \cdot F_{iz} \cdot |v_{ixv}| =$$

$$= \underbrace{2 \cdot \min\left(CC_y \cdot \left(\frac{\delta_{ToeIn}}{2} \right)^2,\ \mu \cdot \frac{\delta_{ToeIn}}{2} \right)}_{TRC} \cdot F_{iz} \cdot |v_{ixv}|; \qquad [3.5]$$

Toe Resistance Coefficient TRC is such that the additional power due to cornering is $TRC \cdot m \cdot g \cdot v_x$. The TRC is defined for an axle, per wheel. It is comparable with the mean value of the rolling resistance coefficient RRC for two wheels on an axle. A difference is that TRC is a speed loss, while RRC is a torque loss.

The friction saturation (μ dependency) only becomes active if very slippery road and stiff tyres, e.g., $\mu = 0.1$ and $CC_y = 25$ and $|\delta_{ToeIn}| >\approx 0.5\ deg$, which is a large toe angle.

Similar power losses due to (wheel and road) *camber* can be found. They are also per axle, not per wheel or per vehicle.

3.2.4.3.3.2 Steady state turning with single unit with Ackermann

Similar as in 3.2.4.3.3.1, power losses from lateral tyre slip, caused by non-Ackermann geometry, can be found during turning. For single units, it can be studied for steady state, i.e. constant radius and constant speed. In many cases, the models can be used also as momentaneous power loss during slowly varying radius or speed. Low speed turning fall out as a special case of high speed turning, because centrifugal force will approach zero when $a_y = v_x^2/R$ approaches zero.

First we take the example of a two-axle vehicle, studied with a one-track model. It has, intrinsically, Ackermann geometry.

On the tyre level, we will use the power loss model in2.2.10. On the vehicle level, we will use 4.3.7.3.1. When combined, it is important to differ between the tyre slip stiffness C_{iyTyre} and the axle slip stiffness C_{iyTot}.

Power Losses (from Eq [2.75]): $$P_{loss,y} = \left(\frac{F_{fy}^2}{C_{fyTyre}} + \frac{F_{ry}^2}{C_{ryTyre}}\right) \cdot |v_x| = \left(\frac{F_{fy}^2}{CC_y} \cdot \frac{1}{F_{fz}} + \frac{F_{ry}^2}{CC_y} \cdot \frac{1}{F_{rz}}\right) \cdot |v_x| = \\ = \frac{L}{CC_y \cdot m \cdot g} \cdot \left(\frac{F_{fy}^2}{l_r} + \frac{F_{ry}^2}{l_f}\right) \cdot |v_x|;$$

Note that the model with CC instead of C is used in the following, to include the influence from vertical tyre force.

Vehicle model (from 4.3.7.3.1).

Solving both the models, tyre and vehicle, as one system of equations gives:

$$P_{Loss,y} = \frac{C_{fyTyre} \cdot l_f^2 + C_{ryTyre} \cdot l_r^2}{C_{fyTyre} \cdot C_{ryTyre} \cdot L^2} \cdot m^2 \cdot v_x^3 \cdot \omega_z^2 = \\ = \underbrace{\frac{C_{fyTyre} \cdot l_f^2 + C_{ryTyre} \cdot l_r^2}{C_{fyTyre} \cdot C_{ryTyre} \cdot L^2} \cdot \frac{m \cdot v_x^2 \cdot \omega_z^2}{g}}_{CRC} \cdot m \cdot g \cdot v_x; \quad [3.6]$$

or

$$P_{Loss,y} = \frac{m \cdot v_x^3 \cdot \omega_z^2}{CC_y \cdot g} = \underbrace{\frac{1}{CC_y} \cdot \left(\frac{v_x \cdot \omega_z}{g}\right)^2}_{CRC} \cdot m \cdot g \cdot v_x = \underbrace{\frac{1}{CC_y} \cdot \left(\frac{v_x^2}{R_p \cdot g}\right)^2}_{CRC} \cdot m \cdot g \cdot v_x;$$

Cornering Resistance Coefficient $CRC = PPS_{TyreLatSlip,Loss}/(m \cdot g)$ gives the additional propulsion power due to cornering. The CRC for a vehicle is comparable with the mean rolling resistance coefficient RRC for all wheels on a vehicle. A difference is that CRC is a loss of rotational speed, while RRC is a torque loss.

Note that the expression for $P_{loss,y}$ does neither contain β_i, δ_{sw} nor distribution of steering angle between axles. This should be understood as that, for each operating condition $\{v_x, \omega_z\}$, the driver will steer with a specific δ_{sw} and the vehicle will run with a specific β.

During a transport operation, the cornering in each time instant is typically described by two variables, e.g. $\{v_x, R_p\}$, but only the combined scalar measure $a_y \approx v_x \cdot \omega_z \approx v_x^2/R_p$ influences CRC. Hence, we can plot the graph in Figure 3-19.

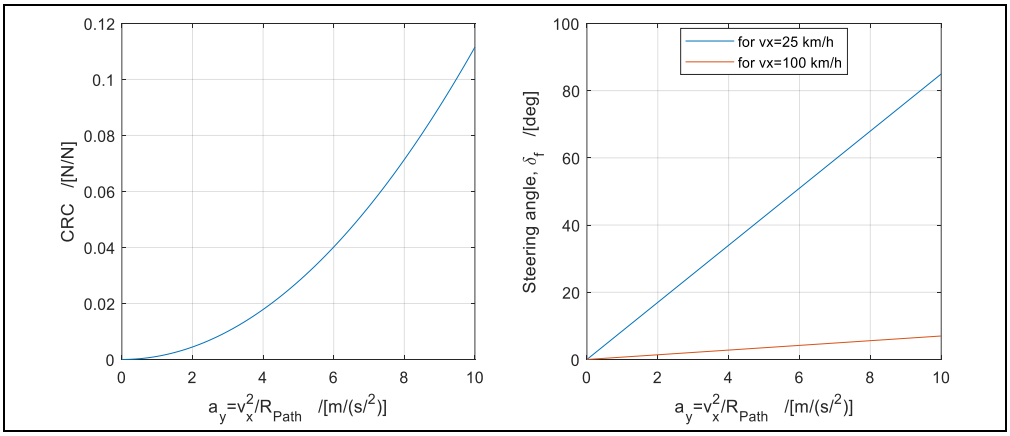


Figure 3-19: Left: Cornering Resistance Coefficient. Right: Required steer angle. Vehicle data: $m = 1500\ kg$; $L = 3$; $l_f = 1.25$; $C_f = 60\ [kN/1]$; $C_r = 80\ [kN/1]$.

Notes:

- We see no influence of path radius R_p and longitudinal velocity v_x, only from a_y, which is built up by both as $a_y = v_x^2/R_p$.
- The model used above is not advanced enough to differ between which axle is driven. For such purpose, one would need e.g., the model in Figure 4-16.
- Normal driving is often below 2 or 3 m/s^2, so the coefficient typically stays below 0.01. So, the influence on energy consumption, during such "maximum normal" negotiation of corners, is still of the same magnitude as rolling resistance coefficient $RRC \approx 0.005..0.010$.
- For ideally tracking axles, see 2.2.7, $C_f \to \infty$ and $C_r \to \infty$, which gives that $f_{CRC} \to 0$ and consequently no power loss and no required propulsion force. Therefore, high cornering stiffness is fuel efficient when cornering.
  When driving extreme cornering, such as driving as fast as possible in a circle on a test-track, one will experience that the top speed is much lower than driving straight ahead. To explain that one has to include combined tyre slip.

To take the tyre lateral slip losses into account in energy consumption over a transport task, one would need to find out how it affects the torque and rotational speed on the wheels $\{T_{Whl}, \omega_{Whl}\}$. For this, we need a more detailed model where we know which wheels are driven, etc. However, for a one-wheel model (which is often used in energy computations) and normal driving (far from tyre friction limit and far from large lateral load transfer), we can approximate by no effect on ω_{Whl} and the following effect on T_{Whl}, using Eqs [3.4] and [3.6]:

$$T_{Whl} = \underbrace{F_x \cdot R_{Whl}}_{Accel,Grade,Air} + \underbrace{RRC \cdot R_{Whl} \cdot F_z}_{Rolling\ resistance} + \underbrace{\frac{F_x^2}{CC_x \cdot F_z} \cdot \left|\frac{v_x}{\omega_{Whl}}\right|}_{Long.TyreSlip} + \underbrace{\frac{F_z}{CC_y} \cdot \left(\frac{v_x^2}{R_p \cdot g}\right)^2 \cdot \left|\frac{v_x}{\omega_{Whl}}\right|}_{Lat.TyreSlip}; \quad [3.7]$$

For most driving cycles, additional term from the lateral tyre slip becomes neglectable. Note that this statement is about single unit vehicles with Ackermann geometry.

3.2.4.3.4 Power losses due to combined tyre slip

(This section requires knowledge from Chapter 4 for full understanding.)

Tyre slip causes power losses, 0. In this section we consider all slip, i.e., combined tyre-longitudinal and tyre-lateral slip.

Combined slip losses can appear in all vehicle operation conditions as covered in 3.2.4.3.2 and 3.2.4.3.3, but in the following we only study the extension with longitudinal tyre slip to 3.2.4.3.3.2 Steady state turning .

3.2.5 Functions after start

Figure 3-25 shows how the functions can be found in a traction diagram.

3.2.5.1 Top speed *

*Function definition: **Top speed** is the maximum longitudinal forward speed the vehicle can reach and maintain on level and rigid ground without headwind.*

Top speed is the speed where the sum of all driving resistance terms is equal to the available propulsion forces.

3.2.5.2 Gradeability *

Function definition: ***Grade-ability*** *is the maximum grade that a vehicle is capable to maintain the forward motion on an uphill road at a certain constant speed, at a certain road friction level and with a certain load. (from Reference (Kati, 2013))*

For vehicles with high installed propulsion power per weight, the road friction can be limiting, but this is not visualised in Figure 3-25. Since the speeds are higher than for start-ability, the air resistance cannot be neglected.

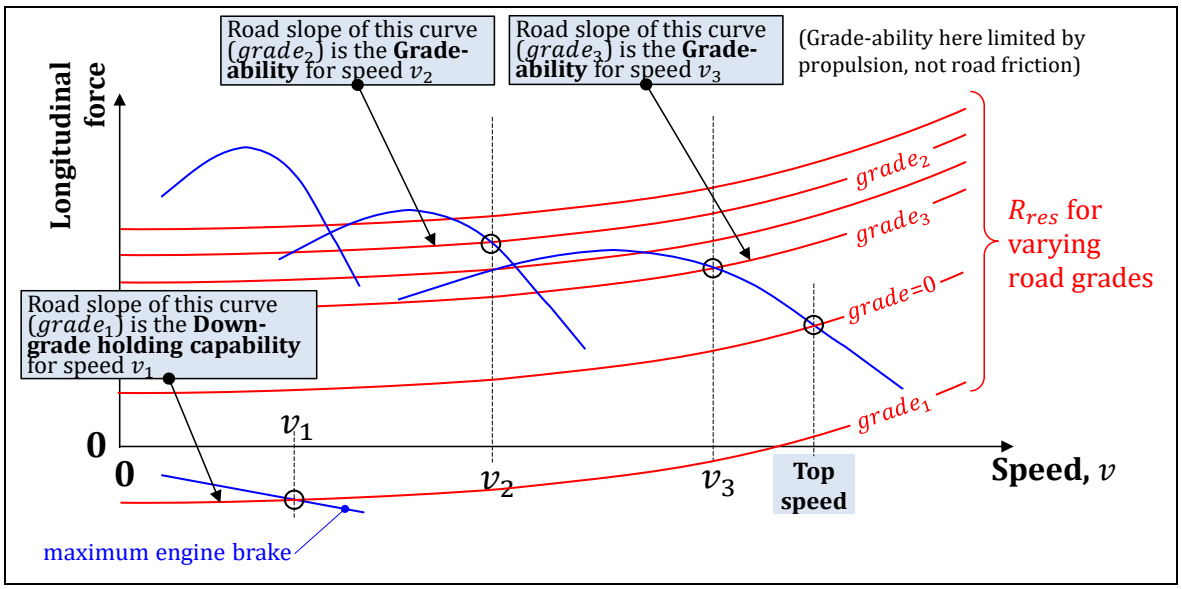


Figure 3-25: How Top speed, Gradeability and Down grade holding capability is read-out from Traction diagram.

3.2.5.3 Down-grade Holding Capability *

Function definition: ***Down-grade holding capability*** *is defined as the maximum down-grade in which the vehicle with certain weight is able to maintain a certain speed without using friction brakes.*

The function is typically of interest for heavy trucks and certain typical certain weight and certain speed is payload corresponding to maximum allowed weight and 80 km/h downhill.

The function is defined assuming there are clear friction brakes and other brakes, where the other brakes are typically engine brake and retarders. For newer vehicle concepts having electric propulsion, also regenerative braking via reversed electric propulsion motors can be discussed to be allowed. However, because sometimes the energy storage will be full so that regenerative braking cannot be applied. Also, a small energy storage will have a limited downhill length, which might call for also prescribing a certain downhill distance.

3.2.5.4 Constant Operating Conditions Energy Consumption *

Function definition: ***Constant Operating Conditions Energy (or Fuel) Consumption*** *is the amount of energy* $[J]$ *(or fuel* $[kg]$ *or* $[litre]$*) consumed by the vehicle per performed transportation amount in constant operating conditions (speed, road grade, wind, ambient temperature, etc.). Transportation amount can e.g. be measured in km,* $km, person \cdot km, ton \cdot km,$ *or* $m^3 \cdot km$.

Vehicles are typically defined for typically varying operating conditions. So, the function is not often so relevant to set requirements on. But for some uses, such as long transports on flat road and relatively constant speeds it is a relevant and simple function to set requirements on.

A closely related function is:

> *Function definition:* ***Constant Operating Conditions Minimum Energy (or Fuel) Consumption Speed*** *is the speed* $[m/s]$ *where energy consumption* $[J/m = N]$ *is as lowest. Constant operating conditions (speed, road grade, wind, ambient temperature, etc.) has to be defined.*

3.2.6 Starting (the vehicle) with Slipping Clutch

This section is about when the vehicle should be started from stand-still and the prime mover is an ICE and is on.

As seen in previous traction diagrams for an ICE, there is no available positive propulsion force at zero speed. This means that the diagram can still not explain how we can start a vehicle from stand-still.

The concepts in Figure 3-1 were used to create the force-velocity diagram in

Figure 3-26. It shows the smooth curve of a Continuously Variable (ratio) Transmission (CVT) in comparison to the stepped transmission. The CVT is the ideal situation for the engine since it can always let the engine work at a maximum power or minimum fuel consumption (minimum for the momentarily required power). If the CVT has unlimited high ratio, it can actually have a non-zero propulsion force at zero vehicle speed. Without losses, this force would be infinite, but in reality, it is limited, but still positive, so the vehicle can start from stand-still.

A stepped transmission, as well as a CVT with limited ratio range, instead needs a clutch to enable starting from vehicle stand-still. This is shown in Figure 3-26. The highest force level on each curve can be reached at all lower vehicle speeds, because the clutch can slip. It requires the clutch to be engaged carefully to the torque level just below the maximum the engine can produce. In traditional automatic transmissions, the slipping clutch is replaced with a hydrodynamic torque converter, to enable start from stand-still.

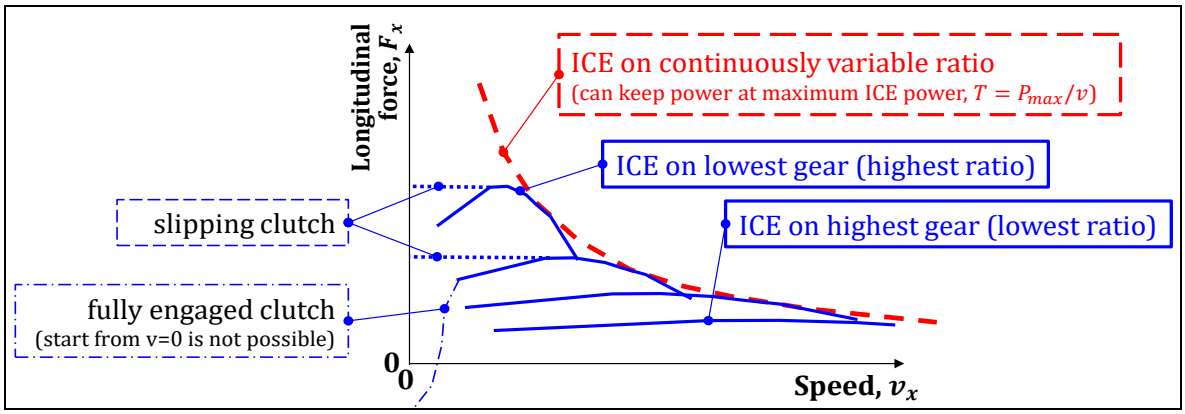


Figure 3-26: Force/Speed Curves for a Multiple Gear Transmission and for CVT.

3.2.7 Starting (an ICE) with starter (start motor) at vehicle stand-still

This section is about when vehicle is in stand-still and the prime mover is an ICE and is off but should be started.

An ICE can only output power on its shaft if it has a rotational speed within a certain range on the positive part of the speed axis, see Figure 2-99. Therefore, the vehicles are typically equipped with a starter (start motor) or, in older times, a crank for manually adding power.

Traditionally, cars and heavy trucks have the starter before the clutch. With that design, the ICE can be cranked without putting the gearbox in neutral. However, (one-track) two-wheelers typically have the starter (or crank) after the clutch. This forces the driver to put the gear in neutral before cranking. This reduces the risk of unintended accelerations of the vehicle which is less controllable on a (one-track) two-wheeler than in a two-track vehicle. Such a design consideration is an example of safety case, see 1.4.5.

3.2.8 Steady State Vertical Force Distribution between Axles

The vehicle performance discussed previously does not rely on knowing the distribution of (vertical) load between the axles. To be able to introduce limitations due to road friction, this distribution must be known. Hence, we set up the free-body diagram in Figure 3-27.

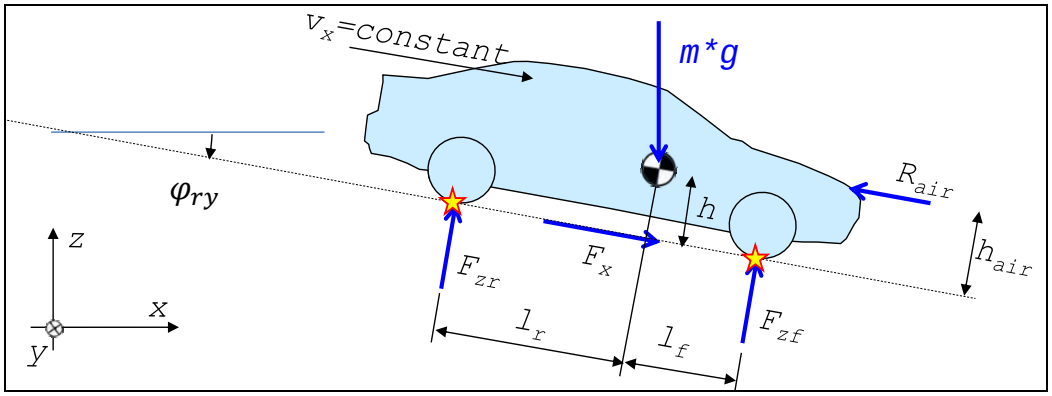


Figure 3-27: Free Body Diagram for steady state vehicle. With ISO coordinate system, the road gradient is positive when downhill. (Rolling resistance force on non-driven axles is included in F_x.)

From the free-body diagram we can set up the equilibrium equations as follows and derive the formula for load on front and rear axle:

Moment equilibrium, around rear contact with ground (✯):

$$m \cdot g \cdot \left(l_r \cdot \cos(\varphi_{ry}) + h \cdot \sin(\varphi_{ry})\right) - R_{air} \cdot h_{air} - F_{zf} \cdot (l_f + l_r) = 0; \Rightarrow$$

$$\Rightarrow F_{zf} = m \cdot g \cdot \frac{l_r \cdot \cos(\varphi_{ry}) + h \cdot \sin(\varphi_{ry})}{l_f + l_r} - R_{air} \cdot \frac{h_{air}}{l_f + l_r}$$

Moment equilibrium, around front contact with ground (✯):

$$F_{zr} \cdot (l_f + l_r) - m \cdot g \cdot \left(l_f \cdot \cos(\varphi_{ry}) - h \cdot \sin(\varphi_{ry})\right) - R_{air} \cdot h_{air} = 0; \Rightarrow$$

$$\Rightarrow F_{zr} = m \cdot g \cdot \frac{l_f \cdot \cos(\varphi_{ry}) - h \cdot \sin(\varphi_{ry})}{l_f + l_r} + R_{air} \cdot \frac{h_{air}}{l_f + l_r}$$

[3.10]

For most vehicles and reasonable gradients, one can neglect $h \cdot \sin(\varphi_{ry})$ since it is $\ll \left|l_f \cdot \cos(\varphi_{ry})\right| \approx \left|l_r \cdot \cos(\varphi_{ry})\right|$.

3.2.9 Friction Limit

With a high-powered propulsion system, there is a limitation to how much the vehicle can be propelled, due to the road friction limit. It is the normal load and coefficient of friction, which limits this. For a vehicle which is driven only on one axle, it is only the normal load on the driven axle, $F_{z,driven}$, that is the limiting factor:

$$F_x = \min\left(F_{x,PropSyst}\ ;\ \mu \cdot F_{z,driven}\right) \qquad [3.11]$$

One realises, from Figure 2-24, that the rolling resistance on the driven axle works as a torque loss and that the road friction limitation will be limiting $T_{eng} \cdot ratio - e \cdot F_{z,driven}$ rather than limiting $T_{eng} \cdot ratio$. Expressed using the rolling resistance coefficient, f_{roll}, gives:

$$F_x = \min\left(F_{x,PropSyst}\ ;\ \mu \cdot F_{z,driven}\right) = \min\left(\frac{T_{eng} \cdot ratio}{radius} - f_{roll} \cdot F_{z,driven}\ ;\ \mu \cdot F_{z,driven}\right) \quad [3.12]$$

This is shown in the traction diagram in Figure 3-28, where it should also be noted that the rolling resistance curve only consists of the rolling resistance on the non-driven axles. See also Figure 2-24.

3.2.10Start Functions

3.2.10.1 Start-ability *

*Function definition: **Start-ability** is the maximum grade that a vehicle is capable to start in and maintain the forward motion at a certain road friction level and a certain load. (Reference (Kati, 2013))*

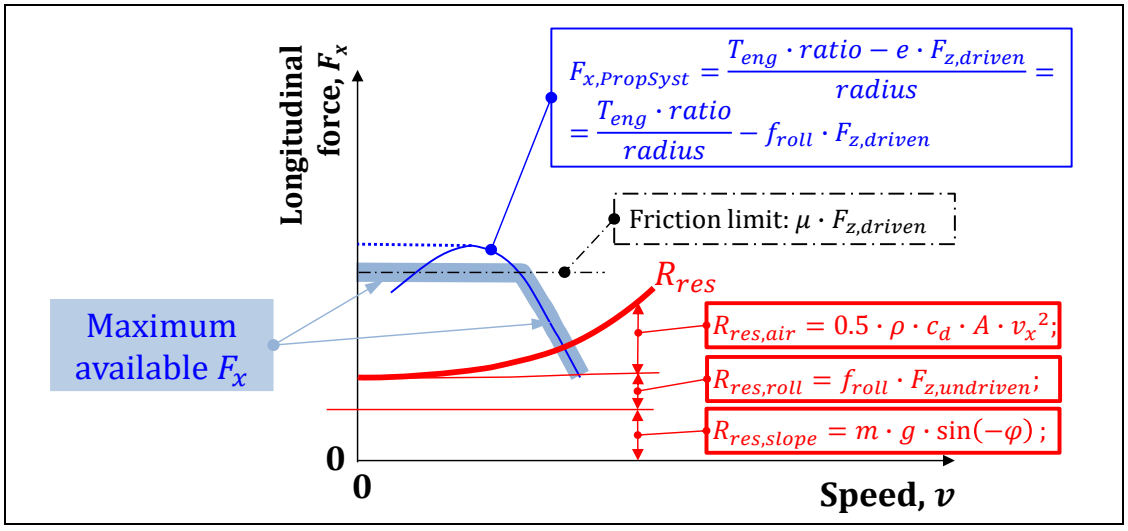


Figure 3-28: Traction diagram with Road Friction limitation and Driving Resistance curves.

Figure 3-29 shows how we find the start-ability in the traction diagram. There are two phenomena that can limit start-ability: propulsion system or road friction. Also, in each case, we can theoretically reach somewhat higher start-ability by allowing clutch or tyre to slip. However, in practice the start-ability has to require "forward motion without significant slip in clutch or tyre", because there will be a lot of wear and heat in the slipping clutch or tyre. Hence, the lower curves in Figure 3-29 are used. The reduction is however very small, since the resistance curves does not change very much in this speed interval (the resistance curves in the figure have exaggerated slope; the air resistance can typically be neglected for start-ability).

However, the energy loss (heat, wear) in clutch and tyre should be limited also **during the starting sequence**. This can limit the start-ability more severely than the slope of the resistance curves, but it cannot be shown in the traction diagram, since it is limited by energy losses in clutch or tyre, which is a time integral of $T \cdot \omega_{clutch}$ and $T_{wheel} \cdot \omega_{wheel}$. There can also be quite other limitations of start-ability, such as deliberately limited engine torque at low gears, to save drive shafts.

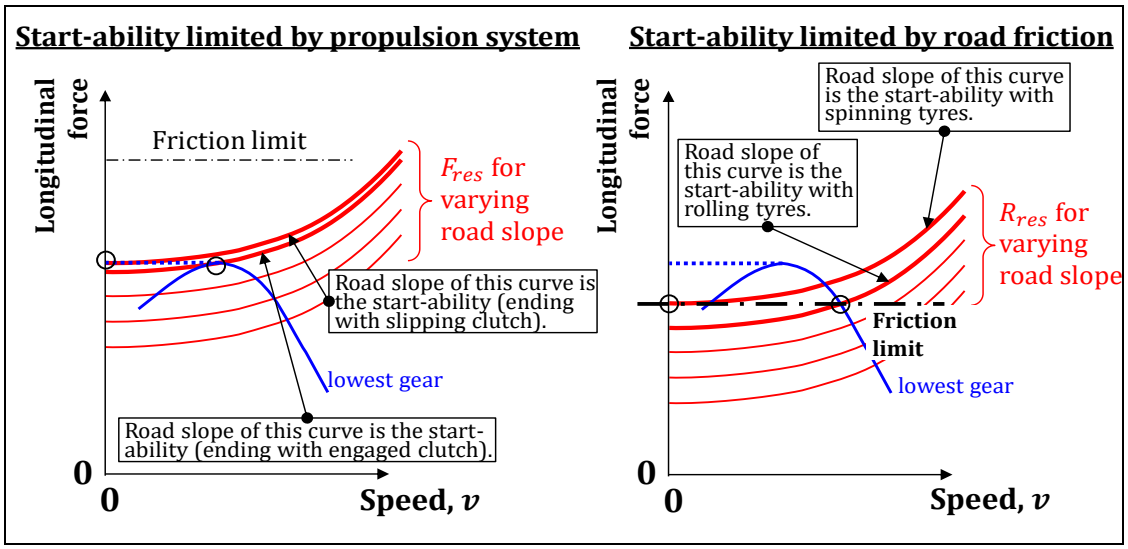


Figure 3-29: How Start-ability is read-out from Traction diagram.

3.2.10.2 Towing Capacity *

*Function definition: **Towing capacity** is the maximum vehicle-external longitudinal force the vehicle can have on its body and start and maintain a certain forward speed at a certain road friction and a certain up-hill gradient.*

The driving situation for defining towing capacity is similar to the one for defining grade-ability. Towing capacity describes how much load the vehicle can tow, P_x in Figure 3-30, on a certain up-hill gradient. Since towing a load is more relevant as part of a longer transport mission, it is normally also for a particular constant speed, typically in range 80 to 100 km/h. Since the speed is that large, the air resistance may not be neglected. It is also important consider air resistance of the trailer and that axle loads can change, which changes both friction limitation and rolling resistance. A free-body diagram is shown in Figure 3-30. It is noticeable, that there can also be an additional air resistance of the trailer which will influence in a test of Towing capacity.

For pure off-road vehicles and agriculture tractors, the term "towing" can mean the maximum pulling force at very low forward speeds at level ground. This is related but different to the above described towing capacity for road vehicles.

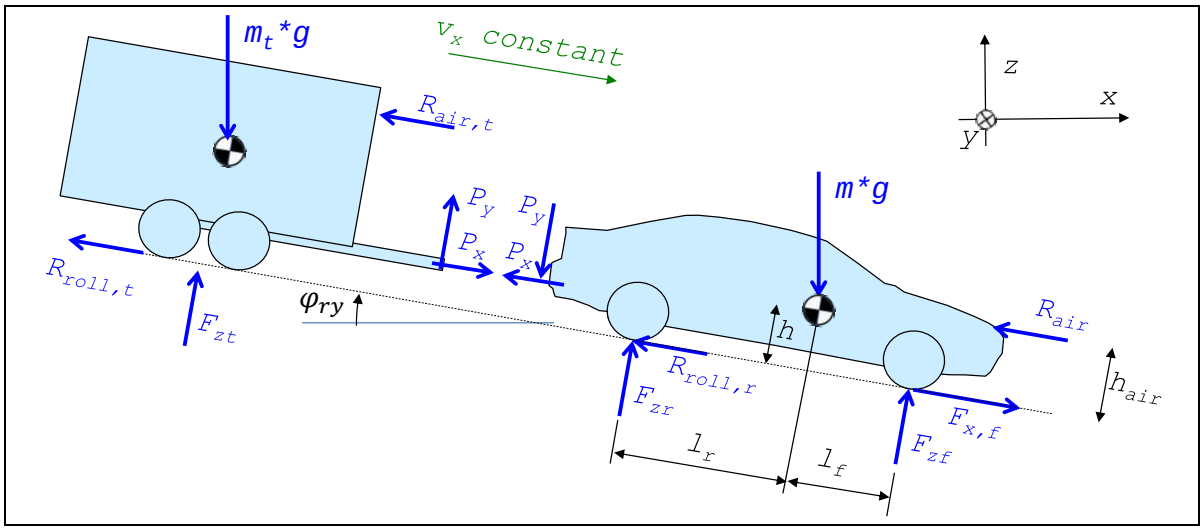


Figure 3-30: Towing Loads. The towing vehicle is front axle driven.

3.3 Functions for (longer) transports

Functions as fuel or energy consumption and emissions are relevant only over longer periods of driving, typically some minutes to hours of driving. A collective name for this kind of driving can be cycles. But one should be aware of that there are different ways of defining such cycles.

3.3.1 Description formats of transports

This section could alternatively fit in 2.10, from where it is also referred to.

This section is about how to describe "all except the vehicle", e.g. road, traffic, driver and payload. The overall idea is to model the vehicle operation as *independent of the vehicle*, so that different vehicles, or different designs or configurations of a certain vehicle, can be compared in a fair way.

3.3.1.1 (Traditional) Driving cycles

One way to describe (model) transports is a so-called driving cycle; where the vehicle speed is defined as function of time or distance along the route. If defined as function of distance along the route, it can also make sense to define other parameters of the road, such as road grade as function of distance along the route. Examples of commonly used driving cycles are given in Figure 3-31 to Figure 3-32. In addition, it can also be relevant to give road inclination as function of time. Engine temperature and selected gear as functions of time may also be defined. For hybrid vehicles, the possibility to regenerate energy via electric machines is limited in curves, so curvature radius can also be prescribed as function of time. For heavy vehicles, the weight of transported goods can be another important measure to prescribe.

FTP and HFTP are examples of cycles derived from logging actual driving, mainly used in North America. NEDC is an example of a "synthetically compiled" cycle, mainly used in Europe. Worldwide harmonized Light duty driving Test Cycle (WLTC) is a work with intention to be used world-wide, see Figure 3-34. WLTC exists in different variants for differently powered vehicle [power/weight].

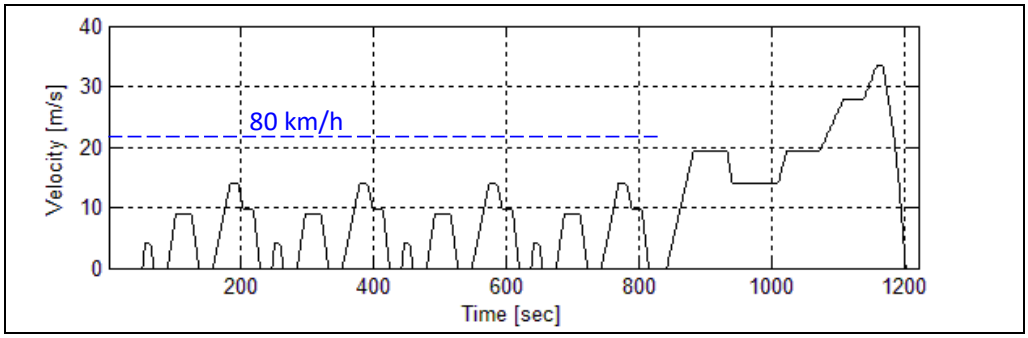


Figure 3-31: New European Driving Cycle (NEDC). From (Boerboom, 2012)

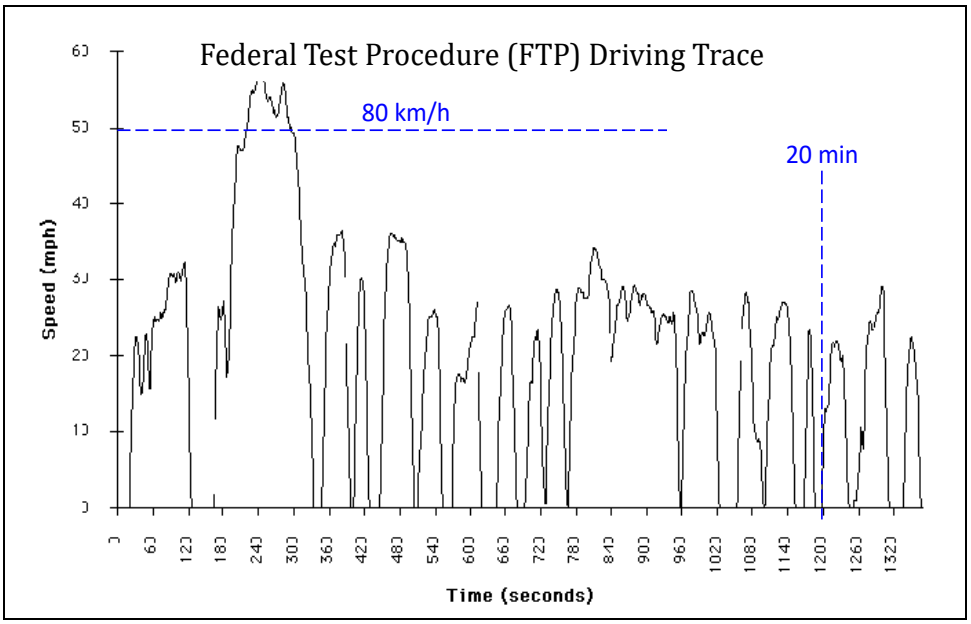


Figure 3-32: FTP cycle from http://www.epa.gov/oms/regs/ld-hwy/ftp-rev/ftp-tech.pdf

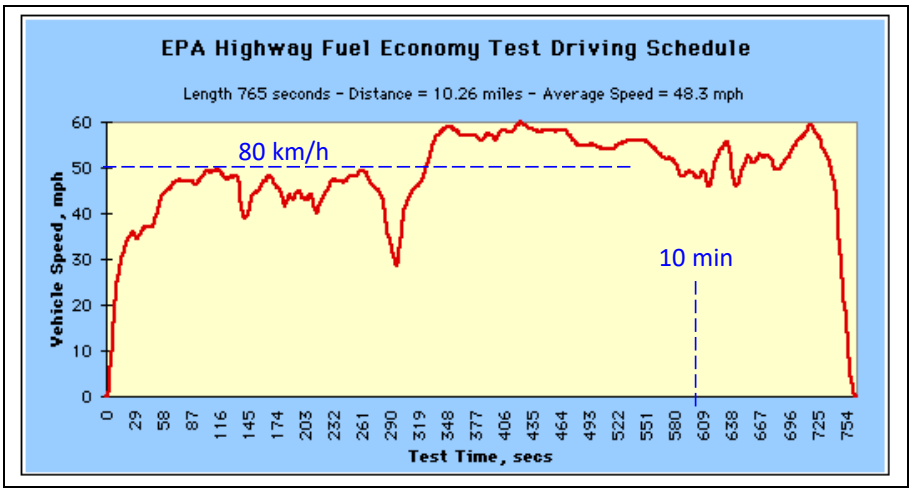
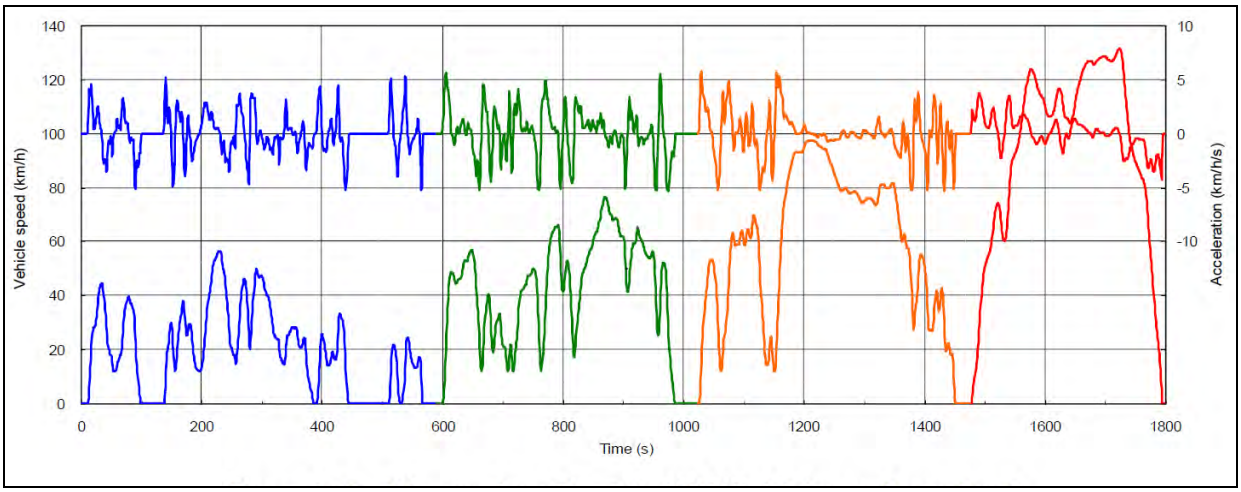


Figure 3-33: HFTP cycle from http://www.epa.gov/nvfel/methods/hwfetdds.gif



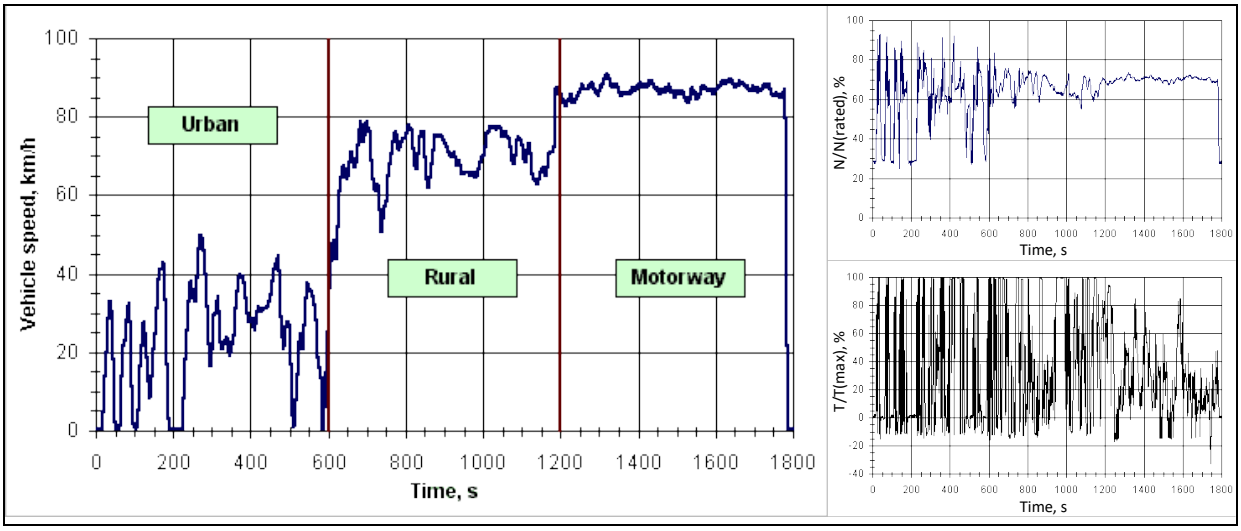


Figure 3-34: Top: WLTC cycle from http://www.unece.org, from 2015, for light vehicles. Bottom: European Transient Cycle (ETC) for heavy commercial vehicles. The engine variants, $T_{e(t)}$ and $\omega_e(t)$, are used for certification from 2000. https://www.dieselnet.com/standards/cycles/etc.php

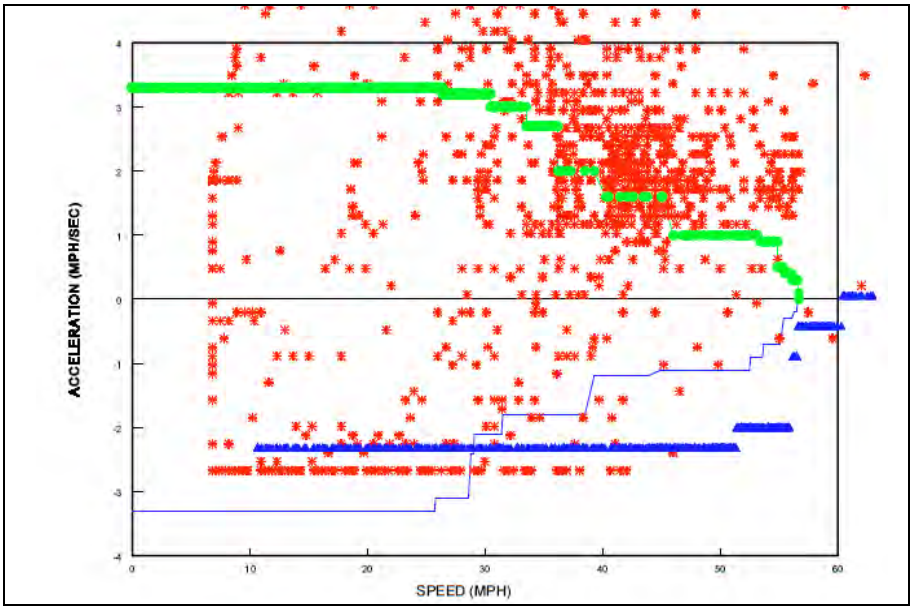


Figure 3-35: FTP cycle converted to a Driving pattern, i.e. a distribution of operating duration in speed and acceleration domain. Each marker marks a duration, e.g. each marker can represent that the vehicle operates 10 s in that point. From http://www.epa.gov/oms/regs/ld-hwy/ftp-rev/ftp-tech.pdf.

3.3.1.2 Driving Pattern

A driving cycle can be condensed into a Driving pattern, i.e. function with duration of operation in combinations of {speed, acceleration}, as shown in Figure 3-35. Note that the chronological order is no longer represented in such representation; it is not a dynamic model. Figure 3-35 shows simply a scatter plot of time-sampled combinations of speed and acceleration. Using the same diagram axis, such information can also be shown as durations (in seconds or fractions of total time (frequency)). A Driving pattern can only be combined with a steady state model of the vehicle, such as "*fuel consumption=function(speed, acceleration)*", as opposed to a dynamic model of the vehicle. The Driving pattern itself includes the driver, so no driver model is needed.

Driving patterns can use more than 2 dimensions, such as [speed, acceleration, road gradient]. In principle, they can also use less than 2 dimensions, maybe only [speed]. The (steady state) vehicle model has to reflect the corresponding dimensions.

This description of vehicle operation is the simplest. It can even collapse to be used to describe constant speed operation, used to define the function in "0

Table 3.1: Quantities for energy (consumption) and power (losses)

Overall definition of different consumptions	**When modelling as losses in physical parts or phenomena, i**	**Note**
Energy, E_{Cons} • in $[J]$, • is an **accumulation** over a time interval: $E_{Cons} = \int P_{Cons} \cdot dt$;	E_{iLoss} is the energy loss in part, or phenomenon, i. If all $(\forall i)$ are modelled: $E_{Cons} = \sum_{\forall i} E_{iLoss}$;	P_{Cons} is the power from the energy storages which we have a cost [€] to fill up, such as fuel tanks and batteries. For a battery, $E_{Cons} = \int \frac{d(E_{Stored})}{dt} \cdot dt$; E_{iLoss} is the energy "loss" in a part or phenomena, where loss means that we cannot use the energy for transport. Important to include in "$\forall i$" are: energy storages, prime movers, transmissions, wheels, friction brakes, aerodynamic resistance, road grades, and auxiliary loads.
Energy per distance, EPD • in $[J/m = N]$, • is an **average** over a time interval: $EPD = E_{Cons}/(\int \dot{s} \cdot dt) = = E_{Cons}/\int ds$;	$EPD_i = E_{iLoss}/(\int \dot{s} \cdot dt) = E_{iLoss}/(\int ds)$; If all $(\forall i)$ parts or phenomena are modelled: $EPD = \sum_{\forall i} EPD_i$;	EPD and EPD_i can be seen as the "equivalent" **average** resistance forces, $R_{iEquivAv}$ $[N]$. These are averaged over a distance interval. $R_{iEquivAv}$ is equivalent with respect to the **energy** loss. Losses E_{iLoss} can be replaced by a constant force acting on the vehicle body, counter-directed to the route direction. $R_{iEquivAv}$ cannot be measured in a real-world test but are useful for comparison between losses in different parts or phenomena.
Power, P_{Cons} • in $[J/s = W]$, • is defined for the vehicle in its transport operation • is a **momentaneous** quantity (for a time **instant**, not an average over a short time interval)	If all $(\forall i)$ parts or phenomena are modelled: $P_{Cons} = \sum_{\forall i} P_{iLoss}$;	Note the difference between the **momentaneous** quantity P_{Cons} and the **average** over a time interval, $P_{ConsAv} = E_{Cons}/(\int dt) = (\int P_{Cons} \cdot dt)/(\int dt)$;. $P_{iLoss} = P_{iIn} - P_{iOut}$; During driving, some (as storages) have $P_{iIn} \equiv 0$, and some (as aerodynamic resistance) have $P_{iOut} \equiv 0$, while some (as prime movers, transmissions and wheels) can have both $P_{iIn} \neq 0$ and $P_{iOut} \neq 0$.
Power per speed, PPS • in $[(J/s)/(m/s) = N]$ • is defined for the vehicle in its transport operation or for a part or phenomenon in the vehicle • is a **momentaneous** quantity: $PPS = P/\dot{s}$;	$PPS_i = P_{iLoss}/\dot{s}$; If all $(\forall i)$ parts or phenomena are modelled: $PPS = \sum_{\forall i} PPS_i$;	PPS and PPS_i can be seen as "equivalent" **momentaneous** resistance forces R_{iEquiv}. These are mot averaged but momentaneous at a time instant. R_{iEquiv} is equivalent with respect to the **power** loss. Losses P_{iLoss} can be replaced by a force acting on the vehicle body, counter-directed to the route direction. R_{iEquiv} cannot be measured in a real-world test but are useful for comparison between losses in different parts or phenomena.

Energy consumption for constant operating conditions".

3.3.1.3 Operating Conditions

Traditional driving cycles typically prescribe only a velocity trajectory during a transport operation. Such trajectory is rather a result from a certain combination of {{*road*, *traffic*, *weather*, *mission}*, *driver, vehicle}* than a description of the operating conditions. An Operation Condition (OC) format can describe the environment in concrete physical quantities, structured in {*road*, *traffic*, *weather*, *mission}*. These parameters should be independent of the {*vehicle*} and of the {*driver*}. This makes it useful for different vehicle types, including but not limited to passenger cars and heavy vehicles. It is difficult to find parameters which are completely independent of the {*vehicle*}, e.g. rolling resistance depends on both tyre and ground. A complete independency of the {*driver}* is even more difficult.

Traditional driving cycles are used for certification of road vehicles, historically mainly for passenger cars but nowadays also for heavy vehicles, e.g. through Vecto, see Reference (European Comission, accessed 2026-10-04)**Error! Reference source not found.**. OC formats are more useful for comparisons between vehicle designs during vehicle development and between vehicles during vehicle purchase/selection. With the OC format, different vehicles will do the same transport operation but with relatively different velocity trajectories. A third use of the OC format is in real-time functions for each individual vehicle, such as *Residual range prediction* and *Predictive cruise control*.

An OC format can contain both a deterministic and a stochastic description of the route ahead, for instance: An example of a concrete physical variable is the legal speed in [m/s]. It changes in steps where a new speed limit is posted along the route. The parameter in a deterministic description is a stepwise changing trajectory $v_{Posted}(s)$, typically hundreds of parameters for a transport operation. In a stochastic description, $v_{Posted}(s)$ is not given explicitly but a stochastic model is given for where the distance between the steps follows a probability function. The mean value and variance, both in the concrete physical variable length in [m], are the parameters of the stochastic OC. The stochastic OC can describe the same real transport operation but has typically much fewer parameters than the deterministic OC. The stochastic OC format can be seen as describing the uncertainties of a transport operation.

Also, other parameters, like road grade, weight of transported goods etc. are defined in position rather than time. For stops along the route, the stop duration or departure time then must be separately defined. This leads to a more realistic description (model) of the vehicle usage, here called Operating cycle or Operating conditions. Important is that an Operating cycle becomes vehicle independent, so that different vehicles or different vehicle configurations can be fairly compared. See (Pettersson, 2017) and (Romano, 2023).

Simulation with an Operating cycle requires a driver model. This is to reduce speed, e.g., $v_{Req} = \min\left(v_{Legal}, \sqrt{Radius \cdot a_{yDrvr}}\right)$; and control it, e.g. $F_{Req} = Gain_{Drvr} \cdot \left(v_{Actl} - v_{Req}\right)$;. A consequence is that different driver models (both driver equations and values of driver parameters, e.g., $\left\{a_{yDrvr}, Gain_{Drvr}\right\}$) will give different results, i.e. different $v_{Actl}(t)$ as well as different energy consumption and transport time. Hence, the driver model itself can be seen as a part of the vehicle usage definition. With increased use of automated functions, such as advanced cruise controllers, the influence of the human driver, and hereby the need to it, can be reduced in future.

Vehicle and Driver is part of a Transport Operation, see 2.10.1, but not part of the Operating conditions. Operating conditions for a transport operation can be described (modelled) in 4 parts (sub-models), see Table 3-36. The ***Mission*** (or Transport Mission) is the purpose of one transport operation, such as what payload (cargo) to transport and where and when to stop and load/unload it. Table 3-36 shows proposed parameters in an Operating Condition description from (Pettersson, 2019) and (Romano, 2023).

Table 3-36: Some proposed parameters to model an Operating Cycle (OC) or Operating Conditions (OC).

Part of OC	Parameter		Independent variable		Notes.
	Name	Unit	Position along route	Time	
Road	Legal speed	m/s	1	0	Typically varies in segments. Valid for passenger cars and saturated to lower for other vehicle types.
Road	Altitude	m	1	0	Can be modelled as piecewise linearly with position.
Road	Curvature	1/m	yes	no	Influences transport costs mainly through velocity adaptation for safe and comfortable lateral acceleration
Road	Ground type	discrete	yes	no	Discrete state representing ground softness. To be more concrete.
Road	Roughness		yes	no	Discrete state representing ground roughness. To be more concrete.
Road	Coverage		yes	possibly	Discrete state representing what is on the road (water, snow, …). To be more concrete.
Road	Stop signs	boolean	yes	no	
Road	Traffic lights		yes	no	
Road	Give way signs		yes	no	
Road	Speed bumps		yes	no	
Weather	Ambient temperature		yes	possibly	
Weather	Atmospheric pressure		yes	possibly	
Weather	Precipitation		yes	possibly	
Weather	Wind velocity		yes	possibly	Velocity magnitude and direction
Weather	Relative humidity		yes	possibly	
Traffic	Traffic density		yes	possibly	
Mission	Mission stops	s	yes	no	Quantified with each stop's time duration
Mission	Cargo weight	kg	yes	possibly	Typically only varied at mission stops
Mission	Power take-off	kW	yes		
Road	example: Charging power				Possibility to re-fill energy, e.g. fossil fuel or electric charge of batteries

3.3.2 Energy consumption

3.3.2.1 Recap and develop quantities

To prepare ourselves for "3.3.5.1 Energy consumption over cycle*", we need to recap and develop Table 3.1 and Table 3.2. In 3.2.2 and 3.2.3, they were only used for steady state, which has constant operating conditions.

3.3.2.1.1 Energy Consumption for varying operating conditions *

3.3.2.1.2 Energy consumption for constant operating conditions, with given speed variation *

Function definition: ***Energy (or Fuel) consumption*** *is the amount of energy* $[J]$ *(or fuel* $[kg]$ *or* $[litre]$*) consumed by the vehicle per performed transportation amount. Transportation amount can e.g. be measured in* $[km], [person \cdot km], [ton \cdot km]$*, or* $[m^3 \cdot km]$*. The vehicle operation conditions are given as:* ***Given***

speed variation *(a.f.o. time or distance) as well as given other conditions: road gradient, head wind, cargo load, road surface conditions, etc. (also a.f.o. time or distance).*

3.3.2.1.3 Energy consumption for constant operating conditions, with given signed speed variation *

Function definition: ***Energy (or Fuel) consumption*** *is the amount of energy* $[J]$ *(or fuel* $[kg]$ *or* $[litre]$*) consumed by the vehicle per performed transportation amount. Transportation amount can e.g. be measured in* $[km], [person \cdot km], [ton \cdot km]$*, or* $[m^3 \cdot km]$*. The vehicle operation conditions are given as:* ***Given signed speed variation*** *(a.f.o. time or distance, typically stepwise) as well as given other conditions: road gradient, head wind, cargo load, road surface conditions, etc. (also a.f.o. time or distance). A driver model also needs to be specified to follow the signed speed variation in a realistic way.*

3.3.3 Rotating Inertia Influence on Acceleration

Contribution by Alireza Marzbanrad, Volvo Trucks

In Figure 3-18 it was shown that the acceleration cannot be found directly as a force difference (distance between curves) divided by vehicle mass. This is because the Traction Diagram cannot well represent an event over a time interval and the inertial phenomena contains not only translational acceleration of the vehicle mass but also the rotational acceleration of parts, such as wheel and rotating parts in the driveline. The phenomenon that occurs is referred to here as "Rotating Inertia Influence on Acceleration". If no velocity losses, the rotating part of the propulsion system, e.g. engine and wheels, must be synchronically accelerated with the vehicle mass. This "steals" some of the power in the propulsion system. The "stolen" power is stored as rotational kinetic energy and the transmitted power as kinetic energy of the vehicle translation and for overcoming driving resistance through body-forces. So, also this "stealing" of power affects how much power is required when following accelerations in a driving cycle.

Consider a wheel (without vehicle!) rolling which is ideally rolling (no slip), with a free-body diagram and notations as in Figure 3-37. The wheel becomes simply a rolling cylinder. Setting up 2 equilibrium equations and 1 compatibility equation gives Eq [3.13].

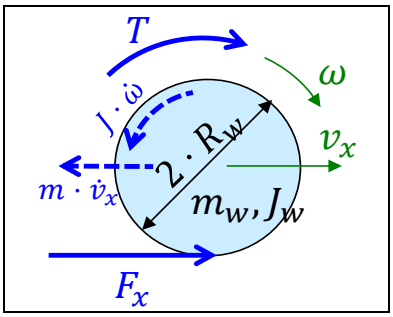


Figure 3-37: Rolling wheel (without vehicle, which is why no forces in the wheel centre)

$$\begin{aligned} m_w \cdot \dot{v}_x &= F_x; \\ J_w \cdot \dot{\omega} &= T - F_x \cdot R_w; \\ v_x &= R_w \cdot \omega \Rightarrow \dot{v}_x = R_w \cdot \dot{\omega}; \end{aligned} \qquad [3.13]$$

3 equations and 3 unknown variables (v_x, ω, F_x, while T is considers as known). Elimination of ω gives:

$$\underbrace{\left(m_w + \frac{J_w}{R_w^2}\right)}_{k \cdot m_w} \cdot \dot{v}_x = T/R_w; \quad and$$

$$F_x = \frac{R_w \cdot m_w}{m_w \cdot R_w^2 + J_w} \cdot T = \frac{1}{k} \cdot \frac{T}{R_w}; \qquad [3.14]$$

Note that F_x becomes proportional to T. This is because we have neglected slip ($v_x = R_w \cdot \omega - v_x \equiv 0$). Therefore, if simulating, we gain by having only one of $\{v_x, \omega\}$ as state variable. In more theoretical mechanics, one call the neglection of slip a *(motion) constraint* and F_x a *constraint force*.

So, the rotating inertia makes the mass m_w appear as scaled up with a factor k. Also, the force F_x becomes scaled down (compared to T/R_w) with the same factor k. The reduction of F_x is what we called "stealing power" above. We call the factor k the "rotational inertia coefficient".

A vehicle with total mass m will appear to have larger mass due to inertias in the propulsion system. There are rotational inertias at two places: before transmission, i.e. rotating with same speed as

engine: J_e and after transmission, i.e. rotating with same speed as the wheel: J_w. The rotational inertia coefficient k, will be dependent on the main transmission ratio r as well. In the following, we include the wheel mass in the total vehicle mass m.

$$k \cdot m \cdot \dot{v}_x = T_e \cdot \frac{r}{R_w};$$
$$where\ k \cdot m = m + \frac{J_w}{R_w^2} + \frac{J_e \cdot r^2}{R_w^2};$$

[3.15]

Typically for a passenger car with traditional ICE propulsion, $k = 1.3..1.4$ in the first gear and $k = 1.1$ in the highest gear ($J_e \approx 0.2\ [kg \cdot m^2], r \approx\ 4 \cdot 4 = 16, R_w = 0.3\ [m]$). Typically, the influence of the J_w term is smaller, also after one have considered that all wheels contribute. Anyway, typically, $k = 1.3..1.4$ is significant!

Typically for electrical propulsion of the same vehicle, J_w is smaller and there are fewer gears, so k can typically be lower than for an ICE vehicle on low gear, but higher than for an ICE vehicle on high gear. So, it might require redesign/retuning of ABS and TC. But the electrical propulsion systems have not reached a mature design yet, so it is worth checking in each case, using Eq [3.15].

We can now learn how to determine acceleration from the Traction Diagram, see Figure 3-38.

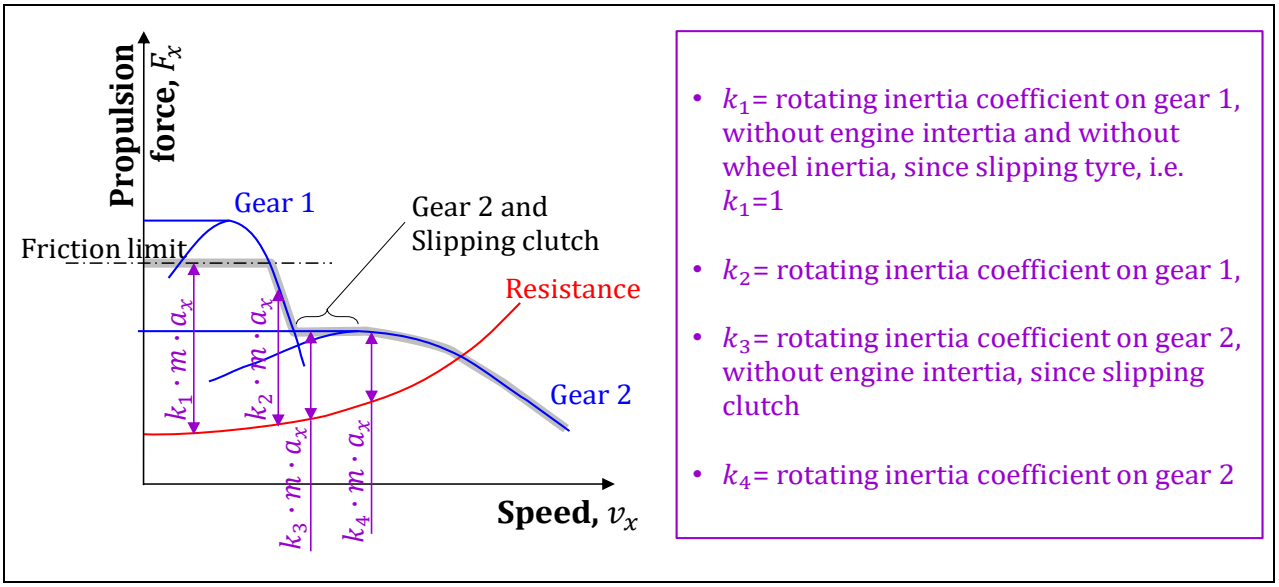


Figure 3-38: Acceleration in Traction Diagram. Rotating inertia effects are shown assuming that the engine is operated on its maximum curve and gear selection and clutch operation are made for highest acceleration.

When the clutch is slipping, there is no constraint between engine speed and vehicle, so the term with J_e disappears from Equation [3.15]. If the wheel spins, both terms J_e and J_w disappear. It should therefore be noted that, if tyre slip is modelled, the effect of rotating inertia is regarded without using the k factor above. That is, if the mathematical model in [3.16] is used instead of [3.13]. Eq [3.16] gives an explicit form model with two states $[v, \omega]$ and it becomes increasingly computational demanding the larger C_x is. (Similar decoupling between inertias J_e and J_w happens if torque converter or elastic driveshafts are modelled between engine inertia and wheel.)

$$m \cdot \dot{v} = F_x;$$
$$J \cdot \dot{\omega} = T - F_x \cdot R_w;$$
$$F_x = C_x \cdot s_x;\quad where\quad s_x = \frac{R_w \cdot \omega - v_x}{|R_w \cdot \omega|};$$

[3.16]

3.3.4 Four Quadrant Traction Diagram

When the driving cycle shows a deceleration, which is larger than can be achieved with resistance force, we need to brake with a combination of engine braking and friction brakes. If only friction braking is used, it can be with engaged or disengaged clutch. That influences the rotating inertia coefficient by using or not using the J_e term in Equation [3.15], respectively. The traction diagram can be extended to also cover engine braking and friction braking. However, the friction brake system is seldom limiting factor for how negative the longitudinal force can be. But the road friction is, see Figure 3-39.

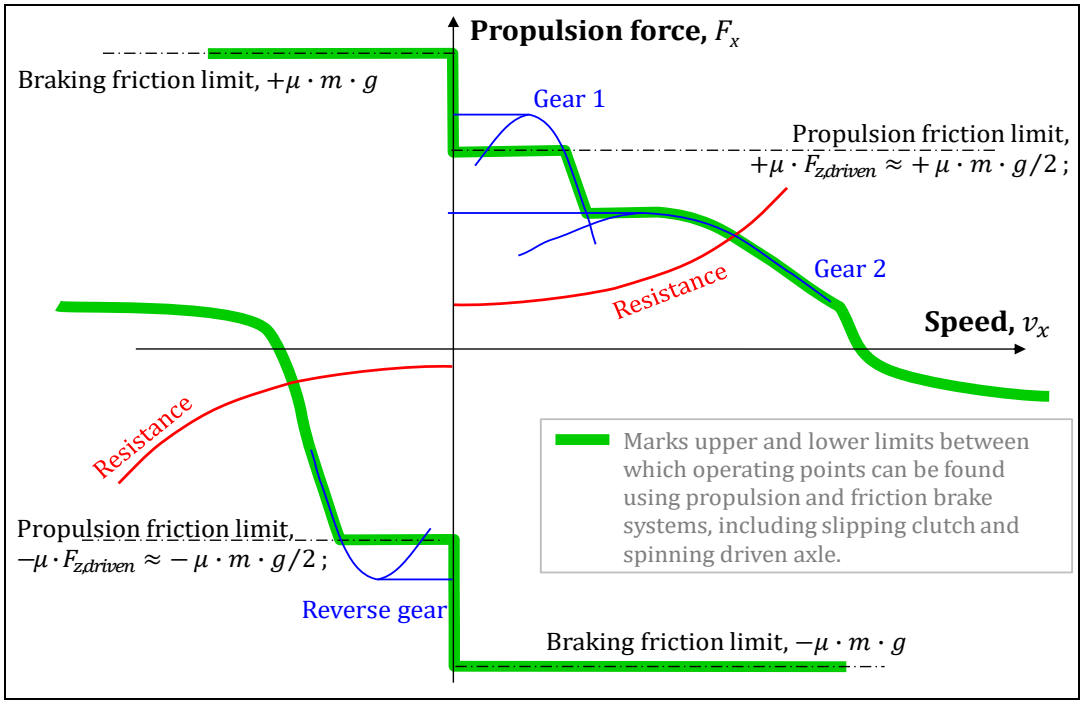


Figure 3-39: Traction Diagram in 4 quadrants. One of two axles is assumed driven, which limits propulsion to ≈half of braking friction limit. Up-hill slope is assumed, which is seen as asymmetric resistance.

3.3.5 Functions Over Cycles

3.3.5.1 Energy consumption over cycle*

> *Function definition:* ***Energy (or Fuel) Consumption*** *is the amount of energy* $[J]$ *(or fuel* $[kg]$ *or* $[litre]$*) consumed by the vehicle per performed transportation amount. Transportation amount can e.g. be measured in* $[km]$, $[person \cdot km]$, $[ton \cdot km]$, *or* $[m^3 \cdot km]$. *The vehicle operation has to be defined, e.g. with certain operating conditions, such as a driving cycle (speed as function of time or position), including road gradient, cargo load, road surface conditions, etc.*

The consumption arises in the prime mover, see Figure 2-101 and Figure 2-102, but as a cycle measure it is dependent of the overall vehicle operation.

Driving cycles are used for legislation and rating for passenger cars. For commercial vehicles, the legislation has been for the engine alone, and not for the whole vehicle. CO_2-rating for commercial vehicles is newly introduced, see http://ec.europa.eu/clima/events/docs/0096/vecto_en.pdf.

Fuel consumption in [litre/km] can be thought of as the **area** (volume per distance) of an imagined fuel hose along the road. Energy consumption in [J/km] can be thought of as the **force** (energy per distance) of an imagined resistance force on the vehicle body. The metaphor with force is useful to compare influence of all different power losses.

3.3.5.2 Transport time *

Function definition: ***Transport Time*** *is the time* $[s]$ *or* $[h]$ *for the vehicle to perform a certain transportation mission. Transportation mission can e.g. be defined in terms of distance, payload, road topography, etc.*

Transport Time is often in conflict with Energy Consumption. Either, one have independent requirements (constraints), but one can also formulate the total transport cost and minimize it, e.g.: $Cost = EnergyCost[€/J] \cdot EnergyConsumption[J] + TimeCost[€/h] \cdot TransportTime[h]$;. (That cost model is for exemplification and very simplified. Important other costs are investment and maintenance.)

For commercial freight traffic, $TimeCost$ is mainly the driver salary, so it can be quantified. For person transport, especially private travels, it is much more difficult to motivate a number of the cost. One can typically find studies which uses travel time cost$\approx 120\ SEK/h \approx 12\ €/h$ for private travels in Sweden.

3.3.5.2.1 Transportation time cost

The transport time cost (for the vehicle user, driver or owner) is very difficult to quantify. Still, for goods transportation, it is most straight-forward and consists mainly of driver salary cost and wear of the vehicle, possibly also depreciation of investments in the vehicle.

The travel time cost (per hour) for transport of persons is very debatable how to quantify. When it is needed, one should think of that it depends on transport mean. For instance, it is higher for air travels than for train because the traveller is less free to do other things; travel with passenger car is in between. Increased driving automation, e.g. adding automatic steering to automatic longitudinal control, should probably reduce the travel cost for passenger cars. References:

- Swedish Transport Administration (Trafikverket), *Analysmetod och samhällsekonomiska kalkylvärden för transportsektorn: ASEK 6.1, Kapitel 7 Värdering av kortare restid och transporttid,* https://www.trafikverket.se/contentassets/4b1c1005597d47bda386d81dd3444b24/asek-6.1/07_restid_o_transporttid_a61.pdf , in Swedish, 2018.
- Lyons and Urry, *Travel time use in the information age*, Transportation Research Part A 39 (2005) 257–276, doi:10.1016/j.tra.2004.09.004, 2004.

3.3.5.3 Emissions *

Function definition: As Energy consumption but amount of certain substance instead of amount of energy.

There are emission maps where different emission substances (NOx, HC, etc.) per time or per produced energy can be read out for a given speed and torque. This is conceptually the same as reading out specific fuel consumption or efficiency from maps like in Figure 2-101 and Figure 2-102. A resulting value can be found in mass of the emitted substance per driven distance.

Noise is also sometimes referred to as emissions. It is not relevant to integrate noise over the time for the driving cycle, but maximum or mean values can have relevance. Noise emissions are very peripheral to vehicle dynamics.

3.3.5.4 Tyre Wear *

Function definition: ***Tyre wear*** *is the worn-out tyre tread depth on a vehicle per performed transportation amount. Tyre wear as a vehicle function has to consider all tyres on the vehicle, e.g., as maximum over the wheels (assuming that all tyres are changed when one is worn out) or average (assuming that single tyres are exchanged when worn out).*

There are models for tyre wear (e.g., outputting “worn tread depth per time”), see Equation [2.70]. For a certain driving cycle, we can integrate the $WearRate$ [in mass/s or mm tread depth/s], over time similar to energy consumption rate, which becomes worn material [in mass or mm tread depth]. The

wear rate per wheel is a function of the total slip, so it can include both longitudinal slip (propulsion and brake) and lateral slip (from cornering and toe angles).

Generally, the worn material will be different for different axles, or wheels, so a tyre change strategy might be necessary to assume to transform the worn material on several axles into one cost. The cost will depend on whether one renews all tyres on the vehicle at once or if one change per axle. The tyre wear is a cost which typically sums up with energy cost and cost of transport time (e.g. driver salary, for commercial vehicles).

3.3.5.5 Range *

Function definition: ***Range*** *[km] is the inverted Energy consumption [kg/km, litre/km, or J/km], multiplied with energy storage size [kg, litre, or J].*

The range is how far the vehicle can be driven without refilling the energy storage, i.e., filling up fuel tank or charging the batteries from the grid. This is in principle dependent on how the vehicle is used, so the driving cycle influences the range. In principle, the same prediction method as for energy consumption and substance emissions can be used. In the case of predicting range, you must integrate speed to distance, so that you in will know the travelled distance.

3.3.5.6 Acceleration Reserve *

Function definition: ***Acceleration reserve*** *is the additional acceleration the vehicle will achieve within a certain time (typically 0.1..1 s) without manual gear-shifting by pressing accelerator pedal fully, when driving in a certain speed on level ground without headwind. For vehicles with automatic transmissions or CVTs the certain time set can allow automatic gearshift (or ratio-change) or not. The reserve can also be measured in propulsion force.*

In general terms, the lowest consumption is found in high gears. However, the vehicle will then tend to have a very small reserve in acceleration. It will, in practice, make the vehicle less comfortable and less safe to drive in real traffic, because one will have to change to a lower gear to achieve a certain higher acceleration. The gear shift gives a time delay.

Figure 3-40 shows one way of defining a momentary acceleration reserve. The reserve becomes generally larger the lower gear one selects. A characteristic of electric propulsion systems is that an electric motor can be run at higher torque for a short time than stationary, see Figure 2-99. On the other hand, the stationary acceleration reserve is less gear dependent, since an electric motor can work at certain power levels in large portions of its operating range.

One can calculate the acceleration reserve at each time instant over a driving cycle. However, integration of acceleration reserve, as we did with fuel, emissions and wear, makes less sense. Instead, a mean value of acceleration reserve tells something about the vehicle's driveability. Minimum or maximum values can also be useful measures.

Acceleration reserve was above described as limited by gear shift strategy. Other factors can be limiting, such as energy buffer state of charge for parallel hybrid vehicles or how much overload an electric machine can take short term, see right part of Figure 3-40.

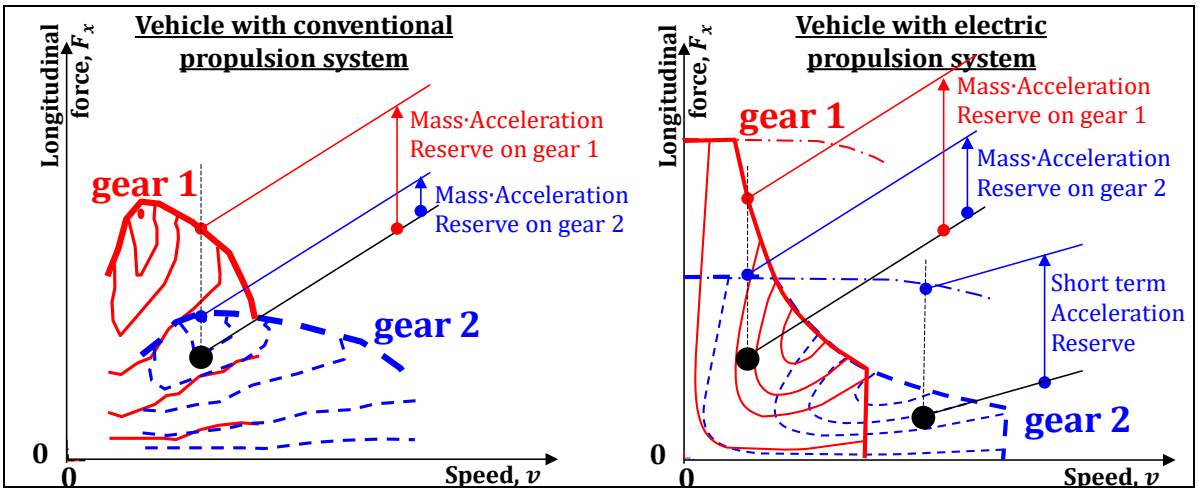


Figure 3-40: Acceleration reserves for different gears. Large dots mark assumed operating points.

3.3.5.7 Computation of cycle measures

The measures of all functions mentioned in 3.3.5 can be assessed in some sort of driving cycle/operation cycle computation. Such computations are described in the following, as exemplified by only one measure, the Energy Consumption.

How to predict the consumption for a vehicle during a certain driving cycle is rather straight-forward using what has been presented earlier in this chapter. Since a driving cycle is a prediction of how the vehicle is moving, it stipulates the acceleration of a mass, which calls for an "inverse dynamic analysis". In such one assumes that the driving cycle is met exactly, which means that both required wheel speed and required wheel torque can be calculated for each time instant. Then, via a propulsion and brake system model, the corresponding fuel consumption in the engine can also be found for each time instant. A summary of such an inverse dynamic algorithm for prediction of fuel or energy consumption is given in Equation [3.17].

```
For each time step in the driving cycle:
```

- Calculate operating point for vehicle (speed and acceleration) from driving cycle. Acceleration is found as slope of v(t) curve. Other quantities, such as road slope, also needs to be identified;
- Select gear (and clutch state, tyre spin, friction brake state, etc) to obtain this operating point. Also select friction brake, especially for operating points which can be reached using only friction brake. If the vehicle has an energy buffer, regenerative braking is also an option;
- Calculate required actuation from propulsion system on the driven wheel, i.e. rotational speed and shaft torque;
- Calculate backwards through propulsion system, from wheel to prime motor. It gives the operating point for prime mover (rotational speed and torque);
- Read prime mover consumption [in kg/s or W=J/s, not specific consumption, not efficiency] from prime mover consumption map;
- Sum up consumption [in kg or J] with earlier time steps, e.g. using the Euler forward integration method: AccumulatedConsumption = AccumulatedConsumption + Consumption*TimeStepLength;

```
end;
```

[3.17]

The final accumulated consumption [in kg or J] is often divided by the total covered distance in the driving cycle, which gives a value in kg/km or J/km. If the fuel is liquid, it is also convenient to divide by fuel density, to give a value in litre/(100*km). It can also be seen as a measure in m^2, which is the area of the "fuel pipe" which the vehicle "consumes" on the way.

For hybrid vehicles (with energy buffers) the same driving cycle can be performed (same $v(t)$) but ending with different level of energy in the buffer. Also, the level when starting the driving cycle can be

different. This makes it unfair to compare energy consumption only as fuel consumption, one should rather weight it to energy cost, €/km or €/(ton·km).

3.3.5.7.1.1 Forward and Backward Simulation

We should note that the calculation scheme in Equation [3.17] does not always guarantee a solution. An obvious example is if the driving cycle prescribes such high accelerations at such high speeds that the propulsion system is not enough, i.e. we end up outside maximum torque curve in engine diagram. This is often the case with "inverse dynamic analysis", i.e. when acceleration of inertial bodies is prescribed, and the required force is calculated.

The alternative is to do a "forward dynamic analysis", a.k.a. simulation with "natural causality", which means that a driver model calculates the pedals to follow the driving cycle speed approximately, but not exactly.

Inverse dynamic analysis is often less computational demanding, but limits what can phenomena that can be modelled in the propulsion and brake system. The computational benefit is especially large if state variables can be omitted, which is often the case but not always. The velocity v_x and position s along the route does not have to be state variables since they are prescribed through the driving cycle. But other variables can remain state variables also for an "inverse dynamic simulation", such as warm-up dynamics of tyres and other states which are not stipulated by the driving cycle.

Inverse dynamics and dynamic simulations are sometimes referred to as backward and forward simulation, respectively; see Reference (Wipke, Cuddy, & Burch, 1999).

3.3.5.7.1.1.1 Causality

The causality (data flow directions) in an Explicit form model changes a lot if changing between Forward and Backward simulation. However, the Mathematical model experiences minimal changes, basically only the parameter t_{Gain} changes from $t_{Gain} > 0$ to $t_{Gain} = 0$, i.e. the driver is modelled as "ideal", i.e., in some "magic" way, making the vehicle follow what the Environment stipulates: $v = v_r$. The Environment is where the Driving Cycle $v_r(t)$ or $v_r(s)$ is modelled. A big difference is that the Backward simulation can often lack solution, e.g. if propulsion system or brake system is weaker than driving cycle demands. Backward simulations where the control algorithms, such as the pedal map in Figure 3-41, can also suffer from that these algorithms not necessarily can be inverted; a unique input signal cannot always be calculated from a known given output signal.

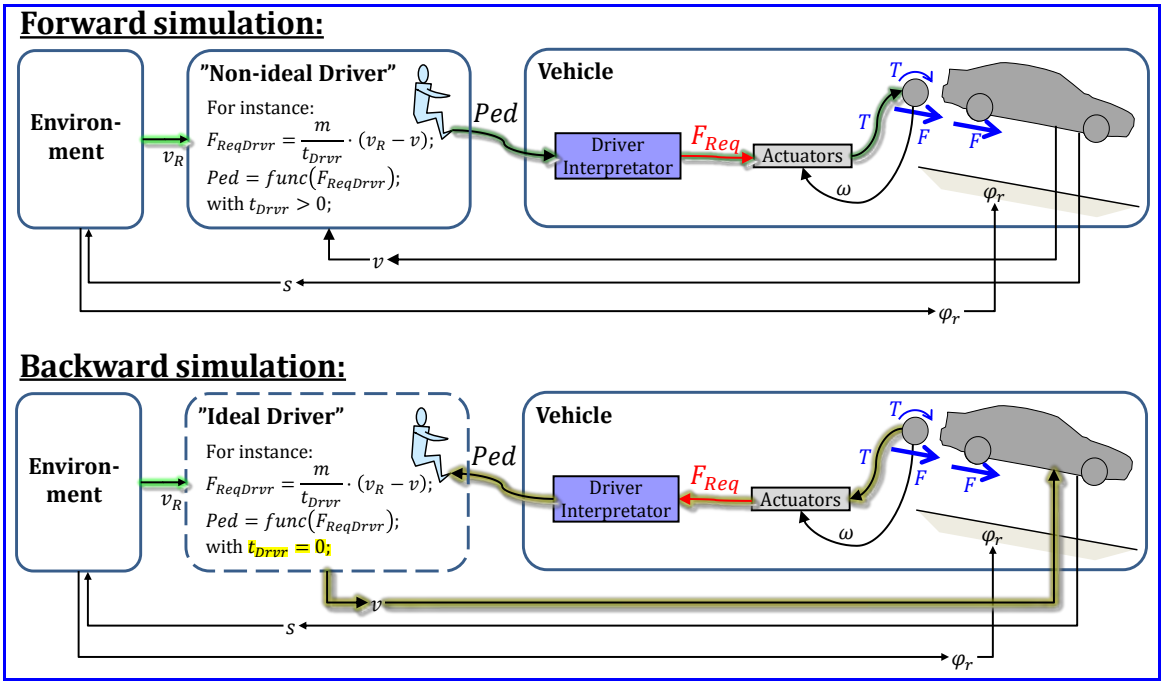


Figure 3-41: Data flow diagrams showing causality for Forward and Backward simulation. Backward leads to changes marked with yellow and that integration $v = \int \dot{v} \cdot dt$; changes to differentiation $\dot{v} = dv/dt$; in Vehicle.

3.3.5.7.1.2 Stepped, CVT and Energy Buffering Main Transmissions

For a given driving cycle $v_x(t)$ there is a certain $[F_x, v_x]$ for each time instant. For different types of main transmissions, one can select operating point $[T_e, \omega_e]$ in prime mover diagram differently, see Figure 3-42. CVTs (or tightly stepped transmissions) enables operation close to optimal curve of engine. However, CVTs typically have more losses than stepped transmissions. So, for commercial vehicles, a higher number of gears is more realistic than real CVTs.

As mentioned in Figure 3-42, one can operate in the optimal point by an energy buffer or by propelling intermittent with a varying vehicle speed. The latter case can be seen as if the vehicle's own kinetic energy ($m \cdot v^2/2$) is used to buffer energy, see (Hedman, 1994) which shows fuel savings in the magnitude of 10%. Intermittent operation is on market as part of predictive cruise, see 3.5.2.3.1.

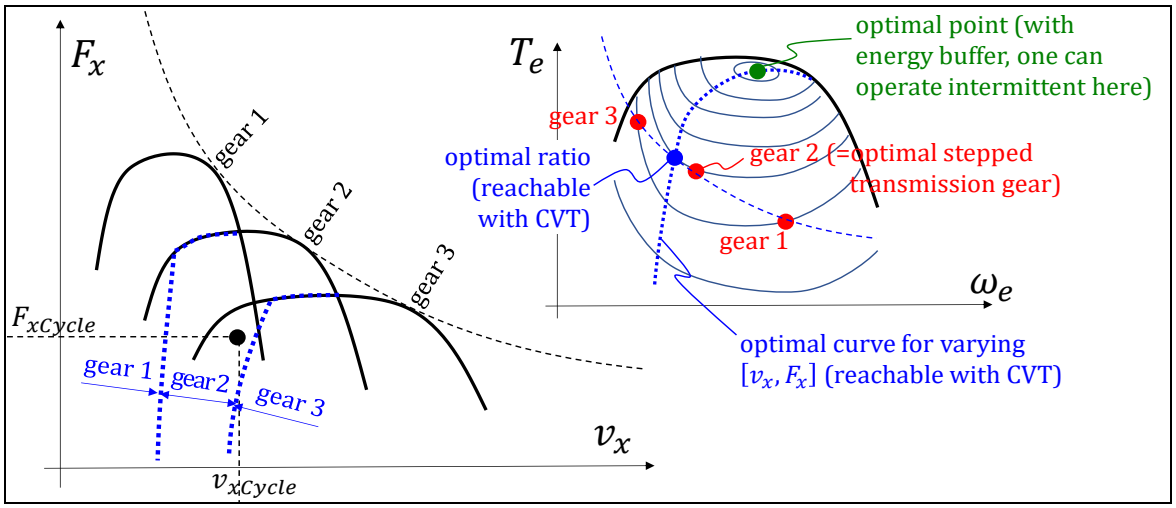


Figure 3-42: Conceptual difference between Stepped, Continuously Variable and Energy Buffering transmission. Operating intermittent would only follow the driving cycle with same average speed.

3.3.6 Load Transfer with Rigid Suspension

Longitudinal load transfer redistributes vertical force from one axle to the other. The off-loaded axle can limit the traction and braking. This is because the propulsion and brake systems are normally designed such that axle torques cannot always be ideally distributed.

For functions over longer events it is often reasonable to consider the suspension as rigid. We start with the free-body diagram in Figure 3-43, which includes acceleration, a_x.

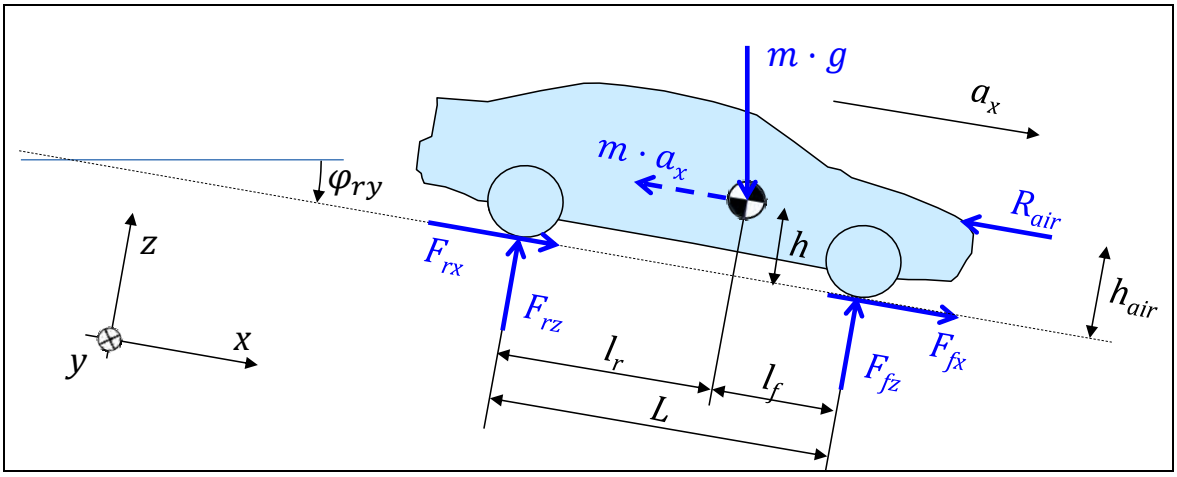


Figure 3-43: Free Body Diagram for accelerating vehicle. Rolling resistance in F_{fx} and F_{rx}.

Note that the free-body diagram and the following derivation is very similar to the derivation of Equation [3.10], but we now include the fictive force $m \cdot a_x$.

Moment equilibrium, around rear contact with ground:

$$-F_{fz} \cdot L + m \cdot g \cdot \left(l_r \cdot cos(\varphi_{ry}) + h \cdot sin(\varphi_{ry})\right) - R_{air} \cdot h_{air} - m \cdot a_x \cdot h = 0; \Rightarrow$$

$$\Rightarrow F_{fz} = m \cdot \left(g \cdot \frac{l_r \cdot cos(\varphi_{ry}) + h \cdot sin(\varphi_{ry})}{L} - a_x \cdot \frac{h}{L}\right) - R_{air} \cdot \frac{h_{air}}{L};$$

Moment equilibrium, around front contact with ground:

$$+F_{rz} \cdot L - m \cdot g \cdot \left(l_f \cdot cos(\varphi_{ry}) - h \cdot sin(\varphi_{ry})\right) - R_{air} \cdot h_{air} - m \cdot a_x \cdot h = 0; \Rightarrow$$

$$\Rightarrow F_{rz} = m \cdot \left(g \cdot \frac{l_f \cdot cos(\varphi_{ry}) - h \cdot sin(\varphi_{ry})}{L} + a_x \cdot \frac{h}{L}\right) + R_{air} \cdot \frac{h_{air}}{L};$$

[3.18]

These equations confirm what we know from experience, the front axle is off-loaded under acceleration with the load shifting to the rear axle. The opposite occurs under braking.

The load shift has an effect on the tyre's grip. If one considers the combined slip conditions of the tyre (presented in Chapter 2), a locked braking wheel limits the amount of lateral tyre forces. The same is true for a spinning wheel. This is an important problem for braking as the rear wheels become off-loaded. This can cause locking of the rear wheels if the brake pressures are not adjusted appropriately. See more in 3.4.4.

3.3.6.1 Influence of Aerodynamic Resistance

Influence of Aerodynamic Resistance becomes different depending on the engineering problem. For instance, assuming $\varphi = 0$ and $l_f = l_r$, the influence on F_{rz} from R_{air} can be expressed as $\frac{\partial F_{rz}}{\partial R_{air}} = \frac{\partial}{\partial R_{air}}\left(\frac{m \cdot g}{2} + \frac{R_{air} \cdot h_{air}}{L} + \frac{m \cdot a_x \cdot h}{L}\right) = \frac{\partial}{\partial R_{air}}\left(\frac{R_{air} \cdot h_{air}}{L} + \frac{m \cdot a_x \cdot h}{L}\right)$.

For an "inverse dynamic" problem, a_x is given (independent). Then $\frac{\partial a_x}{\partial R_{air}} = 0$ because a change in R_{air} is assumed to be compensated with $F_x = F_{fx} + F_{rx}$. Therefore $\frac{\partial F_{rz}}{\partial R_{air}} = \frac{h_{air}}{L}$.

If the problem is instead a "natural causality" problem, e.g. simulation of acceleration. Then F_x is given (independent) and a_x is dependent of R_{air}, via $a_x = \frac{F_x - R_{air}}{m}$; hence $\frac{\partial F_{rz}}{\partial R_{air}} = \frac{h_{air} - h}{L}$.

So, depending on which of these engineering problems one has in mind, it can either be true that R_{air} influences F_{rz} only if $h_{air} \neq 0$ or only if $h_{air} \neq h$.

3.3.6.2 Influence of Acceleration of Rotational Parts

The influence of $J_f \cdot \dot{\omega}_f$ and $J_r \cdot \dot{\omega}_r$ on load transfer will now be studied. See the FBD (and equilibrium) of the whole vehicle in Figure 1-30. If included, it will appear as terms $J_f \cdot \dot{\omega}_f$ and $J_r \cdot \dot{\omega}_r$ in negative pitch direction. If we simplify to assume flat ground and $l_f = l_r = l_a = L/2$ and $R_{air} = 0$:

Moment equilibrium, around rear contact with ground:

$$-F_{fz} \cdot L + m \cdot g \cdot \frac{L}{2} - m \cdot a_x \cdot h - J_f \cdot \dot{\omega}_f - J_r \cdot \dot{\omega}_r = 0; \quad \Rightarrow$$

$$\Rightarrow \quad F_{fz} \approx \left\{ \begin{matrix} \dot{\omega}_f \approx \dot{\omega}_r \approx a_x / R_w \, ; \\ J_f \approx J_r \approx J_a; \end{matrix} \right\} \approx m \cdot \left(\frac{g}{2} - a_x \cdot \frac{h}{L} \cdot \left(1 - \frac{2 \cdot J_a}{m \cdot h \cdot R_w} \right) \right);$$

With realistic values for a passenger vehicle, $m \approx 1500\ kg$ and $J_a = 0.5\ kg \cdot m^2$, the influence from wheel rotational inertia is $= (2 \cdot J_a)/(m \cdot h \cdot R_w) = (2 \cdot 0.5)/(1500 \cdot 0.5 \cdot 0.3) \approx 0.005 = 0.5\%$ on the load transfer which in most cases can be considered as neglectable. In a strong take-off or brake apply, when $\dot{\omega}_i \gg a_x / R_w$, the equation would give a much higher influence but just for a short while. To capture the short transient in such cases, one should model also suspension as in 3.4.5.2.2.

3.3.6.3 Varying Road Pitch

The model in 3.4.4..3.4.5.2 assumes flat but not level road, i.e. φ_{ry} is constant. An example where φ_{ry} varies is when passing a *crest* or a *sag*, see Figure 3-44. If negotiating a curve at the same time as a crest, a vehicle can lose vertical force under tyres so that lateral grip is affected.

Moment equilibrium, around rear and front wheel contact with ground gives:

$$F_{zf} = m \cdot \left((g + z'' \cdot v_x^2) \cdot \frac{l_r \cdot \cos(\varphi) + \mathrm{h} \cdot \sin(\varphi)}{L} - a_x \cdot \frac{h}{\mathrm{L}} \right) - R_{air} \cdot \frac{h_{air}}{\mathrm{L}};$$

$$F_{zr} = m \cdot \left((g + z'' \cdot v_x^2) \cdot \frac{l_f \cdot \cos(\varphi) - \mathrm{h} \cdot \sin(\varphi)}{L} + a_x \cdot \frac{h}{L} \right) + R_{air} \cdot \frac{h_{air}}{L};$$

[3.19]

This assumes that we have the road as $z(s)$, then $\varphi = -\arctan\left(\frac{dz}{ds}\right) \approx -\frac{dz}{ds}$; and $z'' = \frac{d^2 z}{ds^2}$;.

Note that this model is assuming that vertical variations of road are much larger than wheelbase and track width and same on left and right side of the road/vehicle. Else the variation would be called road unevenness, which will be more treated in Chapter **5**.

If models with body vertical and pitch motion and suspension springs, such as in 3.4.5 and 3.4.5.2 it is often suitable to express the vertical fictive force, $m \cdot \ddot{z}$, with $v_x \cdot \omega_y$ instead of $m \cdot z'' \cdot v_x^2$. The fictive force downwards will then be $-m \cdot v_x^2 \cdot \kappa_y = -m \cdot v_x \cdot \omega_y$ instead. This can be understood from basic geometry, $z'' \approx -\kappa_y$, where κ_y is the road pitch curvature $[1/length]$, see Figure 3-44.

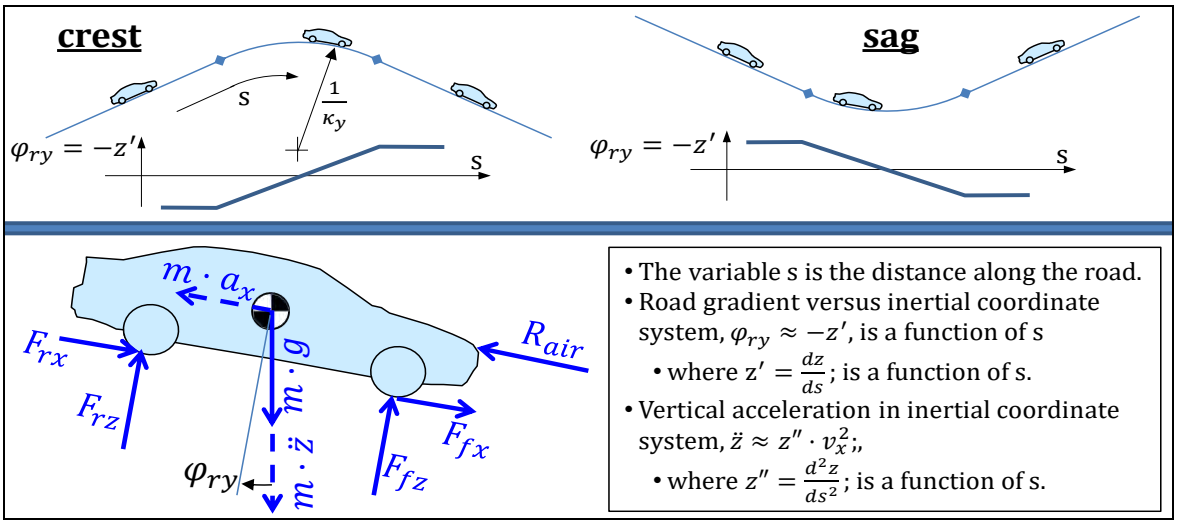


Figure 3-44: Free Body Diagram for driving over non-flat vertical road profile.

3.3.7 Acceleration

Acceleration performance like, typically, 0-100 km/h over 5..10 s, will be addressed in this section. These accelerations are relatively steady state (vehicle pitch and heave are relatively constant), so the suspension compliance is not considered.

Accelerations will also be covered in 0, as being shorter events. The vehicle pitch and heave vary more and, consequently, the suspension compliance becomes important to model. This modelling is also more suited for braking, which typically involve suspension more than propulsion.

3.3.7.1 Acceleration Performance *

*Function definition: **Acceleration performance** is the time needed to, with fully applied accelerator pedal, increase speed from a certain speed to another certain higher speed, at certain road friction on level ground without headwind and certain load.*

3.3.7.2 Solution using Integration over Time

A front-wheel-drive passenger car with a stepped gearbox should accelerate from 0 to 100 km/h. A Matlab code is given in Equation [3.20], which simulates the acceleration uphill from stand-still, using simple numerical integration. The code calculates the possible acceleration in each of the gears, and one mode with slipping clutch. In each time step it selects that which gives the highest acceleration. The numerical data and results are not given in the code, but some diagrams are shown in Figure 3-45. The code is not fully documented, only using equations so far presented in this book.

```
dt=0.1; t_vec=[0:dt:10]; vx_vec(1)=0;
for i=1:length(t_vec)
    vx=vx_vec(i);
    Rres=-m*g*sin(p)+froll*m*g*cos(p)+0.5*roh*A*cd*vx*vx;

    %if gear 1 (clutch engaged)
    ratio=ratios(1);
    we=vx*ratio/radius;
    Te=interp1(Engine_w,Engine_T,we);
    Fx=Te*ratio/radius;
    ax=(Fx-Fres)/(m+(Jw+Je*(ratio^2))/(radius^2));
    Ffz=m*(g*lr/L-ax*h/L);
    if Fx>mu*Ffz

    %if gear 2
        Fx=mu*Ffz;
        ax=(Fx-Rres)/m;
    end
    ax1=ax;   %(clutch engaged)
    ratio=ratios(2);
    … then similar as for gear 1
```

[3.20]

```
    ax2=ax;

    %if gear 3 (clutch engaged)
    ratio=ratios(3);
    … then similar as for gears 1 and 2
    ax3=ax;

    %if clutch slipping on gear 2
    ratio=ratios(2);
    wc=vx*ratio/radius; %speed of output side of clutch
    Te=max(Engine_T);
    we=Engine_w(find(Engine_T>=Te)); %engine runs on speed where max torque
    Fx=Te*ratio/radius;
    ax=(Fx-Fres)/(m+Jw/(radius^2));
    Ffz=m*(g*lr/L-ax*h/L);
    if Fx>mu*Ffz
        Fx=mu*Ffz;
        ax=(Fx-Rres)/m;
    end
    if wc>we %if vehicle side (wc) runs too fast, we cannot slip on clutch
        ax=-inf;
    end
    ax0=ax;

    [ax,gear_vec(i)]=max([ax0,ax1,ax2,ax3]);  vx_vec(i+1)=vx+ax*dt;
end
```

Phenomena that are missing in this model example are:

- Gear shifts are assumed to take place instantly, without any duration
- The option to use slipping clutch on 1st and 3rd gear is not included in model
- The tyre slip is only considered as a limitation at a strict force level, but the partial slip is not considered for simplification. The code line "`we=vx*ratio/radius;`" is hence not fully correct. Including the slip, the engine would run at somewhat higher speeds, leading to that it would lose its torque earlier, leading to worse acceleration performance.
- Load transfer is assumed to take place instantly quick; delays due to Suspension compliance, as described in 3.3, are not included.

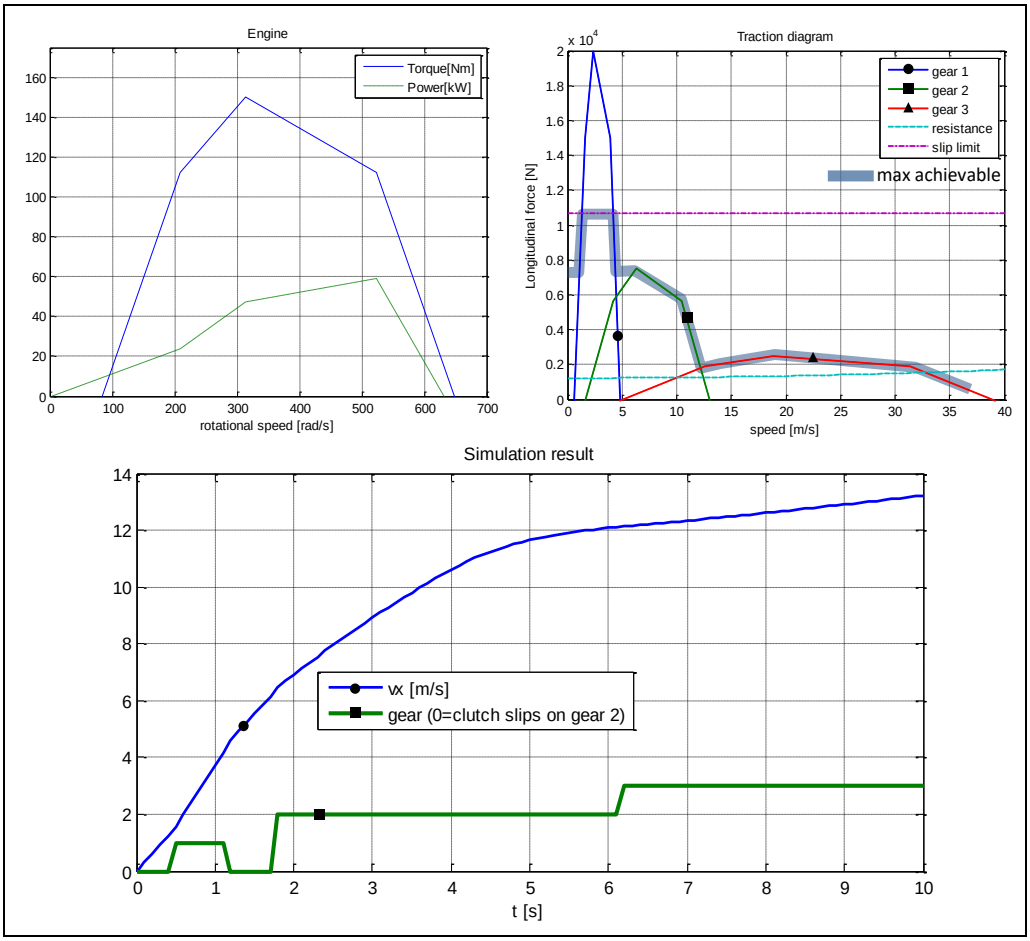


Figure 3-45: Example of simulation of acceleration, using the code in Equation [3.20].

3.3.7.3 Solution using Integration over Velocity

In some cases, with simple vehicle models and monotonously varying velocity, there is an alternative way to find the relation between v_x and t is to separate the differential equation:

$$m \cdot a_x = m \cdot \frac{dv_x}{dt} = F_x(v_x) - R_{res}(v_x); \Rightarrow \frac{m \cdot dv_x}{F_x(v_x) - R_{res}(v_x)} = dt \Rightarrow$$

$$\Rightarrow \int_0^{v_{x,end}} \frac{m \cdot dv_x}{F_x(v_x) - R_{res}(v_x)} = \int_0^{t_{end}} dt \Rightarrow \quad t_{end} = \int_0^{v_{x,end}} \frac{m \cdot dv_x}{F_x(v_x) - R_{res}(v_x)};$$

If simple mathematic functions can be used to describe $F_x(v_x)$ and $F_{res}(v_x)$ the solution can even be on closed form.

3.3.7.4 Solution using Simulation over Position

In some cases, with simple vehicle models and monotonously varying position s, we rewrite to a, initial value problem with position instead of time. The following table shows an example of driving over a crest and set speed is reduced on the way down. The $'$ denotes d/ds.

With time t as independent variable	*With position s as independent variable*
$m \cdot \dot{v}_x = F_x - R_{res};$	$m \cdot v_x' \cdot v_x = F_x - R_{res};$
$F_x = m \cdot (v_{xReq} - v_x)/t_{Drvr}\,;$	$F_x = m \cdot (v_{xReq} - v_x)/t_{Drvr}\,;$
$R_{res} = R_{res}(s, v_x);$	$R_{res} = R_{res}(s, v_x);$
$\dot{s} = v_x;$	$t' = 1/v_x\,;$
$a_x = \dot{v}_x;$	$a_x = v_x' \cdot v_x;$

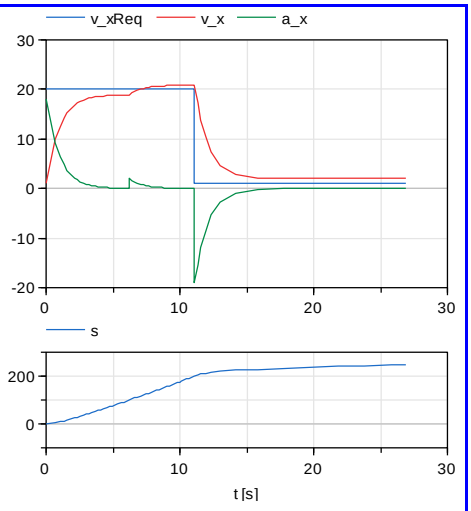


Figure 3-46: Comparing simulation with time and position as independent variable.

It is often possible to study transport missions between two positions with s as independent variable. An advantage is in those cases one does not have to solve the state variable t. If one need to solve for t, the model has the drawback of being singular for stand-still ($v_x = 0$) due to $t' = 1/v_x\,;$. It can be overcome by using t as independent variable for velocities close to 0. Generally, the step selection can be difficult also if only close to $v = 0$; it can then be an idea to judge which time step Δt would be suitable if time was independent variable, and then select a varying position step $\Delta s = v \cdot \Delta t$.

3.4 Functions in (shorter) events

This section targets models and methods to define and verify functions in a certain and shorter time frame, typically 0.5 to 5 seconds. These are functions which rather influence safety risks than transport costs.

Since in the Chapter 3 “Longitudinal Dynamics”, mainly longitudinal acceleration and deceleration are considered. (Friction) Brake system and phenomena as load transfer then becomes important, why these are presented early. But first, some typical driving manoeuvres are presented.

3.4.1 Typical Test Manoeuvres

When applying the longitudinal actuator systems (propulsion system and brake system) there are a couple of different situations which are typical to consider:

- Straight line maximum braking from, typically 100 km/h to stand-still for passenger cars.
- Braking in curve with significant lateral acceleration, see References (ISO, 2006) and (ISO, 2011).
- Straight line acceleration, typically 0 to 100 km/h and 80-100 km/h.
- Accelerating in curve with significant lateral acceleration.

For these four main situations, one can also vary other, typically:

- At high road friction and at low friction, often called "hi-mu" and "lo-mu"
- At different road friction left and right, often called "split-mu"
- At sudden changes in road friction, called "step-mu" or "step-up" and "step-down" when going to higher and lower friction, respectively.
- At high speed, typically 200 km/h, for verifying lateral stability
- At different up-hill/down-hill gradients
- At different road banking (slope left to right)

A propelled or braked wheel or axle develops a longitudinal force, F_x, counter-acting the rotation. F_x is limited by the road friction: $|F_x|_{max} = \mu \cdot F_z$;. (**not** $|F_x|_{max} = \mu \cdot F_z - f_r \cdot F_z$, see Figure 2-24).

Braking Coefficient $= -F_x/F_z$, is a property defined for an axle or a single wheel. It can be seen as the utilized friction coefficient, μ_{util} = brake force/normal load. The μ_{util} should not be mixed up with (available) friction coefficient, μ; the relation between them is $\mu_{util} \leq \mu$.

3.4.2 Deceleration Performance

There are some different functions that measures braking performance or deceleration performance.

3.4.2.1 Braking Efficiency *

> *Function definition:* ***Braking Efficiency*** *is the ratio of vehicle deceleration and the best brake-utilized axle (or wheel), while a certain application level of the brake pedal at a certain speed straight ahead, at certain road friction on level ground without head-wind and certain load at a certain position in the vehicle.*

In equation form, the Braking Efficiency becomes $= \frac{-a_x}{g \cdot \max_{\forall i}(\mu_{i,util})} = \frac{-a_x}{g \cdot \max_{\forall i}(F_{ix}/F_{iz})}$;. If Braking Efficiency = 1 = 100%, the **distribution** of braking is optimal.

An alternative definition which is only relevant for maximum brake pedal apply is Braking Efficiency $= \frac{-a_x}{g \cdot \mu_{peak}}$. This definition requires that all tyres have the same and known characteristics at the particular ground. The value of 100% then means that the **braking** is maximum.

3.4.2.2 Braking Distance *

> *Function definition:* ***Braking Distance*** *is the distance travelled during braking with fully applied brake pedal from a certain speed straight ahead to another certain lower speed, at certain road friction on level ground without headwind and certain load at a certain position in the vehicle.*

For passenger cars one typically brakes fully from 100 km/h and then the braking distance is typically around 40 m (average $a_x = -9.65\ m/s^2$). For a truck it is typically longer, 51..55 m ($-7.5..-7\ m/s^2$).

3.4.2.3 Stopping Distance *

> *Function definition:* ***Stopping Distance*** *is the distance travelled from that an obstacle becomes visible to driver have taken the vehicle to stand-still. Certain conditions, as for Braking Distance, have to be specified, but also a certain traffic scenario and a certain driver to be well defined.*

Stopping Distance is the braking distance + the "thinking/reaction distance", which depends on the speed and the reaction time. The reaction time of a driver is typically 0.5..2 seconds.

3.4.3 Pedal Functions

3.4.3.1 Pedal Response *

Function definition: ***Accelerator pedal response*** *is how vehicle acceleration varies with accelerator pedal position, for a certain vehicle speed and possibly certain gear, on level ground without pressing the brake pedal.*

Function definition: ***Brake pedal response*** *is how vehicle deceleration varies with brake pedal force, for a certain vehicle speed, on level ground without pressing the accelerator pedal.*

These functions, together with the functions in 3.4.3.2, enable the driver to operate the vehicle longitudinally with precision and in an intuitive and consequent way. The requirements based on above function definitions, are typically that the translation of pedal position (or force) to vehicle acceleration (or deceleration) should be consistent, progressive and oscillation-free.

For accelerator pedal steps, there should be enough acceleration, but also absence of "shunt and shuffle" (driveline oscillations). When accelerator pedal is suddenly lifted off, there shall be certain deceleration levels, depending on vehicle speed and gear selected.

3.4.3.2 Pedal Feel *

Function definition: ***Accelerator pedal feel*** *is the pedal's force response to pedal position.*

Function definition: ***Brake pedal feel*** *is the pedal's position response to pedal force.*

These functions, together with the functions in 0, enable the driver to operate the vehicle longitudinally with precision and in an intuitive and consequent way.

3.4.4 Brake and traction distribution

For braking performance, it is important that both axles are used as much as possible during braking, without that any wheel is locked ($\omega = 0$). But one also should consider that, in most driving situations, it is preferred that the front wheels lock first, because:

- A vehicle with **locked front** (steered) wheels ($\omega_f = 0$) tends to be yaw **stable**. However, steering ability is lost, so vehicle continues straight, **incapable of curving its path**.
- A vehicle with **locked rear** wheels ($\omega_r = 0$) tends to be yaw **unstable**. It starts to **flip around** to end up sliding with the rear first.

To understand why these modes appear, one need to understand combined slip tyre models 2.2.5 and lateral dynamic 4.3, 4.4, 4.5. When locking an axle, the lateral grip margin is totally lost. But already when mild braking is applied, the lateral slip stiffness is reduced, which can harm the steering capability or reduce the yaw stability. In present section, we will only consider the extreme, i.e., locking, which we identify as $when\ \sqrt{F_{ix}^2 + F_{iy}^2} = \begin{Bmatrix} if\ straight \\ line\ driving \end{Bmatrix} = |F_{ix}| < -\mu \cdot F_{iz}$.

So, braking performance has a conflict with either steerability or yaw stability, depending on how we distribute braking between front and rear axle.

(A similar problem is to distribute wheel torques for strong propulsion, except that "locked" ($F_{ix} < -\mu \cdot F_{iz}$) is then replaced by "spin" ($F_{ix} > \mu \cdot F_{iz}$). As for locking, spinning an axle eliminates its lateral grip margin totally. And, as for locking, spin at front reduces steerability while spin at rear reduces yaw stability. So, acceleration performance has a conflict with either steerability or yaw stability, depending on how we distribute propulsion between front and rear axle.)

In Chapter 4, we will find that a vehicle can lose yaw stability while straight line driving and $K_u = (C_{ry} \cdot l_r - C_{fy} \cdot l_f)/(C_{fy} \cdot C_{ry} \cdot L) < 0$ and $v_x > v_{xCrit} = \sqrt{L/(-K_u \cdot m)}$. If $K_u > 0$, instead the steerability is strongly reduced when $v_x > v_{xChar} = \sqrt{L/(+K_u \cdot m)}$. In present chapter, we use an extreme combined tyre slip model where the lateral slip stiffness is either a constant or zero: $dF_y/dv_y = C_y = if\ \sqrt{F_x^2 + F_y^2} < \mu \cdot F_z\ then\ C_{y0}\ else\ 0$;. It means that the

influence of v_x disappears, or $v_{xCrit} = v_{xChar} = 0$. The vehicle becomes yaw instable if $|F_{rx}| = \mu \cdot F_{rz}$ and loses steerability if $|F_{fx}| = \mu \cdot F_{fz}$, for any $v_x > 0$.

Wheel torques is influenced simultaneously by both propulsion system and (friction) brake system, especially if regenerative braking with electric propulsion system. So, coordination of brake and propulsion systems is important.

The basic function of a brake system is that brake pressure (hydraulic on passenger cars and pneumatic on trucks) is activated so that it applies brake pads towards brake discs or drums. In a first approximation, the pressure is distributed with a certain fraction on each axle. For passenger cars this is typically 60..70% of axle torque front. In heavy trucks, the distribution varies a lot, e.g. 90% for a solo tractor and 30% for heavy off-road construction rigid truck. The intention is to utilize road friction in proportion to the normal load but not brake too much rear to avoid yaw instability.

We can generalise to the following **concept of axle torque coordination for equal friction utilization**:

Coordinate axle torques T_i so that friction circle is reached (F_{ixy} reaches $\mu \cdot F_{iz}$) on both axles $i = \{f, r\}$ at the same longitudinal force $F_x = F_{fx} + F_{rx}$.

Notes:

- This does **not** require that we know the friction coefficient, just that it is **same** under all axles ($\mu_f = \mu_r = \mu$;).
- This can be extended to coordination of different actuators for **wheel** torque.
- This does **not** guarantee constant understeering since understeering is determined by slip stiffnesses rather than friction circles. See disclaimer in 3.4.4.1. However, if the slip stiffnesses are unknown, it helps to keep retain approximately a constant understeering.

To give simplest possible example, we consider a two-axle vehicle. We assume a one-track model. We neglect aerodynamic forces and road grade in Eq [3.18]. Add driving resistance R_x acting on vehicle body in CoG (road grade and aero drag, no aero lift, and no rolling resistance). Change a_x to an expression with F_x and R_x.

$$\frac{F_{fx}}{\mu_f \cdot F_{fz}} = \frac{F_{rx}}{\mu_r \cdot F_{rz}} \quad \text{"Concept of axle torque coordination for equal friction utilization";}$$

$$\mu_f = \mu_r = \mu \quad \text{"Assume same coefficient of friction";}$$

$$\frac{F_{fz}}{F_{rz}} = \frac{m \cdot g \cdot \frac{l_r}{L} - m \cdot a_x \cdot \frac{h}{L}}{m \cdot g \cdot \frac{l_f}{L} + m \cdot a_x \cdot \frac{h}{L}} = \frac{g \cdot l_r - (F_x - R_x) \cdot \frac{h}{m}}{g \cdot l_f + (F_x - R_x) \cdot \frac{h}{m}} \quad \text{"Longitudinal load transfer";}$$

$$where \quad F_x = F_{fx} + F_{rx} \quad \text{"Definition of } F_x\text{";}$$

Combining these equations, we get expressions for the optimal F_{fx} and F_{rx}:

either as expressed in F_x, each other, or $\{a_x, R_x\}$:

$$F_{fx} = \frac{l_r}{L} \cdot F_x - \frac{h}{m \cdot g \cdot L} \cdot F_x^2; \text{ and } F_{rx} = \frac{l_f}{L} \cdot F_x + \frac{h}{m \cdot g \cdot L} \cdot F_x^2;$$

or

$$F_{fx} = -\frac{(R_x + a_x \cdot m) \cdot (R_x \cdot h + m \cdot a_x \cdot h - m \cdot g \cdot l_r)}{m \cdot g \cdot L}; \text{ and } F_{rx} = \frac{(R_x + a_x \cdot m) \cdot (R_x \cdot h + m \cdot a_x \cdot h + m \cdot g \cdot l_f)}{m \cdot g \cdot L}; \quad [3.21]$$

Eq [3.21] is plotted for variation in centre of gravity height and longitudinal position in Figure 3-47. The distribution of brake between axles is regulated, see Figure 3-48 and left part of Figure 3-54

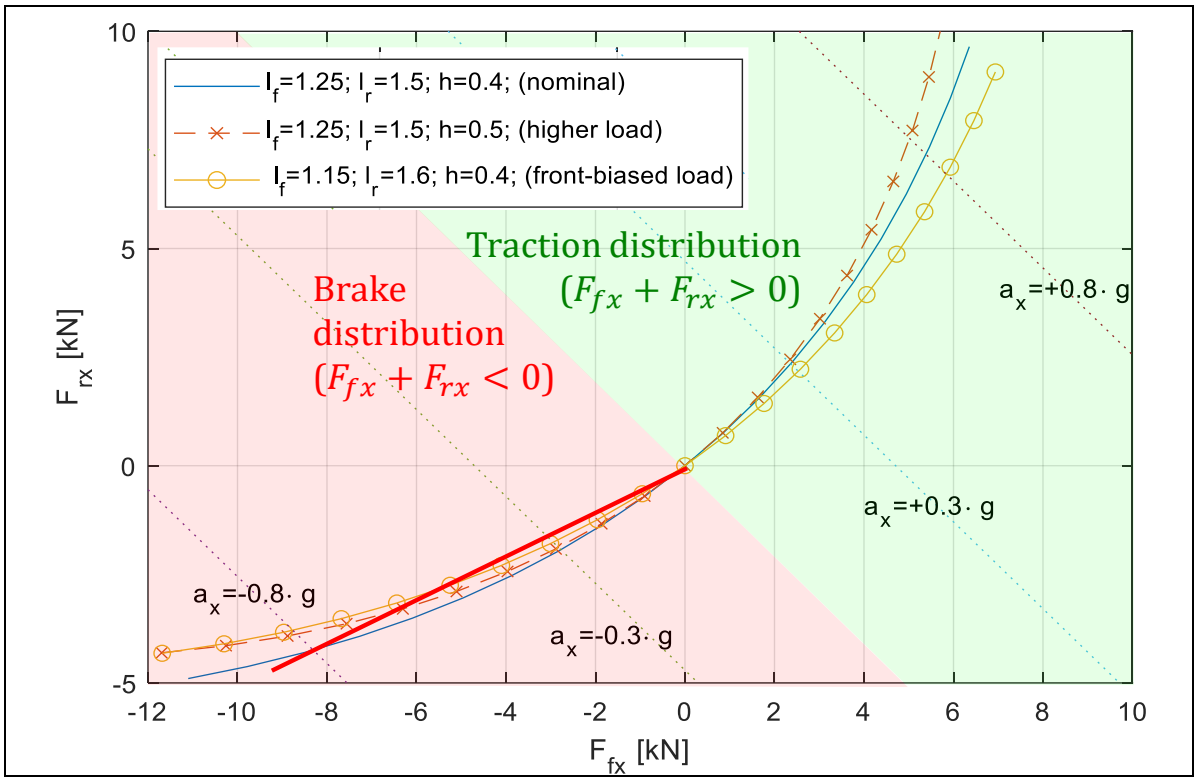


Figure 3-47: Traction and Brake Distribution diagram. The 3rd quadrant is often used alone, for braking, with $\{-F_{fx}, -F_{rx}\}$ on the axes. The thin curves mark optimal distribution for some variation in position of centre of gravity. The bold curve shows one actual brake distribution, assuming hydrostatic brake distribution with certain hydraulic piston areas and brake disk radii. Driving resistance R_x is zero.

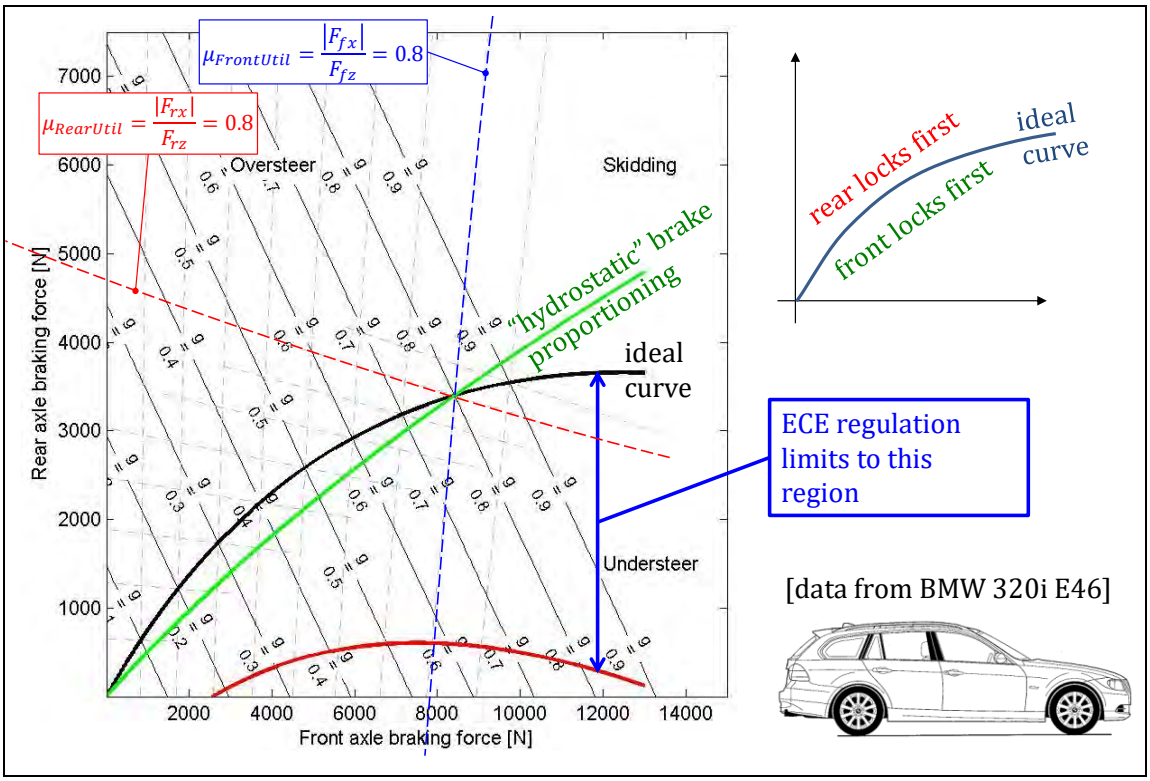


Figure 3-48: Brake Distribution. Built on figure from (Boerboom, 2012). The "hydrostatic curve" is generally a straight line. But, in this case it is weakly digressive, thanks to a brake pad material with pressure dependent friction coefficient. The curves for utilized friction are slightly curved.

The distribution is done by selecting pressure areas for brake callipers, so the base distribution will be a straight line, marked as "hydrostatic brake distribution". For passenger cars, one typically designs this so that front axle locks first for friction below 0.8 for lightest vehicle load and all variants. For heavier braking than $0.8 \cdot g$, or higher (or front-biased) centre of gravity, the rear axle will lock first, if only hydrostatic distribution. But there are more advanced design concepts that counteract such rear axle locking. One is to restrict the brake pressure to the rear axle. This is done by pressure limiting valve, brake pads with pressure dependent friction coefficient or Electronic Brake Distribution (EBD). In principle, it bends down the hydrostatic curve as shown in Figure 3-47. With pressure dependent values one gets a piece-wise linear curve, while pressure dependent friction coefficient gives a continuously curved curve. EBD is an active control using same mechatronic actuation as ABS. EBD is the design used in today's passenger cars, since it comes with ABS, which is a legal requirement on most markets.

On heavy vehicles with EBS (Electronic Brake System) and vertical axle load sensing, the brake pressure for each axle can be tailored. For modest braking (deceleration $\leq 2\ m/s^2$) all axles are braked in proportion to brake pad wear, because it is so important to keep vehicle maintenance cost low. This means to brake in proportion to brake pad area and brake pad radius, which often means same torque on each axle. First when braking more (e.g. above a certain threshold of $-F_{xReq}$ or $-s_{ix}$), the brake pressure is distributed more in proportion to each axle's vertical load.

3.4.4.1 Braking for yaw balance

A **disclaimer** to the analysis so far in 3.4.4, is that the analysis only takes the friction circle edge, $|F_{ixy}| = \mu_i \cdot F_{iz}$, into account. In 4.3, especially 4.3.5.1, we will find that lateral instability, for high longitudinal velocity, can occur also due to changed lateral slip stiffness per axle group $C_{iy} = CC_y \cdot F_{iz};\quad for\ i = \{f, r\}$. We will find, so called, *critical speed* and *characteristic speed* for two axle vehicles and *zero-damping speed* for articulated vehicles. We can draw lines for different v_{xCrit} and v_{xChar} in the brake distribution diagram. We then must give also numerical parameters for the tyres, e.g. μ and CC_{y0}. We also must add these equations:

$$Eq\ [4.19] \quad \Rightarrow \quad v_{xCrit} = \sqrt{\frac{L}{-K_u \cdot m}};\quad and\quad v_{xChar} = \sqrt{\frac{L}{+K_u \cdot m}};$$

$$where\ K_u = \{Eq\ [4.10]\} = \frac{l_r}{C_{fy} \cdot L} - \frac{l_f}{C_{ry} \cdot L} = \frac{l_r}{CC_{fy} \cdot F_{fz} \cdot L} - \frac{l_f}{CC_{ry} \cdot F_{rz} \cdot L};$$

$$where\ CC_{iy} = \{Eq\ [2.62]\} = \sqrt{1 - \left(\frac{F_{ix}(s_{ix})}{\mu \cdot F_{iz}}\right)^2} \cdot CC_{y0};$$

$$where\ F_{fz} = m \cdot g \cdot \frac{l_r}{L} - \left(F_{fx} + F_{rx}\right) \cdot \frac{h}{L};\quad and\quad F_{rz} = m \cdot g \cdot \frac{l_f}{L} + \left(F_{fx} + F_{rx}\right) \cdot \frac{h}{L};$$

Now we can add the v_{xCrit} and v_{xChar} in the Traction and Brake Distribution diagram, see Figure 3-49..Figure 3-51. For a given speed, one can find a safe part of the ideal curve, a safe area, and a safest point and safest line. The safest point and safest line mark where $v_{xCrit} = v_{xChar} = \pm\infty$. The safest line is only known if we know the friction μ, while the ideal curve only assumes $\mu_f = \mu_r$.

A similar diagram can be found (and called Dynamic square) in Reference (Klomp & Thomson, 2010), and there it is pointed out that not only the v_{xCrit} and v_{xChar} but also the lateral acceleration varies over the $\{F_{fx}, F_{rx}\}$-plane.

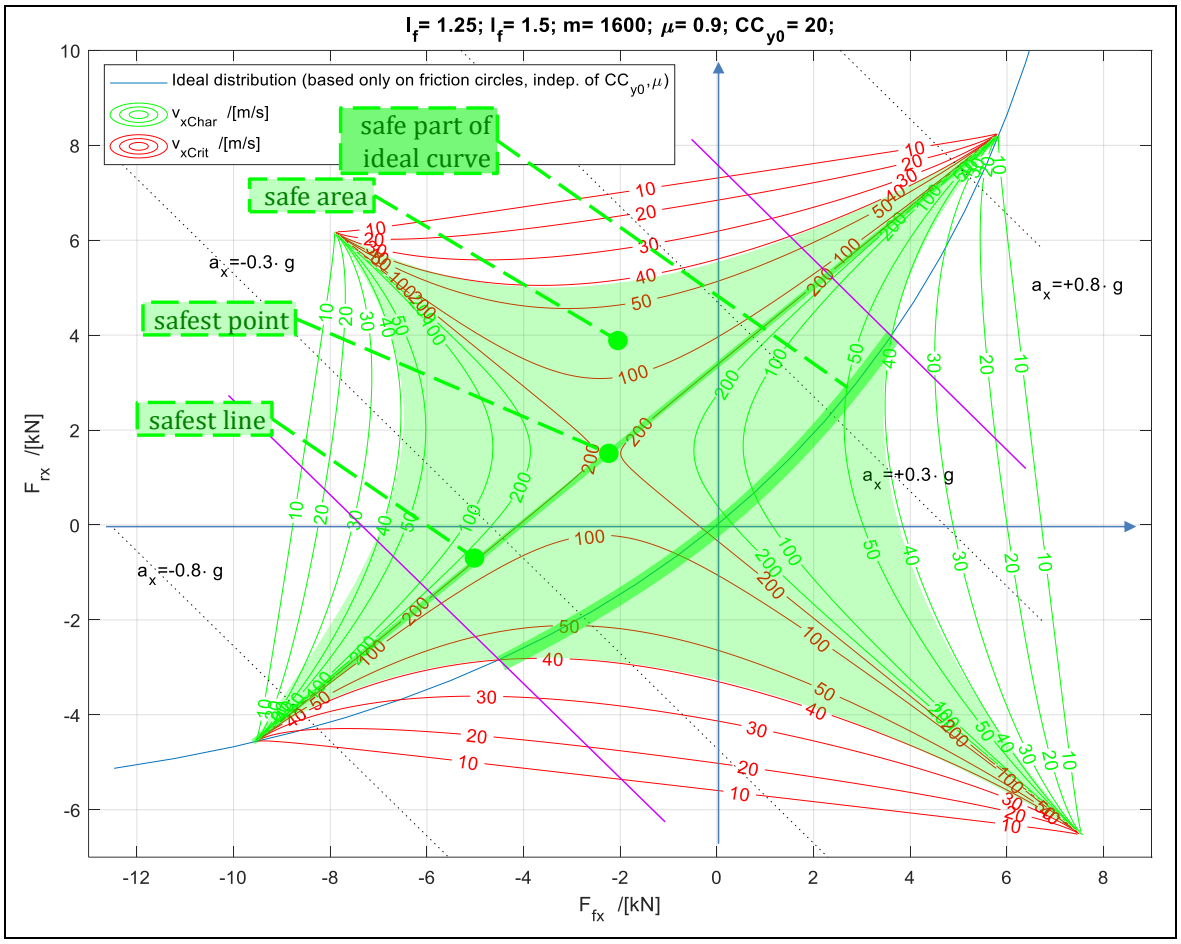


Figure 3-49: Traction and Brake Distribution diagram with yaw balance for straight-line driving, expressed as v_{xChar} and v_{xCrit}. Safe part, safe area, and safest point is marked for $v_x = 40\ [m/s]$. The lines for constant a_x can also be marked with a constant F_x. Friction $\mu = 0.9$.

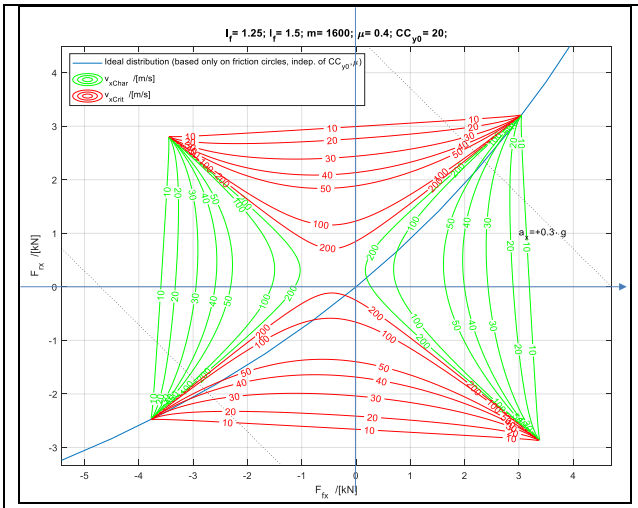


Figure 3-50: Traction and Brake Distribution diagram, as Figure 3-49 but lower friction, $\mu = 0.4$.

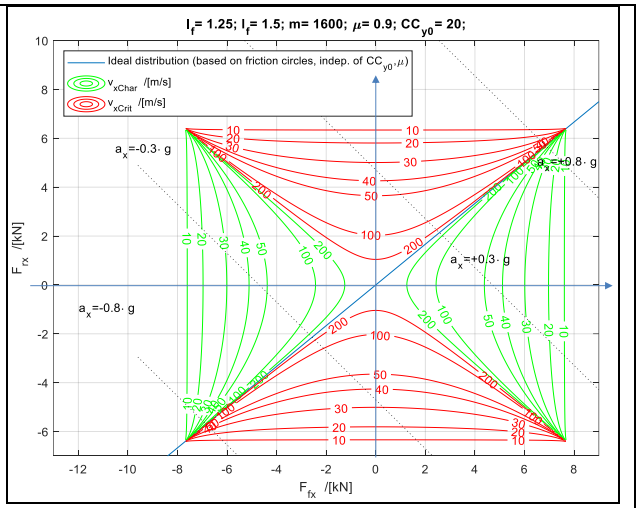


Figure 3-51: Traction and Brake Distribution diagram, as Figure 3-49 but CoG at ground, i.e. h=0.

The diagrams, Figure 3-49..Figure 3-51, are useful for stability-limitation of longitudinal force between front and rear axle group, for a given v_x, but only for straight-line driving. Note that the $\{\beta_f, \beta_r\}$ are identical to zero, which is implicitly modelled and not even explicitly included in the mathematical model. For limitation while driving in a curve, one can do a model which is linearized around a certain steady state cornering condition, see 3.4.4.2. When doing that, we can draw the limit either in a

$\{F_{fx}, F_{rx}\}$-diagram as in Figure 3-49..Figure 3-51, or in a $\{\beta_f, \beta_r\}$-diagram, or $\{\beta, \omega_z\}$-diagram, which can be more robustly interfaced with a closed-loop control on body side slip angles. Such diagrams also are more easily understood and compared with the relatively well-established phase portraits, see 4.5.5.

The above models can be used as "model for control design" for a control of how wheel torques should be coordinated between the axles. It becomes a feedforward control, while there is often needed to add a closed loop part. To arbitrate (switch or sum) the feedforward and closed loop, there must be a control error. The control error should be formulated in something measurable. The F_{fx} and F_{rx} are not well measurable, but the s_{fx} and s_{rx} are better. So, it is of interest to plot the same data as in Figure 3-49, but in a diagram with $\{s_{fx}, s_{rx}\}$. Then we must engage a tyre model which includes the longitudinal slip:

$$F_{ix} = +\mu \cdot F_{iz} \cdot \text{sign}(s_{ix}) \cdot \text{tanhyp}\left(\frac{CC}{\mu} \cdot \left|1 - \frac{v_x}{R \cdot \omega_i}\right|\right);$$

$$F_y = 0;$$

$$C'_{iy,sx0} = \begin{cases} = \mu \cdot F_{iz} \cdot \left|1 - \frac{1}{s_{ix0}}\right| \cdot \text{tanhyp}\left(\frac{CC}{\mu} \cdot |s_{ix0}|\right); & if\ \omega > 0 \\ = \mu \cdot F_{iz} \cdot \left|1 + \frac{1}{s_{ix0}}\right| \cdot \text{tanhyp}\left(\frac{CC}{\mu} \cdot |s_{ix0}|\right); & else \end{cases}$$

[3.22]

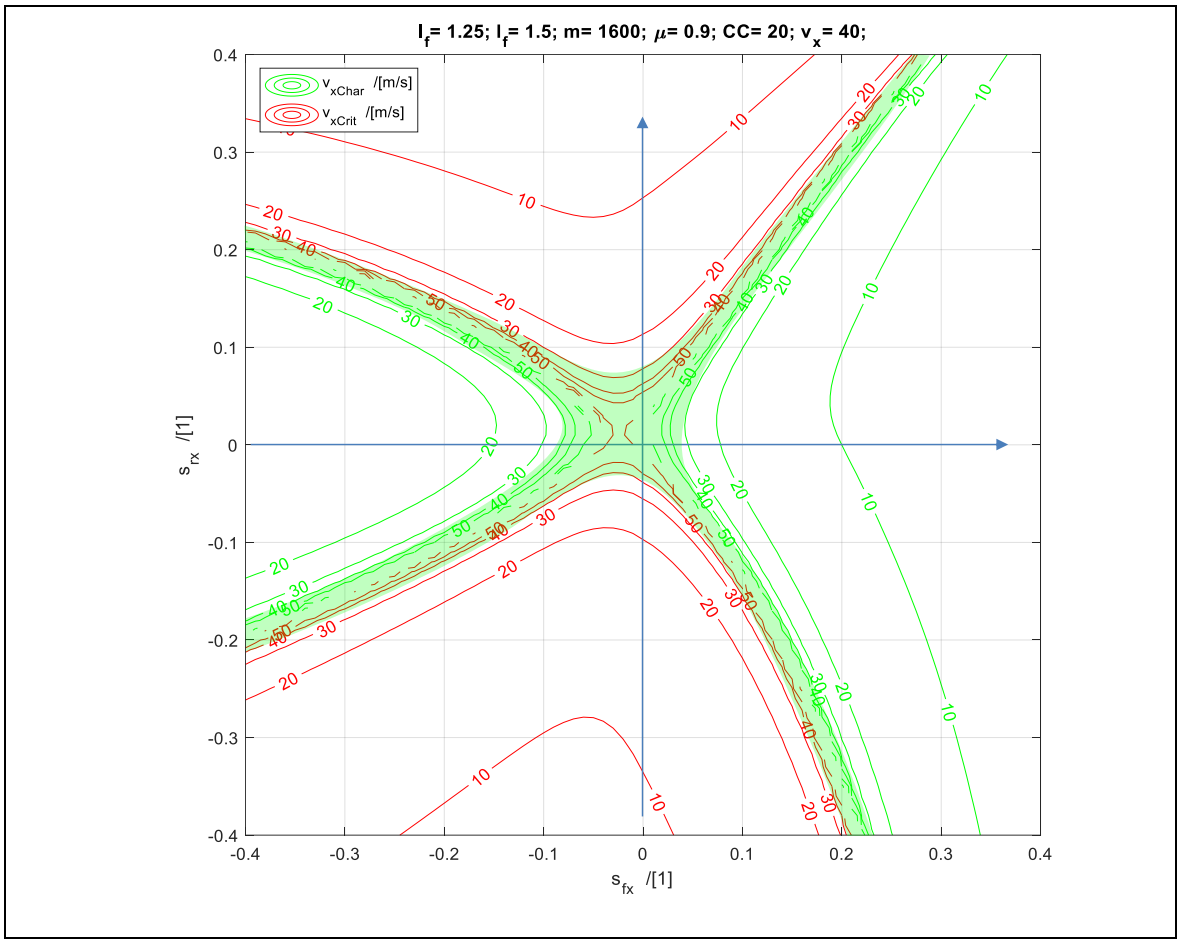


Figure 3-52: Traction and Brake Distribution diagram (in longitudinal slip) with yaw balance for straight-line driving, expressed as v_{xChar} and v_{xCrit}. Safe area for $v_x \leq 40\ [m/s]$ is (approximately) marked with shaded green.

3.4.4.2 Braking from steady state cornering

In 3.4.4.2, we will use some lateral dynamics, even if it is before lateral dynamics in Chapter 4.

We assume that the braking takes place from a *steady state cornering (SSC)*, instead of from straight line driving (SLD). SSC means that the vehicle has a non-zero but constant lateral (or centrifugal) acceleration a_y, but $\dot{v}_y = \dot{\omega}_z = 0$. We can no longer assume that lateral forces $\{F_{fy}, F_{ry}\}$ are zero. So, we must include them and, therefore, add the 2 lateral equilibrium equations:

$$m \cdot a_y = F_{fy} + F_{ry} \qquad \text{“Lateral”;}$$
$$F_{fy} \cdot (L - l_r) - F_{ry} \cdot l_r = 0 \qquad \text{“Yaw”;}$$

The equal utilization of friction must be formulated as follows:

$$\frac{\sqrt{F_{fx}^2+F_{fy}^2}}{\mu \cdot F_{fz}} = \frac{\sqrt{F_{rx}^2+F_{ry}^2}}{\mu \cdot F_{rz}} \qquad \text{"Concept of axle torque coordination for equal friction utilization";}$$

(instead of $\frac{F_{fx}}{\mu \cdot F_{fz}} = \frac{F_{rx}}{\mu \cdot F_{rz}}$;)

Figure 3-54 and Figure 3-55 show results for both straight line driving and steady state cornering.

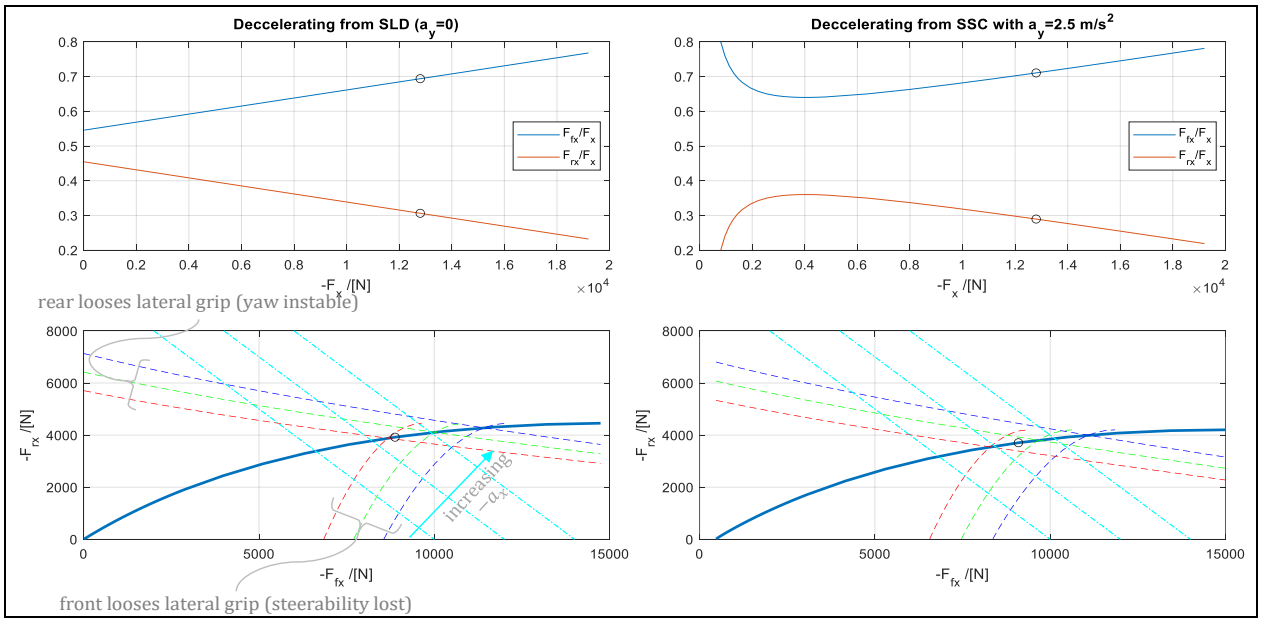


Figure 3-54: Ideal brake distribution for straight line driving (left) and steady state cornering (right). Dashed curves in lower diagrams shows where axles reach friction levels $\mu = \{0.8,\ 0.9,\ 1.0\}$, or we can see them as curves for μ_{fUtil} and μ_{rUtil}. Dash-dotted cyan lines show constant a_x. Parameters: $L = 2.75\ [m];\ l_r = 1.5\ [m];\ m = 1600\ [kg];\ h = 0.5\ [m];$.

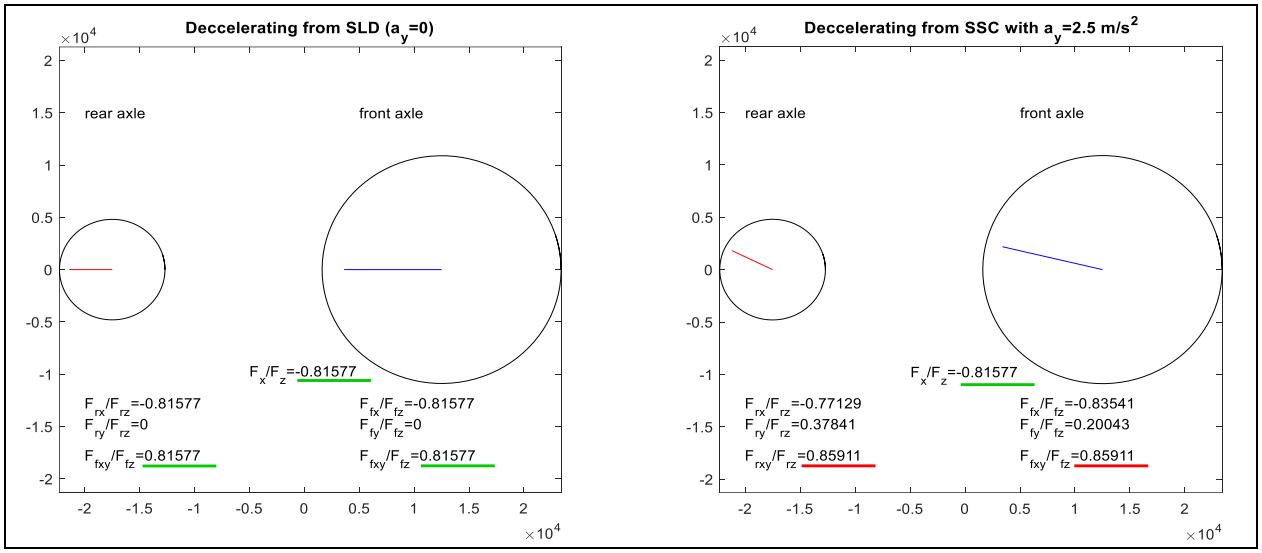


Figure 3-55: Ideal brake distribution for SLD (left) and SSC (right) for the circle-marked deceleration in Figure 3-54. Both SLD and SSC develop same longitudinal force, so they have same longitudinal deceleration. SLD requires only $\mu = 0.81577$, but SSC requires $\mu = 0.85911$.

Note that ideal distribution for SSC suggests different signs of F_{fx} and F_{rx}, for $-F_x$ close to zero, see upper right diagram in Figure 3-54.

We will now connect back to the first brake distribution diagrams, Figure 3-47 and Figure 3-48, where the ideal curve for $a_y = 0$. Let us add the line for some non-zero $|a_y|$ in same diagram as Figure 3-47. We then get Figure 3-56.

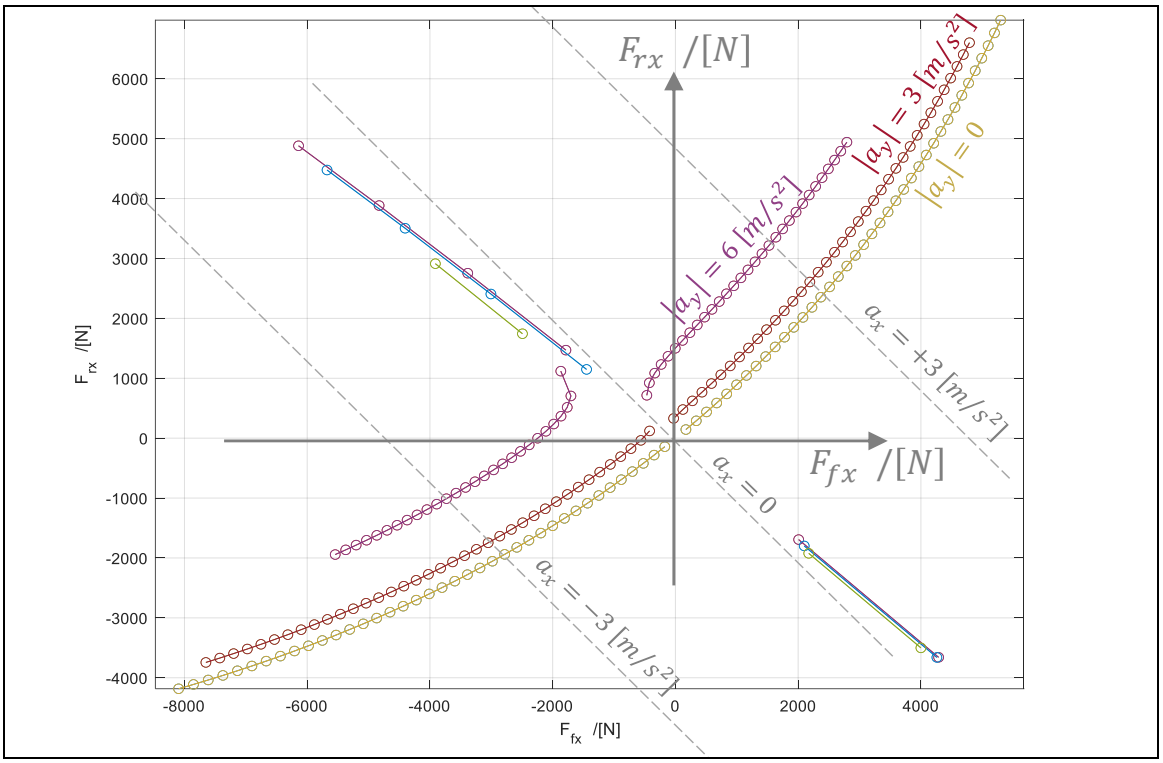


Figure 3-56: Traction and Brake Distribution diagram for both straight line driving ($a_y = 0$) and steady state cornering ($a_y \neq 0$). Parameters used: $m = 1600\ [kg]$, $g = 9.80665\ [m/s^2]$; $l_f = 1.25\ [m]$; $l_r = 1.5\ [m]$; $h = 0.4\ [m]$. The curves are ending where one axle becomes saturated by friction, using $\mu = 0.8$.

3.4.4.3 Heavy vehicles and articulated vehicles

A speciality for heavy vehicle is that there are often trailing units. The couplings make the distribution of vertical forces on one unit dependent of the braking on the other. If the coupling is of fifth wheel type, this is very strong dependence.

Another speciality is that heavy vehicle often have multiple axles in axle groups.

3.4.4.3.1 Articulated with lumped axle groups

In the following, a brake distribution diagram for a tractor with semi-trailer is constructed, as comparison with the two-axle vehicle, Figure 3-47. Figure 3-57 shows some simplifying assumptions.

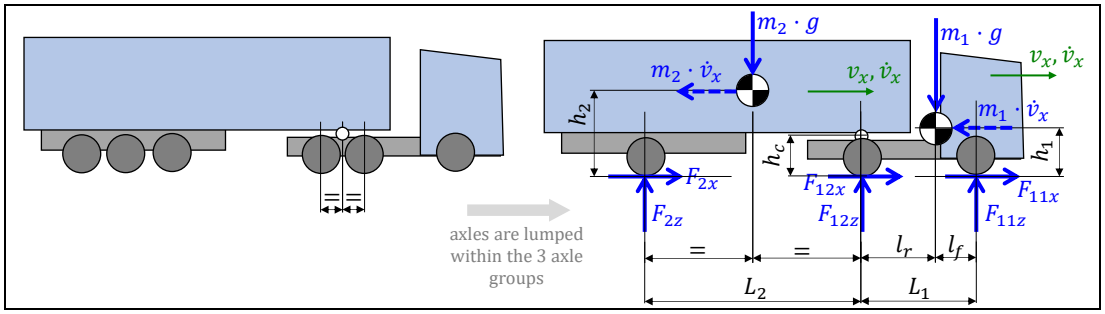


Figure 3-57: Example of combination vehicle to study brake distribution. Simplifications are shown.

First, the concept of equal friction utilization is one alternative:

$$\frac{F_{11x}}{\mu \cdot F_{11z}} = \frac{F_{12x}}{\mu \cdot F_{12z}} = \frac{F_{2x}}{\mu \cdot F_{2z}};$$

A second alternative concept is also formulated:

$$F_{11x} = 0; \quad \text{and} \quad \frac{F_{12x}}{\mu \cdot F_{12z}} = \frac{F_{2x}}{\mu \cdot F_{2z}};$$

The latter is motivated from maximum regeneration of energy, if electric propulsion on the tractor's rear axle group and on the trailer.

So, we have two alternative control concepts to compare, with 2 equations each. Both must, of course, obey the equilibrium, which gives 4 additional equations:

- $(m_1 + m_2) \cdot g = F_{11z} + F_{12z} + F_{2z}$ "Vertical force on whole combination vehicle";
- $(m_1 + m_2) \cdot \dot{v}_x = F_{11x} + F_{12x} + F_{2x}$ "Longitudinal force on whole combination vehicle";
- $m_1 \cdot g \cdot l_r - m_1 \cdot \dot{v}_x \cdot (h_1 - h_c) - (F_{11x} + F_{12x}) \cdot h_c - F_{11z} \cdot L_1 = 0$ "Pitch moment on tractor, around coupling";
- $-m_2 \cdot g \cdot L_2/2 - m_2 \cdot \dot{v}_x \cdot (h_2 - h_c) - F_{2x} \cdot h_c + F_{2z} \cdot L_2 = 0$ "Pitch moment on semi-trailer, around coupling";

Note that, it is not obvious that the load transfer should be modelled as instantaneous as the equation suggest. Anyway, the modelling above suggests so, which implicitly is an assumption that load transfer is much quicker than the critical motion modes (trailer swing-out and jack-knife). To check this assumption, one must study the case in time domain.

In total 2+4=6 equations and 6 unknowns ($F_{11x}, F_{12x}, F_{2x}, F_{11z}, F_{12z}, F_{2z}$). An algebraic solution can be found but we only show numerical diagrams for an example set of parameters, see Figure 3-58.

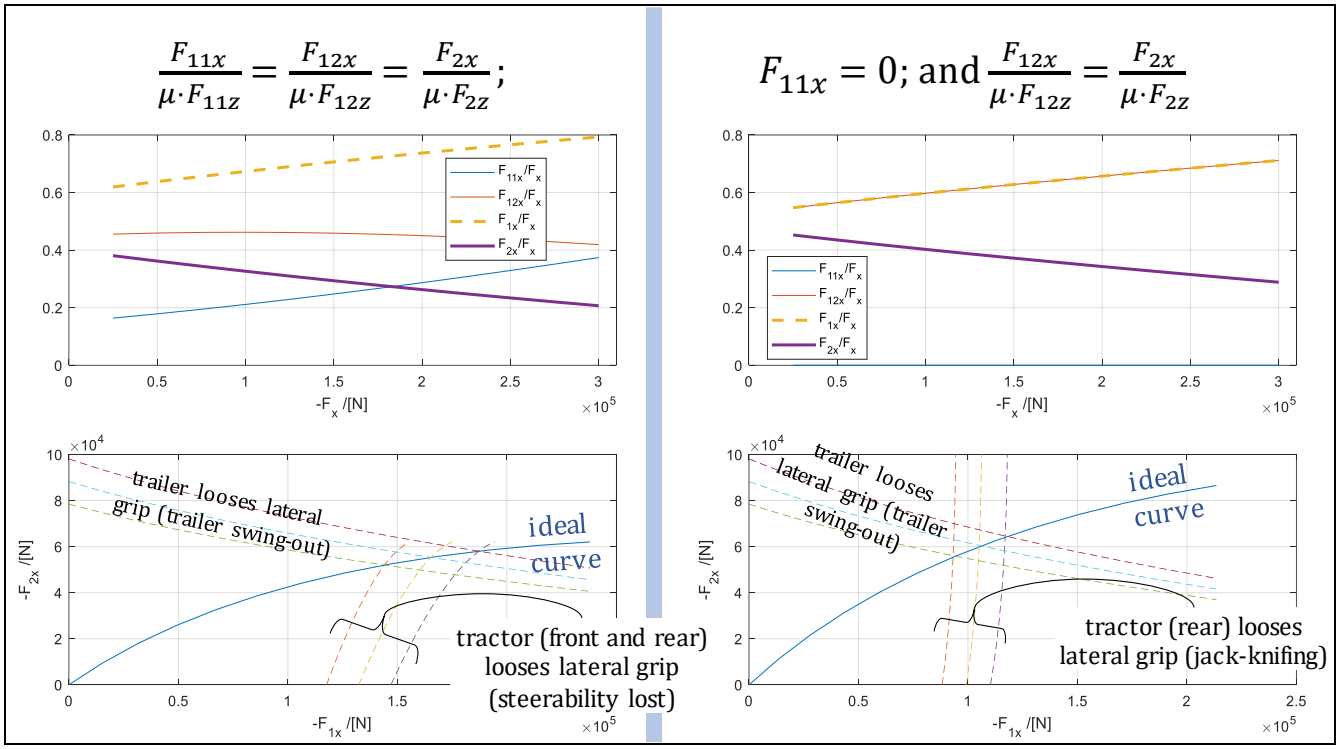


Figure 3-58: Two brake distribution concepts for tractor with semi-trailer in Figure 3-57. Left: Friction braking on all axles. Right: Regeneration on axle groups 12 and 2. Dashed curves in lower diagrams shows where axle groups reaches friction levels $\mu = \{0.8,\ 0.9,\ 1.0\}$. Parameters: $L_1 = 4\ [m];\ l_r = 3\ [m];\ L_2 = 6\ [m];\ h_c = 1.1\ [m];\ m_1 = 5\ [ton];\ h_1 = 0.4\ [m];\ m_2 = 20\ [ton];\ h_2 = 2\ [m];$

3.4.5 Heave and Pitch

So far, in 3.3.5.7 and 3.4.4, we modelled transfer of vertical forces between axles, but neither heave and pitch motion nor displacement. This will be added in 3.4.5. In 3.4.5.1, the load transfer is steady state and the linkage "trivial". In 3.4.5.2, the load transfer is transient and the linkage "non-trivial".

3.4.5.1 Steady State Load Transfer and Trivial Linkage

Additional to that the axle vertical loads change due to acceleration a_x, there are also change in out-of-road-plane motion (heave and pitch). In the following section, we study constant acceleration, e.g.

when mild braking for a long time. We propose the steady state model in Figure 3-59. The model differs between the "unsprung mass" (wheels and the part of the suspension that does not heave) and the "sprung mass" or "body" (parts that heaves and pitches as one rigid body). The wheels are assumed to be linked to the body through "trivial linkage" as in Figure 2-90.

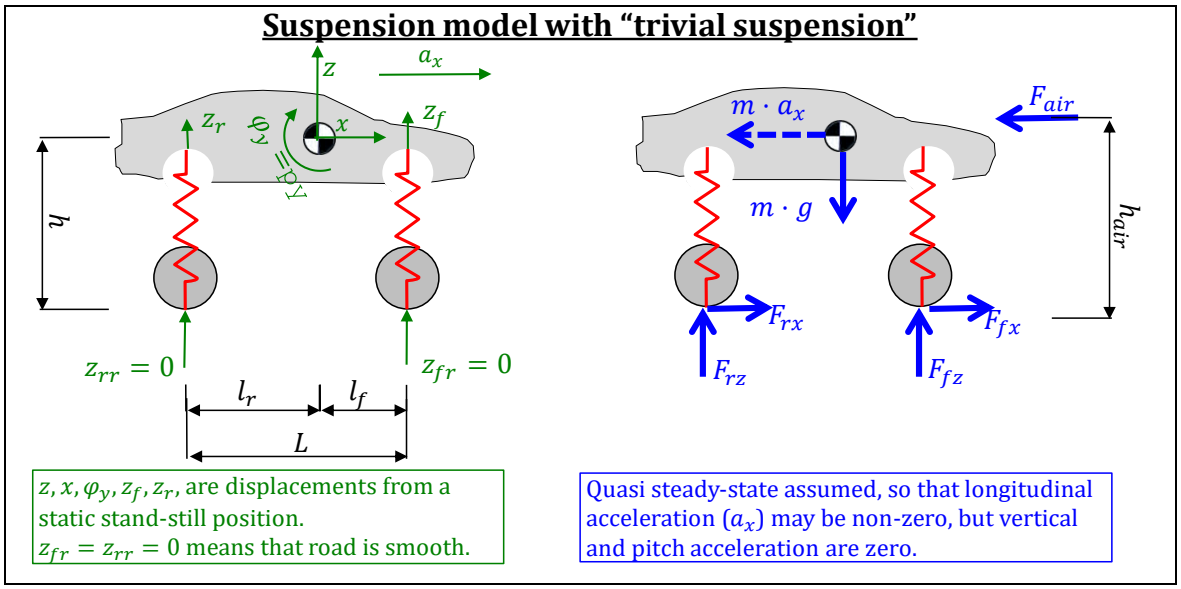


Figure 3-59: Model for steady state heave and pitch due to longitudinal wheel forces.

There is no damping included in model, because their forces would be zero, since there is no displacement velocity, due to the steady-state assumption. As **constitutive equations** for the compliances (springs) we assume that displacements are measured from a static condition and that the compliances are linear. The road is assumed to be smooth, i.e. $z_{fr} = z_{rr} = 0$.

$$F_{fz} = F_{fz0} + c_f \cdot (\cancel{z_{fr}} - z_f); \quad and \quad F_{rz} = F_{rz0} + c_r \cdot (\cancel{z_{rr}} - z_r);$$
$$where\ F_{fz0} + F_{rz0} = m \cdot g; \quad and \quad F_{fz0} \cdot l_f - F_{rz0} \cdot l_r = 0; \qquad [3.24]$$

We see already in free-body diagram that F_{fx} and F_{rx} always act together, so we rename $F_{fx} + F_{rx} = F_{wx}$, where w refers to wheel. The assumption of "trivial linkage" explains how longitudinal forces are transferred between wheels and body. **Equilibrium** then gives:

$$-F_{air} - m \cdot a_x + F_{wx} = 0;$$
$$m \cdot g - F_{fz} - F_{rz} = 0;$$
$$F_{rz} \cdot l_r - F_{fz} \cdot l_f - F_{wx} \cdot h - F_{air} \cdot (h_{air} - h) = 0; \qquad [3.25]$$

Compatibility, to introduce body displacements, z and p_y, gives:

$$z_f = z - l_f \cdot \varphi_y; \quad and \quad z_r = z + l_r \cdot \varphi_y; \qquad [3.26]$$

Solving constitutive relations, equilibrium, compatibility using Matlab Symbolic toolbox gives:

```
>> clear, syms zf zr Ffz Frz Ffz0 Frz0 ax z py
>> sol=solve( ...
    'Ffz=Ffz0-cf*zf', ...
    'Frz=Frz0-cr*zr', ...
    'Ffz0+Frz0=m*g', ...
    'Ffz0*lf-Frz0*lr=0', ...
    '-Fair-m*ax+Fxw=0', ...
    'm*g-Ffz-Frz=0', ...
    'Frz*lr-Ffz*lf-Fxw*h-Fair*(hair-h)=0', ...
    'zf=z-lf*py', ...
    'zr=z+lr*py', ...
    zf, zr, Ffz, Frz, Ffz0, Frz0, ax, z, py);
```

The solution is given in Eq [3.27]:

$$a_x = \frac{F_{wx} - F_{air}}{m};$$
$$z = -\frac{c_f \cdot l_f - c_r \cdot l_r}{c_f \cdot c_r \cdot L^2} \cdot \left(F_{wx} \cdot h + F_{air} \cdot (h_{air} - h)\right)$$
$$p_y = -\frac{c_f + c_r}{c_f \cdot c_r \cdot L^2} \cdot \left(F_{wx} \cdot h + F_{air} \cdot (h_{air} - h)\right) \qquad [3.27]$$

In agreement with intuition and experience the body dives (positive pitch) when braking (negative F_{xw}). Further, the body centre of gravity is lowered (negative z) when braking and weaker suspension front than rear ($c_f \cdot l_f < c_r \cdot l_r$), which is normally the chosen design for cars.

The air resistance force is brought into the equation. It can be noted that for a certain deceleration, there will be different heave and pitch depending on how much of the decelerating force that comes from air resistance and from longitudinal wheel forces. But, as already noted, heave and pitch does not depend on how wheel longitudinal force is distributed between the axles.

3.4.5.2 Transient Load Transfer and Non-Trivial Linkage

Compared to 3.4.5.1, we will now model also the transients of load transfer. If we study longer events when the wheel force is applied and then kept constant for a longer time (1-5 s), it is often a good enough model. But if the wheel forces vary more, we need to capture the transients better. Then it is important to consider that the linkage can transfer some of the wheel longitudinal forces. When studying the transients, it is also relevant to consider the damping.

There are basically two modelling ways to include the suspension linkage in the load transfer: through a pitch centre or through a pivot point for each axle, see Figure 3-60.

3.4.5.2.1 Model with Pitch Centre

This model will not be deeply presented in this book. It has drawbacks in that it has only one suspended degree of freedom. Also, it does not take the distribution of longitudinal wheel forces between the axles into account. These shortcomings is not very important for studying dive and squat, but they are essential when studying rapid individual wheel torque changes in time frames of 0.1 s, such as studying ABS or traction control. So, since the model with axle pivot points is more generally useful and not much more computational demanding (and probably easier intuitively), that model is prioritized in this book.

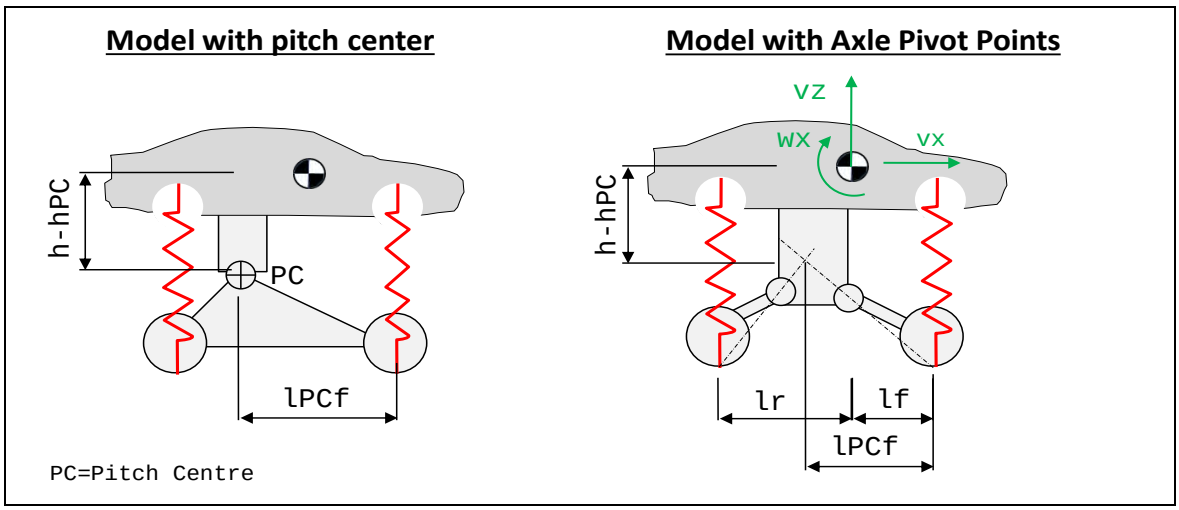


Figure 3-60: Models for including suspension effects in longitudinal load transfer

3.4.5.2.2 Model with Axle Pivot Points

Behold the free-body diagram in Figure 3-61. The road is assumed flat, $z_{fr} = z_{rr} \equiv 0$. The force play in the rear axle is shown in more detail. P_{xr} and P_{zr} are reaction forces in the pivot point. The F_{sr} is the force in the elasticity, i.e. where potential spring energy is stored. The torque T_{sr} is the shaft torque, i.e. from the propulsion system. Both torque from propulsion and brake system contribute to F_{xr}. But torque from friction brake $T_{reac,r}$ is not visible in free-body diagram, unless decomposed in suspension and wheel, as in the right-most part of Figure 3-61. This is because the friction braking appears as internal torque (or, depending on the brake design, probably forces) between brake pad and brake calliper. Any part of the longitudinal wheel force that is applied via reaction torque to unsprung parts will not add to shaft torque, such as an electric motor mounted on unsprung parts or propulsion via longitudinal propeller shaft to a final gear (as usual for rigid propelled axles).

The term $\omega_y \cdot v_x$ is easy to forget, but it does influence especially when v_x is large. The term can be explained as the other centripetal accelerations (giving centrifugal (fictive) forces) in 4.4.2.2.3. The term $\omega_y \cdot v_z$ is generally much smaller. Both the terms appear due to that velocities and accelerations are expressed as components in the vehicle fix (and hence rotating) coordinate system. We could introduce also velocities and accelerations in ground fix coordinate system, with subscripts differing between $[v_{xv}, v_{yv}]$ and $[v_{xg}, v_{yg}]$ and between $[a_{xv}, a_{yv}]$ and $[a_{xg}, a_{yg}]$, in a similar way shown in 4.4.2.2.3.3 for yaw rotation where it is much more important to differ between vehicle and ground fix.

We assume that displacements are measured from the forces F_{sf0} and F_{sr0}, respectively, and that the compliances are linear. The total constitutive equations become:

$$F_{sf} = F_{sf0} + c_f \cdot (\cancel{z_{fr}} - z_f); \quad and \quad F_{sr} = F_{sr0} + c_r \cdot (\cancel{z_{rr}} - z_r); \qquad [3.28]$$

Now, there are two ways of representing the dynamics in spring-mass systems: Either as second order differential equations in position or first order differential equations in velocity and force. We select the latter, because it is easier to select suitable initial values. Then we need the differentiated versions of the compliance's constitutive equations:

$$\dot{F}_{sf} = 0 + c_f \cdot (\cancel{\dot{z}_{fr}} - \dot{z}_f) = -c_f \cdot v_{zf}; \quad and \quad \dot{F}_{sr} = 0 + c_r \cdot (\cancel{\dot{z}_{rr}} - \dot{z}_r) = -c_r \cdot v_{zr}; \qquad [3.29]$$

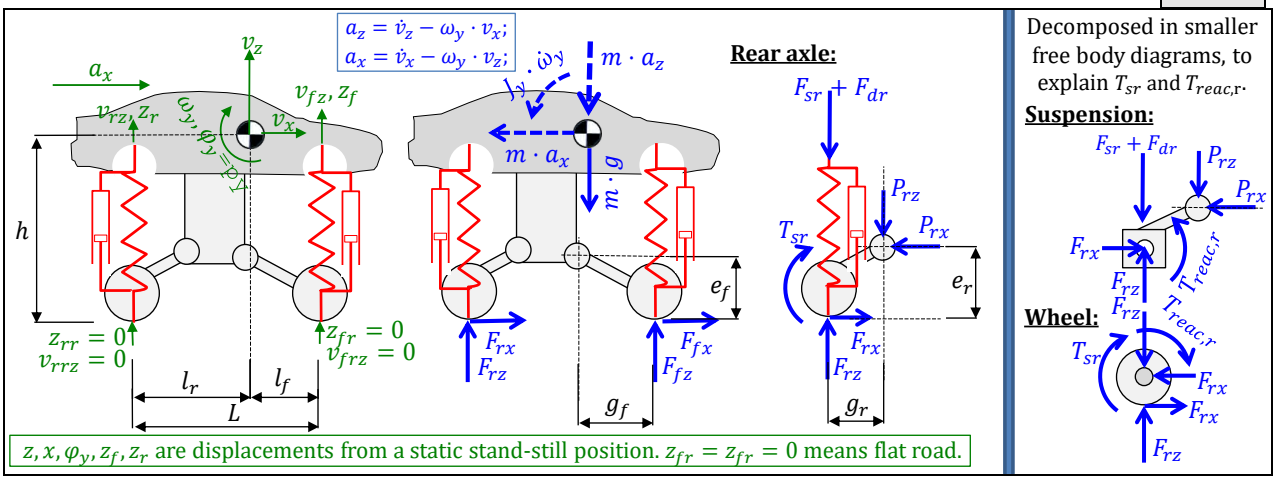


Figure 3-61: Free-body diagram for model with Axle Pivot Points. (The model assumes drive shafts from propulsion system mounted on body. If rigid shaft with longitudinal propeller shaft, $T_{sr} = 0$.)

The damper forces are denoted F_{df} and F_{dr}. They will appear in the equilibrium equations quite similar to F_{sf} and F_{sr}. Note that the damping coefficients, d_f and d_r, are the effective ones, i.e. the ones defined at the wheel contact point with ground, as opposed to the physical ones defined for the actual physical damper. C.f. effective stiffness in 3.4.5.

$$F_{df} = d_f \cdot (\cancel{\dot{z}_{fr}} - \dot{z}_f) = -d_f \cdot v_{zf}; \quad and \quad F_{dr} = d_r \cdot (\cancel{\dot{z}_{rr}} - \dot{z}_r) = -d_r \cdot v_{zr}; \qquad [3.30]$$

Now, 3 equilibria for whole vehicle and 1 moment equilibria for each axle around its pivot point gives:

$$\begin{aligned}
&-m\cdot a_x + F_{fx} + F_{rx} = 0; \quad (with\ a_x = \dot{v}_x - \omega_y \cdot v_z \approx \dot{v}_x;)\\
&-m\cdot a_z - m\cdot g + F_{fz} + F_{rz} = 0; \quad (with\ a_z = \dot{v}_z - \omega_y \cdot v_x;)\\
&-J_y\cdot \dot{\omega}_y + F_{rz}\cdot l_r - F_{fz}\cdot l_f - \left(F_{fx}+F_{rx}\right)\cdot h = 0;\\
&\left(F_{rz} - F_{sr} - F_{dr}\right)\cdot g_r - F_{rx}\cdot e_r + T_{sr} = 0;\\
&\left(F_{sf} + F_{df} - F_{fz}\right)\cdot g_f - F_{fx}\cdot e_f + T_{sf} = 0;
\end{aligned} \qquad [3.31]$$

It can be noted that the unsprung parts are considered massless. Also note, that a "trivial suspension model" (as used in Eq [3.24] and see also Figure 2-90) is a special case which falls out from the equations by letting $g_i \to \infty$, so that $F_{zi} = F_{si} + F_{di};$. With such trivial suspension, there is no difference in vehicle motion if F_{xi} actuation is done with shaft torque T_{si} or via reaction to unsprung parts, $T_{reac,i}$.

Equilibria for wheels on each axle:

$$\begin{cases} T_{sr} + T_{reac,r} - F_{rx}\cdot R_w - J_{rw}\cdot\dot{\omega}_r - RRC\cdot F_{rz}\cdot R_w = 0;\\ T_{sf} + T_{reac,f} - F_{fx}\cdot R_w - J_{fw}\cdot\dot{\omega}_f - RRC\cdot F_{fz}\cdot R_w = 0; \end{cases} \Rightarrow$$

$$\Rightarrow \begin{Bmatrix} \text{neglect rotational inertia,}\\ \text{neglect rolling resistance} \end{Bmatrix} \Rightarrow \begin{cases} T_{sr} + T_{reac,r} - F_{rx}\cdot R_w = 0;\\ T_{sf} + T_{reac,f} - F_{fx}\cdot R_w = 0; \end{cases} \qquad [3.32]$$

If eliminating F_{fx} and F_{rx} from the equilibria of the axles and the wheels one see how shaft torques and reaction torques influence differently:

$$\begin{aligned}
F_{fz} &= \left(F_{sf} + F_{df}\right) - \frac{e_f - R_w}{g_f}\cdot\frac{T_{sf}}{R_w} - \frac{e_f}{g_f}\cdot\frac{T_{reac,f}}{R_w};\\
F_{rz} &= \left(F_{sr} + F_{dr}\right) + \frac{e_r - R_w}{g_r}\cdot\frac{T_{sr}}{R_w} + \frac{e_r}{g_r}\cdot\frac{T_{reac,r}}{R_w};
\end{aligned} \qquad [3.33]$$

Compatibility, to connect to body displacements, z and φ_y, gives:

$$\begin{aligned}
&v_{fz} = v_z - l_f\cdot\omega_y; \quad and \quad v_{rz} = v_z + l_r\cdot\omega_y;\\
&z_f = z - l_f\cdot\varphi_y; \quad and \quad z_r = z + l_r\cdot\varphi_y;\\
&\dot{z} = v_z; \quad and \quad \dot{\varphi}_y = \omega_y;
\end{aligned} \qquad [3.34]$$

By combining constitutive relations, equilibrium and compatibility we can find explicit function so:

- $StateDerivatives = ExplicitFormFunction(States, Inputs)$;
- States: $[v_x \quad v_z \quad \omega_y \quad F_{sf} \quad F_{sr} \quad z \quad \varphi_y]$;
- State Derivatives: $\left[\dot{v}_x \quad \dot{v}_z \quad \dot{\omega}_y \quad \dot{F}_{sf} \quad \dot{F}_{sr} \quad \dot{z} \quad \dot{\varphi}_y\right]$; (if wheel rotational inertias neglected)
- Inputs: $[T_{reac,f} \quad T_{reac,r} \quad T_{sf} \quad T_{sr}]$; or $[F_{xf} \quad F_{xr} \quad T_{sf} \quad T_{sr}]$;

The *ExplicitFormFunction* can be integrated with well-established methods for numerical ODE. Such simulation of is shown in 3.4.8.1. Note that the model is linear.

3.4.5.2.3 Additional Phenomena

It is relevant to point out the following, which are not modelled in this book:

- **Stiffness** and **damping** may be dependent of **wheel (vertical) displacement** and **wheel steer angle**. One way of inserting this in the model is to make the coefficients varying with spring force, which is a measure of how much compressed the suspension is. Here, non-linearity within spring working range, as well as bump stops, can be modelled. Also, **position of pivot points (or pitch and roll centres)** can be dependent of wheel displacement steer angle.
- Dampers are often **deformation direction dependent**, i.e. different damping coefficients are suitable to use for compression and rebound. Typical is 2..4 times softer (smaller d [N/(m/s)]) in compression than in rebound.

3.4.6 Steady State Heave and Pitch, Non-Trivial Linkage

If we study long term steady state for the model described in 3.4.5.2.2 we will find a steady state model comparable with the model in 3.4.5. So, Equations [3.28] to [3.34] are combined. We also neglect air resistance force for clarity of equations. Equation [3.28] becomes, in Matlab format:

```
>> sol=solve( ...
    Fsf==Fsf0-cf*zf,   Fsr==Fsr0-cr*zr, ...
    Fsf0+Fsr0==m*g,      Fsf0*lf-Fsr0*lr==0, ...
    -m*ax+Ffx+Frx==0,   -m*0-m*g+Ffz+Frz==0, ...
    -J*0+Frz*lr-Ffz*lf-(Ffx+Frx )*h==0, ...
    (Frz-Fsr-0 )*gr-Frx*er+Tsr==0,   ...
    (Fsf+0-Ffz )*gf-Ffx*ef+Tsf==0, ...
    zf==z-lf*py, zr==z+lr*py, ...
    Fsf0,Fsr0, Ffz, Frz, zf,zr, ax, Fsf,Fsr, z,py)

%Results:
% sol.ax = (Ffx+Frx)/m
% sol.z  = -(Tsr*cf*gf*lf^2 -Tsf*cr*gr*lr^2 +Tsr*cf*gf*lf*lr
      -Tsf*cr*gr*lf*lr -Frx*cf*er*gf*lf^2 +Ffx*cr*ef*gr*lr^2
      +Ffx*cf*gf*gr*h*lf +Frx*cf*gf*gr*h*lf -Ffx*cr*gf*gr*h*lr
      -Frx*cr*gf*gr*h*lr -Frx*cf*er*gf*lf*lr +Ffx*cr*ef*gr*lf*lr)
      /(cf*cr*gf*gr*(lf + lr)^2)
% sol.py = -(Tsr*cf*gf*lf +Tsr*cf*gf*lr +Tsf*cr*gr*lf
      +Tsf*cr*gr*lr +Ffx*cf*gf*gr*h +Frx*cf*gf*gr*h
      +Ffx*cr*gf*gr*h +Frx*cr*gf*gr*h -Frx*cf*er*gf*lf
      -Ffx*cr*ef*gr*lf -Frx*cf*er*gf*lr -Ffx*cr*ef*gr*lr)
      /(cf*cr*gf*gr*(lf+lr)^2)
% sol.Ffz = -(Ffx*h +Frx*h -g*lr*m)/(lf+lr)
% sol.Frz = +(Ffx*h +Frx*h +g*lf*m)/(lf+lr)
```

[3.35]

The solution can be compared with corresponding solution in Equation [3.27]. The a_x is exactly the same. Then, a general reflection is that the displacement, z and py, in Equation [3.35] follows a complex formula, but that they are dependent on how the $F_{xw} = F_{xf} + F_{xr}$ is applied: both dependent on distribution between axles and dependent on how much of the axle forces (F_{xf} and F_{xr}) that are actuated with shaft torques (T_{sf} and T_{sr}, respectively). In Figure 3-62, dashed lines show the solutions from Equation [3.27].

3.4.7 Pitch Functions at Transient Wheel Torques

3.4.7.1 Dive at Braking *

Function definition: ***Dive at braking*** *is pitch angle of the vehicle body when applying a step in deceleration request to a certain level. Either peak pitch or quasi-steady state pitch angle can be addressed.*

Now, study the suspension at front axle in Figure 3-61. When the axle is braked, F_{xf} will be negative and push the axle rearwards, i.e. in under the body. The front of the vehicle will then be lifted as in pole jumping. This means that this design counter-acts the (transient) dive of the front. (Only the transient dive will be reduced, while the dive after a longer time of kept braking is dependent only on the stiffnesses according to Equation [3.27].) The design concept for front axle suspension to place the pivot point behind axle and above ground is therefore called “anti-dive”.

If the braking is applied without shaft torque T_{sf}, a good measure of the Anti-dive mechanism is e_f/g_f. This is the normal way for braking, since both the action and reaction torque acts on the axle. For in-board brakes, or braking via propulsion shaft, the reaction torque is not taken within the axle, but the

reaction torque is taken by the vehicle body. The action torque T_{sf} then appears in the equilibrium equation for the axle, as shown in Equation [3.31]. If we neglect the wheel rotational dynamics for a while, we can insert $T_{sf} = F_{xf} \cdot R_w$ in the equation with T_{sf} in Equation [3.31]:

$$\begin{aligned}&\left(F_{sf} + F_{df} - F_{fz}\right) \cdot g_f - F_{fx} \cdot e_f + T_{sf} = 0; with\ T_{sf} = F_{fx} \cdot R_w;\ \Rightarrow \\ &\Rightarrow \left(F_{sf} + F_{df} - F_{fz}\right) \cdot g_f - F_{fx} \cdot e_f + F_{fx} \cdot R_w = 0; \Rightarrow \\ &\Rightarrow \left(F_{sf} + F_{df} - F_{fz}\right) \cdot g_f - F_{fx} \cdot \left(e_f - R_w\right) = 0;\end{aligned} \qquad [3.36]$$

We can then see that a good measure of the Anti-dive mechanism is $\left(e_f - R_w\right)/g_f$ instead.

3.4.7.2 Squat at Propulsion *

Function definition: ***Squat at propulsion*** *is pitch angle of the vehicle body when applying a step in acceleration request to a certain level. Either peak pitch or quasi-steady state pitch angle can be addressed.*

Now, study the suspension at rear axle in Figure 3-61. When the axle is propelled, F_{xr} will push the axle in under the body. This means that this design reduces the rear from squatting (transiently). The design concept for rear axle suspension to place the pivot point ahead of axle and above ground is therefore called “anti-squat”.

3.4.7.3 Anti-dive and Anti-Squat Designs

With Anti-dive front and Anti-squat rear, we avoid front lowering at braking and rear lowering at acceleration, respectively. But how will the designs influence the parallel tendencies: that rear tend to lift at braking and front then to lift at propulsion? Well, they will luckily counteract also these: Braking at rear axle will stretch the rear axle rearwards and upwards relative to the body. When propelling the front axle, the propulsion force will stretch the front axle forwards and upwards relative to the body. (If one brakes at one axle and propels at the other, the reasoning is not valid. This mode can be desired for a hybrid vehicle with ICE on front axle and electric motor on rear axle, if one would like to charge batteries “via the road”.)

In summary: Anti-dive and anti-squat refer to the front diving when braking and the rear squatting when acceleration. Anti-dive and anti-squat can be measured in fractions: Anti-dive is measured by e_f/g_f or $\left(e_f - R_w\right)/g_f$ and Anti-squat is measured by e_r/g_r or $(e_r - R_w)/g_r$, see Eq [3.33]. Normal values are typically 0.05..0.15.

3.4.8 Acceleration and Deceleration

Acceleration performance like, typically, 0-100 km/h over 5..10 s, was addressed in 3.3.7. In present Section we address the similar functionality but include larger transients, such as when wheel longitudinal wheel force is changed more rapidly, typically changing $\pm\mu \cdot F_z/2$ during 0.2-0.5 s.

3.4.8.1 Deceleration Performance *

Function definition: See 3.4.2.2.

Deceleration performance can now be predicted, including the suspension mechanisms. It is a very important function, and every decimetre counts when measuring braking distance in standard tests like braking from 100 to 0 km/h. The active control of the brake torques (ABS function) is then very important, and this is so fast dynamics that the suspension mechanisms of Anti-lift and Anti-dive influences. The position of the load in the vehicle will influence, since it influences the load transfer.

We will now set up a mathematical model, see Equation [3.37], which shows how the normal forces change during a braking event. It is based on the physical model in Figure 3-61. Driving resistance contributes normally with a large part of the deceleration, but we will neglect this for simplicity, just to show how the suspension mechanism works. The equations in the model are presented in the dynamic

modelling standardized format “Modelica”, and are hence more or less identical to Equation [3.29] to [3.34]. (The term $\omega_y \cdot v_z$ is included but makes no visible difference.)

```
//Actuation:
  Ffx = if 1 < time and time < 3 then -0.4*m*g else 0;
  Frx = if 3 < time and time < 7 then -0.4*m*g else 0;
  Tsf/Rw = 0;
  Tsr/Rw = if 5 < time and time < 7 then -0.4*m*g else 0;

//Motion equations:
  der(z) = vz;   der(py) = wy;
//Constitutive equations for the springs:
  der(Fsf) = -cf*vfz;   der(Fsr) = -cr*vrz;
//Constitutive equations for the dampers:
  Fdf = -df*vfz;   Fdr = -dr*vrz;
//(Dynamic) Equilibrium equations:
  -m*(der(vx)+vz*wy) + Ffx + Frx = 0;
  -m*(der(vz)-vx*wy) - m*g + Ffz + Frz = 0;
  -Jy*der(wy) + Frz*lr - Ffz*lf - (Ffx + Frx)*h = 0;
  (Frz - Fsr - Fdr)*gr - Frx*er + Tsr = 0;
  (Fsf + Fdf - Ffz)*gf - Ffx*ef + Tsf = 0;
//Compatibility:
  zf = z - lf*py;     zr = z + lr*py;
  vfz = vz - lf*wy;   vrz = vz + lr*wy;
```

[3.37]

The simulation results are shown in Figure 3-62. It shows a constant deceleration, but it is changed how the decelerating force is generated. At time=3 s, there is a shift from braking solely on front axle to solely on rear axle. The braking is, so far, only done with friction brakes, i.e. generating torque by taking reaction torque in the axle itself. At time=5 s, there is a shift from braking with friction brakes to braking with shaft torque. It should be noted that if we shift axle or shift way to take reaction torque, gives transients even if the deceleration remains constant.

One can also see, at time=1 s, that the normal load under the braked axle first changes in a step. This is the effect of the Anti-dive geometry. Similar happens when braking at rear axle, due to the Anti-squat geometry. Since brake performance is much about controlling the pressure rapidly, the transients are relevant, and the plots should make it credible that it is a control challenge to reach a high braking efficiency.

3.4.8.2 Acceleration Performance *

Function definition: See 3.3.7.1.

The model presented in Eq [3.37] can also be used to predict acceleration performance in a more accurate way compared to 3.3.7. Especially, the more accurate model is needed when propelling or braking on the limit of tyre to road adhesion, since the normal load of each tyre then is essential. It is a challenge to control the propulsion and brake wheel torques to utilize the varying normal loads under each axle.

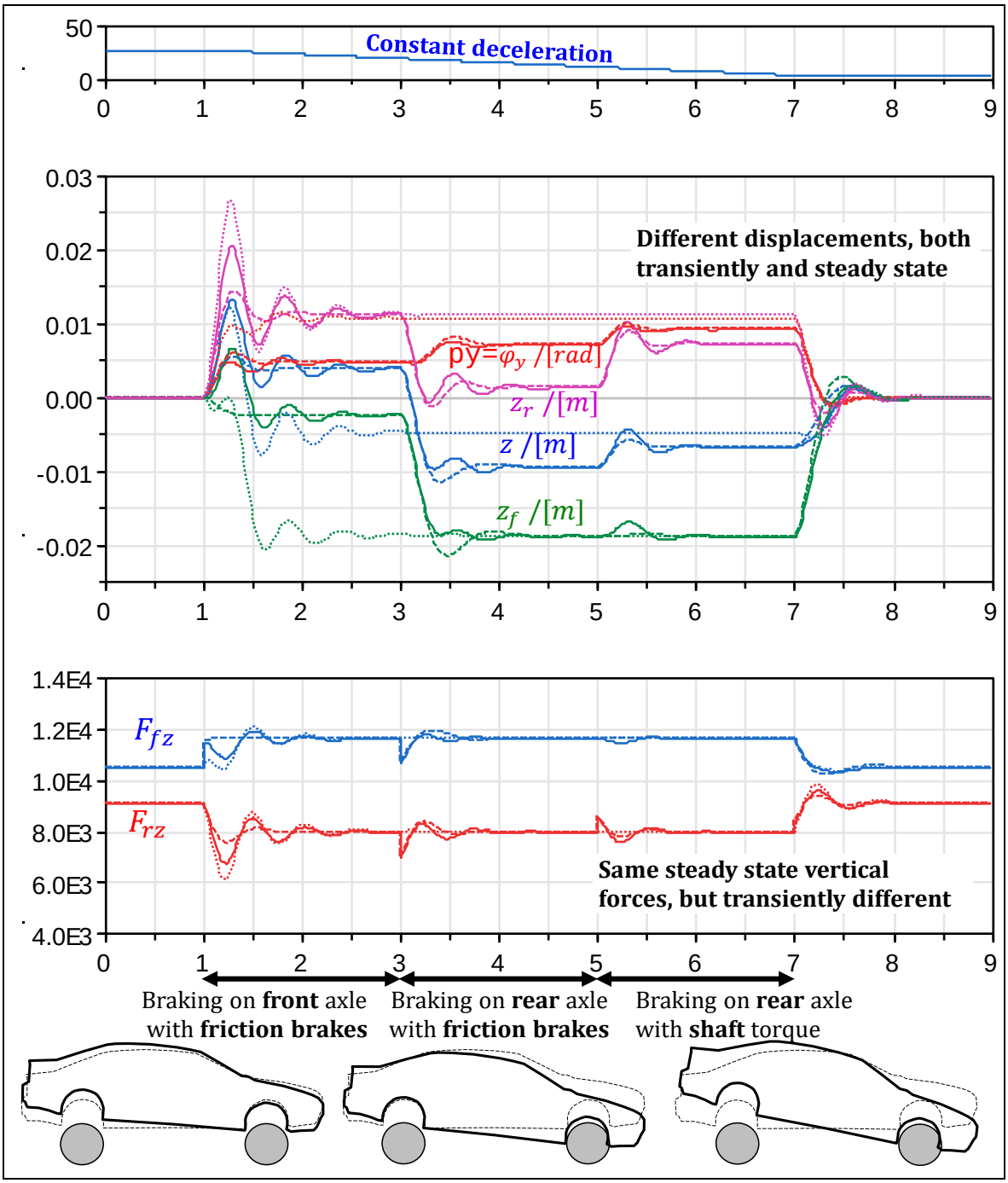


Figure 3-62: Deceleration with constant vehicle deceleration but varying ways of actuation. (Eq [3.37]. With the centripetal term $\omega_y \cdot v_x$ (solid) and without (dashed). Dotted shows without anti-dive/-squat geometry, i.e. $g_f = g_r = \infty$. The term $\omega_y \cdot v_z$ makes no visible difference.)

3.4.9 Other Functions

There are many more longitudinal functions, originating from the attribute Driving dynamics, which could have fitted in 0. Examples of such:

- Off-road accessibility: Ability to pass obstacles of different kind, such as uneven ground, extreme up- and down-hills, mud depth, snow depth, etc.
- Shift quality: Quick and smooth automatic/automated gear shifts
- Shunt & shuffle: Absence from oscillation for quick pedal apply, especially accelerator pedal.

3.5 Control Functions

Some control functions will be described. First, some general aspects on control are given.

3.5.1 Longitudinal Control

Some of the most important sensors available in production vehicles and used mainly for longitudinal control are listed below. (Sensors for instrumented vehicles for testing can be many more.)

- **Wheel Speed Sensors**, WSS. For vehicle control design, one can often assume that "sensor-close" software also can supply information about longitudinal vehicle speed.
- **Vehicle body inertial sensors.** There is generally a yaw velocity gyro and a lateral accelerometer available, but sometimes also a longitudinal accelerometer. The longitudinal accelerometer is useful for longitudinal control and longitudinal velocity estimation.
- **Pedal sensors**. Accelerator pedal normally has a position sensor and brake pedal force can be sensed via brake system main pressure sensor. Heavy vehicles often have both a brake pedal position and brake pressure sensors.
- Today's vehicles have **environment sensors** (camera, radar, GPS with electronic map, etc.) that can give information (relative distance and speed, etc.) about objects ahead of subject vehicle. It can be both fixed objects (road edges, curves, hills, …) and moving objects (other road users, animals, …). See also *2.7.*
- Information about what actuation that is **actually applied at each time instant** is available, but it should be underlined that the confidence in that information often is questionable. Information about axle propulsion torque is generally present, but normally relies on imprecise models of the whole combustion process and torque transmission, based on injected amount of fuel and gear stick position. (Electric motors can typically give better confidence in estimation, especially if motor is close to the wheel without too much transmission in between.) Wheel individual friction brake torque is available, but normally rely on imprecise models of the brake systems hydraulic/pneumatic valves and disc friction coefficient, based on brake main cylinder pressure.
- Information about what **actuation levels that are possible** upon request (availability or capability) is generally not so common. It is difficult to agree of general definitions of such information, because different functions have so different needs, e.g. variations in accepted time delay for actuation.
- Sometime **wheel/axle forces** can be sensed. One case is when pneumatic suspension. More extreme variants are under development, such as sensors in the wheel bearings which can sense forces (3 forces and roll and yaw moment) and sensors in shafts.

3.5.2 Longitudinal Control Functions

3.5.2.1 Range Estimator *

For all vehicles which carry their own energy for propulsion, the user needs to know when the energy storage needs to be refilled or charged.

Function definition: ***Distance left to travel before recharge is needed.***

For fossil fuel, there is a well-established infrastructure of fuelling stations and the refill does not take long time, so the function is not so important and a tank volume meter can be enough. For battery electric vehicles, BEVs, the function is more important, especially due to a sparse infrastructure of recharging stations and long charging time. It is also not so easy to measure the amount of stored energy in batteries.

3.5.2.2 Pedal Driving *

Function definition: See 3.4.3.

Pedal driving is often not seen as comparable with other control functions, but they become more and more relevant to define as such, since both accelerator and brake pedals tend to be electronically controlled, and hence they become increasingly tuneable. Also, more and more functions, such as those below in 3.5.2, will have to be arbitrated with the pedals.

In modern passenger vehicles, Accelerator pedal is normally electronically controlled but the Brake pedal is basically mechanical. In modern heavy commercial vehicles, both functions are electronically controlled.

The functions in "3.4.3.2 Pedal Feel *" are normally not actively controlled, but in there are concept studies with active pedals, where also the pedal feel can be actively changed to give feedback to driver.

3.5.2.2.1 Automatic gear shifting *

Function definition: ***Automatic gear shifting*** *shifts gear only based the driver's operation of the pedals.*

Automatic gear shifting has been on market for a long time. It makes only momentaneous considerations, except for that some hysteresis is normally built in. The algorithms take pedals and vehicle speed into account and select the gear which is optimal in some sense, e.g., for good fuel economy or for good acceleration reserve. See "3.2.1.1 Gear selection".

Automatic gear shifting is also used by the virtual driver, CC and ACC.

3.5.2.2.2 Automatic coordination of other longitudinal actuators *

Function definition: ***Automatic coordination of actuators*** *while driver only must operate pedals.*

This section is not any established single function, but generalised and envisioned future functions, from driver and algorithm design like in 3.5.2.2.1.

Coordinated control of wheel torque actuators (such as multiple electric drivetrains or wheel-/axle-individual friction brakes) or controllable distribution transmission actuators (such as differential locks) can be automated, while the vehicle follows the request from driver's pedals equally or better. It is a function of value for the driver because it is enough for him to operate the pedals.

These functions are typically momentaneous. However, they can possibly be predictive with a short horizon (0.5..2 s or 5..20 m).

See also "4.6.2.1 Automatic coordination of other lateral actuators *".

Also, suspension actuators (such as air suspension and active antiroll bars) can be correspondingly coordinated.

3.5.2.3 Cruise Control and Adaptive Cruise Control (CC, ACC) *

Function definition: ***Cruise Control, CC,*** *controls the vehicle's longitudinal speed. Driver can activate the function and decide desired speed.*

Function definition: ***Adaptive Cruise Control, ACC,*** *is an addition to CC. ACC controls the vehicle's time gap to a lead vehicle. Driver can activate the function and decide desired gap. When there is no lead vehicle, CC controls the vehicle's speed.*

The purpose of CC is to keep the vehicle at a driver selected longitudinal speed, so that driver does not need to adjust the accelerator pedal himself. The actuator used is the propulsion system. In heavy vehicles, also the braking system (both retarders and service brakes) is used to maintain or regulate the vehicle speed.

ACC is an addition to CC. The purpose of ACC is to keep a safe distance to the lead vehicle (vehicle ahead of subject vehicle). ACC also uses friction brake system as actuator, but normally limited to a deceleration of $2..4\ m/s^2$.

The safe distance which ACC aims for, is often expressed as a time gap, driver adjustable in the range $2..3\ s$. A model behind this is that the time gap is the driver reaction time, and the subject vehicle can

decelerate as much as the object vehicle. More advanced models can allow smaller time gap in certain situations. This is desired because it reduces the risk that other vehicles cut in between subject and leading object vehicle. Such models can consider, e.g., acceleration of the object vehicle, pedal operation of subject vehicle, road gradient, road curvature, road friction and deceleration capabilities of subject and object vehicles. ACC can be designed and tuned differently, and influences transport efficiency, comfort, safety, and energy consumption.

Pedals and CC/ACC must be arbitrated. Typically, accelerator pedal wins temporarily if pressed to higher request than CC/ACC, while any use of brake pedal turns off (wins permanently over) the CC/ACC.

CC is normally only working down to 30.. 40 km/h. ACC can have same limitation, but with automatic transmission, good forward-looking environment sensors, brake actuators and speed sensing, ACC can be allowed down to stand-still.

3.5.2.3.1 Predictive CC

Contribution from Toheed Ghandriz

A development of CC uses a varying set speed trajectory ahead. The trajectory is typically optimized for a horizon, typically a kilometre or a minute ahead. In future, one can imagine a longer horizon, covering a whole transport mission, e.g., uploaded from a navigator application.

The optimization typically considers road topography. Intermittent propulsion ("pulse and glide") and traffic are other phenomena that can be considered in optimization. Examples of products on the market are Volvo iSee and Scania Active Prediction, both for heavy vehicles. Future extensions could be that the optimization considers weather, speed limits, and traffic density over several km ahead (see (Pettersson, 2017)). Another extension could be that the optimization considers other road users and curves with road friction some hundreds of meters ahead (see (Ghandriz, 2020)).

A predictive CC works in principle as Figure 3-64. It is an automated longitudinal driving function. It selects an optimal trajectory for a certain horizon ahead, e.g., 1 km ahead and minimizing transport cost including energy cost. The figure assumes it defines candidates to select by trying different $v(s)$, but there are also many other ways to define candidates, such as different driver model parameters. The figure indicates an optimization by trial-and-error, but more sophisticated methods can be used, such as Dynamic Programming, Quadratic Programming, Linear Programming, MPC, etc. Other quantities, such as gear shifting, including Neutral gear selection, $gear(s)$ and state of charge $SoC(s)$ if the vehicle is a hybrid vehicle, can be treated in primarily two different ways. They can be part of candidate definition, which increases the search space for the optimization. Alternatively, they can be calculated (e.g., to give momentaneous optimum) in the model used for optimization, which makes them available as additional optimum trajectories beside $v_{Opt}(s)$.

Macro-level information about traffic density and traffic mean velocity or the route ahead can be considered in optimization. But taking micro-level traffic information, such as nearest vehicle ahead, is more challenging, especially predicting the velocity of the object vehicles.

Figure 3-64 shows an example using the Matlab optimization function `fmincon`, which is a shooting method, see 1.5.1.1.9.3.1.2. The candidates are defined as $a(s)$. This shortcuts the driver dynamics. The actuators limitations in force level is modelled, but not their limitations due to time delays. Other ways of defining the candidate can be considered, such as $v(s)$ or $F(s)$. See (Ghandriz, 2020).

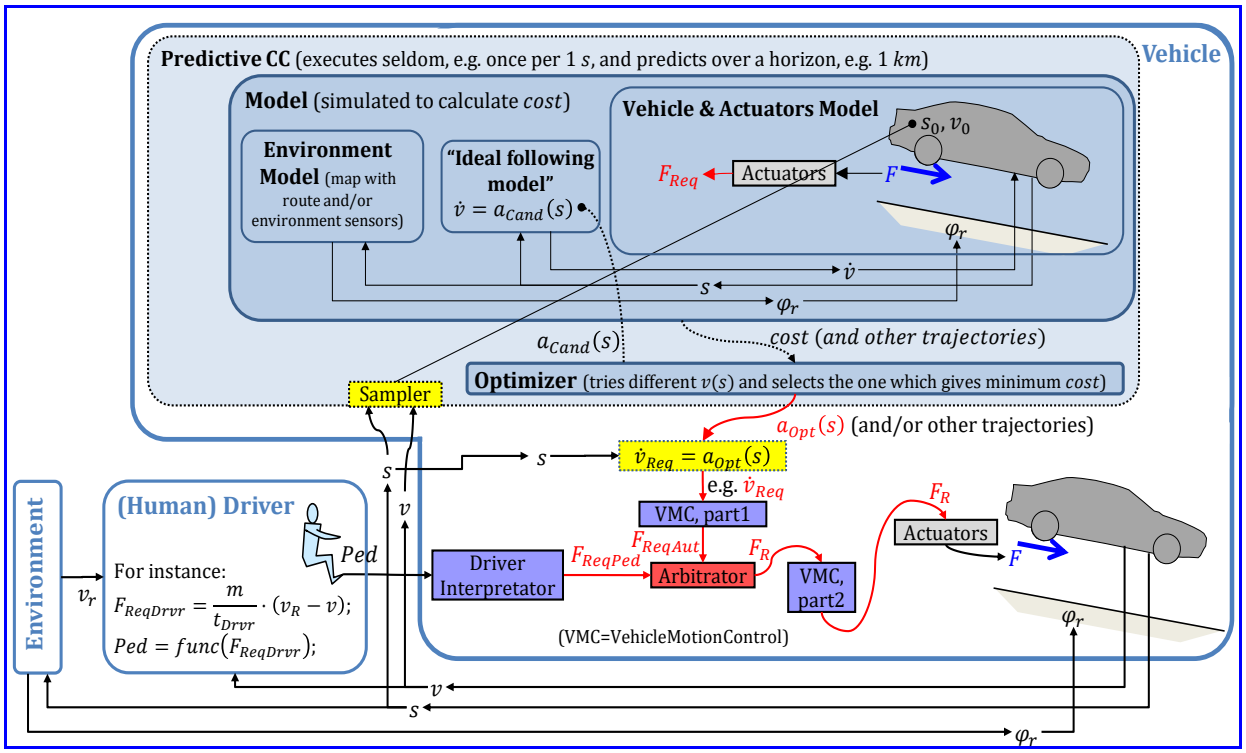


Figure 3-64: Environment, Driver, and Vehicle, where the vehicle has a Predictive CC. The optimization is: $a_{Opt}(s) = arg(min_{a(s)}(Cost(a(s))))$.

3.5.2.3.1.1 Optimization by Varying Acceleration Trajectory

An example of how the cost (as sum of energy cost and fuel cost) can be reduced is given in the 3 following figures.

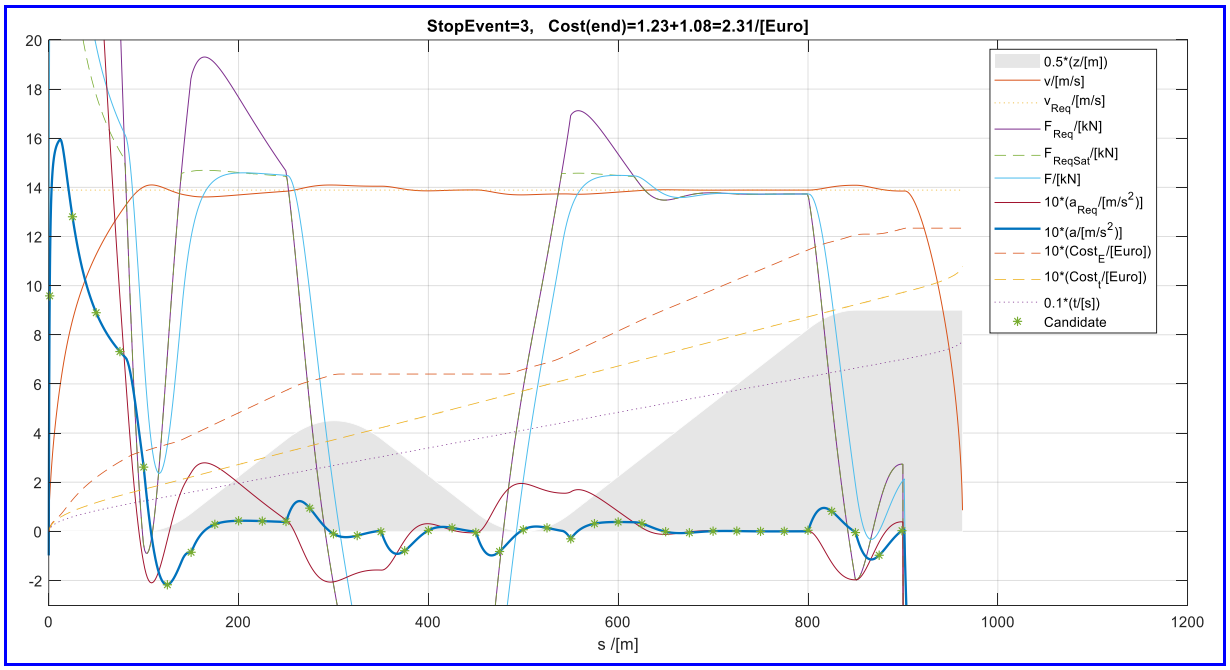


Figure 3-65: Simulation with full model, including a driver model and actuator delays.

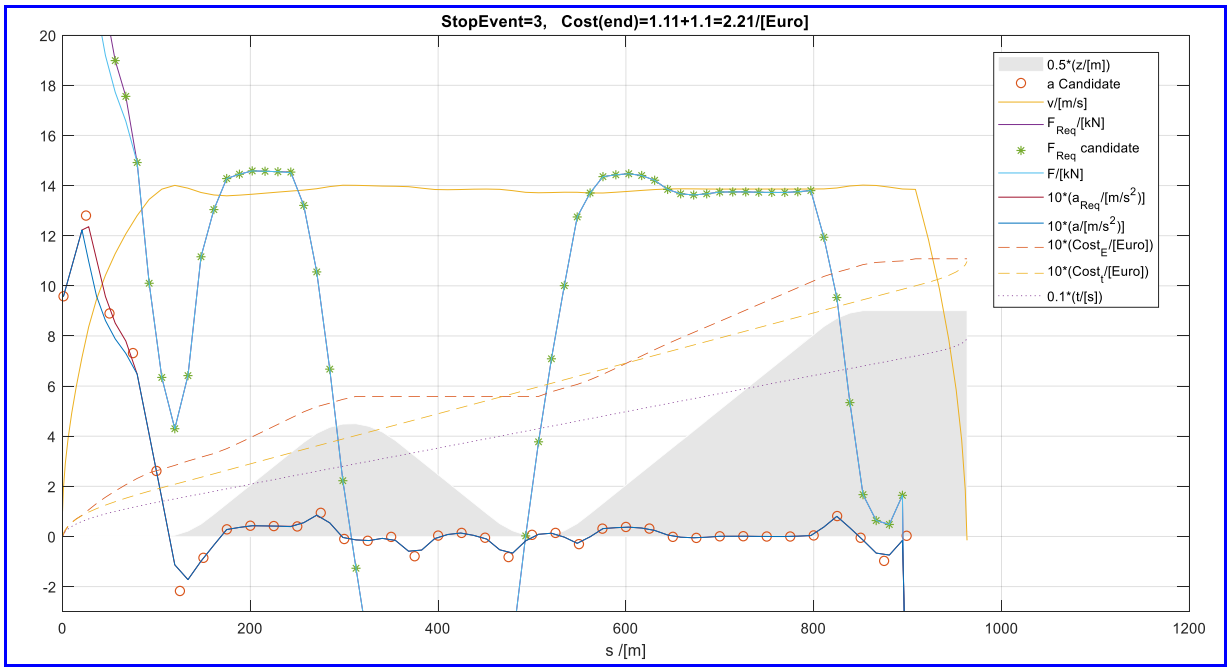


Figure 3-66: Simulation with the model used for optimization with varying $a_{Cand}(s)$. The acceleration trajectory from previous figure used, discretized every 25 m.

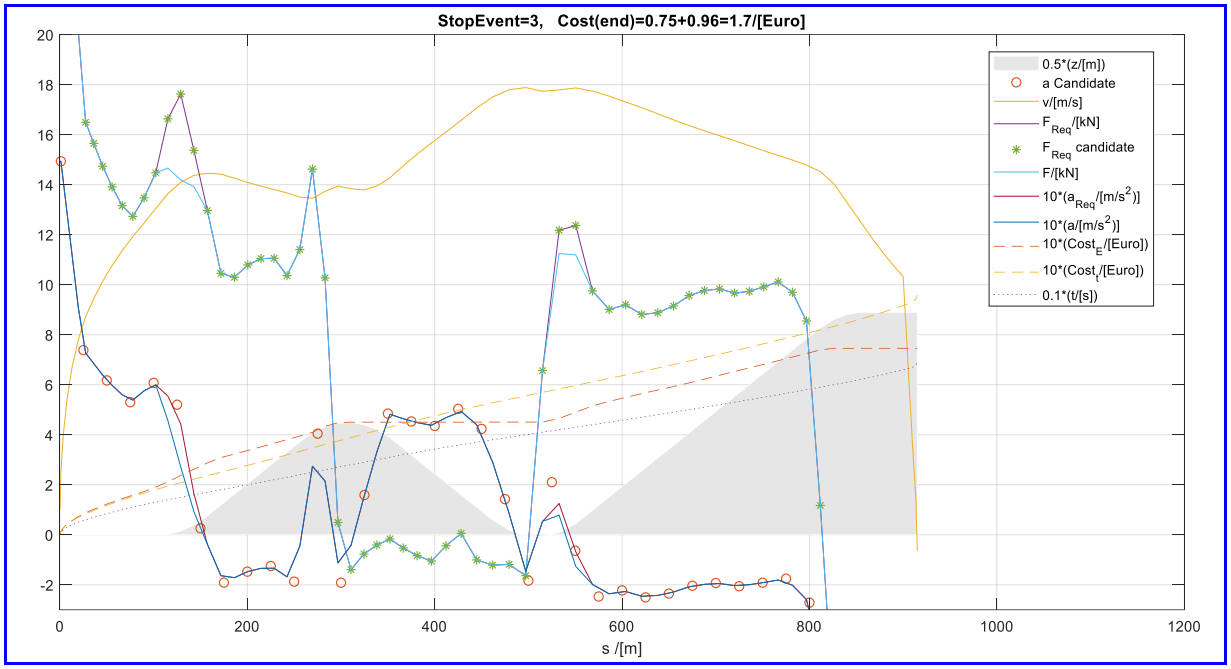


Figure 3-67: Simulation with the model used for optimization with varying $a_{Cand}(s)$. The acceleration trajectory from optimization used, discretized every 25 m. Cost reductions of ≈40% and ≈10%, respectively, is found with the parameters used in this example. The F_{Req} candidates are marked to envision that a next step optimization could be done with a model including actuator dynamics.

The optimizations are made with Matlab function `fmincon`, with $a(s)$ (discretized to parameters $[a(s_1), \cdots, a(s_N)]$) as parameters to vary. The cost function included a simulation of the system, including calculation of cost and constraints. Note that the simulations in the cost functions can include "inverse dynamics" if the candidate prescribe the whole trajectory of a state, which can enable more stable derivative approximations.

Note also that the above figure with optimisation result is not using the full model, i.e. delays in VMC2 and actuators are not considered. So, the end result in cost reduction will not be seen until running it in a more accurate vehicle model or a real vehicle.

3.5.2.3.1.2 Optimization by Varying Force Request Trajectory

If we instead use the $F_{Req}(s)$ as the way to define the candidate. The optimization is: $F_{Req,Opt}(s) = \arg\left(\min_{F_{Req}(s)}\left(F_{Req}(s)\right)\right)$. The advantages is that the simulation becomes "forward" as shown in Figure 3-68, and as opposed to "backward", a.k.a. inverse dynamic. It makes the actuator limitations easier to consider in the algorithms.

If we model the driver and pedal map, it appears as "inverse". This means that data on how the driver should operate or how the pedal map should be designed becomes spin-off from the optimization.

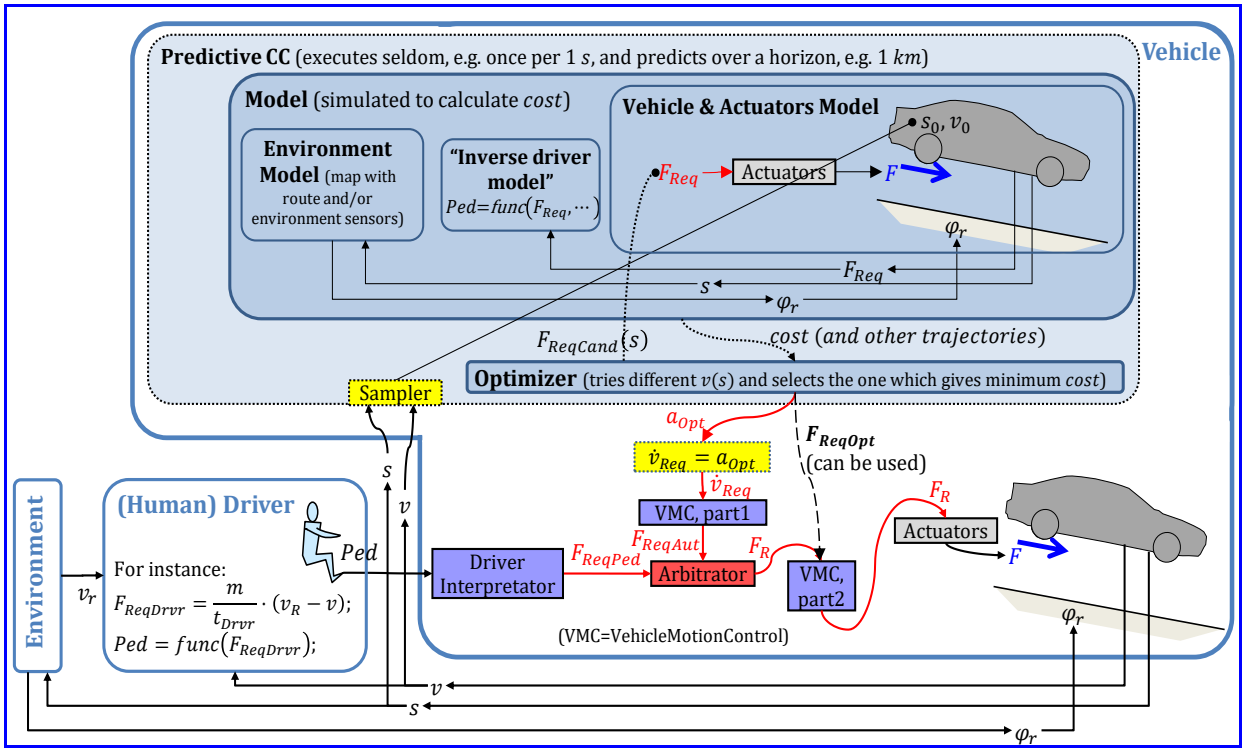


Figure 3-68: Environment, Driver, and Vehicle, where the vehicle has a Predictive CC. The optimization is: $F_{Req}(s) = arg\left(min_{F_{Req}(s)}\left(Cost\left(F_{Req}(s)\right)\right)\right)$. Note causality difference to Figure 3-64.

In our example we pick an initial guess from same simulation as before, to make the solutions comparable.

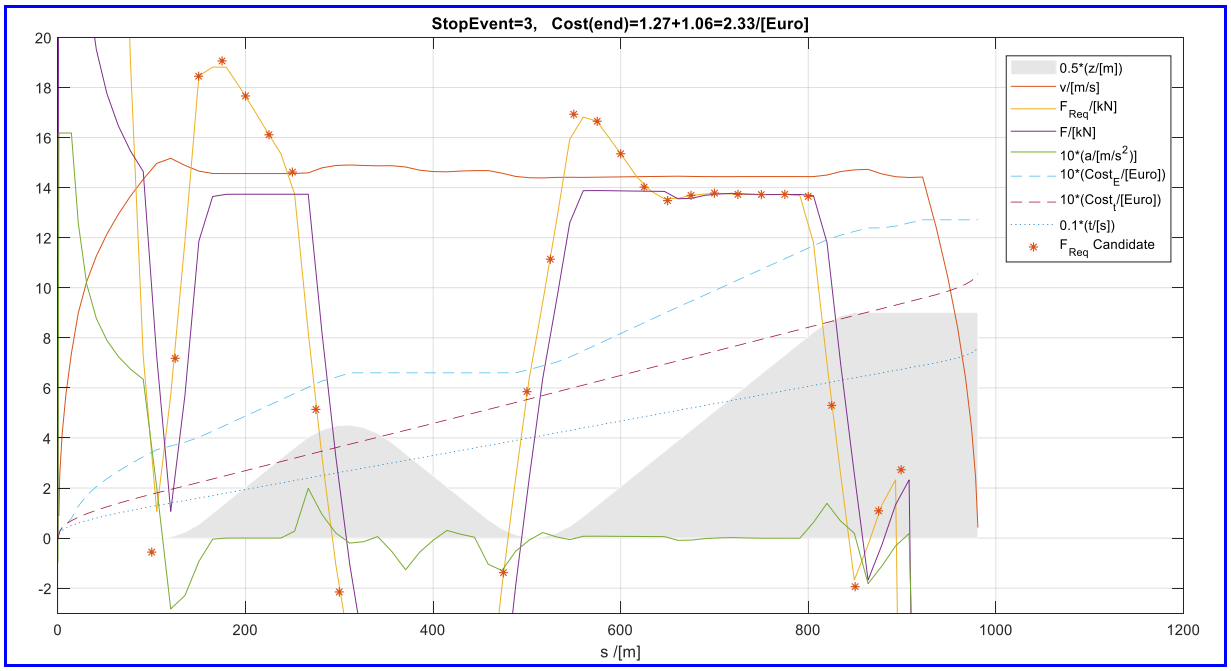


Figure 3-69: Simulation with the model used for optimization with varying $F_{ReqCand}(s)$, discretized every 25 m.

3.5.2.3.1.3 Optimization of over-actuated vehicles by Multiple force request trajectories

Now, consider a vehicle which is over-actuated in longitudinal direction. It can be two axles which each are actuated with both an electric machine and a friction brake. Then, there are 4 request trajectories:

$$\boldsymbol{F_{Req}}(s) = \{F_{FrntProp,Req}(s), F_{FrntBrk,Req}(s), F_{RearProp,Req}(s), F_{RearBrk,Req}(s)\};$$

The optimization can be made in 1 step or 2 steps, as described in the following.

3.5.2.3.1.3.1 The 1-step optimization:

See Figure 3-70. It is very similar to Figure 3-68 with one exception: there must be a "Coordinator", which in turn calls for a separation of notations: F_{Req} and $\boldsymbol{F_{Req}}$. With 1-step optimization, we define the candidates as $\boldsymbol{F_{ReqCand}}$ (not $F_{ReqCand}$).

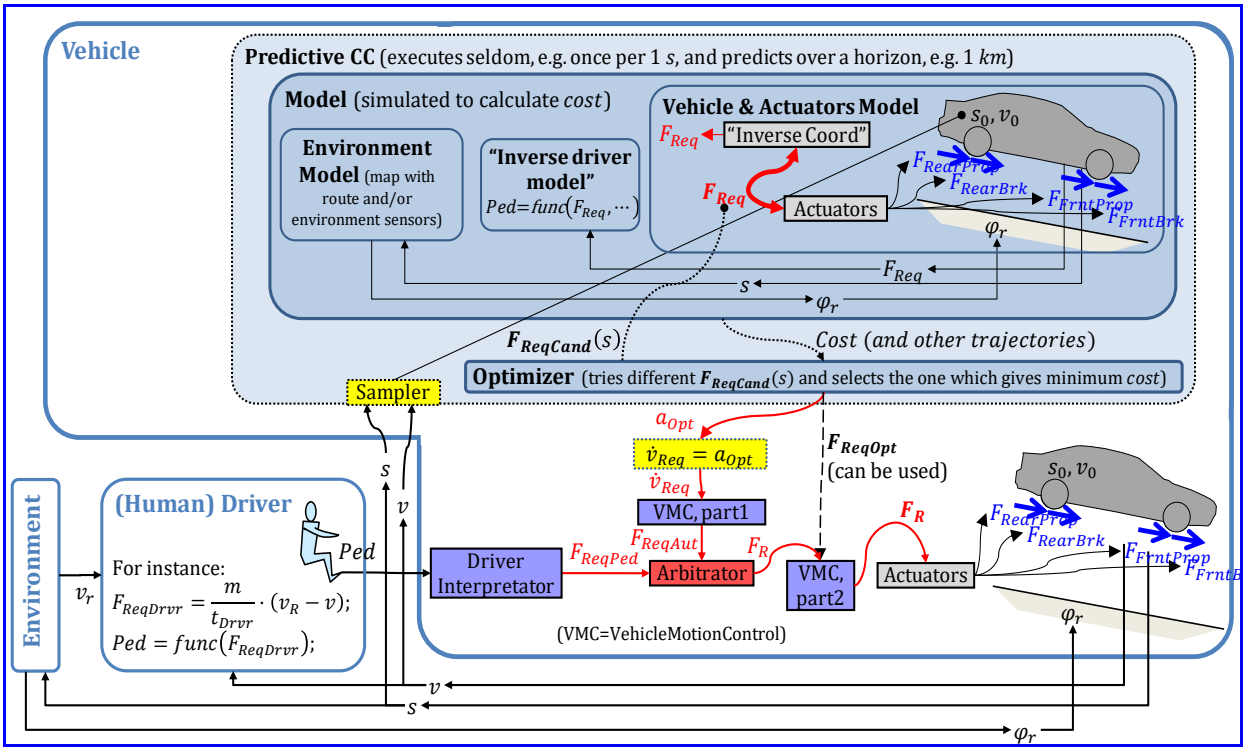


Figure 3-70: Environment, Driver and Vehicle, where the vehicle has a Predictive CC, with 1-step optimization: $\boldsymbol{F_{Req}}(s) = arg\left(min_{\boldsymbol{F_{Req}}(s)}\left(Cost\left(\boldsymbol{F_{Req}}(s)\right)\right)\right)$;. Note that the vehicle is over-actuated, so a "Coordinator" is needed, which was not the case in Figure 3-68.

The 1-step optimization becomes:

$$\boldsymbol{F_{Req,Opt}}(s) \leftarrow \arg\left(\min_{\boldsymbol{F_{Req}}(s)}(Cost)\right);$$

where the "cost model": $Cost = \int CostRate\left(\boldsymbol{F_{Req}}(s), \cdots\right) \cdot ds$;

and the "control design model": $\dot{\boldsymbol{x}} = \boldsymbol{f_1}\left(\boldsymbol{x}, s, \boldsymbol{F_{Req}}\right)$; and $CostRate = f_2\left(\boldsymbol{x}, s, \boldsymbol{F_{Req}}\right)$;

So, as it is described in this book, the 1-step approach is easy to understand. However, the drawback is that the space for candidates becomes much larger to search.

The optimization will not only give the optimal F_{Req} but also the optimal $\boldsymbol{F_{Req}}$. The first is the main result, to be used as a request. The latter can either be forgotten or used as input to the downstreams coordination in "VMC part 2".

If we model the Coordinator, it appears as "inverse". This means that can extract data on how the Coordinator should be designed as a kind of spin-off from the optimization.

3.5.2.3.1.3.2 The 2-step optimization:

The 2-step optimization is more difficult to explain. A new figure is draw, Figure 3-71:

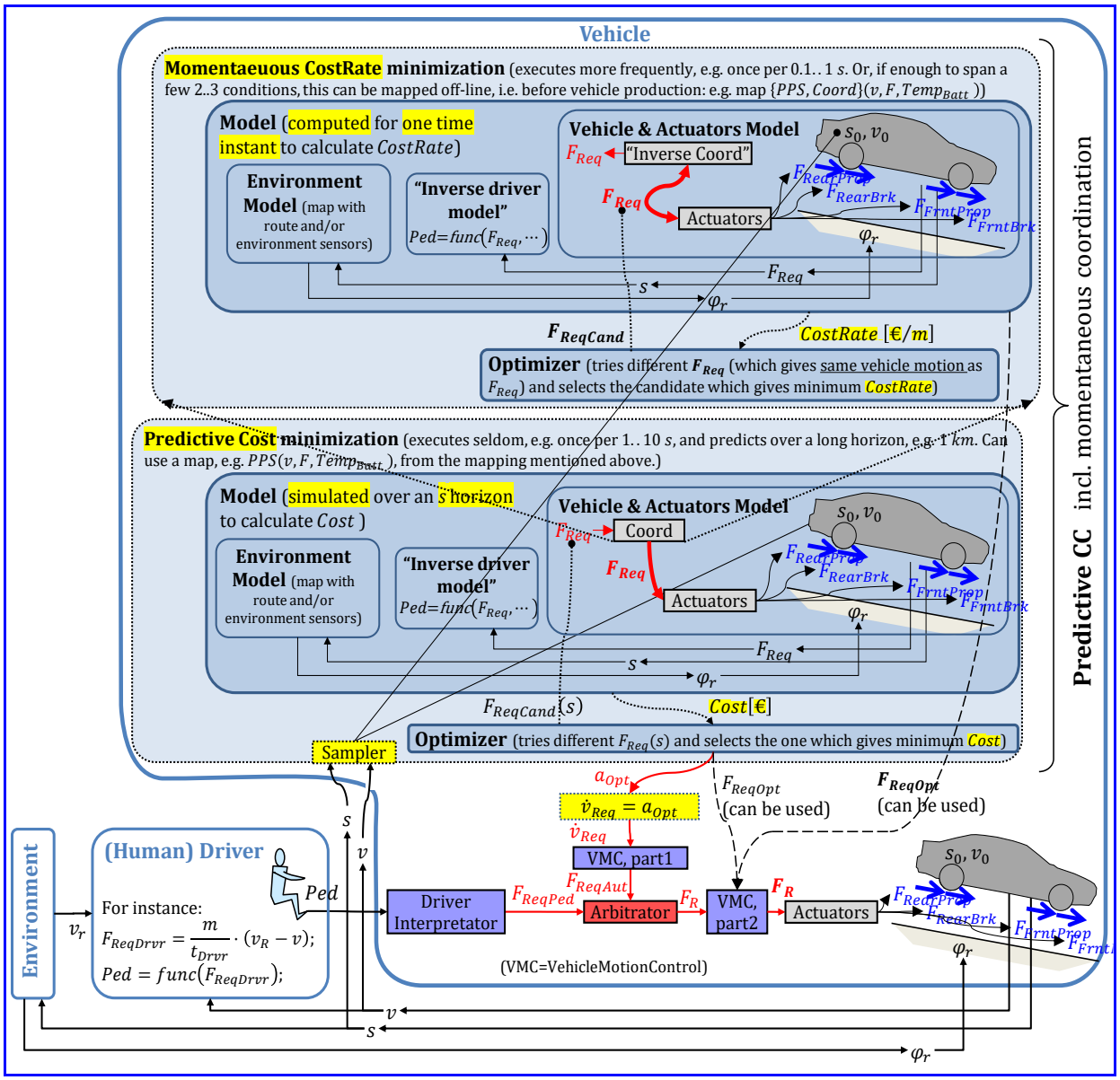


Figure 3-71: Environment, Driver and Vehicle, where the vehicle has a Predictive CC, with 2-step optimization: $F_{Req}(s) = arg\left(min_{F_{Req}(s)}\left(Cost\left(F_{Req}(s)\right)\right)\right)$; *and* $\boldsymbol{F_{Req}} = arg\left(min_{\boldsymbol{F_{Req}}}\left(CostRate\left(\boldsymbol{F_{Req}}, \cdots\right)\right)\right)$;.

Some important differences are highlighted with yellow in the figure. The upper optimization is momentaneous, so it optimized CostRate for a time instant, as opposed to Cost for a horizon in travelled distance s. That makes the function to minimize algebraic, as opposed to an integral or a simulation of a time interval.

Note that the 2-step method has advantages in that the space to search for minimum $Cost$ has less dimensions, only $F_{Req}(s)$ instead of $\boldsymbol{F_{Req}}(s) = \{F_{FrntProp,Req}(s), F_{FrntBrk,Req}(s), F_{RearProp,Req}(s), F_{RearBrk,Req}(s)\}$ and the $CostRate$ optimization has potential to be done off-line before vehicle is used. Also, the $CostRate$ optimization has to handle a constraint that the motion should be the same as for F_{Req}. If this is fulfilled, the solution from 1-step and 2-step is identical.

The 2-step optimization becomes:

$$F_{Req,Opt}(s) \leftarrow \arg\left(\min_{F_{Req}(s)}\left(Cost\left(F_{Req}(s), \cdots\right)\right)\right);$$

where the "cost model": $Cost = \int CostRate\left(\boldsymbol{F_{Req,Opt}}(s), \cdots\right) \cdot ds$;

where $\boldsymbol{F_{Req,Opt}} \leftarrow \arg\left(\min_{\boldsymbol{F_{Req}}}\left(CostRate\left(\boldsymbol{F_{Req}}, \cdots\right)\right)\right)$;

$s.t.$ "$same\ vehicle\ motion$" (e.g., $\sum \boldsymbol{F_{Req}} = F_{Req}$;)

and the "control design model": $\dot{\boldsymbol{x}} = \boldsymbol{f_1}\left(\boldsymbol{x}, s, \boldsymbol{F_{Req}}\right)$; and $CostRate = f_2\left(\boldsymbol{x}, s, \boldsymbol{F_{Req}}\right)$;

Note that $\min_{F_{Req}(s)}\left(Cost\left(F_{Req}(s), \cdots\right)\right)$ is an optimization of a trajectory, the 2D-curve $F_{Req}(s)$, while $\min_{\boldsymbol{F_{Req}}}\left(CostRate\left(\boldsymbol{F_{Req}}, \cdots\right)\right)$ is a optimization of a finite number of values, the scalar components in $\boldsymbol{F_{Req}}$.

3.5.2.3.1.3.3 Comparison between 1-step and 2-step optimization

The 2-step optimization has the advantage of easier to do job split between development teams, with regards to a clear signal interface. It is also more modular, e.g., for inheritance within a vehicle platform. It can also be easier to arbitrate with other functions, such as pedal driving which typically gives a scalar F_{Req} as opposed to a decomposed request $\boldsymbol{F_{Req}}$. It also opens for using maps for the $CostRate$ optimizations, which reduces the amount of computation in the vehicles.

The 2-step optimization has a possible disadvantage of being more complex, both teams need to understand what they should not do. And, if using a mapped $CostRate$ optimization, one can never map for all conditions (those denoted "⋯" in equations above).

3.5.2.4 Anti-Lock Braking System, ABS *

Function definition: ***Anti-lock Braking System, ABS****, prohibits driver to lock the wheels while braking. The wheel brake torques requested are limited by ABS in a way that each individual wheel's longitudinal slip stays above a certain (negative) value. An extended definition of ABS also includes vehicle deceleration requested by other functions than pedal braking, such as AEB.*

The purpose of ABS is to avoid losing vehicle brake force due to that the tyre force curve drops at high slips AND to leave some friction for steering and cornering, see 2.2.1.6 and 2.2.4.7.5. ABS is a wheel slip closed loop control, active when driver brakes via brake pedal. It keeps the slip above a certain value, typically -15..-20 %. ABS uses the friction brakes as actuator.

Each wheel is controlled individually, but all wheels' speed sensors contribute to calculation of vehicle longitudinal speed, for calculation of actual slip. In the ABS function, it may be included how slip are distributed between the wheels, such as normally the front axle is controlled to a slip closer to locking than the rear axle. Also, a sub-function called "select-low" which makes the wheel closest to locking decide the pressure also for the other wheel at the same axle. Select-low is typically used at rear axles.

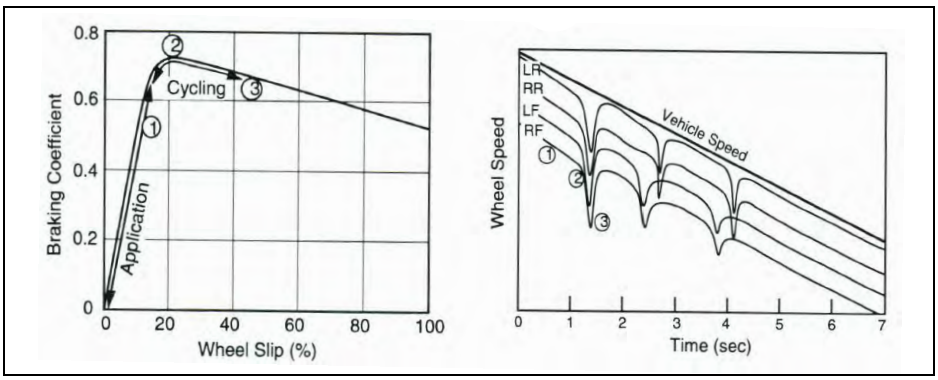


Figure 3-73: ABS control. Principle and control sequence, from Ref (Gillespie, 1992)

3.5.2.5 Electronic Brake Distribution, EBD *

Function definition: ***Electronic Brake Distribution*** *prohibits driver to over-brake the rear axle while braking. An extended definition of EBD also includes vehicle deceleration requested by other functions than pedal braking, such as AEB. EBD only uses friction brake as actuator.*

With a fix distribution between front and rear axle braking, there is a risk to over-brake rear axle when friction is very high, since rear axle is unloaded so much then. Before electronic control was available, it was solved by hydraulic valves, which limited the brake pressure to rear axle when pedal force became too high. In today's cars, where electronic brake control is present thanks to legislation of ABS, the software base function EBD fulfils this need. EBD is primarily a feedforward control of $a_{x,Request}$ and $v_{x,Actual}$. Good estimates of mass, CoG location in x and z direction would be useful, but these are seldom available. EBD can also have feedback of longitudinal slip difference between axles. In heavy vehicles, pneumatic valves are used that limits the brake pressure in relation to the rear axle load (deflection of mechanical spring suspension or air pressure in air suspension).

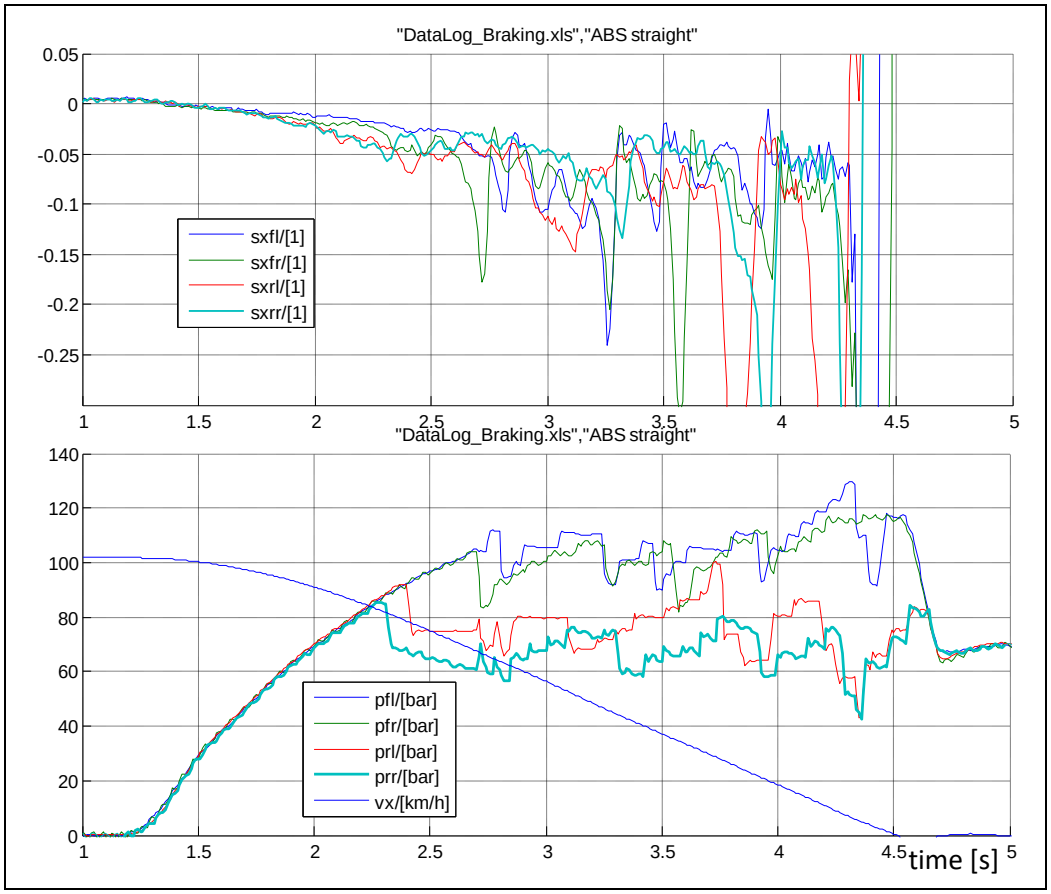


Figure 3-74: ABS control, Data log from passenger car test.

There are other side functions enabled by having ABS on-board. Such are "select low", which means that the brake pressure to both wheels on an axel is limited by the one with lowest pressure allowed from ABS. So, if one wheel comes into ABS control, the other gets the same pressure. This is most relevant on rear axle (to reduce risk of losing side grip) but one tries to eliminate the need of it totally, because it reduces the brake efficiency when braking in curve or on different road friction left/right.

It is often difficult to define strict border between functions that is a part of ABS and which is part of EBD, which is why sometimes one say ABS/EBD as a combined function.

3.5.2.6 Traction Control, TC *

*Function definition: **Traction Control** prohibits driver to spin the driven axle(s) in positive direction while accelerating. An extended definition of TC also includes vehicle acceleration requested by other functions than pedal braking, such as CC. TC uses both friction brakes and propulsion system as actuators.*

The purpose of Traction Control is to maximise traction AND to leave some friction for lateral forces for steering and cornering. Traction control is similar to ABS, but for keeping slip below a certain value, typically +(15..20)%.

Traction control can use different ways to control slip, using different actuators. One way is to reduce engine torque, which reduces slip on both wheels on an axle if driven via differential. Another way is to apply friction brakes, which can be done on each wheel individually. Vehicles with propulsion on several axles can also redistribute propulsion from one axle to other axles, when the first tends to slip. Vehicles with transversal differential clutch or differential lock can redistribute between left and right wheel on one axle.

3.5.2.7 Engine Drag Torque Control, EDC *

*Function definition: **Engine Drag Torque Control** prohibits over-braking of the driven axle(s) while engine-braking. EDC uses both friction brakes and propulsion system as actuators.*

The purpose of Engine Drag Torque Control is as the purpose of ABS, but the targeted driving situation is when engine braking at low road friction, when engine drag torque otherwise can force the wheels to slip too much negative. Similarly to ABS, it keeps the slip above a certain negative value. However, it does it by increasing the engine torque from negative (drag torque) to zero (or above zero for a short period of time).

3.5.2.8 Automatic Emergency Brake, AEB *

*Function definition: **Automatic Emergency Brake** decelerates vehicle without driver having to use brake pedal when probability for forward collision is predicted as high.*

The purpose of AEB is to eliminate or mitigate collisions where subject vehicle collides with a lead vehicle. AEB uses friction brake system as actuator, up to full brake which would be typically 10 m/s2. An AEB system is often limited by not trigger too early, because driver would be disturbed, or it could actually cause accidents. Therefore, in many situations, AEB will rather mitigate than avoid collisions.

Conceptually, an AEB algorithm can be assumed to know physical quantities as marked in Figure 3-75. The quantity time-to-collision, TTC, can then be defined as $TTC = x_o/(v_{sx} - v_{ox})$, which means the time within a collision will appear if no velocities changes. Subscript s and o means subject and object vehicle, respectively.

Also, one can define enhanced time-to-collision measure, eTTC, which considers the present accelerations of the lead vehicle. TTC shall not be mixed up with “time gap” (TG), which is the time when subject vehicle will reach the present position of the lead vehicle, $TG = x_o/v_{sx}$;.

AEB function shall, continuously, decide whether or not to trigger AEB braking. AEB shall intervene by braking when driver can be assumed to collide without intervention. If no other information, this can be predicted as when driver can NOT avoid by normal driving. Avoidance manoeuvres that have to be considered are (normal) deceleration and (normal) lateral avoidance to the left and to the right. What to assume as normal driving is a question of tuning; here the following limits are used $|\dot{v}_{sx}| < a_{sxn} = e.g. 4\ m/s^2$ and $|\dot{v}_{sy}| < a_{syn} = e.g. 6\ m/s^2$. The concept of a physical model-based algorithm is this:

- Normal **deceleration** ($\dot{v}_{sx} = -a_{sxn} = -4\ m/s^2$) leads to **collision if**:
  $\min_{t>0}(x_o(t)) < 0 \quad \Rightarrow \quad \min_{t>0}(x_o + v_{ox} \cdot t - (v_{sx} \cdot t + a_{sxn} \cdot t^2/2)) < 0 \quad \Rightarrow$

$\Rightarrow \quad \left(x_o + v_{ox}\cdot t - (v_{sx}\cdot t + a_{sxn}\cdot t^2/2)\right)\Big|_{t=\frac{v_{ox}-v_{sx}}{a_{sxn}}} < 0 \quad \Rightarrow$

$\Rightarrow \quad x_o - \frac{1}{2\cdot(-a_{sxn})}\cdot(v_{sx}-v_{ox})^2 < 0 \quad \Rightarrow \quad \frac{x_o}{v_{sx}-v_{ox}} < \frac{v_{sx}-v_{ox}}{2\cdot(-a_{sxn})} \quad \Rightarrow \quad \boldsymbol{TTC < \frac{v_{sx}-v_{ox}}{8}};$

- Normal **avoidance to the left** ($\dot{v}_{sy} = a_{syn} = 6\ m/s^2$) leads to **collision if**:
  $\left(y_{ol}(t) + \frac{w}{2}\right)\Big|_{x_o=0} < 0 \quad \Rightarrow \quad \left(y_{ol} - a_{syn}\cdot\frac{t^2}{2} + \frac{w}{2}\right)\Big|_{t=\frac{x_o}{v_{sx}-v_{ox}}} < 0 \quad \Rightarrow$

  $\Rightarrow \quad \frac{x_o}{v_{sx}-v_{ox}} < \sqrt{2\cdot\frac{y_{ol}+w/2}{a_{syn}}} = \{e.g.\} = \sqrt{\frac{0.6+1.8/2}{3}} \approx 0.4\ s \quad \Rightarrow \quad \boldsymbol{TTC < 0.4\ s};$
- Normal **avoidance to the right** ($\dot{v}_{sy} = -a_{syn} = -6\ m/s^2$) leads to **collision if**:
  $\cdots \quad \Rightarrow \quad \frac{x_o}{v_{sx}-v_{ox}} < \sqrt{2\cdot\frac{-y_{or}-w/2}{a_{syn}}} = \cdots \quad \Rightarrow \quad \boldsymbol{TTC < 0.4\ s};$
- Assuming that the AEB intervention decelerates the vehicle with $-\dot{v}_{sx} = a_{sxAEB} = -8\ m/s^2$, a forward collision can be avoided if AEB intervenes AND if:
  $\cdots \Rightarrow \frac{x_o}{v_{sx}-v_{ox}} > \frac{\boldsymbol{v_{sx}-v_{ox}}}{\boldsymbol{2\cdot(-a_{sxAEB})}} = \frac{v_{sx}-v_{ox}}{16} \quad \Rightarrow \boldsymbol{TTC > \frac{v_{sx}-v_{ox}}{16}};$

Figure 3-75 shows a diagram where different condition areas are marked. The sectioned area shows where AEB will be triggered, using above rules. The smaller of the sectioned areas shows where it also will be possible to trigger AEB so timely that a collision is actually avoided; with the assumed numbers, this is for speeds up to 6.4 m/s≈23 km/h.

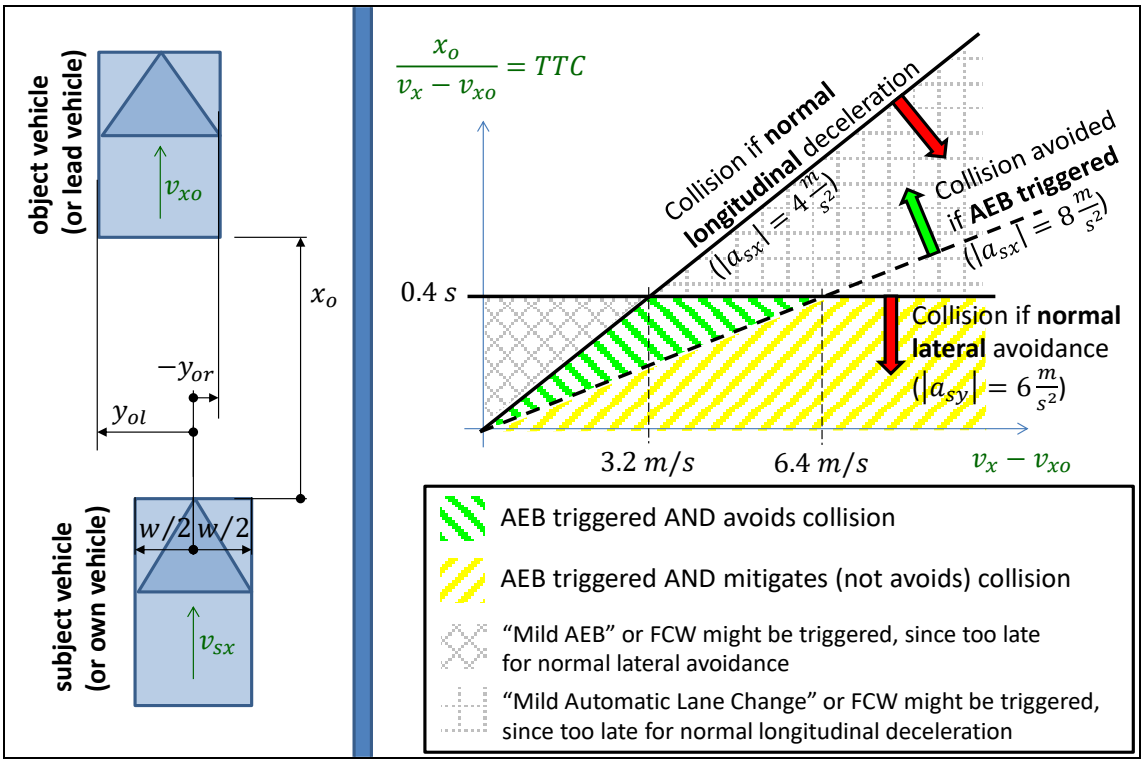


Figure 3-75: Left: Quantities known for an AEB algorithm in the subject vehicle, assuming "symmetrically behind" ($y_{ol} = -y_{or}$). Right: Model based decision of triggering AEB and effectiveness of AEB if triggered.

The reasoning above is very simplified. Additional information can improve effectiveness of AEB, such as knowing if a lateral avoidance on one side of object vehicle is blocked, the acceleration of the object vehicle, pedal operation of subject vehicle, road gradient, road curvature and road friction is. The vehicle dynamics model used is simply a point mass with predicted constant velocity and certain assumed acceleration capability, which of course can be extended a lot; both with taking actual accelerations into account and more advanced vehicle dynamics models. The decision to intervene is dependent of many pieces of information and simple models; vehicle dynamics and driver behaviour (in both subject and object vehicles) as well as road characteristics. AEB function has to be designed together with other similar functions, such as ACC and Forward Collision Warning (FCW).

AEB is legal requirement for both passenger vehicles and heavy vehicles (ISO19377, 2017).

Related functions are, e.g., an automatic extra force assistance in brake pedal when driver steps quickly onto brake. Another related function is automatic braking triggered by a first impact and intended to mitigate or avoid secondary accident events, starts to appear at market, see Reference (Yang, 2013). In semantic meaning, this could be seen as AEB, but they are normally not referred to as AEB; AEB normally refers to functions that use environment sensors (forward directed radar, camera, etc.).

When designing and evaluating AEB, it is important to also know about the function Forward Collision Warning, FCW. FCW is a function that warns the driver via visual and/or audio signals when a forward collision is predicted. FCW is typically triggered earlier than AEB.

AEB as described above could be called “Rear-end AEB”. Another similar functionality, not included in today’s AEB, could be called “Intersection AEB” and include braking for intersecting traffic, see (Sander, 2018).

3.5.3 Longitudinal Motion Function Architecture

All control functions controls have to cooperate, and they have to be transferable between platforms and vehicle variants. It is very complex to take all functions into consideration, but with a scope limited to the longitudinal Motion functionality

Figure 3-76 can be drawn as a solution within the reference architecture.

By using a reference architecture, it can be illustrated that Adaptive Cruise control and cruise control can be seen as part of Traffic Situation Layer (ACC=CC if no vehicle ahead). The Traffic Situation Layer has the purpose and scope to understand the ego vehicle’s surrounding traffic by looking at e.g. Forward Sensors. The forward-looking sensor is in this case part of Vehicle Environment sensors.

Vehicle Motion and Coordination Layer would include the arbitration of Driver’s Acceleration and Brake pedal input and Traffic functionality, see Figure 3-76. In addition, Vehicle Motion and Coordination Layer would perform the powertrain coordination and brake distribution. The coordinated requests are then sent to Motion Support Device Layer.

The Human Machine Interface would include the services available for the driver to activate or request, E.g. ACC activation to Traffic Situation or Deceleration by pressing the brake pedal.

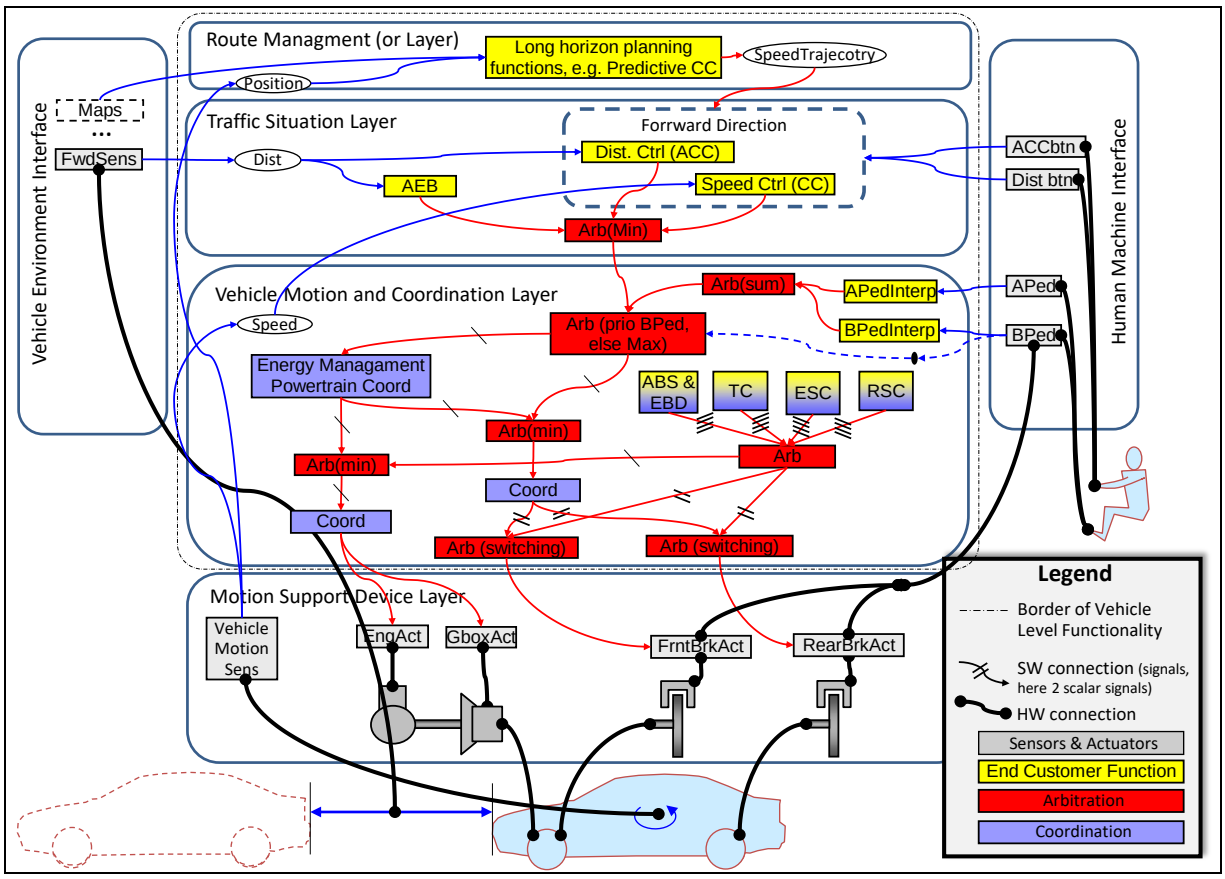


Figure 3-76: Functional architecture for conventional front axle driven passenger car. Mainly longitudinal functions (plus ESC, RSC) are shown, e.g. no steering. Cf. ***Figure 1-73****.*

If a reference architecture is used, it can assist function developers from OEM's Electrical, Powertrain, and Chassis departments and suppliers to have a common view of how vehicle's embedded motion functionality is intended to be partitioned and to understand how different functions relate and interact with each other and what responsibilities they have.

4 LATERAL DYNAMICS

4.1 Introduction

The lateral motion of a vehicle is needed to follow the road curves, select route in intersections and laterally avoid obstacles, which all involve steering. Vehicle steering is studied mainly through the vehicle degrees of freedom: yaw rotation ω_z and lateral translation v_y.

A vehicle can be steered in different ways:

- Applying steer angles on road wheels. Normally both of front wheels are steered with approximately same angle.
- Applying longitudinal forces on road wheels; directly by unsymmetrical between left and right side of vehicle, e.g. one-sided braking, or indirectly by deliberately use up much friction longitudinally on one axle in a curve, so that that axle loses lateral force.
- Articulated steering, where the axles are fixed mounted on the vehicle body, but the vehicle itself can bend.

The turning manoeuvres of vehicles encompass two sub-attributes. Handling is the driver's perception of the vehicle's response to the steering input. Cornering is the physical response (open loop) of the vehicle independent of how it influences the driver.

The lateral dynamics of vehicles is often experienced as the most challenging for the new automotive engineer. Longitudinal dynamics is essentially motion in one plane and rectilinear. Vertical dynamics may be 3 dimensional, but normally the displacements are small and in this book the vertical dynamics is mainly studied in one plane as rectilinear. However, lateral dynamics involves motion in the vehicle coordinate system which introduces curvilinear motion since the coordinate system is rotating as the vehicle yaws.

The chapter introduces the models, more or less, in order of increasing number of states. For some readers, it might be comprehensive to start with a look-ahead on the "linear one-track model" in 4.4.2. This is the simplest model which yet captures the essential lateral motion quantities v_y and ω_z as states. The models earlier in the chapter can then be seen as simplifications.

4.1.1 Lateral Model Categorization

The chapter is organised as shown in Table 4.1. The table also shows a high-level categorization of functions/models in the sections. Typically, the input is steer angle δ and the output is yaw rate ω_z and lateral velocity v_y. The longitudinal speed v_x is often treated as a parameter ($\dot{v}_x \equiv 0$).

Table 4.1: Approximate high-level categorization of lateral functions/models

Section	Longitudinal velocity v_x	Typical input variables or parameters	Typical output variables
4.2 Low-speed	Parameter, $v_x \equiv 0^+ \text{ or } 0^- \ [m/s]$	Path limitations, like road width and radius	Path $x(s), y(s), \varphi_z(s)$, i.e. v_x, v_y, ω_z integrated over the manoeuvre
4.3 Steady State Cornering at High Speed	Parameter, $v_x = 10..30 \ [m/s]$	v_x and Path radius R_p	Steady states $\delta(R_p, v_x)$, $v_y(\delta, v_x), \omega_z(\delta, v_x)$ and $a_y(\delta, v_x)$
4.4 Stationary Oscillating Steering	Parameter, $v_x = 10..30 \ [m/s]$	v_x, Steering amplitude $\hat{\delta}$, Frequency f	Stationary oscillating responses $\hat{\omega}_z(\hat{\delta}, f)$ and $\hat{a}_y(\delta, v_x)$
4.5 Transient Driving	Variable, $\dot{v}_x \neq 0$	Initial v_{x0}, Steering $\delta(t)$, Wheel torques $(\boldsymbol{T}(t))$	<Numerous and various>
	Parameter, $v_x = 0..30 \ [m/s]$	Pure and simplified handling manoeuvres, such as 4.5.4	

There are other categorizations in 1.6.2, such as *irp/oorp* and one-*track/two-track*. Categorization of *tyre* models is found in 2.2.7.

4.1.1.1 A cavalcade of vehicle modelling concepts

A cavalcade of one-track modelling concepts for lateral motion is given in the figure below. Vertical dimension spans different dynamic operating conditions and some simplifications downward. Horizontal spans from single unit to multi-unit.

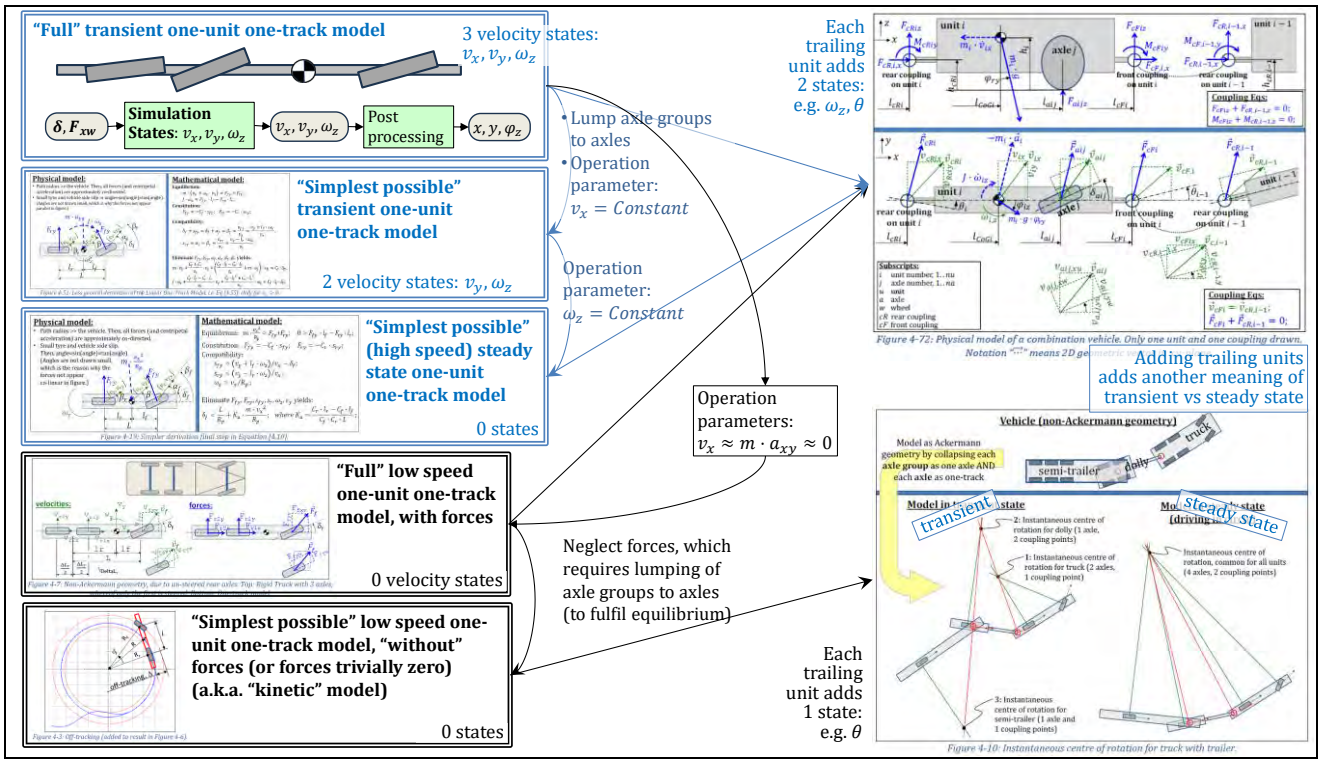


Figure 4-1: A cavalcade of one-track modelling concepts for lateral motion. Left: One-unit vehicles. Right: Adding trailing units. The small figures are copies of pictures from the book: Figure 4-51, Figure 4-19, Figure 4-7, Figure 4-3, Figure 4-72, and Figure 4-10.

Changing to 2-track models requires some representation of the suspension within the axle, very much like how axles within an axle group are suspended (mechanically and controlled) within the axle group. For "full" low speed models, it can motivate adding force or torque states to represent

suspension steering: side force-steering, and roll-/bump-steering beside above influence from tyre force vs tyre slip models.

4.1.2 References for this chapter

- *"Chapter 25 Steering System"* in Ref (Ploechl, 2013).
- *"Chapter 27 Basics of Longitudinal and Lateral Vehicle Dynamics"* in Ref (Ploechl, 2013).
- "*Chapter 8: Electronic Stability Control*" in Ref (Rajamani, 2012)

4.2 Low-speed manoeuvres

This section is about operating vehicles in low speeds, including stand-still and reverse. Specific for low-speed models is that inertia effects can be neglected, i.e. one neglect the fictive forces $m \cdot a_x$, $m \cdot a_y$ and $J_z \cdot \dot{\omega}_z$ in the equilibrium. The function measures often requires that one find the paths $[x(s), y(s)]$ of the vehicles body edges or wheels. The paths can be obtained from 1.6.1.7.

Functions are presented in 4.2.1 and the section that follows explains models with subsequently increasing number of phenomena, ending with reversing. A large divider between models is whether all forces or moments are modelled as zero or not, e.g. the difference between "4.2.2 Low Speed Model, Ackermann, without Forces" and "4.2.3 Low Speed Model, Ackermann, with Forces".

4.2.1 Low-speed functions

4.2.1.1 Turning Diameter *

> *Function definition:* ***Turning diameter*** *is the diameter of the smallest possible circular path obtained steady state at low speed, measured to a certain point at the vehicle. The certain point can be either outer-most point on wheel (Kerb Turning diameter) or outer-most point on body (Wall Turning diameter).*

The end of the simulation in Figure 4-6 is made with constant steer angle. If we assume that it is the maximum steer angle, the circle actually shows the turning circle for centre of gravity. If we add the path for the outermost wheels, we get the kerb turning diameter, see Figure 4-2. If we add the path for the outermost point at the vehicle body we get the wall turning diameter, also shown in Figure 4-2. The outermost point at the vehicle body is normally the front outer corners of the vehicle body.

4.2.1.2 Swept Path Width, SPW *

> *Function definition:* ***Swept path width*** *is the distance between the outermost and innermost paths of wheels (or body points). The paths are then from a certain turning or lane change manoeuvre at a certain speed.*

For manoeuvrability, there is a function which is complementary to turning diameter. It is "Swept Path Width" (SPW), see Figure 4-2. It can be defined for circle driving with maximum steering angle, as Turning diameter, but also for any other certain manoeuvre. It can be defined for kerb and wall; distance between wheels or body points. The SPW should be small for good manoeuvrability.

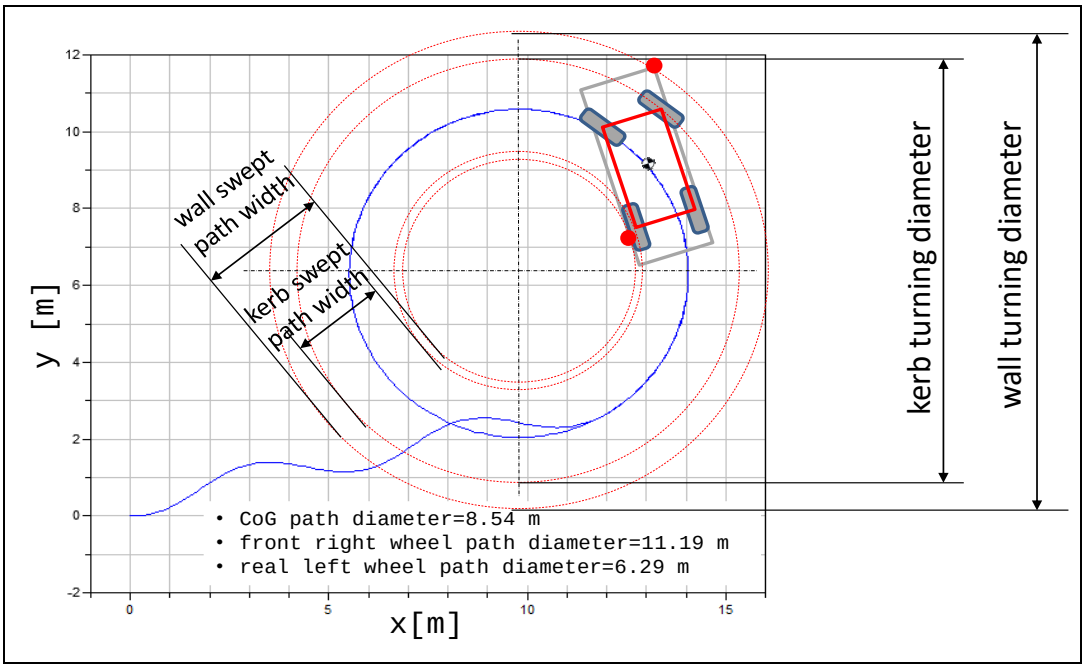


Figure 4-2: Paths for wheels and body points (added to result in Figure 4-6).

4.2.1.3 Low Speed Off-Tracking, LSOT *

*Function definition: **Off-tracking** is the distance between the outermost and innermost paths of mid-points of axles. The paths are then from a certain turning or lane change manoeuvre at a certain speed.*

Another measure of manoeuvrability is "Off-tracking", see Figure 4-3. It is like Swept Path Width, but for the mid points of the axles. It is also used for higher speeds, and then the rear axle often tracks on a larger radius than front axle. A variant of definition of Off-Tracking uses (lateral) midpoints of body and it can be much larger than the first definition for vehicles with long front or rear overhangs.

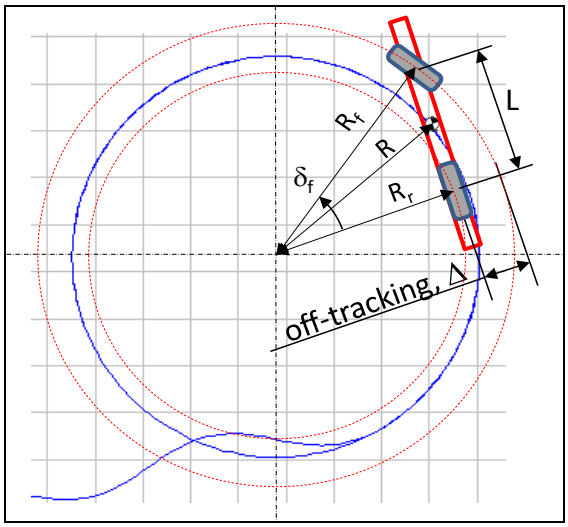


Figure 4-3: Off-tracking (added to result in Figure 4-6).

4.2.1.4 Circle and Manoeuvre Measures

SPW and Off-tracking is most relevant for vehicles with several units, such as truck with trailer. They can be defined for driving several rounds in a circle with constant steering angle ("**Circle** SPW/Off-tracking"). It is a well-defined measure since it is a steady state with respect to articulation angle. However, circle driving is seldom the most relevant manoeuvre. So, one often set requirements on "**Manoeuvre** SPW/Off-tracking", e.g. when driving from straight, via curve with certain outer radius, to a new straight in a certain angle from the first straight, e.g. 12.5 m and 90 deg is common. A way to predict SPW/Off-tracking for such a manoeuvre is to simulate with time integration, see 4.2.5.2. One can integrate in travelled distance s instead of time, but time is often easier and allows stand-still parts in the manoeuvre. The states in the simulation are the path coordinates with orientation (x, y, φ_z) and articulation angles $(\theta_1, \theta_2, \ldots)$.

The steady state is typically approached asymptotically, so the corresponding circle values requires either long simulations or inserting state derivatives zero and algebraic solution. From geometry in Figure 4-3 on can find an expression for (Circle) Off-tracking Δ:

$$\Delta(R_f, L) = R_f - R_r = R_f - \sqrt{R_f^2 - L^2};$$
$$\Delta(\delta_f, L) = R_f - R_r = L/\sin(\delta_f) - L/\tan(\delta_f);$$

[4.1]

Note: The force equilibrium also must be fulfilled, so it is recommended that we realize that this model *implicitly* includes the 3 equilibrium equation in ground plane (involving $F_{fx}, F_{fy}, F_{rx}, F_{ry}$) and the wheel torque coordination $F_{fy} \cdot F_{ry} \approx 0$ (no fighting between axles), but with the *trivial solution* that $F_{fx} \equiv F_{fy} \equiv F_{rx} \equiv F_{ry} \equiv 0$. So, we typically do not, formally, include these equations and these forces. The reason to still realize that these equations exist, even if trivially fulfilled, is that it is easier to recognize/accept why they are needed to formally include for other low-speed models, where forces cannot be neglected.

4.2.1.5 Steering Effort at Low Speed *

Function definition: ***Steering effort at low speed*** *is the steering wheel torque needed to turn the steering wheel a certain angle at a certain angular speed at vehicle stand-still on high road friction.*

At low or zero vehicle speed, it is often difficult to reach a low steering wheel torque, due to:

- Castor offset in Figure 2-138 gives the wheel a side slip when steering and hence a tyre lateral force is developed. Tyre lateral forces times castor offset increases the steering wheel torque.
- Additionally, there is a spin moment in the contact patch, M_{ZT} in Figure 2-7. It does not influence very much, except for at very low vehicle speed. Quantitative models for M_{ZT} are not presented in this book.

A critical test for steering effort at low speed is to steer a parked vehicle with a certain high steering wheel rotational speed, typically some hundred deg/s. The steering wheel torque is then required to stay under a certain design target value, normally a couple of Nm. The torque needed will be dependent on lateral force, spin moment and steering geometry and dependent on the capability of the power steering system (which is dependent on steering, due to delays in the steering assistance actuator). A failure in this test is called "catch-up", referring to that driver catches up with the power steering system. It can be felt as a soft stop and measured as a step in steering wheel torque.

4.2.2 Low Speed Model, Ackermann, without Forces

Low speed manoeuvres are characterised by that the inertial forces are neglected, i.e. $m \cdot a = 0$. If the steering geometry is according to Ackermann, the forces on the vehicle body are small, and there is no significant longitudinal wheel forces, it means that the equilibrium is trivially fulfilled with all forces zero. Then we can use *ideally tracking* tyre model for all wheels, see 2.2.7. We can see this as Eq [2.48] with infinite cornering stiffness: Eq [2.48] $\Rightarrow F_y = -C_y \cdot s_y \to \infty \cdot s_y; \Rightarrow s_y = 0; \Rightarrow v_{yw} = 0;$. The tyre force F_y can be any (finite) value, determined by other part of the system than the tyre. This tyre model can be seen as a compatibility relation (or "kinematic model"), since it relates velocities to each other without involving any force. However, in this book we still consider it as a constitutive model, keeping in mind that it is definitely invalid if $F_y > \mu \cdot F_z;$.

The effects of ideal tracking are that the intersection point of the wheels rotational axes coincides with the instantaneous centre of vehicle rotation in ground plane. This directly relates steer angles and path radius to each other. For the one-track model in Figure 1-70 this relation becomes:

$$\left.\begin{aligned}\tan(\delta_f) &= \frac{L}{R_r};\\ R^2 &= {R_r}^2 + {l_r}^2;\end{aligned}\right\} \Rightarrow \delta_f = \arctan\left(\frac{L}{\sqrt{R^2 - {l_r}^2}}\right) \cdot \text{sign}(R) \approx \frac{L}{\sqrt{R^2 - {l_r}^2}} \cdot \text{sign}(R) \approx \frac{L}{R};$$

where $R > 0$ *means that instantaneous centre of rotation is left of the vehicle*

[4.2]

4.2.3 Low Speed Model, Ackermann, with Forces

In previous models we have not included force equilibria, which is an implicit (or unconscious) modelling of that the forces are zero, so the equilibrium is trivially fulfilled. Sometimes we have to bring in forces, and with those, constitutive equations. Reasons for including forces could be many, such as:

- **Additional axles, not friction steered**, so that the steering geometry is not Ackermann. Then the additional constitutive equations are of the type $F_{iy} = -C_{iy} \cdot s_{iy}$; and they are typically needed for all axles, because the whole vehicle has to fulfil equilibrium.
- Body forces, such as gravity forces from significant **road pitch or road roll** angles. It can also be that the vehicle **towing** something. Possibly there can be cases with strong wind, so we get **aerodynamic forces** without large vehicle speed.
- **Wheel individual wheel torque** and/or **locked differentials** also requires involvement of forces. The additional constitution will have to describe the yaw moment M_{iz} from the axle due to different forces left/right, involving the tyre longitudinal constitution, $F_{ijx} = C_{ijx} \cdot s_x$;.
- Significant **rolling resistance**, where the additional constitutive equation is of type: $T_{iRR} = F_{ix} \cdot R + F_{iz} \cdot RRC \cdot R$; The coordination of wheel torques between the axles then need to be given also.

When forces are added, it often changes the model from relatively simple geometric formulas (typical triangles and trigonometry) to relatively difficult algebraic equation systems.

4.2.3.1 Implications of Forces on Turning Circle

If we have a vehicle with Ackermann geometry, it is tempting to model without involving forces, using Eq [4.2]. But forces can influence low speed paths. When introducing rolling resistance, the force equilibrium is obtained by counter-directed tyre-longitudinal forces on the two axles. Due to the steer angle, a lateral force on the front wheel is required, which gives a lateral tyre slip, $\alpha_f \neq 0$, see Figure 4-4. This changes the motion compared to **Figure 1-70**. Road (pitch) grade resistance influences in a very similar way through longitudinal gravity force and road (roll) inclination influences by adding lateral gravity force.

For heavy combination vehicles, these effects can be significant, adding also rolling resistance from towed units and non-Ackermann effects of several non-steered axles on some units. The function to turn can be quantified by required road friction on steered and driven axle, as opposed to radius at maximum steer angle.

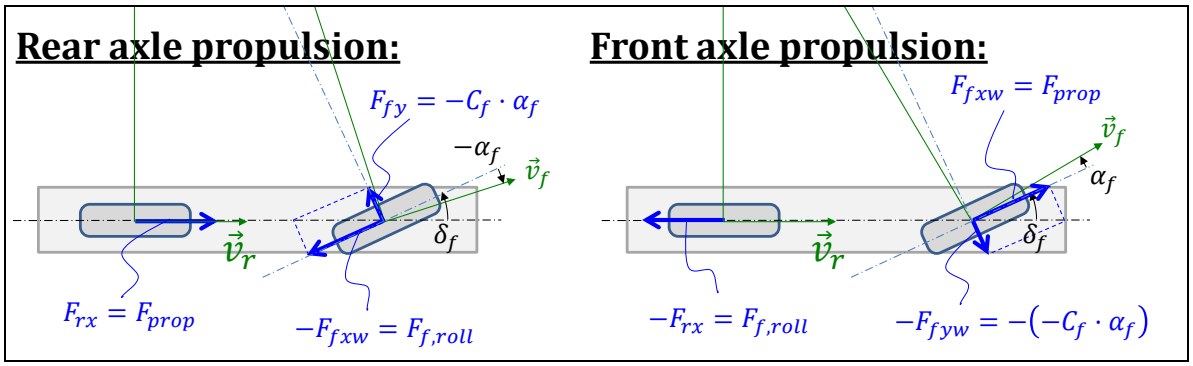


Figure 4-4: Smaller turning circle diameter for front axle propulsion, as compared to rear axle propulsion due to rolling resistance on the un-driven axle.

4.2.3.2 Model

The model in Eq [4.2] predicts a motion without involving forces, or actually assuming forces are zero. To get a more complete model, where more variables can be extracted, we can set up the model in Figure 4-5.

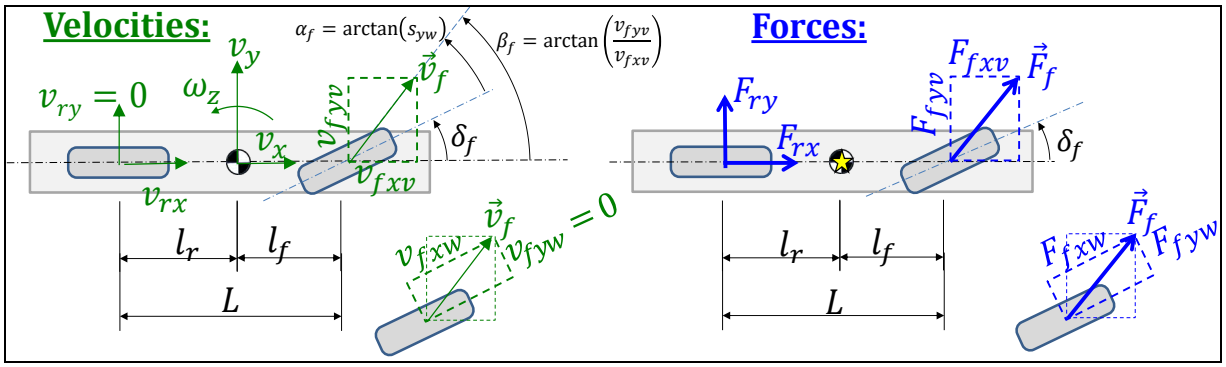


Figure 4-5: One-track model with ideally tracking axles. Lower view of front wheel shows conversion between wheel and vehicle coordinate systems. Note that the reference point is selected as the centre of gravity, to be more comparable with high speed models, but the location of centre of gravity does not influence the overall vehicle motion in low-speed.

The "physical model" in Figure 4-5 gives the following "mathematical model":

Equilibrium (longitudinal, lateral and yaw around CoG):

$$0 = F_{fxv} + F_{rx};$$
$$0 = F_{fyv} + F_{ry};$$
$$0 = F_{fyv} \cdot l_f - F_{ry} \cdot l_r;$$

Transformation between vehicle and wheel coordinate systems:

$$F_{fxv} = F_{fxw} \cdot \cos(\delta_f) - F_{fyw} \cdot \sin(\delta_f);$$
$$F_{fyv} = F_{fxw} \cdot \sin(\delta_f) + F_{fyw} \cdot \cos(\delta_f);$$
$$v_{fxv} = v_{fxw} \cdot \cos(\delta_f) - v_{fyw} \cdot \sin(\delta_f);$$
$$v_{fyv} = v_{fxw} \cdot \sin(\delta_f) + v_{fyw} \cdot \cos(\delta_f);$$

Compatibility between CoG and axles:

$$v_{fxv} = v_x; \quad and \quad v_{fyv} = v_y + l_f \cdot \omega_z;$$
$$v_{rx} = v_x; \quad and \quad v_{ry} = v_y - l_r \cdot \omega_z;$$

Ideal tracking (Constitutive relation, but with infinite lateral slip stiffness):

$$v_{fyw} = 0; \quad and \quad v_{ry} = 0;$$

Path with orientation (compatibility), from Eq [1.9]:

$$\dot{x} = v_x \cdot \cos(\varphi_z) - v_y \cdot \sin(\varphi_z);$$
$$\dot{y} = v_y \cdot \cos(\varphi_z) + v_x \cdot \sin(\varphi_z);$$
$$\dot{\varphi}_z = \omega_z;$$

Controls (driver or actuation):

$$\delta_f = \begin{cases} = (35 \cdot \pi/180) \cdot \sin(0.5 \cdot 2 \cdot \pi \cdot t); & if\ t < 4.5; \\ = 35 \cdot \pi/180; & else \end{cases}$$

driver also decides driving direction, $DrivDir = \text{sign}(v_x)$

Constitution (Rear axle undriven, which gives drag from roll resistance):

$$F_{rx} = -100 \cdot \text{sign}(v_x);$$

[4.3]

Overall, if we assume known $v_x(t)$ and known $\delta_f(t)$ we can simulate the solution from an explicit form of the model: $\{\dot{x}, \dot{y}, \dot{\varphi}_z\} = func(states, input\ variables) = func(\{x, y, \varphi_z\}, \{v_x(t), \delta_f(t)\})$;. For low-speed manoeuvres, it can often be easier to change independent variable from time to travelled longitudinal distance s, e.g., defined by $\dot{s} = |v_x|$. The dynamics then becomes: $\{x', y', \varphi_z', t'\} = \{dx/ds, dy/ds, d\varphi_z/ds\} = func(\{x, y, \varphi_z\}, \{v_x(s), \delta_f(s)\})$; and the connection to time domain (if interesting): $t' = 1/|v_x|$;.

Note that the real location of CoG does not influence the overall motion, meaning that $\{l_f, l_r\}$ can be any values, or any reference point, where we want to calculate the vehicle location $\{x, y, \varphi_z\}$.

Note also that, since we have Ackermann geometry, we can (mathematically) use the ideal tracking tyre model ($v_{iyw} = 0$;) even if forces are now introduced. For some problems, it might be motivated to use $F_{iyw} = -C_{iy} \cdot s_{iy} = -C_{iy} \cdot v_{iyw}/|R \cdot \omega| \approx -C_{iy} \cdot v_{iyw}/|v_{ixw}|$;, but we leave this to 4.2.4.

The compatibility in Eq [4.3] neglects the influence of steering axis offsets at ground, see 0. The terms neglected are of the type $LateralOffset \cdot \dot{\delta}$; in the equation for v_{fxv} and $LongitudinalOffset \cdot \dot{\delta}$ in the equation for v_{fyv}. This is generally well motivated for normal road vehicles, except for very quick steering when vehicle is close to stand-still.

Equation [4.3] is written in Modelica format in Equation [4.4]. Comments are marked with //. The subscripts v and w refer to vehicle coordinate system and wheel coordinate system, respectively. The actual assumption about ideal tracking lies in that $v_{fyw} = v_{ry} = 0$. Global coordinates from Figure 1-66 is also used. A driving resistance of 100 N is assumed on the rear axle ($F_{rx} = -100$;) to exemplify that forces do not need to be zero.

```
//Equilibrium:
  0 = Ffxv + Frx;
  0 = Ffyv + Fry;
  0 = Ffyv*lf - Fry*lr;
//Ideal tracking (Constitutive relation, but without connection to forces):
  vfyw = 0;     vry = 0;
//Compatibility:
  vfxv = vx;    vfyv = vy + lf*wz;
  vrx = vx;     vry = vy - lr*wz;
//Transformation between vehicle and wheel coordinate systems:
  Ffxv = Ffxw*cos(df) - Ffyw*sin(df);
  Ffyv = Ffxw*sin(df) + Ffyw*cos(df);
  vfxv = vfxw*cos(df) - vfyw*sin(df);
  vfyv = vfxw*sin(df) + vfyw*cos(df); //or atan(vfyv/abs(vfxv))=df+atan(sfy); sfy=0;
//Path with orientation:
  der(x) = vx*cos(pz) - vy*sin(pz);
  der(y) = vy*cos(pz) + vx*sin(pz);
  der(pz) = wz;
// Prescription of actuation:
  df = if time < 4.5 then (35*pi/180)*sin(0.5*2*pi*time) else 35*pi/180;
//Rear axle undriven, which gives drag from roll resistance:
  Frx = -100;
```

[4.4]

4.2.3.3 Simulation

The longitudinal speed is a parameter, $v_x = 10\ km/h$. A simulation result from the model is shown in Figure 4-6. It shows the assumed steer angle function of time, which is an input. It also shows the resulting path, $y(x)$.

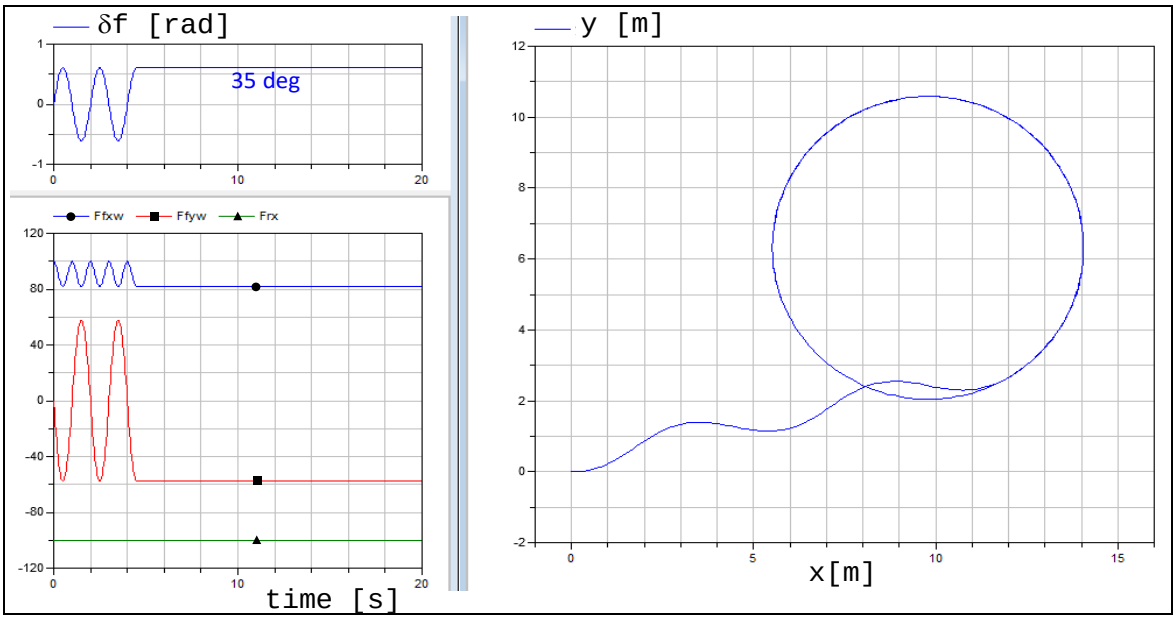


Figure 4-6: Simulation results of one-track model with ideal tracking tyres.

The variables $x, y, p_z = \varphi_z$ are the only state variables of this simulation. If not including the path model (Eq [1.9]), the model would be only an algebraic system of equations. That system of equations could be solved isolated for any value of steer angle without knowledge of time history.

4.2.4 Low Speed Model, Non-Ackermann

If Non-Ackermann geometry, we have to include the forces. Non-Ackermann geometry can be seen as lateral wheel or tyre forces fight each other; either between left and right wheels or between axles. Examples are a two-axle vehicle which has parallel steering and truck with 3 axles, whereof the two rear are non-steered, respectively.

4.2.4.1 Non-Ackermann between Axles

We will go through model changes needed for the latter example. In order to compare the models as closely as possible, we simply split the rear axle into two rear axles, in the example in 4.2.1. The physical model becomes as in Figure 4-7. The measures appear in Figure 4-9, and you see that it is not a typical truck, but a very unconventional vehicle of passenger car size but with two rear axles.

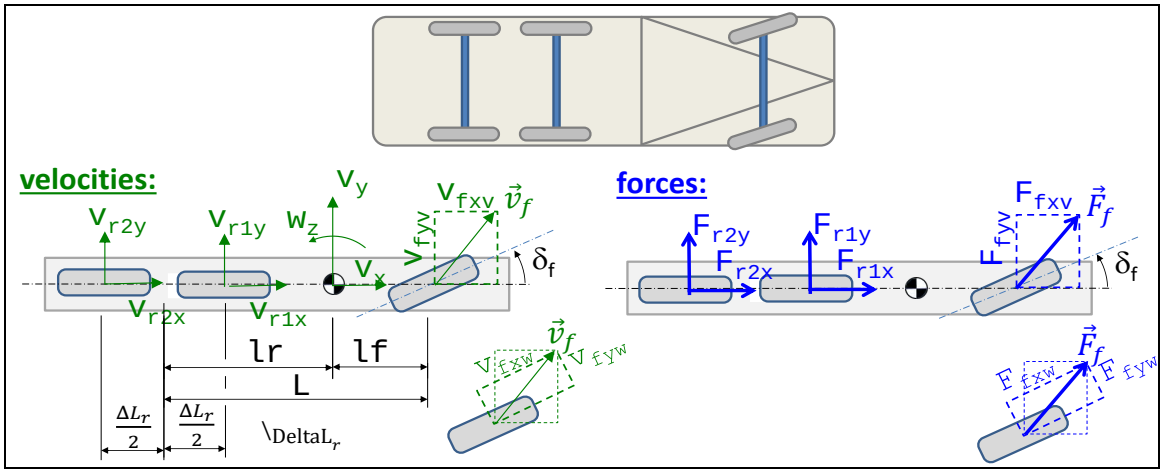


Figure 4-7: Non-Ackermann geometry, due to un-steered rear axles. Top: Rigid Truck with 3 axles, whereof only the first is steered. Bottom: One-track model.

The changes we have to do in the model appear as underlined in Equation [4.5]. There has to be double variables for v_{rx}, v_{ry}, F_{rx}, F_{ry}, denoted 1 and 2 respectively. Also, we cannot (mathematically) use $v_{fyw} = v_{ry} = 0$ anymore, but instead we introduce a lateral tyre force model, as described in 2.2.4.

```
//Equilibrium:
  0 = Ffxv + Fr1x + Fr2x; //grade resistance could be added here, e.g. "+500"
  0 = Ffyv + Fr1y + Fr2y;
  0 = Ffyv*lf - Fr1y*(lr - DLr/2) - Fr2y*(lr + DLr/2);
//Constitutive relation (with slip, as opposed to Ideal tracking):
  Ffyw = -Cf*sfy;    sfy = vfyw/abs(vfxw);
  Fr1y = -Cr1*sr1y;  sr1y = vr1y/abs(vr1x);
  Fr2y = -Cr2*sr2y;  sr2y = vr2y/abs(vr2x);
//Compatibility:
  vfxv = vx;
  vfyv = vy + lf*wz;
  vr1x = vx;
  vr2x = vx;
  vr1y = vy - (lr - DLr/2)*wz;
  vr2y = vy - (lr + DLr/2)*wz;
//Transformation between vehicle and wheel coordinate systems:
  Ffxv = Ffxw*cos(df) - Ffyw*sin(df);
  Ffyv = Ffxw*sin(df) + Ffyw*cos(df);
  vfxv = vfxw*cos(df) - vfyw*sin(df);
  vfyv = vfxw*sin(df) + vfyw*cos(df);
//Path with orientation:
  der(x) = vx*cos(pz) - vy*sin(pz);
  der(y) = vy*cos(pz) + vx*sin(pz);
  der(pz) = wz;
// Prescription of steer angle:
  df = if time < 4.5 then (35*pi/180)*sin(0.5*2*pi*time) else 35*pi/180;
//Rear axles undriven, which gives drag from rolling resistance:
  Fr1x = -100/2*sign(vx);
  Fr2x = -100/2*sign(vx);
```

[4.5]

The new result is shown in Figure 4-8, which should be compared to Figure 4-6. The radius in the circle increases a little, which is intuitive, since the double rear axle makes turning less easy.

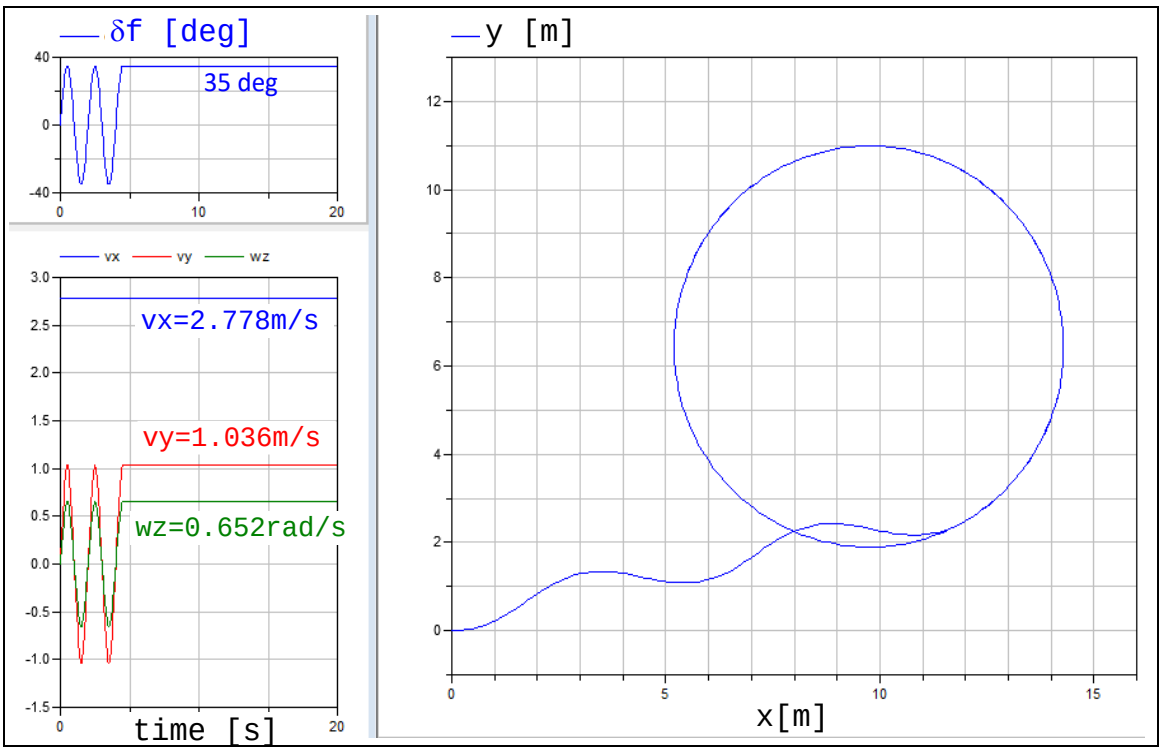


Figure 4-8: Simulation results of one-track model. Non-Ackermann geometry due to two non-steered rear axles. Tyres models are linear, as opposed to ideally tracking.

4.2.4.1.1 Equivalent Wheelbase

We can also draw the different locations of the instantaneous centre for both cases. This is shown, in scale, in Figure 4-9.

We could tune the steer angle required to reach exactly the same path radius as for the 2-axle reference vehicle. Then, we would have to steer a little more than the 35 degrees used, and we could find a new instantaneous centre, and we could identify a so-called Equivalent wheelbase. This leads us to a definition: The equivalent wheelbase of a multi-axle vehicle is the wheel base of the corresponding two-axle vehicle which would exhibit the same turning behaviour as exhibited by the multi-axle vehicle, given same steer angle and similar axle cornering stiffnesses. In 4.2.4 it is shown that ideally tracking tyre model is not enough for non-Ackermann geometry; at least a linear tyre model is needed with $C_y \neq \infty$.

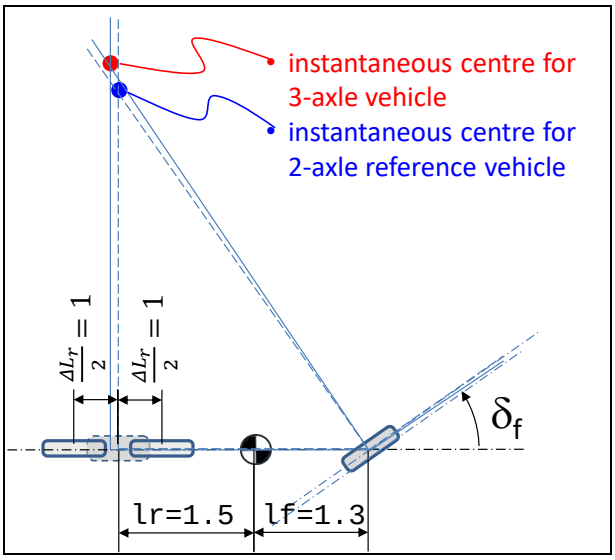


Figure 4-9: Instantaneous centre with a 3-axle vehicle, with corresponding 2-axle vehicle as reference.

4.2.5 Articulated Vehicles

4.2.5.1 Ackermann Geometry for Articulated vehicles

For vehicle without articulation, there has to be one common instantaneous centre for all points on the vehicle body. For articulated vehicles, each unit can have its own instantaneous centre. But these are dependent of each other through the coupling points. So, adding units with one axle does **not** disqualify the Ackermann property of the resulting combination vehicle. See "transient state" in Figure 4-10.

4.2.5.2 Transients in Articulation Angle

For articulated vehicles, also the low speed case has transients in the sense that the articulation angles change transiently. The models are steady state with respect to velocities, but transient with respect to articulation angle, see "transient state" in Figure 4-10. Consider the case of instantaneous step steer. For a vehicle without articulation, a steady state is reached directly, since inertia is not considered. But for an articulated vehicle it takes some time (or travelled distance, since it can be studied independent of speed and time) before a steady state articulation angle is achieved, see "steady state" in Figure 4-10.

So, for articulated vehicles, a scalar requirement on turning radius is not so relevant as for two axle vehicles. The functions "4.2.1.2 Swept Path Width, SPW *" and "4.2.1.3 Low Speed Off-Tracking, LSOT *" are better, assuming one defines a certain road geometry, e.g. through outer radius and total angle of turning.

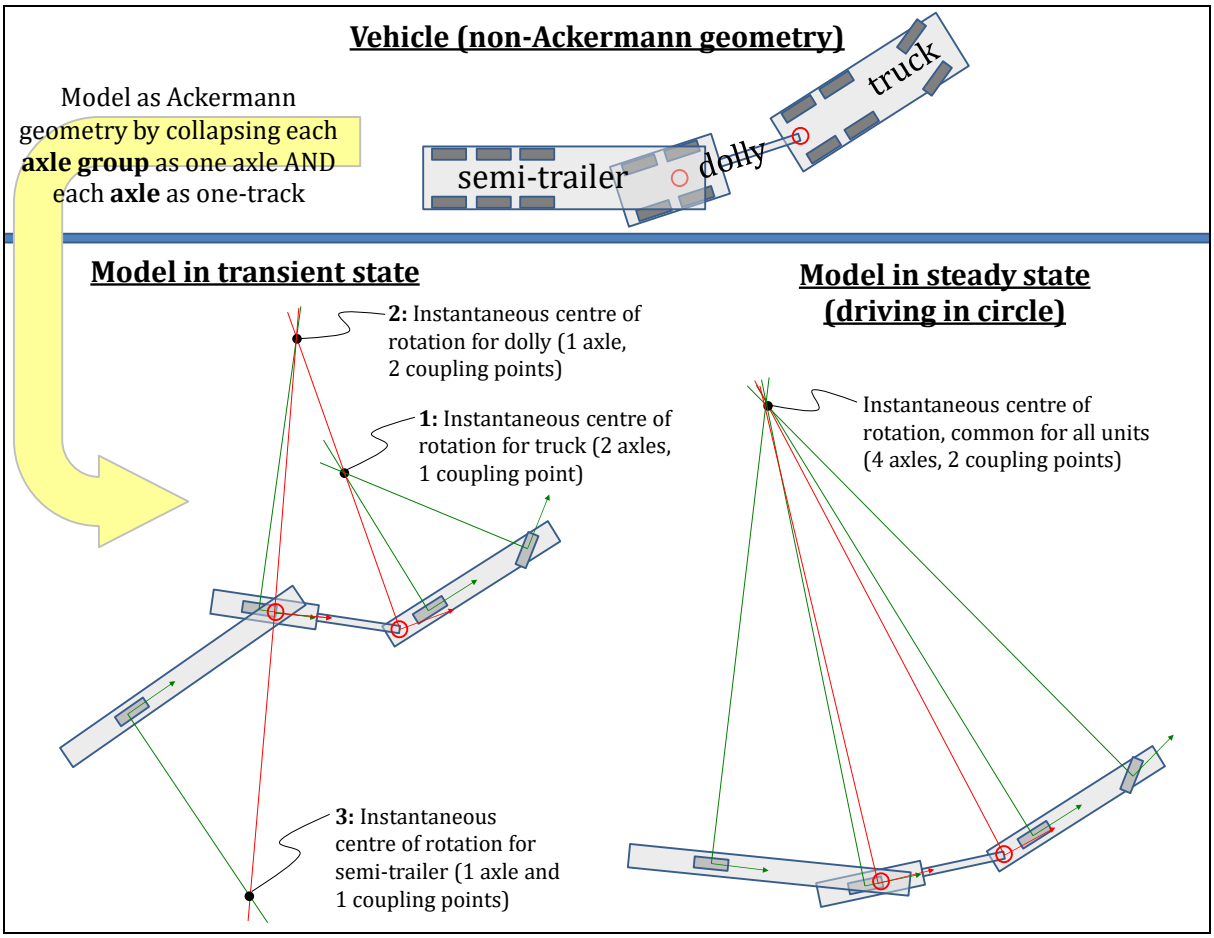


Figure 4-10: Instantaneous centre of rotation for truck with trailer.

A general model, covering arbitrarily many units and Non-Ackermann or forces, is presented in 4.5.2.2.2.2.

4.2.5.3 Model for Ackermann, without forces

Articulated vehicles with Ackermann and without forces moves as indicated in left lower part of Figure 4-10; they have one instantaneous centre of motion per unit and these centres are related through the coupling points. Figure 4-10 is therefore very close to a simulation model, it is just to set up the geometrical relations and they will be just many enough:

- If formulated as dynamic system with time as independent variable: input variables will be one steering angles for each steered axle (group) and the longitudinal velocity of one unit, e.g. the first towing unit. At least each articulation angle will be a state variable. If adding Eq [1.9], also positions of any selected point and orientation of each unit can be solved for and then they also become state variables.
- The model can be reformulated to a dynamic system with position (travelled distance) s of a point at the vehicle as independent variable instead of time, see Eq [1.10]. The time then disappears. The input longitudinal velocity of first unit, $v_{1x}(t)$, is replace by the discrete variable $\text{sign}(v_{1x}(t))$.

4.2.5.3.1 Lack of steady state solution

The "steady state" in Figure 4-10 can lack (real) solution. Generally, it appears if a far-rear unit has its rear axles so far rear that there is no articulation angle where one can find an intersection with the momentaneous centre defined by the front units. Typically, the mathematics will tell us through square root of a negative number. Then, there is no *steady state* solution, i.e., a motion with constant articulation angles. Instead, there will be a *stationary oscillating* motion, something like a crankshaft motion.

4.2.6 Reversing

Contributions from Zhaohui Ge, Chalmers

Low speed manoeuvring is often about both driving forward and reversing. The previous models work formally also for $v_x < 0$. Assume that, after some driving forward, v_x is changed to a negative value. Assume that steering is same for same position along the path, $\delta = \delta(s)$. The vehicle will then reverse in approximately same path as it first drove forward. If ideal tracking tyres, such as Eq [4.2], the paths will be identical. If adding forces to the model, the reverse path can deviate from forward path. A small such deviation can be seen in figure due to a large rolling resistance coefficient ($RRC = 0.10$).

The reverse path for a real articulated vehicle often differs more from the forward path. This is mainly due to back-lash in couplings, even if only some centimetre backlash it can influence a lot. The backlash can be modelled by letting coupling point position be dependent of sign(*coupling force*).

4.2.6.1 Stability when Reversing

Single unit vehicles do not become unstable in low speed, neither for forward nor reverse driving. But articulated vehicles do, when reversing. To study this, we derive a linear model, by assuming small angles. Note that the stability analysis for low speed differs from stability analysis at higher speeds, see 4.4.3.4, in that the low speed models do not include inertial terms $mass \cdot acceleration$.

4.2.6.2 Linear Low Speed Model for Tractor with Semi-trailer

Figure 4-11 shows a physical model for tractor with trailer, assuming small angles φ_{1z}, δ and θ.

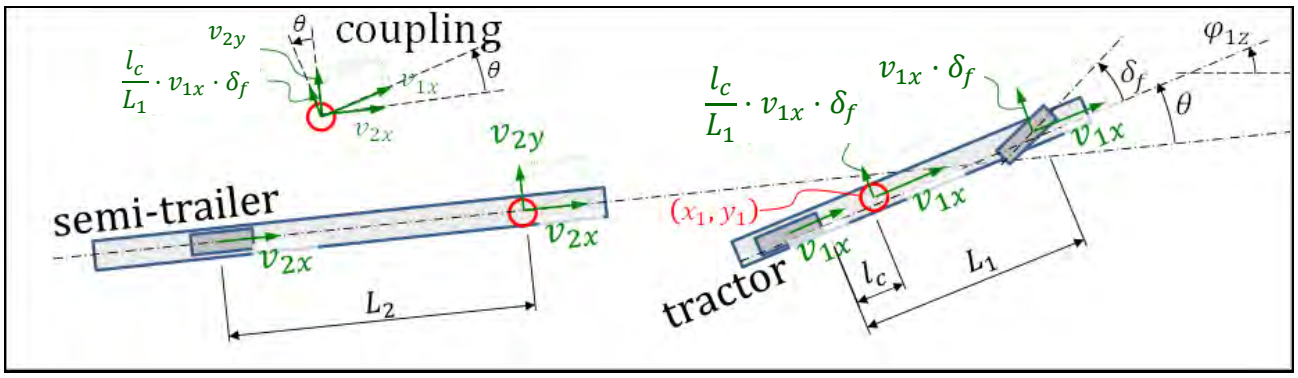


Figure 4-11: A low-speed model of tractor with semi-trailer. Small angles $\varphi_{1z}, \theta, \delta_f$ are assumed.

The mathematical model for lateral position variables $(y_1, \varphi_{1z}, \theta)$ becomes:

$\dot{y}_1 = \frac{l_c}{L_1} \cdot v_{1x} \cdot \delta_f + v_{1x} \cdot \varphi_{1z}$; (from Eq **[1.9]**, with small φ_{1z})

$\dot{\varphi}_{1z} = \frac{v_{1x} \cdot \delta}{L_1}$; (rotational velocity = tangential speed / radius to instantaneous centre)

$\dot{\theta} = \frac{v_{1x} \cdot \delta}{L_1} - \frac{v_{2y}}{L_2}$; (articulation angle is difference between units)

$v_{2y} = v_{1x} \cdot \theta + \frac{l_c}{L_1} \cdot v_{1x} \cdot \delta$; (units have same velocity in coupling point, small θ, small δ_f)

Eliminating v_{2y} gives:

$$\begin{bmatrix} \dot{y}_1 \\ \dot{\varphi}_{1z} \\ \dot{\theta} \end{bmatrix} = \underbrace{\begin{bmatrix} 0 & v_{1x} & 0 \\ 0 & 0 & 0 \\ 0 & 0 & -v_{1x}/L_2 \end{bmatrix}}_{\boldsymbol{A}} \cdot \begin{bmatrix} y_1 \\ \varphi_{1z} \\ \theta \end{bmatrix} + v_{1x} \cdot \begin{bmatrix} l_c/L_1 \\ 1/L_1 \\ 1/L_1 - l_c/(L_1 \cdot L_2) \end{bmatrix} \cdot \delta_f;$$

The eigenvalues to $\boldsymbol{A}$ becomes $\lambda_{1,2} = \pm 0$; $\lambda_3 = -v_{1x}/L_2$;. So, the system is unstable when $v_{1x} < 0$, because it makes $\mathrm{Re}(\lambda_3) > 0$. It is probably intuitive for may readers that the vehicle is unstable, as the semi-trailer pushed rearwards via a moment-free joint. However, note that the analysis shows how stability appears without the inertial terms $mass \cdot acceleration$. The model can be extended with

other multiple-unit vehicles, multiple axles in axle groups and driver models. The state variables will remain as y_1, φ_{1z} and one articulation angle θ_i for each coupling.

A common initial (but wrong) intuitive feeling is that instability when reversing depends on which axle or unit that is steered or propelled. However, the previous model shows that instability is due to number of axles on the units, or where the two-axle unit is in direction of travel. For today used road vehicles, the above model will always have exactly two axles on the first unit and one axle is added after each added articulation point. Such vehicle will always be stable when driving low-speed forward and unstable when reversing low-speed.

Note 1: This is for the basic case that forces can be regarded as small. A common reason that one need to add forces is that there are multiple axles in an axle group so they fight laterally. Those vehicles become less instable.

Note 2: Expanding the model to more than 2 vehicle units is not done in this book but see Reference (Zhaohui Ge, 2024) for up to 4 vehicle units (3 articulation points).

Note 3: Reducing the model to only one axle per unit is neither included, because such vehicle is not controllable with a single driver device (one steering wheel). It is instable in two modes. However, there are similar vehicles, like articulated steering of dumpers, but the articulation angle is controllable by a hydraulic piston. With such (controllable=given) articulation angle, this will be stable and as stable as a two-axle vehicle.

4.3 Steady State Cornering at High Speed

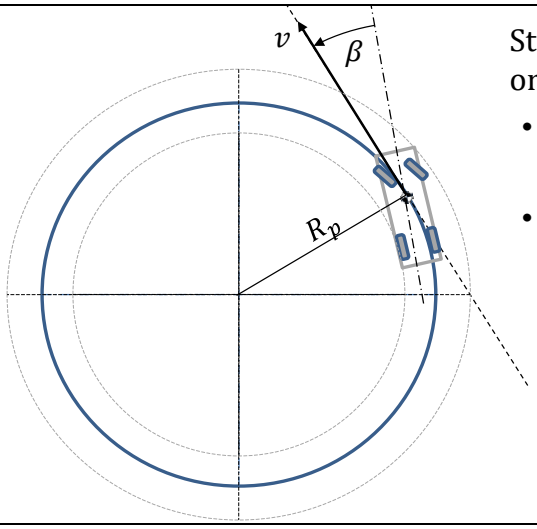
Steady state cornering refers to that all time derivatives of vehicle speeds (v_x, v_y, ω_z) are zero. The physical understanding is then that the vehicle drives on a circle with constant yaw velocity, see Figure 4-12. Alternatively, this can be described as driving with constant tangential speed (v), on a constant path radius (R) and with a constant side slip angle (β).

4.3.1 Steady State Driving Manoeuvres

When testing steady state function, one usually runs on a so called “skid-pad” which appears on most test tracks, see Figure 1-70. It is a flat circular surface with typically 100 m diameter and some concentric circles marked. A general note is that tests in real vehicles are often needed to be performed in simulation also, and normally earlier in the product development process.

Typical steady state tests are:

- Constant path radius. Driven for different longitudinal speeds.
- Constant longitudinal speed. Driven for different path radii.
- Constant steering wheel angle. Then increase accelerator pedal (or apply brake pedal) gently. (If too quick, the test would fall under transient handling instead.)



Steady state cornering can be defined by either 3 or 2 quantities, depending on assumptions:

- For a **general vehicle** it is fully defined only by all **3 quantities**, e.g. $[v_x, v_y, \omega_z]$ or $[v, \beta, R_p]$.
- For a **certain vehicle** it is often considered as fully defined by **2 inputs from driver**: accelerator pedal and steering wheel. (Then, one have neglected other inputs from driver, such as brake pedal and parking brake. One have also neglected other possible automatic actuation, such as all wheel drive distribution and ESC-braking one wheel.)

Figure 4-12: Steady state cornering. (β will be negative for larger v_x, i.e. vehicle will point inwards.)

Relevant standards for these test manoeuvres are: References (ISO 4138) and (ISO 14792).

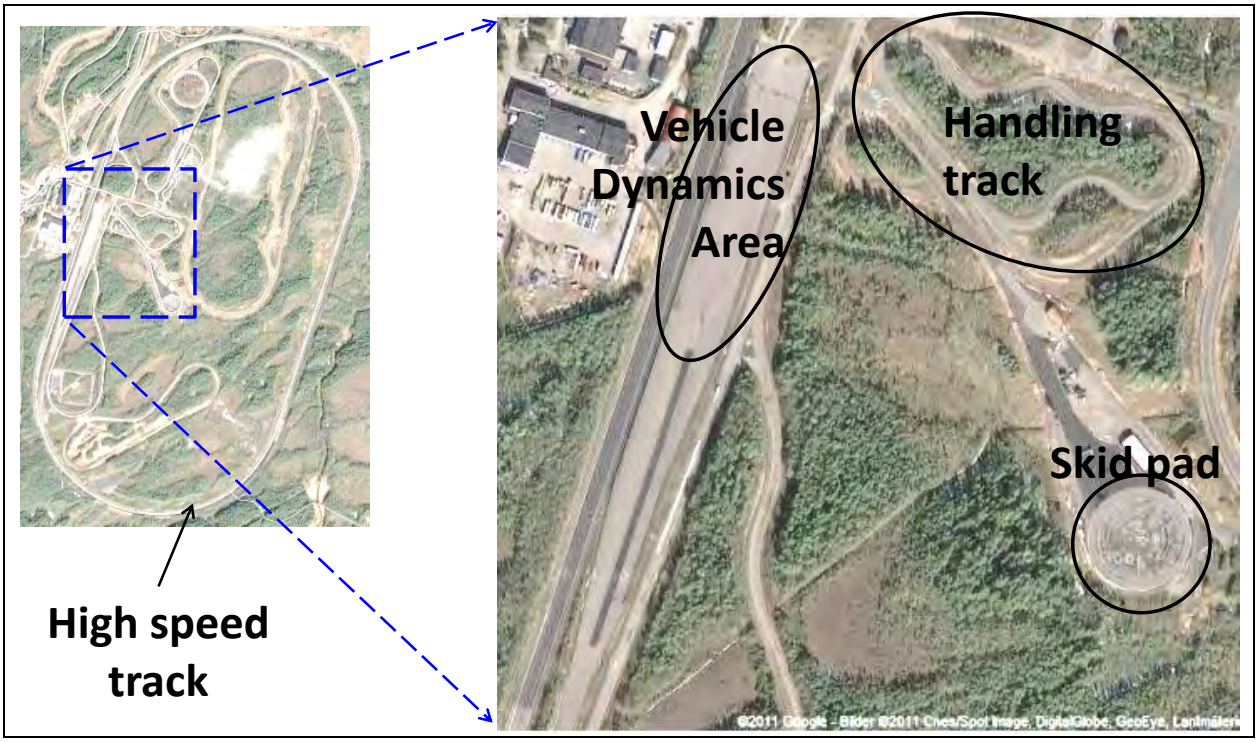


Figure 4-13: An example of test track and some parts with special relevance to Vehicle Dynamics. The example is Hällered Proving Ground, Volvo Car Corporation.

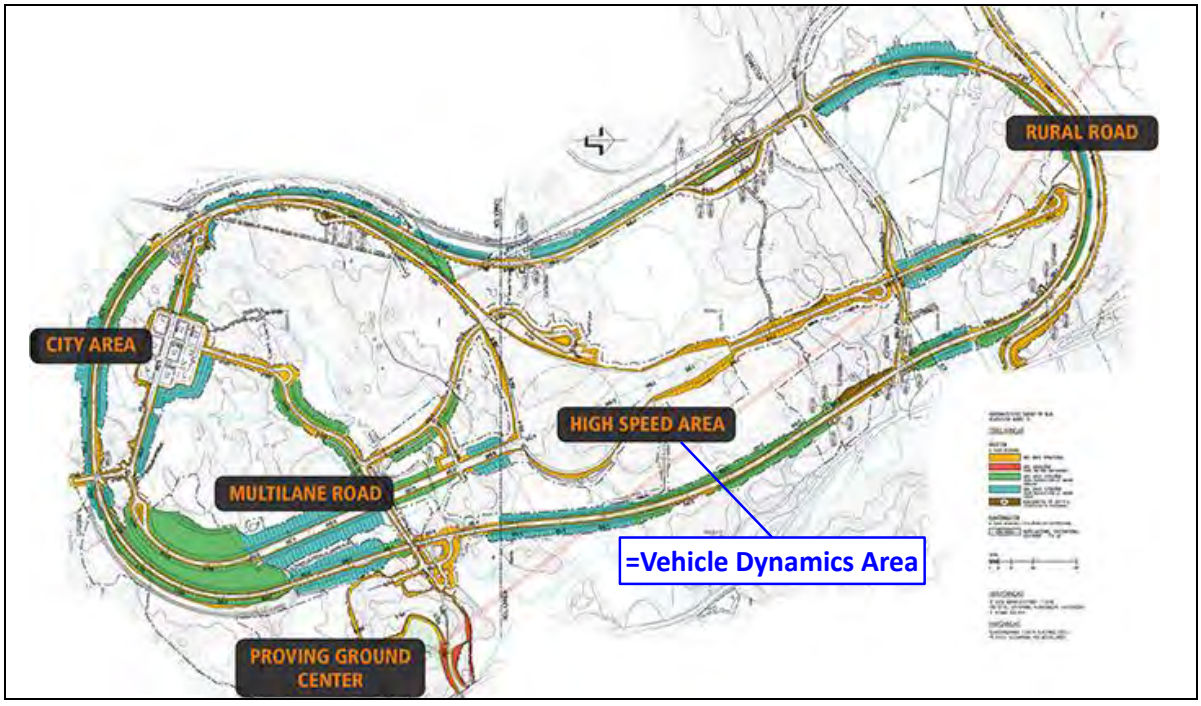


Figure 4-14: An example of test track. The example is AstaZero (Active Safety Test Arena), owned by Research Institute of Sweden (RISE) and Chalmers University of Technology.

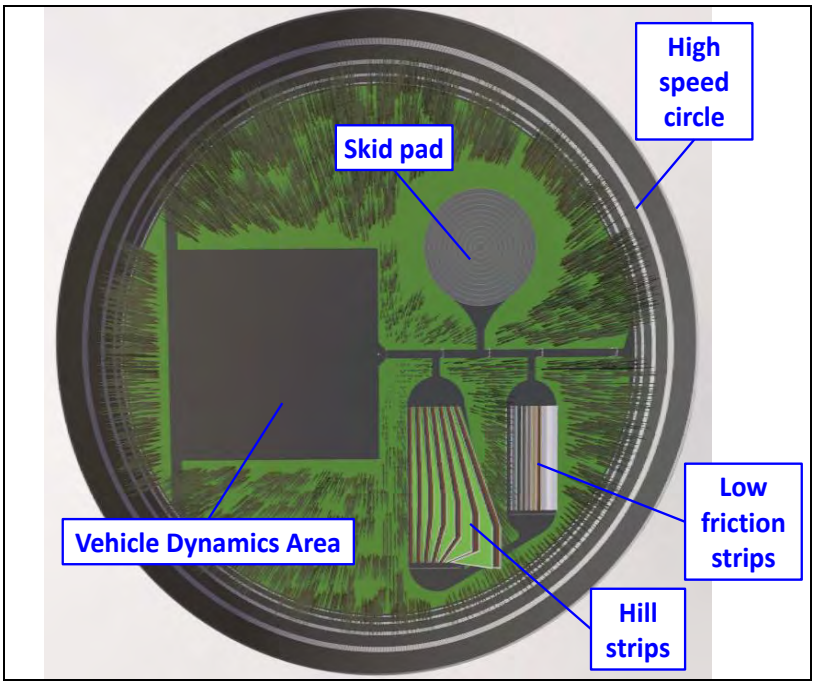


Figure 4-15: An example of test track. The example is CASTER's (virtual) test track. Used for CASTER's driving simulator at Chalmers University of Technology.

4.3.2 Steady State One-Track Model

In steady state we have neither inertial effect from changing the total vehicle speed ($v = \sqrt{v_x^2} + v_y^2 = constant$) nor from changing the yaw velocity ($w_z = constant$). However, the inertial "centrifugal" effect of the vehicle must be modelled. The related acceleration is the centripetal acceleration, $a_c = R_p \cdot {\omega_z}^2 = v^2/R_p = \omega_z \cdot v$.

A vehicle model for this is sketched in Figure 4-16. The model is a development of the model for low-speed in Figure 4-5 and Equation [4.4], with the following changes:

- Longitudinal and lateral accelerations are changed from zero to components of centripetal acceleration, ac, as follows (see Figure 4-16):
  - $a_x = -a_c \cdot \sin(\beta) = -\omega_z \cdot v \cdot \sin(\beta) = -\omega_z \cdot v_y$;
  - $a_y = +a_c \cdot \cos(\beta) = +\omega_z \cdot v \cdot \cos(\beta) = +\omega_z \cdot v_x$;
- The constitutive relations for the axles are changed from ideal tracking to a (linear) relation between lateral force and lateral slip:
  - $F_{fyw} = -C_f \cdot s_{fy}$; where $s_{fy} = v_{fyw}/|R_w \cdot \omega_f| \approx v_{fyw}/|v_{fxw}|$;
  - $F_{ry} = -C_r \cdot s_{ry}$; where $s_{ry} = v_{ry}/|R_w \cdot \omega_r| \approx v_{ry}/|v_{rx}|$;

The constitutive relations above capture the slip characteristics for the tyres, see 2.2.4, but they can also capture steering system compliance, side force steering, and roll steering, see 4.3.7.3.

Note that v_y, v_{fyw} and v_{ry} in Figure 4-16 are drawn as positive for the sign convention of (ISO 8855). It can help understanding to note that these velocities get negative values if vehicle steady state turns to the left, as indicated by the drawn steering angle δ_f.

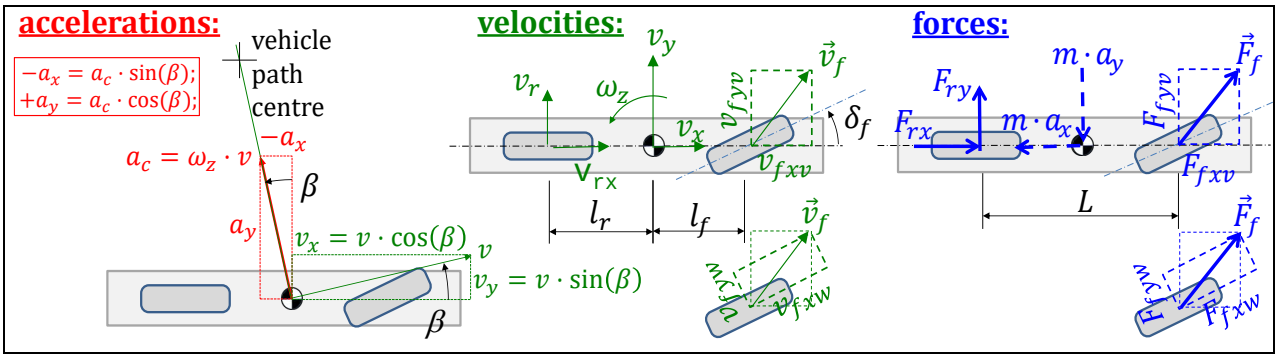


Figure 4-16: One-track model for Steady State Cornering. Dashed forces are "fictive forces".

The model in Figure 4-16 has the mathematical form in Eq [4.6] (in Modelica format). Longitudinal speed v_x is assumed to be positive. The subscripts *v* and *w* refer to vehicle coordinate system and wheel coordinate system, respectively. A driving resistance of 100 N is assumed on the rear axle (`Frx=100;`). The longitudinal speed is a parameter, $v_x = 100\ km/h$.

```
//Equilibrium:
  m*ax = Ffxv + Frx;    //Air and grade resistance neglected
  m*ay = Ffyv + Fry;    Jz*0 = Ffyv*lf - Fry*lr;    // der(wz)=0
  -ax = wz*vy;    +ay = wz*vx;
//Constitutive relation, i.e. Lateral tyre force model:
  Ffyw = -Cf*sfy;   sfy = vfyw/vfxw;
  Fry = -Cr*sry;    sry = vry/vrx;
//Compatibility:
  vfxv = vx;    vfyv = vy + lf*wz;
  vrx = vx;     vry  = vy - lr*wz;
//Transformation between vehicle and wheel coordinate systems:
  Ffxv = Ffxw*cos(df) - Ffyw*sin(df);
  Ffyv = Ffxw*sin(df) + Ffyw*cos(df);
  vfxv = vfxw*cos(df) - vfyw*sin(df);
  vfyv = vfxw*sin(df) + vfyw*cos(df);
//Path with orientation (from Eq [1.9]):
  der(x) = vx*cos(pz) - vy*sin(pz);
  der(y) = vy*cos(pz) + vx*sin(pz);
  der(pz) = wz;
// Prescription of steer angle:
  df = if time < 2.5 then (5*pi/180)*sin(0.5*2*pi*time) else 5*pi/180;
// Rear axle undriven, which gives drag from roll resistance:
  Frx = -100;
```

[4.6]

A simulation result from the model is shown in Figure 4-17. Note that steering start to the left, but vehicle path starts bending to the right. This comes from that it is a steady state model but used in a transient manoeuvre. The steady state cornering condition is found directly and turning left has the steady state v_y directed outwards, to the right, due to centrufugal force.

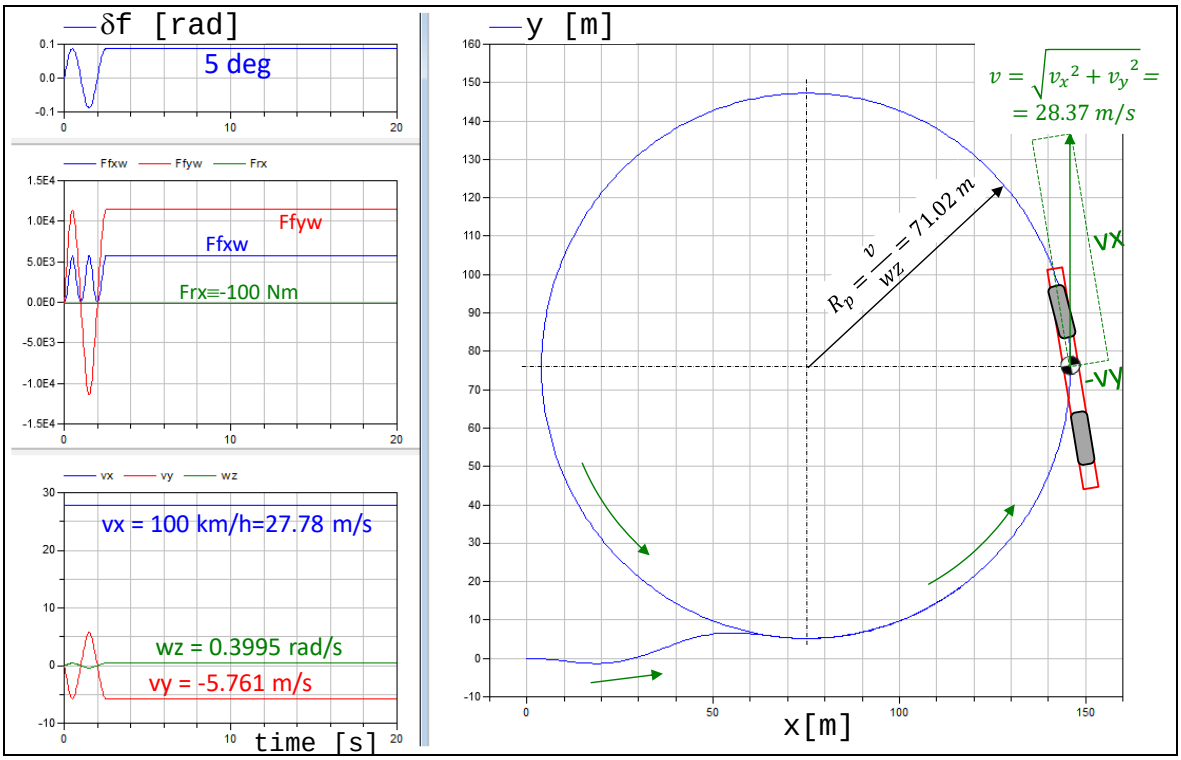


Figure 4-17: Simulation results of steady state one-track model. The vehicle sketched in the path plot is not in scale, but correctly oriented.

Now, the validity of a model always has to be questioned. There are many modelling assumptions which could be checked, but in the following we only check the assumption $a_y = \omega_z \cdot v_x$; instead of the more correct $a_y = \dot{v}_y + \omega_z \cdot v_x$;, which we will learn in "4.4.2 One-Track Model". Comparison of the terms gives $|\dot{v}_y|_{max} \approx |\omega_z \cdot v_x|_{max} \approx 10\,m/s^2$, so $|\omega_z \cdot v_x|$ is large and this jeopardizes the validity. Large $|\omega_z \cdot v_x|$ happens during $0 < t <\approx 2\ s$, so the model is not very valid there. But, at $t >\approx 2\ s$, the model is valid, at least in this aspect, since there $|\dot{v}_y| \approx 0 \ll |\omega_z \cdot v_x|$. So, the model is not so valid during the initial sinusoidal steering. This shows that a steady state *models* should not be trusted outside steady state *conditions*.

Eq [4.6] is a complete model suitable for simulation, but it does not facilitate understanding very well. We will reformulate it assuming small δ_f (i.e. $\cos(\delta_f) = 1$, $\sin(\delta_f) = 0$, and $\delta_f^2 = 0$). Eliminate slip, all forces that are not wheel longitudinal, and all velocities that are not CoG velocities:

$$
\begin{aligned}
&-m \cdot \omega_z \cdot v_y \cdot \left(v_x + \left(v_y + l_f \cdot \omega_z\right) \cdot \delta_f\right) = \\
&\quad = F_{fxw} \cdot \left(v_x + \left(v_y + l_f \cdot \omega_z\right) \cdot \delta_f\right) + C_f \cdot \left(v_y + l_f \cdot \omega_z\right) \cdot \delta_f + F_{rx} \cdot \left(v_x + \left(v_y + l_f \cdot \omega_z\right) \cdot \delta_f\right); \\
&m \cdot \omega_z \cdot v_x \cdot \left(v_x + \left(v_y + l_f \cdot \omega_z\right) \cdot \delta_f\right) = \\
&\quad = -C_f \cdot \left(-v_x \cdot \delta_f + \left(v_y + l_f \cdot \omega_z\right)\right) + F_{fxw} \cdot \delta_f \cdot v_x - C_r \cdot \frac{v_y - l_r \cdot \omega_z}{v_x} \cdot \left(v_x + \left(v_y + l_f \cdot \omega_z\right) \cdot \delta_f\right); \\
&C_f \cdot \left(-v_x \cdot \delta_f + \left(v_y + l_f \cdot \omega_z\right)\right) \cdot l_f - F_{fxw} \cdot \delta_f \cdot l_f \cdot v_x = \\
&\quad = C_r \cdot \frac{v_y - l_r \cdot \omega_z}{v_x} \cdot l_r \cdot \left(v_x + \left(v_y + l_f \cdot \omega_z\right) \cdot \delta_f\right);
\end{aligned}
\qquad [4.7]
$$

Eq [4.7] is a complete model, which we can see as a dynamic system without state variables.

- Actuation: Steering and wheel torque on each axle: $\delta_f, F_{fxw}, F_{rx}$.
- Motion quantities: v_x, v_y, ω_z

For propulsion on both axles, it can be a reasonable case that we know δ_f, F_{fxw}, v_x and want to calculate F_{rx}, v_y, ω_z. Eq [4.8] is a rearrangement of Eq [4.7] for this purpose. It can be used for rear axle

drive using $F_{fxw} = 0$ and calculating how large F_{rx} needs to be. Front axle drive requires more rearrangements.

$$\omega_z = \frac{C_f \cdot C_r \cdot L + C_r \cdot L \cdot F_{fxw}}{C_f \cdot C_r \cdot L^2 + \left(C_r \cdot l_r - C_f \cdot l_f\right) \cdot m \cdot v_x^2} \cdot v_x \cdot \delta_f;$$

$$v_y = \frac{C_f \cdot \left(C_r \cdot L \cdot l_r - l_f \cdot m \cdot v_x^2\right) + \left(C_r \cdot L \cdot l_r - l_f \cdot m \cdot v_x^2\right) \cdot F_{fxw}}{C_f \cdot C_r \cdot L^2 + \left(C_r \cdot l_r - C_f \cdot l_f\right) \cdot m \cdot v_x^2} \cdot v_x \cdot \delta_f;$$

$$F_{rx} = -m \cdot \omega_z \cdot v_y - F_{fxw} - \frac{C_f \cdot \left(v_y + l_f \cdot \omega_z\right) \cdot \delta_f}{\left(\left(v_y + l_f \cdot \omega_z\right) \cdot \delta_f + v_x\right)};$$

[4.8]

Eq [4.8] approximates Eq [4.6]. For instance, the figure to the right shows the difference in yaw velocity in same simulation as in Figure 4-17. The approximation is good for small front axle steering angle δ_f.

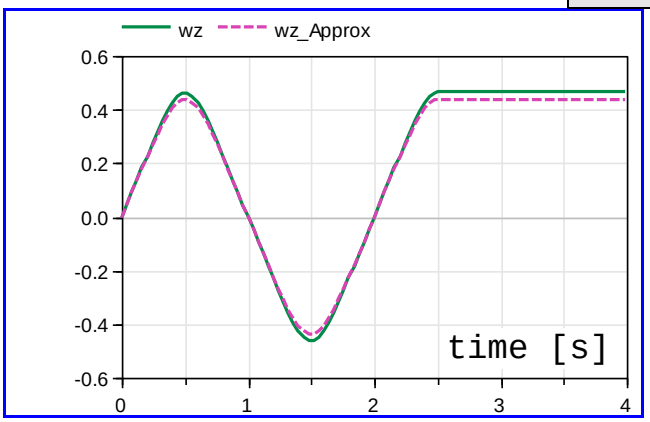


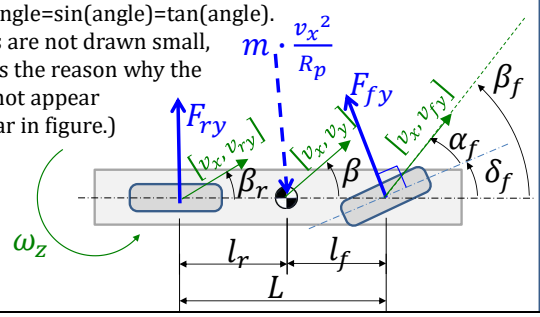
Figure 4-18: Difference between Eq [4.6] and Eq [4.8]

4.3.2.1 Less general model

A less general and more intuitive way to reach almost same expression as first expression in Eq [4.8] is given in Figure 4-19. Here, the simplifications are introduced earlier, already in physical model, which means e.g. the influence of F_{fxw} is not captured. The simpler compatibility from 1.6.1.6 is used and $v_x > 0$ is assumed.

Physical model:

- Path radius >> the vehicle. Then, all forces (and centripetal acceleration) are approximately co-directed.
- Small tyre and vehicle side slip. Then, angle=sin(angle)=tan(angle). (Angles are not drawn small, which is the reason why the forces not appear co-linear in figure.)



Mathematical model:

Equilibrium: $m \cdot \frac{v_x^2}{R_p} \approx F_{fy} + F_{ry}; \quad 0 \approx F_{fy} \cdot l_f - F_{ry} \cdot l_r;$

Constitution: $F_{fy} = -C_f \cdot s_{fy}; \quad F_{ry} = -C_r \cdot s_{ry};$

Compatibility:

$s_{fy} \approx \left(v_y + l_f \cdot \omega_z\right)/v_x - \delta_f;$

$s_{ry} \approx \left(v_y - l_r \cdot \omega_z\right)/v_x;$

$\omega_z \approx v_x/R_p;$

Eliminate $F_{fy}, F_{ry}, s_{fy}, s_r, \omega_z, v_y$ yields:

$$\delta_f \approx \frac{L}{R_p} + K_u \cdot \frac{m \cdot v_x^2}{R_p}; \quad where\ K_u = \frac{C_r \cdot l_r - C_f \cdot l_f}{C_f \cdot C_r \cdot L};$$

Figure 4-19: Simpler derivation final step in Equation [4.10].

Note that α_f and α_r in Figure 4-19 are drawn as positive for the sign convention of (ISO 8855). It can help understanding to note that these angles get negative values if vehicle steady state turns to the left, as indicated by the drawn steering angle δ_f.

4.3.2.1.1 With 2-axle steering

Introduce steering on both axles: $\delta_f = \delta_{sw}/SteRat_f;\ \delta_r = \delta_{sw}/SteRat_r;$. Then:

$$\delta_{sw} \cdot \left(\frac{1}{SteRat_f} - \frac{1}{SteRat_r} \right) = L \cdot \frac{\omega_z}{v_x} + K_u \cdot m \cdot \omega_z \cdot v_x; \quad [4.9]$$

4.3.2.2 Relations between δ_f, v_x, R_p, and β

4.3.2.2.1 Relation δ_f, v_x and R_p

Solving the first equation in Equation [4.8] yields:

$$\begin{aligned}
\delta_f &= \frac{C_f \cdot C_r \cdot L^2 + (C_r \cdot l_r - C_f \cdot l_f) \cdot m \cdot v_x^2}{C_f \cdot C_r \cdot L + (C_r \cdot l_f + C_r \cdot l_r) \cdot F_{fxw}} \cdot \frac{\omega_z}{v_x} \approx \left\{ \begin{matrix} assume\ small\ v_y \Rightarrow \\ \Rightarrow v_x/\omega_z \approx R_p \end{matrix} \right\} \approx \\
&\approx \frac{1}{1 + F_{fxw}/C_f} \cdot \frac{L}{R_p} + \frac{C_r \cdot l_r - C_f \cdot l_f}{(C_f + F_{fxw}) \cdot C_r \cdot L} \cdot \frac{m \cdot v_x^2}{R_p} \approx \left\{ \begin{matrix} assume: \\ F_{fxw}/C_f \approx 0 \end{matrix} \right\} \approx \\
&\approx \frac{L}{R_p} + \frac{C_r \cdot l_r - C_f \cdot l_f}{C_f \cdot C_r \cdot L} \cdot \frac{m \cdot v_x^2}{R_p} = \left\{ use: K_u = \frac{C_r \cdot l_r - C_f \cdot l_f}{C_f \cdot C_r \cdot L} = \frac{l_r}{C_f \cdot L} - \frac{l_f}{C_r \cdot L} \right\} = \\
&= \frac{L}{R_p} + K_u \cdot \frac{m \cdot v_x^2}{R_p};
\end{aligned} \quad [4.10]$$

The coefficient K_u is the *understeer gradient* and it will be explained more in 4.3.3.

4.3.2.2.2 Relation δ_f, v_x and β

Solving the second equation in Equation [4.8] yields:

$$\begin{aligned}
\delta_f &= \frac{C_f \cdot C_r \cdot L^2 + (C_r \cdot l_r - C_f \cdot l_f) \cdot m \cdot {v_x}^2}{C_f \cdot (C_r \cdot L \cdot l_r - l_f \cdot m \cdot {v_x}^2) + (C_r \cdot L \cdot l_r - l_f \cdot m \cdot v_x^2) \cdot F_{fxw}} \cdot \frac{v_y}{v_x} \approx \\
&\approx \{use: F_{fxw} = 0\} \approx \frac{C_f \cdot C_r \cdot L^2 - (C_f \cdot l_f - C_r \cdot l_r) \cdot m \cdot {v_x}^2}{C_f \cdot C_r \cdot l_r \cdot L - C_f \cdot l_f \cdot m \cdot {v_x}^2} \cdot \frac{v_y}{v_x} \approx \\
&\Rightarrow \begin{cases} \delta_f \xrightarrow[v_x \to 0]{} \frac{L}{l_r} \cdot \frac{v_y}{v_x}; \\ \delta_f \xrightarrow[v_x \to \infty]{} \frac{C_f \cdot l_f - C_r \cdot l_r}{C_f \cdot l_f} \cdot \frac{v_y}{v_x} = -K_u \cdot C_r \cdot \frac{L}{l_f} \cdot \frac{v_y}{v_x}; \end{cases}
\end{aligned} \quad [4.11]$$

We can see that there is a speed dependent relation between steer angle and side slip, $\frac{v_y}{v_x}$. The side slip can also be expressed as a side slip angle, $\beta = \arctan\left(\frac{v_y}{v_x}\right)$. Since normally $K_u > 0$, the side slip changes sign, when increasing speed from zero to sufficient high enough. This should feel intuitively correct, if agreeing on the conceptually different side slip angles at low and high speed, as shown in Figure 4-20. We will come back to this equation in context of Figure 4-31.

4.3.2.2.3 Relation v_x, R_p and β

If we approximate $F_{fxw} = 0$ and use both equations in Equation [4.8] to eliminate δ_f we get:

$$\begin{aligned}
&\frac{C_r \cdot L \cdot l_r - l_f \cdot m \cdot v_x^2}{C_r \cdot L} = l_r - \frac{l_f \cdot m \cdot v_x^2}{L \cdot C_r} = \frac{v_y}{\omega_z} = \frac{v_x}{\omega_z} \cdot \frac{v_y}{v_x} \approx R_p \cdot \tan(\beta); \Rightarrow \\
&\Rightarrow \frac{v_y}{v_x} = \tan(\beta) = \left(l_r - \frac{l_f \cdot m \cdot v_x^2}{L \cdot C_r} \right) \cdot \frac{1}{R_p};
\end{aligned} \quad [4.12]$$

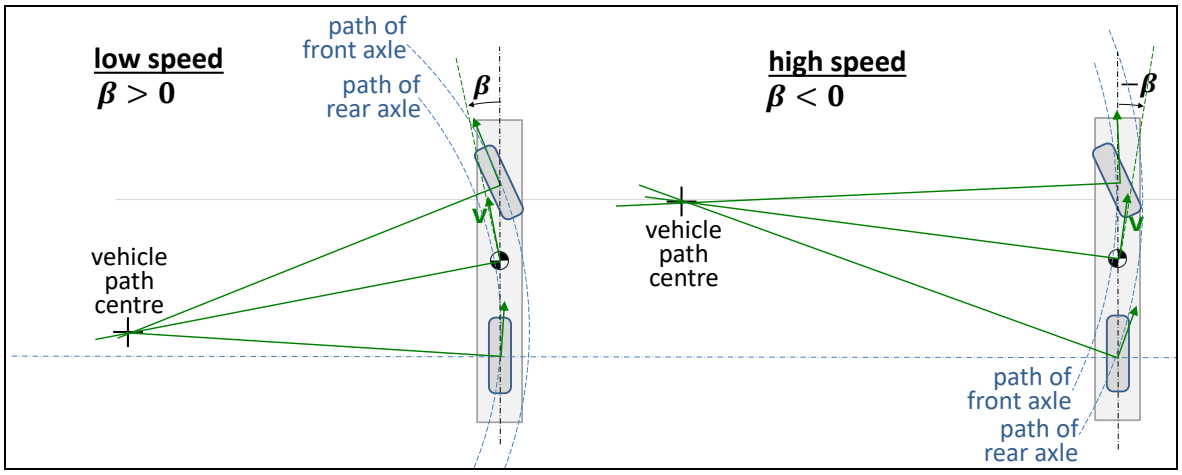


Figure 4-20: Body Slip Angle for Low and High Speed Steady State Curves

4.3.2.3 Steady State Cornering for Non-Ackermann Geometry

Ackermann geometry has been assumed above. We will now try a vehicle like in 4.2.4 and Figure 4-7. Further on, we assuming $F_{fxw} = 0;, l_r = (l_{r1} + l_{r2})/2;,\ \Delta L_r = l_{r2} - l_{r1};, L = l_f + l_r;, and\ C_{r1} = C_{r2} = C_{ra}/2;$. This gives an equation, comparable with Eq [4.10], as follows:

$$\delta_f = \underbrace{\frac{L}{R_p} + \left(\frac{\Delta L_r}{2 \cdot L}\right)^2 \cdot \left(1 + \frac{C_{ra}}{C_f}\right) \cdot \frac{L}{R_p}}_{\delta_A} + K_u \cdot \frac{m \cdot v_x^2}{R_p};\quad where\ and\ K_u = \frac{C_{ra} \cdot l_r - C_f \cdot l_f}{C_f \cdot C_{ra} \cdot L};$$

[4.13]

Note: We can still identify an K_u, but the reference angle δ_A, see also 4.3.3, is not as simple as L/R_p.

4.3.2.4 Model Validity

The validity of the steady state models described in 4.3.2, is of course limited by if the manoeuvre is transient which would mean that steady state is not reached, e.g. if driving above critical speed. But it is also limited by if the assumption of linear tyre characteristics, $F_y = -C \cdot s_y;$, is violated. Therefore, one should check if some axle uses too much of available friction, $F = \sqrt{F_x^2 + F_y^2} > fraction \cdot \mu \cdot F_z;$.

Referring to the tyre brush model with uniform pressure distribution one can argue for using 0.5 as this limiting fraction, since the tyre force is linear with slip up to this value.

4.3.3 Under-, Neutral- and Over-steering *

Function definition: ***Understeering (gradient)*** *is the additional steer angle needed per increase of lateral force (or lateral acceleration) when driving in high-speed steady state cornering on level ground and high road friction. Additional refers to low speed. The gradient is defined at certain high-speed steady state cornering conditions, including straight-line driving. Steer angle can be either road wheel angle or steering wheel angle.*

The first term in Eq [4.10], L/R, is a reference steer angle δ_A, where subscript A stands for Ackermann. The (ISO 8855) defines δ_A as the steer angle which would be needed to give same instantaneous centre of rotation if the vehicle would have had two axles, perfect Ackermann steering and no tyre side slip. So, δ_A is L/R for the simplest one-track model with two axles. If one only have a test vehicle, and no specific vehicle model, the corresponding definition of δ_A, is the steering angle required for a certain curvature $1/R_p$ at low speed. The understeer gradient is then understood as a measure of how the required steering angle changes with increasing speed v_x.

The understeering gradient, K_u, is normally positive, which means that most vehicles require more steer angle for a given curve, the higher the speed is. Depending on the sign of K_u a vehicle is said to be oversteered (if $K_u < 0$), understeered (if $K_u > 0$) and neutral steered ($if\ K_u = 0$). In practice, all

vehicles are designed as understeered, because over steered vehicle would become unstable and difficult to control.

The K_u in Eq [4.10] is called "understeer gradient" and has hence the unit $[1/N]$ (some see it as $[rad/N]$). Sometimes one can see other definitions of what to include in definition of understeer gradient, which have different units, see K_{u2} and K_{u3} in Eq [4.14].

$$\delta_f = \frac{L}{R} + \frac{C_r \cdot l_r - C_f \cdot l_f}{C_f \cdot C_r \cdot L} \cdot \frac{m \cdot g \cdot {v_x}^2}{g \cdot R} = \left\{ K_{u2} = m \cdot g \cdot \frac{C_r \cdot l_r - C_f \cdot l_f}{C_f \cdot C_r \cdot L} [1 \text{ or } rad] \right\} = \frac{L}{R} + K_{u2} \cdot \frac{{v_x}^2}{g \cdot R};$$

$$\delta_f = \frac{L}{R} + \frac{C_r \cdot l_r - C_f \cdot l_f}{C_f \cdot C_r \cdot L} \cdot \frac{m \cdot {v_x}^2}{R} = \left\{ K_{u3} = m \cdot \frac{C_r \cdot l_r - C_f \cdot l_f}{C_f \cdot C_r \cdot L} \left[\frac{1}{m/s^2} or \frac{rad}{m/s^2} \right] \right\} = \frac{L}{R} + K_{u3} \cdot \frac{{v_x}^2}{R};$$

[4.14]

K_{u3} is the definition used in (ISO 8855). For K_{u3}, one can sometimes see the unit "rad/g" used, which present book recommended to not use.

If vertical loads on axles are only due to gravity ($F_{iz} = m \cdot g \cdot (L - l_i)/L$) and tyres linear with vertical load ($C_{iy} = CC_{iy} \cdot F_{iz}$) we can express $K_{u2} = 1/CC_f - 1/CC_r$;.

4.3.3.1 Understeering as a Fix Built-In Measure

The understeering gradient K_u can be understood as how much additionally to the reference steer angle one has to steer, to reach a certain centrifugal force, $F_c = m \cdot {v_x}^2/R$ (or, if using K_{u3}, a certain acceleration $a_c = {v_x}^2/R$):

$$\delta_f = \delta_A + K_u \cdot F_c = \delta_A + K_u \cdot \frac{m \cdot {v_x}^2}{R}; \quad \Rightarrow \quad K_u = \frac{\delta_f - \delta_A}{F_c} = \frac{\Delta\delta_f}{F_c}; \quad or \quad K_{u3} = \frac{\Delta\delta_f}{a_c}$$

Assuming steering on both axles the corresponding expression would be:

$$\delta_f - \delta_r = (\delta_{Af} - \delta_{Ar}) + K_u \cdot F_c = (\delta_{Af} - \delta_{Ar}) + K_u \cdot \frac{m \cdot {v_x}^2}{R}; \quad \Rightarrow \quad K_u = \frac{(\delta_f - \delta_r) - (\delta_{Af} - \delta_{Ar})}{F_c} = \frac{\Delta\delta}{F_c}; \quad or \quad K_{u3} = \frac{\Delta\delta}{a_c}$$

Using the model from before, we can calculate the value of K_u as $K_u = \frac{C_r \cdot l_r - C_f \cdot l_f}{C_f \cdot C_r \cdot L}$;. So, K_u does not depend on whether the vehicle is steered on front or rear axle, see Figure 4-21.

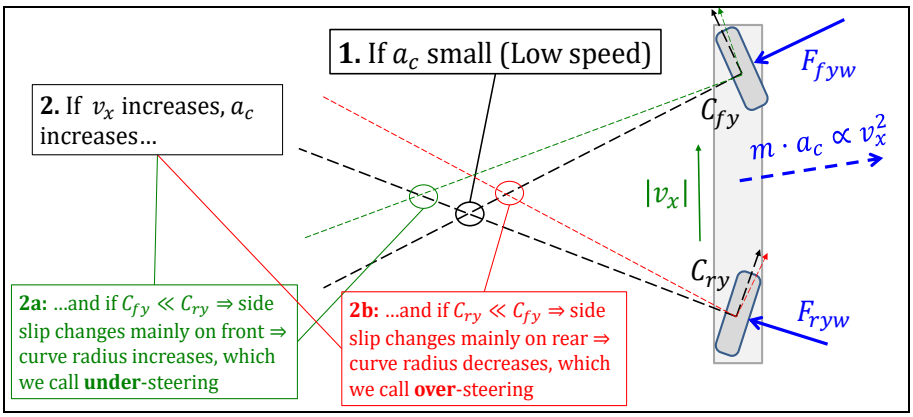


Figure 4-21: Under- and over-steering for a two-axle vehicle with $l_f = l_r$ and steering on both axles. With given C_f, C_r, l_f, l_r, the understeering does not depend on which axle is steered, but which axle is first in the direction of motion. Figure drawn for vehicle driving forward.

4.3.3.2 Understeer Gradient Varying with Steady State Lateral Acceleration

So far, the understeering gradient is presented as a fix vehicle parameter. This makes sense for the model used, but a definition which works also for a real vehicle is better. So, K_u should be defined as a measure, defined by the vehicle motion in a certain steady state driving, i.e., certain curve radius and certain v_x. Therefore, K_u is defined as how much additional steer angle, $\Delta\delta_f$, is needed per increased centrifugal force, F_c, or per increased centrifugal acceleration, a_c:

$$K_u = \frac{\partial(\Delta\delta_f)}{\partial F_c} = \frac{\partial}{\partial F_c}(\delta_f - \delta_A) = \frac{\partial\Delta\delta_f}{\partial F_c}; \quad or \quad K_{u3} = \frac{\partial(\Delta\delta_f)}{\partial a_c} = \frac{\partial\delta_f}{\partial a_c}; \qquad [4.15]$$

Eq [4.15] shows the understeering gradient as a function of a_c, so it is rather a variable than a parameter. But the variable becomes constant during a certain steady state driving (fix curve radius and fix v_x). If assessing understeering for lateral forces up to near road friction limit, Eq [4.15] is more relevant than Eq [4.10], because it reflects that understeering gradient changes.

4.3.3.3 Understeering Variable during Transient Manoeuvres

A third understanding of the word understeering is quite different and less strictly defined. It is to see the understeering as a variable during a transient manoeuvre. For instance, a vehicle can be said to understeer if tyre side slip is larger on front axle than on rear axle, $|\propto_f| > |\propto_r|$, and over-steer if opposite, $|\propto_r| > |\propto_f|$. This way of defining understeering and oversteering is not built-in in vehicle but varies over time through a (transient) manoeuvre. E.g., when braking in a curve a vehicle loses grip on rear axle due to temporary load transfer from rear to front. Then the rear axles can slide outwards significantly, and the vehicle can be referred to as over-steering at this time instant, although the built-in understeering gradient is >0. This "instantaneous" under-/over-steering (binary, not an understeer gradient) can be approximately found from log data with this simple approximation:

$$\delta_{neutral} = \frac{L}{R} \approx \{v_x \approx R \cdot \omega_z\} \approx \frac{L \cdot \omega_z}{v_x} \approx \{a_y \approx v_x \cdot \omega_z\} \approx \frac{L \cdot a_y}{v_x^2}; \qquad [4.16]$$

If the actual vehicle has $|\delta_f| < |\delta_{neutral}|$ the vehicle oversteers, and vice versa. This is often very practical since it only requires simply logged data, δ_f, v_x and a_y. Note that when δ_f and $\delta_{neutral}$ have different signs, neither understeer nor oversteer is suitable as classification, but it can sometimes be called "counter-steer". An example of applying Eq [4.16] is shown in Figure 4-22, where one also see that the ESC system does not follow the Eq [4.16] when deciding ESC interventions; ESC has more advanced "reference models", see 4.6.2.2.

A second look at Equation [4.10] tells us that we have to assume absence of propulsion and braking on front axle, $F_{fxw} = 0$, to get the relatively simple final expression. When propulsion on front axle ($F_{fxw} > 0$), the required steer angle, δ_f, will be smaller; the front propulsion pulls in the front end of the vehicle. When braking on front axle ($F_{fxw} < 0$), the required steer angle, δ_f, will be larger; the front braking hinders the front end to turn in. To keep v_x constant, which is required within definition of steady state, one have to propel the vehicle because there will always be some driving resistance to overcome. Driving fast on a small radius is a situation where the driving resistance from tyre lateral forces becomes significant, which is a part of driving resistance which was only briefly mentioned in 3.2.

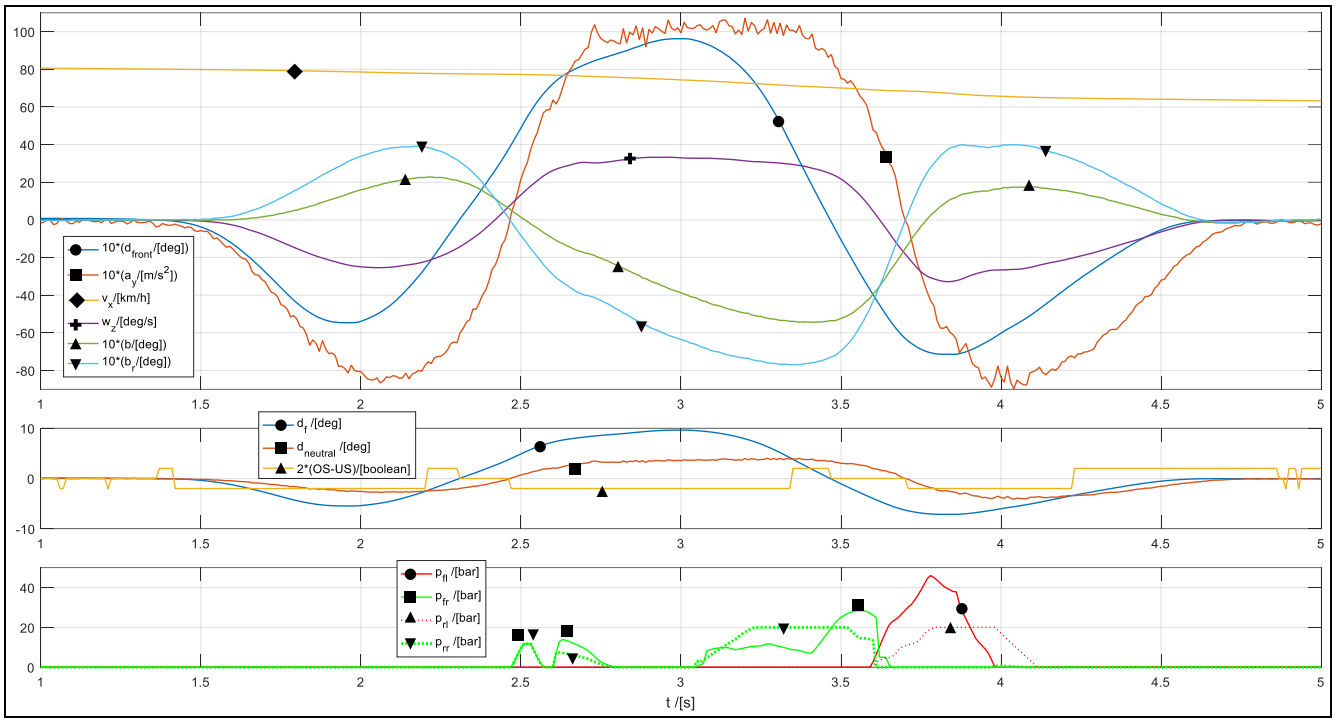


Figure 4-22: Log data from passenger car with ESC in a double lane change. Upper: Vehicle motion. Middle: $\delta_{neutral}$ from Eq [4.16] used to define "instantaneous under-/over-steering" (US/OS). Lower: Pressure to each wheel brake.

4.3.3.4 Neutral Steering Point

An alternative measure to understeering coefficient is the longitudinal position of the *neutral steering point*. The point is defined for lateral force disturbance during steady state **straight-ahead** driving, as opposed to steady state cornering without lateral force disturbance. The point is where a vehicle-external lateral force, such as wind or impact, can be applied on the vehicle without causing a yaw velocity ($\omega_z = 0$), i.e. only causing lateral velocity ($v_y \neq 0$). From this definition, we can derive a formula for calculating the position of the neutral steering point, see Figure 4-23.

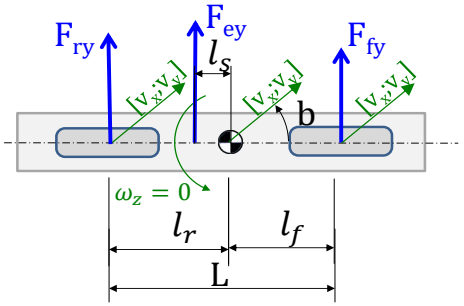
The result is condensed in Eq [4.17].

$$l_s = \frac{C_r \cdot l_r - C_f \cdot l_f}{C_f + C_r} = K_u \cdot \frac{C_f \cdot C_r}{C_f + C_r} \cdot L; \quad where\ K_u = \frac{C_r \cdot l_r - C_f \cdot l_f}{C_f \cdot C_r \cdot L}; \qquad [4.17]$$

We can see that the understeer gradient from steady state cornering model appears also in the formula for neutral steering point position, l_s. Since $C_f, C_r\ and\ L$ are positive, the neutral steering point is behind of CoG for understeered (two-axle) vehicles, and in front of CoG for oversteered (two-axle) vehicles. This is why l_s and K_u can be said to be alternative measures for the same vehicle function/character, the yaw balance.

Physical model:

- Steady state ($\dot{v}_x = \dot{v}_y = \dot{\omega}_z = 0$)
- Straight ahead driving ($\omega_z = 0$)
- No steering
- Small tyre and vehicle side slip. Then, angle=sin(angle)=tan(angle).



Mathematical model:

Equilibrium:

$$0 = F_{fy} + F_{ry} + F_e;$$

$$0 = F_{fy} \cdot l_f - F_{ry} \cdot l_r - F_e \cdot l_s;$$

Constitution: $F_{fy} = -C_f \cdot s_{fy}; and\ F_{ry} = -C_r \cdot s_{ry};$

Compatibility: $s_{fy} = s_{ry} = \frac{v_y}{v_x};$

Eliminate $F_{fy}, F_{ry}, s_{fy}, s_{ry}, F_e$ yields: $l_s = \frac{C_r \cdot l_r - C_f \cdot l_f}{C_f + C_r};$

Identify understeering gradient, $K_u = \frac{C_r \cdot l_r - C_f \cdot l_f}{C_f \cdot C_r \cdot L}$

Then:

$$l_s = K_u \cdot \frac{C_f \cdot C_r}{C_f + C_r} \cdot L;$$

Figure 4-23: Model for definition and calculation of neutral steering point.

4.3.4 Required Steer Angle

A fundamental property of the vehicle is what steer angle that is required to negotiate a certain curvature (=1/path radius = $1/R_p$). This value can vary with longitudinal speed and it can be normalized with wheelbase, L. From Eq [4.10], we can conclude:

$$\textbf{\textit{Normalized required steering angle}} = \frac{\delta_f \cdot R_p}{L} = 1 + K_u \cdot \frac{m \cdot {v_x}^2}{L}; \quad [4.18]$$

The normalized required steer angle is plotted for different understeering gradients Figure 4-24. It is the same as the inverted and normalized curvature gain, see 4.3.6.2.

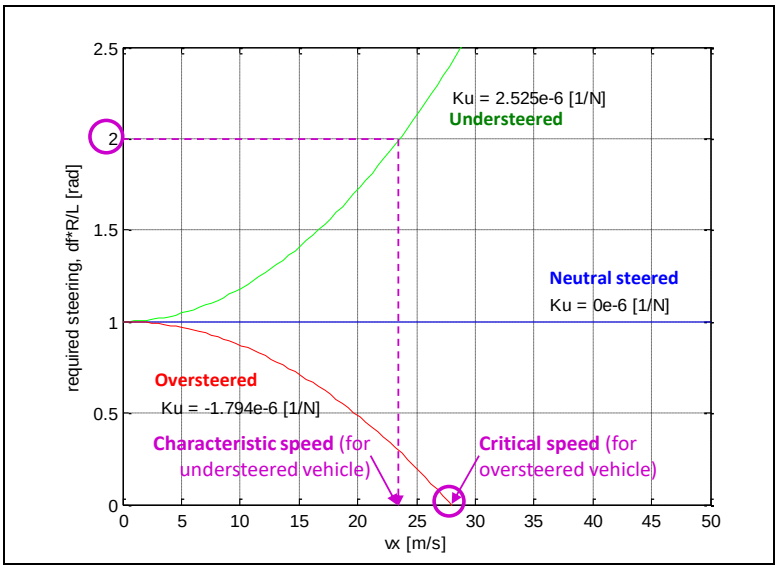


Figure 4-24: Normalized steer angle ($\delta_f \cdot R/L$) for Steady State Cornering

4.3.5 Critical and Characteristic Speed *

*Function definition: **Critical speed** is the speed above which the vehicle becomes unstable in the sense that the yaw velocity grows largely for a small disturbance in, e.g., steer angle.*

*Function definition: **Characteristic speed** is the speed at which the vehicle requires twice as high steer angle for a certain path radius as required at low speed (Figure 4-24). (Alternative definitions: The speed at which the yaw velocity gain reaches maximum (Figure 4-28). The speed at which the lateral acceleration gain per longitudinal speed reaches its highest value. (Figure 4-30).)*

It can be noted that Eq [4.10] leads to $\delta_f < 0$ for an oversteered vehicle driving faster than a certain speed, the *critical speed* $v_{xCrit} = \sqrt{L/(-K_u \cdot m)}$, see also 4.3.5. At $v_x > v_{xCrit}$, we still have steady state operating conditions but **unstable** such. Such conditions are often better studied and understood using a transient model.

We see that zero steering angle is required for the over-steered vehicle at 28 m/s. This is the critical speed, which is the speed where the vehicle becomes unstable. It can be noted that one must steer in the opposite direction, often referred to as "drifting". Normal vehicles are built understeered, which is why a critical speed is more of a theoretical definition. However, if studying (quasi-steady state) situations where the rear axle is heavily braked, the cornering stiffness rear is reduced, and a critical speed can be relevant.

For understeered vehicles, we can instead read out another measure, the *characteristic speed*. The understanding of characteristic speed is, so far just that required steering increases to over twice what is needed for low speed at the same path radius. A better understanding of characteristic speed is suggested in 4.3.6.3.

The vehicle is unstable for speeds above the critical speed. Instability is further discussed in 4.4.3.4. From Equation [4.10], we can find a formula for critical and characteristic speeds:

$$\delta_f = \frac{L}{R_p} + K_u \cdot \frac{m \cdot v_{x,crit}{}^2}{R_p} = 0 \;\Rightarrow\; v_{x,crit} = \sqrt{\frac{L}{-K_u \cdot m}} = \sqrt{\frac{C_f \cdot C_r \cdot L^2}{(C_f \cdot l_f - C_r \cdot l_r) \cdot m}};$$

$$\delta_f = \frac{L}{R_p} + K_u \cdot \frac{m \cdot v_{x,char}{}^2}{R_p} = 2 \cdot \frac{L}{R_p} \;\Rightarrow\; v_{x,char} = \sqrt{\frac{L}{K_u \cdot m}} = \sqrt{\frac{C_f \cdot C_r \cdot L^2}{(C_r \cdot l_r - C_f \cdot l_f) \cdot m}};$$

[4.19]

For articulated vehicles, there are several modes of yaw instability. The critical speed is when the first of instable modes is reached and it is often called "zero damping mode".

4.3.5.1 Quasi-Steady State Longitudinal Acceleration

We will now leave the strict steady state, by claiming that longitudinal load transfer due to $a_x = \dot{v}_x \neq 0$, although v_x is constant. This is refered to as *Quasi-Steady State*.

4.3.5.1.1 Influence of longitudinal load transfer

Longitudinal load transfer show that braking increases over-steering tendency. It is actually so, that the critical speed $v_{x,crit} = \sqrt{L/(-K_u \cdot m)}$ (see Equation [4.19]) can come down to quite reachable levels when braking hard; i.e. hard braking at high speed may cause instability. This is especially so for front biased CoG location. See Figure 4-25, inspired by Reference (Drenth, 1993).

Using definition of understeer gradient:

$$K_u = \frac{l_r}{C_f \cdot L} - \frac{l_f}{C_r \cdot L} = \frac{l_r}{CC_f \cdot F_{fz} \cdot L} - \frac{l_f}{CC_r \cdot F_{rz} \cdot L} = \begin{Bmatrix} longitudinal \\ load\ transfer \\ m \cdot a_x \cdot h/L \end{Bmatrix} =$$

$$= \frac{l_r}{CC_f \cdot \left(m \cdot g \cdot \frac{l_r}{L} - m \cdot a_x \cdot \frac{h}{L}\right) \cdot L} - \frac{l_f}{CC_r \cdot \left(m \cdot g \cdot \frac{l_f}{L} + m \cdot a_x \cdot \frac{h}{L}\right) \cdot L} =$$

$$= \frac{1}{m \cdot g} \cdot \left(\frac{l_r}{CC_f \cdot \left(l_r - \frac{a_x}{g} h\right)} - \frac{l_f}{CC_r \cdot \left(l_f + \frac{a_x}{g} h\right)} \right) = \begin{Bmatrix} if\ CC_f = \\ = CC_f = CC_y \end{Bmatrix} =$$

$$= \frac{1}{m \cdot g \cdot CC_y} \cdot \left(\frac{1}{\left(1 - \frac{a_x}{g} \cdot \frac{h}{l_r}\right)} - \frac{1}{\left(1 + \frac{a_x}{g} \cdot \frac{h}{l_f}\right)} \right) = \begin{Bmatrix} if \\ a_x = 0 \end{Bmatrix} = 0;$$

[4.20]

However, the cornering stiffness varies digressively, e.g. $C_i = k_{ip} \cdot F_{iz} - k_{id} \cdot {F_{iz}}^2$. This is further studied in Reference (Drenth, 1993).

If taking the digressiveness of tyre cornering stiffness into account, the weight distribution plays a role also without longitudinal load transfer; front biased weight distribution gives under-steered vehicles and vice versa. Also, the number of wheels per axle influence stronger; single wheel front (or double-mounted rear) gives under-steered vehicles and vice versa.

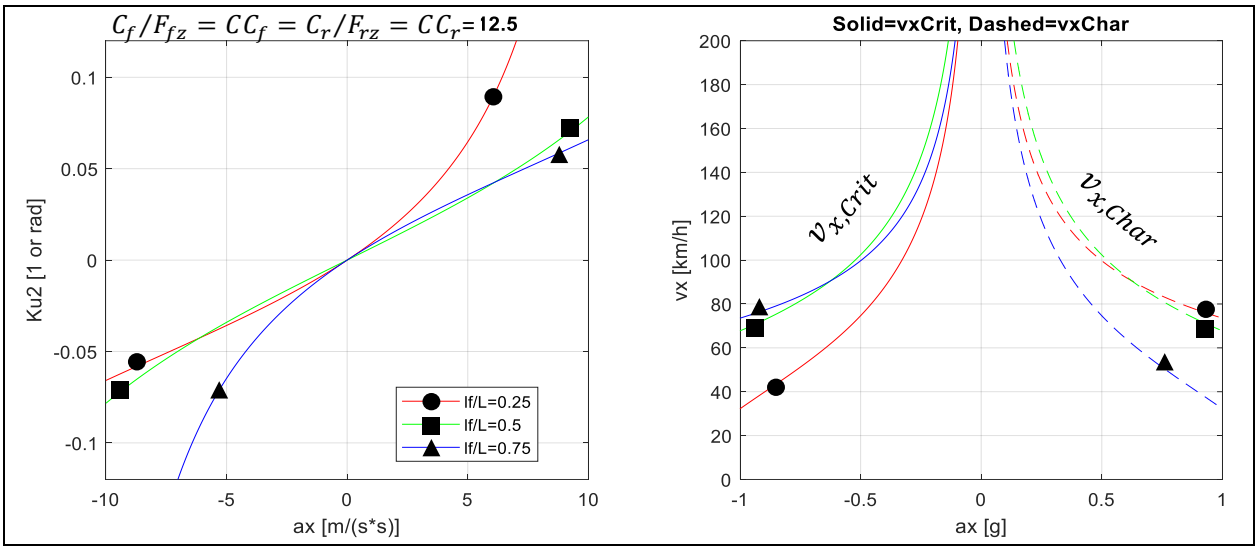


Figure 4-25: Left: Under-steering gradient as function of longitudinal acceleration, a_x, and static load distribution, l_f/L. Right: Critical and characteristic velocity as function of acceleration and load distribution.

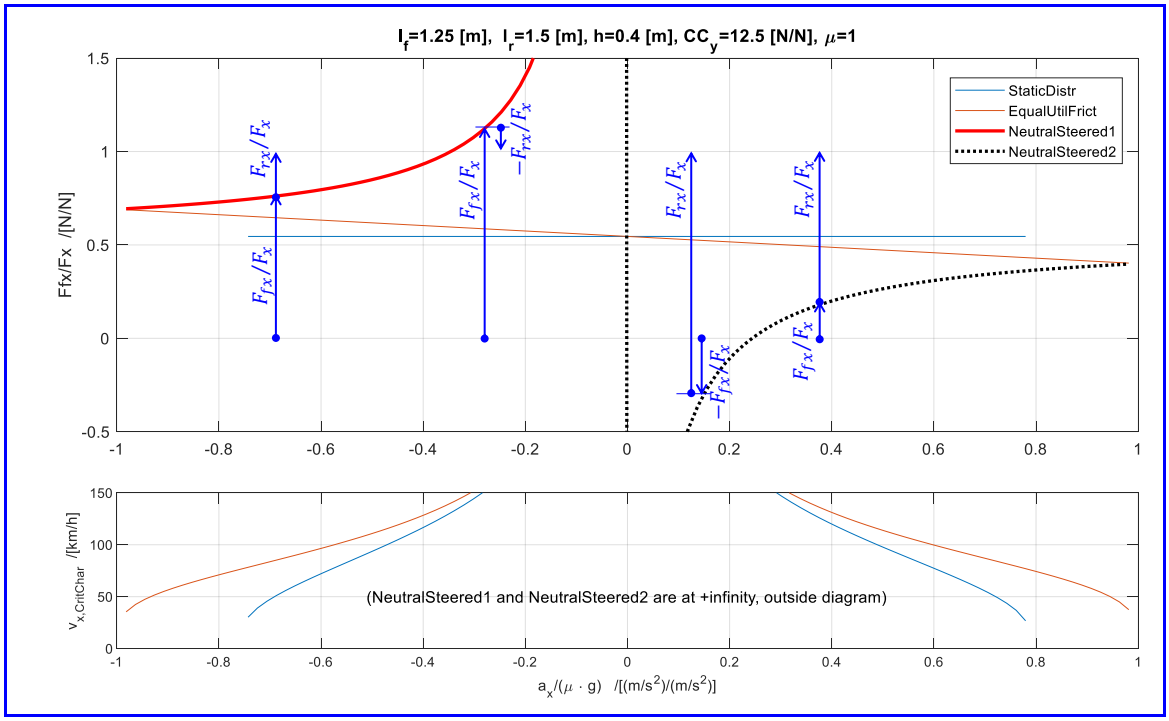


Figure 4-26: Three wheel torque distribution strategies: Distribution as static distribution of vertical forces, Equal utilization of $\mu \cdot F_{iz}$ (as "ideal curve" in 3.4.4) and Neutral steered. There are two ways of making the vehicle neutral steered, with same and opposite sign of F_{fx} and F_{rx}.

4.3.5.1.2 Influence of combined tyre slip

It should be noted that if the longitudinal acceleration is due to wheel torques, as opposed to road grade or aerodynamic forces, the tyre combined slip effects, see 2.2.5, will influence the curves which

is not considered in Figure 4-25; the cornering stiffness of an axle will decrease with increased longitudinal force.

With known combined slip effect, we could distribute longitudinal force so that K_u is unchanged and/or we could avoid braking so that $v_{x,crit}$ becomes lower than the actual speed v_x. To examplify this, we use the simple combined slip model in Eq [2.63] and require $K_u = 0$. We also assume flat road and no air resistance. Resulting distribution is compared with two other distribution rules in next figure. For low $|a_x|$, we must apply wheel torque in different directions to keep $K_u = 0$.

One could also add curves for $F_{fx} = 0$ (WheelTorqueOnlyRear) and $F_{rx} = 0$ (WheelTorqueOnlyFront). This would show that WheelTorqueOnlyRear have a tendency of making the vehicle oversteered. This is a very relevant study for electric propulsion on one axle where there are energy saving reasons to regenerate instead of friction braking.

4.3.6 Steady State Cornering Gains *

Function definition: ***Steady state cornering gains*** *are the amplification from steer angle to certain vehicle response measures for steady state cornering at a certain longitudinal speed.*

From Equation [4.10], we can derive some interesting ratios. We put steer angle in the denominator, so that we get a gain, in the sense that the ratio describes how much of something we get "per steer angle". If we assume $F_{fxw} = 0$, we get Equation [4.21].

$$\textbf{\textit{Yaw velocity gain}} =$$

$$\frac{\omega_z}{\delta_f} = \left\{use: \frac{\omega_z}{v_x} \approx \frac{1}{R_p}\right\} \approx \frac{v_x/R_p}{\frac{L}{R_p} + K_u \cdot \frac{m \cdot {v_x}^2}{R_p}} = \frac{v_x}{L + K_u \cdot m \cdot {v_x}^2};$$

$$\textbf{\textit{Curvature gain}} =$$

$$= \frac{\kappa}{\delta_f} = \frac{1/R_p}{\delta_f} = \frac{1/R_p}{\frac{L}{R} + K_u \cdot \frac{m \cdot {v_x}^2}{R_p}} = \frac{1}{L + K_u \cdot m \cdot {v_x}^2};$$

$$\textbf{\textit{Lateral acceleration gain}} =$$

$$= \frac{a_y}{\delta_f} = \left\{\begin{matrix} use: \\ a_y = \omega_z \cdot v_x; \\ and\ \frac{\omega_z}{v_x} \approx \frac{1}{R_p}; \end{matrix}\right\} \approx \frac{\frac{{v_x}^2}{R_p}}{\frac{L}{R_p} + K_u \cdot \frac{m \cdot {v_x}^2}{R_p}} = \frac{{v_x}^2}{L + K_u \cdot m \cdot {v_x}^2};$$

[4.21]

Yaw velocity gain is also derived for $F_{fxw} \neq 0$, and then we get Equation [4.22].

$$\textbf{\textit{Yaw velocity gain}}\ (with\ F_{fxw}\ taken\ into\ account) =$$

$$= \frac{\omega_z}{\delta_f} = \left(1 + \frac{F_{fxw}}{C_f}\right) \cdot \frac{v_x}{L + K_u \cdot m \cdot {v_x}^2};$$

[4.22]

4.3.6.1 Yaw Velocity Gain

The yaw velocity gain gives us a way to understand Characteristic Speed. Normally one would expect the yaw velocity to increase if one increases the speed along a circular path. However, the vehicle will also increase its path radius when speed is increased. At the Characteristic Speed, the increase in radius cancel out the effect of increased speed, so that yaw velocity in total decrease with increased speed. One can find the characteristic speed as the speed where one senses or measures the highest value of yaw velocity for a fix steer angle. The curves for $F_{fxw} = +0.25 \cdot F_{fz}$ and $F_{fxw} = -0.25 \cdot F_{fz}$ in

Figure 4-28 are generated using Eq [4.22]. Note that critical and characteristic speed is independent of F_{fxw}.

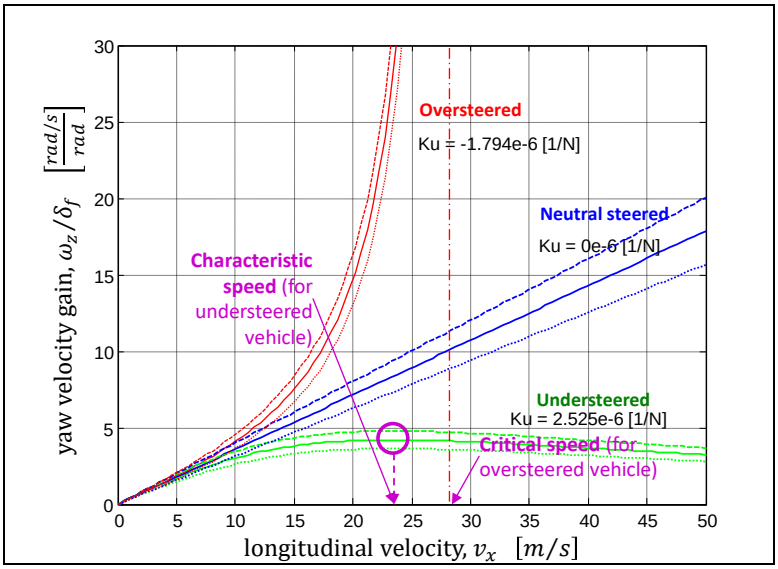


Figure 4-28: Yaw velocity gain (ω_z/δ_f) for Steady State Cornering. Each "cluster of 3 curves": Mid curve $F_{fxw} = 0$. Upper $F_{fxw} = +0.5 \cdot F_{fz}$. Lower $F_{fxw} = -0.5 \cdot F_{fz}$.

4.3.6.2 Curvature Gain

If driving on a constant path radius, and slowly increase speed from zero, an understeered vehicle will require more and more steer angle ("steer-in"), to stay at the same path radius. For an over-steered vehicle, one has to steer less ("open up steering") when increasing the speed.

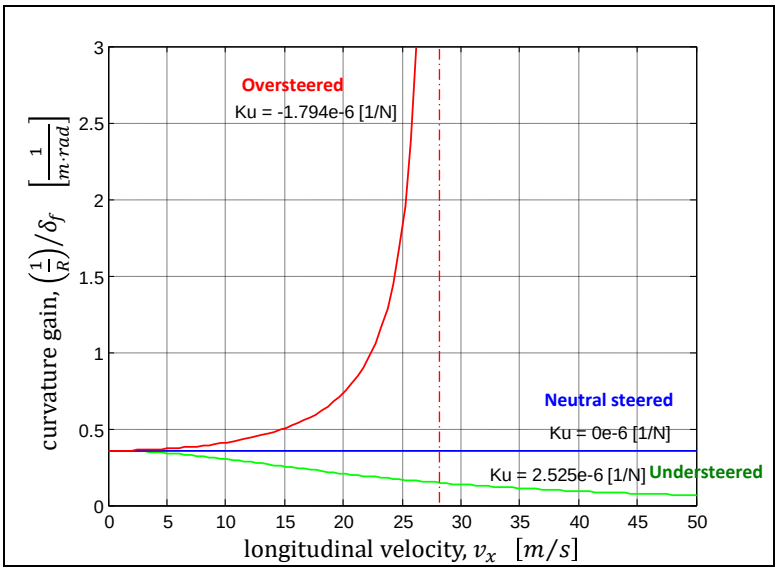


Figure 4-29: Curvature gain ($\frac{1/R}{\delta_f}$) for Steady State Cornering

4.3.6.3 Lateral Acceleration Gain

Figure 4-31 shows the lateral acceleration gain as function of vehicle speed. The characteristics speed is once again identified in this diagram, and now as the speed when lateral acceleration per longitudinal speed ($(a_y/\delta_f)/v_x$) reaches its highest value. This is an alternative definition of characteristic speed, c.f. 4.3.5.

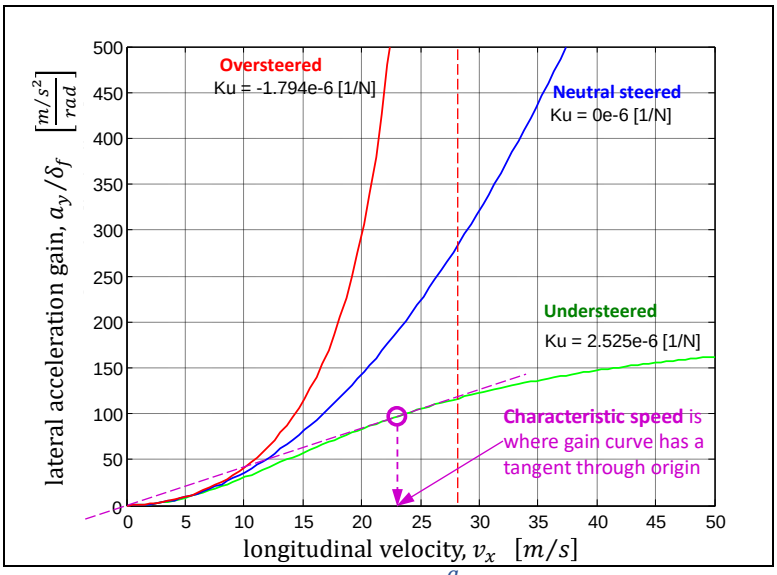


Figure 4-30: Lateral acceleration gain ($\frac{a_y}{\delta_f}$) for Steady State Cornering

From the previous figures the responsiveness of the vehicle can be identified for different understeer gradients. In all cases the vehicle which is understeered is the least responsive of the conditions. Both the yaw velocity and lateral acceleration cannot achieve the levels of the neutral steered or over-steered vehicle. The over-steered vehicle is seen to exhibit instability when the critical speed is reached since small changes in the input result in excessive output conditions. In addition, the over-steered vehicle will have a counter-intuitive response for the driver. To maintain a constant radius curve, an increase in speed requires that the driver turns the steering wheel opposite to the direction of desired path. The result of these characteristics leads car manufacturers to produce understeered vehicles that are close to neutral steering to achieve the best stability and driver feedback.

4.3.6.4 Side Slip Gain

All gains above can be found from solving ω_z from Eq [4.10]. So far, we have quantified the yaw performance. A scalar measure which captures most of this is K_u. If instead solving the other unknown, v_y, we can quantify the lateral velocity (or side slip) performance. It will be a "side slip gain" instead. Eq [4.23] shows the formula for this.

$$\frac{v_y}{v_x \cdot \delta_f} = \frac{C_f \cdot C_r \cdot l_r \cdot L - C_f \cdot l_f \cdot m \cdot {v_x}^2}{C_f \cdot C_r \cdot L^2 - \left(C_f \cdot l_f - C_r \cdot l_r\right) \cdot m \cdot {v_x}^2} \qquad [4.23]$$

It is not solely the understeering gradient that sets the curve shape, but we can still plot for some realistic numerical data, which are under-, neutral, and over-steered, see Figure 4-31.

All cases in Figure 4-31 goes from positive to negative side slip when speed increases. This is the same as we expected already in Figure 4-20. The (ISO 8855) defines the *side slip gradient*= $K_\beta = \partial\beta/\partial a_y$. If one plot in Figure 4-31 with a_y on abscissa axis instead of v_x, the curves will be close to straight lines, i.e., the K_β is almost a constant for a certain vehicle.

4.3.6.4.1 Other related gradients

If front and rear axle are steered proportional to each other, there is a certain longitudinal position where the side slip is zero at low speed. We use ZSSLS (zero side slip at low speed) as subscript for this point. If steering only on front axle, this is at the rear axle and the side slip here becomes: $\beta_{ZSSLS} = \beta_r = \frac{l_f}{L \cdot C_r} \cdot m \cdot a_y = \frac{l_f}{L \cdot C_r} \cdot m \cdot \frac{{v_x}^2}{R_p}$; The gradient $\frac{l_f}{L \cdot C_r}$ or $\frac{l_f}{L \cdot C_r} \cdot m$ can be called *rear axle (body) side slip gradient*. A similar relation for the front axle is $\alpha_f = \frac{l_r}{L \cdot C_f} \cdot m \cdot a_y = \frac{l_r}{L \cdot C_f} \cdot m \cdot \frac{{v_x}^2}{R_p}$; The gradient $\frac{l_r}{L \cdot C_f}$ or

$\frac{l_r}{L \cdot C_f} \cdot m$ can be called *front axle tyre side slip gradient*. Note the difference between **body** side slip gradient in ZSSLS and **tyre** side slip gradient for an axle.

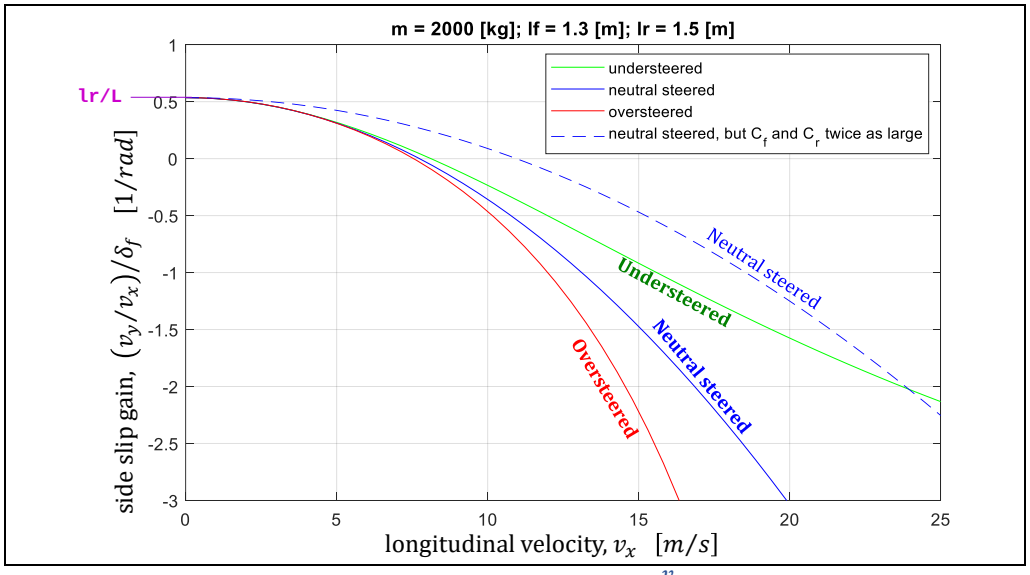


Figure 4-31: Side slip gain ($\frac{v_y}{v_x \cdot \delta_f}$).

We can also calculate and plot the longitudinal location of the motion centre, i.e. $x_{MC} = -v_y/\omega_z$, by combining Eqs [4.23] and [4.21]. Note that R_x is independent of δ_f, while the longitudinal location of the motion centre, $y_{MC} = v_x/\omega_z$, is not. See Figure 4-32.

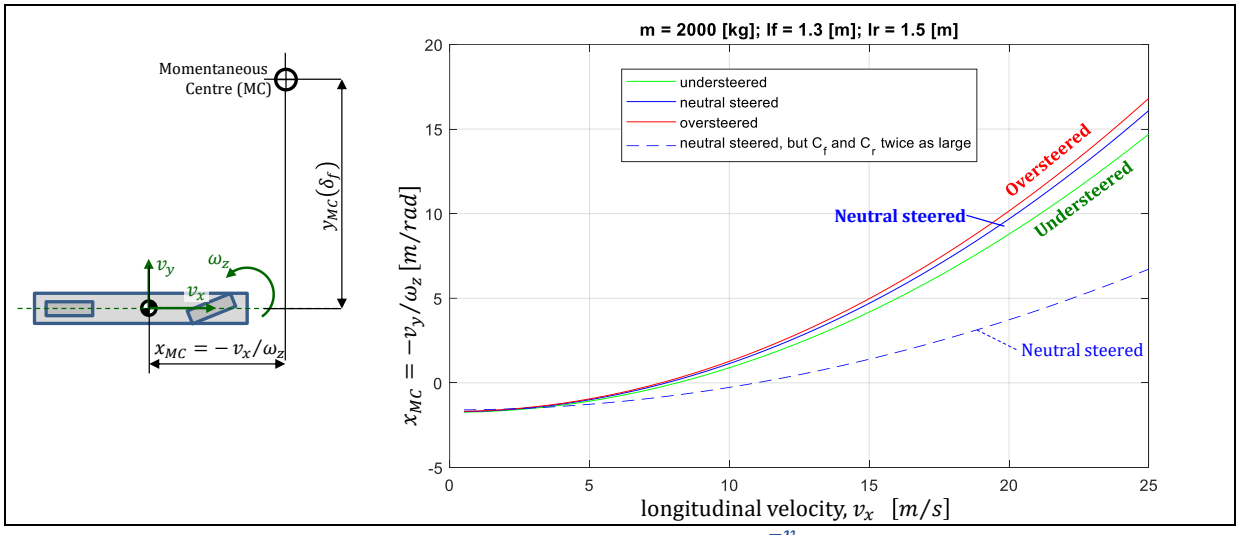


Figure 4-32: Motion centre longitudinal location ($x_{MC} = \frac{-v_y}{\omega_z}$). For Steady State Cornering.

4.3.6.5 Limitations due to Road Friction

The formulas with the gains in Eq [4.21] do not include the limitation due to maximum road friction, i.e. the peak of the tyres' $F_{iy}(s_{iy})$ curves. This limitation is a lateral acceleration $a_{y,max}$ where on of the axles reach friction limit. Yaw and lateral equilibrium requires $F_{fy} = m \cdot a_y \cdot l_r/L$; and $F_{ry} = m \cdot a_y \cdot l_f/L$;, so the limit due to front axle is $m \cdot a_{y,max,f} \cdot l_r/L = \mu_f \cdot F_{fz} = \mu_f \cdot m \cdot g \cdot l_r/L \Rightarrow a_{y,max,f} = \mu_f \cdot g$; and corresponding for rear axle. The total limit is $a_{y,max} = \min(\mu_f, \mu_r) \cdot g$; Inserting this in Eq [4.21] and eliminate δ_f, one finds:

$$v_{x,max} = \sqrt{a_{y,max} \cdot R_p} = \sqrt{\min(\mu_f, \mu_r) \cdot g \cdot R_p}; \quad [4.24]$$

For example, if negotiating a curve with $R = 100\ m$ and $\mu_f = \mu_r = 1$ gives $v_{x,max} \approx 31\ m/s \approx 113\ km/h$ and if either (or both) of μ_f and μ_r are just 0.5, $v_{x,max} \approx 22\ m/s \approx 80\ km/h$. So, we should see the curves in Figure 4-24 and in Figure 4-28 to Figure 4-31 as invalid over certain speed $v_{x,max}$, which depends on max road friction and curvature.

Reaching $v_{x,max}$ means loss of steerability if $\mu_f < \mu_r$, and loss of yaw stability if $\mu_r < \mu_f$. So, also an under-steered vehicle becomes unstable, if $\mu_r < \mu_f$ and driving faster than $v_{x,max}$. And, an oversteered vehicle might be limited from reaching its critical speed if $\mu_f < \mu_r$ and driving on a certain radius R.

4.3.7 How Design Influences Steady State Gains

The cornering stiffness for each axle are only abstract design parameters which influence steady state gains. The cornering stiffness is a combined effect from various, more concrete, design parameters. Such more concrete design parameters are presented in 4.3.7. Also, some vehicle operation which affects understeering gradient, such as hard braking in 4.3.7.1, is mentioned.

4.3.7.1 Tyre Design, Inflation Pressure and Number of Tyres

The cornering stiffness of each tyre is an obvious parameter which influences the axle cornering stiffness. The cornering stiffness of an axle is influenced by the sum of cornering stiffness for all tyres. There are normally two tyres per axle, but there are also vehicles with one tyre per axle (e.g., bicycles) or 4 (2 double mounted tyres on each side on heavy trucks).

Tyre design influences, which is geometrical dimensions and material selection. Inflation pressure is in here to be seen as a design parameter; a vehicle is sold with a recommended tyre inflation pressure.

In a first approximation, tyre cornering stiffness is approximately proportional to vertical load: $C_{iy} = CC_{iy} \cdot F_{iz}$. For a vehicle with same tyres front and rear ($CC_{fy} = CC_{ry}$), this means that it will be neutral steered, neglecting body forces (air and grade). This is because, in steady state cornering, vertical loads are distributed over the axles in the same relation as lateral loads.

4.3.7.2 Roll Stiffness Distribution between Axles

During cornering, the vertical load is shifted towards the outer wheels. Depending on the roll stiffness of each axle, the axles take differently much of this lateral load transfer. This also influences the yaw balance. The more roll stiff an axle is, the more of the lateral load shift it takes. Tyre cornering stiffness varies digressively with vertical load. Together, this means that increasing the roll stiffness on the front axle, leads to less front cornering stiffness, see Figure 2-60, and consequently more understeered vehicle. Increasing roll stiffness on rear axle makes the vehicle more oversteered. The total roll stiffness of the vehicle does not influence the understeering gradient. Normally one makes the front axle more roll stiff than the rear axle. This means that vehicle becomes more and more understeered for increased lateral acceleration, e.g. more steer angle is needed to maintain a certain path radius if speed increases. One can change the roll stiffness of an axle by changing roll centre height, wheel stiffness rate and anti-roll bar stiffness.

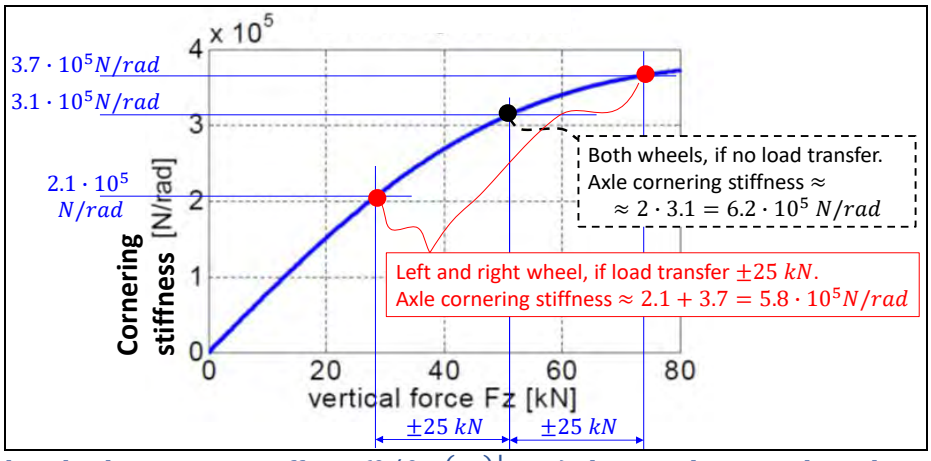


Figure 4-33: The wheels cornering stiffness ($\partial/\partial\alpha\,(F_y)|_{s_y=0}$) changes digressively with vertical load. The axle cornering stiffness therefore decreases with increased load transfer.

4.3.7.3 Suspension Steering

4.3.7.3.1 One-track model with suspension steering

In 4.3.7.2 and 4.3.7.3 some suspension steering phenomena shows to be important additional phenomena which determines the total axle slip stiffness C_{iyTot}. The C_{iyTot} can be inserted into the one-track model, e.g., in Figure 4-19, to compute the proper motion during steady state high speed cornering. But, to compute the proper power loss, it is important to distinguish between C_{iyTot} and C_{iyTyre}. Therefore, we will now derive an extended version of the one-track model in Figure 4-19, which makes difference between these two slip stiffnesses.

4.3.7.3.1.1 Model of vehicle

We will also add a steering on rear axle δ_r and $SteRat_r$. We also add 2 torque vectoring moments M_{fz} and M_{rz}. **In-road-plane**:

Equilibrium, lateral and yaw, solve for $\{F_{fy}, F_{ry}\}$:

$$\begin{bmatrix} F_{fy} \\ F_{ry} \end{bmatrix} = \begin{bmatrix} l_r \\ l_f \end{bmatrix} \cdot \frac{1}{L} \cdot m \cdot v_x \cdot \omega_z + \begin{bmatrix} -1 \\ 1 \end{bmatrix} \cdot \underbrace{(M_{fz} + M_{rz})}_{M_z};$$

Constitution and Compatibility, if s_{iyTyre} and β_i are eliminated:

$$\begin{bmatrix} F_{fy} \\ F_{ry} \end{bmatrix} = -\begin{bmatrix} C_{fyTyre} & 0 \\ 0 & C_{ryTyre} \end{bmatrix} \cdot \left(\begin{bmatrix} 1/v_x & l_f/v_x \\ 1/v_x & -l_r/v_x \end{bmatrix} \cdot \begin{bmatrix} v_y \\ \omega_z \end{bmatrix} - \begin{bmatrix} \delta_f \\ \delta_r \end{bmatrix} \right);$$

If we neglect the suspension steering, we would have:

$$\begin{bmatrix} \delta_f \\ \delta_r \end{bmatrix} = \begin{bmatrix} 1/SteRat_f \\ 1/SteRat_r \end{bmatrix} \cdot \delta_{sw};$$

And **In-road-plane** (roll):

Equilibrium: $$0 = (F_{fy} + F_{ry}) \cdot h - \underbrace{(M_{fx} + M_{rx})}_{M_x};$$

Eliminate $\{\delta_f, \delta_r\}$:

$$\begin{bmatrix} F_{fy} \\ F_{ry} \end{bmatrix} = \begin{bmatrix} l_r \\ l_f \end{bmatrix} \cdot \frac{1}{L} \cdot m \cdot v_x \cdot \omega_z + \begin{bmatrix} -1 \\ 1 \end{bmatrix} \cdot M_z;$$
$$\begin{bmatrix} F_{fy} \\ F_{ry} \end{bmatrix} = -\begin{bmatrix} C_{fyTyre} & 0 \\ 0 & C_{ryTyre} \end{bmatrix} \cdot \left(\begin{bmatrix} 1/v_x & l_f/v_x \\ 1/v_x & -l_r/v_x \end{bmatrix} \cdot \begin{bmatrix} v_y \\ \omega_z \end{bmatrix} - \begin{bmatrix} 1/SteRat_f \\ 1/SteRat_r \end{bmatrix} \cdot \delta_{sw} \right);$$
$$0 = [1 \quad 1] \cdot \begin{bmatrix} F_{fy} \\ F_{ry} \end{bmatrix} \cdot h - M_x;$$

[4.25]

So far, this model is similar to our initial steady state cornering model in Figure 4-19 plus the last roll equation. Note that we do not use any slip variables s_{iy}. Instead, we use $\beta_i - \delta_{sw}/SteRat_i$, which are the tyre side slip angles that **would** appear for same vehicle motion if no suspension steering. This is to prepare for adding the suspension steering, by which $\beta_i - \delta_{sw}/SteRat_i$ is not identifiable as a physical quantity; it is neither measurable as an angle in the model nor in a real vehicle.

5 equations, so we can solve for 5 unknowns. E.g., for a case where the vehicle motion $\{v_x, v_y, \omega_z\}$ is known (or requested), we can solve for the 5 unknowns $\delta_{sw}, M_z, F_{fy}, F_{ry}, M_x$:

$$\begin{bmatrix} \delta_{sw} \\ M_z \end{bmatrix} = \begin{bmatrix} C_{fyTyre}/SteRat_f & 1 \\ C_{ryTyre}/SteRat_r & -1 \end{bmatrix}^{-1} \cdot \left(\begin{bmatrix} C_{fyTyre} & 0 \\ 0 & C_{ryTyre} \end{bmatrix} \cdot \begin{bmatrix} 1/v_x & l_f/v_x \\ 1/v_x & -l_r/v_x \end{bmatrix} \cdot \begin{bmatrix} v_y \\ \omega_z \end{bmatrix} + \begin{bmatrix} l_r \\ l_f \end{bmatrix} \cdot \frac{1}{L} \cdot m \cdot v_x \cdot \omega_z \right);$$
$$\begin{bmatrix} F_{fy} \\ F_{ry} \end{bmatrix} = \begin{bmatrix} l_r \\ l_f \end{bmatrix} \cdot \frac{1}{L} \cdot m \cdot v_x \cdot \omega_z + \begin{bmatrix} -1 \\ 1 \end{bmatrix} \cdot M_z;$$
$$M_x = [1 \quad 1] \cdot \begin{bmatrix} F_{fy} \\ F_{ry} \end{bmatrix} \cdot h;$$

[4.26]

The case is relevant if we want an inverse model control of both ω_z and v_y by using both δ_{sw} and torque vectoring ($M_z \neq 0$). If we do not have torque vectoring ($M_z \equiv 0$), the unknowns would instead be $\delta_{sw}, v_y, F_{fy}, F_{ry}, M_x$, where you can note that the v_y (or sideslip $\arctan(\beta) = v_y/v_x$) is no longer controllable controllable.

4.3.7.3.1.2 Model of suspension steering

First, we model the roll-steering:

Constitution: $M_{fx} = c_{fx} \cdot \varphi_x;$
$M_{rx} = c_{rx} \cdot \varphi_x;$

Then, we model the rest of the suspension steering. We start with the physical model in Figure 4-34.

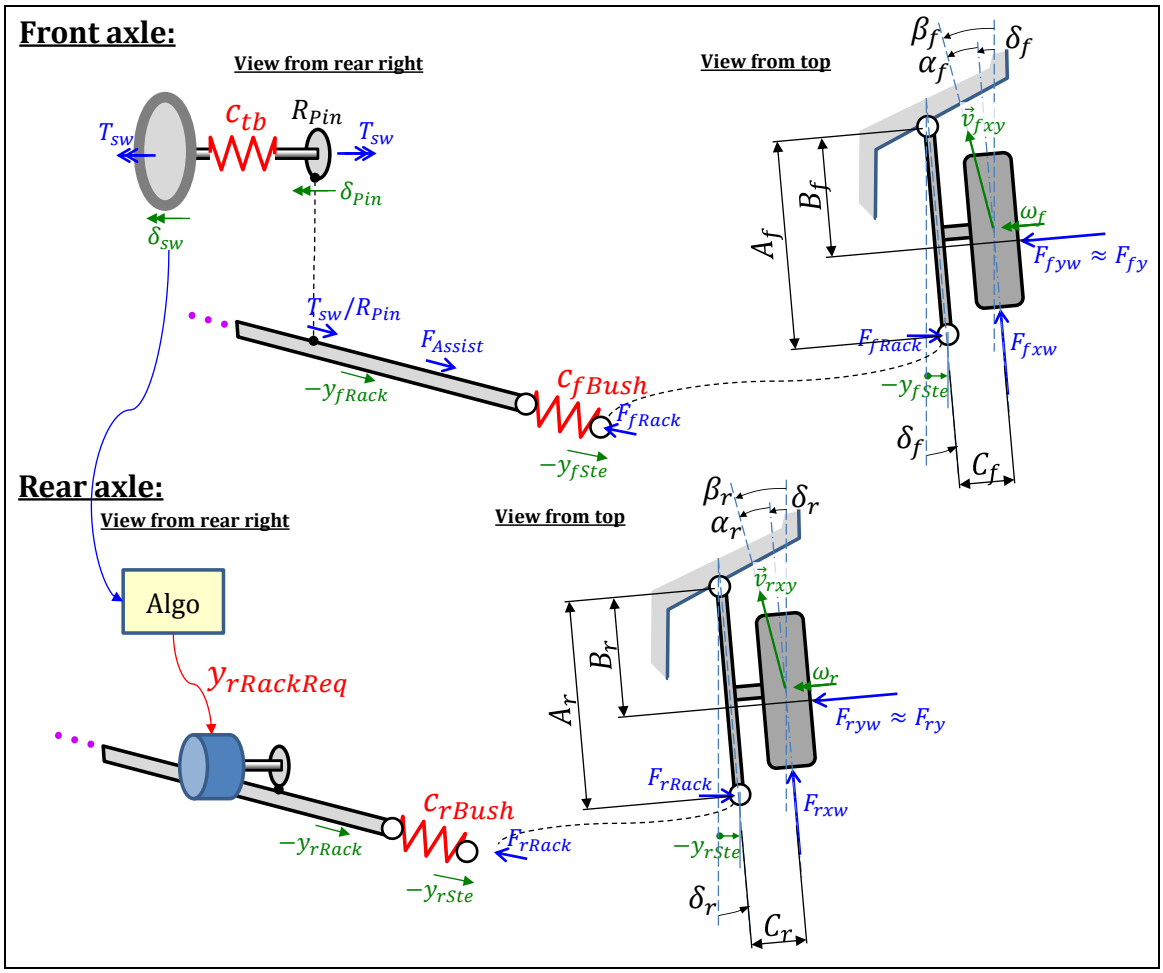


Figure 4-34: Front and rear suspension steering. Note: Roll steering is not visualised. Each axle has 2 wheels with symmetric geometry, but not necessarily symmetry in forces. The B_f and B_r vary due to the variation of pneumatic trail.

The mathematical model becomes:

Front Suspension and Steering:

$$\delta_f = \frac{\left(\delta_{sw} - \frac{T_{sw}}{c_{tb}}\right) \cdot R_{Pin} - \frac{F_{fRack}}{c_{fBush}}}{A_f} + c_{fRS} \cdot \varphi_x;$$

$$where\ F_{fRack} = \frac{T_{sw}}{R_{Pin}} + F_{Assist};$$

$$where\ F_{Assist} = f_{Assist}(T_{sw}, \cdots) \approx \frac{k_{Assist}}{R_{Pin}} \cdot T_{sw};$$

$$and\ F_{fRack} \cdot A_f + \left(F_{frxw} - F_{flxw}\right) \cdot C_f = F_{fy} \cdot B_f;$$

$$and\ SteRat_f = \frac{A_f}{R_{pin}};$$

$$and\ \left(F_{frxw} - F_{flxw}\right) = M_{fz}/(W/2);$$

Rear Suspension and Steering:

$$\delta_r = \frac{y_{rRack} - \frac{F_{rRack}}{c_{rBush}}}{A_r} + c_{rRS} \cdot \varphi_x;$$

$$where \quad y_{rRackReq} = f_{Algo}(\delta_{sw}, \cdots) \approx \frac{A_r}{SteRat_r} \cdot \delta_{sw};$$

$$and \quad y_{rRack} = y_{rRackReq}; \quad \text{(ideal sensor and actuator assumed)}$$

$$and \quad F_{rRack} \cdot A_r + (F_{rrxw} - F_{rlxw}) \cdot C_r = F_{ry} \cdot B_r;$$

$$and \quad SteRat_r = \frac{A_r}{\partial f_{Algo}/\partial \delta_{sw}} \approx \frac{A_r}{k_r};$$

$$and \quad (F_{rrxw} - F_{rlxw}) = M_{rz}/(W/2);$$

Solving 12 equations from the out-of-road-plane and suspension and steering for $\{M_z, \varphi_x, \ \delta_f, \delta_r, T_{sw}, F_{fRack}, F_{Assist}, R_{Pin}, y_{rRackReq}, y_{rRack}, F_{rRack}, k_r\}$ gives:

$$\delta_f = \underbrace{\frac{\delta_{sw}}{SteRat_f}}_{\text{base steering}} + \underbrace{\frac{c_{fRS} \cdot h}{c_x} \cdot (F_{fy} + F_{ry})}_{\text{roll steering}} - \underbrace{\left(\frac{1}{A_f^2 \cdot c_{fBush}} + \frac{1}{SteRat_f^2 \cdot c_{tb} \cdot (1 + k_{Assist})}\right) \cdot B_f \cdot F_{fy}}_{\text{sideforce steering}}$$
$$\underbrace{- \left(\frac{1}{A_f^2 \cdot c_{fBush}} - \frac{1}{SteRat_f^2 \cdot c_{tb} \cdot (1 + k_{Assist})}\right) \cdot \frac{C_f \cdot M_{fz}}{W/2}}_{\text{wheel torque steering}};$$

$$\delta_r = \underbrace{\frac{\delta_{sw}}{SteRat_r}}_{\text{base steering}} + \underbrace{\frac{c_{rRS} \cdot h}{c_x} \cdot (F_{fy} + F_{ry})}_{\text{roll steering}} - \underbrace{\frac{1}{A_r^2 \cdot c_{rBush}} \cdot B_r \cdot F_{ry}}_{\text{sideforce steering}} - \underbrace{\frac{1}{A_r^2 \cdot c_{rBush}} \cdot \frac{C_r \cdot M_{rz}}{W/2}}_{\text{wheel torque steering}};$$

To understand the expressions for δ_f and δ_r it is easiest to first look at expression for δ_r. Different phenomena are identified under the brackets. The name *wheel torque steering* is a collective name for brake steering and (propulsion) torque steering. For front axle, both the torsion bar compliance $1/c_{tb}$ and the steering assistance f_{Assist} influence *side force steering* and wheel torque steering. It is noteworthy that steering assistance influences also if only the first order term of f_{Assist} is considered k_{Assist}. Typically, f_{Assist} is progressive, e.g., $\frac{\partial f_{Assist}}{\partial T_{sw}} \propto T_{sw}$. An expression with a general $f_{Assist}(T_{sw}, \cdots)$ would become very complicated and require an inverted function $T_{sw} = f_{AssistInv}(F_{Assist}, \cdots)$;.

On matrix form:

$$\begin{bmatrix}\delta_f \\ \delta_r\end{bmatrix} = \begin{bmatrix}1/SteRat_f \\ 1/SteRat_r\end{bmatrix} \cdot \delta_{sw} + \boldsymbol{C_{SuspSte}} \cdot \begin{bmatrix}F_{fy} \\ F_{ry}\end{bmatrix} + \mathbf{diag}(\boldsymbol{c_{SuspSte}}) \cdot \begin{bmatrix}M_{fz} \\ M_{rz}\end{bmatrix};$$

4.3.7.3.1.3 Model of vehicle with suspension steering

Now, we recall the vehicle model. Also add the model for suspension steering. Also introduce $\Delta M_{zf} = M_{fz} - M_{rz}$:

$$\begin{bmatrix}F_{fy} \\ F_{ry}\end{bmatrix} = \begin{bmatrix}l_r \\ l_f\end{bmatrix} \cdot \frac{1}{L} \cdot m \cdot v_x \cdot \omega_z + \begin{bmatrix}-1 & 0 \\ 1 & 0\end{bmatrix} \cdot \begin{bmatrix}M_z \\ \Delta M_{zf}\end{bmatrix};$$

$$\begin{bmatrix}F_{fy} \\ F_{ry}\end{bmatrix} = -\begin{bmatrix}C_{fyTyre} & 0 \\ 0 & C_{ryTyre}\end{bmatrix} \cdot \left(\begin{bmatrix}1/v_x & l_f/v_x \\ 1/v_x & -l_r/v_x\end{bmatrix} \cdot \begin{bmatrix}v_y \\ \omega_z\end{bmatrix} - \begin{bmatrix}\delta_f \\ \delta_r\end{bmatrix}\right);$$

$$0 = [1 \quad 1] \cdot \begin{bmatrix}F_{fy} \\ F_{ry}\end{bmatrix} \cdot h - M_x;$$

$$\begin{bmatrix}\delta_f \\ \delta_r\end{bmatrix} = \begin{bmatrix}1/SteRat_f \\ 1/SteRat_r\end{bmatrix} \cdot \delta_{sw} + \boldsymbol{C_{SuspSte}} \cdot \begin{bmatrix}F_{fy} \\ F_{ry}\end{bmatrix} + \mathbf{diag}(\boldsymbol{c_{SuspSte}}) \cdot \frac{1}{2} \cdot \begin{bmatrix}1 & 1 \\ 1 & -1\end{bmatrix} \cdot \begin{bmatrix}M_z \\ \Delta M_{zf}\end{bmatrix};$$

[4.27]

We can now eliminate $\{\delta_f, \delta_r\}$ in Eq [4.27] and get similar model as in Eq [4.25], but the suspension steering is included through $\boldsymbol{C_{SuspSte}}$ and $\boldsymbol{c_{SuspSte}}$.

If $\boldsymbol{C_{SuspSte}} = \mathbf{0_{4\times4}}$ and $\boldsymbol{c_{SuspSte}} = \mathbf{0_2}$, the model in Eq [4.27] collapses to Eq [4.25]. The dimensions of the components in $\boldsymbol{C_{SuspSte}}$ and $\boldsymbol{c_{SuspSte}}$ are compliance=1/stiffness, so it means infinite stiffness, which makes sense if one want to disregard the suspension steering.

With Eq [4.27] one has one more variable ΔM_{zf} to actuate, but there is no more degree of freedom in motion to actuate. However, one can elaborate with it to minimize something, such as power losses, see 3.2.4.3.3.2. and 0.

4.3.7.3.2 Roll Steering

This section studies roll steering separate from other suspension steering effects, which were combined in 4.3.7.3.1.2.

Roll steer gradient, k_{iRS}, is defined for an axle and it is how much the wheels on an axle steers [deg] per vehicle roll angle [deg]. Also, a non-steered axle can steer due to roll-steering. Roll-steering depends on the suspension linkage geometry. The added steer angle can be expressed: $\Delta\delta_i = k_{iRS} \cdot \varphi_x$;.

We will now derive the influence on steady state cornering. Add steering on rear axle to Eq [4.10]:

$$\delta_f - \delta_r \approx \frac{L}{R_p} + K_{u,noRS} \cdot \frac{m \cdot {v_x}^2}{R_p};\ K_{u,noRS} = \frac{C_r \cdot l_r - C_f \cdot l_f}{C_f \cdot C_r \cdot L};\ \text{(subscript "}noRS\text{" means "}no\ Roll\text{-}Steer\text{")}$$

If we see δ_i as built up by one angle from the steering system δ_{i0} and one part coming from the suspension, via roll-steering $\Delta\delta_i$:

$$\left(\delta_{f0} + \Delta\delta_f\right) - \left(\delta_{r0} + \Delta\delta_r\right) \approx \frac{L}{R_p} + K_{u,noRS} \cdot \frac{m \cdot {v_x}^2}{R_p};$$

Then, we can express $\Delta\delta_i$ in φ_x:

$$\Delta\delta_i = \{\Delta\delta_i = k_{iRS} \cdot \varphi_x\} = k_{iRS} \cdot \varphi_x; \quad for\ i = f, r.$$

If one limit validity to steady state cornering ($\dot{v}_x = \dot{v}_y = \dot{\omega}_z = 0$; but also $\dot{v}_z = \dot{\omega}_x = 0$;), there is a algebraic relation between a_y and φ_x:

$$\Delta\delta_i = k_{iRS} \cdot \varphi_x = \begin{Bmatrix} M_x = \left(m \cdot a_y\right) \cdot h = \\ = c_x \cdot \varphi_x \end{Bmatrix} = k_{iRS} \cdot \frac{m \cdot a_y \cdot h}{c_x} = \left\{a_y = \frac{v_x^2}{R}\right\} = \frac{h \cdot k_{iRS}}{c_x} \cdot \frac{m \cdot v_x^2}{R_p};\ \ for\ i = f, r.$$

Insertion identifying an understeering gradient with roll-steering gives:

$$\delta_{f0} - \delta_{r0} \approx \frac{L}{R_p} + K_{u,RS} \cdot \frac{m \cdot v_x^2}{R_p}; \quad where\ K_{u,RS} = K_{u,noRS} + \frac{h \cdot \left(k_{rRS} - k_{fRS}\right)}{c_x}; \qquad [4.28]$$

Note that M_x, c_x and φ_x are for the whole vehicle including both axles. So, roll steering k_{iRS} $[deg/deg]$ is per axle, while the c_x $[Nm/deg]$ is for the whole vehicle, i.e., from both axles.

4.3.7.3.2.1 Bump Steering

Above has cornering on flat road in mind, where the vehicle body rolls so that compression of suspension= $z_{road} - z_{body} = 0 - z_{body}$. If driving over a one sided road bump, the suspension compression will rather be $= z_{road} - z_{body} \approx z_{road} - 0$. Then one use the axle measure *bump steering*, instead of roll steering, which linearized can be modelled:

$$\Delta\delta_{ijBump} = k_{ijBump} \cdot z_{ij};$$

Defining $k_{iLeftBump}$ and $k_{iRightBump}$ and symmetry ($k_{iLeftBump} = -k_{iRightBump} = k_{iBump}$) defines the roll steering gradient:

$$\Delta\delta_i = \frac{\Delta\delta_{iLeftBump} + \Delta\delta_{iRightBump}}{2} = \frac{k_{iLeftBump} \cdot z_{iLeft} + k_{iRightBump} \cdot z_{iRight}}{2} =$$
$$= \frac{k_{iBump} \cdot \left(z_i + \varphi_x \cdot \frac{W}{2}\right) - k_{iBump} \cdot \left(z_i - \varphi_x \cdot \frac{W}{2}\right)}{2} = k_{iBump} \cdot \frac{W}{2} \cdot \varphi_x = k_{iRS} \cdot \varphi_x;$$

4.3.7.3.3 Side-Force Steering

This section studies side-force steering separate from other suspension steering effects, which were combined in 4.3.7.3.1.2.

Side-force steer gradient, c_{iSFS}, is defined for an axle and it is how much the wheels on an axle steers [deg] negatively per lateral force [N]. Negative is chosen since the normal case is that pivot point is ahead of wheel, so that wheel steers negative for a positive force. Also, a non-steered axle steers due to side force steering, which depends on the compliance of the suspension bushings.

It can be modelled as an extra compliance, with the constitutional equations: $F_{fy} = -c_{fSFS} \cdot \Delta\delta_f$; and $F_{ry} = -c_{rSFS} \cdot \Delta\delta_r$;, where the Δ marks additional steer angle due to the lateral force. These extra compliances come into play as series connected with the tyre cornering compliances. If we update Equation [4.10] with side force steering it becomes:

$$\delta_f = \frac{L}{R} + K_u \cdot \frac{m \cdot {v_x}^2}{R};$$

$$where\ K_u = \frac{l_r}{C_{f,tot} \cdot L} - \frac{l_f}{C_{r,tot} \cdot L} = \frac{C_{r,tot} \cdot l_r - C_{f,tot} \cdot l_f}{C_{f,tot} \cdot C_{r,tot} \cdot L};$$

$$where\ C_{f,tot} = \frac{1}{\frac{1}{C_f} + \frac{1}{c_{fSFS}}} \quad and \quad C_{r,tot} = \frac{1}{\frac{1}{C_r} + \frac{1}{c_{rSFS}}};$$

[4.29]

For vehicles with largely varying vertical axle load (such as heavy trucks), one has to consider that the contribution from tyre to axle cornering stiffness is rather proportional to vertical axle load, while the contribution from side-force steering comes from suspension elasticities and is rather constant. So, utilizing side-force steering makes the vehicles lateral manoeuvrability inconsistent with vertical load.

If we use $C_i = CC \cdot F_{iz}$, from Eq [2.50], we can derive the following:

$$K_u = \frac{l_r}{C_{f,tot} \cdot L} - \frac{l_f}{C_{r,tot} \cdot L} = \frac{C_{r,tot} \cdot l_r - C_{f,tot} \cdot l_f}{C_{f,tot} \cdot C_{r,tot} \cdot L} = \frac{\frac{l_r}{C_{f,tot}} - \frac{l_f}{C_{r,tot}}}{L} = \left\{ \frac{l_j}{C_{i,tot}} = \left(\frac{1}{C_i} + \frac{1}{c_{iSFS}}\right) \cdot l_j = \right.$$

$$\left. \left(\frac{1}{CC \cdot F_{iz}} + \frac{1}{c_{iSFS}}\right) \cdot l_j = \frac{L}{CC \cdot m \cdot g} + \frac{l_j}{c_{iSFS}} \right\} = \frac{\left(\frac{L}{CC \cdot m \cdot g} + \frac{l_r}{c_{fSFS}}\right) - \left(\frac{L}{CC \cdot m \cdot g} + \frac{l_f}{c_{rSFS}}\right)}{L} = \frac{l_r}{c_{fSFS} \cdot L} - \frac{l_f}{c_{rSFS} \cdot L};$$

[4.30]

This explains that the influence from the tyres to a large extent disappears if we have same tyres (same CC) front and rear. Instead, the side force steering influence remains.

4.3.7.3.3.1 Influence of Translatory Compliance

One way to deliberately design for side-force steering is to let the axle or wheels have yaw pivot points ahead or behind. This also leads to a lateral translatory compliance of the axle or wheels which, mathematically, gives one more state variable. For lower frequencies, such as for handling, this compliance can often be neglected.

4.3.7.3.4 Steering system compliance

This section studies steering system compliance separate from other suspension steering effects, which were combined in 4.3.7.3.1.2.

The steering system is also compliant: $\delta_f = \delta_{f0} + \Delta\delta_{SteCompl}$; where $\delta_{f0} = SteRatio \cdot \delta_{stw}$ and $\Delta\delta_{SteCompl} = -F_{fy}/c_{SteCompl}$; where $c_{SteCompl}$ $[N/rad]$ is the stiffness between a lateral force on the front axle and the steering (hand) wheel. The steering system compliance and the side-force steering compliance are very related. Without steering assistance, they are two series coupled mechanical compliances: compliance in steering system (e.g. steering column torsion bar) and in suspension (e.g. bushings), respectively.

With steering assistance, the compliance becomes a combined mechanical and algorithmic phenomenon.

If we assume $\delta_{SteWhl} = 0$:

$$T_{Pinion} = (F_{Rack} - F_{Assist}) \cdot r_{Pinion}; \quad F_{Rack} = \frac{a}{b} \cdot F_{fy};$$

$$\delta_{Pinion} = -\frac{y_{Rack}}{r_{Pinion}}; \quad y_{Rack} = -b \cdot \Delta\delta_{SteCompl}; \quad \left(SteRatio = \frac{b}{r_{Pinion}}\right);$$

$$T_{Pinion} = c_{TorsionBar} \cdot (\delta_{SteWhl} - \delta_{Pinion}) = c_{TorsionBar} \cdot (0 - \delta_{Pinion});$$

If $F_{Assist} = 0$:

$$\Delta\delta_{SteCompl} = -F_{fy}/c_{SteCompl}; \quad where\ c_{SteCompl} = c_{TorsionBar} \cdot SteRatio^2/a;$$

If $F_{Assist} = \frac{k_{Assist}}{R_{Pin}} \cdot T_{sw}$ get a model as in 4.3.7.3.1.2.

But if we try a more realistic assistance function, such as $F_{Assist} = Boost \cdot T_{Pinion}^3$, we see that the relationship between $\Delta\delta_{SteCompl}$ and F_{fy} is no longer linear. We can still linearize and find a value of $-\partial F_{fy}/\partial\Delta\delta_{SteCompl}$ as something to comparable with $c_{SteCompl}$. The value will depend on the assistance function; in the example above, it will depend on $Boost$. In most modern passenger car, the steering assistance is electrical, so the $c_{SteCompl}$ will be dependent on both mechanical design and control algortihms.

4.3.7.3.5 Quantified Combined Effect

Side force steering and roll-steering are similar but have different time scales. Roll-steering requires that sprung body changes roll angle, which takes significantly longer time; typically roll eigen-frequency is 1..2 Hz. Side force steering does not require a roll angle change, so side-force steering has much less time delay. Roll-steering also comes into play for one-sided road unevenness, i.e. also without cornering and without body roll.

The combined effect from side force steering (4.3.7.3.2), roll-steering (0) and steering system compliance, often represent a significant part of the front axle cornering compliance, e.g. reduces compliance with 20..40% compared to tyre cornering compliance only, Reference (Wedlin, Tillback, & Bane, 1992). Most of this is due to steering system compliance.

On rear axles on passenger cars, the influence is typically less and in opposite direction, e.g. increase 1..5% compared to tyre cornering compliance only.

Rear axles on heavy vehicles are typically designed without significant side-force steering. However, the frame compliance can cause a relevant amount of side-force oversteering due to that the whole frame steers curve-outwards rear and curve-inwards front. The frame compliance is especially influential on a tractor with fifth wheel ahead of rear axle(s); clearly larger than sideforce compliance on a single axle and on a rigid truck about the same, depending on the body-build on the frame.

Patents exist for making the rear axle suspension on heavy vehicle's trailers sideforce steering so that axle becomes less cornering compliant, reducing compliance with typically 1/3 compared to tyre cornering compliance only. This increases yaw stability, which is very much same concept as using side-force understeering rear at a two-axle vehicle. Using this concept can lead to very yaw stable vehicles. The drawback is reduced yaw agility. If really exaggerated, it can take the rear axle to effectively negative cornering stiffness, which makes vehicle unstable.

4.3.7.4 Camber Steer

Negative camber (wheel top leaning inwards) increases the cornering stiffness. One explanation to this is that curve outer wheel gets more vertical load than the curve inner wheel. Hence, the inwards directed camber force from outer wheel dominates over outwards directed camber force from the inner wheel. Negative camber is often used at rear axle at passenger cars. Drawback with non-zero camber is tyre wear.

4.3.7.5 Toe Angle

Toe has some, but limited effect on an axle's cornering stiffness. Non-zero toe increases tyre wear. Toe-angle: When rolling ahead, tyre side forces pre-tension bushes.

If toe (=toe-in) is positive there are tyre-lateral forces on each tyre already when driving straight ahead, even if left and right cancel out each other: $F_{ay} = \left(C_{left} - C_{right}\right) \cdot \frac{toe}{2} = 0$;. Then, if the axle takes a side force, the vertical loads of the wheels are shifted between left and right wheel, which also changes the tyre cornering stiffnesses. The outer wheel will get more cornering stiffness. Due to positive toe, it will also have the largest steer angle. So, the axle will generate larger lateral force than with zero toe. For steady-state cornering vehicle models, this effect comes in as an increased axle cornering stiffness, i.e. a linear effect.

4.3.7.6 Wheel Torque Effects

Wheel torque give tyre longitudinal force, directed as the wheel is directed. If the wheel is steered, the wheel longitudinal forces can influence the yaw balance, see also F_{fxw} in Equation [4.10].

Unsymmetrical wheel torques (left/right) will give a *direct yaw moment* in the yaw equilibrium in Equation [4.6]. The actuated yaw moment around CoG is then of the magnitude of wheel longitudinal wheel force times half the track width. ESC and Torque vectoring interventions have such effects.

High longitudinal utilization of friction on an axle leads to that lateral grip is reduced on that axle. The changed yaw moment, compared to what one would have without using friction longitudinally, can be called an *indirect yaw moment*. The actuated change in yaw moment around CoG is then of the magnitude of change in wheel lateral wheel force times half the wheelbase. It influences the yaw balance. That is the reason why a front axle driven vehicle may be more understeered than a rear axle driven one. On the other hand, the wheel-longitudinal propulsion force on the front axle does also help the turn-in, which acts towards less understeering.

4.3.7.7 Transient Vehicle Motion Effects on Yaw Balance

The effects presented here are not so relevant for steady state understeering coefficient. However, they affect the yaw balance in a more general sense, why it is relevant to list them in this section.

- Longitudinal load transfer changes normal forces. E.g., strong deceleration by wheel forces helps against under-steering, since front axle gets more normal load. This effect has some delay. Also, it vanishes after the transient.
  (This effect can be compared with the effect described in 4.3.7.2, which is caused by tyre cornering stiffness varying digressively with vertical load, while the longitudinal load transfer effect can be explained solely with the proportional variation.)
- Change of longitudinal velocity v_x helps later in manoeuvre., because the term $\omega_z \cdot v_x$ is reduced. E.g., deceleration early in a manoeuvre makes the vehicle easier to manoeuvre later in the manoeuvre.

4.3.7.8 Some Other Design Aspects

High cornering stiffness is generally desired for controllability.

Longer wheelbase (with unchanged yaw inertia and unchanged steering ratio) improves the transient manoeuvrability, because the lateral forces have larger levers to generate yaw moment with.

4.3.7.9 Manoeuvrability and Stability

The overall conclusion of previous section is that all gains become higher the more over-steered (or less understeered) the vehicle is. Higher gains are generally experienced as a sportier vehicle and they also improve safety because they improve the manoeuvrability. A higher manoeuvrability makes it

easier for the driver to do avoidance manoeuvres. This motivates a design for low understeering gradient.

However, there is also the effect that a vehicle with too small understeer gradient becomes very sensitive to the steering wheel angle input. In extreme, the driver would not be able to control the vehicle. This limits how small the understeering gradient one can design for. Generally, vehicles are built understeered.

It is not impossible for a driver to keep an unstable vehicle ($K_u < 0$ and $v_x > v_{x,crit}$) on an intended path, but it requires an active compensation with steering wheel. If adding support systems, such as yaw damping by steering support or differentiated propulsion torques, it can be even easier. If one could rely on a very high up time for such support systems, one could move today's trade-off between manoeuvrability and stability. This conceptual design step has been taken for some airplanes, which actually are designed so that they would be unstable without active control. See also 4.4.3.4.

4.3.7.10 Handling Diagram

There are many frequently used graphical tools or diagrams to represent vehicle characteristics. One is the "handling diagram". A handling diagram tells maximum cornering a_{yMax} and understeering gradient at different a_y. A handling diagram is essential a plot of same data as in Lateral Acceleration gain in Figure 4-30, but the curve $a_y(\delta_f)$ for one v_x instead of $a_y/\delta_f\ (v_x)$. For the linear model it would be a straight line, with $da_y/d\delta_f = constant = {v_x}^2/(L + K_u \cdot m \cdot {v_x}^2)$. But for a real vehicle test, or a more advanced model, it becomes more different.

A handling diagram is constructed as follows. Same simplifying assumptions are done as in Figure 4-19, with the exception that we don't assume linear tyre models.

Equilibrium:

$$\left\{ m \cdot \frac{{v_x}^2}{R} = m \cdot a_y = F_{fy} + F_{ry};\quad 0 = F_{fy} \cdot l_f - F_{ry} \cdot l_r; \right\} \Rightarrow F_{fy} = \frac{l_r}{L} \cdot m \cdot a_y;\ F_{ry} = \frac{l_f}{L} \cdot m \cdot a_y;$$

Constitution:

$$F_{fy} = F_{fy}(\alpha_f) \Rightarrow \alpha_f = {F_{fy}}^{-1}(F_{fy});\quad F_{ry} = F_{ry}(\alpha_r) \Rightarrow \alpha_r = {F_{ry}}^{-1}(F_{ry});$$

Solving for $\alpha_f - \alpha_r$ yields:

$$\alpha_r - \alpha_f = {F_{ry}}^{-1}(F_{ry}) - {F_{fy}}^{-1}(F_{fy}) = {F_{ry}}^{-1}\left(\frac{l_f}{L} \cdot m \cdot a_y\right) - {F_{fy}}^{-1}\left(\frac{l_r}{L} \cdot m \cdot a_y\right);$$

So, we can plot $\alpha_r - \alpha_f$ as function of a_y. This relation is interesting because compatibility ($\delta_f + \alpha_f - \alpha_r = L/R$;) yields $\alpha_r - \alpha_f = \delta_f - L/R = \delta_f - \delta_A$. And $\delta_f - \delta_A$ is connected to one of the understandings of K_u in Equation [4.15], ($K_u = \frac{\partial}{\partial a_y}(\delta_f - \delta_A)$;). If we plot $\alpha_r - \alpha_f = \delta_f - \delta_A$ on abscissa axis and a_y on ordinate axis, we get the most common way of drawing the handling diagram, see Figure 4-35. The axle's constitutive relations can be used as graphical support to construct the diagram, but then the constitutive relations should be plotted as: $a_{yi}(\alpha_i) = \frac{L}{L-l_i} \cdot \frac{1}{m} \cdot F_{iy}(\alpha_i)$;. The quantity a_{yi} can be seen as the lateral force scaled with a certain fraction of vehicle mass, where the certain fraction is such that both axles' values correspond to the same vehicle lateral acceleration.

Figure 4-35 shows the construction of a handling diagram from axle slip characteristics. Figure 4-36 show examples of handling diagrams constructed via tests with simulation tools. Handling diagrams can be designed from real vehicle tests as well. The slope in the handling diagram corresponds to understeering gradient K_{u3} in Equation [4.14].

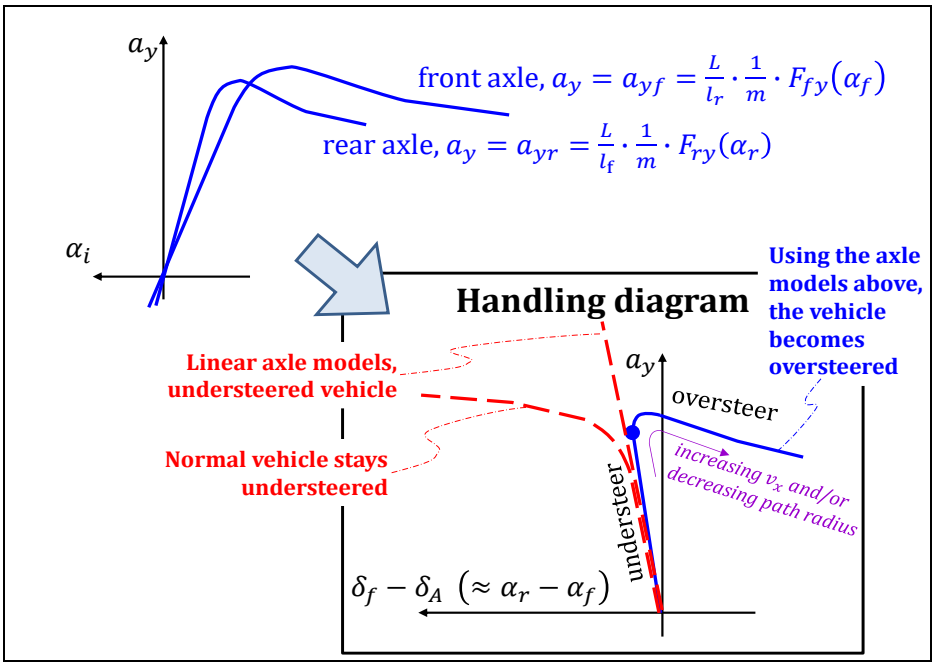
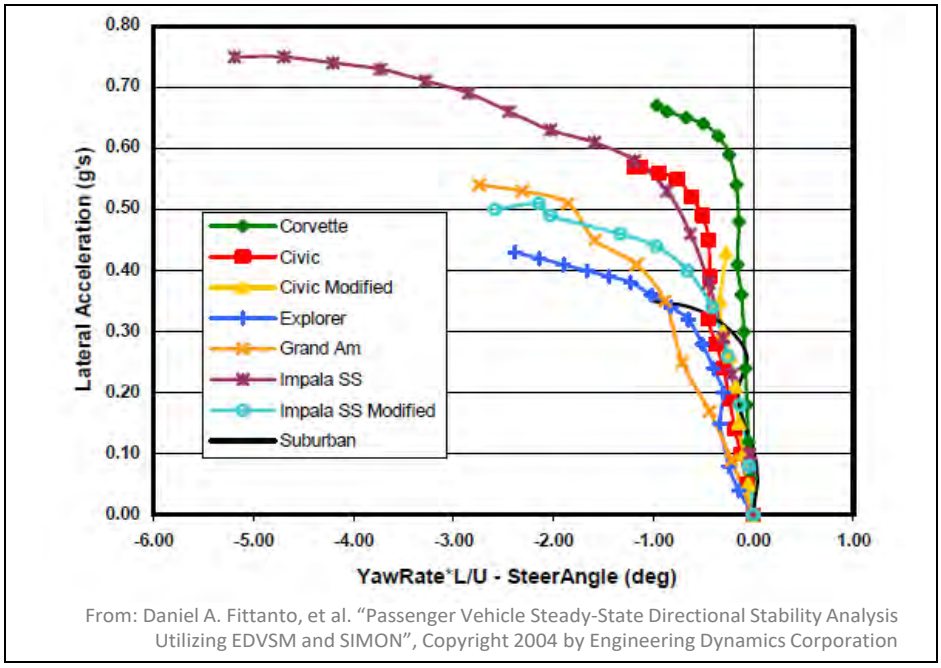


Figure 4-35: Construction of the "Handling diagram". The axle's slip characteristics (upper diagram) are chosen so that vehicle transits from understeer to over-steer with increased longitudinal speed, v_x. The dashed shows two other slip characteristics.



From: Daniel A. Fittanto, et al. "Passenger Vehicle Steady-State Directional Stability Analysis Utilizing EDVSM and SIMON", Copyright 2004 by Engineering Dynamics Corporation

Figure 4-36: Example of handling diagram.

4.3.7.11 Lateral Load Transfer in Steady State Cornering

In the chapter about longitudinal dynamics, we studied (vertical tyre) load transfer between front and rear axle. The corresponding issue for lateral dynamics is load transfer between left and right side of the vehicle. Within the steady state lateral dynamics, we will cover some of the simpler effects, but save the more complex suspension linkage dependent effects to 4.4.3.4.

The relevance to study the load transfer during steady state cornering is to limit the roll during cornering (for comfort) and yaw balance (understeering gradient, see 4.3.7.2). Additionally, the load transfer influence the transient handling; see 4.4 and 4.4.3.4.

4.3.7.11.1 Load Transfer between Vehicle Sides

Without resolving into front and rear, we do not need to involve suspension in model:

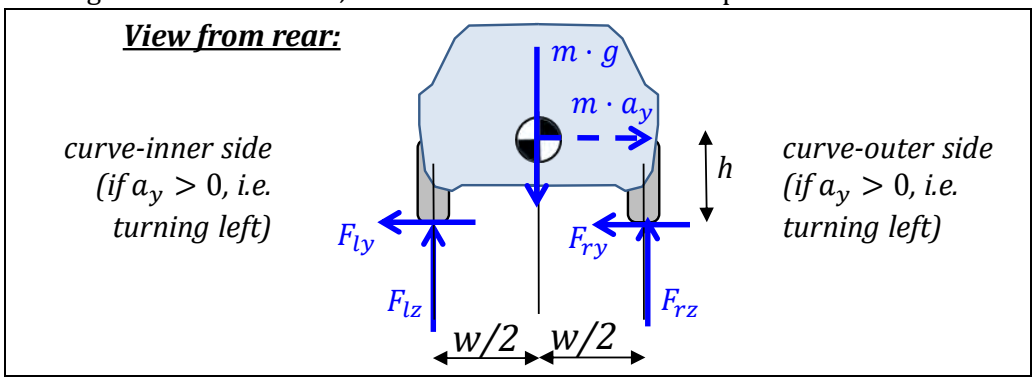


Figure 4-37: A cornering vehicle. The $m \cdot a_y$ is a fictive force. Subscript l and r mean left and right.

Moment equilibrium, around left contact with ground: ⇒

$$\Rightarrow m \cdot g \cdot \frac{w}{2} + m \cdot a_y \cdot h - F_{rz} \cdot w = 0 \Rightarrow F_{rz} = m \cdot \left(\frac{g}{2} + a_y \cdot \frac{h}{w}\right);$$

Moment equilibrium, around right contact with ground: $\Rightarrow F_{lz} = m \cdot \left(\frac{g}{2} - a_y \cdot \frac{h}{w}\right);$ [4.31]

These equations confirm what we know from experience, the curve-inner side if off-loaded.

4.3.7.11.2 Body Heave and Roll Due to Lateral Wheel Forces

Now, we shall find out how much the vehicle rolls and heaves during steady state cornering. First, we decide to formulate the model in "effective stiffnesses", in the same manner as for longitudinal load transfer in previous chapter.

There is no damping included in model, because their forces would be zero, since there is no displacement velocity, due to the "quasi-steady-state" assumption. As constitutive equations for the compliances (springs) we assume that displacements are measured from a static condition and that the compliances are linear. The road is assumed to be smooth, i.e. $z_{lr} = z_{rr} = 0$ (2nd subscript means *road*).

$$\begin{aligned} F_{lz} &= F_{lz0} + c_{side} \cdot (z_{lr} - z_l) + c_{arb} \cdot \big((z_{lr} - z_l) - (z_{rr} - z_r)\big) = \\ &= \{z_{lr} = z_{rr} = 0\} = F_{lz0} - (c_{side} + c_{arb}) \cdot z_l + c_{arb} \cdot z_r; \\ F_{rz} &= \cdots = F_{rz0} - (c_{side} + c_{arb}) \cdot z_r + c_{arb} \cdot z_l; \\ &where\ F_{lz0} + F_{rz0} = m \cdot g; \quad and \quad F_{lz0} \cdot w/2 - F_{rz0} \cdot w/2 = 0; \end{aligned} \qquad [4.32]$$

The stiffnesses c_{side} and c_{arb} (arb means *anti-roll bar*) are effective stiffnesses as measurable under the wheels. The physical springs are mounted inside in some kind of linkage and have different stiffness values, but their effect is captured in the effective stiffnesses. Some examples of different physical spring and linkage design are given in 2.3.3.1 and 2.3.4.1.

We see already in free-body diagram in Figure 4-38 that F_{yl} and F_{yr} always act together, so we rename $F_{yl} + F_{yr} = F_y$. We see in Figure 2-90 that we have to assume something about how the lateral forces are transferred from road to body. The "trivial linkage" from Figure 2-90 is assumed. **Equilibrium** then gives:

$$\begin{aligned} &F_y - m \cdot a_y = 0; \\ &m \cdot g - F_{zl} - F_{zr} = 0; \\ &F_{zl} \cdot (w/2) - F_{zr} \cdot (w/2) + F_y \cdot h + m \cdot g \cdot (-y) = 0; \end{aligned} \qquad [4.33]$$

The term $m \cdot g \cdot (-y)$ is taken as $m \cdot g \cdot (h - h_{RC}) \cdot \sin(\varphi_x) \approx m \cdot g \cdot (h - h_{RC}) \cdot \varphi_x$. It assumes a height for the point where the roll takes place, h_{RC}. We don't know the value of it, until below where we study the suspension design, but it can be mentioned already here that most vehicles have an $h_{RC} \ll h$. This

causes a "(roll) pendulum effect", especially significant for heavy commercial vehicles due to their large h..

Compatibility, to introduce body displacements, z and φ_x, gives:

$$z_l = z + (w/2)\cdot\varphi_x; \quad and \quad z_r = z - (w/2)\cdot\varphi_x; \qquad [4.34]$$

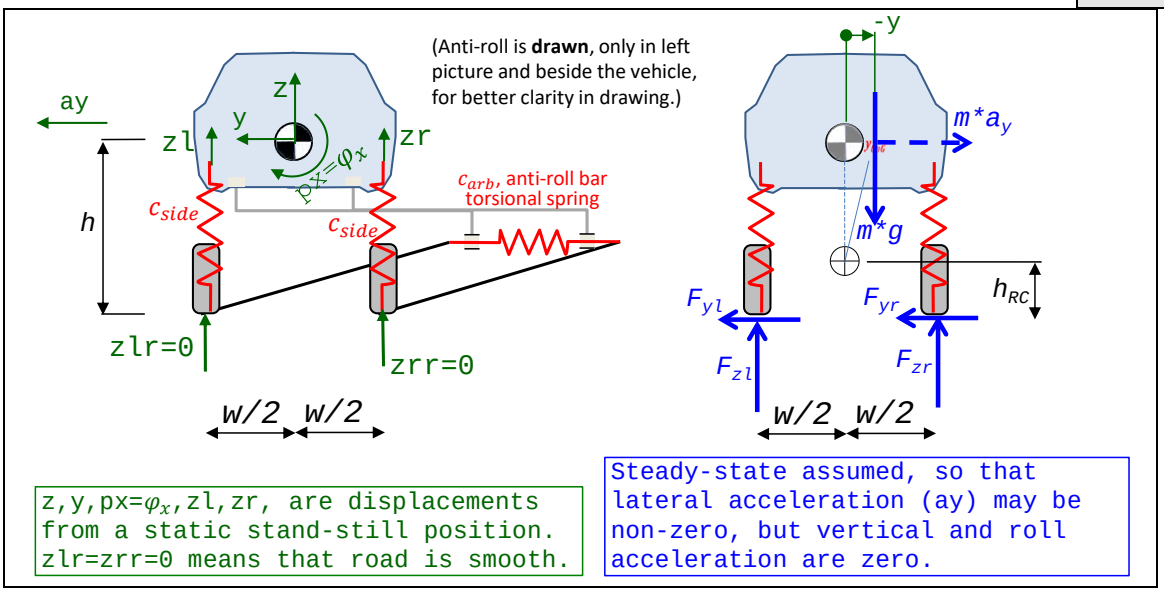


Figure 4-38: Model for steady state heave and roll due to lateral acceleration. Suspension model is no linkage (or "trivial linkage") and without difference front and rear.

Combining constitutive relations, equilibrium and compatibility, gives, as Matlab script:

```
syms …; sol=solve( ...
    Flz==Flz0-cside*zl+carb*(zr-zl), ...
    Frz==Frz0-cside*zr+carb*(zl-zr), ...
    Flz0+Frz0==m*g,  Flz0*w/2-Frz0*w/2==0, ...
    Fy-m*ay==0, ...
    m*g-Flz-Frz==0', ...
    Flz*(w/2)-Frz*(w/2)+Fy*h+m*g*(h-hRC)*px==0, ...
    zl==z+(w/2)*px,  zr==z-(w/2)*px, ...
    Fzl1==-1/((Fzl/m-g/2)*w/(ay*h)), ...
    zl, zr, Flz, Frz, Flz0, Frz0, Fy, z, px);
```

[4.35]

The results from the Matlab script in Equation [4.35]:

$$F_y = m\cdot a_y; \quad z = 0;$$

$$p_x = \varphi_x = \frac{2\cdot m\cdot a_y\cdot h}{(c_{side}+2\cdot c_{arb})\cdot w^2 - 2\cdot m\cdot g\cdot(h-h_{RC})};$$

$$F_{lz} = m\cdot\left(\frac{g}{2} - \frac{a_y\cdot h}{w}\Big/\left(1 - \frac{2\cdot m\cdot g}{c_{side}+2\cdot c_{arb}}\cdot\frac{h-h_{RC}}{w^2}\right)\right);$$

$$F_{rz} = m\cdot\left(\frac{g}{2} + \frac{a_y\cdot h}{w}\Big/\left(1 - \frac{2\cdot m\cdot g}{c_{side}+2\cdot c_{arb}}\cdot\frac{h-h_{RC}}{w^2}\right)\right);$$

[4.36]

In agreement with intuition and experience the body rolls with positive roll when steering to the left (positive F_{yw}). Further, the body centre of gravity is unchanged in heave (vertical motion, z). The formula uses h_{RC} which we cannot estimate without modelling the suspension. Since front and rear axle normally are different, we could expect that h_{RC} is expressed in some similar quantities for each of front and rear axle, which also is the case, see Equation [4.43].

4.3.7.11.2.1 Steady-State Roll-Gradient *

*Function definition: **Steady state roll-gradient** is the body roll angle per lateral acceleration for the vehicle during steady state cornering with a certain lateral acceleration and certain path radius on level ground.*

4.3.7.11.3 Lateral Load Transfer Models of Suspension Linkage

For longitudinal load transfer, during purely longitudinal dynamic manoeuvres, the symmetry of the vehicle makes it reasonable to split vertical load on each axle equally between the left and right wheel of the axle. However, for lateral dynamics it is not very realistic to assume symmetry between front and rear axle. Hence, the suspension has to be considered separately for front and rear axle. The properties that are important to model for each axle is not only left and right elasticity (as we modelled the whole vehicle in Figure 4-38). It is also how the lateral tyre forces are transmitted from road contact patches to the vehicle body. We end up with conceptually the same two possible linkage modelling concepts as we found for longitudinal load transfer, see Figure 3-60. Either we can introduce 1 roll centre heights for each axle (c.f. pitch centre in 0) or we can introduce two pivot points for each axle (1 per wheel if individually suspended wheels or 2 per axle if rigid axle) (c.f. axle pivot points in 0). A difference for lateral load transfer, compared to longitudinal load transfer, is that it is significant also at steady state (due to centrifugal force). The two modelling ways to include the suspension in the lateral load transfer are shown in Figure 4-39. Generally speaking, they can be combined, so that one is used on front axle and the other on rear axle. In this book, we will select the roll-centre model when modelling.

One should differ between roll-centre heights and roll-centres. One can say that roll-centre heights exists while roll-centres is only a model concept. If a vehicle was actually designed with a roll-centre as being a real pivot point between axle and body, that vehicle would be totally rigid in vertical direction.

4.3.7.11.3.1 Load Transfer Model with Two Pivot Points per Axle

This model will not be deeply presented in this book. However, it should be mentioned as having quite a few advantages:

- The model has both heave and roll degree of freedom. (Roll centre model is restricted to roll around roll centre.)
- If wheel independent suspension, the distribution of lateral wheel forces between left and right side is considered. (Roll centre model only uses the sum of lateral forces per axle and needs involvement of tyre model to resolve into individual left and right side forces.)

Generally spoken, this model is more accurate and not much more computational demanding and probably easier to intuitively understand, since it does not constrain heave motion.

Note that non-individual, rigid axles or beam axles, the pivot-point model does not have one pivot point for each wheel, but instead two pivot points for the whole axle: heave and roll. The roll-centre height affects as the height where lateral force is transferred between axle and body.

Cases when this model is recommended as opposed to the model with roll centres are:

- Steady state and transient manoeuvres where the heave displacement is important.
- When large differences between lateral load on left and right wheels are present, such as:
  - Large load transfer, i.e. high CoG and large lateral accelerations. One example is when studying wheel lift and roll-over tendencies.
  - Large differences between longitudinal slip, while axle skids sideways. Then one wheel might have zero lateral force, due to that friction is used up longitudinally, while the other can have a large lateral force.
  - If individual steering within an axle would be studied. One could think of an extreme case if actuating a sudden toe-in or toe-out, which would cause large but counter-directed lateral forces on left and right wheel.

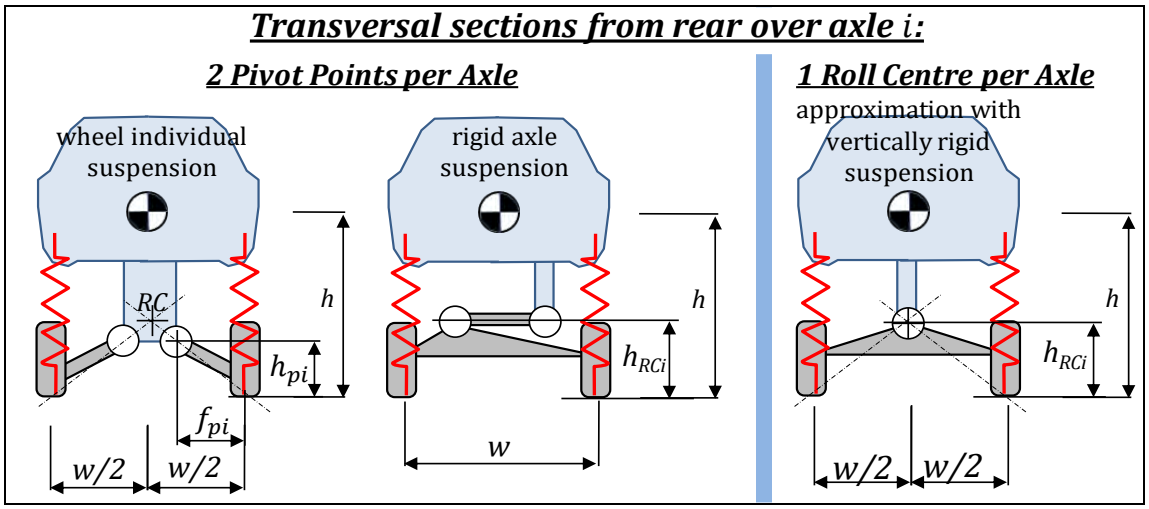


Figure 4-39: Two alternative models for including suspension linkage effects (kinematics) in lateral load transfer. Anti-roll bars not drawn.

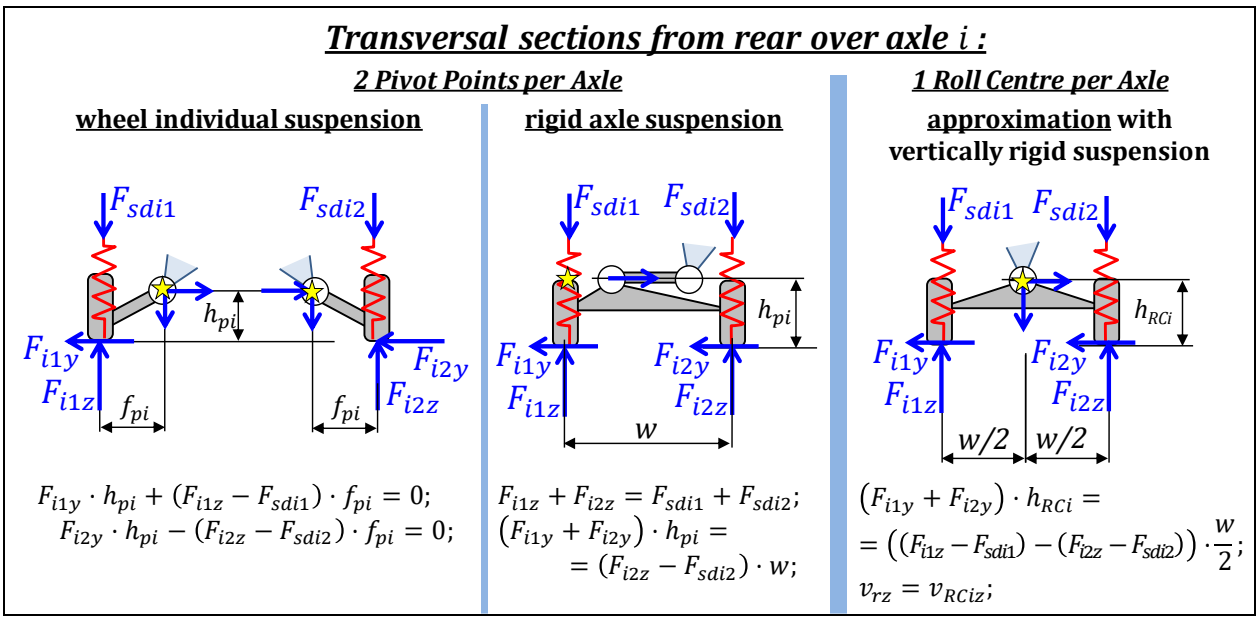


Figure 4-40: The there are equally many (2) equations generated in each model in Figure 4-39.

4.3.7.11.3.2 Load Transfer Model with Roll Centre (One Pivot Point) per Axle

The model with 1 roll centres has some drawback as listen before. To mention some advantages, it is somewhat less computational demanding. However, the main reason why the book uses this model is to cover two different concepts with longitudinal and lateral load transfer.

Study the free-body diagrams in Figure 4-41.

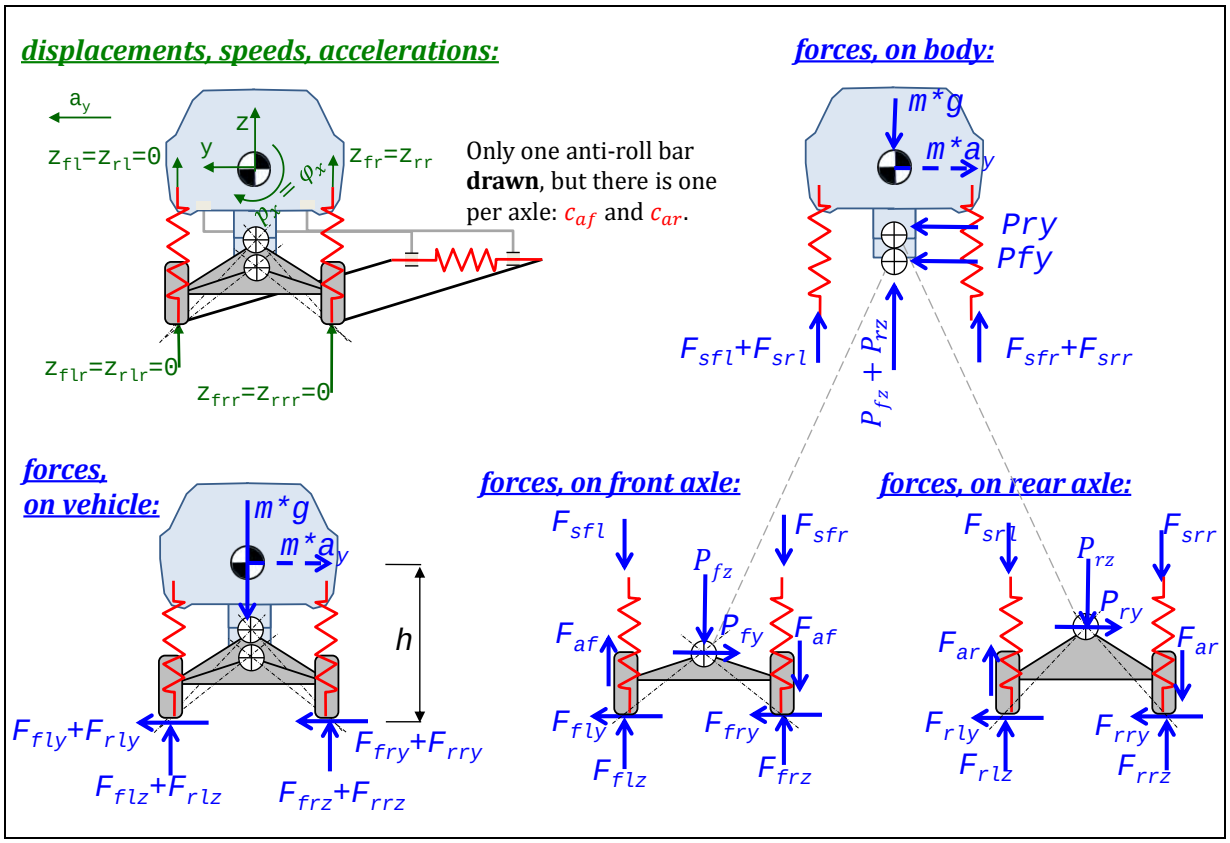


Figure 4-41: Model for steady state heave and roll due to lateral acceleration, using roll centres, which can be different front and rear.

The road is assumed to be flat, $z_{flr} = z_{frr} = z_{rlr} = z_{rrr} = 0$. In free-body diagram for the front axle, P_{fz} and P_{fy} are the reaction force in the rear roll-centre. Corresponding reaction forces are found for rear axle. Note that roll centres are free of roll moment, which is the key assumption about roll centres. The $F_{sfl}, F_{sfr}, F_{srl}$ and F_{srr} are the forces in the compliances, i.e. where potential spring energy is stored. One can understand the roll-centres as also unable to take vertical force, as opposed to constraining vertical motion (as drawn). Which of vertically force-free or vertically motion-free depends on how one understands the concept or roll-centre, and it does not influence the equations.

Note carefully that the "pendulum effect" is NOT included here, in 4.3.7.11.3, as it was in 4.3.7.11.2. The motivation is to get simpler equations for educational reasons.

There is no damping included in model, because their forces would be zero, since there is no displacement velocity, due to the steady-state assumption. As constitutive equations for the compliances (springs) we assume that displacements are measured from a static condition and that the compliances are linear. Note that there are two elasticity types modelled: springs per wheel (c_{fw} per front wheel and c_{rw} per rear wheel) and anti-roll bars per axle (c_{af} front and c_{ar} rear). The road is assumed to be smooth, i.e. $z_{flr} = z_{frr} = z_{rlr} = z_{rrr} = 0$. The stiffnesses c_{fw}, c_{rw}, c_{af} and c_{ar} are effective stiffnesses per wheel. We see already in free-body diagram that F_{fly} and F_{fry} always act together, so we rename $F_{fly} + F_{fry} = F_{fy}$ and $F_{rly} + F_{rry} = F_{ry}$.

$$
\begin{aligned}
&F_{sfl} = F_{sfl0} + c_{fw} \cdot (\cancel{z_{flr}} - z_{fl});\\
&F_{sfr} = F_{sfr0} + c_{fw} \cdot (\cancel{z_{frr}} - z_{fr});\\
&F_{srl} = F_{srl0} + c_{rw} \cdot (\cancel{z_{rlr}} - z_{rl});\\
&F_{srr} = F_{srr0} + c_{rw} \cdot (\cancel{z_{rrr}} - z_{rr});\\
&F_{af} = 0 + c_{af} \cdot \left((\cancel{z_{flr}} - z_{fl}) - (\cancel{z_{frr}} - z_{fr}) \right);\\
&F_{ar} = 0 + c_{ar} \cdot \left((\cancel{z_{rlr}} - z_{rl}) - (\cancel{z_{rrr}} - z_{rr}) \right);\\
&where\ F_{sfl0} = F_{sfr0} = \frac{m \cdot g \cdot l_r}{2 \cdot L};\ \ and\ \ F_{srl0} = F_{srr0} = \frac{m \cdot g \cdot l_f}{2 \cdot L};
\end{aligned}
\qquad [4.37]
$$

Equilibrium for whole vehicle (vertical, lateral, yaw, pitch, roll) neglecting body forces (air resistance and gravity components in road plane) gives:

$$
\begin{aligned}
&F_{flz} + F_{frz} + F_{rlz} + F_{rrz} = m \cdot g;\\
&m \cdot a_y = F_{fy} + F_{ry};\\
&0 = F_{fy} \cdot l_f - F_{ry} \cdot l_r;\\
&-(F_{flz} + F_{frz}) \cdot l_f + (F_{rlz} + F_{rrz}) \cdot l_r = 0;\\
&(F_{flz} + F_{rlz}) \cdot \frac{w}{2} - (F_{frz} + F_{rrz}) \cdot \frac{w}{2} + (F_{fy} + F_{ry}) \cdot h = 0;
\end{aligned}
\qquad [4.38]
$$

Equilibrium for each axle (roll, around roll centre). Note that the axles are considered massless:

$$
\begin{aligned}
&(F_{flz} - F_{sfl} + F_{af}) \cdot \frac{w}{2} - (F_{frz} - F_{sfr} - F_{af}) \cdot \frac{w}{2} + F_{fy} \cdot h_{RCf} = 0;\\
&(F_{rlz} - F_{srl} + F_{ar}) \cdot \frac{w}{2} - (F_{rrz} - F_{srr} - F_{ar}) \cdot \frac{w}{2} + F_{ry} \cdot h_{RCr} = 0;
\end{aligned}
\qquad [4.39]
$$

Compatibility, to introduce body displacements, z, φ_x and φ_y, gives:

$$
\begin{aligned}
&z_{fl} = z + \frac{w}{2} \cdot \varphi_x - l_f \cdot \varphi_y;\ \ and\ \ z_{fr} = z - \frac{w}{2} \cdot \varphi_x - l_f \cdot \varphi_y;\\
&z_{rl} = z + \frac{w}{2} \cdot \varphi_x + l_r \cdot \varphi_y;\ \ and\ z_{rr} = z - \frac{w}{2} \cdot \varphi_x + l_r \cdot \varphi_y;\\
&z_{fl} + z_{fr} = 0;\ \ and\ \ z_{rl} + z_{rr} = 0;
\end{aligned}
\qquad [4.40]
$$

The measure Δh is redundant and can be connected to the other geometry measures as follows. The geometrical interpretation is given in Figure 4-42.

$$
\Delta h = h - \frac{l_r \cdot h_{RCf} + l_f \cdot h_{RCr}}{L};
\qquad [4.41]
$$

Combining Equations [4.37] to [4.41] gives, as Matlab script and solution:

```
syms …; sol=solve( ...
    Fsfl==Fsfl0-cfw*zfl,  Fsfr==Fsfr0-cfw*zfr, ...
    Fsrl==Fsrl0-crw*zrl,  Fsrr==Fsrr0-crw*zrr, ...
    Faf==0-caf*(-zfl+zfr),  Far==0-car*(-zrl+zrr), ...
      Fsfl0==(1/2)*m*g*lr/L,  Fsfr0==(1/2)*m*g*lr/L, ...
      Fsrl0==(1/2)*m*g*lf/L,  Fsrr0==(1/2)*m*g*lf/L, ...
    Fflz+Ffrz+Frlz+Frrz==m*g, ...
    m*ay==Ffy+Fry, ...
    0==Ffy*lf-Fry*lr, ...
    -(Fflz+Ffrz)*lf+(Frlz+Frrz)*lr==0, ...
    (Fflz+Frlz)*w/2-(Ffrz+Frrz)*w/2+(Ffy+Fry)*h==0, ...
      (Fflz-Fsfl+Faf)*w/2-(Ffrz-Fsfr-Faf)*w/2+Ffy*hRCf==0, ...
      (Frlz-Fsrl+Far)*w/2-(Frrz-Fsrr-Far)*w/2+Fry*hRCr==0, ...
    zfl==z+(w/2)*px-lf*py,  zfr==z-(w/2)*px-lf*py, ...
    zrl==z+(w/2)*px+lr*py,  zrr==z-(w/2)*px+lr*py, ...
      zfl+zfr==0,  zrl+zrr==0, ...
    dh==h-(lr*hRCf+lf*hRCr)/(lf+lr), ...
    zfl, zfr, zrl, zrr, Fsfl, Fsfr, Fsrl, Fsrr, ...
    Faf, Far, Fsfl0, Fsfr0, Fsrl0, Fsrr0, ...
```

[4.42]

```
Fflz, Ffrz, Frlz, Frrz, Ffy, Fry, z, px, py, h);
```

The result from the Matlab script in Equation [4.42], but in a prettier writing format:

$$
\begin{aligned}
&F_{fy} = m \cdot a_y \cdot \frac{l_r}{L}; \quad and \quad F_{ry} = m \cdot a_y \cdot \frac{l_f}{L};\\
&z = 0; \quad and \quad p_x = \frac{m \cdot a_y \cdot \Delta h}{c_{vehicle,roll}} = \frac{(F_{fy}+F_{ry}) \cdot \Delta h}{c_{vehicle,roll}}; \quad and \quad p_y = 0;\\
&F_{flz} = m \cdot \left(\frac{g \cdot l_r}{2 \cdot L} - a_y \cdot \left(\frac{h_{RCf} \cdot l_r}{L \cdot w} + \frac{\Delta h}{w} \cdot \frac{c_{f,roll}}{c_{vehicle,roll}} \right) \right);\\
&F_{frz} = m \cdot \left(\frac{g \cdot l_r}{2 \cdot L} + a_y \cdot \left(\frac{h_{RCf} \cdot l_r}{L \cdot w} + \frac{\Delta h}{w} \cdot \frac{c_{f,roll}}{c_{vehicle,roll}} \right) \right);\\
&F_{rlz} = m \cdot \left(\frac{g \cdot l_f}{2 \cdot L} - a_y \cdot \left(\frac{h_{RCr} \cdot l_f}{L \cdot w} + \frac{\Delta h}{w} \cdot \frac{c_{r,roll}}{c_{vehicle,roll}} \right) \right);\\
&F_{rrz} = m \cdot \left(\frac{g \cdot l_f}{2 \cdot L} + a_y \cdot \left(\frac{h_{RCr} \cdot l_f}{L \cdot w} + \frac{\Delta h}{w} \cdot \frac{c_{r,roll}}{c_{vehicle,roll}} \right) \right);
\end{aligned}
\qquad [4.43]
$$

where, roll stiffnesses are:

$$
\begin{aligned}
&c_{f,roll} = 2 \cdot \left(c_{fw} + 2 \cdot c_{af}\right) \cdot \left(\frac{w}{2}\right)^2 \quad \left[\frac{Nm}{rad}\right];\\
&c_{r,roll} = 2 \cdot \left(c_{rw} + 2 \cdot c_{ar}\right) \cdot \left(\frac{w}{2}\right)^2 \quad \left[\frac{Nm}{rad}\right];\\
&c_{vehicle,roll} = c_{f,roll} + c_{r,roll} \quad \left[\frac{Nm}{rad}\right];
\end{aligned}
$$

The axle roll stiffnesses, $c_{f,roll}$ and $c_{r,roll}$ are identified beside vehicle roll stiffness $c_{vehicle,roll}$. We should compare Equation [4.43] with Equation [4.36]. Eq [4.36] considers the "(roll) pendulum effect", but not the differentiation between front and rear suspension. Eq [4.43] does the opposite.

Assume $h = h_{RC}$ and look at the sum of vertical force on one side, F_{lz} in Eq [4.36]. Compare F_{zl} in Eq [4.36] and $F_{flz} + F_{rlz}$ in Eq [4.43]; the equations agree if:

$$
\begin{aligned}
&F_{flz} + F_{rlz} = F_{zl} \Rightarrow \; m \cdot \left(\frac{g}{2} - a_y \cdot \left(\frac{h_{RCf} \cdot l_r + h_{RCr} \cdot l_f}{L \cdot w} + \frac{\Delta h}{w} \right) \right) = m \cdot \left(\frac{g}{2} - a_y \cdot \frac{h}{w} \right) = F_{zl} \Rightarrow\\
&\Rightarrow \frac{h_{RCf} \cdot l_r + h_{RCr} \cdot l_f}{L \cdot w} + \frac{\Delta h}{w} = \frac{h}{w} \Rightarrow h_{RCf} \cdot l_r + h_{RCr} \cdot l_f = (h - \Delta h) \cdot L;
\end{aligned}
$$

This is exactly in agreement with the definition of the redundant geometric parameter Δh, see Eq [4.41]. This means that a consistent geometric model of the whole model is as drawn in Figure 4-42. Here the artefact roll axis is also defined.

The terms of type $h_{RCi} \cdot l_j/(L \cdot w)$ in Eq [4.43] can be seen as the part of the lateral tyre forces that goes via the stiff linkage. The terms of type $(\Delta h/w) \cdot \left(c_{iw}/\left(c_{iw} + c_{jw}\right)\right)$ in Eq [4.43] can be seen as the part of the lateral tyre forces that goes via the compliance. The latter part is distributed in proportion to roll stiffness of the studied axle, as a fraction of the vehicle roll stiffness. This should agree with intuition and experience from other preloaded mechanical systems (load distributes as stiffness).

Body rolls with positive roll when steering to the left, as long as CoG is above roll axle. Further, the body centre of gravity is unchanged in heave (vertical z) because the model does not allow any vertical displacements, which is a drawback already mentioned.

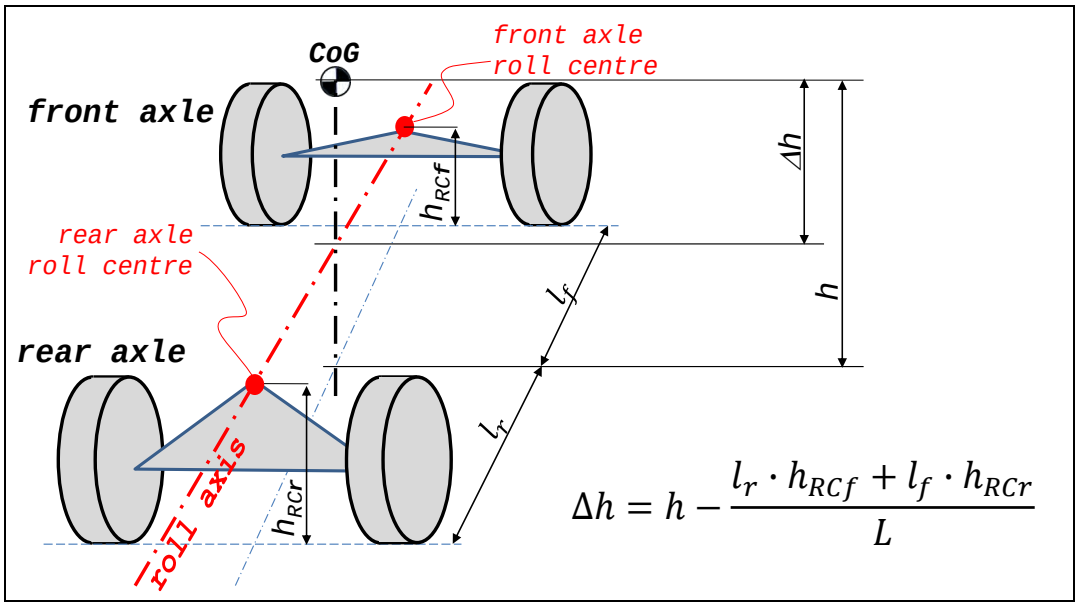


Figure 4-42: Roll axis for a two-axle vehicle. (Note that the picture may indicate that the roll centres and roll axis are above wheel centre, but this is normally not the case.)

Eq [4.49] was derived as a *steady state out-of-road-plane* model, but only the ratio between roll stiffnesses influence the lateral load transfer. So, if the roll stiffnesses are large, they can be neglected (considered infinite), if the ratios are given. Then, Eq [4.49] works also for transient manoeuvres.

4.3.7.11.3.3 Steady State Longitudinal and Lateral Distribution

If the vehicle has a steady state acceleration with combined a_x and a_y, we can combine Eqs [4.43]and [3.35] (with $(F_{fx} + F_{rx}) = m \cdot a_x$) to Eq [4.44]. Note:

- Body forces (air resistance and gravity components in road plane) are neglected.
- We have also assumed symmetric longitudinal load transfer. This is reasonable if no roll pre-tension. Pre-tension could appear if uneven ground or unusual suspension, e.g. pre-tensioned (or "active") anti-roll bar.

$$
\begin{aligned}
F_{flz} &= m \cdot \left(\frac{g \cdot l_r}{2 \cdot L} - a_x \cdot \frac{h}{2 \cdot L} - a_y \cdot \left(\frac{h_{RCf} \cdot l_r}{L \cdot w} + \frac{\Delta h}{w} \cdot \frac{c_{f,roll}}{c_{vehicle,roll}} \right) \right); \\
F_{frz} &= m \cdot \left(\frac{g \cdot l_r}{2 \cdot L} - a_x \cdot \frac{h}{2 \cdot L} + a_y \cdot \left(\frac{h_{RCf} \cdot l_r}{L \cdot w} + \frac{\Delta h}{w} \cdot \frac{c_{f,roll}}{c_{vehicle,roll}} \right) \right); \\
F_{rlz} &= m \cdot \left(\frac{g \cdot l_f}{2 \cdot L} + a_x \cdot \frac{h}{2 \cdot L} - a_y \cdot \left(\frac{h_{RCr} \cdot l_f}{L \cdot w} + \frac{\Delta h}{w} \cdot \frac{c_{r,roll}}{c_{vehicle,roll}} \right) \right); \\
F_{rrz} &= m \cdot \left(\frac{g \cdot l_f}{2 \cdot L} + a_x \cdot \frac{h}{2 \cdot L} + a_y \cdot \left(\frac{h_{RCr} \cdot l_f}{L \cdot w} + \frac{\Delta h}{w} \cdot \frac{c_{r,roll}}{c_{vehicle,roll}} \right) \right);
\end{aligned}
\qquad [4.44]
$$

4.3.7.12 High Speed Steady State Vehicle Functions

4.3.7.12.1 Steering Feel *

*Function definition: **Steering feel** is the steering wheel torque response to steering wheel angle. The function is used in a very wide sense; on a high level, it is a measure of steering wheel torque, or its variation, for certain driving situations. Often, it can only be subjectively assessed.*

At steady state driving at high speed, there are basically three aspects of steering feel:

- Lateral steering feel feedback at cornering: The steering wheel torque is normally desired to increase monotonously with lateral forces on the front axle. This is basically the way the mechanics work due to castor trail. Some specifications on steering assistance system is however needed to keep the steering wheel torque low enough for comfort.

- Steering torque drop when cornering at low friction: It is built into the mechanics of the castor trail and the pneumatic trail that steering wheel torque drops slightly when one approaches the friction limit on front axle. This is normally a desired behaviour because it gives driver feedback that the vehicle is approach the limits.
- On-centre feel in straight line driving: When the vehicle is driven in straight line, the steering wheel is normally desired to return to centre position after small perturbations. This is a comfort function, which OEMs works a lot with, and it is often rather subjectively assessed.

4.3.7.12.2 High Speed Steady-State Off-tracking *

Function definition: ***High speed steady-state off-tracking*** *is the lateral offset between the paths of the centre of the front axle and the centre of the most severely off-tracking axle of any unit in a steady turn at a certain friction level and a certain constant longitudinal speed. From Reference [(Kati, 2013)].*

The function is mainly of interest for long combination vehicles, as illustrated in Figure 4-43. Off-tracking was also mentioned in 4.2. It measures the lateral road space required. High speed Off-tracking, which is an outboard off-tracking, can be either determined in a steady state turn or in a transient manoeuvre such as lane change; the latter is termed as high speed transient off-tracking, see 4.5.6.2.

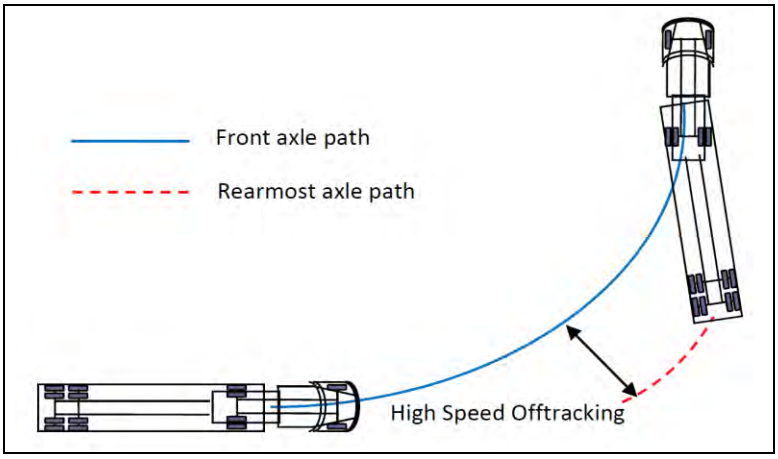


Figure 4-43: Illustration of high speed off-tracking. From (Kharrazi , 2012).

4.3.7.12.3 Tracking-Ability on Straight Path, TASP *

Function definition: ***Tracking-ability on straight path, TASP*** *is the swept width between outer-most axle centres when driving at a road with certain cross-fall and certain road friction at a certain speed.*

The axles on any vehicle driving at a road with cross-fall will not track exactly in each other axle's trajectories. This is especially pronounced if long vehicles with many articulation points. The driving situation is straight steady state low or high speed.

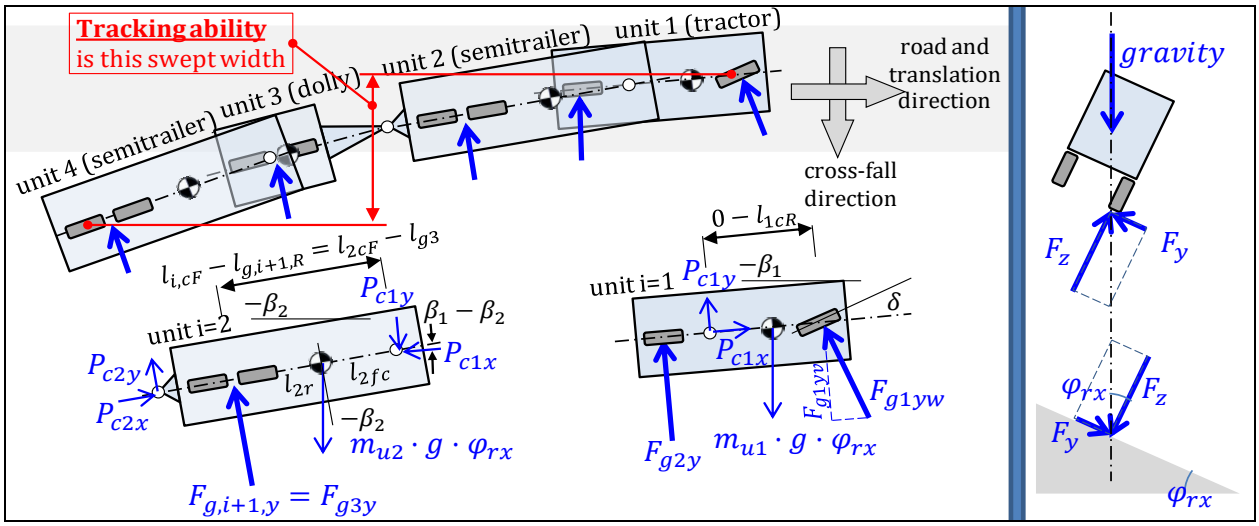


Figure 4-44: Tracking ability on straight path, TASP, for an "A-double". Longitudinal forces neglected. Axles within an axle group lumped together, $g1, g2, \cdots, g5$. (Longitudinal dimensions as in Figure 1-67.)

An example is seen in Figure 4-44. If we neglect combined tyre slip and assume same cornering coefficient, CC, on all axles we can derive these equations, one for each axle group:

- $F_{g1yw} = -CC \cdot F_{g1z} \cdot (\beta_1 - \delta)$;
- $F_{g2y} = -CC \cdot F_{g2z} \cdot \beta_1$;
- $F_{g,i+1,y} = -CC \cdot F_{g,i+1,z} \cdot \beta_i$; $\quad for\ unit\ i = 2..4$

Since the levers for moment equilibria in road xy-plane and in road xz-plane are equal, the distribution of the axles' vertical forces and lateral forces becomes identical. So, relation between lateral force and vertical force becomes $\frac{F_{gjy}}{F_{gjz}} = \tan(\varphi_{rx}) \approx \varphi_{rx}$ for all axle groups $j = 2..5$ and $\frac{F_{g1yv}}{F_{g1z}} \approx \frac{F_{g1yw}}{F_{g1z}} \approx \varphi_{rx}$:

- $\frac{F_{g1yw}}{F_{g1z}} \approx \varphi_{rx} \approx -CC \cdot (\beta_1 - \delta)$;
- $\frac{F_{g2y}}{F_{g2z}} \approx \varphi_{rx} \approx -CC \cdot \beta_1$;
- $\frac{F_{g,i+1,y}}{F_{g,i+1,z}} \approx \varphi_{rx} \approx -CC \cdot \beta_i$; $\quad for\ unit\ i = 2..4$

Solving for side slip angles and steer angle:

- $\beta_i \approx \frac{-\varphi_{rx}}{CC}$; $\quad for\ unit\ i = 1..4$
- $\delta \approx \frac{\varphi_{rx}}{CC} + \beta_1 \approx \frac{\varphi_{rx}}{CC} + \frac{-\varphi_{rx}}{CC} \approx 0$; (the model is too approximative to give a good values of δ)

The swept width becomes: $SweptWidth = TASP \approx$

$$\approx (0 - l_{1cR}) \cdot \beta_1 + (l_{2cF} - l_{g3}) \cdot \beta_2 + (l_{3cF} - l_{g4}) \cdot \beta_3 + (l_{4cF} - l_{g5}) \cdot \beta_4 \approx$$

$$\approx \left((0 - l_{1cR}) + (l_{2cF} - l_{g3}) + (l_{3cF} - l_{g4}) + (l_{4cF} - l_{g5})\right) \cdot \frac{-\varphi_{rx}}{CC};$$

This can be summarized as:

$$TASP \approx [distance\ between\ first\ and\ last\ axle\ group] \cdot \frac{\varphi_{rx}}{CC}; \qquad [4.45]$$

The model is very approximative, since it does **not** take the following aspects into account:

- Axles within an axle group can take different vertical force.
- Axles can have different cornering coefficient CC.
- Large road grades. This can influence via longitudinal forces and both articulation angles and combined tyre slip. The effect would be larger if combined with low road-friction.

More accurate value of TASP can be found by simulation to a steady-state pose of the vehicle.

4.3.7.13 Roll-Over in Steady State Cornering

When going in curves, the vehicle will have roll angles of typically some degrees. At that level, the roll is a comfort issue. However, there are manoeuvres which can cause the vehicle to roll-over, i.e. roll ≥ 90 deg so that vehicle body crashes into ground. Roll-over can be seen as a special event, but if sorting into the chapters of this book it probably fits best in present chapter, about lateral dynamics.

One can categorize roll-overs in e.g. 3 different types:

- **Tripped roll-over**. This is when the car skids sideways and hits an edge, which causes the roll-over. It can be an uprising edge, e.g. pavement or refuge. It can be the opposite, a ditch or loose gravel outside road. In both these cases, it is strong lateral forces on the wheels on one side of the vehicle that causes the roll-over. Tripped roll-over can also be when the vehicle is exposed to large one-sided vertical wheel forces, e.g. by running over a one-sided bump. A third variant of tripped roll-over is when the vehicle is hit by another vehicle so hard that it rolls over.
- **Un-tripped roll-over** or on-road roll-overs. These happen on the road and triggered by high tyre lateral forces. This is why they require high road friction. For sedan passenger cars, these events are almost impossible, since road friction seldom is higher than approximately 1. For SUVs, un-tripped roll-overs can however occur but require dry asphalt roads, where friction is around 1. For trucks, un-tripped roll-over, can happen already at very moderate friction, like 0.4, due to their high CoG in relation to track width. Within un-tripped roll-overs, one can differ between:
  - **Steady state roll-over**. If lateral acceleration is slowly increased, e.g. as running with into a hairpin curve or a highway exit, the vehicle can slowly lift off the inner wheels and roll-over. This is the only case of roll-over for which a model is given in this book.
  - **Transient roll-over**. This is when complex manoeuvres, like double lane changes or sinusoidal steering, are made at high lateral accelerations. This can trigger roll eigen-modes, which can be amplified due to unlucky timing between the turns. Models from 4.4.3.4 can be used as a start, but it is required that load transfer is modelled carefully and includes wheel lifts, suspension end-stops and bump stops.

4.3.7.13.1 Roll-Over Threshold Definitions

An overall requirement on a vehicle is that the vehicle should not roll-over for certain manoeuvres. Heavy trucks will be possible to roll-over on high-mu conditions. The requirement for those is based on some manoeuvres which not utilize the full road friction. For passenger cars, it is often the intended design that they should be impossible to roll-over, even at high mu. Any requirement needs a definition of what exactly roll-over is, i.e. a Roll over threshold definition. Candidates for Roll over threshold definition are:

- **One wheel** lifts from ground
- All wheels on **one side** lift from ground
- Vehicle **CoG** reaches its **highest point** (point of no-return towards roll ≥ 90 deg)

Note that:

- It is the 3rd threshold which really is the limit, but other can still be useful in requirement setting. To use the 3rd for requirement setting makes the verification much more complex, of course in real vehicles but also in simulation.
- The 1st is not a very serious situation for a conventional vehicle with 4 wheels. However, for a 3-wheeled vehicle, such as small “Tuctucs” or a 3-wheel moped, it is still a relevant threshold.
- The 2nd threshold is probably the most useful threshold for two-tracked vehicles, because it defines a condition from which real roll-over is an obvious risk, and still it is relatively easy to test and simulate. For 3-wheeled vehicle, 2nd and 3rd threshold generally coincide. The 2nd threshold will be used in this book.

Figure 4-45 shows how the inner wheels lift off subsequently during a slowly increasing lateral force (or lateral acceleration) build-up. Before any wheel is lifted, the load transfer is proportional to roll-centre heights and roll stiffnesses, as shown in Equation [4.43]. But every time a wheel lifts, the distribution changes, so that a "knee" on the curves appears, see Figure 4-45. So, the relation of type as Equation [4.43] is no longer valid. For instance, it is not physically motivated to keep the roll-centre model for an axle which has lifted one side. So, the prediction of critical lateral acceleration for roll-over is not trivial, especially for heavy vehicles which has many axles, and often also a fifth wheel which can transfer roll-moment to a certain extent. There are approximate standards for how to calculate steady state roll-over thresholds for such vehicle, e.g. UN ECE 111 (http://www.unece.org/fileadmin/DAM/trans/main/wp29/wp29regs/r111e.pdf).

```
model Vehicle_1Unit_NAxles
  …
equation
  //Test case (Steady state cornering, incr. a_y, until left lifts):
  der(p_x)=1; // p_x=0.01; //
  when sum(Lift)>=na then
    terminate("Both left wheels lifted");
  end when;

//Whole unit (=vehicle in this case):
  //Equilibria irp:  //Lateral:
  0= sum(F_ay) - m*a_y;
  //Yaw:
  0 = sum(F_ay.*(x_a-x_CoG*ones(na)));
  //Equilibria oorp:  //Vertical:
  0 = sum(F_alz+F_arz) - m*g;
  //Pitch:
  0 = sum((F_alz+F_arz).*(x_a-x_CoG*ones(na)));
  //Roll, around mid ground:
  0=m*a_y*h + sum(F_alz)*w/2 - sum(F_arz)*w/2;

//For each axle:
  for i in 1:na loop
    //Equilibria:    //Roll, around pivot point:
    0 = F_ay[i]*h_aRC[i] + (F_alz[i] - F_arz[i])*w/2 - M_ax[i];
    //Constitution:    //Tyre:
    F_ay[i]=-CC_y*(F_alz[i]+F_arz[i])*s_ay[i];
    s_ay[i]=v_ay[i]/v_x;
    v_ay[i]=v_y+(x_a[i]-x_CoG)*w_z;
    //Suspension:
    der(M_ax[i]) = c_a[i]*(der(p_ax[i]) - der(p_x));
     if Lift[i] > 0.5 then
       der(F_alz[i]) = 0;
     else       der(p_ax[i]) = 0;       end if;
    when (pre(Lift[i]) < 0.5) and F_alz[i] < 0 then
      Lift[i] = 1;       reinit(p_ax[i], 0);          end when;
  end for;

//Suspension Ctrl. Generates eqs only if number of axles=na>2:
  for i in 2:(na-1) loop
    der(F_alz[i])+der(F_arz[i])=der(F_alz[i+1])+der(F_arz[i+1]);
  end for;

end Vehicle_1Unit_NAxles;
```

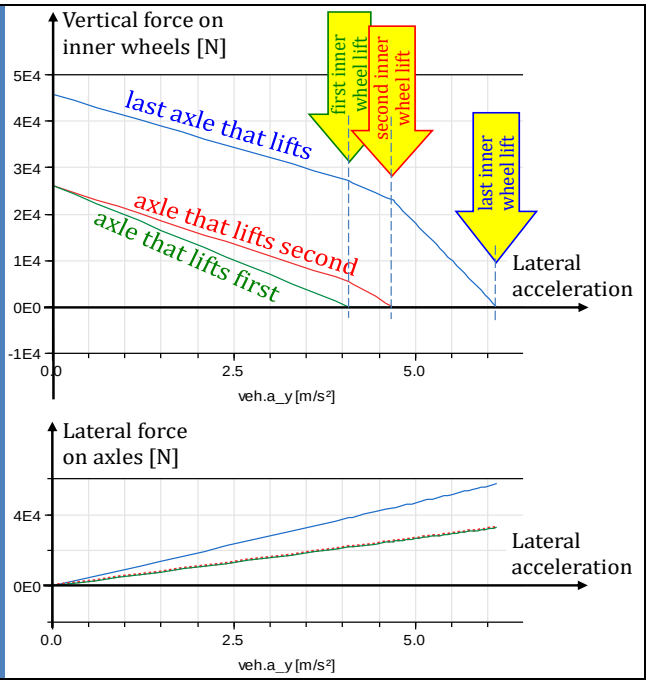


Figure 4-45: Example of 3-axle vehicle steady state roll-over wheel lift diagram.

4.3.7.13.1.1 Roll-Over Model

One way to assess the steady state roll-over lateral acceleration is to model a dynamic system with roll angle as independent variable (instead of time) and then simulate (i.e. study over a lapse with increasing roll angle). When all wheels on one side lifts from ground, we define it as steady state roll-over lateral acceleration. The model is then much more intuitively physical than, e.g. UN ECE 111 formulas.

Figure 4-45 shows a Modelica model of a 1-unit N-axles vehicle. Note that, since 3 axles means non-Ackermann steering geometry, it necessarily involves the lateral tyre slip stiffnesses also. The model can, with maintained physical interpretation, be extended to more units with roll-free or roll-rigid connections. Phenomena as (roll) pendulum effect and lateral deformation of tyres can also be added.

An alternative way of computing the critical lateral acceleration is to use the same model, but not simulate it. Instead one could solve the states where assume that all axles except one are lifted and then see how much lateral acceleration is needed to lift the last axle. Trying each axle to be the last to lift gives several lateral acceleration values, whereof the smallest is the critical lateral acceleration.

4.3.7.13.2 Static Stability Factor, SSF

One very simple measure of the vehicles tendency to roll-over is the Static Stability Factor, SSF. It is proposed by NHTSA, http://www.nhtsa.gov/cars/rules/rulings/roll_resistance/, and it is simply defined as:

$$\text{SSF} = \frac{Half\ TrackWidth}{HeigthOfCoG} = \frac{w/2}{h}; \qquad [4.46]$$

A requirement which requires *SSF>number* cannot be directly interpreted in terms of certain manoeuvre and certain roll-over threshold. It is not a *performance-based requirement*, but a *design-based* (or *prescriptive*) *requirement*. However, one of many possible performance-based *interpretations* is that the vehicle shall not roll-over for steady-state cornering on level ground with an enough friction coefficient. Another is that it should not roll-over in a tilt-table. Since the requirement is not truly performance based, each interpretation will also stipulate a certain verification method; here it would be theoretical verification using a rigid suspension model. Such model and threshold are shown in Figure 4-46.

The derivation of the SSF based requirement looks as follows:

$$\left.\begin{array}{l} Model: \left\{\begin{array}{c} F_{iz}\cdot w + m\cdot a_y \cdot h = m\cdot g\cdot \frac{w}{2}; \\ F_{iz} + F_{oz} = m\cdot g; \\ m\cdot a_y = F_y = \mu\cdot(F_{iz}+F_{oz}); \end{array}\right\} \Rightarrow F_{iz} = m\cdot g\cdot\left(\frac{1}{2} - \frac{h\cdot\mu}{w}\right); \\ Requirement: F_{iz} \geq 0; \end{array}\right\} \Rightarrow$$

$$\Rightarrow Requirement: \frac{1}{2} > \frac{h\cdot\mu}{w} \Rightarrow \frac{w}{2\cdot h} = SSF > \mu; \qquad [4.47]$$

Maximum road friction, μ, is typically 1, which is why SSF>μ=1 would be a reasonable. However, typical values of SSF for passenger vehicles are between 0.95 and 1.5. For heavy trucks, it can be much lower, maybe 0.3..0.5, much depending on how the load is placed. There are objections to use SSF as a measure, because SSF ignores suspension compliance, handling characteristics, electronic stability control, vehicle shape and structure.

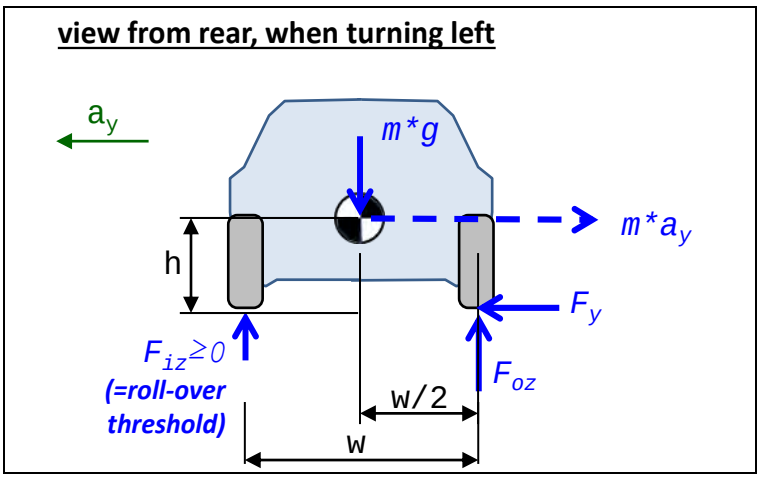


Figure 4-46: Model for verification of requirement based on Static Stability Factor, SSF.

4.3.7.13.3 Steady-State Cornering Roll-Over *

A function defined for requirement setting can be:

> *Function definition:* ***Steady state cornering roll-over acceleration*** *is the maximum lateral acceleration the vehicle can take in steady state cornering without lifting all inner wheels. On level ground with enough road friction and certain weight and position of payload.*

For a long combination-vehicle with several articulation points, one often need to drive a long distance after a steer angle change before steady state values on articulation angles are reached. Hence, it can be more relevant to formulate a corresponding roll-over function in terms of curvature to follow, total yaw angle for turn and longitudinal speed. A common way is also the, somewhat artificial, tilt-table test, which means that one measure steady-state roll-over with a (real or virtual) tilt-table where the

maximum road pitch angle before wheel lift on one side is the measure to set requirement on. An even simpler way to handle steady-state roll-over is to set requirement on the SSF.

Consider a roll-stiff vehicle in steady state cornering. Assume lateral acceleration is subsequently increased. If the vehicle is a two-axle vehicle, Eq [4.43] is valid until first axle lifts its inner wheel, since for larger lateral accelerations, the constitutive equation Eq [4.37] is invalid for the inner wheel, since the lifted inner wheel has zero force from ground. We can identify the terms of one of the inner wheels (if $a_y > 0$) equations in Eq Eq [4.43] as follows:

$$F_{flz} = m \cdot \left(\frac{g \cdot l_r}{2 \cdot L} - a_y \cdot \left(\frac{h_{RCf} \cdot l_r}{L \cdot w} + \frac{\Delta h}{w} \cdot \frac{c_{f,roll}}{c_{roll,vehicle}} \right) \right) =$$

$$= \frac{1}{2} \cdot \underbrace{\frac{m \cdot g \cdot l_r}{2 \cdot L}}_{VerticalForceOnAxle} - \underbrace{m \cdot a_y \cdot \frac{l_r}{L}}_{LateralForceOnAxle} \cdot \frac{h_{RCf}}{w} - \underbrace{m \cdot a_y}_{LateralForceOnVehicle} \cdot \frac{\Delta h}{w} \cdot \underbrace{\frac{c_{f,roll}}{c_{roll,vehicle}}}_{RollStiffnessFractionOnAxle} =$$

$$= \frac{F_{iz}}{2} - F_{iy}(a_y) \cdot \frac{h_{RCi}}{w} - F_y(a_y) \cdot \frac{\Delta h}{w} \cdot \frac{c_{i,roll}}{c_{roll,vehicle}};$$

If the vehicle has more axles, Eq [4.43] is generalized to Eq [4.48], which also is valid until first inner wheel lifts from ground.

For axle i of a roll-stiff vehicle:

$$F_{ilz} = \frac{F_{iz}}{2} - F_{iy}(a_y) \cdot \frac{h_{RCi}}{w} - F_y(a_y) \cdot \frac{\Delta h_i}{w} \cdot \frac{c_{i,roll}}{c_{roll,vehicle}}; \quad [4.48]$$

For a vehicle with >2 axles, the parameter Δh_i can not be calculated from Eq [4.41], but can still be understood as the vertical distance between roll axis and the axles roll centre. It should be noted that the pendulum effect is **not** included in Eq [4.48], and this is often a significant approximation if applied on high CoG vehicles, like heavy trucks.

4.3.7.13.3.1 Model Assuming All Inner Wheels Lift at the Same Lateral Acceleration

An approximation of Steady state cornering roll-over acceleration $a_{y,crit}$ (lateral acceleration when all inner wheels lifted) can be found for vehicles where Eq [4.48] gives $F_{ilz} = 0$ for all axles at same a_y. Then, summing the Eq [4.48] for all axles leads to the Eq [4.49] which is the same $a_{y,crit}$ as the simple SSF model in Figure 4-46 and 4.3.7.13.2 gives.

$$a_{y,crit} = \frac{w \cdot g}{2 \cdot h}; \quad [4.49]$$

In the following, we will elaborate with 4 additional effects, which marked in Figure 4-47.

- The tyre will take the vertical load on its **outer edge** in a roll-over situation. This suggests a change of performance and requirement to: $\frac{a_y}{g} < \frac{w+w_{tyre}}{2 \cdot h}$ and $\frac{w+w_{tyre}}{2 \cdot h} > \mu$. This effect is accentuated when low tyre profile and/or high inflation pressure. This effect **decreases** the risk for roll-over.
- Due to suspension and tyre **lateral deformation**, the body will translate laterally outwards, relative to the tyre. This could motivate $\frac{a_y}{g} < \frac{w-Def_y}{2 \cdot h}$ and $\frac{w-Def_y}{2 \cdot h} > \mu$. This effect **increases** the risk for roll-over.
- Due to suspension linkage and compliances, the **body will roll**. Since the CoG height above roll axis, Δh, normally is positive, this could motivate $\frac{a_y}{g} < \frac{w-\Delta h \cdot \varphi_x}{2 \cdot h}$ and $\frac{w-\Delta h \cdot \varphi_x}{2 \cdot h} > \mu$. This effect **increases** the risk for roll-over. At heavy vehicle this "(roll) pendulum effect" is large.
- Due to suspension linkage and compliances, the body will also heave. This requires a suspension model with pivot points per wheel, as opposed to roll-centre per axle. The heave is

normally positive. This could motivate $\frac{w}{2 \cdot (h+z)} > \mu$ and $\frac{a_y}{g} < \frac{w}{2 \cdot (h+z)}$. The effect is sometimes called "jacking" and it **increases** the risk for roll-over.

- Road leaning left/right (road banking) or driving with one side on a different level (e.g. outside road or on pavement) also influence the roll-over performance.

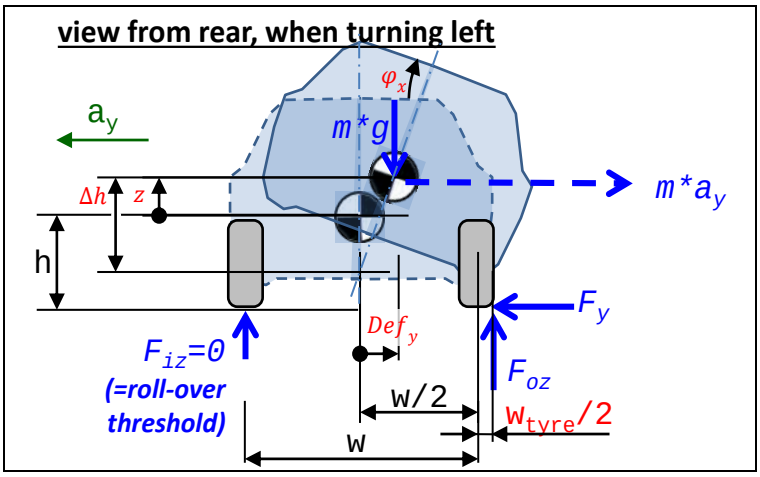


Figure 4-47: Steady-state roll-over model, with fore/aft symmetry. The measures w_{tyre}, Def_y, $\Delta h \cdot \varphi_x$ and z mark effects additional to what is covered with a simple SSF approach.

4.3.7.13.3.2 Model with Sequential Lifts of Inner Wheels

A model which does not assume wheel lift at same lateral acceleration will be sketched. For each axle that has lifted, the equations have to be changed. Instead of simply the constitutive equation $(F_{ilz} - F_{irz}) \cdot w/2 = c_{i,roll} \cdot \varphi_x$; one need to assure $F_{ilz} = 0$;. The axle will then position itself so that it keeps $F_{ilz} + F_{irz} = F_{iz,static}$;. That means both roll and vertical translation of the axle centre, why also the vertical suspension compliance needs to be modelled. A new position variable has to be declared, e.g. the lift distance of the inner wheel, $lift_{ilz}$. This variable is constrained to $lift_{ilz} = 0$; before lift, but after lift the constraint is $F_{ilz} = 0$;. So, the model is suitably implemented as a state event model with the event "*when* F_{ilz} *becomes* < 0". If a_y is swept from zero and upwards, the result will be something like shown in Figure 4-45.

4.3.7.13.3.3 Using a Transient Model for Steady-State Roll-Over

Another work-around to avoid complex algebra is to run a fully transient model, including suspension, and run it until a steady state cornering conditions occur. If then, the lateral acceleration is slowly increased, one can identify when or if the roll-over threshold is reached. Lateral acceleration increase can be through either increase of longitudinal speed or steer angle. It should be noted that the model should reasonably be able to manage at least lift of one wheel from the ground. This way of verifying steady state cornering roll-over requirements has the advantage that, if using tyre models with friction saturation, the limitation discussed in 4.3.7.13.3.2 does not have to be checked separately.

4.3.7.13.4 Roll-Over and Understeering/Propulsion

With the above formulas for roll-over there will always be a certain lateral acceleration that leads to roll-over, because neither limitation due to road friction nor propulsion power modelled yet. Since vehicles generally are understeered, they are limited to develop lateral acceleration, see Figure 4-30. For propulsion-weak vehicles, there is also the limitation of lateral acceleration due to limited longitudinal speed, which in turn is due to driving resistance from the steered wheels (=wheel lateral force * sin(steer angle)) and loosing propulsion power due to longitudinal wheel slip. However, one should consider that the propulsion limitation is less in down-hill driving, which increases the roll-over risk again. Also, if the vehicle goes relatively quickly into steady state cornering, the longitudinal speed will not have time to decelerate to its real (longitudinal) steady state value.

For heavy trucks, the critical lateral acceleration is typically $(0.3..0.4) \cdot g$, which is quite possible to reach during normal road conditions, because road friction is around 1. For passenger cars, the critical

lateral acceleration is typically in the region of 1, so it is often not possible to reach the roll-over-critical lateral acceleration. This is also the case for heavy trucks on low road friction.

4.4 Stationary Oscillating Steering

In between steady state and transient manoeuvres, one can identify stationary oscillations as an intermediate step. Generally, a mechanical system can be excited with a stationary oscillating excitation. The response of the system is, after possible transients are damped out, a stationary oscillation. How this response vary with excitation frequency will be called Frequency Response. If staying within the linear region for the system and the excitation is harmonic (sinus and cosine), the ratio between the response amplitude and the excitation amplitude is only dependent of the frequency. The ratio is called *transfer function*.

For lateral vehicle dynamics, the excitation is typically steering wheel angle and the response is amplitudes of yaw velocity, curvature or lateral acceleration. The corresponding transfer functions are a frequency version of the gains defined in Equation [4.21]. Also, there will be a delay between excitation and response. This is another important measure, beside the amplitude ratio.

4.4.1 Stationary Oscillating Steering Tests

When testing stationary oscillating steering functions, one usually drives on a longer part of the test track. It might be a high-speed track, see Figure 1-70, because the track rather needs to be long than wide, since one is often not too close to lateral grip limits. If the available Vehicle Dynamics Area, see Figure 1-70, is long enough this is of course a safer option. A Vehicle Dynamics Area is a flat surface with typically 100..300 m diameter. It normally has entrance roads for accelerating up to a certain speed.

Typical tests for Stationary oscillating steering functions:

- Sweeping frequency (chirp) and/or amplitude
- Random frequency and amplitude

There are ISO standards for sweeping and random tests. The Frequency Response will be very dependent of the vehicle longitudinal speed, why the same tests are typically done at different such speeds.

4.4.2 One-Track Model for Two-Axle Vehicle for Transient Dynamics

Stationary oscillating steering can often be of interest also with so small amplitudes that a linear model is accurate enough. Such linear model will be derived in 4.4.2. A transient one-track model will first be derived and then approximated to become linear. The resulting linear model is found Eq [4.55] and a less general derivation of it is found in Figure 4-51. Note that road is assumed to be level, i.e. down-grade (or pitch grade) of road $\varphi_{ry} = 0$. Therefore, neither φ_{ry} or yaw angle φ_z appears in model.

The vehicle model is sketched in Figure 4-49. The model is similar to the model for steady state cornering in Figure 4-16, with the following changes:

- Longitudinal and lateral accelerations have both components of centripetal acceleration ($\omega_z \cdot v_y$ and $\omega_z \cdot v_x$) and the derivatives $\dot{v}_x$ and $\dot{v}_y$:

$$a_x = \dot{v}_x - \omega_z \cdot v_y; \qquad a_y = \dot{v}_y + \omega_z \cdot v_x; \qquad [4.50]$$

  (Often, $v_y \ll v_x$, why $\omega_z \cdot v_y$ is more neglectable than $\omega_z \cdot v_x$.)

- The yaw acceleration, $\dot{\omega}_z$, is no longer zero.

- The speed v_x is no longer defined as a parameter, but a variable. Then, one more prescription is needed to be a consistent model. For this purpose, an equation that sets front axle propulsion torque to 1000 Nm is added.

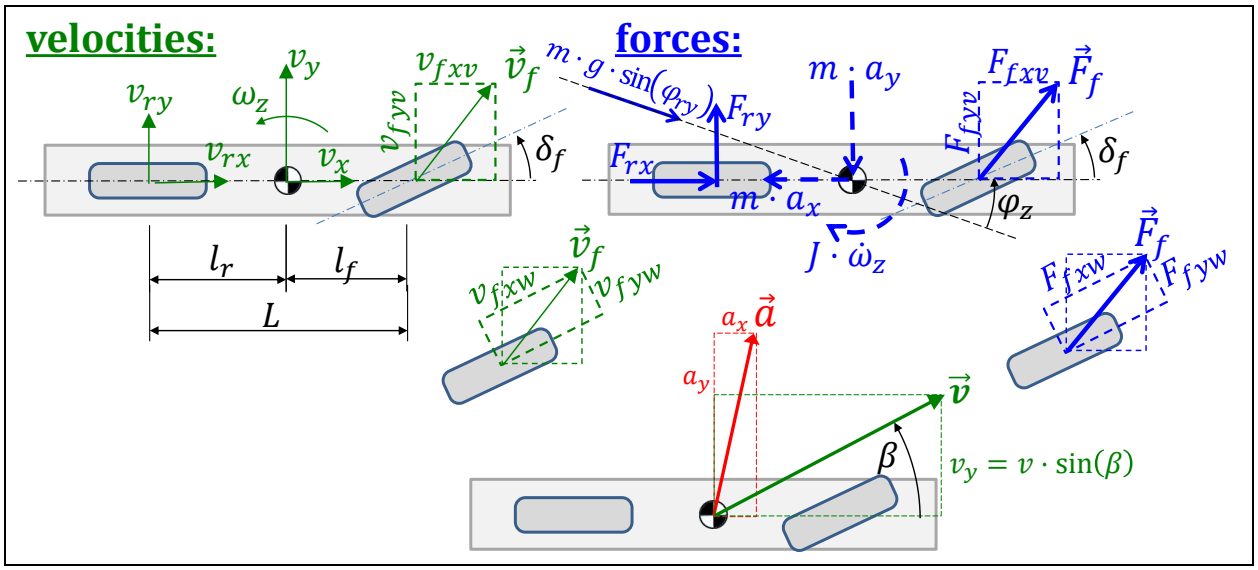


Figure 4-49: One-track model for transient dynamics. Dashed show fictive forces. Compare to Figure 4-16. Note that road is assumed to be level in 4.4, i.e. $\varphi_{ry} = 0$.

It is assumed that the longitudinal tyre forces and slips are small, so $F_{iyw}(s_{iyt}) \approx F_{iyw}(s_{iyw})$. It is also assumed that lateral tyre forces are far below road friction saturation, $F_{iyw}(s_{iyw}) \approx C_{iy} \cdot s_{iyw}$.

It can be difficult to understand the difference between acceleration $[a_x; a_y]$ and derivatives $[\dot{v}_x; \dot{v}_y]$ of velocities $[v_x; v_y]$. Some explanations are proposed in 4.4.2.3.

The Mathematical model shown in Eq [4.51] in Modelica format. The subscript v and w refers to **v**ehicle coordinate system and **w**heel coordinate system, respectively. The model is developed from the model for steady state in Eq [4.6], with the changes marked with yellow and underlined text.

```
//(Dynamic) Equilibrium:
m*ax = Ffxv + Frx;    m*ay = Ffyv + Fry;    J*der(wz) = Ffyv*lf - Fry*lr;
ax=der(vx)-wz*vy;    ay=der(vy)+wz*vx;

//Constitutive relation (Lateral tyre force model):
Ffyw=-Cf*sfyw;     Fry=-Cr*sryw;
sfyw=vfyw/vfxw;    sryw=vry/vrx;

//Compatibility:
vfxv = vx;    vfyv = vy + lf*wz;
vrx = vx;     vry = vy - lr*wz;

//Transformation between vehicle and wheel coordinate systems:
Ffxv = Ffxw*cos(df) - Ffyw*sin(df);
Ffyv = Ffxw*sin(df) + Ffyw*cos(df);
vfxv = vfxw*cos(df) - vfyw*sin(df);
vfyv = vfxw*sin(df) + vfyw*cos(df); //can be exactly replaced with
       // atan2(vfyv,vfxv)=df+atan(sfyw); or approximately with vfyv/vfxv=df+sfyw;

//Path with orientation:
der(x) = vx*cos(pz) - vy*sin(pz);
der(y) = vy*cos(pz) + vx*sin(pz);
der(pz) = wz;

// Prescription of steer angle:
df = if time < 2.5 then (5*pi/180)*sin(0.5*2*pi*time) else 5*pi/180;
//Shaft torques:
```

[4.51]

```
Ffxw = +1000; // Front axle driven.
Frx  = -100; // Rolling resistance on rear axle.
```

Position variables $[x, y, \varphi_y{=}\text{pz}]$ and speed variables $[v_x, v_y, \omega_z{=}\text{wz}]$ are selected state variables. The input variables are $\delta_f, F_{fxw}, F_{rx}$. The only non-zero initial value is $v_x = 100\ km/h$. Simulation result is shown in Figure 4-50. The manoeuvre selected is same steering wheel function of time as in Figure 4-17, for better comparison of the different characteristics of the models.

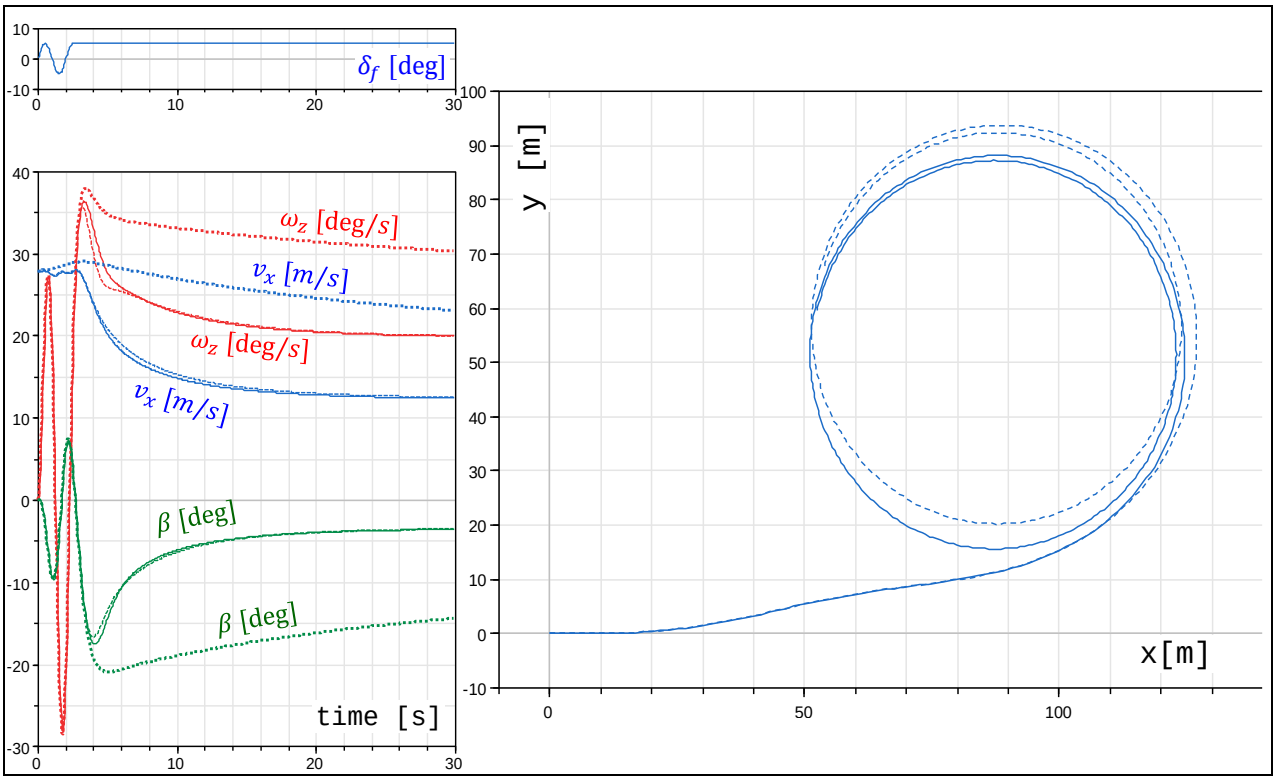


Figure 4-50: Simulation results of transient one-track models. Solid: Eq [4.51] or [4.52]. Dashed: Eq [4.53], which employs the small angle approximation. Dotted: Eq[4.51]=[4.52] but without the term $v_x \cdot \omega_z$.

Eq [4.51] is a complete model suitable for simulation. Removing $[x, y, \varphi_y{=}\text{pz}]$ and the 3 equations for "path with orientation", eliminating some variable and rewrite (no added approximations) gives:

$$
\begin{aligned}
&\text{Equilibrium:} && m \cdot (\dot{v}_x - \omega_z \cdot v_y) = F_{fxw} \cdot \cos(\delta_f) - F_{fyw} \cdot \sin(\delta_f) + F_{rx};\\
& && m \cdot (\dot{v}_y + \omega_z \cdot v_x) = F_{fxw} \cdot \sin(\delta_f) + F_{fyw} \cdot \cos(\delta_f) + F_{ry};\\
& && J \cdot \dot{\omega}_z = (F_{fxw} \cdot \sin(\delta_f) + F_{fyw} \cdot \cos(\delta_f)) \cdot l_f - F_{ry} \cdot l_r;\\
&\text{Constitution:} && F_{fyw} = -C_f \cdot s_{fyw};\ \ F_{ry} = -C_r \cdot s_{ryw};\\
& && s_{fyw} = v_{fyw}/|v_{fxw}|\,; \blacksquare\\
& && s_{ryw} = (v_y - l_r \cdot \omega_z)/|v_x|\,;\\
&\text{Compatibility:} && v_{fxw} = (v_y + l_f \cdot \omega_z) \cdot \sin(\delta_f) + v_x \cdot \cos(\delta_f)\,; \blacksquare\\
& && v_{fyw} = (v_y + l_f \cdot \omega_z) \cdot \cos(\delta_f) - v_x \cdot \sin(\delta_f)\,; \blacksquare
\end{aligned}
\qquad [4.52]
$$

Typically, this model is used for simulation, where δ_f, F_{fxw} and F_{rx} are input variables. Suitable state variables are v_x, v_y and ω_z. It is a non-linear model suitable for arbitrary transient manoeuvres, and we will come back to this in 4.4.3.4.

4.4.2.1 Known longitudinal velocity and small angles and small longitudinal tyre slip

Contribution from Mats Jonasson, Volvo Cars and Vehicle Dynamics at Chalmers

Model in Eq [4.52] is not linear, but we will derive a linear model from it now, through some approximations. Eliminating v_{fxw}, v_{fyw} by using the 2 last ■ equations. This gives:

Equilibrium:
$$m\cdot\left(\dot{v}_x-\omega_z\cdot v_y\right)=F_{fxw}\cdot\cos\left(\delta_f\right)-F_{fyw}\cdot\sin\left(\delta_f\right)+F_{rx};$$
$$m\cdot\left(\dot{v}_y+\omega_z\cdot v_x\right)=F_{fxw}\cdot\sin\left(\delta_f\right)+F_{fyw}\cdot\cos\left(\delta_f\right)+F_{ry};$$
$$J\cdot\dot{\omega}_z=\left(F_{fxw}\cdot\sin\left(\delta_f\right)+F_{fyw}\cdot\cos\left(\delta_f\right)\right)\cdot l_f-F_{ry}\cdot l_r;$$

Constitution:
$$F_{fyw}=-C_f\cdot s_{fyw};\quad F_{ry}=-C_r\cdot s_{ryw};$$

Compatibility:
$$s_{fyw}=\frac{\left(v_y+l_f\cdot\omega_z\right)\cdot\cos\left(\delta_f\right)-v_x\cdot\sin\left(\delta_f\right)}{\left|\left(v_y+l_f\cdot\omega_z\right)\cdot\sin\left(\delta_f\right)+v_x\cdot\cos\left(\delta_f\right)\right|};$$
$$s_{ryw}=\left(v_y-l_r\cdot\omega_z\right)/\left|v_x\right|;$$

Now we assume "not too sharp turning". We also use that $\beta_f=\arctan2\left(v_y+l_f\cdot\omega_z,\left|v_x\right|\right)$; and $\beta_r=\arctan2\left(v_y-l_r\cdot\omega_z,\left|v_x\right|\right)$;. Assume $v_x>0$, $\delta_f\approx\alpha_i\approx\beta_i\approx0$ (or $v_x<0$, $\delta_f\approx0$ and $|\alpha_i|\approx|\beta_i|\approx\pi$, see Figure 1-65). These become "trigonometric approximations" during the Mathematical modelling stage:

Equilibrium:
$$m\cdot\left(\dot{v}_x-\omega_z\cdot v_y\right)=F_{fxw}-F_{fyw}\cdot\delta_f+F_{rx};$$
$$m\cdot\left(\dot{v}_y+\omega_z\cdot v_x\right)=F_{fxw}\cdot\delta_f+F_{fyw}+F_{ry};$$
$$J\cdot\dot{\omega}_z=\left(F_{fxw}\cdot\delta_f+F_{fyw}\right)\cdot l_f-F_{ry}\cdot l_r;$$

Constitution:
$$F_{fyw}=-C_f\cdot s_{fyw};\quad F_{ry}=-C_r\cdot s_{ryw};$$

Compatibility:
$$\frac{v_y+l_f\cdot\omega_z}{|v_x|}\approx\operatorname{sign}(v_x)\cdot\delta_f+s_{fyw};\quad s_{ryw}=\frac{v_y-l_r\cdot\omega_z}{|v_x|};$$

[4.53]

Figure 4-50 shows a simulation with model in Eq [4.53], for comparison with the model without small angle approximations, i.e. from Eq [4.52].

Eliminating $F_{fyw}, F_{ry}, s_{fyw}, s_{ry}, \beta_f$ gives:

$$m\cdot\left(\dot{v}_x-\omega_z\cdot v_y\right)=F_{fxw}+C_f\cdot\left(\frac{v_y+l_f\cdot\omega_z}{|v_x|}-\delta_f\cdot\operatorname{sign}(v_x)\right)\cdot\delta_f+F_{rx};$$
$$m\cdot\left(\dot{v}_y+\omega_z\cdot v_x\right)=F_{fxw}\cdot\delta_f-C_f\cdot\left(\frac{v_y+l_f\cdot\omega_z}{|v_x|}-\delta_f\cdot\operatorname{sign}(v_x)\right)-C_r\cdot\frac{v_y-l_r\cdot\omega_z}{|v_x|};$$
$$J\cdot\dot{\omega}_z=\left(F_{fxw}\cdot\delta_f-\left(C_f\cdot\left(\frac{v_y+l_f\cdot\omega_z}{|v_x|}-\delta_f\cdot\operatorname{sign}(v_x)\right)\right)\right)\cdot l_f+C_r\cdot\frac{v_y-l_r\cdot\omega_z}{|v_x|}\cdot l_r;$$

Yet another approximation which we can do is to assume that centripetal acceleration is directed purely lateral in vehicle and hence remove the term $\omega_z\cdot v_y$. Figure 4-50 shows a simulation of Eq [4.52] without the term $\omega_z\cdot v_y$ for judging the importance of it; it has considerable influence on v_x over time. Also, the influence of the force $F_{fyw}\cdot\delta_f$ in longitudinal direction can be neglected. Eq [4.54] shows the resulting model.

$$m\cdot\dot{v}_x=F_{fxw}+F_{rx};$$
$$m\cdot\left(\dot{v}_y+\omega_z\cdot v_x\right)=F_{fxw}\cdot\delta_f-C_f\cdot\left(\frac{v_y+l_f\cdot\omega_z}{|v_x|}-\delta_f\cdot\operatorname{sign}(v_x)\right)-C_r\cdot\frac{v_y-l_r\cdot\omega_z}{|v_x|};$$
$$J\cdot\dot{\omega}_z=\left(F_{fxw}\cdot\delta_f-C_f\cdot\left(\frac{v_y+l_f\cdot\omega_z}{|v_x|}-\delta_f\cdot\operatorname{sign}(v_x)\right)\right)\cdot l_f+C_r\cdot\frac{v_y-l_r\cdot\omega_z}{|v_x|}\cdot l_r;$$

[4.54]

For stationary oscillation steering, $\dot{v}_x=0$, so v_x can be seen as a manoeuvre-parameter. This is often a good approximation also when turning during mild acceleration and deceleration. But, instead of setting $\dot{v}_x=0$, we keep it more generic: v_x is considered as a known function of time $v_x(t)$, i.e. v_x and

$\dot{v}_x$ are known functions of time, or $\dot{v}_x$ is an input and v_x a state. So, we can continue to select v_x, v_y, ω_z as states, but inputs become $\delta_f, F_{fxw}, \dot{v}_x$:

The first scalar equation (the longitudinal equilibrium) in Eq [4.54] can be used to calculate what F_{rx} is needed to keep the prescribed $v_x(t)$: $F_{rx} = m \cdot \dot{v}_x(t) - F_{fxw}$;. Note that neither aerodynamic, grade nor rolling resistance are considered.
The two latter scalar equations can be written as a linear model on matrix form, with 2 states v_y, ω_z and 2 inputs $\delta_f, F_{fxw} \cdot \delta_f$, see Eq [4.55], where the output is chosen as $\boldsymbol{y^T} = [\omega_z, a_y] = [\omega_z, \dot{v}_y + \omega_z \cdot v_x]$. The $v_x(t)$ is often a scalar constant v_x.

$$\begin{cases} \begin{bmatrix} \dot{v}_y \\ \dot{\omega}_z \end{bmatrix} = \boldsymbol{A} \cdot \begin{bmatrix} v_y \\ \omega_z \end{bmatrix} + \boldsymbol{B} \cdot \begin{bmatrix} \delta_f \\ F_{fxw} \cdot \delta_f \end{bmatrix}; \\ \begin{bmatrix} \omega_z \\ a_y \end{bmatrix} = \boldsymbol{C} \cdot \begin{bmatrix} v_y \\ \omega_z \end{bmatrix} + \boldsymbol{D} \cdot \begin{bmatrix} \delta_f \\ F_{fxw} \cdot \delta_f \end{bmatrix}; \end{cases} \text{ or } \begin{cases} \dot{\boldsymbol{x}} = \boldsymbol{A} \cdot \boldsymbol{x} + \boldsymbol{B} \cdot \boldsymbol{u}; \\ \boldsymbol{y} = \boldsymbol{C} \cdot \boldsymbol{x} + \boldsymbol{D} \cdot \boldsymbol{u}; \end{cases}$$

$$\textit{Where } \boldsymbol{A} = -\begin{bmatrix} m & 0 \\ 0 & J \end{bmatrix}^{-1} \cdot \begin{bmatrix} \frac{C_f + C_r}{|v_x(t)|} & \frac{C_f \cdot l_f - C_r \cdot l_r}{|v_x(t)|} + m \cdot v_x(t) \\ \frac{C_f \cdot l_f - C_r \cdot l_r}{|v_x(t)|} & \frac{C_f \cdot {l_f}^2 + C_r \cdot {l_r}^2}{|v_x(t)|} \end{bmatrix};$$

$$\textit{and } \boldsymbol{B} = \begin{bmatrix} m & 0 \\ 0 & J \end{bmatrix}^{-1} \cdot \begin{bmatrix} C_f \cdot \text{sign}(v_x) & 1 \\ C_f \cdot l_f \cdot \text{sign}(v_x) & l_f \end{bmatrix};$$

$$\textit{and } \boldsymbol{C} = \begin{bmatrix} 0 & 0 \\ 1 & 0 \end{bmatrix} \cdot \boldsymbol{A} + \begin{bmatrix} 0 & 1 \\ 0 & v_x(t) \end{bmatrix}; \textit{ and } \boldsymbol{D} = \begin{bmatrix} 0 & 0 \\ 1 & 0 \end{bmatrix} \cdot \boldsymbol{B};$$

[4.55]

The model above is approximated only for driving situation where tyre forces are far from saturation and angles are small, such as straight-line driving. If studying other driving conditions, we can still approximate with linearized models if variation from the driving condition is small. The method to linearize would be to use only the first terms in a Taylor series expansion of the model $\dot{\boldsymbol{x}} = \boldsymbol{f}(\boldsymbol{x}, \boldsymbol{u})$; around $[\boldsymbol{x}, \boldsymbol{u}] = [\boldsymbol{x_0}, \boldsymbol{u_0}]$:

$$\dot{\boldsymbol{x}} = \boldsymbol{f}(\boldsymbol{x}, \boldsymbol{u}) \approx \boldsymbol{f}(\boldsymbol{x_0}, \boldsymbol{u_0}) + \underbrace{\left.\frac{\boldsymbol{df}}{\boldsymbol{dx}}\right|_{\boldsymbol{x_0}, \boldsymbol{u_0}}}_{\boldsymbol{A_{lin}}} \cdot (\boldsymbol{x} - \boldsymbol{x_0}) + \underbrace{\left.\frac{\boldsymbol{df}}{\boldsymbol{du}}\right|_{\boldsymbol{x_0}, \boldsymbol{u_0}}}_{\boldsymbol{B_{lin}}} \cdot (\boldsymbol{u} - \boldsymbol{u_0}) =$$

$$= \underbrace{\left(\boldsymbol{f}(\boldsymbol{x_0}, \boldsymbol{u_0}) - \left.\frac{\boldsymbol{df}}{\boldsymbol{dx}}\right|_{\boldsymbol{x_0}, \boldsymbol{u_0}} \cdot \boldsymbol{x_0} - \left.\frac{\boldsymbol{df}}{\boldsymbol{du}}\right|_{\boldsymbol{x_0}, \boldsymbol{u_0}} \cdot \boldsymbol{u_0}\right)}_{\boldsymbol{f_0}} + \underbrace{\left.\frac{\boldsymbol{df}}{\boldsymbol{dx}}\right|_{\boldsymbol{x_0}, \boldsymbol{u_0}}}_{\boldsymbol{A_{lin}}} \cdot \boldsymbol{x} + \underbrace{\left.\frac{\boldsymbol{df}}{\boldsymbol{du}}\right|_{\boldsymbol{x_0}, \boldsymbol{u_0}}}_{\boldsymbol{B_{lin}}} \cdot \boldsymbol{u};$$

If the driving condition around which we linearize is steady state cornering, $\boldsymbol{f_0} = \boldsymbol{0}$ and $\boldsymbol{u} = \boldsymbol{u_0} = \boldsymbol{u_{SS}}$. It can also be used for finding conditions where the motion grows exponentially also without any input, i.e. when the vehicle becomes unstable. Then we find the eigenvalues $\{\lambda_1, \lambda_2\}$, defined by $\det(\boldsymbol{A} - \lambda \cdot \boldsymbol{v}) = 0$;. If any real part of $\{\lambda_1, \lambda_2\}$ is positive, the vehicle is unstable. We find that one eigenvalue is $\lambda = 0$ (which cannot indicate instability). But the other is

$$\lambda = \frac{\left(\sqrt{\begin{matrix} C_f^2 J^2 + 2C_f^2 J l_f^2 m + C_f^2 l_f^4 m^2 + 2C_f C_r J^2 - 2C_f C_r J l_f^2 m - 8C_f C_r J l_f l_r m - 2C_f C_r J l_r^2 m + \\ +2C_f C_r l_f^2 l_r^2 m^2 + 4C_f J l_f m^2 v_x^2 + C_r^2 J^2 + 2C_r^2 J l_r^2 m + C_r^2 l_r^4 m^2 - 4C_r J l_r m^2 v_x^2 \end{matrix}}\right) + C_f J + C_r J + C_f l_f^2 m + C_r l_r^2 m}{-2Jmv_x};$$

This eigenvalue can have a positive real part which should be interpreted as instability. The same expression gives instability also for non-steady state conditions.

4.4.2.1.1 Convert to 2nd Order Single State Model

We can eliminate one of the 2 states (v_y, ω_z) in Eq [4.55], but then we have to accept that the ODE becomes 2nd order. We can start from the last 2 scalar equations in Eq [4.54]. We here simplify by

limiting to $\dot{v}_x = 0$ and $F_{fxw} = 0$. To eliminate $v_y(t)$, we first eliminate v_y in the eq "$J \cdot \dot{\omega}_z = \cdots$" using the eq "$m \cdot (\dot{v}_y + \omega_z \cdot v_x) = \cdots$":

$$\begin{aligned}&(C_r \cdot l_r - C_f \cdot l_f) \cdot m \cdot |v_x| \cdot \dot{v}_y + (C_f + C_r) \cdot J \cdot |v_x| \cdot \dot{\omega}_z + \\ &+ \left(C_f \cdot C_r \cdot (l_f + l_r)^2 - (C_f \cdot l_f - C_r \cdot l_r) \cdot m \cdot v_x \cdot |v_x|\right) \cdot \omega_z = C_f \cdot C_r \cdot (l_f + l_r) \cdot |v_x| \cdot \delta_f; \quad \blacksquare\end{aligned}$$

To eliminate $v_y(t)$ completely, we also need to eliminate $\dot{v}_y$. For this reason, we need to differentiate the eq "$J \cdot \dot{\omega}_z = \cdots$", which gives:

$$J \cdot \ddot{\omega}_z = -C_f \cdot \left(\frac{\dot{v}_y + l_f \cdot \dot{\omega}_z}{|v_x|} - \dot{\delta}_f\right) \cdot l_f + C_r \cdot \frac{\dot{v}_y - l_r \cdot \dot{\omega}_z}{|v_x|} \cdot l_r;$$

With equation "$J \cdot \ddot{\omega}_z = \cdots$" and ■, we can now eliminate $\dot{v}_y$:

$$\begin{aligned}&J \cdot m \cdot {v_x}^2 \cdot \ddot{\omega}_z + \\ &+ \left((C_f + C_r) \cdot J + (C_f \cdot l_f^2 + C_r \cdot l_r^2) \cdot m\right) \cdot |v_x| \cdot \dot{\omega}_z + \\ &+ \left(C_f \cdot C_r \cdot (l_f + l_r)^2 + (C_r \cdot l_r - C_f \cdot l_f) \cdot m \cdot v_x \cdot |v_x|\right) \cdot \omega_z = \\ &\qquad = -C_f \cdot l_f \cdot m \cdot {v_x}^2 \cdot \dot{\delta}_f - (l_f + l_r) \cdot C_f \cdot C_r \cdot |v_x| \cdot \delta_f;\end{aligned}$$

The coefficients in front of $\ddot{\omega}_z, \dot{\omega}_z, \omega_z, \dot{\delta}_f$ and δ_f can be compared with coefficients in simpler damped mass and spring systems, see 1.5.2.3. Note, for instance, that the coefficients are dependent of v_x and that C_f and C_r cannot be simply identified as either springs or dampers.

Fourier transform gives:

$$\begin{aligned}&-J \cdot m \cdot {v_x}^2 \cdot \omega^2 \cdot \mathcal{F}(\omega_z) + \\ &+ \left((C_f + C_r) \cdot J + (C_f \cdot l_f^2 + C_r \cdot l_r^2) \cdot m\right) \cdot |v_x| \cdot j \cdot \omega \cdot \mathcal{F}(\omega_z) + \\ &+ \left(C_f \cdot C_r \cdot (l_f + l_r)^2 + (C_r \cdot l_r - C_f \cdot l_f) \cdot m \cdot v_x \cdot |v_x|\right) \cdot \mathcal{F}(\omega_z) = \\ &= -C_f \cdot l_f \cdot m \cdot {v_x}^2 \cdot j \cdot \omega \cdot \mathcal{F}(\delta_f) - (l_f + l_r) \cdot C_f \cdot C_r \cdot |v_x| \cdot \mathcal{F}(\delta_f); \;\Rightarrow\end{aligned}$$

$$\Rightarrow H_{\delta_f \to \omega_z}(\omega) = \frac{\mathcal{F}(\omega_z)}{\mathcal{F}(\delta_f)} =$$

$$= \frac{C_f \cdot l_f \cdot m \cdot {v_x}^2 \cdot j \cdot \omega + (l_f + l_r) \cdot C_f \cdot C_r \cdot |v_x|}{J \cdot m \cdot {v_x}^2 \cdot \omega^2 - \left((C_f + C_r) \cdot J + \left(C_f \cdot l_f^2 + C_r \cdot l_r^2\right) \cdot m\right) \cdot |v_x| \cdot j \cdot \omega - \left(C_f \cdot C_r \cdot (l_f + l_r)^2 + (C_r \cdot l_r - C_f \cdot l_f) \cdot m \cdot v_x \cdot |v_x|\right)};$$

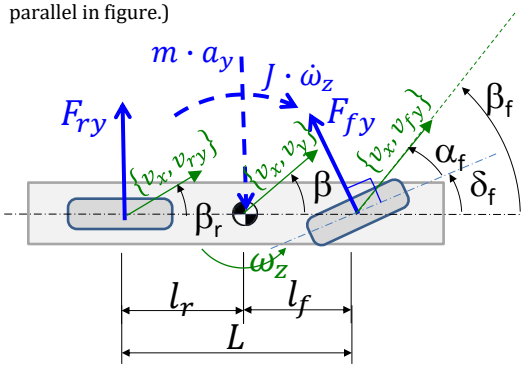
This gives the same transfer function as in 0, which is derived with matrix formula for the "1st order, 2 state model". A single state, 2nd order model for v_y can be derived similarly.

4.4.2.2 Less General Derivation of Linear One-Track Model

A less general and more intuitive derivation of Eq [4.55] is made in Figure 4-51. The approximations are introduced earlier, already in the physical model. Therefore, the influence of F_{fxw} is not reflected and the longitudinal equilibrium is neglected. It is also assumed that $v_x > 0$.

Physical model:

- Path radius >> the vehicle. Then, all forces (and centripetal acceleration) are approximately co-directed.
- Small tyre and vehicle side slip ⇒ angle=sin(angle)=tan(angle). (Angles are not drawn small, which is why the forces not appear parallel in figure.)



Mathematical model:

Equilibrium:

$$m \cdot (\dot{v}_y + \omega_z \cdot v_x) \approx F_{fy} + F_{ry};$$
$$J \cdot \dot{\omega}_z \approx F_{fy} \cdot l_f - F_{ry} \cdot l_r;$$

Constitution:

$$F_{fy} = -C_f \cdot s_{fy}; \quad F_{ry} = -C_r \cdot s_{ry};$$

Compatibility:

$$\delta_f + s_{fy} \approx \delta_f + \alpha_f = \beta_f \approx \frac{v_{fy}}{v_x} = \frac{v_y + l_f \cdot \omega_z}{v_x};$$
$$s_{ry} \approx \alpha_r = \beta_r \approx \frac{v_{ry}}{v_x} = \frac{v_y - l_r \cdot \omega_z}{v_x};$$

Eliminate $F_{fy}, F_{ry}, \alpha_f, \alpha_r, \beta_f, \beta_r$ **yields:**

$$m \cdot \dot{v}_y + \frac{C_f + C_r}{v_x} \cdot v_y + \left(\frac{C_f \cdot l_f - C_r \cdot l_r}{v_x} + m \cdot v_x\right) \cdot \omega_z \approx C_f \cdot \delta_f;$$
$$J \cdot \dot{\omega}_z + \frac{C_f \cdot l_f - C_r \cdot l_r}{v_x} \cdot v_y + \frac{C_f \cdot {l_f}^2 + C_r \cdot {l_r}^2}{v_x} \cdot \omega_z \approx C_f \cdot l_f \cdot \delta_f;$$

Figure 4-51: Less general derivation of the Linear One-Track Model, i.e. Eq [4.55]. Only for $v_x > 0$.

One can add more axles to the derivation. E.g., a truck with double rear axle will get an added term proportional to ω_z in the moment equilibrium.

4.4.2.3 Accelerations and Velocity Derivatives

Contribution from Toheed Ghandriz

See Equation [4.50]. This section provides some explanations to the difference between acceleration $[a_x; a_y]$ and derivatives $[\dot{v}_x; \dot{v}_y]$ of velocities $[v_x; v_y]$.

4.4.2.3.1 Theoretical explanation

First, think of $\vec{a}$ and $\vec{v}$ as geometric vectors (acceleration and velocity are vectors in physics). Acceleration $\vec{a}$ is acceleration in inertial frame, i.e. accelerations over ground. Velocity $\vec{v}$ is velocity in inertial frame, i.e. velocity over ground. A driver or accelerometers, attached to the vehicle body, will experience $[a_x; a_y]$. The ground, observed from the vehicle through a hole in the floor, would be experienced as moving with $[-v_x; -v_y]$.

It is suitable to decompose $\vec{a}$ and $\vec{v}$ in vehicle directions, since most equations (tyres, steering, propulsion, braking, etc) are expressed in those directions. With $\vec{u}_x$ and $\vec{u}_y$ as unit vectors in vehicle directions: $\vec{a} = a_x \cdot \vec{u}_x + a_y \cdot \vec{u}_y$ and $\vec{v} = v_x \cdot \vec{u}_x + v_y \cdot \vec{u}_y$, or shorter, $[a_x; a_y]$ and $[v_x; v_y]$, which are mathematical vectors. Now, it is important to remember that the vehicle is rotating with ω_z.

The accelerations are used in equilibrium equations, where the fictive force is $m \cdot \vec{a} = m \cdot \frac{d}{dt}\vec{v};$. Since we express $\vec{v}$ in components in vehicle coordinate system directions, the differentiation is **not** as simple as differentiation component by component, $[\dot{v}_x; \dot{v}_y]$. Instead: $[a_x; a_y] = [\dot{v}_x; \dot{v}_y] + [-\omega_z \cdot v_y;\ \omega_z \cdot v_x];$. The terms proportional to ω_z are centrifugal accelerations.

This can be mathematically shown as differentiation of the geometrical vector $\vec{v}$:

$$\vec{a} = \frac{d}{dt}\vec{v} = \frac{d}{dt}(v_x \cdot \vec{u}_x + v_y \cdot \vec{u}_y) = \left(\dot{v}_x \cdot \vec{u}_x + v_x \cdot \frac{d}{dt}\vec{u}_x\right) + \left(\dot{v}_y \cdot \vec{u}_y + v_y \cdot \frac{d}{dt}\vec{u}_y\right) =$$
$$= (\dot{v}_x \cdot \vec{u}_x + v_x \cdot \omega_z \cdot \vec{u}_y) + (\dot{v}_y \cdot \vec{u}_y - v_y \cdot \omega_z \cdot \vec{u}_x) = \underbrace{(\dot{v}_x - v_y \cdot \omega_z)}_{a_x} \cdot \vec{u}_x + \underbrace{(\dot{v}_y + v_x \cdot \omega_z)}_{a_y} \cdot \vec{u}_y;$$

The constitutive and compatibility equations are typically expressed in velocities, not accelerations. For high index models, some of the compatibility equations (a.k.a. constraint equations) also needs to be differentiated, see example in 4.5.2.2.

4.4.2.3.2 Practical Explanation

Another explanation is given in left part of Figure 4-52 and the following reasoning. We can express the velocity in direction of the x axis at time t, at two time instants:

- Velocity at time $= t$: v_x
- Velocity at time $= t + \Delta t$: $(v_x + \Delta v_x) \cdot \cos(\Delta\psi) - (v_y + \Delta v_y) \cdot \sin(\Delta\psi) = (v_x \cdot \cos(\Delta\psi) + \Delta v_x \cdot \cos(\Delta\psi)) - (v_y \cdot \sin(\Delta\psi) + \Delta v_y \cdot \sin(\Delta\psi)) \approx \{\Delta\psi\ small\} \approx (v_x + \Delta v_x) - (v_y \cdot \Delta\psi + \Delta v_y \cdot \Delta\psi) \approx \{\Delta v_y \cdot \Delta\psi\ small\} \approx (v_x + \Delta v_x) - v_y \cdot \Delta\psi$

Using these two expressions, we can express a_x as the change of that speed per time unit:

- Acceleration=Velocity change per time $= a_x = \frac{\{(v_x+\Delta v_x)-v_y\cdot\Delta\psi\}-v_x}{\Delta t} = \frac{\Delta v_x - v_y\cdot\Delta\psi}{\Delta t} = \frac{\Delta v_x}{\Delta t} - v_y\frac{\Delta\psi}{\Delta t} \approx \dot{v}_x - v_y \cdot \dot{\psi} = \dot{v}_x - v_y \cdot \omega_z$

Corresponding for the lateral direction gives the Equation [4.50]. In Equation [4.50], the term $\omega_z \cdot v_x$ is generally more important than the term $\omega_z \cdot v_y$. This is because v_x is generally much larger than v_y.

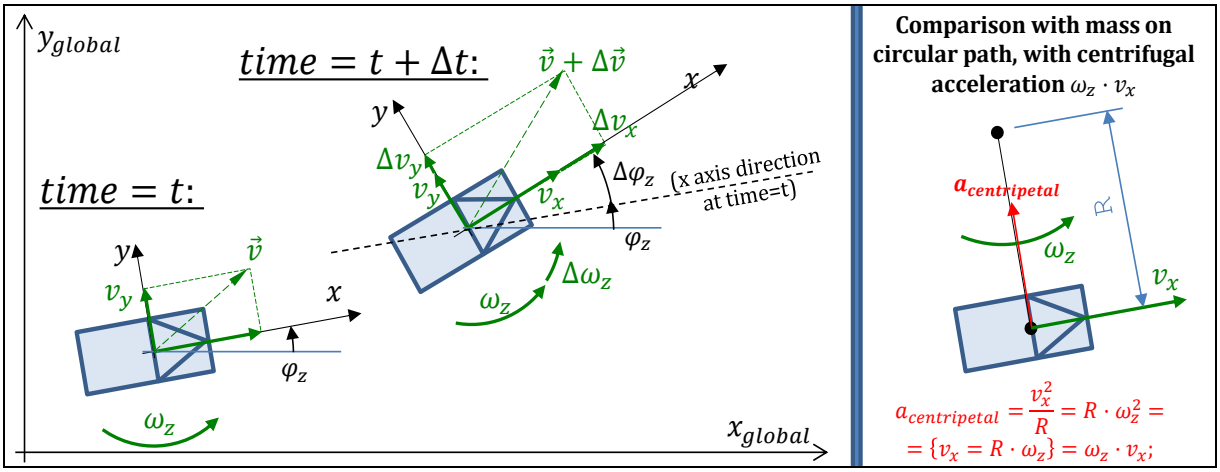


Figure 4-52: How to understand the acceleration term $\omega_z \cdot v_x$ for vehicle motion in ground plane. Left: Two consecutive time instants. Right: Comparison with circular motion, to identify the centripetal acceleration.

4.4.2.3.3 Model with Velocity Components in Ground Fixed Directions

An alternative mathematical model is to express the velocity in components in ground fix (inertial) directions ($\vec{v} = v_{xg} \cdot \vec{u}_{xg} + v_{yg} \cdot \vec{u}_{yg}$, subscript g for *ground*) instead of vehicle fix directions ($\vec{v} = v_{xv} \cdot \vec{u}_{xv} + v_{yv} \cdot \vec{u}_{yv}$, subscript v for *vehicle*). The fictive forces are till $m \cdot \frac{d}{dt}\vec{v}$, but we should express $\frac{d}{dt}\vec{v}$ in $[v_{xg}, v_{xg}]$ instead of $[v_{xv}, v_{yv}]$, which becomes: $\vec{a} = \frac{d}{dt}(v_{xg} \cdot \vec{u}_{xg} + v_{yg} \cdot \vec{u}_{yg}) = \dot{v}_{xg} \cdot \vec{u}_{xg} + \dot{v}_{yg} \cdot \vec{u}_{yg};$. This is a simpler differentiation than using the rotating unit vectors $\vec{u}_{xv}$ and $\vec{u}_{yv}$. We get $a_{yg} = \dot{v}_{yg};$ and $a_{xg} = \dot{v}_{xg};$ instead of $a_{yv} = \dot{v}_{yv} + v_{xv} \cdot \omega_z;$ and $a_{xv} = \dot{v}_{xv} - v_{yv} \cdot \omega_z;$.

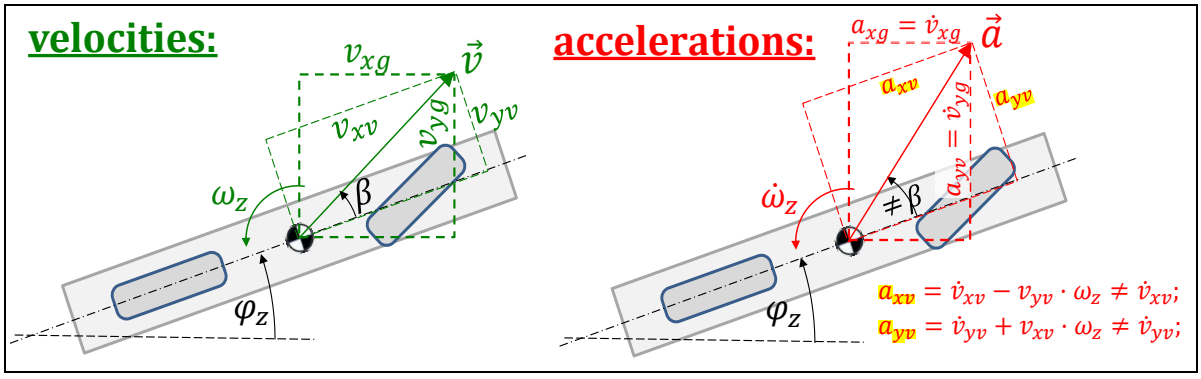


Figure 4-53: Velocity and Acceleration Components in Vehicle fix and Ground Fixed Directions.

Then, we replace the 2 translation equilibrium equations in Eq [4.52]. We also add 2 transformation equations and a compatibility in yaw. The remaining equations can be kept, but it is proposed to add subscript v to v_x, v_y and F_{rx}. The two models, side-by-side becomes as in Table 4-54.

Table 4-54: Comparison between model with velocities in vehicle fixed and ground fixed directions.

Model in…	**…vehicle fix directions,** Eq [4.52]	**… ground fixed directions**
Translation Equilibrium	$m \cdot (\dot{v}_{xv} - \omega_z \cdot v_{yv}) = = F_{fxv} + F_{rxv};$ $m \cdot (\dot{v}_{yv} + \omega_z \cdot v_{xv}) = = F_{fyv} + F_{ryv};$	$m \cdot \dot{v}_{xg} = (F_{fxv} + F_{rxv}) \cdot \cos(\varphi_z) - (F_{fyv} + F_{ryv}) \cdot \sin(\varphi_z);$ $m \cdot \dot{v}_{yg} = (F_{fxv} + F_{rxv}) \cdot \sin(\varphi_z) + (F_{fyv} + F_{ryv}) \cdot \cos(\varphi_z);$
Velocity Transformation, ground to vehicle	<not needed>	$v_{xv} = +v_{xg} \cdot \cos(\varphi_z) + v_{yg} \cdot \sin(\varphi_z);$ $v_{yv} = -v_{xg} \cdot \sin(\varphi_z) + v_{yg} \cdot \cos(\varphi_z);$
Yaw Compatibility	<not needed>	$\dot{\varphi}_z = \omega_z;$ (adds φ_z as state)
Yaw Equilibrium	$J \cdot \dot{\omega}_z = F_{fyv} \cdot l_f - F_{ryv} \cdot l_r;$	
Constitution	$F_{fyw} = -C_f \cdot s_{fyw}; \quad F_{ryv} = -C_r \cdot s_{ry};$	
Compatibility	$\delta_f + s_{fyw} \approx (v_{yv} + l_f \cdot \omega_z)/\lvert v_{xv}\rvert; \quad s_{ry} = (v_{yv} - l_r \cdot \omega_z)/\lvert v_{xv}\rvert;$	
Force transformation, steered wheels to vehicle	$F_{fxv} = F_{fxw} - F_{fyw} \cdot \delta_f; \quad F_{fyv} = F_{fxw} \cdot \delta_f + F_{fyw};$	
Path with orientation:	From Eq [4.51]: $\dot{x} = v_{xv} \cdot cos(\varphi_z) - v_{yv} \cdot sin(\varphi_z);$ $\dot{y} = v_{yv} \cdot \cos(\varphi_z) + v_{xv} \cdot sin(\varphi_z);$ $\dot{\varphi}_z = \omega_z;$	$\dot{x} = v_{xg};$ $\dot{y} = v_{yg};$ $\dot{\varphi}_z = \omega_z;$ (already included in yaw compatibility, above)

Using the velocity components in inertial directions brings yaw angle φ_z into the differential equations for velocities. So, we have to add φ_z as state: we get 4 states $(v_{xg}, v_{yg}, \omega_z, \varphi_z)$ instead of 3 $(v_{xv}, v_{yv}, \omega_z)$. The need of transformation manifests that vehicle directions is more natural directions for the constitutive equations (tyre models). However, the equations for path becomes simpler with the ground fixed directions. The two models gives, of course, the same result, e.g. $v_{xg}(t) \equiv v_{xv}(t) \cdot \cos(\varphi_z(t)) - v_{yv}(t) \cdot \sin(\varphi_z(t))$, but the model in vehicle fixed directions is more frequently used.

A similar comparison between model in vehicle and ground fix v and a components can be done for pitch rotation in 3.4.5 and 5.7.2 but the difference there is less important since pitch angle is much more limited than yaw angle.

4.4.2.4 Validity of Model

When only studying the Frequency Response as yaw velocity and curvature response, it is easy to forget that one very easily comes into manoeuvres where road friction is limited, i.e. where the linear tyre model is not valid. Hence it is good to look at lateral acceleration Frequency Response, because we can roughly say that for $\lvert a_y\rvert$ in the same magnitude as $\mu \cdot m \cdot g$, it is doubtful if the model is valid. If the

wheel torques are significant, the validity limit is even lower. For high CoG vehicles, another invalidating circumstance is wheel lift, which can be approximately checked by checking that $|a_y| \ll SSF = g \cdot w/(2 \cdot h)$.

If one needs to include nonlinear tyre models in stationary oscillation response, one can simulate using time integration (same method as usually used for transient handling) over several excitation cycles, until the response shows a clear stationary oscillation. This consumes more computational efforts and the solutions become approximate and numerical.

4.4.3 Using the One-Track Model

Use the linear matrix model in Eq [4.55] to study "stationary oscillating steering":

$$\begin{bmatrix} \dot{v}_y \\ \dot{\omega}_z \end{bmatrix} = A \cdot \begin{bmatrix} v_y \\ \omega_z \end{bmatrix} + B \cdot \delta(t) = A \cdot \begin{bmatrix} v_y \\ \omega_z \end{bmatrix} + B \cdot \hat{\delta} \cdot \cos(\omega \cdot t)$$

(Note similar notation for vehicle yaw velocity, ω_z, and steering angular frequency, ω.) Knowing $\hat{\delta}$ and ω, it is possible to calculate the responses $\hat{v}_y$, $\hat{\omega}_z$, φ_y and φ_z:

$$\begin{bmatrix} v_y \\ \omega_z \end{bmatrix} = \begin{bmatrix} \hat{v}_y \\ \hat{\omega}_z \end{bmatrix} \cdot \cos\left(\omega \cdot t - \begin{bmatrix} \varphi_{v_y} \\ \varphi_{\omega_z} \end{bmatrix}\right); \quad and \quad \begin{bmatrix} \omega_z \\ a_y \end{bmatrix} = \begin{bmatrix} \hat{\omega}_z \\ \hat{a}_y \end{bmatrix} \cdot \cos\left(\omega \cdot t - \begin{bmatrix} \varphi_{\omega_z} \\ \varphi_{a_y} \end{bmatrix}\right);$$

Different methods are available for calculation of the Frequency Responses:

- **Fourier** transform
- **Complex mathematics**, using $e^{j \cdot \omega \cdot t}$
- **Real trigonometry**, using $\cos(\omega \cdot t + phase)$, $\sin(\omega \cdot t + phase)$ or $\cos(\omega \cdot t) + \sin(\omega \cdot t)$.

Typically, the problem has at least dimension 2, which makes matrix algebra efficient. Matrix formulation and Fourier transform is very convenient with tools as Matlab if numerical solutions are accepted.

4.4.3.1 Single Frequency Response

4.4.3.1.1 Solution with Fourier Transform

Eq [4.55] can be transformed to the frequency domain ($\mathcal{F}$ denotes Fourier transform, i.e. $\mathcal{F}(\xi(t)) = \int_{-\infty}^{\infty} e^{-j \cdot \omega \cdot t} \cdot \xi(t) \cdot dt$):

$$\begin{cases} j \cdot \omega \cdot \boldsymbol{\mathcal{F}}\left(\begin{bmatrix} v_y \\ \omega_z \end{bmatrix}\right) = \boldsymbol{A} \cdot \boldsymbol{\mathcal{F}}\left(\begin{bmatrix} v_y \\ \omega_z \end{bmatrix}\right) + \boldsymbol{B} \cdot \begin{bmatrix} \mathcal{F}(\delta_f) \\ \mathcal{F}(F_{fxw} \cdot \delta_f) \end{bmatrix}; \\ \boldsymbol{\mathcal{F}}\left(\begin{bmatrix} \omega_z \\ a_y \end{bmatrix}\right) = \boldsymbol{C} \cdot \boldsymbol{\mathcal{F}}\left(\begin{bmatrix} v_y \\ \omega_z \end{bmatrix}\right) + \boldsymbol{D} \cdot \begin{bmatrix} \mathcal{F}(\delta_f) \\ \mathcal{F}(F_{fxw} \cdot \delta_f) \end{bmatrix}; \end{cases}$$

Solving for states and outputs, using $\mathcal{F}(\dot{z}) = j \cdot \omega \cdot \mathcal{F}(z)$;, gives:

$$\begin{cases} \begin{bmatrix} v_y \\ \omega_z \end{bmatrix} = \mathcal{F}^{-1}\left(\boldsymbol{\mathcal{F}}\left(\begin{bmatrix} v_y \\ \omega_z \end{bmatrix}\right)\right) = \mathcal{F}^{-1}\left((j \cdot \omega \cdot \boldsymbol{I} - \boldsymbol{A})^{-1} \cdot \boldsymbol{B} \cdot \begin{bmatrix} \mathcal{F}(\delta_f) \\ \mathcal{F}(F_{fxw} \cdot \delta_f) \end{bmatrix}\right); \\ \begin{bmatrix} \omega_z \\ a_y \end{bmatrix} = \mathcal{F}^{-1}\left(\boldsymbol{\mathcal{F}}\left(\begin{bmatrix} \omega_z \\ a_y \end{bmatrix}\right)\right) = \mathcal{F}^{-1}\left(\boldsymbol{C} \cdot \boldsymbol{\mathcal{F}}\left(\begin{bmatrix} v_y \\ \omega_z \end{bmatrix}\right) + \boldsymbol{D} \cdot \begin{bmatrix} \mathcal{F}(\delta_f) \\ \mathcal{F}(F_{fxw} \cdot \delta_f) \end{bmatrix}\right); \end{cases}$$

We now look at the response to only on δ_f, not $F_{fxw} \cdot \delta_f$:

$$\begin{cases} \begin{bmatrix} v_y \\ \omega_z \end{bmatrix} = \mathcal{F}^{-1}\left(\boldsymbol{\mathcal{F}}\left(\begin{bmatrix} v_y \\ \omega_z \end{bmatrix}\right)\right) = \mathcal{F}^{-1}\left((j \cdot \omega \cdot \boldsymbol{I} - \boldsymbol{A})^{-1} \cdot \boldsymbol{B} \cdot \begin{bmatrix} 1 \\ 0 \end{bmatrix} \cdot \mathcal{F}(\delta_f)\right); \\ \begin{bmatrix} \omega_z \\ a_y \end{bmatrix} = \mathcal{F}^{-1}\left(\boldsymbol{\mathcal{F}}\left(\begin{bmatrix} \omega_z \\ a_y \end{bmatrix}\right)\right) = \mathcal{F}^{-1}\left(\boldsymbol{C} \cdot \boldsymbol{\mathcal{F}}\left(\begin{bmatrix} v_y \\ \omega_z \end{bmatrix}\right) + \boldsymbol{D} \cdot \begin{bmatrix} 1 \\ 0 \end{bmatrix} \cdot \mathcal{F}(\delta_f)\right); \end{cases}$$

Expressed as transfer functions:

$$\boldsymbol{H}_{\delta_f\to\begin{bmatrix}v_y\\ \omega_z\end{bmatrix}} = \frac{1}{\mathcal{F}(\delta_f)}\cdot\boldsymbol{\mathcal{F}}\left(\begin{bmatrix}v_y\\ \omega_z\end{bmatrix}\right) = \left(\frac{(j\cdot\omega\cdot\boldsymbol{I}-\boldsymbol{A})^{-1}\cdot\boldsymbol{B}\cdot\mathcal{F}(\delta_f)}{\mathcal{F}(\delta_f)}\right)\cdot\begin{bmatrix}1\\0\end{bmatrix} = (j\cdot\omega\cdot\boldsymbol{I}-\boldsymbol{A})^{-1}\cdot\boldsymbol{B}\cdot\begin{bmatrix}1\\0\end{bmatrix};$$

$$\boldsymbol{H}_{\delta_f\to\begin{bmatrix}\omega_z\\ a_y\end{bmatrix}} = \frac{1}{\mathcal{F}(\delta_f)}\cdot\boldsymbol{\mathcal{F}}\left(\begin{bmatrix}\omega_z\\ a_y\end{bmatrix}\right) = \boldsymbol{C}\cdot\boldsymbol{H}_{\delta_f\to\begin{bmatrix}v_y\\ \omega_z\end{bmatrix}} + \boldsymbol{D}\cdot\begin{bmatrix}1\\0\end{bmatrix} = (\boldsymbol{C}\cdot(j\cdot\omega\cdot\boldsymbol{I}-\boldsymbol{A})^{-1}\cdot\boldsymbol{B}+\boldsymbol{D})\cdot\begin{bmatrix}1\\0\end{bmatrix};$$

[4.56]

We have derived the transfer functions. The subscript tells that the transfer function is for the vehicle operation with excitation=input= δ_f and response=output= $[v_y \quad \omega_z]^T$ and output= $[v_y \quad a_y]^T$. The transfer function has dimension 2x1 and is complex. It operates as follows:

$$\text{Amplitudes: } \begin{cases}\begin{bmatrix}\hat{v}_y\\ \hat{\omega}_z\end{bmatrix} = \left|H_{\delta_f\to\begin{bmatrix}v_y\\ \omega_z\end{bmatrix}}\right|\cdot\hat{\delta}_f;\\ \begin{bmatrix}\hat{\omega}_z\\ \hat{a}_y\end{bmatrix} = \left|H_{\delta_f\to\begin{bmatrix}\omega_z\\ a_y\end{bmatrix}}\right|\cdot\hat{\delta}_f;\end{cases}$$

$$\text{Phase delays: } \begin{cases}\begin{bmatrix}\varphi_{v_y}\\ \varphi_{\omega_z}\end{bmatrix} = \begin{bmatrix}\arg(v_y)\\ \arg(\omega_z)\end{bmatrix} - \begin{bmatrix}1\\1\end{bmatrix}\cdot\arg(\delta_f) = \begin{Bmatrix}\arg(\delta_f)\\ =0\end{Bmatrix} = \arg\left(H_{\delta_f\to\begin{bmatrix}v_y\\ \omega_z\end{bmatrix}}\right);\\ \begin{bmatrix}\varphi_{\omega_z}\\ \varphi_{a_y}\end{bmatrix} = \begin{bmatrix}\arg(\omega_z)\\ \arg(a_y)\end{bmatrix} - \begin{bmatrix}1\\1\end{bmatrix}\cdot\arg(\delta_f) = \begin{Bmatrix}\arg(\delta_f)\\ =0\end{Bmatrix} = \arg\left(H_{\delta_f\to\begin{bmatrix}\omega_z\\ a_y\end{bmatrix}}\right);\end{cases}$$

[4.57]

4.4.3.1.2 Solution with Complex Mathematics

This section avoids requiring skills in Fourier transform. This makes the derivation quite long to reach the final results Eqs [4.62] and [4.61]. With Fourier Transform, the expression for the Transfer Function, H, can be reached with less algebra. Knowing H, it can be used in Eq [4.61].

The fundamental situation for steering frequency response is that the excitation is: $\delta_f = \hat{\delta}_f \cdot \cos(2\cdot\pi\cdot f\cdot t) = \{e^{j\cdot a} = \cos(a) + j\cdot\sin(a)\} = \mathrm{Re}(\hat{\delta}_f\cdot e^{j\cdot 2\cdot\pi\cdot f\cdot t})$, where f is the (time) frequency in Hz and j is the imaginary unit. We rewrite $2\cdot\pi\cdot f$ as ω (angular frequency), which has to be carefully distinguished from ω_z (yaw velocity). Insert this in Eq [4.55] and neglecting the longitudinal force F_{fxw}. The full (complex) equation is used:

$$\mathrm{Re}\left[\begin{bmatrix}m & 0\\ 0 & J\end{bmatrix}\cdot\begin{bmatrix}\dot{v}_{yc}\\ \dot{\omega}_{zc}\end{bmatrix} + \begin{bmatrix}\frac{C_f+C_r}{v_x} & \frac{C_f\cdot l_f - C_r\cdot l_r}{v_x} + m\cdot v_x\\ \frac{C_f\cdot l_f - C_r\cdot l_r}{v_x} & \frac{C_f\cdot {l_f}^2 + C_r\cdot {l_r}^2}{v_x}\end{bmatrix}\cdot\begin{bmatrix}v_{yc}\\ \omega_{zc}\end{bmatrix} = \begin{bmatrix}C_f\\ C_f\cdot l_f\end{bmatrix}\cdot\hat{\delta}_f\cdot e^{j\omega\cdot t}\right];$$

[4.58]

We intend to solve the complex equation, and then find the solutions as real parts: $v_y = \mathrm{Re}[v_{yc}]$; and $\omega_z = \mathrm{Re}[\omega_{zc}]$;. (Subscript c means complex.)

If only interested in the stationary solution, which is valid after possible initial value dependent transients are damped out, we can assume a general form for the solution.

$$\begin{bmatrix}v_{yc}\\ \omega_{zc}\end{bmatrix} = \begin{bmatrix}\hat{v}_{yc}\\ \hat{\omega}_{zc}\end{bmatrix}\cdot e^{j\cdot\omega\cdot t} \quad\Rightarrow\quad \begin{bmatrix}\dot{v}_{yc}\\ \dot{\omega}_{zc}\end{bmatrix} = j\cdot\omega\cdot\begin{bmatrix}\hat{v}_{yc}\\ \hat{\omega}_{zc}\end{bmatrix}\cdot e^{j\cdot\omega\cdot t};$$

[4.59]

Inserting the assumption in the differential equation gives:

$$\begin{bmatrix} m & 0 \\ 0 & J \end{bmatrix} \cdot j \cdot \omega \cdot \begin{bmatrix} \hat{v}_{yc} \\ \hat{\omega}_{zc} \end{bmatrix} \cdot e^{j \cdot \omega \cdot t} + \\ + \begin{bmatrix} \frac{C_f + C_r}{v_x} & \frac{C_f \cdot l_f - C_r \cdot l_r}{v_x} + m \cdot v_x \\ \frac{C_f \cdot l_f - C_r \cdot l_r}{v_x} & \frac{C_f \cdot {l_f}^2 + C_r \cdot {l_r}^2}{v_x} \end{bmatrix} \cdot \begin{bmatrix} \hat{v}_{yc} \\ \hat{\omega}_{zc} \end{bmatrix} \cdot e^{j \cdot \omega \cdot t} = \begin{bmatrix} 1 \\ l_f \end{bmatrix} \cdot C_f \cdot \hat{\delta}_f \cdot e^{j \cdot \omega \cdot t} \Rightarrow$$

$$\Rightarrow \begin{bmatrix} \hat{v}_{yc} \\ \hat{\omega}_{zc} \end{bmatrix} =$$

$$= \left(\begin{bmatrix} m & 0 \\ 0 & J \end{bmatrix} \cdot j \cdot \omega + \begin{bmatrix} \frac{C_f + C_r}{v_x} & \frac{C_f \cdot l_f - C_r \cdot l_r}{v_x} + m \cdot v_x \\ \frac{C_f \cdot l_f - C_r \cdot l_r}{v_x} & \frac{C_f \cdot {l_f}^2 + C_r \cdot {l_r}^2}{v_x} \end{bmatrix} \right)^{-1} \cdot \begin{bmatrix} 1 \\ l_f \end{bmatrix} \cdot C_f \cdot \hat{\delta}_f =$$

$$= H_{\delta_f \to \begin{bmatrix} v_y \\ \omega_z \end{bmatrix}} \cdot \hat{\delta}_f; \qquad [4.60]$$

Then, we can assume we know $\hat{v}_{yc}$ and $\hat{\omega}_{zc}$ from Equation [4.60], and consequently we know v_{yc} and ω_{zc} from Eq [4.59]. We have derived the transfer function, $H_{\delta_f \to \begin{bmatrix} v_y \\ \omega_z \end{bmatrix}}$. The subscript tells that the transfer function is for the vehicle operation with excitation=input= δ_f and response=output= $\begin{bmatrix} v_y \\ \omega_z \end{bmatrix}$ case. This transfer function has dimension 2x1 and it is complex. It operates as follows:

$$\text{Amplitudes: } \begin{bmatrix} \hat{v}_y \\ \hat{\omega}_z \end{bmatrix} = \begin{bmatrix} |v_y| \\ |\omega_z| \end{bmatrix} = \left| H_{\delta_f \to \begin{bmatrix} v_y \\ \omega_z \end{bmatrix}} \right| \cdot |\delta_f|;$$

$$\text{Phase delays: } \begin{bmatrix} \arg(v_y) \\ \arg(\omega_z) \end{bmatrix} - \begin{bmatrix} 1 \\ 1 \end{bmatrix} \cdot \arg(\delta_f) = \{\arg(\delta_f) = 0\} = \arg\left(H_{\delta_f \to \begin{bmatrix} v_y \\ \omega_z \end{bmatrix}} \right) \qquad [4.61]$$

However, we can derive expressions for v_{yc} and ω_{zc} on a real (non-complex) form, $amplitude \cdot \cos(angular\ frequency \cdot t - phase\ delay)$, without involving transfer function. That is done in the following:

$$v_y = \mathrm{Re}(v_{yc}) = \mathrm{Re}(\hat{v}_{yc} \cdot e^{j \cdot \omega \cdot t}) = \cdots = |\hat{v}_{yc}| \cdot \cos(\omega \cdot t + \arg(\hat{v}_{yc}));$$

The same rewriting can be done with ω_z, so that in total:

$$\begin{bmatrix} v_y \\ \omega_z \end{bmatrix} = \begin{bmatrix} \hat{v}_y \cdot \cos(\omega \cdot t - \varphi_{vy}) \\ \hat{\omega}_z \cdot \cos(\omega \cdot t - \varphi_{\omega z}) \end{bmatrix} = \begin{bmatrix} |\hat{v}_{yc}| \cdot \cos\left(\omega \cdot t - (-\arg(\hat{v}_{yc}))\right) \\ |\hat{\omega}_{zc}| \cdot \cos(\omega \cdot t - (-\arg(\hat{\omega}_{zc}))) \end{bmatrix} \qquad [4.62]$$

Equation [4.60] and Equation [4.62] now gives us the possibility to find vehicle response amplitude and phase delay. The ratios between amplitude of responses and amplitude of excitation, $\hat{v}_y/\hat{\delta}_f$ and $\hat{\omega}_z/\hat{\delta}_f$, are called gains. The difference in argument is the phase delay.

4.4.3.2 Frequency Responses on Steering *

Function definition: ***Frequency Responses on Steering*** *are amplification and delay of steer angle to vehicle responses' measures (yaw velocity, lateral acceleration etc.), for stationary oscillating harmonic steering at certain longitudinal speed and varying steering frequency.*

Solutions to harmonic excitation of linear dynamic systems are superimposable. This is also why the response from a mixed frequency excitation can be spliced into separate frequencies, e.g. using Fourier transformation. Hence, a common way to measure the frequency response diagrams is to log data from a **random** steering test, where the excitation frequency and amplitude is randomly varying. Another

way is to sweep the frequency slowly over an interval. The frequency response diagram can then be extracted from either of those tests.

4.4.3.2.1 Lateral Velocity and Yaw Velocity Frequency Response *

The frequency response for the two states, Lateral Velocity and Yaw velocity, can be plotted using Eq [4.56] and only one input ($\boldsymbol{u} = \delta_f$; instead of $\boldsymbol{u} = [\delta_f \quad F_{fxw} \cdot \delta_f]^T$), see Figure 4-55. The curves show Frequency Response for same vehicle, but different speed. The yaw velocity gain curve has a knee at 0.5..1 Hz. The decrease after that is a measure of yaw damping. The curve for high speed actually has a weak peak just before the knee. This is not desired, because the vehicle might feel a bit nervous. Yaw damping can also be how fast yaw velocity decays after a step response, see 4.4.3.4.

From Equation [4.19] we can calculate that characteristic speed for the vehicle is 120 km/h. With another understeering coefficient, we could have calculated a critical speed. Studying Figure 4-55 to Figure 4-58, one can find these special speeds in another appearance:

- For an understeered vehicle, speeds above the characteristic speed gives a negative yaw velocity delay for low steering frequencies will be negative.
- For over-steered vehicles, speeds above the critical speed gives a yaw velocity delay larger than 180 deg and yaw velocity amplitudes which are very large for low steering frequencies.

From Equation [4.19] we can calculate that characteristic speed for the vehicle is 120 km/h.

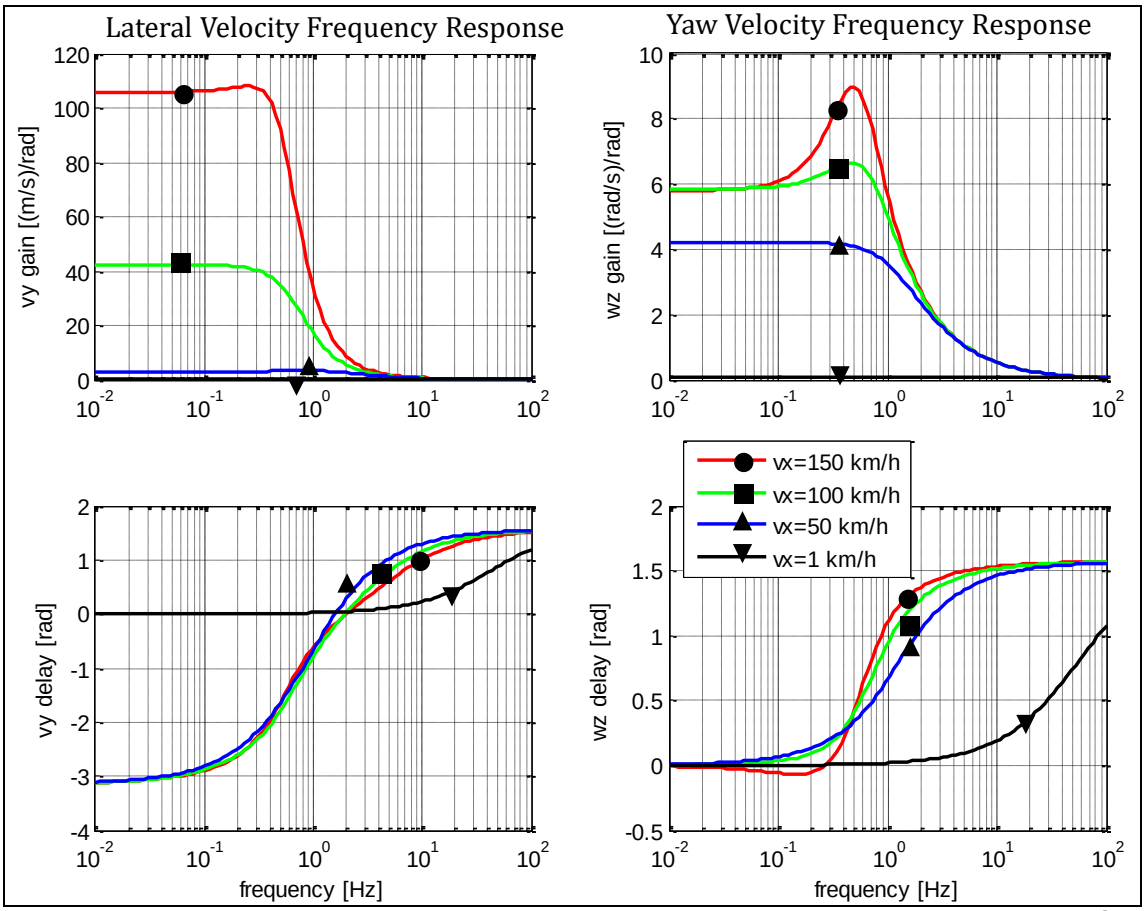


Figure 4-55: Frequency response to steer angle. Vehicle data: $m = 2000\ kg$; $J = 3000\ kg \cdot m^2$; $l_f = 1.3\ m$; $l_r = 1.5\ m$; $C_f = 81400\ N/rad$; $C_r = 78000\ N/rad$; ($K_u = 1.26\ rad/MN$).

In Figure 4-56 the curves are for same speed and constant understeering gradient, but they show the Frequency Response for different sums of cornering stiffness $C_f + C_r$. Increasing the stiffness increases the yaw velocity gain (agility) at high frequencies.

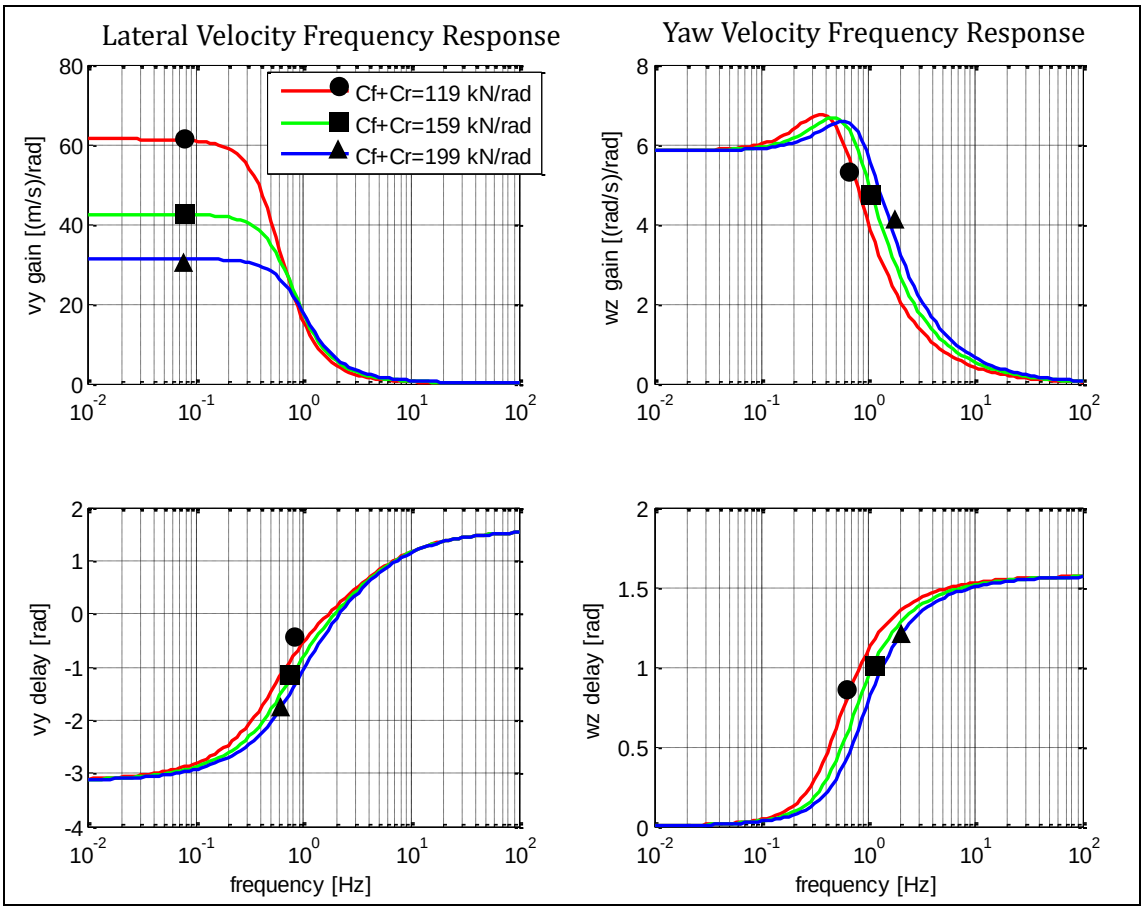


Figure 4-56: Frequency response to steer angle. Same vehicle data as in Figure 4-55, except varying C_f and C_r but keeping understeering gradient K_u constant. Vehicle speed = 100 km/h.

In Figure 4-57 the curves are for same speed and constant sum of cornering stiffness ($C_f + C_r$), but they show the Frequency Response for different values of understeering gradient (Ku). Increasing understeer gradient decreases the yaw velocity gain (agility) at low frequencies. But, also note that increased understeering increases the peak in YVFR at around 0.5 Hz, which means low yaw damping.

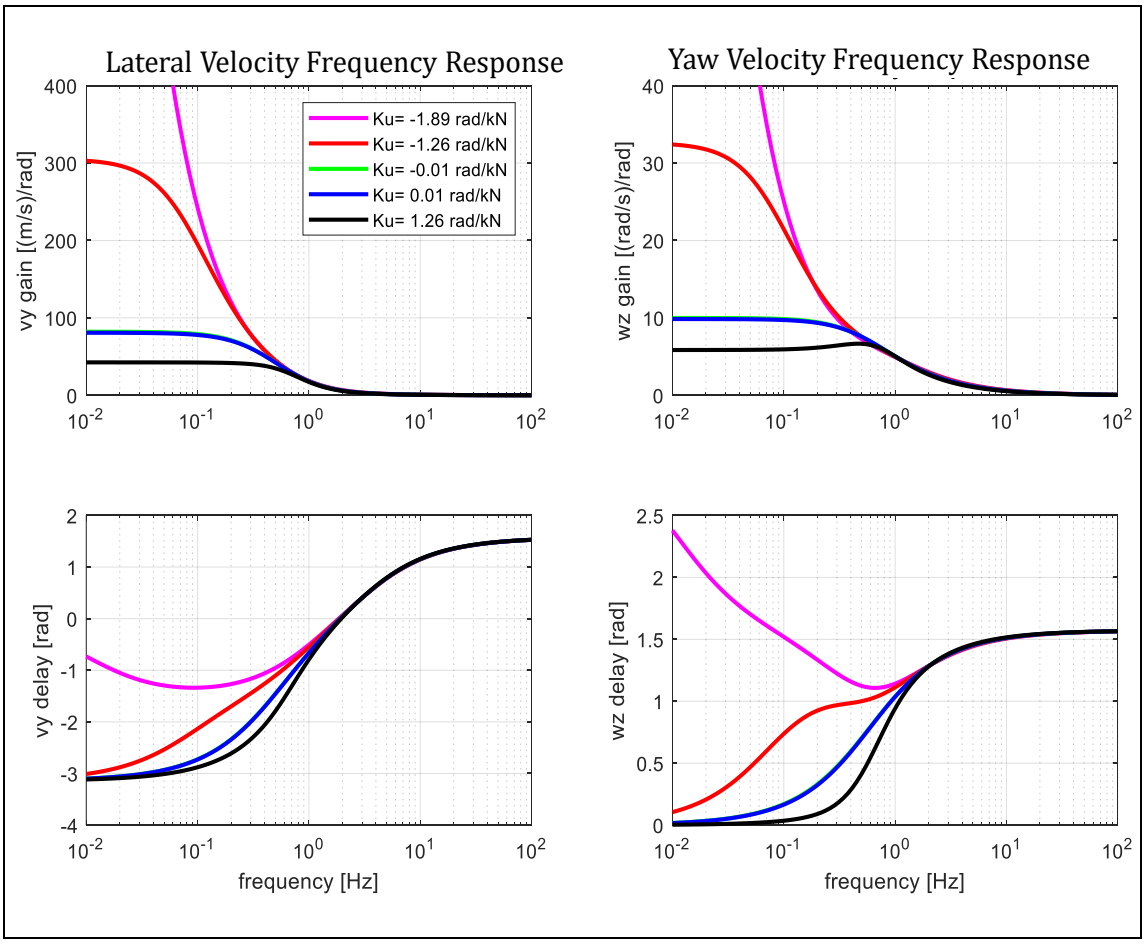


Figure 4-57: Frequency response to steer angle. Same vehicle data as in Figure 4-55, except varying understeering gradient Ku but keeping $C_f + C_r$ constant. Vehicle speed $v_x = 100$ km/h. The $K_u = -1.89$ gives $v_{xCrit} \approx 98$ km/h $< v_x$.

4.4.3.2.2 Lateral Acceleration Frequency Response *

The lateral acceleration Frequency Response is another useful measure to study and set requirements on. Actually, yaw velocity and lateral acceleration are the most frequently used measures, since they are easily measured, e.g. from ESC sensors in most vehicles.

The transfer function is found (here using Fourier transform and previous results):

$$\text{Amplitude: } \hat{a}_y = |a_{yc}| = \left\{use: a_y = \frac{\dot{v}_y + \omega_z \cdot v_x}{m}\right\} = \left|\frac{j\cdot\omega\cdot v_{yc} + \omega_{zc}\cdot v_x}{m}\right| =$$
$$= \left|\frac{1}{m}\cdot[j\cdot\omega \quad v_x]\cdot H_{\delta_f\to\begin{bmatrix}v_y\\ \omega_z\end{bmatrix}}\cdot\delta_f\right| = \left|[j\cdot\omega \quad v_x]\cdot H_{\delta_f\to\begin{bmatrix}v_y\\ \omega_z\end{bmatrix}}\right|\cdot\frac{\delta_f}{m};$$
$$\text{Phase delay: } \arg(a_y) - \arg(\delta_f) = \{use: \arg(\delta_f) = 0\} = \arg\left([j\cdot\omega \quad v_x]\cdot H_{\delta_f\to\begin{bmatrix}v_y\\ \omega_z\end{bmatrix}}\right); \qquad [4.63]$$

Lateral acceleration Frequency Response is plotted for different vehicle speeds in Figure 4-58.

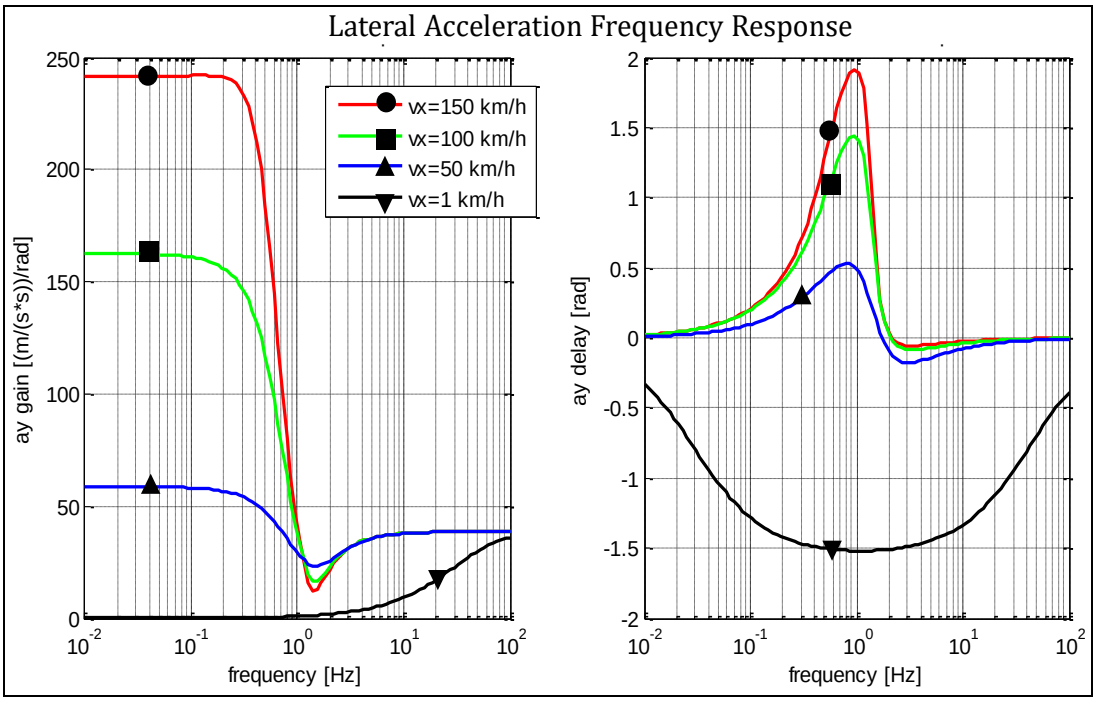


Figure 4-58: Lateral acceleration frequency response to steer angle. Vehicle data: $m = 2000\ kg;\ J = 3000\ kg \cdot m^2;\ l_f = 1.3\ m;\ l_r = 1.5\ m;\ C_f = 81400\ N/rad;\ C_r = 78000\ N/rad;\ (K_u = 1.26\ rad/MN)$.

4.4.3.2.2.1 Influence of Tyre Relaxation

If relaxation is taken into account using 0 and $L_r = 50\%\ of\ wheel\ circumference = 0.5 \cdot 2 \cdot \pi \cdot R; R = 0.3\ m;$, we get the following versions of the diagrams in Figure 4-55 .. Figure 4-58:

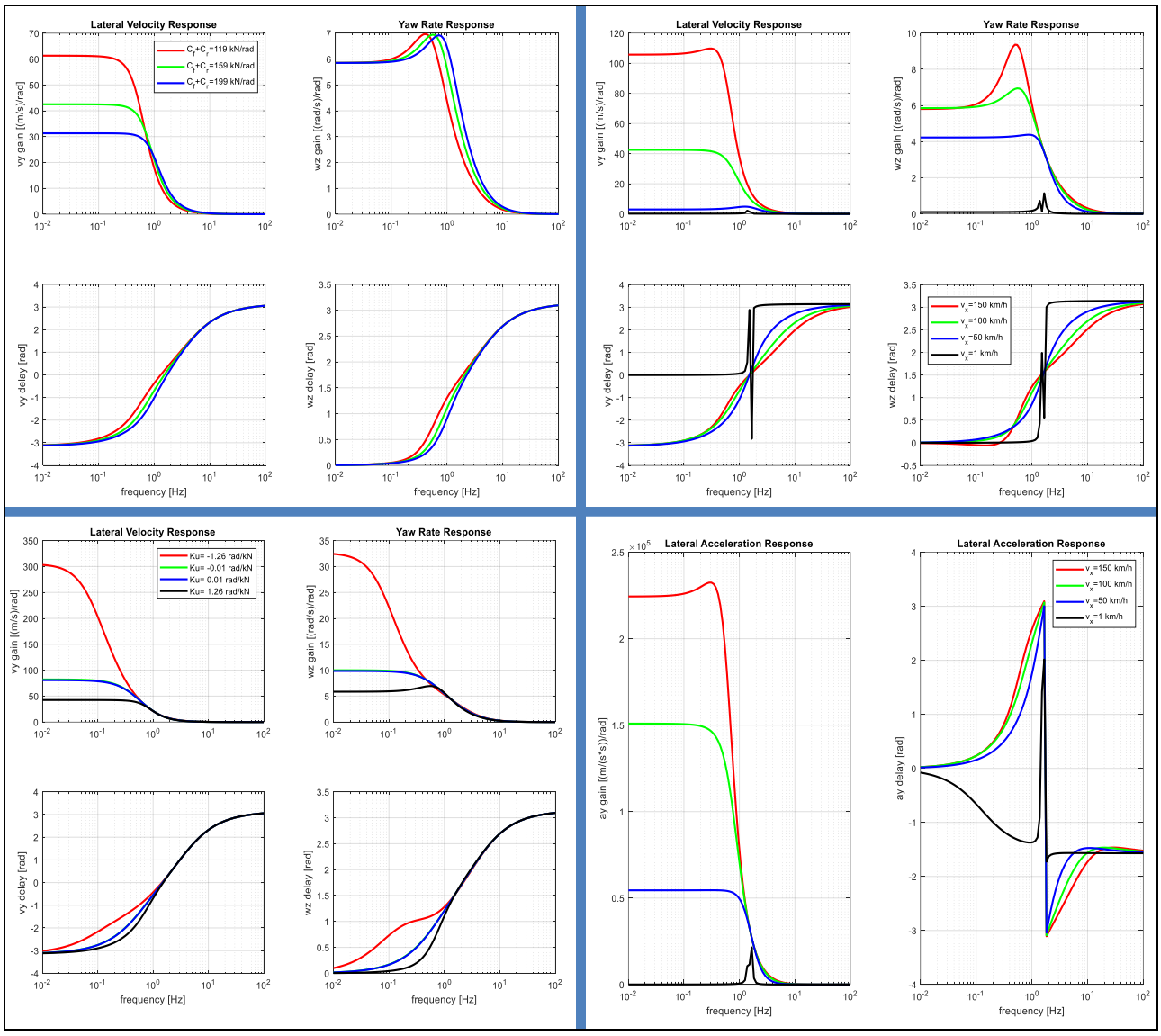


Figure 4-59: Frequency responses if model includes tyre relaxation.

We see that we get similar frequency responses, but the gain peaks at $f \approx 0.3..08\ Hz$ becomes a bit higher. This is expected, since we add a delay in the system. The delay influence generally more if the vehicle is articulated, such as long heavy combination vehicles.

It should be noted that the Lateral Acceleration Frequency Response gain approaches zero asymptotically when frequency increases, which was not the case without relaxation. The approach to zero is truer and more intuitive since, with relaxation, the steered axle will not have time to develop forces when its steering angle oscillates with high frequency.

4.4.3.3 Other Frequency Responses to Oscillating Steering *

In principle, it is possible to study a lot of other responses, such as Path Curvature Frequency Response, Side slip Frequency Response and Lateral Path Width Frequency Response etc. For combination-vehicles it is common to plot Rearward amplification (RA) as function of frequency. The book identifies some alternative definitions: $RA_{\omega z} = \max_i(\hat{\omega}_{iz}/\hat{\omega}_{1z})$; where i numbers the vehicle units. If the manoeuvre is not stationary oscillations, but e.g. a single lane change, we instead propose $RA_{\omega z} = \max_i\left(\max_t|\omega_{iz}|/\max_t|\omega_{1z}|\right)$;. RA can also be defined for the worst frequency, e.g. $RA_{\omega z} =$

$\max_f\left(\max_i(\hat{\omega}_{iz}/\hat{\omega}_{1z})\right)$;. (Some argue for alternative definitions with a_y instead of ω_z. However, these are more difficult to agree on; which point, vertical and longitudinal, one should measure a_y in.)

4.4.3.4 Lateral Stability

Eq [4.55] can explain instability. If one of the eigen solutions grows unlimited, v_y and/or ω_z grows unlimited. We call the property of such growth *lateral instability*. Simplified, instability can have two modes: Front axle maintains grip but rear axle slides sideways (oversteering in 4.3.3.3) and vice versa which makes vehicle unsteer-able (understeering in 4.3.3.3),

4.4.3.4.1 Locking One Axle

Locking one axle, i, can be modelled by replacing C_i with $\mu \cdot F_{iz}$;. This can be proven by linearization of Eq [4.52] with the locked axle's constitution replaced by "$F_{iy} = -\mu \cdot F_{iz} \cdot v_{iy}/|v_{ix}|$;". Since $C_i \approx CC_i \cdot F_{iz}$ and cornering compliance, CC_i, is typically 5..10 (trucks) and 10..15 (passenger cars), we can conclude that $\mu \cdot F_{iz}$ is normally $\ll C_i$. Realistic variation of road friction coefficient μ is 0.2..1. So, a locked axle can be seen as having much (typically 5..75 times) lower cornering stiffness on the locked axle. So, locking front gives extreme under-steering and locking rear gives extreme over-steering.

4.4.3.4.2 Frequency Responses for Different Understeering Gradients

Eq [4.55] can explain instability. Instability means here that vehicle gets infinitely growing solutions although $\delta_f \equiv 0$. Eq [4.73] shows the explicit solution. We set $\delta_f \equiv 0$; and a small yaw disturbance as initial conditions: $[v_{y0} \quad \omega_{z0}] = [0 \quad \varepsilon]$; and get the following expression for the solution:

$$\begin{bmatrix} v_y \\ \omega_z \end{bmatrix} = \begin{bmatrix} \hat{v}_{y1} & \hat{v}_{y2} \\ \hat{\omega}_{z1} & \hat{\omega}_{z2} \end{bmatrix} \cdot \begin{bmatrix} e^{\lambda_1 \cdot t} & 0 \\ 0 & e^{\lambda_2 \cdot t} \end{bmatrix} \cdot \begin{bmatrix} \hat{v}_{y1} & \hat{v}_{y2} \\ \hat{\omega}_{z1} & \hat{\omega}_{z2} \end{bmatrix}^{-1} \cdot \begin{bmatrix} v_{y0} \\ \omega_{z0} \end{bmatrix};$$

$$where \left[\begin{bmatrix} \hat{v}_{y1} & \hat{v}_{y2} \\ \hat{\omega}_{z1} & \hat{\omega}_{z2} \end{bmatrix}, \begin{bmatrix} \lambda_1 & 0 \\ 0 & \lambda_2 \end{bmatrix}\right] = \text{eig}(\boldsymbol{A});$$

In Figure 4-60 we sweep v_x for normal passenger car data and try the following cornering stiffnesses:

- Locked front axle: $C_f \cdot l_f \approx 0.1 \cdot C_r \cdot l_r$; (extremely under-steered)
- Under-steered: $C_f \cdot l_f \approx 0.9 \cdot C_r \cdot l_r$; (moderatly under-steered
- Neutral-steered: $C_f \cdot l_f \approx 1 \cdot C_r \cdot l_r$;
- Over-steered: $C_f \cdot l_f \approx 1.1 \cdot C_r \cdot l_r$; (moderatly over-steered
- Locked rear axle: $C_f \cdot l_f \approx 10 \cdot C_r \cdot l_r$; (extremely over-steered)

In Figure 4-60 we see that only over-steered (incl. lock rear) gives an unstable vehicle. And that only under-steered vehicles (incl. lock front) give oscillating solutions. Also, we see that all vehicles are stable for low enough speed.

Limit to instability (subscript $crit$) is when $\text{Real}(\lambda_{crit}) = 0$. Since $\lambda = \lambda(v_x)$, we can find $v_{x,crit} = \sqrt{C_f \cdot C_r \cdot L^2/(C_f \cdot l_f - C_r \cdot l_r) \cdot m}$;. This is the same expression as we found already with the steady state model in Eq [4.19]. An advantage with using the transient model in Eq [4.55] is that we can also express how fast the solutions grows towards infinity, if they are oscillating or exponential and how the eigenmodes look.

We can express the condition for instability in other quantities. An example is when we want to limit regenerative braking with electric motor on rear axle. Then we solve for $C_{r,crit}$: $C_{r,crit} = l_f/(L^2/m \cdot v_x^2 - l_f/C_f)$;. Together with a combined slip tyre model (e.g. Eq [2.63]), we can express instability in: $F_{x,crit} = \sqrt{(\mu \cdot F_z)^2 - \left(\mu \cdot F_z \cdot l_f/\left((L^2/m \cdot v_x^2 - l_f/C_f) \cdot C_{ry}\big|_{s_x=0}\right)\right)^2}$;.

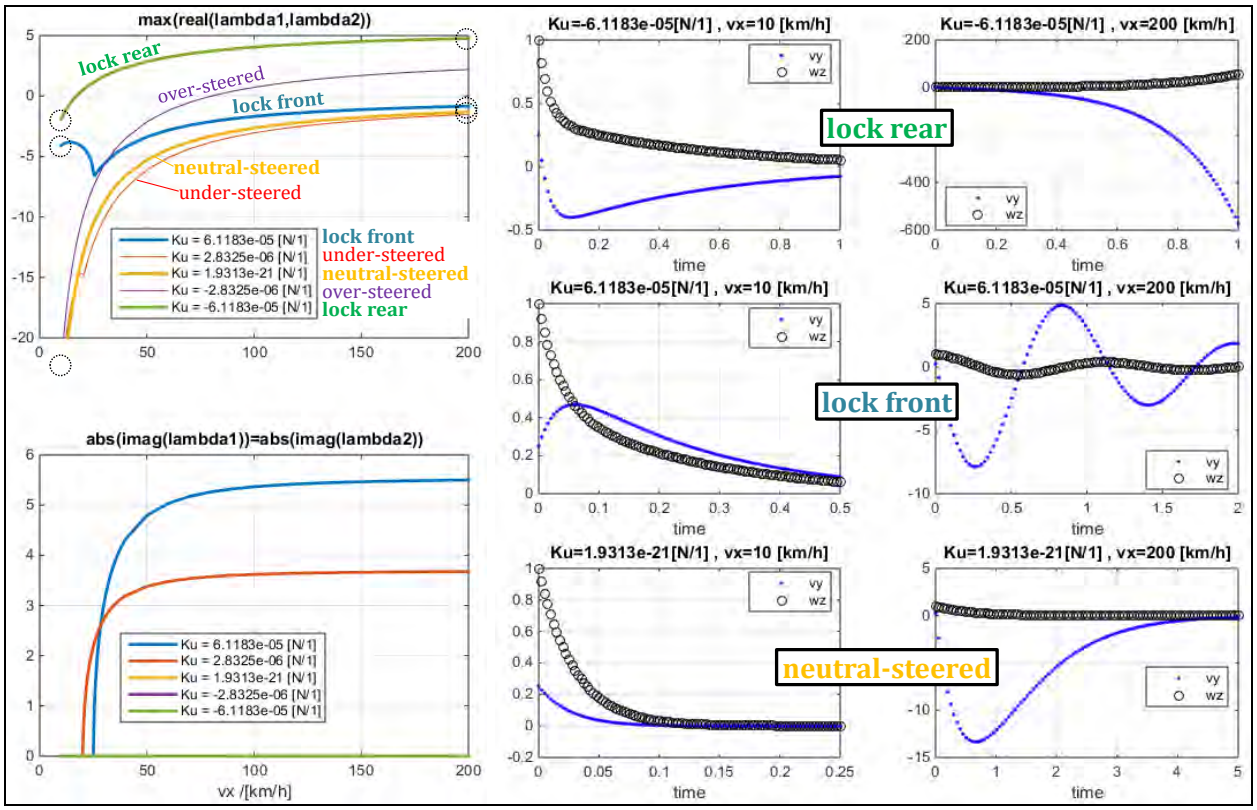


Figure 4-60: Stability analysis of passenger car with varying cornering stiffnesses.

4.4.3.5 Driver Influence on Stability

A driver can improve or disturb the vehicle. The gains for steady state cornering and the frequency responses for stationary oscillating steering does not measure the real stability since they do not include the dynamics of the driver, neither human nor automated driver. However, studying critical speed through a transient model enables to add a dynamic driver model and quantify the influence of driver.

A driver model can be, e.g.: $\delta_f = k \cdot (\omega_{z,Req} - \omega_z) = k \cdot \left(\frac{v_x}{R_{Path}} - \omega_z\right) = k \cdot \frac{v_x}{R_{Path}} + k \cdot [0 \quad -1] \cdot \begin{bmatrix} v_y \\ \omega_z \end{bmatrix}$;

This is for a constant radius turn, where R_{Path} is the radius with positive sign if turning left.

Adding this equation to Eq [4.55] gives:

$$\begin{bmatrix} \dot{v}_y \\ \dot{\omega}_z \end{bmatrix} = \boldsymbol{A} \cdot \begin{bmatrix} v_y \\ \omega_z \end{bmatrix} + \boldsymbol{B} \cdot \delta_f = (\boldsymbol{A} + \boldsymbol{B} \cdot k \cdot [0 \quad -1]) \cdot \begin{bmatrix} v_y \\ \omega_z \end{bmatrix} + \boldsymbol{B} \cdot k \cdot \frac{v_x}{R_{Path}};$$

We assume v_x as given constant, so the interesting eigenvalue is for the matrix $(\boldsymbol{A} + \boldsymbol{B} \cdot k \cdot [0 \quad -1])$. Eigenvalue analysis for different speed v_x and driver gain k gives the Figure 4-61.

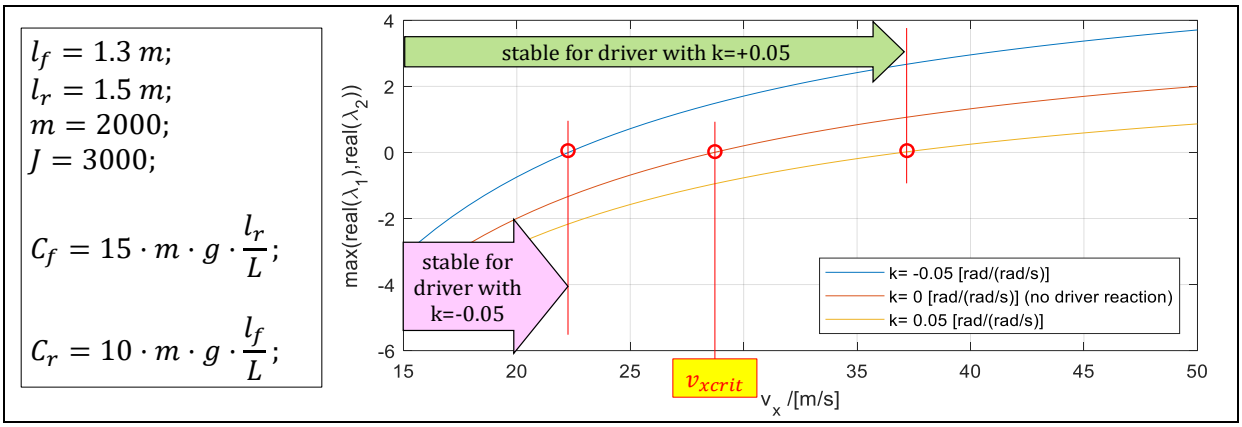


Figure 4-61: Influence of driver on stability on an oversteered vehicle.
Driver model used: $\delta_f = k \cdot (\omega_{z,Req} - \omega_z)$. Straight line, $\omega_{zReq} = 0$, is used as example.

Involvement of such a driver model makes it possible to compute a continuous stability measure k, not only a Boolean, stable or instable.

4.5 Transient Driving

This section addresses both transient handling and arbitrary transient driving, where the first is mainly lateral, while longitudinal dynamics is added in the latter. Generally, this can be turning and braking/accelerating at the same time through a manoeuvre.

4.5.1 Transient Driving Manoeuvres *

From the manoeuvres defined in this section, there are a large number of relevant function possible to define. Here, only a few is mentioned:

> *Function definition:* ***Double Lane Change Capability*** *is the highest entry speed that a certain driver (or driver model) can manage without hitting any cones. A certain cone pattern (e.g. as Figure 4-62 or Figure 4-63) and a certain road friction has to be defined. A certain operation principle of pedals needs to be specified, e.g. release both pedals at entry or full brake pedal apply.*
>
> *Function definition:* ***Over-speed into Curve Capability*** *is the highest entry speed that a certain driver (or driver model) can manage without hitting any cones. A certain cone pattern e.g. as Figure 4-64) and a certain road friction has to be defined. A certain operation principle of pedals needs to be specified, e.g. release both pedals at entry or full brake pedal apply.*
>
> *Function definition:* ***Steer-In and Release Accelerator Pedal stability*** *is a measure (e.g. side slip rear axle peak) after a certain simultaneous steer-in and release of accelerator pedal, starting from a steady state cornering at a certain path radius and speed. A certain road friction has to be defined.*

When testing Transient driving manoeuvres, the typical part of the test track is the Vehicle Dynamics Area or a Handling Track, see Figure 1-70. A Handling Track is a normal width road, intentionally curved and with safety areas beside the curves for safety in case of run-off road during tests.

Typical transient tests are:

- Step steer, where one can measure transient versions of
  - Yaw velocity response
  - Lateral acceleration response
  - Curvature response
  - Yaw damping
- Lateral avoidance manoeuvres:
  - Single Lane Change SLC cone track
  - Double Lane Change DLC cone track, see Figure 4-22, Figure 4-62, and Figure 4-63
  - Lane change while full braking

  - Sine with dwell
  - Steering effort in evasive manoeuvres
- Tests from steady state cornering
  - Brake or accelerate in curve
  - Lift accelerator pedal and steer-in while cornering
  - Over-speeding into curve, see Figure 4-64
- Handling type tests
  - Slalom between cones
  - Handling track, general driving experience
- Roll-over tests

Standards which are relevant to these test manoeuvres are, e.g. References (ISO 3888), (ISO 7401), (ISO 7975, 2006), (ISO 11026), (ISO 14791), (ISO 14793), (ISO 14794, 2011) and (NHTSA).

There are many standards for DLC beside ISO, such as Consumer Union. Generally speaking, the DLCs with short distance in 2nd lane is often used for ESC-like tests.

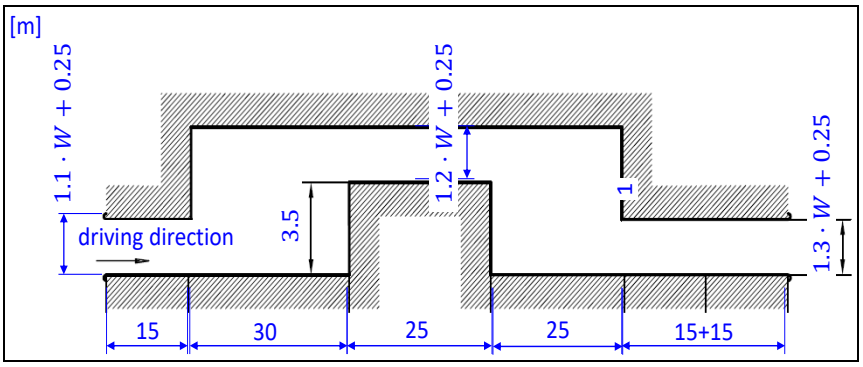


Figure 4-62: Passenger cars - Test track for a severe lane-change manoeuvre - Part 1: Double lane-change. Reference (ISO 3888).

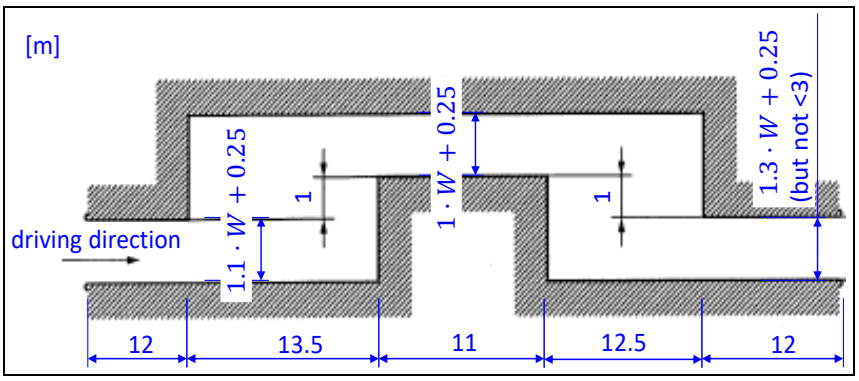


Figure 4-63: Passenger cars - Test track for a severe lane-change manoeuvre - Part 2: Obstacle avoidance. Reference (ISO 3888).

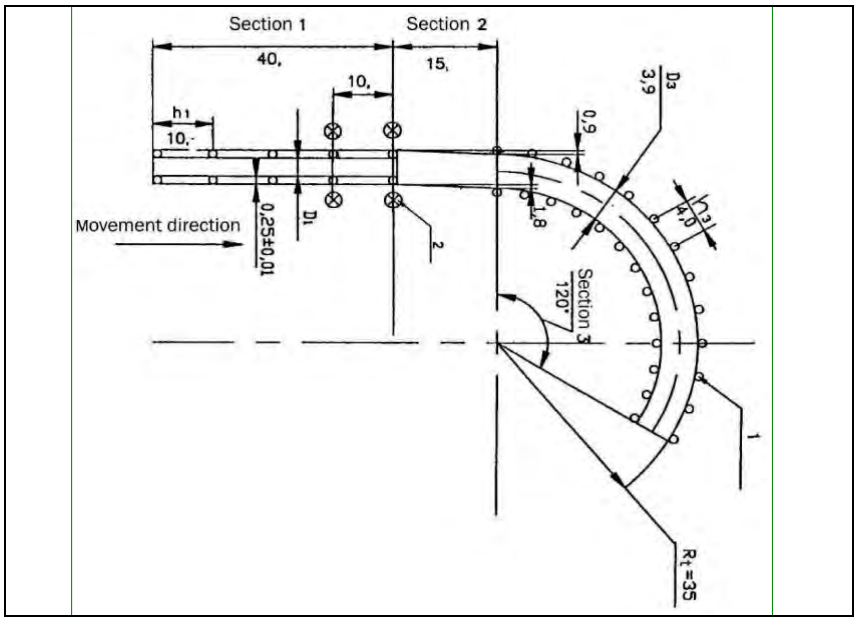


Figure 4-64: Cone track for one standardized test of Over-speeding into curve

4.5.2 One-Track Models, without Lateral Load Transfer

4.5.2.1 Two-Axle Vehicle

This section starts from the model derived in 4.4.2 and Figure 4-49 and Equations [4.51] and [4.52]. However, in the context of transient dynamics it is more relevant to use the model for more violent manoeuvres, and also active control such as ESC interventions. Hence, we extend the model in three ways:

- The constitutive relation is saturated, to reflect that each axle may reach friction limit, friction coefficient times normal load on the axle. See max functions in Equation [4.64].
- To be able to do mentioned limitation, the longitudinal load transfer is modelled, but only in the simplest possible way using stiff suspension models. Basically, it is the same model as given in Equation [3.18].
- A yaw moment representing (left/right) unsymmetrical braking/propulsion. See the term $M_{act,z}$ in yaw equilibrium in Equation [4.64]. This is much better modelled in a two-track model, where $M_{act,z}$ does not appear, but we instead can have different longitudinal tyre forces on left and right side.

It should be noted that the model lacks lateral load transfer and the transients in longitudinal load transfer and the reduced cornering stiffness and reduced max friction due to load transfer and utilizing friction for wheel longitudinal forces.

Equilibrium in road plane (longitudinal, lateral, yaw):

$$m \cdot (\dot{v}_x - \omega_z \cdot v_y) = F_{fxw} \cdot \cos(\delta_f) - F_{fyw} \cdot \sin(\delta_f) + F_{rx};$$
$$m \cdot (\dot{v}_y + \omega_z \cdot v_x) = F_{fxw} \cdot \sin(\delta_f) + F_{fyw} \cdot \cos(\delta_f) + F_{ry};$$
$$J \cdot \dot{\omega}_z = (F_{fxw} \cdot \sin(\delta_f) + F_{fyw} \cdot \cos(\delta_f)) \cdot l_f - F_{ry} \cdot l_r + M_{act,z};$$

Equilibrium out of road plane (vertical, pitch):

$$F_{fz} + F_{rz} - m \cdot g = 0;$$
$$-F_{fz} \cdot l_f + F_{rz} \cdot l_r - (F_{fxw} \cdot \cos(\delta_f) - F_{fyw} \cdot \sin(\delta_f) + F_{rx}) \cdot h = 0;$$

Constitution:

$$F_{fyw} = -\text{sign}(s_{fy}) \cdot \min(C_f \cdot |s_{fy}|;\ \mu \cdot F_{fz});$$
$$F_{ry} = -\text{sign}(s_{ry}) \cdot \min(C_r \cdot |s_{ry}|;\ \mu \cdot F_{rz});$$

Compatibility, slip definitions:

$$s_{fy} = \frac{v_{fyw}}{v_{fxw}};\quad and\quad s_{ry} = \frac{v_y - l_r \cdot \omega_z}{v_x};$$

Compatibility, transformation from vehicle to wheel coordinate system:

$$v_{fxw} = (v_y + l_f \cdot \omega_z) \cdot \sin(\delta_f) + v_x \cdot \cos(\delta_f);$$
$$v_{fyw} = (v_y + l_f \cdot \omega_z) \cdot \cos(\delta_f) - v_x \cdot \sin(\delta_f);$$

[4.64]

A Modelica model is given in Eq [4.65]. Changes compared to Eq [4.51] are marked as underlined code.

```
//Equilibrium, in road plane:
  m*(der(vx)-wz*vy) = Ffxv + Frx;
  m*(der(vy)+wz*vx) = Ffyv + Fry;
  J*der(wz) = Ffyv*lf - Fry*lr + Mactz;
//Equilibrium, out of road plane:
  Ffz + Frz - m*g = 0;
  -Ffz*lf + Frz*lr -(Ffxv + Frx)*h = 0;
//Compatibility:
  vfxv = vx;    vfyv = vy + lf*wz;
  vrx = vx;     vry = vy - lr*wz;
//Lateral tyre force model:
  Ffyw = -sign(sfy)*min(Cf*abs(sfy), mu*Ffz);   sfy = vfyw/vfxw;
  Fry  = -sign(sry)*min(Cr*abs(sry), mu*Frz);   sry = vry/vrx;
//Transformation between vehicle and wheel coordinate systems:
  Ffxv = Ffxw*cos(df) - Ffyw*sin(df);
  Ffyv = Ffxw*sin(df) + Ffyw*cos(df);
  vfxv = vfxw*cos(df) - vfyw*sin(df);
  vfyv = vfxw*sin(df) + vfyw*cos(df);
//Shaft torques
  Ffxw = +1000; // Front axle driven.
  Frx  = -100; // Rolling resistance on rear axle.
  Mactz=0;
```

[4.65]

A simulation of this model is seen in Figure 4-65. Same steering input as used in Figure 4-50. $M_{act,z}$ is zero. Cornering stiffnesses are chosen so that the vehicle is understeered in steady state. Road friction coefficient is 1. We can see that the vehicle now gets unstable and spins out with rear to the right. This is mainly because longitudinal load transfer unloads the rear axle, since the kept steer angle decelerates the vehicle. In this manoeuvre, it would have been reasonable to model also that the rear cornering stiffness decreases with the decreased rear normal load, and opposite on front. Such addition to the model would make the vehicle spin out even more. On the other hand, the longitudinal load shift is modelled to take place immediately. With a suspension model, this load shift would require some more time, which would calm down the spin-out. In conclusion, the manoeuvre is violent enough to trigger a spin-out, so a further elaboration with how to control $M_{act,z}$ could be of interest. However, it is beyond the scope of this book.

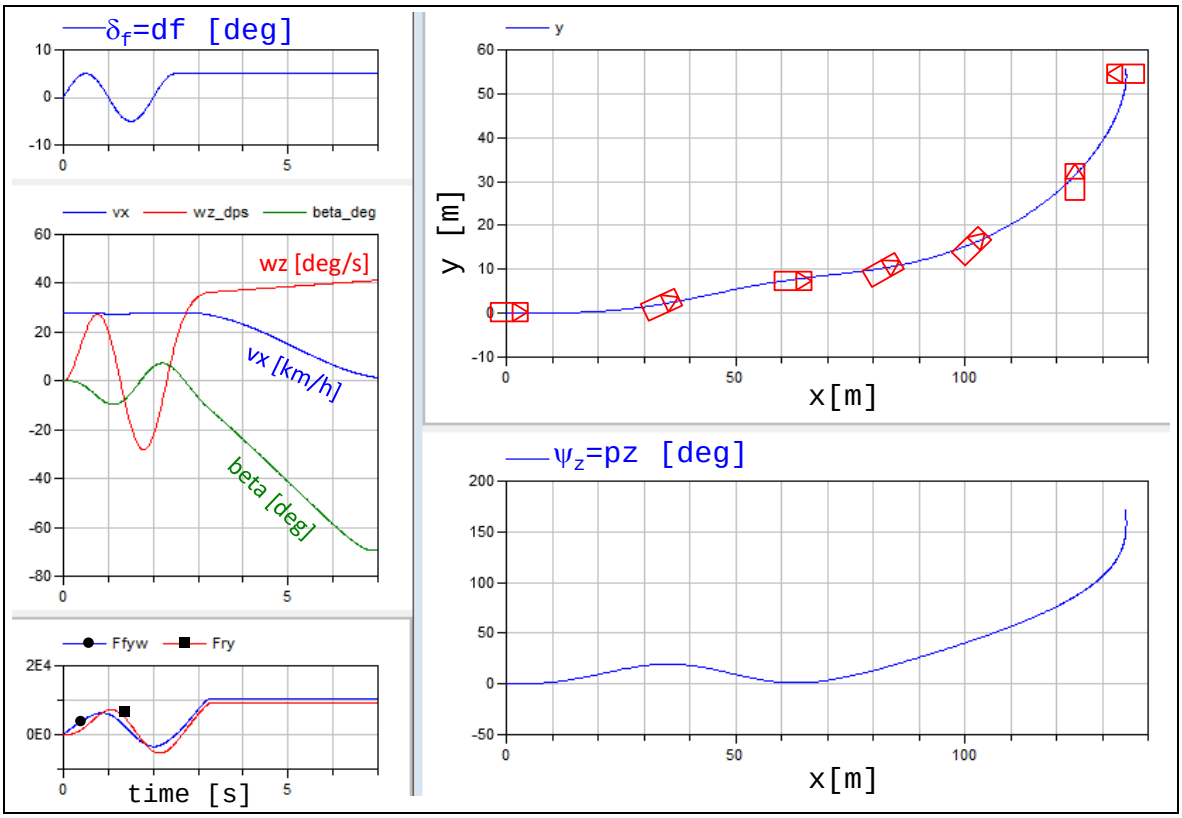


Figure 4-65: Simulation results of one-track model for transient dynamics. The vehicle drawn in the path plot is not in proper scale, but the orientation is approximately correct.

The vehicle reaches zero speed already after 7 seconds, because the wide side slip decelerates the vehicle a lot. The simulation is then stopped, because the model cannot handle zero speed. That vehicle models become singular at zero speed is very usual, since the slip definition becomes singular due to zero speed in the denominator. The large difference compared to Figure 4-50 is due to the new constitutive equation used, which shows the importance of checking validity region for any model one uses.

A simplified version of the mathematical model in Eq [4.64] follows in Eq [4.66]; assuming constant v_x and small angles and small propulsion force and no $M_{act,z}$.

Equilibrium in road plane (lateral, yaw):

$$m \cdot (\dot{v}_y + \omega_z \cdot v_x) = F_{fy} + F_{ry};$$
$$J \cdot \dot{\omega}_z = F_{fy} \cdot l_f - F_{ry} \cdot l_r;$$

Equilibrium out of road plane (vertical, pitch):

$$F_{fz} + F_{rz} - m \cdot g = 0;$$
$$-F_{fz} \cdot l_f + F_{rz} \cdot l_r = 0;$$

Constitution:

$$F_{fy} = -\text{sign}(s_{fy}) \cdot \min(C_f \cdot |s_{fy}|;\ \mu \cdot F_{fz});$$
$$F_{ry} = -\text{sign}(s_{ry}) \cdot \min(C_r \cdot |s_{ry}|;\ \mu \cdot F_{rz});$$

Compatibility:

$$\delta_f + s_{fy} = \frac{v_y + l_f \cdot \omega_z}{v_x};\quad and\quad s_{ry} = \frac{v_y - l_r \cdot \omega_z}{v_x};$$

[4.66]

4.5.2.2 Articulated Vehicles

A model for an articulated vehicle will now be derived in the same spirit as in 4.4.2. The model can represent a car with trailer or rigid truck with centre-axle trailer or tractor with semitrailer (if $l_{1c} < L_1$).

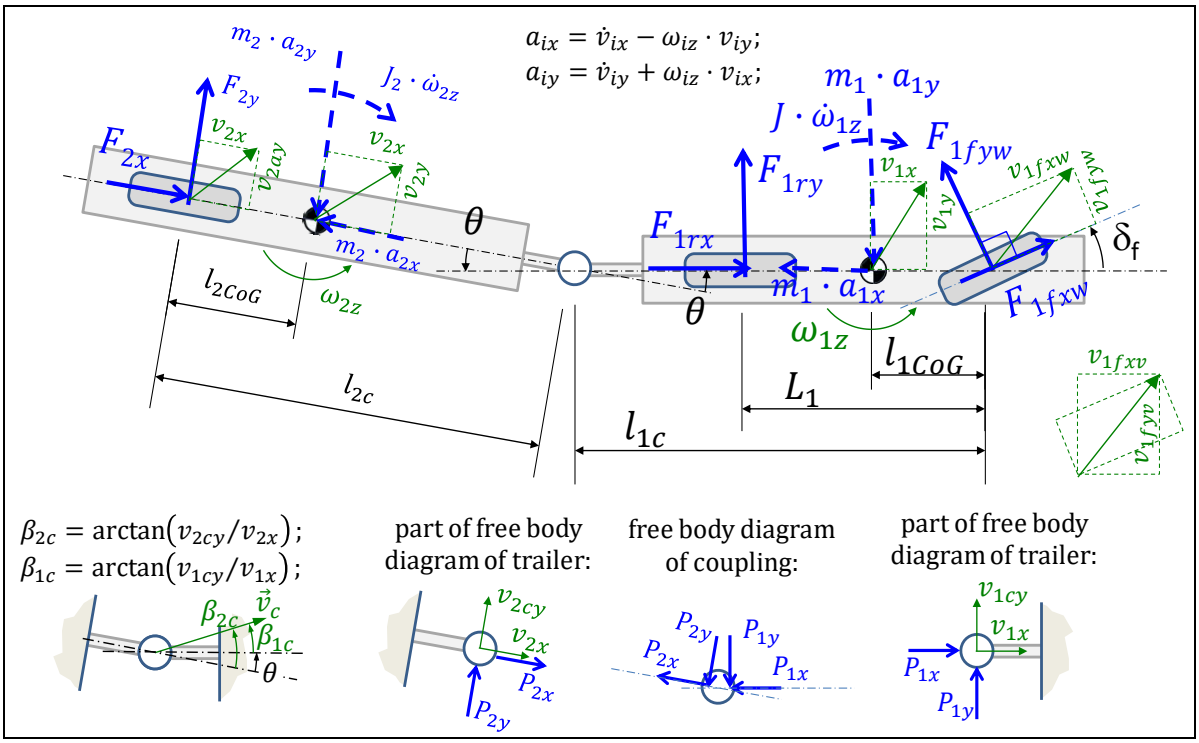


Figure 4-66: Model of two-unit articulated vehicle.

Model equations for the 1st unit:

Equilibrium of 1st unit (longitudinal, lateral, yaw around CoG):

$$m_1 \cdot (\dot{v}_{1x} - \omega_{1z} \cdot v_{1y}) = \cos(\delta_f) \cdot F_{1fxw} - \sin(\delta_f) \cdot F_{1fyw} + F_{1rx} + P_{1x};$$
$$m_1 \cdot (\dot{v}_{1y} + \omega_{1z} \cdot v_{1x}) = \sin(\delta_f) \cdot F_{1fxw} + \cos(\delta_f) \cdot F_{1fyw} + F_{1ry} + P_{1y};$$
$$J_1 \cdot \dot{\omega}_{1z} = (\sin(\delta_f) \cdot F_{1fxw} + \cos(\delta_f) \cdot F_{1fyw}) \cdot l_{1CoG} - F_{1ry} \cdot (L_1 - l_{1CoG}) + + (-P_{1y}) \cdot (l_{1c} - l_{1CoG});$$

Compatibility, within 1st unit:

$$v_{1fyv} = v_{1y} + \omega_{1z} \cdot l_{1CoG};$$
$$v_{1ry} = v_{1y} - \omega_{1z} \cdot (L_1 - l_{1CoG});$$
$$v_{1cy} = v_{1y} - \omega_{1z} \cdot (l_{1c} - l_{1CoG}); \quad \blacksquare$$
$$v_{1fxw} = +\cos(\delta_f) \cdot v_{1x} + \sin(\delta_f) \cdot v_{1fyv};$$
$$v_{1fyw} = -\sin(\delta_f) \cdot v_{1x} + \cos(\delta_f) \cdot v_{1fyv};$$

Constitution for axles on 1st unit:

$$F_{1fyw} = -C_{1f} \cdot s_{1fy}; \quad F_{1ry} = -C_{1r} \cdot s_{1ry};$$
$$s_{1fy} = v_{1fyw}/|v_{1fxw}|; \quad s_{1ry} = v_{1ry}/|v_{1x}|;$$

[4.67]

Model equations for the 2nd unit:

Equilibrium of 2nd unit (longitudinal, lateral, yaw around CoG):

$$m_2 \cdot (\dot{v}_{2x} - \omega_{2z} \cdot v_{2y}) = F_{2x} + P_{2x};$$
$$m_2 \cdot (\dot{v}_{2y} + \omega_{2z} \cdot v_{2x}) = F_{2y} + P_{2y};$$
$$J_2 \cdot \dot{\omega}_{2z} = -F_{2y} \cdot l_{2CoG} + P_{2y} \cdot (l_{2c} - l_{2CoG});$$

Compatibility, within 2nd unit:

$$v_{2cy} = v_{2y} + \omega_{2z} \cdot (l_{2c} - l_{2CoG}); \quad \blacksquare$$
$$v_{2ay} = v_{2y} - \omega_{2z} \cdot l_{2CoG};$$

Constitution for axles on 2nd unit:

$$F_{2y} = -C_2 \cdot s_{2y}; \quad s_{2y} = v_{2ay}/|v_{2x}|;$$

[4.68]

Model equations for the coupling (see also1.6.1.1):

Equilibrium of coupling (x, y in 1st unit's coordinates):

$$P_{1x} + \cos(\theta) \cdot P_{2x} + \sin(\theta) \cdot P_{2y} = 0;$$
$$P_{1y} - \sin(\theta) \cdot P_{2x} + \cos(\theta) \cdot P_{2y} = 0;$$

Compatibility of coupling:

$$v_{1x} = +\cos(\theta) \cdot v_{2x} + \sin(\theta) \cdot v_{2cy}; \quad \blacksquare$$
$$v_{1cy} = -\sin(\theta) \cdot v_{2x} + \cos(\theta) \cdot v_{2cy}; \quad \blacksquare$$
$$\dot{\theta} = \omega_{1z} - \omega_{2z};$$

[4.69]

Let us assume $\boldsymbol{u} = \left[\delta_f; F_{1fxw}; F_{1rx}; F_{2x}\right]^T$ are known inputs. Eqs [4.67].. [4.69] is a DAE system in with 24 equations and 24 unknowns: $v_{1x}, v_{1y}, \omega_{1z}, v_{2x}, v_{2y}, \omega_{2z}, \theta, F_{1fyw}, F_{1ry}, F_{2y}, s_{1fy}, s_{1ry}, s_{2y}, P_{1x}, P_{1y}, P_{2x}, P_{2y}, v_{1fxw}, v_{1fyw}, v_{1fyv}, v_{1ry}, v_{2ay}, v_{1cy}, v_{2cy}$. The equations can be written as they are into a Modelica tool, which can find a possible state selection $\boldsymbol{x}$ (such as $\boldsymbol{x} = \left[v_{1x} v_{1y}, \omega_{1z}, \omega_{2z}, \theta\right]$), an explicit form and perform simulations. Note that not only velocities but also an (relative angular) position becomes states, as opposed to a one-unit vehicle. The use of a DAE tool, e.g., a Modelica tool, is very motivated for articulated vehicles, since the articulation points makes the DAE system of equation to be of "high index", meaning that the Modelica tool identifies the constraints equations, i.e. the equations which have to be differentiated, cf. 3.3.2.1.1. In this case, it is the equations marked with ■ in Eqs [4.67]..[4.69]. The result is an explicit algorithm, possibly with iterations, for computing $\dot{\boldsymbol{x}} = \boldsymbol{f_{ODE}}(\boldsymbol{x}, \boldsymbol{u})$;

4.5.2.2.1 Explicit Form Model without DAE Tool

Contribution by Toheed Ghandriz, Vehicle Dynamics at Chalmers

It will now be explained how the explicit form model can be found using manual equation manipulations or simpler symbolic tools, unable to handle DAEs (e.g. Matlab Symbolic Toolbox). We have to differentiate the equations marked with ■ in Eqs [4.67]..[4.69]. It leads to:

$$\dot{v}_{1cy} = \dot{v}_{1y} - \dot{\omega}_{1z} \cdot (l_{1c} - l_{1CoG});$$
$$\dot{v}_{2cy} = \dot{v}_{2y} + \dot{\omega}_{2z} \cdot (l_{2c} - l_{2CoG});$$
$$\dot{v}_{1x} = \left(-\sin(\theta) \cdot \dot{\theta} \cdot v_{2x} + \cos(\theta) \cdot \dot{v}_{2x}\right) + \left(\cos(\theta) \cdot \dot{\theta} \cdot v_{2cy} + \sin(\theta) \cdot \dot{v}_{2cy}\right);$$
$$\dot{v}_{1cy} = \left(-\cos(\theta) \cdot \dot{\theta} \cdot v_{2x} - \sin(\theta) \cdot \dot{v}_{2x}\right) + \left(-\sin(\theta) \cdot \dot{\theta} \cdot v_{2cy} + \cos(\theta) \cdot \dot{v}_{2cy}\right);$$

So, we regard it as an ODE with 24+4=28 equations: States and inputs as above DAE. The states are regarded as known and we can count to 28 unknown variables, with notations as in 1.5.1.1.5.2.2:

$$\{\boldsymbol{x}, \boldsymbol{y_1}, \dot{\boldsymbol{y}}_2, \boldsymbol{y_2}\} = \left\{ \begin{matrix} \{v_{1x} v_{1y}, \omega_{1z}, \omega_{2z}, \theta\}, \\ \{F_{1fyw}, F_{1ry}, F_{2y}, s_{1fy}, s_{1ry}, s_{2y}, P_{1x}, P_{1y}, P_{2x}, P_{2y}, v_{1fxw}, v_{1fyw}, v_{1fyv}, v_{1ry}, v_{2ay}\}, \\ \{\dot{v}_{1cy}, \dot{v}_{2cy}, \dot{v}_{2x}, \dot{v}_{2y}\}, \{v_{1cy}, v_{2cy}, v_{2x}, v_{2y}\} \end{matrix} \right\}$$

The expressions for state derivatives $\dot{v}_{1x}, \dot{v}_{1y}, \dot{\omega}_{1z}, \dot{\omega}_{2z}, \dot{\theta}$ and output variables (remaining of the 28 variables) can be found through algebraic manipulations, but in this case the symbolic tools will generate huge expressions (hundreds of thousands of tokens) or even fail. Therefore, we will reformulate model and introduce approximations in 4.5.2.2.1.1.

A way to keep symbolic expressions smaller (still large, but not huge) without approximations is to stay at the implicit form, and solve it with special time integration methods, see 1.5.1.1.5.2.2:

$$\boldsymbol{residual} \leftarrow \boldsymbol{f_{implicit}}(\dot{\boldsymbol{x}}, \boldsymbol{x}, \boldsymbol{y_1}, \dot{\boldsymbol{y}}_2, \boldsymbol{y_2}, \boldsymbol{u}(t), t); \quad \textit{where } \boldsymbol{y_2} = \{v_{1cy}, v_{2cy}, v_{2y}, v_{2x}\}$$

4.5.2.2.1.1 Reformulated Model with Approximations

We will derive a model without introducing the constraint forces $P_{1x}, P_{1y}, P_{2x}, P_{2y}$. We select intuitively the 5 states $v_{1x} v_{1y}, \omega_{1z}, \omega_{2z}, \theta$ and find the equations to express their derivatives: 4 equilibria and 1 compatibility relations which involves $\dot{\theta}$. We also introduce approximations as for the two axle one-track model in 4.4.2: small angles $\delta_f, \beta_{ij}, \alpha_{ij} = \arctan\left(v_{ijyw} / \left|v_{ijxw}\right|\right)$, centrifugal acceleration

perpendicular to each unit ($v_{ix} \cdot \omega_{iz} = 0$) and steered axle lateral tyre force does not influence whole vehicle longitudinally ($F_{fyw} \cdot \delta_f = 0$). Some new, but conceptually same, approximations can be done especially for articulated vehicles: small articulation angle θ and lateral tyre force on axles on 2nd unit does not influence whole vehicle longitudinally ($F_{2y} \cdot \theta = 0$).

Equilibrium of whole vehicle (all units together: longitudinal to 1st unit, lateral to 1st unit):

$$\begin{aligned}0 = & -m_1 \cdot a_{1x} + F_{1fxw} \cdot \cos(\delta_f) - F_{1fyw} \cdot \sin(\delta_f) + F_{1rx} + (F_{2x} - m_2 \cdot a_{2x}) \cdot \cos(\theta) \\ & + (F_{2y} - m_2 \cdot a_{2y}) \cdot \sin(\theta) \\ & \approx -m_1 \cdot a_{1x} + F_{1fxw} - 0 + F_{1rx} + (F_{2x} - m_2 \cdot a_{2x}) + (0 - m_2 \cdot a_{2y}) \cdot \theta; \\ 0 = & -m_1 \cdot a_{1y} + F_{1fxw} \cdot \sin(\delta_f) + F_{1fyw} \cdot \cos(\delta_f) + F_{1ry} - (F_{2x} - m_2 \cdot a_{2x}) \cdot \sin(\theta) \\ & + (F_{2y} - m_2 \cdot a_{2y}) \cdot \cos(\theta) \\ & \approx -m_1 \cdot a_{1y} + F_{1fxw} \cdot \delta_f + F_{1fyw} + F_{1ry} - (F_{2x} - m_2 \cdot a_{2x}) \cdot \theta \\ & + (F_{2y} - m_2 \cdot a_{2y});\end{aligned}$$

$$\begin{aligned}&where\ a_{1x} = \dot{v}_{1x} - \omega_{1z} \cdot v_{1y} \approx \dot{v}_{1x}; \quad a_{2x} = \dot{v}_{2x} - \omega_{2z} \cdot v_{2y} \approx \dot{v}_{2x}; \\ & a_{1y} = \dot{v}_{1y} + \omega_{1z} \cdot v_{1x}; \quad a_{2y} = \dot{v}_{2y} + \omega_{2z} \cdot v_{2x};\end{aligned}$$

Equilibrium of 1st unit (yaw around coupling):

$$\begin{aligned}0 = & +(F_{1fxw} \cdot \sin(\delta_f) + F_{1fyw} \cdot \cos(\delta_f)) \cdot l_{1c} + F_{1ry} \cdot (l_{1c} - L_1) - m_1 \cdot a_{1y} \cdot (l_{1c} - l_{1CoG}) - J_1 \cdot \dot{\omega}_{1z} \approx \\ \approx & +(F_{1fxw} \cdot \delta_f + F_{1fyw}) \cdot l_{1c} + F_{1ry} \cdot (l_{1c} - L_1) - m_1 \cdot a_{1y} \cdot (l_{1c} - l_{1CoG}) - J_1 \cdot \dot{\omega}_{1z};\end{aligned}$$

Equilibrium of 2nd unit (yaw around coupling):

$$0 = -F_{2y} \cdot l_{2CoG} + m_2 \cdot a_{2y} \cdot (l_{2c} - l_{2CoG}) - J_2 \cdot \dot{\omega}_{2z};$$

Compatibility in coupling:

$$\dot{\theta} = \omega_{1z} - \omega_{2z};$$

(Note: The same concept works for a vehicle with *N* units: 2 translational equilibria for the whole vehicle and 2 rotational equilibria (fore and aft part) per coupling point: $2 + 2 \cdot N$ equilibria.)

Now, we realize that we have to find 2 compatibility relations that eliminate $\dot{v}_{2x}, \dot{v}_{2y}$. These may not involve any new derivatives, only $\dot{v}_{2x}, \dot{v}_{2y}$ and the state derivatives:

Differentiated Compatibility (to *eliminate* $\dot{v}_{2x}, \dot{v}_{2y}$):

$$\begin{aligned}\dot{v}_{2x} = & \frac{d}{dt}(v_{1x} \cdot \cos(\theta) - v_{1cy} \cdot \sin(\theta)) = \frac{d}{dt}\left(v_{1x} \cdot \cos(\theta) - \left(v_{1y} - \omega_{1z} \cdot (l_{1c} - l_{1CoG})\right) \cdot \sin(\theta)\right) \\ & = +\dot{v}_{1x} \cdot \cos(\theta) - v_{1x} \cdot \sin(\theta) \cdot \dot{\theta} - \left(\dot{v}_{1y} - \dot{\omega}_{1z} \cdot (l_{1c} - l_{1CoG})\right) \cdot \sin(\theta) \\ & - \left(v_{1y} - \omega_{1z} \cdot (l_{1c} - l_{1CoG})\right) \cdot \cos(\theta) \cdot \dot{\theta} \approx \\ & \approx +\dot{v}_{1x} - v_{1x} \cdot \theta \cdot \dot{\theta} - \left(\dot{v}_{1y} - \dot{\omega}_{1z} \cdot (l_{1c} - l_{1CoG})\right) \cdot \theta - \left(v_{1y} - \omega_{1z} \cdot (l_{1c} - l_{1CoG})\right) \cdot \dot{\theta}; \\ \dot{v}_{2y} = & \frac{d}{dt}\left(v_{2cy} - \omega_{2z} \cdot (l_{2c} - l_{2CoG})\right) = \frac{d}{dt}\left(v_{1cy} \cdot \cos(\theta) + v_{1x} \cdot \sin(\theta) - \omega_{2z} \cdot (l_{2c} - l_{2CoG})\right) = \\ & = \frac{d}{dt}\left(\left(v_{1y} - \omega_{1z} \cdot (l_{1c} - l_{1CoG})\right) \cdot \cos(\theta) + v_{1x} \cdot \sin(\theta) - \omega_{2z} \cdot (l_{2c} - l_{2CoG})\right) = \\ & = \left(\dot{v}_{1y} - \dot{\omega}_{1z} \cdot (l_{1c} - l_{1CoG})\right) \cdot \cos(\theta) - \left(v_{1y} - \omega_{1z} \cdot (l_{1c} - l_{1CoG})\right) \cdot \sin(\theta) \cdot \dot{\theta} + \dot{v}_{1x} \\ & \cdot \sin(\theta) + v_{1x} \cdot \cos(\theta) \cdot \dot{\theta} - \dot{\omega}_{2z} \cdot (l_{2c} - l_{2CoG}) \approx \\ \approx & \left(\dot{v}_{1y} - \dot{\omega}_{1z} \cdot (l_{1c} - l_{1CoG})\right) - \left(v_{1y} - \omega_{1z} \cdot (l_{1c} - l_{1CoG})\right) \cdot \theta \cdot \dot{\theta} + \\ & + \dot{v}_{1x} \cdot \theta + v_{1x} \cdot \dot{\theta} - \dot{\omega}_{2z} \cdot (l_{2c} - l_{2CoG});\end{aligned}$$

Now the constitution can be involved:

Constitution for axles (to *eliminate* lateral forces $F_{1fyw}, F_{1ry}, F_{2y}$):

$$F_{1fyw} = -C_{1f} \cdot s_{1fyw};$$

$$F_{1ry} = -C_{1r} \cdot s_{1ry};$$

$$F_{2y} = -C_2 \cdot s_{2y};$$

We now eliminate the slips $s_{1fyw}, s_{1ryw}, s_{2y}$ and express them in state variables:

Compatibility (to *eliminate* s_{fyw}):

$\arctan2(v_{1fyv}, |v_{1x}|) = \delta_f + \arctan(s_{1fyw}) \Rightarrow s_{1fyw} \approx v_{1fyv}/|v_{1x}| - \delta_f$;

where $v_{1fyv} = v_{1y} + \omega_{1z} \cdot l_{1CoG}$;

Compatibility (to *eliminate* s_{1ry}):

$s_{1ry} = v_{1ry}/|v_{1x}|$;

where $v_{1ry} = v_{1y} - \omega_{1z} \cdot (L_1 - l_{1CoG})$;

Compatibility (to *eliminate* s_{2y}):

$s_{2y} = v_{2ay}/|v_{2x}|$;

where $v_{2ay} = v_{2cy} - \omega_{2z} \cdot l_{2c}$;

where $v_{2cy} = v_{1cy} \cdot \cos(\theta) + v_{1x} \cdot \sin(\theta) \approx v_{1cy} + v_{1x} \cdot \theta$;

where $v_{1cy} = v_{1y} - \omega_{1z} \cdot (l_{1c} - l_{1CoG})$;

and $v_{2x} = +v_{1x} \cdot \cos(\theta) - v_{1cy} \cdot \sin(\theta) \approx +v_{1x} - v_{1cy} \cdot \theta$;

If we perform the *eliminations,* we get 5 equations:

$$\boldsymbol{f_{DAE}}(\dot{\boldsymbol{x}}, \boldsymbol{x}, \boldsymbol{u}) = \boldsymbol{0}; \quad where\ \boldsymbol{x} = [v_{1x}; v_{1y}; \omega_{1z}; \omega_{2z}; \theta],\ \ \boldsymbol{u} = [\delta_f; F_{1fxw}; F_{1rx}; F_{2x}];$$

Using the exact (grey text) expressions, this is exactly same model as in Eqs [4.67]..[4.69].

4.5.2.2.1.2 Symbolically Linearized Explicit Form Model

We can reformulate to explicit form: $\dot{\boldsymbol{x}} = \boldsymbol{f_{ODE}}(\boldsymbol{x}, \boldsymbol{u})$; but this is the same huge expression, mentioned above. Using the approximate (black text) expressions, the solution will be somewhat smaller, but still very large. However, we can linearize around an operation point $(\boldsymbol{x_0}, \boldsymbol{u_0})$:

$$\begin{aligned}\dot{\boldsymbol{x}} &\approx \boldsymbol{f_{ODE}}(\boldsymbol{x_0}, \boldsymbol{u_0}) + \boldsymbol{A}(\boldsymbol{x_0}, \boldsymbol{u_0}) \cdot (\boldsymbol{x} - \boldsymbol{x_0}) + \boldsymbol{B}(\boldsymbol{x_0}, \boldsymbol{u_0}) \cdot (\boldsymbol{u} - \boldsymbol{u_0}) = \\ &= \boldsymbol{f_0} + \boldsymbol{A_0} \cdot (\boldsymbol{x} - \boldsymbol{x_0}) + \boldsymbol{B_0} \cdot (\boldsymbol{u} - \boldsymbol{u_0}) = \\ &= (\boldsymbol{f_0} - \boldsymbol{A_0} \cdot \boldsymbol{x_0} - \boldsymbol{B_0} \cdot \boldsymbol{u_0}) + \boldsymbol{A_0} \cdot \boldsymbol{x} + \boldsymbol{B_0} \cdot \boldsymbol{u} = \boldsymbol{k_{\dot{x}}} + \boldsymbol{A_0} \cdot \boldsymbol{x} + \boldsymbol{B_0} \cdot \boldsymbol{u};\end{aligned}$$

It is most common to linearize around a $(\boldsymbol{x_0}, \boldsymbol{u_0})$ which is a steady state operating point,. Then $\boldsymbol{f_{ODE}}(\boldsymbol{x_0}, \boldsymbol{u_0}) = \boldsymbol{f_0} = \boldsymbol{0}$.

The elements of the matrices $\boldsymbol{A_0}, \boldsymbol{B_0}$ is: $A_{0,ij} = \left.\frac{\partial f_{ODE,i}}{\partial x_j}\right|_{\boldsymbol{x_0}, \boldsymbol{u_0}}$; and $B_{0,ij} = \left.\frac{\partial f_{ODE,i}}{\partial u_j}\right|_{\boldsymbol{x_0}, \boldsymbol{u_0}}$;

4.5.2.2.1.2.1 Linearize around steady state straight-line driving

As example of relevant operating condition to linearize around, we take steady state straight-line driving without significant longitudinal tyre forces: $\boldsymbol{x_0} = [v_{1x0}; 0; 0; 0; 0]^T, \boldsymbol{u_0} = [0; 0; 0; 0]^T$. Note that we could have used another distribution of longitudinal forces, because the vehicle is over-actuated, e.g.. $\boldsymbol{u_0} = [0; 0; 10000; -10000]^T$ where propulsion and brake are fighting but still result in zero total force. Note also that we do not have to solve the model for the operating condition to linearize around, because we know the solution.

Then we get symbolic expressions of only $\boldsymbol{A_0}, \boldsymbol{B_0}$ of around 15 thousand tokens, which is manageable, but not worth writing out in this book, except on this overviewing way:

$$\boldsymbol{A_0} = \begin{bmatrix} 0 & 0 & 0 & 0 & 0 \\ 0 & 0 & \neq 0 & \neq 0 & \neq 0 \\ 0 & 0 & \neq 0 & \neq 0 & \neq 0 \\ 0 & 0 & \neq 0 & \neq 0 & \neq 0 \\ 0 & 0 & 1 & -1 & 0 \end{bmatrix}; \quad \boldsymbol{B_0} = \begin{bmatrix} 0 & \neq 0 & \neq 0 & \neq 0 \\ \neq 0 & 0 & 0 & 0 \\ \neq 0 & 0 & 0 & 0 \\ \neq 0 & 0 & 0 & 0 \\ 0 & 0 & 0 & 0 \end{bmatrix};$$

Now, we can simulate to compare the different models:

- "*Exact*" ("Modular" Eqs [4.67]..[4.69], which is identical to the equations with black text above)
- "*Small Angles*" (the equations above, with a mixture of black and grey text so that only using the small angle approximations, but not using the "zeros")
- "*With All Physical Approximations*, but not linearized" (the equations with black text above)
- *"(Symbolically) Linearized*" ($\dot{\boldsymbol{x}} = \boldsymbol{k_{\dot{x}}} + \boldsymbol{A_0} \cdot \boldsymbol{x} + \boldsymbol{B_0} \cdot \boldsymbol{u}$; as described above in 4.5.2.2.1.2)

A simulation with these 4 models is shown in Figure 4-67.

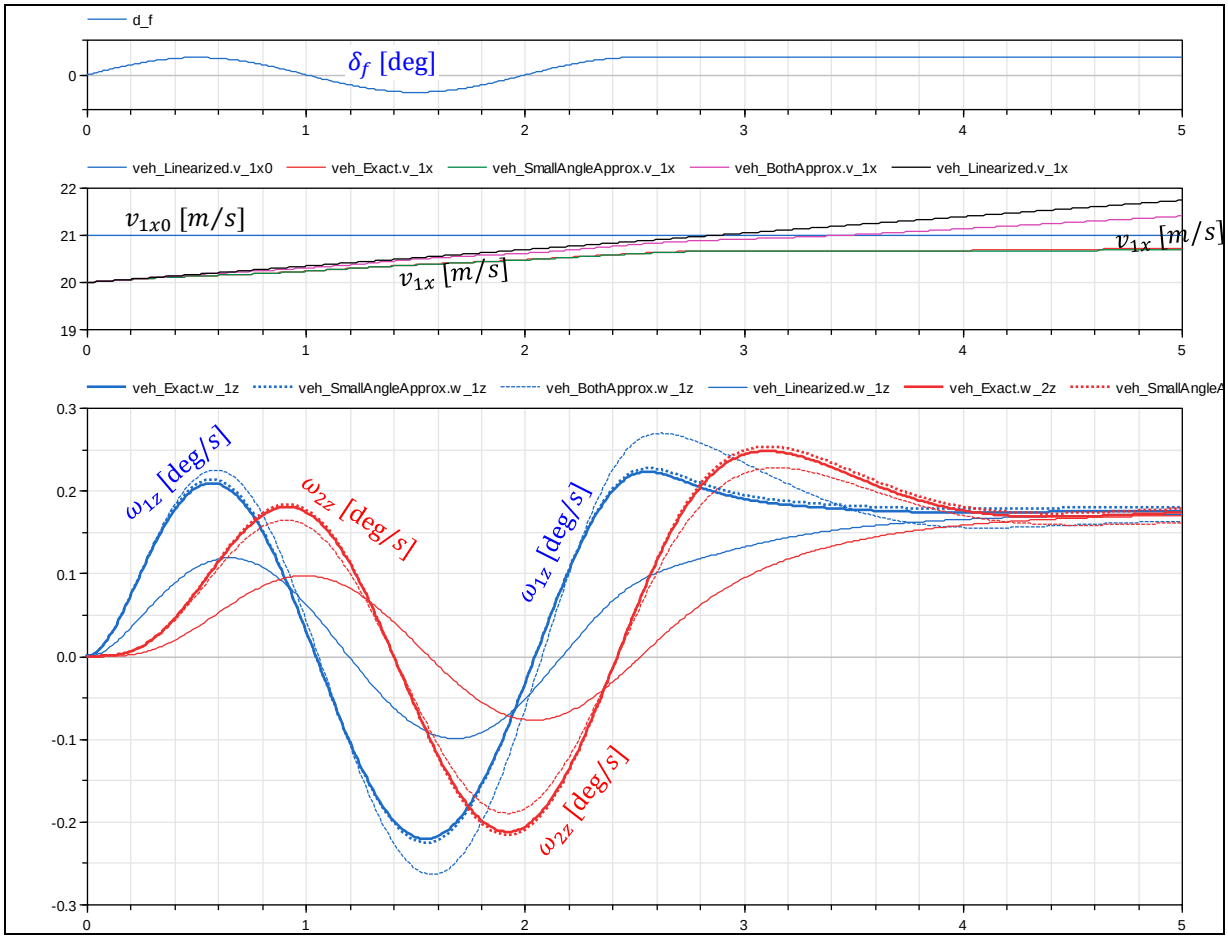


Figure 4-67: Tractor and semitrailer. Comparison of simulations with the 4 models (thick solid: "Exact", thick dotted: "Small Angles", thin dashed: "With All Physical Approximations, but not linearized", thin solid: "(Symbolically) Linearized").

A similar linearization is done for a longer combination vehicle (A-double, i.e. Tractor+Semitrailer+Fulltrailer) in https://research.chalmers.se/publication/192958.

4.5.2.2.1.3 Eigen value analysis

The $\boldsymbol{A_0}$ matrix is of special interest because it can tell something about the eigenmodes, through eigenvalue analysis. We will use an example and do one linearization for steady state straight-line driving and one for steady state cornering. We will use the following numerical parameters:

$$CC_y = 6;$$

$$C_{1f} = CC_y \cdot m_1 \cdot g \cdot \frac{l_{1CoG}}{L_1};\ C_{1r} = CC_y \cdot \left(m_1 \cdot \left(\frac{L_1 - l_{1CoG}}{L_1}\right) + \frac{m_2}{2}\right) \cdot g);\ C_2 = CC_y \cdot \frac{m_2}{2} \cdot g;$$

$$l_{1CoG} = \frac{L_1}{3};\ l_{1c} = L_1 - 1;\ l_{2CoG} = \frac{l_{2c}}{2};\ L_1 = 5\ [m];\ l_{2c} = 8\ [m];$$

$$m_1 = 7500\ [kg];\ m_2 = 20000\ [kg];\ J_1 = 22500;\ J_2 = 200000\ \ [kg\ m^2];$$

$$v_{1x0} = 21\ [m/s];\ \ g = 9.80665\ \ [m/s^2];$$

4.5.2.2.1.3.1 Steady state straight-line driving

For this operation, we already know the matrix $\boldsymbol{A_0}$ from 4.5.2.2.1.2.1. With numerical values it becomes:

$$\begin{bmatrix} \dot{v}_{1x} \\ \dot{v}_{1y} \\ \dot{\omega}_{1z} \\ \dot{\omega}_{2z} \\ \dot{\theta} \end{bmatrix} = \underbrace{\begin{bmatrix} 0 & 0 & 0 & 0 & 0 \\ 0 & 0 & -23.6272 & -9.4633 & 24.8413 \\ 0 & 0 & -5.2208 & 7.3604 & -19.3210 \\ 0 & 0 & 0.4641 & -7.5466 & 19.8098 \\ 0 & 0 & 1 & -1 & 0 \end{bmatrix}}_{\boldsymbol{A_0}} \cdot \underbrace{\begin{bmatrix} v_{1x} \\ v_{1y} \\ \omega_{1z} \\ \omega_{2z} \\ \theta \end{bmatrix}}_{\boldsymbol{x}};$$

An eigen solution analysis of $\boldsymbol{A_0}$ gives:

$$\lambda_{1,2,3,4,5} = \{0,\ -5.5491 + 5.0790 \cdot i,\ -5.5491 - 5.0790 \cdot i,\ -1.6691,\ 0\};$$

$$\boldsymbol{x_{eig1}} = \begin{bmatrix} 0 \\ 1 \\ 0 \\ 0 \\ 0 \end{bmatrix}; \boldsymbol{x_{eig2}} = \begin{bmatrix} 0 \\ 0.9327 \\ 0.1534 - 0.2473 \cdot i \\ 0.0248 + 0.2023 \cdot i \\ -0.0530 + 0.0325 \cdot i \end{bmatrix}; \boldsymbol{x_{eig2}} = \begin{bmatrix} 0 \\ 0.9327 \\ 0.1534 + 0.2473 \cdot i \\ 0.0248 - 0.2023 \cdot i \\ -0.0530 - 0.0325 \cdot i \end{bmatrix};$$

$$\boldsymbol{x_{eig4}} = \begin{bmatrix} 0 \\ 0.9915 \\ 0.0587 \\ 0.1117 \\ 0.0318 \end{bmatrix}; \boldsymbol{x_{eig5}} = \begin{bmatrix} 1 \\ 0 \\ 0 \\ 0 \\ 0 \end{bmatrix};$$

We recall from mathematics, similarly as in 4.5.4.1.1, that $\boldsymbol{x} = \boldsymbol{x}_\infty + e^{\lambda_1 \cdot t} \cdot \boldsymbol{x_{eig1}} + \cdots + e^{\lambda_5 \cdot t} \cdot \boldsymbol{x_{eig5}}$; where $\boldsymbol{x}_\infty = -\mathbf{A}^{-1} \cdot \mathbf{B} \cdot \delta_f = \mathbf{0}$.

The modes 1 and 5 are rigid body modes. They can be understood as if the vehicle moves as a rigid pose from start, it simply continues. Mode 1 corresponds to all units moves forward with constant speed without changing heading angle or articulation angle. Mode 2 corresponds the same but sideways. With the initial values we have from the operating condition linearized around, this means that $v_{1x} \equiv v_{2x} \equiv v_{1x0}$ and $\omega_{1z} \equiv \omega_{2z} \equiv \theta \equiv 0$.

The modes 2 and 3 are complex conjugated, which means that the sum of them becomes real, while each mode contains imaginary results. We should not try to interpret any imaginary results to real world, so we analyse mode 2 and 3 together as:

$$\boldsymbol{x_2} + \boldsymbol{x_3} = e^{-5.5491 \cdot t} \cdot \underbrace{\begin{bmatrix} 0 \\ +0.9327 \\ +0.1534 \\ +0.0248 \\ -0.0530 \end{bmatrix}}_{\mathrm{Re}(\boldsymbol{x_{eig2}}) = \mathrm{Re}(\boldsymbol{x_{eig3}})} \cdot \sin(5.0790 \cdot t + \varphi);$$

The mode is damped, so it is no instability. It is rather strongly damped: it decays to 37% of initial values in $1/5.5491 \approx 0.2$ s. The oscillation frequency is fast: 5.07090 $[rad/s] \approx 291$ $[Hz]$. So, this eigen solution is probably not suitable to study with this model. However, we can understand the mode shape of the combination vehicle if we draw the position of some points at the vehicle. If we assume that the initial pose is with all those points at $y = 0$, their position after a small time t_ε becomes the integral $[x; y] = \int [\dot{x}; \dot{y}] \cdot dt = \int [\dot{x}; \dot{y}] \cdot dt = \left[v_x; v_y\right] \cdot t_\varepsilon$. However, we do not move the points in x direction, but instead we assume "the camera" moves with the speed v_{1x0} above the y axis.

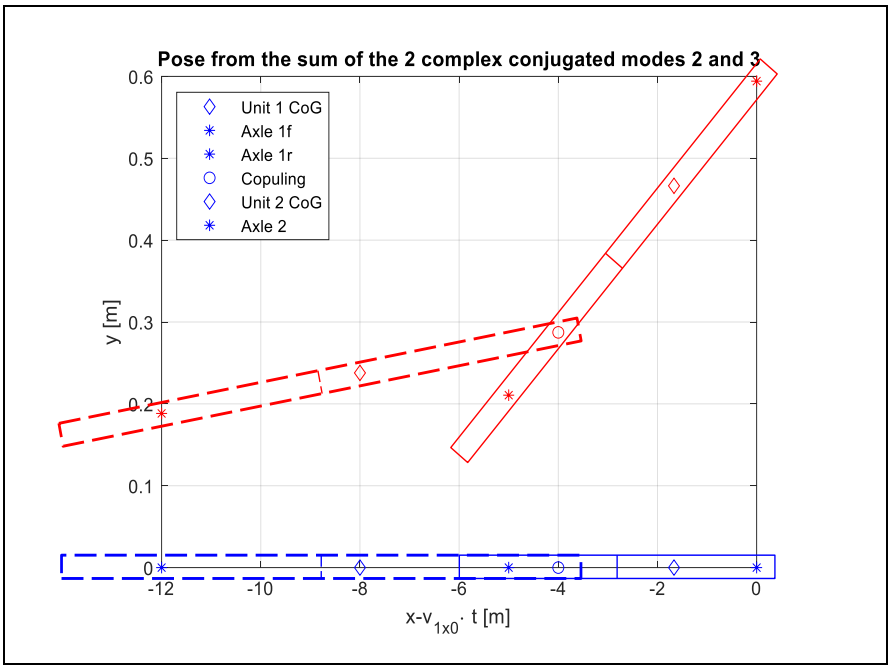


Figure 4-68: Mode pose from (complex conjugated) modes 2 and 3 from straight-line driving. $\lambda_{2,3} = -5.5491 \pm 5.0790 \cdot i;$

The last mode to analyse is Mode 4. This mode is exponentially stable. We can draw similar figure for this mode. The solutions decay to 37% of initial values in $1/1.6691 \approx 0.6$ s.

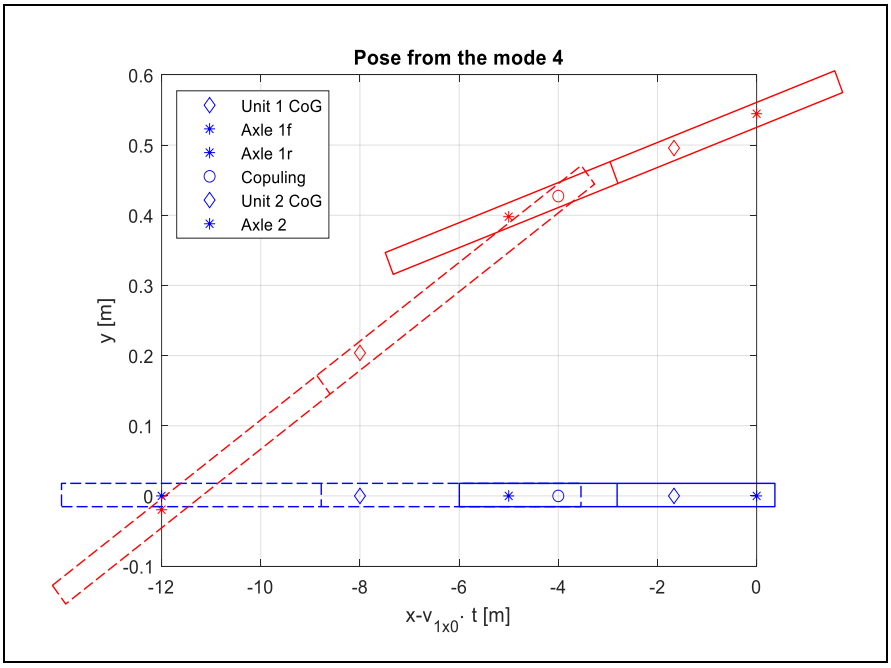


Figure 4-69: Mode pose from mode 4 from straight-line driving.

4.5.2.2.2 Model Library for Articulated Vehicles

The first model (Eqs [4.67].. [4.69]) for articulated vehicle is written so that each equation belongs to either a unit or a coupling. This opens up for systematic treatment of combination vehicles with more than one articulation point. There are basically two conceptual ways:

- Modular library from which parts can be graphically dragged, dropped and connected.
- Vectorised formulation, see Reference (Sundström, Jacobson, & Laine, 2014) and 4.5.2.2.2.2.

4.5.2.2.2.1 Modular Library

A modular library is shown in figure below. Eq [4.67] is declared in "Unit" and Eq [4.69] in "Coupling".

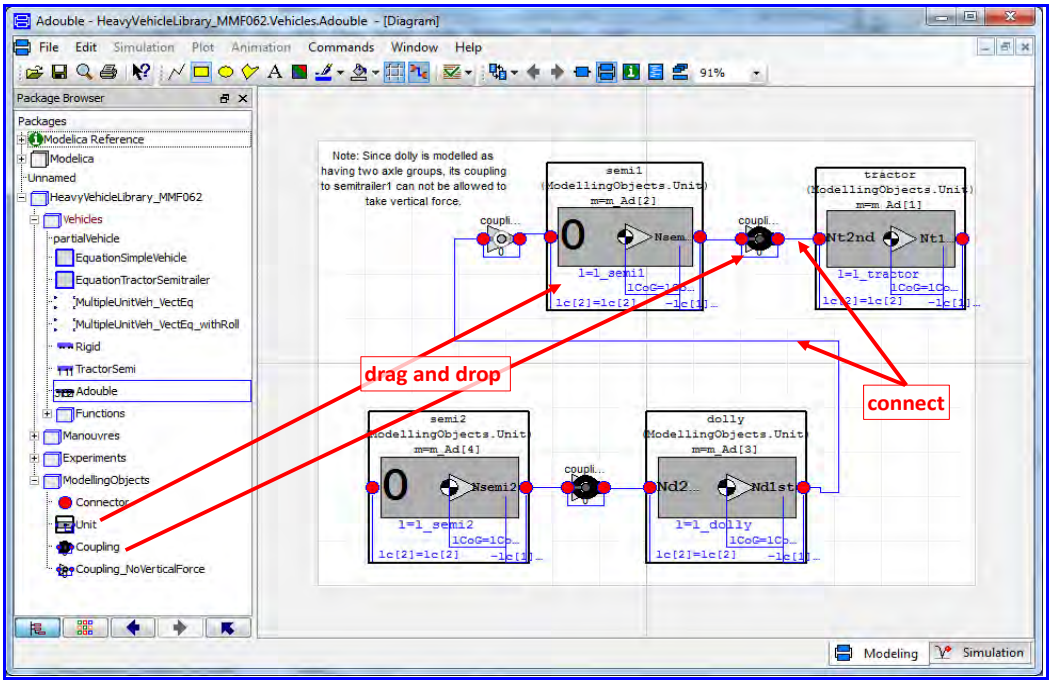


Figure 4-70: Drag, drop and connect library for heavy combination vehicles. The model example shows a so-called A-double, Tractor+SemiTrailer+Dolly+SemiTrailer.

An example of lane change manoeuvre, defined as lateral acceleration on 1st axle follows a single sine-wave, is shown in Figure 4-71. The natural input is prescribed steer angle ($\delta_f = \sin(time)$;), but since modelled in Modelica, it is as easy to prescribe something else, e.g. lateral acceleration on first axle ($a_{f1y} = \sin(time)$;).

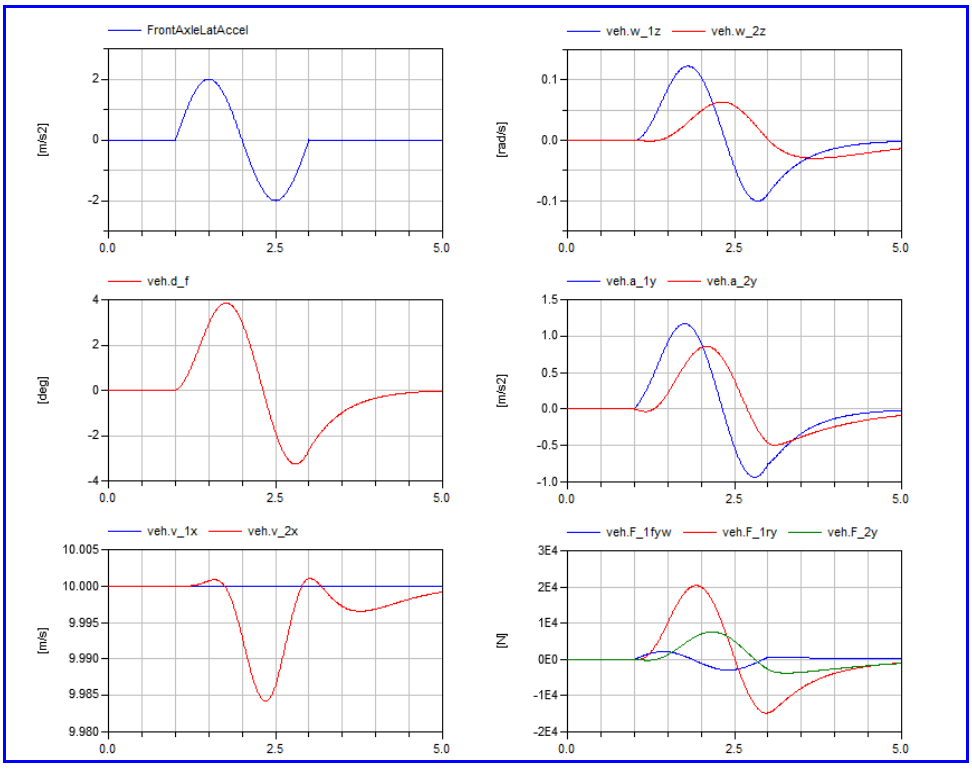


Figure 4-71: One period sinus test of a Tractor+SemiTrailer.

4.5.2.2.2.2 Vectorised Model Format

Contribution from Toheed Ghandriz, Vehicle Dynamics at Chalmers and Mikko Karisaari, Oulo University, Finland

The model presented in this section can be run in 3 different modes (set by parameter `DynOpCond`): Transient, SteadyState and LowSpeed.

When modelling combination vehicles, there is a value of being able to use same model for vehicles with different number of units. The following figure shows the physical model for a unit $i = 1..nu$, where nu is the number of units. Only one axle $j = 1..na$, where na is the maximum number of axles per unit. There are $nu - 1$ couplings. The inputs to a model can be, e.g., $nu \cdot na$ steering angles δ_{ij} and $nu \cdot na$ wheel-longitudinal forces $F_{a,ij,xw}$. The latter can be actuated as $F_{a,ij,xw} = (T_{Prop,ij} + T_{Brk,ij})/R_{whl}$.

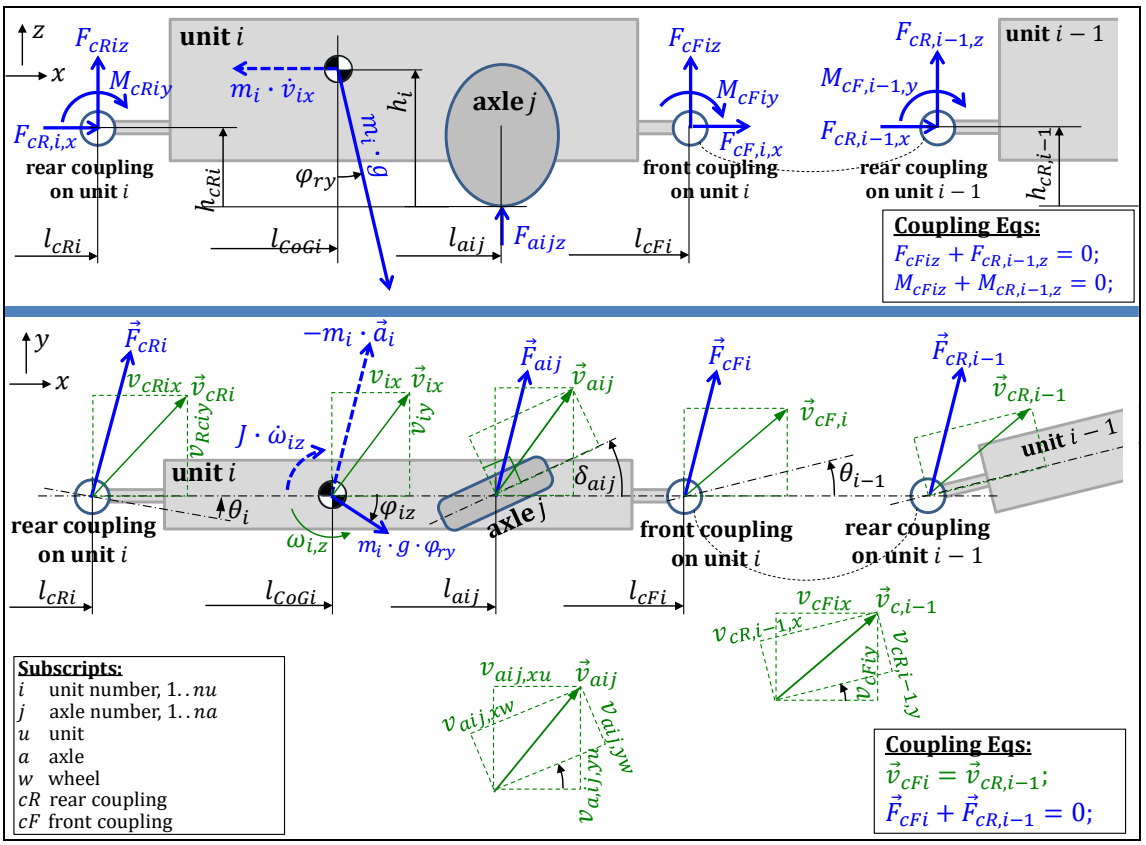


Figure 4-72: Physical model of a combination vehicle. Only one unit and one coupling drawn. Notation "⇀⋯" means 2D geometric vector in xy-plane.

The Modelica model becomes rather compact, using Modelica's `vector`, `for` and `if` notation:

```
model vehModel_LateralOneTrack
…  //Vectorised parameters, e.g. nu=number of units, na=max number of axles per unit, m[nu], …
…  //Vectorised variables, e.g. v_x[nu], F_az[nu,na], …
equation
  //For each unit:
  for i in 1:nu loop
    //In-road-plane Equilibrium of units (longitudinal, lateral, yaw around CoG):
    if DynOpCond==3 or DynOpCond==2 then
      KinEnForce_x[i] =m[i]*((if DynOpCond==3 then der(v_x[i]) else 0) - w_z[i]*v_y[i]);
      KinEnForce_y[i] =m[i]*((if DynOpCond==3 then der(v_y[i]) else 0) + w_z[i]*v_x[i]);
      KinEnMoment_z[i]=J_z[i]*der(w_z[i]);
    else  // if DynOpCond==1 then
      KinEnForce_x[i] =0;
      KinEnForce_y[i] =0;
      KinEnMoment_z[i]=0;
    end if;
    KinEnForce_x[i] = sum(F_axu[i,:]) +F_cRx[i] +F_cFx[i] +m[i]*g*sin(phi_ry)*sin(phi_z[i])
                      -(if i==1 then HalfRhoACd*v_x[i]^2 else 0);
    KinEnForce_y[i] = sum(F_ayu[i,:]) +F_cRy[i] +F_cFy[i] -m[i]*g*sin(phi_ry)*cos(phi_z[i]);
    KinEnMoment_z[i]= sum(F_ayu[i,:].*(l_a[i,:]-l_CoG[i]*ones(na)))
```

```
                    +F_cRy[i]*(l_cR[i]-l_CoG[i]) +F_cFy[i]*(l_cF[i]-l_CoG[i]);
    a_x[i]=der(v_x[i]) - w_z[i]*v_y[i];
    a_y[i]=der(v_y[i]) + w_z[i]*v_x[i];
    //Out-of-road-plane Equilibrium of units (vertical, pitch around point on ground under CoG):
    0 = +sum(F_az[i,:]) +F_cRz[i] +F_cFz[i] -m[i]*g*cos(phi_ry);
    0 = -sum(F_az[i,:].*(l_a[i,:]-l_CoG[i]*ones(na)))   -F_cRz[i]*(l_cR[i]-l_CoG[i])
        -F_cFz[i]*(l_cF[i]-l_CoG[i])   +F_cRx[i]*h_cR[i] +F_cFx[i]*h_cF[i]
        +M_cRy[i]   +M_cFy[i] -m[i]*(der(v_x[i])-g*sin(phi_ry)*sin(phi_z[i])) *h[i];
    //Compatibility for rear and front couplings:
    v_cRx[i] = v_x[i];    v_cRy[i] = v_y[i] + w_z[i]*(l_cR[i] - l_CoG[i]);
    v_cFx[i] = v_x[i];    v_cFy[i] = v_y[i] + w_z[i]*(l_cF[i] - l_CoG[i]);
    //Constitution (suspension)
    for j in 1:na loop
      if AxleGroupNumber[i,j] == 0 then
          F_az[i,j] = 0;
      elseif j >= 2 then
        if AxleGroupNumber[i,j] == AxleGroupNumber[i,j-1] then
          F_az[i,j] = F_az[i,j-1];
        end if;
      end if;
    end for;
    //Front coupling on 1st unit and Rear coupling on last unit not coupled:
    if i == 1 then
      F_cFx[1] = 0;      F_cFy[1] = 0;      F_cFz[1] = 0;      M_cFy[1] = 0;
    end if;
    if i == nu then
      F_cRx[i] = 0;      F_cRy[i] = 0;
    end if;
    //Rear coupling degrees of freedoms:
    if VertFree_RearCoupl[i] or i == nu then
      F_cRz[i] = 0;
    end if;
    if PitchFree_RearCoupl[i] then
      M_cRy[i] = 0;
    end if;
  end for;

  //For each coupling:
  for i in 2:nu loop
    //Compatibility of coupled couplings:
    theta[i - 1] = phi_z[i - 1] - phi_z[i]; // der(theta[i - 1]) = w_z[i - 1] - w_z[i];
    v_cFx[i] = +cos(theta[i - 1])*v_cRx[i - 1] - sin(theta[i - 1])*v_cRy[i - 1];
    v_cFy[i] = +sin(theta[i - 1])*v_cRx[i - 1] + cos(theta[i - 1])*v_cRy[i - 1];
    //Equilibrium of coupled couplings (longitudinal, lateral):
    F_cFx[i] +(+cos(theta[i-1])*F_cRx[i-1] -sin(theta[i-1])*F_cRy[i-1]) = 0;
    F_cFy[i] +(+sin(theta[i-1])*F_cRx[i-1] +cos(theta[i-1])*F_cRy[i-1]) = 0;
    F_cFz[i] +F_cRz[i-1] = 0;
    M_cFy[i] +M_cRy[i-1] = 0;
  end for;

  //For each axle:
  for i in 1:nu loop
    for j in 1:na loop
      Rw[i, j] = R_w*w[i, j];
      //Wheel Torque Actuation:
      F_aa[i, j] = sign(F_aaReq[i, j])*min(abs(F_aaReq[i, j]),
                                           min(F_aaMax,P_aaMax/max(abs(Rw[i, j]), v_eps)));

// if WhlTyreMod == 2 then
      //Wheel, Rotational Equilibrium:
      J_w*der(w[i, j]) = (F_aa[i, j] - RRC*F_az[i, j] - F_axw[i, j])*R_w;
      //Tyre Constitution:
      (F_axw[i, j],F_ayw[i, j]) = F_xy_RotatingWhl(F_z=max(F_az[i, j], F_eps), w=w[i, j],
                                     v_xw=v_axw[i, j],v_yw=v_ayw[i, j],R_w=R_w,mu_peak=mu_peak);
      s_x[i, j] = (Rw[i, j] - v_axw[i, j])/max(abs(Rw[i, j]), v_eps);
      s_yt[i, j] = v_ayw[i, j]/max(abs(Rw[i, j]), v_eps);
      alpha[i, j] = atan2(v_ayw[i, j], v_axw[i, j]);

      //Compatibility for each axle:
      v_axu[i, j] = +cos(delta[i, j])*v_axw[i, j] - sin(delta[i, j])*v_ayw[i, j];
      v_ayu[i, j] = +sin(delta[i, j])*v_axw[i, j] + cos(delta[i, j])*v_ayw[i, j];
      v_axu[i, j] = v_x[i];
      v_ayu[i, j] = v_y[i] + w_z[i]*(l_a[i, j] - l_CoG[i]);
      //Force equivalence or transformation:
      F_axu[i, j] = +cos(delta[i, j])*F_axw[i, j] - sin(delta[i, j])*F_ayw[i, j];
      F_ayu[i, j] = +sin(delta[i, j])*F_axw[i, j] + cos(delta[i, j])*F_ayw[i, j];
    end for;
  end for;
end vehModel_LateralOneTrack;
```

Note that the tyre model used takes the influence of vertical tyre load into account. This is important for heavy vehicles which typically have large variation of load and position of load. It requires that also the out-of-road-plane equilibria, vertical and pitch, are included. It also requires that different coupling degrees of freedom and axle lifting are modelled. Therefore, the coupling also have the parameters "`Boolean VertFree_RearCoupl[nu]`", "`Boolean PitchFree_RearCoupl[nu]`" and "`Integer AxleGroupNumber[nu,na]`". Based on these parameters, and an assumption about the suspension control, e.g. same vertical forces within an axle group, the vertical forces can be solved for. It cannot be guaranteed to work for all combination vehicles, but it works e.g. for the "A-double with Dolly" and "A-double with FullTrailer" in Figure 1-76. The change is only to change `VertFree_RearCoupl[2]` from `false` to `true` and `PitchFree_RearCoupl[3]` from `true` to `false`. This gives a change due to that vertical force is taken slightly different, see figure below.

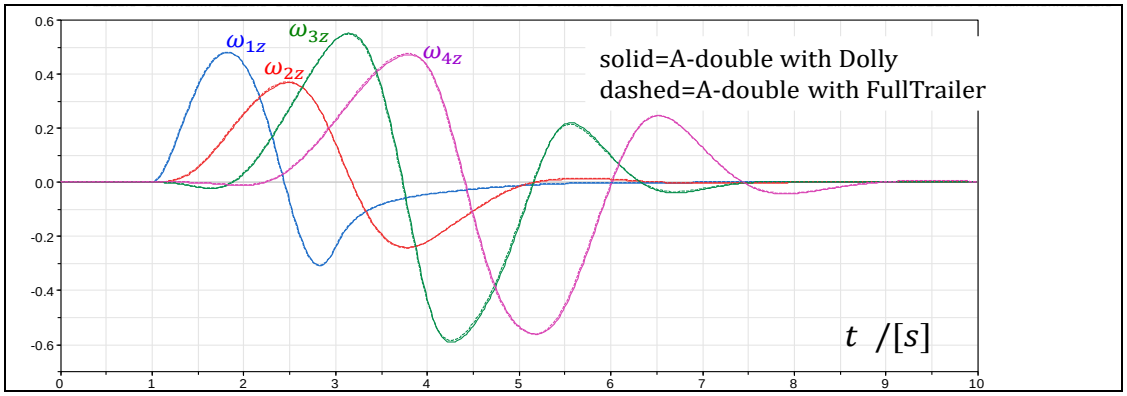


Figure 4-73: Difference between "A-double with Dolly" and "A-double with FullTrailer", see Figure 1-76 . Single sine steering during $1 < t < 3$ at 20 m/s. The drawbar coupling carries no vertical force in a FullTrailer, but some (here $\approx$ 3 kN) in the other case. Lateral acceleration, peaking around 7..8 m/s^2, is unrealistic for roll-over, but reducing to realistic 2..4 m/s^2 gives hardly any visible difference.

The difference does not become so large because the pitch moment of the dolly is taken by either the pitch-rigid drawbar or the turntable of the 2nd SemiTrailer. The dynamic longitudinal load transfer is considered by adding the term `m[i]*der(v_x[i])*h[i]` in pitch equilibrium of the units. This generates more simultaneous equations (algebraic loops). So, neglecting the dynamic longitudinal load transfer is an option for a simpler explicit form model.

4.5.2.3 Cambering Vehicles

The model below shows how a cambering vehicle can be modelled. The model is mainly made for lateral dynamics, but it allows also longitudinal acceleration. The drawing shows a two-wheeler, but any or both of the axles could have two wheels, as long as the suspension linkage is such that the axle does not take any roll moment. The model is shown in Eq [4.70] in Modelica format. It is not modelled that driver moves within the vehicle, which is why the inertial data is constant. Also, the chassis (frame) is modelled as stiff and steering system as massless. The model lacks two equations, which is logical since a driver model can add prescribed steer angle and prescribed F_{rx}.

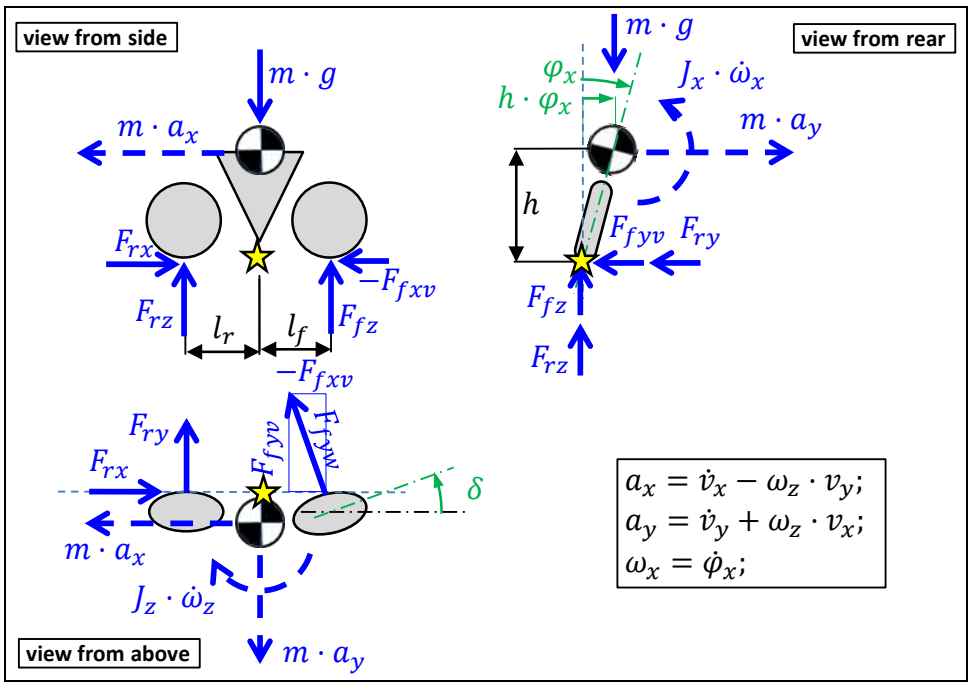


Figure 4-74: Model of cambering vehicle. (The stars marks point of moment equilibria in the "mathematical model" derived from this "physical model".)

```
//Equilibrium in road plane (x,y,rotz):
  m*ax = Ffxv + Frx;
  m*ay = Ffyv + Fry;
  Jz*der(wz) = Ffyv*lf - Fry*lr - m*ax*h*px;
  ax = der(vx) - wz*vy;
  ay = der(vy) + wz*vx;
//Equilibrium out of road plane (z, rotx, roty):
  m*g = Ffz + Frz;
  Jx*der(wx) = m*g*h*px + m*ay*h;
  0 = -Ffz*lf + Frz*lr - m*ax*h;
  wx = der(px);
//Constitution:
  Ffyw = -CC*Ffz*sfy;   Fry = -CC*Frz*sry;
//Compatibility, slip definition:
  atan(sfy) = atan2(vy + lf*wz + h*wx, vx - h*px*wz) - d;
  atan(sry) = atan2(vy - lr*wz + h*wx, vx - h*px*wz) - 0;
//Force coordinate transformation:
  Ffxv = -Ffyw*sin(d);
  Ffyv = +Ffyw*cos(d);
```

[4.70]

When entering a constant radius curve from straight driving one has to first steer out of the curve to tilt the vehicle a suitable amount for the coming path curvature, R_p. The suitable amount is hence $\varphi_{x,suitable} = -a_y/g = -\omega_z \cdot v_x/g = -v_x^2/(R_p \cdot g)$;. Then one steers with the turn and balances (closed loop controls) to the desired roll angle. Systems like this, which has to be operated in opposite direction initially is called "Non-minimum phase systems". It is generally difficult to design a controller for such systems. The two simulations shown in Figure 4-92 are done with the above model. Initial speed is $v_x = 10\ m/s$ and $F_{rx} = 0$. Path radius, $R_p(t) = step\ function\ at\ t = 0.1$, representing a suddenly curving road or path.

- One simulation (`veh_driver`) uses a closed loop driver model which first steers outwards ($\delta < 0$) and then continuously calculates the steer angle as a closed loop controller: $\delta = Gain \cdot (\varphi_{x,req} - \varphi_x)$;. It is not claimed that the driver model is representative for real drivers.
- In the other simulation (`veh_inverse`), the roll angle is prescribed as $\varphi_x = -v_x^2/(R_p \cdot g)$;. To prescribe the roll angle, instead of steer angle, is a way to avoid the "Non-minimum phase" difficulties. The system becomes a normal Minimum phase system if actuated with roll angle instead of steer angle. A price one has to pay for this is that the model equations has to go through a more advanced symbolic manipulation, e.g. differentiation, to solve for all variables,

including the steer angle δ. However, with a Modelica tool the symbolic manipulation is done automatically. One can see this as a way to avoid a controller design and instead use an optimal driver; optimal in the sense that it follows the path curvature with optimal yaw agility. The road path curvature is a step function but has to be filtered twice (time constant 0.1 s is used in Figure 4-92) to become differentiable.

The latter, optimal driver, negotiates the turn without overshot in yaw velocity, so it follows a suddenly curving path better.

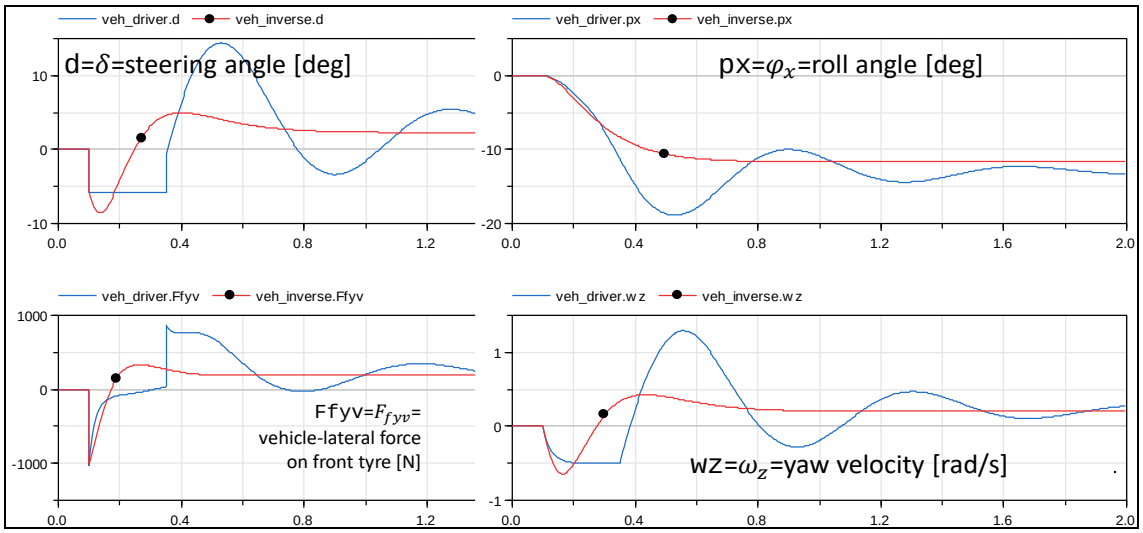


Figure 4-75: Simulations of entering a curve with a cambering vehicle. Blue solid curves without dot-marker show a closed-loop driver model which actuates δ. Red curves with dot-marker shows an optimal/inverse driver model which actuates φ_x.

Both driver models above only exemplify the low-level, roll-balancing, part of a driver. To run the model in an environment with obstacles, one would also need a high-level, path selecting, part which outputs desired, e.g., δ or φ_x. Additional driver model for longitudinal actuation is also needed.

It can be noted that the roll influences in two ways, compared to the non-cambering (roll-stiff) vehicles previously modelled in the book:

- The roll motion itself is a dynamic motion, where the roll velocity becomes a state variable carrying kinetic energy.
- The roll influences the tyre slip, e.g. rear: $s_{ry} = \left(v_y - l_r \cdot \omega_z + h \cdot \omega_x\right)/(v_x - h \cdot \varphi_x \cdot \omega_z)$;. The term $h \cdot \omega_x$ can generally be neglected for non-cambering vehicles, but for a cambering vehicle, such as a bike, it is essential. The term $h \cdot \varphi_x \cdot \omega_z$ is only important at large roll angles, it is for instance used as lever for longitudinal wheel forces in ESC-like control systems for motorbikes.

4.5.3 Two-Track Models, with Lateral Load Transfer

Contribution from Umur Erdinc, Volvo Trucks and Chalmers

The models in this section model both transients longitudinal load transfer (as in 3.4.5.2) and transient lateral load transfer (extension from 4.3.7.11.3, with transients and wheel-individual suspension).

4.5.3.1 Physical and Mathematical Model

Compared to the model presented in Figure 4-41 and Equations [4.37]..[4.43], we add the following:

- Inertial term for roll rotation, i.e. $J_{sx} \cdot \dot{\omega}_x$. Note that sprung body roll inertia ($J_{s,x}$), not whole vehicle roll inertia (J_x), is used in roll equilibrium because the unsprung parts does not participate in roll motion.
- Damping forces in parallel to each spring force, i.e. adding F_{dfl}, F_{dfr}, F_{drl}, and F_{drr}.

Due to the axle roll centre model, as opposed to wheel pivot point model, the heave acceleration is zero. Hence, no inertial force $m \cdot a_z$ needs to be introduced.

The free-body diagrams are given in Fig below, which should be compared to Figure 4-41.

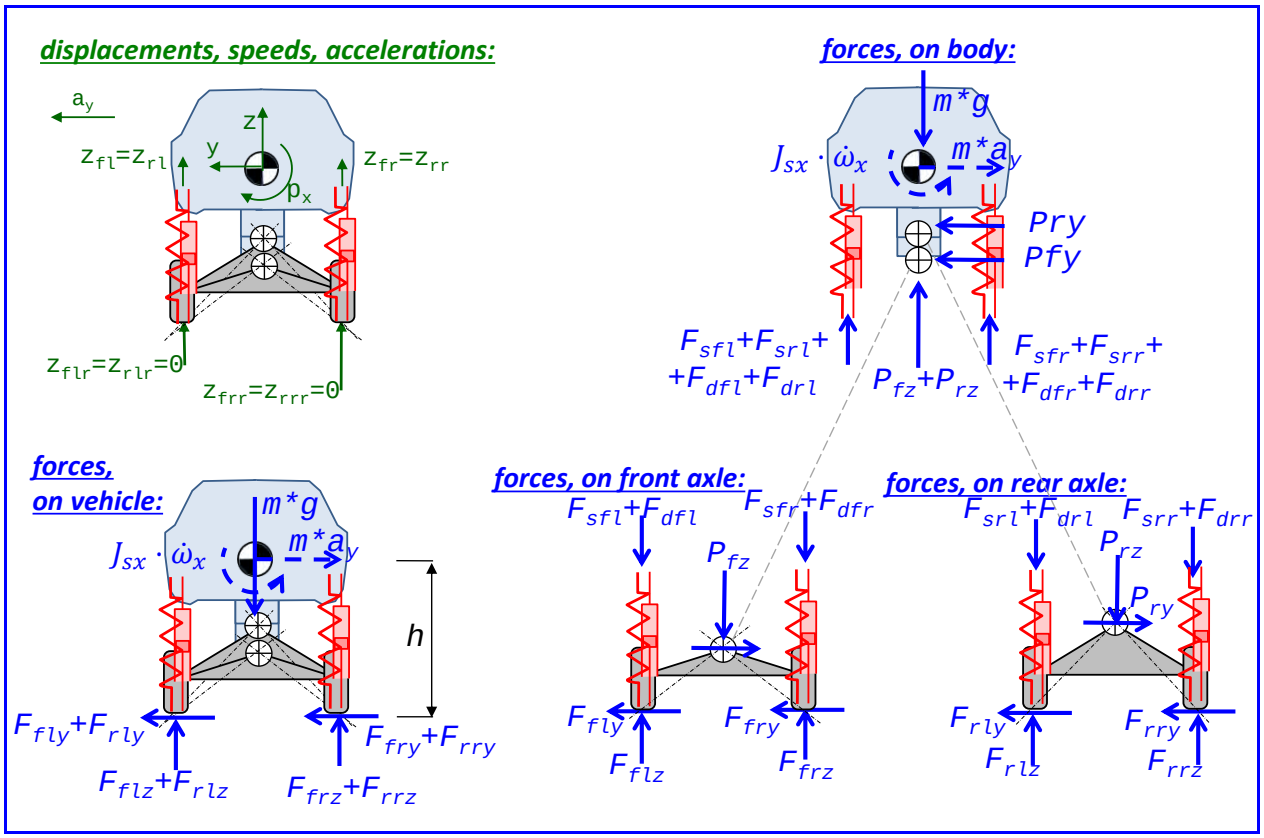


Figure 4-76: Model for transient load transfer due to lateral acceleration, using axle roll centres.

The constitutive equations for the compliances (or springs) are as follows, see Eq [4.36]. Note that the **anti-roll bars are not modelled**. Note also that we differentiate, since we will later use the spring forces as state variables in a simulation.

$$F_{sfl} = F_{sfl0} + c_{fw} \cdot (\cancel{z_{flr}} - z_{fl}); \Rightarrow \dot{F}_{sfl} = -c_{fw} \cdot \dot{z}_{fl} = -c_{fw} \cdot v_{flz};$$
$$F_{sfr} = F_{sfr0} + c_{fw} \cdot (\cancel{z_{frr}} - z_{fr}); \Rightarrow \dot{F}_{sfr} = -c_{fw} \cdot \dot{z}_{fr} = -c_{fw} \cdot v_{frz};$$
$$F_{srl} = F_{srl0} + c_{rw} \cdot (\cancel{z_{rlr}} - z_{rl}); \Rightarrow \dot{F}_{srl} = -c_{rw} \cdot \dot{z}_{rl} = -c_{rw} \cdot v_{rlz};$$
$$F_{srr} = F_{srr0} + c_{rw} \cdot (\cancel{z_{rrr}} - z_{rr}); \Rightarrow \dot{F}_{srr} = -c_{rw} \cdot \dot{z}_{rr} = -c_{rw} \cdot v_{rrz};$$
$$where\ F_{sfl0} = F_{sfr0} = \frac{m \cdot g \cdot l_r}{2 \cdot L};\ and\ \ F_{srl0} = F_{srr0} = \frac{m \cdot g \cdot l_f}{2 \cdot L};$$

The constitutive equations for the dampers have to be added:

$$F_{dfl} = -d_{fw} \cdot v_{flz};$$
$$F_{dfr} = -d_{fw} \cdot v_{frz};$$
$$F_{drl} = -d_{rw} \cdot v_{rlz};$$
$$F_{drr} = -d_{rw} \cdot v_{rrz};$$

As comparable with Equation [4.37], we get the next equation to fulfil the equilibrium. The change compared to Equation [4.37] is that we also have a roll and lateral inertia terms and 4 damper forces, acting in parallel to each of the 4 spring forces. Actually, when setting up equations, we also understand that a model for longitudinal load transfer is needed, which is why the simplest possible such, which is the stiff suspension on in Equation [3.18].

In-road-plane: Equilibrium for vehicle (longitudinal, lateral, yaw): [4.71]

$$m \cdot a_x = m \cdot (\dot{v}_x - \omega_z \cdot v_y) = F_{fx} + F_{rx};$$
$$m \cdot a_y = m \cdot (\dot{v}_y + \omega_z \cdot v_x) = F_{fy} + F_{ry};$$
$$J_z \cdot \dot{\omega}_z = F_{fy} \cdot l_f - F_{ry} \cdot l_r;$$

Out-of-road-plane: Equilibrium for vehicle (vertical, pitch, roll):

$$F_{flz} + F_{frz} + F_{rlz} + F_{rrz} - m \cdot g = 0;$$
$$-(F_{flz} + F_{frz}) \cdot l_f + (F_{rlz} + F_{rrz}) \cdot l_r - (F_{fx} + F_{rx}) \cdot h = 0;$$
$$J_{s,x} \cdot \dot{\omega}_x = (F_{flz} + F_{rlz}) \cdot \frac{w}{2} - (F_{frz} + F_{rrz}) \cdot \frac{w}{2} + (F_{fy} + F_{ry}) \cdot h;$$

Equilibrium for each axle (pitch, around roll centre):

$$\left(F_{flz} - (F_{sfl} + F_{dfl})\right) \cdot \frac{w}{2} - \left(F_{frz} - (F_{sfr} + F_{dfr})\right) \cdot \frac{w}{2} + F_{fy} \cdot h_{RCf} = 0;$$
$$\left(F_{rlz} - (F_{srl} + F_{drl})\right) \cdot \frac{w}{2} - \left(F_{rrz} - (F_{srr} + F_{drr})\right) \cdot \frac{w}{2} + F_{ry} \cdot h_{RCr} = 0;$$

Compatibility gives, keeping in mind that ω_x is the only non-zero out-of road plane velocity (i.e. $\dot{z} = \omega_y = 0$):

$$\dot{z}_{fl} = v_{flz} = +\frac{w}{2} \cdot \omega_x; \quad and \quad \dot{z}_{fr} = v_{frz} = -\frac{w}{2} \cdot \omega_x;$$
$$\dot{z}_{rl} = v_{rlz} = +\frac{w}{2} \cdot \omega_x; \quad and \quad \dot{z}_{rr} = v_{rrz} = -\frac{w}{2} \cdot \omega_x;$$

Constitution for tyre forces versus slip in ground plane becomes per wheel, as opposed to per axle in previous model:

$$F_{fyw} = -\text{sign}(s_{fy}) \cdot \left(\min\left(\frac{C_f}{2} \cdot |s_{fy}|;\ \mu \cdot F_{flz}\right) + \min\left(\frac{C_f}{2} \cdot |s_{fy}|;\ \mu \cdot F_{frz}\right)\right);$$

$$F_{ry} = -\text{sign}(s_{ry}) \cdot \left(\min\left(\frac{C_r}{2} \cdot |s_{ry}|;\ \mu \cdot F_{rlz}\right) + \min\left(\frac{C_r}{2} \cdot |s_{ry}|;\ \mu \cdot F_{rrz}\right)\right);$$

Eqs above give a model very similar to the one in Eq [4.65]. Only the additional equations from this new model are shown in Eq below. Note especially the new lateral tyre force model equations, which now have one term per wheel, because one wheel on an axle can saturate independent of the other on the same axle.

```
//Equilibrium, roll
  Jsx*der(wx) = (Fflz+Frlz)*w/2 - (Ffrz+Frrz)*w/2 + (Ffyv+Fry)*h;
//Equilibrium for each axle (roll, around roll centre):
  (Fflz-(Fsfl+Fdfl))*w/2 - (Ffrz-(Fsfr+Fdfr))*w/2 + Ffyv*hRCf = 0;
  (Frlz-(Fsrl+Fdrl))*w/2 - (Frrz-(Fsrr+Fdrr))*w/2 + Fry*hRCr = 0;
//Constitutive relation for tyres (Lateral tyre force model):
  Ffyw = -sign(sfy)*
     (min((Cf/2)*abs(sfy), mu*Fflz) + min((Cf/2)*abs(sfy), mu*Ffrz));
  Fry  = -sign(sry)*
     (min((Cr/2)*abs(sry), mu*Frlz) + min((Cr/2)*abs(sry), mu*Frrz));
  sfy = vfyw/vfxw;      sry = vry/vrx;
//Constitution for springs:
  der(Fsfl) = -cfw*vflz;   der(Fsfr) = -cfw*vfrz;
  der(Fsrl) = -crw*vrlz;   der(Fsrr) = -crw*vrrz;
//Constitution for dampers:
  Fdfl = -dfw*vflz;   Fdfr = -dfw*vfrz;
  Fdrl = -drw*vrlz;   Fdrr = -drw*vrrz;
//Compatibility, out of road plane:
  vflz = +w/2*wx;  vfrz = -w/2*wx;  vrlz = +w/2*wx;  vrrz = -w/2*wx;
```

[4.72]

A simulation of this model is shown in Figure 4-77 and should be compared with the simulation in Figure 4-50. When comparing these, we see a slight difference, which is that the axles saturate gradually during 3<time<3.5, instead of both at once at time=3.25.

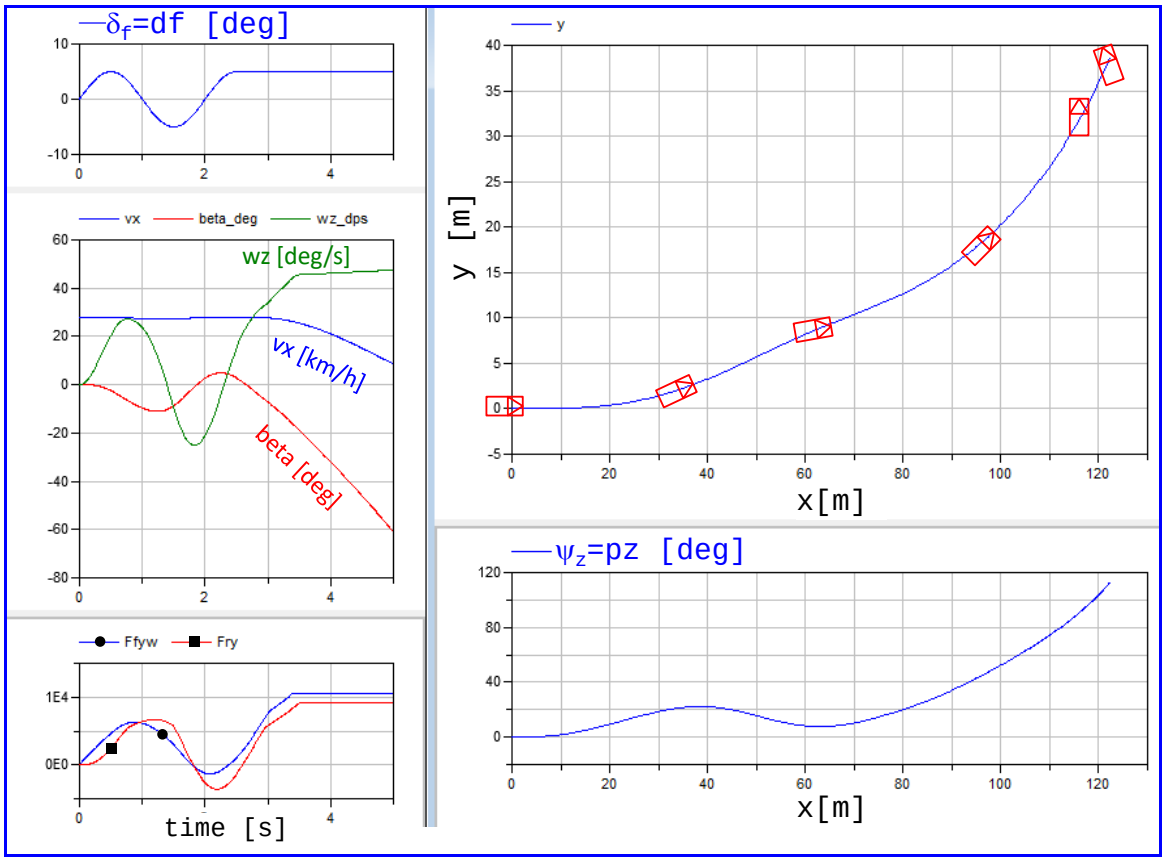


Figure 4-77: Simulation results of one-track model for transient dynamics with lateral load transfer. The vehicle drawn in the path plot is not in proper scale, but the orientation is approximately correct.

Even if the load transfer model does not influence the vehicle path a lot in this case, it may be important to include it to validity check the model through checking wheel lift. Wheel lift can be identified as negative vertical wheel forces, which are why we plot some vertical wheel forces, see Figure 4-78. In this case we see that we have no wheel lift (which would disqualify the simulation). In the right part of the figure we can also see the separate contribution from spring (F_{srr}), damper (F_{drr}) and linkage ($F_{link}, f_{l,z} = F_{flz} - F_{sfl} - F_{dfl}$).

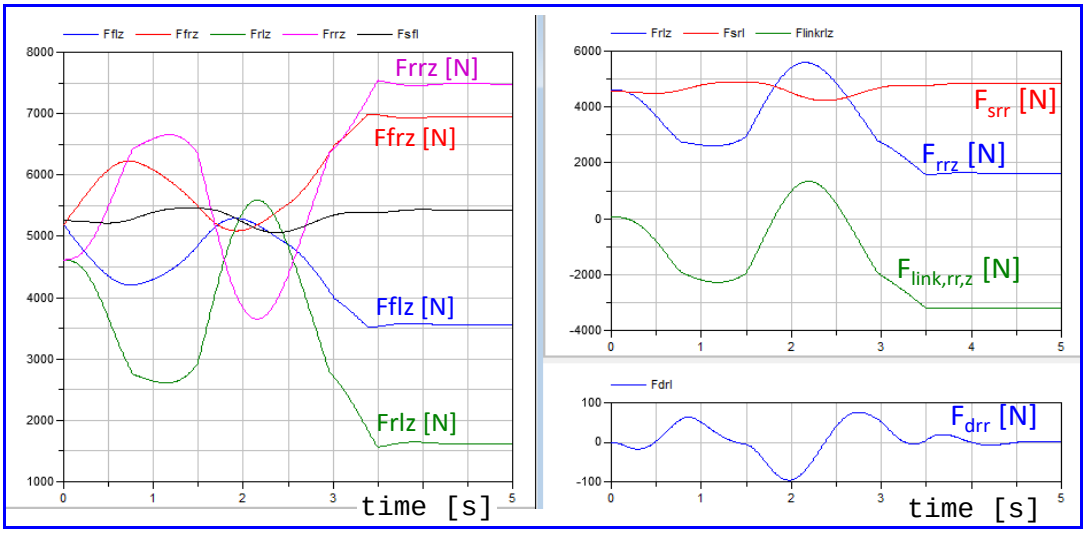


Figure 4-78: Suspension vertical force plots from simulation with one-track model for transient dynamics with lateral load transfer dynamics (same simulation as Figure 4-77). Left: Road contact forces for all wheels. Right: Forces for one wheel, rear left.

4.5.3.2 Example of Explicit Form Model; Two-Axle Vehicle, Driver and Environment

The implementation of the model in 4.5.2.3 was done in Modelica. A Modelica tool automatically transforms the model to explicit form which can be simulated, which is very efficient. But, as mentioned in 1.5.4.1.5, explicit form models can sometimes facilitate the understanding of the vehicle's dynamics. Therefore, the following model is presented. It is implemented in the data flow diagram tool Simulink. This section explains how the **states** (or state variables) together with **inputs** (or input variables), influence the **derivatives** (or state derivatives).

The example model in this section is similar, but not identical, to the model in 4.5.2.3. The aim is to model in-road-plane motion, due to transient actuation (wheel torques and wheel steer angles). Limitations in this example model are:

- Influence from vertically uneven road is NOT modelled.
- Neither wheel lift nor suspension bump stop are modelled
- Control functions (such as ABS, TC and ESC) are NOT modelled
- The (roll) pendulum effect is NOT modelled, see 4.3.7.11.2
- Wheel camber and steer angle change with suspension travel is NOT modelled.

The model is a typical passenger vehicle, with driver and environment, see Figure 4-79. The driver interface is the normal, 2 pedals, 1 steering wheel and a boolean request for direction of propulsion, `LongDir` (=-1 or +1). The interface to environment is motion (variable position) in surrounding world. To try out the vehicle model, driver and environment is also modelled. This includes also the interface between them, which is motion of obstacles in environment, relative to subject vehicle. The suspension is exemplified with wheel-individual suspension on both axles.

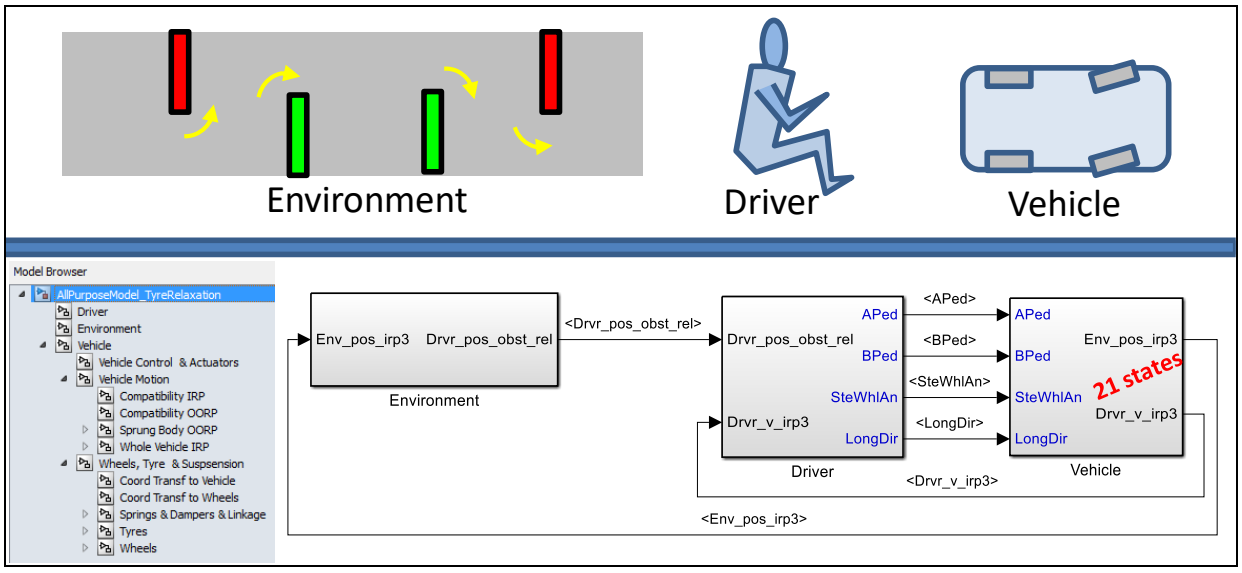


Figure 4-79: Top level of model with model tree structure. The Environment is a track test with cone walls to go left and right around. Notation "irp" and "oorp" refers to in-road-plane and out-of-road-plane, respectively.

As an initial overview, the states are presented. There are **21 states** in total, and distributed:

- Driver: 0 states
- Vehicle:
  - Vehicle Control & Actuation: 0 states
  - **Wheels, Tyres & Suspension: 12 states** (4 wheels' rotational speed, 4 Elastic parts of vertical wheel forces, 4 Longitudinal tyre forces, 4 Lateral tyre forces)
  - **Vehicle Motion: 9 states** (6 velocities and 3 positions)
- Environment: 0 states

The 4+4 tyre force states arise from modelled tyre relaxation, see 0.

4.5.3.2.1 Submodel Environment

Generally, the environment model is where the surrounding to the driver and the vehicle should be defined: road/road network, obstacles, other road users and the "driving task"/"driving instructions". In this example, it is very small and simple; it only captures stand-still point obstacles, each with instructions whether to be passed as obstacle left or right of the vehicle. Inputs to environment model is the (subject) vehicles position, including orientation in global coordinates. Outputs are the relative position (x, y) to each obstacle, in (subject) vehicle coordinate system.

4.5.3.2.2 Submodel Driver

In this example, the driver model is very small and simple. Briefly described, it treats the longitudinal dynamics very simple, as closed loop control towards a constant desired speed forward. The lateral dynamics is divided into two parts:

- Driver planning: Based on how driver perceives the obstacles relative to the vehicle, one of the objects is selected to mind for, which leads to where to be aim. Basically, the nearest obstacle ahead of vehicle is selected as mind for and aim is, in principle, either half a vehicle width left (or right) of this obstacle.
- Driver operation: Based on the driver's motorics, the steering wheel angle is calculated. In the example, it is simply an inverse model of an ideally tracking two-axle vehicle which calculates which constant steering wheel angle that would be needed to make front axle run over the aim obstacle.

It can be noted that a Driver model would also be a logical model part where to include calculation of driver's perception, such as steering effort and perceived safety during manoeuvre, etc. It can also be noted that the border between Environment and Driver is sometimes not obvious, especially when it comes to modelling the "driving task" in the Environment model, which can also be seen as a "driver high-level decision" and then be a logical part of the Driver model. If Environment model includes surrounding vehicles (object vehicles), it also includes driver models for those. For automatic functionality, anything from cruise control to automated driving, there should also be a "button HMI output" from Driver model, not only pedals and steering wheel. Such interface would turn on/off such functionality in the Vehicle model.

4.5.3.2.3 Submodel Vehicle

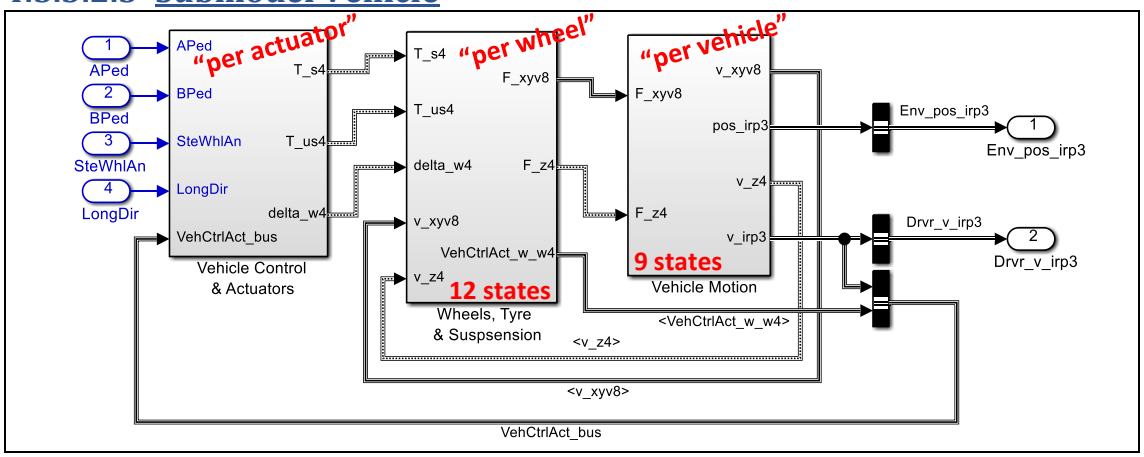


Figure 4-80: Vehicle submodel.

The figure shows the decomposition of the vehicle into 3 parts:

- Submodel **"Vehicle Control & Actuation"** models the actuators (Propulsion system, Brake system and Steering system, including "control functions") that respond on requests from the driver with wheel torques (`T_s` and `T_us`) and wheel steer angles (`delta_w`). The notation ending "4" refers to that the quantities are vectors with 4 components, one per wheel. `T_s` is

shaft torque and `T_us` is torque applied from unsprung parts, e.g. friction brake torque from brake calliper. One can think of very advanced models of these actuator systems, including e.g. propulsion system dynamics and control functions (ABS, ESC, TC, …). However, in this example model it is only modelled very simple:

  - Propulsion system outputs a fraction (determined by `APed`) of a certain maximum power, distributed equally on front left and front right wheel. If brake pedal is applied, the propulsion system outputs zero torque.
  - Brake system outputs a fraction (determined by `BPed`) of a maximum brake torque ($\mu \cdot m \cdot g/R_w$), distributed in a certain fix fraction between front and rear axle (70/30). The distribution within each axle is equal on left and right wheel.
  - There are **no states** modelled in the vehicle Control & Actuator submodel.
- Submodel **"Wheels, Tyre & Suspension"** models the part which pushes the tyres towards the ground and consequently transforms the wheel torques and wheel steer angles, via the tyre, to forces on the whole vehicle. `F_xyv8` is the x and y forces in each of the 4 wheels, 2x4=8. `F_z4` is the 4 vertical forces under each wheel. Submodel "Wheels, Tyre & Suspension" is **further explained** in 4.5.3.2.5.
- Submodel "**Vehicle Motion**" models the motion of the whole vehicle in-road-plane and motion of sprung body out-of-road-plane. The inertial effects (mass·acceleration) of the unsprung parts are considered for in-road-plane but not for out-of-road-plane. This submodel includes integrators for the 3+3+3=9 **states**:
  - Velocities in-road-plane, v_x, v_y, ω_z: **`v_irp3`** (which is transformed to x- and y-velocities of each wheel and then fed back as `v_irpv8`)
  - Position in-road-plane, x, y, φ_z: **`pos_irp3`** (which is only fed forward to "Environment")
  - Velocities out-of-road-plane, v_z, ω_x, ω_y: **`v_oorp3`** (which is transformed to z-velocities of sprung body over each wheel and then fed back as `v_z4`)

4.5.3.2.4 Submodel Vehicle Control and Actuators

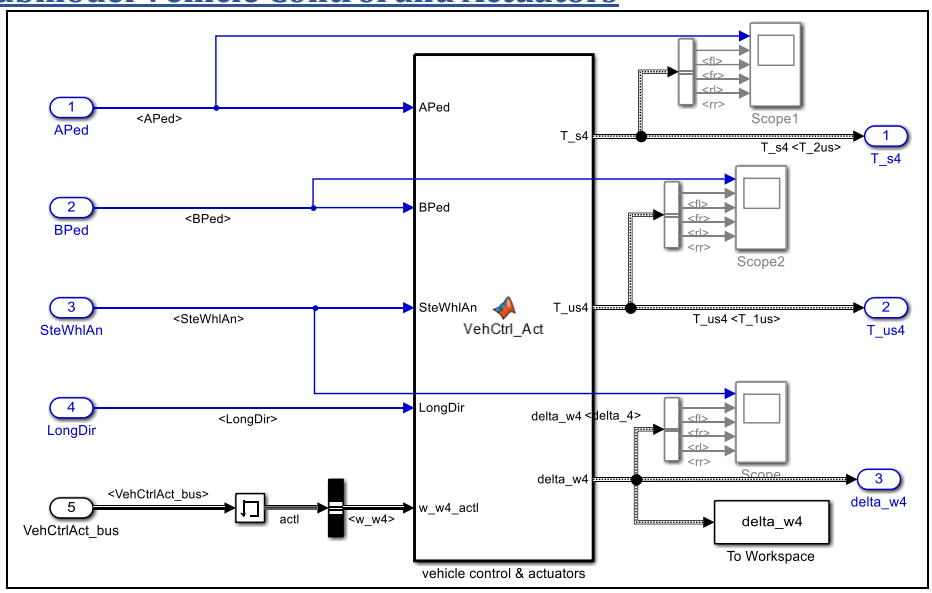


Figure 4-81: Vehicle Control & Actuators sub-model.

The example content of this sub-model is very minimalistic but can still be explained as two parts:

- **Interpret** pedals (including **arbitrate** between accelerator and brake pedal) to a sum over wheels longitudinal force request ($F_{x,req}$) and steering wheel angle to a front road wheel angle request ($\delta_{f,req}$).
- **Coordinate** and **actuate** propulsion and brake, i.e. allocate $F_{x,req}$ to 4 wheels' propulsion torques and brake torques. Also allocate $\delta_{f,req}$ to each of left and right front wheels.

Vehicle variables used for the control are wheel rotational speeds. Since front axle propulsion is assumed, the front rotational speeds are also input to the propulsion actuator modelling. No state variables are present in this minimalistic example, but in a more advanced actuation model there could typically be states such as: engine speed, gear (discrete state), delay states for brake system and elastic forces in steering system.

4.5.3.2.5 Submodel Wheels, Tyres and Suspension

This submodel is shown in Figure 4-82.

- The 2 sub-models "**Coord Transf to Vehicle**" and "**Coord Transf to Wheels**" are straight-forward coordinate transformations, see Eq [1.7].
- The sub-model "**Wheels**" is also relatively straight-forward. For each wheel, the rotational equilibrium is used as model: $J \cdot \dot{\omega} = T_{us} + T_s - F_x \cdot R_w - \text{sign}(\omega) \cdot RRC \cdot F_z \cdot R_w$; where R_w is wheel radius and RRC is rolling resistance coeeficient. The submodel will hence contain the 4 **states**: Rotational speeds of each wheel: **`w_w4.`**
- The sub-model "**Springs, Dampers & Linkage**" models the springs (incl. anti-roll-bars) and dampers and the linkage. For each wheel:
  - Four **states**: Elastic part of vertical tyre force under each wheel: **`F_s4`**
  - The derivatives are governed by the differentiated constitution of the springs: Conceptually $\dot{F}_s = -c \cdot v_z$; but involving both wheel spring and anti-roll-bar.
  - The force in damper is governed by the damper's constitutive relation: $F_d = -d \cdot v_z$;
  - The contact forces F_z are calculated in submodel "Suspension Equilibrium" in Figure 4-83. They are calculated from moment equilibrium of unsprung parts around a 3-dimensional pivot axis. The pivot axis is defined by two points, the pivot point in longitudinal load transfer (see Figure 3-60) and the pivot point in longitudinal load transfer (see Figure 4-39). The scalar equilibrium equation for one wheel can be expressed, with vector (cross) and scalar (dot) products, in $F_{xv}, F_{yv}, F_s, F_d, T_s, F_z$ and point coordinates. From this, F_z can be solved. It should be noted that the general relation should use a screw joint along the pivot axis, see https://en.wikipedia.org/wiki/Screw_theory, which is why the *lead* of the screw appears in equations.

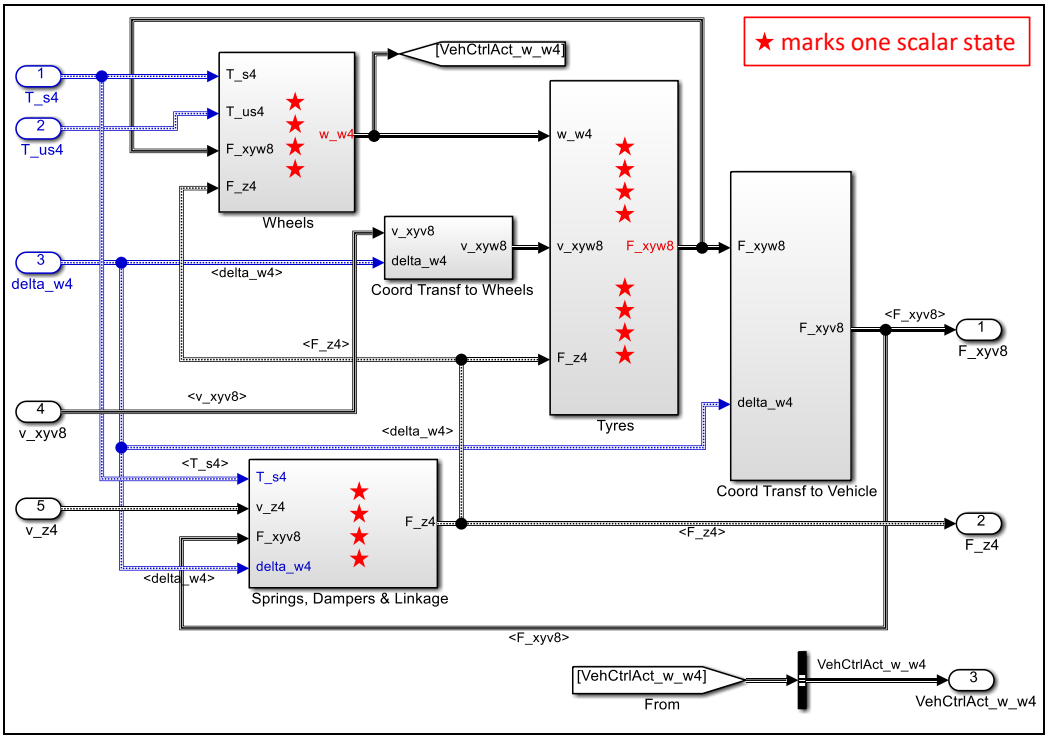


Figure 4-82: Wheels, Tyres & Suspension sub-model.

- The sub-model "**Tyres**" models the tyre mechanics, very much like the combined slip model in Equation [2.59] and a relaxation model. For each wheel:

- Four **states**: Magnitudes of tyre forces in ground plane (F_{xy}) for each wheel: **F_xyw4**
- Unfortunately, the tyre forces F_x and F_y depend on F_z. This could easily create algebraic loops. However, since we also model relaxation, the tyre forces become state variables which breaks such algebraic loops. Another way of getting rid of the algebraic loops could have been to use "memory blocks". "Memories" are such that value from last time instant is used to calculate derivatives in present time instant. This is generally NOT a recommended way of modelling.

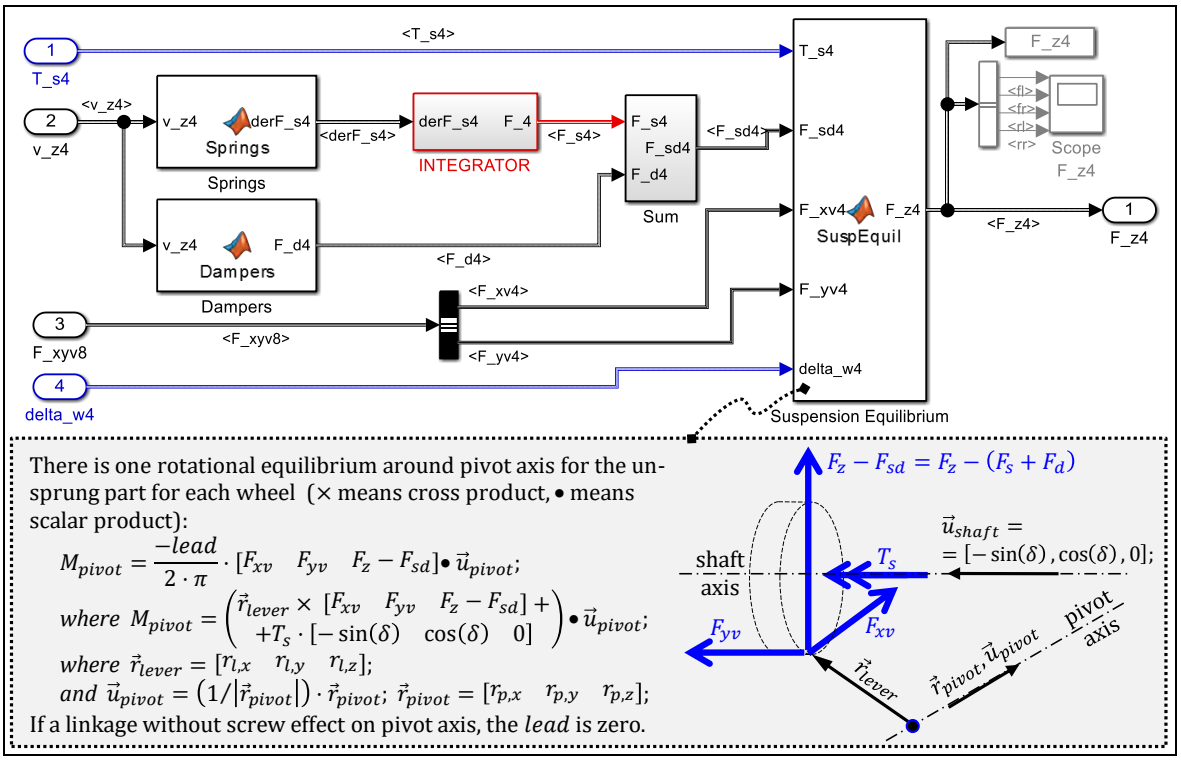


Figure 4-83: Sub-model "Springs, Dampers & Linkage".

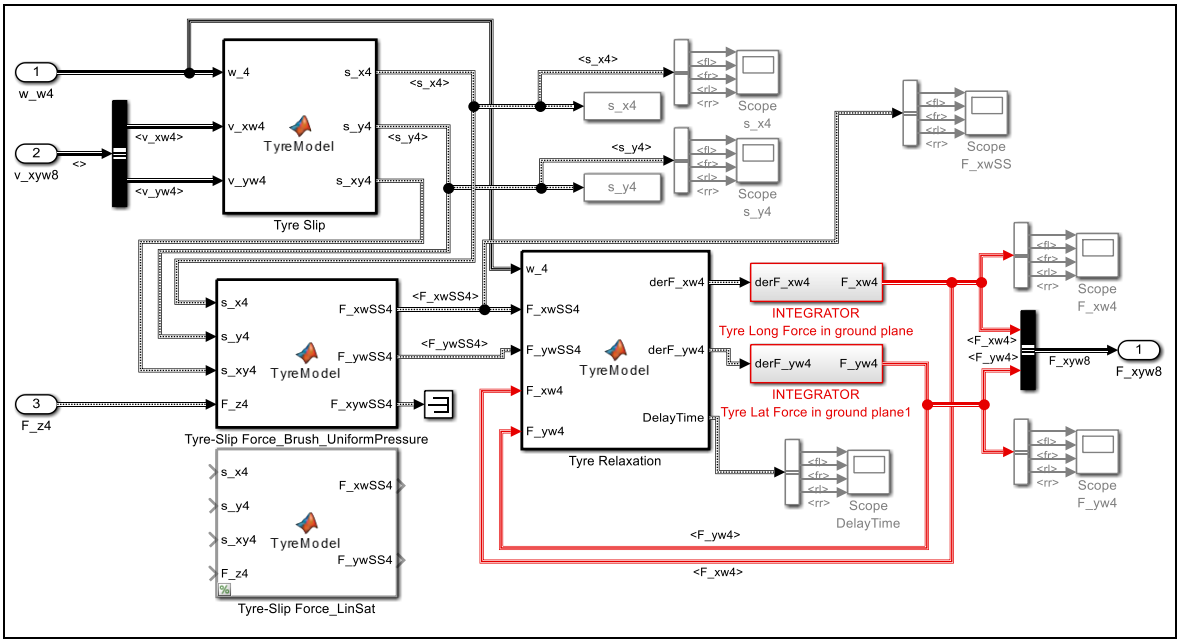


Figure 4-84: Sub-model "Tyres".

4.5.3.2.6 Sub-model Vehicle Motion

The sub-model is shown in Figure 4-85. It is divided in upper part in-road-plane (irp) and lower part out-of-road-plane (oorp). The velocities in road plane (v_irp3= $[v_x, v_y, \omega_z]$) is needed also in Sprung body OORP because of the centripetal term, $\omega_y \cdot v_x$, identified in 3.3.6.3 and used in 3.4.8.1.

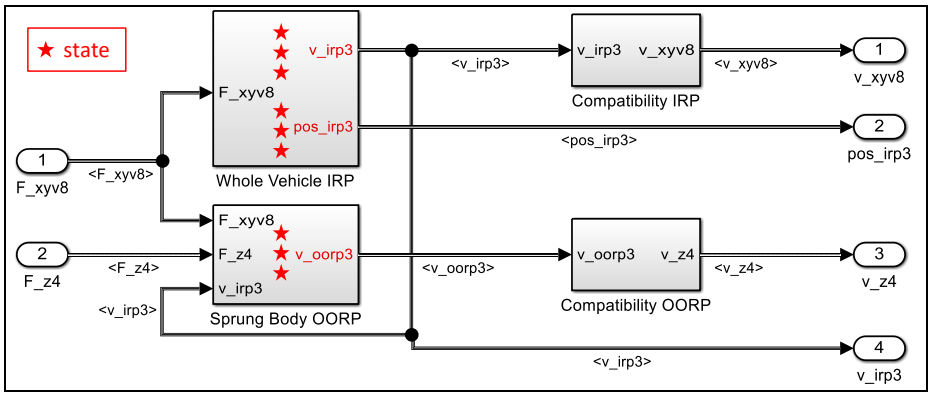


Figure 4-85: Vehicle Motion.

4.5.3.2.7 Simulation Example Double Lane Change

A double lane change between cones is used as simulation example, see Figure 4-86. The cones are run over and even passed on the wrong side because the driver model is very simple.

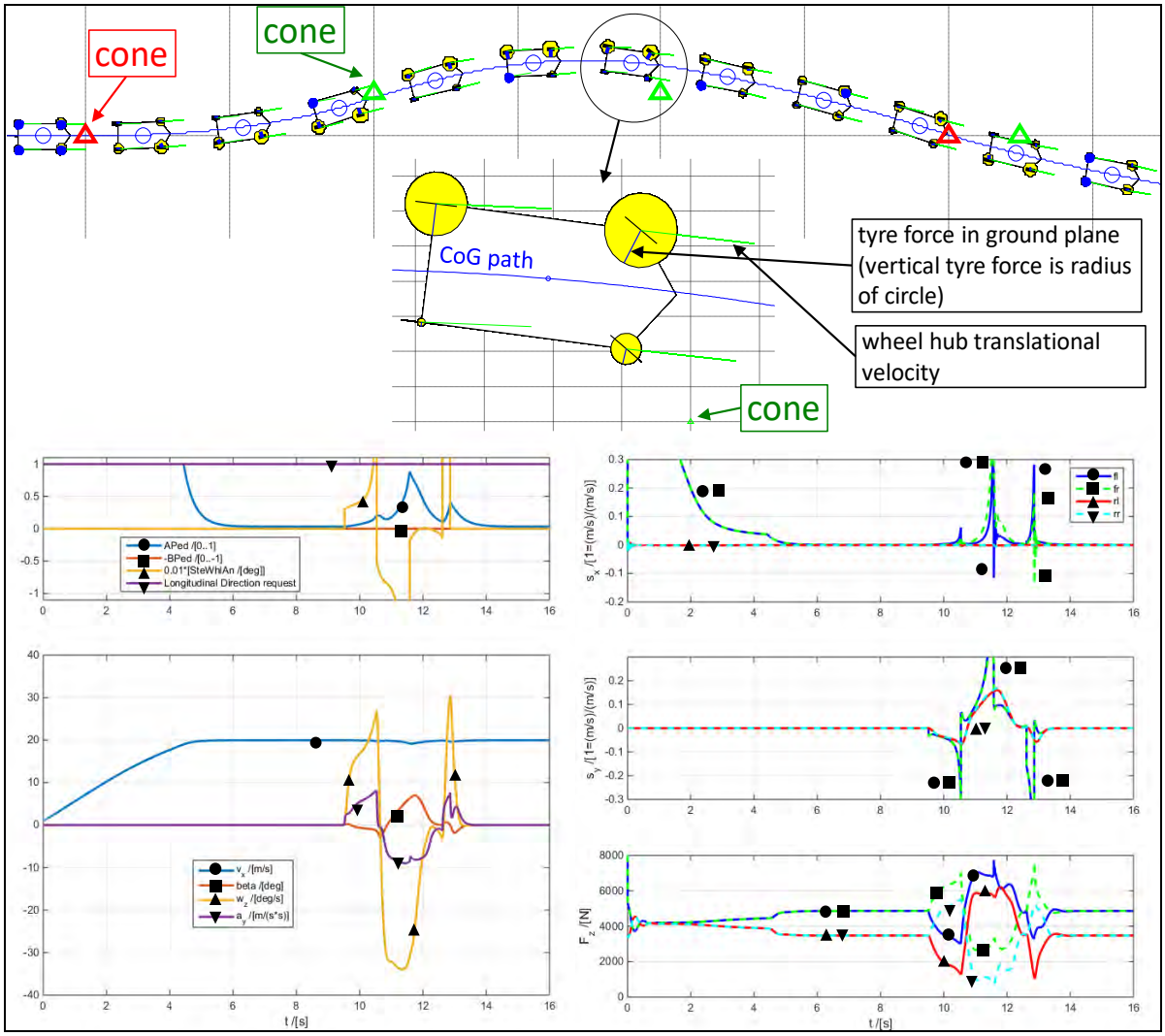


Figure 4-86: Simulation results of a double lane change between cones.

4.5.3.3 Additional Phenomena

It is relevant to point out the following, which are not modelled in this book:

- Same as pointed out as missing for longitudinal load transfer, see 3.4.5.2.3.
- Additionally, anti-roll arrangements (elastic connections between left and right wheel on one axle, often built as torsion bar) are not modelled in this book. With same modelling concept as used above, each such would be treated as a separate spring with one state variable, e.g. F_{af} (Force-antiroll-front). This force will act in parallel with F_{sf} and F_{df} on each side. Note that it will be added on one side and subtracted on the other.

4.5.3.4 Transient Roll-Over *

Function definition: ***Transient roll-over resistance*** *is the most severe measure of a certain transient manoeuvre that the vehicle can manage without lifting all wheels on inner side. The manoeuvre is typically on level ground with high road friction and certain payload, loaded high.*

The manoeuvre can typically be a double lane change, since the double triggers roll oscillations. The severity measure of the manoeuvre can be the peak lateral acceleration, or a lane change width or longitudinal speed for given lane width.

If applying the function on articulated vehicles, it is often relevant to define the threshold as lifting all inner wheels on a roll-stiff unit. Two units connected by a fifth wheel constitutes one roll-stiff unit, since the fifth wheel is conceptually roll rigid.

The function is not relevant for cambering vehicles. These could rather roll-over inward in curve, triggered by tyre loses lateral grip, which would be a completely different situation.

4.5.4 Step Steering Response *

Function definition: ***Step steering response*** *is the response to a step in steering wheel angle measured in certain vehicle measures. The step is made from a certain steady state cornering condition to a certain steering wheel angle. The response can be the time history or certain measures on the time history, such as delay time and overshoot.*

In a simple model as the linear one-track model, a step from straight-line driving results in an initial rotation around a point $l_{initial} = J_z/(m \cdot l_f)$ behind the vehicle CoG. For most vehilces, $J_z \approx m \cdot (L/2)^2 \approx m \cdot l_f^2$, $l_{initial} \approx (L/2)^2/l_f \approx L/2$, so the initial rotation appears somewhere close to rear axle. In more detail: if $J_z < m \cdot l_f \cdot l_r$, we get $l_{initial} < l_r$, which means that F_{ry} will initially be directed in same direction as F_{fy}, which means that rear axle rather helps a_y than $\dot{\omega}_z$ rotation. If smaller J_z, the the rear axle will help $\dot{\omega}_z$ rather than a_y.

4.5.4.1 Mild Step Steering Response

This section is to be compared with 4.5.4.2, which uses a more advanced model. In present section a less advanced model will be used, which is enough for small steering steps.

The model used for single frequency stationary oscillating steering can also be used for other purposes, as long as limited lateral accelerations. Most common interpretation is to make the steering step from an initial straight-line driving. In reality, the step will be a quick ramp. Equation [4.55] allows an explicit solution prediction of stationary oscillating steering, but also for step response.

Results for step steer to +3 deg are shown in Figure 4-87. Left diagram shows step steer from straight line driving, while right diagram shows a step from steady state cornering with -3 deg steer angle. It can be noted that, if the steering step is sized so that same steady state path radius, i.e. same steady state yaw velocity, the understeered vehicle will require larger steering step, but it will respond quicker in yaw velocity and lateral acceleration.

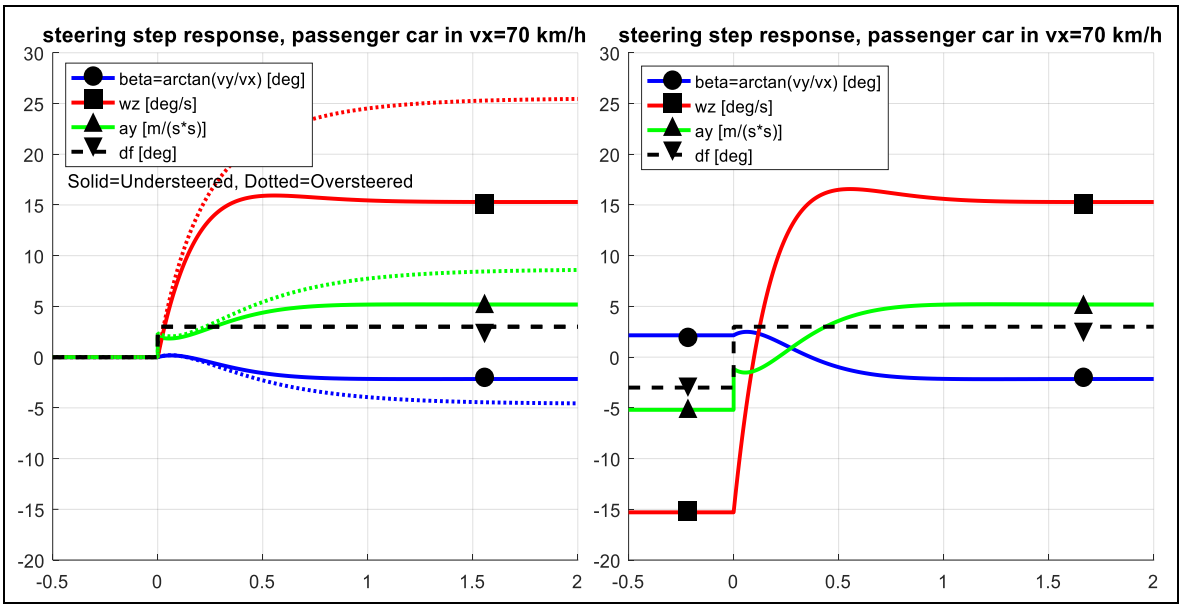


Figure 4-87: Steering step response. Simulation with model from Equation [4.73].

4.5.4.1.1 Solution with Ansatz

Start from Equation [4.55] (assuming $F_{fxw} \equiv 0$): $\begin{bmatrix} \dot{v}_y \\ \dot{\omega}_z \end{bmatrix} = \mathbf{A} \cdot \begin{bmatrix} v_y \\ \omega_z \end{bmatrix} + \mathbf{B} \cdot \delta_f;$

With steady state **initial conditions**: $\begin{bmatrix} v_y(0) \\ \omega_z(0) \end{bmatrix} = \begin{bmatrix} v_{y0} \\ \omega_{z0} \end{bmatrix}$; or $\begin{bmatrix} v_{y0} \\ \omega_{z0} \end{bmatrix} = -\mathbf{A}^{-1} \cdot \mathbf{B} \cdot \delta_{f0};$

Make an **ansatz**: $\begin{bmatrix} v_y \\ \omega_z \end{bmatrix} = \begin{bmatrix} v_{y\infty} \\ \omega_{z\infty} \end{bmatrix} + \begin{bmatrix} \hat{v}_{y1} & \hat{v}_{y2} \\ \hat{\omega}_{z1} & \hat{\omega}_{z2} \end{bmatrix} \cdot \begin{bmatrix} e^{\lambda_1 \cdot t} & 0 \\ 0 & e^{\lambda_2 \cdot t} \end{bmatrix} \cdot \begin{bmatrix} a_1 \\ a_2 \end{bmatrix};$ $\Rightarrow$

$$\Rightarrow \begin{bmatrix} \dot{v}_y \\ \dot{\omega}_z \end{bmatrix} = \begin{bmatrix} \hat{v}_{y1} & \hat{v}_{y2} \\ \hat{\omega}_{z1} & \hat{\omega}_{z2} \end{bmatrix} \cdot \begin{bmatrix} \lambda_1 \cdot e^{\lambda_1 \cdot t} & 0 \\ 0 & \lambda_2 \cdot e^{\lambda_2 \cdot t} \end{bmatrix} \cdot \begin{bmatrix} a_1 \\ a_2 \end{bmatrix};$$

Insert: $\begin{bmatrix} \hat{v}_{y1} & \hat{v}_{y2} \\ \hat{\omega}_{z1} & \hat{\omega}_{z2} \end{bmatrix} \cdot \begin{bmatrix} \lambda_1 \cdot e^{\lambda_1 \cdot t} & 0 \\ 0 & \lambda_2 \cdot e^{\lambda_2 \cdot t} \end{bmatrix} \cdot \begin{bmatrix} a_1 \\ a_2 \end{bmatrix} =$

$$= \mathbf{A} \cdot \left(\begin{bmatrix} v_{y\infty} \\ \omega_{z\infty} \end{bmatrix} + \begin{bmatrix} \hat{v}_{y1} & \hat{v}_{y2} \\ \hat{\omega}_{z1} & \hat{\omega}_{z2} \end{bmatrix} \cdot \begin{bmatrix} e^{\lambda_1 \cdot t} & 0 \\ 0 & e^{\lambda_2 \cdot t} \end{bmatrix} \cdot \begin{bmatrix} a_1 \\ a_2 \end{bmatrix} \right) + \mathbf{B} \cdot \delta_f;$$

Solve for each time function term (constant, $e^{\lambda_1 \cdot t}$ and $e^{\lambda_2 \cdot t}$ terms):

$$\begin{bmatrix} v_{y\infty} \\ \omega_{z\infty} \end{bmatrix} = -\mathbf{A}^{-1} \cdot \mathbf{B} \cdot \delta_f; \quad and \quad \left[\begin{bmatrix} \hat{v}_{y1} & \hat{v}_{y2} \\ \hat{\omega}_{z1} & \hat{\omega}_{z2} \end{bmatrix}, \begin{bmatrix} \lambda_1 & 0 \\ 0 & \lambda_2 \end{bmatrix} \right] = \text{eig}(\mathbf{A});$$

The function ”eig” is identical to function ”eig” in Matlab. It is defined as eigenvalues and eigenvectors for the matrix input argument. The eigenvalues are typically complex, which gives harmonic parts in solution. The eigenvectors are also typically complex, so that the solution of physical variables becomes real.

Initial conditions: $\begin{bmatrix} v_{y0} \\ \omega_{z0} \end{bmatrix} = \begin{bmatrix} v_{y\infty} \\ \omega_{z\infty} \end{bmatrix} + \begin{bmatrix} \hat{v}_{y1} & \hat{v}_{y2} \\ \hat{\omega}_{z1} & \hat{\omega}_{z2} \end{bmatrix} \cdot \begin{bmatrix} a_1 \\ a_2 \end{bmatrix};$ $\Rightarrow$

$$\Rightarrow \begin{bmatrix} a_1 \\ a_2 \end{bmatrix} = \begin{bmatrix} \hat{v}_{y1} & \hat{v}_{y2} \\ \hat{\omega}_{z1} & \hat{\omega}_{z2} \end{bmatrix}^{-1} \cdot \left(\begin{bmatrix} v_{y0} \\ \omega_{z0} \end{bmatrix} - \begin{bmatrix} v_{y\infty} \\ \omega_{z\infty} \end{bmatrix} \right);$$

The solution in summary:

$$\begin{cases} \begin{bmatrix} v_y \\ \omega_z \end{bmatrix} = \begin{bmatrix} v_{y\infty} \\ \omega_{z\infty} \end{bmatrix} + \begin{bmatrix} \hat{v}_{y1} & \hat{v}_{y2} \\ \hat{\omega}_{z1} & \hat{\omega}_{z2} \end{bmatrix} \cdot \begin{bmatrix} e^{\lambda_1 \cdot t} & 0 \\ 0 & e^{\lambda_2 \cdot t} \end{bmatrix} \cdot \begin{bmatrix} a_1 \\ a_2 \end{bmatrix}; \\ a_y = \dot{v}_y + v_x \cdot \omega_z = \lambda_1 \cdot \hat{v}_{y1} \cdot e^{\lambda_1 \cdot t} \cdot a_1 + \lambda_2 \cdot \hat{v}_{y2} \cdot e^{\lambda_2 \cdot t} \cdot a_2 + v_x \cdot \omega_z; \end{cases} \quad [4.73]$$

$$\text{where: } \begin{bmatrix} v_{y\infty} \\ \omega_{z\infty} \end{bmatrix} = -\boldsymbol{A}^{-1} \cdot \boldsymbol{B} \cdot \delta_f; \text{ and } \left[\begin{bmatrix} \hat{v}_{y1} & \hat{v}_{y2} \\ \hat{\omega}_{z1} & \hat{\omega}_{z2} \end{bmatrix}, \begin{bmatrix} \lambda_1 & 0 \\ 0 & \lambda_2 \end{bmatrix} \right] = \text{eig}(\boldsymbol{A});$$

$$\text{and } \begin{bmatrix} a_1 \\ a_2 \end{bmatrix} = \begin{bmatrix} \hat{v}_{y1} & \hat{v}_{y2} \\ \hat{\omega}_{z1} & \hat{\omega}_{z2} \end{bmatrix}^{-1} \cdot \left(\begin{bmatrix} v_{y0} \\ \omega_{z0} \end{bmatrix} - \begin{bmatrix} v_{y\infty} \\ \omega_{z\infty} \end{bmatrix} \right);$$

Another way to express or compute this is the "matrix exponential", mentioned in 1.5.1.1.6.

4.5.4.1.2 Solution with Laplace transform

By Mats Jonasson, Volvo Cars and Vehicle Dynamics at Chalmers

Solution of same mathematical model as 4.5.4.1.1. But we use special case $\begin{bmatrix} v_{y0} \\ \omega_{z0} \end{bmatrix} = \mathbf{0}$;.

Laplace transforms, 1.5.1.1.4.1, gives: $s \cdot \mathcal{L}\left(\begin{bmatrix} v_y \\ \omega_z \end{bmatrix}\right) - \begin{bmatrix} v_{y0} \\ \omega_{z0} \end{bmatrix} = \mathcal{L}\left(\mathbf{A} \cdot \begin{bmatrix} v_y \\ \omega_z \end{bmatrix} + \mathbf{B} \cdot \delta_f(t)\right); \Rightarrow$

$$\Rightarrow \left\{ \begin{bmatrix} v_{y0} \\ \omega_{z0} \end{bmatrix} = \mathbf{0} \right\} \Rightarrow \quad s \cdot \mathcal{L}\left(\begin{bmatrix} v_y \\ \omega_z \end{bmatrix}\right) - \mathbf{0} = \mathbf{A} \cdot \mathcal{L}\left(\begin{bmatrix} v_y \\ \omega_z \end{bmatrix}\right) + \mathbf{B} \cdot \mathcal{L}\left(\delta_f(t)\right); \Rightarrow$$

$$\Rightarrow \quad (\mathbf{A} - s \cdot \boldsymbol{I}) \cdot \mathcal{L}\left(\begin{bmatrix} v_y \\ \omega_z \end{bmatrix}\right) = -\mathbf{B} \cdot \mathcal{L}\left(\delta_f(t)\right); \Rightarrow \quad \mathcal{L}\left(\begin{bmatrix} v_y \\ \omega_z \end{bmatrix}\right) = \underbrace{-(\mathbf{A} - s \cdot \boldsymbol{I})^{-1} \cdot \mathbf{B}}_{\boldsymbol{H}(s)} \cdot \mathcal{L}\left(\delta_f(t)\right); \Rightarrow$$

$$\Rightarrow \quad \{\mathcal{L}(step) = step/s\} \Rightarrow \quad \mathcal{L}\left(\begin{bmatrix} v_y \\ \omega_z \end{bmatrix}\right) = \underbrace{-(\mathbf{A} - s \cdot \boldsymbol{I})^{-1} \cdot \mathbf{B}}_{\boldsymbol{H}(s)} \cdot \frac{\delta_f}{s}; \Rightarrow \quad \mathcal{L}\left(\begin{bmatrix} v_y \\ \omega_z \end{bmatrix}\right) = \frac{\boldsymbol{H}(s)}{s} \cdot \delta_f; \Rightarrow$$

$$\Rightarrow \quad \begin{bmatrix} v_y \\ \omega_z \end{bmatrix} = \mathcal{L}^{-1}\left(\frac{\boldsymbol{H}(s)}{s} \cdot \delta_f\right); \Rightarrow$$

$$\Rightarrow \quad \begin{bmatrix} v_y \\ \omega_z \end{bmatrix} = \mathcal{L}^{-1}\left(\frac{\boldsymbol{H}(s)}{s}\right) \cdot \delta_f = \cdots \begin{Bmatrix} \text{inverse Laplace transform} \\ \text{e.g. using Matlab command} \\ \texttt{ilaplace}\text{, see 1.5.4.1.1} \end{Bmatrix} = \begin{bmatrix} c_1 \\ c_2 \end{bmatrix} - \begin{bmatrix} c_3 \\ c_4 \end{bmatrix} \cdot e^{-c_5 \cdot t} \cdot \begin{bmatrix} \cos(c_6 \cdot t + c_7) \\ \cos(c_6 \cdot t + c_8) \end{bmatrix};$$

where $c_1, c_2, \cdots, c_8$ are real parameters, expressed in model parameters l_f, l_r, m, J, C_f, C_r, initial conditions and size of step in input variable δ_f. So, $v_y(t)$ and $\omega_z(t)$ can be computed and plotted, overlapping in Figure 4-87. Note:

- The $\boldsymbol{H}(s)$ is the Laplace transfer function. Each component of $\boldsymbol{H}(s)$ is a surface over the complex space $[Re(s), Im(s)]$. Compare with Fourier transfer function $\boldsymbol{H}(\omega)$ of which each component is a one-dimensional curve over ω.
- Laplace transform can also handle other transient vehicle problems, such as engine torque step or vertical road step. Laplace can also handle other transient disturbances, such as ramps.
- For stationary oscillations, Fourier transform is often enough and easier to use.

4.5.4.2 Violent Step Steering Response

This section is to be compared with 4.5.4.1 Mild Step Steering Response, which uses a model with linear tyre models without saturation. In present section, a more advanced model will be used, which might be needed when the step steering is more violent.

Most common interpretation is to make the steering step from an initial straight-line driving. In reality, the step will be a quick ramp. In simulations, an ideal step can be used.

The transients can easily be that violent that a model as Eq in 4.5.3 is needed. If ESC is to be simulated, even more detailed models are needed (full two-track models, which are not presented in this book). Anyway, if we apply a step steer to the model in 4.5.3, we can simulate as in Figure 4-88.

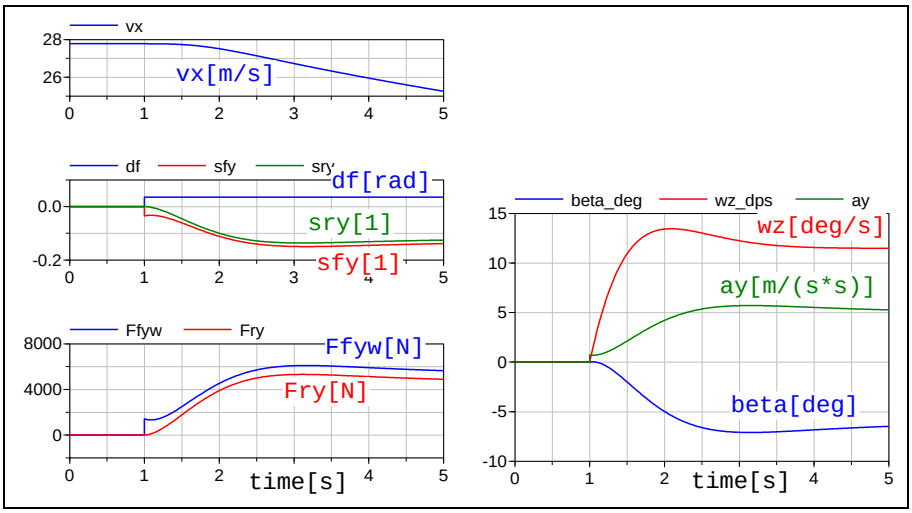


Figure 4-88: Step steer. 2 deg on road wheels at $v_x = 100$ km/h. Simulation with model in 4.5.3.

4.5.4.3 Steering Effort at High Speed *

*Function definition: **Steering effort at high speed** is the steering wheel torque (or subjectively assessed effort) needed to perform a certain avoidance manoeuvre at high road friction.*

At higher vehicle speeds, the steering effort is normally less of a problem since unless really high steering wheel rate. Hence, steering wheel torque in avoidance manoeuvres in e.g. 70 km/h can be a relevant requirement. In these situations, the subjective assessment of steering effort can also be the measure. Then, steering effort is probably assessed based on both steering wheel rate and steering wheel torque.

4.5.5 Phase Portrait

The transient from one steady state to another is seen after the steps in Figure 4-87 and Figure 4-88. Plotting several such transients as trajectories in a β, ω_z-diagram gives a phase portrait, which is a graphical representation of how a vehicle stabilize itself or gets unstable. For transients that stays within unsaturated tyre slip, the linear one-track model can be used, and the trajectories can then be explicit time expressions using Eq[4.73]. This is exemplified in left part of Figure 4-89. Some states can be confirmed stable already from this simple model. Simulations with higher fidelity model is exemplified in right part of Figure 4-89. With that one can confirm some more stable areas.

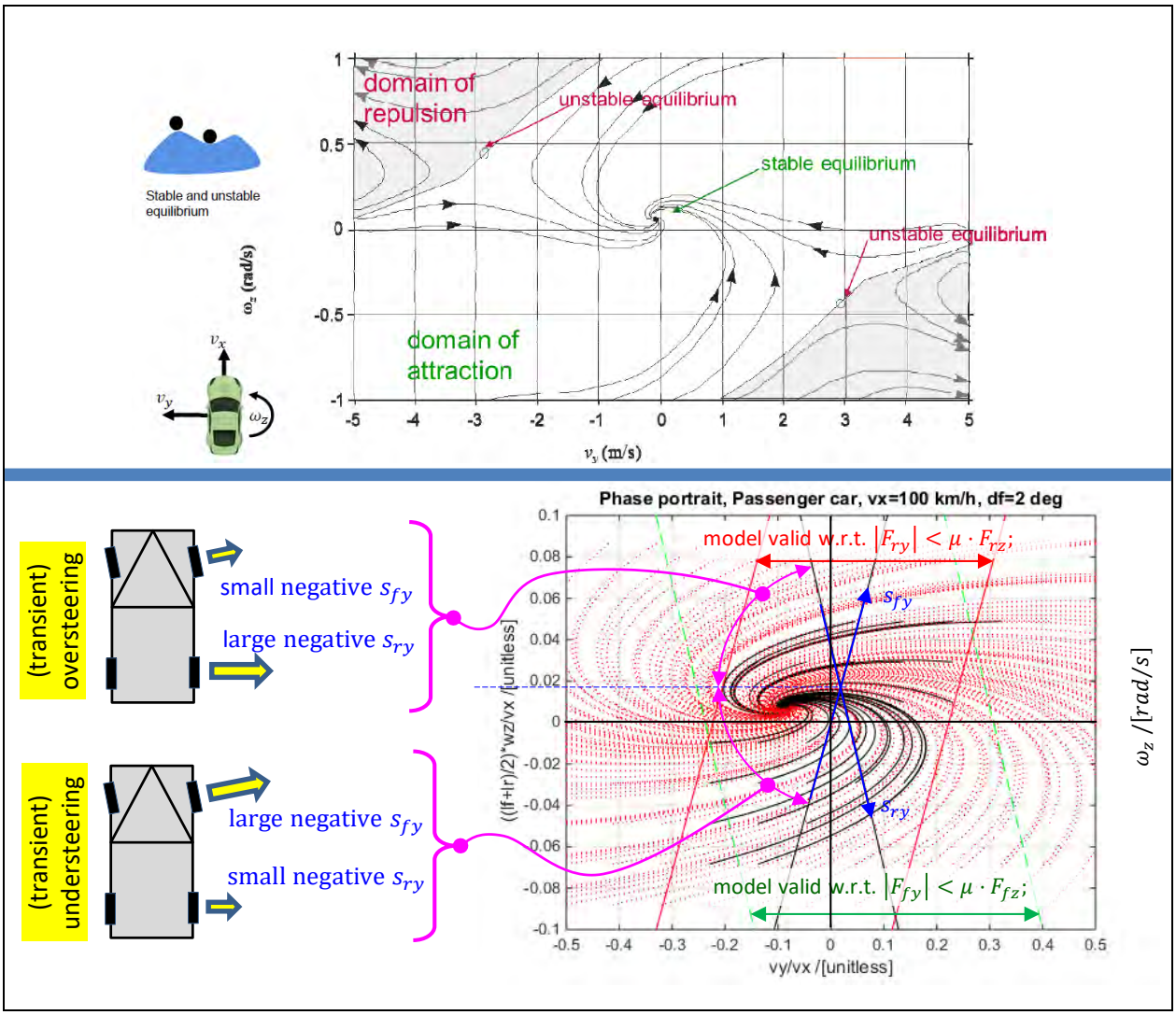


Figure 4-89: Phase portrait for constant v_x and constant steer angle δ_f. Bottom: Using simple model in Eq [4.55]. Only black solid trajectories credible, since they are completely within model validity. Upper: Using a model with larger validity. From Mats Jonasson, VCC.

There is a linear transformation between the variables $\{v_y, \omega_z\}$ and $\{v_{fy}/v_x\,, v_{ry}/v_x\} \approx$ $\approx \{\tan(\beta_f)\,, \tan(\beta_r)\}$. The phase portrait can be given in dimensionless units by selecting the latter, see Figure 4-90.

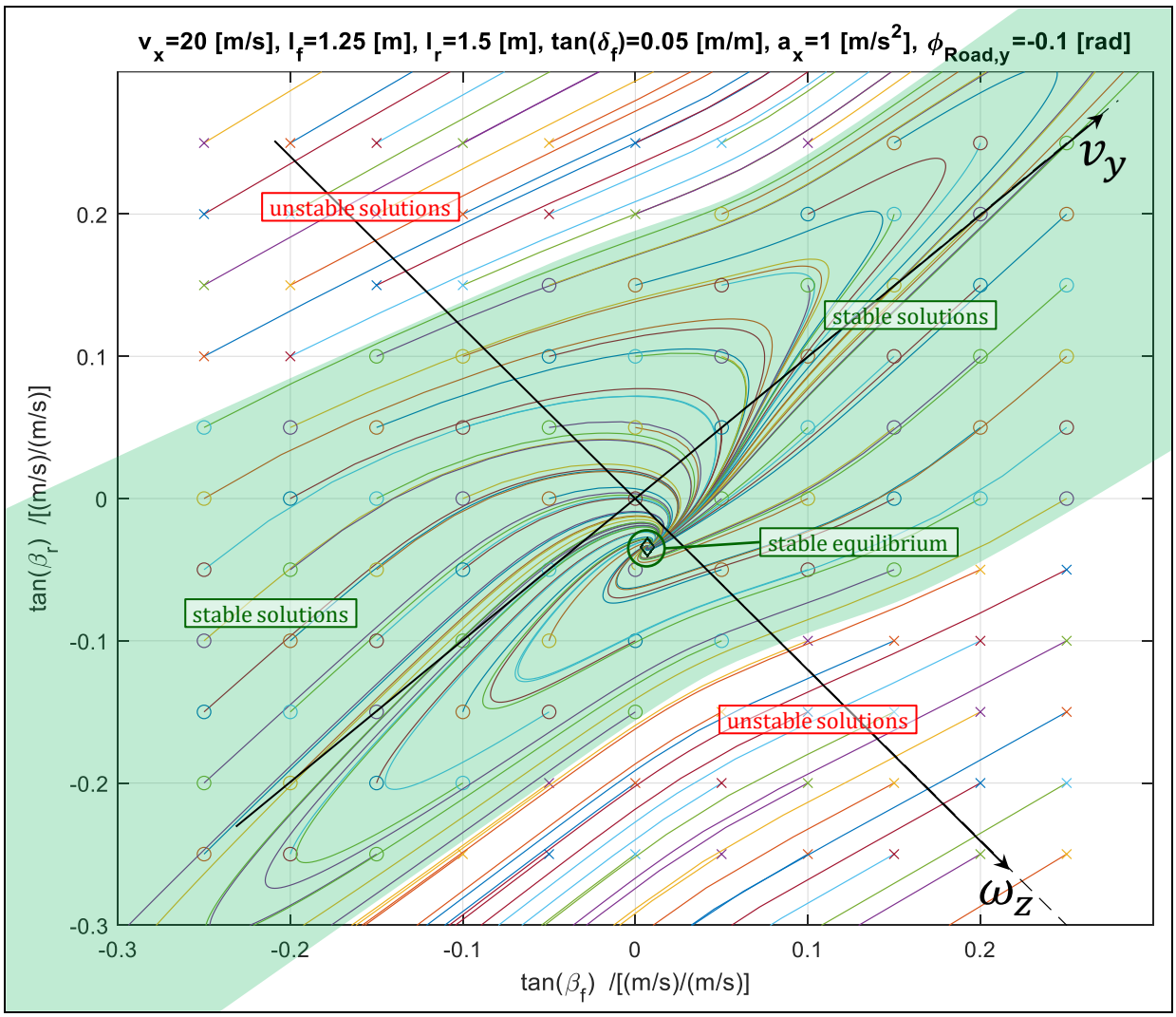


Figure 4-90: Phase portrait of a one-track model with two axles. Tyre model used is Eq [2.59] with $tanhyp(\cdots)$. No suspension steering. Equal utilization of "longitudinal friction": $F_{fx}/F_{fz} = F_{rx}/F_{rz}$. Solutions that reach β_f or β_r larger than $arctan(0.5) \approx 27\ deg$ are considered as unstable.

4.5.6 Long Heavy Combination Vehicles High Speed Functions

It is sometimes irrelevant to apply functions/measures from two axle vehicles on combinations of units. This can be the case for passenger cars with a trailer, but it is even more obvious for long combinations of heavy vehicles. Some typical measures for multi-unit combination vehicle are given in this section.

4.5.6.1 Rearward Amplification, RA *

> *Function definition:* ***Rearward Amplification for long heavy combination vehicles*** *is the ratio of the maximum value of the motion variable of interest (e.g. yaw velocity or lateral acceleration of the centre of gravity) of the worst excited following vehicle unit to that of the first vehicle unit during a specified manoeuvre at a certain friction level and constant speed. From Reference [(Kati, 2013)].*

Figure 4-91 illustrates Rearward Amplification, RWA. RWA is defined for a special manoeuvre, e.g. a certain lane change or step steer. RWA is the ratio of the peak value of yaw velocity or lateral acceleration for the rearmost unit to that of the lead unit. This performance measure indicates the increased risk for a swing out or rollover of the last unit compared to what the driver is experiencing in the lead unit.

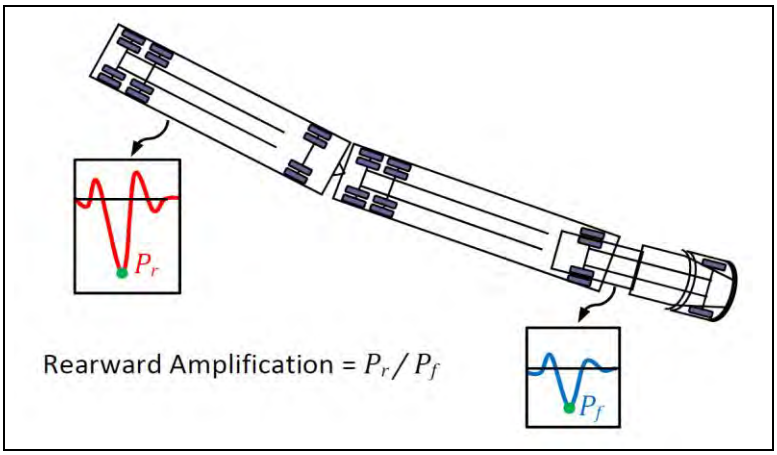


Figure 4-91: Rearward amplification, P is peak value of motion variable of interest. From (Kharrazi , 2012).

An alternative definition of RA is via the frequency response: $RA = \left|H_{\delta\to\omega_1}/H_{\delta\to\omega_{last}}\right|$, where H denots transfer functions, so $H(f)$, where f is the frequency of an harmonic variation of δ. So, either we see $RA = RA(f)$ or $RA = \max_f\left(RA(f)\right)$. The f where max appears is typically 0.4..0.6 Hz. The frequency response definition is better (independent of δ amplitude) for measuring how difficult it is for driver to keep the lateral stability of the last unit when driving straight ahead with small lateral disturbances. It is a relevant measure both for human driver and virtual driver, such as LKA, 4.6.2.4.

4.5.6.2 High Speed Transient Off-tracking, HSTO *

Function definition: ***High speed transient off-tracking for long heavy combination vehicles*** *is the overshoot in the lateral distance between the paths of the centre of the front axle and the centre of the most severely off-tracking axle of any unit in a specified manoeuvre at a certain friction level and a certain constant longitudinal speed. From Reference [(Kati, 2013)].*

Figure 4-43 illustrates a manoeuvre where this Off-tracking can be defined. Off-tracking can be either determined in a steady state turn or in a transient manoeuvre such as lane change. The steady state version is described in 4.3.7.12.2.

4.5.6.3 Yaw Damping, YD *

Function definition: Yaw Damping for long heavy combination vehicles is the ratio of decay of the least damped articulation joint's angle of the combination vehicle during free oscillations excited by actuating the steering wheel in a certain transient way, e.g. a step or single sine wave at a certain friction level. From Reference [(Kati, 2013)].

Figure 4-92 illustrates Yaw Damping. It is the ratio of two subsequent peaks, $YD = \left|\hat{\theta}_{i,j}/\hat{\theta}_{i,j+1}\right|$; where i=ordinal of coupling and j=ordinal of "half period" after steering disturbance has ended. Assuming linear model, it should not matter which two half periods one uses and, then it can give less sensitive definition to use several peaks, e.g. $YD = \left|\hat{\theta}_{i,j}/\hat{\theta}_{i,j+5}\right|/5$;. Sometimes other qualtities than articulation angle in coupling points, such as yaw velocity of units, can be used.

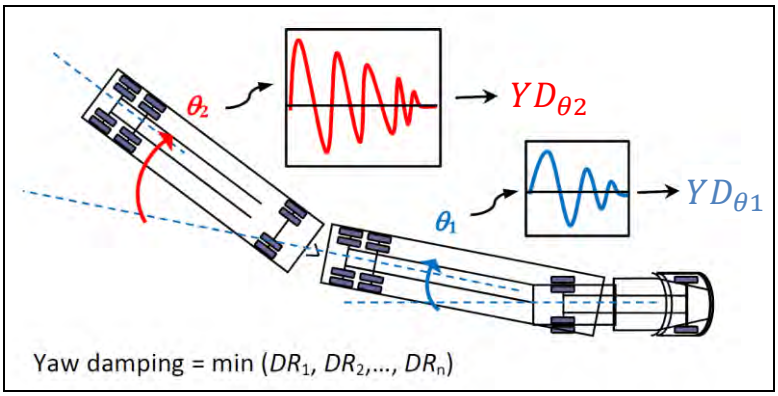


Figure 4-92: Yaw damping, YD_i denotes damping ratio of the articulation joint. From (Kharrazi , 2012).

4.5.6.4 Zero-Damping Speed *

Function definition: Zero-damping speed for long heavy combination vehicles is the longitudinal speed at which a yaw disturbance leads to undamped response.

The measure can be calculated from a linear model as the longitudinal speed when the damping coefficient, for any mode involving yaw velocity, equals zero. If the measure is applied on a two-axle vehicle it is same as critical speed.

4.6 Lateral Control Functions

Some control functions involving lateral vehicle dynamics will be presented briefly. There are more, but the following are among the most well-established ones. But initially, some general aspects of lateral control are given.

4.6.1 Lateral Control

Sensors available in production vehicles and used for lateral control are, generally those mentioned as available for Longitudinal Control, see 3.5 plus some more:

Steering wheel sensors gives at least steering wheel angle, if the vehicle is equipped with ESC (which is a legal requirement on many markets). Additionally, if the steering assistance is electrical, the steering wheel torque can be sensed.

High specification modern vehicles also have environment sensors (camera, radar, etc) that can give laterally interesting information, such as: Subject vehicle lateral position versus lane markers ahead and other vehicles to the side or rear of subject vehicle.

As general considerations for actuators, one can mention that interventions with friction brake normally have to have thresholds, because interventions are noticed by driver and also generate energy loss. Interventions with steering are less sensitive and can be designed without thresholds.

4.6.2 Lateral Control Functions

4.6.2.1 Automatic coordination of other lateral actuators *

Function definition: ***Automatic coordination of actuators*** *while driver only must operate steering wheel.*

This section has the very same purpose as "3.5.2.2.2 Automatic coordination of other longitudinal actuators *". But here it is added:

If multiple steered axles or wheels, the corresponding automatic coordination can be designed for those, while the vehicle still will follow how the driver operate the steering wheel.

Also, suspension actuators (such as air suspension and active antiroll bars) can be correspondingly coordinated.

4.6.2.2 Electronic Stability Control, ESC *

*Function definition: **Electronic Stability Control** directs the vehicle to match a desired yaw behaviour, when the deviation from desired behaviour becomes above certain thresholds. ESC typically monitors vehicle speed, steer angle and yaw velocity to calculate a yaw velocity error and uses friction brakes as actuator to reduce it.*

There are 3 parts of ESC: Over-steer control, Under-steer control, Over-speed control. The actual control error that the vehicle reacts on is typically the yaw velocity error between a desired yaw velocity and the sensed yaw velocity. Desired yaw velocity is calculated from a so-called reference model. Some of today's advanced ESC also intervenes on difference between desired and estimated side slip.

Desired yaw velocity and side-slip is calculated using a reference model and a closed loop control on the reference, see Figure 4-94. The reference model requires at least steer angle and longitudinal velocity as input. The reference model could conceptually use an *ideally tracking* model:

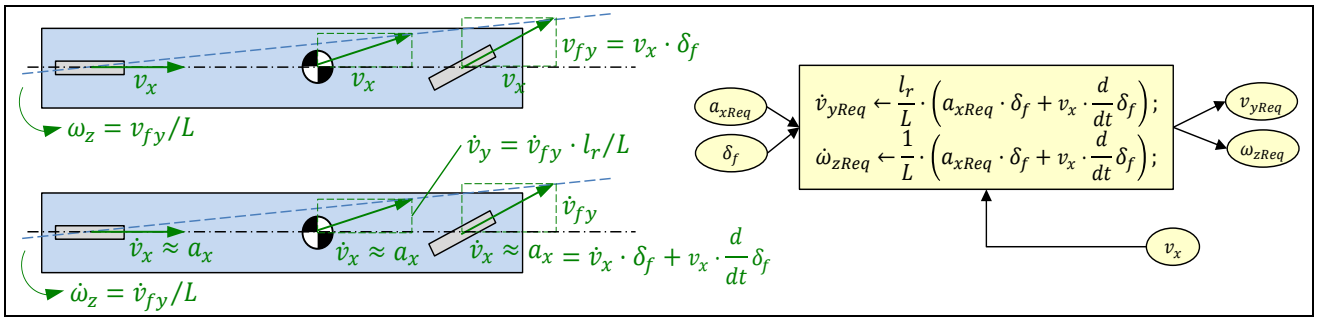


Figure 4-93: Concept for reference model. Idealised, using ideally tracking model. The a_{xReq} comes from pedals or cruise. The δ_f comes from steering wheel or lane assistance.

However, the reference model is typically either of *steady state* type (approximately as Eq [4.21] or the [4.16]) or *transient* (approximately as Eq [4.55]). The vehicle modelled by the reference model should rather be a desired vehicle than the controlled vehicle. Figure 4-94 does NOT show: Slide slip control, Reduction of C_f due to low friction detection, Coordination with Engine/Steering interventions, Arbitration with Pedal/ACC/ABS braking. (For single unit vehicles, $\dot{\omega}_{z,req}$ can be seen as a yaw moment.)

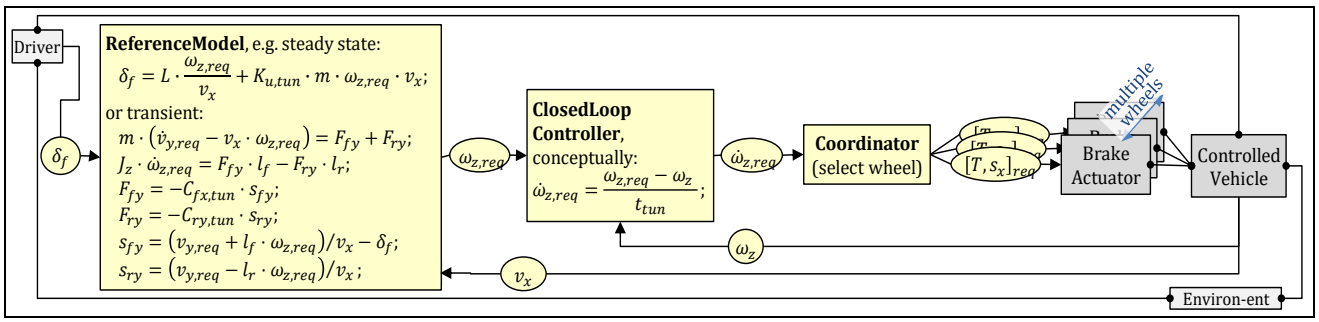


Figure 4-94: Concept for ESC.

The manoeuvre in Figure 4-22 shows an example of ESC interventions. But, in order to avoid too much friction brake interventions; the reference model cannot be too different. Also, in order to avoid that vehicle yaws more than its path curvature; the reference model cannot be much less understeered than the controlled vehicle, which typically can be arranged by saturating lateral tyre forces on the front axle in the reference model. This requires some kind of friction estimation, especially for low-mu driving.

When controlling yaw via wheel torques, one can identify some different concepts such as direct and in-direct yaw moment, see 4.3.7.6. For ESC there is also a "pre-cautious yaw control" which aims at reducing speed, see 4.6.2.2.3. The coordination of wheel torques handles these aspects, which are far from trivial. Often, a dual-request concept for each wheel is used, see Figure 4-94 and 4.6.2.2.4. A simplest possible coordinator can be to request braking only on one wheel at the time:

4.6.2.2.1 Over-Steer Control

Over-steer control was the first and most efficient concept in ESC. When a vehicle over-steers, ESC will typically coordinate wheel torques so that outer front wheel is braked. It can brake to deep slip levels (typically -50%) since losing side grip on front axle is desired in an over-steer situation. More advanced ESC variants also brake outer rear, but less and not to same deep slip level.

For combination vehicles with trailers that have controllable brakes, also the trailer is braked to avoid jack-knife effect, see upper part of Figure 4-95, or swing-out of the towed units.

4.6.2.2.2 Under-Steer Control

Under-steer control means that inner rear is braked when vehicle under-steers. This helps the vehicle turn-in. This intervention is most efficient on low mu, because on high mu the inner rear wheel normally has very little normal load. Also, the slip levels are not usually as deep as corresponding over-steer intervention, but rather -10%. This is because there is always a danger in braking too much on rear axle, since it can cause over-steering. More advanced ESC variants also brake inner front. The more wheels that are braked, the more similar the understeer intervention becomes with the function in 4.6.2.2.3.

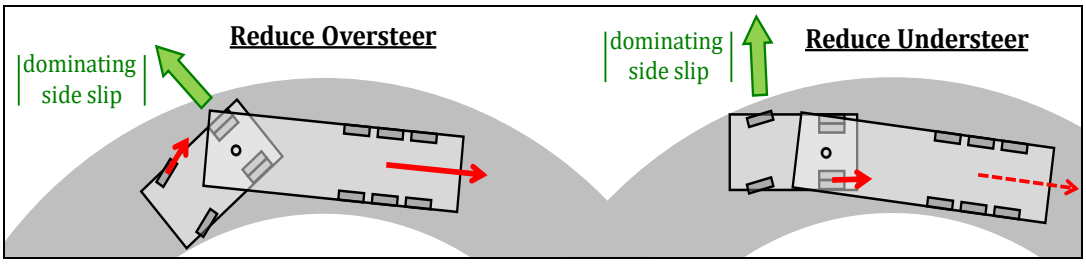


Figure 4-95: ESC brake interventions when oversteer and understeer, on a tractor with trailer.

4.6.2.2.3 Over-Speed Control

Over-speed control is not always recognised as a separate concept, but as a part of under-steer control. The actuation is that propulsion is reduced, or more than just inner rear wheels are braked. In this text, we identify this as done to decrease speed, which has a positive effect later in the curve.

4.6.2.2.4 Wheel-Level Control with dual-request-interface

A pre-requisite for all controls mentioned above in 4.6.2.2 is that the wheel torque actuator primarily responds to a torque request. However, one need to have a "dual-request-interface", with both torque (or F_x) request and longitudinal slip request. This gives control over the lateral force margin. See Figure 4-94 and Figure 4-96. The slip request is generally used as a "safety net" to avoid lock-up the wheel too much; so, it is a "max $|s_x|$ request". Typically, s_x is $-0.2..-0.1$, for braking, but at RSC interventions (see 4.6.2.3) the lateral grip should be braked away, so a deeper slip request is then used, typically 50-70%.

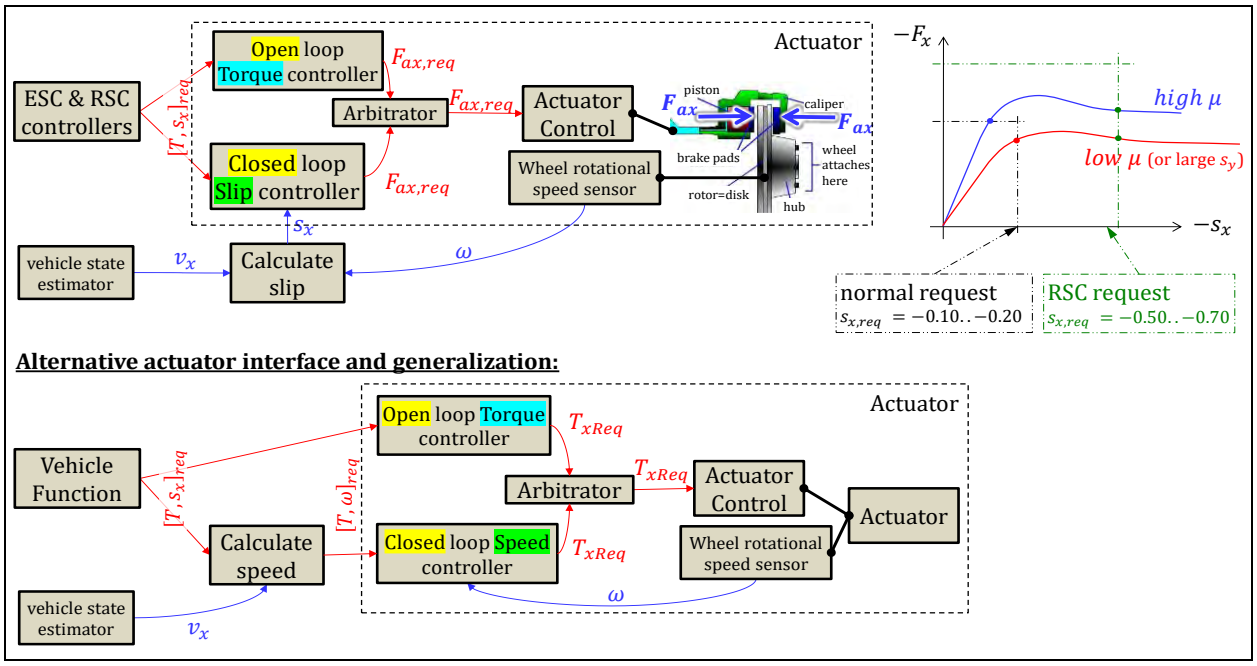


Figure 4-96: Individual wheel control by friction brakes for ESC-type functions.

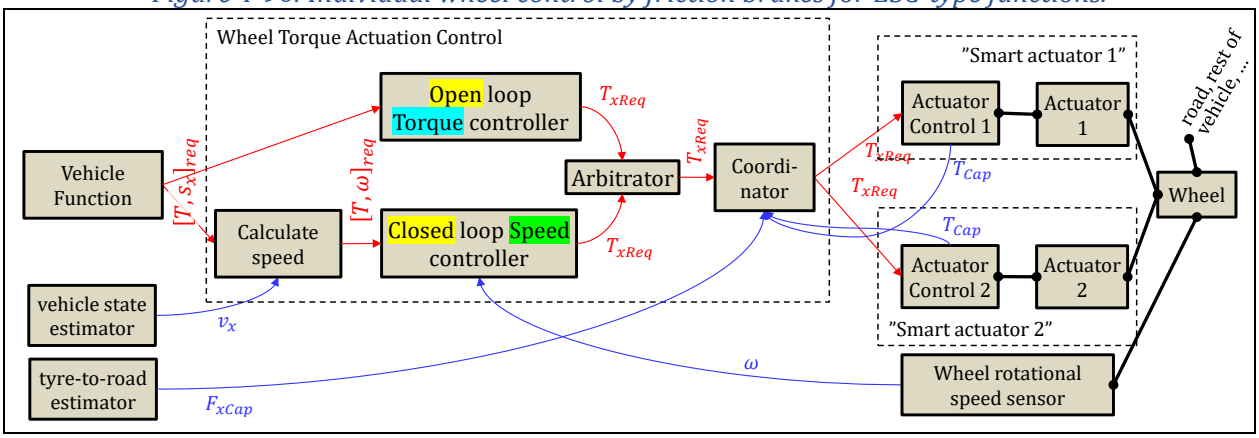


Figure 4-97: Alternative to Figure 4-96 when 2 wheel-torque actuators, propulsion, and friction brakes.

Expansion from "wheel-torque actuation control" to "axle or axle group F_x and M_z actuation control" can be motivated if propulsion is not wheel-individual, e.g., via differential. See Figure 1-38 and Figure 1-39.

The dual-interface-request secures that we have a lateral force margin, but it also gives a larger "local slip stiffness" $C'_{ysx} > C'_{yFx}$, see 2.2.5.4.

4.6.2.2.5 Other Intervention than Individual Wheel Brakes

4.6.2.2.5.1 Balancing with Propulsion per Axle

For vehicles with controllable distribution of propulsion torque between the axles, ESC can intervene also with a request for redistribution of the propulsion torque. If over-steering, the propulsion should be redistributed towards front and opposite for understeering.

4.6.2.2.5.2 Torque Vectoring

For vehicles with controllable distribution of propulsion torque between the left and right, ESC can intervene also with a request for redistribution of the propulsion torque. If over-steering, the propulsion should be redistributed towards inner side and opposite for understeering.

4.6.2.2.5.3 Steering Guidance

For vehicles with controllable steering wheel torque, ESC can intervene also with a request for additional steering wheel torque. The most obvious function is to guide driver to open up steering

(counter-steer) when the vehicle over-steers. Such functions are on market in passenger cars today. Less obvious is how to guide the driver when vehicle is under-steering.

4.6.2.2.6 ESC using Environment Information / ESC for the Virtual Driver

A prognosis of the future development of ESC like functions is that environment sensors can be used to better predict what driver tries to do; presently ESC can only look at steering wheel angle.

Related to this, but still somewhat different, would be to utilize the automated driving development by utilizing that a "virtual driver" can be much better predicted than a "manual driver". So, a predictive ESC control is more possible.

4.6.2.3 Roll Stability Control, RSC *

Function definition: ***Roll Stability Control, RSC****, prohibits vehicle to roll-over due to lateral wheel forces from road friction. RSC uses friction brake as actuator.*

The purpose of RSC is to avoid un-tripped roll-overs. The actuator used is the friction brake system. When roll-over risk is detected, via lateral acceleration sensor (or in some advanced RSC implementations, also roll velocity sensor), the outer front wheel is braked. RSC can brake to deep slip levels (typically -70%..-50%) since losing side grip on front axle is positive in this situation. To lock the wheels (slip= $-\infty$) is undesired since wheel rotational inertia makes it difficult to quickly regain lateral grip when needed after the intervention.

On heavy vehicles, RSC intervenes earlier and similar to function described in 4.6.2.2.3 Over-Speed Control. Future RSC might be developed towards also using steering, and potentially counteract also some tripped roll-overs.

4.6.2.4 Lane Keeping Aid, LKA *

Function definition: ***Lane Keeping Aid*** *steers the vehicle without driver having to steer, when probability for lane departure is predicted as high. It is normally actuated as an additional steering wheel torque. Conceptually, it can also be actuated as a steering wheel angle offset.*

Lane Keeping Aid (or *Lane Departure Prevention*) has the purpose to guide the driver to keep in the lane. Given the lane position from a camera, the function detects whether vehicle tends to leave the lane. If so, the function requests a mild steering wheel torque (typically 1..2 Nm) in appropriate direction. Driver can easily overcome the additional torque. Function does not intervene if too low speed or turning indicator (blinker) is used. There are different concepts whether the function continuously should aim at keeping the vehicle in centre of lane, or just intervene when close to leaving the lane, see Figure 4-98.

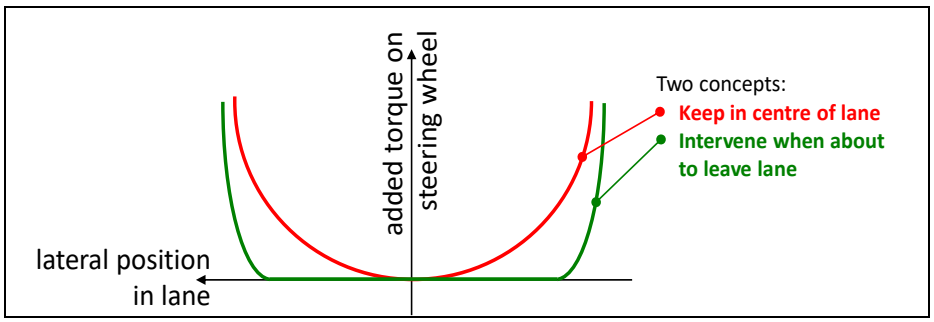


Figure 4-98: Two concepts for Lane Keeping Aid.

4.6.2.5 Lateral Collision Avoidance/Automatic Emergency Steering, LCA/AES *

Function definition: ***Lateral Collision Avoidance/Automatic Emergency Steering,*** *supports the driver when he has to do late lateral obstacle avoidance, when probability for forward collision is predicted as high.*

There are systems on the market for Automatic Emergency Brake, see 3.5. These do Longitudinal Collision Avoidance. Automotive industry also aims at AES/LCA functions, which would automatically steer away laterally from an obstacle ahead of subject vehicle. The market introduction is cautious, since many things can go wrong with such functions. However, the first systems on market triggers only if driver initiates steering. Another would be to trigger on a first collision impact, see Reference (Yang, 2013), when driver is less capable of steering by himself. A future similar situation could be AES/LCA functions active only during automated driving, when driver also is less likely to steer.

4.6.2.6 Automated Driving (AD)

Combining longitudinal control (such as ACC, in 3.5.2.3) with a lateral control (such as LKA, see 4.6.2.2) results in functionality which clearly approaches automated driving (AD). AD is a very general expression but are sometimes interpreted as more specific, but specific in different ways depending on context. In a way, AD is already reality since there are vehicles on the road which can have ACC and LKA active at the same time. On the other hand, AD can be seen as very futuristic, since completely driverless vehicle which can operate in all situations is far from mass-production.

It is not obvious if AD will mean higher or lower requirements on vehicle dynamics. Some (of many more!) examples of changes, relevant for vehicle dynamics are:

- The vehicle control can better **predict** the next few seconds of a virtual driver (AD algorithms) than of a (human) driver. This can facilitate loss-of-grip functions, such as ABS & ESC.
- There will be new requirements on vehicle response on **requests from the virtual driver**, in parallel with requirements on response on human drivers pedal and steering wheel operation.
- There will be new requirements on vehicle **relative** motion, relative to surrounding road and traffic, such as lane edges and other road users. These will be in synergy or conflict to corresponding requirement for absolute motion response.
- The motion actuation will have to be more **redundant**, since driver is less likely to take back control quickly. Emergency functions to reach safe stop will need to work with partly faulty sensors and actuators. Failures needs to be designed according to (ISO 26262, 2011-2012)
- The **maximum speed** for which the vehicle is designed can possibly be lower, since reduced transport efficiency could be accepted if driver can do something else or is not needed at all.
- Estimation of Road friction, Controlling to Safe stop, Self-Diagnose, etc.

5 VERTICAL DYNAMICS

5.1 Introduction

The vertical dynamics are needed since vehicles are operated on real roads, and real roads are not perfectly smooth. Also, vehicle can be operated off-road, where the ground unevenness is even larger.

The irregularities of the road can be categorized. A **transient** disturbance, such as a pothole or bump, can be represented as a step input or ramp. Undulating surfaces like grooves across the road may be a type of sinusoidal or other **stationary oscillating** (or periodic) input. More natural input like the random surface texture of the road may be a **random** noise distribution. In all cases, the same mechanical system must react when the vehicle travels over the road at varying speeds including doing manoeuvres in longitudinal and lateral directions.

The chapter is organised around the 3 complete vehicle functions: 5.5.1 Ride Comfort *, 5.5.2 Fatigue Life *, and 5.5.3 Road Grip *. It is, to a larger extent than Chapters 3 and 4, organised with mathematical theory first followed by the vehicle functions. In Figure 5-1 shows the 3 main functions. It explains the importance of the vehicle's dynamic structure. The vehicle's dynamic structure calls for a pretty extensive theory base, described mainly in 5.2.

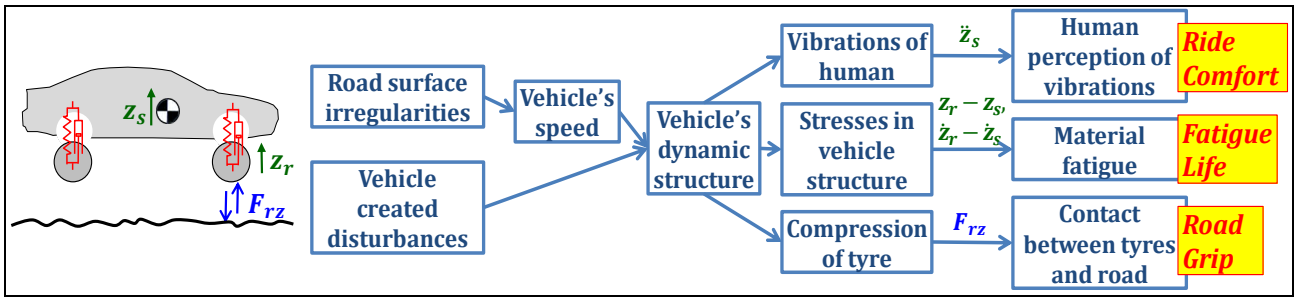


Figure 5-1: Different types of knowledge and functions in the area of vertical vehicle dynamics, organised around the vehicle's dynamic structure.

Models in this chapter focus the disturbance from vertical irregularities from the road, i.e. only the vertical forces on the tyre from the road and **not** the forces in road plane. This enables the use of simple models which are independent of exact wheel and axle suspension, such as pivot axes and roll centres. Only the wheel stiffness rate (effective stiffness) and wheel damping rate (effective damping), see Figure 2-90, influence. This has the benefit that the chapter becomes relatively independent of previous chapters, but it has the drawback that the presented models are **not** really suitable for studies of steep road irregularities (which have longitudinal components) and sudden changes in wheel torque or tyre side forces. Also, noise ($>\approx 25Hz$) is not covered in this book.

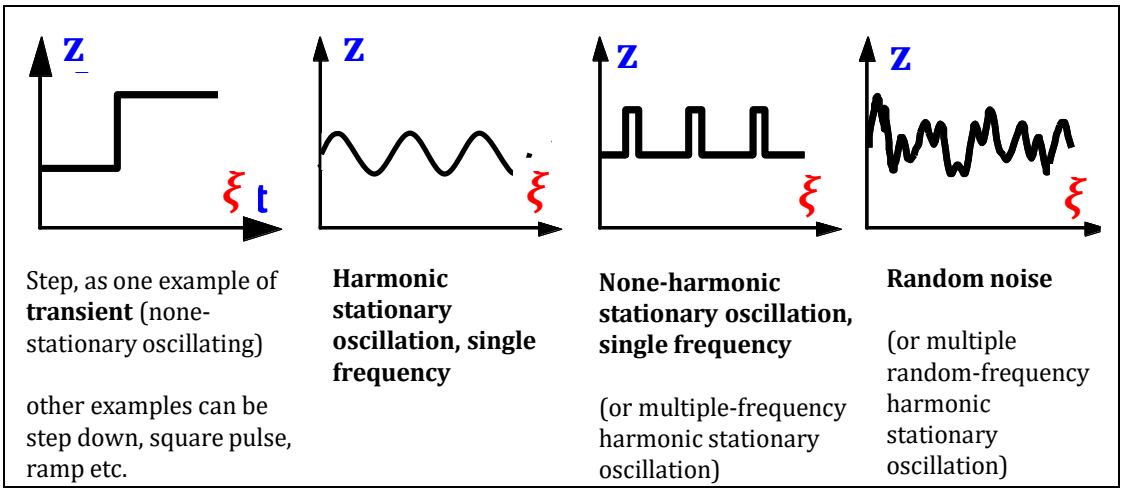
5.1.1 References for this Chapter

- 2.3 Suspension and *"Chapter 21 Suspension Systems"* in Ref (Ploechl, 2013)
- *"Chapter 29 Ride Comfort and Road Holding"* in Ref (Ploechl, 2013)

5.2 Stationary Oscillations Theory

Many vehicle functions in this chapter will be studied using stationary oscillations (cyclic repeating), as opposed to transiently varying. An example of transiently varying quantity is a single step function or single square pulse. A stationary oscillation can be as a sum of several harmonic terms, a multiple frequency harmonic stationary oscillation. The special case with only one frequency is called a single frequency harmonic stationary oscillation. See Figure 5-2 and Equation [5.1].

Harmonic stationary oscillations:
Single frequency : $z(\xi) = \hat{z} \cdot \cos(\omega \cdot \xi + \varphi)$;
Multiple frequencies : $z(\xi) = \sum_{i=1}^{N} \hat{z}_i \cdot \cos(\omega_i \cdot \xi + \varphi_i)$;
where ξ *is the independent variable.* [5.1]



Step, as one example of **transient** (none-stationary oscillating)

other examples can be step down, square pulse, ramp etc.

Harmonic stationary oscillation, single frequency

None-harmonic stationary oscillation, single frequency

(or multiple-frequency harmonic stationary oscillation)

Random noise

(or multiple random-frequency harmonic stationary oscillation)

Figure 5-2: Different types of variables, both transient and stationary oscillating. The independent variable ξ can, typically, be either time or distance.

The most intuitive is probably to think of time as the independent variable, i.e. that the variation takes place as function of time and that $\xi = t$ in Equation [5.1]. However, for one specific road, the vertical displacement varies with longitudinal position, rather than with time. This is why we can either do analysis in **time domain** ($\xi = t$) and **space domain** ($\xi = x$).

Since the same oscillation can be described either as a function of ξ ($z = z(\xi)$) or as a function of frequency ω ($\hat{z} = \hat{z}(\omega)$), we can do analysis either in the **independent variable domain** (ξ) or in **frequency domain** (ω).

The four combinations of domains are shown in Figure 5-3.

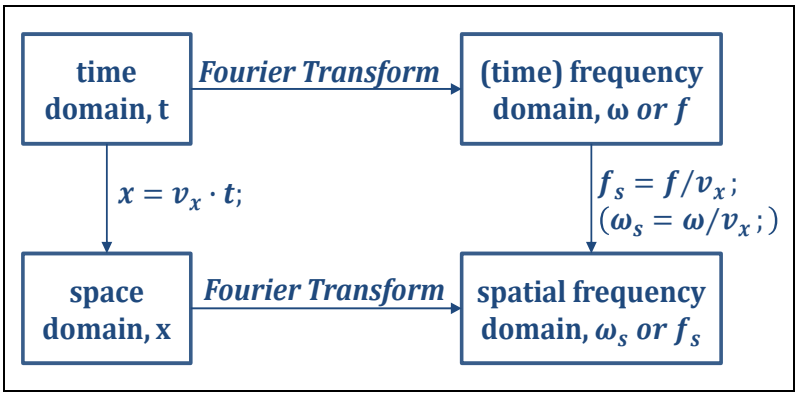


Figure 5-3: Four domains and transformations between them.

Time and space domains are treated in 5.2.1 and 5.2.2. In addition to the domains, we also need to differ between discrete and continuous representations in both domains.

5.2.1 Time as Independent Variable

With time as independent variable, the frequency has the meaning of "how often per time". Even so, there are two relevant ways to measure frequency: angular (time) frequency, and (time) frequency.

$$\omega = 2 \cdot \pi \cdot f;$$
$$where \quad \omega\,[rad/s] = angular\ (time)\ frequency;$$
$$and \quad f\,[1/s = oscillations/s] = (time)\ frequency; \qquad [5.2]$$

The time for one oscillation is called the period time. It is denoted T:

$$T = 1/f = 2 \cdot \pi/\omega\,; \qquad [5.3]$$

5.2.1.1 Mean Square (MS) and Root Mean Square (RMS)

For a variable, z, we can define MS and RMS values as follows:

$$Variable: \quad z = z(t);$$
$$MeanSquare: \quad MS(z) = \frac{\int_0^{t_{end}} z^2 \cdot dt}{t_{end}};$$
$$RootMeanSquare: \quad RMS(z) = \sqrt{\frac{\int_0^{t_{end}} z^2 \cdot dt}{t_{end}}}; \qquad [5.4]$$

If the variable is written as a single frequency harmonic stationary oscillation:

$$Variable: \quad z = \hat{z} \cdot \cos(\omega \cdot t + \varphi)\,;$$
$$MeanSquare: \quad MS(z) = \frac{\int_0^{t_{end}} z^2 \cdot dt}{t_{end}} = \frac{\int_0^{t_{end}} (\hat{z} \cdot \cos(\omega \cdot t + \varphi))^2 \cdot dt}{t_{end}} =$$
$$= \frac{\hat{z}^2 \cdot \left[\frac{t}{2} + \frac{\sin(2 \cdot \omega \cdot t)}{4 \cdot \omega}\right]_{t=0}^{t=t_{end}}}{t_{end}} = \frac{\hat{z}^2 \cdot \left(\frac{t_{end}}{2} + \frac{\sin(2 \cdot \omega \cdot t_{end})}{4 \cdot \omega}\right)}{t_{end}} \xrightarrow[t_{end} \to \infty]{} \frac{\hat{z}^2}{2};$$
$$RootMeanSquare: \quad RMS(z) = \sqrt{\frac{\int_0^{t_{end}} z^2 \cdot dt}{t_{end}}} = \sqrt{MS(z)} = \frac{|\hat{z}|}{\sqrt{2}}; \qquad [5.5]$$

If the variable is written as a multiple frequency harmonic stationary oscillation:

$$Variable: \quad z = \sum_{i=1}^{N} z_i = \sum_{i=1}^{N} \hat{z}_i \cdot \cos(\omega_i \cdot t + \varphi_i)\,;$$
$$MeanSquare: \quad MS(z) = \frac{\int_0^{t_{end}} z^2 \cdot dt}{t_{end}} = \frac{\int_0^{t_{end}} \left(\sum_{i=1}^{N} z_i\right)^2 \cdot dt}{t_{end}} =$$
$$= \frac{\int_0^{t_{end}} \left(\sum_{i=1}^{N} \hat{z}_i \cdot \cos(\omega_i \cdot t + \varphi_i)\right)^2 \cdot dt}{t_{end}} \xrightarrow[t_{end} \to \infty]{}$$
$$\xrightarrow[t_{end} \to \infty]{} \frac{\int_0^{t_{end}} \sum_{i=1}^{N} \hat{z}_i{}^2 \cdot (\cos(\omega_i \cdot t + \varphi_i))^2 \cdot dt}{t_{end}} = \sum_{i=1}^{N} MS(z_i) = \sum_{i=1}^{N} \frac{\hat{z}_i{}^2}{2};$$
$$RootMeanSquare: \quad RMS(z) = \sqrt{MS(z)} = \sqrt{\sum_{i=1}^{N} \frac{\hat{z}_i{}^2}{2}} = \sqrt{\sum_{i=1}^{N} MS(z_i)} = \sqrt{\sum_{i=1}^{N} \left(RMS(z_i)\right)^2}; \qquad [5.6]$$

5.2.1.2 Power Spectral Density and Frequency Bands

So far, the frequency has been a discrete number of frequencies, $\omega_1, \omega_2, \cdots, \omega_N$. There are reasons to treat the frequency as a continuous variable instead. The discrete amplitudes, $\hat{z}_1, \hat{z}_2, \cdots, \hat{z}_N$, should then

be thought of as integrals of a "continuous amplitude curve", $\hat{z}_c$, where the integration is done over a small frequency interval, centred around a mid-frequency, ω_i:

$$\hat{z}_i = \int_{\omega=\frac{\omega_{i-1}+\omega_i}{2}}^{\frac{\omega_i+\omega_{i+1}}{2}} \hat{z}_c \cdot d\omega = \hat{z}_c(\omega_i) \cdot \frac{\omega_{i+1}-\omega_{i-1}}{2} = \hat{z}_c(\omega_i) \cdot \Delta\omega_i; \Rightarrow \hat{z}_c(\omega_i) = \frac{\hat{z}_i}{\Delta\omega_i}; \quad [5.7]$$

We realize that the unit of $\hat{z}_c$ has to be same as for z, but per [rad/s]. So, if z is a displacement in [m], $\hat{z}_c$ has the unit [m/(rad/s)]. Now, $\hat{z}_c$ is a way to understand the concept of a spectral density. A similar value, but more used, is the Power Spectral Density, PSD (also called Mean Square Spectral Density).

$PSD(\omega)$ which is a continuous function, while $\hat{z}_i$ is a discrete function. That means that $PSD(\omega)$ is fully determined by a certain measured or calculated variable $z(t)$, while $\hat{z}_i$ depends on which discretization (which ω_i or which $\Delta\omega$) that is chosen.

$$PSD(z(t), \omega, \Delta\omega) = \frac{MS\big(filter(z(t), \omega, \Delta\omega)\big)}{\Delta\omega} = G(\omega); \quad [5.8]$$
$$where \text{ filter} is\ a\ bandpass\ filter\ centered\ around\ \omega\ and\ with\ band\ width\ \Delta\omega;$$

PSD can also be defined with band width in time frequency instead of angular frequency. Eq [5.8] is the same but replacing $\Delta\omega$ with Δf.

When the variable to study (z) is known and the band width is known, one often writes simply $PSD(\omega)$ or $G(\omega)$. G has the same unit as z^2, but per [rad/s] or per [oscillations/s]. So, if z is a displacement in [m], G has the unit $[m^2/(rad/s)]$ or $[m^2/(1/s) = m^2 \cdot s]$.

RMS is square root of the area under the PSD curve:

$$RMS(z) = \sqrt{\sum_{i=1}^{N} MS(z_i)} = \sqrt{\sum_{i=1}^{N} G(\omega_i) \cdot \Delta\omega_i} = \sqrt{\int_{\omega=0}^{\infty} G(\omega) \cdot d\omega}; \quad [5.9]$$

5.2.1.2.1 Differentiation of PSD

Knowing the PSD of a variable, we can easily obtain the PSD for the derivative of the same variable:

$$G_{\dot{z}}(\omega) = \omega^2 \cdot G_z(\omega); \quad [5.10]$$

5.2.1.3 Transfer Function

In a minimum model for vertical dynamics there is at least one excitation, often road vertical displacement, z_r, and one response, e.g. vertical displacement of sprung mass (=vehicle body), z_s. A Transfer function, $H = H(j \cdot \omega)$, is the function which we can use to find the response, given the excitation:

$$Z_s(\omega) = H(\omega) \cdot Z_r(\omega); \quad \Leftrightarrow \quad \mathcal{F}\big(z_s(t)\big) = H(\omega) \cdot \mathcal{F}\big(z_r(t)\big); \quad [5.11]$$
$$where\ \mathcal{F}\ is\ the\ Fourier\ operator: Z(\omega) = \mathcal{F}\big(z(t)\big) = \int_0^{\infty} e^{-j\cdot\omega\cdot t} \cdot z(t) \cdot dt;$$

H is complex, with magnitude, $|H| = \sqrt{(\mathrm{Re}(H))^2 + (\mathrm{Im}(H))^2}$, and phase, $\arg\big(H(\omega)\big) = \arctan(\mathrm{Im}(H)/\mathrm{Re}(H))$.

$$Amplitude:\ \hat{z}_s(\omega) = |H(\omega)| \cdot \hat{z}_r(\omega);$$
$$Phase:\ \varphi_s(\omega) - \varphi_r(\omega) = \arg\big(H(\omega)\big);$$
$$where\ z = \sum_{i=1}^{N} \hat{z}(\omega_i) \cdot \cos(\omega_i \cdot t + \varphi_i);$$

[5.12]

Since there can be different excitations and responses in a system, there are several transfer functions. To distinguish between those, a subscripting of H is often used: $H_{excitation \to response}$, which would be $H_{z_r \to z_s} = H_{road\ displacement \to sprung\ mass\ displacement}$ in the example above. Other examples of relevant transfer functions in vertical vehicle dynamics are:

- $H_{road\ displacement \to sprung\ mass\ acceleration}$ $[(m/s^2)/m]$, see 5.5
- $H_{road\ displacement \to suspension\ deformation}$ $[m/m]$, see 5.5.2
- $H_{road\ displacement \to tyre\ force}$ $[N/m]$, see 5.5.2

When transfer function for one derivative is found, it is often easy to convert it to another:

$$H_{z_1 \to \dot{z}_2} = j \cdot \omega \cdot H_{z_1 \to z_2};$$
$$H_{z_1 \to \ddot{z}_2} = j \cdot \omega \cdot j \cdot \omega \cdot H_{z_1 \to z_2} = -\omega^2 \cdot H_{z_1 \to z_2};$$
$$H_{z_1 \to z_2 - z_3} = H_{z_1 \to z_2} - H_{z_1 \to z_3};$$

[5.13]

The usage of the transfer function is, primarily, to easily obtain the response from the excitation, as shown in Equation [5.12]. Also, the transfer function can operate on the Power Spectral Density, PSD=G, as shown in the following:

$$G_{z_s}(\omega) = \frac{MS(z_s(t), \omega)}{\Delta\omega} = \frac{\big(\hat{z}_s(\omega)\big)^2/2}{\Delta\omega} = \frac{\big(|H(\omega)| \cdot \hat{z}_r(\omega)\big)^2/2}{\Delta\omega} =$$
$$= \big|H_{z_r \to z_s}(\omega)\big|^2 \cdot \frac{\big(\hat{z}_r(\omega)\big)^2/2}{\Delta\omega} = \big|H_{z_r \to z_s}(\omega)\big|^2 \cdot G_{z_r}(\omega);$$

[5.14]

Using Equation [5.9], we can then express $RMS(z_s)$ (sprung mass), from knowing $G_{z_r}(\omega)$ (road):

$$RMS(z_s) = \sqrt{\int_{\omega=0}^{\infty} \big|H_{z_r \to z_s}(\omega)\big|^2 \cdot G_{z_r}(\omega) \cdot d\omega};$$

[5.15]

5.2.2 Space as Independent Variable

All transformations, in this book, between time domain and space domain requires a constant longitudinal speed, v_x, so that:

$$x = v_x \cdot t + x_0;$$

[5.16]

The offset (x_0) is the phase (spatial) offset (x_0) is the correspondence to the phase angle (φ).

The corresponding formulas as given in Equations [5.2]..[5.13] can be formulated when changing to space domain, or spatial domain. It is generally a good idea to use a separate set of notations for the spatial domain. Hence the formulas are repeated with new notations, which is basically what will be done in present section.

In space domain, the frequency has the common understanding of "how often per **distance**". Even so, there are two relevant ways to measure frequency: spatial angular frequency and spatial frequency.

$$\Omega = 2 \cdot \pi \cdot f_s;$$
$$where\quad \Omega\ [rad/m] = angular\ spatial\ frequency;$$
$$and\quad f_s\ [1/m = oscillations/m] = spatial\ frequency;$$

[5.17]

The correspondence to period time is wavelength, denoted λ:

$$\lambda[m] = 1/f_s = 2 \cdot \pi/\Omega\,; \qquad [5.18]$$

Now, the basic assumption in Equation [5.16] and definitions of frequencies gives:

$$\omega = v_x \cdot \Omega; \quad and \;\; f = v_x \cdot f_s; \qquad [5.19]$$

The relation between the phase (spatial) offset (x_0) and the phase angle (φ) is:

$$x_0 = \frac{\lambda \cdot \varphi}{2 \cdot \pi}; \qquad [5.20]$$

5.2.2.1 Spatial Mean Square and Spatial Root Mean Square

In space domain, a variable, z, varies with distance, x. We can define Mean Square and Root Mean Square values also in space domain. We subscript these with s for space.

$$\begin{aligned} &Variable: && z && = z(x); \\ &MeanSquare: && MS_s(z) && = \frac{\int_0^{x_{end}} z^2 \cdot dx}{x_{end}}; \\ &RootMeanSquare: && RMS_s(z) && = \sqrt{\frac{\int_0^{x_{end}} z^2 \cdot dx}{x_{end}}}; \end{aligned} \qquad [5.21]$$

Because v_x is constant, the Mean Square and Root Mean Square will be the same in time and space domain. If the variable is written as a single frequency harmonic stationary oscillation, these values becomes as follows:

$$\begin{aligned} &Variable: && z && = \hat{z} \cdot \cos(\Omega \cdot x + x_0)\,; \\ &MeanSquare: && MS_s(z) && = \cdots = \frac{\hat{z}^2}{2} = MS(z); \\ &RootMeanSquare: && RMS_s(z) && = \cdots = \frac{|\hat{z}|}{\sqrt{2}} = RMS(z); \end{aligned} \qquad [5.22]$$

If the variable is written as a multiple frequency harmonic stationary oscillation:

$$\begin{aligned} &Variable: && z && = \sum_{i=1}^{N} z_i = \sum_{i=1}^{N} \hat{z}_i \cdot \cos(\Omega_i \cdot x + x_{0i})\,; \\ &MeanSquare: && MS_s(z) && = \sum_{i=1}^{N} \frac{\hat{z}_i{}^2}{2} = MS(z); \\ &RootMeanSquare: && RMS_s(z) && = \sqrt{MS_s(z)} = \sqrt{\sum_{i=1}^{N} \left(RMS(z_i)\right)^2} = RMS(z); \end{aligned} \qquad [5.23]$$

5.2.2.2 Spatial Power Spectral Density and Frequency Bands

A correspondence to Power Spectral Density in space domain is denoted PSD_s in the following:

$$PSD_s(z(x), \Omega, \Delta\lambda) = \frac{MS(filter(z(x), \Omega, \Delta\lambda))}{\Delta\lambda} = \Phi(\Omega); \qquad [5.24]$$

where "filter" is a band pass filter centred around ω and with band width Δf;

When the variable to study z is known and the band width is known, one often writes simply $PSD_s(\Omega)$ or $\Phi(\Omega)$. The Φ has the same unit as z^2, but per [rad/m] or per [oscillations/m]. So, if z is a displacement in [m], Φ has the unit $[\frac{m^2}{rad/m} = \frac{m^3}{rad}]$ or $[\frac{m^2}{1/m} = m^3]$.

5.3 Road Models

In general, a road model can include ground properties such as coefficient of friction, damping/elasticity of ground and vertical position. The independent variable is either one, along an assumed path, or generally two, x and y in ground plane. In vertical dynamics in this book, we only assume vertical displacement as function of a path. We use x as independent variable along the path, meaning that the road model is: $z_r = z_r(x)$. The function $z_r(x)$ can be either of the types in Figure 5-2. We will concentrate on stationary oscillations, which by Fourier series, always can be expressed as multiple (spatial) frequency harmonic stationary oscillation. This can be specialized to either single (spatial) frequency or random (spatial) frequency. Hence, the general form of the road model is multiple (spatial) frequencies:

$$z_r = z_r(x) = \sum_{i=1}^{N} \hat{z}_i \cdot \cos(\Omega_i \cdot x + x_{0i}) \; ; \qquad [5.25]$$

5.3.1 One Frequency Road Model

For certain roads, such as roads built with concrete blocks, a single (spatial) frequency can be a relevant approximation to study a certain single wavelength. Also, the single (spatial) frequency road model is good for learning the different concepts. A single (spatial) frequency model is the same as a single wave length model ($\lambda = 2 \cdot \pi/\Omega$, from Equation [5.17]) and it can be described as:

$$z_r = z_r(x) = \hat{z} \cdot \cos(\Omega \cdot x + x_0) \; ; \qquad [5.26]$$

5.3.2 Multiple Frequency Road Models

Based on the general format in Equation [5.25], we will now specialise to models for different road qualities. In Figure 5-4, there are 4 types of road types defined. The 3 upper ones of those are also defined as PSD-plots in Figure 5-5. The mathematical formula is given in Equation [5.27] and numerical parameter values are given in Equation [5.28].

$$\Phi = \Phi(\Omega) = \Phi_0 \cdot \left(\frac{\Omega}{\Omega_0}\right)^{-w} = \frac{MS_s(z_r, \Omega)}{\Delta\Omega}; \qquad [5.27]$$

$where \;\; \Phi_0 \;=\; \text{road severity} \left[\frac{\text{m}^2}{\text{rad/m}}\right];$

$\text{w} \;=\; \text{road waviness [1]};$

$\Omega \;=\; \text{spatial angular frequency [rad/m]};$

$\Omega_0 \;=\; 1 \text{ [rad/m]};$

Typical values are:

Very good road: $\Phi_0 = 1 \cdot 10^{-6} \left[\frac{\mathrm{m}^2}{\mathrm{rad/m}}\right]$;

Bad road : $\Phi_0 = 10 \cdot 10^{-6} \left[\frac{\mathrm{m}^2}{\mathrm{rad/m}}\right]$;

Very bad road : $\Phi_0 = 100 \cdot 10^{-6} \left[\frac{\mathrm{m}^2}{\mathrm{rad/m}}\right]$;

The waviness is normally in the range of $w = 2..3$ [1],
where smooth roads have larger waviness than bad roads.

[5.28]

The decreasing amplitude for higher (spatial) frequencies (i.e. for smaller wavelength) can be explained by that height variation over a short distance requires large gradients. On micro-level, in the granular level in the asphalt, there can of course be steep slopes on each small stone in the asphalt. These are of less interest in vehicle vertical dynamics, since the wheel dimensions filter out wave length << tyre contact length, see Figure 2-85. Reference (ISO 8608) uses road waviness, w=2 for all roads. Figure 5-5 is based on measurements on real roads, which shows that waviness actually varies with road severity, Φ_0. A certain road can be described with:

- $\Omega_1, \cdots, \Omega_N$
- $\hat{z}_1, \cdots, \hat{z}_N$
- $x_{01}, \cdots, x_{0N}$

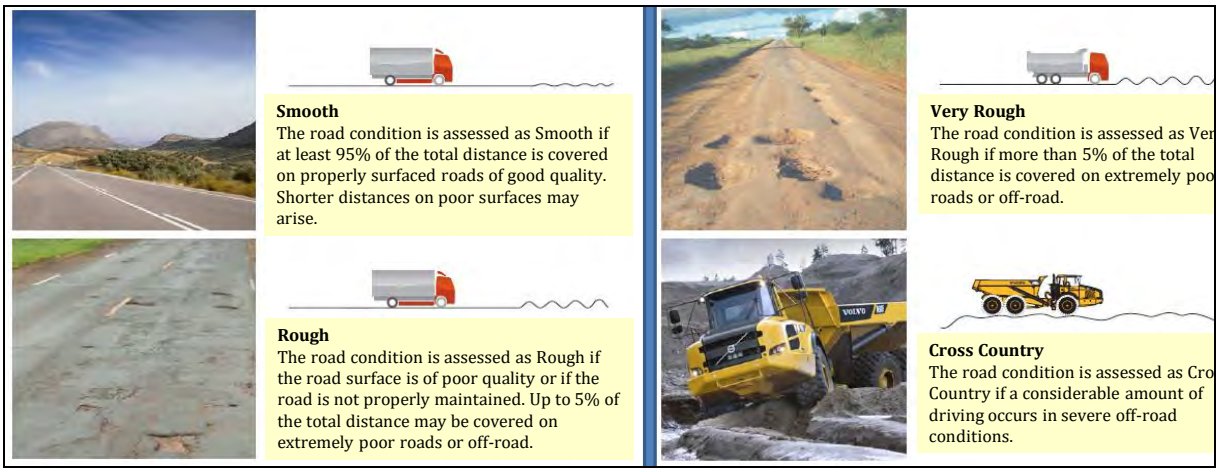


Figure 5-4: Four typical road types. From (AB Volvo, 2011).

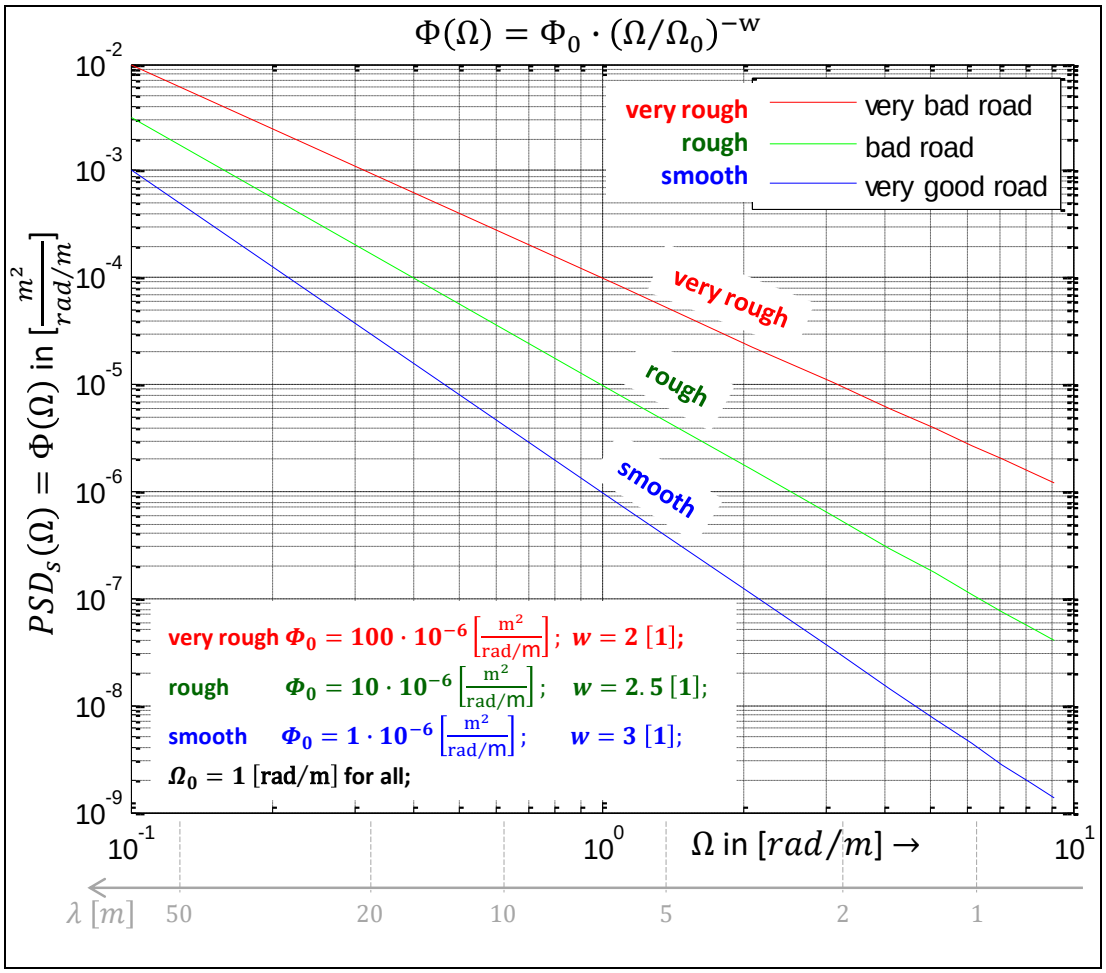


Figure 5-5: PSD spectra for the three typical roads in Figure 5-4.

Number of frequency components, N, to select is a matter of accuracy or experience. The offsets, $x_{01}, \cdots, x_{0N}$, can often be assumed to be zero. If phase is to be studied, as in Figure 5-5, a random generation of offsets is suitable. See also Reference (ISO 8608).

There is also a well-established measure of a road unevenness which is called *International Roughness Index* (IRI). It is defined by calculating the vertical motion of the vehicle body of a specified quarter car model (see 5.4) with parameters for a typical passenger car, driving in 80 km/h. Here is the formula:

$$IRI = \frac{\int |v_z| \cdot dt}{\int v_x \cdot dt}; where\ v_x = 80\ km/h;$$

We can generate $z_r(x)$ curves for the 3 road types in Figure 5-5 as shown in Figure 5-6. To generate those plots, we have assumed different number of harmonic components (N in Equation [5.25]) and also randomly generate the phase for each component (each x_{0i}).

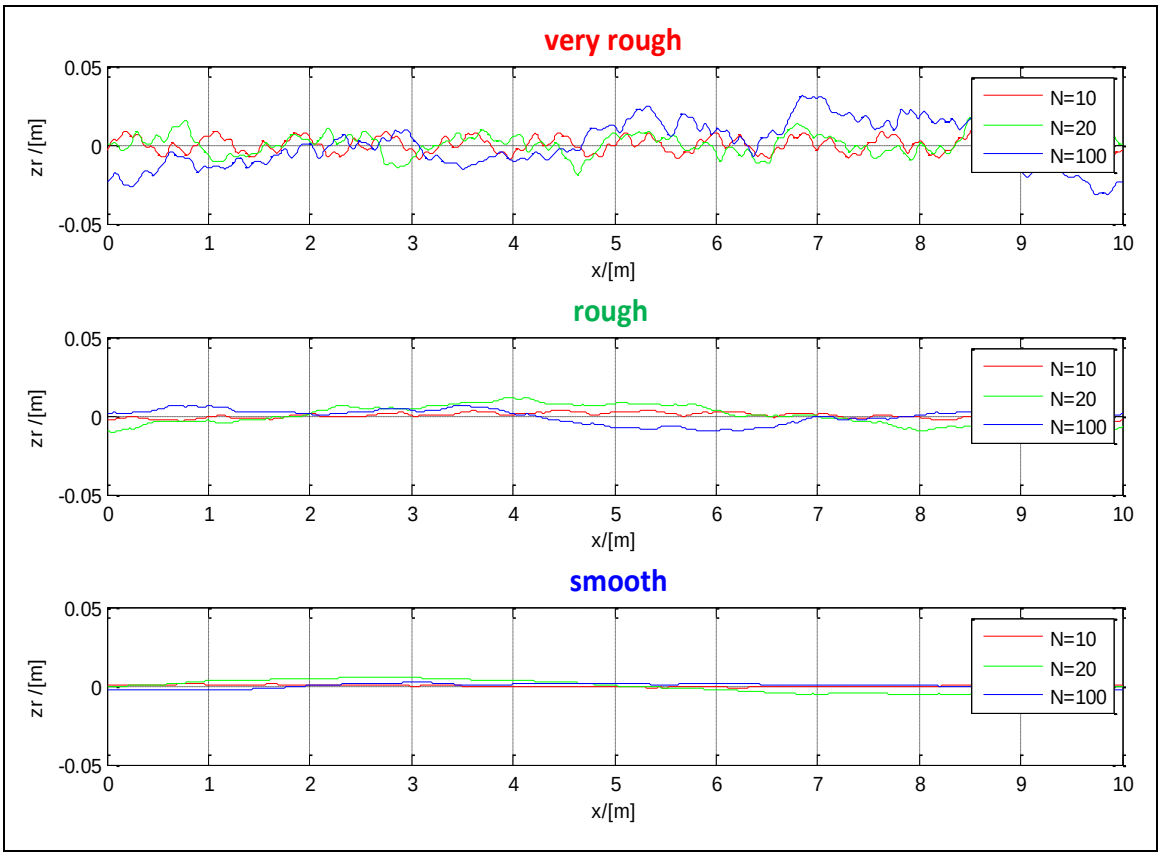


Figure 5-6: Road profiles, $z_r(x)$, for the three typical roads in Figure 5-4.

5.3.2.1 Transfer Function from Road Spectrum in Spatial Domain to System Response in Time Domain

Since we assume constant longitudinal velocity, v_x, the road spectrum can be transformed to the time-frequency domain:

$$G_{z_r}(\omega) = \frac{MS(z_r,\omega)}{\Delta\omega} = \{use: \omega = v_x \cdot \Omega\} = \frac{MS_s(z_r,\Omega)}{v_x \cdot \Delta\Omega} =$$

$$= \left\{use: \Phi_0 \cdot \left(\frac{\Omega}{\Omega_0}\right)^{-w} = \frac{MS_s(z_r,\Omega)}{\Delta\Omega}\right\} = \frac{\Phi_0 \cdot \left(\frac{\Omega}{\Omega_0}\right)^{-w}}{v_x} =$$

$$= \frac{\Phi_0 \cdot \Omega^{-w}}{{\Omega_0}^{-w} \cdot v_x} = \frac{\Phi_0}{{\Omega_0}^{-w}} \cdot \frac{\left(\frac{\omega}{v_x}\right)^{-w}}{v_x} = \frac{\Phi_0}{{\Omega_0}^{-w}} \cdot {v_x}^{w-1} \cdot \omega^{-w}; \quad [5.29]$$

Then, we can use Equation [5.14] to obtain the responsez_s:

$$G_{z_s}(\omega) = \left|H_{z_r \to z_s}(\omega)\right|^2 \cdot G_{z_r}(\omega) = \left|H_{z_r \to z_s}(\omega)\right|^2 \cdot \frac{\Phi_0}{{\Omega_0}^{-w}} \cdot {v_x}^{w-1} \cdot \omega^{-w}; \quad [5.30]$$

Then we can use Equation [5.9] to obtain the RMS of the response z_s:

$$RMS(z_s) = \sqrt{\sum_{i=1}^{N} G_{z_s}(\omega_i) \cdot \Delta\omega} = \sqrt{\frac{\Phi_0}{{\Omega_0}^{-w}} \cdot {v_x}^{w-1} \cdot \sum_{i=1}^{N} \left|H_{z_r \to z_s}(\omega_i)\right|^2 \cdot {\omega_i}^{-w} \cdot \Delta\omega}\,;$$

or

$$RMS(z_s) = \sqrt{\int_{\omega=0}^{\infty} G_{z_s}(\omega) \cdot d\omega} = \sqrt{\frac{\Phi_0}{{\Omega_0}^{-w}} \cdot {v_x}^{w-1} \cdot \int_{\omega=0}^{\infty} \left|H_{z_r \to z_s}(\omega)\right|^2 \cdot \omega^{-w} \cdot d\omega}\,;$$

[5.31]

5.4 1D vehicle models

"One-dimensional" (1D) refers to pure vertical motion. We can directly identify some weaknesses with this kind of models:

- These one-dimensional models do **not** filter away wave lengths smaller than (approximately) the wheel's radius, as real wheels do, see Figure 2-85. This filtering can be called *wheel radius filtering*.
- These one-dimensional models **do** filter away wave lengths around the vehicle wheelbase, which real vehicles do, see 5.7.2. This filtering can be called *wheelbase filtering*.
- These one-dimensional models **do** filter away unevenness in ground roll, i.e. when the ground has a height difference between left and right wheel. See 5.7.2.

This can be seen as that the whole vehicle mass, m, is modelled as suspended by the sum of all wheels' vertical forces, $F_z = F_{flz} + F_{frz} + F_{rlz} + F_{rrz}$. However, the model can sometimes be referred to as a "quarter-car-model". That is because one can see the model as a quarter of the vehicle mass, $m/4$, which is suspended by one of the wheel's vertical force, F_{ijz}. The exact physical interpolation of a quarter car is less obvious, since one can argue whether the fraction ¼ of the vehicle mass is the proper fraction or from which point of view it is proper. Using the fraction ¼ is as least debatable if the vehicle is completely symmetrical, both left/right and front/rear.

5.4.1 1D Model without Dynamic dofs

"Without dynamic degree of freedom" refers to that the (axle) suspension is modelled as ideally stiff. The model can be visualised as in Figure 5-7.

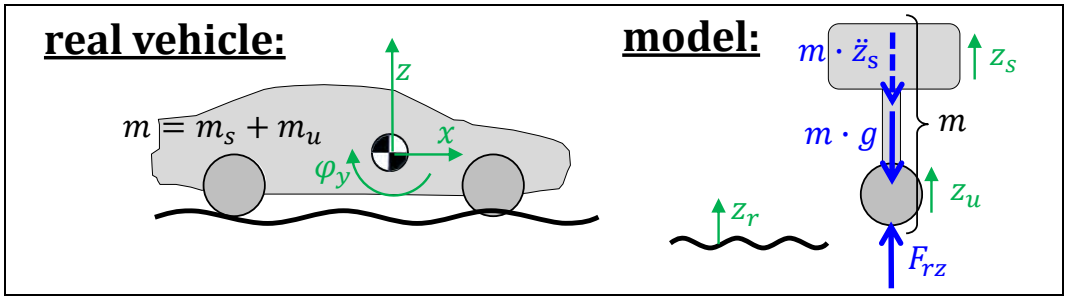


Figure 5-7: One-dimensional model without dynamic degree of freedom

The equations could be set up directly ($m \cdot \ddot{z}_s = F_{rz};\ \ and\ \ z_s = z_r(t);$), but the following equations gives a formalism which will be useful for the more complex models in 5.4.2 and 5.4.3.

$$\begin{aligned} &\textbf{\textit{Equilibrium}}: && m \cdot \ddot{z}_s + m \cdot g = F_{rz}; \\ &\textbf{\textit{Compatibility}}: && z_r = z_s;\ \ and\ \ z_r = z_u; \\ &\textbf{\textit{Excitation}}: && z_r = z_r(t); \end{aligned}$$

[5.32]

5.4.1.1 Response to a Single Frequency Excitation

Assume that the road has only one (spatial) frequency, i.e. one wavelength. Then the excitation is as follows:

$$\left.\begin{array}{c} z_r = z_r(x) = \hat{z}_r \cdot \cos(\Omega \cdot x + x_0) = \hat{z}_r \cdot \cos\left(\frac{2 \cdot \pi}{\lambda} \cdot x + x_0\right); \\ x = v_x \cdot t; \\ Assume\ x_0 = 0; \end{array}\right\} \Rightarrow$$

$$\Rightarrow z_r(t) = \hat{z}_r \cdot \cos\left(\frac{2 \cdot \pi \cdot v_x}{\lambda} \cdot t\right) = \hat{z}_r \cdot \cos(\omega \cdot t)\,; \Rightarrow$$

$$\Rightarrow \dot{z}_r(t) = -\frac{2 \cdot \pi \cdot v_x}{\lambda} \cdot \hat{z}_r \cdot \sin\left(\frac{2 \cdot \pi \cdot v_x}{\lambda} \cdot t\right) = -\omega \cdot \hat{z}_r \cdot \sin(\omega \cdot t)\,; \Rightarrow$$

$$\Rightarrow \ddot{z}_r(t) = -\left(\frac{2 \cdot \pi \cdot v_x}{\lambda}\right)^2 \cdot \hat{z}_r \cdot \cos\left(\frac{2 \cdot \pi \cdot v_x}{\lambda} \cdot t\right) = -\omega^2 \cdot \hat{z}_r \cdot \cos(\omega \cdot t)\,; \quad [5.33]$$

Insertion in the model in Equation [5.32] (with eliminated z_u) gives directly the solution:

$$\begin{cases} F_{rz}(t) = m \cdot g + \Delta F(t) = m \cdot g + \widehat{\Delta F}_{rz} \cdot \cos(\omega \cdot t)\,; \\ z_r(t) = z_s(t) = \hat{z}_r \cdot \cos(\omega \cdot t); \quad and \quad \ddot{z}_r(t) = \ddot{z}_s(t) = \hat{a} \cdot \cos(\omega \cdot t)\,; \end{cases} \quad [5.34]$$

$$where \quad \hat{F}_{rz} = -m \cdot \omega^2 \cdot \hat{z}_r; \quad and \quad \hat{a} = -\omega^2 \cdot \hat{z}_r;$$

We can identify the magnitude of the transfer functions H. The negative sign in Equation [5.35] means 180 degrees phase shift:

$$H_{z_r \to z_s} = \left\{H_{z_r \to z_s} = \frac{\mathcal{F}(z_s)}{\mathcal{F}(z_r)}\right\} = \{z_r(t) = z_s(t)\} = 1 + j \cdot 0;$$

$$H_{z_r \to z_r - z_s} = \left\{H_{z_r \to z_r - z_s} = H_{z_r \to z_s} - H_{z_s \to z_s} = H_{z_r \to z_s} - 1\right\} = 0 + j \cdot 0;$$

$$H_{z_r \to \ddot{z}_s} = \left\{H_{z_r \to \ddot{z}_s} = (j \cdot \omega)^2 \cdot H_{z_r \to z_s} = -\omega^2 \cdot H_{z_r \to z_s}\right\} = -\omega^2 + j \cdot 0;$$

$$H_{z_r \to \Delta F_{rz}} = \left\{H_{z_r \to \Delta F_{rz}} = m \cdot H_{z_r \to \ddot{z}_s}\right\} = -m \cdot \omega^2 + j \cdot 0; \quad [5.35]$$

The motivation to choose exactly those transfer functions is revealed later, in 5.5, 5.5.2 and 5.5.2. For now, we simply conclude that various transfer functions can be identified and plotted. The plots are found in Figure 5-8. Numerical values for m and λ are chosen.

5.4.1.1.1 Example Analysis

An example of how to use Figure 5-8 is: A certain road has amplitude of 1 cm ($\hat{z}_r = 0.01\ m$). The vehicle drives on it with a longitudinal velocity of 50 km/h ($v_x \approx 14\ m/s \mathrel{\widehat{=}} \approx 2.8 Hz$):

- $\left|H_{z_r \to \ddot{z}_s}(v_x)\right| \approx 305;\ \Rightarrow\ |\hat{a}| = 305 \cdot \hat{z}_r = 305 \cdot 0.01 = 3.05\ m/s^2;$. From this we can calculate $RMS(\ddot{z}_s) = |3.05|/\sqrt{2} \approx 2.16\ m/s^2$. The RMS value of acceleration will later be related to ride **comfort**, see 5.5.
- $\left|H_{z_r \to z_u - z_s}(v_x)\right| = 0;$ is the transfer function to deformation of suspension, which later will be related to **fatigue life**, see 5.5.2. The model in 5.4.1 is not good for measuring fatigue, since the $\hat{z}_u - \hat{z}_s$ is intrinsically zero because of no compliance between unsprung and sprung mass.
- $\left|H_{z_r \to \Delta F_{rz}}(v_x)\right| \approx 487000;\ \Rightarrow\ \widehat{\Delta F}_{rz} = 487000 \cdot \hat{z}_r = 487000 \cdot 0.01 = 4870\ N;$. If $\widehat{\Delta F}_{rz} > m \cdot g \approx 16000\ N$, the model is outside its validity region, because it would require pulling forces between tyre and road. If changing to $\hat{z}_r = 0.1\ m$, this limit is defined by $\left|H_{z_r \to \Delta F_{rz}}(v_x)\right| > \approx \frac{16000}{0.1} = 1.6 \cdot 10^5\ [N/m]$, which is used to examplify the validity limit in Figure 5-8; model becomes invalid for $v_x > \approx 300\ m/s$. The variation in tyre road contact force will be related to **road grip**, see 5.5.2.

The phases for the studied variables can be found in Equation [5.35]. With this model, the phases become constant and $\pm 90\ deg$.

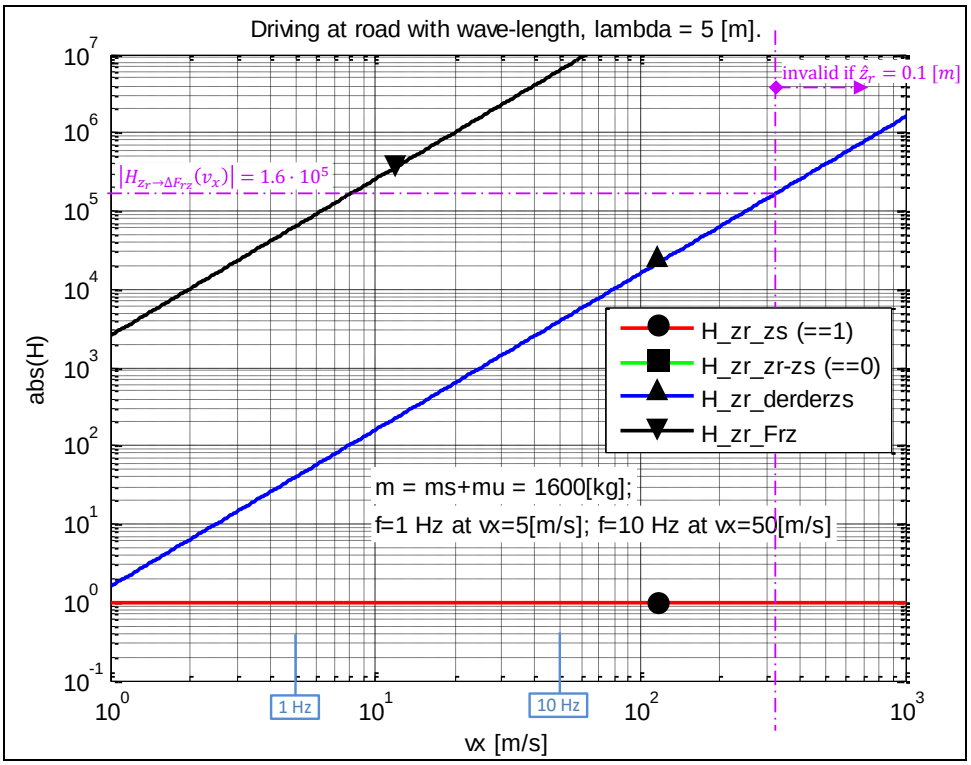


Figure 5-8: Transfer functions from model in Figure 5-7, excited with single frequencies.

5.4.1.2 Response to a Multiple Frequency Excitation

Using Eq [5.31], Eq [5.42] and values for road type "rough" in Figure 5-5, we can conclude:

$$RMS(z_s) = \sqrt{\frac{\Phi_0}{\Omega_0^{-w}} \cdot {v_x}^{w-1} \cdot \int_{\omega=0}^{\infty} \left|H_{z_r \to z_s}(\omega)\right|^2 \cdot \omega^{-w} \cdot d\omega} =$$

$$= \sqrt{\frac{10 \cdot 10^{-6}}{1} \cdot {v_x}^{2.5-1} \cdot \int_{\omega=0}^{\infty} \left|H_{z_r \to z_s}(\omega)\right|^2 \cdot \omega^{-2.5} \cdot d\omega}\,; \quad [5.36]$$

For now, we simply note that it is possible to calculate this (scalar) RMS value for each vehicle speed over the assumed road. In corresponding way, an RMS value can be calculated for any of the oscillating variables, such as $\ddot{z}_s$, $z_r - z_s$ and F_{rz}. We will come back to Equation [5.36] in 5.5.1.2.

5.4.2 1D Model with 1 Dynamic dof

"With 1 dynamic dof" refers to that the axle suspension is modelled as a linear spring and linear (viscous) damper in parallel. Compared to the model in 5.4.1, the tyre is still stiff, but the unsprung parts are assigned a mass m_u. The model can be visualised as in Figure 5-9.

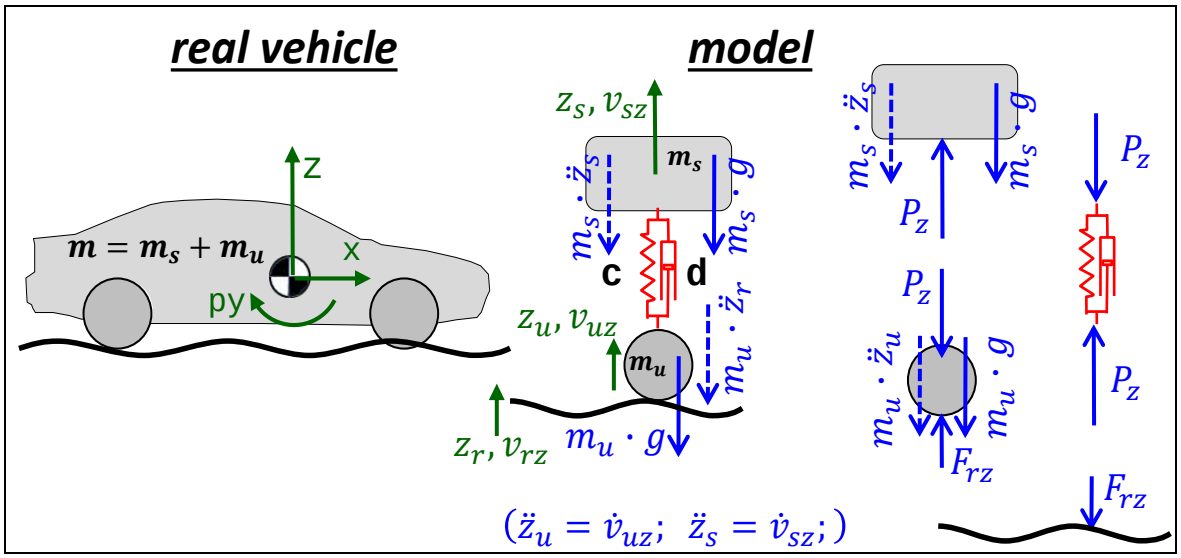


Figure 5-9: One-dimensional model with 1 dynamic degree of freedom.

The mathematical model becomes as follows:

$$\begin{aligned}
&\textbf{\textit{Equilibrium sprung mass}}: P_z - m_s \cdot \ddot{z}_s - m_s \cdot g = 0;\\
&\textbf{\textit{Equilibrium unsprung mass}}: F_{rz} - P_z - m_u \cdot \ddot{z}_r - m_u \cdot g = 0;\\
&\textbf{\textit{Constitution}}: P_z = \underbrace{c \cdot (z_u - z_s) + P_{zs0}}_{\text{linear spring } c} + d \cdot (\dot{z}_u - \dot{z}_s);\\
&\qquad \text{where } z_u \text{ and } z_s \text{ are measured from positions such that } P_{zs0} = m_s \cdot g;\\
&\textbf{\textit{Compatibility}}: z_u = z_r;\\
&\textbf{\textit{Excitation}}: z_r = z_r(t);
\end{aligned} \qquad [5.37]$$

The z_u and z_s can also be measured from other positions. However, the shown way is practical since the constant term in the total system of equations will vanish. The shown way can be physically understood as measuring from the positions for the system in static equilibrium, i.e. when the vehicle is stand-still or driving on a perfectly flat road.

5.4.2.1 Response to a Single Frequency Excitation

Eliminating P_z, z_u and z_r gives:

$$\begin{aligned}
&m_s \cdot \ddot{z}_s = c \cdot (z_r(t) - z_s) + d \cdot (\dot{z}_r(t) - \dot{z}_s);\\
&\underbrace{F_{rz} - (m_s + m_u) \cdot g}_{\Delta F_{rz}} = c \cdot (z_r(t) - z_s) + d \cdot (\dot{z}_r(t) - \dot{z}_s) + m_u \cdot \ddot{z}_r(t);
\end{aligned} \qquad [5.38]$$

Note that since we measure z_u and z_s from the static equilibrium, the static load, $m_s \cdot g$, disappears when constitution is inserted in equilibrium. The ΔF_{rz} denotes the variation from static contact force between road and tyre.

Assume that the road has only one (spatial) frequency, i.e. one wavelength. Then the excitation is as in Equation [5.26], in which we assume $x_0 = 0$. So, we can insert $z_r(t) = \hat{z}_r \cdot \cos(\omega \cdot t) \Rightarrow \dot{z}_r(t) = -\omega \cdot \hat{z}_r \cdot \sin(\omega \cdot t) \Rightarrow \ddot{z}_r(t) = -\omega^2 \cdot \hat{z}_r \cdot \cos(\omega \cdot t)$; in Equation [5.38] and solve it for $z_s(t)$ and $\Delta F_{rz}(t)$ with trigonometry or Fourier transform.

In 4.4.3.1.1, we applied Fourier transform on the linear explicit form model. To show a slightly other way, we do not rewrite to explicit form, but apply Fourier transform on Eq [5.38] directly:

$$\begin{aligned}
&m_s \cdot \left(-\omega^2 \cdot \mathcal{F}(z_s)\right) = c \cdot \left(\mathcal{F}(z_r) - \mathcal{F}(z_s)\right) + d \cdot j \cdot \omega \cdot \left(\mathcal{F}(z_r) - \mathcal{F}(z_s)\right);\\
&\mathcal{F}(\Delta F_{rz}) = c \cdot \left(\mathcal{F}(z_r) - \mathcal{F}(z_s)\right) + d \cdot j \cdot \omega \cdot \left(\mathcal{F}(z_r) - \mathcal{F}(z_s)\right) - m_u \cdot \omega^2 \cdot \mathcal{F}(z_r);
\end{aligned} \qquad [5.39]$$

From this, we can then solve for the transfer functions:

$$H_{z_r \to z_s} = \frac{\mathcal{F}(z_s)}{\mathcal{F}(z_r)} = \frac{c + j \cdot d \cdot \omega}{c + j \cdot d \cdot \omega - m_s \cdot \omega^2};$$

$$H_{z_r \to \Delta F_{rz}} = \frac{\mathcal{F}(\Delta F_{rz})}{\mathcal{F}(z_r)} = (c + j \cdot \omega \cdot d - m_u \cdot \omega^2) - (c + j \cdot \omega \cdot d) \cdot \frac{\mathcal{F}(z_s)}{\mathcal{F}(z_r)} =$$
$$= (c + j \cdot \omega \cdot d - m_u \cdot \omega^2) - (c + j \cdot \omega \cdot d) \cdot H_{z_r \to z_s};$$

[5.40]

We can elaborate further with the 1st equation in Eq [5.40]:

Amplitude: $\left|H_{z_r \to z_s}\right| = \frac{\hat{z}_s}{\hat{z}_r} = \left|\frac{c+j \cdot d \cdot \omega}{(c - m_s \cdot \omega^2) + j \cdot d \cdot \omega}\right| = \left\{\left|\frac{z_1}{z_2}\right| = \frac{|z_1|}{|z_2|}\right\} = \sqrt{\frac{c^2 + d^2 \cdot \omega^2}{(c - m_s \cdot \omega^2)^2 + d^2 \cdot \omega^2}};$

Phase: $\varphi_s(\omega) - \varphi_r(\omega) = \arg\left(\frac{c+j \cdot d \cdot \omega}{-m_s \cdot \omega^2 + c + j \cdot d \cdot \omega}\right) = \left\{\arg\left(\frac{z_1}{z_2}\right) = \arg(z_1) - \arg(z_2)\right\} =$

$\arg(c + j \cdot d \cdot \omega) - \arg(-m_s \cdot \omega^2 + c + j \cdot d \cdot \omega) = \cdots = \arctan\left(\frac{m_s \cdot d \cdot \omega^3}{c^2 - m_s \cdot c \cdot \omega^2 + d^2 \cdot \omega^2}\right);$

[5.41]

Equation [5.13] now allows us to get the magnitudes of the other transfer functions as well:
05/10/2026

$H_{z_r \to z_s}$ = from Equation [5.40];

$H_{z_r \to z_r - z_s} = H_{z_r \to z_r} - H_{z_r \to z_s} = 1 - H_{z_r \to z_s};$

$H_{z_r \to \ddot{z}_s} = -\omega^2 \cdot H_{z_r \to z_s};$

$$H_{z_r \to \Delta F_{rz}} = \left\{\begin{matrix} \Delta F_{rz} = m_u \cdot \ddot{z}_u + P_z = m_u \cdot \ddot{z}_r + P_z = \\ = m_u \cdot \ddot{z}_r + c \cdot (z_r - z_s) + d \cdot (\dot{z}_r - \dot{z}_s) \end{matrix}\right\} =$$
$$= m_u \cdot H_{z_r \to \ddot{z}_r} + c \cdot \left(H_{z_r \to z_r} - H_{z_r \to z_s}\right) + d \cdot \left(H_{z_r \to \dot{z}_r} - H_{z_r \to \dot{z}_s}\right) =$$
$$= m_u \cdot (j \cdot \omega)^2 + (c + j \cdot d \cdot \omega) \cdot \left(H_{z_r \to z_r} - H_{z_r \to z_s}\right) =$$
$$= -m_u \cdot \omega^2 + (c + j \cdot d \cdot \omega) \cdot \left(1 - H_{z_r \to z_s}\right);$$

[5.42]

The motivation to choose exactly those transfer functions is revealed later, in 5.5. The transfer function to acceleration, $\ddot{z}_s$, is of special interest for comfort:

$$\left|H_{z_r \to \ddot{z}_s}\right| = \omega^2 \cdot \sqrt{\frac{c^2 + d^2 \cdot \omega^2}{(c - m_s \cdot \omega^2)^2 + d^2 \cdot \omega^2}};$$

$$\left|H_{z_r \to \Delta F_{rz}}\right| = \sqrt{\begin{matrix} \left(c - m_u \cdot \omega^2 + \frac{(c^2 - (d \cdot \omega)^2) \cdot (c - m_s \cdot \omega^2) + 2 \cdot c \cdot (d \cdot \omega)^2}{(d \cdot \omega)^2 - (c - m_s \cdot \omega^2)^2}\right)^2 + \\ + \left(\left(1 + \frac{2 \cdot c \cdot (c - m_s \cdot \omega^2) - (c^2 - (d \cdot \omega)^2)}{(d \cdot \omega)^2 - (c - m_s \cdot \omega^2)^2}\right) \cdot d \cdot \omega\right)^2 \end{matrix}};$$

[5.43]

5.4.2.1.1 Example Analysis

The transfer functions in Equation [5.41] are plotted in Figure 5-10 and Figure 5-11. Numerical values for m and λ have been chosen. If we use Figure 5-10 as the example in 5.4.1:

- Ride comfort related: $\left|H_{z_r \to \ddot{z}_s}(v_x)\right| \approx 120; \Rightarrow |\hat{a}| = 120 \cdot \hat{z}_r = 120 \cdot 0.01 = 1.20\, m/s^2$;. From this we can calculate $RMS(\ddot{z}_s) = |1.20|/\sqrt{2} \approx 0.8485\, m/s^2$.
- Fatigue life related: $\left|H_{z_r \to z_r - z_s}(v_x)\right| \approx 1.11; \Rightarrow |\hat{z}_r - \hat{z}_s| = 1.11 \cdot \hat{z}_r = 1.11 \cdot 0.01 = 0.0111\, m = 1.11\, cm$;.
- Road grip related: $\left|H_{z_r \to \Delta F_{rz}}(v_x)\right| \approx 59795; \Rightarrow |\Delta F_{rz}| = 59795 \cdot \hat{z}_r = 59795 \cdot 0.01 = 598\, N$;.

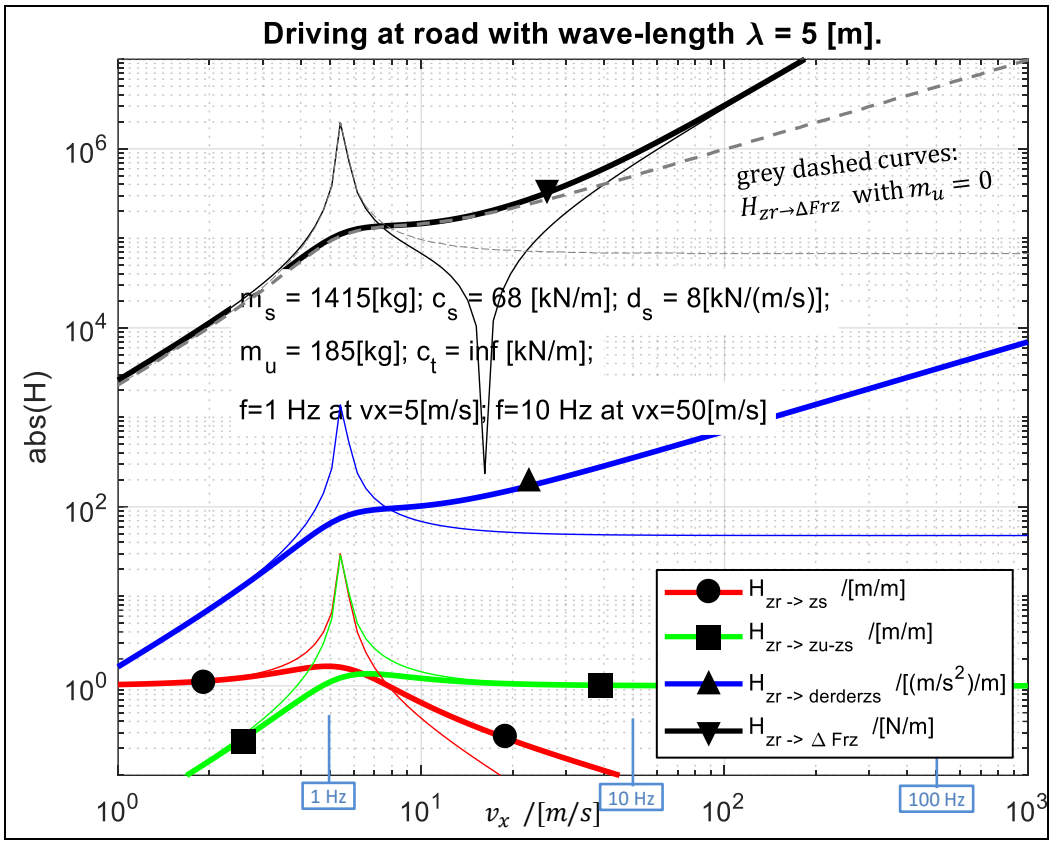


Figure 5-10: Transfer functions for amplitudes from model in Figure 5-9, excited with single frequencies. Thin lines are without damping. Notation: $H_{a\to b}$ is denoted H_a_b.

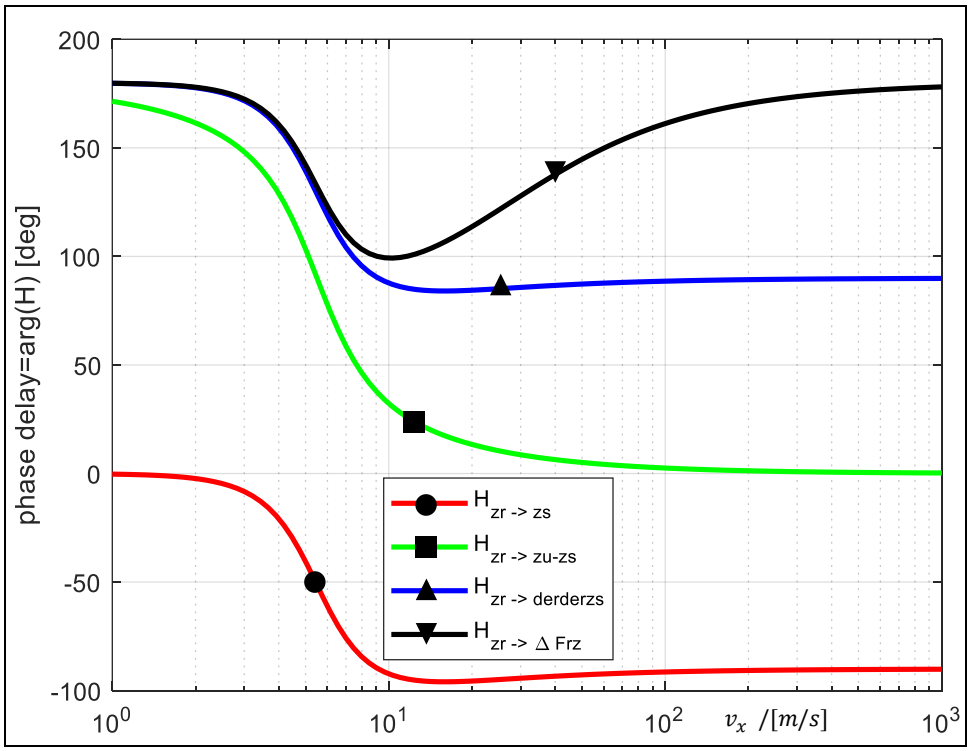


Figure 5-11: Transfer functions for phase delays from model in Figure 5-9, excited with single frequencies.

We compare these numbers with the corresponding numbers for the simpler model in 5.4.1. The comfort is better. The fatigue life and road grip have become more realistic.

Figure 5-10 also shows the curves for the undamped system (d=0). The highest peaks appear at approximately $v_x = 5..6$ m/s. This corresponds to the speed where the natural (=undamped) eigen frequency appears ($v_{x,crit} = \lambda \cdot f_{crit} = \lambda \cdot \omega_{crit}/(2 \cdot \pi) = \lambda \cdot \sqrt{c/m}/(2 \cdot \pi) \approx 5.5\ m/s$).

Figure 5-11 shows the phase angles for the different responses.

5.4.2.1.2 Solution with Trigonometry

The purpose with 5.4.2.1.2 is that it might help some readers to better/intuitively understand what the previously used, more efficient, Fourier transform method does.

One way to solve the mathematical model in Eq [5.37] is to assume a real solution, insert the assumption and find expressions for the coefficients in the assumption. Assume such solution (and that $x_0 = 0$ in Equation [5.26]): $z_r = \hat{z}_r \cdot \cos(\omega \cdot t)$. Insertion in 1st scalar equation in Eq [5.37] gives:

$$m \cdot \ddot{z}_s + d \cdot \dot{z}_s + c \cdot z_s = \hat{z}_r \cdot (c \cdot \cos(\omega \cdot t) - d \cdot \omega \cdot \sin(\omega \cdot t));$$

Assumed solution:

$z_s = \hat{z}_s \cdot \cos(\omega \cdot t - \varphi)\ ; \Rightarrow$
$\Rightarrow\ \{use\colon\ \cos(a-b) = \cos a \cdot \cos b + \sin a \cdot \sin b\} \Rightarrow$
$\Rightarrow\ z_s = \hat{z}_s \cdot [\cos(\omega \cdot t) \cdot \cos\varphi + \sin(\omega \cdot t) \cdot \sin\varphi];\ \Rightarrow$
$\Rightarrow\ \dot{z}_s = \hat{z}_s \cdot \omega \cdot [-\sin(\omega \cdot t) \cdot \cos\varphi + \cos(\omega \cdot t) \cdot \sin\varphi];\ \Rightarrow$
$\Rightarrow\ \ddot{z}_s = -\hat{z}_s \cdot \omega^2 \cdot [\cos(\omega \cdot t) \cdot \cos\varphi + \sin(\omega \cdot t) \cdot \sin\varphi];$

Insertion:

$$\begin{aligned}
&-m \cdot \hat{z}_s \cdot \omega^2 \cdot [\cos(\omega \cdot t) \cdot \cos\varphi + \sin(\omega \cdot t) \cdot \sin\varphi] + \\
&+d \cdot \hat{z}_s \cdot \omega \cdot [-\sin(\omega \cdot t) \cdot \cos\varphi + \cos(\omega \cdot t) \cdot \sin\varphi] + \\
&+c \cdot \hat{z}_s \cdot [\cos(\omega \cdot t) \cdot \cos\varphi + \sin(\omega \cdot t) \cdot \sin\varphi] = \\
&= \hat{z}_r \cdot (c \cdot \cos(\omega \cdot t) - d \cdot \omega \cdot \sin(\omega \cdot t));\ \Rightarrow \\
&\Rightarrow \begin{cases} \boldsymbol{cos\ terms}\colon\ -m \cdot \hat{z}_s \cdot \omega^2 \cdot \cos\varphi + d \cdot \hat{z}_s \cdot \omega \cdot \sin\varphi + c \cdot \hat{z}_s \cdot \cos\varphi = \hat{z}_r \cdot c; \\ \boldsymbol{sin\ terms}\colon\ -m \cdot \hat{z}_s \cdot \omega^2 \cdot \sin\varphi - d \cdot \hat{z}_s \cdot \omega \cdot \cos\varphi + c \cdot \hat{z}_s \cdot \sin\varphi = -\hat{z}_r \cdot d \cdot \omega; \end{cases} \Rightarrow \\
&\Rightarrow \begin{cases} \varphi = \arctan\left(\dfrac{m \cdot d \cdot \omega^3}{c^2 - m \cdot c \cdot \omega^2 + d^2 \cdot \omega^2}\right); \\ \dfrac{\hat{z}_s}{\hat{z}_r} = \dfrac{d \cdot \omega}{(m \cdot \omega^2 - c) \cdot \sin\varphi + d \cdot \omega \cdot \cos\varphi} = \left|H_{z_r \to z_s}\right|; \end{cases} \\
&where\ \ \omega = \frac{2 \cdot \pi \cdot v_x}{\lambda};
\end{aligned}$$

We have identified $\left|H_{z_r \to z_s}(v_x)\right|$, which can be compared to $\left|H_{z_r \to z_s}(v_x)\right|$ in Eq [5.35]. The other transfer functions in Eq [5.35] are more difficult to derive using the method with trigonometry.

5.4.3 1D Model with 2 Dynamic dofs

The expression "2 dynamic dofs" refers to that both elasticity between road and wheel (unsprung mass) as well as between wheel (unsprung mass) and sprung mass is modelled. The model can be visualised as in Figure 5-12. No damping is modelled in tyre (in parallel with elasticity c_t) because it is generally relatively low.

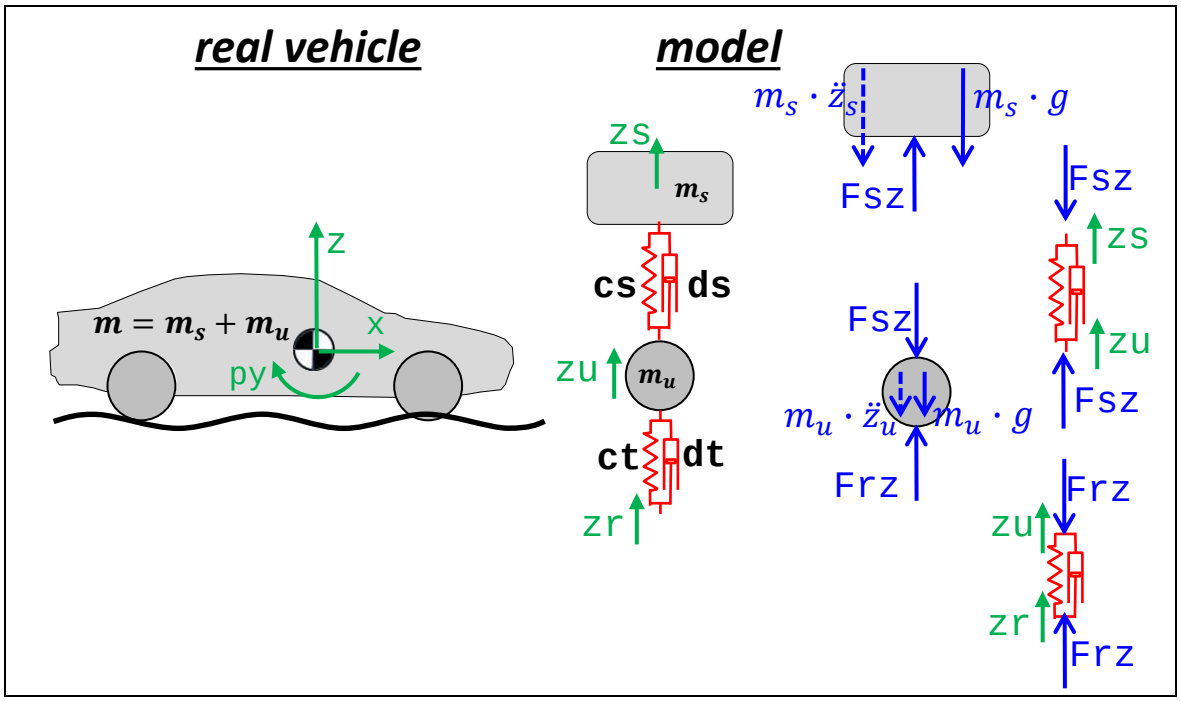


Figure 5-12: One-dimensional model with two dynamic degrees of freedom

The corresponding mathematical model becomes as follows:

Equilibrium:

$$m_s \cdot \ddot{z}_s = F_{sz} - m_s \cdot g;$$
$$m_u \cdot \ddot{z}_u = F_{rz} - F_{sz} - m_u \cdot g;$$

Constitution (displacements measured from static equilibrium):

$$F_{sz} = \underbrace{c_s \cdot (z_u - z_s) + m_s \cdot g}_{\text{linear spring } c_s} + d_s \cdot (\dot{z}_u - \dot{z}_s);$$
$$F_{rz} = \underbrace{c_t \cdot (z_r - z_u) + (m_s + m_u) \cdot g}_{\text{linear spring } c_t} + d_t \cdot (\dot{z}_r - \dot{z}_u);$$

Excitation: $z_r = z_r(t);$

[5.44]

The same can be formulated with matrices and Fourier transforms:

$$\begin{bmatrix} m_s & 0 \\ 0 & m_u \end{bmatrix} \cdot \begin{bmatrix} \ddot{z}_s \\ \ddot{z}_u \end{bmatrix} + \begin{bmatrix} d_s & -d_s \\ -d_s & d_s + d_t \end{bmatrix} \cdot \begin{bmatrix} \dot{z}_s \\ \dot{z}_u \end{bmatrix} + \begin{bmatrix} c_s & -c_s \\ -c_s & c_s + c_t \end{bmatrix} \cdot \begin{bmatrix} z_s \\ z_u \end{bmatrix} = \begin{bmatrix} 0 \\ d_t \end{bmatrix} \cdot \dot{z}_r + \begin{bmatrix} 0 \\ c_t \end{bmatrix} \cdot z_r + A; \Rightarrow$$

$$\Rightarrow \boldsymbol{M} \cdot \begin{bmatrix} \ddot{z}_s \\ \ddot{z}_u \end{bmatrix} + \boldsymbol{D} \cdot \begin{bmatrix} \dot{z}_s \\ \dot{z}_u \end{bmatrix} + \boldsymbol{C} \cdot \begin{bmatrix} z_s \\ z_u \end{bmatrix} = \boldsymbol{D_r} \cdot \dot{z}_r + \boldsymbol{C_r} \cdot z_r + A; \Rightarrow$$

$$\Rightarrow \boldsymbol{M} \cdot \left(-\omega^2 \cdot \begin{bmatrix} \mathcal{F}(z_s) \\ \mathcal{F}(z_u) \end{bmatrix}\right) + \boldsymbol{D} \cdot \left(j \cdot \omega \cdot \begin{bmatrix} \mathcal{F}(z_s) \\ \mathcal{F}(z_u) \end{bmatrix}\right) + \boldsymbol{C} \cdot \begin{bmatrix} \mathcal{F}(z_s) \\ \mathcal{F}(z_u) \end{bmatrix} = \boldsymbol{D_r} \cdot \left(j \cdot \omega \cdot \mathcal{F}(z_r)\right) + \boldsymbol{C_r} \cdot \mathcal{F}(z_r) + \mathcal{F}(A); \Rightarrow$$

$$\Rightarrow (-\omega^2 \cdot \boldsymbol{M} + j \cdot \omega \cdot \boldsymbol{D} + \boldsymbol{C}) \cdot \begin{bmatrix} \mathcal{F}(z_s) \\ \mathcal{F}(z_u) \end{bmatrix} = (j \cdot \omega \cdot \boldsymbol{D_r} + \boldsymbol{C_r}) \cdot \mathcal{F}(z_r);$$

[5.45]

Note that, if we do not measure displacements from static equilibrium, we get a constant term in Eq [5.45].

5.4.3.1 Response to a Single Frequency Excitation

We can find the transfer functions via Fourier transform, starting from Eq [5.45]:

$$\begin{bmatrix} H_{z_r \to z_s} \\ H_{z_r \to z_u} \end{bmatrix} = \begin{bmatrix} \mathcal{F}(z_s) \\ \mathcal{F}(z_u) \end{bmatrix} \cdot \frac{1}{\mathcal{F}(z_r)} = (-\omega^2 \cdot \boldsymbol{M} + j \cdot \omega \cdot \boldsymbol{D} + \boldsymbol{C})^{-1} \cdot (j \cdot \omega \cdot \boldsymbol{D_r} + \boldsymbol{C_r}); \quad [5.46]$$

This format is very compact, since it includes both transfer functions for amplitude and phase. For numerical analyses, the expression in Eq [5.46] is explicit enough, since there are tools, e.g. Matlab, which do numerical matrix inversion and complex mathematics. Symbolic solution is rather lengthy, but one can use symbolic tools, e.g. Mathematica or Matlab Symbolic Toolbox.

Expression in real (without phase information) can be derived, see Eq [5.47].

$$\begin{aligned}
&\left|H_{z_r \to \ddot{z}_s}\right| = \omega^2 \cdot \frac{\sqrt{(c_s \cdot c_t - d_s \cdot d_t \cdot \omega^2)^2 + \left(\omega \cdot (d_s \cdot c_t + d_t \cdot c_s)\right)^2}}{\sqrt{A^2 + B^2}}; \\
&\left|H_{z_r \to z_u - z_s}\right| = \frac{m_s \cdot \sqrt{(c_t \cdot \omega^2)^2 + (d_t \cdot \omega^3)^2}}{\sqrt{A^2 + B^2}}; \\
&\left|H_{z_r \to z_r - z_u}\right| = \frac{\sqrt{(-m_s \cdot m_u \cdot \omega^4 + \omega^2 \cdot (m_s + m_u) \cdot c_s)^2 + (\omega^3 \cdot (m_s + m_u) \cdot d_s)^2}}{\sqrt{A^2 + B^2}}; \\
&A = \omega^4 \cdot m_s \cdot m_u - \omega^2 \cdot (m_s \cdot c_t + m_s \cdot c_s + d_s \cdot d_t + c_s \cdot m_u) + c_s \cdot c_t; \\
&B = \omega^3 \cdot (m_s \cdot d_t + m_s \cdot d_s + m_u \cdot d_s) - \omega \cdot (d_s \cdot c_t + d_t \cdot c_s);
\end{aligned} \quad [5.47]$$

With $d_t = 0$, the solutions (with phase information, i.e. complex) becomes as follows:

$$\begin{aligned}
H_{z_r \to z_s} &= \frac{\mathcal{F}(z_s)}{\mathcal{F}(z_r)} = \frac{\dfrac{(-m_u \cdot \omega^2 + j \cdot d_s \cdot \omega + c_t + c_s) \cdot c_t}{-m_u \cdot \omega^2 + j \cdot d_s \cdot \omega + c_t + c_s - \dfrac{(c_s + j \cdot d_s \cdot \omega)^2}{-m_s \cdot \omega^2 + j \cdot d_s \cdot \omega + c_s}} - c_t}{c_s + j \cdot d_s \cdot \omega}; \\
H_{z_r \to z_u} &= \frac{\mathcal{F}(z_u)}{\mathcal{F}(z_r)} = \frac{c_t}{-m_u \cdot \omega^2 + j \cdot d_s \cdot \omega + c_t + c_s - \dfrac{(c_s + j \cdot d_s \cdot \omega)^2}{-m_s \cdot \omega^2 + j \cdot d_s \cdot \omega + c_s}}; \\
&\text{where } \omega = \tfrac{2 \cdot \pi \cdot v_x}{\lambda};
\end{aligned} \quad [5.48]$$

Equation [5.13] now allows us to get the magnitudes of the other transfer functions as well:

$$\begin{aligned}
H_{z_r \to z_s} &= \{\text{use Eq [5.48]}\}; \\
H_{z_r \to z_u} &= \{\text{use Eq [5.48]}\}; \\
H_{z_r \to z_r - z_u} &= H_{z_r \to z_r} - H_{z_r \to z_u} = 1 - H_{z_r \to z_u}; \\
H_{z_r \to z_u - z_s} &= H_{z_r \to z_u} - H_{z_r \to z_s}; \\
H_{z_r \to \ddot{z}_s} &= -\omega^2 \cdot H_{z_r \to z_s}; \\
H_{z_r \to \Delta F_{sz}} &= \{\Delta F_{sz} = c_s \cdot (z_u - z_s) + d_s \cdot (\dot{z}_u - \dot{z}_s)\} = \\
&\quad = c_s \cdot \left(H_{z_r \to z_u} - H_{z_r \to z_s}\right) + d_s \cdot j \cdot \omega \cdot \left(H_{z_r \to z_u} - H_{z_r \to z_s}\right) = \\
&\quad = (c_s + j \cdot d_s \cdot \omega) \cdot \left(H_{z_r \to z_u} - H_{z_r \to z_s}\right); \\
H_{z_r \to \Delta F_{rz}} &= \{\Delta F_{rz} = c_t \cdot (z_r - z_u)\} = c_t \cdot \left(H_{z_r \to z_r} - H_{z_r \to z_u}\right) = c_t \cdot \left(1 - H_{z_r \to z_u}\right);
\end{aligned} \quad [5.49]$$

The transfer functions in Equation [5.49] are plotted in Figure 5-13.

5.4.3.1.1 Example Analysis

If we use Figure 5-13 as the example in 5.4.1:

- Ride comfort related: $\left|H_{z_r \to \ddot{z}_s}(v_x)\right| \approx 123; \Rightarrow |\hat{a}| = 123 \cdot \hat{z}_r = 123 \cdot 0.01 = 1.23\ m/s^2$;. From this we can calculate $RMS(\ddot{z}_s) = |1.23|/\sqrt{2} \approx 0.8697\ m/s^2$.
- Fatigue life related: $\left|H_{z_r \to z_u - z_s}(v_x)\right| \approx 1.14; \Rightarrow\ |\hat{z}_u - \hat{z}_s| = 1.14 \cdot \hat{z}_r = 1.14 \cdot 0.01 = 0.0114\ m = 1.14\ cm$;.

- Road grip related: $\left|H_{z_r \to \Delta F_{rz}}(v_x)\right| \approx 177470; \Rightarrow \left|\Delta F_{rz}\right| = 177470 \cdot \hat{z}_r = 177470 \cdot 0.01 = 1775\ N;$.

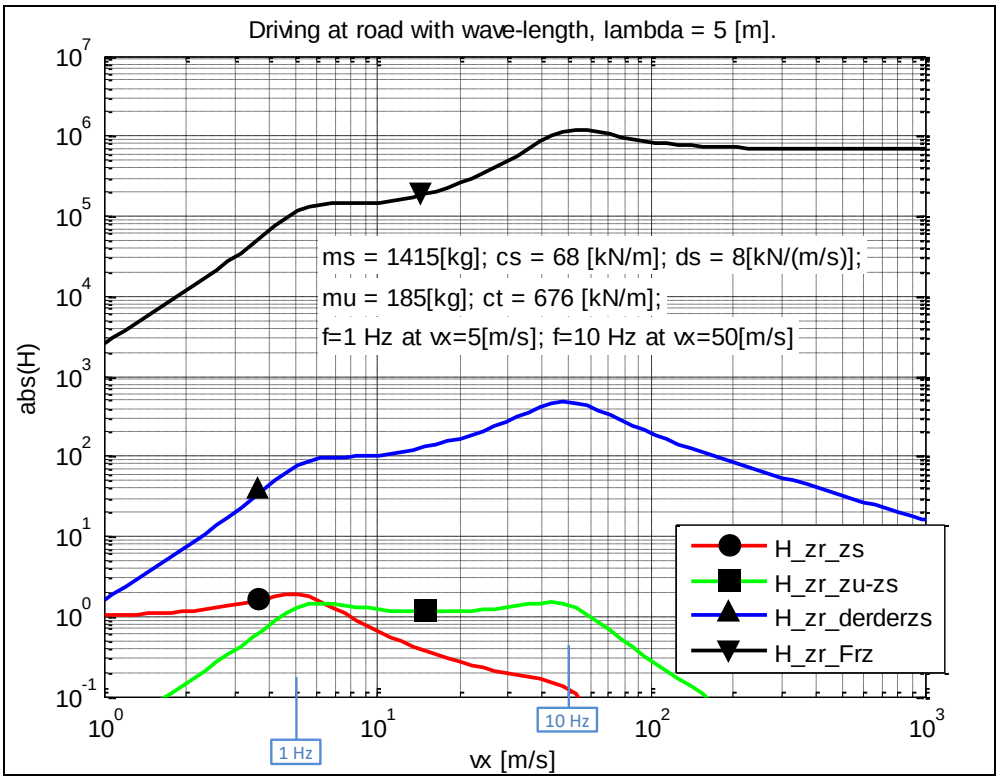


Figure 5-13: Transfer functions for amplitudes from model in Figure 5-12, excited with single frequencies.

This analysis can be compared with the analysis in 5.4.2.1.1. Ride comfort and fatigue does not change a lot, but road grip does. This indicates that the more advanced model is only needed for road grip evaluation.

Figure 5-14 shows the phase angles for the different responses.

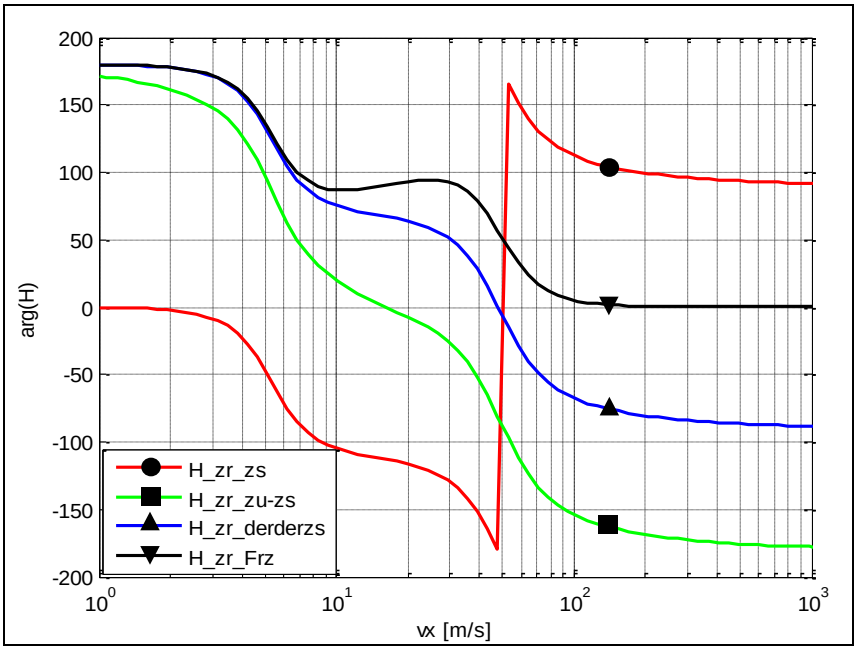


Figure 5-14: Transfer functions for phase delays. Same model and data as in Figure 5-13.

Figure 5-15, shows the amplitude gains for the corresponding un-damped system. Natural frequencies are around 5 m/s and 50 m/s. These two speeds correspond to frequencies $v_{x,crit}/\lambda$, i.e.

approximately 1 Hz and 10 Hz. The 1Hz frequency is an oscillation mode where the both masses move in phase with each other, the so called "heave mode" or "bounce mode". The 10 Hz frequency comes from the mode where the masses are in counter-phase, the so called "wheel hop mode". In the wheel hop mode, the sprung mass is almost not moving at all. We will come back to these modes in 5.4.4.

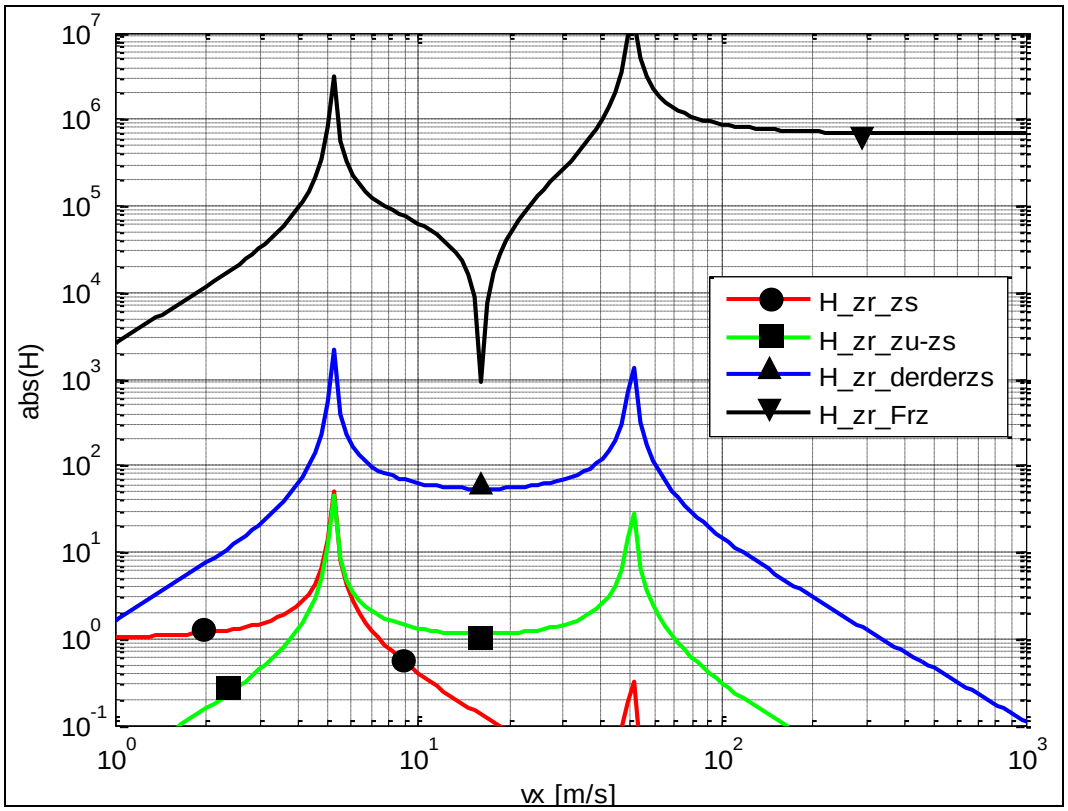


Figure 5-15: Un-damped transfer functions. Same model and data as in Figure 5-13, except $d_s = 0$.

5.4.3.2 Active Damping using Skyhook Control

Contribution from Waltteri Koskinen, student at Tampere University, Finland

A traditional damper follows $F_{push} = d_s \cdot v_{cpr}$;, where subscript *cpr* means compression. Since d_s comes from flow losses of oil in the damper, d_s will always be > 0. Taking into account that pressure losses are proportional to hydraulic flow in square, a better model is $F_{push} = d_{s2} \cdot \text{sign}(v_{cpr}) \cdot v_{cpr}^2 = d_{s2} \cdot v_{cpr} \cdot |v_{cpr}|$;. But, regardless of the exact curve form, we can conclude that a traditional damper can only dissipate energy. A step towards controllable suspension is to use a semi-active damper, which has varying hydraulic orifices. It can still only dissipate energy, but the curve shape is variable. If adding energy via a hydraulic pump, one can take one more step, called a "active damper". In principle, an active damper can generate both positive and negative force $F_d = F_{ad}$ (subscript *ad* for *active damper*) for any sign on v_{cpr}. A common way to design control algorithms for such dampers is to use the F_{ad} to mimick a virtual "Skyhook damper" connected between vehicle unsprung parts and "the sky", i.e. a fix inertial system.

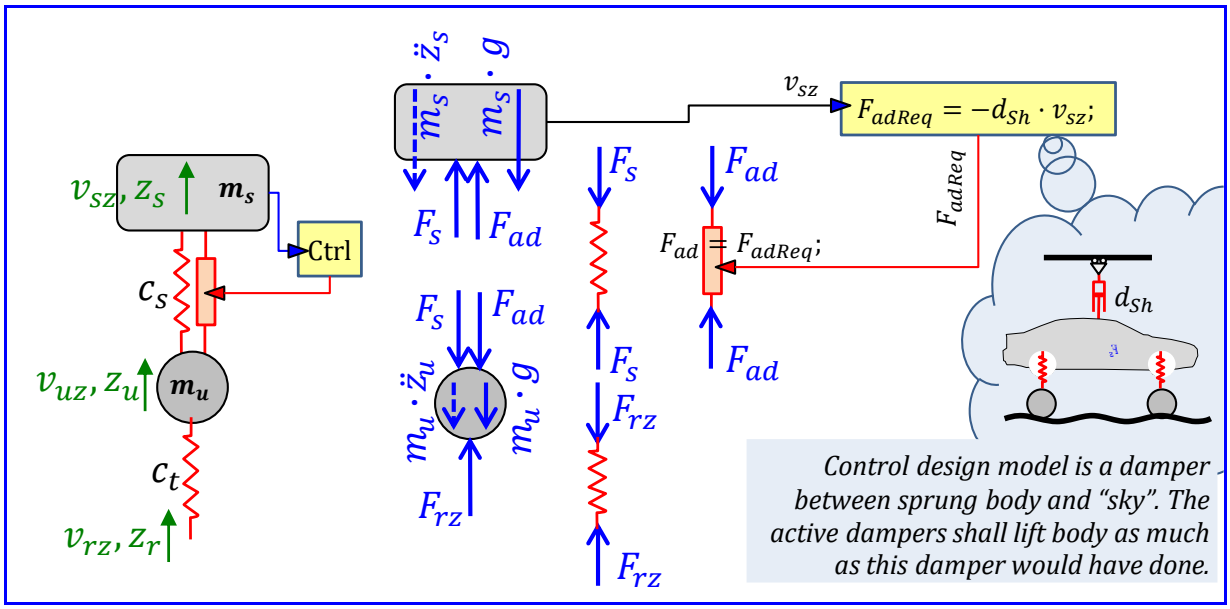


Figure 5-16: One-dimensional model with two dynamic degrees of freedom and with the traditional dampers replaced by a Skyhook controlled active damper (ideal sensing, computation and actuation). Tyre damping neglected.

The corresponding mathematical model becomes as follows:

Equilibrium:

$$m_s \cdot \ddot{z}_s = F_s + F_{ad} - m_s \cdot g;$$
$$m_u \cdot \ddot{z}_u = F_{rz} - F_s - F_{ad} - m_u \cdot g;$$

Constitution (displacements counted from static equilibrium):

$$F_s = c_s \cdot (z_u - z_s) + m_s \cdot g;$$
$$F_{rz} = c_t \cdot (z_r - z_u) + (m_s + m_u) \cdot g;$$

Control and actuation: $F_{ad} = -d_{Sh} \cdot v_{sz} = -d_{Sh} \cdot \dot{z}_s;$

Excitation: $z_r = z_r(t);$

The same can be formulated with matrices and Fourier transforms:

$$\begin{bmatrix} m_s & 0 \\ 0 & m_u \end{bmatrix} \cdot \begin{bmatrix} \ddot{z}_s \\ \ddot{z}_u \end{bmatrix} + \begin{bmatrix} d_{Sh} & 0 \\ -d_{Sh} & 0 \end{bmatrix} \cdot \begin{bmatrix} \dot{z}_s \\ \dot{z}_u \end{bmatrix} + \begin{bmatrix} c_s & -c_s \\ -c_s & c_s + c_t \end{bmatrix} \cdot \begin{bmatrix} z_s \\ z_u \end{bmatrix} = \begin{bmatrix} 0 \\ c_t \end{bmatrix} \cdot z_r;$$

Eq [5.46] is still valid with same matrix names, but the definition of matrix ***D*** is different. No transfer functions are plotted here, but in 5.6.5.

5.4.4 One-Mode Models

The sprung mass is typically around 10 times larger than the unsprung mass and the suspension spring is usually around 10 times lower than the tyre stiffness. Hence, there are the 2 distinguished modes, identified in 0. If only interested in a certain frequency range around one of the eigenfrequencies, one can split the model in 2 models, which explains one mode each, see Figure 5-17.

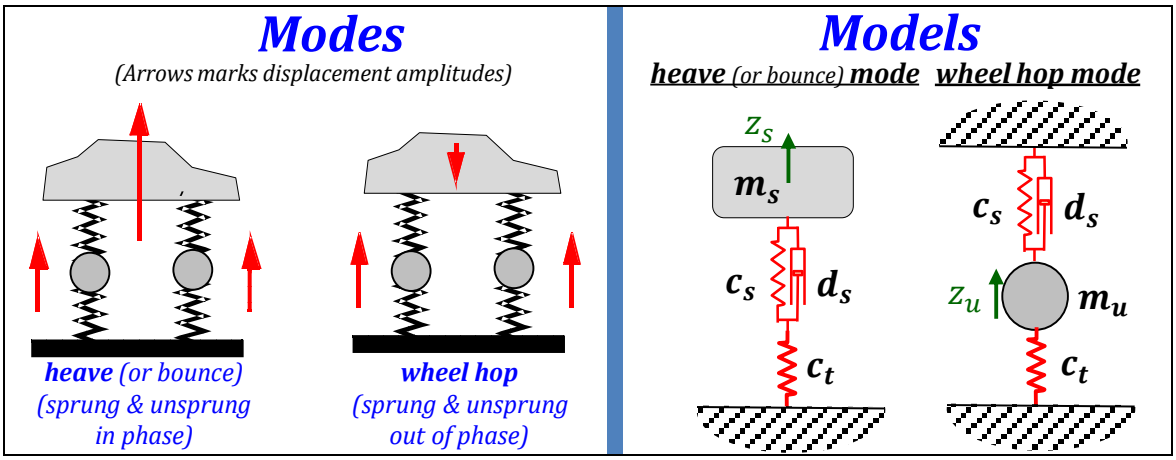


Figure 5-17: Modes and approximate models.

We will now derive the natural frequencies for the two models and compared with the natural frequencies ($d_s = 0$) found for the combined model, in Figure 5-15. Both models are one degree of freedom models with mass and spring, why the eigenfrequency is $\sqrt{\text{stiffness/mass}}$.

For the heave model, the mass is m_s. Stiffnesses c_s and c_t are series connected, which means that the total stiffness$= 1/\big((1/c_s) + (1/c_t)\big)$.

For the wheel hop model, the mass is m_u. Stiffnesses c_s and c_t are parallel connected, which means that the total stiffness$= c_s + c_t$.

$$\omega_{Bounce} = \sqrt{\frac{1/\left(\frac{1}{c_s}+\frac{1}{c_t}\right)}{m_s}} = 6.61\,\frac{\text{rad}}{\text{s}} = 1.05\text{ Hz};\quad \omega_{WheelHop} = \sqrt{\frac{c_s+c_t}{m_u}} = 63.4\,\frac{\text{rad}}{\text{s}} = 10.1\text{ Hz};\qquad [5.50]$$

Numerical values from 5.4.3 is used ($m_s = 1415\ kg; m_u = 185\ kg; c_s = 68\ \ kN/m; c_t = 676\ \ kN/m;$) and eigenfrequencies coincide well with Figure 5-15.

Heave (or Bounce) refers to the mode where the sprung mass has the greatest amplitude and wheel hop is related to the case when the unsprung mass exhibits the greatest amplitude. For a passenger car, the spring mass has the lowest frequency, typically around 1 Hz while tyre hop is more prevalent at frequencies around 10 Hz.

5.5 Functions for Stationary Oscillations

5.5.1 Ride Comfort *

Function definition: ***(Stationary) Ride comfort*** *is the comfort that vehicle occupants experience from stationary oscillations when the vehicle travels over a road with certain vertical irregularity in a certain speed. The measure is defined at least including driver (or driver seat) vertical acceleration amplitudes.*

Ride comfort is sometimes divided into:

- ***Primary Ride*** – the vehicle body on its suspension. Heave (Bounce), Pitch and Roll ≈0..4 Hz
- ***Secondary Ride*** – same but above body natural frequencies, i.e. ≈4..25 Hz

5.5.1.1 Single Frequency

It is generally accepted for stationary vibrations, that humans are sensitive to the RMS value of the acceleration. However, the sensitivity is frequency dependent, so that highest discomfort appears for a certain range of frequencies. Some human tolerance curves are shown in Figure 5-18 and Figure 5-19.

The curves can be considered a threshold for acceptance where everything above the line is unacceptable and points below the curve are acceptable. Discomfort is a subjective measure, and this is why the different diagrams cannot be directly compared to each other. The SAE has suggested that frequencies from 4 to 8 Hz are the most sensitive and the accepted accelerations for these are no higher than 0.025 g (RMS).

The curves in Figure 5-18 mostly represent an extended exposure to the vibration. As one can expect, a human can endure exposure to more severe conditions for short periods of time. The SAE limits presented are indicative of 8 hours of continuous exposure. Curves for different exposure times can also be obtained from ISO, (ISO 2631). The ISO curves are from the first version of ISO 2631 and were later modified, see Figure 5-19.

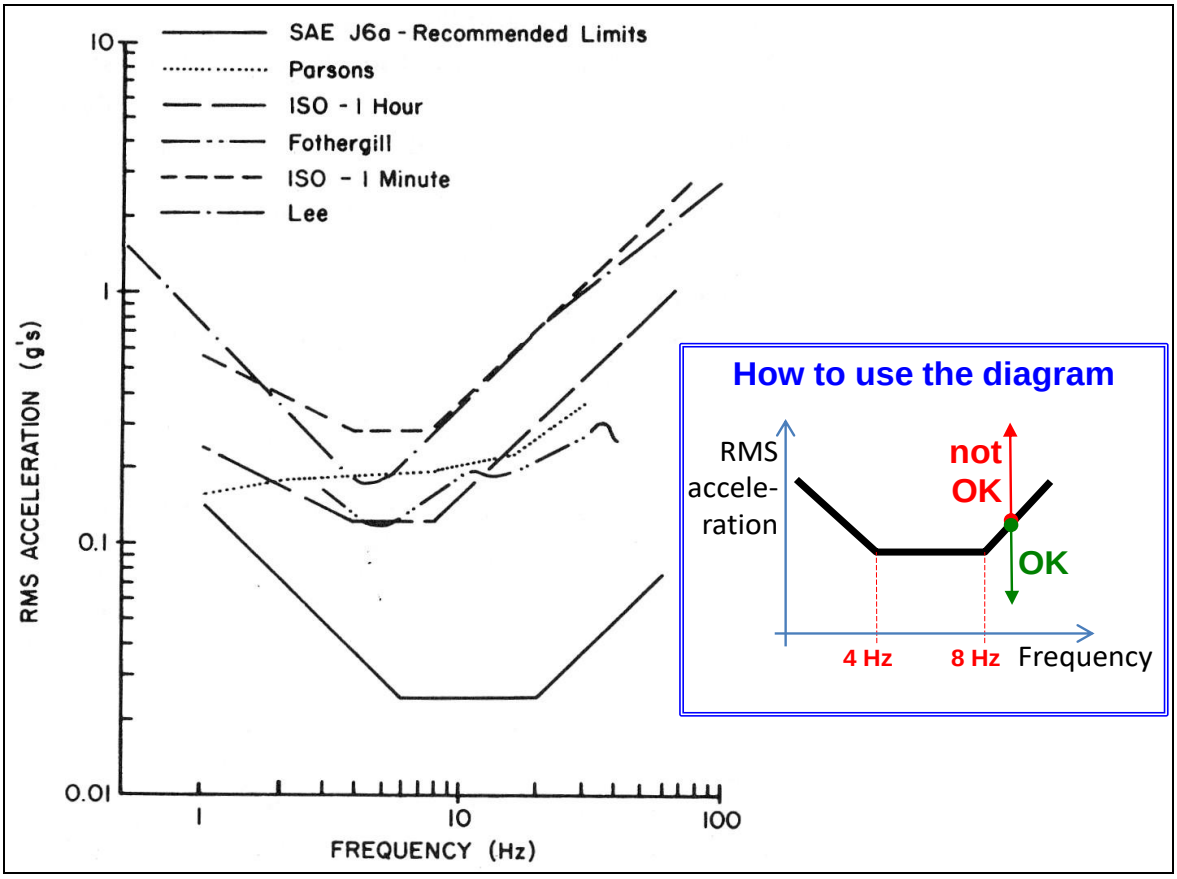


Figure 5-18: Various Human Tolerance Curves to Vertical Vibration, (Gillespie, 1992)

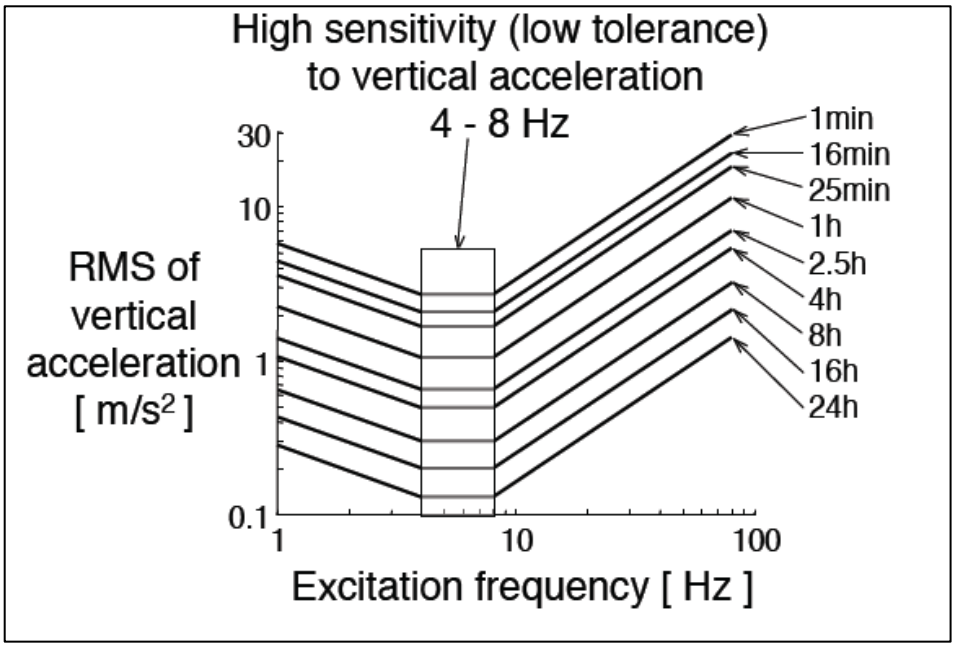


Figure 5-19: ISO 2631 Human Tolerance Curves

5.5.1.2 Multiple Frequencies

The curves in Figure 5-18 and Figure 5-19 can be interpreted as a filter, where the response of the human is influenced by the frequencies they are exposed to. This leads to the concept of a Human Filter Function $W_k(f)$. (W_k refers to vertical whole human body vibration sensitivity, while there are other for sensitivities for other directions and human parts.) This can be seen as a transfer function from driver seat to somewhere inside the driver's body or brain, where discomfort is perceived.

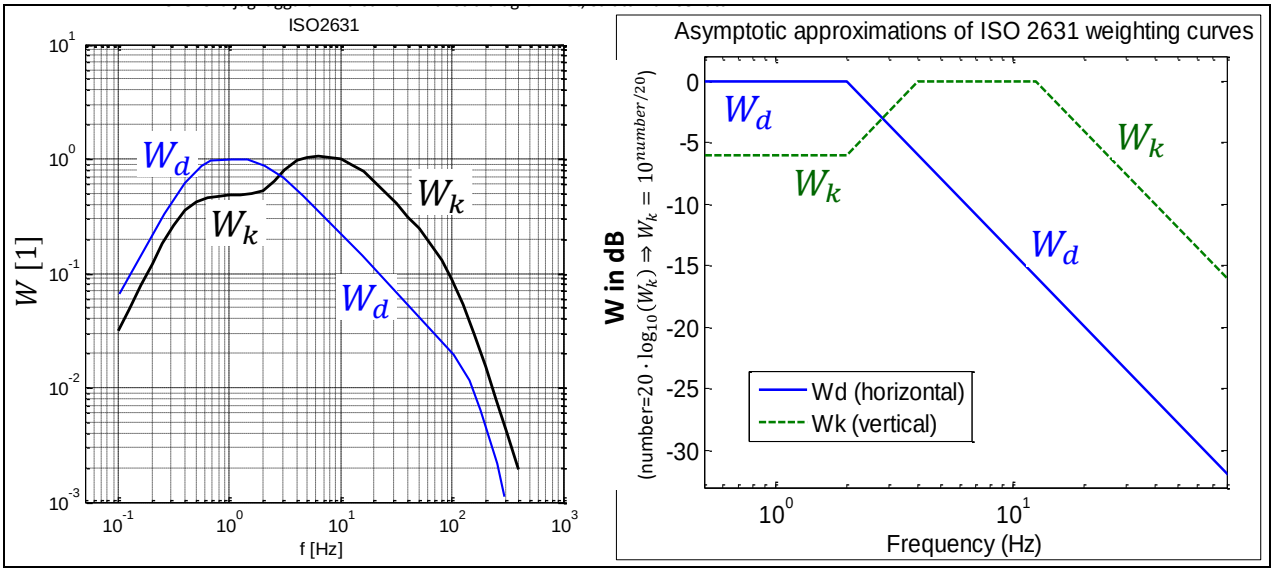


Figure 5-20: Human Sensitivity Filter Function. From (ISO 2631). Right: Asymptotic approximation

Frequency f Hz	W_k factor × 1 000	W_k dB
0,02		
0,025		
0,031 5		
0,04		
0,05		
0,063		
0,08		
0,1	31,2	− 30,11
0,125	48,6	− 26,26
0,16	79,0	− 22,05
0,2	121	− 18,33
0,25	182	− 14,81
0,315	263	− 11,60
0,4	352	− 9,07
0,5	418	− 7,57
0,63	459	− 6,77
0,8	477	− 6,43
1	482	− 6,33
1,25	484	− 6,29
1,6	494	− 6,12
1,6	494	− 6,12
2	531	− 5,49
2,5	631	− 4,01
3,15	804	− 1,90
4	967	− 0,29
5	1 039	0,33
6,3	1 054	0,46
8	1 036	0,31
10	988	− 0,10
12,5	902	− 0,89
16	768	− 2,28
20	636	− 3,93
25	513	− 5,80
31,5	405	− 7,86
40	314	− 10,05
50	246	− 12,19
63	186	− 14,61
80	132	− 17,56
100	88,7	− 21,04
125	54,0	− 25,35
160	28,5	− 30,91
200	15,2	− 36,38
250	7,90	− 42,04
315	3,98	− 48,00
400	1,95	− 54,20

Figure 5-21: Human Filter Function for vertical vibrations. Table from (ISO 2631).

With formulas from earlier in this chapter we can calculate an RMS value of a signal with multiple frequencies, see Equation [5.6]. Consequently, we can calculate RMS of multiple frequency acceleration. Since humans are sensitive to acceleration, it would give one measure of human discomfort. However, to get a measure which is useful for comparing accelerations with different frequency content, the measure has to take the human filter function into account. The Weighted RMS Acceleration, a_w, in the following formula is such measure:

$$a_w = a_w\left(\ddot{z}(t)\right) = \left\{use: RMS\left(\ddot{z}(t)\right) = \sqrt{\sum_{i=1}^{N} \frac{\hat{\ddot{z}}_i^{\,2}}{2}}\right\} = \sqrt{\sum_{i=1}^{N} \frac{\left(W_k(\omega_i)\cdot \hat{\ddot{z}}_i\right)^2}{2}}; \quad \text{or}$$

$$a_w = a_w\left(\ddot{z}(t)\right) = \left\{use: RMS\left(\ddot{z}(t)\right) = \sqrt{\int_{\omega=0}^{\infty} G_{\ddot{z}}(\omega)\cdot d\omega}\right\} = \sqrt{\int_{\omega=0}^{\infty} \left(W_k(\omega)\right)^2 \cdot G_{\ddot{z}}(\omega)\cdot d\omega}\,; \qquad [5.51]$$

Equation [5.51] is written for a case with only vertical vibrations, hence W_k and $G_{\ddot{z}}$. If vibrations in several directions, a total a_w can still be calculated, see (ISO 2631).

In (ISO 2631) one can also find the following equation, which weights together several time periods, with different vibrations spectra. Time averaged whole-body vibration exposure value is denoted $a_{w,av}$.

$$a_{w,av} = \sqrt{\frac{\sum_i {a_{wi}}^2 \cdot T_i}{\sum_i T_i}}; \qquad [5.52]$$

The a_w in Eq [5.52] is used both for vehicle customer requirement setting at OEMs and governmental legislation. One example of legislation is (DIRECTIVE 2002/44/EC, 2002). This directive stipulates that a_w in Eq [5.52] in any direction, normalized to 8 hours, may not exceed 1.15 m/s², and if the value exceeds 0.5 m/s² action must be taken.

5.5.1.2.1 Certain Combination of Road, Vehicle and Speed

Now we can use Equation [5.36] without assuming road type. However, we must identify $\hat{\ddot{z}}_s$ and multiply it with $W_k(\omega)$, according to Equation [5.51]. Then we get [5.53].

Using Equation [5.53], we can calculate the weighted RMS value for the different models in 5.4.1, 5.4.2 and 5.4.3. For each model, it will vary with speed, v_x. A plot, assuming a certain road type ("Rough" from Figure 5-5) is shown in Figure 5-30. We can see that the simplest model "*stiff tyre, no unsprung mass*" gives much different comfort value than the two others, so the simplest is not goof to estimate comfort. However, the two other models give approximately same result, which indicates that the medium model, "*stiff tyre, no unsprung mass*", is enough for comfort evaluation. This is no general truth but an indication that the most advanced model, "*two masses, elastic tyre*", is not needed for comfort on normal roads. The advanced model is more needed for road grip.

We can also see that the comfort decreases, the faster the vehicle drives. If we read out at which speed we reach $a_w = 1\ m/s^2$ (which is a reasonable value for long time exposure) we get around $v_x \approx 70\ m/s \approx 250\ km/h$ on this road type ("Rough") with the medium (and advanced) model. With the simplest model, we get $v_x \approx 1\ m/s \approx 3..4\ km/h$.

$$RMS(\ddot{z}_s) = \left\{ \begin{matrix} \text{Eq} \\ [5.31] \end{matrix} \right\} = \sqrt{\frac{\Phi_0}{{\Omega_0}^{-w}} \cdot {v_x}^{w-1} \cdot \int_{\omega=0}^{\infty} \left| H_{z_r \to \ddot{z}_s}(\omega) \right|^2 \cdot \omega^{-w} \cdot d\omega} = \left\{ \begin{matrix} H_{z_r \to \ddot{z}_s} = \\ = -\omega^2 \cdot H_{z_r \to z_s} \end{matrix} \right\}$$

$$= \sqrt{\frac{\Phi_0}{{\Omega_0}^{-w}} \cdot {v_x}^{w-1} \cdot \int_{\omega=0}^{\infty} \left| \omega^2 \cdot H_{z_r \to z_s}(\omega) \right|^2 \cdot \omega^{-w} \cdot d\omega} =$$

$$= \sqrt{\frac{\Phi_0}{{\Omega_0}^{-w}} \cdot {v_x}^{w-1} \cdot \int_{\omega=0}^{\infty} \left| H_{z_r \to z_s}(\omega) \right|^2 \cdot \omega^{4-w} \cdot d\omega} ; \Rightarrow \left\{ \begin{matrix} \text{Eq} \\ [5.51] \end{matrix} \right\} \Rightarrow$$

$$\Rightarrow a_w = \sqrt{\frac{\Phi_0}{{\Omega_0}^{-w}} \cdot {v_x}^{w-1} \cdot \int_{\omega=0}^{\infty} \left(W_k(\omega) \right)^2 \cdot \left| H_{z_r \to z_s}(\omega) \right|^2 \cdot \omega^{4-w} \cdot d\omega} ;$$

[5.53]

5.5.1.3 Other Excitation Sources

Present chapter focuses on the influence of excitation from vertical displacement of the road. Examples of other, but often co-operating, excitation sources are:

- Powertrain vibrations, non-uniform rotation in engine. Frequencies will be proportional to engine speed
- Wheel vibrations, e.g. due to non-round wheels or otherwise unbalanced wheels. Frequencies will be proportional to vehicle speed.
- Special machineries mounted on vehicles (e.g. climate systems or concrete mixers)

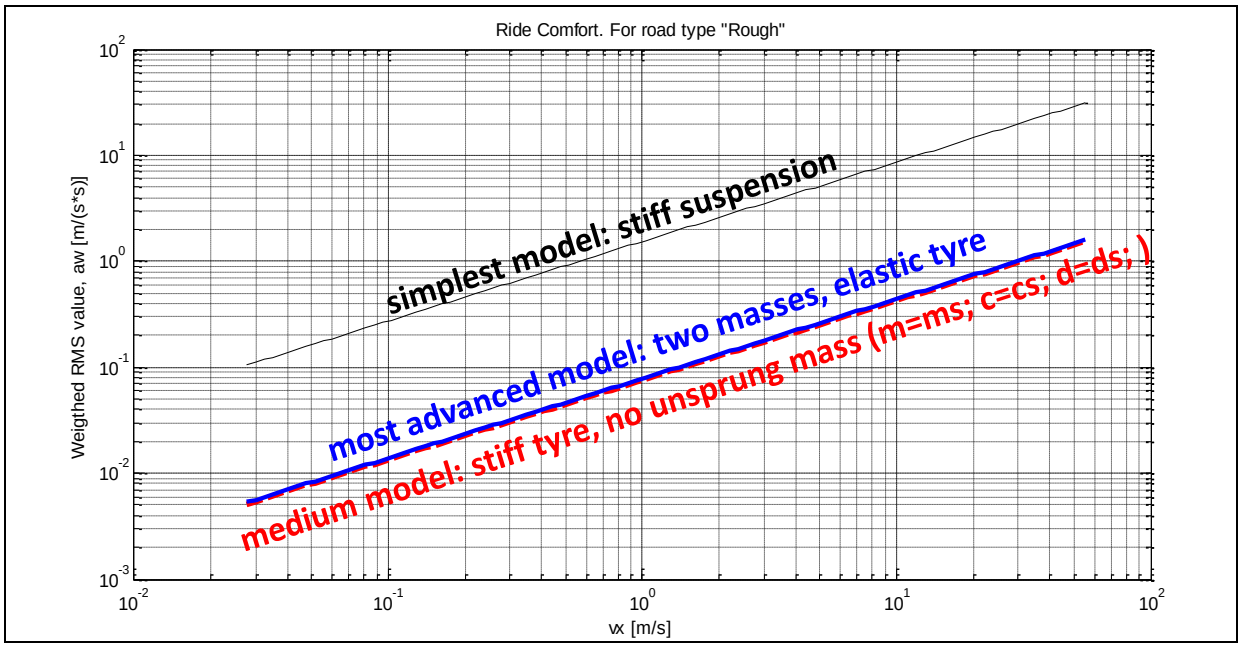


Figure 5-22: Weighted RMS values for road type "Smooth" from Figure 5-5. The 3 curves show 3 different models: Simplest (from 1.5.1), Medium (from 1.5.2) and Most advanced (from 1.5.3).

5.5.2 Fatigue Life *

Function definition: ***(Vehicle) Fatigue life*** *is the life that the vehicle, mainly suspension, can reach due to stationary oscillations when vehicle travels over a road with certain vertical irregularity in a certain speed. One measure is the suspension vertical deformation amplitude.*

Beside human comfort, the fatigue of the vehicle structure itself is one issue to consider in vertical vehicle dynamics.

5.5.2.1 Single Frequency

5.5.2.1.1 Loads on Suspension Spring

In particular, the suspension spring may be subject to fatigue. The variation in spring material stress is dimensioning, which is why the force variation or amplitude in the springs should be under observation. Since spring force is proportional to deformation, the suspension deformation amplitude is proposed as a good measure (at least if spring design is not varied). This is the explanation to why the amplitude of $z_u - z_s$ is plotted in Figure 5-10.

Beside fatigue loads, $z_u - z_s$ is also relevant for judging whether suspension bump-stops become engaged or not. At normal driving, that limit should be far from reached, except possibly at high loads (many persons/much payload).

It can be noted that $z_u - z_s$ represents the variation in material stress only if spring is not changed. So, if different spring designs are compared, it is not sufficient to study only $z_u - z_s$.

5.5.2.1.2 Fatigue of Other Components

Fatigue of other parts may require other amplitudes.

One other example can be the damper fatigue. Damper fatigue would be more relevant to judge from amplitude of $\dot{z}_u - \dot{z}_s$, which determines the force level and hence the stress level.

Another example is to judge the force amplitude in parts that carry both spring and damper forces. For those it is motivated to consider $\Delta F_{sz} = c_s \cdot (z_u - z_s) + d_s \cdot (\dot{z}_u - \dot{z}_s)$; as in Eq [5.49].

Yet another example is the load of the road itself. For heavy trucks, it is relevant to consider how much they wear the road. At some roads with legislated maximum (static) axle load, one can be allowed to

exceed that limit if the vehicle has especially road friendly suspensions. For these judgements, it is the contact force between tyre and road, $\hat{F}_{rz}$, which is important. These considerations are primarily for road authorities but becomes aspects for vehicle developers as legal requirements.

5.5.2.2 Multiple Frequencies

If the excitation is of one single frequency, the stress amplitude can be used when comparing two designs. However, for spectra of multiple frequencies, one cannot look at amplitudes solely, $[\hat{z}_1, \hat{z}_2, \cdots, \hat{z}_N]$, because the amplitudes will depend on how the discretization is done, i.e. the number N. Some kind of integral of a spectral density is more reasonable. In this book, it is proposed that a very approximate measure of fatigue load is calculated as follows, exemplified for the case of fatigue of the spring:

$$\begin{aligned} &Measure\ for\ spring\ fatigue\ life = RMS\big(z_u(t) - z_s(t)\big) = \\ &= \sqrt{\frac{\Phi_0}{\Omega_0{}^{-w}} \cdot v_x{}^{w-1} \cdot \int_{\omega=0}^{\infty} \left|H_{z_r \to z_u - z_s}(\omega)\right|^2 \cdot \omega^{-w} \cdot d\omega} = \\ &\left\{ \begin{matrix} use: H_{z_r \to z_u - z_s} = \\ = H_{z_r \to z_u} - H_{z_r \to z_s} \end{matrix} \right\} = \\ &= \sqrt{\frac{\Phi_0}{\Omega_0{}^{-w}} \cdot v_x{}^{w-1} \cdot \int_{\omega=0}^{\infty} \left|H_{z_r \to z_u}(\omega) - H_{z_r \to z_s}(\omega)\right|^2 \cdot \omega^{-w} \cdot d\omega}\,; \end{aligned} \qquad [5.54]$$

Equation is written for application to a known road spectra (Φ_0, w) and vehicle dynamic structure ($H_{z_r \to z_u}, H_{z_r \to z_s}$), but the first expression ($RMS\big(z_u(t) - z_s(t)\big)$) is applicable on a measured or simulated time domain solution.

5.5.3 Road Grip *

Function definition: ***Road grip (on undulated roads)*** *is how well the longitudinal and lateral grip between tyres and road is retained due to stationary oscillations when the vehicle travels over a road with certain vertical irregularity in a certain speed.*

In **3.3** and **0**, the brush model explains how the tyre forces in the ground plane appears. It is a physical model where the contact length influences how stiff the tyre is for longitudinal and lateral slip. There is also a brief description of relaxation models for tyres. This together motivates that a tyre has more difficult to build up forces in ground plane if the vertical force varies. We can understand it as when contact length varies, the shear stress builds up has to start all over again. As an average effect, the tyre will lose more and more grip, the more the vertical force varies.

5.5.3.1 Multiple Frequencies

If the excitation is of one single frequency, the force amplitude can be used when comparing two designs. However, for spectra of multiple frequencies, one cannot look at amplitudes solely, $[\hat{z}_1, \hat{z}_2, \cdots, \hat{z}_N]$, because the amplitudes will depend on how the discretization is done, i.e. the number N. Some kind of integral of a spectral density is more reasonable. In this book, it is proposed that a very approximate measure of road grip is calculated as follows:

$$\begin{aligned} &Measure\ for\ (bad) road\ grip = RMS\big(\Delta F_{rz}(t)\big) = \\ &= \sqrt{\frac{\Phi_0}{\Omega_0{}^{-w}} \cdot v_x{}^{w-1} \cdot \int_{\omega=0}^{\infty} \left|H_{z_r \to \Delta F_{rz}}(\omega)\right|^2 \cdot \omega^{-w} \cdot d\omega} = \\ &= \left\{ use: H_{z_r \to z_u - z_s} = c_t \cdot \left(1 - H_{z_r \to z_u}\right) \right\} = \\ &= \sqrt{\frac{\Phi_0}{\Omega_0{}^{-w}} \cdot v_x{}^{w-1} \cdot \int_{\omega=0}^{\infty} \left|c_t \cdot \left(1 - H_{z_r \to z_u}\right)\right|^2 \cdot \omega^{-w} \cdot d\omega}\,; \end{aligned} \qquad [5.55]$$

Equation is written for application to a known road spectrum (Φ_0, w) and vehicle dynamic structure ($H_{z_r \to z_u}$), but the first expression ($RMS(\Delta F_{rz}(t))$) is applicable on a measured or simulated time domain solution.

5.5.4 Other Functions

Present chapter focuses on the functions, (vertical) ride comfort, fatigue and road grip. Examples of other functions are:

- An area of functions that encompasses the vertical dynamics is **Noise, Vibration, and Harshness – NVH**. It is similar to ride comfort, but the frequencies are higher, stretching up to sound which is heard by humans.
- **Ground clearance** (static and dynamic) between vehicle body and ground. Typically, important for off-road situations.
- **Longitudinal comfort**, due to drive line oscillations and/or vertical road displacements. Especially critical when driver cabin is separately suspended to the body. This is the case for heavy trucks.
- **Disturbances in steering wheel feel**, due to one-sided bumps. Especially critical for rigid steered axles. This is often the design of the front axle in heavy trucks.
- There are of course an infinite number of combined manoeuvres, in which functions with requirements can be found. Examples can be **bump during strong cornering** (possibly destabilizing vehicle) or **one-sided bump** (exciting both heave=bounce, pitch and roll modes). When studying such transients, the vertical dynamics is not enough to capture the comfort, but one often need to involve also **longitudinal** dynamics; the linkage with ant-dive/anti-squat geometry from Chapter **3** becomes important as well as tyre vertical (radial) deflection characteristics.
- Energy is dissipated in suspension dampers, which influence **energy consumption** for the vehicle. This energy loss is much related, but not same as, to (tyre) rolling resistance. One can define a *Suspension resistance coefficient* $SRC = PPS_{Susp}/(m \cdot g)$ which can be compared directly to *Rolling resistance coefficient* RRC. So, suspension characteristics do influence this energy loss, but normally $SRC \ll RRC$, unless driving very fast on very uneven road.

5.6 Variation of Suspension Design

The influence of design parameters on vehicle functions Ride comfort, Suspension fatigue and Road grip can now be made. E.g., it is important to not only use the transfer function, but also take the road and human sensitivity into account, which calls for different weighting for different frequencies.

Transfer function for the model in 5.4.3 is shown as dashed lines in

Figure 5-23. Same figure also shows the Road- and Human-weighted versions. Studying how these curves change with design parameters gives a quantitative understanding of how different suspension design parameters influence. Such variations will be done in 5.6.1 to 5.6.4.

There are two particular frequency intervals of the graphs to observe. These are the 2 peaks around the two the natural frequencies of the sprung and unsprung masses, the peak at lower frequency is mainly a resonance in heave mode, while the higher one is in wheel hop mode.

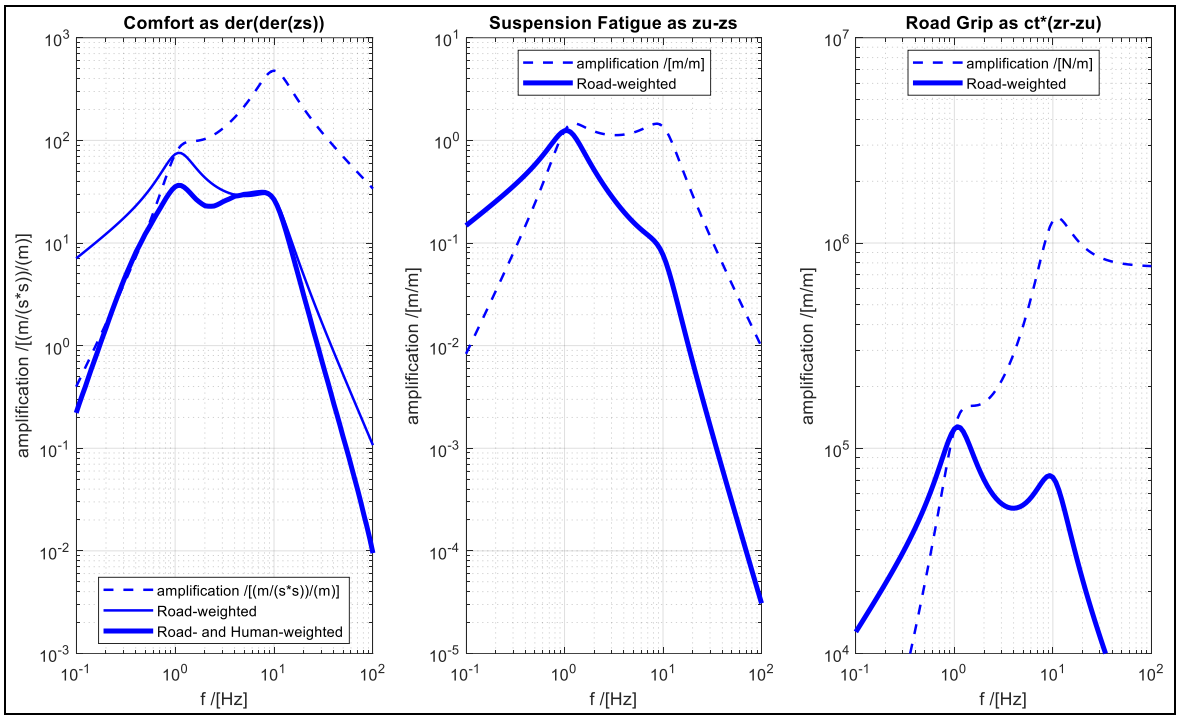


Figure 5-23: For a passenger car with $m_s = 1600\ [kg], m_u = 200\ [kg], c_s = 76\ [kN/m],\ d_s = 9\ [kN/(m/s)], c_t = 764\ [kN/m], d_t = 0$. Left is vertical acceleration (amplitude) of sprung mass for Ride Comfort. Middle is relative displacement (amplitude) between sprung and unsprung mass for Suspension Fatigue. Right is deformation (amplitude) of tyre spring for Road Grip. Weightings for typical road and for human sensitivity is shown.

5.6.1 Varying Suspension Stiffness

In Figure 5-24 the benefits of the low suspension stiffness (1 Hz) is seen for suspension travel and comfort without much change in the road grip performance.

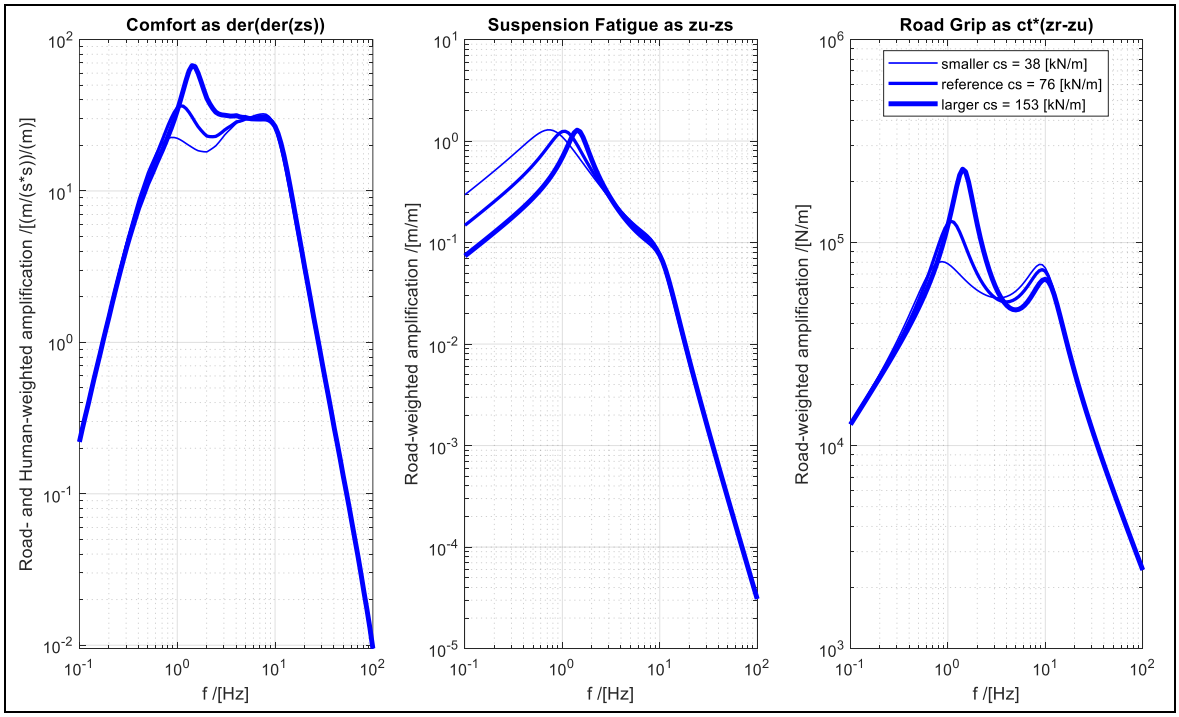


Figure 5-24: Variation of suspension stiffness, c_s

Regarding Figure 5-24 and Figure 5-25 we see that there is a large influence of the acceleration gain at low frequencies with little change at the wheel hop and higher frequencies. The suspension stiffness and damping were seen to have little influence on the ride comfort / road grip response around 10 Hz.

5.6.2 Varying Suspension Damping

In Figure 5-25, we see that the changes in suspension damping have opposite effects for the heave and wheel hop frequency responses. High damping is good for reducing heave, but not so effective for wheel hop.

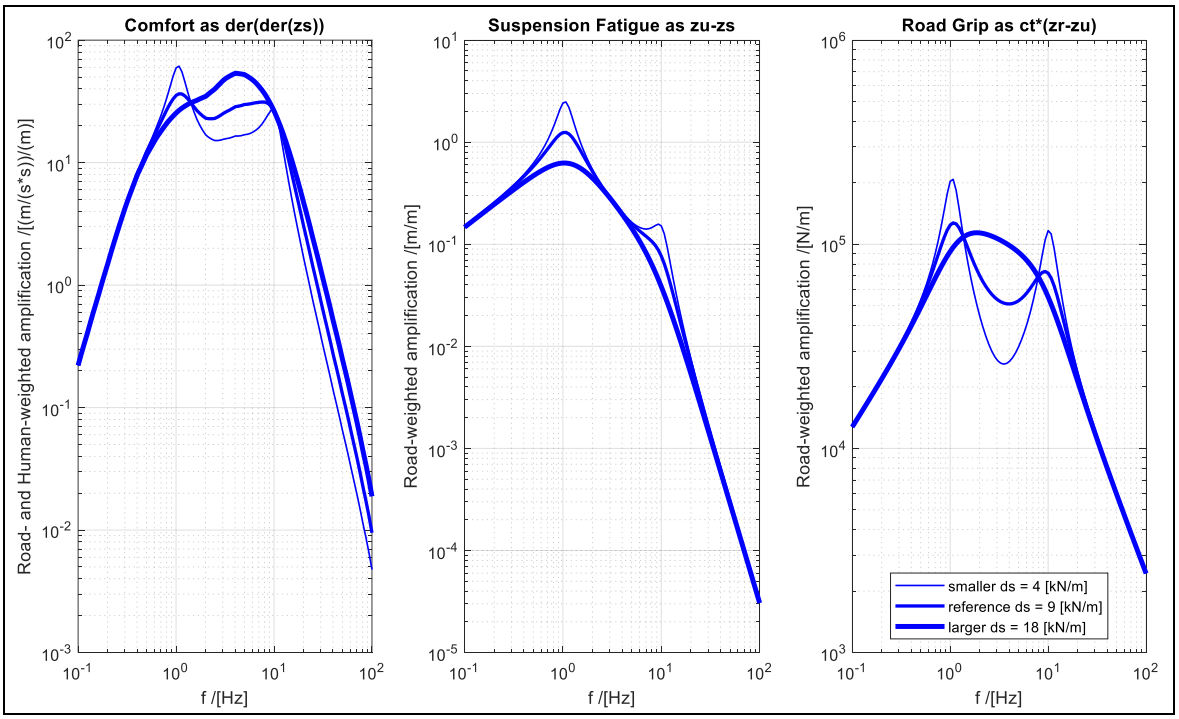


Figure 5-25: Variation of suspension damping, d_s

5.6.3 Varying Unsprung Mass

In Figure 5-26, we see that if the response around the wheel hop frequency is to be changed, the unsprung mass is one of the most influential parameters. The unsprung mass is usually in the range of 10% of the sprung mass. Opposite to the suspension parameters, the unsprung mass influences frequencies around the wheel hop frequency with little influence around the heave frequency.

In Figure 5-26, the case with $m_u = 0$ is added. This is to demonstrate what a model with neglected mass gives and can be nearly compared with the model in 5.4.2.

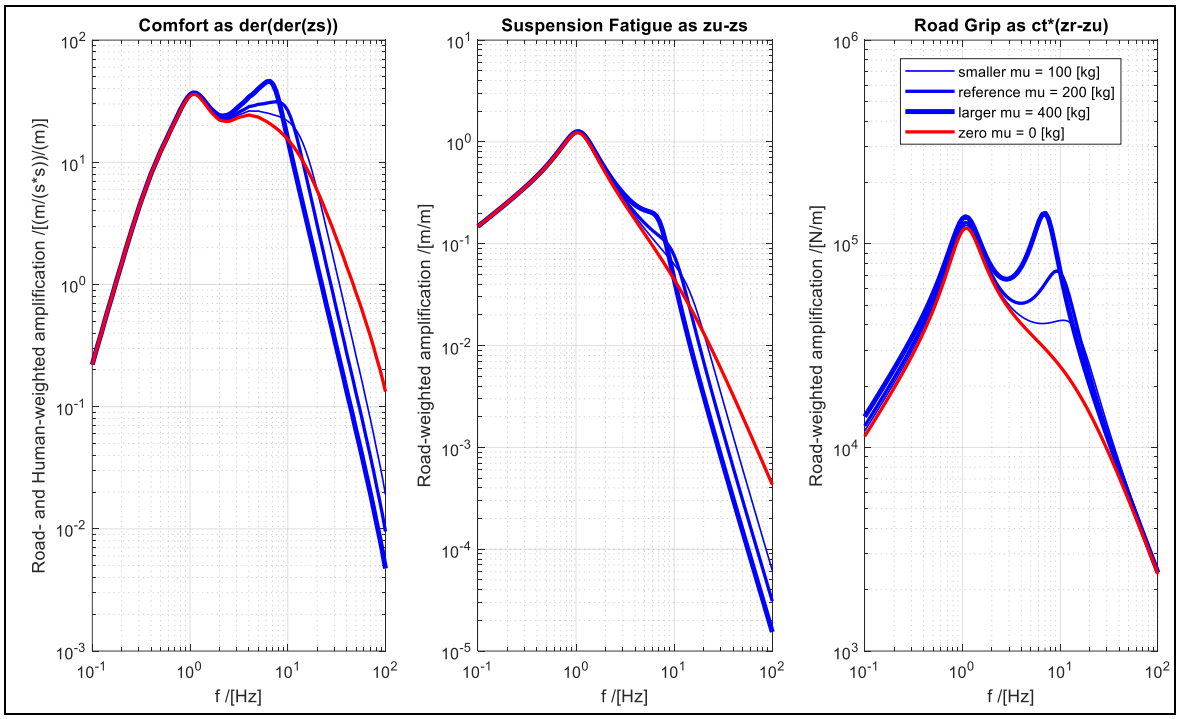


Figure 5-26: Variation of unsprung mass, m_u

5.6.4 Varying Tyre Stiffness

In Figure 5-27 a general observation is that low sprung mass natural frequencies are preferred for comfort considerations. Another parameter that has a strong affect near the wheel hop frequency is the tyre stiffness. The strongest response is noticed for the road grip function. (Note that, since c_t is now varying, we have to express road grip as $c_t \cdot (z_r - z_u)$; only $z_r - z_u$ does not give a fair comparison.)

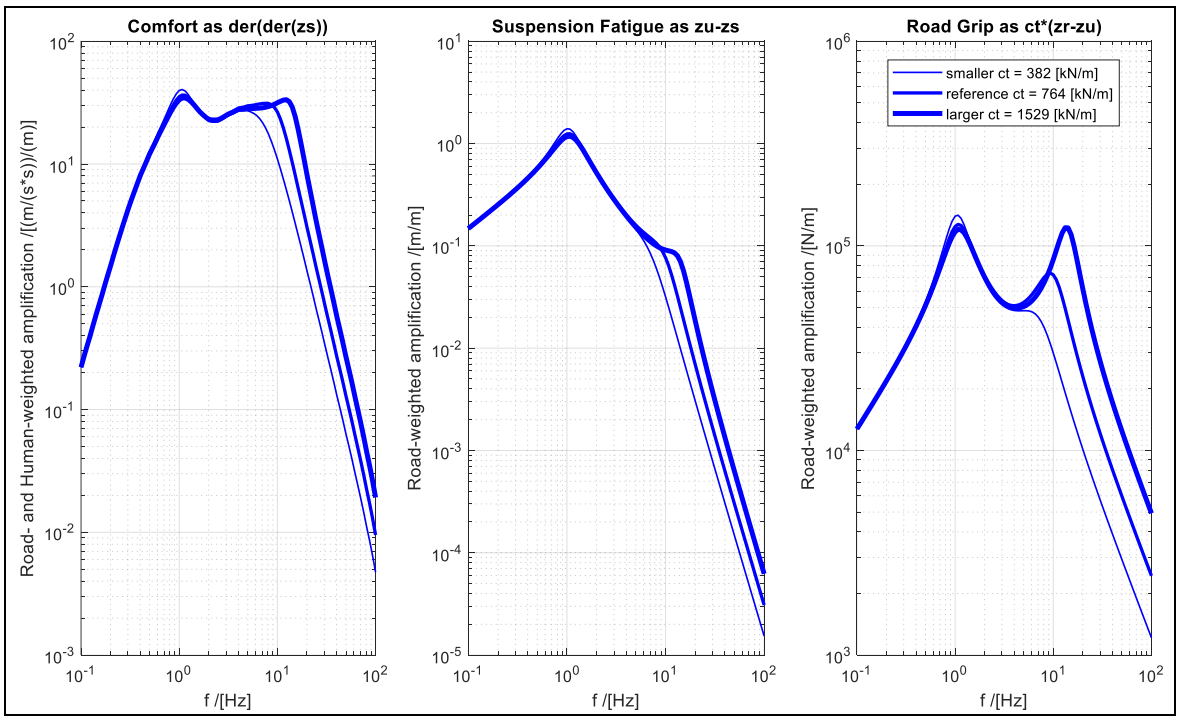


Figure 5-27: Variation of Tyre Stiffness, c_t

5.6.5 Varying Skyhook Damping

Contribution from Waltteri Koskinen, student at Tampere University, Finland

In figure below, the suspension dampers are replaced by ideal active dampers (ideal sensing, control algorithm computation and actuation), see 2.3.1.4. One can compare with how variation of (traditional) damper in Figure 5-25. The active dampers improve comfort and road grip, except for at wheel hop frequency around 10 Hz. The fatigue is generally worse. The transfer functions are plotted using the model in 5.4.3.2.

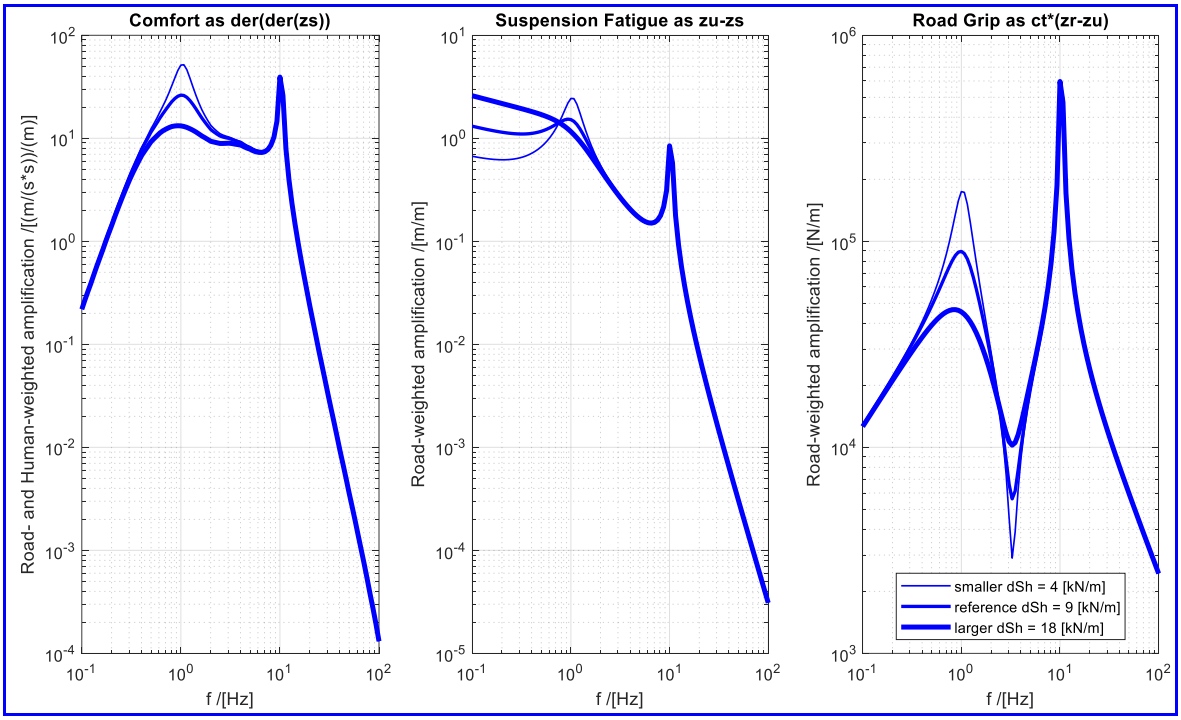


Figure 5-28: Variation of Skyhook damping, d_{Sh}

5.7 Two Dimensional Oscillations

The one-dimensional models (only heave) do not represent pitch and roll. Here, other models are needed, such as Figure 5-30 and Figure 5-29.

5.7.1 Heave and Roll

A model like in Figure 5-29 is proposed. We have been studying Heave (bounce) and pitch before, in 4.3.7.11 and 4.5.2.3. In Chapter 4, the excitation was lateral tyre/axle forces, while the vertical displacement of the road was assumed to be zero. In vertical vehicle dynamics, it is the opposite. That means that the linkage geometry (roll centre or wheel pivot points) is not so relevant here. So, the model can be somewhat simpler.

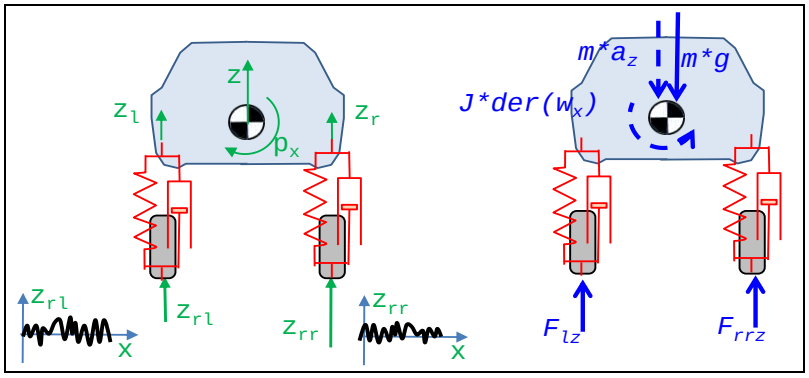


*Figure 5-29: Heave and roll model. Anti-roll bar not drawn but can be included in equations in matrix **C**.*

No equations are formulated for this model in this book, but a model will typically show two different modes, the heave and roll. Heave Eigen frequency is typically 1-1.5 Hz for a passenger car, as mentioned before. The roll frequency is similar or somewhat higher.

If modelling unsprung masses without inertia, we still get 2 state variables, heave z and roll φ_x. Using same mathematical form of equations as in Eq [5.45] we get this model (subscripts rl for "road left" and rr for "road right"):

$$\boldsymbol{M}\cdot\ddot{\boldsymbol{z}}+\boldsymbol{D}\cdot\dot{\boldsymbol{z}}+\boldsymbol{C}\cdot\boldsymbol{z}=\boldsymbol{D_r}\cdot\dot{\boldsymbol{z}}_{\boldsymbol{r}}+\boldsymbol{C_r}\cdot\boldsymbol{z_r};$$

$$where\ \boldsymbol{z}=\begin{bmatrix}z\\ \varphi_x\end{bmatrix}\ and\ \boldsymbol{z_r}=\begin{bmatrix}z_{rl}\\ z_{rr}\end{bmatrix};$$

The disturbances from the road are two independent ones, so the transfer functions will be a 2 × 2 matrix:

$$\begin{bmatrix}\mathcal{F}(z)\\ \mathcal{F}(\varphi_x)\end{bmatrix}=\boldsymbol{H}\cdot\begin{bmatrix}\mathcal{F}(z_{rl})\\ \mathcal{F}(z_{rr})\end{bmatrix}=\begin{bmatrix}H_{z_{rl}\to z} & H_{z_{rr}\to z}\\ H_{z_{rl}\to\varphi_x} & H_{z_{rr}\to\varphi_x}\end{bmatrix}\cdot\begin{bmatrix}\mathcal{F}(z_{rl})\\ \mathcal{F}(z_{rr})\end{bmatrix};$$

[5.56]

Note that the restoring matrix C might need to include both elastic restoring (wheel springs and anti-roll-bars) and (roll) pendulum effects, see 4.3.7.11.2 and Reference (Mägi, The Significance of System Pre-Load at Modal Analysis of Low-Resonant Mechanical Systems, 1988). For high-loaded trucks, the pendulum effect is really relevant, while it often can be omitted for a low sportscar.

5.7.2 Heave and Pitch

A model like in Figure 5-30 is proposed. We have been studying heave (or bounce) and pitch before, in 3.4.5.2. Hence compare with corresponding model in Figure 3-61. In Chapter **3**, the excitation was longitudinal tyre forces, while the vertical displacement of the road was assumed to be zero. In vertical vehicle dynamics, it is the opposite. The importance of model with linkage geometry (pitch centre or axle pivot points above ground level) is that tyre forces are transferred correctly to the body. That means that the linkage geometry is not so relevant for vertical vehicle dynamics in Chapter 5. So, the model can be somewhat simpler.

A mathematical model would typically show two different modes, see Figure 5-31. The heave eigen-frequency is typically 1-1.5 Hz for a passenger car. The pitch frequency is somewhat higher.

We should reflect on that the models in 5.4 and 5.7.1 refer to the same bounce mode. But the models will most likely give different numbers of, e.g., Eigen frequency. A total model, with all degrees of freedom, would align those values, but the larger a model is the more data it produces which often leads to less easy design decisions.

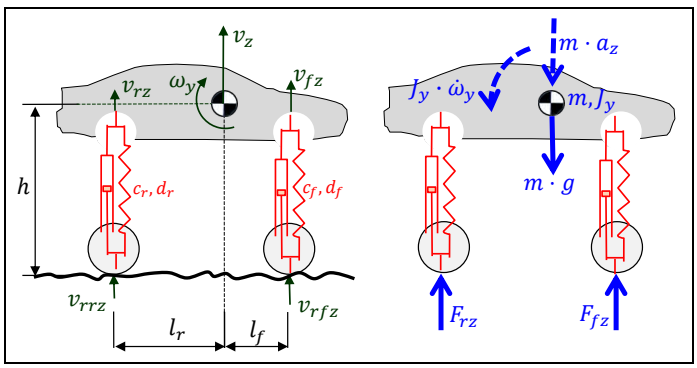


Figure 5-30: Heave and pitch physical model.

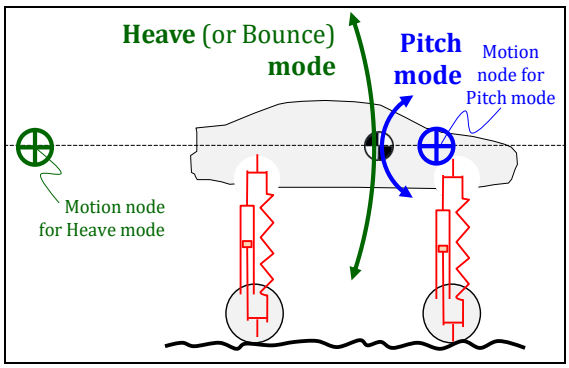


Figure 5-31: Oscillation modes of a Heave and Pitch model.

5.7.2.1 Wheelbase Filtering

See Figure 5-32. If the wheelbase is an integer multiple of the wavelength, only heave (bounce) will be excited. If wavelength is in the middle between those, only pitch will be excited. This phenomenon is called "wheelbase filtering".

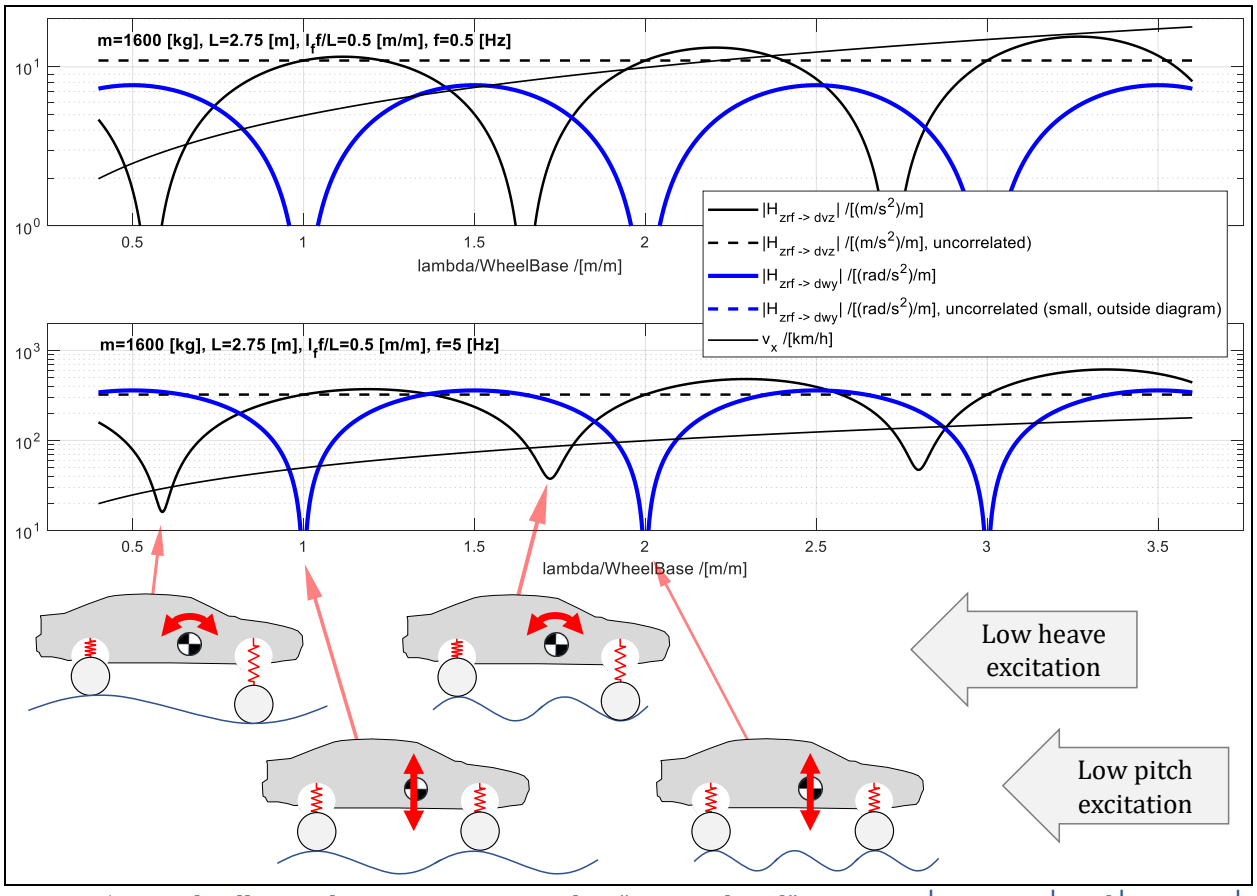


Figure 5-32: Wheelbase Filtering, as compared to "uncorrelated". Response $|H_{zrf\to vzg}|$ and $|H_{zrf\to\dot{\omega}y}|$. Two frequencies, 0.5 and 5 Hz. Varying Road Wavelengths, so also v_x has to vary.

5.7.2.2 Mathematical Model

From Figure 5-30 we can derive the following mathematical models:

Equilibrium: $F_{fz} + F_{rz} - m \cdot g - m \cdot a_z = 0;\quad and\quad -F_{fz} \cdot l_f + F_{rz} \cdot l_r - J_y \cdot \dot{\omega}_y = 0;$

Compatibility: $v_{fz} = v_z - l_f \cdot \omega_y;\quad and\quad v_{rz} = v_z + l_r \cdot \omega_y;$

Constitution: $F_{fz} = F_{fs} + d_f \cdot (v_{rfz} - v_{fz});\quad and\quad \dot{F}_{fs} = c_f \cdot (v_{rfz} - v_{fz});\quad and$
$F_{rz} = F_{rs} + d_r \cdot (v_{rrz} - v_{rz});\quad and\quad \dot{F}_{rs} = c_r \cdot (v_{rrz} - v_{rz});$

Above model is formulated on first order form ($m \cdot \dot{v} \cdots$; and $\dot{F}_s = c \cdot (\cdots)$;) to show an alternative to second order differential equation form ($m \cdot \ddot{z} \cdots$;) used in 5.4.

We need to express a_z in differentiated variables. Then we can either assume $[v_x, v_z] = [v_{xg}, v_{zg}]$; (velocity components in ground fixed directions) or $[v_x, v_z] = [v_{xv}, v_{zv}]$; (vehicle fixed directions). Both are correct, in similar way as for the yaw rotation, see 4.4.2.3.3. If ground fix: $[a_{xg}, a_{zg}] = [\dot{v}_{xg}, \dot{v}_{zg}]$;. If ground fix: $[a_{xv}, a_{zv}] = [\dot{v}_{xv} + v_{zv} \cdot \omega_y \approx \dot{v}_{xv}, \dot{v}_{zv} - v_{xv} \cdot \omega_y]$;. The intention for 5.7.2 is to study constant speed over ground, so we know $\dot{v}_{xg} = 0$;. Therefore it is easiest to use ground fix directions. We can compare with the pitching model in 3.4.5, which is typically used for longitudinal acceleration and braking. Then it is most natural to use vehicle fix and solve v_{xv} and v_{zv} as state variables in an ode.

We formulate the matrix form of the model in ground fix direction:

$$\underbrace{\begin{bmatrix} m & 0 & 0 & 0 \\ 0 & J_y & 0 & 0 \\ 0 & 0 & 1/c_f & 0 \\ 0 & 0 & 0 & 1/c_r \end{bmatrix}}_{\boldsymbol{MC}} \cdot \begin{bmatrix} \dot{v}_{zg} \\ \dot{\omega}_y \\ \dot{F}_{fs} \\ \dot{F}_{rs} \end{bmatrix} =$$

$$= \underbrace{\begin{bmatrix} -d_f - d_r & d_f \cdot l_f - d_r \cdot l_r & 1 & 1 \\ d_f \cdot l_f - d_r \cdot l_r & -d_f \cdot l_f^2 - d_r \cdot l_r^2 & -l_f & +l_r \\ -1 & +l_f & 0 & 0 \\ -1 & -l_r & 0 & 0 \end{bmatrix}}_{\boldsymbol{D}} \cdot \underbrace{\begin{bmatrix} v_{zg} \\ \omega_y \\ F_{fs} \\ F_{rs} \end{bmatrix}}_{\boldsymbol{z_{vF}}} + \underbrace{\begin{bmatrix} -m \cdot g \\ 0 \\ 0 \\ 0 \end{bmatrix}}_{\boldsymbol{g}} + \underbrace{\begin{bmatrix} d_f & d_r \\ -d_f \cdot l_f & d_r \cdot l_r \\ 1 & 0 \\ 0 & 1 \end{bmatrix}}_{\boldsymbol{D_r}} \cdot \underbrace{\begin{bmatrix} v_{rfz} \\ v_{rrz} \end{bmatrix}}_{\boldsymbol{z_{vr}}};$$

Variable substitution $\boldsymbol{z_{vF} = z_{vF0} - D^{-1} \cdot g}$; gives: $\boldsymbol{MC \cdot \dot{z}_{vF0} = D \cdot z_{vF0} + D_r \cdot z_{vrz}}$;.

Fourier transform gives: $\boldsymbol{j \cdot \omega \cdot MC \cdot \mathcal{F}(z_{vF0}) = D \cdot \mathcal{F}(z_{vF0}) + D_r \cdot \mathcal{F}(z_{vrz})}$;The Transfer functions in Figure 5-32 can now be plotted. Note that the driver comfort, earlier measured in vertical acceleration amplitude $\hat{a}_z = \text{amplitude}(\dot{v}_z)$;, now has two possibilities: $\hat{a}_{zg} = \text{amplitude}(\dot{v}_{zg}) = \hat{\dot{v}}_{zg}$; or $\hat{a}_{zv} = \text{amplitude}(\dot{v}_{zv} - v_{xv} \cdot \omega_y)$;. The latter one makes most sense, since seat and driver rotates with the vehicle. With this measure of driver comfort, the transfer function for a_z in Figure 5-32, $|H_{zrf \to \dot{v}z}| = |H_{zrf \to \dot{v}zg}|$, should be adjusted to $|H_{zrf \to \dot{v}zv}|$, for driver comfort measure.

If eliminating the forces, in the model in vehicle directions, we get the 2nd order differential equation:

$$\begin{bmatrix} m & 0 \\ 0 & J_y \end{bmatrix} \cdot \begin{bmatrix} \ddot{v}_{zg} \\ \ddot{\omega}_y \end{bmatrix} = \begin{bmatrix} -d_f - d_r & d_f \cdot l_f - d_r \cdot l_r \\ d_f \cdot l_f - d_r \cdot l_r & -d_f \cdot l_f^2 - d_r \cdot l_r^2 \end{bmatrix} \cdot \begin{bmatrix} \dot{v}_{zg} \\ \dot{\omega}_y \end{bmatrix} + \begin{bmatrix} 1 & 1 \\ -l_f & l_r \end{bmatrix} \cdot \begin{bmatrix} c_f & 0 \\ 0 & c_r \end{bmatrix}$$
$$\cdot \left(\begin{bmatrix} -1 & l_f \\ -1 & -l_r \end{bmatrix} \cdot \begin{bmatrix} v_{zg} \\ \omega_y \end{bmatrix} + \begin{bmatrix} v_{rfzg} \\ v_{rrzg} \end{bmatrix} \right) + \begin{bmatrix} d_f & d_r \\ -d_f \cdot l_f & d_r \cdot l_r \end{bmatrix} \cdot \begin{bmatrix} \dot{v}_{rfzg} \\ \dot{v}_{rrzg} \end{bmatrix};$$

5.7.2.2.1 Correlated or Wheelbase Filtered

Front and rear are excited with same frequencies, but delayed at the rear:

$$\boldsymbol{\mathcal{F}(z_{vrz})} = \begin{bmatrix} \mathcal{F}(v_{rfz}) \\ \mathcal{F}(v_{rrz}) \end{bmatrix} = \boldsymbol{\mathcal{F}}\left(\frac{d}{dt} \begin{bmatrix} z_{rf} \\ z_{rr} \end{bmatrix} \right) = \boldsymbol{\mathcal{F}}\left(\frac{d}{dt} \begin{bmatrix} \hat{z}_r \cdot \cos(\omega \cdot t) \\ \hat{z}_r \cdot \cos(\omega \cdot t - 2 \cdot \pi \cdot \lambda / L) \end{bmatrix} \right) =$$
$$= \begin{bmatrix} 1 \\ \cos(2 \cdot \pi \cdot \lambda / L) - j \cdot \sin(2 \cdot \pi \cdot \lambda / L) \end{bmatrix} \cdot \mathcal{F}(\hat{z}_r \cdot \cos(\omega \cdot t)) =$$
$$= \begin{bmatrix} 1 \\ \cos(2 \cdot \pi \cdot \lambda / L) - j \cdot \sin(2 \cdot \pi \cdot \lambda / L) \end{bmatrix} \cdot \mathcal{F}(v_{rfz}) =$$
$$= j \cdot \omega \cdot \begin{bmatrix} 1 \\ \cos(2 \cdot \pi \cdot \lambda / L) - j \cdot \sin(2 \cdot \pi \cdot \lambda / L) \end{bmatrix} \cdot \mathcal{F}(z_{rf}) = j \cdot \omega \cdot \boldsymbol{d_\lambda} \cdot \mathcal{F}(z_{rf});$$

Insertion gives: $\boldsymbol{j \cdot \omega \cdot MC \cdot \mathcal{F}(z_{vF0}) = D \cdot \mathcal{F}(z_{vF0}) + D_r \cdot j \cdot \omega \cdot d_\lambda \cdot \mathcal{F}(z_{rf})}$; $\Rightarrow$

$$\Rightarrow \boldsymbol{\mathcal{F}(z_{vF0})} = (\boldsymbol{j \cdot \omega \cdot MC - D})^{-1} \cdot \boldsymbol{D_r} \cdot j \cdot \omega \cdot \boldsymbol{d_\lambda} \cdot \mathcal{F}(z_{rf}) = \begin{bmatrix} H_{z_{rf} \to v_z} \\ H_{z_{rf} \to \omega_y} \\ H_{z_{rf} \to F_{fs}} \\ H_{z_{rf} \to F_{rs}} \end{bmatrix} \cdot \mathcal{F}(z_{rf}) = \boldsymbol{H_{z_{rf} \to v_z, corr}} \cdot \mathcal{F}(z_{rf});$$

All H depend on ω (or λ) and v_x.

5.7.2.2.2 Uncorrelated

We now assume that front and rear are excited "uncorrelated". This is wrong if driving on a road where rear axle follows front axle, but it is correct for a vehicle with independent excitation under each axle, which can be achieved e.g. in a shake rig.

$$\boldsymbol{\mathcal{F}(z_{vr})} = \begin{bmatrix} \mathcal{F}(v_{rfz}) \\ \mathcal{F}(v_{rrz}) \end{bmatrix} = \begin{bmatrix} \mathcal{F}(\dot{z}_{rf}) \\ \mathcal{F}(\dot{z}_{rr}) \end{bmatrix} = j \cdot \omega \cdot \begin{bmatrix} \mathcal{F}(z_{rf}) \\ \mathcal{F}(z_{rr}) \end{bmatrix};$$

$$\boldsymbol{\mathcal{F}}(\boldsymbol{z_{vF0}}) = (j \cdot \omega \cdot \boldsymbol{MC} - \boldsymbol{D})^{-1} \cdot \boldsymbol{D_r} \cdot j \cdot \omega \cdot \begin{bmatrix} \mathcal{F}(z_{rf}) \\ \mathcal{F}(z_{rr}) \end{bmatrix} = \begin{bmatrix} H_{z_{rf}\to v_z,uncorr} & H_{z_{rr}\to v_z,uncorr} \\ H_{z_{rf}\to \omega_y,uncorr} & H_{z_{rr}\to \omega_y,uncorr} \\ H_{z_{rf}\to F_{fs},uncorr} & H_{z_{rr}\to F_{fs},uncorr} \\ H_{z_{rf}\to F_{rs},uncorr} & H_{z_{rr}\to F_{rs},uncorr} \end{bmatrix} \cdot \begin{bmatrix} \mathcal{F}(z_{rf}) \\ \mathcal{F}(z_{rr}) \end{bmatrix};$$

If z_{rf} and z_{rf} have the same amplitude(frequency) content, and is called z_r, we can write:

$$\boldsymbol{\mathcal{F}}(\boldsymbol{z_{vF0}}) = \begin{bmatrix} H_{z_{rf}\to v_z,uncorr} & H_{z_{rr}\to v_z,uncorr} \\ H_{z_{rf}\to \omega_y,uncorr} & H_{z_{rr}\to \omega_y,uncorr} \\ H_{z_{rf}\to F_{fs},uncorr} & H_{z_{rr}\to F_{fs},uncorr} \\ H_{z_{rf}\to F_{rs},uncorr} & H_{z_{rr}\to F_{rs},uncorr} \end{bmatrix} \cdot \begin{bmatrix} 1 \\ 1 \end{bmatrix} \cdot \mathcal{F}(z_r) = \boldsymbol{H_{z_r\to v_z,uncorr}} \cdot \mathcal{F}(z_r);$$

The elements in H depend on ω (or λ) and v_x.

5.8 Three Dimensional Oscillations

A real road generates motion in all out-of-road-plane dimensions: heave z, roll φ_x and pitch φ_y. One can, for instance, use [5.27] to generate a vertical profile for each side of the vehicle, but then randomly generate different phases for each side. Another way is to record a certain piece of a road, typically at the vehicle manufacturer's test track. One then gets wheelbase filtering one each side and a roll influence due to that left and right side are not in phase with each other.

If modelling unsprung masses without inertia, we still get 3 state variables: heave z, pitch φ_y and roll φ_y. Using same form of equations as in Eq [5.45] we get this model (subscripts rfl for "road front left" and so on):

$$\boldsymbol{M} \cdot \ddot{\boldsymbol{z}} + \boldsymbol{D} \cdot \dot{\boldsymbol{z}} + \boldsymbol{C} \cdot \boldsymbol{z} = \boldsymbol{D_r} \cdot \dot{\boldsymbol{z}}_{\boldsymbol{r}} + \boldsymbol{C_r} \cdot \boldsymbol{z_r};$$

$$where\ \boldsymbol{z} = \begin{bmatrix} z \\ \varphi_x \\ \varphi_y \end{bmatrix};$$

$$and\ \boldsymbol{z_r} = \begin{bmatrix} z_{rfl} \\ z_{rfr} \\ z_{rrl} \\ z_{rrr} \end{bmatrix} = \begin{bmatrix} 1 & 0 \\ 0 & 1 \\ \cos(\varphi) + j \cdot \sin(\varphi) & 0 \\ 0 & \cos(\varphi) + j \cdot \sin(\varphi) \end{bmatrix} \cdot \begin{bmatrix} z_{rfl} \\ z_{rfr} \end{bmatrix};$$

$$where\ \varphi = 2 \cdot \pi \cdot L / v_x\ ;$$

The disturbances from the road are two independent ones, so the transfer functions will be a 3 × 2 matrix:

$$\begin{bmatrix} \mathcal{F}(z) \\ \mathcal{F}(\varphi_x) \\ \mathcal{F}(\varphi_y) \end{bmatrix} = \boldsymbol{H} \cdot \begin{bmatrix} \mathcal{F}(z_{rfl}) \\ \mathcal{F}(z_{rfr}) \end{bmatrix} = \begin{bmatrix} H_{z_{rfl}\to z} & H_{z_{rfr}\to z} \\ H_{z_{rfl}\to \varphi_x} & H_{z_{rfr}\to \varphi_x} \\ H_{z_{rfl}\to \varphi_y} & H_{z_{rfr}\to \varphi_y} \end{bmatrix} \cdot \begin{bmatrix} \mathcal{F}(z_{rl}) \\ \mathcal{F}(z_{rr}) \end{bmatrix};$$

[5.57]

5.9 Transient Vertical Dynamics

Most of the chapter you read now, considers driving for during long time periods on roads with repetitive unevenness. This is one relevant use case, and the functions are then suitably analysed using frequency analysis, since the quantities vary as stationary oscillations.

However, vertical vehicle dynamics also have transient disturbances to consider. Test cases can be one-sided or two sides road bumps or potholes. Two-sided bump is envisioned in Figure 5-33. It can represent driving over a speed bump or a low obstacle.

The models from earlier in this chapter are all relevant for two-sided bumps or holes, but the presented computations earlier in this chapter is only for stationary oscillations. The models can be used also for transient response, e.g. by simulating a step road height z_r. However, it should be mentioned that one also might need to model non-linearities such as bump stops or wheel lift as well as different damping in compression and rebound. Also, the longitudinal force play often becomes important to model, such as suspension kinematics and compliance, more careful models of tyre deformation, and sometimes wheel torque. The function measures (and requirements) should be shifted somewhat:

- Human **comfort** for transients is often better described as time derivative of acceleration (called "jerk"). Peak-to-peak values of the variables can be used. Reference (ISO 2631) is primarily for stationary oscillations, but it has some about transient comfort. However, it is difficult to apply.
- The material **loads** are more of maximum load type than fatigue life dimensioning, i.e. higher material stress but fewer load cycles during vehicle lifetime.
- **Road grip** studies over road bumps and potholes are challenging. Qualitatively, the tyre models often must include relaxation, because that is the mechanism which reduces road grip when vertical load shifts. To get quantitatively correct tyre models is beyond the goal of the book you presently read.
- **Roll-over** can be tripped by large one-sided bumps. This kind of roll-overs is unusual and requires complex models.

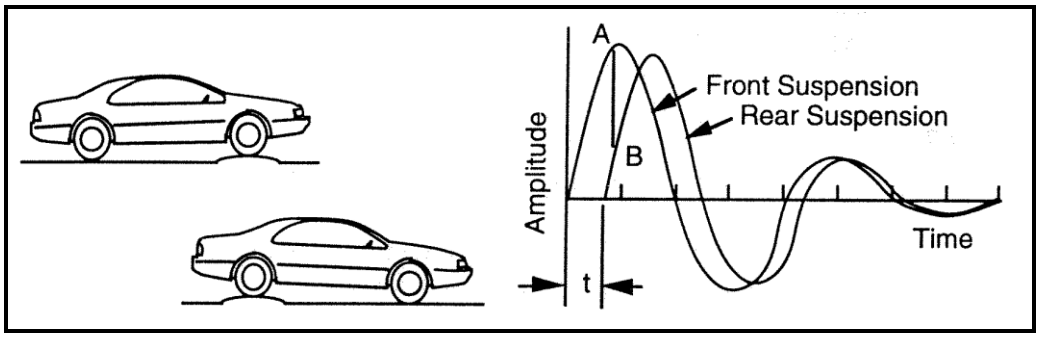


Figure 5-33: Response of Vehicle for Front and Rear Axle Impulses, (Gillespie, 1992)

Models for studying transient vertical dynamics can, in general be categorized as the stationary oscillation models, 1D, 2D and 3D. But they cannot generally be linear, so they require simulation, not frequency analysis. One typically need to add inertia of unsprung parts and vertical elasticities in each tyre. And "trivial linkage" suspension is generally not enough if sharp road unevenness, but instead one might identify the pivot axis in space for each wheel linkage.

A 3D model according to these concepts gets the states $\boldsymbol{z}$ containing $z,\ \varphi_x,\ \varphi_y,\ z_{fl},\ z_{fr},\ z_{rl},\ and\ z_{rr}$ if modelled with a second order differential equation ($\boldsymbol{f}(\ddot{\boldsymbol{z}}, \dot{\boldsymbol{z}}, \boldsymbol{z}, \boldsymbol{u}, t) = 0$;). If modelled with first order differential equations ($\boldsymbol{f}(\dot{\boldsymbol{z}}, \boldsymbol{z}, \boldsymbol{u}, t) = 0$;) and the concept of using forces in elasticities as states, see 1.5.2.1.2, the states z will instead contain $z,\ \varphi_x,\ \varphi_y,\ v_{flz},\ v_{frz},\ v_{rlz},\ v_{rrz},\ F_{sfl},\ F_{sfr},\ F_{srl},\ and\ F_{srr}$, where v_{ijz} is vertical velocity of unsprung mass in wheel ij and F_{sij} is elastic part of vertical force under wheel ij. The inputs (disturbance) $\boldsymbol{u} = \boldsymbol{z_r}$ will contain $z_{rfl},\ z_{rfr},\ z_{rrl},\ and\ z_{rrr}$.

5.10 Control Functions

This section about Control functions for vertical dynamics is much smaller than corresponding for other direction, 3.5 and 4.6. Vertical Control Functions do exist, e.g., levelling control, active anti-rollbars, and active damper control. However, they are less common and generally influence less than the stronger propulsion, brake, and steering control functions. The book does not go deep into this area, but some is covered in 2.3.1.4 and 5.4.3.2.

BIBLIOGRAPHY

AB Volvo. (2011). *Global Transport Application.*

Andreasson, J. (2007). *On Generic Road Vehicle Motion Modelling and Control.* Stockholm: KTH.

Askerdal, M. (2023). *On motion resistance estimation and modeling for heterogeneous road vehicles.* Licentiate thesis. Hämtat från https://research.chalmers.se/en/publication/535577

Bakker, E. N. (1987). *Tyre Modelling for use in Vehicle Dynamics Studies.*

Barnard, R. (2010). *Road Vehicle Aerodynamic Design.* Mechaero Publishing.

Barnard, R. H. (u.d.). *Road Vehicle Aerodynamic Design.* Mechaero Publishing.

Besselink, I. J. (2011). Experiences with the TYDEX standard tyre interface and file format. *Vehicle System Dynamics*. doi:https://doi.org/10.1080/00423110500109299

Blundell, M., & Harty, D. (2014). *The Multibody Systems Approach to Vehicle Dynamics.* Elsevier Science & Technology. Retrieved from https://ebookcentral.proquest.com/lib/chalmers/detail.action?docID=1790885

Boerboom, M. (2012). *Electric Vehicle Blended Braking maximizing energy recovery while maintaining vehicle stability and maneuverability.* Göteborg, Sweden: Chalmers University of Technology.

Brian Bole, e. a. (2012). *Energy Management Control of a Hybrid Electric Vehicle with Two-Mode Electrically Variable Transmission.* Los Angeles: 2012 Electric Vehicle Symposium, EVS26. doi:10.13140/2.1.2827.6480

Bruzelius, F. (2004). *Linear Parameter-Varying Systems - an approach to gain scheduling* (Vol. Doctoral thesis). Chalmers University of Technology.

Clark, S. (. (1971). *Mechanics of Pneumatic Tires, Monograph 122.* National Bureau of Standards, USA.

Cooper Tire & Rubber Co. (den 16 September 2007). *Passenger radial tire cutaway. Online Art.* (Cooper Tire & Rubber Co.) Hämtat från http://deantires.com/us/en/information/info-construction.asp

DIRECTIVE 2002/44/EC. (2002). *DIRECTIVE 2002/44/EC OF THE EUROPEAN PARLIAMENT AND OF THE COUNCIL.*

Drenth, E. F. (1993). *Brake Stability of Front Wheel Driven Cars at High Speed.* Delft, Netherlands: Delft University of Technology.

Dugoff, H., Fancher, P., & Segel, L. (1969). *Tire performance characteristics affecting vehicle response to steering and braking control inputs. Final report.* Washington, US. Hämtat från http://hdl.handle.net/2027.42/1387

Ejsmont, J. A., & et al. (2017). Road texture influence on tyre rolling resistance. *Road Materials and Pavement Design*, 181-198.

Elmqvist, H. (2014). A short history of Modelica. *10th International Modelica Conference*, ss. 1-12. Hämtat från https://ep.liu.se/ecp/096/001/ecp14096001.pdf

Encyclopædia Britannica Online. (2007, September 16). *belted tire: tire designs." Online Art. Encyclopædia Britannica Online.* Retrieved from http://www.britannica.com/eb/art-7786

European Comission, D.-G. (accessed 2026-10-04). *Vehicle Energy Consumption calculation TOol - VECTO.* European comission. Hämtat från https://climate.ec.europa.eu/areas-

action/transport-decarbonisation/road-transport/vehicle-energy-consumption-calculation-tool-vecto_en

Ghandriz, T. (2020). *Transportation Mission-Based Optimization of Heavy Combination Road Vehicles and Distributed Propulsion, Including Predictive Energy and Motion Control.* Göteborg, Sweden: Chalmers University of Technology. Retrieved from https://research.chalmers.se/en/publication/520358

Gillespie, T. (1992). *Fundamentals of Vehicle Dynamics.* Society of Automotive Engineers.

Grosch, K., & Schallamach, A. (1961, September–October). Tyre wear at controlled slip. *Wear, Volume 4*(Issue 5), pp. Pages 356–371.

Happian-Smith, J. (2002). *An Introduction to Modern Vehicle Design.* Butterwoth-Heinemann, ISBN 0-7506-5044-3.

Hedman, A. (1994). *Intermittent Engine Operation -- A Way to Reduce Vehicle Fuel Consumption.* Beijing: FISITA, XXV FISITA Congress, 17-21 October 1994.

Hirschberg, W., Rill, G., & Weinfurter, H. (2007). Tire model TMeasy. *Vehicle System Dynamics, 45:1*, pp. 101 — 119. doi:10.1080/00423110701776284

Huang, Y. (2025). *Artificial Intelligence supported road vehicle suspension design.* Göteborg, Sweden: Chalmers University of Technology. Hämtat från https://research.chalmers.se/en/publication/547459

Hucho, W.-H. (1998). *Aerodynamics of Road Vehicles.* SAE International.

Hyttinen, J. (2023). *Modelling and experimental testing of truck tyre rolling resistance.* Stockholm: KTH. Hämtat från https://kth.diva-portal.org/smash/record.jsf?pid=diva2%3A1794138&dswid=2648

ISO 11026. (u.d.). *ISO 11026 Heavy commercial vehicles and buses - Test method for roll stability - Closing-curve test.* International Organization for Standardization, Genève, Switzerland.

ISO 11992. (2003). *ISO 11992 Road vehicles – Interchange of digital information on electrical connections between towing and towed vehicles.* ISO.

ISO 14791. (u.d.). *ISO 14791 Road vehicles - Heavy commercial vehicle combinations and articulated buses - Lateral stability test methods.* International Organization for Standardization, Genève, Switzerland.

ISO 14792. (u.d.). *ISO 14792 Road vehicles - Heavy commercial vehicles and buses - Steady-state circular tests.* International Organization for Standardization, Genève, Switzerland.

ISO 14793. (u.d.). *ISO 14793 Road vehicles – Heavy commercial vehicles and buses – Lateral transient response test methods.* International Organization for Standardization, Genève, Switzerland.

ISO 14794. (2011). *ISO 14794 Heavy commercial vehicles and buses - Braking in a turn - Open-loop test methods.* International Organization for Standardization, Genève, Switzerland.

ISO. (2006). *Passenger cars – Braking in a turn – Open-loop test method.* ISO.

ISO. (2011). *ISO 14794 Heavy commercial vehicles and buses - Braking in a turn - Open-loop test methods.* ISO.

ISO 26262. (2011-2012). *Road vehicles – Functional safety, 1-10.* International Organization for Standardization, Genève, Switzerland.

ISO 2631. (n.d.). *ISO 2631 – Evaluation of Human Exposure to Whole-Body Vibration.* International Organization for Standardization, Genève, Switzerland.

ISO 3888. (u.d.). *ISO 3888 Passenenger Cars -- Test track for severe lane change manouvre -- Part 2: Obstacle Avoidance.* International Organization for Standardization, Genève, Switzerland.

ISO 4130. (u.d.). *ISO 4130: Road vehicles -- Three-dimensional reference system and fidicial marks -- Definitions, 1979.*

ISO 4138. (u.d.). *ISO 4138 Passenger cars – Steady-state circular driving behaviour - Open-loop test methods.* International Organization for Standardization, Genève, Switzerland.

ISO 7401. (u.d.). *ISO 7401 Lateral transient response test methods - Open-loop test methods.* International Organization for Standardization, Genève, Switzerland.

ISO 7975. (2006). *ISO 7975 Passenger cars – Braking in a turn – Open-loop test method.* International Organization for Standardization, Genève, Switzerland.

ISO 80000-1. (2013). *ISO 80000 - Quantities and units - Part 1: General.* International Organization for Standardization (ISO), Geneva, Switzerland.

ISO 80000-3. (2013). *ISO 80000 – Quantities and units – Part 3: Space and time.* International Organization for Standardization, Genève, Switzerland.

ISO 8608. (u.d.). *ISO 8608 Mechanical vibration - Road surface profiles - Reporting of measured data.* International Organization for Standardization, Genève, Switzerland.

ISO 8855. (n.d.). *ISO 8855 – Road vehicle – Vehicle dynamics and road holding ability – Vocabulary.* International Organization for Standardization, Genève, Switzerland.

ISO19377. (2017). *ISO 19377 Heavy commercial vehicles and buses - Emergency braking on a defined path - Test method for trajectory measurement.* ISO.

ISO28580. (2018). *Passenger car, truck and bus tyre rolling resistance measurement method -- single point test and correlation of measurement results.* ISO.

J. Lepine, X. N. (2022). An empirical tire-wear model for. *Tire Sci. Technol., vol. 50, no. 3*, 211-229.

Jacobson, B. (1993). *Gear Shifting with Retained Power Transfer.* Göteborg, Sweden: Chalmers Univeristy of Technology. Hämtat från https://research.chalmers.se/en/publication/1485

Jacobson, B. e. (2014). *Vehicle Dynamics Compendium for Course MMF062.* Göteborg, Sweden: Chalmers University of Technology.

Jacobson, B. e. (2020). *Vehicle Dynamics Compendium.* Göteborg, Sweden: Chalmers University of Technology.

Jacobson, B., & Spickenreuther, M. (2003). Gearshift sequence optimisation for vehicles with automated non-powershifting transmissions. *International Journal of Vehicle Design, Vol. 32, Nos. 3/4*, 187-207. Hämtat från https://research.chalmers.se/publication/191083

Jacobson, B., Sundström, P., Kharrazi, S., Fröjd, N., & Islam, M. (2017). *An Open Assessment Tool for Performance Based Standards of Long Combination Vehicles.* Hämtat från https://research.chalmers.se/en/publication/251269

Jonasson, M. (2009). *Exploiting individual wheel actuators to enhance vehicle dynamics and safety in electric vehicles* (Vol. Doctoral thesis). Stockholm: Royal Insitute of Technology.

Jonsson, A., & Olsson, E. (2016). *A Methodology for Identification of Magic Formula Tire Model Parameters from In-Vehicle Measurements.* Chalmers University of Technology. Hämtat från http://studentarbeten.chalmers.se/publication/239258-a-methodology-for-identification-of-magic-formula-tire-model-parameters-from-in-vehicle-measurements

Kati, M. S. (2013). *Definitions of Performance Based Characteristics for Long Heavy Vehicle Combinations.* Signals and Systems. Chalmers University of Technology. Hämtat från http://publications.lib.chalmers.se/records/fulltext/176464/176464.pdf

Kharrazi , S. (2012). *Steering Based Lateral Performance Control of Long Heavy Vehicle Combinations.* Göteborg, Sweden: Chalmers University of Technology.

Kiencke, U. a. (2005). *Automotive Control Systems.*

Klomp, M., & Thomson, R. (2010). *Influence of Front/Rear Drive Force Distribution on the Lateral Grip and Understeer of All-Wheel Drive Vehicles.* Chalmers University of Technology, Göteborg, Sweden. Hämtat från https://research.chalmers.se/en/publication/122777

Kopplow, H. W. (2023). AXLE DESIGN AS A KEY FACTOR FOR GREENING ROAD FREIGHT. *HVTT17 conference: Technology Convergence 2023, Setting the Wheels In Motion: Reimagining the future of heavy vehicles, roads and freight.* Brisbane: HVTT. Hämtat från https://hvttforum.org/wp-content/uploads/2023/12/HVTT17_paper_5155_Kopplow.pdf

Lex, C. (2015). *Estimation of the Maximum Coefficient of Friction between Tire and Road based on Vehicle State measurements.* Graz: Graz University of Technology.

Lidberg, M., & Alfredsson, J. (2009). Control of the Direction Sensitive Locking Differential (DSLD) for a Front Wheel Drive Passenger Car in Transient Cornering. Proceedings of the IAVSD'09 Conference.

Ludwig, C., & Kim, C. (2017). *Influence of testing surface on tire lateral force characteristics.* München: Springer Fachmedien.

Mahmoudi, A., Soong, W. L., Pellegrino, G., & Armando, E. (2015). Efficiency maps of electrical machines. Hämtat från https://iris.polito.it/handle/11583/2627142

Metzler, M., Tavernini, D., Gruber, P., & Sorniotti, A. (2020). On Prediction Model Fidelity in Explicit Nonlinear Model Predictive Vehicle Stability Control. *IEEE Transactions on Control Systems Technology*. doi:10.1109/TCST.2020.3012683

Michelin. (2003). *The tyre Rolling resistance and fuel savings.* Michelin.

Mägi, M. (1988). *The Significance of System Pre-Load at Modal Analysis of Low-Resonant Mechanical Systems.* Århus, Denmark: Modal Testing & FEM Seminar in Århus.

Mägi, M., Jacobson, B., & Resev, J. (1998). *DYNAMIC ANALYSIS OF PLANETARY GEAR TRAINS.* Tallin. Hämtat från https://research.chalmers.se/en/publication/191074

Newton, I. (1687-07-05). *Philosophiæ Naturalis Principia Mathematica.*

NHTSA. (u.d.). *Electronic Stability Control Systems.* NHTSA.

Pacejka, H. (2005). *Tyre and Vehicle Dynamics, 2nd ed.* Elsevier.

Pettersson, P. (2017). *On Numerical Descriptions of Road Transport Missions.* Gothenburg, Sweden: Chalmers University of Technology. Hämtat från https://research.chalmers.se/en/publication/249525

Pettersson, P. (2019). *Operation cycles representations for road vehicles.* Göteborg: Chalmers University of Technology.

Ploechl, M. (Red.). (2013). *Road and Off-Road Vehicle System Dynamics Handbook.* CRC Press.

Rajamani, R. (2012). *Vehicle Dynamics and Control.* Springer. Hämtat från http://link.springer.com/book/10.1007%2F978-1-4614-1433-9

Rhyne, T. B. (2005). *Development of a Vertical Stiffness Relationship for Belted Radial Tires.* Tire Science and Technology, TSTCA, Vol. 33, no. 3, July-September 2005.

Rill, G. (2006). *FIRST ORDER TIRE DYNAMICS.* Lisbon, Portugal: III European Conference on Computational Mechanics Solids, Structures and Coupled Problems in Engineering, 5–8 June 2006. Hämtat från https://hps.hs-regensburg.de/~rig39165/paper/First_Order_Tire_Dynamics.pdf

Robert Bosch GmbH. (2004). *Bosch Automotive Handbook 6th Edition.* Bentley Publishes.

Romano, L. (2022). *Advanced Brush Tyre Modelling.* Springer. doi:10.1007/978-3-030-98435-9_3

Romano, L. (2022). *Brush model simulator (Matlab code)*. Hämtat från https://research.chalmers.se/publication/531276

Romano, L. (2023). *The operating cycle representation of road transport missions.* Chalmers university of technology. Hämtat från www.research.chalmers.se

Romano, L., Bruzelius, F., & Jacobson, B. J. (2020). Unsteady-state brush theory. *Vehicle System Dynamics*. Retrieved from https://research.chalmers.se/publication/517277

Ross, I. M. (2015). *A Primer on Pontryagin's Principle in Optimal Control.*

Rösth, M. (2007). *Hydraulic Power Steering System Design in Road Vehicles: Analysis, Testing and Enhanced Functionality.* Linköping: Linköping Univeristy, Department of Management and Engineering, Fluid and Mechatronic Systems.

SAE J1441. (2016.). *Standard J1441, Subjective Rating Scale for Vehicle Ride and Handling.* SAE International, .

SAE_J3016. (2016). *SAE J3016 Taxonomy and Definitions for Terms Related toDriving Automation Systems for On-Road Motor Vehicles.* SAE International.

SAEJ670. (u.d.). *SAE J670e - Vehicle Dynamics Terminology.* Society of Automotive Engineers, Warrendale, PA, USA.

Sander, U. (2018). *Predicting Safety Benefits of Automated Emergency Braking in Intersections -- Virtual simulations based on real-world accident data.* Göteborg: Chalmers University of Technology, PhD thesis.

Schuetz, T. (2015). *Aerodynamics of Road Vehicles, Fifth Edition.* SAE.

Schuring, D. (1980). *The Rolling Loss of Pneumatic Tires.* doi:10.5254/1.3535054

Sivaramakrishnan, P., Madhava Prakash, A., Sekulic, D., Jacobson, B., Selvi, C., & Moe Johannesen, S. (2023). Methods to introduce floating bridge motion and wind excitation on a model for the investigation of heavy vehicle dynamics. *Applied Mathematical Modelling, 117*, 118-141. doi:https://doi.org/10.1016/j.apm.2022.11.038

Sundström, P., Jacobson, B., & Laine, L. (2014). Vectorized single-track model in Modelica for articulated vehicles with arbitrary number of units and axles. Lund, Sweden: Modelica conference 2014, March 10-12, 2014. Hämtat från http://publications.lib.chalmers.se/publication/190501

Svendenius, J. (2003). *Tire Models for Use in Braking Applications.* Licentiate Thesis, Lund Insitute of Technology. Hämtat från https://portal.research.lu.se/files/4386030/8840416.pdf

Svendenius, J. (2007). *Tire Modeling and Friction Estimation.* Lund, Sweden: Department of Automatic Control, Lund University.

Tagesson, K. (2017). *Driver-centred Motion Control of Heavy Trucks.* Gothenburg, Sweden: Chalmers University of Technology.

Tagesson, K., & Cole, D. (2017). Advanced emergency braking under split friction conditions and the influence of a destabilising steering wheel torque. *Vehicle System Dynamics, 55*. doi:http://dx.doi.org/10.1080/00423114.2017.1278779

Tiller, M. (2019). *Modelica by example*. Hämtat från https://mbe.modelica.university/ den 4 June 2019

UN ECE 111. (2001). *UNIFORM PROVISIONS CONCERNING THE APPROVAL OF TANK VEHICLES OF CATEGORIES N AND O WITH REGARD TO ROLLOVER STABILITY.* UNITED NATIONS. Hämtat från http://www.unece.org/fileadmin/DAM/trans/main/wp29/wp29regs/r111e.pdf

Utbult, J., Jonasson, M., Yang, D., & Jacobson, B. (2020). Energy reduction by power loss minimisation through wheel torque allocation in electric vehicles. *Vehicle Systems Dynamics*.

Weber, R. (1981). *Reifen Führungskräfte bei schnellen Änderungen von Schräglauf und Schlupf.* Karlsruhe: University of Karlsruhe.

Wedlin, J., Tillback, L.-R., & Bane, O. (1992). *Combining Properties for Driving Pleasure and Driving Safety: A Challenge for the Chassis Engineer.* SAE. doi:10.4271/921595

Wipke, K. B., Cuddy, M. R., & Burch, S. D. (1999). ADVISOR 2.1: A User-Friendly Advanced Powertrain Simulation Using a Combined Backward/Forward Approach. *IEEE TRANSACTIONS ON VEHICULAR TECHNOLOGY, 48*(6), ss. 1751-1761.

Wong, J. (2001). *Theory of Ground Vehicles (3rd ed.).* John Wiley and Sons, Inc., New York.

Yang, D. (2013). *Vehicle Dynamics Control after Impacts in Multiple-Event Accidents.* Göteborg: Chalmers University of Technology. Hämtat från http://publications.lib.chalmers.se/publication/182012-vehicle-dynamics-control-after-impacts-in-multiple-event-accidents

Zhaohui Ge, F. B. (2024). Long Combination Vehicles Reverse Strategies Based on Articulation Angle Gradient. *16th International Symposium on Advanced Vehicle Control, Proceedings of AVEC'24 –.* Society of Automotive Engineers of Japan. Hämtat från https://research.chalmers.se/en/publication/543376

Åberg, E. (2021). *Modelica Series*. Retrieved from Eradity: https://www.eradity.com/blog/29-modelica-series-introduction-to-modelica

COURSE MMF062 VEHICLE MOTION ENGINEERING

This Appendix is for the (MSc) course MMF062 Vehicle Motion Engineering at Chalmers University of Technology, Göteborg, Sweden. Course web (autumn 2025: https://canvas.chalmers.se/courses/36728). It covers each *Module* in the course, referring to sections, equations, and figures in the book.

Modules on Chapter 1 INTRODUCTION

Module 1:1 The subject Vehicle dynamics and the course

Learning Objectives	Reading
• The subject *Vehicle dynamics*, and the book *Vehicle motion engineering*, cover more than the course. • The ***teaching & learning*** is organised in 26 *Modules* and 3 *Design tasks*. There are *Lectures*, *Problem solving sessions (Räknestugor)*, and *Design task sessions*. • The course ***examination*** consists of 1 Written Examination and 3 Design task reports. • Most administrative information is found in **Course Memo**	• Course Memo
• Know the major sub-systems by name. • Explain and exemplify *Attribute, Function* and *Requirement* on complete vehicle level. • Describe where Vehicle Dynamics is used in the vehicle development: *Requirement setting, Design/Re-design, Verification*. • Explain *Virtual Verification* and how it appears in the development "V process" for sub-systems and complete vehicle.	• 1.1 What is Vehicle Motion Engineering • 1.2 About this book • Figure 2-2 • 1.4 Requirement Setting • Figure 1-2
• Understand the difference between *Design parameters* and *Operation/Manoeuvre parameters*.	• Figure 1-10

Module 1:2 Modelling

Learning objectives	Reading
• Explain and exemplify the 3 modelling stages: Physical (≈FBD), Mathematical (≈DAE) and Explicit form (≈ODE) modelling. • Explain how an Explicit form model is used to do a simulation with the Euler forward as example of integration method. • Recognize *Dataflow diagrams* (or Block diagrams) as a graphical representation of an Explicit form model. • Differ between *parameters/constants* and *variables/signals* in a dynamic model. • Realize that *causality* is the information flow direction (or calculation order) in an explicit form model and that causality of a submodel depends on the surrounding submodels in the superior model.	• 1.5.1.1 Stages in (Dynamic) Model Based Engineering • Figure 1-12

• Do *Physical models* (drawings), especially including FBDs for mechanical systems. • Deduct *Mathematical models* (equations) for small systems. • Understand that the drawings lead to the equations, not the other way around. • Know that fictive forces can be drawn in FBD (and in book they are drawn with dashed arrows). • Understand that "Equilibrium with fictive forces, $m \cdot a - F = 0$;" is just an **alternative** way to formulate "Equations of motion, $m \cdot a = F$;". • Categorize equations: *Equilibrium*, *Compatibility*, *Constitution,* and "*Algorithms*". • Understand that one can select "Force in elastic part" as state variables, as an **alternative** to "Position of inertial body".	• 1.5.2 Mechanical/ Machine Engineering • Figure 1-30 • Figure 1-31
• Recognize the terms *algebraic loop* and *high index* as difficulties that can appear in modelling.	• Figure 1-24 • Figure 1-25

Module 1:3 Vehicle coordinates, types, terminology

Learning objectives	Reading
• Know vehicle motion degrees of freedom and the ISO8855 vehicle-fix coordinate system. • Explain difference between models that captures *in-road-plane* and *out-of-road-plane* motion. • Transform velocities and forces between vehicle-fix and wheel-fix coordinate system	• 1.6.1 Vehicle Motions and Coordinate Systems • Figure 1-59 • Figure 1-60 • Figure 1-64 • Eq[1.7]
• Understand the difference between the operating conditions *static/low speed, steady state, stationary oscillating* and *transient*. • Explain difference between one-track and two-track models. • Know that centrifugal acceleration appears due to vehicle fix (rotating) coordinate system.	• 1.6.2 Complete Vehicle Modelling Concepts • Figure 1-69 • Eq [1.11]
• Recognize and explain terms in "1.6.3 Vehicle Dynamics Terms" • Recognize and explain the concept "Function architecture"	• 1.6.3 Vehicle Dynamics Terms • 1.6.4 Vehicle Architectures
• Explain the major differences, relevant for vehicle dynamics, between passenger cars and heavy vehicles	• 1.7 Heavy Trucks

Module 1:4: Virtual Verification

Learning objectives	Reading
• Understand the business value in virtual verification as alternative to building pre-series real vehicle prototypes. • Name and describe differences and similarities between verification methods: Off-line simulation, MIL, SIL, HIL simulation, Driving simulator, Test track, Testing/Logging in real traffic/operation. • Understand that different requirement on vehicle model for virtual verification of functions that actuate vehicle motion and functions that does not. Examples from the latter: Warning/information and Supporting functions, such as estimators. • Understand opportunities and challenges with modularization and reuse/exchange of submodels for a vehicle manufacturer and a vehicle supplier. • Name and describe the standard Modelica. • Name and describe the standard FMI	• 1.6.5 Verification Methods with Real Vehicle • 1.6.6 Verification Methods with Virtual Vehicle • Table 1-75 • 1.5.4 Tools • Figure 1-51 • Figure 1-52 • Figure 1-53 • Figure 1-54 • 1.6.4.3 Virtual Vehicle Architecture

Modules on Chapter 2 VEHICLE INTERACTIONS AND VEHICLE SUBSYSTEMS

Module 2:1 Tyre Design and Rolling

Learning objectives	Reading
• Wheels & Tyres are both interaction elements to vehicle environment and a subsystem. • Sketch how a tyre model can be interfaced to a model of the rest of the vehicle.	• Figure 2-1, Figure 2-2 • 2.2 Wheels and Tyre • Figure 2-8

- Know how to explain rolling resistance (on rigid ground) from offset in contact pressure.
- Know how rolling resistance comes in when relating wheel longitudinal force F_x to actuated wheel torque T
- Definition of longitudinal slip $s_x = (R \cdot \omega - v_x)/|R \cdot \omega|$;

- 2.2.1.6 How Tyres Carries Vertical Load
- 2.2.1.7 The wheel as a transmission
- 2.2.1.7.2 Efficiencies
- Efficiency η often means power efficiency, it is $\eta = P_{useful}/P_{used}$. For a tran
  such when power is coming out in the intended output end and when powe
  the intended output end. For a wheel, with subscript $Prop$ for intended pow
  propulsion system to vehicle body and Brk for intended power transfer fro
  propulsion system (for reduction of vehicle speed and/or regeneration of e

$$\eta_{Prop} = \frac{P_{useful}}{P_{used}} = \frac{+F_x \cdot v_x}{+T \cdot \omega}; \quad and \quad \eta_{Brk} = \frac{P_{useful}}{P_{used}} = \frac{-T \cdot \omega}{-F_x \cdot v_x};$$

With those definitions and the equations from 2.2.1.7.1 these power efficiencies

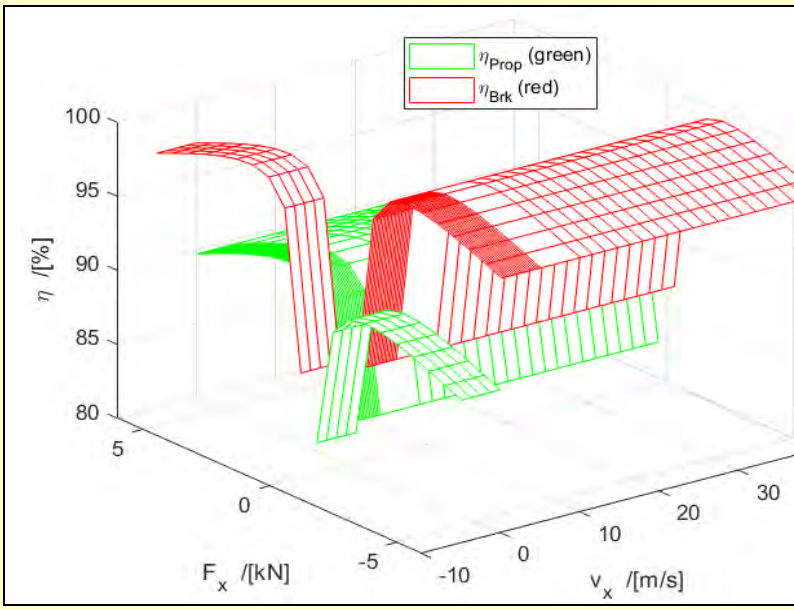


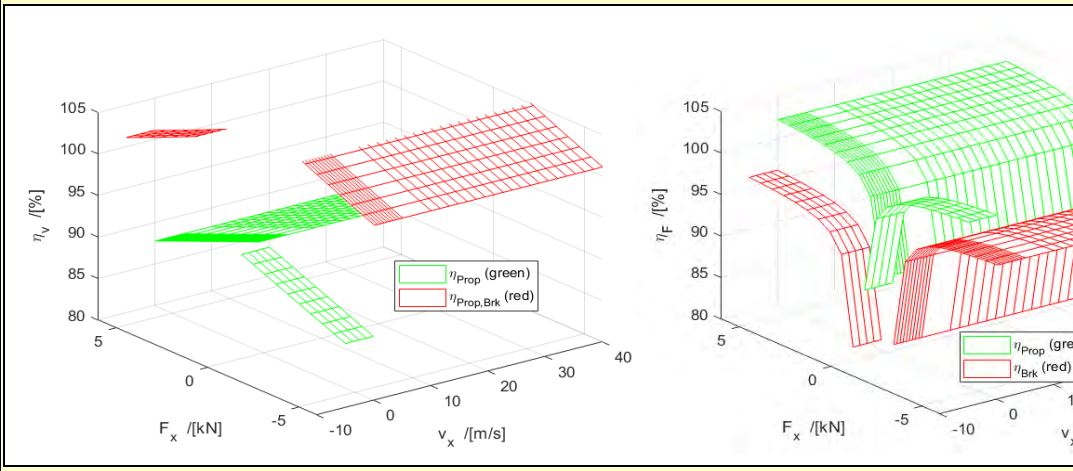
Figure 2-14: Power efficiencies for a wheel. Parametrized with numerical values car. Note that saturation due to road friction is not included, which would decrea dramatically for large $|F_x|$.

For transmissions, one often factorizes the (power) efficiency η in speed and tor $\eta_\omega \cdot \eta_T$. The η is always $\leq 1 = 100\%$ and the distribution of losses between η_ω a what nominal ratio is assumed. For a wheel and tyre, the corresponding become

$\eta = \eta_v \cdot \eta_F$; (if, as below, same nominal radius R_{Nom} is used in velocity ar

$$where \begin{bmatrix}\eta_v \\ \eta_F\end{bmatrix} = \begin{cases} = \{F_x \cdot v_x > 0\} = \begin{bmatrix}\eta_v \\ \eta_F\end{bmatrix}_{Prop} = \begin{bmatrix}\frac{v_x}{v_{xNom}} = \frac{v_x}{R_{Nom} \cdot \omega} \\ \frac{F_x}{F_{xNom}} = \frac{F_x}{T/R_{Nom}}\end{bmatrix}; \\ = \{F_x \cdot v_x < 0\} = \begin{bmatrix}\eta_v \\ \eta_F\end{bmatrix}_{Brk} = \begin{bmatrix}\frac{\omega}{\omega_{Nom}} = \frac{\omega}{v_x/R_{Nom}} \\ \frac{T}{T_{Nom}} = \frac{T}{R_{Nom} \cdot F_x}\end{bmatrix}; \end{cases}$$

Check: $\eta_{Propv} \cdot \eta_{PropF} = \frac{v_x}{R_{Nom} \cdot \omega} \cdot \frac{F_x}{T/R_{Nom}} = \frac{+v_x \cdot F_x}{+\omega \cdot T} = \eta_{Prop}$; and $\eta_{Brkv} \cdot \eta_{BrkF} = \frac{-\omega \cdot T}{-v_x \cdot F_x} = \eta_{Brk}$;. This was expected and, hopefully, it gave an understanding of the velocity and force efficiency.

	Note that R_{Nom} is a 3rd "ratio-like" parameter for a wheel, beside R_L and r_E. The value on what one expects from the wheel, which can be different.  *Figure 2-15: Velocity and force efficiencies for a wheel. Parametrized with numerical va passenger car. Note that saturation due to road friction is not included, which would dec and η_{vBrk} dramatically for large $\|F_x\|$.* • Tyre Rolling and Radii • Eq [2.2] • Eq[2.10]
• Understand that contact length is an intermediate variable, not a design parameter, e.g.: $[DesignParameters, F_z] \Rightarrow L \Rightarrow [RRC, C_x]$ • Know difference between free-rolling and pure rolling wheel. • Know typical numerical value of rolling resistance coefficient for passenger cars and trucks	• 2.2.1.9 Tyre Contact Length • 2.2.2 Rolling resistance of tyres • Figure 2-24

Module 2:2 Tyre Longitudinal Force and Slip

Learning objectives	Reading
• Explain similarities and differences between how friction force varies with sliding speed for "sliding block" and for "rolling wheel of rubber". • Know that generation of longitudinal force F_x requires longitudinal slip s_x • Know that longitudinal tyre slip models are only valid if lateral slip and forces are low. • Be able to follow a derivation of simplest possible brush model that explains the gradual transition between low slip and high slip	• Figure 2-32 • 2.2.3.1.1 Uniform Pressure Distribution and Known Contact Length • Figure 2-34 • Eq[2.13]
• Know tyre model for low force F_x (far below saturation): $F_x \approx C_x \cdot s_x = CC_x \cdot F_z \cdot s_x$; • Know tyre model for high force F_x (saturated): $F_x \approx \mu \cdot F_z \cdot \text{sign}(s_x)$;	• 2.2.3.1.2 Longitudinal slip stiffness • Eq[2.16] • Eq[2.17]
• Know that pressure distribution assumption changes the $F_x(s_x)$ curve. • Find and use the brush model with formula for $F_x(s_x)$ • Know that there are many empirical tyre models. • Find and use the "Magic tyre formula" for $F_x(s_x)$	• 2.2.3.1.5 Different pressure distribution • Eq[2.22] • 2.2.3.4 Curve Fit Tyre Models

Module 2:3 Tyre Lateral and Combined Slip

Learning objectives	Reading
• Know that lateral force and slip relation is conceptually same as longitudinal, but with $F_y(s_y)$ instead of $F_x(s_x)$. • Brush model concept can also be used for lateral. • Far below saturation: $F_y = -C_y \cdot s_y = -CC_y \cdot F_z \cdot s_y$; • Near or on saturation: $F_y \approx -\mu \cdot F_z \cdot \text{sign}(s_y)$; • Lateral tyre models are only valid if longitudinal slip is low.	• 2.2.4.1.1 Model with Independent Bristles • Figure 2-56 • Eq[2.44] • Eq[2.43]
• Know the difference between lateral wheel slip $s_{yw} = v_y/\lvert v_x\rvert = \tan(\alpha)$ and lateral tyre slip $s_{yt} = v_y/\lvert R \cdot \omega\rvert$. • Know the relation between s_{yv} and slip angle α: $\alpha = \text{arctan2}(v_y, v_x)$; or $\alpha = \arctan(s_{yw})$;.	• 2.2.4.2 Lateral Tyre Slip Stiffness • Eq[2.49] • Eq[2.50]
• Know that a version of Magic Tyre Formula is for lateral slip. • Know that C_y is digressively varying with F_z	• 0 Note that C'_x has an important variation with longitudinal utilization of tyre contact, e.g., C'_y s_y,Fx. This is not included in present section but in === • Influence of Vertical Load
• Explain combined slip with the two main principles: $F_x^2 + F_y^2 < (\mu \cdot F_z)^2$; and $F_x/F_y = -s_x/s_y$; • F_y and C_y can be quasi-physically modelled as "downscaled due to utilisation of F_x, inspired by friction circle". • Know that a version of Magic Tyre Formula is for combined slip	• 2.2.5.3.1 Scalar force function • Eq[2.59] • Figure 2-73 • 2.2.5.3 Approximate combined slip model • Eq[2.55] • Eq[2.61]

Module 2:4 Tyre Vertical and other Vehicle Interactions

Learning objectives	Reading
Explain tyre slip models categories: • Longitudinal/Lateral/Combined • Ideal/Linear to slip and vertical force/Saturated. A tyre vertical constitution is relatively well modelled as linear around its static load: $F_z \approx F_{z0} + c_z \cdot z$;	• 2.2.7 Summary of Tyre Force vs Slip Models • 2.2.8 Vertical Properties of Tyres
• List the subsystems relevant for vehicle dynamics. • Propose simplest possible models for the subsystems and how they can be interfaced to the model of "vehicle body with wheels"	*Browse:* • *2.3 Suspension* • *2.4 Propulsion* • *2.5 Braking System* • *2.6* Steering System • 2.7 Combined effects of subsystems on axles' and axle groups' road grip
• Use aerodynamic force models with given "c coefficients": $F_{air} = 0.5 \cdot c \cdot \rho \cdot A \cdot {v_{rel}}^2$; • Understand that a vehicle model needs "driver" and "environment" models to form a simulateable model.	• 2.9 Vehicle aerodynamics • Figure 2-142 • Eq[2.91] • 2.10 Driving and transport application

Modules on Chapter 3 LONGITUDINAL DYNAMICS

Module 3:1 *Longitudinal:* Steady State

Learning objectives	Reading
• Describe propulsion system as *prime mover, transmission* and sometimes *energy buffer*. It actuates torques on driven wheels. • Describe $[torque, speed]$ characteristics for different prime movers: $T = f(\omega)$; • Know transmissions transformation of $[T, \omega\ ]$ to $[F_{xw}, v_{xw}]$ with different ratios on different gears. • Know approximate forms on energy consumption characteristics: $dE_{cons}/dt = P_{cons} = f(\omega, T, gear)$; (or $\eta = \frac{T \cdot \omega}{P_{cons}}$)	• 2.4 Propulsion • 2.4.2 Prime movers • Figure 2-99 • 2.4.3 Transmissions • Eq[2.83] • Eq[2.84]
• Construct *traction diagram* from given propulsion system, vehicle, and road. • Use a traction diagram to explain functions, such as *Top Speed* and *Gradeability*.	• 3.2.1 Traction diagram • Figure 3-1 • 3.2.2 Energy consumption and power losses • Figure 3-18 • 3.2.5 Functions after start • Figure 3-25
• Calculate *steady state vertical force distribution* over axles. • Calculate when *road friction limits propulsion* force on an axle (for steady state). • Calculate *Startability* and *Gradeability*.	• 3.2.7 Starting (an ICE) with starter (start motor) at vehicle stand-still • 3.2.8 Steady State Vertical Force Distribution between Axles • Eq[3.10] • 3.2.9 Friction Limit, Eq[3.12] • 3.2.10 Start Functions • Figure 3-28, Figure 3-29

Module 3:2 *Longitudinal:* Long Cycles

Learning objectives	Reading
• Know that $v_x(t)$ is a *traditional driving cycle*, used for legislation and vehicle development. • Know that traditional driving cycles $v(t)$ or $v(s)$ have shortcomings. Alternatives are more physical models of the transport operations, e.g., describing legal speed, road gradient and curves, traffic and driver. • With *Backward simulation* it is easy to miss saturations and dynamic phenomena, as compared to *Forward simulation*.	• 3.3.1 Description formats of transports • 3.3.5.7.1.1 Forward and Backward Simulation
• Calculate influence on acceleration from *rotating inertias* on vehicle longitudinal acceleration. • Understand that influence from rotating parts can be modelled with either a "k-factor", slipping tyres or clutch or compliant shafts.	• 3.3.2.1.1 Energy Consumption for varying operating conditions * • 3.3.3 Rotating Inertia Influence on Acceleration • Eq[3.15]
• Calculate cycle measures (such as energy consumption) for simple and short cycles. • Understand how more complex and longer cycles can be analysed, using a programming/simulation tool.	• 3.3.5 Functions Over Cycles • Eq[3.17]
• Calculate longitudinal load transfer due to F_x and body forces (gravity and aerodynamics) assuming rigid suspension, • Calculate acceleration performance for vehicle models with rigid suspension	• 3.3.5.7 Functions Over Cycles • • Figure 3-43, Eq[3.18] • 3.3.7 Acceleration • Eq[3.20]

Module 3:3 *Longitudinal:* Short Events

Learning objectives	Reading
• Know the principles of a brake system: Hydraulic or pneumatic pressure applied on a friction brake. Applied via Brake pedal or request from Control algorithms. • List some complete vehicle manoeuvres which are relevant for brake system verification	• Figure 2-129 • Figure 2-130 • 3.4.1 Typical Test Manoeuvres • 3.4.2 Deceleration Performance
Front/rear axle locking: • Know that locking (or spinning) *rear* axle tends to make a two-axle vehicle *yaw-unstable*. • Know that locking (or spinning) *front* axle tends to *reduce steerability* of a two-axle vehicle; vehicle ploughs straight ahead. Brake proportioning diagram: • Construct *Brake proportioning diagram* from brake system and vehicle. • Use a Brake proportioning diagram to propose *Brake Distribution* when. • Calculate for which deceleration or brake force one axle locks and whether it is front or rear axle.	• 3.4.4 Brake and traction distribution • Eq[3.21] • Figure 3-47

Module 3:4 *Longitudinal:* Control Functions and Heavy Vehicle Brake System and ABS

Learning objectives	Reading
• *List sensors relevant for longitudinal control: WSS, a_x, pedals, fwd looking, estimated torques from propulsion and braking systems.* • *Know that propulsion and braking system are main actuators for longitudinal control function.*	*Browse:* • *3.5.1 Longitudinal Control* • *3.5.3 Longitudinal Motion Function Architecture*
• Describe the difference between CC (speed control) and ACC (adding distance control) • Understand that arbitration is needed between CC (or ACC) and Pedal driving	• 3.5.2.3 Cruise Control and Adaptive Cruise Control (CC, ACC) *
• Explain ABS control in a tyre force-vs-slip diagram. • Understand that ABS has two purposes to be balanced: Large longitudinal brake forces and maintained margin for lateral tyre forces	• 3.5.2.4 Anti-Lock Braking System, ABS * • Figure 3-73
• Describe differences between passenger car and heavy vehicle brake systems (media, pressure levels, "by-wire level", …) • Describe differences in ABS function between heavy vehicles and passenger cars	• Figure 2-131 • 3.5.2.4 Anti-Lock Braking System, ABS *

Modules on Chapter 4 LATERAL DYNAMICS

Module 4:1 *Lateral:* Linear One-Track Model

Learning objectives	Reading
Explain main assumptions for these categories of lateral models: • Low speed: Neglect all inertial forces $m \cdot (\dot{v}_y + v_x \cdot \omega_z)$, Steady state at high-speed cornering: Neglect $m \cdot v_x \cdot \omega_z$, or Transient: Include all $m \cdot (\dot{v}_y + v_x \cdot \omega_z)$ • In road plane (irp) or Out-of-road plane (oorp) • One-track or Two-track Models • Tyre models: Ideal-tracking, Linear, Saturated and Combined slip	• 4.1.1 Lateral Model Categorization • *Repeat: 1.6.2 Complete Vehicle Modelling Concepts*
• Derive the (transient, lateral dynamics) "linear one-track model", at least the simpler way in Figure 4-51 • Write the "linear one-track model" on matrix form • Derive and use the "linear one-track model" for simulation with known $\delta(t)$. • Discuss validity limits for "linear one-track model" above: level ground, 2 axles, low CoG, tyre forces in ground plane far from saturation, small variations in v_x, no yaw torque from individual wheel torque actuation.	• 4.4.2 One-Track Model • Figure 4-49 • Eq [4.52] • Figure 4-51 • Eq[4.55]

Module 4:2 *Lateral:* Low Speed, Ackermann

Learning objectives	Reading
• Know that left and right (road) wheels are normally geometrically constrained to each other and to steering (hand) wheel. • Explain and draw Ackermann steering geometry: between left and right wheel and between axles. • Recap that we can postprocess a solution $v_{x(t)},\ v_{y(t)},\ \omega_z(t)$ to a path $x(t), y(t)$ with orientation $\varphi_z(t)$ • Recap lateral tyre model: $F_y = -C_y \cdot s_y$;	*Repeat:* • *1.6.1.7.1 Path with Orientation* • *2.6.1 Chassis Steering Geometry* • *Figure 2-133,* • *Figure 2-134* • *2.2.7 Summary of Tyre Force vs Slip Models*
Explain the functions: Turning radius, Swept Path Width and Off-Tracking	• 4.2.1 Low-speed functions • Figure 4-2, • Figure 4-3 • 4.2.1 Low-speed functions
Derive and use low speed models without forces of a two-axle vehicles.	• 4.2.2 Low Speed Model, Ackermann, without Forces • Eq[4.2] • Eq [4.1]
Understand how forces can be included in low-speed model. And, if Ackermann geometry, either as $s_y = 0$; or $F_y = -C_y \cdot s_y$;.	• 4.2.3 Low Speed Model, Ackermann, with Forces • Figure 4-5 • Eq[4.3]

Module 4:3 *Lateral:* Low Speed, Non-Ackermann, Articulation

Learning objectives	Reading
• Understand how Non-Ackermann or manoeuvre with large forces requires/proposes to include forces with $F_y = -C_y \cdot s_y$;.	• 4.2.4 Low Speed Model, Non-Ackermann • Figure 4-7 • Eq[4.5] • Figure 4-9
• Understand that articulated vehicles have a transient (in articulation angle) which distinguish between circle and transient low speed driving. • Construct instantaneous points of rotation for an articulated vehicle modelled without tyre forces. Derive and use such models. • Reason about how non-zero forces (due to non-Ackermann geometry or other) affect low speed manoeuvres of articulated vehicles	• 4.2.5 Articulated Vehicles

Module 4:4 *Lateral:* Steady State Cornering without Load Transfer

Learning objectives	Reading
• Understand that 3 scalar measures fully define a Steady State Cornering operating condition for a general vehicle, e.g., R_p, v_x, β. • Understand that, with a certain vehicle, the driver is limited to 2 "request channels": Pedals + SteeringWheel. • So, with a certain vehicle, the driver can select radius R_p with steering and speed v_x with pedals, while the side slip angle β is a result of how vehicle (and road surface) is built.	• 4.3.1 Steady State Driving Manoeuvres • Figure 4-12
• Derive and use model for steady state cornering. Derivation either from transient model "linear one-track" (by neglecting terms) or from Physical model (at least the simpler way in Figure 4-19). • Find and use the model for steady state for cornering	• 4.3.2 Steady State One-Track Model • Figure 4-16 • Figure 4-19 • Eq[4.10]

Module 4:5 *Lateral:* Steady State Cornering Functions

Learning objectives	Reading
• Understeer gradient is a steady state cornering measure, but maybe be defined differently: $[1/N]$, $[1]$ or $[1/(m/s^2)]$ • Understeer gradient can be defined for straight ahead driving (linearized around zero lateral acceleration) or linearized around a non-zero lateral acceleration. • Understeering is sometimes used as a momentaneous measure during an arbitrary transient manoeuvre	• 4.3.3 Under-, Neutral- and Over-steering *
Sketch these steady state diagrams with v_x as abscissa: • Steering Wheel Angle • Yaw Velocity Gain • Lateral Acceleration Gain *Know that Handling diagram is a way to visualize steady state cornering behaviour*	• 4.3.4 Required Steer Angle • Eq[4.18] • Figure 4-24 • Eq[4.19] • 4.3.5 Critical and Characteristic Speed * Figure 4-28 • Figure 4-30 • *Browse: 4.3.7.10 Handling Diagram*
Understand that understeering can be varied in many ways, e.g.: • Longitudinal load transfer due to tyre longitudinal forces, acceleration and deceleration • Roll stiffness distribution between axles (stiffer front gives understeered) • Side-force-steering and roll-steering • Wheel torque distribution, left-right and front-rear (more wheel torque front gives understeered) *Understand that yaw responsiveness can be both too low and too high*	• 4.3.7 How Design Influences • Figure 4-25 • Figure 4-33 • *Browse: 4.3.7 How Design Influences Steady State Gains*

Module 4:6 *Lateral:* Steady State Cornering with Load Transfer

Learning objectives	Reading
• Describe wheel/axle suspension as consisting of: Linkages, Elasticities (springs, anti-roll bars, bushings, flexible links) and Dampers (shock absorbers, friction). • Know that each wheel can be individually suspended, or each axle suspended as one unit.	• 2.3 Suspension • Figure 4-39
• Lateral load transfer on each axle depends on suspension linkage and elasticities. Dampers does not influence in steady state. • One can model suspension with 2 pivot points (wheel-individual pivot points or 2 points for a rigid axle) or with 1 roll centre height for each axle. • If roll centre was in ground plane, the load transfer appears first when a roll angle appears; Force play would go "via elasticities". • If roll centre was at CoG height, the load transfer happens directly without a roll angle; Force play would go "via linkage".	• 4.3.7.11.3 Lateral Load Transfer • Figure 4-41 • Eq [4.43]
• Know that Off-Tracking can be defined for also high speed (it was defined for low speed before) • Know that wheel-lift appears at different lateral acceleration for different axles	• 4.3.7.12 High Speed Steady State Vehicle Functions • Figure 4-43

Module 4:7 *Lateral:* Stationary Oscillating Steering

Learning objectives	Reading
• Understand that stationary oscillating steering requires a transient model, but the solutions are stationary (constant amplitude, frequency and phase) • Know how to use “linear one-track model” and Fourier-transform to find frequency responses	• 4.4.1 Stationary Oscillating Steering Tests • *Repetition: 4.4.2 One-Track Model* • Eq [4.55] • *Repetition (of Mathematics): Fourier and Laplace transform in 1.5.1.1.4.1 Mathematics and Notation*/Naming Conventions • 4.4.3.1.1 Solution with Fourier Transform • Eq [4.56]
• Sketch Yaw Rate amplitude response as function of steering frequency for different v_x • Sketch Lateral Acceleration response as function of steering frequency for different v_x	• 4.4.3.2.2 Lateral Acceleration Frequency Response • 4.4.3.3 Other Frequency Responses to Oscillating Steering • Figure 4-55 • Figure 4-58

Module 4:8 *Lateral:* Transient Manoeuvres, incl. Step Steer

Learning objectives	Reading
• Transient driving is used as most arbitrary way of driving • Expanding the "linear one-track model" to varying v_x and saturated tyres gives a useful model for many transient driving manouvres	• *Browse: 4.5.1 Transient Driving Manoeuvres ** • 4.5.2 One-Track Models, without Lateral Load Transfer • Figure 4-49 • Eq [4.64]
• Articulated vehicles: o Each articulation point is represented in mathematical model: 2 equilibrium Eqs and 2 compatibility Eqs o The articulation points make the explicit form model much harder to find, due to "high index" o For each added unit: 2 additional states appear: θ and $\dot{\theta}$ • For cambering vehicles, the roll angle is important to model	*Browse:* • *4.5.2.2 Articulated Vehicles* • *Figure 4-66* • *4.5.2.3 Cambering Vehicles* • *Figure 4-74*
The load transfer in transient models adds, compared to steady state cornering and transient one-track model: • Forces in dampers • Roll dynamics $J_x \cdot \dot{\omega}_z$ • Heave and Pitch Dynamics depending on suspension models Example model: • There is an example of relatively complete model (driver, vehicle environment) with proposed modularity and interfaces. • The model shows how Control and Actuation can be modelled as a separate module.	*Browse:* • *4.5.3.2 Example of Explicit Form Model; Two-Axle Vehicle, Driver and Environment* • *Figure 4-79* • *Figure 4-80*
If tyres are far below grip limit, step steering response can be evaluated with the linear one-track model. Solutions can be on closed form.	• 4.5.4.1 Mild Step Steering Response • Eq [4.73]
If tyres are closer to grip limit, step steering response requires more advanced models. Solutions generally requires time simulation.	• 4.5.4.2 Violent Step Steering Response
Long articulated vehicles have special functions/measures defined. Rearward amplification is one, which often reveals that yaw velocity is amplified to typically the double for the rear-most unit.	• *Browse: 4.5.6 Long Heavy Combination Vehicles*

Module 4:9 *Lateral:* Vehicle Simulator as Verification Tool

Learning objectives	Reading
• Understand the cons and pros with driver in the loop simulators (DIL) compared to "**office-simulations**" (MIL, SIL, HIL) • Understand the cons and pros with driver in the loop simulators (DIL) compared to **real test-vehicles** • Understand the cons and pros with driver in the loop simulators with and without motion platform • Understand that Motion-queuing bridges the inevitable gap between simulated vehicle motion and motion platform motion. • Know state of the art for in-vehicle-programme use of simulators. How far have simulators come? • Know some research questions on the research/development front for simulators.	• 1.6.6.1 Testing with Real Driver • Figure 1-74

Module 4:10 *Lateral:* Control Functions

Learning objectives	Reading
ESC is a function which corrects the yaw velocity when lateral grip is lost on one axle (under- or oversteering situation). • Outer front wheel is primary wheel to brake when detecting over-steering. • Inner rear wheel is primary wheel to brake when detecting under-steering. • RSC brakes away lateral grip on front axle. • Brakes are main actuator for ESC and RSC, but development towards using more actuators is on-going.	• 4.6.2.2 Electronic Stability Control, ESC * • 4.6.2.3 Roll Stability Control, RSC *
LKA, LCA/AES and AD are functions with automatic lateral interventions in increasing levels. • LKA is a relatively stand-alone function. • LCA/AES needs to be designed together with (longitudinal) AEB. • AD is a very wide term. AD ranges from allowing LKA and (longitudinal) ACC at the same time to full AD with selection of route and absent driver.	• 4.6.2.4 Lane Keeping Aid, LKA * • 4.6.2.5 Lateral Collision Avoidance/Automatic Emergency Steering, LCA/AES * • 4.6.2.6 Automated Driving (AD)

Modules on Chapter 5 VERTICAL DYNAMICS

Module 5:1 *Vertical:* Suspension and Stationary Oscillation theory

Learning objectives	Reading
• Understand that vertical dynamics often is studied in frequency domain • Know that 3 areas of functions are: Comfort, Road grip and Fatigue	• 5.1 Introduction • Figure 5-1
• Two frequency domains: time frequency $z(t)$ and spatial frequency $z(x)$ • Definition and usage of Root Mean Square, $RMS(z)$ $[unit: same\ as\ z]$ • Definition and usage of Power Spectral Density, PSD: o $PSD(z,\omega)$ and $PSD(z,\Omega)$, $[unit: \frac{same\ as\ z}{rad/m}]$ • Definition and usage of Transfer Function $H_{z_a \to z_b}(\omega) = \hat{z}_b/\hat{z}_a$;	• 5.2 Stationary Oscillations Theory • Figure 5-3 • Eq [5.4] • Eq [5.8] • Eq [5.11] • Eq [5.13]

Module 5:2 *Vertical:* Road Models, 1D Vehicle Models

Learning objectives	Reading
• Typical roads have large amplitude $[m]$ for long waves (=low spatial frequency) and small amplitudes for short waves (=high spatial frequency) • Calculate RMS value of a response variable z_s if knowing: road (Φ_0, Ω_0, w), Vehicle speed v_x and Transfer function $H_{z_r \to z_s}$, using Eq [5.31].	• 5.3 Road Models • Eq [5.27] • Figure 5-5 • Eq [5.31]
• Derive, and use transfer functions, for "1D model with 2 dynamic dofs" • Understand that different models used to study 1D (vertical) motion	• 5.4.3 1D Model with 2 Dynamic dofs • Figure 5-12 • Figure 5-13

Module 5:3 *Vertical:* Comfort and Grip

Learning objectives	Reading
• Understand that human's sensitivity to accelerations is different for different frequencies, with maximum sensitivity for $f = 4..8\ Hz$ • Calculate a_w value of a response variable z_s if knowing: road (Φ_0, Ω_0, w), Vehicle speed v_x and Transfer function $H_{z_r \to z_s}$, using Eq [5.53]. • Calculate Time averaged whole-body vibration exposure value $a_{w,av}$ if knowing a_w for the time periods using Eq [5.52] • Understand that Road grip can be measured with amplitude of vertical force in tyre contact patch ΔF_{rz}	• 5.5 Functions for Stationary Oscillations • Figure 5-20 • Eq [5.51] • Eq [5.52] • Eq [5.53]
Plot and use frequency response diagrams to analyse for which frequencies Comfort, Fatigue and Road grip becomes worse or better for variations of suspension design parameters.	• 5.6 Variation of Suspension Design • Figure 5-23 • Figure 5-24 • Figure 5-25

Design Tasks

Learning objectives	Reading

Design Task 1: Longitudinal • Functions: Acceleration (uphill, various road friction) • What to engineer: Distribution of propulsion between front and rear axle (FWD/RWD) • Method: Modelling and simulation • Tools: "Home-solved" and "Home-coded" time-integration (for conceptual understanding of simulation)	• Figure 2-32, 2.2.3.4.1 Magic Formula Tyre Model, Eq [2.2] • 1.5.1.1.3 Physical Modelling • 1.5.1.1.4 Mathematical modelling, 1.5.2.1 Free-Body Diagrams • 1.5.1.1.5 Explicit Form Modelling, 1.5.1.1.6 Computation • Figure 3-43, Eq [3.18] • 3.5.2.6 Traction Control, TC * • 1.5.4.1.1 General Mathematics Tools
Design Task 2: Lateral • Functions: Yaw balance in steady state high speed, Step steer response, Brake in curve • What to engineer: Distribution of roll-stiffness and brake force between front and rear axle • Method: Simulation, Driving experience, model integration and log data analysis • Tools: Simulink (for learning one commonly used tool for simulation), Motion platform driving simulator (for driving experience and log data analysis)	• Figure 4-12 • Figure 4-16 • Figure 4-19 • 0 • 4.3.6 Steady State Cornering Gains * • Eq [1.1][4.18] • Eq [4.19] • Figure 4-51 • 1.5.1.1.4.5 Affine and Linear form (ABCD form) • Figure 4-42, Eq [4.43] • Eq [2.61]
Design Task 3: Vertical • Functions: Comfort for stationary vibrations, Road grip due to stationary varying vertical tyre force • What to engineer: Wheel suspension stiffness and damping • Method: Frequency analysis • Tools: Matlab (for learning one commonly used tool for matrix computations)	• Figure 5-1, Figure 5-12, [5.44] • Figure 5-3, Eq [5.4], Eq [5.13], 4.4.3.1.1 Solution with Fourier Transform • Eq [5.45] • Figure 5-5, Figure 5-20

COURSE TME102 VEHICLE MOTION AND CONTROL

This appendix is for the (MSc) course TME102 Vehicle Motion and Control at Chalmers University of Technology, Göteborg, Sweden. Course web (spring 2025: https://chalmers.instructure.com/courses/28962). It covers some *Modules* in the course, in terms of *Learning Objectives* and *(Recommended) Reading*, referring to sections, equations and figures in the book.

- Darker grey highlight marks repetition.
- Strike-through text is "stretched target".

Complementing *Preparation* material is found on the course web: Some *Videos*, beside the *Classroom Session* material: *Classroom Lecture* and *Classroom Problem*.

The Learning objectives for the course *MMF062 Vehicle Motion Engineering* are assumed to be pre-knowledge for the course participants.

Module Modelling

About the module

- *Modelling is how to derive the models from physical/engineering interpretation (deductive, as opposed to inductive, modelling).* ***Deductive*** *modelling gives a wider model validity (and, hopefully, better understanding) for variations in design and operational parameters. The modelling aims at complete vehicle verification.*
- ***Modelica*** *is used for terminology and for an (executable) Mathematical model format.*
- *Simulink and FMU are used as examples of (executable) Explicit form model format.*
- *Modularity is important for* ***model exchange****, which is important for virtual development of complex products, such as vehicles, where many organisations and engineers must contribute to complete vehicle models.*
- *Modelling of* ***Discrete dynamics*** *is a base for modelling of Mechatronics (and pure control algorithms).*

The "sub-modules" below are in chronological order of the 4 × 45 minutes Classroom sessions. The last sub-module gives the learning objectives for the Hand-in.

2025 Bengt Jacobson*, Chalmers and 2021 Peter Sundström, Modelon*

Context

Learning Objectives	Reading
• **Explain** how Vehicle Engineering (in comparison to engineering of many other products) is especially complex in product structure, use cases and demands on product costs and development time. • **Exemplify** the terms and their relations to each other: *Attribute, Function, Requirement, Verification.* • **Exemplify** how a design decision is becomes a requirement on the next lower (product structure) level, e.g., front and rear axles or engine and gearbox. • **Explain** how and why *Virtual verification* is, and can be increasingly, useful for efficient product development. • **Distinguish** between model validation, analyse influence of design, and check requirement fulfilment	• Figure 1-2, Figure 1-7, Figure 1-10 • 1.4 Requirement Setting • 1.4.4 Requirement Setting in Hierarchical Products, Figure 1-5, Figure 1-6 • Figure 1-19, Figure 1-20, Figure 1-21

Terminology and concepts

Learning Objectives	Reading
• **Exemplify** the following terms: o Physical, Mathematical and Explicit form modelling, o *Causality* is (here) computation order, which is sometimes the direction of data flow between blocks. *Causality* is a result of the whole (simulateable) model, not the real system. o Modelling for design guidance o Representation of Quantities: *Variables, Parameters, Signals.* o *Design* Parameters and *Operation* Parameters. o Equation origins: *Equilibrium, Compatibility, Constitution, Other* o A physical interface typically has *effort* and *flow* as interface variables, e.g., velocity and force. • **Select** states in a mathematical model and **exemplify** that the selection is ambiguous. • ~~**Know** that *Lagrange*'s "equilibria of projected energy" can replace Newton's "equilibria of forces and moments".~~	• Figure 1-12 • 1.5.1.1 Stages in (Dynamic) Model Based Engineering • 1.5.1.1.9 Modelling for Design Guidance • 1.5.1.3 Constants, Parameters, and Variables of Quantity and Signal • 1.5.2.1 Free-Body Diagrams • 1.5.2.4 Equation Types • 1.5.2.1.2 Physical Connections and Factorized Power Interface • 1.5.2.2 Selection of State Variables • ~~1.5.2.4.1.3 Lagrange Mechanics~~
• Known that the Modelica way to define a differentiated variable is the operator `der(…)` • **Exemplify** *algebraic loops* or *(Simultaneous) Systems of Equations* can be problematic when Explicit form modelling. • **Exemplify** *high index* can be problematic when Explicit form modelling. E.g., when connecting 2 masses or 2 springs rigidly • **Know** that Modelica tools often can solve algebraic loops and high index automatically	• 1.5.1.4 Algebraic Loops or Simultaneous Equations, Figure 1-24 • 1.5.1.5 High Index, Figure 1-25 • Figure 1-53

Formats and tools

Learning Objectives	Reading
• **Examplify** tools where modelling is done in Explicit form and Mathematical form, respectively. E.g., Simulink and Dymola. • ~~**Know** that Modelica is both *EquationOriented* (Acausal) and *ObjectOriented*. Object orientation: *Instantiate, Extend, Replace, Model/Connector/Unit, …* Hence, one can model in Modelica either in *equations* or by instantiation from *libraries*.~~ • **Know** that Modelica terminology is also a useful (complete and strict) for understanding dynamic modelling in general, also if not using Modelica tools. • **Translate** (and **Compare**) simple models between Simulink and Modelica • **Know** that an FMU is an model on Explicit form and facilitates modularity/model exchange (tools, IP, …)	• 1.5.4 Tools, • ~~Figure 1-54, Figure 4-70~~ • Figure 1-51, Figure 1-52 • Figure 1-54

Modelling discrete dynamics

Learning Objectives	Reading
• **Exemplify** Discrete dynamics: *Time sampled, Discretization, Finite State Machines, Physical state events, ~~Event iteration~~* • **Know** that Mechatronic submodels are typically time sampled on signal interfaces but continuous on the physical interface variables • **Model** time-sampling with Modelica operator **`sample`** • ~~Model continuous dynamics as *Discrete*~~ • ~~Model with *Finite State Machines*~~ • ~~Model with *Physical state events* and *Event iteration* with Modelica operator **when**~~	• 1.5.1.4 Algebraic Loops or Simultaneous Equations • 1.5.1.6.1 Discretization of Continuous Models • ~~2.4.4 Clutches and Brakes in Transmission~~ • ~~Figure 2-112~~ • ~~Figure 2-114~~

Modelling mechatronics

Learning Objectives	Reading
• **Exemplify** a *Mechatronics* subsystem and how such contain *Algorithm* and *Signal* interface, beside equations and variables. • **Know** that Modelica treats causal variables (signals) as special case of variables, using the declaration `input`.	• Figure 1-23 • 1.5.2.4.5 Algorithms and Other Equation Types

DAE modelling (Modelica) in automotive industry

Learning Objectives	Reading
• **Know** that: o there are open (free) standard libraries, e.g., 3D Mechanics, Electrical, Thermodynamics, ... o Vehicle Dynamics Library (VDL) is an example of a commercial Modelica library, developed for vehicle dynamics. o a Modelica addition for (parameter and trajectory) optimization, e.g., Optimica and Jmodelica, is worked on but not yet included in many tools yet, if any. o there are "cloud based" Modelica tools, *Modelon Impact* is one example. o the present development of the FMU standard addresses, e.g., multiple FMUs, hierarchical FMUs and co-simulation [Note: These objectives may not fit perfectly with 2026 year's guest lecture. Some updates might appear, 2026 or later.]	• Slides from guest lecturer Mohamed Takkush from VAS • Figure 1-56 • 1.5.4.1.5 Acausal modelling tools • 1.5.4.1.6 FMI Supporting Simulation Tools • Figure 1-57, Figure 1-58 • 1.5.1.1.9.3 Optimization • 1.5.4.1.7 Modularity in Models

Hand-in

Learning Objectives	Reading
• Functions: Straight-line maximum acceleration on flat road on medium slippery road • What to engineer: Driveshaft stiffness • Method: Modelling and simulation. Modelling with Modelica (equations, not using libraries). • Tools: Modelica tools for simulation. Complete vehicle requirement setting and verification.	
• Learn-by-doing how to: o Start from *Physical* modelling (on paper/board/powerpoint) o Do a *Mathematical* model with a *Modelica* tool using equations (as opposed to using Modelica libraries). o Add phenomena to the model (added parameters, variables, and equations) o Use *Computation* (simulation) and *Evaluation* (e.g., plotting and tables) to reflect over validity of the model and requirement fulfilment of the design. • ~~Model using ready **libraries** (graphical)~~ • ~~Model using **object orientation** to reuse models in "experiments"~~ • Model using **object orientation** to build component libraries. Briefly understand connector concept. • ~~**Generate** an FMU and **test-run** it in Matlab (e.g., from script) and/or Simulink~~	• Hand-in instructions on Course web • Figure 1-12 • Eq [1.3], Figure 1-52 • Figure 2-120, Figure 3-61, Figure 4-41 • ~~Figure 1-54~~ • Figure 1-55 • ~~Figure 2-121~~ • ~~Figure 1-51~~

Module SubSystems

Background and Motivation for the Module

- *Subsystems decide the forces on the vehicle, via the tyres. So, the control of the motion (through human driver or algorithms) must consider the subsystems to operate the vehicle.*
- *Simplified:*
  - ***Suspension** controls the **vertical forces** F_{iz} on wheels and tyres.*
  - ***Propulsion and Braking** actuates the wheel torques T_i, and hereby the **longitudinal** F_{ix}.*
  - ***Steering** actuates wheel steering angles on steered wheels, δ_i, and hereby the **lateral** F_{iy}.*
- *Less simplified: Suspension steers both steered and non-steered wheels. Tyre forces F_{ix} and F_{iy} share the road friction $\mu \cdot F_{iz}$. So, tyres and suspension cause an interaction between all subsystems.*
- *For most modern vehicles: Propulsion, Brake and Steering are Mechatronic.*

The subsystems “2.2 Wheels and Tyres” and “2.8 Environment Sensing System” in the book are treated in other Modules in the course.

The “sub-modules” below are in chronological order of the 8×45 *minutes* Classroom Sessions. For each subsystem, the structure: “Design Concepts and Requirement” and “Passenger vehicle suspension #Under construction

New TME102.ModuleSubsystems.Suspension spring 2026:

Learning objectives	Reading
• Learn some concepts for individual suspension (e.g. McPherson, double wishbone, 5-link) • Suspension parts (links, bushings, spring, damper, anti-roll bar). • Understand that both kinematics and compliance cooperate to give an axle its characteristics.	• *Guest lecture presentation from Tobias Brandin, Volvo Cars*

Heavy vehicle suspension #Under construction

Moved from MMF062.Module5:4 autumn 2025 to TME102.ModuleSubsystems.Suspension spring 2026:

Learning objectives	Reading
• Describe differences between passenger car and heavy vehicle suspension systems (number of axles, variation in payload, …) • Qualitatively explain differences between non-reactive and reactive suspension.	• *Guest lecture presentation from Jan Hendrics, Volvo Trucks* • *Repeat/Browse: 2.3 Suspension* • *3.4.5.2 Transient Load Transfer and Non-Trivial Linkage* • *3.4.7 Pitch Functions at Transient Wheel Torques* • *4.3.7.11.3 Lateral Load Transfer*

Modelling Concepts” and is followed.

***2025 Bengt Jacobson** and 2021 Ingemar Johansson, Chalmers*
Tobias Branding (Suspension), Jan Andersson (Propulsion), Matthijs Klomp, Volvo Cars
Leon Henderson (Brake), Volvo Trucks and Chalmers
Anders Eriksson (Propulsion) and Jan Hendrix (Suspension), Volvo Trucks

Vehicle with Subsystems

Learning Objectives	Reading
• **Explain** how a vehicle interacts with driver and environment • **Explain** how the subsystems connect vehicle body with driver and environment • **Understand** that, during use of the vehicle, the vehicle control typically sends *request signals* to the (mechatronic) subsystems. Also that vehicle control have to receive *information signals* from the subsystems. • **Draw** a free-body diagram of a wheel. With this, **explain** how T_{shaft} (from propulsion) and T_{brake} (from brake) sums up to a T_{whl} and how T_{whl} is related to tyre F_x. And **explain** how β and δ (from suspension) sums up to α and how it is related to tyre F_y. • **Understand that** one can elaborate with how requirements on subsystems influence various complete vehicle functions, using a simulation tool, such as IPG CarMaker.	• Figure 2-1, Figure 2-2 • 1.6.4.2 Vehicle Function Architecture, Figure 1-72, Figure 1-73 • Figure 2-7 • 1.5.4.1.3Vehicle Dynamics Specialized Simulation Tools

(Wheel) Suspension Systems

Design Concepts and Requirements

Learning Objectives	Reading
• **Know** that there are typically multiple axles, at least 2, and that an axle typically has 2 wheels and that a wheel has typically 1 tyre. • **Count** (kinematic motion) dofs for a given suspension, by "look&feel/count links" • **Explain** difference between Wheel-Individual and RigidAxle design concepts	• Figure 2-8, 2.3 Suspension System, 2.3.2 Axle and Wheel Rates, Figure 2-88, Figure 2-90, Figure 4-82 • 2.3.3 Suspension -- Heave and Pitch, Figure 2-90, Figure 2-91, Figure 2-92 • 2.3.4 Suspension -- Heave and Roll, Figure 2-93, Figure 2-94, Figure 4-39
• **Exemplify** requirements on complete vehicle functionality where suspension system is essential: Longitudinal and lateral manouvres short manouvres and comfort during longer driving. Use: o Steady state cornering gain diagrams o Frequency responce diagrams for stationary oscillating steering o Transfer function diagrams for vertical comfort and road grip o (Other useful diagrams, e.g. Handling diagram, will be presented in the course module Vehicle Performance and the Design Task)	• 0 #.#.#.#.#.# # • 4.3.6 Steady State Cornering Gains * • 4.4.3.2 Frequency Responses on Steering * • 5.4 1D vehicle models, 5.6 Variation of Suspension Design • 4.3.7.10 Handling Diagram
• **Exemplify** at least 5 "Requirements on suspension system for one axle" (often called "Requirements on Kinematics&Compliance (K&C) parameters") among. The 5 can be: o Anti-dive/-squat geometry [m/m] o Axle Roll Center Heigth [m] o Axle Roll Stiffness [Nm/deg] o Axle Roll Damping [Nm/(deg/s)] o RollSteer [deg/deg] o SideForceSteer [deg/N] o Steering Compliance Steering [deg/N] • **Draw and read** "K&C diagrams" • **Understand** suspension parameters and **set** numerical values of them in a tool like IPG CarMaker	• Figure 3-61 • Figure 4-41 • 4.3.7 How Design Influences Steady State Gains, 4.3.7.3 Suspension Steering • IPG CarMaker "ReferenceManual.pdf"

Passenger vehicle suspension #Under construction

New TME102.ModuleSubsystems.Suspension spring 2026:

Learning objectives	Reading
• Learn some concepts for individual suspension (e.g. McPherson, double wishbone, 5-link) • Suspension parts (links, bushings, spring, damper, anti-roll bar). • Understand that both kinematics and compliance cooperate to give an axle its characteristics.	• *Guest lecture presentation from Tobias Brandin, Volvo Cars*

Heavy vehicle suspension #Under construction

Moved from MMF062.Module5:4 autumn 2025 to TME102.ModuleSubsystems.Suspension spring 2026:

Learning objectives	Reading
• Describe differences between passenger car and heavy vehicle suspension systems (number of axles, variation in payload, …) • Qualitatively explain differences between non-reactive and reactive suspension.	• *Guest lecture presentation from Jan Hendrics, Volvo Trucks* • *Repeat/Browse: 2.3 Suspension* • *3.4.5.2 Transient Load Transfer and Non-Trivial Linkage* • *3.4.7 Pitch Functions at Transient Wheel Torques* • *4.3.7.11.3 Lateral Load Transfer*

Modelling Concepts #Under construction

Learning Objectives	Reading
• **Explain** difference between suspension modelling concepts: o "Component compliances" or "wheel/axle rates" o SteadyState or Transient o Longitudinal Load Transfer o Lateral Load Transfer ▪ Pendulum Effect o Wheel lift and Bump stop o Kinematic or ElastoKinematics (Compliance) models o Unsprung parts with or without inertia o Dampers different in compression and expansion o "Trivial suspension" o 2D in xz plane ▪ **Model** a 2-axle vehicle with independent suspension in xz-plane, for transient and 1 pivot point per axle o 2D in yz plane o **Model** a 2-axle vehicle in yz-plane, for steady state and 1 roll centre per axle ▪ 1 pivot point (RollCentre) or 2 pivot points per axle. ▪ **Model** a 2-axle vehicle in yz-plane, for transient and 1 pivot point per wheel o "2.5D" o ~~Full 3D~~ ▪ Understand that the linear gradients, e.g. BumpSteer=$d\delta/dz$ and 1/SteeringRatio=$d\delta/dRackTravel$, in $\{z, RackTravel\} = \{z_{DesignHeigth}, 0\}$, can be complemented with the nonlinearities through higher order terms. ▪ 5-link as concrete example. Explain how to formulate the kinematics relations (compatibility). ▪ Understand that equilibrium equations can be derived from power equilibrium, assuming one position and no energy dissipation in the suspension mechanism. ▪ Explain which 2D-tables that typically represents the non-linearities in vehicle dynamics models, such as CarMaker. o ~~Active Suspension, Skyhook algos~~ • **Apply** Time domain and Frequency domain analysis	• Figure 2-90 • 3.4.7 Pitch Functions at Transient Wheel Torques, 3.4.8 Acceleration and Deceleration • Figure 4-39, Eqs [4.37]..[4.43] • ~~2.3.2.2 Expansion to 3D~~ • 5.6 Variation of Suspension Design • Figure 3-61, Eq [3.37] • Guest lecture presentations from Yansong Huang, Volvo Cars • 2.3.2.3 Example: Requirements on suspension • Figure 4-41, Eqs [4.37]..[4.43] • ~~5.4.3.2 Active Damping using Skyhook Control, 5.6.5 Varying Skyhook Damping~~

Propulsion System

Design Concepts and Requirements

Learning Objectives / Reading

- **Know** that there are alternative propulsion system design concepts in terms of:
  - Single or Multiple drivetrains
    / Figure 2-96, 2.4.7 Special Topology Propulsion Systems
  - Distribution of propulsion:
    - For passenger cars: FWD, RWD, AWD
    - For heavy vehicle: Which unit(s), which axle group(s), which axle(s)
  - Prime movers (ICE, electric) / 2.4.2 Prime movers
  - Main Transmissions and Gearboxes
    - Clutches, Torque Converters
    - Energy storages
      / 2.4.6 Energy Storages and Energy Buffers, Figure 3-42
    - Gear shifting including Neutral gear
      /3.2.1.1 Gear selection
  - ~~Distribution Transmissions:~~
    - ~~Differential, Differential locks~~
      ~~/ Eq [2.83], Eq [2.84]~~
    - ~~Torque Vectoring differentials and clutches~~

- **Draw and read** Traction diagrams and $a_x(v_x)$ diagrams
  / Figure 3-1, Figure 3-2, Figure 3-3
- **Exemplify** requirements on complete vehicle functionality where propulsion system is essential, e.g.:
  - Steady state
    / Figure 3-25, Figure 3-29,
  - Long cycles
    /Figure 3-31, Figure 3-35, ~~3.3.5.7.1.1 Forward and Backward Simulation~~, 3.5.2.3.1 Predictive CC, Table 3.1: Quantities for energy (consumption) and power (losses),
  - Short events, acceleration and deceleration
    / Figure 3-62
  - 3.4.3.1 Pedal Response *, 3.5.2.6 Traction Control, TC *

- **Exemplify** "Requirements on a propulsion system", e.g.:
  - Torque capability [T for a certain ω] (influences vehicle's top speed, gradeability, etc)
    / Figure 2-99
  - Power loss [P for a certain $\{T, \omega\}$] (influences the vehicle's energy consumption)
    / 2.4.2.3.1 Power loss and efficiencies in electric machines
  - Response time [time for a certain step in T], Smoothness [variations in T during a certain step in T] (influences vehicle's driveability), Accuracy [error $T - T_{Req}$] (influences control functions of the vehicle)
    / Figure 2-120, Figure 2-102
  - ~~Torque vectoring capabilities~~
  - ~~Function Architecture Requirements: Request and information interface to propulsion system, Arbitrations and Coordinations within propulsion system~~
- **Understand** propulsion system parameters ~~and **set** numerical values of them in a IPG CarMaker (as one example of tool)~~
  ~~/ IPG CarMaker "ReferenceManual.pdf"~~
- **Draw and read** Prime mover diagrams: $T_{eMax}(\omega_e), \eta(T_e, \omega_e), \eta(P_e)$

Modelling Concepts

Learning Objectives	Reading
• **Model** propulsion systems with these modelling concepts: o *1D* modelling for rotational dynamics with *Nodes* or *Connectors* o *Power factorized interfaces* $\{T, \omega\}$ as opposed to P o Energy storage in flywheels and torsional springs o Longitudinal slip in tyre as damper ~~o Clutches, Torque converter maps, Backlash, Shifting~~ ~~o Propulsion component suspension~~ ~~• Modeling (Computation) with Forward and Backward Simulation~~	• Figure 1-68 • 1.5.2.1.1 Forces in a Cut or Connection, Figure 2-97 • 1.5.2.1.2 Physical Connections and Factorized Power Interface • 1.5.2.2 Selection of State Variables • 3.4.3.1 Pedal Response *
• **Example Models**: o Open and locked differential while propelling in different path radii. o Torque Vectoring Dual Clutch electric axle o Predictive Speed Control for Cost Minimization of Remaining Mission	• 3.4.3.1 Pedal Response * • 3.5.2.6 Traction Control, TC *

Braking System

Design Concepts and Requirements

Learning Objectives	Reading
• **Describe** alternative braking system designs: o Engine brake, Driveline brake, Friction brakes at wheels o Hydraulic, Pneumatic or Electro-Mechanical Braking system (EMB). Different degrees of "by-wire". o Braking of several units: Standard is that truck decides and sends 1 scalar request rearwards: Fraction "utilized friction"= $\sum F_x / \sum F_z$. The rest of units simply relay same signal rearwards.	• 2.5 Braking System
• **Exemplify** requirements on complete vehicle functionality where braking system is essential, e.g.: o Braking distance on different surfaces, straight-line and in curve o Yaw stability while braking on different surfaces, straight-line and in curve • **Use** Brake Distribution diagram	• 3.4.1 Typical Test Manoeuvres, 3.4.2 Deceleration Performance • Figure 3-47, Figure 3-48
• **Exemplify** at least 3 "Requirements on a braking system". The 3 can be: o Brake distribution between axles for mild braking [torque fraction front/total] o Behaviour for hard braking, ABS/EBD [no single measure value] o Function Architecture Requirements: ▪ Requirements on information from braking system: ω_{whl} per wheel (sometimes also also v_x, ω_z, a_y). ▪ Requirements on actuation requests by braking system: interfaces on vehicle level request (F_x or a_x) and per wheel, typically "dual request" $\{T_{Req}, s_{xLimReq}\}$ per-wheel interface. ▪ ~~Arbitrations and Coordinations within propulsion system~~ • **Understand** braking system parameters and **set** numerical values of them in a IPG CarMaker (as one example of tool)	• 3.4.4 Brake and traction distribution • 4.6.2.2.4 Wheel-Level Control • IPG CarMaker "ReferenceManual.pdf"

Modelling Concepts

Learning Objectives	Reading
• Model of 1 wheel, Vehicle model with individual wheels or lumped wheels, Lumping per vehicle, per unit, per axle group • Brake actuator dynamics, delays and time sampling • Disc friction, continuous dynamics or state event • ~~Tyre model close to $v_x = \omega = 0$ and tyre combined slip~~	• 2.5.1 Wheel Longitudinal Slip Limit Control
• One wheel slip control with brake actuator	• Figure 1-45 • 2.5.1 Wheel Longitudinal Slip Limit Control

Steering System

Design Concepts and Requirements

Learning Objectives	Reading
• **Describe** alternative steering system designs: o Front axle steering, Rear axle steering, Steered trailer, Articulated steering o Hydraulic or Electric assistance. Different degrees of "by-wire", e.g. ActiveFrontSteering • ~~Steering on truck rear axles and on towed units: Only for low speed is common.~~ • Steering feel control: Boost curve or closed loop control (Angle or Torque from Reference Generator) • ~~Active interventions: Angle overlay or Torque Overlay~~	• 2.6 Steering System
• **Exemplify** requirements on complete vehicle functionality where steering system is essential, e.g.: o Turning radius at low speed o Steering response, e.g. step steer $\omega_z(t)$ and $\omega_z(v_x)/\delta_{sw}$ at steady state cornering or oscillating δ_{sw}. o Steering feel, e.g. step steer $T_{sw}(t)$ and $T_{sw}(v_x)/\delta_{sw}$ at steady state cornering or oscillating δ_{sw}. o ~~Automated steering of different levels of automation~~	• 4.2.1.1Turning Diameter *Turning Diameter * • 0 #.#.#.#.#.# # • 4.4.3.2 Frequency Responses on Steering * • Figure 2-137 • ~~4.6.2.4 Lane Keeping Aid, LKA *, 4.6.2.5Lateral Collision Avoidance/Automatic Emergency Steering, LCA/AES *, 4.6.2.6Automated Driving (AD)~~
• **Exemplify** at least 3 "Requirements on a steering system". The 3 can be: o Boost curve o Steering ratio and Ackermann Percentage o Caster offset • **Understand** steering system parameters and **set** numerical values of them in a IPG CarMaker (as one example of tool)	• 2.6.2 Steering System Forces, Figure 2-133 • Figure 2-134, Figure 2-136 • IPG CarMaker "ReferenceManual.pdf"

Modelling Concepts

Learning Objectives	Reading
• **Explain** difference between modelling concepts: o Stiff or compliant steering column o Rack and wheel with or without mass inertia o Simple steering ratio or modelling the kinematics of steering links • **Modelling** the steering assistance with or without time sampled control algorithms • **Briefly understand** the difficulties with co-simulation and HIL for steering assistance systems.	• Figure 2-134, Figure 2-136
• Steering assistance influence on step steering response and feel	• 2.6.2 Steering System Forces